USMCA 2013

12th INTERNATIONAL SYMPOSIUM ON NEW TECHNOLOGIES FOR URBAN SAFETY OF MEGA CITIES IN ASIA

(SEIKEN SYMPSIUM 75)

ISBN4-903661-68-7

USMCA 2013

ICUS Report 2013-03 (serial No.73)

the 12th International Symposium
on New Technologies
for Urban Safety of Mega Cities in Asia

October 9-11, 2013
at
Hilton Hanoi Opera Hotel, Hanoi, Vietnam
and
National University of Civil Engineering, Hanoi, Vietnam

Edited by
Eiko Yoshimoto

Organized by
International Center for Urban Safety Engineering,
Institute of Industrial Science, The University of Tokyo, Japan
National University of Civil Engineering, Vietnam
and
Vietnam Federation of Civil Engineering Association, Vietnam

Sponsored by
The Foundation for the Promotion of Industrial Science, Japan,
National Foundation for Science and Technology Development, Vietnam,
JFE Steel Corporation,
Delta Corporation,
SE Corporation,
Vietnam - Japan Engineering Consultant,
Department of Building and Industrial Engineering, NUCE, Vietnam,
Consultancy Company Limited of University of Civil Engineering,
FECON Foundation Engineering and Underground Construction,
JSC,
Consultant and Inspection Joint Stock Company of Construction,
Technology and Equipment – CONINCO,

Coteccons Group,
Aimil International,
Vietnam Geotechnical Engineering JSC
and
GETECCO Corporation

Cooperated by
Ministry of Construction, Vietnam,
Ministry of Education and Training, Vietnam,
Japan International Cooperation Agency
And
Japan Society of Civil Engineering

SYMPOSIUM ORGANISERS

CHAIRMEN

Le Van Thanh, President of National University of Civil Engineering (NUCE), Vietnam
Kimiro Meguro, Director of ICUS, IIS, The University of Tokyo
Pham Sy Liem, Vice President of VFCEA

STEERING COMMITTEE

Pham Duy Hoa, Vice president of National University of Civil Engineering, Vietnam
Pham Hung Cuong, Vice president of National University of Civil Engineering, Vietnam
Do Huu Thanh, National University of Civil Engineering, Vietnam
Le Trung Thanh, Ministry of Construction, Vietnam
Ha Minh, Coninco, Vietnam
Mehedi Ahmed Ansary, Bangladesh University of Engineering Technology, Bangladesh
Sudhir Misra, Indian Institute of Technology Kanpur, India
Takeo Uomoto, Chief Executive, Public Works Research Institute, Japan
Yoshiaki Nakano, Director, IIS, the University of Tokyo, Japan
Tsuneo Katayama, Real-time Earthquake Information Consortium, Japan
Wei Cheng Fan, CPSR, Tsinghua University, China
Worsak Kanok-Nukulchai, Asian Institute of Technology, Thailand
Yoshifumi Yasuoka, Research Organization of Information and System, Japan
Do Van Hua, VFCEA

TECHNICAL COMMITTEE

Phan Quang Minh, National University of Civil Engineering, Vietnam
Nguyen Huu Dao, National University of Civil Engineering, Vietnam
Nguyen Truong Tien, President of VSSGME, Vietnam
Nguyen Viet Anh, National University of Civil Engineering, Vietnam
Nguyen Hoang Giang, National University of Civil Engineering, Vietnam
Dinh Van Hiep, National University of Civil Engineering, Vietnam
Chayanon Hansapinyo, Chiang Mai University, Thailand
Haruo Sawada, ICUS, IIS, the University of Tokyo, Japan
Kiang Hwee Tan, National University of Singapore, Singapore
Kimiro Meguro, ICUS, IIS, the University of Tokyo, Japan
Mafizur Rahman, Bangladesh University of Engineering Technology, Bangladesh
Pennung Warnitchai, Asian Institute of Technology, Thailand
Somnuk Tangtermsirikul, Thammasat University, Thailand
Srikantha Herath, United Nations University, Japan
Taikan Oki, ICUS, IIS, the University of Tokyo, Japan
Jiro Kuwano, Saitama University, Japan

ORGANIZING COMMITTEE

Reiko Kuwano, ICUS, IIS, the University of Tokyo, Japan
Akiyuki Kawasaki, ICUS, IIS, the University of Tokyo, Japan
Kohei Nagai, ICUS, IIS, the University of Tokyo, Japan
Pham Dang Khoa, National University of Civil Engineering, Vietnam
Dinh Van Thuat, National University of Civil Engineering, Vietnam

Contacts:

Nguyen Hoang Giang, National University of Civil Engineering (NUCE), Vietnam
Eiko Yoshimoto, ICUS, IIS, the University of Tokyo, Japan

PREFACE

On behalf of the Organizing Institutes of the 12th International Symposium on New Technologies for Urban Safety of Mega Cites in Asia (USMCA2013), I expressed our sincere welcome to all symposium participants and distinguished keynote speakers.

In the Asia and Pacific-Rim regions, rapid economic development and population growth and concentration is fast accelerating the pace of urbanization. Unfortunately, the rapid expansion of infrastructure for urbanization is not adequately balanced with appropriate measures for their maintenance and management, and urban disasters have resulted. During the last few years, there were several big disasters in Asia and the Pacific Rim regions, such as killer cyclones Sidr in Bangladesh (2007), Nargis in Myanmar (2008), and Aila in Bangladesh and India (2009), and Typhoon Ketsna in Philippines (2009), flooding in Mongolia (2009) and Pakistan (2010), the devastating earthquakes in Sichuan, China (2008), Sumatra (2009), Samoa (2009) and Tohoku, Japan (2011), and heat waves in Russia and Japan (2010). The number of fatalities and missing reported due to these disasters was well over 200,000. These unprecedented events show us the importance of urban safety.

The International Center for Urban Safety Engineering (ICUS) was established in 2001 at the Institute of Industrial Science (IIS), the University of Tokyo, with the objectives of carrying out researches on urban safety and implementing them towards the realization of safer cities, especially in Asia and the Pacific Rim regions, in the 21st century. For over a decade, ICUS has been actively tackling advanced researches, as well as the enhancement of networking, dissemination and information collection in order to fully realize ICUS's vision. And as a part of ICUS activities, ICUS has been annually co-organizing USMCA since 2002 with its partners in the Asian region. In 2013, ICUS jointly organized the 12th USMCA in Hanoi, Vietnam, with National University of Civil Engineering (NUCE) and Vietnam Federation of Civil Engineering Association (VFCEA).

The objectives of the symposium was to bring together decision makers, practitioners and researchers involved in the field of urban safety to share their expertise, knowledge and experience in tackling the critical issues for safer cities in Asia and the Pacific Rim regions. It also provided an environment to create and reinforce collaborative networks among experts in the fields relevant to urban safety. The symposium focused on disaster response and recovery; risk assessment, prediction, and early-warning; decision-making technologies; planning and development of urban infrastructure systems; life-cycle management of infrastructure systems; climate change mitigation and adaptation; and application of geospatial technologies.

During the two-day symposium, 130 papers in thirteen parallel sessions were presented with five papers by keynote speakers. We also had research exhibitions in 13 booths on the first day. Total participants were 328 from 16 countries such as Vietnam, Thailand, China, Sweden, Bangladesh, Japan, Korea, Mongolia, India, Indonesia, Singapore, Myanmar, Nepal, Pakistan, Canada and USA.

I would like to thank all the members of the Steering, Technical and Organizing Committees as well as the Symposium Secretariat for their hard work, time and effort in putting this symposium together. I would also like to thank all our sponsors for their generous support and contribution. Thanks are also due to all those who have contributed towards making this symposium successful.

Kimiro MEGURO

Director of ICUS, IIS, The University of Tokyo
(Co-Chairman of Organizing Committee, USMCA2013)

Please contact:
International Center for Urban Safety Engineering (ICUS),
Institute of Industrial Science (IIS),
The University of Tokyo, Japan

Tel: +81-3-5452-6472
Fax: +81-3-5452-6476

2013 Program Overview

Time	Tuesday, 8 October
09:00-16:00	Technical visits & sightseeing pre-conference day Van Mieu - Imperial Academy – Nhat Tan Bridge
18:00-19:00	Registration at Hilton Hanoi Hotel
19:30-	Welcome dinner

Time	Wednesday, 9 October	
08:00-08:30	**Registration (Hilton Hanoi Hotel)**	
08:30-08:55 (5*4)	**Opening address (Ballroom)** WELCOME Speech (Dr. Le Van Thanh - President of National University of Civil Engineering) WELCOME Speech (Prof. Kimiro Meguro - Director of ICUS, The University of Tokyo) Opening Remark (Mr. Hideo Suzuki, Deputy Chief of Mission of Japan Embassy in Vietnam) Opening Remark (Dr. Nguyen Thanh Nghi - Deputy Minister of Construction) Opening Remark (Mr Fumihiko Okiura - Senior Representative of JICA Vietnam) **Moderator: Dr. Nguyen Hoang Giang**	
08:55-09:25	**Keynote Speech (Ball room)** **Advanced technologies for safety of underground expressway network in Tokyo metropolitan area** Dr. Hiroshi Dobashi - President, Shutoko Engineering Co., Ltd, Japan **Moderator: Dr. Nguyen Hoang Giang**	
09:25-10:15	**Group photo – Coffee break & Exhibitions**	
10:15-10:45 11:45-11:15 11:15-11:30	**Keynote Speech (Ball room)** **The structural design trend of supertall buildings in Vietnam** Prof. Phan Quang Minh - Dean of Building & Industrial Engineering Department – NUCE **Construction technologies for royal city complex** Mr. Tran Nhat Thanh – President of Delta Corporation **Advanced steel technologies for infrastructure** Dr. Hisaya Kamura- JFE Steel Corporation **Moderator: Dr. Nguyen Hoang Giang**	
11:30-11:40	**Sponsor awards**	
11:40-13:00	**Lunch at Hilton Hanoi Hotel 2nd floor**	
	Lecture hall 1	**Lecture hall 2**
13:00-15:00	**Session 1-A** : *Session Chairs:* *Dr. Takaaki Kaato* *Dr.Dinh Van Thuat*	**Session 2-B** : *Session Chairs:* *Prof. Reiko Kuwano* *Dr. Nguyen Hoang Giang*
15:00-15:30	*Tea-break at Exhibition zone*	
15:30-17:30	**Session 3-C** : *Session Chairs:* *Prof. Taketo Uomoto* *Dr. Nguyen Hung Phong*	**Session 4-D** : *Session Chairs:* *Prof. Haruo Sawada* *Prof. Pham Quang Hung*
18:30-22:00	Symposium dinner Maison Sen Restaurant (bus will be leaving at 18:00)	

Time	Thursday, 10 October		
	NUCE **Library building 2nd floor**	**NUCE** **Environmental Inst: 2nd floor**	**NUCE** **G3 building 1st floor**
09:00-10:30	**Session 5-E1 :** *Session Chairs:* *Prof. Nguyen Viet Anh* *Prof. Sudhir Misra*	**Session 6-F1** *Session Chairs:* *Prof. Jiro Kuwano* *Dr. Le Quang Hanh*	**Session 7-G1 :** *Session Chairs:* *Prof. Mehedi Ahmed Ansary* *Prof. Do Huu Thanh*
10:30-10:45	Tea-break at session area		
	NUCE **Library building 2nd floor**	**NUCE** **Environmental Inst: 2nd floor**	**NUCE** **G3 building 1st floor**
10:45-11:25	**Session 5-E2:** *Session Chairs:* *Dr. Miho Ohara* *Dr. Dinh Van Hiep*	**Session 6-F2 :** *Session Chairs:* *Prof. Tan Kiang Hwee* *Dr. Tran. T. Viet Nga*	**Session 7-G2 :** *Session Chairs:* *Prof. Mikio Koshihara* *Dr. Dao Danh Tung*
11:30-12:00	**Campus tour**		
12:00-13:30	**Lunch at Long Vi restaurant**		
13:30-15:50	**Session 5-E3** *Session Chairs* *Dr. Takaaki Kato* *Prof. Pham Thuy Loan*	**Session 8 :** *Session Chairs:* *Dr. Akiyuki Kawasaki* *Dr. Win Win ZIn*	**Session 9 :** *Session Chairs:* *Dr. Kohei Nagai* *Dr.Pham Hoang Kien*
15:50-16:00	Coffee break at G3 Hall, 2nd floor		
	G3 Hall		
16:00-16:30 16:30-17:00 17:00-17:30	**Keynote Speech (G3 Hall)** **Utilization of unused and/or non-familiar materials for construction** Prof. Taketo Uomoto - Chief Executive, Public Works Research Institute / Professor Emeritus, University of Tokyo **Water management in Vietnamese cities: present status and vision to future** Prof. Nguyen Viet Anh - National University of Civil Engineering **SanrikuTsunami and reconstruction of cities** Prof. Hiroshi Naito - Architect / Emeritus Professor, the University of Tokyo **Moderator: Dr. Nguyen Hoang Giang**		
17:30-18:30	**Closing ceremony (G3 Hall)** Young award ceremony Announcement of USMCA2014 NUCE's closing speech ICUS's closing speech Closing Banquet & Music **Moderator: Dr. Nguyen Hoang Giang**		

Time	Friday, 11 October
08:00-20:00	Excursion Ha Long Bay

Contents

Keynote Session

Oral Sessions

TECHNICAL PROGRAMME – DAY 1

Session 1-A:

Session 2-B:

Session 3-C:

Session 4-D:

TECHNICAL PROGRAMME – DAY 2

Session 5-E1:

Session 5-E2:

Session 5-E3:

Session 6-F1:

Session 6-F2:

Session 7-G1:

Session 9:

Photograph

Welcome boards

View of registration at Hilton Hotel

Inauguration ceremony

View of participants of opening address

View of participants of keynote speech session

Dr. Le Van Thanh,
President, NUCE, Vietnam

Prof. Kimiro Meguro,
Director, ICUS, Japan

Mr. Nguyen Dinh Toan,
Deputy Minister of Construction, Vietnam

Mr. Hirofumi Miyake,
Embassy of Japan in Vietnam

Mr. Fumihiko Okiura,
Senior Representative, JICA Vietnam

Invited speakers (Keynote)

Dr. Hiroshi Dobashi, President, Shutoko Engineering Co., Ltd, Japan

Prof. Phan Quang Minh, Dean, Building & Industrial Engineering Dept. NUCE, Vietnam

Mr. Tran Nhat Thanh, Chairman, DELTA Group, Vietnam

Dr. Hisaya Kamura, General Manager, JFE Steel Corporation, Vietnam

Dr. Taketo Uomoto, Chief Executive Public Works Research Institute, Japan

Prof. Nguyen Viet Anh, NUCE, Vietnam

Prof. Hiroshi Naito, Architect, Professor Emeritus, The Univ. of Tokyo, Japan

Exhibition area

Exhibition area

Invited speakers

Prof. Kiang Hwee Tan,
National University of Singapore,
Singapore

Prof. Sudhir Misra,
IIT, Kanpur, India

Prof. Mehedi Ahmed Ansary,
BUET, Dhaka, Bangladesh

Mr. Khin Maung Maung,
CEC menber,
Myanmar Engineering Society,
Myanmar

Dr. Win Win Zin,
Yangon Technological University,
Myanmar

Second day at National University of Civil Engineering

Closing ceremony

View of closing ceremony

Prof. Pham Hung Cuong, Vice-Rector, NUCE, Vietnam

Young-Researcher- Award recipients
with Prof. Kuwano (left) and Prof. Meguro (right)

Awardees: Mr. Chunri Quan, ,Mr. Tomofumi Ikenaga,
Mr. Tsubasa Sasaki, Ms. Naoc Duyen Nguyen, UTokyo, Japan and Mr. Nguyen Chou Lan, NUCE, Vietnam
(from the second left to the right)

Vietnam student-staff with organizers

Group photos

Press coverage by VTV and Hanoi TV

ICUS members meet with Dr. Le Van Thanh, President of NUCE

Lunch, break, banquet and farewell party










Whole day tour : Visit to Van mieu, Imperial Academy and Nhat Tan Bridge on 8th October

Whole day tour: Visit to Ha Long bay on 11th October

Visit to Vietnam city

Keynote Session

Advanced safety technology for underground expressway in Tokyo metropolitan area

Hiroshi DOBASHI
President, Shutoko Engineering Co., Ltd., Japan
h.dobashi118@shutoko.jp

ABSTRACT

The Metropolitan Expressway network serves as a major traffic facility that supports socio-economic activities in the Tokyo metropolitan area and it currently extends for approximately 300 km. With economic growth and rapid development of the city, effective utilization of urban space is highly required for development of infrastructures such as the Metropolitan Expressway and the subways. In addition, with consideration of environmental conservation, underground structures instead of viaduct structures have been recently employed. As a result, the Central Circular Shinjuku and Shinagawa Routes of the Metropolitan Expressway are mostly comprised of tunnel structures with 18km in total length, which is the longest tunnel in urban areas. Therefore, management and operation system of the urban long tunnel has been developed to secure safety and prevent disasters such as fire or other accidents in addition to development of innovative tunnel construction technology. Advanced safety technology would be expected to contribute further to effective utilization and development of underground space in urban areas.

Keywords: *environmental conservation, safety and disaster prevention system, innovative tunnel construction technology*

1. INTRODUCTION

The Metropolitan Expressway network, on which construction began more than 50 years ago, currently extends for approximately 300 km (Fig.1). In 2011, it carried about 1 million vehicles and about 2 million passengers per day. Although the total length of the network in service is only 15% of the total length of major city roads in the Tokyo metropolitan area, it carries approximately 30% of the total traffic in terms of vehicle-kilometrage, indicating the degree of utilization. Since it carries approximately 28% of freight transportation in the area, it is considered to function approximately twice more in vehicle-kilometrage and approximately three times more in freight transportation than other major city roads. As described above, the Metropolitan Expressway network serves as a major traffic facility that supports socio-economic activities in the Tokyo metropolitan area, and it is a road system that is indispensable to the lifestyle of the people in the area.
The operation of an effective traffic system in the Tokyo metropolitan area requires the creation of a network with a appropriate balance between radial and

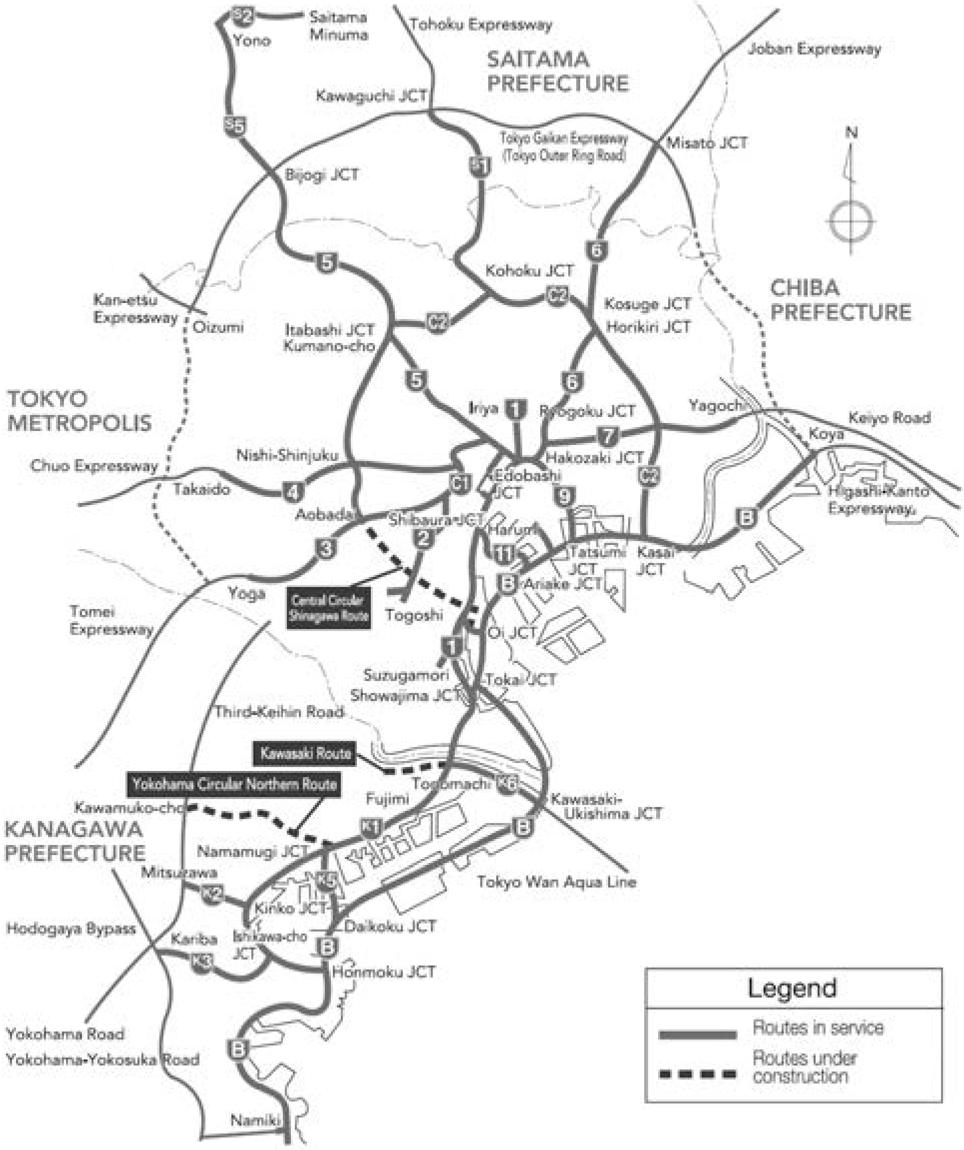

Figure 1: The network of Tokyo Metropolitan Expressway

circular routes. The Metropolitan Expressway Company Limited completed the Central Circular Shinjuku Route in 2009, and is currently in the process of building the Central Circular Shinagawa Route that forms a southern part of the Central Circular Route due to be completed in the fiscal year of 2014.

The Central Circular Shinjuku and Shinagawa Route employ a tunnel structure to accommodate the land use patterns along the route and the concerns for environmental conservation, hence enabling the construction of expressways in densely populated urban areas. In order to secure the financial feasibility of the project, appropriate measures are taken to reduce the costs and construction period based upon the use of the new technology. Furthermore, an important aspect of urban long tunnel construction is the need for safety measures especially against fire. Therefore, traffic and facility operation such as provision of information, ventilation system and so on, are required.

This paper provides the innovative tunnel construction technology, and management and operation system of the urban long tunnel which has been newly developed to secure safety and prevent disasters such as fire or other accidents.

2. THE CENTRAL CIRCULA SHINJUKU AND SHINAGAWA ROUTE

2.1 The Shinjuku Route (Yamate Tunnel)

The Shinjuku Route is an 11 km expressway between Route No.3 and No.5 (as shown in Figure 1) that is designed with two lanes in each direction and has a design speed of 60 km/h. To accommodate the land use patterns along the route, and in order to conserve a surrounding environment and make efficient use of limited public urban space, the Shinjuku Route is designed as a tunnel structure under the circular road Route No.6 (Yamate Dori), which will be widened to 40m in the same period. Therefore, the alignment of the tunnel, the types of underground structures, and the construction methods must take account of constraint conditions such as the crossing of rivers, subways, trunk roads and railways, as well as the accommodation of major existing public utilities. As further characteristic feature of the Shinjuku route, i.e. the short average distance between the access ramps, it has a short average distance between access ramps, with six access ramps to the ground-level street and three junctions connecting the radial routes of other Metropolitan Expressway.

Because of the complicated structure of the ramps and the large number of them, transversal ventilation system is employed with nine ventilation stations installed on this route. Seven of these ventilation stations are installed underneath the circular road No.6, while only the ventilation towers are built above ground. This is due to the limitations in the availability of space above ground. The remaining two ventilation stations are installed above ground in spaces off the road.

2.2 The Shinagawa Route

The Shinagawa Route is an 9.4 km expressway between Route No.3 and Bay-shore Route (as shown in Figure 1) that is designed with two lanes in each direction and has a design speed of 60 km/h. The Shinagawa Route is also employs a tunnel structure under the circular road Route No.6 and beneath Meguro river to accommodate the land use patterns along the route, and in order to conserve a surrounding environment and make efficient use of limited public urban space. The Shinagawa Route has one ramp accessing to the surface street and two junctions with existing routes.

Since less number of the ramp along the route, the longitudinal ventilation system is employed with four ventilation stations installed on this route. Two of these ventilation stations are installed under the circular road No.6. This is due to the limitations in the availability of space above ground. The remaining two ventilation stations are installed above ground beside the road

3. INNOVATIVE TUNNEL CONSTRUVTION TECHNOLOGY

The tunnel construction method for the Shinjuku Route was originally planned to be a cut-and-cover method. However, in the 1990’s, shield tunnels with 14m in diameter were completed and recent developments on shield tunnel have been developed in construction methods for underground junctions and for entrances and exits. As a result, shield tunneling method with a large diameter is employed for approximately 80% of the entire tunnel section instead of a cut-and-cover method. In addition, upon adopting large diameter shield tunneling, the following new design and construction technologies have been developed and/or introduced to reduce construction costs.

3.1 Establishment of a rational design method for shield tunnel segments

In the design of the segment, the structure of joints on a segment is properly evaluated by using the beam-spring model in the calculation method rather than by the conventional two-dimensional ring calculation model. The beam-spring model calculation evaluates reduction of bending rigidity and splice effects of staggered arrangement by using a model in which a segment is considered as a curved beam or a straight beam. A segment joint is considered as a rotational spring and a ring joint is considered as a shear spring.

In addition to above, a system in which the backfill grouting is recently conducted simultaneously or almost simultaneously with shield advancement, has been developed and the backfill grouting materials which achieve the required strength at an early stage after driving, have also come to be used. By employing such a backfill grouting system together with circle shape retaining device and using the thrust force of shield jacks properly, the soil reaction acting on the segments is considered even against the deformation of the segment caused by its self-weight, which has not been taken into account so far.

3.2 Reduction in tunnel diameter by eliminating secondary lining

Since shield tunnel construction, waterproofing of segmental lining itself and sealing materials have been improved, segmental joint bolts have become less exposed and the inside surface of a segmental lining have become flat and smooth. As a result, the secondary lining of the tunnel is eliminated, enabling several percent reduction of tunnel diameter.

On the other hand, installation of fire-resistant material on the inside surface of a tunnel segments shall be planned to prevent spalling of concrete segment from tunnel fires. Fire-resistant material has been tested and selected according to the German Standard, RABT curve. The mortal with fire resistance is sprayed on the surface of RC segment and panel of silicic acid calcium or ceramics is installed on the surface the steel segment. Recently, polypropylene fiber (PP, L=12mm, d=64.8μm, aspect ratio L/d=185), is mixed with concrete to prevent spalling by getting vapor enter into the void of concrete generated by the melt of PP fiber.

3.3 Development of shield tunnel enlargement method

The innovative technology has been developed to connect main tunnel with ramp tunnel. As a result, the structures of underground junction and connection between main and ramp tunnels can be constructed by excavation from the surface with a cut-and-cover method or trenchless method after main shield tunnels are completed.

With development of this method, the distance of a tunnel excavated by one shield machine is dramatically increased, and overall construction cost is reduced and the construction period is shortened. In addition, the adverse effects on surface traffic and the surrounding environment can be reduced by minimizing the width of open excavation. Finally, it would be possible to minimize a risk for delay of construction schedule and reduce environmental impact for surroundings.

4. TUNNEL MANAGEMENT AND OPERATION

4.1 Basic policy for fire prevention and safety measure

The basic policy is that if a fire breaks out, the Metropolitan Expressway Co., Ltd. will put human life first and give top priority to evacuation, while also preventing secondary disasters and ensuring the overall safety of expressways through cooperation with the related organizations. The policy is unique in that it gives consideration to traffic congestion. The aim is to further improve fire prevention and safety by taking multifaceted measures from the viewpoints of both facility planning and management/operation. Such measures include operating road transport systems to reduce traffic congestion on a routine basis and operating the systems in accordance with traffic congestion at the time of fire as well. In order to further improve safety, it is important to take operational measures on a routine basis as well as during time of fire. Based on the following considerations, the comprehensive fire prevention and safety measures shown in Figure 2 will be taken on a routine basis.

- To take measures to prevent accidents, fire and other irregularities on a routine basis
- To take measures to minimize damage to human life and facilities if a fire occurs in the tunnel as well as to minimize the effects of the fire on society as a whole
- To work with users as well as the related organizations, including police, firefighters and other road administrators, making efforts to prevent disasters and ensure the safety of the tunnel
- To Carry out on a routine basis educational activities and fire prevention drills to prevent accidents and fires from developing into serious disasters

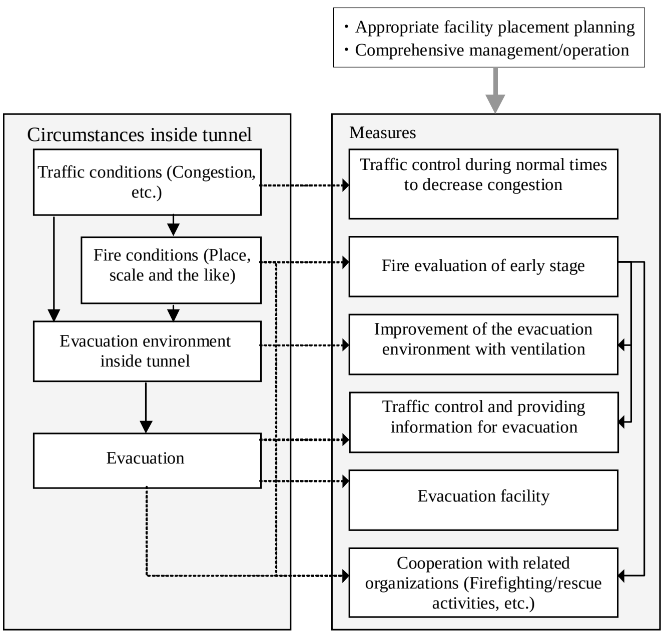

Figure 2: Basic policy of fire prevention

Measures are being studied to provide information on people evacuation and guidance so that evacuation can be completed at an early stage of the fire. With data of the past experimental fires, traffic accidents and other irregularities as a reference, the characteristics of vehicle fires were analyzed and road tunnel fire development was classified into early and late stages. The time targeted to complete evacuation is around 10 minutes for the early stage of a fire. The details will be discussed in 4.2, 4.3 and 4.4.

4.2 Traffic control and management

To ensure safety and comfort on the Tokyo Metropolitan Expressway, traffic control is in operation on a round-the-clock basis. Patrol services are mustered to deal with accidents in a speedy manner and recover fallen objects. Information providing services are also offered to expressway users by processing road data sent at set intervals in real-time. For example, ultrasonic vehicle detectors are installed at intervals of approximately 300m to collect traffic data. In this manner, traffic volume, speed, and occupancy data are collected and processed in real-time to assess traffic conditions. The data is displayed or provided on overhead information panels on the expressway routes and through a roadside radio service. In addition, a personal information service called VICS provides congestion and required travel time information to individual cars via on-board receivers. In tunnels, CCTV cameras are installed at intervals of about 100m. Images from the cameras are used by the control staff to monitor traffic conditions in tunnels around the clock. Emergency telephones and other devices are installed so expressway users can report accidents and other irregularities. In addition, because of the recent spread of cellular phones it is now possible to report to the control room using the #9910 speed dial number.

In conjunction with the construction of the Shinjuku Route, a new Traffic Control and Monitoring Center will be built in addition to the existing one. The objective is to introduce a more advanced and sophisticated system of traffic control. A typical example is the newly developed system capable of detecting traffic extraordinary behaviors instantly by processing CCTV images. The introduction of this type of system will help block vehicular access into the tunnel after a traffic accident has occurred and ensure a smooth flow of traffic through the tunnel. The traffic control system can also be used to prevent traffic jams in tunnels to maintain safety and comfort during normal conditions as well.

4.3 Principles governing the safety of users in case of fire

In the event of a fire outbreak, effective fume control must be provided to withdraw fumes and care has to be taken to improve the escape routing. Appropriate information must be offered to guide people through emergency exit to safe areas. It is also of great importance to provide safe escape routing rapidly, the flow of traffic on the opposite tunnel that is not exposed to fire should be stopped as quickly as possible.

The Shinjuku Route is provided with all emergency facilities laid down by national regulations. Consideration is being given to the creation and operation of facilities designed to improve the escape routing through the earliest possible detection of fire outbreak, accurate assessment of the situation, and effective operation of fume exhaust facilities and to guide people to safer refuge areas. In addition, a tunnel design is planned to permit rapid access of the firefighting services to the site of the fire accident. This may include the construction of a U-turn lane in the tunnel to permit fast rescue and firefighting operations by the firefighting services.

4.3.1 Prohibition of access for vehicles with dangerous loads and emergency equipment

Since the Shinjuku Route is a tunnel of more than 5km in total length, vehicles carrying dangerous loads such as explosives and gasoline are not allowed for access into the tunnel in accordance with the Road Law. Consequently, fire accidents on the Shinjuku Route can only involve vehicles that do not carry dangerous loads.

Emergency facilities in the tunnel are subject to the “Technical Standard on the Tunnel Emergency Equipment” by the central government authorities in accordance with traffic volume and tunnel length. The Shinjuku Route is ranked as Class AA, requiring the installation of all necessary and adequate emergency equipment. Figure 3 shows tunnel classification and Table 1 shows emergency equipment required for Class AA tunnel.

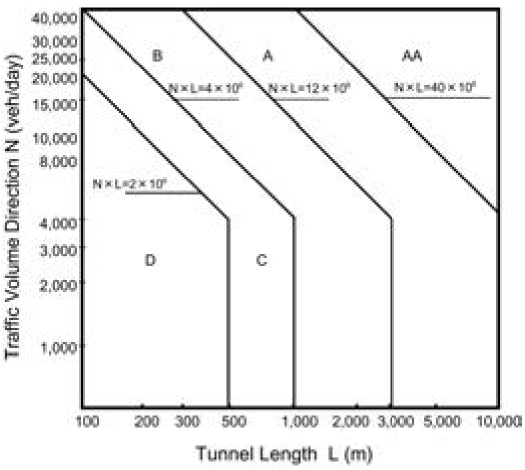

Figure 3: Tunnel classification

Table 1: Emergency equipment for Class AA tunnel

Warning and alarm equipment	Emergency telephone Alarm button Fire detector Emergency alarm Traffic signal
Fire extinguishing equipment	Fire extinguisher Foam hydrant
Escape route guide system	Emergency Exit Escape guide panels Fume exhaust equipment
Other equipment	Water hydrant Sprinkler Radio communications Radio re-broadcasting CCTV camera Uninterrupted power supply Emergency power supply

4.3.2 Arrangement of Escape Routes

Emergency exits in the tunnel are spaced at an interval distance sufficient to allow people to escape safely on foot. There are 39 emergency exits spaced at intervals no longer than about 350m. There are following three types of emergency exits on the Shinjuku Route.

1) Center Evacuation Route Type: The inner and outer lanes of sections built by the open-cut method are designed as an integral structure and five evacuation routes are to be built in the center of this type of structure.
2) Connecting Tube Type: In the section built by the shield method, where the inner and outer tunnels are separate the two tunnels are to be connected with 10 escape tubes to enable people to escape safely to the oppose tunnel.
3) Independent Stairs Type: Where it is structurally difficult to install evacuation route or escape connecting tubes, independent escape stairs are to be provided for access to the ground. These stairs are to be provided in 19 locations. In section in which shields are constructed in the vertical configuration the upper and lower tunnels are to be connected by escape stairs to be provided in five locations.

People who have escaped through 1) the evacuation routes or 2) connecting tube will be able to reach the ground safely through escape stairs (provided in 24 locations) installed in the shield construction shafts where the shield machine is to be started or in the ventilation locations constructed by the open-cut method.

4.4 Safety measures in case of fire

While vehicles carrying dangerous materials are not permitted access to the Shinjuku and Shinagawa urban long tunnels, their traffic volume are expected to reach 60,000 - 80,000 and 57,000 – 75,000 vehicles a day, respectively, with large vehicles to make up about 30%. This means that the traffic volume will be very high and so will the proportion of large vehicles. In view of past traffic conditions and fire accident patterns, careful and detailed considerations are given to the opinions and experiences of other countries in designing other details of tunnel structures. In the event of a fire, its earliest possible detection and ascertaining the situation comes first. It is essential to efficiently extract smoke to improve the evacuation environment, provide appropriate information, and guide evacuees through emergency exits to a safe space.

4.4.1 Improvement of evacuation environment with ventilation

In the early stage of a fire, ventilation facilities will be operated to maintain an environment for evacuating people safely and efficiently. For the Shinjuku and Shinagawa Route tunnels, different methods are being devised for operating ventilation facilities depending on whether there is congestion or not, and specific operation systems are currently under consideration. In the last phase of a fire, the operation of ventilation facilities will be switched to support firefighting operation by firefighting units, and specific operational systems for this stage are also under consideration. The Shinjuku Route tunnel uses the transversal ventilation system based on the specially structured flue method while the Shinagawa Route tunnel uses longitudinal ventilation system with the simplicity of the entire tunnel structure. Model tests, numerical fire simulations and other experiments were conducted to confirm whether or not an evacuation environment could be maintained for around 10 minutes immediately after a fire breaks out, the goal set

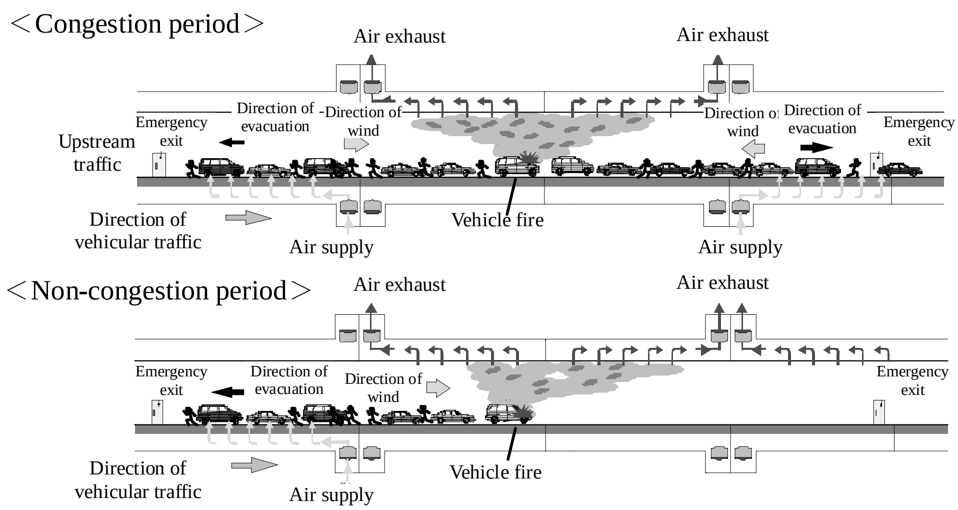

Figure 4: Concept of ventilation operation in case of fire

by the Metropolitan Expressway Co., Ltd. The experimental results confirm that such an evacuation environment can be maintained with the scale of ventilation facilities that is currently planned. (See Figure 4)

4.4.2 Traffic control and providing information for evacuation

Traffic control for the guidance of vehicles involves utilizing entrances and exits effectively to control traffic for certain sectors with the aim of reducing the number of vehicles in the tunnel. The Shinjuku and Shinagawa Route tunnels will have a large volume of traffic, and therefore, in order to guide vehicles more precisely, the Metropolitan Expressway Co., Ltd. plans to install traffic block facilities such as crossing gate, two or more information boards, and signals both at the entrance of the tunnel and at the point where the tunnel diverges (See Figure 5). The ultimate goal of evacuating and guiding people who escape on foot is to guide them up to the ground smoothly and safely, and appropriate ways of providing necessary guidance information along the escape route have been studied. Measures have been considered on how to guide people to emergency exits, the most important measures for evacuating them and ensuring their safety, and how to complete their evacuation in around 10 minutes: the target set by the Metropolitan Expressway Co., Ltd. After a fire is detected, it is important to immediately provide initial information of fire to all people in the tunnel in order to direct their attention to the event. After that, information on fire will be provided to people inside the car through repeated radio broadcasts and to those who are outside the car through public address systems. The evacuation and guidance policy is to provide people with information in two ways: providing visual information by installing guidance lamps pointing to emergency exits and providing auditory information by using public address systems.

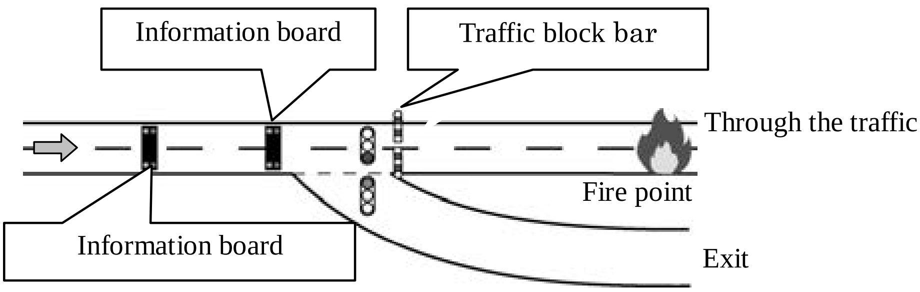

Figure 5: Traffic control equipment at the diverging point in the tunnel

4.4.3 Cooperation with related organizations

Since cooperation with related organizations such as firefighting authorities is important to prevent secondary disasters and check the spread of fire, the road administrator has devised policies on supporting such organizations. The Shinjuku and Shinagawa Route tunnels exist in urban areas, and therefore, fire stations are located relatively close to the route and the time required for firefighters to rush to the scene is not a major problem. It is necessary, however, that firefighters choose an efficient and safe route since the Shinjuku Route tunnel has many entrances and exits. It is of utmost importance to communicate accurate information to fire stations quickly, and plans call for direct telephone lines to be installed and visual images provided by cameras to be exchanged so that the control room can communicate with fire stations easily.

5. CONCLUSION

This paper has described the innovative technologies for the construction of tunnel structures in urban areas, and integrated management and operation system for long urban tunnel to secure safety and prevent disasters.
Based on the results in this paper, the following conclusions can be drawn.

- In order to achieve an efficient operation of traffic network in the Tokyo Metropolitan area, it is essential to develop the circular route.
- Since the Central Circular Shinjuku and Shinagawa Routes are located in highly densely populated city, it is essential to construct these routes underground to accommodate the need for minimizing the environmental impact and complete the routes in a short period.
- These underground projects provide a realistic prospect and sustainable development for reducing construction costs through the use of innovative construction technologies such as a large diameter of shield tunnel and shield tunnel enlargement method which has been newly developed by the Metropolitan Expressway Co., Ltd.
- Safety measures to be taken at the time of fire are being developed with use of the latest knowledge and the overall direction of safety measures is being determined.
- The rapid collection of data and providing information by using traffic control and monitoring systems, and road and traffic control, including restriction of access into the tunnel, will also be an important factor in terms of upgrading service and safety.
- Safety of the Shinjuku and Shinagawa Route tunnels are an important criterion. In view of this, efforts will be made to develop the facilities, tunnel structures and their operation taking account of the latest opinions and studies.
- Considerations described in this paper will contribute to the urban safety of the underground space in mega cities such as Tokyo Metropolitan area.

REFERENCES

Furuki, M., Ando K. and Kurohara, I., 2001. Planning a long urban tunnel -project outline of the Tokyo Metropolitan Expressway Central Circular Shinjuku Route-, *1st World Conference on Urban Road Tunnel, 14th World Congress of the International Road Federation (IRF)*, Paris.
Hamabe, K., Kikkawa, H., Tajima, H., and Tazawa, S., 2005. Safety measures of fire prevention in long urban tunnels –Tokyo Metropolitan Expressway Central Circular Shinjuku Route-, *15th International Road Federation (IRF) World Meeting*, Bangkok.
Ando, K., Ishii, N. and Dobashi, H., 2004. Construction of the Metropolitan Expressway Central Circular Route, which supports Tokyo Metropolis, *The Third Civil Engineering Conference in the Asian Region(CECAR)*, Seoul.
Dobashi, H. 2012, Soil improvement for extra soft ground of offshore reclaimed land and advanced technology for tunnel construction, *International Symposium 'Developing bridge and road construction technology in Viet Nam' VIBRA-MOT*, Hanoi.

The structural design trend of supertall buildings in Vietnam

Phan Quang MINH[1], Pham Thanh TUNG[2]
[1] Professor, Dean, National University of Civil Engineering,Vietnam
minhpq@nuce.edu.vn
[2] Dr., National University of Civil Engineering,Vietnam
ptunguce@yahoo.com

ABSTRACT
This paper describes the tendency of the structural design of supertall buildings in Vietnam. Reference is made to four projects in Hanoi and Ho Chi Minh City. Besides, typhoon, inducing a huge wind load on high-rise buildings, is required to be rigorously considered. The wind tunnel test is applied to determine the impact of typhoon and then the obtained data are used to design both architectural and structural systems of the mentioned above buildings.

Keywords: supertall building, structural system, wind tunnel test

1. INTRODUCTION

Due to the high growth in population and businesses in Vietnam, the demand of supertall buildings has been rapidly increasing. As CTBUH (2012), the Keangnam Landmark Tower, the tallest building in Vietnam, is in Top 100 tallest completed buildings all over the world (38^{th}). A successful design of a building is an achievement of a mutual collaboration among of the architect and the engineer to find out an appropriate architectural and effective structural system. However, difference from the design work of low-rise buildings is the more challenges designers have to deal with high load-bearing foundation, vertical and horizontal structures to make the high-rise building sustain under the more sophisticated lateral load as wind load and the complexity of the mechanical systems: fire distinguisher, vertical transport and human evacuation.
Selecting the structural system has a great impact on both exterior aesthetics and its interior space planning of a building. In this paper, the structural systems of four tallest buildings, mentioned in Table 1, are analyzed to introduce the trend of tall building design in Vietnam.

Table 1: Vietnam's 4 Tallest Building (up to 2013)

Building	**City**	**Height**	**Floors**	**Year**
Bitexco Tower	Ho Chi Minh City	269 m	68	2010
Keangnam Landmark Tower	Hanoi	336 m	72	2011
Lotte Center Tower	Hanoi	267 m	65	2013 (roofing)
Vietinbank Tower	Hanoi	362 m	68	under construction

			
Bitexco Financial Tower	Keangnam Landmark Tower	Lotte Center Tower	Vietinbank Tower

Fig. 1.Four Tallest Buildings in Vietnam (up to 2013)

Besides, the decision of architects on the geometry of the floor plan not only impact upon the interior space planning, exterior building envelope but also to the structural design. Generally, the simpler and more regular the floor plan shape, the easier the demand of the user in floor partitioning is satisfied. Square, rectangular and round floor plans have shown the more efficiency than curved and irregular shapes. The efficiency is based on the ratio of the usable to gross area of a floor (Paul H K HO, 2007). Among of four buildings in the paper, The Vietinbank Tower is an example with the V- shaped plan and other three buildings are with smooth and round plan shapes. For these projects, the ratio is about 70 to 80 %.

2. FOUNDATIONS

A well-designed foundation is an important part of a high-rise structure because its function is to safely transfer the structural loads from the building to the ground. Successful geotechnical engineering remains hidden underground and the importance of a good foundation only becomes visible when errors occur. The foundation is evaluated based on the criteria of allowable settlements, tilting and building damage.

The reinforced concrete mat supported on bored piles was applied for the foundation system of the four projects. For example, the mat foundation of Lotte Project with the dimensions of 92.7 m(W) x 44.1 m(D) x5.7 m(H) was continuously cast in situ in 52 hours. On basis of aforementioned project data, the system is the most practical and economical option.

In Vietnam, the two-level basement is fairly popular but the studied projects have more than 4 underground floors. That required a rigid perimeter diaphragm wall constructed by the slurry method

Bored piles with a wide range of diameter and length based on their design load-bearing capacity are appropriately applied for tall buildings. At the Bitexco Tower, 1500mm diameter bored piles extending to a depth of between 80m to 90m were constructed under the main load-bearing structures, while the podium and basements were supported by bored piles with 1200mm in diameter and 63m in length (Figure 2). At the Vietinbank Tower, bored piles were 2000 mm in diameter, which extended to the depth of about 45 m from the ground surface with the observed load-bearing capacity of 35000kN, so far from limit capacity predicted by the Vietnamese Code.

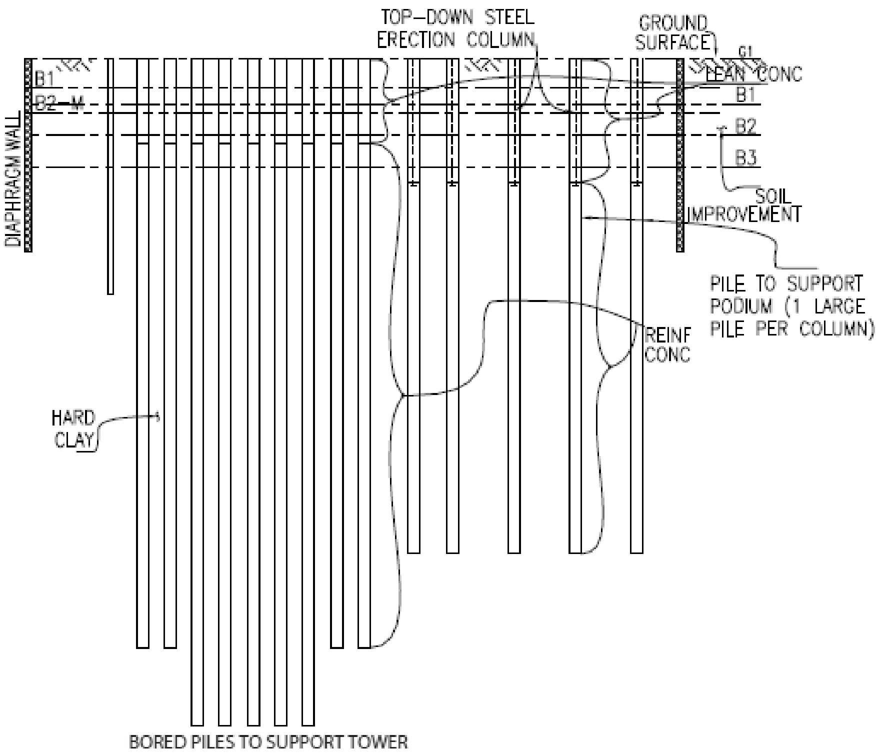

Figure 2.The Bitexco Tower's pile arrangement

3. MATERIALS AND SUPERTALL BUILDINGS

The selection of construction materials may be dependent on the height and function of a building. Each construction material has its own limitations in terms of mechanical properties and economical feasibility. The total structural material quantity and its cost have always been an important determinant for the development of super tall buildings. The structural efficiency can be measured by means of the lowest total construction cost which may be minimized by (1) using local materials and laborers, (2) optimizing the sizes of structural members so as to increase the usable/rentable floor area and thus its future revenue, (3) reducing the structural weight so as to reduce its impact on the foundation, and (4) shortening the overall construction time so as to generate income earlier and also reduce the loan expense. In Vietnam, concrete and steel are two dominant materials used to build tall buildings.

3.1. Concrete

In supertall buildings floor slabs and beams can be made of light weight or normal concrete which reduce their self-weight. The columns are normal or high strength concrete because they are the main load-bearing structures. High strength concrete is highly recommended for high-rise buildings due to high strength and durability. According to the European Norm EN 206-1, high strength concrete is defined as concrete with a strength class above C50 grade equal to B60 in Vietnamese Code TCVN 5574-2012. High strength concrete mix requires strictly quality control on site and is more expensive than normal strength concrete due to the requirement of high cement content and admixtures.
High-strength concrete has not been very common in Vietnam yet, but it was used for all abovementioned above projects with maximum grade of 70 MPa (cylinder). Concrete grades used for The Keangnam Landmark Tower and The Lotte Tower are shown in Table 2 and 3.

Table 2: Concrete strength in The Keangnam Landmark Tower

Keangnam Landmark Tower	**Residental Tower (50fls)** **Concrete grade**	**Hotel Tower (72fls)** **Concrete grade**
Shear walls, columns, beams	23F↓ 70 MPa 24F↑ 50 MPa	27F↓ 70 MPa 47F↓ 60 MPa 48F↑ 50 MPa
PT slab	23F↓ 50 MPa 24F↑ 45 MPa	27F↓ 50 MPa 47F↓ 45 MPa 48F↑ 35 MPa

Table 3: Concrete strength in The Lotte Tower

Lotte Tower	**Tower (65fls)** **Concrete grade**
Shear walls, columns, link beams	34F↓ 60 MPa 41F↓ 50 MPa 42F↑ 40 MPa
Beams, slab	34F↓ 43 MPa 41F↓ 40 MPa 42F↑ 30 MPa

3.2. Steel:

In Vietnam market, there are limited suppliers for quality structural steel and experienced contractors in steel fabrication. Using steel material to construct buildings is normally more expensive than reinforced concrete, when taking account of the additional fire protection cost for structural steel members.

For the Vietinbank Office Tower, a mixed system comprised of structural steel floor framing, perimeter composite columns and concrete core wall was employed (Figure 4). The structural steel grades for rolled shapes are to be as follows: wide flanges: ASTM A992 (f_y = 350 MPa), other rolled shapes: ASTM A36 (f_y = 250 MPa), built-up shapes: ASTM A572 (f_y = 345 MPa).

4. STRUCTURAL SYSTEMS OF TALL BUILDINGS

In addition to transferring the gravity loads to the foundation, another important role of the structural system in a tall building is to resist the lateral loads caused by wind or earthquake. Therefore, main structural systems of tall buildings are classified mostly based on their relative effectiveness in lateral load resistance.
Another classification of structural systems of tall buildings is on basis of the position of the dominant lateral load-resisting system at the floor plan including two broad categories: interior structures and exterior structures (Mir M. Ali and Kyoung Sun Moon, 2007). A system is categorized as an interior structure in which the major part of the lateral load resisting system is located within the interior of the building while in an exterior system if the main lateral load-bearing system is set on the perimeter of the building.

4.1. Interior Structures

The interior structure category consists of two fundamental types as the moment-resisting frames and shear trusses/shear walls. These systems are assembled by a group of planar structures developed in two orthogonal directions. These planar structures interact to form the spatial stiffness of the building to resist the lateral loads.
A derivation of this category is the core-supported outrigger structure, which is widely used for supertall buildings. Outrigger systems have been historically used by sailing ships to help resist the wind forces in their sails, making the tall and slender masts stable and strong. The core in a tall building is analogous to the mast of the ship, with outriggers acting as the spreaders and the exterior columns like the stays. As for the sailing ships, outriggers serve to reduce the overturning moment in the core that would otherwise act as pure cantilever, and to transfer the reduced moment to the outer columns through the outriggers connecting the core to these columns. The core may be centrally located with outriggers extending on both sides or in some cases it may be located on one side of the building with outriggers extending to the building columns on the other side (Taranath, 1998).
In comparison with the tube system which requires diagonals or closely spaced columns, the advantage of the core-outrigger system is that the exterior column spacing can easily meet aesthetic and functional requirements and the buildings perimeter framing system may consist of simple beam-column framing without the need for rigid-frame-type connections. For supertall buildings, connecting the outriggers with exterior megacolumns opens up the facade system more flexible, aesthetic and architectural articulation.
This system has a disadvantage is that the outriggers can interfere with the residential or rentable space and makes the erection process slower due to the lack of the structure unity. Nevertheless, these drawbacks can be overcome by

architectural and structural solutions such as placing outriggers in mechanical floors and improving erection procedure.
The outrigger systems may be formed in any combination of steel, concrete and composite construction. Most of the supertall buildings in Vietnam such as The Keangnam Landmark Tower, The Lotte Tower and The Bitexco Tower have used the system as the main load-bearing structures. Figure 3 shows the structural system of The Keangnam Landmark Tower with details of the outrigger trusses and belt trusses at the floor 23rd (Byung-Ick Yoon et al., 2010).

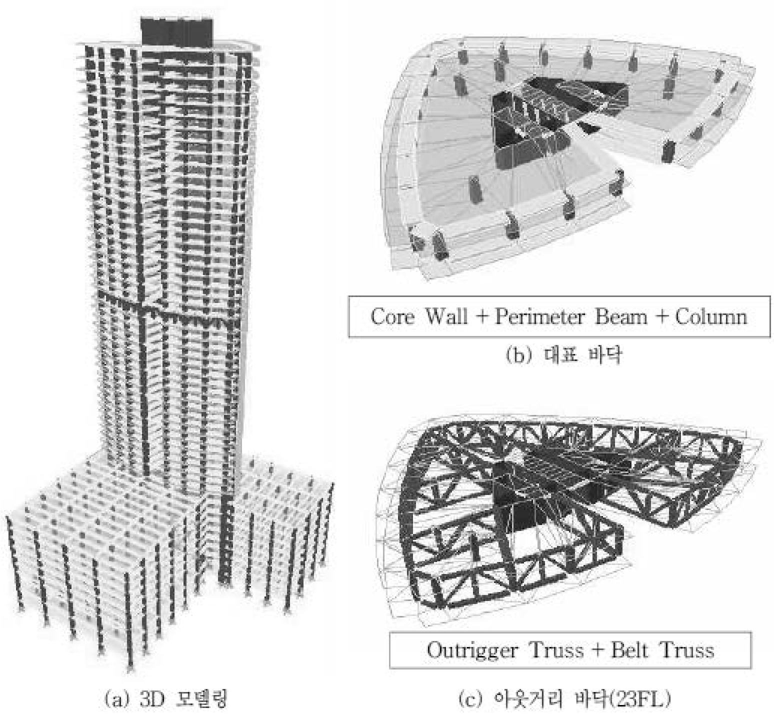

Figure.3. Structural system of Keangnam Landmark Tower

In The Bitexco Tower, for wind load design, the outrigger trusses and belt walls were connected to the core walls and perimeter columns from the floor 29th to 30th. This allows the outrigger and belt wall systems to collaborate with the concrete core walls in resisting lateral loads. To construct the outrigger system, two of the four sets of double-story trusses was set aligned with the two primary core cross walls and the other two trusses was put parallel to the fire stair walls. The connections between the outrigger trusses (1000mm wide) and the cross walls (400mm) is considered to effectively transfer lateral forces (William J. F., 2009).

4.2. Exterior Structures

The exterior structure of the building is supposed to absorb a great proportion of lateral forces especially wind loads. Hence it should be noted that most of the wind resisting system is concentrated on the perimeter of tall buildings. One of the most typical exterior structures is the tubular, which consists of a great number of rigid joints, acting along the periphery, creating a large tube. In framed tube system, the exterior tube carries all the lateral loads and the gravity load is supported by the tube and the interior columns or walls. The columns connected by a deep spandrel are closely packed on the perimeter of the building. In braced tube system instead of using closely spaced perimeter columns, widely spaced columns stiffened by diagonal braces are applied. Another structural system can be formed by clustering the individual tubes. In the system, the tubes are interconnected by common interior panels to generate a perforated multi-cell tube.

A super-frame system is composed of megacolumns combining with braced frames of large dimensions at building corners. The systems are linked by multistory trusses at about every 15 to 20 stories. The designers have been used the concept of super-frame for The Vietinbank Tower. The structural layout at level 5, 27 and 48 of the tower is shown in Figure 4.

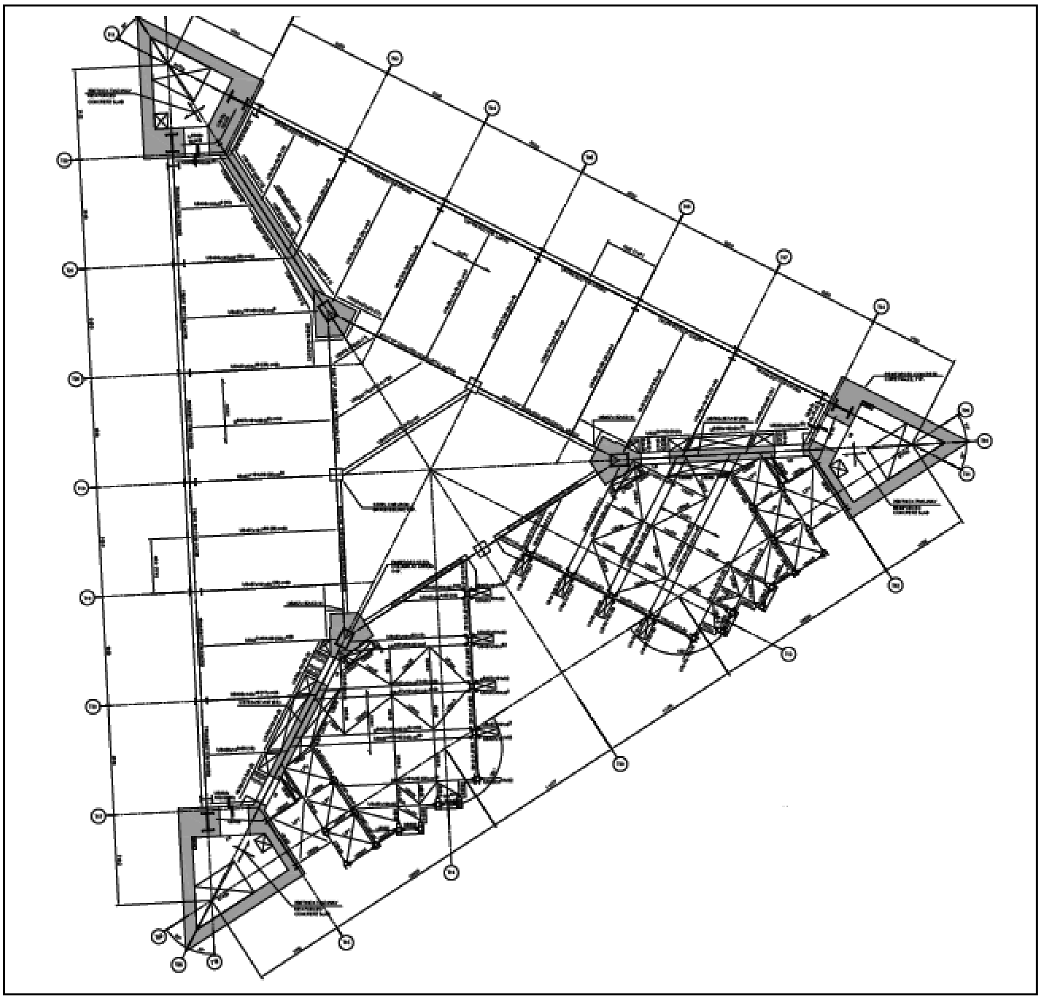

Figure 4. Structural Plan Layout of The Vietinbank Tower at level 5, 27 and 48

As mentioned above, the core-outrigger structures and the megacolumns are going to be dominantly used as the main structural system for supertall buildings. The combination of these systems should be studied to apply in Vietnam in the near future.

4.3. Floors

In terms of structural roles, the floor system is to sustain the self-weighted load and constructing loads in and after erection. This also works as a diaphragm to transfer and redistribute the lateral loads to vertical structural components such as: shear walls, cores, tubes...
When it comes to the service duration of the building, the floor system is used to divide the building space in the vertical direction. It plays a role as an anti fire spreading and sonic insulation components. The floor also carries the mechanical system of the building such as the heating, ventilating and air conditioning systems.

The floor makes up a large portion of the self-weight of the whole building so that the selection of floor system types is really important and greatly influences on the construction cost. In situ concrete floor is very reliable and economical due to the development of concrete pumping technology. This type of floor creates a very stiff diaphragm and effective in terms of transverse load transferring. Precast concrete floor has an advantage because of shortening the construction duration but the requirement of the large crane work makes it more expensive.

4.3.1. Flat slab floor

A flat-slab floor, with the span from 8.5 to 9.5 m, has the thickness from 280 to320 mm. The self-weight of these flat slabs significantly increases the total weight of the structure system.
In The Bitexco Tower, the conventional slab with the thickness of 250mm was constructed for the lower office floors while the upper office floors used the 250 mm thick flat slab system.
In The Vietinbank Tower, the conventional slab with the thickness of 250mm was constructed for the lower office floors while the upper office floors used the 250 mm thick flat slab system.
The flat slab system with the span of 9m combined with the perimeter spandrel beams were employed for The Lotte Tower.

4.3.2. Prestressed concrete floors

Prestressed concrete is an advance technology for long span slabs. The technology is effective when the span of the slab is over 9 m due to the reduction of the thickness. The thickness of the prestressed concrete slab is only about 1/40 of the span length. In The Keangnam Landmark Towers, the PT slab was used as a replacement for the conventional slab system.

4.3.3. Composite floors

A composite floor is a combination of different materials to develop an economic structural system. Steel and concrete composite floors are fairly popular in tall building. To form the composite slab, in situ or precast concrete can be used. The link between two materials is founded by welding shear connector, called shear studs, which is welded to the steel decking and buried on concrete after hardening. The use of composite slab and cast in place concrete beam form an effective system. This was employed by The Steel Deck to design the slab of The

Vietinbank Tower. The slab was 75mm deep galvanized composite deck per ASTM A653 with a minimum yield strength fy= 280 MPa (Figure 4).

5. WIND TUNNEL TESTING

The impact of the winds can be reduced by aerodynamic effects based on the optimization of the shape of the buildings. The building has to design so that the higher stiffness of building s is to resist the dominant wind. To achieve that goal the wind tunnel test is required. The data obtained from the test not only is used to design the structural components including columns, beams, bracing frames and foundation but also to select the façade systems. The wind tunnel test is more effective when the building is taller because this helps to collect the more accurate wind load on the structures. For the high-rise buildings, the serviceability limit state related to wind loading, sometimes, is more concerned than the ultimate limit state.

Vietnam is located in an area where typhoon appears frequently. It is important to study wind climate in Vietnam in order to accurately estimate impact of the wind to the structure and the building's behaviour as well. At the moment, the application of the wind tunnel test for determining the wind load for tall building is not popular and only applied for four abovementioned projects in Vietnam. We will consider the wind tunnel test of The Vietinbank Tower as an illustration of using experimental data in designing work (RWDI, 2011).

A 1:500 scaled model of the tower was set up based on the architectural drawings (Figure 5). 997 pressure tags were mounted on the model to measure the wind pressure. All surroundings within 600m from the centre of the building was modeled to estimate the interaction between the building and the topography. Beyond the modeled area, the influence of the upwind terrain of the planetary boundary layer was simulated in the testing by appropriate roughness on the wind tunnel floor and flow conditioning spires at the upwind end of the working section for each direction.

The wind pressure impacting on the building is a function of the return period. In order to predict the pressure, the wind tunnel data were combined with a statistical model of the local wind climate. The wind climate model was based on measuring local surface wind and simulating local typhoon on the computer at Noi Bai International Airport (Hanoi). Over 100,000 years of tropical storms were simulated to account for variability of typhoon wind speed within direction. The wind climate model was scaled so that the magnitude of the wind velocity for the 50-year return period corresponding to 3-second gust wind speed was 43.2 m/s at a height 10m on the open terrain, equal to a reference pressure of 11.4 kPa. This 50-year reference pressure was obtained by the application of a reliability factor of 1.2 to the code referenced 20-year pressure of 950 kPa. This value is consistent with that defined for Hanoi area in the Vietnamese Standard TCVN 2737:1995. The wind load on the cladding system of these projects was obtained from the wind tunnel test data.

The wind pressures obtained from wind tunnel tests would be lower than code predictions due to the unconventional geometry of buildings, the complexity of the surroundings as well as the wind directionality. However, the changes of the surroundings in the near future need to be controlled and concerned. By that way, an accurate wind load is derived and recommended for design based on wind tunnel tests and code predictions.

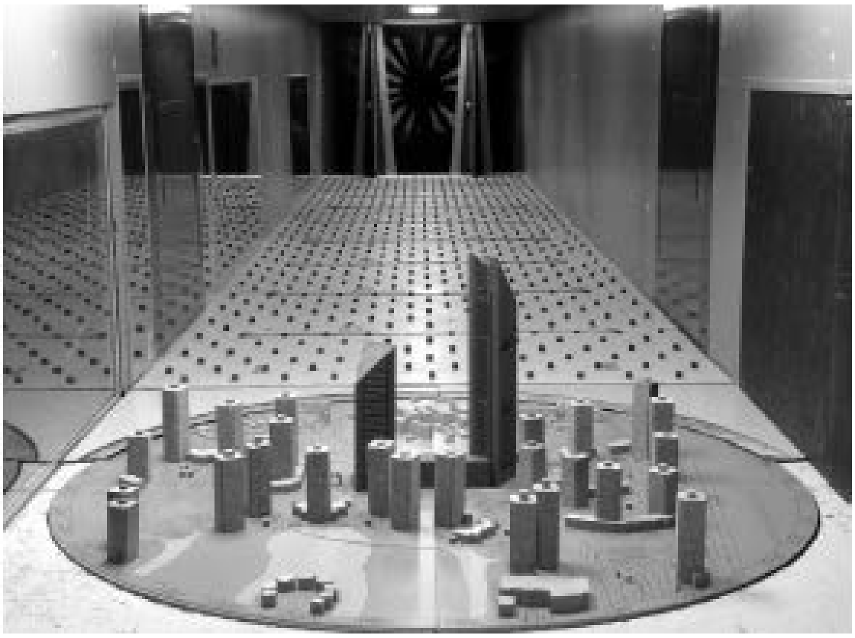

Figure. 5. The wind tunnel test model of The Vietinbank Tower

CONCLUSION

The appearance of supertall buildings is essential for the big cities of Vietnam so that their designs are rigorously concerned by engineers. Presently, the core-outrigger system is widely used for the load-bearing structure of the buildings. Together with the development of concrete technology, high strength concrete is used as a solution to reduce the construction cost for the type of buildings. Moreover, to obtain the accurate wind load on the supertall buildings, the wind tunnel tests are employed. The effectiveness of these applications has been proven based on the analysis data of the four reference projects in Vietnam.

REFERENCES

Byung-Ick Yoon et al., 2010. Design and Construction of Keangnam Hanoi Landmark Tower in Vietnam, *Journal of the Korea Concrete Institute*, vol. 22, issue 2 (in korea).
CTBUH, 2012. *100 tallest completed buidings in the world.* CTBUH. Retrieved 27 April 2012.
Mir M. Ali and Kyoung Sun Moon, 2007. Structural Developments in Tall Buildings: Current Trends and Future Prospects. *Architectural Science Review*, volume 50.3, pp 205-223.
Paul H K HO, 2007. Economics Planning of Super Tall Buildings in Asia Pacific Cities. TS 4G - *Construction Economics and Development*.
Taranath, B.S., 1998. *Steel, Concrete and Composite Design of Tall Buildings*, McGraw-Hill, New York.

RWDI, 2011. Head office of Vietinbank, Draft Final Report. *Wind- Induced Structural Responses*.
William J. F. et al. , 2009. Bitexco-Finacial Tower. *Structure Magazine,* June.

Utilization of unused and/or non-familiar materials for construction

Taketo UOMOTO
Chief Executive,
Public Works Research Institute
Professor Emeritus, University of Tokyo

ABSTRACT

Considering the sustainability of structures, it is important to utilize unused and/or non-familiar materials for construction. In most cases, when the regulations and specifications are used, engineers do not think much about the usage of unused and/or non-familiar materials. It is convenient for the engineers to use familiar materials than unused and/or non-familiar materials. As a result, the engineers construct similar structures without considering the cost and sustainability of the structure. This paper shows an example of constructing a large dam utilizing unused material (CSG) in Japan. The result shows that utilization of unused and/or non-familiar material may give a new way to the future.

Keywords: utilization, unused material, non-familiar material, CSG, dam

1. INTRODUCTION

In the year 2011, a huge Earthquake occurred on March 11, in the north eastern part of Honshu Island. Not only the earthquake, but also the great tsunami hit the East coast of Honshu Island. Due to the tsunami, many houses and structures on the coastal lines were destroyed completely. As a result, tremendous amount of destroyed materials, including wood, concrete, steel, mud, stones, bricks, etc., were damped on the land of Tohoku area It takes about three years to clean up the land from these deposits.

Figure 1 Deposits by Tsunami after the Great East Japan Earthquake

The next problem is how to utilize these deposits: it is difficult to utilize them as construction materials in normal manner. Even after they are separated to sand, stones, bricks, wood, etc., they contain various small sized materials with salt, etc. They cannot meet the requirements of standards of any country to be used as normal construction materials, such as for concrete.

To deal with the problem, one method may be to utilize these material as unused material or non-familiar materials for construction. If they are used as construction materials, we can utilize them to rebuild the structures and land of destroyed area. This paper gives an example of utilizing unused material including river deposits as CSG (Cemented Sand and Aggregate) for dam construction in Japan. For those who have more interest on the technology, the details are given in the following paper: Kenji Sakata: Current Situation of Planning and Construction of Dams in Japan, Foro International de Concreto 2012[2)].

2. TRAPEZOIDAL CSG DAM

The trapezoidal CSG dam[1)] is a new type of dam which differs from the conventional concrete gravity dams and embankment dams, and its dam body is trapezoidal in shape and made of cemented sand and gravel (CSG). In Japan in particular, the quarry conditions of yield ratio and transport required to obtain dam body materials are becoming more severe, with aggregate related costs accounting for approximately 40% of total work costs at recently constructed concrete dams. There is thus an urgent need to rationalize material-use to cut costs and reduce the environmental load imposed by excavated slopes, etc. The trapezoidal CSG dam is a new type of dam which can be realize rationalization of materials, which is currently the biggest challenge to be overcome, and also helps to rationalize the design and execution.

A trapezoidal CSG dam is a trapezoidal shaped dam built using CSG by the CSG method, and has the following characteristics.

[1] Rationalization of materials

The dam body of a trapezoidal CSG dam requires less strength, so the material strength may be low, permitting the use of low-quality materials and expanding the range of materials which can be selected.

[2] Rationalization of design

In addition to the lower strength required for the dam body material, a trapezoidal CSG dam has fewer requirements for the foundation bedrock, increasing the flexibility for dam site selection.

[3] Rationalization of execution

A trapezoidal CSG dam can be built with a simple material manufacturing plant, permitting rapid execution by a continuous mixing system.

Figure 2 shows the standard cross section of trapezoidal CSG dam. A trapezoidal CSG dam is made using CSG for the main part of dam body, and protection concrete is placed on its surface to secure durability and water-tightness. A gallery, structural concrete and a seepage control concrete for securing an appropriate seepage pass length are placed on the upstream side. The CSG on the bottom surface of the dam body is rich-mix CSG prepared to ensure durability. The trapezoidal CSG dam is designed in range of an elastic body behavior, so like a concrete dam, the discharge systems, gallery, etc. can be placed inside the dam body, and the emergency spillway, etc. placed at the crest.

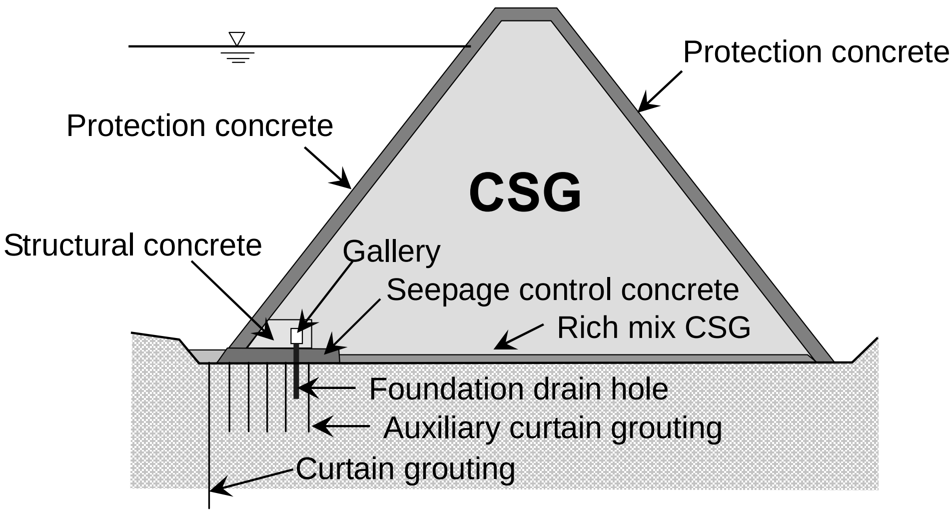

Figure 2 Standard cross-section of a trapezoidal CSG dam [1)]

The differences between a trapezoidal CSG dam and a concrete gravity dam, which are designed as an elastic body, are summarized below. Table 1 explains the basic differences in design, and Figure 3 shows differences in the designing procedures for the two kinds.

CSG is produced using simple equipment by mixing cement and water with material obtainable nearby without classification, gradation adjustment or washing. The CSG method involves spreading CSG with bulldozers, then compacting it with vibrating rollers to build the structure. This method reduces costs, speeds up execution, and reduces the impact on the environment. Figure 4 illustrate CSG manufacturing process, Figure 5 shows an example of CSG mixing facility and Figure 6 shows situation of CSG casting.

Table 1 Differences between designs [1)]

	Trapezoidal CSG dam	Concrete gravity dam
Basic differences in design	- It is not necessary to integrate the dam body and foundation bedrock - The dam body volume is larger	- It is necessary to integrate the dam body with the foundation bedrock - It is possible to minimize the dam body volume
Resistance against overturning	The vertical stress at dam bottom surface is compressive, even during an earthquake, over the entire region.	During an earthquake, tensile stress is occurred on dam bottom surface, and its tensile stress is resisted by integrating the dam body with the foundation.
Resistance against overturning	Friction between the dam body and bedrock can fully resist sliding.	Sliding safety is secured by integrating the dam body with the foundation bedrock to use the shear strength of the bedrock.

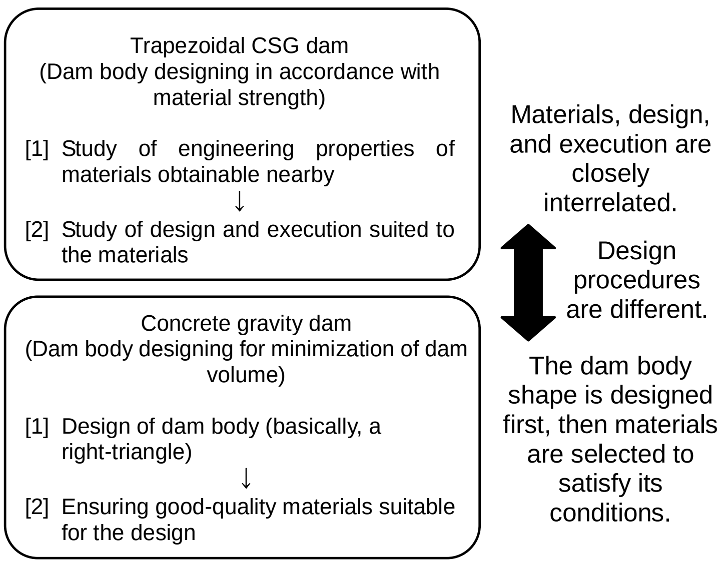

Figure 3 Design procedure [1)]

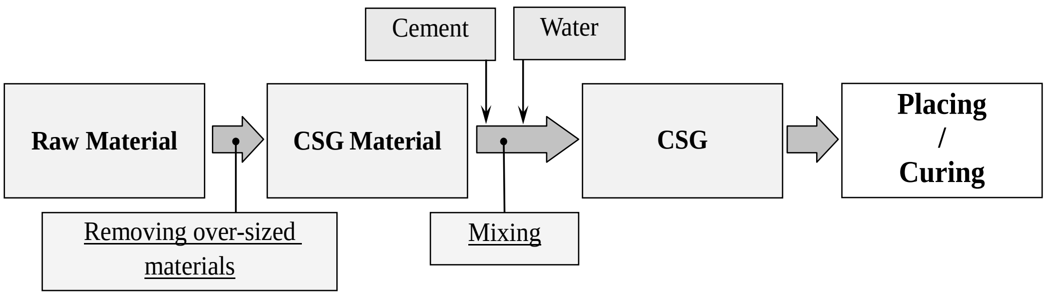

Figure 4 CSG manufacturing process [1)]

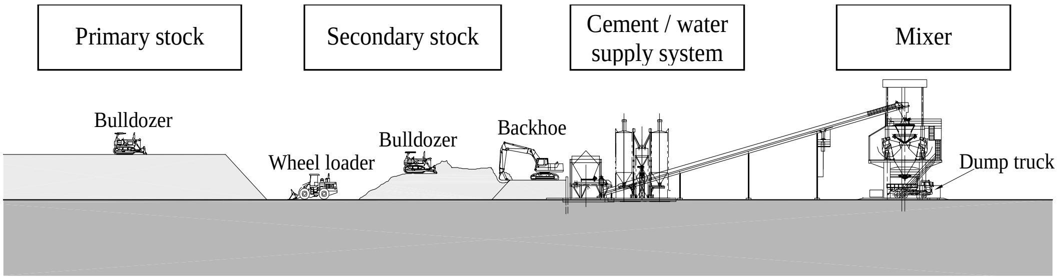

Figure 5 Example of CSG mixing facility [1)]

Figure 6 Casting of CSG

3. EXAMPLES OF CSG DAMS

The first structure made of CSG and by a method using this material, the CSG method, in Japan was the upstream cofferdam at the Nagashima Dam. Since then, CSG and the CSG method have been used to build many upstream cofferdams and other temporary structures such as embankment work for roads, etc., because it is easy both to obtain the materials and to execute the method. In response to this demand, and with accumulated knowledge of the physical properties and execution characteristics of CSG and the CSG method, work began in 1999 on developing a dam design applying a trapezoidal shaped cross section and using CSG, and the proposed design method was completed the following year.

CSG, which can be produced easily by mixing cement and water with material obtained nearby without gradation adjustment and washing, is not as strong as concrete. To overcome this shortcoming, it was combined with a trapezoidal dam shape, which does not require great strength. The newly developed trapezoidal

CSG dam design method was applied to design the seepage control structure (dam volume 34,000 m3, height 30 m, Okinawa General Bureau (OGB)) at the Taiho Dam and the Kawai Sub-dam (dam volume 32,000m3, height 14m, MLIT) of the Haizuka Dam, and both were constructed by the CSG method. Based on these results, the "Engineering Manual for Construction and Quality Control of Trapezoidal CSG Dams (September 2007)" was compiled as the basis for constructing a full-scale dam. As full-scale trapezoidal CSG dams, placing of the body of the Tobetsu Dam (dam volume 813,000m3, height 30m, Hokkaido) and of the sub-dam of Kasegawa Dam (dam volume 68,000m3, height 30m, MLIT) began in 2009, and placing of the body of the Okukubi Dam (dam volume 339,000m3, height 39m, OGB) began in 2010. At all those dams, CSG casting completed within one year. Figures 7 and Figures 8 show Tobetsu Dam and Okukubi Dam, respectively.

Figure 7 Tobetsu dam

Figure 8 Okukubi dam

4. UTILIZATION OF UNUSED AND/OR NON-FAMILIAR MATERIAL

It is difficult to utilize unused and/or non-familiar materials as usual construction material. Even the most familiar construction material; "concrete" has been used and studied for more than 200 years but yet we still encounter many problems. It takes a long period of time to utilize new materials for construction considering both strength and durability aspects of a material, but if we can develop a new method to utilize unused and/or non-familiar materials, we can get a new method even for the newest constructions.

The important point for such utilization is that we have to consider not only the properties of concrete, but also the concept of designing a structure using the new material. In some cases, we have to develop technologies to maintain the quality of the material and develop a new construction method using the material. Considering the sustainability of structures on earth, it will become an important issue to utilize unused and/or non-familiar materials when a large scale disaster happens in the world. I hope we can develop the method in the near future.

REFERENCES

1) The Technical Committee on Engineering Manual For Construction and Quality Control of Trapezoidal CSG Dam: Engineering Manual for Construction and Quality Control of Trapezoidal CSG Dam, Japan Dam Engineering Center, September 2007.
2) Kenji Sakata: Current Situation of Planning and Construction of Dams in Japan, Foro International de Concreto 2012.

Water management in Vietnamese cities: present status and vision to future

Viet Anh NGUYEN
Associate Professor and Vice Director, Institute of Environmental Science and Engineering (IESE), National University of Civil Engineering, Vietnam.
vietanhctn@gmail.com

ABSTRACT

Water is a crucial component for life in any city. The water issue is often becoming more and more crucial in fast growing megacities. Adequate distribution of water among users ensuring water source protection is among most crucial issues in Vietnamese urban water supply. Besides, other hot issues in urban water are analyzed in the paper. Further, analyzing current status and evolution trend in the last 20 years of wastewater management, the author proposes recommendations aiming at sustainable urban water management in Vietnamese urban areas, such as, establishment of a National Strategy and a National Target Program on urban water management, whereas River basin management approach should be realized; increase of wastewater tariff to achieve O&M cost recovery and system sustainability; encouragement of Public-Private Partnerships (PPP) and Private Sector Participation (PSP) in the sector; implementation of Sanitation planning on a citywide or river basin wide basis; application of combination of centralized scheme for dense core urban areas, and decentralized scheme in the remaining parts; implementation of sustainable flood management solutions in combination with selection of appropriate wastewater collection and treatment options; integrated treatment of different waste fractions for resource recovery in the cities.

Keywords: water supply, wastewater, collection, treatment, resource.

1. URBAN WATER SUPPLY

Water is a crucial component for life in any city. The water issue is often becoming more and more crucial in fast growing megacities. Up to June 2013, there are 765 cities and towns in Vietnam providing residence for more than 32% total population of the country. The total design capacity of urban water supply systems is about 6.5 million m^3/day, whereas actual operation capacity of them is 5.7 million m^3/day or 89% of the design capacity. The average ratio of urban population served with centralized water supply systems is 77% or 32.6 million persons. This ratio is ranging from 57% as average for grade V towns, to 80% for cities and towns of grade IV and larger. Non-revenue water is still as high as 27.8 %, ranging from 7.2 to 44.9% from company to company. An average water consumption rate is 101 l/cap/day, ranging from 33 to 213 l/cap/day (Figure 1). Average energy consumption for each cubic meter of water produced is 0.35 KWl/m^3, ranging from 0.18 to 1.0 KWh/m^3. Cost for energy in average is 26.3%, ranging from 4.2% to 47.6% of total water system operation and maintenance costs.

Adequate distribution of water among users ensuring water source protection is among most crucial issues in Vietnamese urban water supply. Master plans for urban and industrial water supply for core development zones in Vietnam are under development and revision. Other key issues in urban water supply in Vietnam include: (1) Surface water scarcity, salt intrusion, usage conflict; (2) Groundwater depletion; (3) Non-revenue water: (4) Water pollution (NOMs, industrial chemicals, pathogens, chlorine disinfection, … in surface water, organic and nitrogen compounds, arsenic, salt intrusion, … in ground water); (5) Poor O&M capacity especially at peri-urban and rural water supply systems; (6) Need in process optimization, energy savings, efficient management; (7) Privatization, self financing capacity and cost recovery at water utilities.

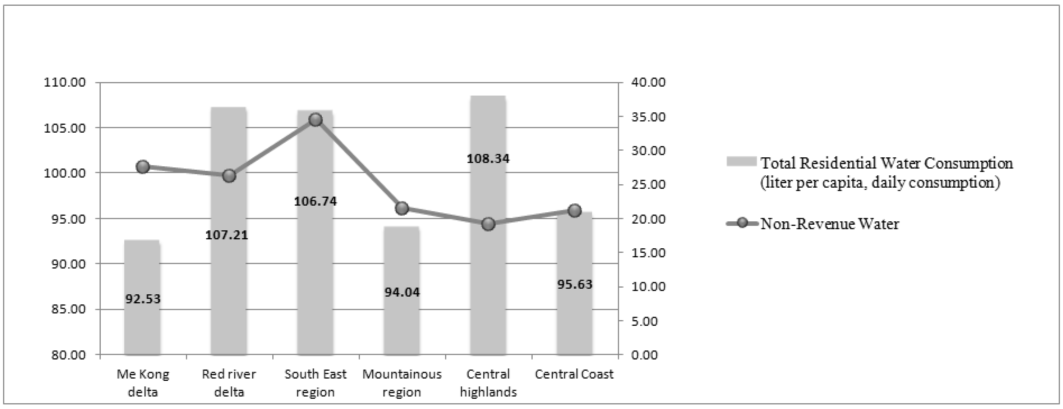

Figure 1. Average water consumption in urban households from 6 regions in Vietnam

(Source: MOC – WB. Urban water sector database, 2013)

2. URBAN WASTEWATER MANAGEMENT

Over last three decades, a legal framework in environmental protection, urban and rural infrastructure development in general, and in sanitation or wastewater management in particular has been making significant steps forward. The first Environment Protection Law has been issued in 1995, and its Revision has been issued in 2005. Since 1998, the Government of Vietnam has initiated policies and provided investment to improve urban sanitation resulting in significant progress in development of the wastewater sector. Provision of wastewater services to the urban poor has been impressive with open defecation now eliminated. Environmental Protection Fee imposed to urban and industrial wastewater has been taken in force in 2003. Important Decrees on Urban and Industrial Water Supply, Wastewater Management, and Solid Waste Management have been issued in 2007. The third National Target Program on Rural water Supply and Sanitation (NTP3) implemented in the period 2011 – 2015 pays more focus on sanitation improvement activities (see Figure 2). Effluent standards for different types of wastewater are being set up. However, number of efforts is required in order to make Vietnamese wastewater related legislations more practical and efficient. Access to toilets is now 94%, with 90% of households using septic tanks as a means of on-site treatment. 60% of households dispose of wastewater to a public sewerage system, primarily comprising combined systems. By September 2013, some 20 urban wastewater systems had been constructed in Hanoi, Ho Chi Minh City and other provincial towns and cities, with a total capacity of 600.000 m^3/day (Figure 3). Besides, some 30 new wastewater systems are in the design/construction phase.

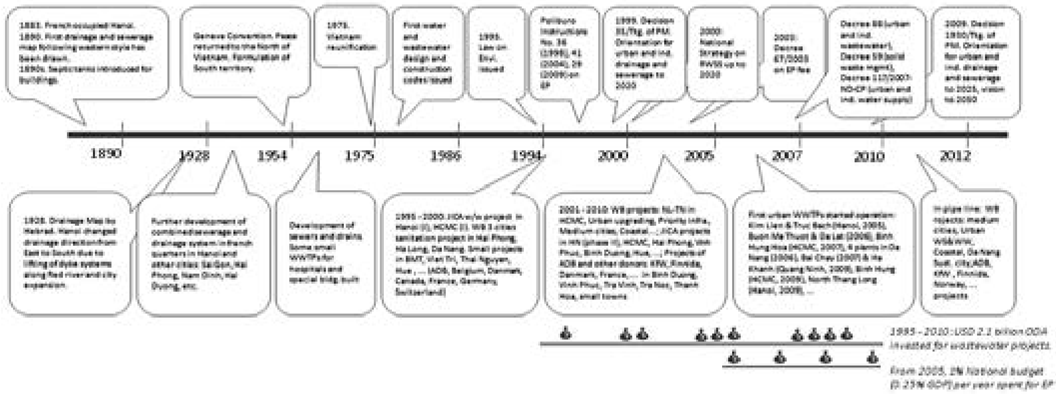

Figure 2. Timeline of development of wastewater management activities in Vietnam

Figure 3. Functioning wastewater treatment plants in Vietnamese urban areas

Despite these impressive initiatives, urban sanitation continues to face critical issues that need to be urgently addressed as follows: (1) Most of urban sewerage and drainage systems are combined (Figure 3), with low household connection rates (especially in low density urban and peri-urban areas and in urban areas of central region where soil is mostly sandy), and whereas only 10% of wastewater is being treated; (2) Only 4% of septage is treated. Fecal sludge management is generally poor in most cities; (3) Cost recovery of the capital and O&M costs of the wastewater systems are generally low (Figure 4); (4) Institutional arrangements do not encourage efficient system operation with the wastewater enterprises having limited autonomy to manage operations and undertake system development; (5) Financing needs are still very high, estimated to be USD 8.3 billion to provide sewerage to the estimated 2025 urban population of 36 million; (6) Lack of understanding by decision makers of appropriate technical solutions and the limited land available for the WWTPs has resulted in construction of expensive treatment facilities with advanced technology and imbalance with household connection and network investment; (7) Integrated, river basin management concept is not applied; (8) Urban sanitation planning is not being included properly in master urban planning and planning of other development plans; (9) Limited participation of private sector in urban wastewater management activities.

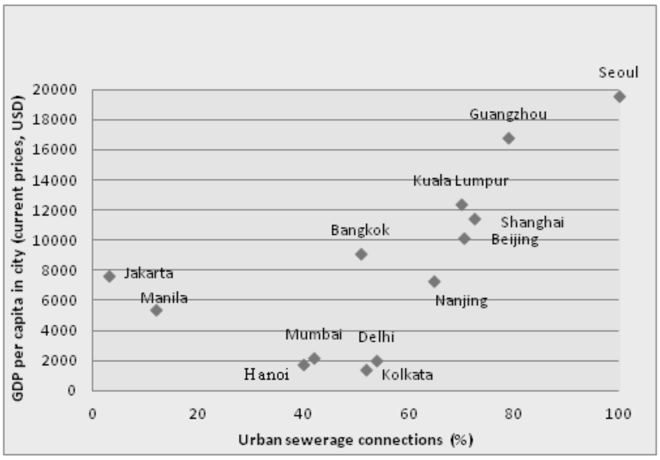

Figure 4. Urban sewerage connections against city GDP per capita
(Source: EAP Sanitation review, WB, 2013)

3. RECOMMENDATIONS FOR SUSTAINABLE URBAN WATER MANAGEMENT IN VIETNAMESE URBAN AREAS

Analyzing current status and evolution trend in the last 20 years, the author would like to propose following recommendations aiming at sustainable urban water management in Vietnamese urban areas.

Establish a National Strategy and a National Target Program on urban water management. River basin management approach should be realized. The principles of integrated water resources management and a river basin approach should be applied as a means of achieving coordination across sectors and reduction of the current sector fragmentation. An integrated approach to implementation with components of water supply, sanitation and hygiene is likely to produce more sustainable results and more benefits. There is a need to promote and develop coordination mechanisms between water resource management and environmental protection agencies, water supply and sanitation companies and community organizations at all stages of project planning and implementation, within a river basin context.

The current commitment by central government to water and sanitation improvement needs to be sustained.

Co-ordination of government-donor dialogue on sector financing at a high level and among government agencies at central and local levels needs to be improved. Besides, additional financing sources, especially for sanitation investment, also clearly need to be mobilized. These may be government grants in the short to medium term, but in the longer run may change to other instruments, such as issuance of government bonds, the introduction of property taxes and the introduction of earmarked increases of personal income taxes. Increase of wastewater tariff is a key tool to achieve O&M cost recovery and system sustainability.

Full recovery of investment and O&M costs should be assured for water supply systems. For wastewater systems, management and O&M of the wastewater collection and treatment systems will be funded mostly through wastewater tariffs paid by households. Besides, financial support for poor households should be maintained (Figure 6).

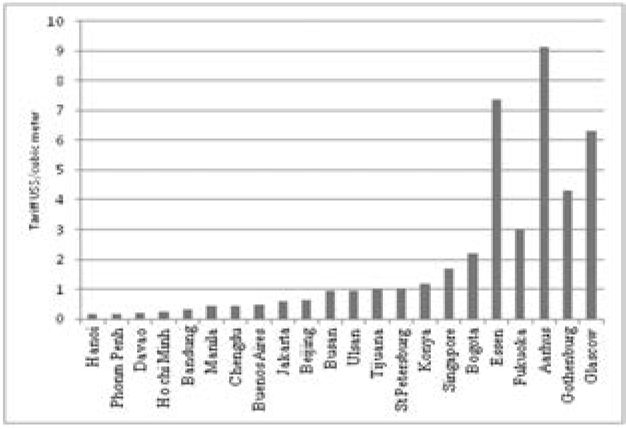

Figure 5. Water and wastewater tariffs in selected cities (data from year 2012)
(Source: EAP Sanitation review, WB, 2013)

Policies to encourage Public-Private Partnerships (PPP) and Private Sector Participation (PSP) are to be developed and implemented. It is critical that investments from the private sector in combination with Government result in a complete wastewater system incorporating connections, network and treatment facilities, and not just the most profitable element. Policies such as favorable loan and tax conditions are needed to encourage the private sector to invest in resource recovery from wastewater and sludge treatment including the use of reclaimed water and production of wastewater-driven electricity and heat for sale the grid.

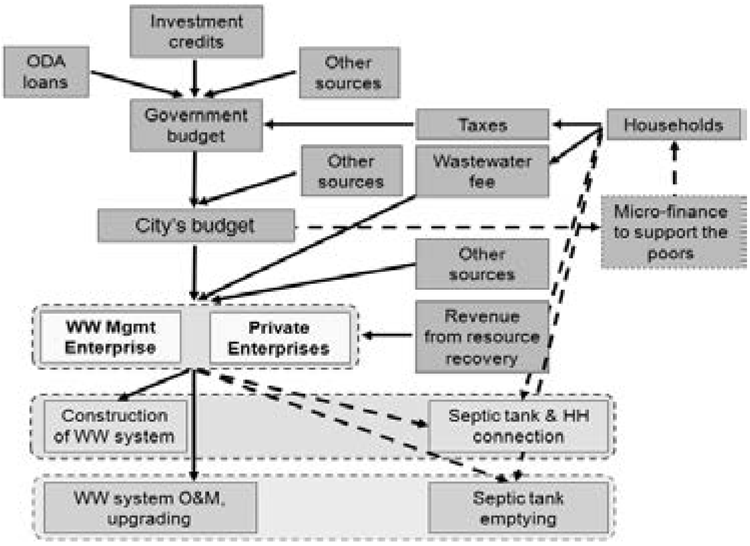

Figure 6. Recommended sources for funding in urban water and wastewater systems

Sanitation planning on a citywide or river basin wide basis should be initially conducted prior to mobilization of investment and implementation. The sanitation plans should carefully consider the performance of low cost technology options and delivery approaches to provide efficient and affordable solutions for the range of physical and socio-economic conditions present in a city or river basin. Safe and efficient resource recovery should be targeted in sanitation planning. The reuse of treated wastewater and sludge in agriculture would bring significant benefits to the integrated sanitation system.

With 60-70% of the cost associated with implementation of a wastewater system resulting from the cost of a sewerage collection system, it is important to consider alternatives, such as decentralized wastewater scheme, which could effectively reduce overall investment costs as well as reduce ongoing operation and maintenance costs. Application of decentralized scheme is site specific, limited to less dense urban areas in which land would be available to site smaller, decentralized WWTPs. The goal here is to localize the collection of sewerage, minimizing the use of long conveyance pipelines and pumping stations, as well as reducing the capacity requirements for WWTPs. Decentralized scheme may not be appropriate for densely populated urban areas, in which locating of even smaller WWTPs becomes challenging as well as extremely costly in terms of site acquisition.

Centralized scheme will cost more in terms of infrastructure improvement, particularly with respect to sewerage collection aspects. However, centralized scheme may be unavoidable in densely populated urban areas, where land is simply unavailable and collection systems may be limited to interception of drains at key locations.

A combination of the use of centralized scheme for dense core urban areas, and decentralized scheme in the remaining parts, with reasonable set of effluent limits would be both a logical and cost effective approach for wastewater collection and treatment for Vietnamese cities. Decisions on project phasing and selection of prioritized areas of investment should be based on comprehensive analysis.

Most of the urban wastewater systems in Vietnam are still employing combined sewerage systems for collecting and conveying wastewater. The reason for this is related to both cost, as CSS is less costly, and to the ease of implementation, as CSS can be implemented with far fewer pipes creating less construction impact in residential neighborhoods. Further, CSS generally utilizes the existing drainage system as secondary sewers for collecting wastewater from household, making it necessary only to intercept that flow by use of combined sewer overflow structures (CSOs) and then transport that flow to a WWTP for treatment. To date, a formalized program for household connections is generally excluded from the implementation of CSS, again making it more attractive to decision-makers due to apparent simplicity of execution. It is important to take into account that CSS-based wastewater will usually have a low organic content, which may mean that treatment is not necessary or at least that only simple treatment processes are required. Where treatment is required, presence of storm drainage and groundwater infiltration and seasonal fluctuation of wastewater flows should be considered. Awareness raising activities for the customers and public associated with proper operation and maintenance of CSS to prevent inclusion of solid waste and solids retention in network in dray season, and to prevent hydraulic overload of system during rainy seasons are to be considered. For some cities, investment in “Flood Storage” facilities allowing “holding” of peak storm water flows which can then be discharged in a more controlled manner to the WWTP can be considered as an promising technical solution (WB, 2012).

Separate sewerage systems (SSS) are designed to collect and convey only sewerage, with drainage and rainwater specifically excluded. Such a system can offer very significant benefits to the end user, in that household septic tanks can be eliminated and households can be connected directly to an enclosed piping system, which is not impacted by either solid waste or rainfall. Neighborhood odors long associated with CSS, can be effectively eliminated with SSS. The quality of the wastewater collected and transported to the WWTP is strictly limited to household sewage and as such, is of high organic load concentration. The amount of flow collected and pumped is less, allowing downstream WWTPs to be designed with lesser capacities. In terms of investment cost, the SSS will be more costly than CSS, as three systems of piping, primary trunk mains, secondary sewers (located in streets) and tertiary sewers (located in sidewalks) will be required. However, the investment in SSS results in the inherent advantages mentioned earlier. The use of separate sewer systems should not be overlooked for consideration during project formulation, as the benefits to the end user are significant.

It is recommended to design SSS for all new urban development areas. Strict urban management measures should take place in order to control construction design, project implementation and system operation to avoid wrong connection of drains and sewers. Household connections, construction of the sewerage network and the downstream WWTP should take place at the same time. *For that*, *staged development of WWTP components should reduce financial pressures keeping high efficiency of the investments.* For existing urban areas where upgrading of CSS and collection of wastewater can't be realized in a short period of time, investment in the WWTP should be carried out in stages following gradually expanding sewerage network and household connections. When warranted, it is proposed to apply in the first stage the first unit of a combination of unit processes. Advancing in stages simplifies the handling of the system and maximizes budget utilization efficiency.

Summary of recommended wastewater collection and treatment schemes is presented in Figure 7.

Present situation 1. On-site sanitation or Open defecation

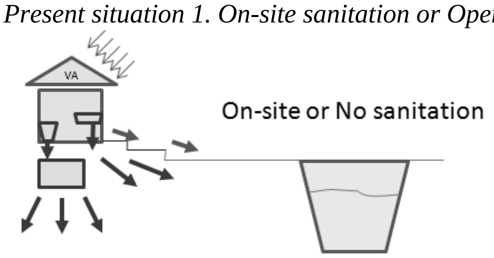

Present situation 2. Septic tank (ST) + Combined Sewerage System (CSS)

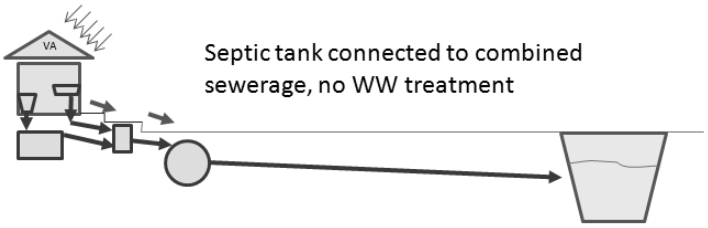

Recommended Option 1a (ST + CSS + Centralized Wastewater Treatment Plant WWTP), 1b (ST + CSS + decentralized WWTP)

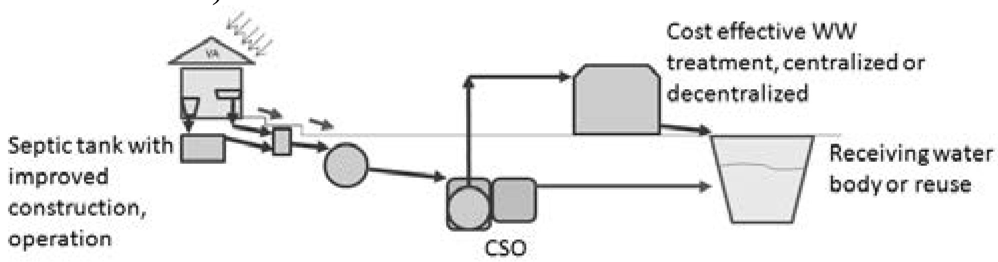

Recommended Option 2a (SSS + Centralized WWTP), 2b (SSS + decentralized WWTP)

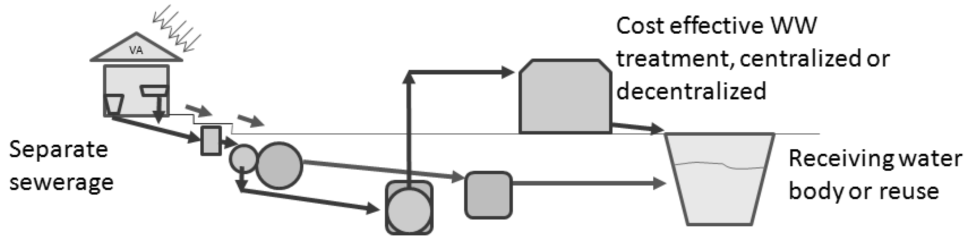

Recommended Option 3a (ST + SSS + Centralized WWTP), 3b (ST + SSS + decentralized WWTP)

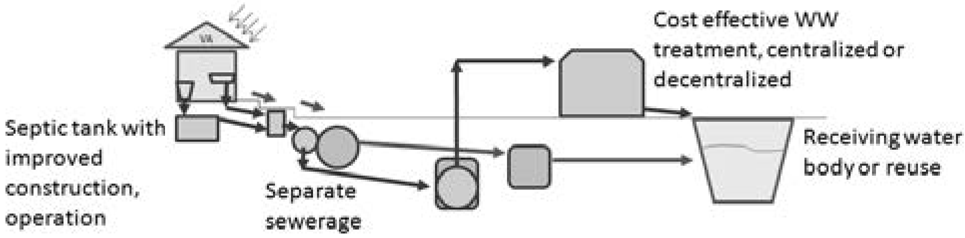

Figure 7. Summary of recommended wastewater collection and treatment schemes

In both CSS and SSS, flood management should be well taken based on river basin management approach where appropriate “less impact development” solutions should be considered. Storm water flow delay and attenuation using natural and constructed systems are now widely used under the concept called “Sustainable urban drainage solutions – SUDS”. Examples of SUDS are given in Figure 8. SUDS should be widely used in urban and transportation drainage in Vietnam. Legal framework and system of design standards should be developed accordingly. Harvesting and storage of storm water can also lead to other benefits such as stored water can be used for fire protection, car and toilet flushing, gardening, air conditioning, etc.

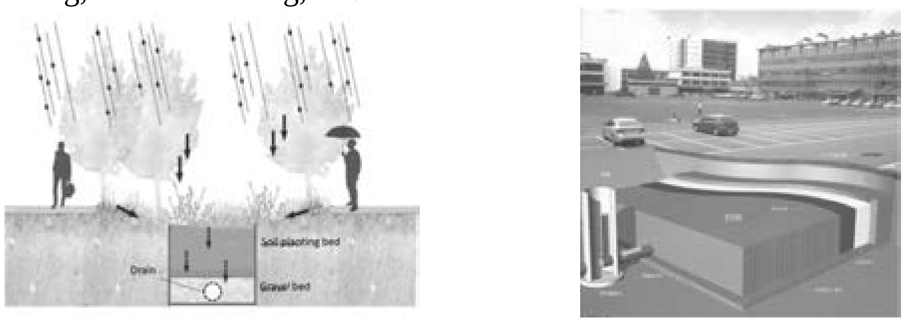

(a) (b)

Figure 8 (a, b). Examples of flood prevention solutions SUDS

Ensure balance between treatment facilities and collection systems in investment programs. Each wastewater project phase should be developed on a holistic basis with an appropriate investment balance among project components, including wastewater and septage treatment facilities, household connections, drainage and wastewater collection. A household connection policy with either combined or separate systems should be identified at each project stage and enforced by regulation. Engineered facilities should be designed together with ‘’soft interventions’’ such as capacity building, management structures and financial mechanisms.

Promote efficient institutional and regulatory arrangements at the local level. Government should encourage local authorities to integrate physical infrastructure development with improving ongoing service delivery. This implies greater efforts to improve public awareness, hygiene promotion and institutional development both at the utility management and regulatory level.

Greater emphasis needs to be placed on the selection of water and wastewater treatment technology. Selection of the most appropriate treatment technology involves technical evaluation of key criteria, namely: (a) land availability; (b) life-cycle costs, incorporating investment and O&M costs; and (c) suitability to achieve discharge requirements. By using appropriate technology treatment processes, savings can be made both in investment and O&M cost.

The technical solutions, with an integrated treatment for the different waste fractions, for example, septic tank sludge, sludge from future wastewater treatment plants, as well as organic waste, should be encouraged. A central aim is a smooth and sustainable operation of the units especially concerning handling of the above mentioned waste flows for public health and environmental protection. The produced biogas caters for an energy self-sufficient operation of the plants. The digested sludge (residue) is further treated and utilized for hygienically safe fertilizer to improve the soil quality, because it contains rich nutrients and organic fibers ideal for plants. In this way integrated solution of sanitation in urbanized area for sludge and organic waste treatment becomes feasible. Furthermore, when farming energy crops in the peri-urban areas, farmers can earn benefit in the new scheme. Once sewage network is established in future in the area, the operation scheme of the anaerobic digestion system is changed to accept sludge produced from the wastewater treatment plants. Thus the existing infrastructure can be continuously used without major additional modification, which saves significant expenditure of the municipality (Figure 9).

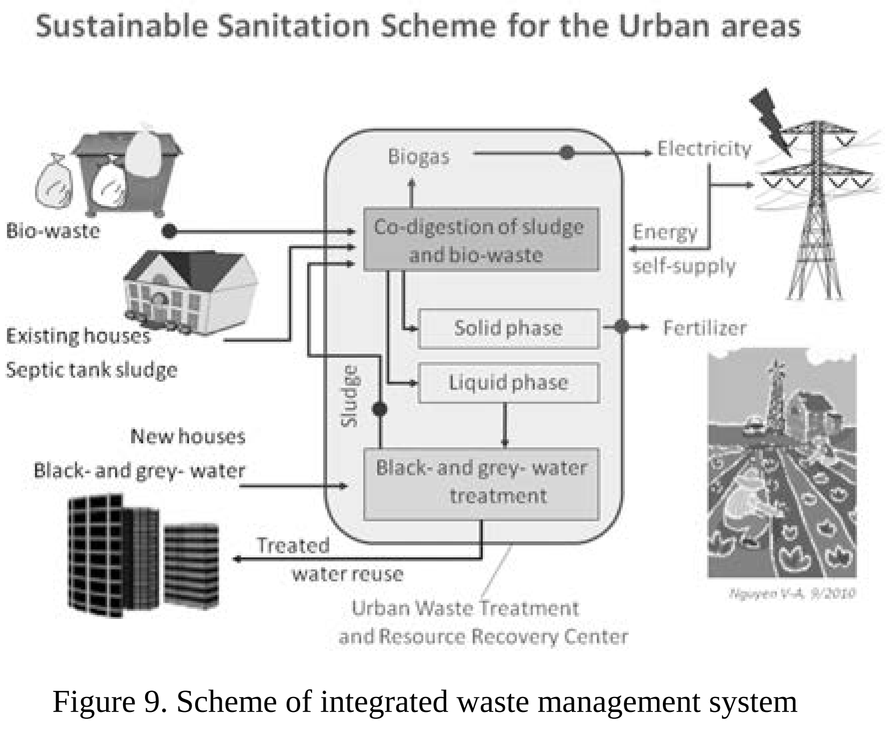

Figure 9. Scheme of integrated waste management system

Engineered facilities should be designed together with ‘’soft interventions’’ such as capacity building, institutional and financial arrangements. Besides, IEC programs to promote behavior change should be implemented to increase public awareness and appreciation of the benefits of water, hygiene practice, and environmental sanitation.

REFERENCES

Le Duy Hung, Corning J, Nguyen Viet Anh, Tran Viet Nga (2013). *Vietnam urban wastewater review*. The World Bank. 2013.

MOC – WB (2013). *Vietnam urban water supply database.* Report of Credit No. 4028-VIE. By Invest Consult Group – Toconet Korea Co. Ltd. March 2013.

Nguyen Viet Anh, Nguyen Hong Sam, Dinh Dang Hai, Nguyen Phuoc Dan, Bui Xuan Thanh (2011). *Landscape Analysis and Business Model Assessment in Fecal Sludge Management: Extraction and Transportation Models in Vietnam.* Final Report. For Bill & Melinda Gates Foundation. December 2011.

Nguyen Viet Anh, Nguyen Khac Hai (2012). *Vietnam water supply and sanitation sector assessment report.* For MOH – WHO – UNICEF (in Vietnamese).

World Bank. *East Asia Pacific urban sanitation flagship study*. 2013.

World Bank. *GFDRR report on Cities and Flooding*. 2012.

Sanriku Tsunami and reconstruction of cities

Hiroshi NAITO

Architect / Emeritus Professor, the University of Tokyo

ABSTRACT

The 2011 Tohoku Earthquake and Fukushima nuclear accident were the largest natural disasters ever experienced in modern Japanese history. As an architect, I am involved in the reconstruction and urban planning of the damaged cities in the Sanriku Region. There, the meaning and significance of Architecture, Urban Planning, Civil Engineering, and our social system surrounding them are being questioned from their basis. This is because ideal disaster prevention and reconstruction of cities attributes to the relationship between the nation and the individual. There is no single answer there. Yet, we need to seriously think about this issue. We would like to share this issue with people of Vietnam who are currently witnessing a rapid change in their urban structure.

Keywords*: Sanriku Tsunami, Reconstruction of cities and urban planning*

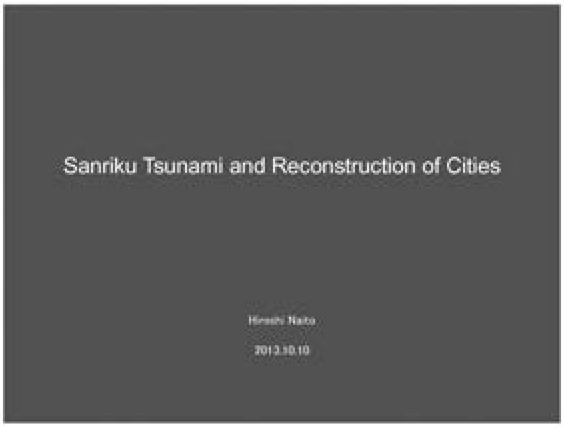
Sanriku Tsunami and Reconstruction of Cities
Hiroshi Naito
2013.10.10


Spring
Summer
Autumn
Winter


Tsunami
Tornado
Typhoon
Heavy Snowfall

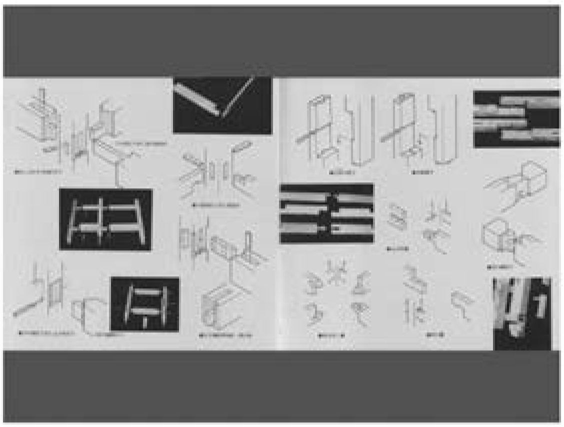

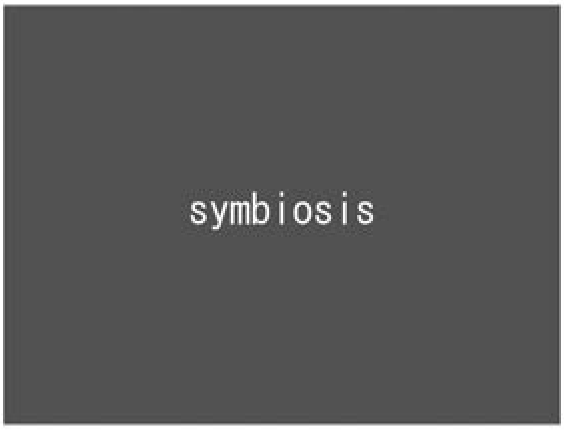
symbiosis

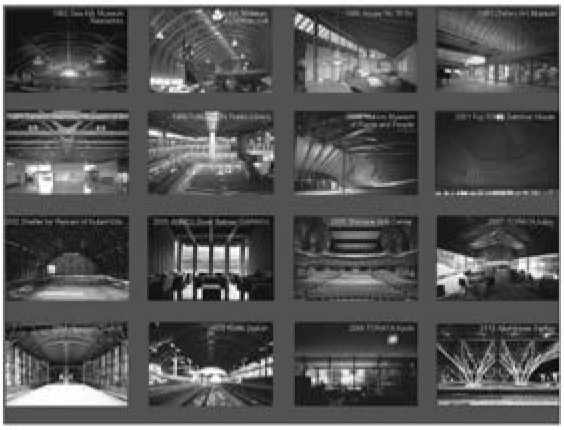

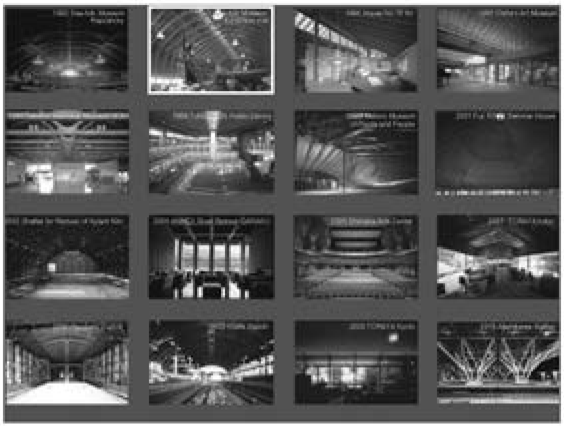


Sea-Folk Museum | 1992

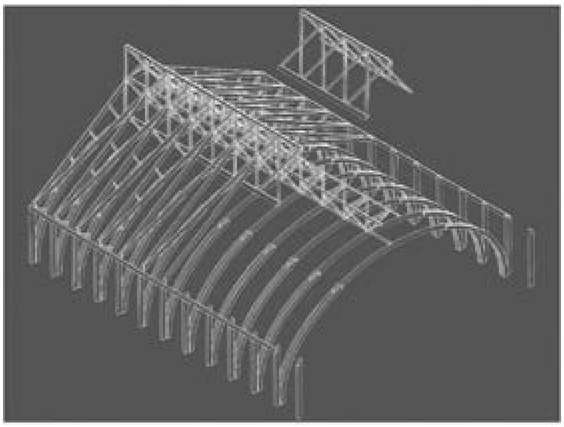

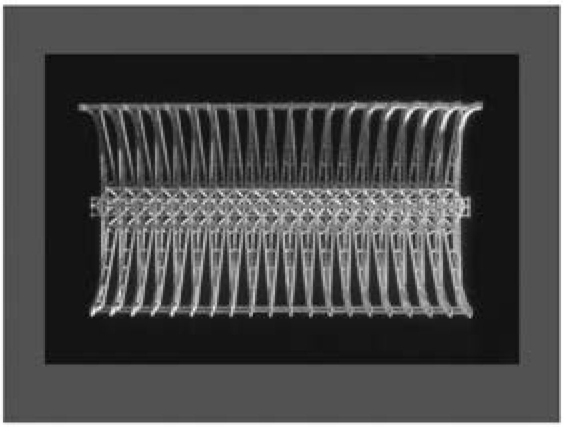

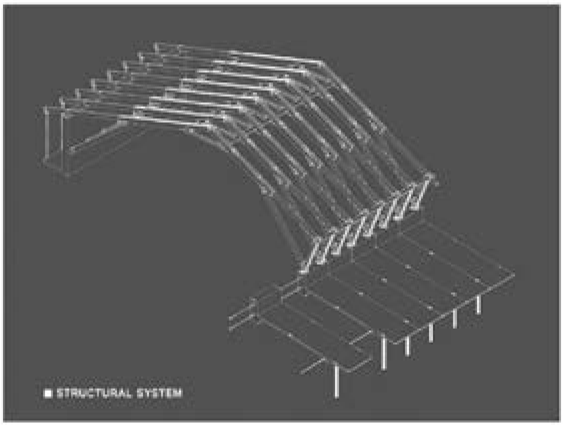
■ STRUCTURAL SYSTEM

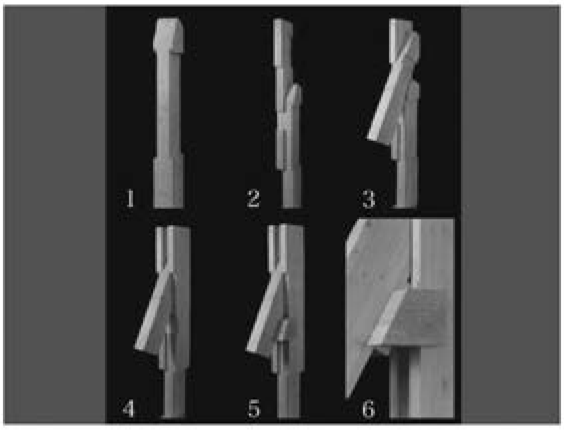
1
2
3
4
5
6


Makino Museum of Plants and People | 1999

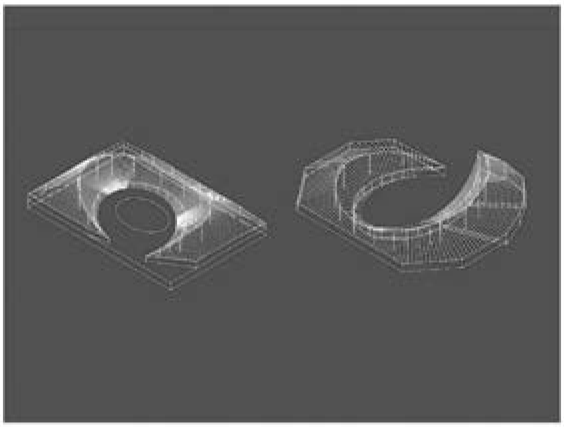
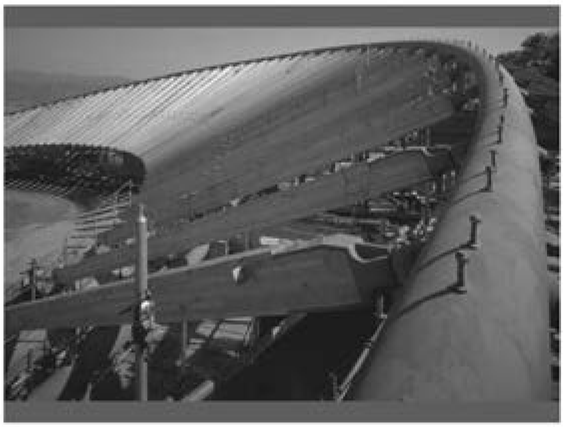




Hyugasji Station | 2008

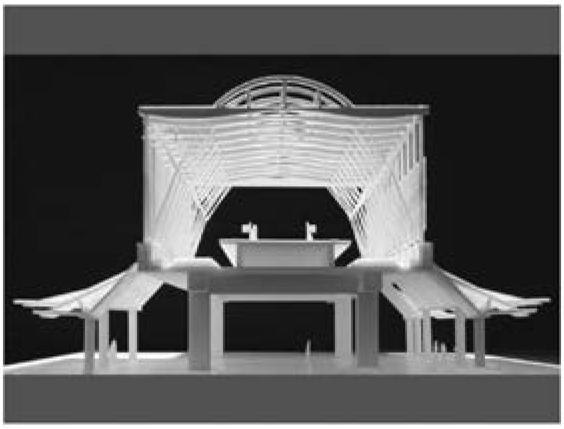


Kochi Station | 2009


Kuji city , Iwate


Rikuzentakata city , Iwate


Greate Tokyo Air Raid (Firebombing of Tokyo , Mar . 10 , 1945)

symbiosis

Oral Sessions

A study on the development of risk assessment method for urban fire according to fire spread phenomena of exterior and wood materials

Young Jin KWON[1], Bong Chan KIM[2], In Hyuk Goo[3]
[1] Professor, Department of Fire & Disaster Protection, Hoseo University, Korea
Jungangman@naver.com
[2] M.Eng., Department of Fire & Disaster Protection, Hoseo University, Korea
[3]Doctoral course, Department of Fire & Disaster Protection, Hoseo University,Korea

ABSTRACT

In Korea, there is a need for the introduction and investigation of Korea urban fire simulation that can assess the risk of fire by local unit with fire prevention districts, fire protect area, and other similar areas vulnerable to fire as targets. In this regard, this study examined the applicability of the urban fire simulation in Korea and conducted wood fire-resistance and aluminum composite panel tests to improve the simulation based on the review of the applicability. A regression analysis of the final carbonization depth was carried out, and the difference of vertical combustion expanded properties of non-combustible aluminum composite panels was identified. In the future, the improvement of urban fire simulation is considered to be needed through modeling.

Keywords: Urban fire, simulation, aluminum composite panel, Douglas-fir

1. INTRODUCTION

With the rapid economic gross and progress of urban congestion, development of Korea has mainly focused on the convenience of living and efficiency of space. As a result, the emergence of high-rise, large and in-depth structures has become more common. However, many deteriorated structures of various structures and uses such as traditional markets, shacks, and traditional village, etc. are also located, and they have characteristics which are vulnerable to disasters and calamities, especially to fire. These areas and districts are specified as fire prevention districts in the 'National Land Planning and Utilization Act' and fire protect area in the 'Fire Safety Law'. However, the fire prevention districts and fire protect area are designated by local governors, and there is no special evaluation method on the designation of fire prevention districts and fire protect area.

The fire prevention districts, fire protect area and similar areas vulnerable to fire have characteristics that lead to the rapid spread of a fire due to overcrowded structures within a certain district, resulting in the collapse of buildings. For instance, a fire that occurred in Insa-dong in February 2013 totally destroyed 23

Figure 1 : Big Fire in Korea

stores as shown in Figure 1, and 13 buildings of a total of 33buildings were burnt down by a fire that occurred in shacks located in Gaepo-dong, Gangnam-gu in June 2011. In a related move, the Seoul City Government plans to equip 'urban fire simulation' that can classify the grade of risks with areas vulnerable to fire as target. However, there are few studies on the urban fire simulations other than international joint research projects implemented by NIST, BRI (Japanese Building Research Institute) and Hoseo University. In this regard, there is a need to introduce and study Korean urban fire simulation that can assess the risk of fire by local unit with fire prevention districts, fire alert districts and other similar districts vulnerable to fire as primary target.

Accordingly, this study attempted to examine the applicability of urban fire simulation improved by the international joint research of Hoseo University, BRI and NIST in Korea. In addition, this study aims to obtain data used as a basis for the improvement of the urban fire simulation by conducting aluminum composite panel test and wood fire-resistance test to improve the simulation based on the review of applicability.

2. REVIEW ON THE APPLICABILITY OF URBAN FIRE SIMULATION

2.1 Overview of the urban fire Simulation

The urban fire simulation was developed by the BRI, and Ministry of land, Infrastructure and Transport for five years from 1998, and it was Improved through and international joint research of Hoseo University, BRI and NIST in 2009. The basic scenario of the urban fire simulation is shown in Figure 2. In the urban fire simulation, a total of five structures can be set, and one kind can be selected among a total of 22 uses. In addition, input is possible with respect to various conditions such as damages from earthquake, and detailed data is required for this.

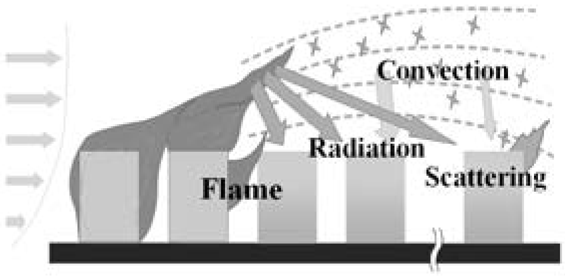

Figure 2 : Basic scenario of urban fire simulation

2.2 Analysis conditions of the urban fire simulation

For the review of the applicability of the urban fire simulation, two kind of case studies were carried at based on fire cases, and a comparison between the fire cases and analysis results was conducted.

2.2.1 Case study 1 –Shacks in Gaepo-dong, Gangnam-gu

In Gaepo-dong, Gangnam-gu, deteriorated shacks are concentrated, and 13 buildings were totally destroyed by a large fire that occurred in 2011. The conditions set for a simulation analysis are shown in Table 1. Originally, wood and sandwich panels were used for most of buildings. However, since the application of sandwich panels is impossible, the buildings were set with wood. Their use was determined to be a residence, and the total analysis times was set to 120 minutes. The fire building, wind speed and wind direction were set in accordance with the same conditions at the time of the fire.

2.2.2 Case study 2 –Area crowded with restaurants in Insa-dong

In case of the area crowded with restaurants in Insa-dong, deteriorated wooden buildings are concentrated, and 19 stores were burnt down by a large fire that occurred in February 2013. The conditions set for a simulation analysis are shown in Table 1. 120 minutes were set as the total analysis time as in the case of shacks in Gaepo-dong, Gangnam-gu, and the fire building, wind speed and wind direction were set in accordance with the same conditions at the time of the fire.

Table 1 : Detail setting conditions of simulation

	Structure	**Use**	**Opening**	**Time**	**Ignition Point**	**Wind**
Case 1	Wooden, Fireproof	Housing	General	120min	Actual ignition point	3.4m/s Northwester
Case 2	Wooden, Fireproof	Sales facility	General	120min	Actual ignition point	4m/s Northwester

2.3 Analysis results of the simulation

2.3.1 Case study 1 –Shacks in Gaepo-dong, Gangnam-gu

The simulation results showed that the fire point and neighboring buildings started to be burnt down in about 60 minutes, and the fire spread to more than 80% of the entire building in about 80 minutes. It can be identified that after 120 minutes, the fire spread to all wooden buildings except for fire-resistance building. The results of the simulation identified over time are shown in Figure3.

2.3.2 Case study 2 –Area crowded with restaurants in Insa-dong

The simulation results found that the range of the fire spread to about 50m radius in 60minutes, and the number of buildings which started to burnt down rapidly increased 70 minutes later. In addition, it was identified that the fire spread to more than 40% of the entire building in the area after 80 minutes, and more than 50% of the buildings 100 minutes later. And finally, 10buildings turned out to be totally destroyed. The results of the simulation identified over time are shown in Figure 4.

Figure 3 : Result of simulation (Case study 1)

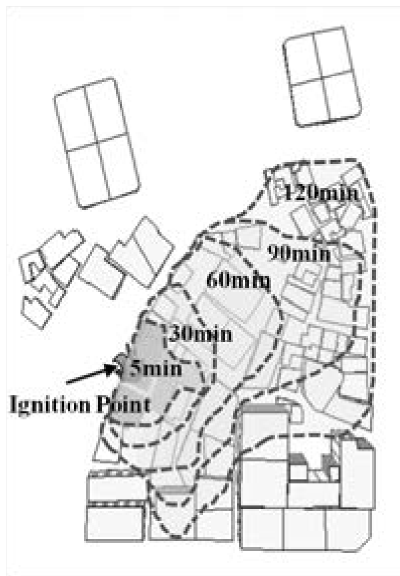

Figure 4 : Result of simulation (Case study 2)

2.4 Comparison of actual and simulated fire

As for the Case Study 1, a comparison between the range of the damages caused by the actual fire after 60 minutes and that of simulation after 60 minutes is shown in Figure 5. In case of the actual fire, the range of the damages was totally destroyed after 60 minutes. On the other hand, the range of the fire expanded was similar, but only some of the buildings turned out to be burnt down in the simulation results.

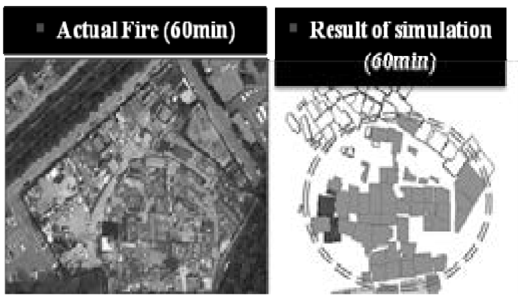

Figure 5 : Comparability of fire spread range

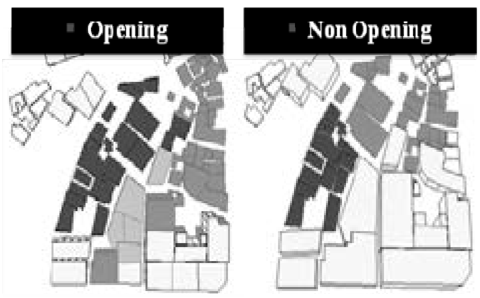

Figure 6 : Fire spread of exterior material by opening

Even in case of the Case Study 2, the range of the damages caused by the actual fire after 60 minutes was found to be similar to that of the analysis on the simulation, but only some part of the buildings were burnt down in the analysis compared to the results from the actual fire. In addition, it turned out that a fire in the outer wall itself does not occur in case an opening is not set as shown in Figure 6.

2.5 Discussions

The results of performing case studies to review the applicability of urban fire simulation found that it can be applicable to the range of fire spread in domestic wooden buildings, but there is a limit to the estimation of the collapse resulting from the total destruction by fire. In addition, it cannot simulate the actual fire in case the spread of fire to the adjacent buildings is caused by the outer wall. In this regard, it is required to conduct experiments and analysis on the estimation on the collapse of wooden buildings and the spread of fire caused by external materials.

3. FIRE-RESISTANCE TEST AND ANALYSIS FOR THE ESTIMATION OF THE COLLAPSE OF WOODEN BUILDINGS

3.1 Experimental purposes and Methods

As a basic experiment for the estimation of collapse of wooden buildings, a fire-resistance test was conducted using a horizontal furnace. For heating conditions, heat was applied for 60 minutes based on the ISO 834 standard heating curve. As a timber used as specimen, Douglas-fir, which has mainly used for building structures, was used. In addition, the specimen was divided into a total of five kinds according to the flame retardant treatment and moisture content as shown in Table 2. And the final carbonization depth was measured by cutting the specimen after the end of the experiment.

Table 2 : Condition of each specimen

	Classification	Moisture content	Weight	Size
Non-treated	General	9.9 %	27.9 kg	300×300×500 (mm)
	Water impregnation	25.3 %	26.8 kg	
Treated	Flame retardant liquid	18.1 %	26.2 kg	
	Oily flame retardant paint	9.6 %	26.6 kg	
	Aqueous flame retardant paint	9.4 %	26.5 kg	

3.2 Experimental results

The results of cutting the specimen after the cooling process after the end of the experiment are shown in the Table 3. In case of the general specimen, the depth of carbonization was measured at 3.8cm, and it was measured at 3.5cm, in case of the water impregnation, 3.7cm in case of the flame retardant liquid, 4.0cm in case of the oily flame retardant paint, and 3.8cm in case of the aqueous flame retardant paint. Figure 7 shows the comparison between the final carbonization depth measured and data obtained from the Kyoto University in Japan. As a result of the regression analysis, 'y=28.31ln(x)-79.088'was deduced, and the coefficient of determination (R^2) turned out to be high (0.9246).

Table 3 : Charring depth of each specimen after cutting

	General	Water impregnation	Flame retardant liquid	Oily flame retardant paint	Aqueous flame retardant paint
Charring depth	3.8 cm	3.5 cm	3.7 cm	4.0 cm	3.8 cm

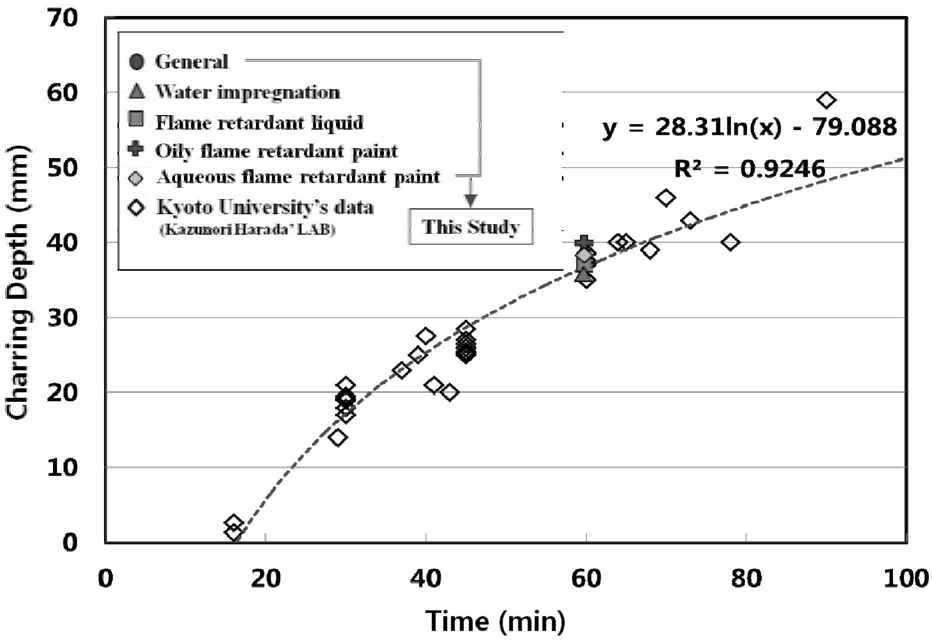

Figure 7 : Regression analysis of charring depth

3.3 Analysis methods

For the estimation of wood carbonization depth, an analysis was conducted using a simple prediction equation of 'Kosuke Kajiyama'. The analysis of wood carbonization depth X can be carried out using the density ρ of the specimen and temperature measured by equation 1.

$$X = \sqrt{\frac{2\lambda_{char}}{\rho L}(T_2 - T_1)(t - t_0)} \quad (1)$$

The carbonization occurrence temperature T_1 was fixed at 288℃, the latent heat of pyrolysis L 4260000J/kg, and the thermal conductivity of coal λ_{char} 0.18W/mk. As for fire-side temperature T_2 and wood density, values measured in the experiment were used.

3.4 Analysis results

As a result of conducting an analysis, the difference between the carbonization depth measured in the experiment and values obtained by the analysis results turned out to be large as shown in Table 4. Through the results of re-estimation of the actual carbonization depth measured in the experiment by applying the correction value f to $\frac{\lambda_{char}}{\rho L}$ of equation 1, the actual carbonization depth was estimated on each specimen as shown in Figure 8.

Table 4 : The analysis results and correction value of each specimen

	General	**Water impregnation**	**Flame retardant liquid**	**Oily flame retardant paint**	**Aqueous flame retardant paint**
Analysis	1.2 cm	1.82 cm	1.84 cm	1.83 cm	1.83 cm
Correction value f	4.5	3.7	4	4.8	4.3

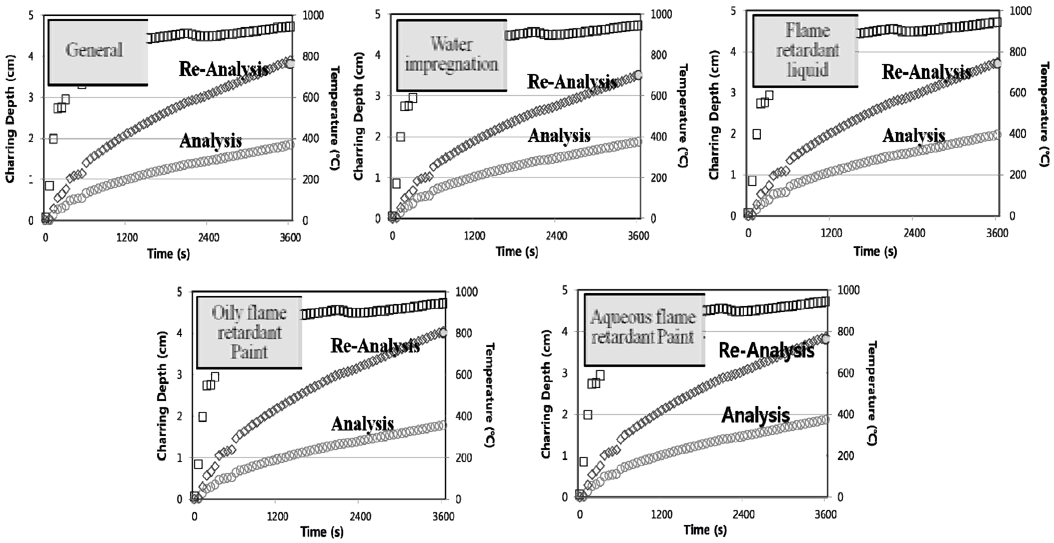

Figure 8 : Re-analysis for prediction equation

3.5 Discussions

The actual carbonization depth that occurs after the experiment is adjudged to have no great relevance with the flame-retardant treatment. In addition, the analysis results showed that it seems to be possible to estimate the carbonization depth using the correction value f according to changes in time, but additional experiments is required for securing reliability. In addition, since the correction value f has a significant impact on the thermal conductivity of the carbonized layer in the analysis, more in-depth analysis on the thermal conductivity of the carbonized layer according to the flame-retardant treatment will be needed.

4. VERTICAL COMBUSTION EXPANSION EXPERIMENT OF ALUMINUM COMPOSITE PANELS

4.1 Experimental purposes and Methods

To identify the fire expansion properties by conducting a vertical combustion expansion experiment of aluminum composite panels, external materials with a consistent increase in the frequency of use in Korea, an experiment was carried out based on the ISO 13785-2 “reaction-to-fire tests for facades –Part 2: Large-scale test”. Characteristics of the specimen are shown in Figure 9, and heat flux and temperature was measured. The experiment was conducted using a propane gas burner with gas flow rate of 0~120g/s for a total of 25 minutes, and it was carried out with two conditions of general aluminum composite panels and semi non-combustible aluminum composite panels. (Figure 10)

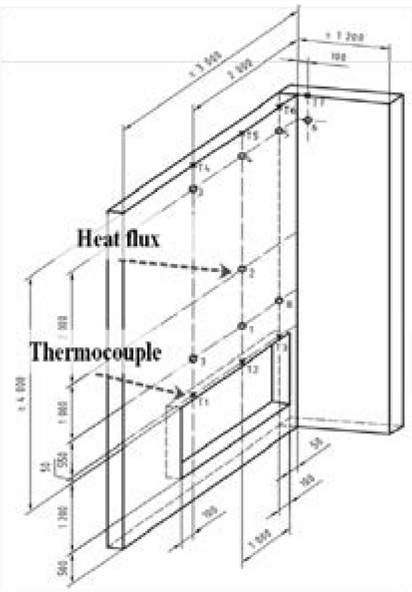

Figure 9 : Installation location of Heat flux and thermocouple

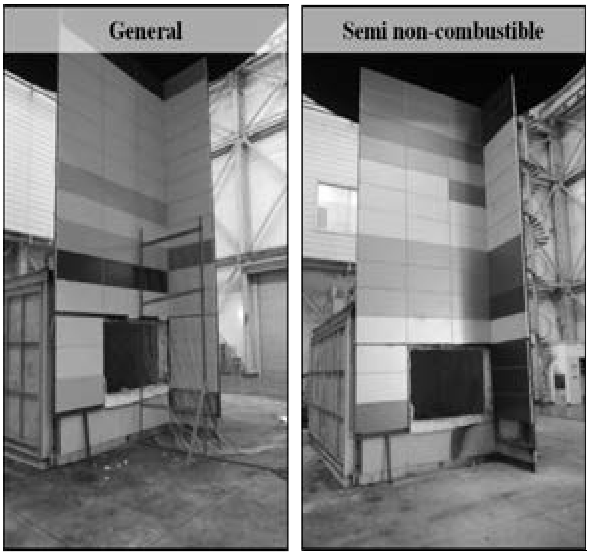

Figure 10 : Installation of aluminum composite panel

4.2 Comparison properties of aluminum composite panels

The combustion of general aluminum composite and semi non-combustible aluminum panels started in 2minutes and 3minutes respectively, and the flames reached the top of the panels after 5 minutes. In case of the general aluminum composite panels, the combustion was rapidly expanded to the top of the opening, along with the side wall after about 8 minutes whereas, a slow process of becoming inflammatory state was found at the part in which the flame did not reach directly in case of the semi non-combustible aluminum composite panels. As for general aluminum composite panels, the experiment was terminated after 9 minutes since the flames soared up to 7m, whereas the experiment lasted for 25 minutes in case of the semi non-combustible aluminum composite panels.

4.3 Comparison of the temperature and heat flux of aluminum composite panels

Figure 11, 12 show a graph that compares the temperature with some of heat flux measured in the experiments of the general aluminum composite panels (Experiment 1) and semi non-combustible aluminum composite panels (Experiment 2). The difference between the two experiments can be identified in about 5 minutes, and the TC-7 of the aluminum composite panels was measured at about 40℃ higher compared to that of the semi non-combustible aluminum composite panels. In case of the heat flux, the highest heat flux of the H/F2 showed a difference of about 20kW/m^2, and a difference of about 3 minutes was found in case of the point of time when the highest heat flux is reached.

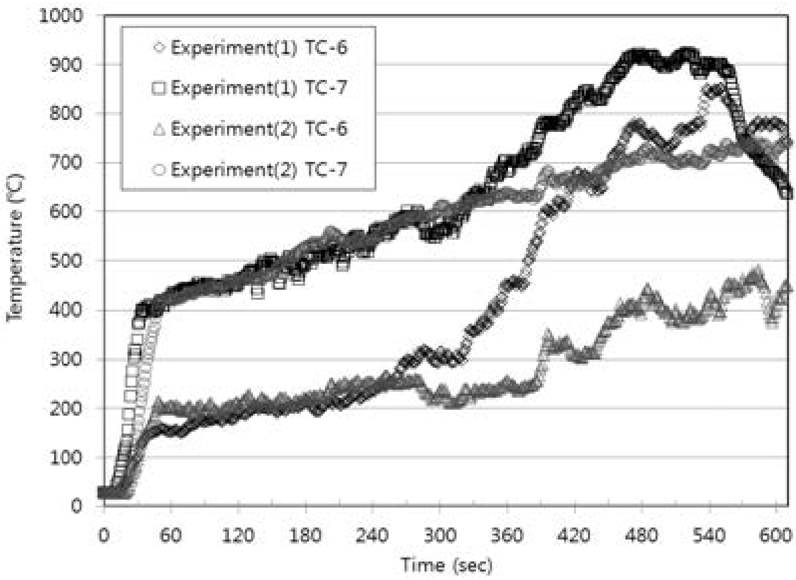

Figure 11 : Comparing the temperature of experiment 1 and 2

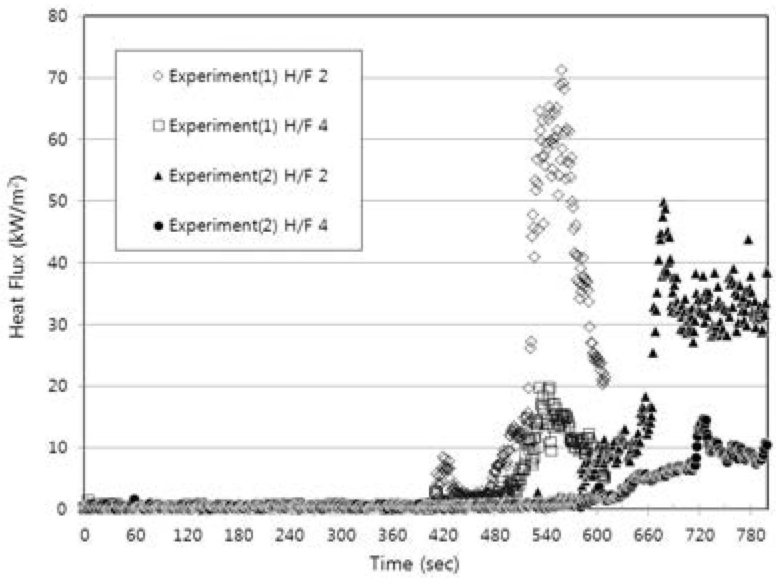

Figure 12 : Comparing the heat flux of experiment 1 and 2

4.4 Discussions

The experimental results of the general aluminum composite panels and semi non-combustible aluminum composite panels found that the flames reached the panels at the top after 5 minutes, which is attributed to the factors of the side wall, not the actual combustion expansion. In case of the semi non-combustible aluminum composite panels, it seems to be possible to delay the combustion expansion at the part in which direct flames are not reached after 13 minutes. However, since the combustion was expanded up to 4m at the corner, the risk of combustion expansions to the upper part is considered to be still great.

5. CONCLUSIONS

From the results of experiments and analysis for the improvement of simulation and review on the applicability of urban fire simulation, the following conclusions were obtained.

1) The range of fire spread in wooden buildings was similar to that the actual fire, and different aspects were found in the collapse and total destruction by fire. In addition, identified that the combustion of the outer wall itself cannot be considered in cased there are no openings.
2) As a result of conducting wood fire-resistance test, it was found that the difference of the carbonization depth according to the flame-retardant treatment does not occur in the actual carbonization depth. In addition, the regression analysis was conducted after comparing the final carbonization depth and data of Japan, subsequently deducing ‘y=28.31ln(x)-79.088’. In addition, the estimation of the carbonization depth was carried out using the correction value f obtained from the results of the analysis using a simple prediction equation.
3) The results of the vertical combustion expansion experiment of the aluminum composite panels found that general aluminum panels were measured about 400℃ higher at the TC-7, and about 20kW/m^2 higher at the H/F2, which indicates that the difference of the vertical combustion expansion according to the internal core materials is great.

In the future, the improvement is required to apply the urban fire simulation to Korea through the fire propagation modeling by the external materials between adjacent buildings, and to conduct analytical research on the vertical combustion expansion of aluminum composite panels, along with the establishment of collapse models through more in-depth experiments and analysis on the carbonization depth and strength degradation of structural members.

REFERENCES

BongChan, Kim, 2012, A study on the fire spread phenomena of aluminium composite panel and Douglas-fir for urban fire risk assessment, Master’s Thesis, Hoseo University, Korea.

Self-help approach in housing reconstruction and beneficiaries' satisfaction in Palestine

Adnan ENSHASSI[1] and Mohammed ABU ZAITER[2]
[1,2]Department of Civil Engineering, IUG, Palestine
aenshassi@gmail.com

ABSTRACT

Everyone has a right to adequate housing. Plans to reconstruct damaged or demolished housing as a result of the conflict remain largely stagnant. Lack of access to raw building materials, remains the major reason for the chronic weakness of progress in reconstruction in Gaza. The main approach which has been used in housing reconstruction process in Gaza strip after the war is Owner-Driven approach which is called "Self-help approach", where conditional financial assistance is given, accompanied by regulations and technical support aimed at ensuring that houses are built back better. More than 90% of the homes have been reconstructed by this method. This paper aims to determine the efficiency of the self-help approach of housing reconstruction in Gaza reconstruction process and to determine the satisfaction of the beneficiaries from this approach. The methodology that is used in this study was direct observations, interviews and questionnaire. It was found that there is significant efficacy of the self-help approach and there is a great satisfaction to the beneficiaries of the reconstruction projects in this way.

Keywords: disaster, housing, post-disaster reconstruction, self-help, Gaza Strip

1. INTRODUCTION

Gaza Strip is a coastal strip of land on the eastern shore of the Mediterranean Sea, bordered on the south by Egypt, on the west by the Mediterranean Sea, and on the north and east by Occupied Palestinian lands between 31 25 N, 34 20 E (CIA 2012). The area of the Gaza Strip is 378 sq km (Encarta 2005). It has one of the highest overall growth rates and population densities in the world. In 2007 PCPS indicated that the population was 1,416,543 where the population density was 3,747 persons per sq km (PCPS 2009), and it is estimated to be 1,710,257 in July 2012 (CIA 2012).

In December 27th 2008 war was launched in the Gaza Strip which was called "Casted Lead". The war stopped on January 18th 2009. The estimated value of all damage caused by Cast Lead war on Gaza Strip is about US$1.1 billion (Barakat et al., 2009). The Palestinian Central Bureau of Statistics (PCBS) reports that 4100 housing buildings destroyed, 17000 houses damaged, 20 mosques, 25 education and health buildings and 1500 factories, shops and other commercial facilities completely destroyed. Shelters will require the construction of about

5000 homes for families who had lived in houses which were destroyed in and before the 2009 war (Al-Qeeq & El-Wazir 2010).

Post-disaster reconstruction, if not well planned and implemented, can create further vulnerabilities in a disaster affected community. According to Schilderman (2004), whilst the number of hazard events does not appear to be increasing greatly, their impact on people is increasing (Chang et al., 2010). Plans to reconstruct housing damaged or demolished as a result of the conflict remain largely stagnant (Shelter Sector-Gaza, 2012). Lack of access to raw building materials, remains the major reason for the chronic lack of progress in reconstruction in Gaza.

A number of strategies and options can be identified based upon previous attempts at reconstruction in Gaza and also upon international best practices. Any project should attempt to find social and physical appropriate planning and design methods to help advancing the post-war reconstruction efforts in the Gaza Strip (Al-Qeeq & El-Wazir 2010). Five predominant approaches are adopted in the contemporary reconstruction practice: Cash Approach, Owner-Driven, Community-Driven, Agency-Driven Reconstruction in-Situ, and Agency-Driven Reconstruction in Relocated Site (Chang et al., 2010; Barakat, 2003; Stephen et al., 2010). The main approach which has been used in reconstruction process in Gaza strip after the war until now is Owner-Driven approach which is called "Self-help approach". In this approach conditional financial assistance is given, accompanied by regulations and technical support aimed at ensuring that houses is built back better. More than 90% of the homes that had been reconstructed by this way. This paper aims to determine the efficiency of the Self-help approach of reconstruction in Gaza reconstruction process in addition to determine the satisfaction of the beneficiaries from this approach.

2. LITERATURE REVIEW

Disasters had great effects on the region and community that they occurred physically, socially, economically and psychologically. The community sometimes uses most of its capacity to overcome the situation and sustain their pre disaster daily life. The most important problem revealed after the emergency phase is especially to meet the shelter needs of the affected population (Arslan & Ünlü 2008).The International Federation of Red Cross and Red Crescent Societies defined disaster as: a sudden overwhelming and unforeseen event. At the household level, a disaster could result in a major illness, death, a substantial economic or social misfortune (Johns 2008). At the community level, it could be a flood, a fire, a collapse of buildings in an earthquake, the destruction of livelihoods, an epidemic or displacement through conflict (Hopkins 2008). Other disaster definition is a widespread human and material or environmental loss which exceeds the ability of the affected society to cope using its own resources (Coppola, 2007, p.25, cited in Mohapatra 2009).

Communities that have faced natural disasters, classifies disasters as Natural (e.g., earth-quakes, hurricanes, floods, wildlife fires etc.) or technological (e.g., terrorism, nuclear power plant emergencies, hazardous materials etc.) (Hristidis, et al., 2010). Conflicts definitely are in need of complicated and interrelated processes and arrangements to go through reconstruction processes, rehabilitation and recovery as well (Barakat et al., 2009). Baradan (2006) explained that post-disaster housing reconstruction is a process of planning, defining strategies, preparation of operation plans, implementations for reconstruction after disasters. Unlike other relief items such as food aid or medicine, housing is a significant, long-term and non-consumable asset (Barakat 2003).

Post-disaster housing reconstruction can be undertaken through different approaches, which vary principally in terms of a household's degree of control over the reconstruction process. Jha et al (2010) defined five reconstruction approaches that may be pursued after a disaster:

- Cash Approach: Unconditional financial assistance is given without technical support.
- Owner-Driven Reconstruction (ODR): Conditional financial assistance is given, accompanied by regulations and technical support aimed at ensuring that houses is built back better.
- Community-Driven Reconstruction: Financial and/or material assistance is channeled through community organizations that are actively involved in decision making and in managing reconstruction.
- Agency-Driven Reconstruction in-Situ: Refers to an approach in which a governmental or nongovernmental agency hires a construction company to replace damaged houses in their predisaster location.
- Agency-Driven Reconstruction in Relocated Site: refers to an approach in which a governmental or nongovernmental agency hires a construction company to build new houses in a new site.

Barakat (2003) indicated that the Post-disaster housing rebuilding priorities require special attention to be paid to the implications of resource availability for reconstruction performance and to underlying resourcing bottlenecks in the reconstruction process. Four predominant resourcing approaches are adopted in the contemporary reconstruction practice: government driven, donor driven, market driven, and owner driven (Chang et al., 2010). The choice of the best reconstruction approach to be employed is context-specific and should take into consideration (1) reconstruction costs; (2) improvement in housing and community safety; (3) restoration of livelihoods; (4) political milieu; (5) cultural context; and (6) people's own goals for well-being, empowerment, and capacity (Jhans et al., 2008). It is very important to make deep consultation with the community and evaluation of requirements and capacities is critical before deciding on any reconstruction approach (Chang et al., 2010).

While people affected by a disaster are the first to engage with the emergency, they are often perceived as victims of the disaster rather than as the critical driving force behind reconstruction (Jhans et al., 2008). Sadiqi, et al., (2011) indicated that local communities and the survivors of a disaster play a crucial role in post disaster reconstruction and their participation ultimately determines project success. Effective community participation in reconstruction process should be instigated. Empowering communities to participate in the reconstruction process can be highly inspiring to the recipient stakeholders of resulting projects and provides an opportunity for members to contribute their knowledge and skills. This is made possible when affected communities are effectively involved in all stages of the post-disaster reconstruction (Sadiqi, et al., 2011). Post-disaster practices must embrace greater involvement of the affected communities and local institutions specially households of destroyed home in the process of reconstruction (Allen 2006). In an ODR approach, people who lost their shelter are given some combination of cash, vouchers, and in-kind and technical assistance to repair or rebuild their houses (Jha et al., 2010). They may undertake the construction or repair work by themselves, by employing family labor, by employing a local contractor or local laborers, or by using some combination of these options. ODR is similar to the "Self-Help approach" (Barakat 2003).

In general, the more intensive the community engagement in reconstruction planning, house design, beneficiary selection and construction management, the greater is the beneficiaries sense of ownership of and satisfaction with their new homes, and the higher are occupancy rates (Westover 2004). ODR requires good oversight and governance, that is, a government capable of establishing and enforcing standards, and some agency (governmental or nongovernmental) to ensure the quality of construction (Jha et al., 2010; Barakat 2003). A self-help approach encourages the active participation of the disaster-affected community; it may be a useful way of restoring a sense of pride and well-being in people who have been through a trauma (Petrini et al., 2012; Barakat 2003).

Success lies in establishing a support system for homeowners appropriate to the local context, Jha et al., (2010) indicated that to make self-help approach more effective and efficient, some conditions should be proceeded which may include:

- Training of trades people and homeowners.
- Technical assistance and construction supervision and inspection.
- Updating and enforcement of building codes and construction guidelines.
- Mechanisms to regulate prices and facilitate access to building materials.
- A system for providing financial assistance in installments as construction progresses.

An owner-driven approach entails some risks and drawbacks These risks can be overcome through the introduction of building codes and adequate technical assistance (Jha et al., 2010). In self-help approach beneficiaries were brought into assessing the hazards and identifying the design features needed as well as were brought into the construction process. The participatory housing design methodology sought beneficiary knowledge through: structured and semi structured interviews; modified participatory and vulnerability mapping and participatory rural appraisal; field observations; focus group discussions and the inclusion of building regulations, donor technical specifications and beneficiary specifications as well as hazard mapping of the individual sites (Ibrahim 2010).

3. METHODOLOGY

Reconstruction destroyed housing program funded by the grant of the Gulf Cooperation Council for the reconstruction of Gaza in cooperation with the Islamic Development Bank, where reconstruction process depended on Self-help approach (Owner-Driven Reconstruction- ODR) was used as a case study. All the records of meetings of the Steering Committee for IDB reconstruction program-Housing Allocation, and final reports of these projects were studied and analyzed. Interviews with members of the Steering Committee and number of interviews were conducted with beneficiaries from these projects.

A questionnaire survey was adopted to determine the extent of satisfaction of the target group (beneficiaries from reconstruction project using Self-help approach). The questionnaires were randomly distributed to 40 beneficiaries of the projects, 33 questionnaires were received.

The questionnaire was divided into two parts:
Section I: This section contains a series of questions related to personal features of individuals of the sample.
Section II: Level of satisfaction and their relationship with some variables which consists of two parts.
The first part: The level of satisfaction in general about the process of reconstruction-based self-help approach.
The second part: The level of satisfaction with the mechanism of reconstruction of the beneficiary's house in particular.

Validity and reliability of the questionnaire had been confirmed.

Structure Validity: All the correlation coefficients in all areas of statistically significant questionnaire when it is all scopes of the questionnaire ratified status measured at the level of significance $\alpha = 0.05$.

The value of Cronbach's alpha coefficient was high for each scope, ranging from (0.657-0.768). As well as the value of the coefficient alpha for all the paragraphs of the resolution was (0.797). This means that the reliability coefficient is high.

4. RESULTS and DISCUSSION

4.1 IDB housing reconstruction program description

The Islamic Development Bank (IDB) is the coordinator for the Program of the Gulf Cooperation Council for the Reconstruction of Gaza, where the reconstruction process depended on Self-help approach (Owner-Driven Reconstruction). A Conditional financial assistance is given to the beneficiaries through payments equal to the reconstruction cost (260\$-300\$/sq meter), accompanied by regulations and technical support aimed at ensuring that houses are built back better. The donor forms a steering committee to manage the process of reconstruction, with the following tasks:

- Developing standards to beneficiaries.
- Directing the projects implementation.
- Solving problems and obstacles during the implementation.
- Monitoring the reconstruction process.

Beneficiaries have built houses with area ranging from (90-180 square meters). The committee policies have given the beneficiaries the flexibility to increase their home's area and improve its quality from their own recourses provided that all specifications and reconstruction conditions must be met. Partners and institutions overseeing the implementation of projects provide technical support and guidance to the beneficiaries to complete the reconstruction process within the planned budget and duration as well as a high quality. Before any financial payment is paid to the beneficiary they have provided the following documents to supervisor: (Drawings which is approved from the Municipal and Engineers Association, time schedule and the implementation mechanism for reconstruction process, providing a legal insurance for using the financial assistance just for reconstruction purpose.

The payments are paid in a line with the progress report and according to the recommendations of supervisors. The final installment is paid when the beneficiary complete the reconstruction of their houses.

Table 1 shows the IDB housing reconstruction program components.

Table 1: IDB housing reconstruction program components

Status	Fund allocation	Number of housing units				total	Budget $M
Executing Agency		Mercy	Housing council	UNDP	UN		
Completed	first	50	51	0	0	101	3,640,000
Completed	second	39	37	46	0	122	5,432,000
In progress	third	71	71	0	260	402	13,227,700
In progress	forth	150	230	0	220	600	29,437,700
In progress	fifth	100	100	0	125	325	10,520,000
Total		410	489	46	605	1550	62,257,400
The average grant for each housing unit		*Totally reconstruction*					*40,000$*
		Rehabilitation					8,860$

4.2 Advantages which is found in this approach (self-help approach)

1- Households have taken an active role in rebuilding, which speeds recovery from disaster psychological and social dependencies.

2- Assistance can be adjusted to the needs of the household related to income, family size, livelihoods, and socio-cultural requirements.

3- Overcoming political problems, which prevent the NGO's to use materials that are entered by the tunnels.

4- Tends to involve local building industry, thereby contributing to restoration of local economy and livelihoods.

5- Allows people to “top up” housing assistance with their own savings and build a house reflecting their specific needs and aspirations.

6- less subjected to disruptions caused by unstable political situation (for example, blockade, closure of the crossings)
7- The beneficiaries are highly motivated and more belonging to their houses in addition to the increasing spirit of cooperation in the community.

4.3 Disadvantages which is found in this approach

1- Beneficiaries' weakness in the management of reconstruction process specially the financial management.
2- Instability of material prices in the market was the major risk faces the beneficiaries
3- Beneficiaries had to bear some additional financial burdens as a result of extensions of the home in excess of the grant.
4- It was more difficult with poor beneficiaries who have not experience in construction.
5- Difficulty to contract with technical construction worker for each home, causing price rises in many cases.

4.4 Beneficiaries' satisfaction in self-help approach

Figure 1 illustrates the level of satisfaction in general about the process of reconstruction-based self-help approach.

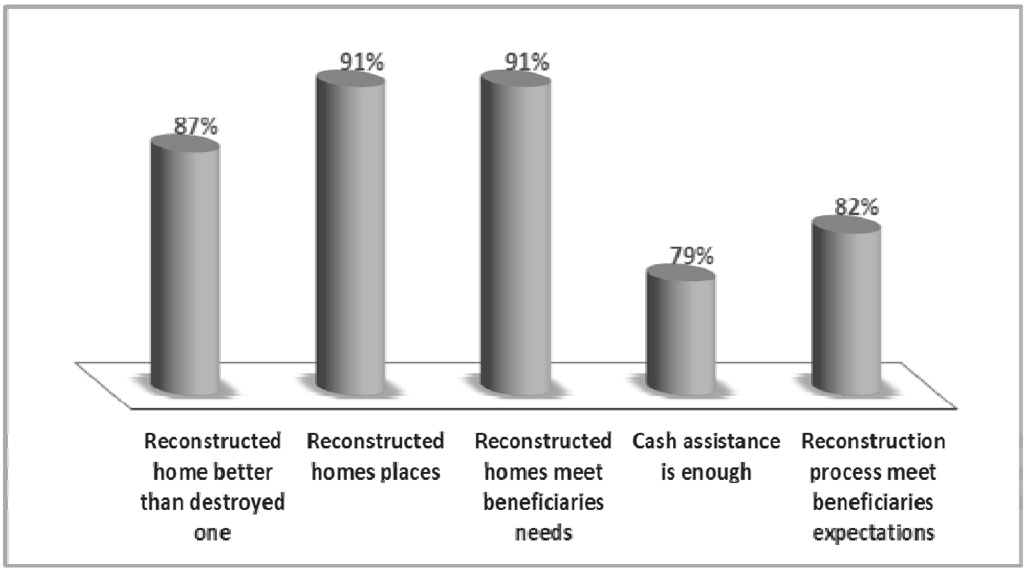

Figure 1: Satisfaction about the process of reconstruction-based self-help approach

The results indicated that there is a high level of satisfaction in general about the process of reconstruction-based self-help approach.

Table 2 shows the level of satisfaction with the mechanism of reconstruction of the beneficiary's house in particular.

Table 2: Beneficiaries satisfaction with the mechanism of reconstruction process

Satisfaction factors	Mostly satisfied	Satisfied	Unsatisfied	Mostly dissatisfied	Degree of satisfaction
Comfort of reconstructed home	46%	46%	6%	3%	83%
Home is hygienic	67%	24%	6%	3%	89%
Home is Safety/security in general	24%	33%	36%	6%	69%
General level of happiness/well-being	55%	27%	12%	6%	83%
Beneficiaries satisfaction with the reconstructed home	70%	21%	6%	3%	89%
Beneficiaries satisfaction with the area of reconstructed home	70%	21%	9%	0%	90%
Beneficiaries satisfaction with the distribution of rooms and services	70%	27%	3%	0%	92%
Beneficiaries satisfaction with Electrical works at home	70%	24%	6%	0%	91%
Beneficiaries satisfaction with Home ventilation	67%	27%	6%	0%	90%
Beneficiaries satisfaction with Speed of execution	42%	49%	9%	0%	83%
Beneficiaries satisfaction with Speed the flow of payments	52%	39%	9%	0%	86%
Beneficiaries satisfaction with Dealing with the	76%	24%	0%	0%	94%

supervisory					
Beneficiaries satisfaction with Technical supervision of the supervising party	76%	24%	0%	0%	94%

The result in the above table indicates that there is a high level of satisfaction with the mechanism of reconstruction of the beneficiary's house in particular.

By analyzing the results of the questioner it can be indicated that:

- There is a clear relationship between the method of reconstruction and satisfaction of target group, since most of the beneficiaries expressed their great satisfaction of this ways of reconstruction (Self-help approach).
- The study showed that there is a clear relationship between the level of satisfaction and area of houses which were reconstructed. Homeowners with small home area less satisfied than others.
- The result also indicated that beneficiaries are satisfied with the distribution of rooms and services and building conditions as a whole, because they are the main responsible for drawings and implementation of construction process.
- Most of the beneficiaries satisfied with the method of supervision applied by the donor.
- Most of the beneficiaries satisfied with the value of financial assistance and the way the flow of payments, although some of them had to pay some money to complete the reconstructed home, in order to cover the increase in the area or the improvement in the specifications of the house.

Finally, the results indicated that there is clear consent of the beneficiaries to the self-help approach as an effective and efficient approach to reconstruct their homes.

5. CONCLUSION and RECOMMENDATION

The aim of this paper was to determine the efficacy of the self-help approach of reconstruction in Gaza housing reconstruction process, in addition to determine the satisfaction of the beneficiaries for this approach. It was found that there is significant efficacy of the self-help approach, and that the beneficiaries are satisfied with this approach.

Communities and households must have a strong voice in determining the post-disaster reconstruction approaches and a central role in the reconstruction process.

Good planning principles and environmental practices should be incorporated, whatever the reconstructions approach.

There should be a plan and a clear strategy for the reconstruction of Gaza in the housing sector. Database of the war damages comparative studied and research results of reconstruction projects should be prepared. Training programs in reconstruction approaches should be organized for policy-makers and practitioners to exchange experiences from recent recovery operations.

REFERENCES

Allen, K. M., 2006. *"Community-Based Disaster Preparedness and Climate Adaptation: Local Capacity Building in the Philippines". Disasters,* Volume 30 (1), pages 81-101.

Al-Qeeq, F. & El-Wazir, M., 2010. *"Sustainable Housing Strategies in Post-war, Reconstruction of the Gaza Strip"*. International Congress: Rehabilitation and Sustainability. The Future is possible", Col·legi d Aparelladors & Tècnics i Enginyers d'Edificació de Barcelona, 4th, October 2010, Barcelona.

Arsalan, H. & Unlu, A., 2008. *"The Role of NGO's in the Context of Post Disaster Housing in Turkey*". 4th International i-REC Conference, "Building Resilience: Achieving Effective Post Disaster Reconstruction", 30 April-2 May 2008, Christchurch.

Baradan, B., 2006. *"The Role of Information and Communication Technologies in The Process of Post-Disaster Housing Reconstruction"*. 1st International CIB Endorsed METU Postgraduate Conference Built Environment & Information Technologies, Ankara, pages 73-84.

Barakat, S., 2003. *"Housing Reconstruction after Conflict and Disaster,"*. Humanitarian Practice Network at ODI, UK.

Barakat, S., Zyck, S. & Hunt, J. E., 2009. *"The reconstruction of Gaza: A Guidance Note for Palestinian and International Stakeholders"*. Regional Human Security Centre, Post- War Reconstruction & development Unit (PRDU).

Central Intelligence Agency, 2012. https://www.cia.gov/library/publications/the-world-factbook/geos/gz.html, Last Accessed date: April 15, 2012.

Chang Y., Wilkinson S., Potangaroa R., & Seville E., 2010. "Resourcing challenges for post-disaster housing reconstruction: a comparative analysis*"*. Building Research & Information, Volume 38(3), Pages 247–264.

Hristidis V., Chen S., Tao Li, Luis S. & Yi D., 2010. *"Survey of Data Management and Analysis in Disaster Situations"*. The Journal of Systems and Software, Volume 83, pp. 1701–1714.

Ibrahim, M., 2010. *"Post-Disaster Housing Reconstruction in a Conflict Affected District, Batticaloa, Sri Lanka"*. Strengthening Climate Resilience Discussion Paper 6, Institute of Development Studies at the University of Sussex Brighton BN1 9RE, UK. www.csdrm.org, Last Accessed date: April 15, 2012.

IDB, Fourth Quarter Report, 2012. *"Grant of the Gulf Cooperation Council for The Reconstruction of Gaza in Cooperation with the Islamic Development Bank – Jeddah"*. April 2012, Gaza, not puplished.

Jha, A., B. Jennifer Duyne, P. Daniel & Stephen, S., 2010. "*Safer Homes, Stronger Communities: a Handbook for Reconstructing after Natural Disasters*". Washington, DC, World Bank.

Johns, H., International Federation of Red Cross & Red Crescent Societies Public Health, 2008. "*Guide for Emergencies*". A textbook, 2008, 2nd Edition, Switzerland.

Mohapatra, R., 2009. "*Community Based Planning in Post-Disaster Reconstruction: A Case Study of Tsunami Affected Fishing Communities in Tamil Nadu Coast of India*". A thesis presented to the University of Waterloo in fulfillment of the thesis requirement for the degree of Doctor of Philosophy in Planning, Waterloo, Ontario, Canada, 2009.

Palestinian Central Bureau of Statistics, 2009."*Main Indicators by Locality Type*". http://www.pcbs.gov.ps/DesktopDefault.aspx?tabID=4151&lang=en, Last Accessed date: April 15, 2012.

Petrini, F., Vannucchi, S., Miraglia A., & Meringol, P., 2012. "*Self-Help Groups in a City of Tuscany: Reconstruction of the Second Generation Model of Work for Professionals and Services*". Global Journal of Community Psychology Practice, Volume 2(3), Pages 1-12.

Sadiqi , Z. Coffey, V. & Trigunarsyah, B., 2011. "*Post-Disaster Housing Reconstruction: Challenges for Community Participation*". *In Proceedings of the International Conference on Building Resilience: Interdisciplinary Approaches to Disaster Risk Reduction and the Development of Sustainable Communities*, Heritance Kandalama, Sri Lanka. http://eprints.qut.edu.au/42177/, Last Accessed date: April 15, 2012.

Schilderman, T., 2004. "*Adapting Traditional Shelter for Disaster Mitigation and Reconstruction: Experiences with Community- Based Approaches*". Building Research & Information, Volume 32(5), Pages 414–426.

Shelter Sector Gaza, 2012. "*Shelter Advocacy Fact Sheet 4*". Unified Shelter Sector Database (USSD), http://www.sheltergaza.org, Last Accessed date: April 15, 2012.

Snider, H. & Takeda, N., 2008. "*Design for All: Implications for Bank Operations*".

Westover, N., 2004. "*Lessons from A Post-Disaster Reconstruction Experiences*". CIDA in consultation with its reconstruction partners in Indonesia following the Asian tsunami of December 2004 .http://www.cowater.com/uploads/English.pdf, , Last Accessed date: April 15, 2012.

Roles of self-help and mutual and local government aid in community-based disaster mitigation

Midori YAMAGUCHI[1], Chiaki TAKEKUMA[2] and Yoko TOWATARI[3]
[1] Project Lecturer, RN, MPH, Kumamoto Health Science University, Japan
yamaguchi.mi@kumamoto-hsu.ac.jp
[2] Professor, BSN, MW, PHN, Ph.D., Kumamoto Health Science University, Japan
[3] Lecturer, RN, MW, PHN, MS (Sociology),
Kumamoto Health Science University, Japan

ABSTRACT

Disaster mitigation means minimizing the damage occurring when a disaster strikes. Whereas "disaster prevention" implies protection against damage, "disaster mitigation" involves the active reduction or control of damage, assuming that it is going to occur. There are two aspects to community-based disaster mitigation. One is the "hardware" aspect, which includes such items as the maintenance and development of social infrastructure. The other is the "software" aspect, which consists of human behaviors directed against disaster. Currently, self-help and mutual and local government aid – for example through cooperative activities – are essential because the human "software" input is essential to managing the social problems that accompany disaster mitigation efforts. Now, in Japan, the numbers of people who need support in time of disaster are increasing because of the "super aging" nature of our society. There is therefore an even greater stronger need for cooperative activities so that we can strengthen the self-help and mutual and local government aid. This report clarifies the roles of these three kinds of aid in community-based disaster mitigation by introducing an example of disaster planning in Fukuoka Prefecture.

Keywords: disaster mitigation, mutual and local government aid, self-help

1. INTRODUCTION

Japan has suffered many disasters, including not only the aftermath of the 2011 Great East Japan Earthquake and Tsunami, but also yearly typhoons, floods, and severe snowstorms. Japan's environmental conditions make the country susceptible to natural disasters, and social factors such as the type of living environment, population density, and type of land use tend to enhance disaster damage. Therefore, emergency response to disaster has become a major concern, and many sectors in this country are now collaborating in disaster management.

Community-based disaster mitigation is an essential part of disaster management. Disaster mitigation means minimizing or controlling the damage that occurs when a disaster strikes. Disasters can destroy communities, and empowering leaders and the public with knowledge of available resources through the planning and development of disaster responses can strengthen a community's resilience.

Self-help and mutual and local government aid play a role in strengthening community resilience. Today, the numbers of people in Japan who need support in times of disaster are increasing because of the "super aging" nature of our society. Therefore, there is an even greater need for cooperation to strengthen the mitigative effects of self-help and mutual and local government aid.

This report clarifies the roles of these three kinds of aid in community-based disaster mitigation by introducing an example of disaster planning in the municipality of Miyama in Fukuoka Prefecture.

2. SELF-HELP AND MUTUAL AND LOCAL GOVERNMENT AID

Self-help and mutual and local governmental aid express the division of roles of the individual, the community, and the administration. Under this principle of subsidiarity, the small units (individuals and the community) take the initiative and make decisions, and the government provides subsidies. These cooperative activities are essential, because human behavior, which can be seen as the "software" input in disaster mitigation, is essential to manage social problems in the face of disaster.

In the Great Hanshin-Awaji Earthquake in 1995, about 80% of the people under the rubble were rescued by families or neighboring residents (Kawada, 1997). One report showed that the rate of self-rescue or rescue by family or neighbors exceeded 90% in certain area. Despite the serious damage, the safety of all residents was checked on the day of the earthquake by neighbors or the fire brigade. These examples show that self-help and mutual aid play a big role in saving lives in times of disaster. Moreover, in the Mano district in the municipality of Kobe, residents used bucket relays to put out post-earthquake fires, thus relying on self-help and the mutual aid of the local community (Araki, 2013). Enhancing the capability of local communities is thus essential for disaster management and recovery. Such examples as those mentioned above show us that daily social connections within neighborhoods and communities are important. Moreover, communities need to develop partnerships with local government. Figure 1 shows the relationships among self-help and mutual and local government aid in community-based disaster mitigation.

Figure 1: Relationships among self-help and mutual and local government aid in community-based disaster mitigation

3. ASSESSING AND SUPPORTING VULNERABILITY

Previously, those who are vulnerable at the time of a disaster were referred to by the acronym "CWAP": Children, Women, Aged people, and the Poor or Patients. In the current Japanese Government's guidelines on disaster vulnerability, the vulnerable are now referred to as those who need support to collect the information they need and evacuate to a safe place in time of disaster. These people include the elderly, the disabled, non-Japanese speakers, infants, children, and pregnant women. Because of the aging of Japan's population and a shift from hospital to home-based care, the vulnerability of our population is increasing. We have learned from previous disasters, including the 1995 Great Hanshin-Awaji Earthquake and the 2011 Great East Japan Earthquake and Tsunami, that the proportion of the elderly who are harmed in such disasters is high. Therefore, it is vital that we assess the vulnerable, support their evacuation, and prevent secondary harm to them.

4. PLAN FOR SUPPORTING THE VULNERABLE IN TIMES OF DISASTER IN MIYAMA MUNICIPALITY, FUKUOKA PREFECTURE

4.1 Aim and persons covered

A plan for supporting the vulnerable in times of disaster was devised as part of Miyama municipality's disaster prevention plan (March, 2011). This plan aims to precisely assess the vulnerable and to support their safe evacuation when a disaster occurs. To do this, self-help among the vulnerable and mutual aid by the community are fundamental, and social connections need to be strengthened. More municipality plans to strengthen connections with other organizations such as community leaders and volunteers. Information on the vulnerable is entered into a register and then shared by stakeholders such as community leaders, volunteers, and the leaders of various groups.

In the Plan, the following people are considered to be vulnerable:

a. Those aged over 65 years and living in households by themselves
b. Those certified as requiring long-term care
c. The disabled
d. Those who have mental disorders

The classification therefore does not apply to people who are receiving support from families, those who are hospitalized, those living in care houses, or those who can evacuate themselves.

4.2 Registration on the Vulnerable list

Those who are prepared to be registered on the list need to fill in private and personal information such as demographic data, disease history, and contact persons. In addition, they must agree to give this information to community or group leaders. The information that is submitted is registered on the Vulnerable list so that individual support plans, with mapping and refuge information, can be compiled. After the registration is complete, a "Information card" for urgent communication is distributed (Figure 2). The registration card, together with the information held by local government and community leaders, can thus be used to give precise information to emergency services. Figure 3 illustrates the system used to support the vulnerable.

Figure 2: “ Information Card ” on the refrigerator
advice to put on a health insurance ID card, a consultation ID card, drug information and own photograph, etc.

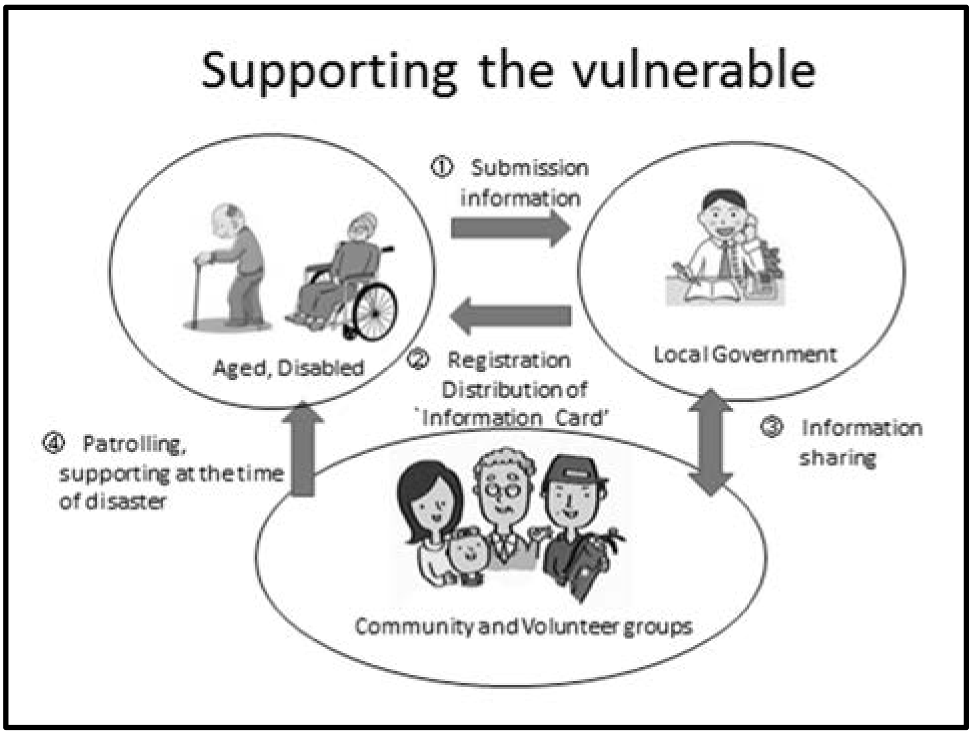

Modified due to Miyama m. information

Figure3: Plan for supporting the vulnerable in times of disaster
in Miyama municipality

5. FLOODS AND LANDSIDES IN NORTHERN KYUSHU IN 2012: THE EXPERIENCE OF MIYAMA MUNICIPALITY

Floods and landslides caused by torrential rain “never before experienced” occurred in 2012 in the prefectures of Fukuoka, Kumamoto, and Oita in northern Kyushu (Fig. 4). Thirty people were killed and 27 were injured.

The municipality of Miyama is located in the southern part of Fukuoka Prefecture. Its population is about 40,000, of which more than 31% of which are over the age of 65. Agriculture is a key industry. The Yabe River flows through the northern part of the municipality. In 1953, floods affected this area and 29 people were killed in the watershed. In the 2012 floods, 2 people were injured and many houses and farms suffered huge amounts of damage. The disaster experience revealed that the main problems were temporary refuge, communication, and support of the vulnerable.

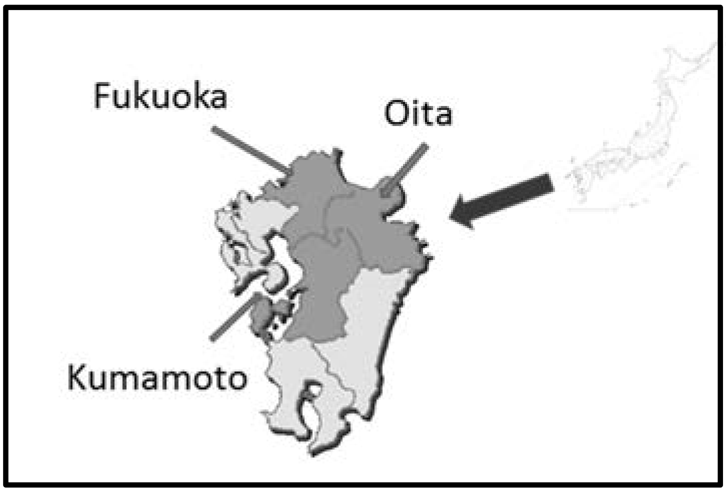

Figure: 4 Map of the Kyushu prefectures affected by floods and landslides in 2012

6. EVACUATION TRAINING BY A VOLUNTARY DISASTER PREVENTION GROUP IN THE HONGO DISTRICT OF MIYAMA MUNICIPALITY

After disastrously heavy rain was experienced in 2012 a local volunteer disaster prevention group in the Hongo district of Miyama municipality performed evacuation training. After refuge information is broadcast, a refuge support person goes to the houses of vulnerable people and guides them to a temporary refuge. When they leave the house they hang a towel on the fence or door post as a marker for the firefighting team (Figure 6). The firefighting team then checks all of the houses to ensure that the occupants are safe. The volunteers say that the training help them to prepare for disaster: they learn to remain calm and are thus better able to act. Training participants who live by themselves say that they feel uneasy and anxious about evacuating in time of disaster and that they feel a need for daily communication.

Figure 5: Evacuation by supporting volunteers

Figure 6: Hanging a towel on the fence or door post as a marker for the occupants are already evacuated

7. DISCUSSION

The Hongo District is located in the sandbank of the river and the area is at high risk of the flood. Resident awareness of disaster was high. The head of the district took the initiative to organize the voluntary disaster prevention group and perform evacuation the training with the cooperation of local government. Residents in the at-risk areas are now aware that they can protect their community by themselves.

This case shows how mutual aid can be reinforced in an aging society. Voluntary disaster prevention groups are especially needed in areas where the disaster risk is high. The organization rate increases after disasters; in 2012 it reached 70% according to research on the status of voluntary disaster prevention groups in southern Fukuoka Prefecture, and it is expected that this rate will increase further with time. However, the organization rate in 5 of 12 cities is less than 50% in southern Fukuoka, so there are substantial differences in organization rates among areas(Tanaka, 2013). A lack of people among the aged who are able to lead groups is a problem. Nevertheless, high levels of awareness and recognition among residents help to promote community-based volunteer activity. It is particularly important to promote the organization of volunteer groups in areas considered to be at high risk of disaster.

Support for the vulnerable is essential and beneficial. Even though such a system has been set up in the Hongo district of Miyama municipality, there have been problems with its proposal in other areas, as some people are hesitant to register because of the need to reveal personal information.

8. CONCLUSION

Many disasters have occurred in our country, and disasters that are unexpected or that we have never experienced before affect us every year. Security and safety are basic human needs, and disaster preparation is indispensable. In disaster responses we must cater to every situation and provide response measures strategically. In community-based mitigation, the organization and continuation of volunteer disaster prevention groups are important activities. We need a system that is based on self-help and mutual aid among local residents, with appropriate support from local government.

REFERENCES

Araki, C., 2013 Earthquake and Disaster Response in the Japanese Community: A Strengths and Community Perspective. *Journal of Social Work in Disability & Rehabilitation.*, 12:1-2, 39-47.

Fire and Disaster Management Agency in Japan., 2011 Jisyubousaisosikinotebiki (Guidelines for volunteer disaster prevention groups) , *http://www.fdma.go.jp/html/life/bousai/bousai_2304-all.pdf*

Kawada, Y., 1997 Prediction of Loss of Human Lives Due to Catastrophic Earthquake Disaster. *Journal of Japan Society for Natural Disaster Science*, Vol.16, N.1, 3-14.

Kawada, Y., 2012 *Korekarano bousai,gennsaiga wakaruhonn (Disaster Prevention and Disaster Mitigation in the Future),* Iwanami Junior Paperbacks

Tanaka, N., 2013, July 14. Preparedness for Disaster, Differences among areas, *Nishinihonn shinnbunn*, p1

Miyama municipality., 2011 *Master Plan*: Plan of supporting the vulnerable at the time of disaster.

Sustainable safety and security in private rental properties for students in Hanoi: the tenants' perspective

Thi Mai NGUYEN [1], Anh Quan PHUNG [2] and The Quan NGUYEN [3]
[1] Undergraduate student in 54KT6 class,
[2] Lecturer, Faculty of Construction Economics and Management,
[3] PhD, Vice Dean, Faculty of Construction Economics and Management,
[1, 2, 3] National University of Civil Engineering, Hanoi, Vietnam
nguyenquan.nuce@gmail.com

ABSTRACT

Sustainable urbanization requires that all forms of development and associated policies be judged on the basis of three criteria: economy, ecology and equity. Therefore, together with developing economic infrastructure supporting economic activities, cities need to provide social infrastructure assets for accommodating social services to secure a better living quality for urban inhabitants. This paper looks into the practices of safety and security in student rentals in Hanoi, using data collected from a survey with participants as students from universities and colleges in the city. The paper investigates the issues in student rentals in order to find out significant influential factors affecting safety and security in this rental market under the tenants' perspective as well as important criteria to their accommodation choice. According to the survey results, the survey participants have experienced thirteen factors causing their safety and security risks in rental accommodation, whose average impact levels are recorded. Among the factors, the most significant influential factors include "security quality of rental properties" and "security issues in neighborhood areas" which bring the highest risks for tenants as students. Among seventeen criteria for rental accommodation choice and their level of contribution to the choice which are presented and analyzed, those relates to safety/security risks belong to the most important group. The influential factors to safety/security risks then are analyzed to measure their level of importance to accommodation choice. The results imply that tenants, landlords and the local government authorities need to pay attentions to those factors in order to contribute to the sustainable development of this rental market as well as this type of urban citizens.

Keywords: *accommodation safety and security, safety/security risks, student rentals, accommodation choice criteria, living quality.*

1. INTRODUCTION

The number of students studying in universities, colleges and vocational schools account for a significant proportion of the population of Hanoi. In 2009, there were about 800.000 students studying in Hanoi, accounting for more than 46% the total number of students all over the country, which was 1.719.499 students in 2009 (Phan Duong, 2009). Since 2009, due to the expansion of existing universities and the entrance of new universities to the market, there are about one million students currently living and studying in Hanoi and the number is still increasing. Consequently, the student population accounts for about one-seventh the total population of Hanoi. This type of citizen also needs a lot of infrastructure in order to ensure their standards of life at a certain and acceptable level for their sustainable development.

Lacking functional areas because of limited land fund is a common feature of universities located in Hanoi. There are several universities with the average land area per student is just around 2m2/student (Phan Duong, 2009). As a result, most of universities in Hanoi do not have a large dormitory that can serve the need of their students. According to (Phan Duong 2009), the total areas of dormitories available in Hanoi can only meet about 15-20% the demand from students. Yet these universities cannot afford an extension of their dormitories due to financial and land fund issues. Most of the universities in Hanoi posses only less than 10 ha of their areas, especially there are three universities having only an area of less than 1 ha. With about 80% students from outside the city, apart from the ones who stay living at home and commute to the universities and the ones who live with their relatives in the city, there is still a lot of unmet demand for rental houses for students in Hanoi (Students from NEU, 2006).

Being provided and managed by households and private developers, private houses for rent, including student rentals in Hanoi has been considered as a complicated and unsafe, low quality sector. This paper, based on an empirical survey, looks into the practices of safety and securities in private student rentals in Hanoi in order to point out factors related to safety and security issues in residential rentals and their impact levels. It then measures the level of risk that each safety and security factors may create to student tenants in Hanoi (hereafter referred to as safety/security risk with its negative meaning) and the role of safety/security risk consideration on their accommodation choice from the tenants' perspective.

2. THE RESEARCH METHODOLOGY

The paper uses results from a survey with respondents who are students from different universities and colleges in the city of Hanoi to investigate the issues in student rentals in terms of safety and security. A total of 30 questions were included in the questionnaire. The factors to be measured in the questions have been developed from interim results collected in a preliminary survey through unofficial talks with 20 students from the researchers' faculty. The respondents are requested to answer the questions regarding their own experience living in private rentals. 184 questionnaires were sent back with a wide range of participants' age, rental location, gender, and hometown (Table 1). Among them, 140 questionnaire were done with self-completion method, the others were filled in an online survey. Participants of the survey age from 18 to 24, with an average a number of 20.95. Among the participants, apart from 40 people (21.74%) refusing to give information on their age, the female respondents account for 33.15% while the male students constitute 45.11%.

Table 1: The survey participants classification

No	Categories	No of respondents	%
1	Gender		
1.1	Male	83	45.11
1.2	Female	61	33.15
1.3	Not answer	40	21.74
2	Hometown		
2.1	Rural areas	96	52.17
2.2	Small towns	26	14.13
2.3	Class II cities	27	14.67
2.4	Class I and special cities	10	5.43
2.5	Not answer	25	13.59
	Total	184	100.00

The collected data was transcribed and analyzed using SPSS software and Excel. The research results are analyzed and discussed in the next sections.

3. INFLUENTIAL FACTORS TO SAFETY AND SECURITY RISKS: CATEGORIES AND LEVELS OF IMPACT TO STUDENT TENANTS

There are 13 factors (generated from the preliminary survey), coded from Factor_A to Factor_N, being investigated in the study to measure their impact on safety and security of the students in rentals properties (Table 2). There are several new factors emerged from the data, but their rates of happening are very low (less than 1%), therefore, they are not included to be analyzed in the study. The figures in Table 2 show the percentage of respondents who claimed that the factors have happened and brought safety/security risks to some or many of the respondents.

Table 2: Common influential factors to safety/security risks of student tenants

No	Factor Code	Influential Factors to Safety/Security Risks	Rate of happening
1	Factor_A	Structural quality and life of rental properties	7.10%
2	Factor_B	Security quality of rental properties (doors, windows, locks, roofs, security equipment provided, etc..)	18.00%
3	Factor_C	Equipment quality in rental properties	9.30%
4	Factor_D	Roommates/flatmates	9.30%
5	Factor_E	Tenants in surrounding rental properties	7.10%
6	Factor_F	Landlords	8.20%
7	Factor_G	People live surrounding the rental properties	6.00%

No	Factor Code	Influential Factors to Safety/Security Risks	Rate of happening
8	Factor_H	Properties' visitors	5.50%
9	Factor_I	Security issues in neighborhood areas	13.10%
10	Factor_K	Location of the properties	8.20%
11	Factor_L	Quality of surrounding buildings/construction works	4.90%
12	Factor_M	The construction of new construction works near the properties	3.90%
13	Factor_N	Natural environment	4.90%

Among the factors, Factor_B (security quality of rental properties) and Factor_I (security issues in neighborhood areas) are the ones to be considered as the most common factors to bring safety/security risk to student tenants with the rate of happening to the survey participants as 18.00% and 13.10% respectively. Other significant and commonly happened factors include Factor_F (landlords), Factor_K (location of the properties), Factor_C (equipment quality in rental properties) and Factor_D (roommates/flatmates). There is a surprise that the landlords have become a common influential factor negatively impacting safety and security issues of student tenants.

Each factor will also be measured its level of influence with three different scales: high impact (score 2), low impact (score 1), no impact (score 0). The average influential levels of each factor then are calculated and presented in Table 3.

Table 3: Impact levels of influential factors

No	Factor Code	No impact	Low Impact	High Impact	Average Impact Level
1	Factor_A	4.35%	35.35%	60.30%	1.56
2	Factor_B	1.10%	6.00%	92.90%	1.92
3	Factor_C	3.30%	44.30%	52.50%	1.49
4	Factor_D	9.20%	32.60%	58.20%	1.49
5	Factor_E	5.45%	49.20%	45.35%	1.40
6	Factor_F	12.60%	40.40%	47.00%	1.34
7	Factor_G	6.60%	54.10%	39.30%	1.33
8	Factor_H	12.50%	53.10%	34.40%	1.22
9	Factor_I	2.20%	12.50%	85.30%	1.83
10	Factor_K	2.70%	40.80%	56.50%	1.54
11	Factor_L	24.00%	54.10%	21.90%	0.98
12	Factor_M	26.25%	55.75%	18.00%	0.92
13	Factor_N	10.90%	47.00%	42.10%	1.31

According to Table 3, most of the influential factors (11 out of 13) are considered as having low to high impacts to the student tenants. Factor_B and Factor_I, the most commonly influential factors are also the ones that have greatest impact with the average impact level of 1.92 and 1.83 respectively. What the survey respondents have experienced with these factors may explain this result, since people tend to judge things more seriously based on their own experiences than prediction. Factor_A, Factor_K are the other two that come into the top five. Factor_L (quality of surrounding buildings/construction works) and Factor_M (the construction of new construction works near the properties) are the ones with the lowest average impact level, of only 0.98 and 0.92 respectively. Though more than 50% of the respondents have considered those factors as having low impact on their safety/security risks, a certain percentage of them do not consider these factors as having high impact, therefore, the factors generally become having very low impact on student tenants' safety and security. The fact that the least number of respondents having experienced consequences of these factors (rate of commonly happening ranked 12^{th} and 13^{th} in Table 2) can explain this research outcome.

Being ranked with the 6^{th} position in Table 2 in terms of rate of commonly happening, Factor_A (structural quality and life of rental properties) jumps up to position 3 in terms of average impact level, passing Factor_C (equipment quality in rental properties), Factor_D (roommates/flatmates), Factor_F (landlords) and Factor_K (location of the properties). "Structural quality and life of rental properties", therefore, is considered as having high impact to student tenants' safety/security risks. "Location of the properties", with average impact level of 1.54, has become the fourth factor harming badly to the survey participants. With the average impact levels ranging from 1.49 down to 1.22, "equipment quality in rental properties", "roommates/flatmates", "tenants in surrounding rental properties", "landlords", "people live surrounding the rental properties", "natural environment" and "properties' visitors" are considered as having average impact on tenants' safety and security. "Equipment quality in rental properties" and "roommates/flatmates", which have both brought safety/security issues to 9.3% of the respondents, have been thought generating comparably high safety impact to the students. The "landlords", then "tenants in surrounding rental properties", as 8.2% and 7.1% respondents have had issues with (see Table 2), are still considered as creating average impact on student tenants' safety/security risk (average impact level 1.34 and 1.40 respectively) .

Taking the past figures of rate of happening as the probability of occurrence for each influential factor to safety/security risks, expected risk level then are calculated and presented in Table 4. Figures in Table 4 are sorted in the descending order of risk levels. Seven factors (Factor_B, Factor_I, Factor_C, Factor_D, Factor_K, Factor_A, Factor_F) have highest risk level, more than 10%. These are the ones which need paying attention to when examining the student rental accommodation. Among them, "security quality of rental properties" and "security issues in neighborhood areas" (Factor_B and Factor_I) are the ones that need to be managed properly due to their substantial high risk levels.

Table 4: Risk levels analysis

No	Factor Code	Probability of occurrence	Average Impact	Risk Level
1	Factor_B	18.00%	1.92	34.52%
2	Factor_I	13.10%	1.83	23.99%

No	Factor Code	Probability of occurrence	Average Impact	Risk Level
3	Factor_C	9.30%	1.49	13.87%
4	Factor_D	9.30%	1.49	13.86%
5	Factor_K	8.20%	1.54	12.61%
6	Factor_A	7.10%	1.56	11.07%
7	Factor_F	8.20%	1.34	11.02%
8	Factor_E	7.10%	1.40	9.93%
9	Factor_G	6.00%	1.33	7.96%
10	Factor_H	5.50%	1.22	6.70%
11	Factor_N	4.90%	1.31	6.43%
12	Factor_L	4.90%	0.98	4.80%
13	Factor_M	3.90%	0.92	3.58%

4. CRITERIA FOR STUDENTS' RENTAL ACCOMMODATION CHOICE AND THE LEVEL OF IMPORTANCE OF SAFETY/SECURITY RISK FACTORS TO THE RENTAL DECISION-MAKING

4.1 Criteria for rental accommodation choice of students in Hanoi

The survey respondents were asked for factors that can influence their rental choice. Seventeen factors have emerged from the survey results as significant criteria for accommodation choice of student tenants in Hanoi (Table 5). There are still several criteria being mentioned by a couple of respondents, yet due to the low rate of emergence (less than 5%), they are excluded from the analysis. There is a surprise that "living with friends/beloved people" is considered as one of the top five important factors by only 22.28% of the respondents, having the lowest rank in the Table. Among those seventeen criteria, there are 10 factors having rate of being mentioned from 50% upward. The results show that, rent is the most significant perceived factor, as being considered by 99.42% of the survey participants as one of the important factors (out of the total number of respondents who answered the relevant question, not including the ones who have refused). For more details, the survey participants have a tendency to look for a property with monthly rental price of under 1,600,000 VND (~76 USD) with approximately 18m2 area. In order to minimize the rent, 83.7% of interviewees choose to share the house with other students. Individual rent, therefore is estimated averagely at 839,505 VND (~40 USD) per person per month. In addition, not many landlords in Hanoi require tenants to pay a deposit or they require only the a minimum deposit of about 600,000 VND, less than a monthly rent.

The next significant factors include "distance to university/college" (Criterion_B), "quality of the property" (Criterion_E), "safety and security issues in the rental properties" (Criterion_R) and "rental area" (Criterion_D). A percentage of 81.87 % of the respondents considered "distance to university/college" as a criterion for rental choice. This is reasonable because students commute mainly by bus and bike. Moreover, because of frequent traffic congestion in capital, tenants want a property in the proximity of the school. "Quality of the property" aspect is also used by 81.87% of the survey participants when choosing a place to rent while 76.02% of them chose to take into account the “rental area”. That sharing a rental property can help tenants to save money means they have to accept smaller area. According to the data, in average, every 2.44 tenant shares a rental property which is 21.65 m2 in area. Therefore, each student haves a limited area of 9.56 m2 for accommodation. Besides “rent”, “quality of the property” and “distance to university/college”, “safety and security issues in the rental properties” is agreed by 81.29% of the respondents who replied to the relevant question as an important factor to be used for rental decision. It is noted that this factor, safety and security issues in the rental properties, belongs to the top five factors that have greatest rate of being considered as important criteria to accommodation choice of student tenants in the research.

Table 5: The criteria for accommodation choice

No	**Criterion Code**	**Accommodation Choice Criteria**	**Rate of being considered as an important criterion**
1	Criterion_A	Rent	99.42%
2	Criterion_B	Distance to university/college	81.87%
3	Criterion_C	Availability of commuting means	56.73%
4	Criterion_D	Rental area	76.02%
5	Criterion_E	Quality of the property	81.87%
6	Criterion_F	Property equipped facilities (equipment, internet access, TV license, etc…)	67.84%
7	Criterion_G	Property regulation level of strict	53.80%
8	Criterion_H	Landlord’s sharing flat	49.71%
9	Criterion_I	Availability and quality of kitchen, WC etc.,	64.33%
10	Criterion_K	Sharing room with others	40.35%
11	Criterion_L	Rate of power cut-off	45.03%
12	Criterion_M	Water supply	50.88%
13	Criterion_N	Tenants in surrounding rental properties	46.20%
14	Criterion_O	People live surrounding the rental properties	33.92%
15	Criterion_P	Surrounding natural environment	36.84%
16	Criterion_Q	Living with friends/beloved people	23.98%
17	Criterion_R	Safety and security issues in the rental properties	81.29%

In terms of the weights that respondents gave to each criterion, it is observed that they have a very wide range. Table 6 shows the maximum value of the weights recorded from the survey for each criterion in terms of contribution to the accommodation decision and their mean values. Data in Table 5 reveals that there is no criterion being considered as important by all of the respondents, even rent (one person did not choose rent as an criterion for his/her accommodation decision). Yet rent is still considered as the most influential factor to the respondents' accommodation decision with the maximum weight of 80% and a mean value of 31.13%, comparably greater than other factors (Table 6). "Safety and security issues in the rental properties" is the next great contributor to accommodation decision with the maximum weight recorded of 50% and a mean value of 12.08%. "Living with friends/beloved people" seems to vary a lot, with the maximum weight noted of 50% but the mean value is only 1.66%. This figure shows different points of view of students in their choices for accommodation.

Table 6: The criteria's weights to accommodation decision

No	Criterion Code	Maximum weight	Mean of weight
1	Criterion_A	80%	31.13%
2	Criterion_B	30%	7.59%
3	Criterion_C	30%	3.62%
4	Criterion_D	30%	6.40%
5	Criterion_E	35%	9.55%
6	Criterion_F	30%	4.33%
7	Criterion_G	40%	3.30%
8	Criterion_H	25%	2.90%
9	Criterion_I	30%	5.67%
10	Criterion_K	30%	2.27%
11	Criterion_L	10%	2.22%
12	Criterion_M	15%	2.79%
13	Criterion_N	20%	2.04%
14	Criterion_O	10%	0.97%
15	Criterion_P	50%	1.66%
16	Criterion_Q	30%	1.48%
17	Criterion_R	50%	12.08%
	Total		100.00%

4.2 Factors that bring safety/security risks to student tenants and their level of importance to accommodation choice

It is noted that besides "safety and security issues in the rental properties", there are a lot of factors that can bring in safety/security risks to student tenants appearing as criteria to accommodation choice of the survey participants, such as "quality of the property", "landlords' sharing flat", "tenants in surrounding rental properties", "people live surrounding the rental properties", "surrounding natural environment" etc., with significant percentage of the respondents considered them as important. Table 7 looks into this further by list out the aspects of safety/security risks (see Table 2 for the description of each factor code) in terms of their importance to accommodation choice. Respondents were asked to choose their own list of top five important factors to their rental choice. Scores are given to the factors with 5 for the most important and 1 for the least important factor. The average level of importance for each factor then is calculated by taking the mean of their importance scores.

Table 7: The safety/security risk factors in terms of level of importance to accommodation choice

No	Factor Code	Frequency to be included in top five important factors	Average level of importance
1	Factor_A	58.64%	2.01
2	Factor_B	89.51%	3.55
3	Factor_C	40.74%	1.09
4	Factor_D	35.19%	1.02
5	Factor_E	43.83%	1.32
6	Factor_F	27.78%	0.65
7	Factor_G	26.54%	0.54
8	Factor_H	22.22%	0.50
9	Factor_I	71.60%	2.56
10	Factor_K	39.51%	0.94
11	Factor_L	5.56%	0.09
12	Factor_M	9.88%	0.19
13	Factor_N	22.84%	0.41

According to the data, the top five most mentioned factors include Factor_B (security quality of rental properties), Factor_I (security issues in neighborhood areas), Factor _A (structural quality and life of rental properties), Factor_E (tenants in surrounding rental properties) and Factor_C (equipment quality in rental properties). These also are the ones which have greatest average level of importance accordingly. Among them, "security quality of rental properties" (Factor_B) and "security issues in neighborhood areas" (Factor_I) become the most important factors which have average level of importance to the rental choice of more than 2.5/5. This has confirmed their high level of impact as discussed in Section 3. Again, Factor_L (quality of surrounding buildings/construction works) and Factor_M (the construction of new construction works near the properties) which are with the lowest average impact level (Table 3), have lowest frequency to be included in the top five important factors as well as the average level of importance. The results show a consistency in the data collected from the survey.

4.3 Trade-off between bearing safety/security risks and selected accommodation choice criteria

A certain percentage of 80.8% of the respondents who replied to a relevant questions in the questionnaire do not choose a location with more safety/security risks to have a lower rent. Other 33 people (19.2%) may consider the trade-off but only with a substantial reduction in rent (33.5%). In terms of leveraging the distance to university/college and safety/security risk, there are 108 out of 173 survey participants (62.4%) refusing to live in low-security areas in proximity of their university/college whereas the others accept. Though a limited number of them (less than 25%) did not consider living with friend/beloved people as very important, 56.40% of 172 people who have responded to the relevant questions may accept a trade-off between bearing more safety/security risks and living with friend/beloved people, 15.12% of them will definitely accept and only 28.49% of them refuse the trade-off.

5. CONCLUSIONS AND RECOMMENDATIONS

Looking into the safety/security risk issues of student rentals in Hanoi under the tenants' perspective, this research has found out that there are thirteen factors that can significantly bring risks to the tenants' life in rental accommodation. Seventeen criteria have been selected by the respondents as important factors influencing their rental accommodation choice. The top six mostly happened influential factors to safety/security risks include "Security quality of rental properties", "Security issues in neighborhood areas", "Equipment quality in rental properties", "Roommates/flatmates", "Location of the properties" and "Landlords" (the last two have the same rate of happening). The top six with highest average impact level are "Security quality of rental properties", "Security issues in neighborhood areas", "Structural quality and life of rental properties", "Location of the properties", "Equipment quality in rental properties" and "Roommates/flatmates" (again, the last two have the same figures). With both greatest impact level and occurrence probability, "security quality of rental properties" and "security issues in neighborhood areas" become the highest risks for tenants as students. "Location of the properties" and "Roommates/flatmates" are the next ones with both great impact level and frequency of happening. This implies that the student tenants need to pay most attention to those issues in order to reduce and manage properly their safety/security risks. The landlords also need to care about those issues to attract and protect their tenants.

Regarding the criteria for rental accommodation choice, besides "rent", "quality of the property" and "distance to university/college ", "safety and security issues in the rental properties" goes in the top five aspects that have been considered as important to accommodation choice. It is noted that there are a lot of criteria that can bring in safety/security risks to student tenants appearing as criteria to accommodation choice of the survey participants. All of these criteria, when being analyzed under the influential factors to safety/security risks, have contributed to the importance of safety/security risks consideration in student rental accommodation choice. Again, "security quality of rental properties" and "security issues in neighborhood areas" become the most important factors which have greatest average level of importance to the rental choice. In addition, students do not care much about trade-off between bearing safety/security risks and selected accommodation choice criteria.

This paper adds in the need of raising attention from the landlords, the tenants and even the government authorities in providing safe and sustainable accommodation to student tenants in order to have their contribution to the development of this rental market as well as the sustainable development of this type of urban citizens.

REFERENCES

Phan Duong, 2009. *Land for universities in Hanoi: too limited.* Vietnam Economy

Students from NEU, 2006. *Student research report: student rentals: practice and solutions.* Hanoi, NEU.

Tsunami evacuation facilities in the damaged areas due to the Great East Japan Earthquake: before and after

Osamu MURAO
Professor, International Research Institute of Disaster Science
Tohoku University, Japan
murao@irides.tohoku.ac.jp

ABSTRACT

Vertical evacuation is a very critical countermeasure to prevent damage to residents in tsunami-prone areas from devastating tsunami. There are two types of tsunami evacuation facilities; tsunami evacuation buildings and towers. How they are used will be a very significant matter in tsunami-prone low-lying areas to reduce tsunami casualties in the future. This paper reports those construction conditions in the damaged areas due to the Great East Japan Earthquake and Tsunami as of March 2011, and how they were used just after the occurrence of tsunamis. It also presents the recent construction situation and tsunami evacuation strategies through the recovery process after the event. The key findings of the research are as follows: (1) there were 111 tsunami evacuation buildings and no tower in the damaged areas as of March 2011, (2) the number of buildings and towers became 255 and 4 respectively, and (3) construction situations vary with the damage and recovery conditions. Problems and recommendations should be shared among every coastal district in Japan.

Keywords: 2011 Great East Japan Earthquake and Tsunami, tsunami evacuation building, tsunami evacuation tower, vertical evacuation, urban recovery

1. INTRODUCTION

The great earthquake on March 11, 2011 caused great tsunamis to the coastal areas in Tohoku Region in Japan. The death toll by the event, mainly by the tsunamis, went up to 18,493, but some victims might have survived the tsunamis if those areas had adopted proper evacuation system according to geographic characteristics. This paper explains the meaning of vertical evacuation system, which mainly employs tsunami evacuation construction, and its background in Japan at first. Then it reports how many tsunami evacuation facilities existed and how they worked in the affected coastal areas, Aomori, Iwate, Miyagi, Fukushima, Ibaraki, and Chiba, when the tsunamis hit. Finally it refers to how they have been increasing since 2011 and examines regional differences of those situations.

2. BACKGROUND OF TSUNAMI DISASTER REDUCTION STRATEGIES WITH EVACUATION CONSTRUCTION IN JAPAN

2.1 Vertical evacuation

There are two types of evacuation from tsunami; horizontal and vertical evacuation. NOAA et.al (2001) define them in "Designing for Tsunamis" as follows:

- horizontal evacuation—moving people to more distant locations or higher ground.
- vertical evacuation—moving people to higher floors in buildings.

2.2 Vertical evacuation

Tsunami evacuation strategies should correspond to each geographical condition and land use regulation. Vertical evacuation systems are necessary for immediate escape in low-lying areas such as Sendai or Natori in Sendai Plain. There are basically two types of vertical evacuation facilities as shown in Figure 1; tsunami evacuation buildings and tsunami evacuation tower.

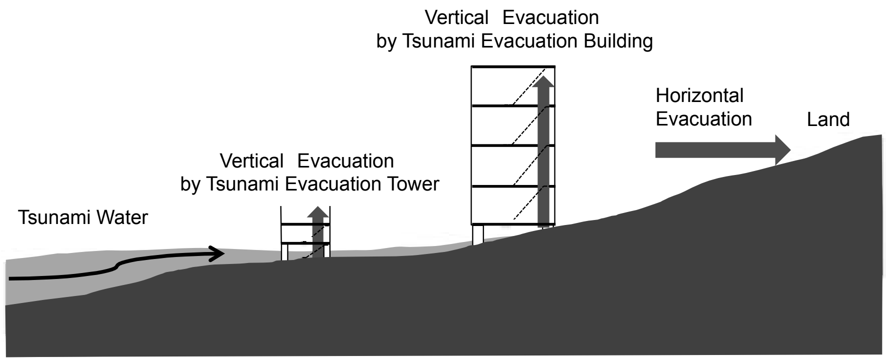

Figure 1: Horizontal evacuation and two types of vertical evacuation

People can escape from coming tsunami into any kind of buildings if it is stronger and higher than the tsunami. However, some of them might be inappropriate to be designated in advance because of lack of space or privacy in daily life. Then local governments usually designate appropriate buildings as "designated tsunami evacuation building" according to estimated tsunami height, building structural type and the number of stories in Japan. It may be an high-rise apartment, an elementary school, a hospital, or a government office building. Figure 2 shows a designated tsunami evacuation building in Fujisawa City, Kanagawa Prefecture.

On the other hand, tsunami evacuation tower is the one constructed by a local government in order to save people in the tsunami high-risk districts. This kind of structure tends to be located in the low-lying areas, where finding existing proper buildings for vertical evacuation is difficult. Figure 3 shows tsunami evacuation towers in Fujisawa City, Kanagawa Prefecture, and Kushimoto, Wakayama Prefecture.

Figure 2: Designated tsunami evacuation building in Fujisawa, Kanagawa

(a) in Fujisawa, Kanagawa (b) in Kushimoto, Wakayama

Figure 3: Tsunami evacuation towers

2.3 Tsunami Disaster Reduction Strategies in Japan

We Japanese people, living in the earthquake-prone country surrounded by ocean, have experienced huge tsunamis since ancient times. The first systematic tsunami disaster strategy in the 20th century was shown in "*Advisory Report for Tsunami Disaster Prevention*" by Council for Earthquake Disaster Prevention (1933). It contains relocation to higher land, seawall, tsunami control forest, piers, building regulation, buffer zone, evacuation route, warning system, and commemoration project. This triggered construction of piers and tsunami control forest in some places.

Tsunami disaster reduction strategies were actively examined after World War II. The tsunami forecast started in the 1950s. The construction for tsunami mitigation such as levees or seawalls was accelerated after the 1960 Chilean Tsunami. In the 1970s, disaster reduction human activities began: tsunami inundation maps were made, tsunami information system was established, and tsunami education activities were carried out. Although the vertical evacuation strategies were not widely employed in the 1980s, Fujisawa City started to conclude MOU for "designated tsunami evacuation buildings" with about fifty private buildings.

In the 1990s, the needs of comprehensive disaster management arose socially, and "*Guideline to Strengthen Tsunami Disaster Management in Local Plan for Disaster Prevention*" was released (National Land Agency et al., 1997). This

contained basic ideas, basic policy, and planning process for tsunami disaster management based on Japanese experience. It refers to tsunami evacuation building utilization, but it is not as a comprehensive vertical evacuation system.
The Great Kobe Earthquake was the most devastating urban disaster that hit modernized cities in the 20th century, and it influenced future disaster management in many fields. One of the remarkable evolutions could be seen in the spatial information technology. The spread of Geographic Information System affected the disaster management field, and it changed the way of making hazard maps in community level. Then Cabinet Office (CAO), et al. (2004) published "*Tsunami and Tidal Wave Hazard Map Making Manual*" for coastal areas. "*Guideline for Management of Tsunami Evacuation Buildings*," which enlarges on tsunami evacuation building management, was released by CAO (2005) next year.
Since then, the local governments facing the Pacific Ocean in East Japan had prepared tsunami evacuation facilities as well as those in West Japan. However, the huge tsunamis caused by the Great East Japan Earthquake attacked those coastal areas.

3. SITUATION OF TSUNAMI EVACUATION CONSTRUCTION AS OF MARCH 2011

3.1 Interview

In order to compile information of the tsunami evacuation construction situation in the damaged areas as of March 2011 and August 2013, telephone interviews with the local governments were conducted as follows:

Date: August 6-19, 2013
Interviewees: 70 local governments located in front of the Pacific Ocean in Aomori, Iwate, Miyagi, Fukushima, Ibaraki, and Chiba Prefecture
Questions:

1. the number of tsunami evacuation facilities as of March 2011
2. what happened concerning tsunami evacuation facilities
3. the number of tsunami evacuation facilities as of August 2013
4. problems they faced

3.2 The number of tsunami evacuation facilities as of March 2011

As a result of the interviews, the number of tsunami evacuation facilities, buildings and towers, as of March 2011 and August 2013 in terms of prefecture is shown in Table 1. The situation as of March 2011 is examined in this chapter.
There was no tower in the seven prefectures in those days. On the other hand, there were 111 tsunami evacuation buildings in the damaged prefectures except Fukushima and Ibaraki. The most buildings, sixty two, existed in Chiba followed by Miyagi with 45. There were only two buildings in Aomori and Iwate respectively.

Table 1: The number of tsunami evacuation facilities as of March 2011 and August 2013 in terms of prefecture

Prefecture	Tsunami Evacuation Buildings		Tsunami Evacuation Towers	
	March 2011	August 2013	March 2011	August 2013
Aomori	2	20	0	0
Iwate	2	1	0	0
Miyagi	45	29	0	1
Fukushima	0	0	0	0
Ibaraki	0	28	0	0
Chiba	62	177	0	3
Total	111	255	0	4

Table 2 demonstrates the number of tsunami evacuation buildings as of March 2011 and August 2013 in terms of local governments, and future challenges. The municipalities with no building is not included in the table.
Focusing on the number of local governments that had the buildings, Chiba prefecture had ten followed by Miyagi with eight. Aomori and Iwate had only one.
As for the number of buildings in each local government, the most buildings, 22, were in Shirako Town, followed by 18 in Tateyama City, in a few damaged Chiba Prefecture. In the devastated Tohoku prefectures, there were 15 buildings in Kesen-numa City and 12 buildings in Tagajo City.

3.3 Evacuation situation just after the tsunamis on March 11, 2011

Most buildings were helpfully used more or less after the event according to the survey. Especially in severely damaged Kesen-numa, Minami-Sanriku, Shiogama, Tagajo, hundreds or thousands of people escaped to the buildings and survived. It means that most existing designated tsunami evacuation buildings functioned as expected.
On the other hand, some buildings did not work for survival because of destruction. One building was washed away in Sendai, and another building was not high enough to save people from the huge tsunami in Natori.
The damage situation was not critical from the viewpoint of evacuation in Chiba, but the data indicates many buildings usefully worked for the affected people. One good practice was the fact that the usual evacuation drill they had carried out was effective to escape in Yokoshiba-hikari.

4. SITUATION OF TSUNAMI EVACUATION CONSTRUCTION AS OF AUGUST 2013

Each local government has increased the number of tsunami evacuation facilities in water front areas since the earthquake, but there are differences depending on their recovery process or geological situation. Hereafter, recent construction situation will be discussed based on the acquired information by the interviews.

Table 2: The number of tsunami evacuation buildings as of March 2011 and August 2013 in terms of local governments, and future challenges

Prefecture	Municipality	Mar-11	Aug-13	Policies and Challenges on Tsunami Evacuation Facilities
Aomori	Hachinohe	2	20	Some Tsunami Evacuation Buildings were newly designated, based on the maximum Tsunami inundation map published by Aomori Prefecture, in October.
Iwate	Hirono	0	1	No new plan to designate due to the lack of tall buildings along the shore.
	Kamaishi	2	0	Prioritize alerting the residents higher ground evacuation over evacuating to Tsunami Evacuation Buildings. Designation of 2 buildings was removed after the disaster.
Miyagi	Kesen-numa	15	2	In the area where people have difficulty in evacuation, Tsunami Evacuation Buildings are planned to be a solution. When the disaster occurred, the evacuees at the Tsunami Evacuation Buildings couldn't get out of the buildings due to the fire that broke out.
	Minami-sanriku	4	0	Higher ground evacuation is more acknowledged than evacuation facilities. It was better if there were stocks and generators at the Evacuation Buildings when the disaster occurred.
	Ishinomaki	3	4	On Tsunami Evacuation Buildings, there are restrictions because of the use of private facilities. To secure enough land and funds is a challenge to build towers. Deal with the specific issues as the reconstruction goes.
	Higashi-matsushima	2	0	Overall evacuation plans are being reconsidered. The designation of the Tsunami Evacuation Buildings was removed due to the damage the buildings got. The use of private facilities are under consideration, including new designations. One of the concerns is if the construction of seawalls will go smoothly.
	Shiogama	4	4	More Tsunami Evacuation Buildings are planned to be constructed since there isn't enough.
	Tagajo	12	16	More designation is planned because of the lack of Tsunami Evacuation Buildings. When the disaster occurred, supply/food stocks weren't enough in these buildings.
	Sendai	2	1	Both of the buildings and towers are needed to be designated/constructed as soon as possible because of the lack of these facilities.
	Natori	3	2	Today, community planning toward reconstruction is progressing, which is related to Tsunami evacuation planning. The current designated Tsunami Evacuation buildings, an elementary school and junior high school, will be broken down.
Ibaraki	Kamisu	0	28	Because of the low land overall, the city proactively call for designation to private companies, and also there were offers to designate from private businesses. The city has 40 more places available for evacuation except the private facilities.
Chiba	Choshi	0	8	If there are facilities willing to be designated, more Tsunami Evacuation Buildings are essential. Communicating information smoothly is a key.
	Asahi	1	8	Response to the residents after evacuating to Tsunami Evacuation Buildings need to be considered.
	Yokoshibahikari	4	4	Some issues need to be solved: ways of guiding evacuees in the case of Tsunami occurrence at night or on holidays, or securing electricity. To raise residents' awareness of evacuation is essential.
	Sanmu	1	5	No plan to designate more buildings. All the tall buildings on the coast were already designated. Stairs are planned to be built attached to 2 schools by the coast for rooftop evacuation. Disaster drills are carried out after the Tsunami.
	Kujukuri	0	5	Had been collecting the basic data. Evacuation procedures will be reconsidered. Plans on concluding an agreement on temporary staffing upon disaster occurrence.
	Oamishirasato	0	4	One of the current designated Tsunami Evacuation Buildings were under discussion when the earthquake hit. Plans on new buildings or towers are on hold since the predicted flood map published by Chiba Prefecture doesn't meet the policy of Ministry of Land, Infrastructure, Transport and Tourism.
	Shirako	22	29	Buildings under construction in the coastal area. Evacuation procedures, including evacuee guidance and evacuation by cars through narrow streets, will be considered.
	Ichinomiya	5	9	No tall buildings in the coastal area, which needs to be improved. Designation of Tsunami evacuation routes is considered. The downside of the designation is it may cause traffic issues on those routs due to a small number of primary roads that goes from the east to the west.
	Isumi	1	4	Problems such as ensuring lands for tower constructions and evacuation roads need to be solved. The priority of the measures is discussed with the residents.
	Onjuku	0	7	Make the use of 7 currently designated Tsunami Evacuation Buildings.
	Katsuura	0	10	Comprehensive evacuation measures need to be considered, including all types of temporal evacuation facilities.
	Kamogawa	1	44	Disaster drills are carried out in the area with not enough land for building Tsunami evacuation facilities. Chiba Prefecture announced the prediction on Tsunami; about 8 meter high Tsunami would reach Tateyama area in 8-10minutes. Based on the prediction, a goal has been set to evacuate to sites with 10 meters above sea level or higher in 10 minutes. In order to raise awareness of evacuation in the daily life, each municipality is putting up sea-level signs (240 signs up in total.)
	Minamiboso	9	22	Finished designation of Tsunami Evacuation Buildings in the city. Planning on designating a Children's Center on higher ground. Measures for big crowds, such as firework events, need to be considered.
	Tateyama	18	18	Each region are holding disaster drills to escape to higher ground than the predicted Tsunami height.
	Total	111	255	

4.1 The number of tsunami evacuation facilities as of August 2013

Table 1 also shows the change of the number of tsunami evacuation facilities between March 2011 and August 2013. The total number of buildings became 255 from 111, which means more than double. Regarding to each prefecture, the number of buildings increased by 18 to 20 in Aomori, by 28 from 0 in Ibaraki, and by 115 to 177 in Chiba; the number decreased by 1 from 2 in Iwate, and by 16 to 29 in Miyagi. In Fukushima remains 0.
As for tsunami evacuation towers, the total number was quite small: one tower was constructed in Miyagi, and three in Chiba.

4.2 Problems and future challenges of tsunami evacuation facilities

Table 2 includes the policies and challenges on tsunami evacuation facilities clarified by the interviews. Because the tendency of the construction and current policy with regard to tsunami evacuation system depends on the circumstances around each district and its recovery plan related to the damage level, this session examines the problems and future challenges prefecture by prefecture.
Municipalities in Fukushima do not have concrete vision on the evacuation facilities because of the difficulty of making recovery plans due to the Fukushima Daiichi nuclear disaster.
In Iwate, there were only two designated evacuation buildings in Kamaishi, but both were cancelled after the event because of the inundation and destruction by the tsunami. Although Hirono Town designated one building, the others did not have a plan to have evacuation buildings yet in near future. It is probably because of the rias geography surrounded by mountains.
Miyagi has Sendai Plain in the south, and this geographic characteristic differentiates its construction situation from Iwate’s. Southern local governments, Matsushima, Shiogama, Tagajo, Sendai had already increased or planned to have tsunami evacuation facilities. However, we can see some similarities to Iwate. They cannot discuss concrete evacuation plans in Kesen-numa, Minami Sanriku, Higashi Matsushima, and Natori City until the new districts are designed concretely.
Following above three prefectures in Tohoku Region, the cities in Ibaraki were also severely damaged. However the damage level was less than those in Tohoku, so their most concern is not the recovery from washed-away districts but improvement of the existing districts. According to Table 2, Hitachinaka and Oarai are focusing on the evacuation to higher lands, and Kamisu City, located on low-lying ground, had already designated 28 tsunami evacuation buildings since 2011.
Damage to the districts by the tsunami in Aomori and Chiba was not significant. However, the construction situation is different. The number of existing tsunami buildings as of March 2011 was only two in Aomori, but it became 18 in August 2013.
Chiba Prefecture had the biggest number of buildings among the objective prefectures. In addition to them, they constructed 115 buildings by August 2013. The active situation may be related to its dense location, close to Tokyo, and geographical condition by the long coast of Kujukuri Beach.

5. CONCLUSION

This paper reports the construction situation of tsunami evacuation buildings and towers in the damaged areas due to the Great East Japan Earthquake and Tsunami as of March 2011, and how they were used just after the occurrence of the tsunamis. It also presents the recent construction situation and tsunami evacuation strategies through the recovery process after the event. The key findings of the research are as follows: (1) there were 111 tsunami evacuation buildings and no tower in the damaged areas as of March 2011, (2) the number of buildings and towers became 255 and 4 respectively, and (3) construction situations vary with the damage and recovery conditions. Problems and recommendations should be shared among every coastal district in Japan.

ACKNOWLEDGEMENTS

This work was supported by the Japan Society for the Promotion of Science (JSPS) through the Grants-in-Aid for Scientific Research No. 25242036 "Resilience of the Urban Recovery System after the 2011 Great East Japan Earthquake and Regional Vulnerability Assessment to Tsunami" and No. 23404019 "Examination of Urban Recovery Plans after the 2004 Indian Ocean Tsunami and Urban Risk Evaluation of Tsunami in Asia Influenced by Global Warming," and by the Organization for Promoting Urban Development Research Grant 2012-2013 "Proposition of Tsunami Evacuation Plan in Katase District in Fujisawa City."

REFERENCES

Council for Earthquake Disaster Prevention, 1933. *Advisory Report for Tsunami Disaster Prevention*. (in Japanese)

Cabinet Office, Government of Japan (CAO), et al., 2004. *Tsunami and Tidal Wave Hazard Map Making Manual* (in Japanese)

Cabinet Office, Government of Japan (CAO), 2005. *Guideline for Management of Tsunami Evacuation Buildings* (in Japanese)

National Land Agency et al., 1997. *Guideline to Strengthen Tsunami Disaster Management in Local Plan for Disaster Prevention*. (in Japanese)

NOAA, USGS, FEMA, NSF, Alaska, California, Hawaii, Oregon, and Washington, 2001. *Designing for Tsunamis Seven Principles for Planning and Designing for Tsunami Hazard*, http://nthmp-history.pmel.noaa.gov/Designing_for_Tsunamis.pdf.

A new parking concept for a living quarter in Hanoi

Quang Minh NGUYEN
PhD, Faculty of Architecture and Urban Planning,
National University of Civil Engineering, Vietnam
ktsquangminh@yahoo.com

ABSTRACT

Parking systems form an integral part of any urban infrastructure, especially in such a mega-city with a very high building density and huge number of private vehicles as Hanoi. Parking has now become an urgent issue as the capital city continues to expand, the number of cars and motorbikes keeps on increasing quickly and many residents have to drive kilometers away to park and spend half an hour or more walking home which is of course not so convenient. In most residential areas, there is an intersection (and also a conflict) between motorized and non-motorized traffic flows. In view of traffic safety, this problem must be solved as soon as possible. The fine concept car-free settlement has been developed in several European towns. Among them, Vauban (Freiburg - Germany) may be the best example and thus selected as a case study. The most important factors for success from this pilot project as well as the applicability to Hanoi are analyzed in the first part of the academic paper. The second part will then focus on the spatial re-organization of a typical living quarter in Hanoi on the basis of the periphery-and-core structure, in which the periphery can be used for parking along with commercial activities while the core will be reserved for walking and cycling only, instead of the mixed zone quarter as often seen nowadays. This new paradigm will ensure a much better living quality and contribute to the long-awaited sustainable city development in the next few decades.

Keywords: *parking system, mixed zone, car-free settlement, periphery-and-core structure*

1. INTRODUCTION

An ecological settlement is usually regarded as a miniature of an ecological city. It is planned and built on certain eco-disciplines and encompasses a broad spectrum of solutions, ranging from traffic, townscape, energy, water, building material and construction technology, recycling of waste, etc. into details such as design of the room plans and structure of the building envelope. In addition, a number of social issues should be considered in order to achieve sustainability in full. A car-free living quarter is an outstanding (but also difficult) facet of this brand new concept.

In the world there have been many eco-towns developed at different levels of success over the past three decades, but very few of them succeeded in solving the traffic problems with private cars and motorbikes based on the three main criteria: safety, convenience and environment-friendliness. Most of the sustainable urban development projects just concentrated on public transport and fuel-saving cars without solving the problem to a further extent. In fact, in those places, car and motorbike areas are mixed with bicycle routes and pedestrian zones. No matter how well planned such a living quarter may be, the local people still feel that their daily lives are affected to a certain degree: either by noise or by exhaust gas, and even more seriously by traffic accidents that could suddenly happen to old people crossing the road or to children playing at the corner of the street if they do not pay due attention to the cars and motorbikes passing and even when their parents stay somewhere around them but do not keep an eye on them. In this circumstance, the city will no longer be a safe place for people to live in. When safety as the very first requirement and a basic condition cannot be fulfilled, sustainability will seem almost unreal.

Car-free concept does not mean living completely without cars or stopping using cars, because cars have become an integral part of a modern city and daily life to a certain number of people. On the contrary, people can still drive in the city but will not park near home. This notion today will lead to the development of a new car and motorbike parking concept in mega-cities tomorrow.

2. LESSONS FROM VAUBAN (FREIBURG, GERMANY)

Vauban is a new neighborhood in central Freiburg - a small town in the southwest of Germany - initially planned in the early 1990s on a 40-hectare site of a former barracks of the French army and built a few years later for about 4,800 inhabitants as a model residential area in terms of sustainability. In Vauban, solar energy is used and all houses as well as public buildings are constructed to low or ultra low energy standards, just like all the other ecological living quarters in Germany. However, Vauban became more successful and better known than the others for its car-free concept - a pilot project of its kind in Europe.

Vauban is very well connected to the center and the other parts of the city with one excellent public transport network which enables everyone to go anywhere in the 153 km^2 urban region within 20 minutes. Inside Vauban, transportation is primarily by bicycle and/or by foot. As of 2008, over 70% of the families in Vauban had no car, according to the statistics of the local authority (Vauban Project Management Board, 2008). The remaining householders would like to rent or sell their cars as quickly as possible, otherwise they have to pay 18,000 EUR per year for one family-owned car in the local garage or 3,500 EUR per year for car-sharing charged by the local authority as an obligatory fee (or tax) for the pollution that the residents' cars may cause. This fee is very high, of course, but adequate, since the environmental treatment costs in fact a great deal of money. The City Council of Freiburg has applied this policy in Vauban in order to make the community become aware of the great advantages of living in a much simpler, happier and healthier way without depending largely on private vehicles.

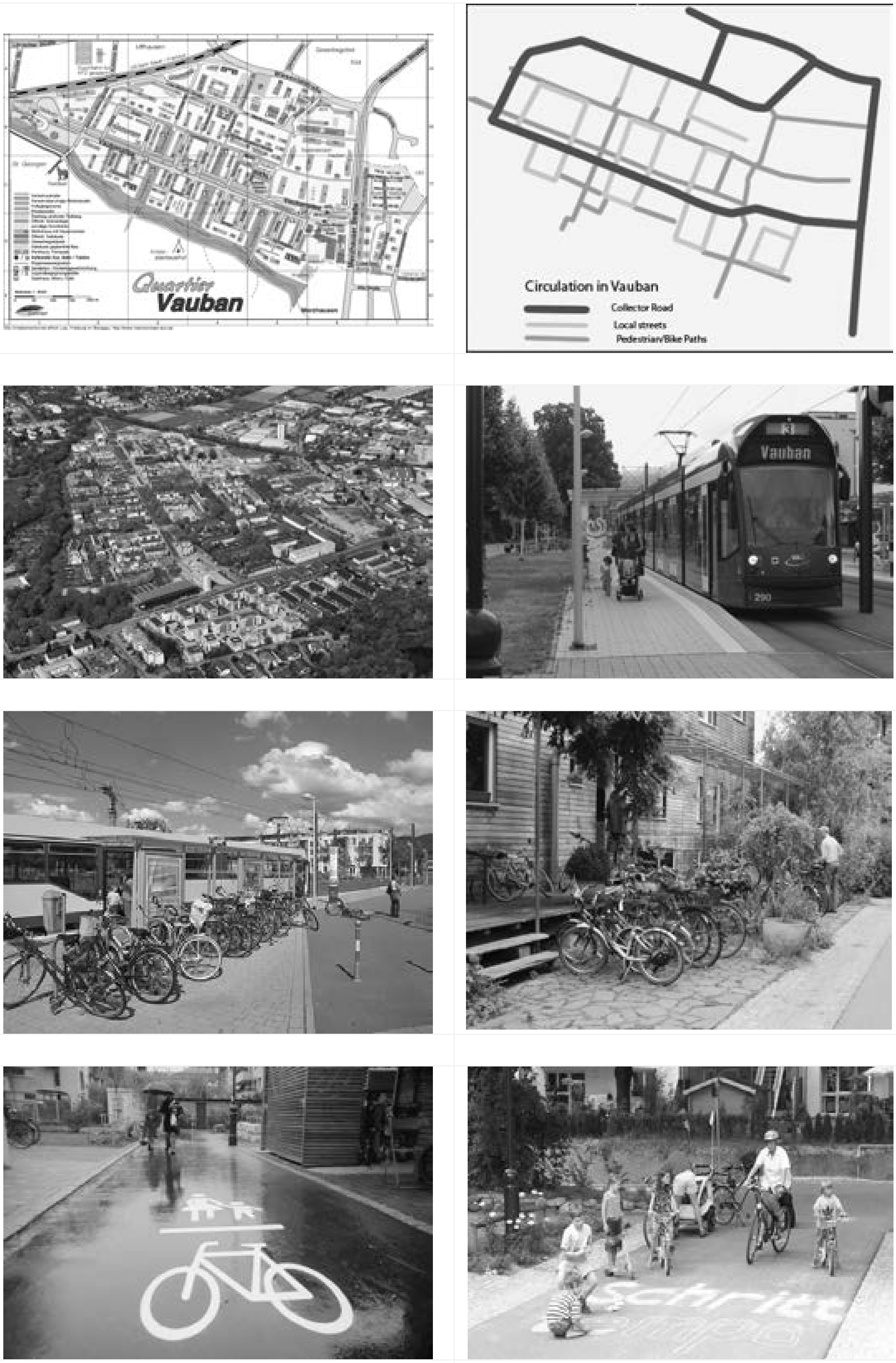

Figure 1: Vauban as the first car-free community in Germany where the residents feel happy and care-free with cycling and walking (Freiburg City Council, 2008)

The Vauban experience is based on simple but very effective solutions as follows:

- Developing an excellent public transport service for external circulation: two options (tram and bus), in operation 24/24 a day. It takes only five minutes to walk from home to the nearest tram or bus stop. There is one tram or one bus every ten minutes on an alternate basis. That means when one person misses a tram, he or she has to wait only five minutes for the forthcoming bus. Another good thing is that the ticket is all-in-one. Furthermore, the monthly ticket fare is very reasonable: 48 EUR for adults, 36 EUR for the old people as well as for students, and 18 EUR for children.
- Encouraging all the inhabitants to cycle and to walk within the neighborhood for a safe, clean and green environment by planning all daily and weekly services within a short walk from home and by charging car owners a very high parking fee. The local supermarket is located in the middle of one main road side to allow easy access for both cargo trucks and shopping-goers. Thus, the local people do not often have to go shopping anywhere else by car, as they can find and purchase almost everything they need near homes. The other public buildings and facilities are not far from home either, just five minutes' walk. With regard to the car parking fee for one four-member family with husband, wife and two children selected as a case study, they have to pay 18,000 EUR a year to own a car - equal to one third of the annual total income of a middle-class family - and several thousand EUR more for fuel, insurance and regular maintenance. As an alternative, car-sharing is more economical than car ownership but not so convenient, because it is possible that two or three families need to use that car at the same time. If people do not own a car, they will spend only (48 x 2 + 18 x 2) x 12 = 1,584 EUR a year on the public transport - a considerable expense-saving option that one must think about. After all, having no car is obviously the best choice and most of the Vauban householders have decided to change their past lifestyle of their own accord, from driving cars into using public transport means, cycling and walking.

3. BACK TO HANOI: WHY NOT CAR AND MOTORBIKE-FREE?

Since August 2008 Hanoi has become a mega-city in Asia in terms of both area (3,340 km^2) and population (6.7 million inhabitants as of 2012), according to the General Statistic Office. The inner city is extremely populous, 12,000 inhabitants per km^2 on average and 36,000 as the highest (Vietnams Press Agency, 2009). The number of cars has kept on increasing very fast over the past ten years while the urban infrastructure has not been properly upgraded. The road systems in Hanoi fail to support the huge number of private motorized vehicles: 370,000 cars and 3.7 million motorbikes (Vietnams Law Newspaper, 2013). As a consequence, traffic congestions occur frequently throughout the city, not only in rush hours, causing a lot of damage to the socio-economic development which cannot be easily estimated or exactly calculated. Hanoi's chaotic traffic situation is reported to frighten foreign tourists, even those who have come back here many times. This also accounts for the fact that Hanoi has never been ranked among the most livable cities in Asia and the capital city's development goals towards 2030 could hardly be achieved, unless a radical and comprehensive action is taken.

Figure 2: Traffic congestions in the early morning and in the late afternoon in Hanoi

Figure 3: 101 reasons for traffic jams in Hanoi: heavy rain and road reconstruction

Figure 4: Hanoi old street night market - an example of a pedestrian zone, but only at weekends, and the surrounding streets become parking areas

On a smaller scale, within a living quarter, many households have problems with parking. Only a few families have a garage (mostly for one car only) or sufficient places for two to three (or more) motorbikes. The others have to park their cars several kilometers away and walk home. Part of the sidewalk or the public courtyard, even the children’s playground, is occupied by day for parking purpose, because at home there is no room for motorbikes. Only at night are motorbikes kept indoors - often in the living room - which is of course troublesome. At certain times of the day, the traffic flow within the living quarter is heavy. Mixed together, motorized vehicles are likely to collide with one another or with bicyclists as well as with pedestrians.

To solve the problems, the city authority in collaboration with the department of urban planning and building tried to prevent accidents, regulate the traffic flows and reduce the traffic jams by broadening the roads and streets, building more footbridges or underground passages, adjusting work time between state-state and state-private organizations and rejecting new registration for cars and motorbikes, etc. But all these measures proved to be short-term or provisional actions and therefore may not be able to deal with the problems to the root.

Back to the success story of Vauban neighborhood, both solutions have already been considered and partially applied to Hanoi over the last few years, but they are not so well implemented in reality. For example: Bus is one of only two public transport options in Hanoi. Compared to taxi, the bus service is much cheaper: only 5,000 VND for a single trip in any direction within the city, while 12,000 to 15,000 VND per kilometer is charged for a taxi ride, the current exchange rate: 1 USD = 21,000 VND (VietcomBank, 2013). For this reason, bus still remains as a popular choice for low-income people and as a favorite transport means for many students, despite the substandard service quality. Another problem is that the bus system has not yet been well planned. In some places there is no (or almost no) bus service while the concentration of five or six bus lines in other parts of the capital city has resulted in traffic jams. The bus is expected to serve a greater number of users in the future and supposed to improve the traffic situation.

Generally, social facilities and everyday life services are not very well organized in Hanoi: either locally available and cheap but poor in quality and polluting or good/high quality, environmental-friendly but not convenient in use and far from home, as seen in the following circumstance: A typical woman working in a state office brought home many things for dinner after work. Shortly before cooking, she realized that she had forgotten to buy some salad onions. Some street vendors passing by or the green groceries near her home offered her the salad onions at a reasonable price but she felt uncertain of the quality, because those salad onions might contain preservatives at a higher level than the same category found in the supermarket which went through a strict quality control. The supermarket was, nevertheless, two kilometers away - too far for her to walk after a long and hard working day. In order to buy some fresh salad onions (only 3,000 VND a bunch), she had to pay 5,000 VND for one motorbike parking lot within 20 minutes and had to wait another 20 minutes just to take her motorbike out of the garage, which was full at the time - during the day’s peak shopping hour.

The inhabitants have had to accept this inconvenience for years, as there has not been any other car parking concept ever proposed than the conventional model mixed zone. The people will, however, move out as soon as they have enough spending power to purchase new houses in another ward where the living conditions and car parking services satisfy their high demand: economical, convenient and safe. A car-free settlement is regarded as a preeminent concept to deal with the current traffic problems. But architects and city planners need to ponder upon the question what makes it work. Otherwise, a car-free living quarter will turn out to be another castles-in-the-air story, just like an eco-house before which sounded very nice at first but nobody could afford at last.

4. HOW DOES THIS NEW CONCEPT WORK?

In phase one, a car-free settlement in Hanoi will provide its inhabitants with a high-quality parking service: not only accessible 24/24 for car owners but also going towards a greener and cleaner urban environment and reaching a more and more comfortable living standard. In this in-depth view, a parking system in one residential area should not be put inside (but next to) the housing blocks.

The other factors should also be taken into consideration. Street houses are highly lucrative in a profit-oriented open market economy. The crucial point of the new living concept to be proposed is that although the two main functions “residence” and “business/service” are separated from each other, so that they will not affect each other so much, they can be combined together - in one building as well as in one block - to ensure a close and/or direct connection. Based on this symbiotic relation, a typical settlement in Hanoi for the future will consist of two zones:

- Periphery: is reserved for non-pollutant general service buildings such as supermarkets, offices, stores or shop houses (large and medium-size) and kiosks (small). Car and motorbike parking houses can also be constructed here. The residents and their guests drive into the garages from the streets, then exit the garages through the doors at the back and walk home.
- Core: is planned for residence with various housing forms such as villas, row-houses, low-rise and high-rise apartments divided into groups, open for pedestrians and bicyclists only, with a small open space in the center of each group of houses and a public place with public buildings and a large open space in the heart of the whole living quarter.

Between the periphery and the core, there is a demarcation line called green line, marking the end of the car zone and the start of the pedestrian zone to the central point of the living quarter. But the fire safety requires an inner ring road for fire engines. In another emergency case - strokes at home and cardiovascular diseases among old people - ambulance cars must approach all the houses or apartment buildings. Similarly, if a family moves to another district or buys new furniture, it needs a cargo van that stops at the front door. Normally, the entrance ways end with iron pillars or concrete posts that prevent motorized vehicles from entering the pedestrian zone. If necessary, these posts can be operated to slide up and down the holes and kept underground until the transport cars go out.

According to this spatial organization and functional separation, all the motorized vehicles are kept in public parking garages that are optimally planned along the periphery, taking into account:

- the distance between two garages as well as between garages and homes to ensure the radius of service and accessibility
- the parking capacity of each garage to accommodate all the vehicles of the residents and their visitors. Underground garages can be built if necessary.

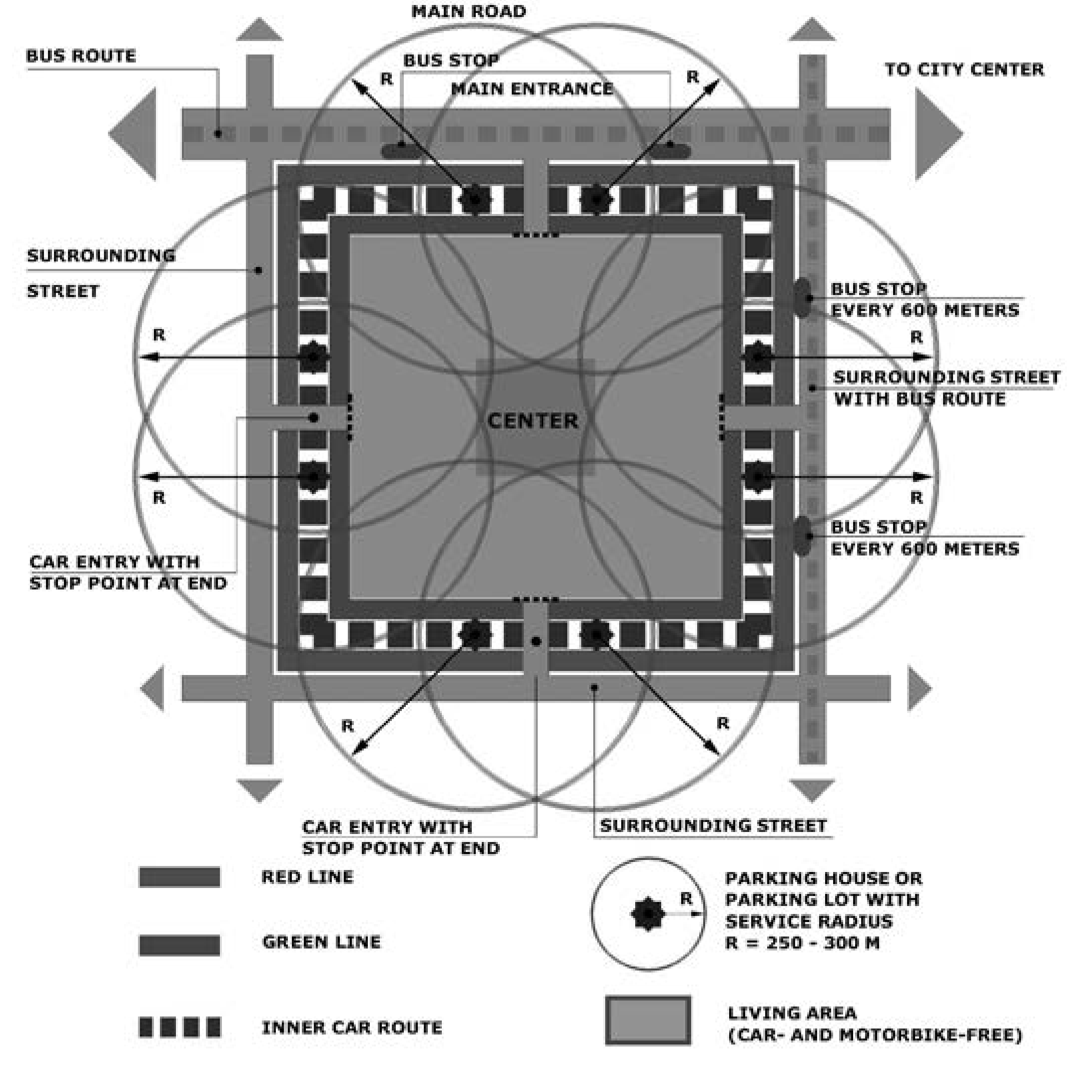

Figure 5: Car and motorbike-free as a new living concept for Hanoi (Nguyen, 2010)

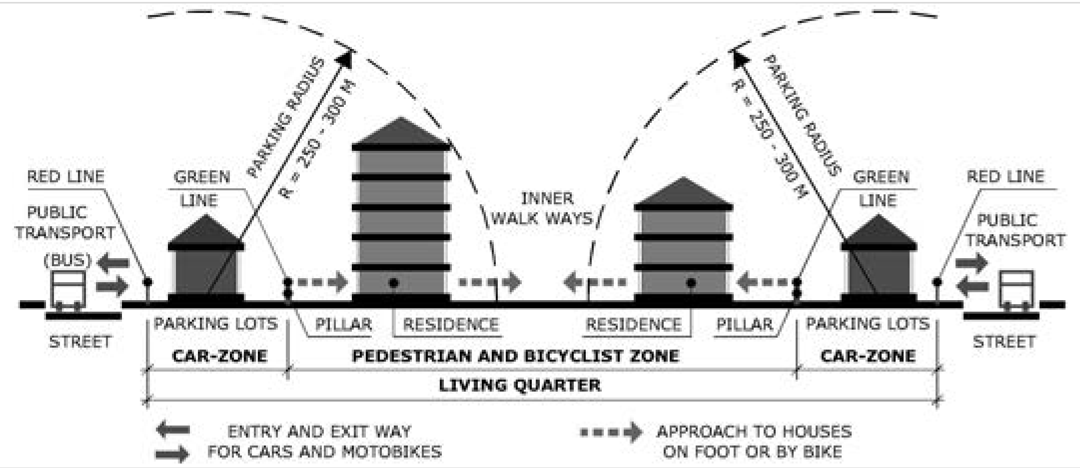

Figure 6: Cross section of a car and motorbike-free living quarter in Hanoi (Nguyen, 2010)

The car parking service radius may vary between 250 and 300 meters based on the experiences from other countries in the South East Asia region and the world. At this distance, the residents do not hesitate to walk between homes and parking lots, because it only takes them less than ten minutes to do so. At the moment, the convenience while using parking services is what people concern the most. That means, aside from paying a reasonable monthly parking fee, people can drive in or out any time they need: 24 hours a day and seven days a week.

In phase two, when the time is right, the number of cars and motorbikes within the living quarter will decrease step by step through a very high car parking fee which would make people eventually sell and/or rent their cars as implemented in Vauban (Freiburg, Germany). Functionally, in view of adaptive use, an old empty garage could be turned into another public building for the local community, for example a fitness center, a restaurant or probably an office for rent.

The periphery-and-core structure described above complies with the guiding principle “simple but effective” and can demonstrate well the main functions that it should perform: trading and parking (periphery) and living (core). In addition, the periphery made up of two to three-storey non-residential buildings can help protect the living space in the core from the negative influences (exhaust gas and noise) of the surrounding streets. Then all the shop houses in the periphery will only be used for commercial purposes. Nevertheless, shop-owners could have a mid-day rest upstairs if they want, and leave their shops at the end of the day for homes just one or two rows behind, and it will take them just a few minutes to go back and forth between homes and workplaces.

At the same time, in order to promote the use of urban public transport with bus and tram as two main options in Hanoi, the current systems should be redeveloped into a city-wide network in line with the enhancement of the service quality. Each settlement has direct access to at least one bus or tram line, with at least one bus stop or tram station every 400 meters along the road which enables local residents to walk to the nearest station within 10 minutes from home. When half of the city population uses public transport means on a daily basis instead of private vehicles, they will not worry any more about getting stuck hours in traffic congestions.

5. HOW LARGE A CAR-FREE LIVING QUARTER SHOULD BE?

Based on the 400-meter distance between two next bus stops and with reference to the right location of a bus stop, for example 100 meters from the crossroads, urban planners can also limit the size of a typical living quarter for easy access, trouble-free traffic circulation and effective management. It should not exceed 36 hectares (in form of a 600 m x 600 m square), quite suitable in terms of area and applicable to most of living quarters in Hanoi at present (30 - 40 hectares). In case of a larger area, mostly in the suburbs, the living quarter may be divided with one or two sub-regional streets or lanes into two or three neighborhoods, about 30 hectares each.

6. A SURVEY FOR CAR PARKING CAPACITY AS A PRE-REQUISITE CONDITION AND PUBLIC PARTICIPATION AS A CRUCIAL FACTOR

For a new urban housing project, before the planning stage begins, the planning team should calculate the parking capacity, based on the following information:

- the number of motorized vehicles within the area at present
- the quantitative increase of private transport means in the future
- how often a household welcomes guests and what kind of vehicle(s) they usually drive to come and visit the family. These cars and motorbikes must be of course added to the local parking capacity.

Without this information as important input data, the parking lots would be either insufficient or surplus. In form of a questionnaire handed out to the householders invited to attend a pre-planning conference, the information can be obtained when people have filled in all the sections in the survey sheets and sent them back at once or a few days later to the professional organization. Each citizen must be responsible for the future development of his or her own living quarter by providing accurate and complete information. The experts will analyze all the information and propose several development scenarios for the living quarter, thereby helping the local people put their wishes for a safer and more sustainable living environment into practice. In a more complicated case - a reconstruction project - a thorough investigation should be conducted in the same way. Local people know what they really need better than anybody else and have always played a decisive role in the success of any urban development program, as also clearly reflected in the second phase of the project, when they can collaborate with the local authority to manage the project after it has been brought into action, according to the bottom-up co-management concept.

7. CONCLUSIONS

There is a fact in Vietnam and in Hanoi that new and breakthrough ideas are not often accepted at the beginning, no matter how good these ideas may be or how much they can contribute to the socio-economic development, because they look very different from what people used to see or imagine and require a significant change in the long-time behavior and customs of the society. In this context, car-free settlement seems to be a tough nut to crack, but this nut keeps in it a truly fine sprout that promises to grow for green. For various reasons, the sprout in the nut has not taken root yet.

A living quarter organized in the periphery-and-core structure will be able to solve the traffic and parking problems that most of the conventional living quarters are coping with. The biggest difficulties while developing this concept will arise in social aspects, such as the awareness and participation of the public together with the cooperation between people and their representatives for a common purpose, etc., rather than in planning and design or in technical solutions. Therefore, in order to make car-free living happen, it is important to start with thinking before acting, but one should not think too long, because time and tide wait for no man.

REFERENCES

Nguyen Q. M., 2010. *A concept for ecological planning and building applied to residential areas in Hanoi with Phung Khoang new town as a case study*, PhD dissertation, Bauhaus University Weimar, Germany, p. 93

Rosenthal E. and Sprecht M., 2009. *In German suburbs life goes on without cars*, The New York Times, published on May 11, 2009. Electronic version retrievable at: http://www.nytimes.com/2009/05/12/science/earth/12suburb.html?_r=0

Freiburg City Council and Vauban Project Management Board, 2008

Vauban Official Website www.vauban.de/info

VietcomBank exchange rate on August 24, 2013 www.vietcombank.com.vn

General Statistic Office (GSO), 2011. *Population and population density in Hanoi and other cities and provinces in Vietnam*, Report retrievable on-line at http://www.gso.gov.vn/default.aspx?tabid=387&idmid=3&ItemID=12875

Vietnams Press Agency, 2009. *The most populous districts in Hanoi.* Electronic version retrievable at http://www.baomoi.com/Quan-Dong-Da-co-mat-do-dan-so-cao-nhat-Ha-Noi/121/3286889.epi

Vietnams Law Newspaper, 2013. *Over 90% of cars in Hanoi are parking in wrong places.* Published on June 8, 2013. Electronic version retrievable at http://www.phapluatvn.vn/xa-hoi/doi-song/201306/Hon-90-xe-o-to-o-Ha-Noi-dang-do-sai-quy-dinh-2078921/

Hoang H., 2009. *Hanoi old street night market becomes busier at the end of the year*. http://vnexpress.net/tin-tuc/xa-hoi/nhon-nhip-cho-dem-pho-co-dip-cuoi-nam-2150967.html

Official traffic information and education websites: www.vovgiaothong.vn, www.luatgiaothong.vn, www.duongbo.vn

Land use of super levees along the Arakawa River in the low-lying areas of Tokyo

Hitoshi NAKAMURAI[1] and Takaaki KATO[2]
[1]Professor, Shibaura Institute of Technology, Japan
nakamu-h@shibaura-it.ac.jp
[2]Associate professor, ICUS, IIS, The University of Tokyo, Japan

ABSTRACT

A super levee is a river embankment with a broad width which can withstand even if overflow. Because a super levee project is often promoted in conjunction with the urban development project along the river, the creation zone will exist discontinuously in the long time. After the super levee project was judged to be "abolishment" by the national budget screening system in 2010, Ministry of Land, Infrastructure and Transport reviewed its policy drastically in August 2011. According to this new policy, the creation zone of super levees is narrowed down to the low-lying area or densely built-up area in the large city where serious human damage is likelier to occur in the large-scale flood. Especially in the low-lying area, it is necessary to create the space that inhabitants can evacuate safely in the large-scale flood. In this view, each super levee can be also utilized as a large-scale upland evacuation area by creating parks and other public facilities on the site. This paper examined the actual land use of super levees in the lower reaches of the Arakawa River in Tokyo and considered the possibilities and problems of promoting a super levee project. Along the Arakawa River, super levee projects have been complete or in progress at 15 sites. As for the land use of these 15 super levees, 8 projects include dwelling houses, 4 projects include public parks, 8 projects include public facilities other than park and 2 projects include others such as commercial buildings. From the standpoint of securing an upland evacuation area, it is desirable to create a public park or public open space on the site, but these cases are only 4 in 15. However, under the certain conditions, it is possible to use public facilities, roads, private open spaces, commercial buildings and high-rise dwelling houses on the super levee as an evacuation area.

Keywords: super levee, land use, flood, evacuation area, low-lying area

1. INTRODUCTION

1.1 Super Levee

A super levee is a high standard river embankment with a broad width which can withstand even if overflow (Stalenberg B. and Kikumori Y., 2008). It is about 30 times as wide (about 200 m to 300 m) as it is high, so that even if it is overtopped,

the flowing water does not breach the levee because it flows slowly across its top surface (Figure 1, Arakawa-Karyu River Office, 2013).
A previous conventional dike can be transformed into a super levee by heightening of the top and by broadening of the slope. The ownership of the land on the super levee special development zone remains unchanged after the project. This special zone can be used for urban land use.
In comparison with the conventional dike, Figure 1 shows various advantages of a super levee such as ground improvement, open space as an evacuation area, gentle slope and easier access to the river, better landscape and living environment.

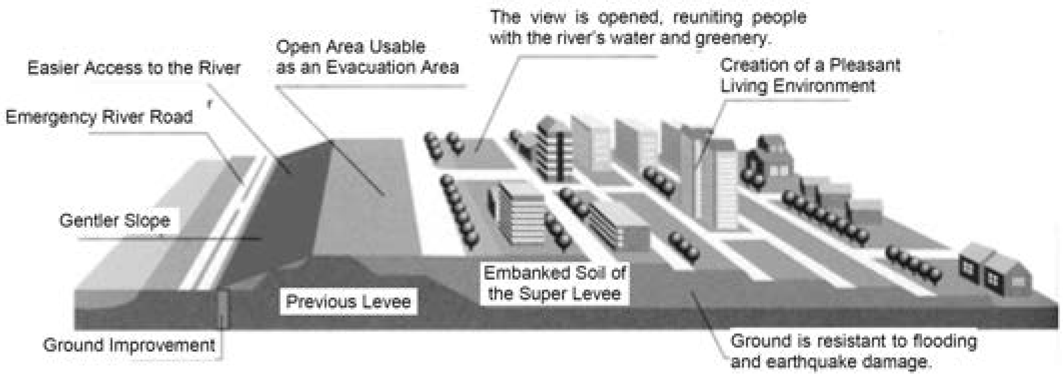

Figure 1: Super levee (Arakawa-Karyu River Office, 2013)

1.2 Super Levee project

A high standard levee improvement project (a super levee project) started in 1987 along the six large rivers in Tokyo and Osaka, i.e., Tonegawa, Edogawa, Arakawa, Tamagawa, Yodogawa and Yamatogawa.
Because a super levee project is often promoted in conjunction with the urban development project along the river, the creation zone will exist discontinuously in the long time. According to the report of the Board of Audit of 2011, as of the end of March 2010, a total length of the districts which enforced projects was 50.6 km (123 districts) and its implementation rate was 5.8 % of a total length of the project zone (872.6 km). As for the project priority zone (223.8 km), a total length of the districts which enforced projects was 27.7 km (59 districts) and its implementation rate was 12.4 %.
By the national budget screening system of 2010, the total project expense of the high standard levee for the past 24 years was estimated for 694 billion yen. In other words when projects are promoted at the same pace, approximately 400 years are necessary before a total project zone is completed, and 12 trillion yen is required for overall project costs. Therefore, in the budget screening, the super levee project was judged with "abolishment."

1.3 Low-lying area

After the judgment by the budget screening in 2010, Ministry of Land, Infrastructure and Transport (MLIT) reviewed its policy drastically in August 2011. According to this new policy, the creation zone of super levees is narrowed

down to the low-lying area or densely built-up area in the large city where serious human damage is likelier to occur in the large-scale flood.
According to MLIT, population in the low-lying areas (the area that the ground is lower than a mean sea level) in three major metropolitan areas, i.e., Tokyo, Osaka and Nagoya in Japan, is said to be more than four million in total. These low-lying areas have been exposed to flood risks and the risks have been increasing due to climate change.
However, recently, few floods have occurred in these areas because of the enhancement of flood control which is sustained mostly by the structural measures. As a result, the awareness of flood risk has been declining and the preparation for the large-scale flood is insufficient for local people in the low-lying areas.
These areas have another flood risk caused by the earthquake. The probability of the conjunction of an earthquake and an extreme weather causing flood may be negligible. However, the possibility of having flood for the restoring term of flood control facilities such as levees damaged by the earthquake cannot be ignored because the recovery of the facilities will take much time.

1.4 Flood hazard map

The revision of flood prevention law in 2005 has obligated municipalities to publish a flood hazard map which has information about the flood hazard and evacuation areas. However, municipalities in the low-lying areas are facing the difficulty to make a reasonable hazard map for citizens because there are not sufficient safe evacuation areas in case of the large-scale flood.
For example, Katsushika ward in the eastern part of Tokyo have no choice but to guide more than 27 thousand people to upland evacuation areas with the distance more than 10 km. In reality, these evacuations will be difficult under the present conditions. And it is estimated that several tens of thousands people cannot evacuate even if all tall buildings including the private buildings are assumed to be evacuation places.
Therefore, especially in the low-lying area, it is necessary to create the space that inhabitants can evacuate safely in the large-scale flood. In this view, each super levee can be also utilized as a large-scale upland evacuation area by creating parks and other public facilities on the site.

1.5 City planning master plan

Examining the description of the city planning master plan of the local governments (5 wards; Sumida, Koto, Adachi, Katsushika, Edogawa) along the Arakawa River in the lowland of eastern Tokyo, every local government specifies the necessity of the flood control measures.
Although super levee project zones are specified in the whole lower reaches of the Arakawa River, they are not specified in the map of the city planning master plan of each ward. Exceptionally, in the Katsushika city master plan (Figure 2), only the generous position of “the evacuation area by the creation of the upland” is shown in a figure of the safety urban development policy (flooding). Some areas along the Arakawa River are designated as the planned upland evacuation area. However, there are no urban planning regulations about super levees.

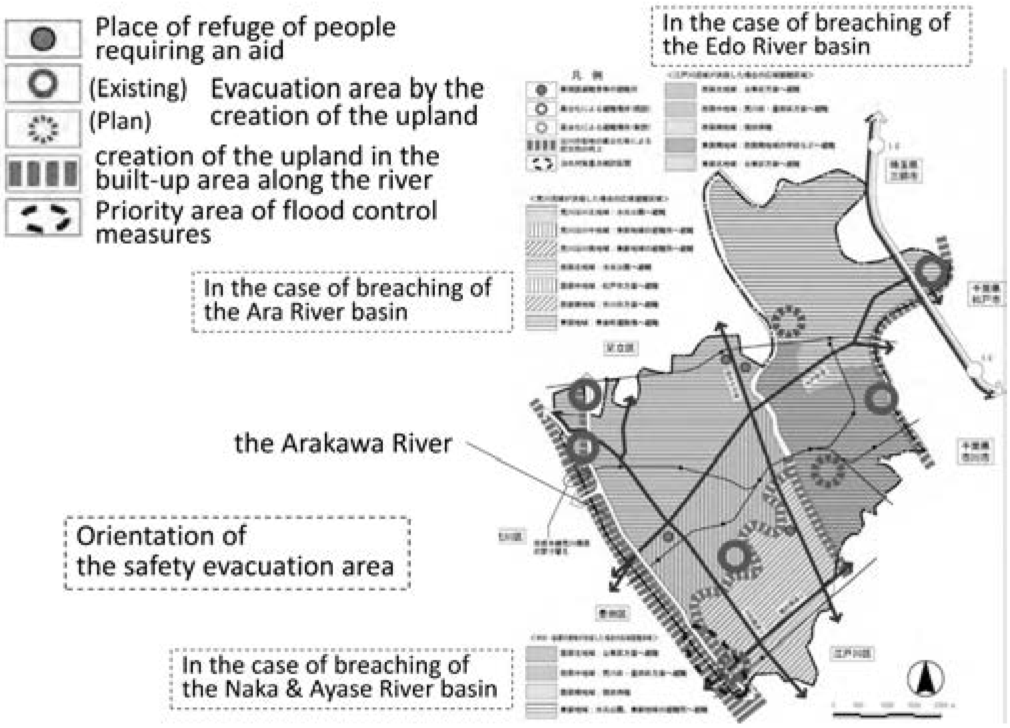

Figure 2: A figure of “safety urban development policy (flooding)” in the Katsushika city master plan (Adapted from Katsushika ward, 2012)

1.6 Purpose

The purpose of this study is to examine the actual land use of super levees in the lower reaches of the Arakawa River in Tokyo and to consider the possibilities and problems of promoting a super levee project.

2. SUPER LEVEES ALONG THE ARAKAWA RIVER

2.1 Super levees along the lower reaches of the Arakawa River

From an interview survey to the Arakawa-Karyu River Office in January 2013, in the lower reaches of the Arakawa River, super levee projects have been complete or in progress at 15 sites, 8.75 km as of March 2012 (Figure 3, Table1). Completed projects are 13 sites, approximately 5.03 km, and projects in progress are 2 sites, approximately 3.72 km. It accounts for about 15 % in a total length of 58.2 km.
It is pointed out that the difficulty of consensus building, the prolongation of the project, the large scale compensation for removal, influences to the surroundings including the sunshine condition are the main disincentive of the project.

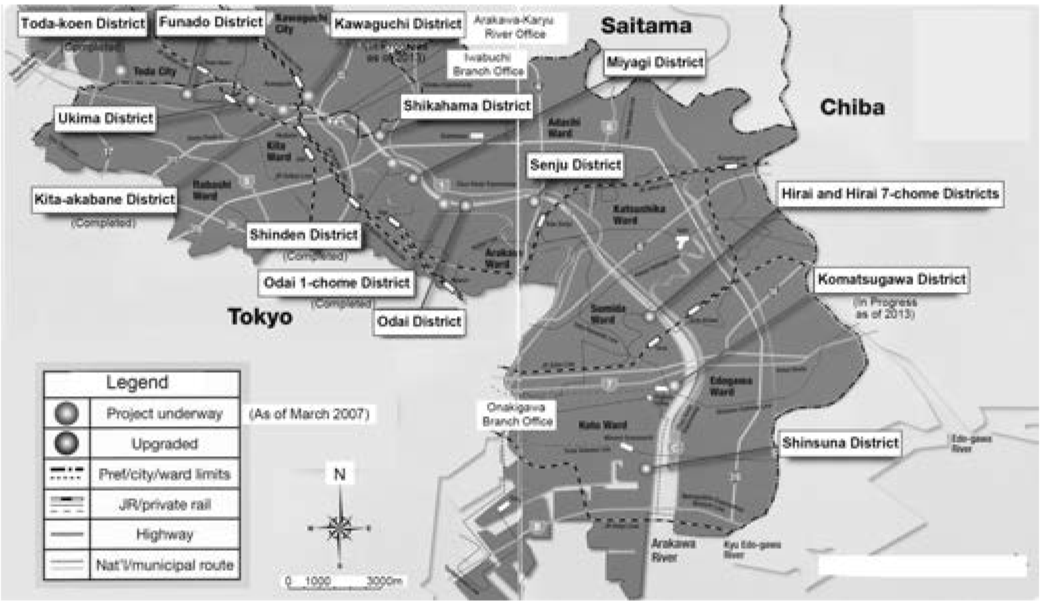

Figure 3: Super levees along the lower reaches of the Arakawa River
(Adapted from Arakawa-Karyu River Office, 2007)

Table 1: Super levees along the lower reaches of the Arakawa River

	Super levee district	Main land use				Length (m)	Area (ha)	Mean width (m)	Filling completion year
		Dwelling house	Public park	Public facility other than park	Ohters				
1	Shinsuna			X		1,140	18	158	2004
2	Komatsugawa	X	X	X		2,380	23	97	in progress
3	Hirai	X				100	1.5	150	2003
4	Hirai 7-chome	X							
5	Senju	X		X		100	1	100	2000
6	Odai	X				100	0.4	40	1991
7	Odai 1-chome	X		X	X	670	12	179	2004
8	Miyagi		X			300	1.6	53	2001
9	Shinden	X		X		1,360	27	199	2007
10	Shikahama		X			300	10	333	1991
11	Kawaguchi	X		X	X	1,340	11.5	86	in progress
12	Kita-akabane			X		500	4.2	84	2003
13	Ukima					provisional completion			
14	Funado			X		70	0.6	86	2006
15	Toda-koen		X			150	2.8	187	2008

Table 2: Public facilities and others on the super levee

	District	Public facilities other than park + Others
1	Shinsuna	Water station, Water treatment plant, Electric power transmission facility
2	Komatsugawa	Junior high school, Pumping station
5	Senju	Community (Lifelong learning) center
7	Odai 1-chome	New transportation system station, Station square + Commercial buildings
9	Shinden	Elementary school, Junior high school, Sewerage facility, Fire fighting center
11	Kawaguchi	Elementary school, Junior high school, Kindergarten + Temple, Driving school
12	Kita-akabane	Disaster prevention station (stockpile warehouse for food and materials)
14	Funado	Recycling facility

2.2 Scale of super levees

The scale of these super levees varies. As for the length of these 14 super levees excluding Ukima district which is regarded as the provisional completion, 5 projects are less than 200 m. 4 projects are more than 200 m and less than 1,000 m. 4 projects are more than 1,000 m.
As for the area of 14 super levees, 6 projects are less than 2 ha. 2 projects are more than 2 ha and less than 5 ha. 6 projects are more than 10 ha.
As for the mean width, 6 projects are less than 100 m. 7 projects are more than 100 m and less than 200 m. According to the concept of a super levee, it should be constructed with about 200 m to 300 m width. However, only one project is more than 200 m.

3. LAND USE OF SUPER LEVEES

As for the land use of these 14 super levees (Table 1), 8 projects include dwelling houses, 4 projects include public parks, 8 projects include public facilities other than park and 2 projects include other land use such as commercial buildings. Public facilities other than park and other land use are shown in Table 2.
The land use of super levees can be roughly classified into 4 types: a dwelling house type, a public park type, a public facility type other than a public park type and a mixed-use type.

3.1 Dwelling house type

A dwelling house type can be further classified into a detached house residential area type, a single high rise apartment type, a mixed-use type including the aggregation of high rise apartments.
Hirai 7-chome district corresponds to a detached house residential area type. Hirai, Senju and Odai district correspond to a single high rise apartment type. But in the Senju district, there is a public facility in the lower story of the apartment.
Komatsugawa, Odai 1-chome, Shinden and Kawaguchi district correspond to a mixed-use type including the aggregation of high rise apartments.

Hirai 7-chome district | Odai District | Shinden district

Figure 4: Dwelling house type

3.2 Public park type

A public park type can be further classified into a single park type and a mixed-use type including a park.
Miyagi, Shikahama and Toda-koen district correspond to a type that is used only as a public park. In particular, Shikahama district is used for an agricultural park. Komatsugawa district corresponds to a mixed-use type including a large evacuation park.

Miyagi District | Shikahama District | Komatsugawa district

Figure 5: Public park type

3.3 Public facility type

A public facility type other than a public park type can be further classified into a single use type with the public facility and a mixed-use type including the public facility.
Shisuna, Kita-akabane and Funado district correspond to a single use type with the public facility. Komatsugawa, Senju, Odai 1-chome, Shinden and Kawaguchi district correspond to a mixed-use type including the public facility.

Kita-akabane district | Funado District | Kawaguchi district

Figure 6: Public facility type

3.4 Mixed-use type

As has already been pointed out, 5 districts (Komatsugawa, Senju, Odai 1-chome, Shinden, Kawaguchi) correspond to a mixed-use type. 4 districts except the Senju district are relatively equivalent to a large-scale super levee.


Komatsugawa district


Odai 1-chome district


Shinden District

Figure 7: Mixed-use type

4. CONCUSION

From the standpoint of securing an upland evacuation area, it is desirable to create a public park or public open space on the site, but these cases are only 4 in 15. However, under the specific conditions, it seems to be possible to use public facilities, roads, private open spaces, commercial buildings and high-rise apartments on the super levee site as small-scale distributed evacuation spaces. From this viewpoint, it is important to reevaluate the need of super levees as the upland evacuation area in the large-scale flood in the low-lying area.
A detailed analysis of possible evacuation spaces on the super levee and evacuation routes to them is the next research theme. And an appropriate cost-benefit analysis of the super levee as the upland evacuation area should be further considered.

REFERENCES

Arakawa-Karyu River Office, 2007. *Super Levees Guidebook*. Ministry of Land, Infrastructure and Transport, Tokyo, Japan.
Arakawa-Karyu River Office, 2013. Activities of our Office: Super Levees. http://www.ktr.mlit.go.jp/arage/english/outline/01.html#1 (accessed 1 July 2013).
Katsushika ward, 2012. *Katsushika city master plan*. Tokyo, Japan.
Stalenberg B. and Kikumori Y., 2008. Urban Flood Control on the Rivers of Tokyo Metropolitan. In Graaf, R. D. and Hooimeijer, F. (editors), *Urban Water in Japan*, Taylor & Francis Group, London, UK, 119-141.

Anomaly detection of seasonal and annual environment changes of the world

Haruo SAWADA
Project Professor, ICUS, IIS, The University of Tokyo, Japan
sawada@iis.u-tokyo.ac.jp

ABSTRACT

This report shows how remote sensing data are used for global environment health monitoring and development of a new processing methodology for anomaly detection. Seasonal changes in a year are common phenomena in the world although they show different severity to human beings. These phenomena continued for a long time and they characterized natural vegetation and human beings whose lives are supported by local ecosystems and global environment. Global environment changes affect the ecosystem services through the changes of vegetation health. Cloud free 10 day composite images of MODIS and SPOT/Vegetation satellite data clearly show not only the seasonal changes of natural environmental parameters but also the anomaly of seasonal changes of Earth surface, which can be used as the influence of environment changes to ecosystem, services.

Keywords: environment health, remote sensing, seasonal change

1. INTRODUCTION

Phenological changes of ecosystem are closely related to the changes of natural environment, such as water, temperature, soil and solar radiation. Even tropical forests show seasonal variations in the presence of new leaves, flowers, and fruits The National Oceanic and Atmosphere Administration (NOAA) reported that warm temperature trends continue near Earth's surface and datasets of NOAA show 2012 was among the 10 warmest years on record (Blunden and Arndt, 2013). This report also explained that the United States and Argentina had their warmest year on record. Many of the events that made 2012 such an interesting year are part of the long-term trends we see in a changing and varying climate - carbon levels are climbing, sea levels are rising, Arctic sea ice is melting, and our planet as a whole is becoming a warmer place.

Rising temperatures add energy to the atmosphere, and computer models warn that this will produce wider and wilder swings in temperature and rainfall and alter prevailing wind patterns. Therefore, global warming will likely increase the number and severity of extreme weather events. These phenomena continued for a long time and they characterized natural vegetation and human beings whose lives are supported by local ecosystems and global environment. We call these supports of ecosystem as "ecosystem services". For example, carbon sequestration, climate regulation and purification of water are considered ones of regulating services.

Mitigation of disasters (ex. flood and drought) is one of preserving services. Global environment changes affect these ecosystem services through the changes of vegetation health. This report shows methodologies for monitoring the trends of long-term influence of Earth environment to ecosystems and for detecting anomaly events on land surface by global observation satellite sensors.

2. SATELLITE ENIVIRONMENT INDICES

Since the 1980s, NOAA’s Polar Orbiting Environmental Satellite have provided daily global coverage of multi-spectral observations of visible and near-infrared surface reflection as well as surface temperature radiation. The TERRA satellite’s MODIS (MODerate resolution Imaging Spectrometer) data with advanced resolutions in both spatial and spectral characteristics have been provided in daily base since 2000. From these satellite data, some indices related to vegetation condition, such as the Normalized Difference Vegetation Index (NDVI) (Justice et al.. 1985) and the Leaf Water Content Index (LWCI) (Anazawa et al. 2001) , can be derived. The NDVI exploits the spectral properties of green vegetation and the LWCI shows the water contents of plant leaves, which are related to the photosynthesis process in leaves. The data, however, are often affected by various atmospheric disturbances (aerosol, water vapor and ozone), cloud cover, solar illumination. Instrument degradation, insufficient calibration and satellite orbit drifts as well as the different characteristics of sensor systems even on the same satellite series. Therefore, appropriate preprocessing to observed data is required to monitor ecosystems for a long period of time with the same quality.

Global NDVI data have been used to clarify trends of seasonal changes of vegetated areas. Myneri et al (1997) investigated the 1981-1991 Advanced Very High Resolution Radiometer (AVHRR) NDVI for northern hemisphere and detected the trends of advance in active growing season of 8±3 days and delay in the declining phase of 4±2 days over this decade. It is an example of processing to detect the trends of seasonal changes of vegetated area in global scale. However, in order to address the issues arising due to the various environmental problems that are currently attracting attention, it is necessary to devise a method that enables monitoring of fluctuations of vegetation conditions such as moisture, temperature and land cover changes.

3. METHODS

Various research projects on global environment utilize the characteristics of the cyclic nature of multi-temporal satellite data. In those research projects, the n-day composite imagery (ex. n=8, 10), which is created by selecting the best data in 8 or 10 days for every pixel, is often used for characterizing seasonal changes. However, the influence of clouds and haze remain even in these 8 or 10-day composite data and this makes the phenology monitoring with 10-day interval complicate (Sawada et al., 2005). Monthly composite data, however, are not appropriate to monitor phenology dynamics because the seasonal changes of vegetation are phenomena taking place in a few weeks for most of cases. Then we developed a novel method for time series modeling and spectrum anomaly detection applicable to SPOT/vegetation and MODIS as well as AVHRR data. Since this methodology can extract a seasonal change model for each pixel separately, it is useful to monitor land-cover change and ecological disasters.

3.1 Generation of spectral codebook and encoding

The batch-learning self-organizing map (SOM) algorithm was introduced in order to generate a spectral codebook which encodes multispectral data. In each pixel, "pure components" (end-members) are extracted throughout the data collection period by the orthogonal projection analysis (OPA) (Cuesta Sanchez et al., 1996) for removing influence of cloud, haze and other noise for observing earth surface. “Pure components” are derived by the batch-learning SOM algorithm. Generated SOM is used as a codebook in the spectral encoding step. In addition, SOM nodes which are assigned as cloud and haze are masked out. Then, multi-temporal and multi-spectral data, such as MODIS data (MOD09A1) and SPOT/VEGETATION (S10) products, are encoded by the nearest-neighbor method. We set the SOM map as 20 x 20 (the total number of codes is 401 including the “NULL” code).

3.2 Generation of spectral codebook and encoding

The observation data vector and the state vector at (x,y) pixel are denoted by o(x,y) and q(x,y), respectively. Assuming that q(x,y) follows Markov process, we get the conditional probability of q(x,y) (Rabiner, 1989).

3.3 Classification of seasonal change profile

Since the element of the state vector q(x,y) is a nominal scale value, we developed a nominal scale vector (and/or strings data) classification method. Firstly, D(q(x,y)) is defined as a characteristic matrix of the state vector q(x,y). The (i,j) element of D(q(x,y)) is equal one when $q_j(x,y)= i$ and otherwise zero. The size of the matrix D(q(x,y)) is N x T. In bioinformatics researches, D is called ‘Position Specific Scoring Matrix’. Next, the centroid of D, q_{cent} (Q), is defined when Q is a set that consists of state vectors. And we define $f_{ij}(X)$ as a function that returns (i,j) element of a matrix X for further convenience. Similarity of Q and another state vector q’ is also defined by a formula.

3.4 Spectral anomaly detection

In general, an anomaly detection methodology is required to clearly distinguish spectral anomaly (i.e. land cover changes) and phenological changes. If the seasonal change profile of the reference year $\mathbf{q}(x,y)$ and clustering results $\mathbf{Q}$ are known, we can define observation probability of encoded spectrum $p(v_t^{(x,y)})$ in another scene *t(time)* at (x,y) pixel. For setting threshold value to identify anomaly, we assume that encoded spectra are generated by random process. Then, the anomaly score of each pixel is compared with the threshold of the anomaly.

4. RESULTS AND DISCUSSION

4.1 Water coverage monitoring

An example of our processing on MODIS (MOD09A1) data is shown in Figure 1. 414 scenes from the early January 2001 until the end of December 2009 were used. The target area is Amazon River basin (10N-20S, 80W-40W). Figure 1a, 1b and 1c are raw composite, time-series modeling results (by HMM) and cluster centroid, respectively. Almost all the influences of cloud and noises are cleaned up. 23 states were obtained and "state 23" is assigned to water spectra which is clearly distinguished from other states in the spectral shape. Then the water coverage period map was obtained from the occurrences of "state 23".

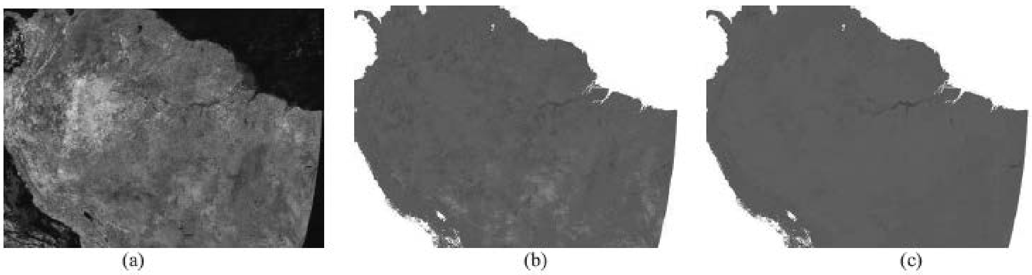

Figure 1 Examples of discrete time-series processed MOD09A1 data (Jan. 12 2009) (a) original MODIS (b) HMM processed (c) cluster centroid image

5.2 Burned area detection

In order to detect burned areas with 10 day interval, the SPOT/vegetation-S10 products were processed. The target area was far-east Russia (50N-54N, 127E-133E). The data collection period as the reference year was from Apr. 1999 to Mar. 2000 (one year, 36scenes). We set the SOM node size to 10 x 10 for clustering of seasonal change profile. As the result, 15 states were obtained and there were mainly four categories, namely "vegetation", "soil", "snow" and "water". The data collection period for anomaly detection was from Jun. to Aug. 2000 (12scenes). For comparison, the products of the same area of the GBA2000 (Global Burned Area, Grégoire et al., 2006) is shown in Figure 2. The comparison shows that our method was effective to identify burned area with pixel bases.

5.3 Forest development area detection

The 10-days composite MODIS data were processed. MODIS data were obtained from Web-MODIS system (Takeuchi et al., 2005). The result shows that it identifies deforestation trends by pixel bases (Figure 3, 13.417N, 106.112E). ASTER VNIR images with 30 m resolution are also used for checking the result.

6. CONCLUSIONS

We developed a discrete time-series model using a self-organizing map (SOM) and a hidden Markov Model (HMM) to reduce the influence of clouds in order to improve the quality of the products. The products can clearly distinguish spectral anomaly and phenological changes. Our method was effective to identify land cover changes (i.e. forest fire and deforestation) with pixel by pixel, but further study will be required to clarify its limitation on usage for land cover change detection. A small land cover changes will not be identified.

ACKNOWLEDGEMENT
This research used ASTER data beta processed by the AIST GEO Grid from ASTER data owned by the Ministry of Economy, Trade and Industry. This study was partially supported by JST

REFERENCES

Anazawa, M., G. Saito, Y. Sawada, and H. Sawada, “Vegetation monitoring study using leaf water content index (LWCI) and NDVI” Processing 22nd Asian Conference on Remote Sensing, vol. CD, pp. 1-6, 2001.

Blunden, J., and D. S. Arndt, Eds., 2013: State of the Climate in 2012. Bull. Amer. Meteor. Soc., 94 (8), S1-S238.

Cuesta Sanchez, F., Toft, J., van den Bogaert, B. and Massart, D. L., 1996. Orthogonal Projection Approach Applied to Peak Purity Assessment. Anal. Chem., 68 (1), pp. 79-85.

Gregoire, J. M., Tansey, K. and Silva, J. M. N., 2003. The GBA2000 initiative: developing a global burnt area database from SPOT-VEGETATION imagery. Int. J. Remote Sens., 24(6), pp. 1369-1376.

Gribskov, M., McLachlan, A. D. and Eisenberg, D., 1987, Profile analysis: detection of distantly related proteins. Proc. Natl. Acad. Sci. USA., 84(13), pp. 4355-4358.

Justice, C.O. J. R. G. Townshend, B. N. Holben, and C. J. Tucker, “Analysis of the phenology of global vegetation using meteorological satellite data,” International Journal of Remote Sensing, vol. 6, no. 8, pp. 1271-1318, 1985.

Kohonen, T., 2000. Self-Organizing Maps (2nd ed.). Springer, Berlin, chapter 3.
Mynenl,R.B., C. D. Keeling, C. J. Tucker, G. Asrar, and R. R. Nemanl, “Increased plant growth in the northern high latitudes from 1981 to 1991,” Nature, vol. 386, pp. 689-702, 1997.

Rabiner, L.R., 1989. A tutorial on hidden Markov models and selected applications in speech recognition. Proc. of the IEEE, 77(2), pp. 257-286.

Sawada, Y and H. Sawada, “Development of a discrete time series model for vegetation” International Archives of the Photogrammetry Remote Sensing and Spatial Information Science, vol. XXXVIII, no. 3, pp. 719-724, 2010.

Sawada, Y., Mitsuzuka, N. and Sawada, H., 2005. Development of a time-series model filter for high revisit satellite data, Proceedings of the Second International VEGETATION User Conference (Veroustraete, F., Bartholome, E. and Verstraeten,W.W. ed.), pp. 83-89, Office for Official Publications of the European Committees, Luxembourg.

Shannon, C., 1948. A Mathematical Theory of Communication. Bell Syst. Tech. J., 27, pp. 379-423.

Takeuchi, W., Nemoto, T., Baruah, P. J. and Yasuoka, Y., 2005. Online satellite data distribution system for the monitoring of environment and disaster over Asia (in Japanese), Photogrammetry and Remote Sensing, 44(2), pp. 68-72.

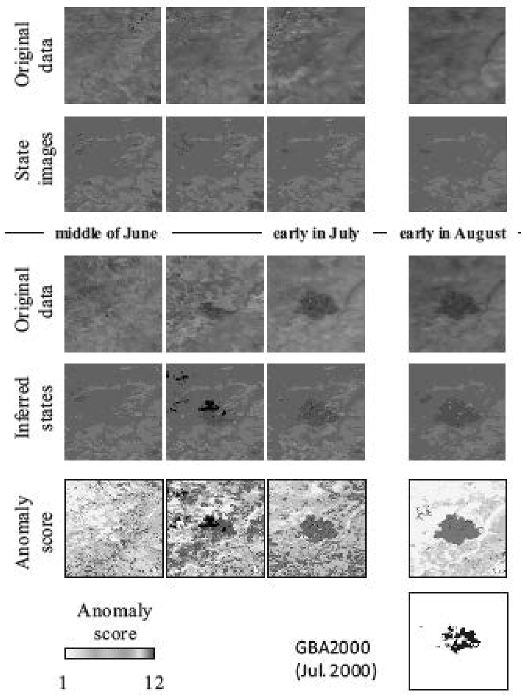

Figure 2 Identification of burned area

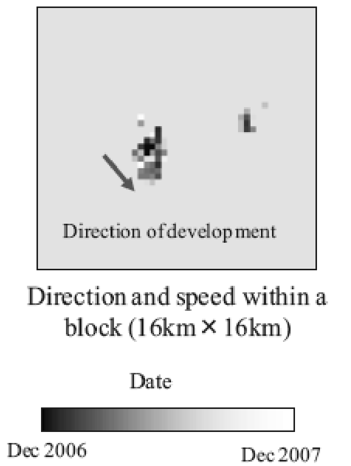

Figure 3 Deforestation detection and trend

Analysis on urban fire hazard and risk zones assessment mapping in Bangkok, Thailand

Praopanitnan CHAIYASANG[1], Nitin Kumar TRIPATHI[2]
[1]Remote Sensing and Geographic Information Systems, Thailand
praopanitnan@hotmail.com
[2]Asian Institute of Technology, Thailand

ABSTRACT

Bangkok is the mega city with high vulnerability because of the urbanization. Many people migrate to urban area because of job opportunity and economic factors, while their quality of life is decreasing. High population density, low quality of housing, and infrastructure shortages can lead to the risk. The problem is they might not know that they are at risk. Therefore, risk identification and the mitigation plan should be considered for coping mechanism. According to the disaster statistics, fire hazard is the one of the main problems in Bangkok. Fire hazards are increasing in Bangkok. It is such a problem which is becoming more intensive. Therefore, Bangkok is also the risk area in case of urban fire hazard because of the urbanization including population and building density, and human activities. Thus, GIS and urban planning knowledge can be used to support Bangkok's abilities to cope with risk, to prevent or reduce the likelihood of this kind of hazard which may result in death, injury, or property damage. The risk zones can be both high density community and urban abandoned land. Most of urban abandoned land in Bangkok is belonging to private sector, thus, government cannot operate or improve this kind of land. Consequently, the private sector should realize that their areas are at risk, they have to manage and give important by their own to avoid from the causes of urban fire. Certainly, co-operation between government, Department of Disaster Prevention and Mitigation (DDPM), private sector, and people, will be required to cope with urban fire as a public hazard. Data about past events may help us to find geospatial pattern/ frequency and hazard hotspots. There are vulnerable communities and infrastructure. These are to be mapped and geodatabase need to be created. These data can be used to develop the model for urban fire risk map and help the urban fire risk management.

Keywords: *Urban Fire Risk, Fire Hazard, Urbanization*

1. INTRODUCTION

Urban fire is the public hazard which can happen anytime. It directly affected to human living such as human health, human property, economy damages, and environment. Urban fire hazard can be classified into two types. The first is naturally occurring fire, for instant, dry leaves friction in the summer or dry season. The other type is fire caused by human such as grass burning, forgetting turn off the lights, and short circuit. There are many factors can lead to fire hazard such as land use, density, building structure, and infrastructure. These factors related to the urban planning approach which controls urban structure. Furthermore, it is necessary to integrate geographical technique to make clear in physical perception. Thus, GIS is the one technique to measure the physical factors. It can be used to prevent the fire hazard and decrease the damages. It is possible to identify the urban fire risk zones by using GIS. People can realize the vulnerable factors of their areas, these factors have to be considered for preparation and prevention.

Bangkok faced fire hazard increased in every year. It's such a problem which is becoming more intensive. Therefore, Bangkok is also the risk area in case of urban fire hazard because of the urbanization including population and building density, and human activities. Thus, GIS and urban planning knowledge can be used to support Bangkok's abilities to cope with risk, to prevent or reduce the likelihood of this kind of hazard which may result in death, injury, or property damage. The risk zones can be both high density community and urban abandoned land. Most of urban abandoned land is belonging to private sector, government cannot operate or improve this kind of land. Thus, if the private sector realizes that their areas are at risk, they might manage and give important by their own to avoid from the causes of urban fire hazard. Moreover, co-operation between government, Department of disaster Prevention and Mitigation (DDPM), private sector, and people, will be required to cope with urban fire as a public hazard.

2. STATEMENT OF PROBLEMS

Urban development in Thailand is likely to grow rapidly especially in Bangkok. Since the industry has driven to be the main country's income, many labors migrate from rural to urban because urban has high job opportunity. It can be the cause of slum which lack of efficiency infrastructure including fire system. Due to lacking of proper urban planning, urban problems have occurred; social, economic, environmental problem, and low quality of life with less standard secure. The one of main problem is the fire risk. Overcrowding communities can be causes of heat-related activities such as cooking, more power usage, and fuel storage in household. Furthermore, fire system in Thailand is still inefficient such as lack of fire mitigation equipment in some area and lack of coordination between the agencies involved. Therefore, the damage will be very intense.

Urban fire hazard often happens in overcrowded communities with high population density, industrial buildings, shopping centers and theaters where these places often have high electric power usage. It can be lead to thermal energy which is cause of fire hazard.

Due to fire risk factors, Bangkok is the one of risk area according to the fire history statistic.

Figure 1: Urban Fire Hazard in Bangkok 1990 - 2011

The development of economic in Thailand has been rapid in the last 20 years. It can be seem from the building increasing especially in Bangkok which is the economic center of Thailand. Bangkok is a modern high-rise building construction increased steadily, particularly in the areas of business growth. Due to the convenient location for the urban lifestyle, the high-rise building is increasing every year. Thus, it is very important to consider structure of the building, it has to be strong and safe follow the building control regulation and engineering standards. According to the disaster statistics, fire was occurred greater than any other disaster. Fire hazard lead to the loss of life and property, especially in a public housing, high-rise buildings, and large buildings. If the buildings do not have the efficiency fire protection and extinguishing systems, such cases will lead to injury, loss of life, and property that may be invaluable.

If fire occurs without fire prevention and efficiency system, it can lead to the high injury, death, and property damages. Hence, the high building should set up the fire prevention system follow the law, they have to maintain the system to be available all the time. Government should realize about this risk and try to solve this problem by using law. It can be used to control the building's owner to do follow the law for more safety. The people who stay in the building have to understand about the fire prevention and mitigation as well. The a fire occurs, they are capable enough to break the cycle of fire spread initially and they also can help themselves or others to escape the danger of fire which is going in the building.

Therefore, the fire risk assessment is the one tool which was created by Department of disaster Prevention and Mitigation (DDPM). They would like to provide this systematic tool for the local area for applying with the particular area or the community. It can be used to identify, predict, and ranking the community's risk. This systematic tool also can help the local government for supporting the efficiency decision making of disaster risk reduction. As well as the geodatabase can be used to develop policies, strategies and plans, projects. This is a truly integrated work. The Department of Disaster Prevention and Mitigation can use the geodatabase from the operation of a fire risk assessment to manage the fire safety program and also apply it for the local scale.

3. OBJECTIVES OF STUDY

The following objectives have been defined in the proposed system;
3.1 To analyze fire hazard status and physical condition in Bangkok
3.2 Mapping the urban fire risk zones of Bangkok

4. METHODOLOGY

This stage involves the collection and gathering of digital thematic maps and statistical data of Bangkok, Thailand relevant to the study. The following thematic layers are used in GIS analysis.

- Administrative Boundary
- Land use
- Source of water
- Road Network (Accessibility)
- Fire Station

4.1 Analytic Hierarchy Process (AHP)

AHP and Weighted Overlay Tool are necessary for this study, the pixel is also important to calculate the weighting score. Thus, the covert feature to raster tool is should be used in this step. The overlay method can only be implementing on raster so that before implementation of the weighted overlay tool, it is necessary to convert the vector data in to the raster by conversion tools (feature to raster).
Due to the result of AHP, it can be used to rank the importance level of five criteria.

Table 1: Analytic Hierarchy Process

Criteria	Land Use	Water Body	Fire Station	Road Surface	Road Lane
Land Use (F1)	1.000	2	0.33	3	2
Water Body (F2)	0.5	1.000	0.33	3	2
Fire Station (F3)	3	3	1.000	4	4
Road Surface (F4)	0.33	0.33	0.25	1.000	0.5
Road Lane (F5)	0.5	0.5	0.25	2	1.000
Sum	**3.33**	**6.85**	**2.16**	**13**	**9.5**

Table 2: Normalized Matrix

Criteria						Sum	Priority Vector
Land Use (F1)	0.300	0.292	0.153	0.231	0.211	1.186	0.212
Water Body (F2)	0.150	0.146	0.153	0.231	0.211	0.891	0.159
Fire Station (F3)	0.900	0.438	0.463	0.308	0.421	2.530	0.452
Road Surface (F4)	0.100	0.048	0.116	0.077	0.053	0.394	0.070
Road Lane (F5)	0.150	0.073	0.116	0.154	0.105	0.598	0.107
					Sum	**5.599**	**1**

Table 3: Estimating Consistency

	F1	F2	F3	F4	F5	Consis-tency	Weight Sum	Consistency Vector (λ)
F1	1.000	2	0.33	3	2	1.186	6.181	5.212
F2	0.5	1.000	0.33	3	2	0.891	4.697	5.272
F3	3	3	1.000	4	4	2.530	12.730	5.032
F4	0.33	0.33	0.25	1.000	0.5	0.394	2.011	5.104
F5	0.5	0.5	0.25	2	1.000	0.598	3.057	5.112
								5.146

Table 4: Inconsistency Indices (RI)

N	1	2	3	4	5	6	7	8	9	10
RI	0.00	0.00	0.58	0.90	1.12	1.24	1.32	1.41	1.45	1.49

$$\text{Consistency Index (CI)} = \frac{\text{Consistency Vector } (\lambda) - N}{N - 1}$$

$$= (5.146 - 5) / 4 = 0.0365$$

$$\text{Consistency Ratio (CR)} = CI / RI$$

$$= 0.0365 / 1.12 = 0.0326$$

Consistency Ratio = 0.0326 (It is less than 0.1, thus, it is acceptable)

4.2 GIS Data Manipulation and Analysis

Factor Rating is required to classify the level of risk in each factor. There are four levels of risk in this study; highest risk, high Risk, moderate risk, and low risk.

Table 5: Risk Level and Its Description

Rating	Risk Level	Description
4	Highest Risk Area	The areas where are at intensive risk, high vulnerability of urban fire hazard
3	High Risk Area	The area have high risk in the factors which lead to fire hazard
2	Moderate Risk Area	The area where fire can occur around 50%
1	Low Risk Area	The area with low risk and fire is difficult to occur, it might be occur a few times

Table 6: Factor Rating

Criteria	Factor Rating			
	4	**3**	**2**	**1**
	Highest Risk	**High Risk**	**Moderate Risk**	**Low Risk**
Land Use	Commercial / Industrial Area	Residential Area, Open Space and Park	Agricultural Area	Infrastructure
Water Body	> 500 M.	250 – 500 M.	100 - 250 M.	< 100 M.
Fire Station	> 10 Km.	5 – 10 Km.	3 – 5 Km.	< 3 Km.
Road Surface	Far from the road > 200 M.	Pedestrian	Soil surface road	Composite Concrete
Road Lane	1	2	3	≥ 4

Table 7: Weighting Criteria

Criteria	Weight
Land Use (F1)	25
Water Body (F2)	20
Fire Station (F3)	30
Road Surface (F4)	10
Road Lane (F5)	15
Sum	**100 %**

4.2.1 Land Use Factor

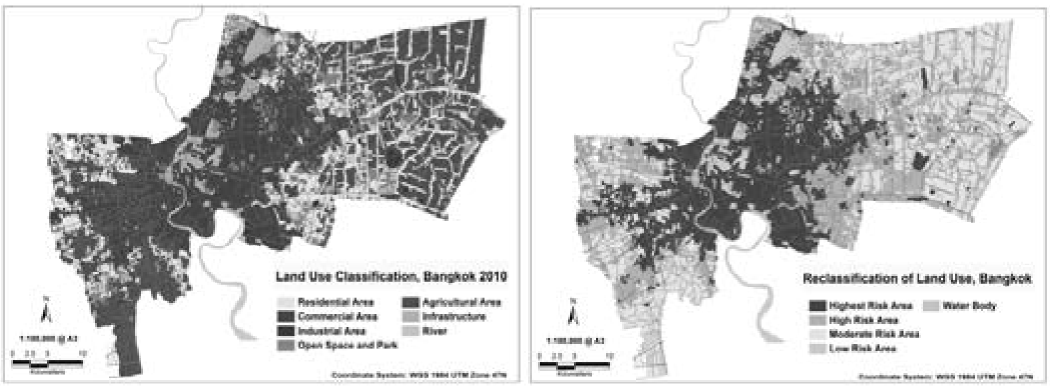

Figure 2: Land Use Classification

4.2.2 Water Body Factor

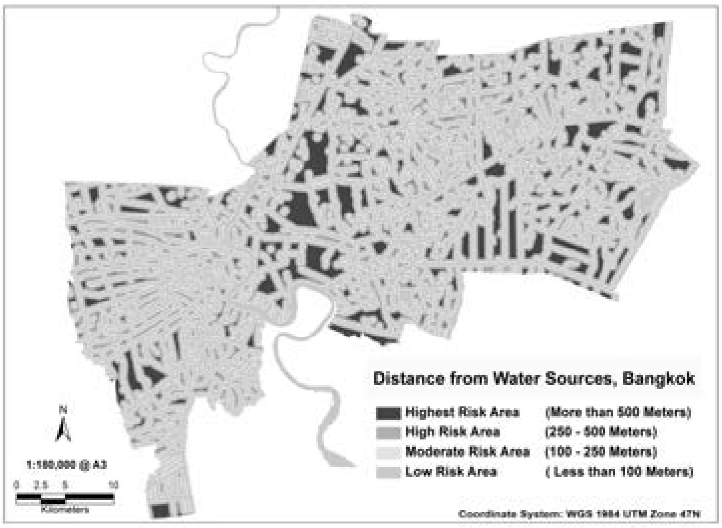

Figure 3: Water Body Classification

4.2.3 Fire Station Factor

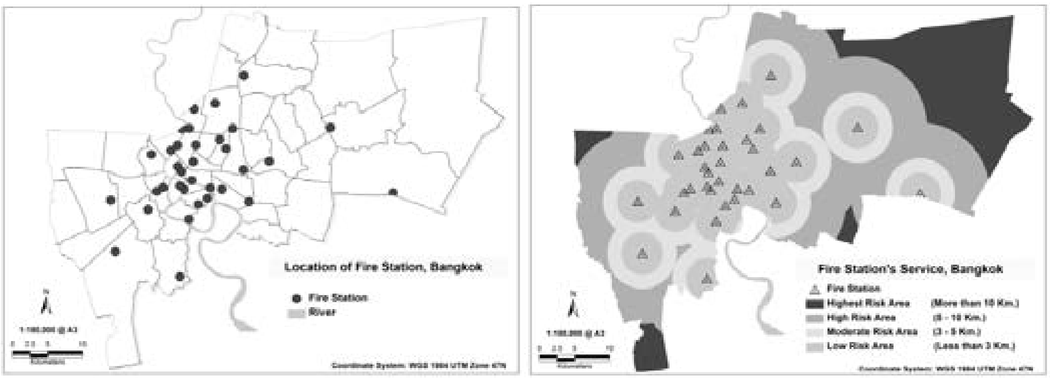

Figure 4: Fire Station Classification

4.2.4 Road Surface Factor

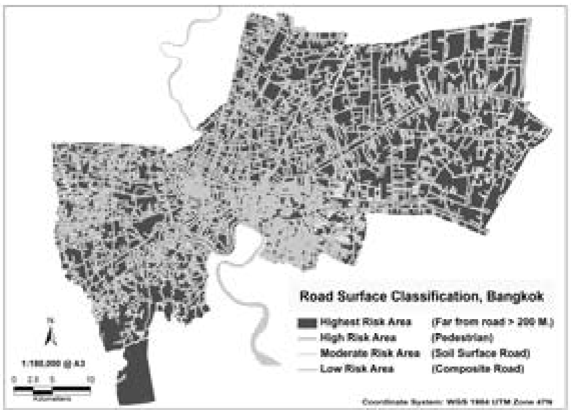

Figure 5: Road Surface Classification

4.2.5 Road Lane Factor

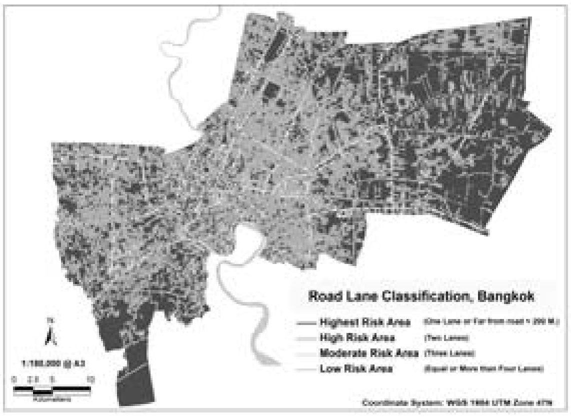

Figure 6: Road Lane Classification

4.2.6 Risk Map

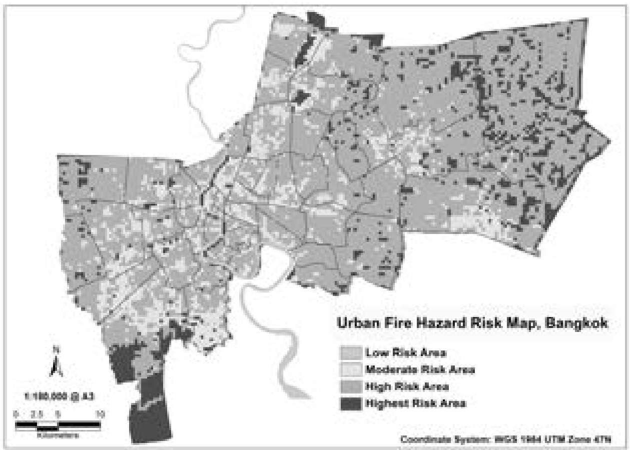

Figure 7: Urban Fire Hazard Risk Map

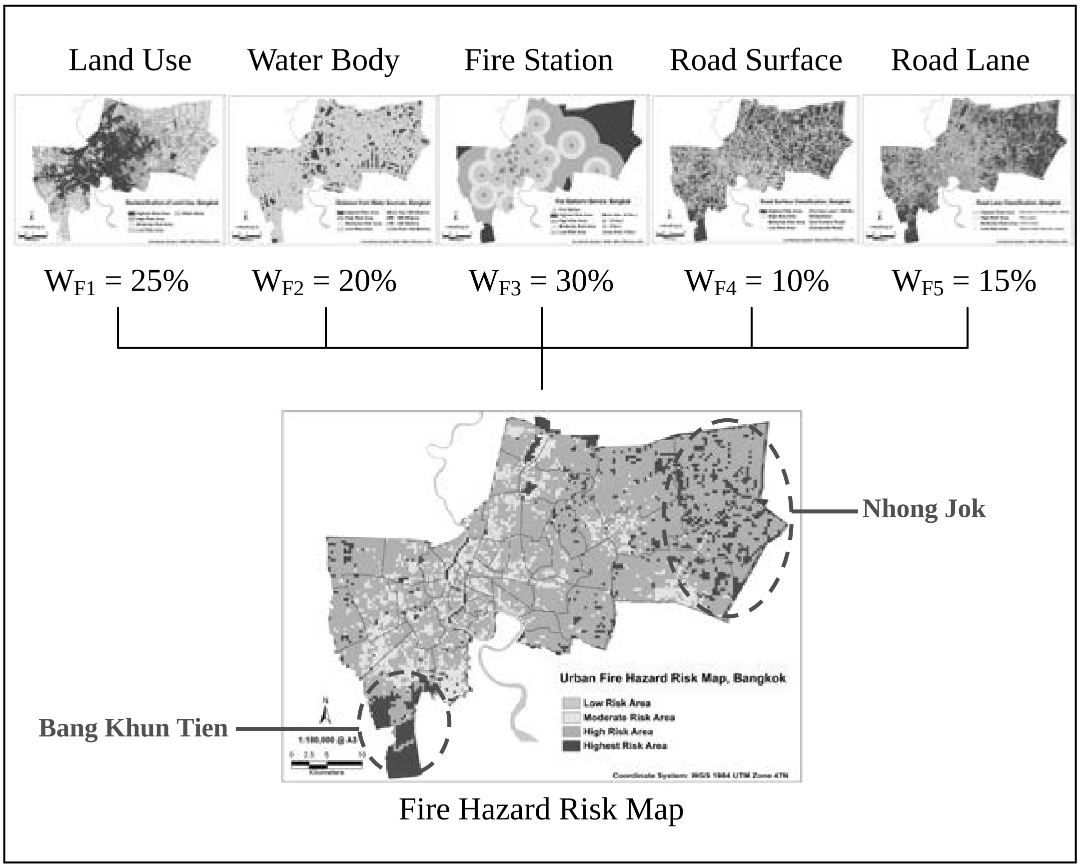

Figure 8: Conceptual Method of Fire Risk Zones Assessment

According to the risk map, the highest risk areas can be identified into two main zones of Bangkok; east (Nhong Jok district) and south-west (Bang Khun Tien district). The five considered factors push these two areas to be the highest risk zones because these zones are located far from the fire station especially Nhong Jok district which does not have even one station and there are many abandoned land which are belonging to the private sectors without the good maintenances. Two main zones also have low accessibility in case of transportation infrastructure.

5. CONCLUSIONS AND RECOMMENDATIONS

This study will be more accuracy to identify the risk area by considering more criteria or factors such as density of building, building height, building material, fire hose location, and available fire trucks. Moreover, it is important to analyst further in the social and economic contexts.

Furthermore, the model or scenario will be required to create the alternative plan for fire prevention and mitigation. The alternative plans can be both structure and non-structure plan. In addition, it is possible to simulate the fire situation. When the fire occurs, any organizations can play their roles including the evacuation route and the route for fire trucks.

6. REFERENCES

Coyle, G. (2004). *The Analytic Hierarchy Process (AHP).*

Hadjisophocleous, G.V. and Fu, Z. (2004). *Literature Review of Fire Risk Assessment Methodologies.* International Journal on Engineering Performance-Based Fire Codes, Volume 6, Number 1, 28-45.

Huo, X. N. (2011). *Spatial Pattern Analysis of Heavy Metals in Beijing Agricultural Soils Based on Spatial Autocorrelation Statistics. Int. J. Environ. Res. Public Health, 2074-2089.*

Hurley, M. J. and Bukowski, R. W. (2008). *Information and Analysis for Fire Protection.*

Jongkroy, P. (2009). *Urbanization and Changing Settlement Patterns in Peri-urban Bangkok*. Kasetsart J. (Soc. Sci) 30, 303-312.

Nour, A. M. (2011). *The Potential of GIS Tools in Strategic Urban Planning Process; as an Approach for Sustainable Development in Egypt.* Journal of Sustainable Development Vol. 4, No. 1, 284-298

Phrommool, S. (2006). *The Study on Behavior and Pattern of fire location distribution within Bangkok District.*

Saaty, T. L. (1977). *A Scaling Method for Priorities in Hierarchical Structures*. Journal of Mathematical Psychology, 15(3), 234-281.

Saaty, T. L. (1980). *The Analytic Hierarchy Process. New York: McGraw-Hill.*

Sopholwit, et al., (2007). *Integrating Remote Sensing and GIS for Fire Hazard Zone Modeling in Kalasin Municipality Area.*

Srivanit, M. (2011). *Community Risk Assessment: Spatial Patterns and GIS-Based Model for Fire Risk Assessment - A Case Study of Chiang Mai Municipality*. JARS 8(2), 113-126.

Srivanit, M. and Kazunori, H. (2011). *Estimating Spatial Disaggregation of Urban Thermal Responsiveness on Summer Diurnal Range with a Numerical Modeling Approach in Bangkok, Thailand*. Journal of World Academy of Science, Engineering and Technology 60, 1125-1134.

Triantaphyllou, E. and Mann, S. H. (1995). *Using the Analytic Hierarchy Process for Decision Making in Engineering Applications: Some Challenge.* Inter'l Journal of Industrial Engineering: Applications and Practice, Vol. 2, No. 1, 35-44.

Y, Jiaqin. And Shi, P. (2002*). Applying Analytic Hierarchy Process in Firm's Overall Performance Evaluation: A Case Study in China.* INTERNATIONAL JOURNAL OF BUSINESS, 7(1), 29-46.

Ground anchors for revetment

Haruka SAITO
SE Corporation, Japan
haruka_saito@se-corp.com

ABSTRACT

Ground anchors have been used in numerous projects for the purpose of landslide control and earth retention at the time of foundation excavation. Today, their applications are expanding into broader areas. For instance, nut-fixed ground anchors are so highly regarded for quake resistance of the anchorage and for corrosion prevention performance of the material that they are used to reinforce abutments, quays, revetments and other existing structures. For example, the quake resistance improvement work for the Kobe Port Island, designed to upgrade the functionality of the super core port, adopted a reinforcement method using ground anchors because of the need to minimize the impact of the work on the surrounding environment as well as the work period, cost and other factors. This paper attempts to introduce the way to design ground anchors to reinforce coastal facilities and cases that ground anchors are utilized for quick recovery from the Great East Japan Earthquake.

Keywords: *ground anchor, revetment*

1. INTRODUCTION

Ground anchor is a system that stabilizes the structure by fixing a tension member such as PC strands to both sides of the underground and the structure and applying pre-stress. In case of reinforcing quays and revetments, anchor heads are fixed at the crest of them. By applying pre-stress, these facilities improved the stability against overturning and sliding. And also displacements caused by an earthquake are repressed. Ground anchor reinforcement can minimize the influence on existing facilities, therefore, it is often used to repair them without disturbing harbor functions.
Through experiments and analyses, the method was appreciated by Coastal Development Institute of Technology in 2009. Items were evaluated are the following 4 points.

1) The effect which controls the displacement of structures caused by an earthquake is recognized.
2) The function of ground anchors can be kept to a seismic impact and vibration by nut-fixed anchor head and compression type of anchor body.
3) Even if a tension fluctuates for an earthquake or environmental change, it is possible to adjust by screwing a nut.
4) Double corrosion protection structure, grease and polyethylene coating, is effective on coastal areas.

2. APPRICATION TO REINFORCEMENT OF STRUCTURES

2.1 Design concept

The method aims to improve the stability against overturning and sliding.
Anchor load T is divided into a horizontal component (T_H : Tcosα) and a vertical component (T_V: Tsinα). Against the risk of sliding, T_H resists directly and T_V adds to friction resistance by increasing of the supposed weight of the structure (equation 1). Against the risk of overturning, both these force generate the opposite moment (equation 2).

$$\frac{\mu\left(\sum V + T_V\right)}{\sum H - T_H} > F_{S1} \quad (1) \qquad \frac{\sum M_V - T_V \cdot x}{\sum M_H - T_H \cdot y} > F_{S2} \quad (2)$$

Where,
ΣV is a vertical force (kN)
ΣH is a horizontal force (kN)
ΣM_V is a vertical component of moment (kN*m)
ΣM_H is a horizontal component of moment (kN*m)
T_V is a vertical component of anchor load (kN)
T_H is a horizontal component of anchor load (kN)
x is horizontal distance from the point applying moment (m)
y is vertical distance from the point applying moment (m)
μ is a coefficient of friction
F_{S1} is a safety factor to sliding (>1.0)
F_{S2} is a safety factor to overturning (>1.2)

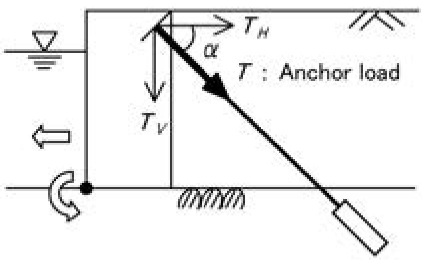

Figure 1: A schematic diagram of ground anchor reinforcement

2.2 Features of ground anchor

There are 3 basis elements of ground anchors (Fig.2).

1) Anchor head – Nut-fixed system
Anchor head is a part which mediates tension between a structure and anchor body. The system is classified into nut-fixed type and wedge-fixed type. This method adopts the former exceeds in seismic resistance.

2) Cable – Double corrosion protection
Maintaining the long-term performance of ground anchor requires reliable corrosion protection. Fig.2 gives a example of double corrosion protection, grease

and polyethylene coating. This structure is considered to be effective under highly corrosive environment as coastal areas.

3) Anchor body – Compression type
Anchor body is a part which bonds to rocks through grout. There are 2 types, tension type and compression type. Fig.2 shows a stress distribution of compression type. Generating stresses from the bottom of anchor body, grout is provided compressive stresses. The structure strongly resists seismic vibrations.

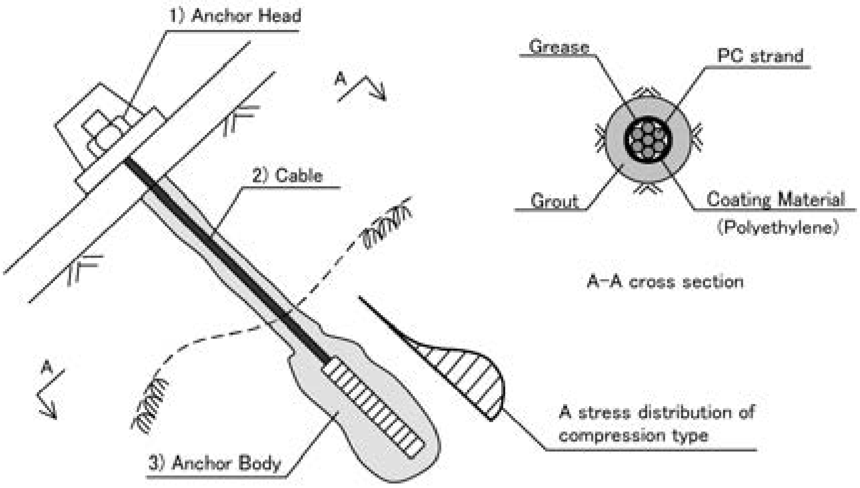

Figure 2: Basis elements of ground anchor

3. Case study 1 ~ Kobe Port Island

Kobe Port Island (2nd) started using from 1998. However, it turned out that their performance was not satisfied with the current seismic design standard by reexamination in 2010. Because quays have already used it is necessary to choose the method considering the utilization of them and also back yards.
The following 3 methods were compared (Fig.3).
a) Ground anchor reinforcement
b) Steel pile connecting with tie-wire
c) Chemical grouting

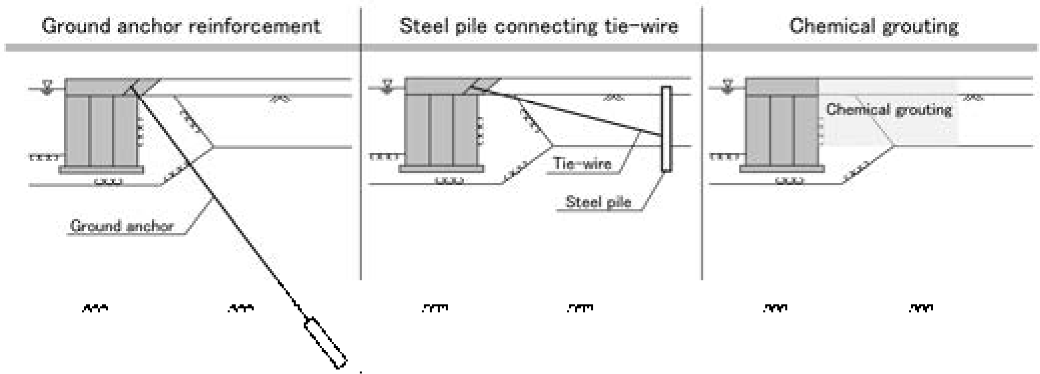

Figure 3: The comparison of reinforcement methods

Ground anchor reinforcement was selected by advantages to minimize the influence on using ports and the cost of the construction. In this site, the layer of clay was distributed thickly and it have not compressed enough. Therefore, the fluctuation of the tension was projected by the settlement of caisson. The structure was designed to regulate the tension easily as changing with time. For example setting load cells, adopting nut-fixed anchor head, putting RC lids and so on.

4. RECOVERY EFFORTS AFTER THE DISASTER

Most of ports located in the pacific side of East Japan were suffered by the great earthquake in 2011. Because of the impact and vibrations, some quays fell down and the ground sank. Case studies was adopted ground anchor reinforcement show below.

Figure 4: Locations of sites

4.1 Case study 2 ~ Funakoshi fishing port

Funakoshi fishing port is located in the middle part of Iwate prefecture. The quay subsided by 0.26 m due to the earthquake, making it necessary to increase its height. However the recovery by mounding up makes it unstable for increasing pressures from back yards. Several reinforcement methods were compared (Fig.5). As against methods widening the quay in concrete which need to excavate and remove ripraps, ground anchor reinforcement minimizes the range, term and cost of the construction. It was chosen as the best method for the rapid recovery. For reinforcing the block quay, anchor heads are fixed at the crest of the block and the blocks are pressd vertically.

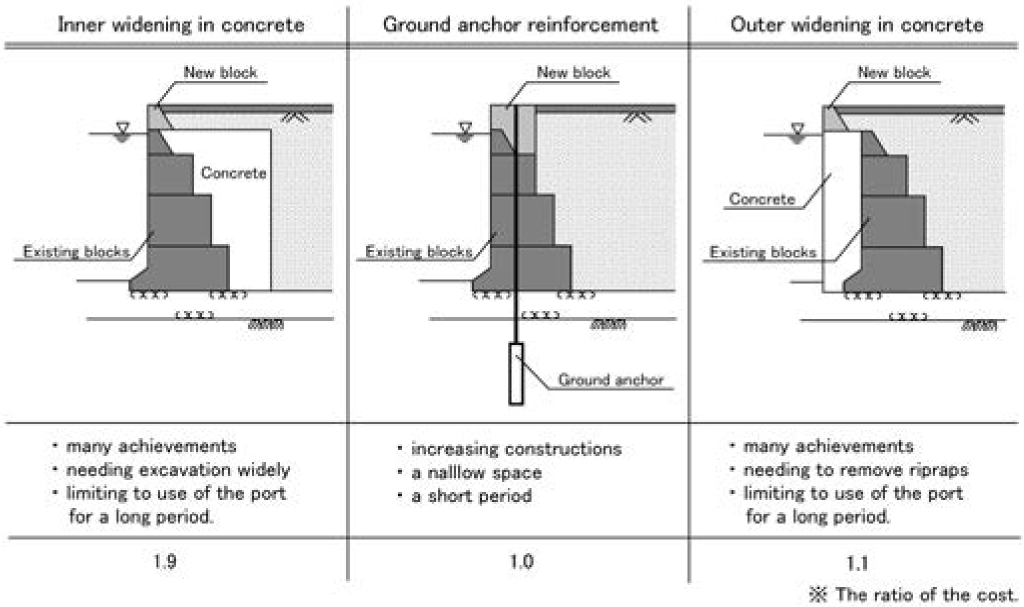

Figure 5: The comparison of reinforcement methods

Figure 6: Funakoshi fishing port, working form the land

4.2 Case study 3 ~ Shibitachi fishing port

Shibitachi fishing port is located in the north part of Miyagi prefecture. Before the earthquake it had the plan to improve the quay which had already become too old for use. However on the way to constructing, the earthquake made a mess of it. After reconsidering it be under reconstruction. For applying the sheet-pile quay, anchor heads are fixed at the crest of the sheet piles using base steel plates and wales.

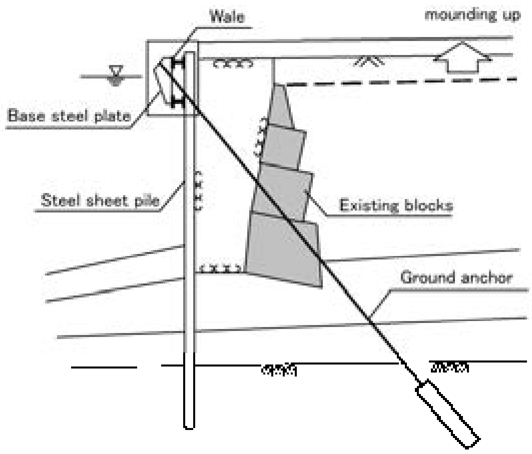

Figure 7: The design of the reconstruction

Figure 8: Shibitachi fishing port, working from the sea

5. CONCLUSION

Ground anchors are useful to reinforce existing structures as using them and to reconstruct quickly. Some quays had already recovered by ground anchor reinforcement and others still are being designed. It is hoped that this method contribute to reconstructions and developments and put the technique to account for disaster control.

REFERENCES

CDIT, 2009. *Technical examination and certification reports of the reinforcement method for quays and revetments applying ground anchor*. Coastal Development Institute of Technology, Japan.

Matsuda, T., Suzuki, K. 2010. Examination of seismic reinforcement techniques utilizing existing revetments. Proceeding of the symposium at Kinki regional development bureau.

Takeya, K., 2013. Ground anchor structure for seismic resistance and its applications. *Earthquake-induced landslides*, pp. 829-838.

Structure maintenance methods and disaster measures of Tokyo Metro

Hiroyuki SHINSAI[1], Shinji KONISHI[2], Kouichi KAWAKAMI[3]
and Yoshihiko MUTOU[4]
[1] Chief Engineer, Structure Engineering Division, Tokyo Metro Co., Ltd., Japan
h.sinsai@tokyometro.jp
[2] Assistant General Manager, Engineering Division, Tokyo Metro Co., Ltd., Japan
[3] Manager, Structure Engineering Division, Tokyo Metro Co., Ltd., Japan
[4] General Manager, Engineering Division, Tokyo Metro Co., Ltd., Japan

ABSTRACT

Tokyo Metro has 9 lines which include Fukutoshin Line open in 2008, total length of the lines is 195.1km. The total length of tunnels is 166.5km, about 85% of all lines. The 6.44 million passengers use our lines each day.
For keeping safety and security feeling of passengers, Tokyo Metro gives high priority to structure maintenance and disaster measures.
This paper describes our activities for them. For former subjects, structure maintenance by inspection, repair and reinforcement methods of subway structures, which Tokyo Metro has been performed, are described. For later subjects, earthquake countermeasures, seismic reinforcement and earthquake early warning system, and anti-inundation measures of Tokyo Metro are described. Lastly, the reliability of the subway is discussed with.

Keywords: subway, tunnel, structure maintenance, earthquake countermeasure, anti-inundation measure

1. INTRODUCTION

Tokyo Metro, it is being checked whether it is normal by round inspection in the daytime. Tokyo Metro has performed inspection, repair and reinforcement efficiently within 1.5 hours at night between the last train and first train of the day, every day.
Moreover, Tokyo Metro has performed the configuration of reinforcement against earthquake or an early earthquake alarm system after the Kobe earthquake which suffered the damage in which the railroad of Kansai district in 1994 was serious.
Recently, the anti-inundation measure is also performed to the guerrilla downpours by weather change in recent years.
This paper describes the reliability and the measures of security on operating Tokyo Metro that is introduced by details of the maintenance management (inspection, repair and reinforcement), the anti-earthquake procedures, and the measure against flood Tokyo Metro has performed.

2. STRUCTURE MAINTENANCE

2.1 Subject and Characteristic

Tokyo Metro has various type structures, for example box tunnel, shield tunnel, viaduct, bridge, each structure (Figure 1). And over 65% of the structures are 40 years old and up. These structures are our targets of maintenance work. It is a special feature that over 85% structures of all length are tunnels. We have to carry out the inspection, repair and reinforcement works within 1.5 hours at night between the last train and first train of the day, every day. For the reason, we maintain them with various devices and keep safety of our train service.

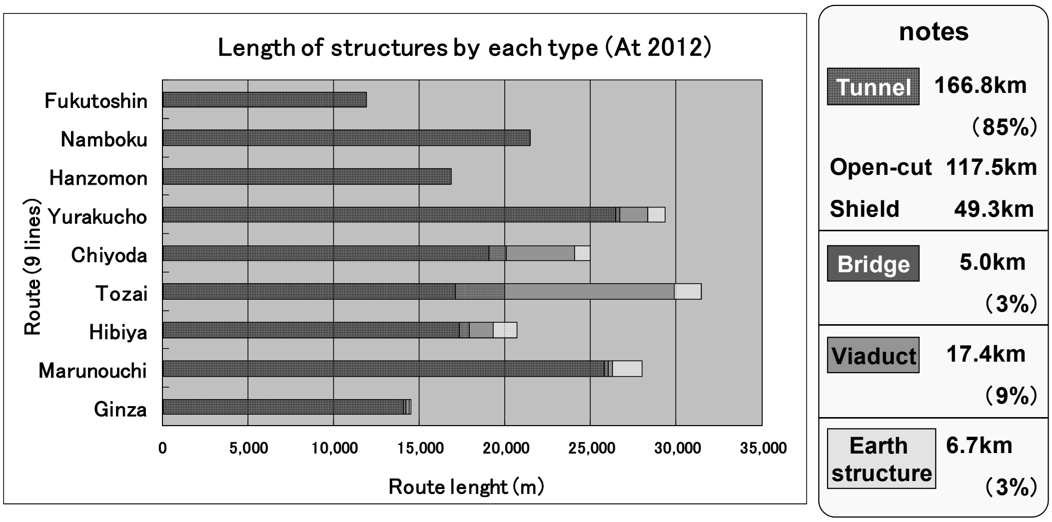

Figure 1: Length of structures by each type

2.2 Inspection

Table 1 shows contents of each inspection for Tokyo Metro's tunnels. We made it with referring to the Maintenance Standards for Railway Structures of the Ministry. In general inspection, we extract and check progress of deformations due to degradation of the lining, for example, crack, leakage and concrete flaking etc., with observation and hammering. The worst influence on the tunnel by occurring and developing of deformations is reinforcement corrosion due to the leakage. Once a reinforcement bar corrodes the swelling pressure due to corrosion sometimes lead to the flaking and spalling of the cover concrete. And the spalling has a bad influence on train safety and service. When leakage water falls on the rails or signal system, some troubles will happen. On the other hand, when a reinforcement bar swells by corrosion or a tunnel deforms severely by a large external force, many cracks will occur. Therefore, in the inspection, we make a tunnel soundness diagnosis with considering state of the structure, risk of a spalling and influence on facilities due to extract and check progress of deformations, for example, crack, leakage and concrete flaking etc. And according to the results of the inspection, we carry repair works on a daily basis, such as leakage water stopping, taking off flaking parts and putting back the shape, to required places. According to the results of the general inspection, we carry out an individual inspection of the place where a detail investigation is needed. In the individual inspection, we investigate and measure by a suitable measuring equipment for detecting the cause and predicting the deterioration progress with high accuracy. Through the activities, for some parts, we take countermeasures of deterioration according to the carefully work-out plan with long term view point.

The regular general inspection, which is performed once every two years, is basically carried out by observation from the floor level. However, on the place within our reach, we carry out a hammering test and knock flaking parts down. For doubtful parts of its soundness on the place without our reach, we inspect in detail by the close range observation and hammering test with a temporary high stage at a later day.

The special general inspection, which is performed once every 20 years, is carried out with the close range observation and hammering test by 4 specialists using a vehicle for high place work. The team has other 6 members, a commander, two drivers, a recorder, a photographer and a worker for cleaning of the tunnel (Figure 2).

Table 2 shows judgments of structure states and standard soundness for structural performance. For example, C rank indicates that the structure state is slight deterioration and A2 rank indicates that the structure state is deterioration which might cause a future performance drop of structures.

Judgment of structure states and standard soundness for spalling, have 3 ranks. α rank indicates the state that there is some possibility of spalling that threatens safety in near future and flaking parts have to be knocked down immediately. β rank indicates the state that there is few possibility of spalling that threatens safety for the moment. But, there is some possibility of spalling that might result in future α rank of soundness. γ rank indicates the state that there is few possibility of spalling that threatens safety.

It is necessary to dicipline and keep skillful inspectors, because the judgment of tunnel soundness is affected heavily by skill of an inspector.

Table 1: Inspection table

Inspection		Purpose	Inspection interval	Item of inspection	Soundness
Initial Inspection		Understand the initial state of the structure	New-construction, Re-construction	Carefully observation +α if necessary	Divide into A･B･C･S For spalling, Divide into α･β･γ
General Inspection	Regular	Extract the deterioration of the structure	2 years	Observation	
	Special	Improve the precision of judgment of Soundness	20 years	Carefully observation +α if necessary	
Individual Inspection		Presume causes of the deterioration, estimate the deterioration, check of the performance demands	–	Carefully observation Detail investigations	Divide A into subdivisions
Extraordinary Inspection		Put into effect, when it needs.	–	Observation +α if necessary	Divide into A･B･C･S For spalling, Divide into α･β･γ

Figure 2: Observation and hammering (special inspection)

Table 2: Structure states by each judgment

Judgment		Structure states
A		State that threatens operational safety of passengers, public safety, guarantee of regular train operation that might cause this state
	AA	Deterioration that threatens operational safety, safety of passengers, public safety, or the guarantee of regular train operation, and require emergency countermeasures
	A1	Progressive deterioration that causes the performance of structures to fall, or heavy rain, floods, or earthquakes that might impair the performance of structures
	A2	Deterioration that might causes future performance of structures fall
B		Deterioration that might result soundness rank of A
C		Slight deterioration
S		Sound

2.3 Repair and Reinforcement

The most severe problem of Tokyo Metro’s tunnels is the trouble due to reinforcement corrosion. The main cause is leakage.

The leakage of cut and cover tunnels occurs from vertical joints between side walls, lateral joints between construction segments and through cracks to the behind side. The leakage of shield tunnel mainly occurs from ring joints and longitudinal joints. In old shield tunnels, leakage is incident to occur, because precision of segments election, backfill grout and water stopping seal of them are poor. Once leakage happens, it’s very difficult to stop it completely.

Figure 3 shows the leakage stopping work by grouting. After the bad part was removed, the place was repaired by polymer cement mortar.

Next, we took reinforcement of a deformed shield tunnel with leakage for 16 years, from 1997 to 1991. We set secondary lining as reinforcement (Figure 4). Because the reinforcement work was performed only midnight due to train service, it took long time. But, it already finished and deformation of the tunnel stopped.

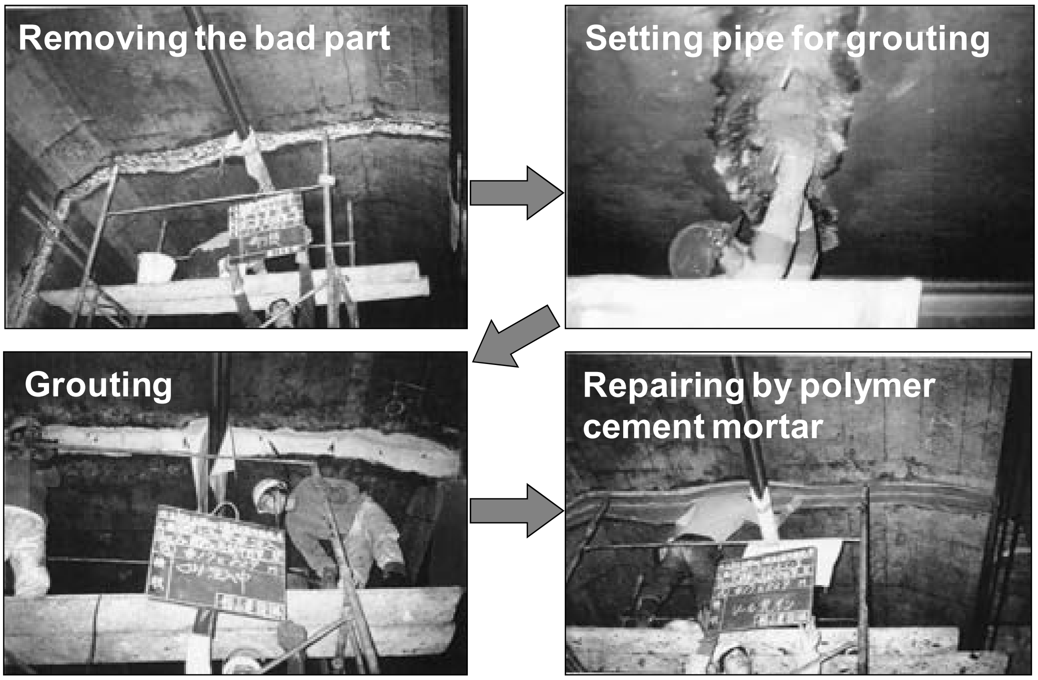

Figure 3: Leakage stopping work by grouting

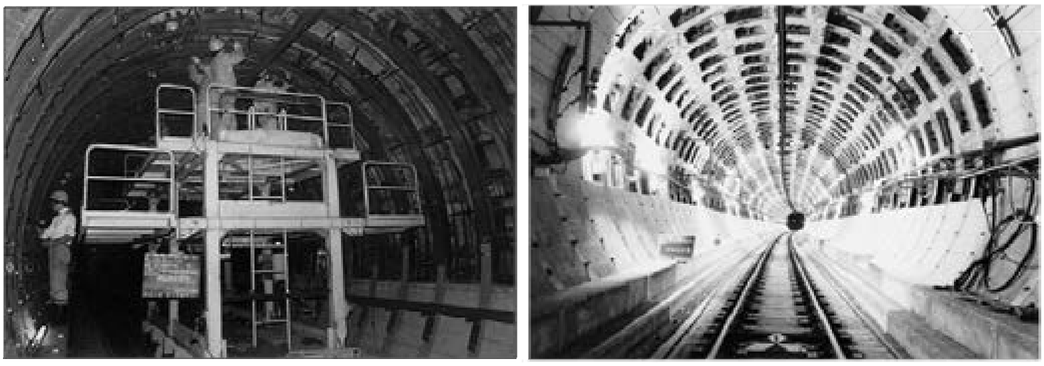

Figure 4: Secondary lining as reinforcement

3. MEASURES AGAINST EARTHQUAKES

3.1 Anti-earthquake reinforcement (Structural measure)

Construction of the oldest tunnel in the Tokyo Metro subway network started in September 1925. It runs from Asakusa Station on the Ginza Line to Ueno Station. It was built after the 1923 Great Earthquake, which means all Tokyo Metro tunnels have been designed to withstand an earthquake equivalent in scale to the 1923 Great Earthquake. However, when the Hyogo-ken-Nanbu Earthquake (magnitude 7.3) occurred in January 1995, a subway tunnel considered to be highly earthquake-resistant collapsed.
In view of this, Tokyo Metro has measured the ground displacement and the yield strength of tunnel center pillars under earthquake conditions and has carried out

pillars reinforcement work where necessary (Figure 5). It is expected that this will prevent tunnel collapse even when an active-fault induced, shallow inland type earthquake equivalent to the Hyogo-ken-Nanbu Earthquake occurs. Consequentially, protection of passengers and securing of the evacuation routes can be assured.
Moreover, we took earthquake resistance of other structures for preventing the big earthquake such as Hyogo-ken-Nanbu Earthquake. Some viaducts were strengthened by steel plate winding method (Figure 6). Some bridges were set brackets as the prevention work for bridge fall.
The Great East Japan Earthquake, which caused approximately 20,000 fatalities and missing persons in March 2011. During the Earthquake, seismic motion of up to 200 gals, with tremors continuing for three minutes or more, occurred in Tokyo. Tokyo Metro had to halt train operation for at least five hours in each case. However, post-quake inspections indicated no substantial damage to underground structures, and train operation could be resumed for all routes.

Figure 5: reinforced pillars

Figure 6: strengthened viaducts

3.2 Early Seismic Alert System (Non-structural measure)

For earthquake countermeasures, we took not only structural measures but also non-structural measures.

3.2.1 Train stop system controlled by seismographs
Regulating train operation is essential to minimizing harm to passengers due to earthquake tremors. In Japan, an earthquake alarm system called “Earthquake Early Warning” has been provided by the Meteorological Agency since October 2007. This system detects P waves initially transmitted when an earthquake occurs. The seismographs used for this, which are under the control of the Meteorological Agency, are connected to alarms that are issued before the arrival of the S wave that causes destruction of structures. Tokyo Metro utilizes an earthquake alarm system based on the Earthquake Early Warning.
Additionally, Tokyo Metro has installed seismographs at six points along its subway lines. If any one of these seismographs detects an earthquake motion exceeding the specified level, the trains on all routes are automatically subject to an emergency stop.

Through the combined use of the systems outlined above, earthquake motion can be detected early enough to stop trains before a substantial tremor occurs (Figure 7). To a great extent, this can prevent derailment due to tremors and reduce possible harm to passengers.

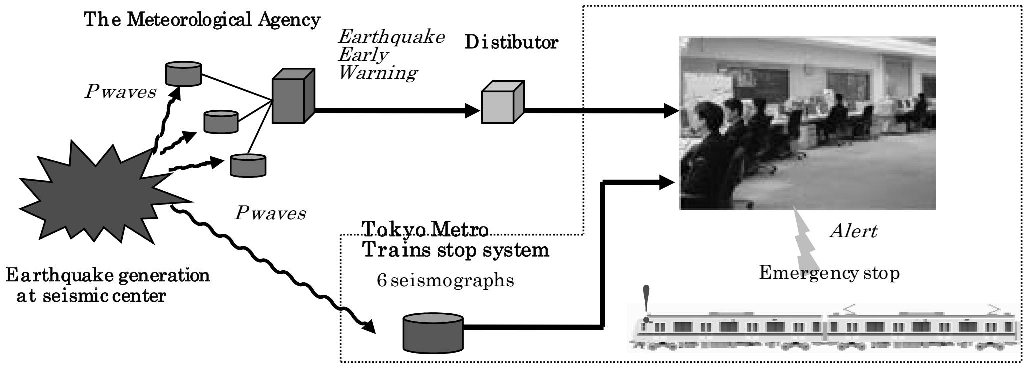

Figure 7: Outline of emergency trains stop system operated in Tokyo Metro

3.2.2 Raising effectiveness of equipment inspection by area seismography's

In addition to the six seismographs that can bring trains to an emergency stop, Tokyo Metro has added "area seismographs" at 36 points along its routes (Figure 8). They are provided for the purpose of efficient inspection and confirmation of the effects of earthquakes on structures.

The area seismographs detect the S waves that exert adverse effects on structures. In areas where earthquake motion exceeded the specified level, inspections will be made by walking through the tunnel after the earthquake, for a detailed investigation to ascertain what damage if any has occurred. In areas where the earthquake motion was less than the specified level, trains will run at reduced speeds to ensure safety.

Once area seismographs were added, inspection efficiency can be enhanced by focusing the inspection on the route section where the earthquake motion is substantial. In this way, the time from the occurrence of the earthquake to resumption of operation can be reduced.

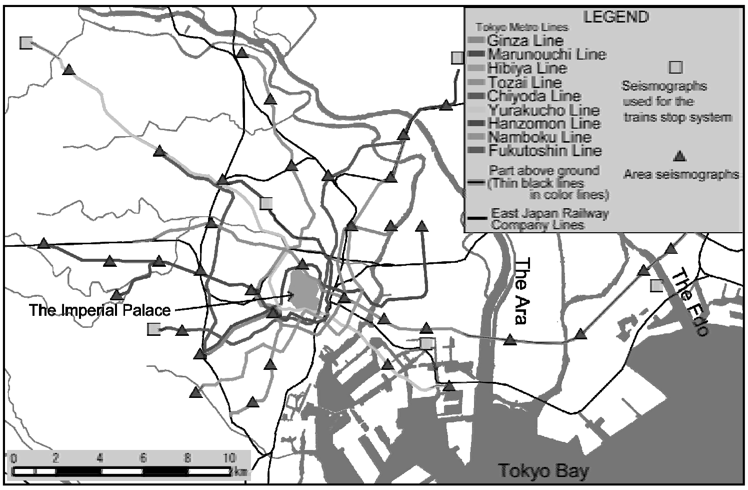

Figure 8: Seismographs installed along Tokyo Metro lines

4. ANTI-INUNDATION MEASURES

4.1 Estimation of Damage and Targeted places

The light green part in Figure 9 indicates the damaged area due to bank rip of the Arakawa River where Ministry supposed. Some color lines show train service lines of Tokyo Metro. The light pink part in Figure 9 indicates flood hazard map of Tokyo Metropolitan Government and the part is the supposed flooded area when Kanda River, Sumida River or other rivers flood by a heavy rain. Because the maps indicate inundation height of each point, we make the plan of anti-inundation measures on the data of the map.

Figure 9: Inundation map of Tokyo

4.2 Anti-Inundation Measures

Subway tunnels are prone to inundation when flooding occurs. Inundation not only makes train operation impossible, it also exposes passengers to harm. Tokyo Metro is taking various measures to prevent inundation. Targeted points of anti-inundation measures are gate ways of underground stations, tunnel entrances and vents.

4.2.1 Cut-off plate and waterproof door at gate way of the station

Cut-off plates or waterproof doors are provided at subway entrances and exits to prevent inundation when flooding occurs. In the normal state, the cut-off plate (Figure 10 left) is housed near the gateway. They are set up to prevent inundation when the risk of inundation increases due to heavy rainfall. The cut-off plates, which are about 70 cm high, can be climbed over by passengers when tunnel evacuation is necessary.

For certain stations located in lowland areas in the eastern parts of Tokyo or near rivers, waterproof doors (Figure 10 right) are also set up at the gateways to prepare for cases in which a cut-off plate would not be enough to prevent inundation. The waterproof doors can protect station entrances and exits, ensuring that inundation of the tunnels will not occur. Stations with low areas have the waterproof doors, and they are provided with elevated gateways for further prevention of inundation.

Figure 10: Cut-off plates and waterproof door at subway entrances and exits

4.2.2 Inundation prevention devices installed at vents

The subway tunnels have vents at various locations. Vents at road surfaces could allow large volumes of water to flow into tunnels when heavy rain or flooding occurs. As a countermeasure, inundation prevention devices (Figure 11) are provided at vent opening on roads. The devices can be remotely controlled from a central operation panel in stations. As they receive information on conditions during heavy rain, station personnel can close the vent before any inundation occurs. In addition, as a means to cope with unexpected localized heavy rainfall, each vent is provided with an inundation sensor that closes the vent automatically when inundation is detected. Improvements are being made to these mechanisms to enable resistance to water pressure at a depth of six meters.

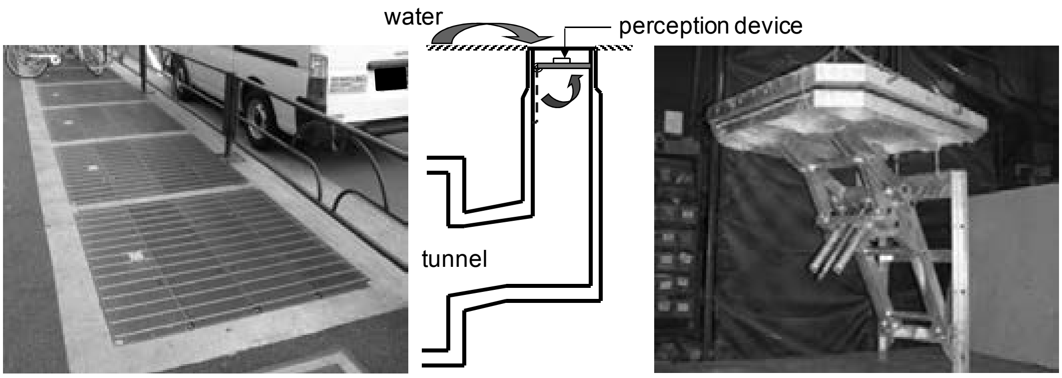

Figure 11: Vents and inundation prevention device

4.2.3 Waterproof gate

The possibility of large-scale floods occurring due to heavy rainfall or a storm surge is high in areas near rivers or in the lowlands spreading to the east of Tokyo. Moreover, these areas could suffer inundation if a tsunami is caused by an earthquake. In the plateaus on the west side of Tokyo, some subway routes have tunnel openings near a river, which poses the risk of water overflowing into the tunnel when localized heavy rainfall occurs.

To prevent large-scale inundation into tunnels, Tokyo Metro has installed waterproof gates (Figure 12) at seven locations in the tunnels. Each of these gates protects the full section of the tunnel to minimize damage and harm to passengers

even in the event of large-scale inundation. These gates are installed around the opening of tunnels in lowland areas, near rivers, and in tunnels running deep below the rivers. Gates can be closed electrically, hydraulically or manually. The time needed to close them is 2 to 4 minutes for hydraulic operation, and 15 to 20 minutes for electric operation. Maintenance work on the waterproof gates is done once a year, using test operation, an air-tightness test, an inspection of electrical equipment parts, and a test of the hydraulic system.
Water entering a tunnel in spite of the waterproof facilities is discharged outside the tunnel by means of drain pumps provided at various locations.

Figure 12: Waterproof gate at normal times and during flooding

5. CONCLUSION

Subway tunnels are a key link in the infrastructure in large cities. Since tunnels are spaces isolated from the ground level and pathways that can be used for evacuation are limited, they are exposed to serious risks in the event of a disaster. Tokyo is frequently hit by typhoons and localized heavy rainfalls every year, and it faces the risk of earthquakes. Therefore, securing the safety of subway tunnels becomes an important and difficult task. Without succumbing to these disadvantages, Tokyo Metro is implementing structural and non-structural measures for the major purpose of securing safe and stable train operations, while assigning top priority to the safety of passengers. Tokyo Metro will not be satisfied with what has been done (as outlined in this paper). It will proceed with efforts to improve and renew disaster-prevention facilities. Tokyo Metro continues efforts daily to enable as many passengers as possible to safely use its subways.

REFERENCES

Tashiro, Y. and Mutou, Y, 2013. *Disaster-Prevention Measures for Tokyo Metro Tunnels*. World Tunnel Congress 2013, Switzerland-Geneva.

For the safety and the sustainable development of Ho Chi Minh City

Ngoc Tran NGUYEN
Professor, Director of Mekong River Delta Development Research Center
nntran2010@gmail.com

ABSTRACT

In every country, a megacity has strong impacts on the economy, the environment and the society, and vice versa is influenced by these factors. Therefore, Ho Chi Minh City, an Asian megacity in a near future, should be approached in terms of economic, social, environmental aspects and governance. The tasks are increasingly necessary in the context of economic globalization and global climate change. This paper refers to a number of urgent issues according to the author's opinion. Science and technology have a lot of tasks to make practical contributions to the safety and the sustainable development of this upcoming megacity.

Key words: Ho Chi Minh City, FDI, rich-poor gap, environment, sustainable development.

I. ABOUT MEGACITIES

A megacity is understood as a city with the population of over 10 million inhabitants. With this understanding, the list of the world's megacities is changing and constantly increasing.

In 2007, *Megacity Challenges* report [1] surveyed 25 cities of which 21 are standard megacities with at least 10 million people.

According to McKinsey Global Institute [2], in 2007, there were 23 megacities in the world. Ranked by population from high downward are: Tokyo, Mumbai, Mexico City, New York, São Paulo, Shanghai, Kolkata, Delhi, Beijing, Chongqing, London, Dhaka, Buenos Aires, Los Angeles, Karachi, Cairo, Rio de Janeiro, Paris, Rhein-Ruhr, Osaka, Manila, Moscow and Istanbul. These 23 megacities account for 5% of the world's population and generate 14% of the global GDP.

Forecasting the growth of megacities by 2025, based on data of 2007, the McKinsey Global Institute (MGI) considers further 600 cities, called *The City 600* by MGI, composed of 23 megacities, 45 large middleweight cities, 143 midsize middleweight cities, and 389 small middleweight cities [1] (Figure 1).

---

[1] A *middleweight city* has a current population between 150,000 and 10 million. *Small*: 150,000–2 million; *Middle*: 2 million–5 million; *Large*: 5 million–10 million).

In 2007, *The city 600* accounted for 22% of the global population and generated 54% of the global GDP.

In *The city 600*, the developing countries had 16 megacities (69.6%), and 407 Cities 600 (67.8%).
To emphasize the importance of megacities, two criteria usually considered are the rate of population and the rate of GDP of megacities over the world population and the global GDP.

For a megacity of a nation, two corresponding criteria are the rates of population and GDP over the population and the GDP of the country.

Figure1. The city 600 in the world (MGI 2007)

Among 23 megacities listed by MGI, the Asia has 11: Tokyo, Mumbai, Shanghai, Kolkata, Delhi, Beijing, Chongqing, Dhaka, Karachi, Osaka, and Manila.

F. Krass and U. Nitschke (2008) [3] introduced their forecast of megacities in Asia in 2015 (Figure 3)

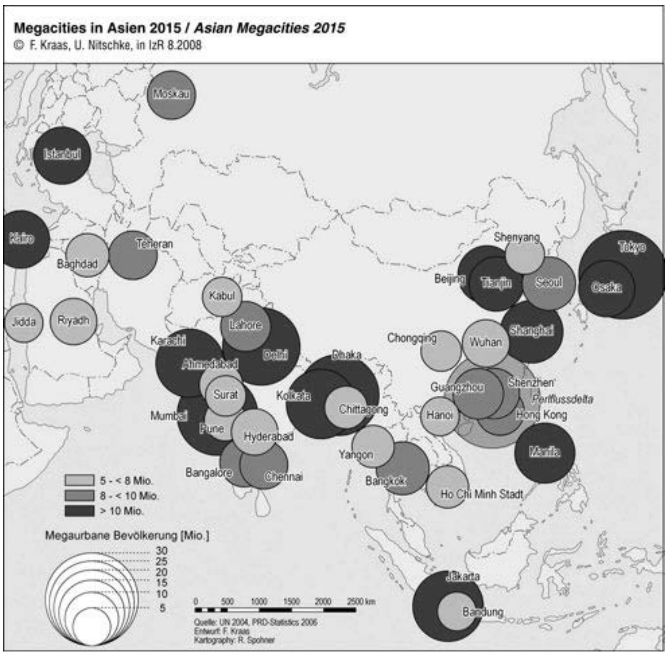

Figure 3. Asian megacities in 2015

It can bee seen that the great majority of megacities (or those soon to become megacities) are in the developing countries. This is true not only in Asia, but also on the global scale, as seen when talking about *The city 600.*

2. HO CHI MINH CITY, A MEGACITY IN A NEAR FUTURE

Table 2 provides the results of the census in the whole country and in Ho Chi Minh City in 1979, 1989, 1999 and 2009.

Table 2. Data of the census in Ho Chi Minh City

POPULATION OF HO CHI MINH CITY OVER 4 CENSUSES				
Ho Chi Minh City	01.10.1979	01.10.1989	01.4.1999	01.04.2009
Total	3,419,978	3,988,124	5,037,155	7,162,864
in urban area	2,700,849	2,946,426	4,204,662	5,968,384
in rural area	2,719,129	1,041,698	832,493	1,194,480
Ratio urban/rural	79.0%	73.9%	73.9%	83.3%
Male	1,622,072	1,890,343	2,424,415	3,435,734
Female	1,797,906	2,097,781	2,612,740	3,727,130

The growth rate of the population every 10 years significantly increased: 16.6% in 1989 compared to 1979, 26.3% in 1999 compared to 1989, 42.2% in 2009 compared to 1999.

The ratio of urban population over total population in Ho Chi Minh city decreased in 1989 compared to that in 1979, and highly increased in 1999 and in 2009.

The above comments are clearly illustrated through the growth of residential built-in land in which construction has been made in the land-use maps in 1985 and 2010 of the city (Figure 4)

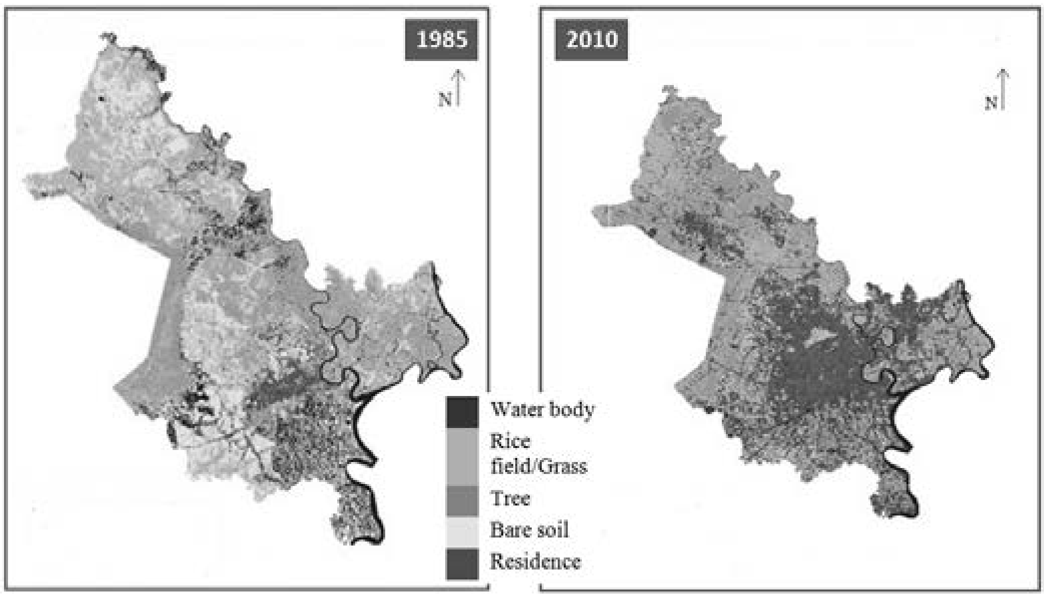

Source: Ho Long Phi et al. (Personal communication of Ho Long Phi)

Figure 4. Map for land use of Ho Chi Minh City in 1985 (left) and 2010 (right)

The GDP growth of Ho Chi Minh City over 20 years (1990-2011) is quite rapid, from 17,993 to 166,423 billion VND (1994 compared value), accounting for national GDP from 13.63% to 28, 49% (Figure 5)

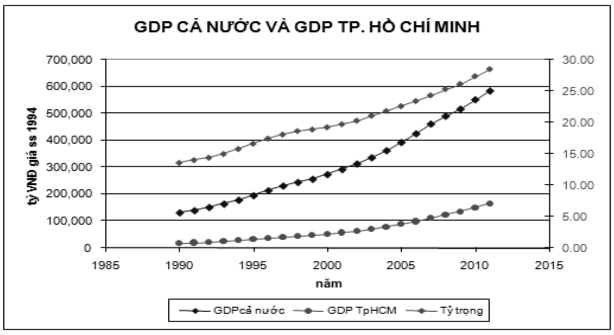

Figure5. National GDP, GDP of Ho Chi Minh City and ratio

In the 1980s, developed countries promoted foreign direct investment with the aim of seeking for high profits from abundant and cheap human resources in the developing countries.

This intention coincides with the "thirst” for capital and technology of the developing countries. This is time for the arrivals of foreign direct investment in these countries in the early 1980s [4].

After that, trade liberalization, economic globalization and the establishment of the *World Trade Organization WTO*, instead of the *General Agreement on Tariffs and Trade GATT*, in 1995, expanded direct investment to the indirect investment. The concept of trade henceforth included goods, intellectual property and services, particularly financial services. This means for the developing countries at the same time opportunities interlaced with challenges to receive investment from outside.

Industrial parks, offices, hotels, villas, luxury apartments and recreational facilities along with transportation infrastructure, communications grew rapidly. Opportunities for employment attract human resources in different qualifications. Thanks to that, the urban appearance has been also more modern and spacious. These are "pushes" for the rapid formation of megacities in developing countries.

It should be also added that some megacities in Asia was formed associated with services in the Vietnam War during the years of 1960 - 1970 and then when Vietnam faced embargo until the mid 1990s.

Law on foreign direct investment in Vietnam was first issued in 1987. However, capital flow of foreign investment actualy arrived into Vietnam in general, and Ho Chi Minh City in particular, only since the mid-1990s after the United States lifted the embargo and normalized relations with Vietnam.

The number of FDI projects and total investment capital valid till 31.12 every year has steadily increased since 1995 so far (Figure 6).

With this momentum of development, in a short time, it is no doubt that Ho Chi Minh City will become an Asia's megacity.

Among causes for the rapid development of Ho Chi Minh City, state management factor has exploited the needs of multinational companies investing into foreign countries, and catched the opportunities opened by the trade liberalization, in combination with promoting resources and the geographical - political - economic position of the City and the country.

However, together with those opportunities, there are a lot of economic, social, environmental and state management challenges.

FDI VALID TO 31/12 ANNUALLY

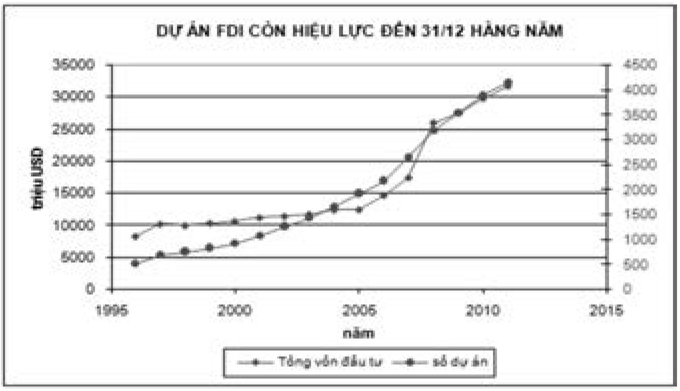

Source: Department of Statistic of Ho Chi Minh

Figure 6.Number of projects valid to 31.12 annually and total corresponding investment

3. SOME FACTORS AFFECTING THE SAFETY OF HO CHI MINH CITY

3.1. With regard to the economy

Since the rapid growth of the economy depends mainly on the foreign investment, this fact itself contains risks of unsafety, when capital flow from outside, for some reason, decreases. Therefore, developing the internal resources of the economy is a task of strategic significance.

In an increasingly globalized economy, the crisis can occur from another country. The 2007 financial crisis started in Thailand and the 2007 economic crisis erupted in the United States have impacted on the worldwide economy, on Vietnam and Ho Chi Minh City in particular. Recently, countries and cities experiencing (or on the edge of) bankruptcy have provided experiences and lessons of how must be an *active integration.*

While focusing the investment for Ho Chi Minh City, the city's leaders take interest for the suburban and the rural areas of the City.

The development of Ho Chi Minh City has to be associated with the Southern major economic area and to link with the Mekong Delta, to promote each other's strengths and cooperation for the mutual development. Moreover, human resources necessary for the development of the City come from all over the country, the southern provinces at first.

The above guidelines, correct and necessary for the safety and the development of Ho Chi Minh City, must be pursued with more and more efficiency.

3.2. With regard to the society

Among number of issues, the one should be paid most consideration is the *poverty of the urban people* because of its significance for the social cohesion, the safety and the sustainable development of the City.

According to the report *Ho Chi Minh City, 35 years of establishment and development* [5], the growth rate of GDP per capita of the City is as follows:

Table 4. Growth rate of GDP per capita of Ho Chi Minh City

Gdp Growth Rate Per Capita Of Ho Chi Minh City						
76-80	81-85	86-90	91-95	96-00	01-05	06-10
1.32	2.96	5.57	9.97	7.16	7.51	7.32

From 1996 to 2008, the proportion of households with usual living facilities increased regularly.

The elimination of a great number of practically insolvable slums, and "black water hamlets" existed before inside the City, is a renown of Ho Chi Minh City.

Paying continuous attention to citizen in general, migrant workers and especially the poor, is a just policy of the City and needs to be continued since many social issues, starting points of social evils, remain to be solved.

Recently, the project "*Monitoring Urban Poverty 2008-2012*" by Oxfam Vietnam has investigated the poverty status of the urban people [6].

According to the project, "in the last 5 years (2008-2012), life of majority of the urban poor at monitoring sites has been improved. (...) Urban poverty in Viet Nam reduces gradually if looked at only income or expenditure terms, even if the poverty line is raised. However, once other dimensions are considered, urban poverty remains a concern."

Multidimensional poverty is understood the lack of basic shortages which prevent uninterruptedly the urban poor from escaping the poverty.

For the native poor, there are five basic shortages: "lack of labor and skill", "lack of capacity to find alternative livelihoods", "lack of social capital", "limited access to public services", "uncomfortable and unsafe living environment”.

Five basic shortages for the migrant poor are: "high living costs", "unstable employment", "lack of social integration", "limited access to public services", “uncomfortable and unsafe living environment”.

The report concludes: If the challenges are not properly dealt with, quality of lives of the local and migrant poor will remain low, their vulnerability will be high, and the inequalities will continue to be increased.

The eight recommendations for action on poverty in urban areas proposed by the report should be paid much concern.

3.3. Environment and flood situation in the City

Traffic congestion, air, sound, water pollutions, flood due to heavy rains and high tides, and greenhouse gases emitted are increasingly urgent issues that Ho Chi Minh City have to solve the sooner the better in order to avoid heavy difficulties encountered by other Asian megacities.

Frequent flood situation in the City causes effectively many obstacles for production activities, business and life of the inhabitants and needs to receive adequate solutions.

Ho Chi Minh City borders with the East Sea at Can Gio district by a dense network of rivers and canals. Its center is 50 km crow-fly far from the sea. Therefore, the City is strongly affected by the climate change and the sea level rise. Preserving the Can Gio mangrove forest in this context not only means conserving the green lungs of the City but also means responding to climate change.

Ho Chi Minh City is at the confluence of Dong Nai, Sai Gon, Vam Co Dong rivers flowing into the East Sea by a network of channels in which the most important are Soai Rap and Long Tau rivers through which the tides come into the City.

In recent years, the situtation of flood in the city has been happened more often along with tides and heavy rains. Water resources institutions have proposed measures to prevent flood such as: placing dikes and sluices along the Vam Co Dong and Soai Rap rivers (Figure 7). These are quite expensive solutions generating the profound environmental changes while effectiveness is yet monitored and evaluated.

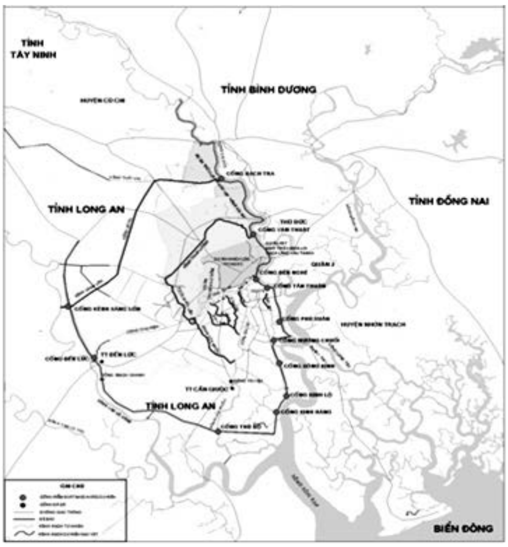

Figure 7.Work solution of irrigation sector (stage 1)

Flood in the city depends on the hydrological regime of the rivers and the tidal amplitude in the estuary. It aslo depends on the water drainage system of the City, on the natural and the accelerated land subsidence in the area.

The designed capacity of the water drainage system of the city depends on many parameters such as population, rainfall in the basin, the area of the water storage and absorption zones etc... Therefore, when the basin surface becomes imperviable where it was pervious and/or capable to store water before, then volume of water drained into the river will be more and more rapid, causing water drainage system and rivers overloaded

Figure 8 shows the remarkable decline of the water storage and absorption since the urbanization of Ho Chi Minh City so far (See also Figure 4 for the rate of urbanization).

Accelerated subsidence is caused by groundwater surexploitation, mining, construction of buildings and urban infrastructures.

Since the 1990s, the City has begun its urbanization, hundreds thousands of cubic meters of groundwater has been exploited every day, especially in new urban areas. Groundwater levels of the city have decreased over 20 meters since 1990, significantly contributing to the deformation of the ground of city.

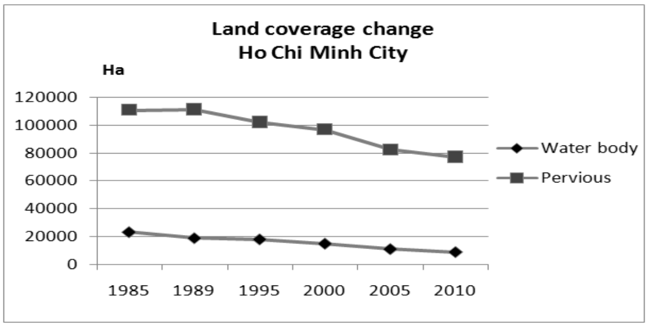

(Personal communication from Ph.D. Ho Long Phi)

Figure 8. Decrease in area of water storage and absorption of Ho Chi Minh city)

The primary measured results of PS InSAR technique shows the strain rate with range from -10 to +8 mm / year (Figure 9) and the subsidence in some areas in the inner City of 30 mm during the period from 1996 to 2003 [7].

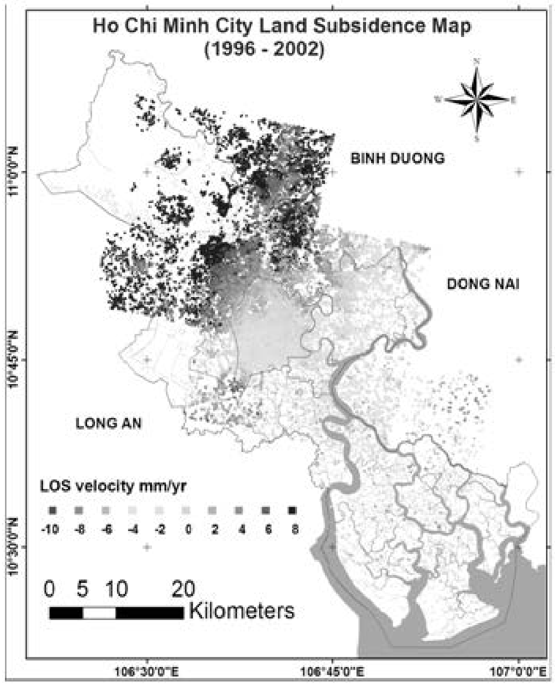

Source: L.V.Trung, H.T.M.Dinh (2009)

Figure 9. Ground deformation in Ho Chi Minh City (1996-2002)

Analyzing hydrological data from 1988 to 2008 shows that during this period at Vung Tau station the increase trend of the highest annual high tide level on average is of 3.88 mm / year while at Phu An station that is 14.23 mm / year, 3.7 times higher than in Vung Tau [8]. Does this increase derives from internal impacts in areas of Saigon and Dong Nai rivers? That is a main question the research of anti-flood measures for HCMC has to clarify.

4. FOR A SUSTAINABLE DEVELOPMENT OF HO CHI MINH CITY

With a population of 7.7509 million people in 2012, excluding the number of residents without registration in the area, the fact that Ho Chi Minh City becomes a megacity in the future is obvious. However, as seen above, to make it a safety megacity with sustainable development, Ho Chi Minh City has to deal with many issues.

The City should refer to the achievements and especially the difficulties and challenges faced by Bangkok, Manila, Jakarta in its development process, to learn therefrom necessary lessons and experiences, particularly in the context of climate change [9].

Global Summit on sustainable development in Johannesburg in 2002 agreed that for sustainable development, it should be based on three main pillars: economic growth, social equity and progress, and environmental preservation [10].

Economic growth and social equity and progress satisfied, but the environment degraded and exhausted will not provide sustainable development.

Economic growth and preserved environment satisfied, but persists and enlarges the fracture between rich and poor, it also will not be able to develop stably.

A development model in which the results of achievements are equally divided for all the people, the environment is protected, but the economy is not growing, this model will not survive long time, especially in a world with fierce competition and large exchanges.

Figure10. Sustainable development model

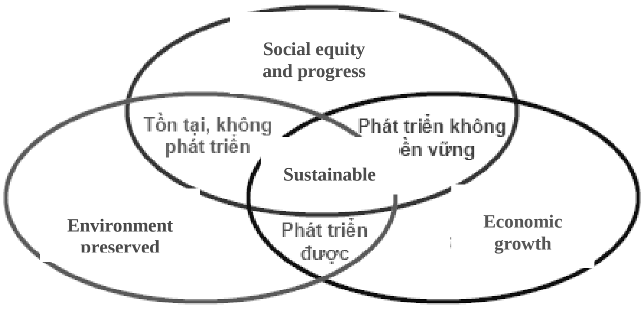

A nation or a city can only develop sustainably when its development model lies in the intersection of three circles *Economy, Society, Environment*, i.e the model must ensure *simultaneously* economic growth, equity and social progress, and environmental preservation (Figure 10).

To develop such a model, the prerequisite is that a nation or city must be *well governed.*

In all four sectors economic growth, environmental protection, equitable, democratic and civilized society, and good governance, as seen above, Science and Technology can participate largely and effectively.

I would like through this paper, share with the Conference some ideas to make Ho Chi Minh City a safe and sustainable megacity.

REFERENCES

[1] GlobeScan and MRC McLean Hazel, *Megacities Challenges*, *A Stakeholder Perspective* (2007), Research Project sponsored by Siemens.

[2] McKinsey Global Institute, *Urban World Mapping the Economic Power of Cities*, 2011.

[3] Krass F., Nitschke U. (2008), *Mega-urbanisation and Global Change in Asia: Processes, Problems and Perspectives*,
Kraas, F. (2007): *Megacities and global change: key priorities*. Geographical Journal 173 (1): 79-82.

[4] Nguyen Ngoc Tran, *Foreign Direct Investment* in *Some of current global economic issues*, 109-184, Thế Giới Publishing House, 2003, in Vietnamese.

[5] Ho Chi Minh city Development Research Institue, *Ho Chi Minh city, 35 years of establishment and development (1975 – 2010)*, 2012, Ho Chi Minh City General Publishing House, in Vietnamese.

[6] Oxfam Vietnam, *Poverty reduction in Vietnam: new challenges, new approach*, 2012, http://oxfaminvietnam.wordpress.com/resourcesbao-cao/

[7] L. V. Trung, H. T. M. Dinh (2009). *Monitoring Land Deformation Using Permanent Scatterer InSAR Techniques (Case study: Ho Chi Minh City)*. The 7th FIG Regional Conference on Spatial Data Serving People: Land Governance and the Environment – Building the Capacity. Hanoi, Vietnam, 19-22 October 2009.

[8] Nguyen Van Dang, Nguyen Ngoc Tran, Changes in rain and water level in Nam Bộ. Analysis of hydrological data in the period of *1988-2008*. Technical report of Mekong Delta Development Research Center (MDDRC), February, 2010.

[9] World Bank, *Climate Risks and Adaptation in Asian Coastal Megacities. A Synthesis Report*, September 2010.

[10] Nguyen Ngoc Tran, *Johannesburg Submit Conference 2002 and Sustainable Development,* in *Small Stones for the Sustainble Development,* p.30-38, Tre Publishing House, 2011.

History and recent trend of Tokyo Metro's tunnel construction technology

Shinji KONISHI[1], Satoshi ITO[2], Takashi HIRANO[3]
and Kazufumi NOYAKI[4]
[1] Assistant General Manager, Engineering Division, Tokyo Metro Co., Ltd., Japan
s.konishi.r4r@tokyometro.jp
[2] Construction Work Office Manager, Renovation & Construction Department, Tokyo Metro Co., Ltd., Japan
[3] Design Section Assistant Manager, Renovation & Construction Department, Tokyo Metro Co., Ltd., Japan
[4] General Manager, Renovation & Construction Department, Tokyo Metro Co., Ltd., Japan

ABSTRACT

The Construction of the first subway in Asia was started in 1925 and operation of it was started in 1927, 87 years ago by the former Tokyo Metro Company. This is a part of the Ginza line, between Asakusa and Ueno in Tokyo. Since the event, we constructed a lot of lines. Now, we operate nine subway lines with 195.1 kilometers of track that predominantly serve Tokyo's 23 wards and carry 6.4 million passengers each day.

The report introduces some topics of our construction history for new subway lines. After that, it describes recent two cases of tunnel construction, The Fukutoshin line and the Kotake-mukaihara bypass tunnel, with discussing trend of recent technology for tunneling.

Keywords: subway, neighboring construction, shield tunnel, traffic networking

1. INTRODUCTION

The chronological table of subway construction in Tokyo Metro is shown in Figure 1 (Renovation & Construction Department, Tokyo Metro Co., Ltd., 2005). Figure 2 shows the distance ratio of cut-and-cover work and shield tunnel construction in each line. Now, 70% of total tunnel length, 166.8km, is cut and cover tunnel and 30% is shield tunnel. The evolution of cut and cover technology in Tokyo Metro is shown in Figure 1. The epoch-making changes are that steel materials started to be used for temporary materials from 1960's and underground diaphragms started to be adopted for earth-retaining wall from 1970's. Owing to the evolutions, wider and deeper underground space can be constructed safely by the cut and cover method. After that, fundamental techniques of cut and cover method haven't evolved remarkably without some auxiliary methods, underpinning method and information-oriented construction.

However, technical innovation of shield tunneling method advanced remarkably in recent years. Therefore, over 70% new tunnels of Tokyo Metro are constructed by shield tunneling method. In this paper, the construction history of Tokyo Metro's tunnel, with focus on shield tunneling method, is described. Then, it describes recent two cases of tunnel construction, the Fukutoshin line and the Kotake-mukaihara bypass tunnel, with discussing trend of recent technology for tunneling, because new technologies were applied for the two tunnels with the object of reducing costs and environmental load.

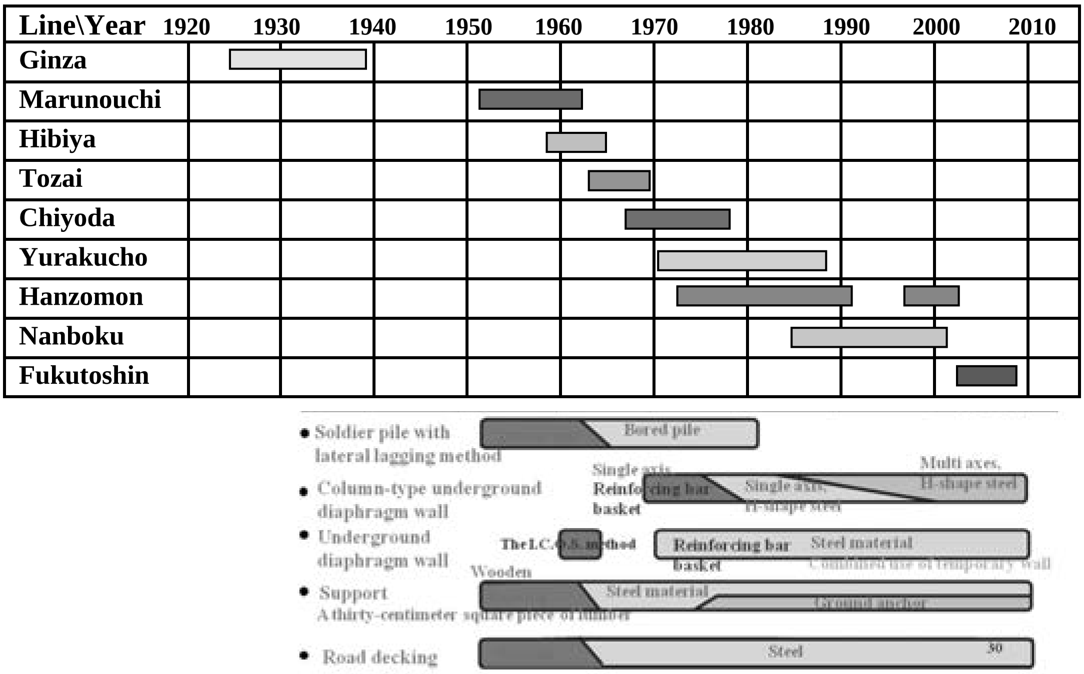

Figure1: Chronological table of subway construction in Tokyo Metro

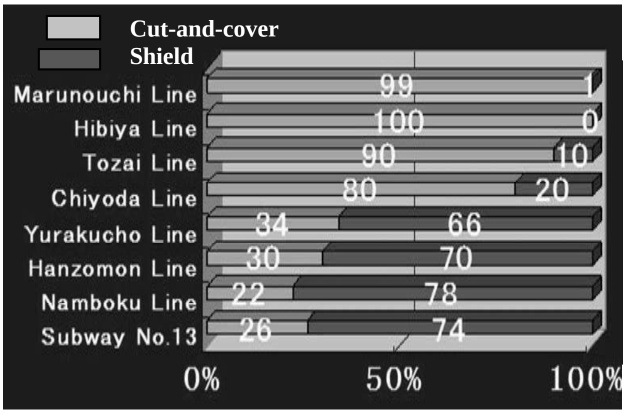

Figure 2: Distance ratio of cut & cover and shield tunnel

Table 1: Number of open type and closed type shield

Year	Open type	Closed type
-1965	3 tunnels	
-1970	16 tunnels	
-1975	21 tunnels	
-1980	20 tunnels	1 tunnels
-1985	1 tunnels	5 tunnels
-1990	-	9 tunnels
-1995	-	11 tunnels
-2000	1 tunnels	22 tunnels
2001-	-	10 tunnels
Total	62 tunnels	58 tunnels

2. HISTORY OF TOKYO METRO'S TUNNEL CONSTRUCTION

2.1 Shield tunnel

Table 1 shows the number of an "open type shield tunnels" and a "closed type shield tunnels" every five years. Tokyo Metro already constructed over 130 shield tunnels. At first, a tunnel of the Marunouchi line was constructed by roof shield method in 1957. Next, full-scale circular shield tunnel was adopted for the Touzai line in 1964. Nowadays, the method is used not only for the tunnels between stations but also stations. Shield tunneling method was used for around 75% of all tunnels recently. Since 1980's, closed type shield started to be applied. The "closed type shield" is the most common type used over the past 20 years.

Recent topics of shield tunnel evolutions are increasing in size of the cross section and diversification of the cross section shape. The 10m across in diameter class shield tunnel, like subway tunnel, had the largest cross section previously. Subsequently, large size tunnels with from 11m to 14m across in diameter were constructed, because the method was adopted for the underground retention basin, underground river and underground road tunnels.

The biggest railway shield tunnel in Japan, which has 13.92m across in diameter and has 3 track lines, was constructed in the Nanboku line of Tokyo Metro, opened in 2000 (Figure 3). Technical summaries of the large scale tunnel are shown in below.

1. To keep tunnel face stability with large difference of earth and water pressure between the crown and bottom of the tunnel face.
2. To have the full mixing capacity in a chamber and earth-removing capacity.
3. To keep high accuracy of the shield machine and segments.
4. To equip the full cutting power coping with increase of cutting torque.

Regarding the diversification of cross section shape, a round shape is the main shape of shield machines as yet, because of advantages of simple rotation structure with one axis and strong ring structure. However, multi circular shield, such as double faced shield and triple faced shield, are applied recently, as shown in Figure 4. Moreover, elliptic-type shield, rectangular-type shield and compound circular shield (Figure 5) were developed for these 10 years due to the necessity.

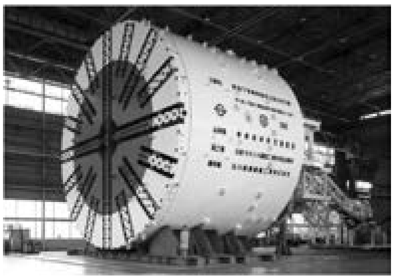

Figure 3: Mother and child shield machine

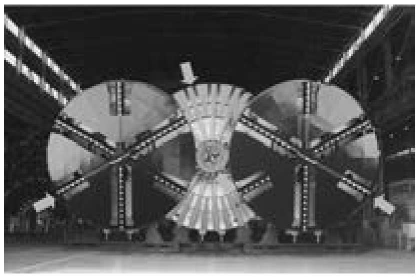

Figure 4: Triple circular type shield machine

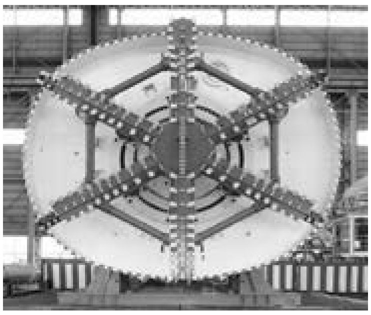

Figure 5: Compound circular shield

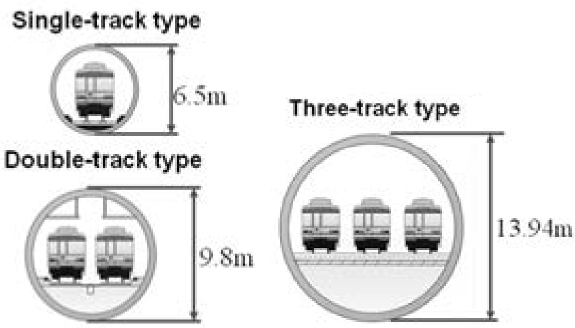

Figure 6: Transition of shield tunnel shape between stations in Tokyo Metro

Figure 6 shows the transition of shield tunnel shape between stations in Tokyo Metro. Circular tunnel of single-track type, double track type and three-track type are standard. However, compound circular shield was developed and applied in Fukutoshin line of Tokyo Metro.

2.2 Station by shield tunnels

Figure 7 shows the transition of shield station tunnel shape. In old times, 1970's, the enlarge method between two shield tunnels by mining were used generally. However, the method need very complicated processes with dangerous work, long term and high cost. The station tunnels come to be constructed at one stroke by a multi circular face shield machines with the advance of technology, because the method can improve safety, term and cost of the construction work.

An example of station tunnel construction method with a removable triple circular shield machine is shown in Figures 8, 9. The method was used for the construction of a part of the Nanboku line in Tokyo Metro and can construct a station and tunnels between stations with one shield machine, because the machine can be changed its cross section with putting on and taking off the both side shields.

Figure 10 shows a construction method of the double track tunnel and triple track tunnel with one shield machine (Figure 3). The machine is the mother and child shield machine. The ultra-large shield machine, the mother shield machine, with a diameter of 14m has a shield machine, the child shield machine, with a diameter of 10m build-in.

The triple circular type shield machine with same diameter, is shown in Figure 4, was used for construction of a station tunnel and triple tracks tunnel in the Hanzomon line of Tokyo Metro. The machine has two circular cutting heads with one axis respectively on both sides and a shaking cutter in the middle part.

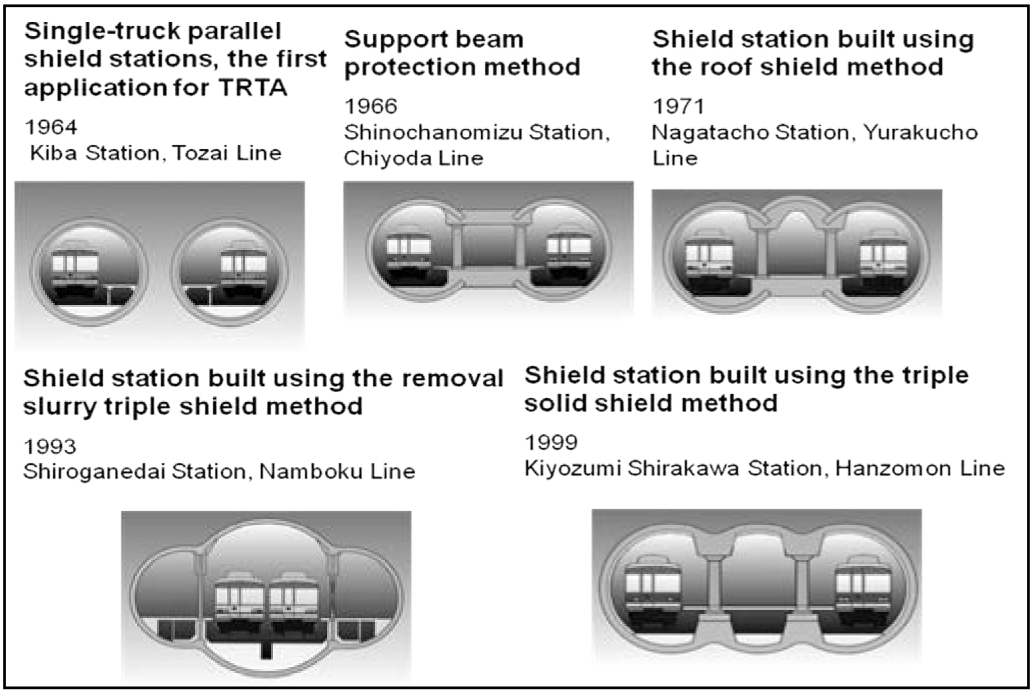

Figure 7: Transition of shield station tunnel shape in Tokyo Metro

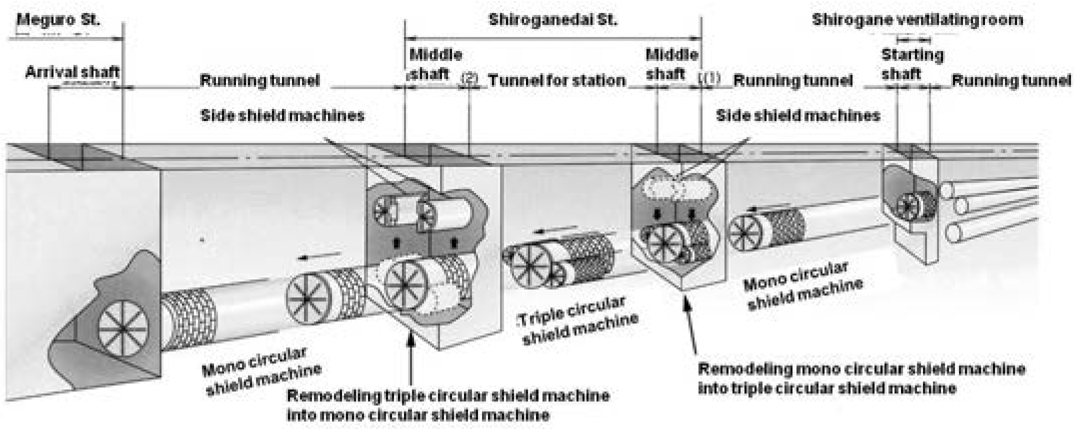

Figure 8: Construction method with the removable triple circular shield machine

Figure 9: Removable triple circular shield machine

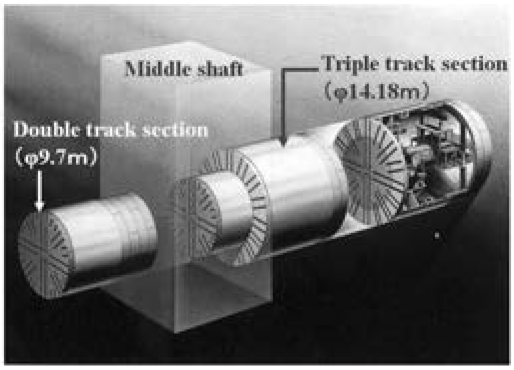

Figure 10: Construction method withir the mother and child shield machine

3. RECENT TREND OF TOKYO METRO’S TUNNEL CONSTRUCTION

3.1 Construction of the Fukutoshin line

The Fukutoshin Line, 11.9km in length and opened Jun.2008, is a subway which connects three leading shopping districts (Ikebukuro, Shinjuku, Shibuya) in Tokyo (Figure 11). Altogether, ten shields were used for tunnel construction including stations (Nishimura, 2012). They include machines for two special shield tunneling methods. They are the compound circular shield and mother-and-child shield.

3.1.1 Compound circular shield

The compound circular shield is the shield made combining circles with three different curvatures. It was adopted for usage in tunnel construction between the Meiji-jingumae station and Shibuya station. Because the width is greater than the height, expand-and-contract cutters at the end of the spoke of the shielding machine are attached (Figure 5). The red portion in the figure is the "expand-and-contract cutter." Although this spoke rotates and it excavates underground, if a spoke comes upwards, the red portion will withdraw.

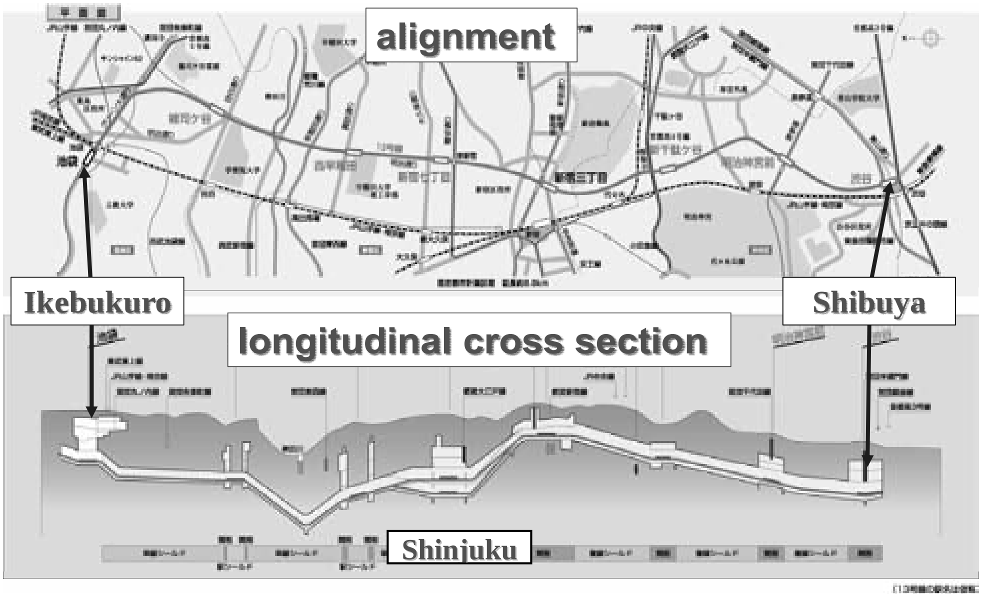

Figure 11: Alignment and longitudinal cross section of the Fukutoshin Line

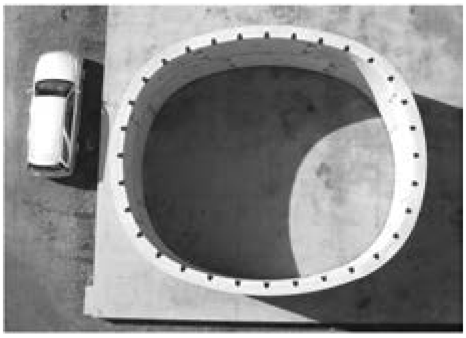

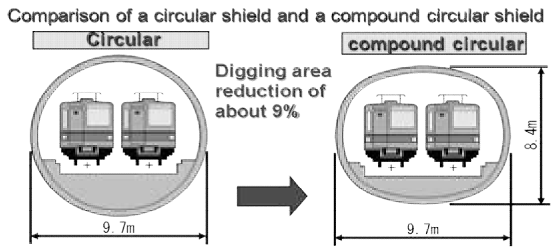

	Space area	Digging area
A : Circular	46.95m^2	73.90 m^2
B : Compound Circular	46.05 m^2	67.30 m^2
A/B	0.98	0.91

Figure.12: Form of compound circular tunnel

Figure13: Comparison with a circular and compound circular shield

Figure 12 shows the tunnel form seen from above. Figure 13 shows a comparison with a circular shield and compound circular shield. The area of the space of a tunnel will be 98% and has almost the same space. However, the digging area will be 91% therefore reducing 9%. So, this shield tunneling method is very good for the environment and cost.

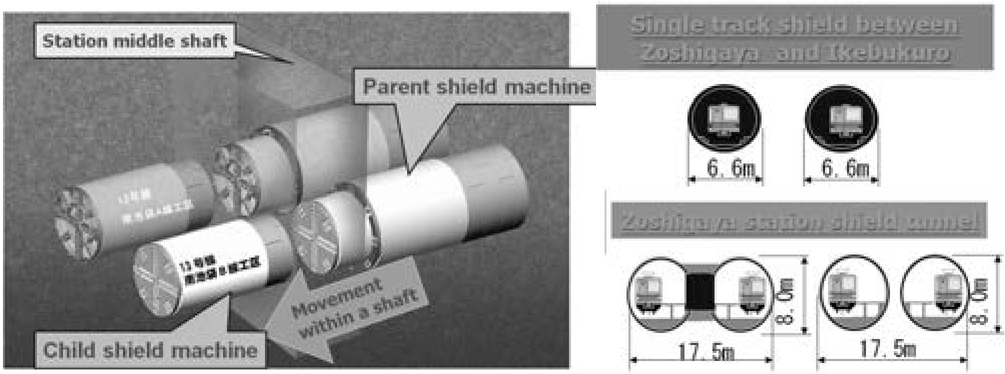

Figure 14: Construction method with the mother & child shield machine

3.1.2 Mother-and-child shield

The mother-and-child shield machine is used for the construction method adopted for construction of both stations and tunnels between stations (Figure 14). By using this one machine, we could reduce cost. With this one mother-and-child shield machine, tunnels of two different sizes can be built. The machine has the structure which included the small shield (called "child shield") inside the large shield (called "mother shield"). When the "mother shield" reaches the intermediate shaft, we extract the "child shield", and re-start the "child shield" to build the structure.

3.2 Construction of the Kotake-mukaihara bypass line

3.2.1 Outline of the Kotake-mukaihara bypass line

The new bypass line is located between the Kotake-mukaihara and Senkawa station on both the Yurakucho and Fukutoshin Lines. Figure 15 shows the present state and the improvement plan of this level crossing section (Noyaki, 2011). Here, the line from the north-western area of Tokyo (Nerima) comes in to join the already existing parallel sections of the Yurakucho and Fukutoshin Lines. The operation pattern here is extremely complicated, including the four routes shown in Table 2. A seamless network has been established by planning the level crossing between Route (2) and Route (3). As the train interval becomes tight between Routes (2) and (3) in this level crossing section, the following train has to stop temporarily before crossing to wait for the preceding train to pass. This causes a delay in the diagram. For this reason, the bypass tunnels for the Yurakuchou line between the Kotaemukaihara and Senkawa station were constructed and the level crossing section was removed.

Table 2: Operation patterns

No	To the starting point	To the terminal point	Level crossing
1	To Nerima Station (Seibu Yurakucho Line)	Shin-kiba Station (Yurakucho Line)	No
2		Shibuya Station (Fukutoshin Line)	Yes
3	To Wakoshi Station	Shin-kiba Station (Yurakucho Line)	Yes
4		Shibuya Station (Fukutoshin Line)	No

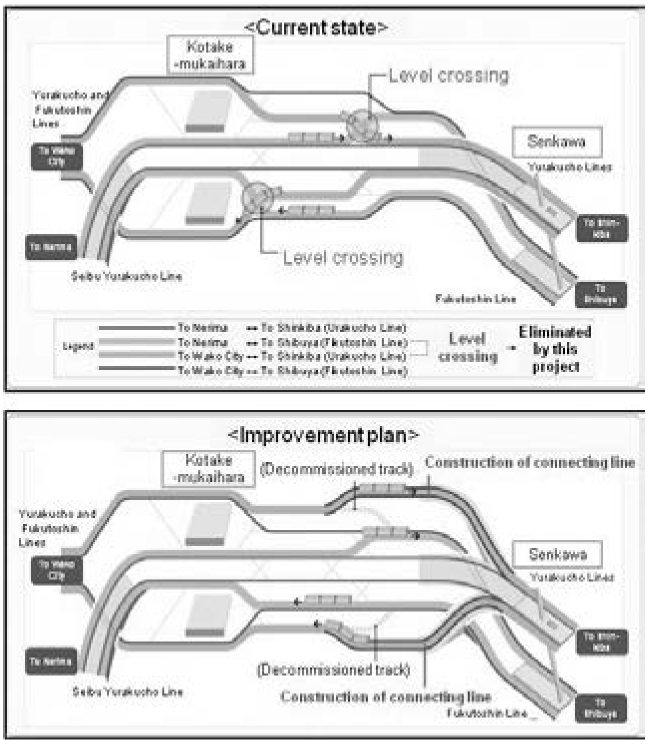

Figure 15: Present state and the improvement plan of this level crossing section

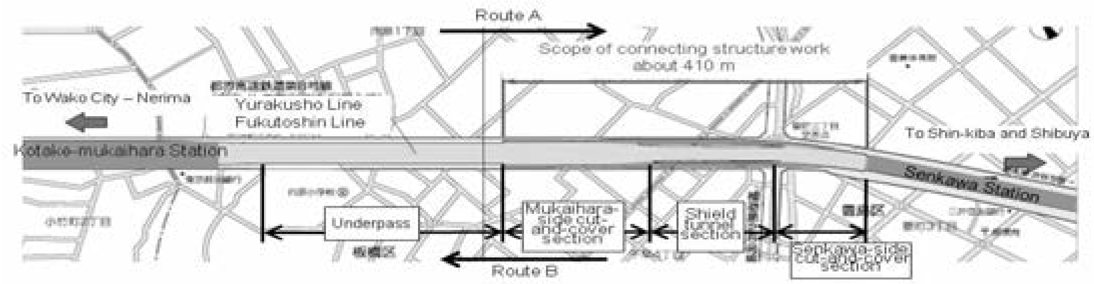

Fig.16: Plan view of the Kotake-mukaihara bypasses line

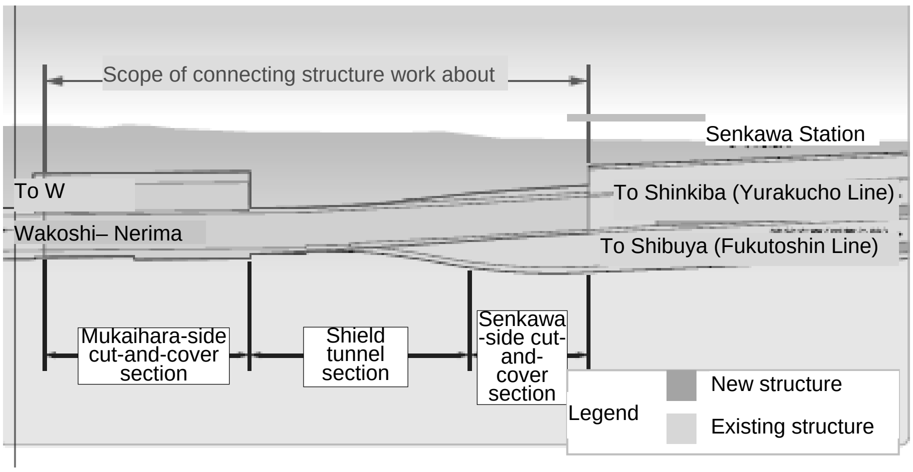

Fig. 17: Vertical sectional view of the Kotake-mukaihara bypasses line

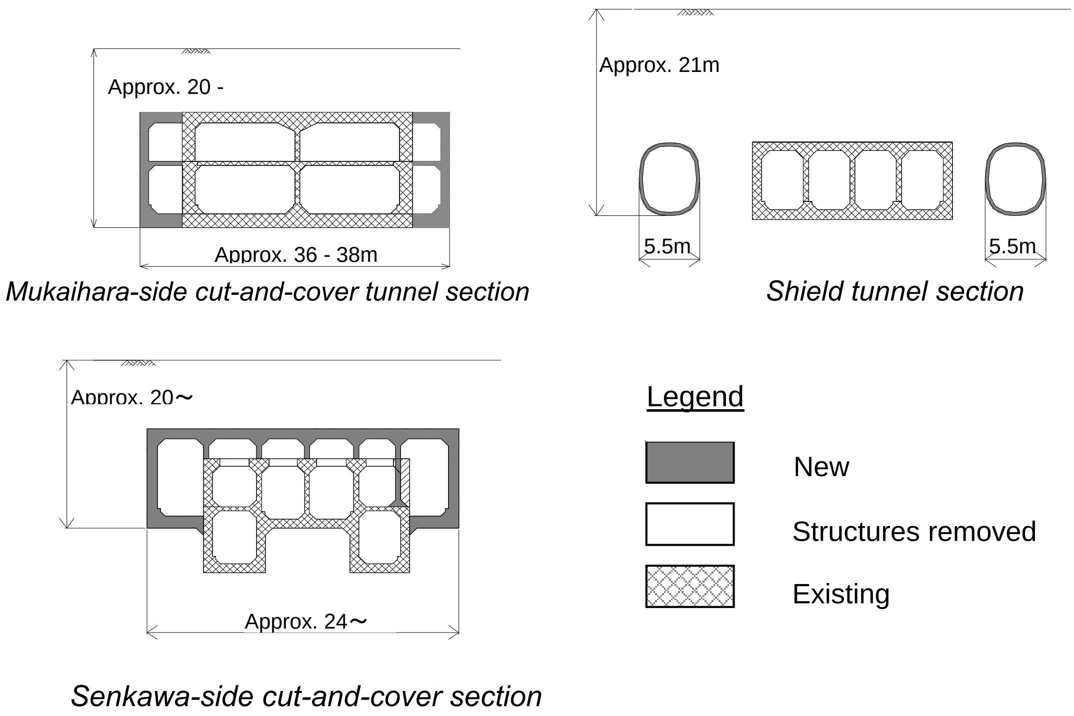

Fig. 18: Sectional view of the structures

Because of the traffic congestion problem, environment problem of noise and vibration, cost reduction and shortening of construction period, the improving area was decided to be approximately 410m and the structures were divided into three sections:

(1) A cut and cover tunnel on the Mukaihara side
(2) A shield tunnel section
(3) A cut and cover tunnel on the Senkawa side

The scope of each structural type is shown in Figures. 16, 17 and a sectional view is shown in Figure. 18

The cut and cover tunnel had to join into the existing tunnel. Therefore, at first the bypass tunnels were set on side or top of the existing tunnels. Then, side walls and upper slabs of the existing tunnel were removed. The work was very difficult, because it was ultra-adjacent construction to the rail track under operation. However, we completed the work without any problem due to the detailed construction plan and suitable process.

3.2.2 Shield tunnel section

The sectional shape of the shield tunnel section was decided to be the combined-circular section as shown in Figure 19. The principal objectives are as follows:

(1) Securing sufficient distance from private land.
(2) Securing sufficient distance from existing structures.
(3) Reducing the environmental impact by reducing the sectional area.

Table 3 shows the comparison of the sectional area relative to the circular section.

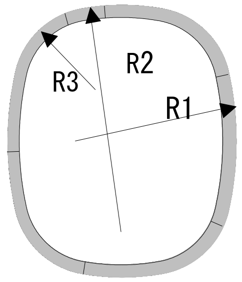

Table 3: Comparison of the sectional area relative to the circular section

	Excavation sectional area	Tunnel internal space area
A: Circular(Φ6.6m)	34.21m^2	26.48m^2
B: Combined-circular	31.15m^2	23.64m^2
B/A	0.91	0.89

R1=5500mm, R2=7800mm, R3=2000mm (Combined-circular: H6.6m x W5.5m)

Figure 19: Combined circular section

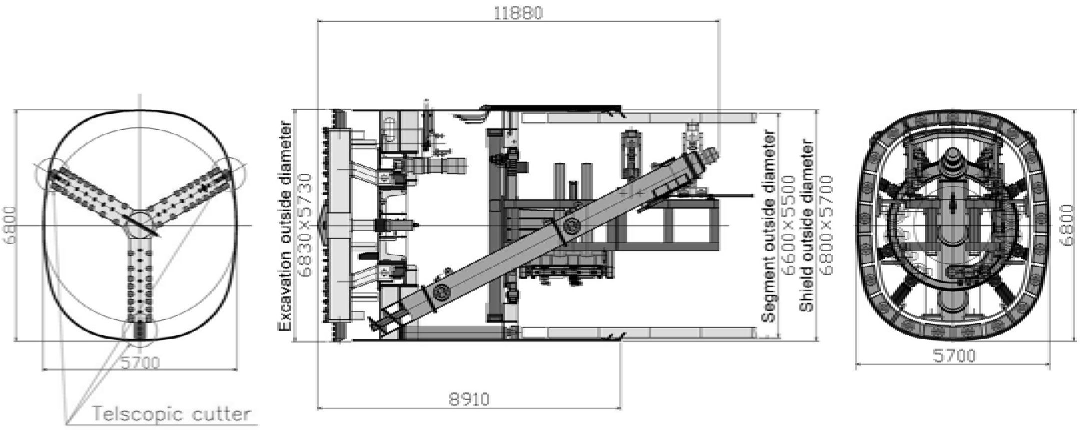

Figure 20: Details of the shield machine

The use of a combined-circular section enables securing trouble-free internal space for subway operation while reducing the sectional area by 10% from the circular section. The segments used were reinforced-concrete designed after considering the working load and economy. The segment thickness was determined on the basis of the thickness needed in terms of design, while attempts were made to reduce the thickness to secure an internal section (construction gauge) needed for subway operation. The thickness was set at 300 mm and width was set at 1,500 mm. For splitting, a six-part unequal split was utilized based on an overall consideration of the assembling workability of K-type segments and to reduce water leaking points after opening for service.

A 5,700 mm W × 6,800 mm H high-density slurry shield machine was used for shield tunnelling (Figure 20). On the purpose of reduction of the construction cost and environment load, we constructed the Route B tunnel by reusing the principal components, such as the cutter head, soil discharge system, erector, shield jack, and shape protection unit that had been used for the preceding Route A.

4. CONCLUSION

The report introduced some topics of our construction history for new subway lines. After that, it describes recent two cases of tunnel construction, The Fukutoshin line and the Kotake-mukaihara bypass tunnel, with discussing trend of recent technology for tunneling.

Lately, Tokyo Metro has been engaged in wide variety of tunnel improvement projects to improve railway services by securing stable transportation, alleviating congestion, and ensuring safety. Our aim is to provide a convenient subway network for the future, thereby contributing to social development. In the situation, construction method shifts to the methods that can be reducing the volume of excavated soil, operation procedures and operation time for the purpose of reducing construction cost and environment load. Moreover, the construction method which can use leaved small underground space is requested now.

Tokyo Metro will continue to make every effort to challenge to develop and apply new techniques and improve the quality of the subway services it provides.

REFERENCES

Nishimura, T., 2012. *Performance of the Construction of Tokyo Metro Line No. 13 -Application of new technology and cost reduction policy-.* The 1st Singapore – Japan Tunnel Seminar 2012, Tunnelling and Underground Construction Society of Singapore, Singapore.

Noyaki, K., 2011. *Link-line Construction to Improve Subway Network Functions ― Link-line Construction between Kotake Mukaihara and Senkawa ―*. Proceedings-World Tunnel Congress2011,ITA-AITES.

Renovation & Construction Department, Tokyo Metro Co., Ltd., 2005. *Construction History of Tokyo Metro (in Japanese)*, Tokyo Metro Co., Ltd., Japan.

High-raised urban expressway to mitigate congested heavy traffic

Yukitake SHIOI[1] and Hiroshi KUDOH[2]
[1]Emeritus Professor, Hachinohe Institute of Technology, Japan
yshioi@blue.plaia.or.jp
[2]Project Manager, Chodai, Japan

ABSTRACT

Many large cities in the developing countries are confronted with traffic heavy congestion, negatively impacting urban functions such as residents' daily lives and socio-economical activities in the future. To mitigate this situation the construction of urban expressways is required besides the existing net of roads. The high-raised viaduct for expressway is more advantageous than the underground motorway in terms of enclosed space, disaster prevention, maintenance fees, construction costs, construction period and so on. Besides, the viaduct should solve the problems of vehicle noise, urban landscape, limited construction spaces, impact on circulation and so on. The authors propose a new design and technology in response to these problems. The viaduct passes over the roadside trees at a height of 30~40 m with spans of 80~100 m, which has attractive design features such as rainbows, colonnades, row of trees and so on. The foundation can be constructed using suspended diaphragm wall machine or the screw pile method. The piers or columns are made of reinforced concrete-filled steel shell (RCFT). The superstructures are fabricated with continuous steel box girders induced pre-stress by out-cables. This proposal enables a relatively economical cost and short construction period to realize the high-raised viaduct.

Keywords: *heavy congestion, high-raised viaduct, urban expressway, RCFT, pre-stressed continuous steel girder*

1. INTRODUCTION

Many megacities in the developing countries are confronted with heavy traffic congestion, damaging their urban functions. It is inevitable that residents of such cities demand improved convenience and better living conditions in line with the development of the economy, as is the influx of people from the country sides seeking jobs in the large cities. As a result, the capacity of existing transportation facilities in urban area is rapidly outstripped by the growing demand for circulation to sustain economic development and modernized lifestyles. The heavy congestion due to the excess traffic damages the urban functions such as residents' daily lives, economic growth and an ongoing range of various developing social activities.

In order to mitigate this situation an expansion of traffic facilities up to an area ratio of 30% is required in such urban areas. However, it is very difficult to construct new roads or railways in the established urban districts. Location for

new traffic facilities must be found in elevated or underground spaces. In case of motorways, some urban expressways are required besides the existing networks of roads. For the urban expressway, the hi-raised viaducts along boulevards are more advantageous than the underground motorways.
Underground ways possess the disadvantages of enclosed space, risk of fire or flooding, exhaust fumes, large daily maintenance fees, high construction costs, long construction periods, disposal of huge amount of excavated soils and so on, though they can offer relatively free selection of route without the demolition of houses. Hi-raised viaducts offer open sight distance, relatively economical construction costs and short construction period. However, they are subject to consideration of urban landscaping, diffusion of noise and gases from vehicles, limited construction space and impact on circulation and so on.
The authors hereinafter explain the advantages and the technical feasibility of the hi-raised viaduct of urban expressway in the case of the megacities in Vietnam.

2. HI-RAISED VIADUCT OF URBAN EXPRESSWAY IN VIETNAM

The streets in Hanoi and Ho Chi Minh are densely crowded with many motorcycles, as shown in Photo 1 and Photo 2. It is forecast that the larger part of this motorcycle traffic will change over to cars in the future. In this case, the number of traffic accidents involving motorcycles may increase apart from issues of the traffic congestion. To secure the smooth circulation and the road safety, the development of the bus networks with the dedicated bus lanes and the separation of the traffics for medium and long distance trips are necessary in urban areas.
In separating traffics for medium and long distance trips, hi-raised viaducts have many advantages over underground motorways. Since the main streets in Hanoi and Ho Chi Minh are wide boulevards or avenues as shown in Photo 3 and Photo 4, it is possible to install the viaduct piers. It is also possible to secure unimpaired view of the sky from the side walks, owing to the minimized sight obstruction by the hi-raised girder of viaduct. This ameliorates the feeling of oppression caused by the low height girder. The cost and period of its construction are much better than for underground motorways, especially on soft ground.
However, because an urban viaduct may potentially damage the quality of street scenery, it is necessary to elevate the girder to a position of 30~40 m high and to

Photo 1: Swarm of motorcycles (1)

Photo 2: Swarm of motorcycles (2)

Photo 3: Boulevard in Hanoi

Photo 4: Avenue in Hanoi

design the girders and piers with attractive design features such as colonnades, woods, rainbow and so on. The hi-raised girder over the roadside trees does not impact the view of the people nearby and it appears as an attractive line in far sight. It does not yield the reflection noise by the bottom face of girder from the cars passing on the lanes at the ground level. The noise and gases from the vehicles widely are widely scattered in air on the oblique fences and the people along the viaduct feel noise and gas only slightly. Finally, the hi-raised viaducts should be a social asset bettering the quality of the townscape.
The design and construction methods of the hi-raised viaduct in an urban area are given below.

3. DESIGN AND CONSTRUCTION METHODS OF SUBSTRUCTURES

The authors propose a new design and technology to construct this hi-raised viaduct along the street.
Firstly, firm foundations are required to sustain the high piers on the soft grounds of Hanoi or Ho Chi Minh. The construction of a reliable foundation is restricted in a limited space so as not to disturb the present circulation. For that purpose the soil improvement diaphragm wall foundation (Figure 1, Photo 5, Figure 2) or the screw pile foundation (Photo 6, Photo 7, Figure 3) are applicable as the construction machines capable of installing a deep foundation.
The soil improvement diaphragm wall foundation is a new type of foundation

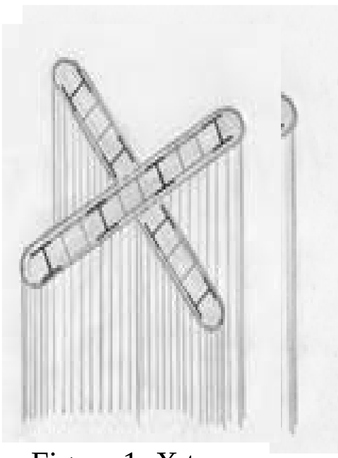

Figure 1: X type diaphragm wall foundation

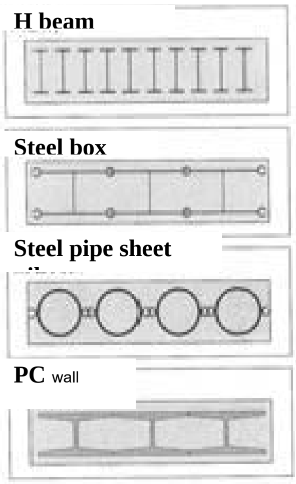

Figure 2: Various bone materials

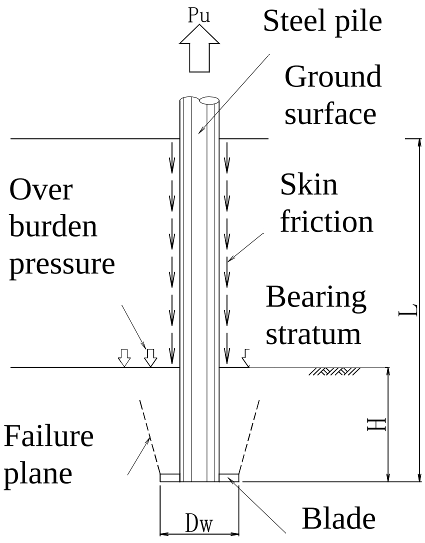

Figure 3: Bearing mechanism

Photo 5: low head soil improvement machine

Photo 6: Shape of tip of screw pile

Photo 7: Casing Rotator

which consists of the soil cement diaphragm wall dug by the suspended machine in Photo 5 and with bone materials as the core of the foundation as in Figure 2. It can reach to a depth of 50 m in a narrow working space and mobilize a large bearing capacity with the skin friction along the surface of wall and the point resistance of the bone materials.

The screw pile foundation is a steel pipe pile with a spiral blade welded at its lower end as illustrated in Photo 6. Using a casing rotator (Photo 7), the screw pile is given a vertical load and a rotating torque, and is twisted into the ground with the wedge effect of the blade up to a depth of 50 m. The screw pile has a larger bearing capacity than the normal steel pipe pile (Figure 3). Its bearing capacity can be confirmed by torque substituting for an in-situ shear test.

Both types of foundation can be constructed in a limited space with little noise and vibration and the minimum surplus soil, and without disturbance to the passing vehicles.

The piers of the hi-raised viaduct mainly receive a major vertical load and sometimes horizontal load. Though the reinforced concrete (RC) pier requires a large section against such major loads, the pier made of reinforced concrete-filled shell (RCFS) shown in Figure 4 can endure such loads with a relatively small section. Reinforcing bars are very effective in keeping concrete in RCFS (Figure

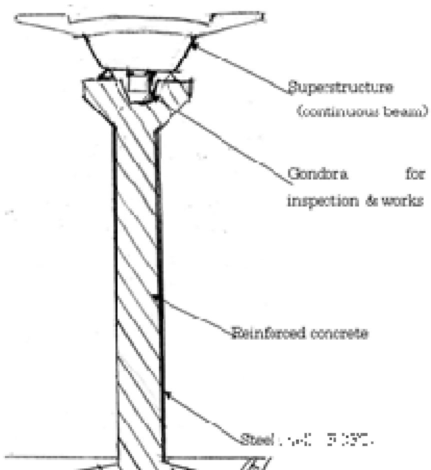

Figure 4: Concept of RCFS pier

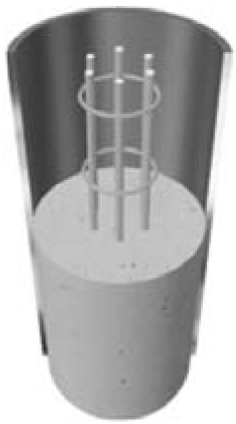

Figure 5: Model of RCFS (RCFT)

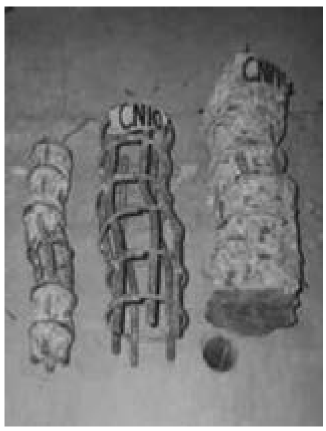

Photo 8: Double reinforcing cage to shear strain

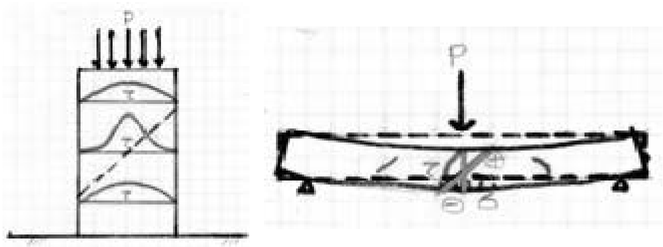

Figure 6: Shear stress at vertical load (left) and bending moment (right)

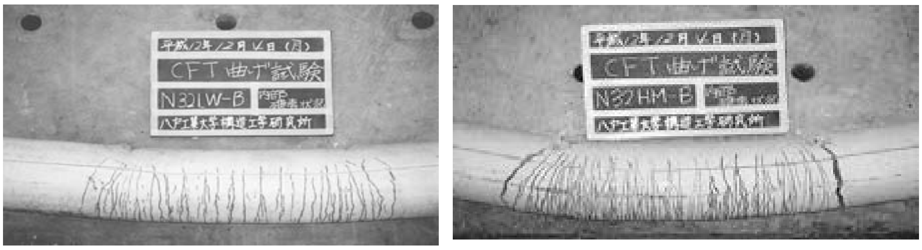

Photo 9: Cracks at RCFT (left) and CFT (right)

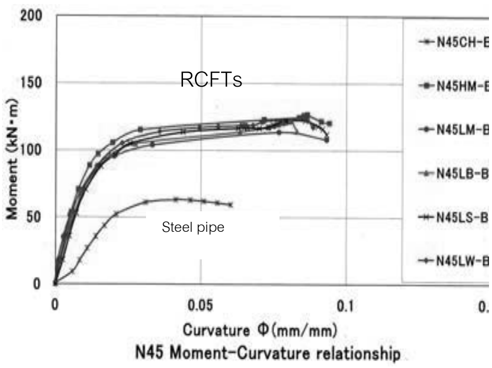

Figure 7: Deformation curves of RCFT for moment

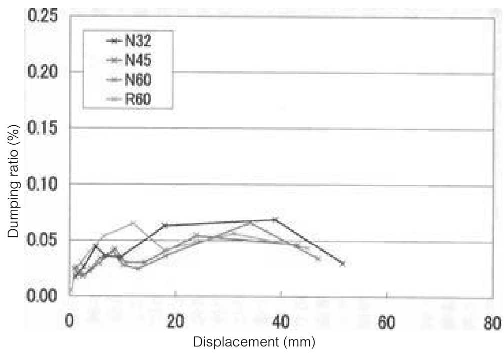

Figure 8: Damping ratios of RCFT for displacement

5) sound under a large load and deflection because the shear strain in RC members caused by the vertical force and the bending moment is the maximum at the central part of the section (Figure 6 and Photo 8) and the binding effect of the outer steel shell becomes week in cases of the larger dimensions. Furthermore, the reinforcing bars in the reinforced concrete-filled tube (RCFT) displayed excellent ductility (Figure 7) and the restoring force characteristics of RCFT superior to the concrete-filled tube (CFT) as shown in Photo 9, and the dumping ratio of RCFT is warranted at 5 % as shown in Figure 8.
The piers may be designed as trees or colonnades to harmonize with the urban landscape and the top of the piers should be Y-type in order to allow passage of a gondola for maintenance of the superstructure (Photo 10).

4. DESIGN AND CONSTRUCTION METHODS OF SUPERSTRUCTURES

The hi-raised viaduct may be erected over the wide streets in the urban areas. To release people nearby the feeling of eyesore or oppression from the wide superstructure or piers, the hi-raised viaduct is effective because the highly

Photo 10: Gondola for maintenance and Y type pier

Photo 11: Hi-raised viaduct (1)

Photo 12: Hi-raised viaduct (2)

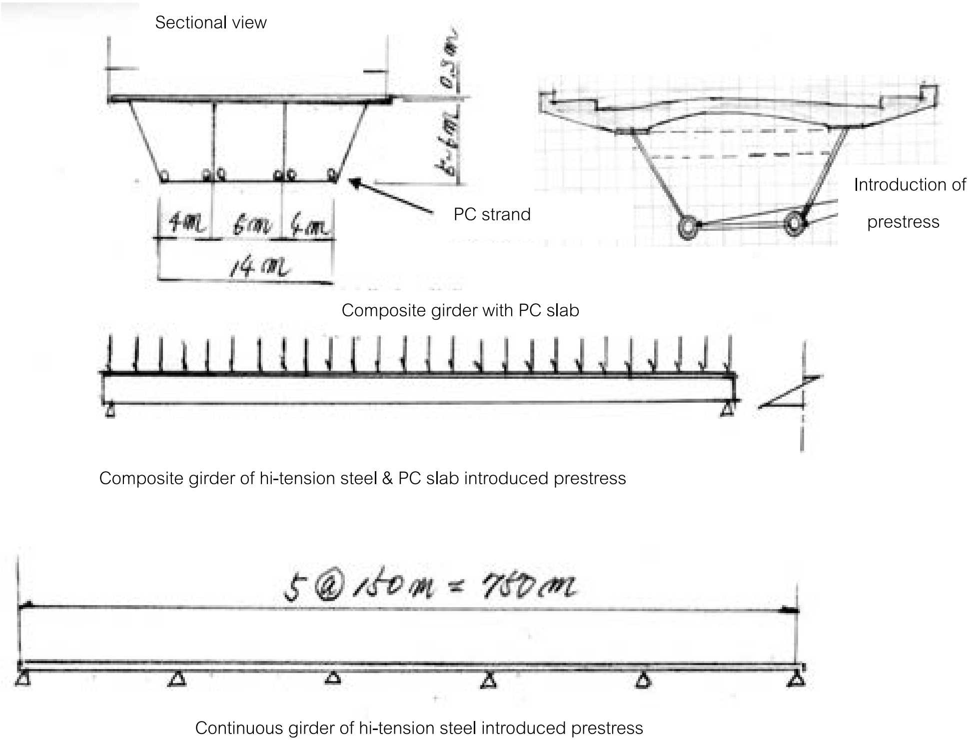

Figure 9: Continuous and composite girders introduced prestress

elevated beam is out of the sight of people nearby and the slender piers designed beautifully supporting the long spans of viaduct are out of the care (Photo 11, Photo 12). The viaducts visible over long sight should be designed in an attractive manner and harmonize with the streets.

To realize the hi-raised viaduct with a long span, a new type of continuous box girder is proposed as shown in Figure 9. The introduced prestress for continuous and composite box girders is indicated in Figure 9 and Figure 10. Figure 10 explains the process of an easily erected composite girder and introduced prestress, with a thick prestressed concrete (PC) slab. The box girder makes reverse deflection by the introduction of prestress to the lower flange. Therefore, the thick PC slab installed on the box girder becomes an important element of the composite girder. The thick slab is also durable and it enables usage of high-tensile-strength steel and strong stiffness of the girder.

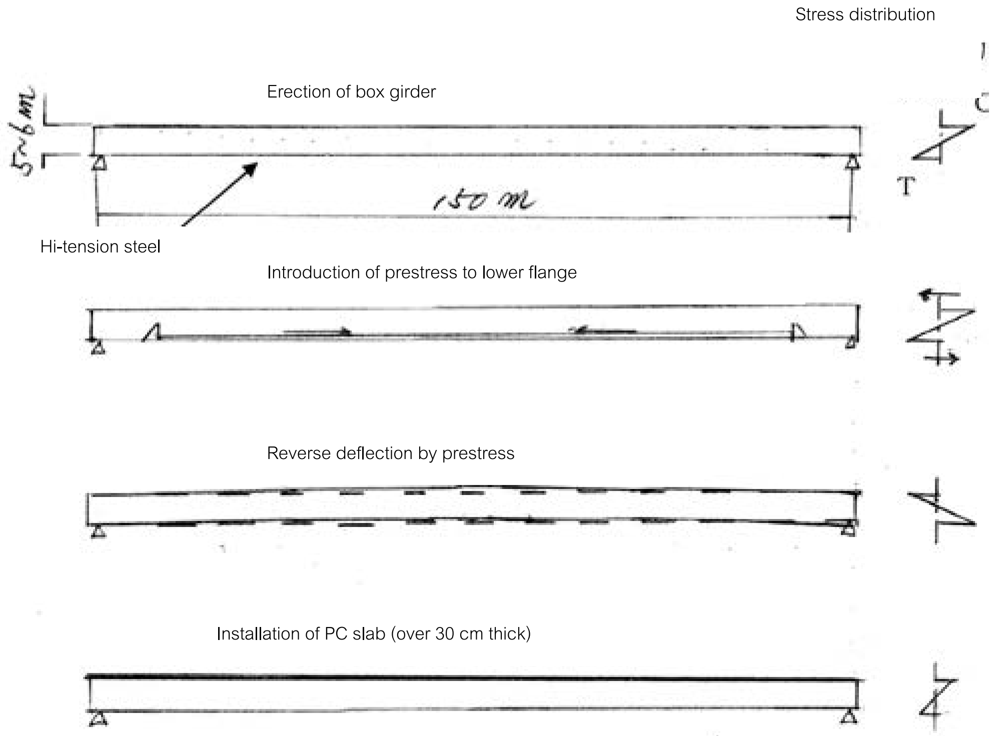

Figure 10: Process of erecting composite girder with introduced prestress

The steel box girder is more advantageous in introducing prestress than the PC girder because it is elastic without creep and drying shrinkage, and it has good rigidity. The prestress is introduced to the girder by the out cables and realizes the spans of 90~150 m. A traveling gondola for maintenance is installed along the rail under the box girder as shown in Photo 10 and a few dryers are set for maintenance free inside of the box girder.

It is necessary for the designs of the box girders and the piers over the trees to match the street configuration and building skyline and to take consideration in avoiding negative impact on residents' daily lives, such disturbance due to noise, vibration, air pollution, etc. emanating from the traffic lanes on the viaduct. To connect the viaduct with the existing road network smoothly, some rational

Photo 13: Example of interchange

Photo 14: Example of junction

interchanges (Photo 13) and junctions (Photo 14) should be disposed in the important points.
These concepts are applicable to the megacities in other developing countries besides Vietnam.

5. SUMMARIES

1. Since, in line with the rapid development of economy, many megacities in the developing countries are confronted with heavy traffic congestion which adversely impacts the urban functions, the expansion of traffic facilities is required in the urban area to mitigate this situation.
2. The hi-raised expressway viaduct is more advantageous than the underground motor way from many viewpoints.
3. The construction of the hi-raised viaduct can be realized with economical cost and short period but its several problem points in relation to the surrounding urban area are to be resolved by the design so as to adverse impacts on residents' daily lives.
4. As the foundation of the hi-raised viaduct, the soil improvement diaphragm wall foundation and the screw pile foundation are recommended in viewpoint of reliable bearing capacity, easy construction in a limited space, less pollution, little disturbance to the passing vehicles and so on.
5. As the pier of the hi-raised viaduct, the reinforced concrete-filled shell (RCFS) is proposed from the viewpoints of major load-carrying capacity, large ductility to vertical load and moment, superior restoring force characteristics and constant value of damping ratio.
6. As the superstructure of the hi-raised viaduct, the continuous and the composite box girders with introduced prestress, with a thick prestressed concrete (PC) slab, is devised to realize long spans, strong stiffness, use of high quality steel, and long durability with a gondola for maintenance and dryers inside.
7. The viaduct composed of box girders and high piers shall be attractively designed to match the street configuration and needs rational interchanges and junctions near the important points.
8. The concept discussed here is applicable to the megacities in other developing countries besides Vietnam.

AKCNOWLEDGEMENT

The authors would like to express their deep gratitude to Messrs. Kiyosi Matsui and Narutoshi Okabe for their cooperation in producing some perspectives of the hi-raised viaduct and Dr. Akira Ohwada who provided materials on screw pile method. Furthermore, the authors would also like to offer their thanks to Prof. Akira Hasegawa who is a co-researcher on RCFT and Dr. Phan Le Binh who offered some pictures of the streets in Hanoi.

Application of water screen fire prevention systems

Hideaki KUWANA[1],
Reiko AMANO[2], Takuzo IDA[3], Osamu IMAZEKI[4],
Toshihide TSUJI[5]
[1] Senior Research Engineer, Technical Research Institute, Kajima Co., Japan
kuwana-hideaki@kajima.com
[2-4] Kajima Co., Japan
[5] Hochiki Co., Japan

ABSTRACT

This study originally aims at understanding the characteristics of water screen systems as one part of the various technologies used in the construction of fire safety systems for structures in deep underground tunnels. The water screen (hereafter referred to as WS) aims at restraining the spread of the heat and smoke generated by fires to other compartments or reducing the speed of their spread as well as controlling the heat release rate during fires in tunnels. Furthermore, the objects of this study are to reduce heat radiation generated from the origin of a fire and to support evacuation and activities for firefighting and rescue utilizing the transparency of water. The WS system has been applied to buildings and civil engineering structures. Several applications are described.

Keywords: *Water Screen, application, fire prevention, evacuation, heat flux, fire safety engineering, performance design*

1. INTRODUCTION

When fires break out in closed tubular spaces such as tunnels or subway stations where air inflows are restricted, heat, smoke and toxic compounds such as carbon monoxide spread throughout the entire spaces. As a result, activities for evacuation, rescue and fire-fighting are retarded by the fires naturally expanding to nonflammable materials.

This study aims at understanding the characteristics of the WS systems as one part of the various technologies used in the construction of fire safety systems for tunnels, offices, stations, etc. The WS aims at restraining the spread of the heat and smoke generated by fires to other compartments or reducing the speed of their spread as well as controlling the heat release rate during fires in compartment. The objects of this study are to reduce heat flux generated from the origin of a fire and to support evacuation and activities for firefighting and rescue utilizing the sight through property of water.

Carrying out of plenty of fire experiments at the Miyagi fire prevention test center of Hochiki Corporation using a 1/2 scaled tunnel model (height 2.7m, width 5.4m, length 43.7m) equipped with the WS assuming a fire for a passenger car has verified the effectiveness of the WS system.

Various fire experiments have resulted in clarifying the high effectiveness of the WS system on the reduction of heat and smoke. In 2000, Kajima Corporation carried forward the technical development with regard to "compartment technology for fire zones using water droplets screen=Water Screen System" as a Kajima's original technology and in 2001 this WS system was authorized first in Japan by the Minister of Land, Infrastructure, Transport and Tourism (MLIT) based on the performance evaluation as a special fire prevention equipment in the architectural field.

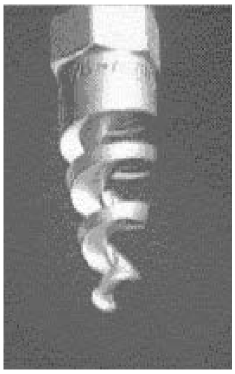

Fig.1
Spiral nozzle

The WS is a system that creates screens of water by spraying water from spiral nozzles (Fig.1) arranged in lines in compartmented positions. This fire prevention system creates the compartments that can restrict the damage of structures to limited areas and support firefighting activities as well as securing the evacuation safety for victims by restraining the spread of heat and smoke and washing out toxic floating particles.

2. PERFORMANCE TESTS

The outline of the tests carried out in 2003 is briefly shown below.

1. Test model (Fig.2): A tunnel space with a section of 2.7m height×5.4m width, 43.7m long.
2. WS equipment: WS pressure 1.0(MPa), average particle diameter 200(μm), water amount 10(Liter/min/nozzle), water spray angle 150 – 170(degrees).
3. Blower equipment: 20 fans installed at the position 2m away from the model end on the air supply side.
4. Measurement details: The heat release rate was obtained using the oxygen consumption law and weight conversion law. In order to understand the effectiveness of the WS in washing out soot generated during fires, the behavior of soot in smoke at high temperatures was studied using a duct installed at the end of the opening of the model. Furthermore, for the purpose of understanding the burning behavior of the fire source, the spray behavior of the WS and flow behavior of the smoke as well as investigating the fire source and evacuation directions during evacuation and fire fighting, observations were carried out using video cameras and thermo-cameras.
5. Test conditions: Test factors were set as ① Wind speed (0.0, 1.4, 1.8, 2.2 (m/sec), ② Fuel (n-heptane, gasoline), ③ The heat release rate (1.5, 5.0 (MW)), ④ Activation of WS equipment. On the basis of the Froude Law under consideration of the reduced scale ratio as a similitude ratio, the heat release rate was set at 1.5(MW) on the assumption that a single automobile burnt. The standard value for the wind velocity which prevents the heat flux from reversing flow on the windward side during a fire under the conditions of having a natural ventilation or a longitudinal ventilation method was set to be 1.4(m/sec).

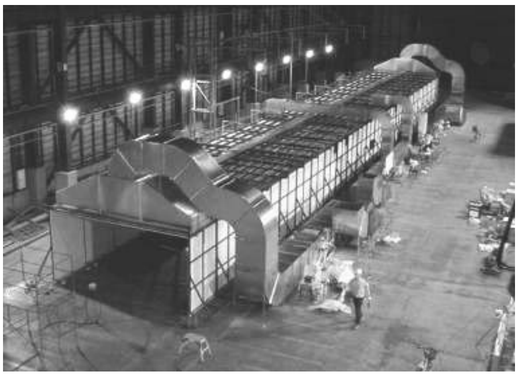

Fig.2 Test model

2.1 Test Results

Tests were carried out in 22 cases by combining test factors. And to report this time, test results are described in cases of [Wind Speed=0.0(m/sec), Fuel=gasoline, Heat release rate=1.5(MW), Case 1=without WS, Case 2= with WS].

2.1.1 Effects on received radiation calorie

Fig.3 shows the time history of the received radiation calorie measured using a radiometer installed on the outside of the model opening. The received radiation calorie in Case 1 (without WS) reached about 120 – 140(W/m^2), in Case 2 (with WS) was about 5(W/m^2). It is indicated that the received radiation ratio becomes small due to the activation of WS.

2.1.2 Effects on heat release rate

Fig.4 shows the time history of the heat release rate. In Case 1, the heat release rate attained a maximum value of 1.5(MW). In Case 2, it was 1.0(MW). In both cases, we have put the same amount of fuel. It can be assumed that the value for the heat release rate became small because of the restraining effect which was produced by the retardation of combustion due to the compartments created by the WS and water particles.

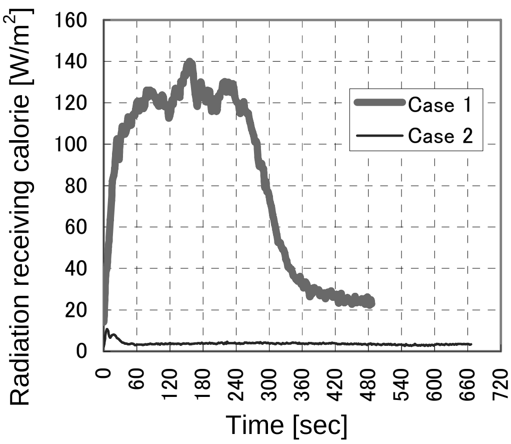

Fig.3 Radiation receiving calorie

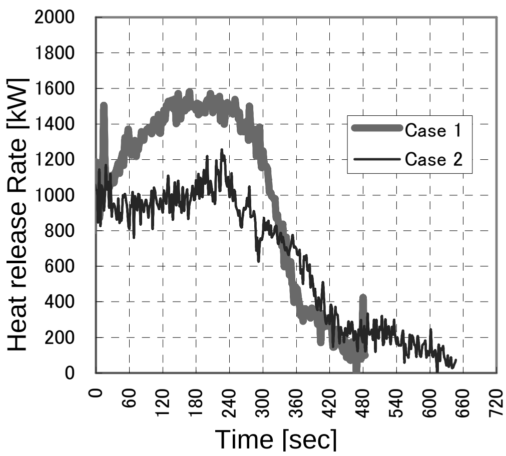

Fig.4 Heat release rate

2.1.3 Effects on gas concentration

Fig.5 shows the time history of CO gas concentration and CO_2 gas concentration. In Case 2, not only the effects of the decrease in the heat release rate upon the restraint of the amount of gas generated, but also the gentle decrease in the latter half period after fire extinguishment were shown. The cause was that the gas confined in the compartments gradually flowed out.

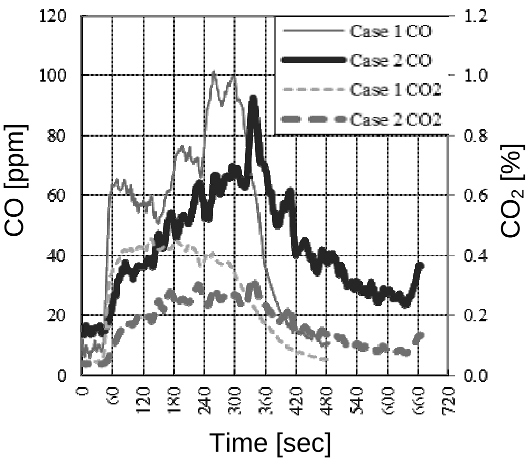

Fig.5 Gas concentration

3. ACQUISITION OF GENERAL AUTHORIZATION

The WS system acquired general authorization as a piece of designated fire preventive equipment in 2005 based on the results obtained from the performance tests.

The designated fire preventive equipment is a piece of fire prevention equipment prescribed in Article 112 of the Building Standards Law Enforcement Order. It must be built ① using the construction methods prescribed by the MLIT or must be ② authorized by the MLIT, under the condition that caloric heat induced by an ordinary fire will never produce flame on any surfaces except the surface of the fire origin within one hour after the heating begins.

3.1 Outline of General Authorization

With regard to the prescribed value for the performance evaluation of special fire prevention equipment, in the case of a fire resistance furnace being heated over one hour, the maximum temperature and average temperature of an unexposed surface (the maximum temperature in the furnace is 945℃) are required to be 200℃ or less and 160℃ or less respectively.

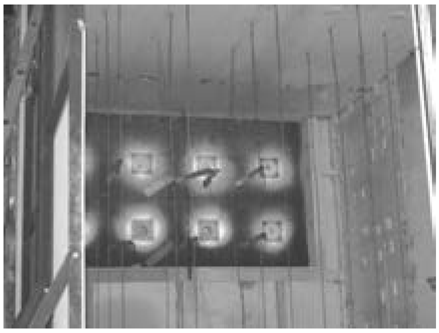

Fig.6 Conditions when heating begins in a furnace (WS not activated)

Fig.6 shows the conditions when the heating begins in the furnace and Fig.7 shows the conditions when the WS are activated 20 minutes after the heating begins.

Fig.7 Conditions during heating in a furnace (WS activated)

It was confirmed from the test results that the maximum temperature was 156℃ and the average temperature was 77℃ in the case of one line arrangement. As the result of confirming that these values from the tests were below the prescribed values, the general authorization was obtained (Fig.8).

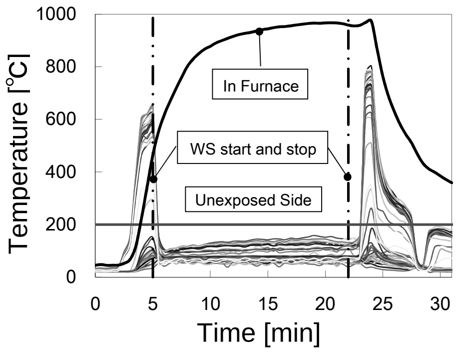

Fig.8 Time history of Temperature

4. APPLICATIONS

Since obtaining the general authorization, the WS system has been applied to buildings and civil engineering structures.

Several applications are described below.

4.1 Rental Office Building

The WS system was applied to the location connecting the 1st basement and the subway concourse for an office building completed in Oct. 2005. This place where many unspecified people pass through was assumed to be a closed space when shutters were pulled down.

It can be seen that the area opposite to the compartment partitioned by the WS is open to the outside. The WS compartment is composed of a height of 4.0m, width of 5.6m and 19 spiral nozzles. Fig.9 shows the entire building to which the WS system is applied and Fig.10 shows the conditions when people pass through in the case of the WS being activated.

Fig.9 WS system is Right side

Fig.10 WS activated

4.2 Office Building for a Construction Equipment Manufacturing Plant

The WS was applied to the compartment between the central atrium and the corridor of the administration building of a construction equipment manufacturing plant. The safety in relation to the spread of smoke in this space was confirmed using the whole building evacuation safety verification method (=performance design).

Before completion of the building, tests were carried out in order to confirm the actual activation conditions of the WS. About 50 people concerned in the jurisdiction fire station and architectural guiding section who participated in the tests confirmed that all the fire victims, including the injured, could easily pass through the compartment by observing the formation of the WS as a compartment or having actual experience of passing through. Fig.11 shows the conditions for those passing through, in the case of the WS being activated. Fig.12 shows the compartment line is indicated with the curved lines not straight one.

Fig.11 Conditions for those passing through in the case of WS activated

Fig.12 Compartment Line indicated with curves

4.3 Utility Shield Tunnel (Demolition work for shield machines)

With regard to the demolition of shield machines after completion of shield excavation work, a method for removing machines that have been broken into small pieces using gas cutting equipment and then lifting the pieces through aboveground openings made for the vertical opening where the machine reaches is mainly used. Before conducting operations using flames generated by gas cutting equipment, oil in the machines is extracted and grease is mostly wiped off. The oil, however, cannot be completely removed beforehand. Due to this, sparks induced by the gas cutting equipment set fire to residual lubricant during demolition work and a large amount of smoke, which is blackish with soot in most cases, is generated.

As for the above mentioned problems, demolition work has been simplified while exhausting the smoke by using dust collectors. However, it has been feared that the working environment deteriorates due to smoke permeating the whole tunnel and that smoke rising up to the above ground has bad effects upon the peripheral environment.

Accordingly, the WS equipment should be installed both in the front and rear of the shield machine for decreasing smoke generated from the demolition work.

Fig.13 shows the conditions on the inside of the tunnel and Fig.14 shows the activation conditions of WS on the vertical opening side where the machine reaches. The smoke concentration decreased by 80% due to the WS. Answers to the questionnaires given after the demolition work such as “Odor of burning and smoking decreased” or “The amount of smoke rising from an opening above ground decreased” were obtained.

Fig.13 Inside of shield machine before demolition

Fig.14 WS Activated

4.4 Subway Station Platform

4.4.1 Fire Prevention for Station Buildings

In February of 2003, a major accident with 192 dead and 148 injured resulted from an incendiary fire in a subway train in Daegu, Korea. Most casualties were confined to the train, but some passengers were killed in front of fire prevention shutters because they had lost their directions of escape in the black smoke. Based on this major accident, the Railway Bureau of the MLIT revised “The ministerial ordinance establishing technological standards with regard to railways" and "The standards for interpreting this ministerial ordinance" and notified the parties concerned with new standards for the prescribed improvement of noncombustible passenger car, fire safety of station yards and evacuation safety.

4.4.2 Process of WS Installation

The space of ceilings for the existing stations is too limited to install fire prevention shutters. Moreover, it is assumed that a number of people would gather in front of stairways during evacuation from fires. The WS equipment was installed in front of the central stairs connecting the platform stairs and the ticket gate stairs. In March, 2009, the WS equipment tests were carried out in the presence of staff of the authorities concerned. Fig.15 shows the activation conditions of WS.

4.4.3 Evacuation Efficiency

The evacuation calculation is carried out under the condition that the effective movement coefficient at the opening part is 1.5[persons/m/sec]. The number of persons passing through per hour can be increased by widening the effective width of the opening part. Although the effective width of a fire door or a side door is about 0.9m, the effective width for the WS equipment can be set to be up to 50m owing to the general authorization. (Fig.16 shows)

Due to the fact that the compartments can be created using only water, the opposite side can be clearly seen and evacuees can move forward while confirming the conditions in the stairways.

Fig.15 WS Activated

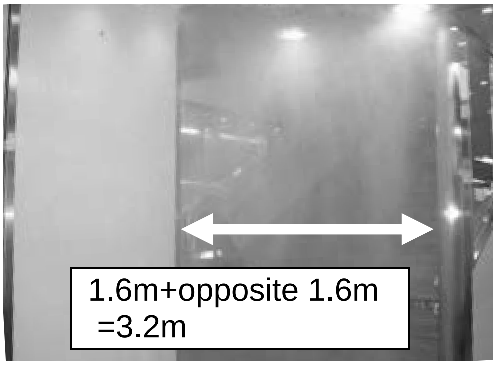

Fig.16 Availability width

4.5 Furniture Factory

The Furniture Factory is connected by a bridge from assembles building to other buildings. The designated fire preventive equipment with WS to be installed to the opening (Area compartment as Article 112, the Building Standard Law Enforcement Order) challenge heat insulation property required for the compartmentation. There is a rail conveyor hanging on to pass through the opening.

The heat insulation property in the opening that the through section can be sufficiently exhibited is the outstanding features of WS, but this time, things have been proven in the practice of the CFD analysis in specific cases.

Fig .17 shows calculation model about these areas and Table.1 shows calculation result from CFD. The heat release rate has given $0.113t^2$ (t<=163(sec)), 3000(kW) (t>163(sec)) in fire sources. Both edges of these areas are free boundary. When WS system activated, the maximum temperature is 88℃. Fig.18 shows that WS nozzles are installed. Fig.19 shows activation conditions of WS. (Imazeki, 2005)

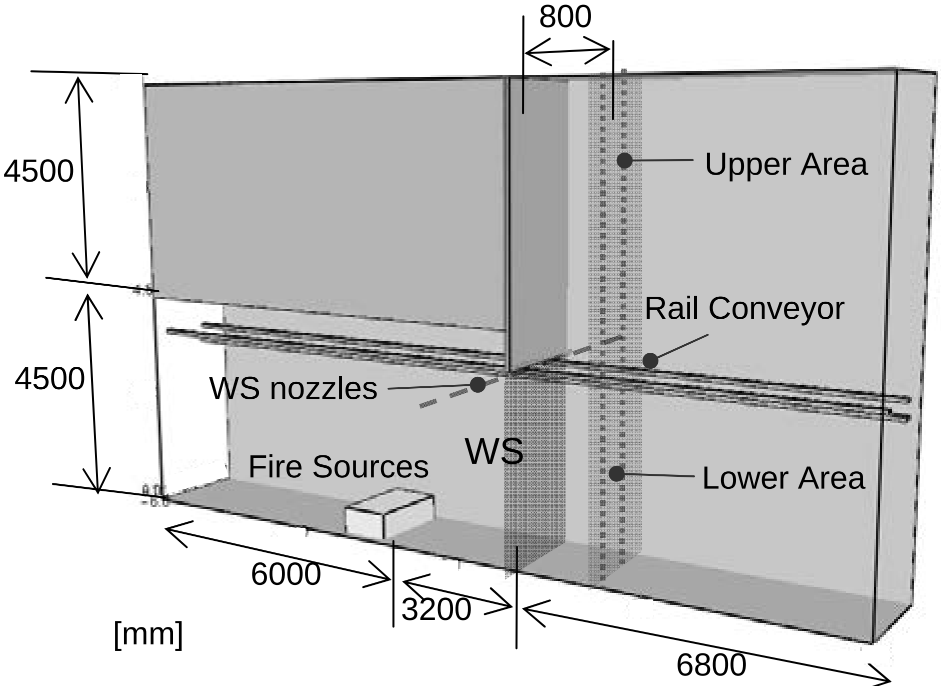

Fig.17 Calculation model

Table.1 CFD Calculation Result (Temperature)

		WS not activated	WS activated
Upper area from WS nozzles	Average	58.6	63.3
	Maximum	194.0	88.0
Lower area from WS nozzles	Average	106.7	39.0
	Maximum	171.5	39.4
Total area	Average	84.8	50.1
	Maximum	194.0	88.0

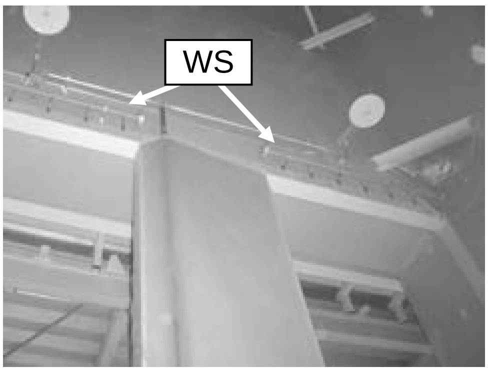

Fig.18 Installed WS nozzles

Fig.19 WS Activated

5. CONCLUSION

It was also confirmed that the occupants could survive in the fire zone partitioned by using the WS and that activities for refuge and fire-fighting could be effectively carried out. As a result, the WS as partitioning technology for a fire is very useful.

The WS has won the award of two major in Japan.

1. Association of Building Engineering and Equipment, Environmental and Equipment Design Award 2007, category 1 (Mechanical and Electrical Equipment/System Design) Best Design Award
2. Architectural Institute of Japan, the Prize of Architectural Institute of Japan 2011, Building Engineering Division Award

REFFERENCES

R.Amano, Y.Izushi, H.Kurioka, H.Kuwana, T.Tsuruda, T.Suzuki, Y.Ogawa, 2004.01, Water Screen Fire Disaster Prevention System -Characteristics of Water Screen as Partitioning Technology-, ICUS/INCEDE Report 2, *New Technologies for Urban Safety of Mega Cities in Asia*, Agra, India

R.Amano, Y.Izushi, H.Kurioka, H.Sato, H.Kuwana, T.Tsuruda, Y.Ogawa, T.Suzuki, 2004.03, Water Screen Fire Disaster Prevention System in Underground Space, *Proceedings of the 6th Asia-Oceania Symposium on Fire Safety and Technology*, Daegu, Korea

Imazeki O., Kurioka H., Oka Y., Takigawa S., Amano R. , 2005.09, Computational Fluid Dynamics of Hot Current from a Fire Source near a Tunnel wall, *8th The International Association for Fire Safety Science Symposium*, Beijing, China

Amano R., Kurioka H., Imazeki O. , 2005.10, Computational Fluid Dynamics Simulation of Thermal Behavior under Working Water Screens in a Tunnel, *the 4th International Symposium on New Technologies for Urban Safety of Mega Cities in Asia*, Nanyang Technological University, Singapore

Amano R., Izushi Y., Kurioka H., Kuwana H., Tsuruda T., Suzuki T., Ogawa Y. , 2006.03, Prevention Measures against Fires in Road Tunnels and Water Screen Fire Prevention System, *The International Symposium on Management Systems for Disaster Prevention*, Kouchi, Japan

Amano R., Kurioka H., Kuwana H., Murakami M., Tsuruda T., Suzuki T., Ogawa Y. , 2006.05, Applicability of Water Screen Fire Disaster Prevention System to Road Tunnels in Japan, *3rd International Conference Tunnel Safety and Ventilation -New Developments in Tunnel Safety*, Graz, Austria

H.Kuwana, H.Kurioka, R.Amano, Y.Izushi, T.Tsuruda, T.Suzuki, Y.OGAWA, 2006.07, Effects of Water Screen system in compartments, *12th International Conference on Aerodynamics and Ventilation of Vehicle Tunnels*, Portoroz, Slovenia

Evaluation of applicability of steel pipe piles in Vietnam

Shunsuke USAMI[1], Dinh Van THUAT[2], Yasushi WAKIYA[3],
Eiji KATAYAMA[4] and Dinh Van HIEP[5]

[1]Senior researcher, Civil Engineering Research Department, JFE Steel Corporation, Japan;
s-usami@jfe-steel.co.jp
[2]Asst. Prof., Department of Steel Structures, National University of Civil Engineering, Vietnam
[3] Deputy General Manager, JFE Steel Vietnam Co., Ltd., Japan
[4]Construction Materials & Business Development Department, JFE Steel Corporation, Japan
[5]Asst. Prof., IPTE Director, National University of Civil Engineering, Vietnam

ABSTRACT

In Vietnam, many infrastructure development projects (e.g., bridges, expressways, port facilities and high-rise buildings) are ongoing now and rapidity, safety and environmental considerations are required for their constructions. These structures are often constructed on the soft surface ground. Therefore, pile foundations need to be used in order to support superstructures. Bored piles and prestressed concrete spun piles are commonly used as pile foundations, while the application of steel pipe piles is not popular yet due to some causes such as the high material cost. However, steel pipe pile has merits such as a high material quality, high strength, easy handling and rapid construction. Therefore, steel pipe pile can be an effective and safe solution for construction of new infrastructure projects. In addition, a standard for design of steel pipe piles has not been completely regulated in Vietnam. In this paper, the applicability of steel pipe piles for bridge and high-rise building foundations is examined. The trial design of steel pipe piles and bored piles is carried out and competitiveness of applying steel pipe piles is clarified. The Vietnamese and Japanese design formulas are applied to steel pipe piles. Bearing capacities obtained from the two formulas are compared and their difference is found. In conclusion, the authors suggest a design method of steel pipe piles in Vietnam.

Keywords: *steel pipe pile, bored pile, design standard, bearing capacity*

1. INTRODUCTION

In Vietnam, a high economic growth is expected in medium and long terms and the infrastructure development is declared as one of high priority policy issues. Curently, some big infrastructure projects such as Nhat Tan Bridge, Lach Huyen Port and Cai Mep - Thi Vai Port are ongoing and there are many other plans required to improve the country’s infrastructures in future. The rapidity, safety, cost and environmental considerations are required in the construction of infrastructures and ground condition is one of the important examination issues. In Vietnam, the soft soil ground often widely spreads on the surface layer. Therefore, deep pile foundations need to be used in order to support superstructures. There are various types of pile foundations as shown in Figure 1 and the features of these pile foundations are given in Table 1. Steel pipe piles have a high quality and high strength compared to concrete bored and spun piles. Steel pipe piles also have a large bearing capacity against axial loads and a large horizontal resistance against horizontal forces such as due to seismic and wind loads.

(a) Steel pipe pile (b) Concrete bored pile (c) Concrete spun pile

Figure 1: Types of pile foundations

Table 1: Features of pile foundations

Items	**Steel pipe pile**	**Bored pile**	**Spun pile**
Material strength	-High reliable -High ductility	-Brittleness	-Brittleness
	-High compression stress -High tensile stress	-High compression stress -Low tensile stress	-High compression stress -Low tensile stress
Bearing capacity	Large	Large	Average
Corrosion	Fair	Little	Little
Construction speed	Rapid	Low	Average
Reliability of construction	Good	Fair (collapse of excavation hole)	Fair
Environmental impact	Little soil removal	So much soil removal	Little soil removal

As for the construction, a construction machine of steel pipe piles is compact. Steel pipe piles can be rapidly driven because some construction procedures such as excavation hole and concrete curing as required for bored piles are not needed. In addition, steel pipe piles are easily handled during transportation and construction because of their light weights. Therefore, steel pipe piles have been recognized as an effective and safe solution for construction in many countries such as Japan. However, the construction technology of steel pipe piles is still new in Vietnam and as a result the application of steel pipe piles is rare. Furthermore, the design standard has not been completely regulated. Therefore, the purpose of this paper is to evaluate the applicability and suggest a design method of steel pipe piles in Vietnam.

2. DESIGN OF STEEL PIPE PILES

The design of steel pipe pile foundations requires considerations of geotechnical and structural capacity, stresses in pile and displacement. There are various calculation methods depending on the country's standard/specification. In particular, the authors focus on the calculation methods of the geotechnical and structural capacity of steel pipe piles in Vietnam and Japan in this paper.

2.1 Design standard/specification

Table 2 summarizes the standard/specification/manual used in the design of steel pipe piles in Vietnam and Japan. In Vietnam, the specification 22TCN272-05 which was compiled based on the AASHTO LRFD 1998 has been applied to bridge design and the construction method of driven piles has been mentioned. The standard TCXDVN 205-1998 has still been limited in calculation of the bearing capacity of steel pipe piles. The book "Pile foundation analysis and design" compiled by Professor Vu Cong Ngu published in 2006 is only a reference design manual. In Japan, the design method of steel pipe piles has already been established and followed the allowable stress design (ASD) approach. The "Specifications for Highway Bridges" for bridge foundations and "Recommendations for Design of Building Foundations" for building foundations are generally used and updated as necessary.

Table 2: Standard/specification/manual for the design of steel pipe piles

Country	**Title**	**Field**	**Design approach**
Vietnam	22TCN272-05 "Specification for bridge design", Section 10.7 Driven pile	Bridges	LRFD
	TCXD 205-1998 "Pile foundation - Specifications for design"		
	Book "Pile foundation analysis and design" by Prof. Vu Cong Ngu		ASD
Japan	"Specifications for highway bridges", Chapter 12: Design of pile foundations	Bridges	ASD
	"Recommendations for design of building foundations"	Buildings	ASD

Notes: ASD: Allowable stress design, LRFD: Load and resistance factor design

2.2 Bearing capacity of ground

The bearing capacity of ground includes the end bearing resistance and shaft friction resistance as given by Equation 1. Allowable bearing capacity in ASD and the factored bearing resistance in LRFD are taken as Equations 2 and 3, respectively. Table 3 summarizes the resistance factor (φ) used in 22TCN207-05 and safety factor (SF) in the Schmertmann SPT and Japanese methods. Moreover, the unit end resistance and unit shaft friction resistance for building and bridge foundations are shown in Tables 4 and 5 and Tables 6 and 7, respectively.

$$Q_u = Q_p + Q_f = q_p A_p + q_f A_f \quad (1)$$

ASD: $$Q_a = Q_u / SF \quad (2)$$

LRFD: $$Q_R = \varphi_p Q_p + \varphi_f Q_f = \varphi_p q_p A_p + \varphi_f q_f A_f \quad (3)$$

where Q_u is the ultimate bearing capacity of ground; Q_a is the allowable bearing capacity of ground; Q_p is the end resistance; Q_f is the shaft friction resistance; q_p is the unit end resistance; q_f is the unit shaft friction resistance; φ_p, φ_f are the resistance factors; A_p is the cross sectional area of pile; A_f is the surface area of pile and SF is the safety factor.

Table 3: Resistance factor (φ) in 22TCN207-05 and safety factor (SF) in Schmertmann SPT method and Japanese method

<table>
<tr><td rowspan="4"></td><td colspan="3">Vietnam</td><td colspan="2" rowspan="2">Japan</td></tr>
<tr><td colspan="2">SPT method (22TCN207-05)</td><td>Schmertmann SPT method</td></tr>
<tr><td colspan="2" rowspan="2">φ</td><td rowspan="2">SF</td><td colspan="2">SF</td></tr>
<tr><td>Bridge</td><td>Building</td></tr>
<tr><td rowspan="3">End resistance</td><td>Sand</td><td>SPT: 0.45
CPT: 0.65</td><td rowspan="3">4</td><td rowspan="3">3 (Ordinary)
2 (Seismic)</td><td rowspan="3">3 (Ordinary)
1.5 (Seismic)</td></tr>
<tr><td>Clay</td><td>0.70</td></tr>
<tr><td>Rock</td><td>0.50</td></tr>
<tr><td rowspan="2">Shaft friction resistance</td><td>Sand</td><td>SPT: 0.45
CPT: 0.65</td><td rowspan="2">2</td><td rowspan="2">3 (Ordinary)
2 (Seismic)</td><td rowspan="2">3 (Ordinary)
1.5 (Seismic)</td></tr>
<tr><td>Clay</td><td>α method: 0.70
β method: 0.50
γ method: 0.55</td></tr>
<tr><td>Formula</td><td colspan="2">$Q_R = \varphi_p Q_p + \varphi_f Q_f$</td><td>$Q_a=(Q_p/2+Q_f)/2$</td><td colspan="2">$Q_a = (Q_p+Q_f)/SF$</td></tr>
</table>

Table 4: Unit shaft friction resistance, q_f (kN/m^2)

Soil types	**Vietnam using Schmertmann SPT method**	**Japan**
Sand	5.55+14.56 lnN_{60}	10/3N (≦100)
Soft limestone, shelly sand	1.72+12.83 lnN_{60}	
Clay	18.58+20.93 lnN_{60}	1/2q_u (≦100)
Mixed clay, powdery fine sand	23.27+14.07 lnN_{60}	

Note: N_{60} is the SPT N value corrected for field procedures

Table 5: Unit end resistance, q_p (kN/m^2)

Soil types	**Vietnam using Schmertmann SPT method**	**Japan**
Sand	46N_{60}	300N (≦18,000)
Soft limestone, shelly sand	92N_{60}	
Clay	126N_{60}	
Mixed clay, powdery fine sand	184N_{60}	

Table 6: Unit shaft friction resistance, q_f (kN/m^2)

Soil types	**Vietnam**		**Japan**
	SPT method (22TCN207-05)	**Schmertmann SPT method**	
Sand	0.0019$\bar{N}$ for driven displacement piles	5.55+14.56 lnN_{60} for sand	2N (≦100)
		1.72+12.83 lnN_{60} for soft limestone, shelly sand	
Clay	—	18.58+20.93 lnN_{60} for clay	C or 10N (≦150)
		23.27+14.07 lnN_{60} for mixed clay, powdery fine sand	

Note: $\bar{N}$ is the average SPT blow count along the pile shaft

Table 7: Unit end resistance, q_p (kN/m^2)

Soil types	Vietnam		Japan
	SPT method (22TCN207-05)	**Schmertmann SPT method**	
Sand	$0.038N_{corr}\,(D_b/D)$ $<0.4N_{corr}$ for sand $<0.3N_{corr}$ for nonplastic silts $N_{corr} = 0.77\log_{10}(\frac{1.92}{\sigma_v'})N$	$46N_{60}$ for sand $92N_{60}$ for soft limestone, shelly sand	$300N$ $*D_b/D \geqq 5$
Clay	—	$126N_{60}$ for clay $184N_{60}$ for mixed clay, powdery fine sand	

Note: D_b is the embedment depth into the bearing layer

2.3 Structural capacity of piles

When the structural capacity of steel pipe pile is calculated in Vietnam, it needs to refer to relevant specifications in foreign countries because the calculation formula has not been regulated adequately. Therefore, the authors refer to the Japanese manual and AASHTO ASD and evaluate the structural capacity of steel pipe piles by using allowable stress design approach. The allowable structural capacity can be given by Equation 4.

$$p = \sigma \times A = \varphi \times F_y \times A \tag{4}$$

where P is the allowable structural capacity, σ is the allowable stress in piles, φ is the reduction factor, F_y is the yield strength of steel and A is the cross sectional area of pile.

The structural capacity of steel pipe pile is reduced from an ultimate value to an allowable value by a reduction factor. Table 8 summarizes the reduction factor used in the Japanese method and AASHTO ASD. The reduction factor used in Japan is determined in consideration of the effect of local buckling based on the results of compressive tests for short steel pipes. In contrast, the reduction factor in the AASHTO ASD accounts for uncertainty in resistance and applied load such as the effects of driving stress levels, eccentricity of applied load, damage to piles due to driving and inherent variability in pile material. The reduction factor in the Japanese method is about twice larger than that in the AASHTO ASD and this means that the AASHTO ASD is much more conservative than the Japanese method. Therefore, it is recommended that the Japanese method is applied to the calculation of the structural capacity of pile when an economical design is required.

Table 8: Reduction factors in the Japanese method and AASHTO ASD

	Japan	AASHTO ASD
Equation	$(0.8+2.5\frac{t}{r})$: $0.01<\frac{t}{r}\leqq 0.08$ 1.0 : $\frac{t}{r}\geqq 0.08$ where: *t*: Thickness of steel pipe *r*: Radius of steel pipe **SF* = 1.5 is considered in the calculation of allowable stress of steel pipe pile.	$\frac{(\varphi)(ecc)(HDF)}{LF}$ where: *φ*: Product manufacturing variability *ecc*: Load eccentricity factor *HDF*: Hidden defect factor due to damage during pile driving *LF*: Load factor
Value	0.55～0.67	Driving damage likely: 0.25 Driving damage unlikely: 0.33

3. TRIAL DESIGNS

The trial design of steel pipe piles and bored piles is examined for bridge and high-rise building foundations in order to evaluate the applicability and suggest a design method of steel pipe piles in Vietnam. Further details can be found in the research report by JFE-IPTE/NUCE in 2012.

3.1 Design of steel pipe piles for building foundations

The trial design is examined for three typical types of 35-story buildings with 3 basements, including reinforced concrete (RC) building, steel building and hybrid building (Figure 2). These buildings are assumed to be constructed in Hanoi and designed in accordance with the Vietnamese standards. A typical ground condition in the Hanoi area as shown in Figure 3 is used as the site condition. The piles are embedded into the gravel layer. The center pile cap and the surrounding pile cap are subjected to axial forces of about 13,300 tons and 1,600 ~ 2,500 tons, respectively. The bearing capacity of bored piles is calculated using the Japanese formula and Meyehof's formula specified in the TCXD 205-1998 while the bearing capacity of steel pipe piles is calculated using the Schmertmann SPT method and Japanese formula. Table 9 summarizes the obtained design results.

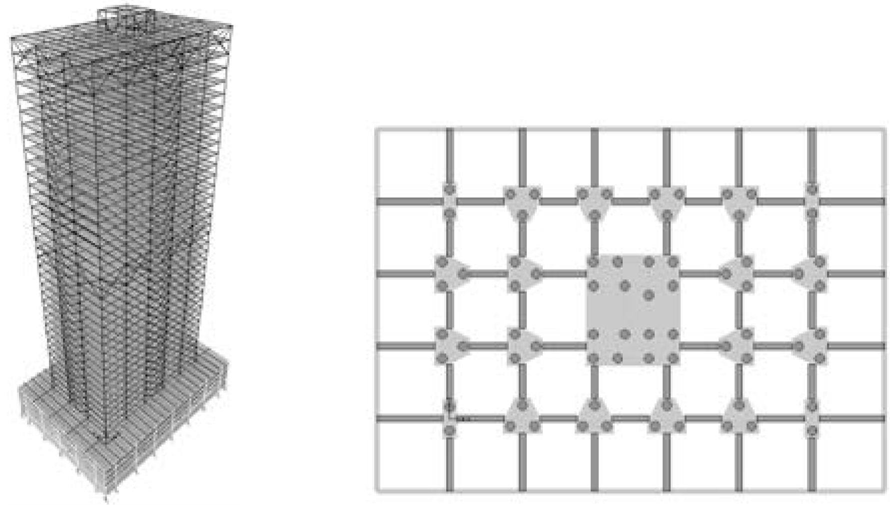

(a) Structural model (b) Plan of pile caps

Figure 2: Structure model and plan for pile caps

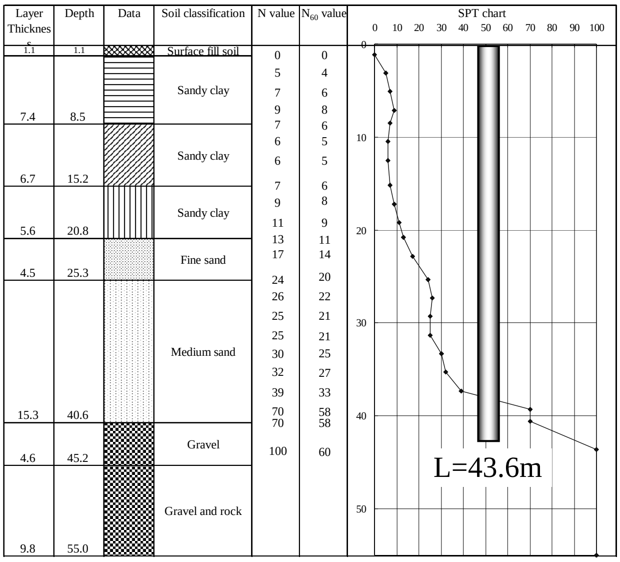

Figure 3: Site condition in Hanoi area

Table 9: Design results of bored and steel pipe piles

a) 35-story steel buildings

		Bored pile	Steel pipe pile		
		TCXD 205-1998	Schmertmann SPT method	Japanese formula	
Dimensions	mm	*D*1200	*D*1200×*t*30	*D*1100×*t*14, 15	
Length	m	43.6	43.6	43.6	
Number of piles		72	72	36	36
Bearing capacity	kN	8500.0	8500.0	9182.9	
Structural capacity	kN	9160.0	9024.5	8249.1	8922.5

b) 35-story RC buildings

		Bored pile	Steel pipe pile		
		TCXD 205-1998	Schmertmann SPT method	Japanese formula	
Dimensions	mm	*D*1200	*D*1200×*t*30	*D*1100×*t*14, 15	
Length	m	43.6	43.6	43.6	
Number of piles		120	120	80	36
Bearing capacity	kN	8500.0	8500.0	9182.9	
Structural capacity	kN	9160.0	9024.5	8249.1	8922.5

c) 35-story hybrid buildings

		Bored pile	Steel pipe pile		
		TCXD 205-1998	Schmertmann SPT method	Japanese formula	
Dimensions	mm	*D*1200	*D*1200×*t*30	*D*1200×*t*14, 15	
Length	m	43.6	43.6	43.6	
Number of piles		86	86	12	56
Bearing capacity	kN	8500.0	8500.0	10583.2	
Structural capacity	kN	9160.0	9024.5	8957.6	9685.6

3.2 Design of steel pipe piles for bridge foundations

The bridge structure comprises of six simple spans with I-shaped girders (A1~P1~P2 and P8~P11~A2) and six continuous spans (P2~P8) with composite pre-stressed RC girders (Figure 4). The total length of the bridge structure is 855.9 m. The pile foundations are calculated for the pier P3 and the load combinations are shown in Table 10. A typical ground condition in the Hanoi area is shown in Figure 5 as the site condition. The piles are embedded into the gravel layer. The bearing capacity of bored piles is calculated using the Japanese formula and Meyehof’s formula specified in the TCXD 205-1998 and that of steel pipe piles is calculated using the SPT method specified in 22TCN207-05, Schmertmann SPT method and Japanese formula.

The bending moment and axial force generated at the top of pile is calculated by using an analysis software. Table 11 summarizes the design results. The diameter of steel pipe piles by the Japanese method is about two-third compared to those of bored piles and steel pipe piles by the 22TCN207-05 and Schmertmann SPT method while remaining the same bearing capacities. The diameter and thickness of steel pipe piles by the Japanese method can be reduced compared to the Vietnamese method since there is about ten times of difference in the bending moment generated at the top of piles as shown in Table 11. The difference in an assumption of the stiffness of footing between Japanese and Vietnamese method is one of the reasons and the further investigation is required.

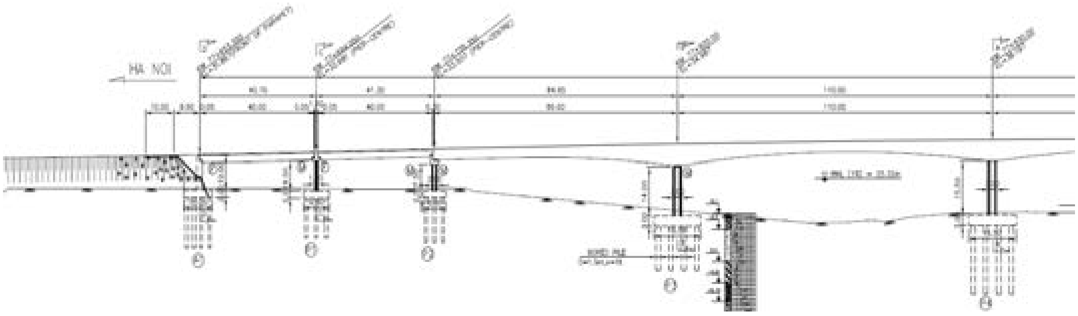

Figure 4: Bridge structure (A1, P1~P4)

Elevation (m)	Depth (m)	Layer Thicknes (m)	Data	Soil classification	N value	N_{60} value
10.5	4.6	4.6		Clay, yellowish grey, light grey very stiff	12 13	9 10
5.5	9.6	5.0		Sandy clay, brownish grey medium stiff	4 5	3 4
-0.8	15.9	6.3		Clay, yellowish grey, light grey very stiff	16 21 22	12 15 16
-6.1	21.2	5.3		Sandy clay, greenish grey very stiff	9 7 9	6 5 6
-18.5	33.6	12.4		Gravel sand, saturated dense to very dense	32 30 34 45 41	24 22 25 33 30
-30.5	45.6	12.0		Gravel, cobble with coarse sand, saturated very dense	53 73 75 78	39 54 56 58

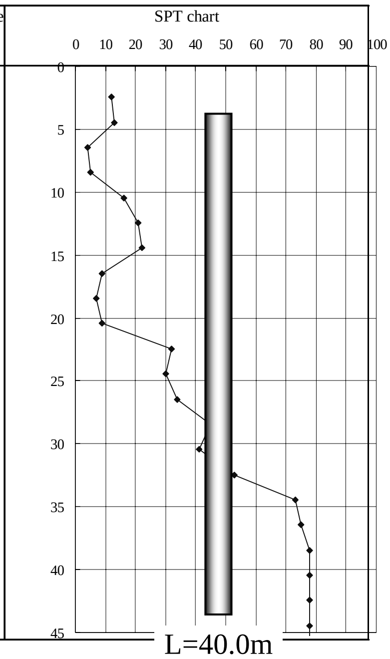

Figure 5: Site condition in Hanoi area

Table 10: Load combination at bottom footing and axial load

	Vertical load	Horizontal load	
	N (kN)	H_x (kN)	M_y (kNm)
Service I (Longitudinal wind load - LWL)	71,880	3,292	57,858
Strength I (LWL - Longitudinal)	94,426	3,293	59,057
Extreme event (Earthquake Longitudinal - LWL)	88,583	11,509	195,714

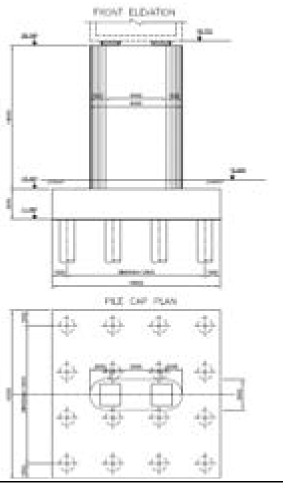

Table 11: Design results

		Bored pile		
		Reese&O'neill	Reese&Wright	Meyerhof
Diameter	mm	φ1500		
Length	m	40.0		
Bending moment	kNm	6331.0		
Axial force	kN	10050.0		
Bearing capacity	kN	23698.6	13583.9	7667.9

		Steel pipe pile		
		Using SPT 22TCN207-05	Schmertmann SPT method	Japanese method
Diameter	mm	φ1500×t28		φ1000×t14
Length	m	40.0		40.0
Bending moment	kNm	6322.0		543.4
Axial force	kN	9185.5		8708.2
Bearing capacity	kN	7935.0	9496.0	10291.9

4. CONCLUSIONS

This study has examined the applicability of steel pipe piles for bridge and high-rise building foundations in Vietnam by means of trial designs. The conclusions and recommendations for the application of steel pipe piles and further studies are as follows.

(1) The 22TCN272-05 specification has been applied to design bridge and driven piles can be designed in accordance with this specification in Vietnam. On the other hand, the design specification of steel pipe piles for high-rise building foundations has not been regulated.

(2) The diameter of steel pipe piles obtained by using the Japanese formula can be equal to or smaller than that of bored piles while remaining the same bearing capacity as that of bored piles.
(3) As for the calculation of structural capacity of piles, the diameter and thickness of steel pipe pile can be reduced by using the Japanese formula since the reduction factor in the calculation of allowable stress in piles is different.
(4) It is recommended that the design specification of steel pipe piles subjected to both axial forces and bending moments can be developed in Vietnam based on the Japanese specification with consideration of constructional and material conditions.

REFERENCES

22TCN272-05, 2005, *Specification for Bridge Design*, The Ministry of Transportation, Hanoi.

Architectural Institute of Japan, 2001, *Recommendations for Design of Building Foundations*, 2nd edition, Japan.

Davisson, M. T., Manuel, F. S., and Armstrong, R. M., 1983. Allowable Stresses in Piles, *FHWA-RD-83-059*, Federal Highway Administration.

Japan Road Association, 2012, *Specifications for Highway Bridges*, Japan.

JFE-IPTE/NUCE, 2012, *Research for Introduction of JFE R&D Steel Products for High-rise Buildings and Bridges in Vietnam*, Research report, Hanoi.

Ngu, V. C., and Thai, N., 2006, *Pile foundation: Analysis and design*, Hanoi. (in Vietnamese)

TCXD 205-1998, 1998, *Pile foundation - Specifications for design*, The Ministry of Construction, Hanoi.

Contemporary timber building in Japan, 2013

Mikio KOSHIHARA
Professor, Institute of Industrial Science,
the University of Tokyo, Japan
kos@iis.u-tokyo.ac.jp

ABSTRACT

Revision of the Building Standards Law 2000 allowed the construction of timber buildings four-story or taller with fire-resistance performance. The possibilities of mid-rise and large timber buildings in Japan are extended.
For fire-resistance three type of members were developed and achieved in Japan. First type is a membrane member covered with fireproof elements like gypsum boards. Second type is a built-in steel member for self-extinguish. Last third type is a fire-stop, 'Moedomri', member covered with wood and non-combustible treat wood. First layer wood functions as a 'Moeshiro' layer for making fire-prevention time and second layer wood functions as a 'Moedomari' layer for self-extinguish.
With membrane member many large timber building have been built from 2005. Typical structural system is 2x4 system and post and beam system. Shimouma building reported in 2012 used this fire-prevention system. M-Bldg. reported in 2012 use a built-in steel system. Finally timber buildings with 'Moedomari' are completed in 2013.
This paper describes the detail of large timber buildings with three fire prevention system in Japan, 2013.

Keywords: *Mid-rise timber building, Large timber building, Fire prevention,*

A useful approach to identify and analyze factors affecting safety on construction site with lifting equipment in Vietnamese environment

Thanh Long NGO[1], Van Gon BUI[2], Dinh Sung PHAM[3]
Quoc Dung NGUYEN[4] and Chi-Chen TSAI[5]
[1] Assistant Professor, Department of Construction Mechanical Engineering, National University of Civil Engineering, Vietnam
ntlongntu@yahoo.com
[2] Lecturer, Department of Construction Mechanical Engineering, National University of Civil Engineering, Vietnam
[3] Lecturer, Department of Construction Mechanical Engineering, National University of Civil Engineering, Vietnam
[4] Lecturer, Department of Construction Mechanical Engineering, National University of Civil Engineering, Vietnam
[5] Ph.D. Candidate, Department of Civil Engineering, National Taiwan University, Taiwan

ABSTRACT

Lifting equipment is the centerpiece of production on today's typical building construction sites. Lifting equipment hoists and transports a variety of loads near and above people and other construction types of equipment, working under the crowded environment, overlapping zones, time, budget, and labor constraints. The safety risk relating to lifting equipment further increases on construction sites in the world, especially in Vietnam, and it has not been paid any adequate attention by researchers and users as well. This paper presents a useful approach to identify and analyze factors affecting safety in lifting equipment environments in construction sites in Vietnam. The research methodology is based on previous studies' results and real construction environment in Vietnam. The proposed approach includes comprehensive questionnaire of experts who have lifting equipment working experience, such as lifting equipment operators, safety managers, equipment managers, and designers in order to identify these factors, and it has been used statistical techniques to analyze and evaluate them. The steps of the proposed approach are showed in this paper. The result of the paper is very useful for future studies in the construction machines safety management field in Vietnam.

Keywords: *lifting equipment, construction sites, fatalities, safety, Vietnam*

1. INTRODUCTION

Vietnam's construction industry has been increasing to meet the needs of its rapid economic growth. The construction sector contributes 42% to Vietnam's gross domestic product (GDP) in 2007 (Bloomberg, 2008). However, safety performance in construction industry has raised concerns in recent years (Mohamed et al., 2009), and construction industry has very high injury and fatality rates compared to other industries (Rivara and Alexander, 1994; Tam and Fung, 2011).

Types of lifting equipment including mobile cranes, tower cranes, and lifts are the really important machines in construction sites in the world and in Vietnam as well. Lifting equipment certainly contributes to the high number of construction injuries and fatalities (Shapiro and Shapiro, 2004; Skinner et al., 2006; Neitzel et al., 2001; Van Hamptom and Lawis, 2008; Shapira et al., 2012). For example, according to the statistics from Occupational Safety and Health in the United States (Kang and Miranda, 2007), there were 137 crane-related fatalities recorded from 1992 to 2001 in the United States. Japan recorded 41 fatalities resulting from crane accidents in 2006 (Kawata, 2007). Tam and Fung (2011) showed that there were 12 accidents of tower cranes from 1998 to 2005 in Hong Kong. A British study found that cranes are involved in 17% of all construction fatalities in British (Health and Safety Executive, 1978). Vietnam reported that there were 74 accidents of lifting equipment from 2000 to 2004 (Ministry of Labour-Invalids and Social Affairs, 2013). However, there had no specific information about the activities or actions leading to these injuries, and they did not identify causal factors or environments (Neitzel et al., 2001).

Identification and analysis of factors affecting safety on construction sites with types of lifting equipment have become urgent issues. As a result, there are some studies in this field, but they have done in American and European construction sites (Shapira and Lyachin, 2009). In addition, these studies have only focused on one or some types of lifting equipment, and it can come across some difficulties during using result of these studies in Vietnamese construction environment. This paper addresses an approach that can be effectively applied to identify and analyze factors affecting safety on construction sites with lifting equipment in Vietnam. The proposed approach includes comprehensive questionnaire of experts, and statistical techniques have been used to analyze and evaluate them.

2. LITERATURE

Construction sites are increasing use of lifting equipment as the dominant machines in recent years, but they have a fairly numerous number of accidents involving types of lifting equipment have occurred (Shapira et al., 2012). Therefore, lifting equipment safety management field at construction sites has attracted some leading studies.

Some studies have used statistics as knowledge source to show major causes of fatalities in the use of crane. Neitzel et al. (2001) reviewed crane related injury data to find and evaluate major causes of fatalities in the use of crane. Beavers et al. (2006) used the Occupational Safety and Health Administration’s (OSHA) case files from crane-related fatality investigations during the years 1997–2003, the paper examined the data to determine the proximal causes and contributing physical factors. In reality, however, statistics suitable to serve the purposes of current study hardly exist-for tower or mobile cranes (Shapira and Lyachin, 2009).

There have been some studies that proposed some quantitative approaches to identify and measure factors affecting crane safety on construction sites. Shapiro and Shapiro (2004) showed that in crane and rigging, most failures arise out of one or ten categories, such as deficient equipment; pressure from cost or time constraints; inexperienced management; lack of training, knowledge, or skill; inadequate planning; unreasonable demands of owner or management; environmental conditions; unclear instructions; operator errors; changed circumstances. Shapira and Lyachin (2009) showed twenty one major factors affecting safety in tower-crane environments and evaluated the degree to which each factor influences ongoing safety on site. Twenty one factors are divided into four factors groups including project conditions factor (ten factors), environment factor (three factors), human factor (five factors), and safety management factor (three factors). The research was based on comprehensive questioning of an expert team that included the safety managers and equipment managers of leading construction companies with Delphi technique. Shapira and Simcha (2009a) used nineteen senior construction equipment and safety experts interviewed and led through the analytic hierarchy process (AHP). The research found out the final weights of thirteen major factors affecting safety on construction sites, and these factors include site-level safety management, operator proficiency, wind, superintendent character, maintenance management, company-level safety management, overlapping cranes, operator character, signalperson experience, blind lifts, type of load, employment source, and length of work shift. These weights can be used to produce a tower crane safety index for any individual site. Shapira and Simcha (2009b) proposed a method, which addresses quantitative measurement and risk scales of safety hazards on construction sites due to the work of tower cranes. The research focused on two factors overlapping cranes and operator proficiency. A probability-based method was prescribed for the measurement of overlapping cranes, while the analytical hierarchy process method and knowledge elicitation from experts were applied to develop metrics for operator proficiency. Shapira et al. 2012 presented an integrative model for quantitative evaluation of safety on construction sites with tower cranes. The model integrated for modules: (1) nonsite-specific relative weights of safety factors, (2) measurement of the magnitude of each safety factor actually present on site, (3) scales to convert each measured magnitude into a value representing the potential risk generated by each factor present on site, and (4) multiplying factors to convert the cumulative risk generated by all factors into actual risk. However, these studies only focus on crane safety management and measurement, and they were done in construction environments with enough information and high levels of reliability while construction environments in Vietnam are different from them. As a result, these models may need to modify during applying them in construction environments in Vietnam.

3. METHODOLOGY

Following approaches from the previous studies and basing on construction environment in Vietnam, the paper analyzes and evaluates them and then proposes a useful approach to identify and analyze factors affecting safety on construction site with lifting equipment in Vietnam. The whole research methodology is presented as in the Figure 1.

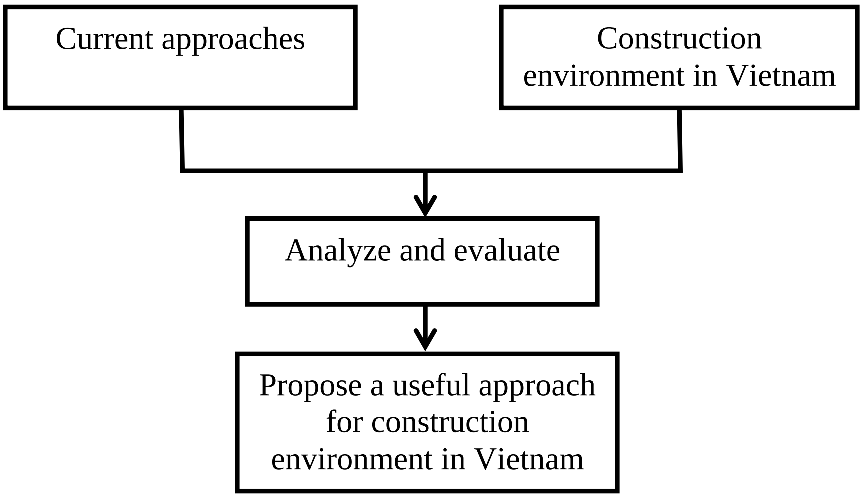

Figure 1: Research methodology

4. A USEFUL APPROACH FOR CONSTRUCTION ENVIROMENT IN VIETNAM

An approach can be effectively used to identify and analyze factors that affect safety on construction sites with lifting equipment in Vietnamese environment including 6 steps described as in Figure 2.

4.1 Step 1: An initial list of factors from literature and the condition of construction site in Vietnam

The valuable studies include Shapiro (2004), Shapira and Lyachin (2009), Shapira and Simcha (2009a, 2009b). These studies offered important factors that affect safety of lifting equipment on construction sites, and in which many factors can be used in Vietnamese Environment. However, in Vietnam, there are some conditions differing from these studies' conditions, such as project conditions, environment, human factor, design and manufacture, and safety management. Thus, initial list of factors need to base on both of literature and Vietnamese environment.

4.2 Step 2: Exploratory interviews

An open-ended questionnaire survey first is conducted with some professionals through face-to-face, e-mail, or phone calls. All these experts are either the safety or equipment managers of leading construction companies in Vietnam. These experts include equipment managers, safety managers, hold both positions, designers and manufacturers, and they have at least five years of working experience in this field (Ling and Poh, 2008; Bo and Chan, 2012). This step is often used to determine the major facets of a set of data, by simply counting the number of times an activity happens, or a topic is depicted (Fellow and Liu, 2008).

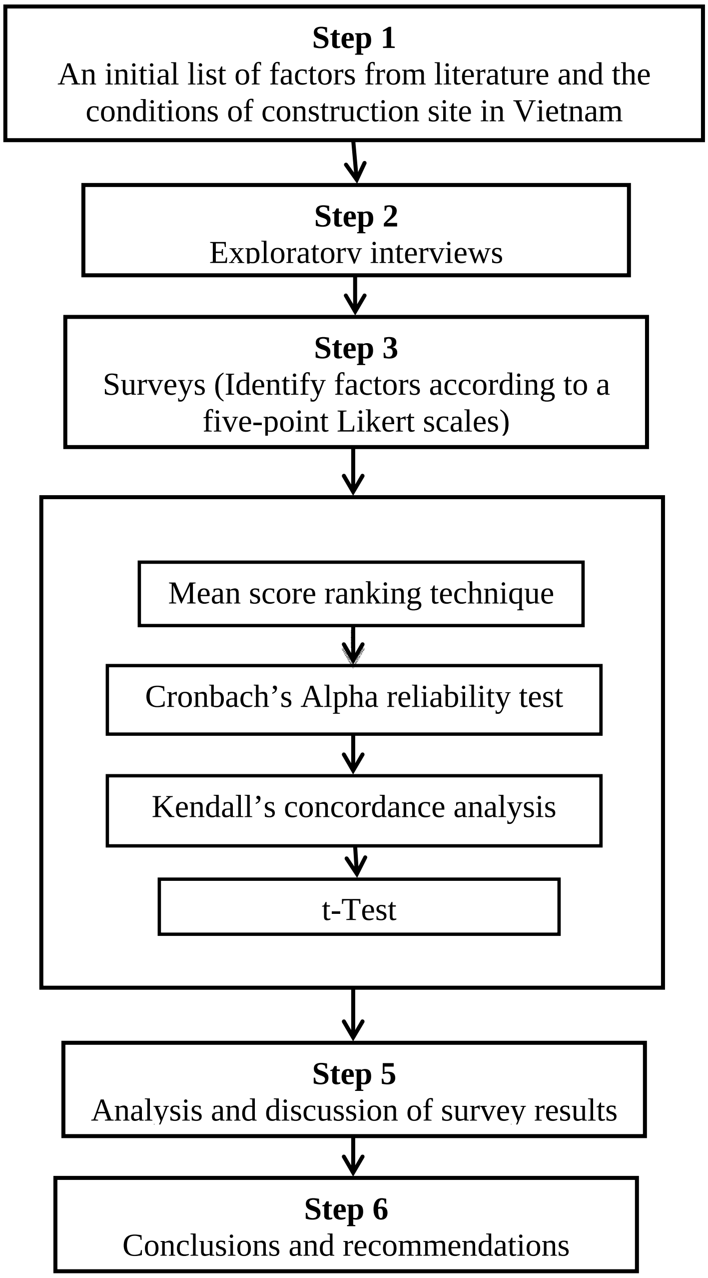

Figure 2: The approach to identify and analyze factors affecting safety on construction site with lifting equipment in Vietnamese environment

4.3 Step 3: Surveys

A three-part questionnaire is designed. The first section comprises general instructions that guide the respondents how to tick in the questionnaire. The second section is to take general information of the respondents. The third section includes a list of factors that affect safety on construction site with lifting equipment. The respondents are asked to rate the extent to which they agree with each statement, where 1 = strongly agree, 2 = agree, 3 = neither agree nor disagree, 4 = disagree, and 5 = strongly disagree. The respondents are invited to state other factors and rate them. Questionnaires can be sent by post and e-mails to about 50 respondents who have working experience in this field.

4.4 Step 4: Methods of data analysis

4.4.1 Mean score ranking technique

Descriptive statistics and the mean score ranking technique is adopted to the relative importance of various factors that affect safety on construction site with lifting equipment using the Statistical Package for Social Sciences (SPSS). The five-point Likert scale described above is used to calculate the mean score for each factor, which is then used to determine their relative ranking in descending order of importance.

4.4.2 Cronbach's alpha reliability test

The Cronbach's alpha reliability (the scale of coefficient) measures are used to verify the internal consistency amongst the respondents under the adopted Likert scale of measurement regarding factors affecting safety on construction site with lifting equipment in Vietnamese environment. The Cronbach's alpha coefficients range from 0 to 1 in value and may be used to show the reliability of factors extracted from multi-point formatted questionnaires or scales (Sanotos, 1999). If the items making up the score are all identical and perfectly correlated, then $\alpha = 1$. If the items are all independent, then $\alpha = 0$. Thus, the higher the score, the more reliable the generated scale will be. Tuckman (1999) and Yip and Poon (2009) recommended acceptable alpha values of 0.5 for attitude/perception assessment. The Cronbach's alpha tests are applied to test the reliability of the scales of factors in the questionnaire survey.

4.4.3 Kendall's condordance analysis

The Kendall's coefficient of concordance (W) is used to measure the agreement of different respondents on their rankings of factors based on mean values within a particular survey group. This analysis aims to find out whether the respondents within an individual group respond in a consistent manner or not (Chan et al., 2011). Values of W can range from 0 to 1, with 1 exhibiting perfect agreement and 0 indicating perfect disagreement. In the other hand, a high or significant value of W reflects that different parties are essentially applying the same standard in ranking factors (Daniel, 1978; Chan et al., 2011). However, according to Siegel and Castellan (1988), W is only suitable when the number of attributes is less than or equal to 7. If the number of attributes is greater than 7, chi-square is used as a near approximation instead. If the actual calculated chi-square value equals or exceeds the critical chi-square value got from the table for a certain level of significance and a particular value of degrees of freedom, then the null hypothesis that the respondents' sets of ranking are unrelated to each other within a survey group can be rejected.

4.4.4 t-Test

t-Test of the mean is carried out with the help of SPSS to ascertain whether the respondents will agree that the factors affecting safety on construction sites with lifting equipment. For each attribute, the null and alternative hypotheses are set out below. μ is the population mean, and μ_0 is fixed at 3, ratings below 3 represented respondents' agree with the problem. Null hypothesis H_0: $\mu \geq \mu_0$. The decision rule was to accept H_0 when $p \geq 0.05$. Therefore, when the calculated t value has significance of ≥ 0.05, it is concluded that the issue is not a significant problem to the owner. Alternative hypothesis H_1: $\mu < \mu_0$. The decision rule was to accept H_1 (and reject H_0) when $p < 0.05$ and the t value is negative. Thus, when the calculated t value has significance of < 0.05, it is concluded that the factor has a significant influence of safety on construction site (Ling and Poh, 2008).

4.4.5 Step 5 and 6: Analysis and discussion of survey results; conclusions and recommendations

The results derived from the analysis of empirical questionnaire survey will be cross-referenced to the literature and to complement each other for validation. Finally, valuable conclusions and helpful recommendations for parties involved (e.g., construction firms, regulatory and enforcement authorities, etc.) should be showed.

5. CONCLUSIONS AND FUTURE RESEARCH

This paper presented steps of the useful approach to identify and analyze factors that affect safety in lifting equipment environment in Vietnam. The approach is based on the experience and expertise of safety managers, equipment mangers, and designers and manufacturers. These experts will assess the influence of each of the factors, thus making it possible to distinguish between factors that exert a strong influence and those that exert a moderate influence on site safety. In addition, the proposed approach uses fairly reliable methods of data analysis. However, the proposed approach needs to be verified by some real studies, so it is very important for the research directions in the future.

REFERENCES

Beavers, J. E., Moore, J. R., Rinehart, R., and Schriver, W. R., 2006. Crane-related fatalities in the construction industry. *Journal of Construction Engineering and Management* 132, 901-910.

Bloomberg, 2007. *Vietnam's economy grew by a decade high in 2007*. Bloomberg, Jan. 1, 11.

Bo, X., and Chan, A. P. C., 2012. Investigation of barriers to entry into the design-build market in the people's republic of China. *Journal of Construction Engineering and Management* 138, 120-127.

Chan, D. W. M., Chan, A. P. C., Lam, P. T. I., and Wong, J. M. W., 2011. An empirical survey of the motives and benefits of adopting guaranteed maximum price and target cost contracts in construction, *International Journal of Project Management* 29, 577-590.

Daniel,W.W., 1978. *Applied nonparametric statistics*. Houghton Mifflin, Boston.

Fellow, R., and Liu, A., 2008. *Research methods for construction*, Wiley Blackwell, UK.

Health and Safety Executive, 1978. *One hundred fatal accidents in construction.* Her Majesty's Stationary Office: London, England.

Kang, S., and Miranda, E., 2007. *Physics based model for simulating the dynamics of tower cranes*. Stanford University, United Kingdom.

Kawata, M., 2007. *Safety use of cranes in the construction industry*. Occupational Safety and Health Council, Hong Kong Special Administrative Region.

Ling, F. Y. Y., and Poh, B. H. M., 2008. Problems encountered by owners of design–build projects in Singapore. *International Journal of Project Management* 26, 164-173.

Ministry of Labour-Invalids and Social Affairs, 2013. Labour accidents with causes <http://www.molisa.gov.vn/Default.aspx?tabid=193&temidclicked=342>

Mohamed, S., Ali, T. H., and Tam, W. Y. V., 2009. National culture and safe work behaviour of construction workers in Pakistan. *Safety Science* 47, 29–35.

Neitzel, R. L., Seixas, N. S., and Ren, K. K., 2001. A review of crane safety in the construction industry. *Applied Occupational Environmental Hygiene* 16, 1106–1117.

Rivara, F. P., and Alexander, B. H., 1994. *Occupational injuries in clinical*. Occupational, and Environmental Medicine, Saunders, Philadelphia.

Sanotos, J. R. A., 1999. Cronbach's alpha: a tool for assessing the reliability of scales. *Journal of Extension* 37, 1-5.

Siegel, S., and Castellan Jr, N. J., 1988. *Nonparametric statistics for behavioural sciences*, 2nd ed., McGraw-Hill, New York.

Shapira, A., and Lyachin, B., 2009. Identification and analysis of factors affecting safety on construction sites with tower cranes. *Journal of Construction Engineering and Management* 135, 24-33.

Shapira, A., and Simcha, M., 2009a. AHP-based weighting of factors affecting safety on construction sites with tower cranes. *Journal of Construction Engineering and Management* 135, 307-318.

Shapira, A., and Simcha, M., 2009b. Measurement and risk scales of crane-related safety factors on construction sites. *Journal of Construction Engineering and Management* 135, 979-989.

Shapira, A., Simcha, M., and Goldenberg, M., 2012. Integrative model for quantitative evaluation of safety on construction sites with tower cranes. *Journal of Construction Engineering and Management* 138, 1281-1293.

Shapiro, L. K., and Shapiro J. P., 2004. *Cranes and derricks*, 4th Ed., McGraw-Hill, New York.

Skinner, H., Watson, T., Dunkley, B., and Blackmore, P., 2006. *Tower crane stability*. CIRIA C654, CIRIA, London.

Tam, V. W. Y., and Fung, I. W. H., 2011. Tower crane safety in the construction industry: A Hong Kong study. *Safety Science* 49, 208-215.

Tuckman, B.W., 1999. *Conducting educational research*, 5th ed., Wadsworth Group, Belmont.

Yip, R. C. P., and Poon, C. S., 2009. Cultural shift towards sustainability in the construction industry of Hong Kong. *Journal of Environmental Management* 90, 3616-3628.

Recycled glass concrete beams under bending and shear

Kiang Hwee TAN
Professor, Department of Civil & Environmental Engineering
National University of Singapore, Singapore
tankh@nus.edu.sg

ABSTRACT

As an effort towards the sustainability of concrete as a construction material, waste glass was considered as a substitute for fine aggregates in this study. The flexural and shear behavior of reinforced concrete (RC) beams with recycled glass as 50% and 100% of fine aggregates were investigated. The recycled glass consisted of green and brown glass particles in equal proportions. The beams were examined in terms of cracking and deformation characteristics, as well as ultimate strength and mode of failure. Test results indicated that recycled glass concrete beams similar flexural and shear characteristics as normal concrete beams. The findings therefore demonstrated the technical viability of using waste glass particles as fine aggregates in concrete.

Keywords: *flexure, recycled glass, reinforced concrete, shear, sustainability.*

1. INTRODUCTION

Concrete is the second most used commodity after water, and has been used since the 5th century BC. It is typically mixed with 6% air, 10% cement, 18% water, 25% sand (that is, fine aggregates) and 41% gravel (that is, coarse aggregates). The manufacture of cement, which results in 0.8 to 1.0 ton of CO_2 being released into the atmosphere for every ton of cement production, has raised concerns on its impact on the global carbon footprint. At the same time, the harvesting of sand and gravel which results in deforestation and ecological damage has become an environmental issue in many countries. As such, initiatives have been set up to address the issue of sustainability of concrete as a construction material.

On the other hand, the effluence of society has resulted in more and more urban waste such as paper, plastic and glass, being generated. These wastes have a much lower recycling rate compared to construction waste. The disposal of such waste poses an environmental problem, as landfills are limited. It is therefore natural to consider the use of such waste in the production of concrete. This study was carried out to investigate the feasibility of using waste glass as sand replacement in structural concrete members.

The flexural and shear behavior of reinforced concrete (RC) beams with mixed-color glass as 50% and 100% of fine aggregates were investigated. The mixed-color glass consisted of green and brown glass particles in equal proportions. The beams were examined in terms of cracking and deformation characteristics, as well as ultimate strength and mode of failure. The results were compared to normal RC beams with natural sand as fine aggregates

2. TEST PROGRAM

In this study, soda-lime glass in the form of waste glass bottles were collected from a local recycler. Those bottles were originally used to contain beer or wine. Glass for this purpose is primarily produced in green or brown colors. Green glass is colored by oxides of Cr and Co, while brown glass is produced by adding oxides of Mn, Fe, Ni, and Co (Christensen and Damaggard, 2010). The glass bottles were delivered from the recycling plant in the condition just prior to disposal into landfills.

Before crushing, the glass bottles were cleaned and sorted in the following manner. First, the bottles were immersed in tap water for one day. Next, the metal/plastic caps and neck-caps, wooden corks, as well as plastic/paper labels were removed. Then, the surface of glass bottles was cleaned with tap water, and finally, the glass bottles were separated by color. The green and brown glass bottles were found to have negligible contamination after washing.

The crushing process was done using a jaw crusher, with the output size of the glass particles manually adjusted. Glass bottles were efficiently reduced in size into the range specified by ASTM C 33 (2003) for sand, as shown in Figure 1. The crushed glass particles exhibited angular shape, sharper edge, smooth surface texture and higher aspect ratio than natural sand, because of its brittle characteristics (see Figure 2).

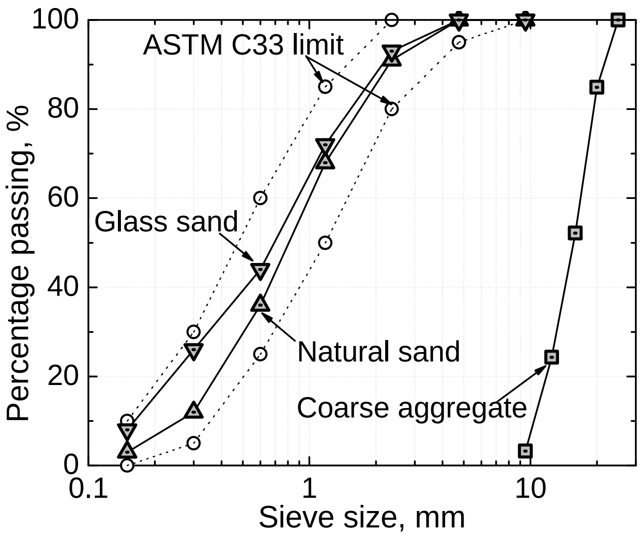

Figure 1: Gradation of glass particles and natural aggregates

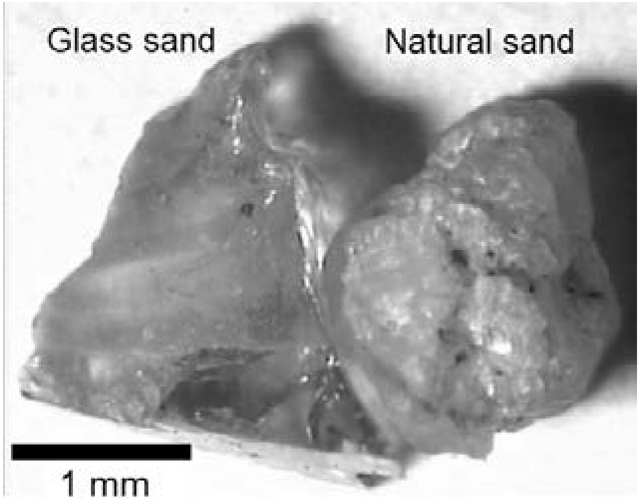

Figure.2: Appearance of typical glass and natural sand

The saturated surface dry (SSD) specific gravity and water absorption capacity of glass particles were determined according to ASTM C 128 (2007) to be 2.53 and 0.07% respectively. Chemical compositions of glasses with different colors were analyzed by energy dispersive spectrum X-ray spectroscopy (EDS) and the results are shown in Table 1 together with those of natural sand and cement..

Table 1: Chemical compositions of glass particles, natural sand and cement

Composition, %	Glass particles		Natural sand	Cement
	Green	Brown		
SiO_2	71.22	72.08	88.54	20.8
Al_2O_3	1.63	2.19	1.21	4.6
Fe_2O_3	0.32	0.22	0.76	2.8
CaO	10.79	10.45	5.33	65.4
MgO	1.57	0.72	0.42	1.3
Na_2O	13.12	13.71	0.33	0.31
K_2O	0.64	0.16	0.31	0.44
TiO_2	0.07	0.1	0.05	—
Cr_2O_3	0.22	0.01	—	—
SO_3	—	—	—	2.2

2.1 Test Specimens

Eighteen beams were fabricated and tested. The beams were divided into two main groups, with nine beams for flexural tests (Group BF) and another nine for shear tests (Group BS), as shown in Table 2. The main test parameter was the tensile steel ratio for former group, and shear span to effective depth ratio for the latter group. For each test parameter, the glass-to-fine-aggregate content was varied as 0%, 50% and 100%. Group GF beams were designated BF*m*-*n*, where *m* denotes the diameter of tensile reinforcing bars, and *n* denotes the glass-to-fine aggregate ratio, in percentage (%). Group BS beams were designated BS*x*-*y*, where x denotes the shear span-to-effective depth ratio, and y the glass-to-fine aggregate ratio (%).

Table 2: Test parameters and results

Gp.	Beam designation	Tensile steel ratio, ρ (%)	Shear span – effective depth ratio, a/d	Glass-to-fine aggregate ratio, g/fa	Concrete compressive strength, f_{cm} (MPa)	Ultimate load, P_u (kN)	Failure mode
BF	BF10-0	1.24	4.7~4.8	0	44.4	39.1	FT
	BF10-50			50	42.0	36.7	FT
	BF10-100			100	39.0	37.2	FT
	BF13-0	2.12		0	48.0	57.2	FT
	BF13-50			50	42.0	51.9	FT
	BF13-100			100	39.0	53.4	FT
	BF16-0	3.24		0	40.0	81.1	FC
	BF16-50			50	39.5	77.8	FC
	BF16-100			100	37.6	65.4	FC
BS	BS1.8-0	1.24	1.8	0	42.0	121.0	FT
	BS1.8-50			50	42.3	122.0	SC
	BS1.8-100			100	39.7	134.3	FT
	BS2.4-0		2.4	0	39.7	36.0	SB
	BS2.4-50			50	42.3	54.7	SB
	BS2.4-100			100	39.7	52.6	SB
	BS3.5-0		3.5	0	39.0	41.6	SB
	BS3.5-50			50	42.3	39.6	SB
	BS3.5-100			100	39.7	49.8	SB

Note: FT – flexural tension; FC – flexural compression; SC – shear-compression; SB – shear-bond.

The concrete mix consisted of cement, fine aggregates, coarse aggregates, and water in the proportion of 1 : 1.90 : 1.61 : 0.49 by weight. The cement content was 460 kg/m^3. The target slump was 100 mm and characteristic cylinder strength was 30 MPa.

The reinforcement cages for the beams are shown in Figure 3. For Group BF beams, each beam measured 2 meters in length. The longitudinal reinforcement consisted of two deformed bars with diameters of 10 mm, 13 mm or 16 mm (see Table 2), and except for the middle third-length, the beams were provided with closed links with a diameter of 6 mm at a spacing of 90 mm. For Group BS beams, the length varied according to the desired shear span-to-effective depth ratio. The longitudinal reinforcement consisted of two deformed bars with a diameter of 10 mm, and no transverse reinforcement was provided.

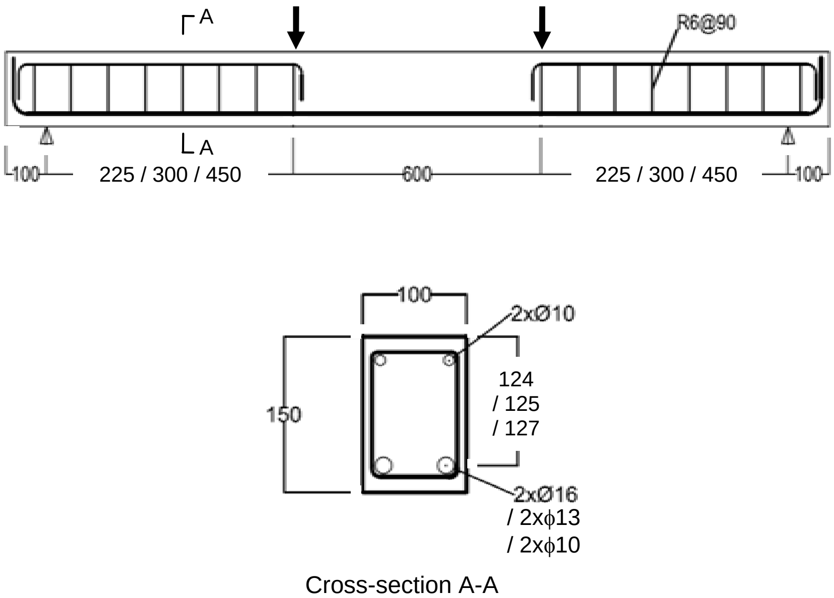

Figure 3: Reinforcement details of test beams (*All dimensions are in mm*)

2.2 Material Properties

Ordinary Portland Cement (OPC) was used. The fine aggregates consisted of both natural sand and waste glass particles. The glass particles were obtained by crushing waste soda lime glass bottles and sieving to remove particles which are larger than 4.75mm. Granite of a maximum size of 10 mm was used as coarse aggregates.

The average yield strength of 6, 10, 13 and 16 mm bars were 452, 573, 480 and 503 MPa, respectively, each determined based on three samples. The corresponding elastic moduli were 199, 205, 193 and 199 GPa, respectively.

2.3 Beam Fabrication and Test Instrumentation

The reinforcement cage was assembled and strain gauges were fixed on the longitudinal steel bars at mid-length and on the closed links as shown in Figure 4. The beams were cast in wooden formwork, which was removed one day later. They were then placed under wet gunny sacks for a week.

Accompanying cubes and cylinders for the determination of concrete compressive strength were prepared at the same time and cured in the same manner. After that, the beams were placed in the laboratory under ambient condition until the day of testing, which was typically 28 days after casting.

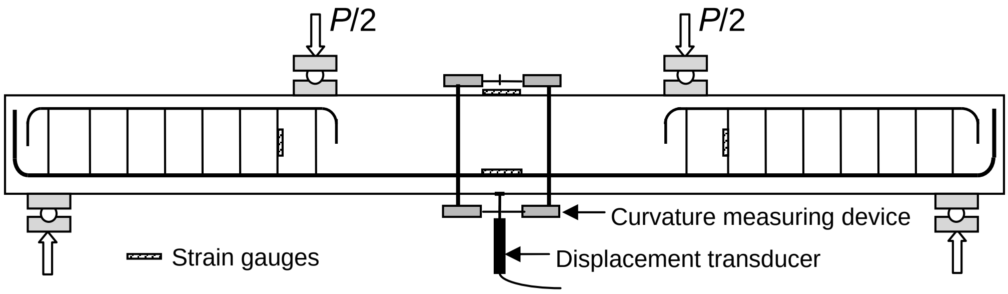

Figure 4: Test set up and instrumentation

The test set-up is also shown in Figure 4, with the beam subjected to four-point bending. Strain gauges were placed on the top of the beam at mid-span and on the side face of the beam in both the transverse and longitudinal directions in the case of Group BS beams, at approximately one effective-depth distance from the loading points. A device using two transducers placed one each above and below the beam was used to measure the beam curvature at mid-span. In addition, the mid-span deflection of the beam was monitored using a linear variable displacement transducer (LDVT). The cracking characteristics were noted as the beam was loaded to failure.

3. TEST RESULTS AND DISCUSSION

In general, the behavior of the beams was found to be similar regardless of the glass-to-fine-aggregate ratio, *g*/*fa*. The appearance of the beams after testing is shown in Figure 5. As indicated in Table 2, the beams exhibited approximately the same ultimate load-carrying capacity, P_u, and the same failure mode, especially for Group BF beams that failed in flexure. For Group BS beams, some difference in shear capacity was observed with different *g*/*fa* ratios, but this was probably due to the scatter nature related to shear resistance of structural concrete, especially for small span-to-effective depth ratio, *a*/*d*. The failure was by shear-bond except for BS1.8-*y* beams. Due to a small *a*/*d* ratio of 1.8, BS1.8-*y* beams failed by shear-compression or flexural tension, as the corresponding beam capacities were close to one another.

3.1 Flexural characteristics

The load versus mid-span deflection curves for BF-10-*n*, BF-13-*n* and BF-16-*n* beams are shown in Figure 6. BF-10 beams with a tensile steel ratio of 1.24%, were designed as under-reinforced beams. In these beams, cracks were first observed at about 6 kN. This was followed by a reduction in beam stiffness as cracks developed further. The longitudinal steel was observed to yield at about 35 kN. The beams exhibited ductile behavior before they finally failed in flexural tension, with the extreme concrete compressive fiber reaching a strain of 0.0035 to 0.0045. There was no difference in the flexural characteristics due to the different *g*/*fa* ratios.

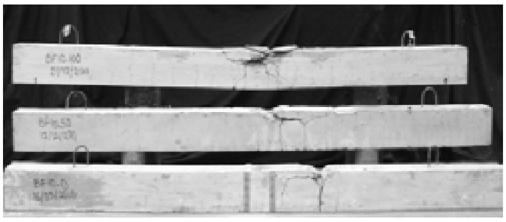

(a) BF-10 beams (ρ = 1.24%)

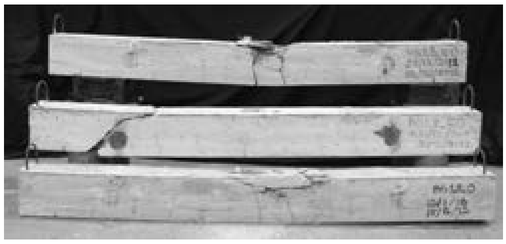

(d) BS-1.8 beams (a/d = 1.8)

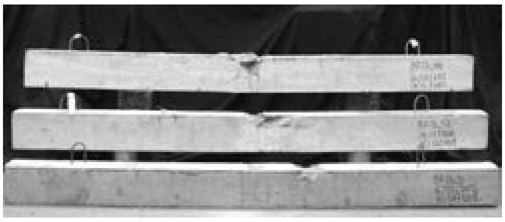

(b) BF-13 beams (ρ = 2.12%)

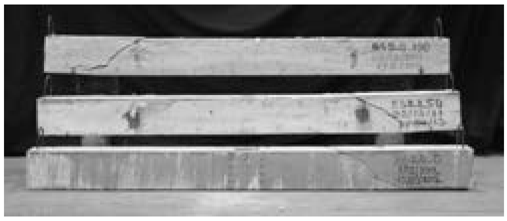

(e) BS-2.4 beams (a/d = 2.4)

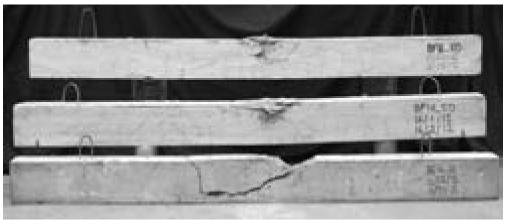

(c) BF-16 beams (ρ = 3.24%)

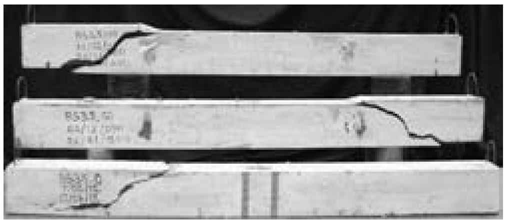

(f) BS-3.5 beams (a/d = 3.5)

Figure 5: Appearance of beams after tests (bottom to top: ***g*/*fa*** = 0, 50, 100%)

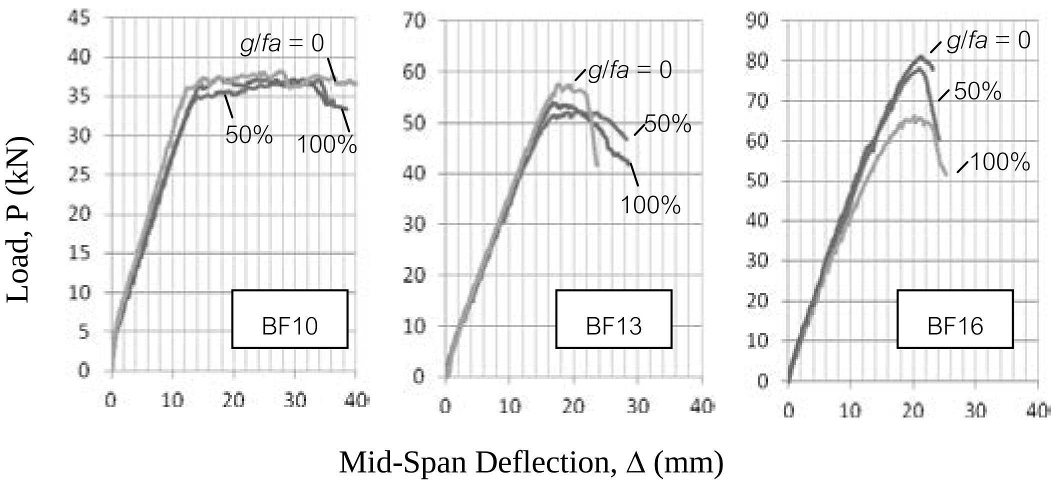

Figure 6: Load versus deflection characteristics of Group BF beams

BF-13 beams had a tensile steel ratio of 2.12%, approximately equal to the balanced steel ratio. The beams exhibited similar behavior as BF-10 beams except for a smaller reduction in beam stiffness after cracking, a higher yield load and a limited ductility at failure. Again, there was no significant difference among the beams. BF-16 beams were designed with a tensile steel ratio of 3.24%, that is, as over-reinforced beams. After cracking at about 8.5 kN, there was a small reduction in beam stiffness, and the beam failed by concrete crushing just prior to the yielding of the longitudinal steel reinforcement. The difference in behavior among the beams was small. The maximum concrete strain measured at the extreme compressive fiber was between 0.003 and 0.004 for these two sub-groups of beams.

Figure 7 shows the observed maximum width of flexural cracks in the beams. The maximum crack width was measured at the level of the tensile longitudinal reinforcement. It is noted the crack widths tend to be smaller with a higher percentage of glass particles; however, the difference is not significant.

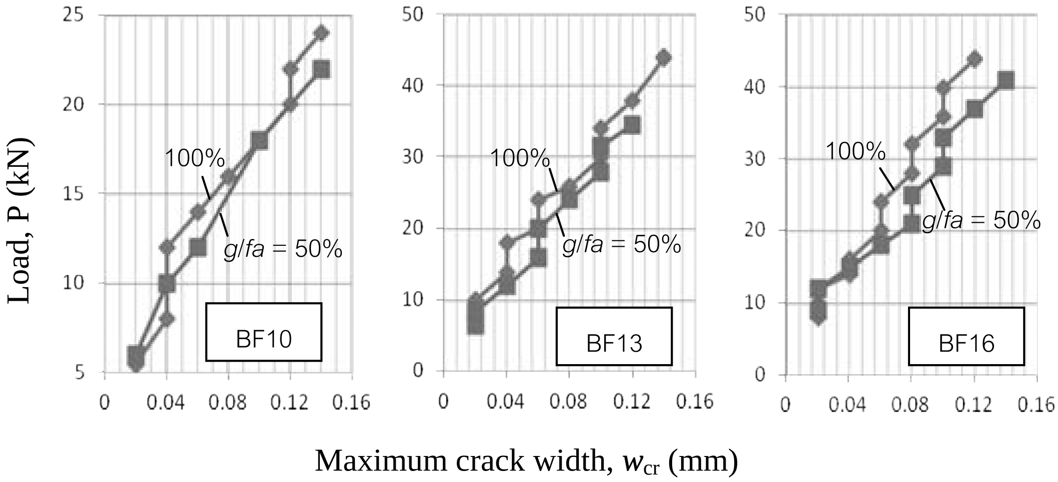

Figure 7: Maximum crack widths in Group BF beams

3.2 Shear characteristics

The load versus mid-span deflection curves for Group BS beams are shown in Figure 8. Except for BS1.8-0 and BS1.8-100, which failed by flexural tension, all beams failed abruptly by shear bond or shear compression. No significant difference due to different glass-to-fine aggregate ratios was observed.

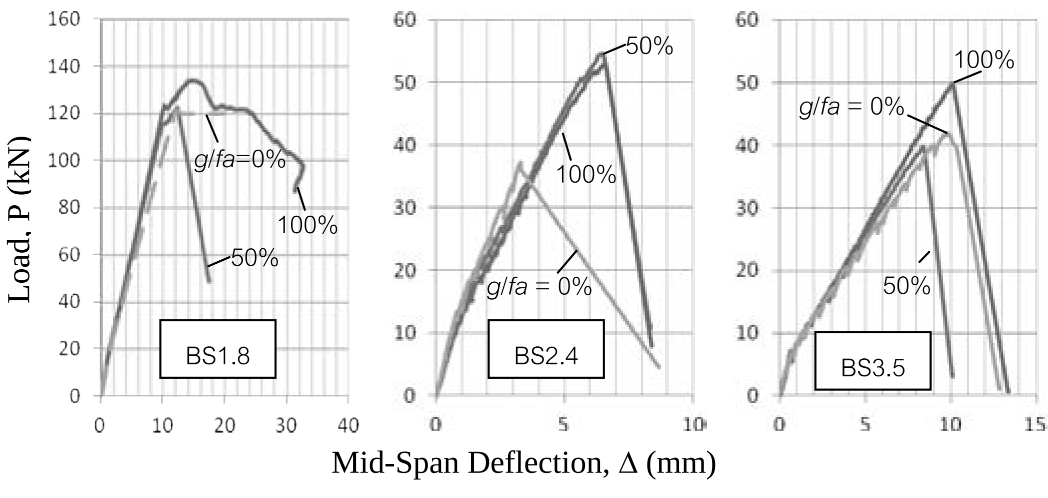

Figure 8: Load versus deflection characteristics of Group BS beams

4. CONCLUDING REMARKS

Previous studies (Du, 2011) have shown that recycled glass concrete with glass particles as fine aggregates do not differ much from normal concrete in properties at the freshly mixed state. Only a slight reduction in fresh density, marginal increase in air content and negligible change in slump, were observed.

Also, the mechanical properties of concrete were not affected by the use of recycled glass particles. On the contrary, there could be an increase in the compressive strength, flexural and splitting tensile strengths, and static modulus. Drying shrinkage was also found to reduce in recycled glass concrete with lower water-cement ratio. Resistance to chloride ion penetration was found to be significantly higher in recycled glass concrete. Furthermore, recycled glass concrete was found to show innocuous alkali-silica expansion in accelerated mortar bar tests using mortar screened from recycled glass concrete.

The tests carried out and reported herein demonstrated that both the flexural and shear behavior of reinforced concrete beams with glass particles as fine aggregates are essentially the same as those of normal reinforced concrete beams. Hence, it is feasible to use waste glass particles in concrete without compromising on the mechanical and structural properties of concrete and concrete members. Further field studies would be appropriate before it can be implemented in practice.

REFERENCES

ASTM C 33-03, 2003. *Standard Specification for Concrete Aggregates.* West Conshohocken, PA: ASTM International.

ASTM C 128-01, 2007. *Standard Test Method for Density, Relative Density (Specific Gravity), and Absorption of Fine Aggregate.* West Conshohocken, PA: ASTM International.

Christensen, T. H., and Damaggard, A., 2010. Recycling of Glass. In Christensen, T. H. (editor), *Solid Waste Technology & Management*, John Wiley & Sons, Chichester.

Du, H., 2011. *Glass Sand Concrete and "Sandless" Concrete*. PhD Thesis, National University of Singapore, Singapore.

Strength of beam-column joint in soft-first story RC buildings

Toshikatsu ICHINOSE[1], Sefatullah HALIM[2], Susumu TAKAHASHI[3], Masaomi TESHIGAWARA[4], Takashi KAMIYA[5] and Hiroshi FUKUYAMA[6]
[1]Professor, Nagoya Institute of Technology, Japan.
ich@nitech.ac.jp
[2]Ph.D Student, Nagoya Institute of Technology, Japan
[3]Assistant Professor, Nagoya Institute of Technology, Japan.
[4]Professor, Nagoya University, Japan.
[5]Chief Research Engineer, Yahagi Construction Co., Ltd, Japan.
[6]Director, Building Research Institute, Japan.

ABSTRACT

This paper describes the strength of reinforced concrete (RC) beam-column joints in buildings with soft-first story. In such a building, the sections of first story columns are usually much larger than those of second story columns. To investigate the strength of the joint, specimens are constructed and tested. Test parameters are hoops in the beam-column joint, beam reinforcements, stirrups in the beam and axial force. The test result shows that the beam reinforcements and stirrups are effective to prevent joint failure. The force-resistant mechanisms of these joints are different from those of usual beam-column joints, because sign of bending moment in the second story column is same as that of the first story columns in these joints. Failure modes of these joints are also different from those of usual beam-column joints. Strut-and-tie models are developed for the specimens. The developed models agreed with the test results.

Keywords: *strength, reinforced concrete, beam-column joint, strut-and-tie model, soft-first story, seismic design*

1. INTRODUCTION

Reinforced concrete (RC) buildings with soft first story are popular because the large space in the first story serves as a parking lot, commercial space, or other similar purposes. However, as shown in Fig. 1, many collapses occurred in soft first story in the 1995 Kobe earthquake. In Japan, researchers proposed to strengthen the columns in the soft first story after the 1995 Kobe earthquake. As a result of such experiences and researches, many RC buildings are being constructed in Japan with a soft first story in which the sectional area of the first-story column is larger than those of the upper stories to prevent story collapse as shown in Fig. 2. In this paper, the joints shown in Figs. 2a and 2b are called "I-type" and "O-type" joints, respectively, where the first-story columns are extended toward the inside and outside of the frame.

In either case, the vertical reinforcements in the extended area of the first-story column are anchored to the beam-column joint. A question arises whether the joint may fail before the column exhibit its strength. In fact, the joint in Fig. 1 is more damaged than the column.

In this study, a test is conducted to investigate the strength and failure modes of both loading directions and both type of joints. In addition, the reinforcements effective in strengthening the beam-column joint in soft first story are discussed.

Figure 1 Joint failure in soft story

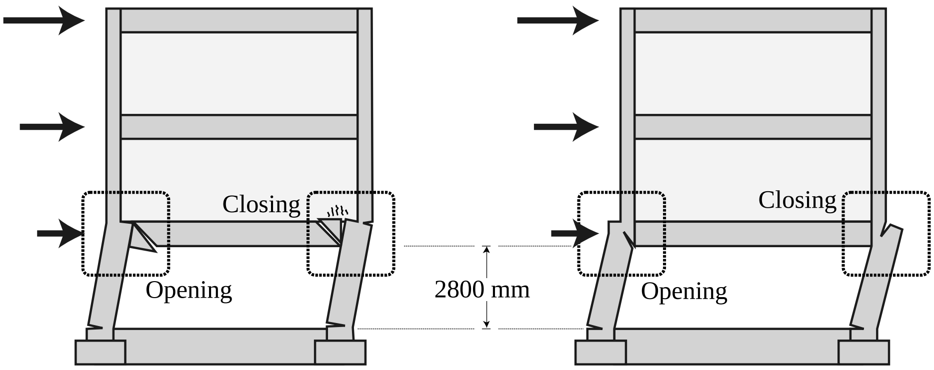

(a) I-type joint (b) O-type joint

Figure 2 Two types of buildings with soft-first story

2. EXPERIMENTAL PROGRAM

Two specimens of each type of building are constructed: Specimens I-1 and I-1t for the building shown in Fig. 2a and Specimens O-1 and O-1t for the building shown in Fig. 2b. The area around the joint denoted by the dashed line in Fig. 2 is used as specimen to investigate the strength of the beam-column joint. The specimens are 1/2 scale models constructed upside down to easily apply the forces. Figure 3 shows the test setup and the dimensions of Specimen I-1, where the specimen and test setup are drawn upside down to treat the specimen as a part of an actual building. The stub column at the left end of the specimen is constructed to prevent the flexural failure of the wall panel that never occurs in real buildings. The loading point is assumed to be the middle point of the clear height of the first story; therefore, 700 mm in Fig. 3 corresponds to one-fourth of the story height (2800 mm in Fig. 2). The displacement is controlled at the lateral loading point. The lateral drift is defined as the ratio of the lateral displacement at the loading point to 700 mm. The applied axial load is shown in Table 1 where the positive value represents compressive axial force. The axial load is constant up to the drift of 0.5%. Considering the overturning mechanism of the building due to larger displacements, the axial load is changed for opening and closing directions.

Figure 4 shows the detail of Specimen O-1t. The detail of Specimen I-1t is reported by Ogawa et al (2012). The shape of Specimens I-1 and O-1 are identical to those of I-1t and O-1t, respectively. However, the numbers of stirrups, hoops in the joint, and beam reinforcements of I-1t and O-1t are larger than those of I-1 and O-1, respectively (red-, blue-, and green-colored reinforcements in Fig. 4 are provided only in I-1t and O-1t). The yield strengths of the steel bars are between 369 and 389 MPa. The pro compressive strengths of concrete are between 25.5 and 26.4 MPa.

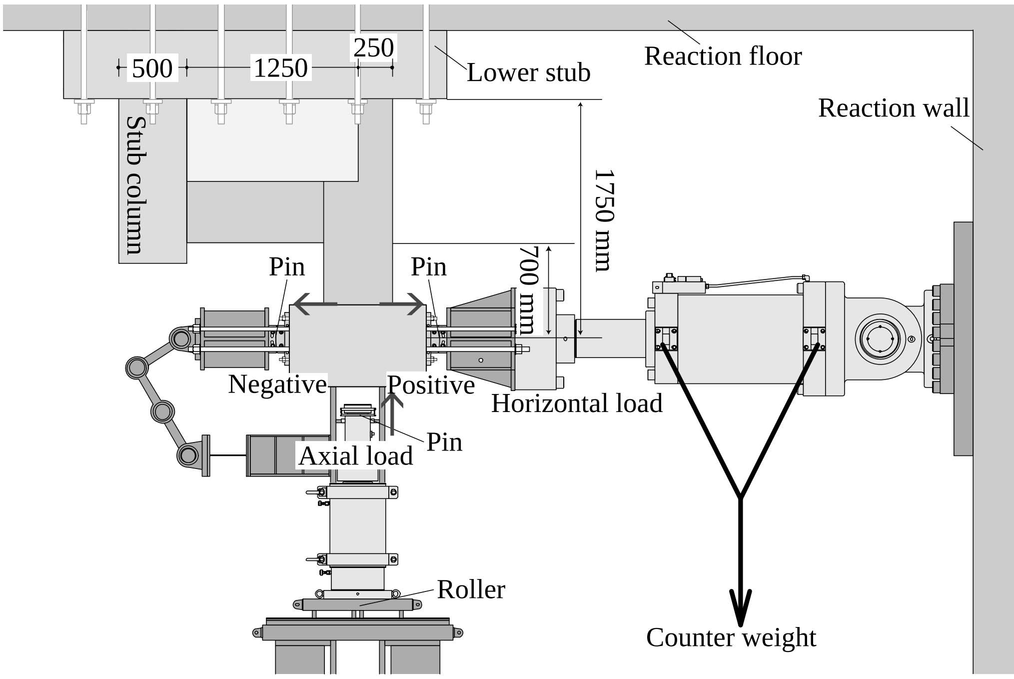

Figure 3 Test set up and dimensions of specimen I-1 [mm]

Table 1 Applied axial load

<table>
<tr><th colspan="2">Specimen</th><th>$R \leq 0.5$ %</th><th>$R > 0.5$ %</th></tr>
<tr><td rowspan="2">I-1
O-1</td><td>Open</td><td rowspan="2">1125 kN
(η = 0.15)</td><td>0 kN</td></tr>
<tr><td>Close</td><td>2250 kN
(η = 0.30)</td></tr>
<tr><td rowspan="2">I-1t
O-1t</td><td>Open</td><td rowspan="2">500 kN
(η = 0.07)</td><td>-450 kN</td></tr>
<tr><td>Close</td><td>1450 kN
(η = 0.20)</td></tr>
</table>

η : Ratio of the axial force to the compressive capacity of the first story column

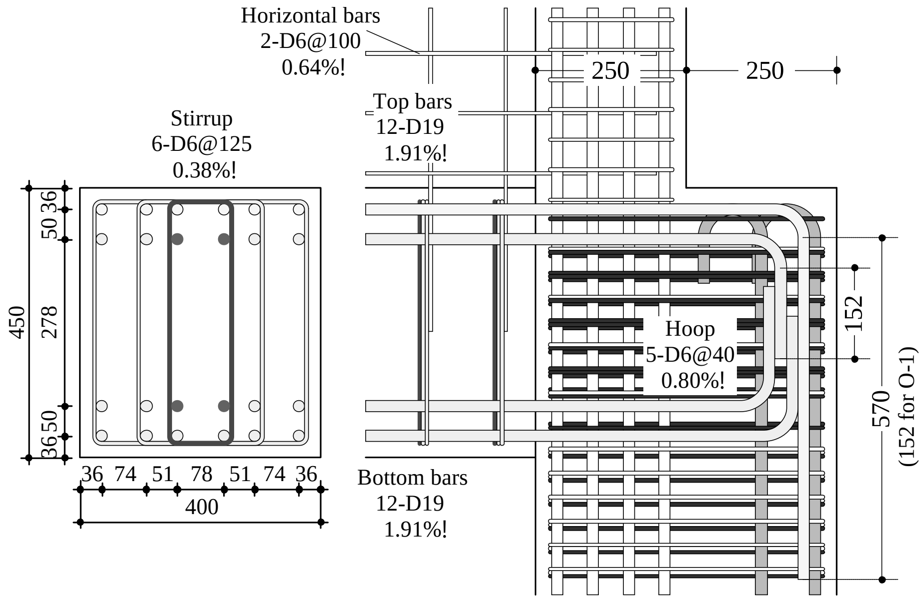

Figure 4 Specimen O-1t [mm]

3. EXPERIMENTAL RESULTS OF SPECIMENS I-1 AND I-1t

The load–drift relationship of I-1 is shown in Fig. 5, where the loading cycles smaller than 0.5% drift are not shown because the scope of this study is to discuss the strength and failure mode of the beam-column joints. Blue lines represent the strengths based on the flexural failure of the first-story column at the beam bottom face. These strengths are computed using the stress–strain relationship of concrete proposed by Hognestad et al. (1955). In the opening (positive) direction, during the cycle to +1% drift, the beam bottom reinforcements and stirrups yielded. The maximum strength is recorded at +2% drift and corresponds to 66% of the computed strength. Figure 7a shows the crack pattern at +2% drift at which the maximum strength is recorded. A crack in the beam (thick line in Fig. 6a) is prominent. This crack proceeds to the joint above the hooks of the vertical reinforcement in the extended area of the first-story column. The vertical reinforcements in the second-story column yielded during the cycle to +2% drift (C4 in Fig. 5). In this failure mode as depicted in Fig. 6b, the beam bottom reinforcements and the vertical reinforcements in the second-story column are yielded. In the following, the failure associated with the yielding of the beam reinforcements and vertical reinforcements in the second-story column is called joint failure. The arrows in Fig. 6b represent the sign of the bending moments of the first-story column (M_{c1}), the beam (M_b), and the second-story column (M_{c2}). The bending moment of the second-story column is opposite to that in the usual beam-column joints. Therefore, the force-resistant mechanism of this joint is different from that of the usual beam-column joints. The failure mode of Specimen I-1 in the opening direction is a joint failure and it has large ductility. The strength remains almost constant up to +5% lateral drift.

In the closing direction, during the cycle to -2% drift, the beam-top reinforcements yielded (B4 in Fig. 5). Figure 7a shows the crack pattern at −2% drift. In addition, the lateral strength degraded during this cycle as shown in Fig. 5.

The compressive failure of the wall panel was observed. As discussed above, the force-resistant mechanism of this joint is different from that of the usual beam-column joints; the failure of the wall panel triggered strength degradation (see the photo in Fig. 7a). An inclined crack in the beam is prominent in the closing direction. On the basis of these results, as shown in Fig. 7b, the failure mode corresponds to the joint failure, which is a brittle failure mode, and the lateral load decreases rapidly when the wall panel fails under compression (Fig. 5).

The load–drift relationship of I-1t is shown in Fig. 8. In the opening direction, the vertical reinforcements in the first-story column yielded prior to the beam bottom reinforcements during the cycle to +1% drift. The maximum strength is recorded at +2% drift, which corresponds to 92% of the analytical strength based on the flexural capacity of the first-story column. In the closing direction (the left half of Fig. 9), the vertical reinforcements in the first-story column yielded during the cycle to −1% drift. The yielding of the beam-top reinforcements and the compressive failure in the wall panel are not observed in I-1t. The specimen I-1t has large ductility in the closing direction as well as in the opening direction.

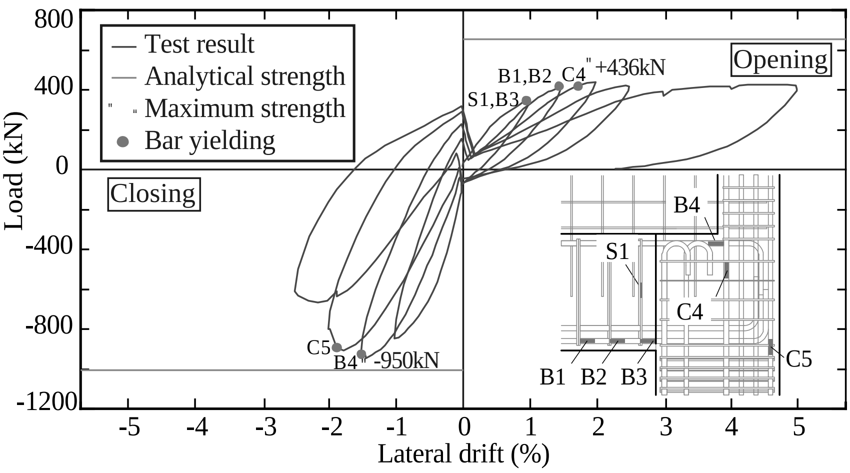

Figure 5 Load-drift relationship of I-1

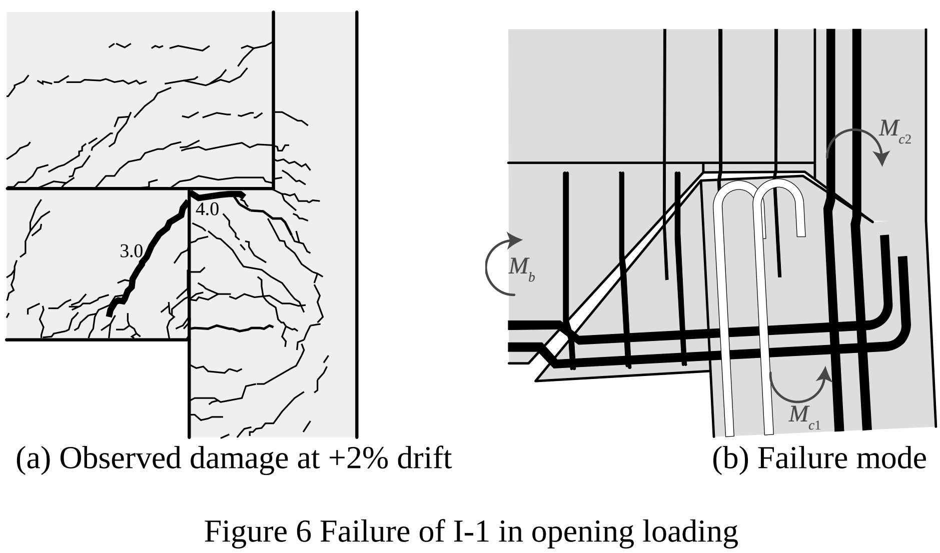

(a) Observed damage at +2% drift (b) Failure mode

Figure 6 Failure of I-1 in opening loading

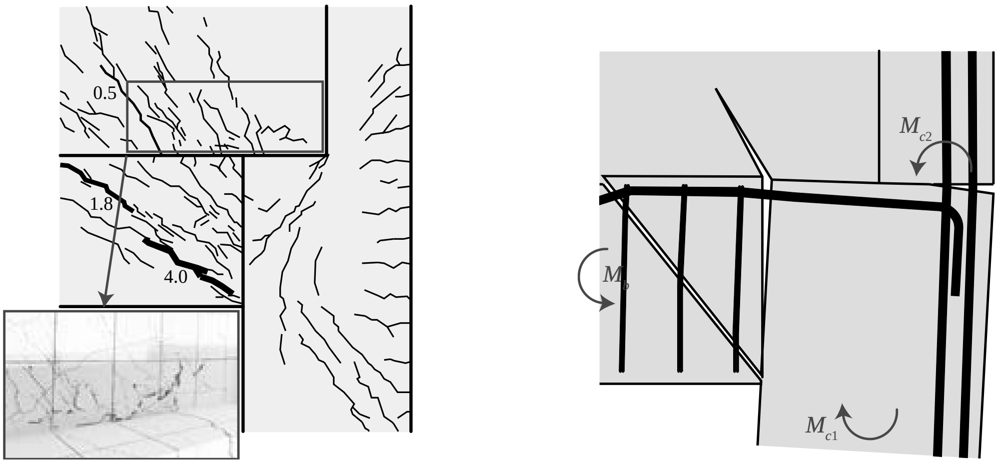

(a) Observed damage at -2% drift (b) Failure mode

Figure 7 Failure of I-1 in closing loading

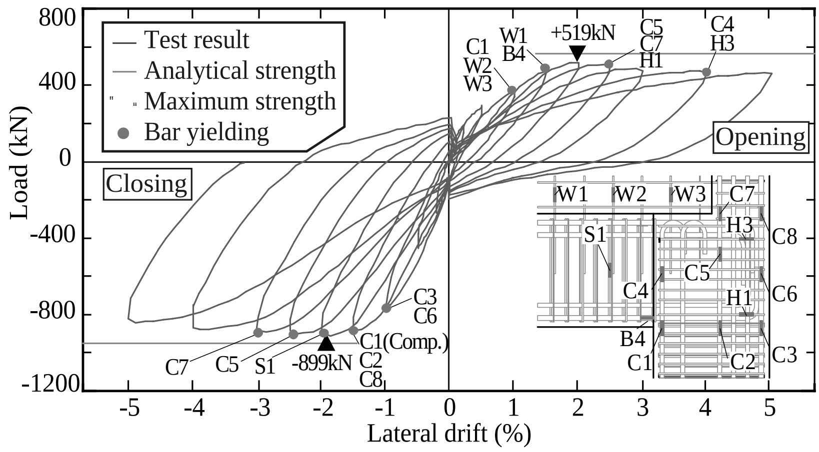

Figure 8 Load-drift relationship of I-1t

4. EXPERIMENTAL RESULTS OF SPECIMENS O-1 AND O-1t

The load–drift relationship of O-1 is shown in Fig. 9. In the opening (positive) direction, during the cycle to +1.5% drift, the beam bottom reinforcements yielded while the stirrups yielded during the cycle to +2% drift. Figure 10a shows the crack pattern at +2.5% drift at which the maximum strength is recorded. The three cracks depicted in Fig. 10b are prominent. Therefore, the failure mode in the opening direction is regarded as joint failure. The strength of the failure is 72% of the computed strength, but it has large ductility similar to Specimen I-1. The failure modes of I-1 (Fig. 6b) and O-1 (Fig. 10b) in the opening direction appear different. However, the strengths of these failures are similar to each other because they are governed by the beam bottom reinforcements and vertical reinforcements in the second-story column, contributing to M_b and M_{c2} (Figs. 6b and 10b, respectively) as discussed later.
In the closing direction, the beam-top reinforcements yielded during the cycle to −2% drift at which the maximum strength is recorded. Figure 11a shows the crack

pattern at the maximum strength. The crack at the reentrant corner above the joint is more prominent than those in the beam and column. Figure 11b shows the failure mode of the closing direction, which is again a joint failure and has a larger ductility than that of Specimen I-1 in the closing direction. The compressive failure of the wall panel was not observed in O-1. The maximum strength of O-1 is also larger than that of I-1 in the closing direction.

The load–drift relationship of O-1t is shown in Fig. 12. In the opening direction, during the cycle to +1.5% drift, the reinforcements in the first-story column and the beam yielded. The maximum strength is recorded at +4% drift, which is close to the analytical strength of the first-story column. In the closing direction, during the cycle to −1.5% drift, the reinforcements near the reentrant corner above the joint yielded (B9 and C8 in Fig. 12), indicating joint failure. The maximum strength is recorded at −2.5% drift and the hoop reinforcements in the upper part of the joint (H3 in Fig. 18) yielded during this loading cycle. During the cycle to −3% drift, the vertical reinforcements in the first-story column (C3) yielded, indicating column failure.

The failure modes of the specimens are summarized in Table 2. Because the joint failure of Specimen I-1t is prevented in both directions of the loading, it is concluded that the stirrups and beam reinforcements increase the strength of the joint failure of the I-type joints. Because the joint failure of Specimen O-1t is prevented in the opening loading and reduced in the closing direction, it is concluded that the hoops in the joint and beam reinforcements increase the strength of the joint failure of the O-type specimen.

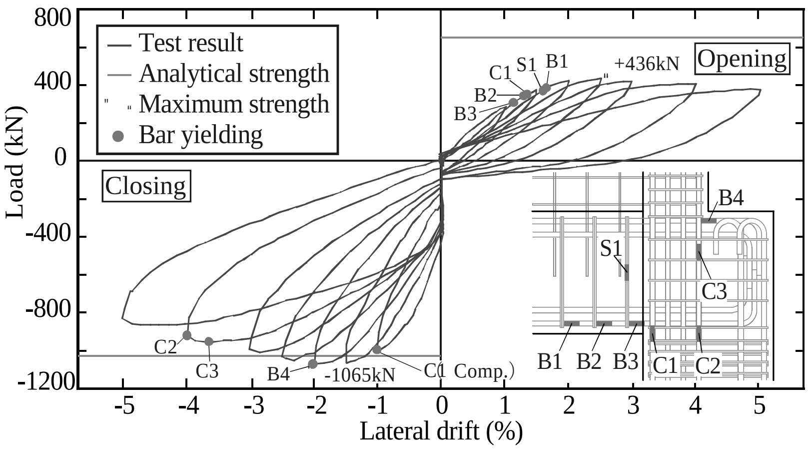

Figure 9 Load-drift relationship of O-1

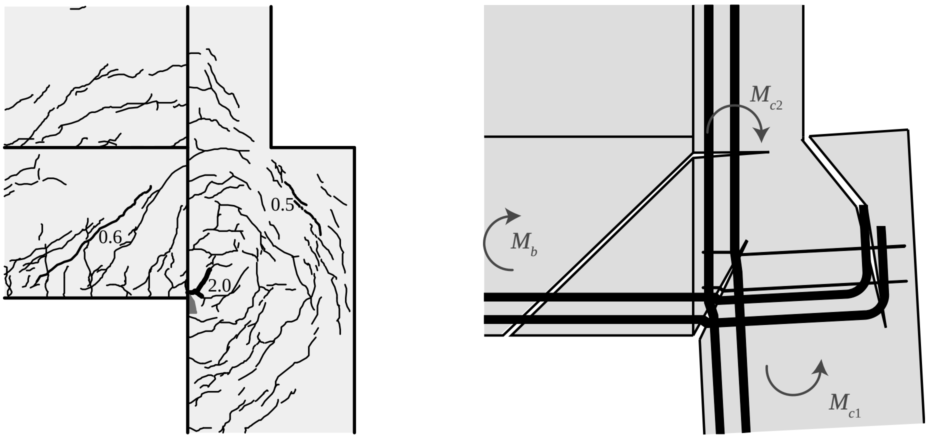

(a) Observed damage at +2% drift (b) Failure mode

Figure 10 Failure of O-1 in opening loading

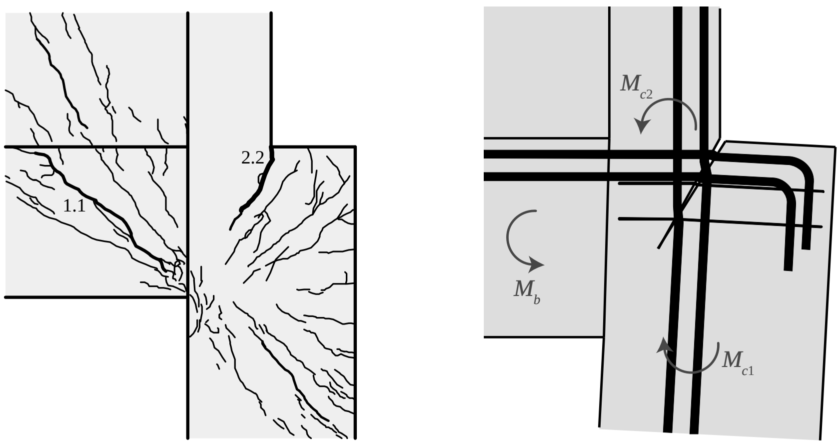

(a) Observed damage at -2% drift (b) Failure mode

Figure 11 Failure of O-1 in closing loading

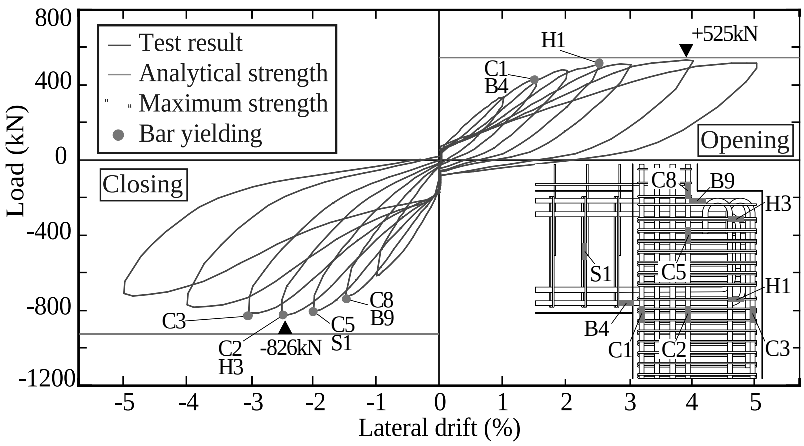

Figure 12 Load-drift relationship of O-1t

Table 2 Failure modes of specimens

Specimen	Open	Close
I-1	Joint	Joint
I-1t	Column	Column
O-1	Joint	Joint
O-1t	Column	Joint*

*The degree of joint failure was reduced and some symptoms of column failure is observed.

5. STRUT-AND-TIE ANALYSES

Figures 13 and 14 show the strut-and-tie models for I-1 and O-1 specimens. Solid blue lines indicate the bars in the tensile yielding, while dashed lines indicate below the yield point. Red zones indicate struts in compression. The effective compression strength of concrete to determine strut's width is assumed to be 85% of the concrete strength. Because the thickness of the wall panel was 100 mm and 1/4 of the width of the beam (400 mm), the width of each strut widens by four times at the boundary of the beam and the wall panel. Similar changes also occur at the boundary of the beam and the column. The strut distribution agreed with the crack pattern observed in the test. The lateral load carrying capacity based on STM agreed with the test result with error less than 10% (Fig. 15).

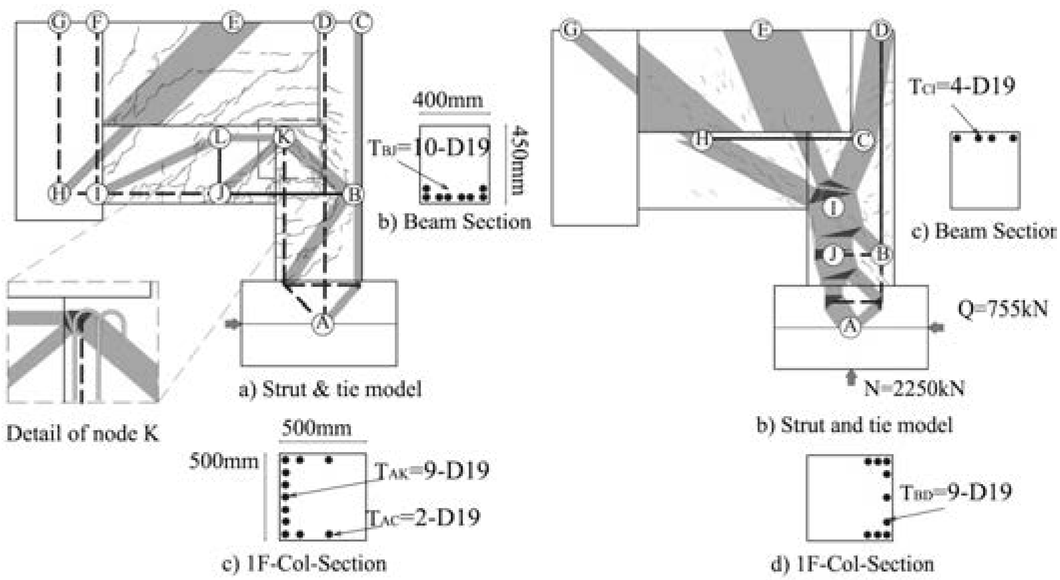

Figure 13 Strut-and-tie models for I-1 specimen

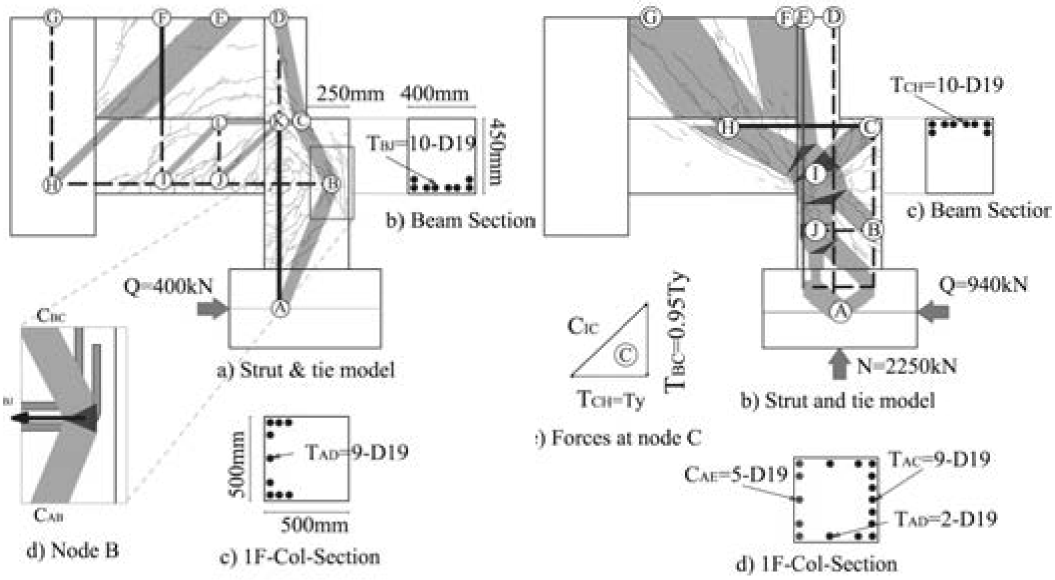

Figure 14 Strut-and-tie models for O-1 specimen

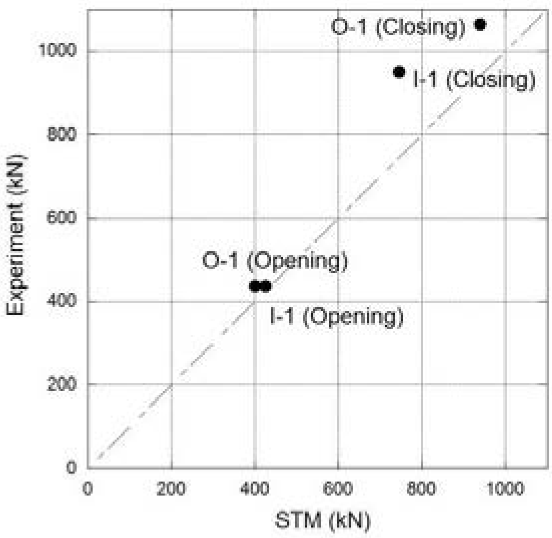

Figure 15 Observed strengths vs. strut-and-tie models

6. CONCLUSIONS

The strength of the joints in soft first story is experimentally investigated. Two types of joints are tested: 1) first-story column is extended toward the inside of the building (I-type joint; Specimens I-1 and I-1t) and 2) first-story column is extended toward the outside of the building (O-type joint; Specimens O-1 and O-1t). On the basis of the test results, the following conclusions are obtained:

1. In Specimens I-1 and O-1, the failures associated with the yielding of the beam reinforcements and cracks in the joint (Figs. 7b, 8b, 16b, and 17b) are observed in both directions of the loading. These failures are called “joint failures.” The

strengths of these failures are much smaller than those of the flexural strength of the first-story column.
2. In both types of specimens, the beam-top and bottom reinforcements are effective to prevent the joint failure in the closing and opening directions, respectively.
3. The stirrups in the beam are effective to prevent the joint failure of I-type joint.
4. The hoops in O-type joint are effective to prevent the joint failure both in the opening and closing loads.
5. The observed crack pattern and the strut-and-tie analyses indicate that the force-resistant mechanisms of these joints are different from those of the usual beam-column joints because, in contrast with the usual beam-column joints, the sign of the bending moment of the second-story column is the same as that of the first-story column.

REFERENCES

Ogawa, T., Teshigawara, M., Ichinose, T., and Kamiya, T., 2012. *The effects of haunches, axial force and anchorages on the beam-column joint of soft first story. Transactions of JCI,* Vol. 34, No. 2, 269-264 (in Japanese).

Parametric study for displacement based analysis of unreinforced brick masonry walls subjected to lateral loads

Archanaa DONGRE[1] and Pradeep K RAMANCHARLA[2]
[1]Associate Professor, Civil Engineering Department, IPEC Ghaziabad, Ghaziabad-201010, India
raut@research.iiit.ac.in
[2]Professor of Civil Engineering, Earthquake Engineering Research Centre, IIIT Hyderabad, Gachibowli, Hyderabad-500032, India
ramancharla@iiit.ac.in

ABSTRACT

Brick masonry construction can be widely seen in Asian countries as well as globally. Past earthquakes proved the vulnerability of brick houses. Research is going on worldwide to understand the behavior of brick masonry buildings.

In this research work, in order to understand the behavior of brick masonry buildings during earthquake and damage to such buildings, a numerical study is conducted to understand the level of damage by crack occurrences, their evolution, block separation and material loss before collapse and mitigation measures of retrofitting of weak buildings can be suggested. In this parametric study; three cases have been considered i.e. Effect of mortar volume, effect of span ratio and effect of opening on strength and stiffness of wall.

Keywords: *Displacement based analysis, mortar volume, span ratio*

1. INTRODUCTION

Masonry buildings are brittle structures and one of the most vulnerable when compared with the all building types under strong earthquake shaking. Ground vibrations during earthquakes cause inertia forces at locations of mass in the building. These forces travel through the roof and walls to the foundation. Masonry building consist of three main components i.e. wall, roof and foundation, in which walls are most vulnerable to damage caused by horizontal forces due to earthquake. As, during earthquake ground shakes simultaneously in vertical as well as horizontal direction and horizontal vibrations are the most damaging to normal masonry buildings. Horizontal inertia force developed at the roof transfers to the walls acting either in the weak or in the strong direction. To ensure good seismic performance, all walls must be joined properly to the adjacent walls. In this way, walls loaded in their weak direction can take advantage of the good lateral resistance offered by walls loaded in their strong direction. Walls also need to be tied to the roof and foundation to preserve their overall integrity.

2. NUMERICAL STUDY USING APPLIED ELEMENT METHOD

2.1 Description:

In AEM, structure is assumed to be virtually divided into small square elements each of which is connected by pairs of normal and shear springs set at contact locations with adjacent elements. These springs bear the constitutive properties of the domain material in the respective area of representations (Fig. 1). Global stiffness of structure is built up with all element stiffness contributed by that of springs around corresponding element. Global matrix equation is solved for three degrees of freedom of these elements for 2D problem. Stress and strain are defined based on displacement of spring end points of element edges. Details of Applied Element scheme can be found in literatures by Meguro et al (1998).

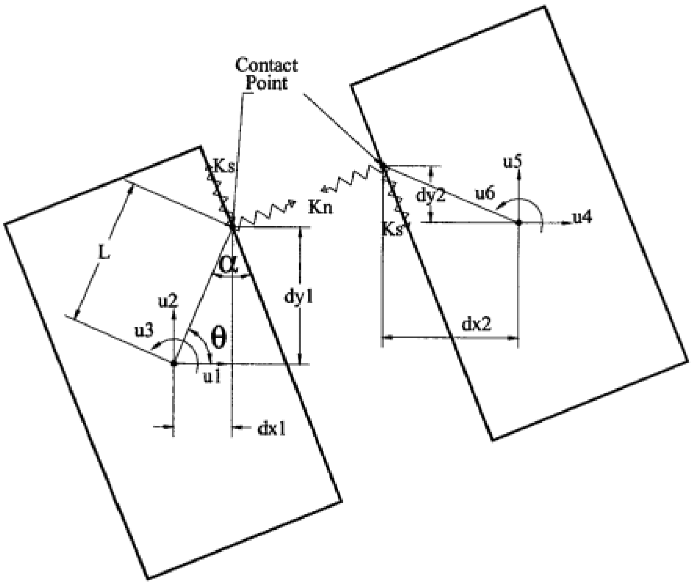

Figure 1. Element shape, contact point and degrees of freedom (Meguro et al, 1998)

2.2 Discretization for brick masonry:

Anisotropy of the masonry is accounted by considering masonry as a two phase material with brick units and mortar joint set in a regular interval. Structure is discretized such that each brick unit is represented by a set of square elements where mortar joints lie in their corresponding contact edges (see Figure 2).
In spring level, springs that lie within one unit of brick are termed as ‘unit springs’. For those springs, the corresponding domain material is brick as isotropic nature and they are assigned to structural properties of brick. Springs those accommodate mortar joints are treated as ‘joint springs’. They are defined by equivalent properties based on respective portion of unit and mortar thickness. Figure 2 shows the configuration of brick units, joints and their representation in this study. The initial elastic stiffness values of joint springs are defined as in Eq. 1 and 2 (Bishnu, 2004).

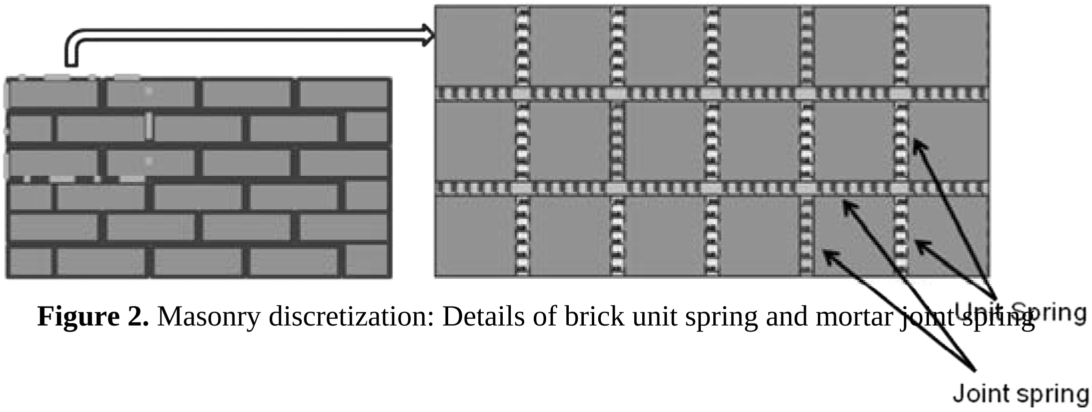

Figure 2. Masonry discretization: Details of brick unit spring and mortar joint spring

$$K_{nunit} = \frac{E_u\ t\ d}{a};\ \ K_{njo\text{int}} = \frac{E_u\ E_m t\ d}{E_u\ \text{x}\ \text{t}_h + E_m(a - t_h)} \tag{1}$$

$$K_{sunit} = \frac{G_u\ t\ d}{a};\ \ K_{sjo\text{int}} = \frac{G_u\ G_m t\ d}{G_u\ \text{x}\ \text{t}_h + G_m(a - t_h)} \tag{2}$$

Where E_u and E_m are Young's modulus for brick unit and mortar, respectively, whereas G_u and *Gm* are shear modulus for the same. Thickness of wall is denoted by 't' and 't_h' is mortar thickness. Dimension of element size is represented by 'a' and '*d*' is the fraction part of element size that each spring represent. While assembling the spring stiffness for global matrix generation, contribution of all springs around the structural element are added up irrespective to the type of spring. In the sense, for global solution of problem, there is no distinction of different phase of material but only their corresponding contribution to the stiffness system.

2.3 Masonry material model

Material model used was a composite model that takes into account of brick and mortar with their respective constitutive relation with elastic and plastic behavior of hardening and softening. Brick springs were assumed to follow principal stress failure criteria with linear elastic behavior. Once there is splitting of brick reaching elastic limit, normal and shear stress are assumed not to transfer through cracked surface in tensile state. The brick spring's failure criterion is based on a failure envelope given by Eq. 3:

$$\frac{f_b}{f_b^{'}} + \frac{f_t}{f_t^{'}} = 1 \tag{3}$$

Where f_b and f_t are the principal compression and tensile stresses, respectively, and f'_b and f'_t are the uniaxial compression and tensile strengths, respectively.

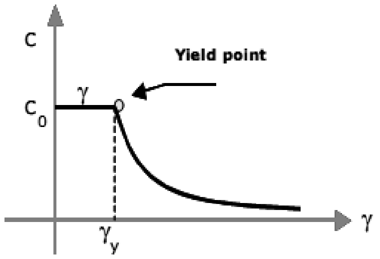

Figure 3: Cohesion degradation (Bishnu Pandey, 2002)

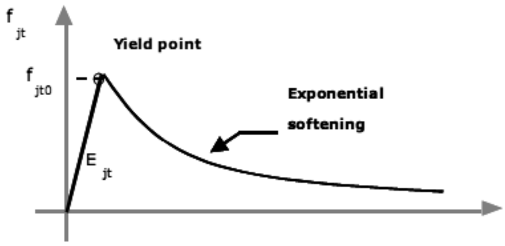

Figure 4: Bond degradation (Bishnu Pandey, 2002)

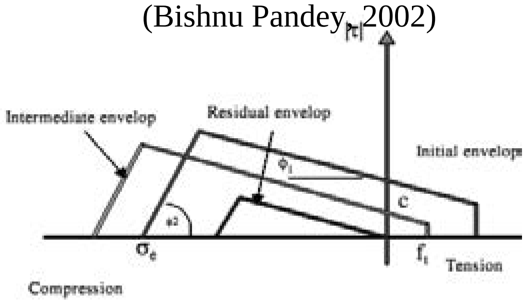

Figure 5: Failure criteria for joint spring (Sutcliffe et al, 2001) (Lourenco, 1996)

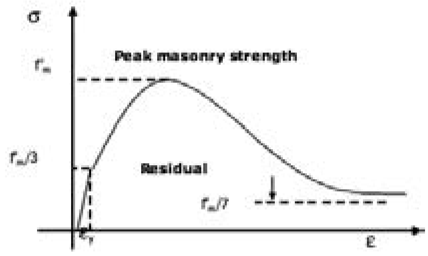

Figure 6: Hardening and softening applied for joint spring in compression cap (Lourenco, 1996)

Coulomb's friction surface with tension cut-off is used as yield surface after which softening of cohesion and maximum tension takes place in exponential form as a function of fracture energy values and state variables of damage. The cohesion and bond values are constant till the stress first time when stress exceeds the respective failure envelopes. Figure 3 and 4 shows the degradation scheme of bond and cohesion. Failure modes that come from joint participation of unit and mortar in high compressive stress is considered by liberalized compression cap as shown in Figure 5. The effective masonry compressive stress used for cap mode follows hardening and softening law as shown in Figure 6. The tension cut-off, f_1, and the sliding along joints, f_2, exhibit softening behavior whereas the compression cap experiences hardening at first and then softening. The failure surfaces used in this study derived from Lourenço, (1997), with some simplification are as given in Eqs. (4), (5) and (6). (Figure 5)

$$f_1(\sigma, K_1) = \sigma - f_t \ \exp\left(-\frac{f_t}{G_f^I} K_1\right) \tag{4}$$

$$f_2(\sigma, K_2) = |\tau| + \sigma \ \tan(\phi_1) - c\exp\left(-\frac{c}{G_f^{II}} K_2\right) \tag{5}$$

$$f_3(\sigma, K_3) = |\tau| + \sigma \ \tan(\phi_2)\left\{\left(\sigma_3(K_3) - \sigma\right)\right\} \tag{6}$$

In above equations, K_1, K_2 and K_3 are hardening and softening parameters for tension, shear and compression behavior respectively. $G^I{}_f$ and $G^{II}{}_f$ is fracture energy in tension and shear respectively.

2.3.1 Material model for concrete and steel:

As a material modeling of concrete under compression condition, Maekawa compression model (Okamura and Maekawa, 1991), as shown in Figure 7 (a), is adopted. The tangent modulus is calculated according to the strain at the spring location and whether the spring is in loading or unloading process. For more details, refer to (Okamura and Maekawa, 1991). After reaching the peak compression stresses, stiffness is assumed as a minimum value (1% of initial value) to avoid having a singular stiffness matrix. The difference between calculated spring stress and stress corresponding to the strain at the spring location are redistributed each increment. And for shear springs, model is assumed. Till the cracking point stresses are assumed to be proportional to strains and after that stiffness is assumed as minimum value (1% of initial value) to avoid having a singular stiffness matrix. For reinforcement, bilinear stress strain relation is assumed. After yield of reinforcement, steel spring stiffness is assumed as 1% of the initial stiffness as shown in Figure 7(b). No model is used, up to this stage, for cut of reinforcement because the behavior of the structure becomes mainly dynamic behavior and the static stiffness matrix becomes singular.
It should be emphasized that some other failure phenomena, like buckling of reinforcement and spalling of concrete cover, are not considered in the analysis in this analysis. However, the shear transfer and shear softening are approximately considered in the analysis. For more details about material models used and the results in case of monotonic loading conditions, refer to [Meguro and Tagel-din, 2001]

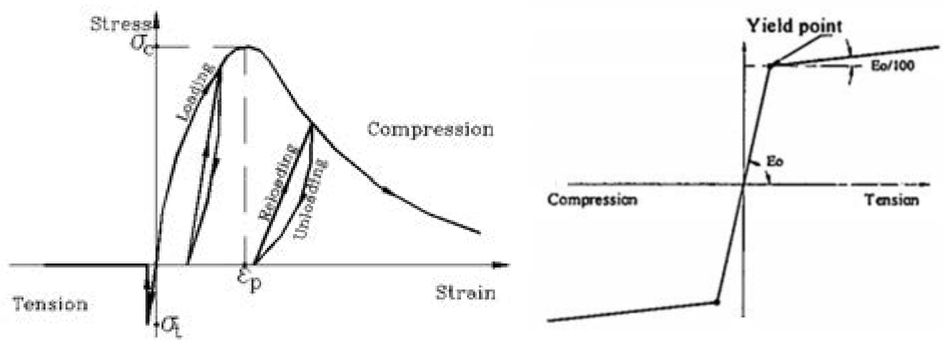

(a) Concrete in Tension and compression (b) Steel

Figure 7: Material models for concrete and steel

3. PARAMETRIC STUDY OF URM BUILDING USING AEM

Description of geometry: Building considered for the analysis is as shown in Figure 8. Building height is 4m and width is 3.9m. Column and beam cross section is considered as 0.3m X 0.3m. Reinforcement is provided as per the requirement. Brick wall panel has dimension of 3.3m X 3.7m X 0.3m. Brick size is considered as per the local brick in practice. In this study, initially a framed wall building (see Figure 8) with reinforcement (see Figure 9 (a) and (b)) is considered and it has been studied under displacement control cases for Monotonic static condition. Displacement control is capable to give the response

of building in post yield. Response of the Infill wall in terms of Base shear versus drift ratio is plotted and structures behavior is studied through this response.
Loading Parameters: A displacement control technique for monotonic static case has been considered, as this method is capable of giving post peak behavior. A lateral displacement of 0.02m is applied in 100 increments on the wall.
Geometry boundary conditions and loading are as below:
Geometry:

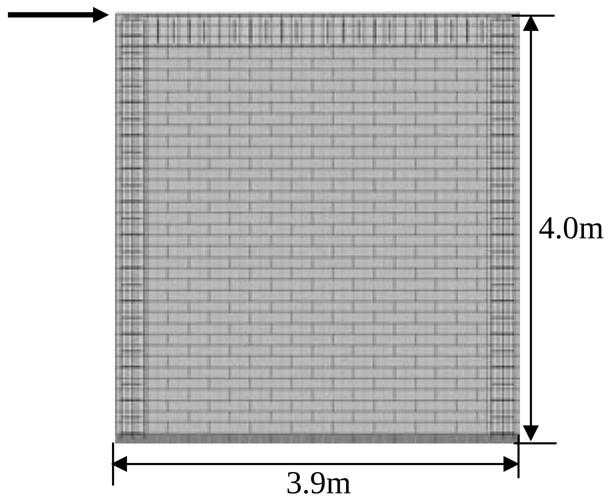

Figure 8 Numerical model of brick infill wall

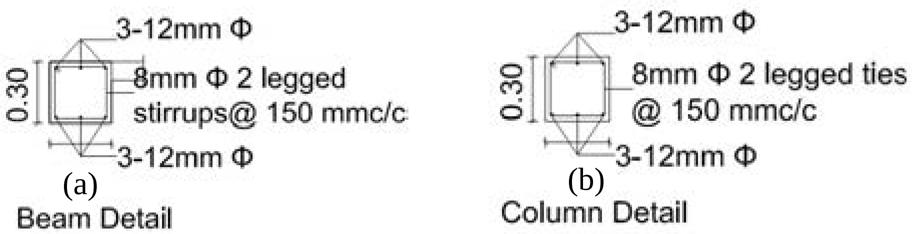

Figure 9: Reinforcement details for (a) Beam (b) Column

Boundary conditions: Base elements are considered as fixed
Loading: Displacement control used. 0.02m displacement applied in 100 loading steps.

3.1 Parameters Considered: Three parametric studies have been considered in this analysis. i.e. Effect of span ratio, effect of opening and mortar volume.

3.1.1 Effect of span ratios: In order to study effect of wall span ratio (h/w) on strength of the wall, four cases have been considered in this analysis as shown in Figure 10. Span ratio (h/w) of 0.5, 1.0, 2.0 and 4.0 is considered and displacement of 0.02m is applied laterally in 100 increments.
Geometry, boundary conditions and loading are as given below:
Geometry: Geometry is as shown in Figure 10
Boundary conditions: Base elements are considered as fixed
Loading conditions: Displacement control used.0.02m displacement applied in 100 loading steps

Effect of aspect ratio can be observed in above Figure 11. Aspect ratio of 0.5 shows more loads carrying capacity than other cases; this is due to high stiffness of wall pertaining to less aspect ratio. Shear is predominant in this case. Case 2 having aspect ratio 1 shows lesser load carrying capacity than case 1, as in this case though shear is predominant but stiffness of wall is less when compared to case 1 due to high aspect ratio. Strut action can be observed in this case. Case 3

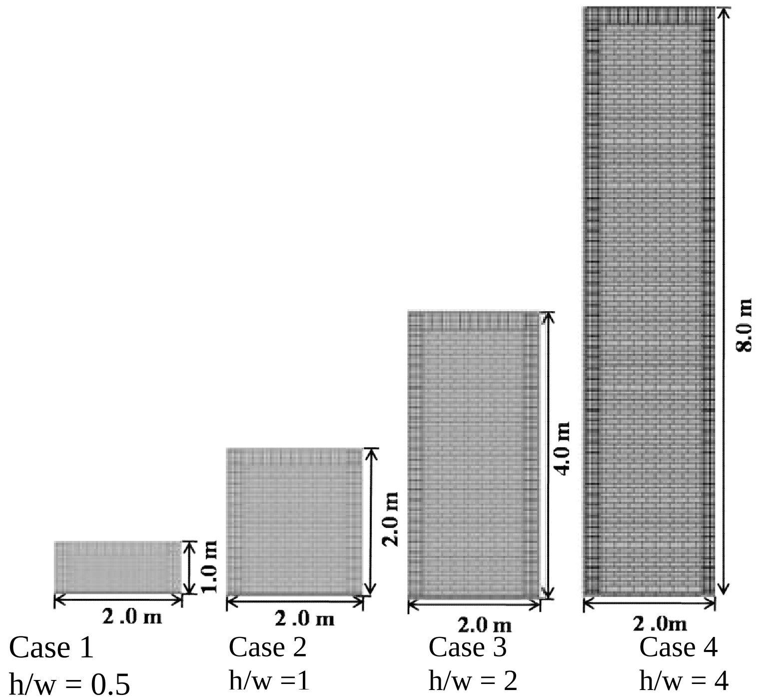

Figure 10: Cases considered for understanding effect of Aspect ratio

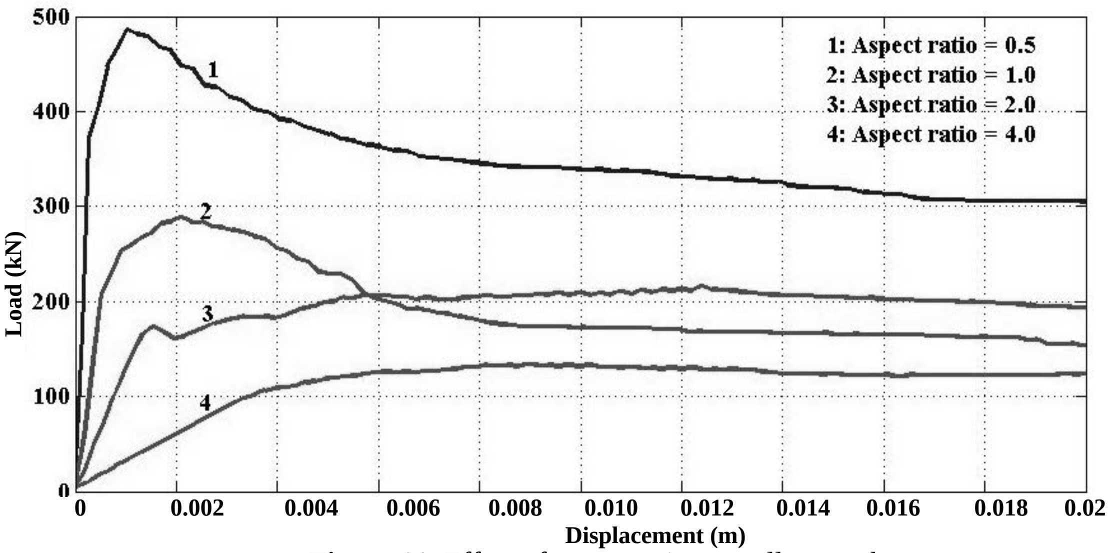

Figure 11. Effect of aspect ratio on wall strength

shows lesser load carrying capacity as aspect ratio is higher at 2, still shear is predominant in this case, but strut action cannot be observed here. Case 4 shows very less load carrying capacity as in this case bending is predominant. In such cases provision of horizontal bands should be considered to avoid weaker sections. From this analysis, It is understood that with increase in aspect ratio, load carrying capacity of the wall decreases (see Figure 11)

3.1.2 Effect of openings

In order to understand the effect of opening on behavior of wall, an Infill wall of size 3.9m X 4.0m is considered in the analysis. Five cases were considered for the study. In first case, full infill wall without opening is considered. In second case, opening in the centre of wall has been considered. In third case, door opening in left side is considered whereas in fourth case door opening in the middle has been considered. In fifth case lintel has been provided on door opening.

Geometry, boundary conditions and loading are as given below (Figure12 and 13):

Boundary conditions: Base elements are considered as fixed

Loading: Displacement control used.

0.02m displacement applied in 100 loading steps.

Details of opening:

Case 2: Central opening of size 1.2m X 1.2m

Case 3: Door opening of size 1.0m X 2m

Case 4: Door opening of size 1.0m X 2m

Case 5: Lintel of size 75mm provided. Main reinforcement in Lintel is of 2-8mm dia. bars and hooks of 6mm dia. used.

Figure 12 shows base shear versus drift ratio relation for the four cases considered. It can be clearly seen that infill wall without opening having more load carrying capacity due to more strength and stiffness of wall when compared with other cases. For second case of central opening shows lesser load carrying capacity than other cases. In this case, at first diagonal zigzag cracks arise along opening in compression diagonal, as loading increases these cracks progress further. As shear is predominant in this case, central opening in wall makes it weaker.

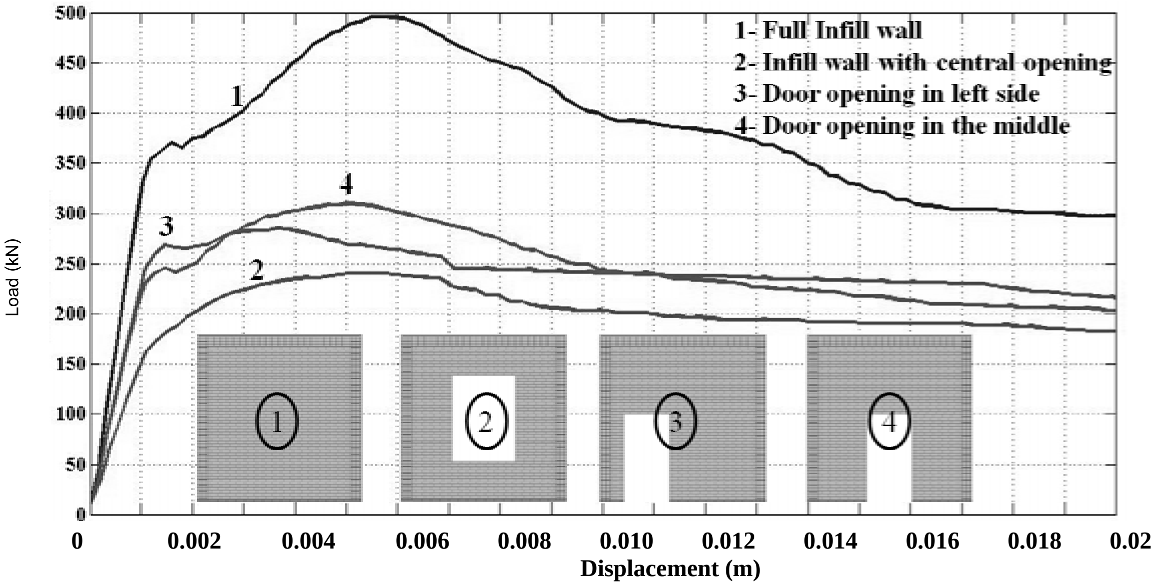

Figure 12. Effect of opening on capacity of wall

For case 3 and 4, positioning of door is considered in left side and in the middle. In case 3, at the initial stages of loading wall shows better load carrying capacity (270kN) as opening does not fall in the middle of the tension diagonal but in later stages stiffness of the wall is continuously decreasing due to weaker pier at left side where stresses are more at the base. Whereas in case 4, as opening is in the middle, cracks initiated in the left diagonal at first due to which load carrying capacity can be seen less initially in Figure 12, but as loading increases, load is distributed in both the piers which makes wall to carry more load (310kN), but at later stage decrease in strength and stiffness can be seen due to progressing cracks in piers due to tensile stresses.

3.1.3 Effect of Mortar Volume

Boundary conditions: Base elements are considered as fixed
Loading: Displacement control used.
0.02m displacement applied in 100 loading steps.
Overall four cases have been considered:
Case1: Brick size 0.21m X 0.10m X 0.07m with mortar thickness 10mm
Case2: Brick size 0.21m X 0.10m X 0.07m with mortar thickness 20mm
Case3: Brick size 0.40m X 0.20m X 0.10m with mortar thickness 10mm
Case4: Brick size 0.40m X 0.20m X 0.10m with mortar thickness 20mm
Mortar thickness is considered as 10mm and 20mm respectively for the brick size of 0.21m X 0.10m X 0.07m. In case 1, mortar volume accounts as 0.448m^3 and for case 2 it is 0.630m^3 this due to high mortar thickness considered in this case. Considering high mortar thickness actually reduces strength of the wall, as mortar being weaker bond in the wall, further increase in thickness increases weaker zone in the wall which reduces strength of the wall. Case 3 and 4; mortar thickness is considered as 10mm and 20mm respectively for the brick size of 0.40m X 0.20m X 0.1m. In case 3, mortar volume accounts as 0.525m^3 and for case 4 it is 0.784 m^3 this due to high mortar thickness considered in case4.

Table 1 illustrates about mortar volume and brick size considered for each case and their respective volumetric ratio. For case1 and 3 for different brick sizes with mortar thickness as 10mm volumetric ratio is lesser when compared with case 2 and 4 where mortar thickness is 20mm.

Table 1 Volumetric ratio for masonry and mortar

Cases	**Brick sizes (m)**	**Mortar thickness (m)**	**Mortar Volume (m^3)**	**Masonry Volume (m^3)**	**Volumetric ratio (= Mortar volume/ Masonry volume)**
1	0.21 X 0.1 X 0.07	10	0.448	1.324	0.338
2	0.21 X 0.1 X 0.07	20	0.629	1.324	0.475
3	0.40 X 0.2 X 0.1	10	0.525	1.324	0.394
4	0.40 X 0.2 X 0.1	20	0.784	1.324	0.588

Effect of mortar thickness contributes in strengthening of wall. But the mortar thickness if not considered properly or if considered in higher side then it can create a weaker zone in wall, whereas a very thin mortar in brick wall will lead to improper bonding between the bricks. To understand how the volume of mortar affects the strength of the wall under loading following study has been done. In this study, effect of mortar volume on brick masonry wall has been studied by considering 2 different sizes of bricks and two different mortar thicknesses. Brick sizes considered were 0.21m X 0.10m X 0.07m and 0.40m X 0.20m X 0.10m and mortar thickness considered were 10mm and 20mm for each case.

4. CONCLUSIONS:

Past earthquake witness most of the disasters in brick masonry building. In view of this there is a need to study the behavior and damage to brick masonry structures and to explore the mitigation measures of retrofitting of weak buildings. In this work, a numerical study has been done to understand the behavior of brick masonry building. A brick masonry wall is modeled using AEM (Applied element method) and parametric study has been done by considering different parameters as, effect of mortar volume, effect of span ratios and effect of opening on strength of wall. More span ratio is responsible for less strength and vice versa. Effect of opening makes it difficult to form a diagonal strut action which causes its strength to degrade with the more opening in the wall. Effect of mortar thickness causes a weaker zone in masonry wall, so mortar thickness used in construction should be appropriate as per IS code.

REFERENCES

Bishnu Pandey, Meguro, Kimiro, 2004, “Simulation of brick masonry wall behavior under in-plane lateral loading using Applied Element method”, *13th World Conference on Earthquake Engineering, Canada.*

K.S Nanjunda Rao, IISC Bangalore, 2008, “Structural masonry properties and behavior” IISC Bangalore seminar

Lourenco and Rots, 1997, “Multi surface interface model for analysis of masonry structures”, Journal of engineering mechanics, ASCE

Meguro K. and Hakuno M., 1989, “Fracture analyses of structures by the modified distinct element method”, Structural Eng./Earthquake Eng., Japan Society of Civil Engineers, Vol. 6. No. 2, pp. 283s-294s.

Meguro K. and Tagel-Din H.,1998, “A new simple and accurate technique for failure analysis of structures”, Bulletin of Earthquake Resistant Structure Research Center, IIS, University of Tokyo, No. 31, pp. 51-61.

Page, A.W., 1978, “Finite element model for masonry”, J. Struc. Div., ASCE, Vol. 104(8), pp. 1267-1285.

Paola Mayorca, 2006, “Report on the state – of-the art in the seismic retrofitting of unreinforced masonry houses by PP-Band meshes”.

Sutcliffe DJ, Yu H.S, Page AW., 2001, "Lower Bound Limit Analysis of Unreinforced Masonry Shear Walls." Computer & Structures 2001; (79):1295-1312

A study of the influence of the bending radius of reinforcement bar on the failure mechanism of L-shaped beam column joint by 3D discrete model

Kohei NAGAI [1], Liyanto EDDY[2], and Koichira IKUTA[3]
[1]Associate Professor, International Center for Urban Safety Engineering
Institute of Industrial Science, the University of Tokyo, Japan
nagai325@iis.u-tokyo.ac.jp
[2]Doctoral Student, Department of Civil Engineering
The University of Tokyo, Japan
[3]Project Engineer, JGC Corporation, Japan

ABSTRACT

The reduction of reinforcement congestion, mainly located in beam column joints where reinforcements meet from many directions, is required as the reinforcement congestion at beam column joints can cause difficulties during the compaction of concrete inside the beam column joint during the casting of concrete, especially when larger bending radius of reinforcement bar is used. On the other hand, the influence of the reinforcement bar, especially the bending radius of the reinforcement bar, on the failure mechanism of the beam column joint has not been clarified well. In this study, in order to reduce the reinforcement congestion at beam column joints, the influence of the bending radius of the reinforcement bar, on the failure mechanism of L-shaped beam column joints, is investigated. Thus, 3-dimensional models of the L-shaped beam column joints with simple reinforcement bars are simulated by using a discrete analysis, called Rigid Body Spring Model and the bending radius of the reinforcement bar is varied. Furthermore, the analysis results, including load-displacement relationships and crack propagations, are also compared with the experimental observations. Based on the analysis results, the load-displacement relationships and the crack propagations are roughly the same with the experimental investigations. Eventually, based on both the analysis results and the experimental investigations, it is concluded that the strength of the beam column joint depends on the bending radius of the reinforcement bar. When a smaller bending radius of the reinforcement bar is used, the strength of the beam column joint will be smaller as the compression region inside the radius of the reinforcement bar becomes smaller. Thus, the compressive force will concentrate in the small region and causes crushing of concrete.

Keywords: *rigid body spring model, L-shaped beam column joint, bending radius, local failure.*

1. INTRODUCTION

Nowadays, the performance requirements of the building in the seismic code are more stringent. To satisfy the strict requirement, large numbers of reinforcement bars must be placed in the reinforced concrete members. As a result, reinforcement congestion, especially located in a beam column joint where reinforcement bars of beams are anchored into a column, occurs. Furthermore, reinforcement congestion may cause difficulties during the compaction of concrete inside the beam column joint during the casting of concrete, especially when a larger bending radius of reinforcement bars is used.

The requirement of the large bending radius of reinforcement bars is one of the causes of the reinforcement congestion in beam column joints, particularly when large diameter of reinforcement bars are used. In Japan Code (2007&2011), i.e. for the beam column joint of viaduct structures, the bending radius of reinforcement bars is determined by 10 times of the diameter of the embedded longitudinal bars. However, there is no clarification why the value is determined. In order to reduce the bending radius of reinforcement bars of beams, a study of the influence of the bending radius of reinforcement bars on the failure mechanism of L-shaped beam column joints, is needed.

Through the experimental work, Yoshitake *et al.* (2012) studied the effect of the bending radius of reinforcement bars on the failure mechanism of L-shaped beam column joints, and found that both the maximum load and the failure behavior of the beam column joint will not change as the bending radius of the reinforcement bars is different. On the other hand, Hotta *et al.* (2012) also studied the effect of the bending radius of reinforcement bars on the failure mechanism of L-shaped beam column joints, and found contrary that both the maximum load and the failure behavior of the beam column joint will change as the bending radius of reinforcement bars of beams is different. Thus, the influence of reinforcement bars, especially the bending radius of reinforcement bars, on the failure mechanism of the beam column joint has not been clarified well yet. Furthermore, more studies are needed to clarify the effect of the bending radius of reinforcement bars on the failure mechanism of L-shaped beam column joints.

Our research groups have used a 3-dimensional discrete analysis, Rigid Body Spring Model (RBSM), to simulate the behavior of concrete by 3-dimensional models, such as Nagai *et al.* (2005); Hayashi *et al.* (2012), and others. In this study, by using Rigid Body Spring Model (RBSM), the influence of the bending radius of reinforcement bars on the failure mechanism of L-shaped beam column joints is studied, including the load-displacement relationship, the internal strain and stress inside the L-shaped beam column joint, and the crack distribution propagated on the L-shaped beam column joint.

2. ANALYSIS METHOD

In this study, the simulation was carried out by a 3-dimensional discrete analysis, Rigid Body Spring Model (RBSM), proposed by Kawai *et al.* (1978). In RBSM, a 3-dimensional reinforced concrete model is meshed into some rigid bodies. Each rigid body consists of 6 degree of freedoms, i.e. 3 transitional degrees of freedom and 3 rational degrees of freedom within its interior and connects with other rigid bodies by 3 springs i.e. 2 shear springs and 1 normal spring (Figure 1).

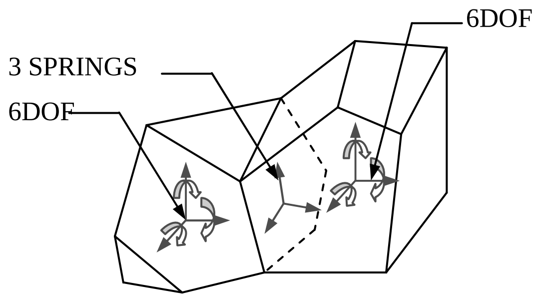

Figure 1: Mechanical Model of 3-D RBSM

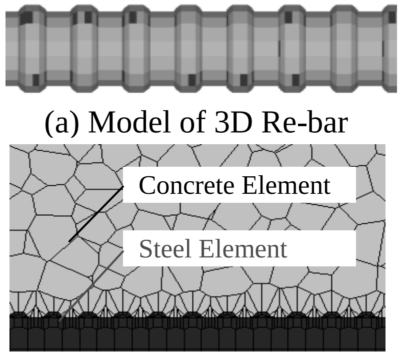

(a) Model of 3D Re-bar

(b) Cross Section of Elements

Figure 2: Mesh Arrangements of Concrete and Re-bar

As the propagation of cracks in the reinforced concrete is one of the most importance factors in investigating the behavior of reinforced concrete members, the mesh arrangement of the model in RBSM is important. In order to prevent cracks propagated in a non-arbitrary direction, a random geometry, called Voronoi Diagram, is used for the element meshing. The size of the concrete element was set to about 1000 mm^3, similar to the size of the coarse aggregate. The geometry of steel elements is modeled in an accurate manner, by modeling a 3-dimensional arrangement of the reinforcement bar, to properly account for the interlock between the reinforcement bar and concrete. Mesh arrangement of concrete and the reinforcement bar at meso-scale in this study is shown in Figure 2. To model a 3-dimensional reinforced concrete member, two types of elements are used, i.e. concrete element and steel element. The properties of the spring are determined so that the elements, while combined together, enable to predict the behavior of the model as accurate as that of the experimental result. In this study, the simulation system, developed by Nagai *et al.* (2005), is used and the constitutive models of the elements are described below.

2.1 Concrete Element

The constitutive model of a normal spring and a shear spring of the concrete element is shown in Figure 3. In the compression zone, the normal spring of the concrete element behaves elastically as crack, between 2 rigid bodies, occurs when the tensile strength of the normal spring exceeds the tensile strength of the concrete (f_t). After exceeding the tensile strength (f_t), the tensile strength of a normal spring is assumed to decrease linearly, depending on the maximum crack width between 2 rigid bodies (w_{max}), which is assumed 0.003 mm (see Figure 3(a)). An elastic-plastic behavior is assumed for the spear spring of the concrete element (see Figure 3(b)), that the value of τ_{max} can be calculated based on equation 1, adopted from Muto *et al.* (2004) (see Figure 3(c)). Here, the value of Φ is assumed 37^{o}.

$$\tau = c - \sigma \tan\Phi \qquad \text{if } \sigma \geq 0.5\, f_c \qquad (1)$$
$$\tau = c - 0.5 f_c \tan\Phi \qquad \text{if } \sigma > 0.5\, f_c$$

where: $c = ft\,(1\text{-}\tan\Phi)$

Moreover, when fracture occurs in the normal spring, the shear stress is reduced according to the reduction ratio of the normal stress. As the result, the shear spring

cannot carry the stress when the crack width of the normal spring reaches w_{max} (see Figure 3(d)).
Generally, the behavior of the normal spring of the interface element, between the concrete element and the steel element, is assumed to be as same as the normal spring of the concrete element. Since the behavior of the interface element, between the concrete element and the steel element is considered more brittle than the concrete element, the tensile strength of the interface element is assumed 0.5 times the tensile strength of the concrete element and the maximum crack width between 2 rigid bodies (w_{max}) for the interface element is assumed 0.001 mm.

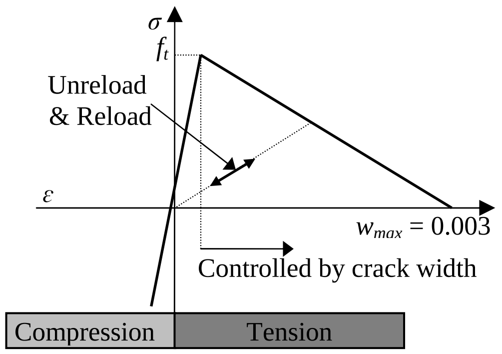

(a) Normal Spring

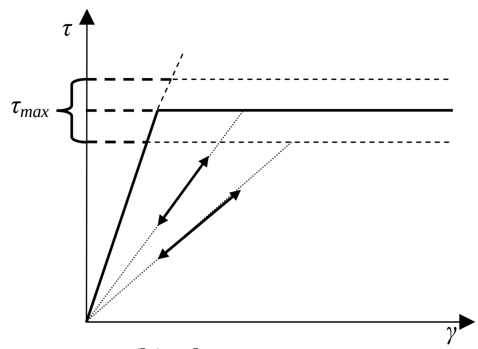

(b) Shear Spring

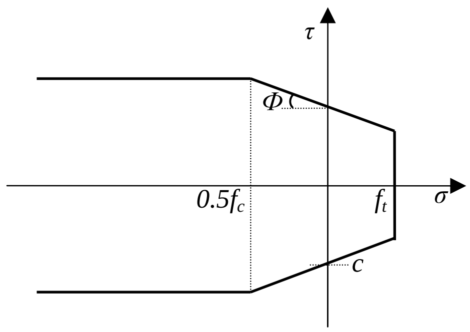

(c) Failure Criterion

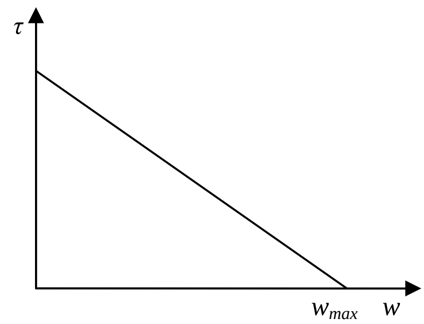

(d) Shear Reduction

Figure 3: Constitutive Model of Concrete

2.2 Steel Element

A bi-linear model, both in the compression zone and the tension zone, was assumed for modeling the normal spring and the shear spring of the steel element.

3. ANALYSIS OF L-SHAPED BEAM COLUMN JOINTS

3.1 Detailed Analysis

In order to clarify the effect of the bending radius of reinforcement bars on the L-shaped reinforced concrete beam column joint, numerical simulations were conducted for experiments carried out by Hotta *et al.* (2012) (Figure 4). Since the experiments were purposed to study the effect of the bending radius of reinforcement bars on the failure mechanism of the L-shaped beam column joints, the bending radius of reinforcement bars in the analysis models was also varied. In order to reduce the computational time, the model of reinforcement bars of the beam and the column were simplified. Eventually, the analysis results will be compared with the experimental results.

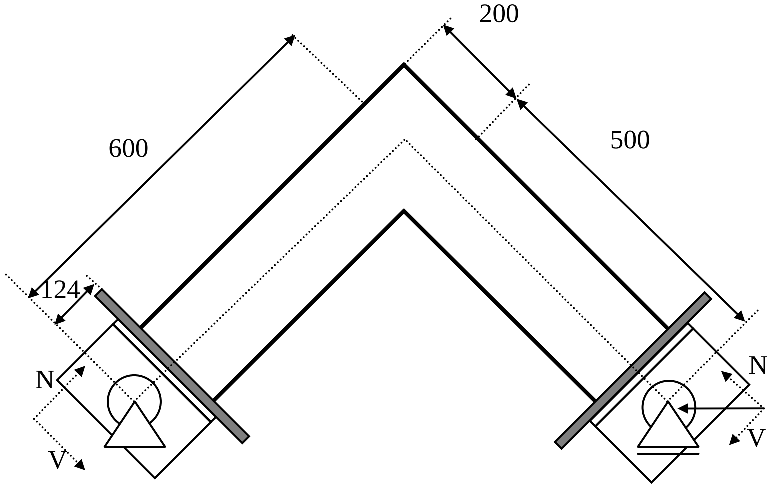

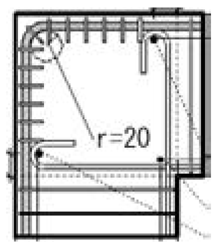

(a) Specimen-1

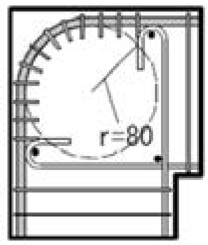

(b) Specimen-2

Figure 4: Experimental Specimens (Hotta *et.al.* (2012))

3.2 Analysis Model

The analysis models are shown in Figure 5. Further, the material properties of concrete and reinforcement bars are shown in Table 1. The dimensions of the L-shaped beam column joint of analysis models were modeled roughly as same as those of experimental specimens and the material properties of the analysis models are as same as those of experimental specimens. The diameter of longitudinal bars of beams and columns of analysis models is as same as experimental specimens, i.e. deformed bars of 10 mm. The diameter of transverse bars of beams and columns of the experimental specimens, i.e. plain bars of 6 mm, was changed, becoming deformed bars of 10 mm, due to meshing simplification in numerical simulation. For easier recognition of the variables in each model, the following notation was used, i.e. C3, C8, C11.5. The number of 3, 8, and 11.5 of C3, C8, and C11.5, respectively, indicates the bending radius of reinforcement bars of beams, i.e. 3 times diameter of the embedded longitudinal bars for C3 (30 mm), 8 times diameter of the embedded longitudinal bars for C8 (80 mm), and 11.5 times diameter of the embedded longitudinal bars for C11.5 (11.5mm). C3 of the analysis model represents specimen-1 of the experimental specimen and C8 of the analysis model represents specimen-2 of the experimental specimen. In order to simplify the meshing arrangement of the numerical simulation, the bending radius of Specimen 1 of experimental specimens, i.e. 20 mm, is enlarged into 30 mm for the bending radius of C3 of analysis model. The beam column joint of C11.5 was only done by the numerical simulation.

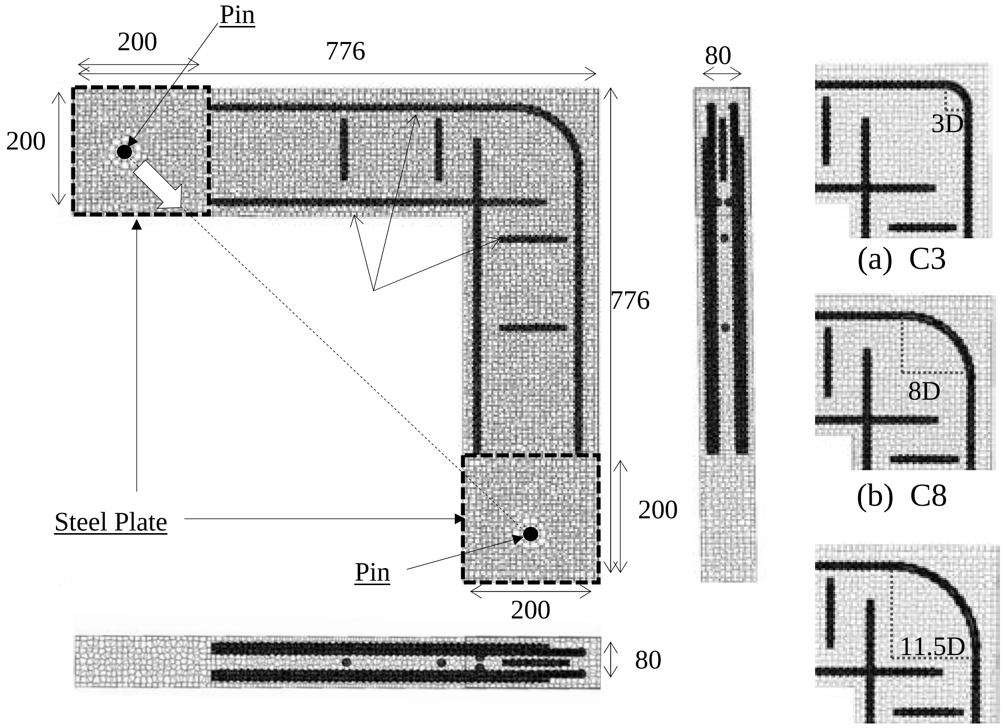

Figure 5: Analysis Models (Units: mm)

Table 1: Material Properties

Model	Bending Radius (mm)	Concrete Properties			Steel Properties		
		Compressive Strength (MPa)	Tensile Strength (MPa)	Modulus of Elasticity (MPa)	Modulus of Elasticity (MPa)	Yield Stress (MPa)	No. of Elements
C3	30	39.3	2.97	29900	190000	457	234393
C8	80						223143
C11.5	115						217541

3.3 Boundary Condition

The boundary condition of analysis models was modeled as similar as possible to the experimental set up. Steel plates, located at the end of the beam and the column (Figure 5), were modeled as same as those of the experimental set up (Figure 4). A random meshing was also used for modeling the steel plates. The stiffness of the steel plates was assumed rigid enough, by increasing the modulus elasticity of shear springs and normal springs of steel plates, so that the deformation of steel plates will be prevented. In order to model the hinged condition of the experimental set up, a pin element is introduced in the analysis models (Figure 5), located in the middle of the steel plates. Furthermore, in the pin element, forces are transferred only through normal springs of the pin element. Similarly to the experimental set up, fix condition in all direction was assumed as the boundary condition of the pin element which is located at the end of the column. Moreover, a monotonically displacement-load controlled was applied to the pin element, which is located at the end of the beam, in a 45-degree diagonal direction, so that a close mode deformation of beam column joint will occur.

4. ANALYSIS RESULT

4.1 Load-displacement Relationship

Load-displacement relationship of the analysis models is shown in Figure 6. Load-displacement relationship of the experimental specimens is shown in Figure 7. Furthermore, Table 2 shows the maximum load of the analysis prediction, compared with the experimental observation. The load-displacement relationship is calculated based on the 45-degree diagonal direction in which direction, load was applied. The maximum load of the analysis model is roughly as same as that of the experimental specimens, about 15% difference between the analysis model and the experimental specimens.

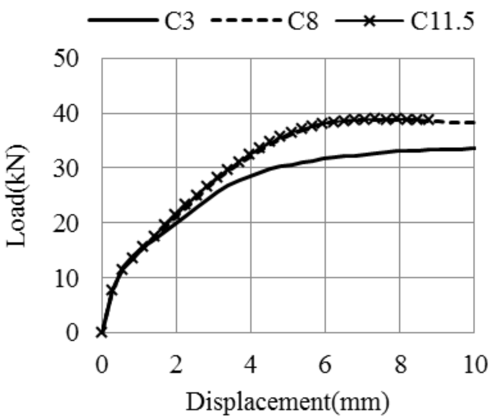

Figure 6: Load-Displacement Relationship of Analysis Models

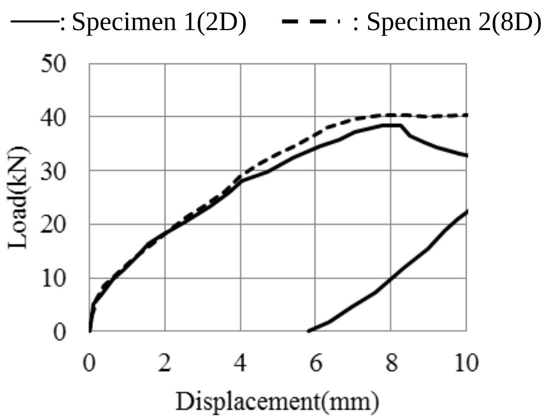

Figure 7: Load-Displacement Relationship of Experimental Specimens (Hotta *et.al.* (2012))

Table 2: The Maximum Load of Analysis Models and Experimental Specimens

Model	Maximum Load		P_{ana}/P_{exp} [%]
	Experimental Specimens P_{exp} [kN]	Analysis Model P_{ana} [kN]	
C3	38.6	33.6	87
C8	39.7	38.8	97.7
C11.5	-	38.9	-

Based on the experimental observation, the reinforcement bars yield first without causing crush of concrete inside the radius of the bending bar when the maximum load of Specimen-2(8D) is reached. Therefore, there is no reduction of load capacity when the displacement is larger than the displacement at the maximum load. The same behavior was observed by the analysis prediction.

Based on the experimental observation, the compressive failure of concrete occurs inside the radius of the bending bar, when the maximum load of Specimen-1 (2D)

is reached, as the result of the stress concentration inside the radius of the bending bar. Therefore, the compressive failure of concrete that occurs inside the radius of the bending bar, causes the maximum load of Specimen-1(2D) is lower than that of Specimen-2 (8D). Lower load capacity was observed when the displacement is larger than the displacement at the maximum load.
Based on the analysis prediction, the same diagonal cracks also occur inside the radius of the bending bar as the result of the stress concentration inside the radius of the bending bar. But, the load capacity of C3 increases as the displacement is larger than the displacement at the maximum load. There are 2 reasons that may cause the difference behavior between the experimental observation and the analysis prediction, i.e. the constitutive model of the normal springs of concrete has not modeled perfectly the compressive softening behavior of concrete and the simplification of transverse bars of the beam and the column that may cause the shear deformation of the beam and the column is larger than that of experiment.
In addition, in case of C11.5, a beam column joint model that was only done by the numerical simulation shows the same behavior with C8. Compressive failure does not occur inside the radius of the bending bar. Therefore, it can be concluded that after a certain value of the bending radius of reinforcement bars, the stress concentration will occur inside the radius of the bending bar and further, causes the compressive failure inside the radius of the bending bar. Moreover, it also can be concluded that if the compressive failure occurs inside the radius of the bending bar, the maximum load of the beam column joint will be reduced.

4.2 Internal Strain-Stress and Crack Propagation

Stress condition of the beam column joint at the displacement of 2.8 mm and cracks of the beam column joint at the displacement of the maximum load will be described below. In addition, the displacement of 2.8 mm was chosen, since the difference of the load-displacement relationships, among C3, C8, and C11.5, starts to occur when the displacement is larger than this value.

4.2.1 Stress condition of the beam column joint at the displacement of 2.8 mm

Figure 8 shows the internal stress of the analysis model of C3. When a close mode deformation of the beam column joint occurs, compressive stresses will be generated along the inner portion of the beam and the column (1) and from the bending part of the reinforcement bars to the corner of the beam column joint (2).
The compressive stresses, which are generated along the inner portion of the beam and the column, were also observed the same in all analysis cases. On the other hand, the compressive stresses, which are generated from the bending part of the reinforcement bars to the corner of the beam column joint, are different each other, among the analysis model of C3, C8, and C11.5, since the bending radius of the reinforcement bars is also different each other. Furthermore, it is observed that the compression region of concrete, inside the radius of the bending bar, becomes smaller when a smaller bending radius of reinforcement bars is used. Furthermore, the compressive force will concentrate in this small region and causes crushing of concrete. Because of the difference of stress condition inside the radius of the bending bar, the difference of load-displacement relationship, among C3, C8, and C11.5, starts to occur when the displacement is larger than 2.8 mm.

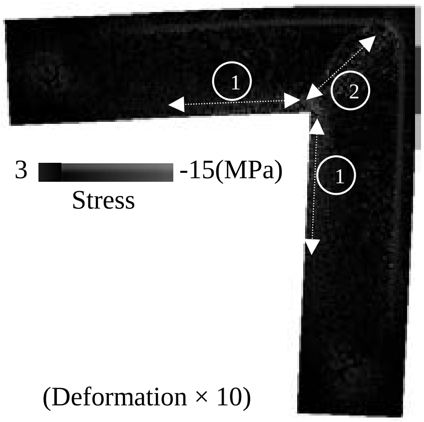

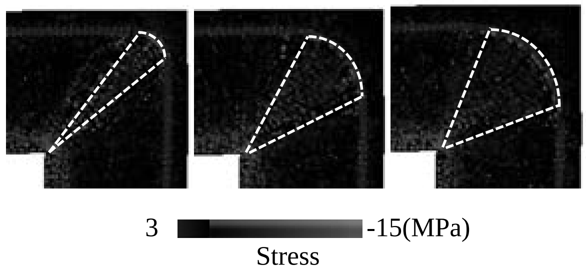

(a)C3 (b) C8 (c) C11.5

Figure 8: Internal Stress of C3 (Displacement of 2.8 mm)

Figure 9: Internal Stress of Beam Column Joint Portion of Analysis Models

4.2.2 Cracks of the beam column joint at the maximum load

Figure 10 shows the surface cracks of the analysis model of C3, C8, C11.5, respectively, at the maximum load.

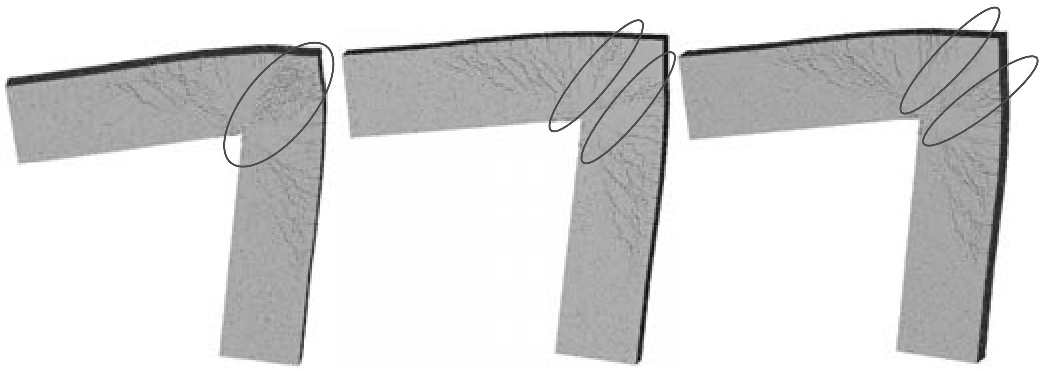

(Deformation × 10)

(a) C3 (b) C8 (c) C11.5

Figure 10: Surface Cracks of the Analysis Models

Based on surface cracks of the analysis model of C3 (Figure 10 (a)), cracks propagate easily inside the radius of the bending bar, as the result of the compressive stress concentration inside the radius of the bending bar. On the other hand, based on surface cracks of the analysis model of C8 and C11.5 (Figure 10(b) & Figure 10(c)), more cracks propagate outside the radius of the bending bar. It is also observed that many shear cracks occur on the surface of the beam and the column as the result of the simplification of the transverse bars of the beam and the column.

Figure 11 shows the internal cracks of the analysis model of C3, C8, C11.5, respectively. Based on internal cracks of the analysis model of C3 (Figure 11(a)), compressive cracks propagate inside the radius of the bending bar. On the other hand, based on the internal cracks of the analysis model of C8 and C11.5 (Figure 11(b) & Figure 11(c)), no compressive crack was observed inside the radius of the bending bar and flexural cracks propagate at the beginning of the bending portion. Thus, the same behavior as the distribution of surface cracks was observed.

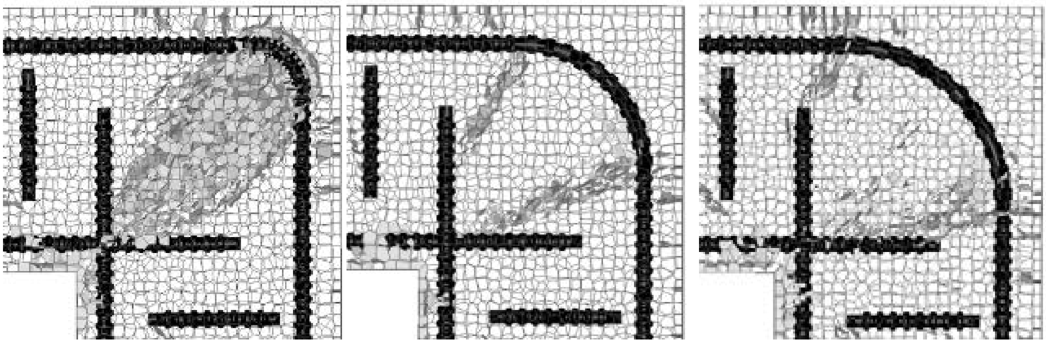

: Crack width = 0.03 mm

(a) C3 (b) C8 (c) C11.5

Figure 11: Internal Crack of the Analysis Models

Figure 12 shows the surface cracks of the experimental specimen of Specimen-1 (2D) & Specimen-2(8D), respectively. The crack propagation of the experimental specimens was observed roughly as same as that of the analysis models, i.e. compressive cracks propagate inside the radius of the bending bar when a smaller bending radius of reinforcement bars is used, however, no compressive crack was observed inside the bending radius of the bending bar and flexural cracks propagate at the beginning of the bending portion when a larger bending radius of reinforcement bars is used. Therefore, the crack propagation of the analysis model is roughly as same as that of experimental specimens and the analysis results can explain well why both the maximum load and the failure behavior of beam column joint will change as the bending radius of reinforcement bars is different.

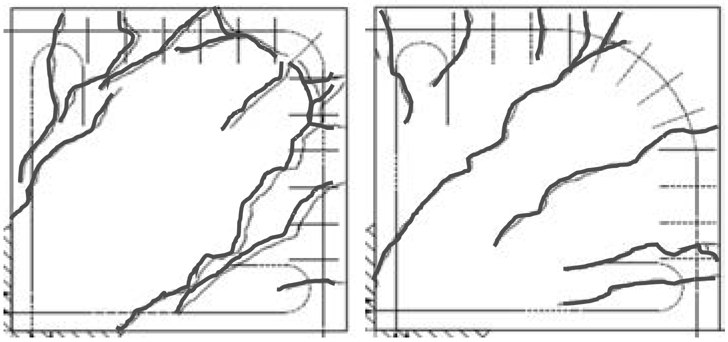

(a) Specimen-1 (2D) (b) Specimen-2 (8D)

Figure 12: Surface Cracks of the Experimental Specimens

5. CONCLUSION

Based on the numerical simulation using a three-dimensional discrete analysis method, 3-dimensional Rigid Body Spring Model (RBSM), the reinforcement bars in the L-shaped beam column joint, especially the bending radius of the reinforcement bars, affects the failure mechanism of the L-shaped beam column joint.

Thus, the following conclusions are made.

1. 3-dimensional discrete analysis method can simulate well the failure mechanism of the L-shaped beam column joint with simple reinforcement. The analysis explains well the failure mechanism inside the beam column joint.
2. By the numerical simulation, the dimension of the bending radius of reinforcement bars affects the failure mechanism of the L-shaped beam column joint. In addition, when a smaller bending radius is used, compressive failure occurs inside the radius of the bending bar and further, decreases the maximum load of the beam column joint. On the other hand, when a larger bending radius is used, the reinforcement bar at the beginning of the bending portion yields and flexural failure may occur at the beginning of the bending portion. The same behavior was also found by the experimental observation.
3. By the numerical simulation, the dimension of the bending radius of reinforcement bars affect the internal strain and stress inside the beam column joint, the crack propagation on the surface of the beam column joint and the crack propagation in the beam column joint. When a smaller bending radius is used, the compressive force is concentrated inside the radius of the bending bar and further, local failure will occur. On the other hand, when a larger bending radius is used, the compressive force may distribute well in the larger area of compression zone and further, local failure will not occur.

REFERENCES

Japan Society of Civil Engineering, 2007. Standard Specification for Concrete Structures.

Concrete Technical Series, 2005. Design System of Reinforced Concrete Structure –Back to the Future-.(*in Japanese*)

Yoshitake, K., Ogawa, A., Ogira, D., and Maezono, T., 2012. The Effect of Bond Behavior of Longitudinal Reinforcement of Beam and Column on Beam Column Joint. JCI Vol.34, No.2, pp. 541-546. (*in Japanese*)

Hotta, H., Nishizawa, N., 2012. An Experimental Study on the Effect of the Position of Longitudinal Reinforcement for Reinforced Concrete Beam-Column L-shaped Joint. JCI Vol.34, No.2, pp. 282.83-282.88. (*in Japanese*)

Nagai, K., Sato, Y., and Ueda, T., 2005. Mesoscopic Simulation of Failure of Mortar and Concrete by 3D RBSM. Journal of Advanced Concrete Technology Vol.3, No.3, pp. 385-402.

Yoshitake, K., Ogawa, A., and Ogira, D., 2010. Bond Performance of Longitudinal Reinforcement of Column and Beam at Joint Part Considering Positional Relation. JSCE Vol-555, pp. 947-948. (*in Japanese*)
Hayashi, D., Nagai, K., Yoshitake, K., and Ogura, D., 2012. Assessment of the Effect of the Reinforcement Spacing on Bond Performance by 3D-RBSM. JCI Vol.34, No.2, 559-564. (*in Japanese*)
Kawai, T., 1978. New Discrete Models and Their Application to Seismic Response Analysis of Structure. Nuclear Engineering Design. 48. pp.207-229.
Muto, S., Worapong, S., Nakamura, H., 2005. Investigation of Bond Behavior of Deformed Bar by Meso Scale Simulation. JCI Vol. 27, No.2, pp. 763-768. (*in Japanese*)

An experimental investigation of a self-oscillating multi-heat pipe using pure water and alumina nanofluid, respectively

Danh Tung DAO [1,3], Shuichi TORII[2]
[1] PhD student, Kumamoto University, Kumamoto, Japan
daodanhtung@gmail.com
[2] Professor, Kumamoto University, Kumamoto, Japan
[3] Lecturer, National University of Civil Engineering, Ha Noi, Viet Nam

ABSTRACT

This experimental study is performed to investigate heat transfer performance of a self-oscillating multi-heat pipe in the condition of different fill charge ratios and different constant heat fluxes. In this experiment, pure water and alumina (Al_2O_3) nanofluid are employed as the working fluid, respectively. The heat pipe is composed of an evaporator section, a condenser section and an adiabatic section. The evaporator and condenser sections have the same size and are connected by four circular parallel tubes. The corresponding external dimensions are 45mm in length, 45mm in width and 8mm in thickness, and the internal dimensions are 42mm, 42mm and 5mm, respectively. The adiabatic section is consisted of four parallel circular tubes whose dimension is ϕ6 (external diameter) x ϕ5 (internal diameter) x 45 (length) mm. A series of experiments with different fill charge ratios and constant heat fluxes were carried out to measure temperature of the heat pipe. It is found that: this self-oscillating multi-heat pipe has capability increasing heat transfer performance corresponding with the increase of heat flux; With this type of heat pipe, from 30% to 100% of fill charge ratio at 10% intervals of working fluid, when applied low heat flux until 10W/cm2, the higher the fill charge ratio is, the higher the heat transfer performance is. When applied higher heat fluxes 15W/cm2 and 20W/cm2, the highest effective thermal conductivity of the multiple-heat pipe appears around 40% of fill charge ratio; the heat transfer performance of this self-oscillating multi-heat pipe is enhanced when working fluid – pure water is replaced by alumina (Al_2O_3) nanofluid 0.1%.

Keywords: *Heat transfer performance; self-oscillating multi-heat pipe; working fluid; alumina nanofluid; fill charge ratio; effective thermal conductivity*

1. INTRODUCTION

One of the most common cooling devices is heat pipe. It works based on boiling heat transfer and condensation heat transfer principles. Working fluid inside the heat pipe absorbs heat and boils at a certain pressure value in the evaporator section. After boiling, working fluid becomes vapor and evaporates to the condenser section and the vapor releases latent heat to this section and is condensed to working fluid again. After that, working fluid travels back the evaporator section with the use of capillary forces in a wick or gravitational, centrifugal, electrostatic, and osmotic forces. The two-phase closed thermosyphon is one of types of heat pipe using gravitational force. It is a simple, but effective heat transfer device. Due to its high equivalent axial thermal conductivity, and cost effectiveness, it has been used in many applications, such as: preservation permafrost, de-icing roadways, turbine blade cooling, and applications in heat exchangers - Faghri [1995].

There were studies that investigated the heat transfer capability of the two-phase closed thermosyphon. S.H. Noie [2005] studied experimentally the effects of input heat transfer rates (100 to 900W at 100W intervals), the working fluid filling ratios (30%; 60%; 90%) on the heat transfer characteristics of a two-phase closed thermosyphon. Yong Joo Park et al. [2002] investigated experimentally the heat transfer characteristics of a two-phase closed thermosyphon on the effects of fill charge ratio 10-70% at 10% intervals and heat flow rate 50-600W … It can be concluded from literatures that the different fill charge ratios and different heat fluxes have effects on the heat transfer performance of the two-phase closed thermosyphon. Wei Guo and Darin W. Nutter [2009] had a deep study and showed the results of an experimental study of axial conduction through a thermosyphon pipe wall. The experimental data showed that the conduction through the pipe wall caused the wall temperature to decrease along the evaporator section. It also increases the overall heat transfer coefficient, evaporation heat transfer coefficient, and condensation heat transfer coefficient of the thermosyphon. However, the heat transfer associated with axial conduction decreased as the heat flux increased.

With the same purpose to develop heat pipe, this study developed and investigated a self-oscillating multi-heat pipe with a very simple structure (Fig. 2). In addition, the heat pipe was investigated with the application of new class fluid - nanofluid.

Modern technology makes it possible to produces particles < 100 nm in diameter for suspending in conventional fluids such as water, engine oil, and ethylene glycol. This new class of fluids is referred to as "nanofluids". Whose term is first named and used by Choi [1995]. Compared with micron-sized particles, nanoparticles have much larger relative surface areas and a great potential for heat transfer enhancement. Based on this idea, many studies were conducted to explore superior properties of nanofluids, such as large surface-area-to-volume ratio, stable suspension, and no flow passage clogging, which are suitable in heat transfer applications. This is because the much larger surface areas of nanophase powders relative to those of conventional powders not only markedly improve conduction heat transfer capabilities but also increase the stability of suspensions. Eastman et al. [1996] demonstrated that oxide nanoparticles such as Al_2O_3 and CuO have excellent dispersion properties in

water, oil, and ethylene glycol and form suspensions. Lee et al. [1999] measured thermal conductivity of fluids containing Al_2O_3 and CuO particles so that for the copper oxide/ethylene glycol system, thermal conductivity can be enhanced by more than 20% at 4 vol %. In particular, they disclosed that the thermal conductivity of nanofluids depends on that of both the base fluids and particles. Lee and Choi [1996] estimated the performance of microchannel heat exchangers with water, liquid nitrogen, and nanofluids as the working fluid and showed the superiority of nanofluid-cooled microchannel heat exchanger. Shuichi Torii and Wen-Jei Yang [2009] also demonstrated the superior property of nanofluid that significant enhancement of heat transfer performance due to suspension of nanodiamond particles in the circular tube flow is observed in comparison with pure water. Tun-Ping Teng et al. [2010] studied about effect of alumina nanofluid particle size on thermal conductivity and showed that adding nanoparticles to fluid can effectively increase the thermal conductivity ratio of the fluid. Applying nanofluid to heat pipe, S.H. Noie et al. [2009] studied about heat transfer enhancement using Al_2O_3 nanofluid in a two-phase closed thermosyphon (TPCT) and the results showed that nanofluids of 1%, 1.5%, 2%, 2.5% and 3% have better thermal performance than pure water. They improved efficiency of the TPCT up to 14.7%. Temperature distributions on the TPCT were lower level using nanofluid compared to pure water. Temperature differences between the evaporator and condenser sections with nanofluid were less than that of pure water.
Based on the foregoing good results of researchers about application of nanofluids to heat exchanger, in this research, Al_2O_3 nanofluid was also applied to the self-oscillating multi-heat pipe to study the heat transfer performance with different fill charge ratios and different constant heat fluxes. The particles used here were Al_2O_3 size less than 30 nm diameter. The base working fluid is pure water.

2. EXPERIMENTAL APPARATUS AND METHOD

2.1 Experimental apparatus

A schematic diagram of experimental apparatus is described in Fig 1. In this figure, the self-oscillating multi-heat pipe was made in Laboratory of Kumamoto University – Japan, the heat pipe was heated on the evaporator section by the heater block made by copper containing 5 heaters (HAKKO) inside with the use of thermo-glue (AINEX) between two surfaces to improve heat transfer (5 heaters are not shown in this figure). 5 heaters were connected with the transformer (YAMABISHI) and its voltage and power were measured by the digital multi-meter (AC/DC POWER HITESTER 3334). The transformer was connected with power supply in the Laboratory. An adequate amount of pure water was filled inside of the self-oscillating heat pipe by the burette (NALJENE). Vacuum pressure inside the self-oscillating multi-heat pipe was generated by the vacuum pump (GHD-030) with the measurement by the vacuum gauge (SMC) and the Power indicator transducer (SMC). The condenser section of the heat pipe was cooled by cooling water set at 15^oC by the thermostatic bath (NCC-1100) with the measurement of flow by the flow meter (RK400). The temperature of the heat pipe was measured by thermocouples type K with the aid of the data logger

(KEYENCE NR-250) and a personal computer. The working fluids in this experimental study were pure water and alumina (Al_2O_3) nanofluid.

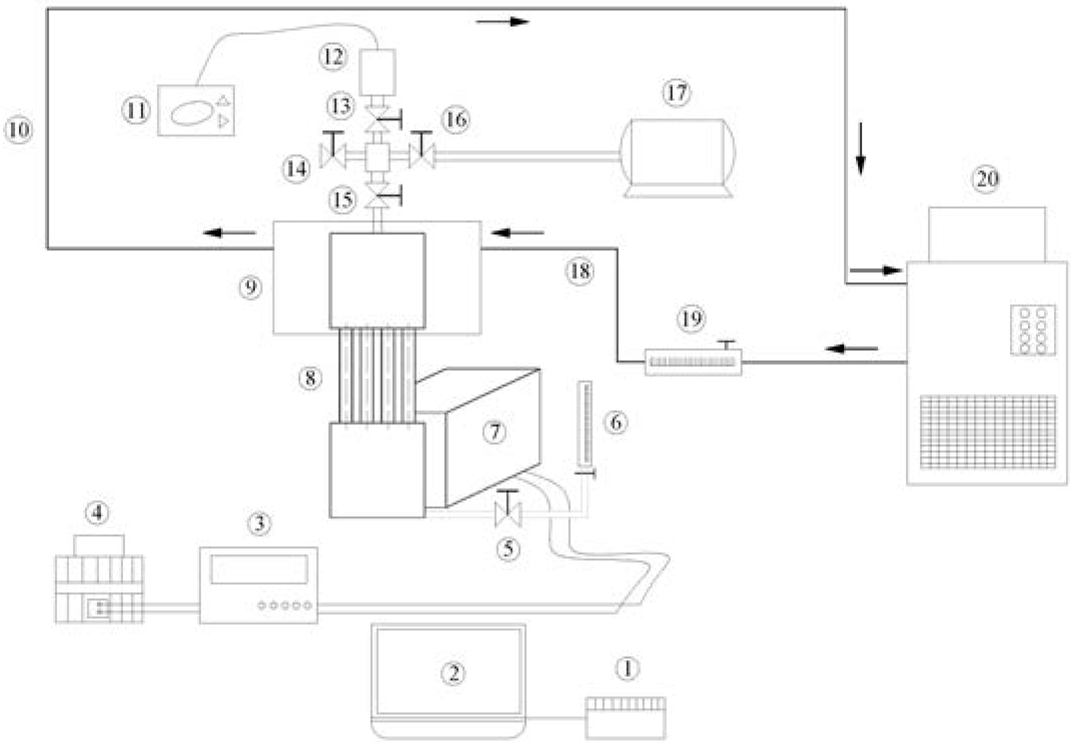

1 Data logger
2 Personal computer
3 Digital multimetter
4 Transformer
5 Vacuum valve
6 Burrette
7 Heater block
8 Heat pipe
9 Water tank
10 Outlet cooling water
11 Power indicator for transducer
12 Pirani gauge Transducer
13 Vacuum valve
14 Vacuum valve
15 Vacuum valve
16 Vacuum valve
17 Vacuum pump
18 Inlet cooling water
19 Flow metter
20 Themostatic bath

Fig.1 Schematic diagram of experimental apparatus

Fig. 2 is detailed drawing of the self-oscillating multi-heat pipe. During experiment, the adiabatic section, the evaporator section and the heater block were insulated with glass fiber to prevent heat loss, the condenser section was inserted to a water tank made by plastic containing cooling water flowed circularly from the thermostatic bath. In order to fill in the working fluid and make vacuum pressure, each link part was manufactured.

2.2 Experimental method

In this experiment, the working fluids were pure water and alumina (Al_2O_3) nanofluid, respectively. The fill charge ratios f_{cr} between fill charge volume of working fluid and internal evaporator section volume were 30%; 40%; 50%; 60%; 70%; 80%; 90% and 100%. The corresponding constant heat fluxes applied to the evaporator section for each case of fill charge ratio were 5W/cm^2 (50kW/m^2); 10W/cm^2 (100kW/m^2); 15W/cm^2 (150kW/m^2) and 20W/cm^2 (200kW/m^2). The angle between heat pipe axis and vertical direction was 0^o (Fig. 3a). As shown in

Fig. 2, the temperature of each section of the heat pipe was measured with thermocouples type K as follows: for the evaporator section: point H_1, H_2, H_3, H_4, H_5; for the condenser section: point C_1, C_2, C_3. The inlet temperature of the cooling water was set at 15^oC using the controllable thermostatic bath and cooling water was supplied to the water tank at a rate of 3.5l/min. After filling an adequate amount of working fluid in the heat pipe, the vacuum pressure would be generated by vacuum pump and its value was maintained at 7400 Pa for all cases. In order to get accurate vacuum pressure value, the vacuum pressure value was read on the power indicator transducer after 20 minutes and when changing from one fill charge ratio to another, the working fluid was filled in when whole experimental system was 25^oC. Temperature was measured until the experiment reached steady state and the steady state time was at least 30 minutes. After finishing all experiments, we could obtain the variation of heat transfer performance of the heat pipe corresponding with the change of the fill charge ratio and heat flux and two results between the use of pure water and nanofluid were compared

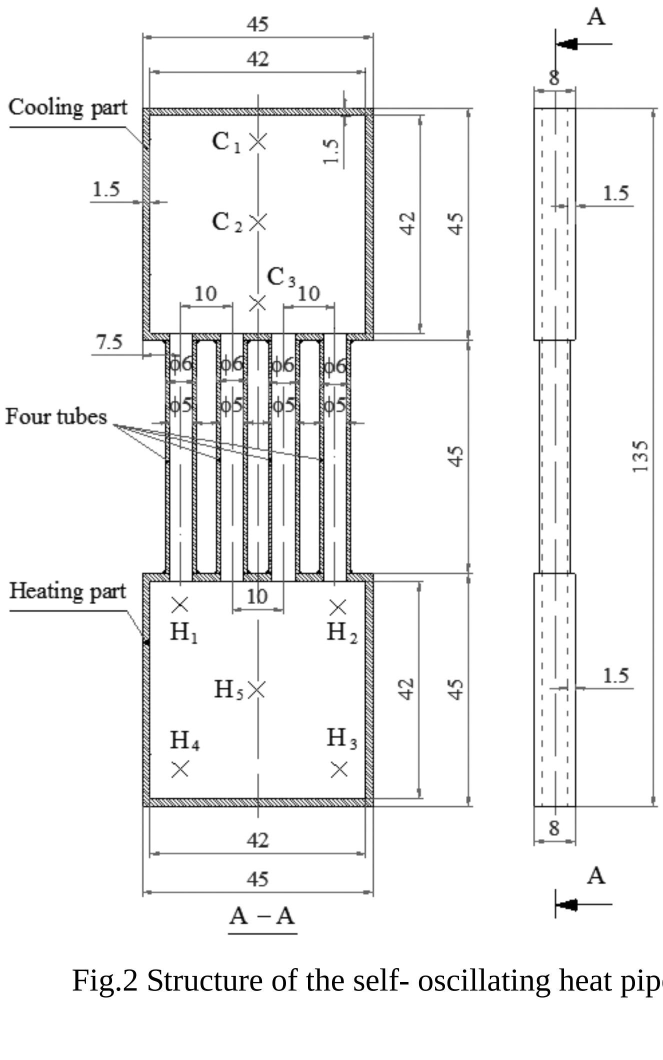

Fig.2 Structure of the self- oscillating heat pipe

3. EXPERIMENTAL RESULTS AND DISCUSSION

3.1 The effect of fill charge ratio and heat flux on the temperature of the heat pipe

Fig. 3b shows how the temperature changes in the evaporator section and the condenser section at fill charge ratio from 30% to 100%.

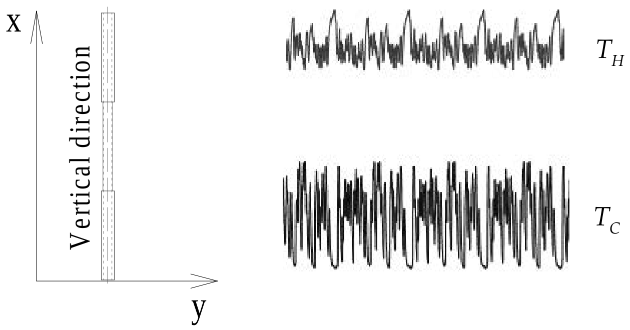

Fig. 3. a) Vertical direction of the heat pipe
b) Temperature form of the evaporator section T_H
and the condenser section T_C

We can see the temperature changes around a certain value. This can be explained briefly as follows: when the heat pipe was heated, the temperature of evaporator section was increased and the working fluid became vapor and it would be evaporated to the condenser section. The evaporator section reached the highest temperature until the working fluid film refluxed and cooled it. When the vapor met the condenser section, it would transfer latent heat to the condenser section and then condensed to working fluid again. Therefore, the temperature of the condenser section would be increased. When the condensed fluid traveled back down the evaporator section, it would absorb heat from the evaporator section and did make the temperature of the evaporator section decreased. At the same time, the condenser section was cooled by circulated cooling water contained in water tank.

Figs.4 and 5 show the effect of fill charge ratio on mean temperatures of the evaporator and condenser section of the heat pipe with the use of pure water and alumina nanofluid 0.1% volume fraction, respectively. To get mean temperature T_H of the evaporator section and T_C of the condenser section, local temperatures were measured and averaged. With the measurement by thermocouples type K, points H_1, H_2, H_3, H_4 and H_5 are for the evaporator section and C_1; C_2; C_3 are for the condenser section. These points were depicted in Fig. 2.
$T_H = \frac{T_{H_1} + T_{H_2} + T_{H_3} + T_{H_4} + T_{H_5}}{5}$; $T_C = \frac{T_{C_1} + T_{C_2} + T_{C_3}}{3}$. As shown in Figs. 4 and 5, we can see that the variation of mean temperature of the evaporator and condenser section corresponding with the increase of fill charge ratio in two cases of working fluid is similar. Mean temperature of the evaporator section tends to decrease corresponding with the increase of fill charge ratio. For the condenser

section, the variation trend has a difference, which is mean temperature also has trend to decrease corresponding with the increase of fill charge ratio, however, at 40% of fill charge ratio, temperature of the condenser section get maximum value when heat flux goes up. From this phenomenon, it can be guessed the heat pipe reaches the maximum of heat transfer performance at 40% of fill charge ratio when applied much much higher heat flux.

Also from this results, we can see that with the same heat flux and fill charge ratio, mean temperature of the evaporator section of the heat pipe using Al_2O_3 nanofluid 0.1% Vol is lower than that of using pure water. In contrast, mean temperature of the condenser section of the heat pipe using Al_2O_3 nanofluid 0.1% Vol is higher than that of using pure water. This demonstrates an excellent sign for this heat pipe when applied nanofluid as working fluid.

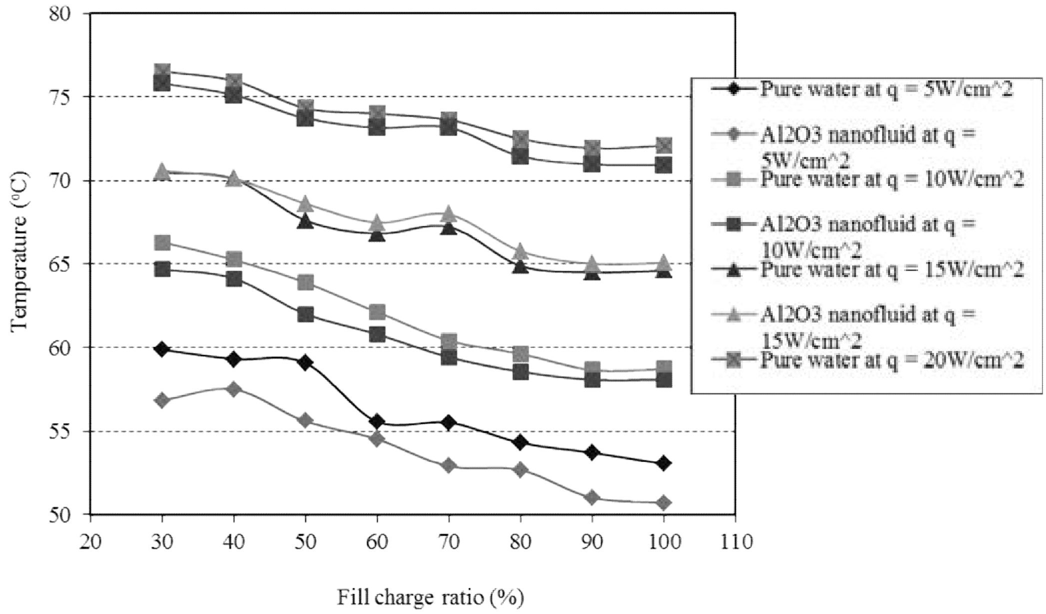

Fig.4 Mean temperature of the evaporator section
versus fill charge ratio with the use of pure water and Al_2O_3 nanofluid 0.1% vol

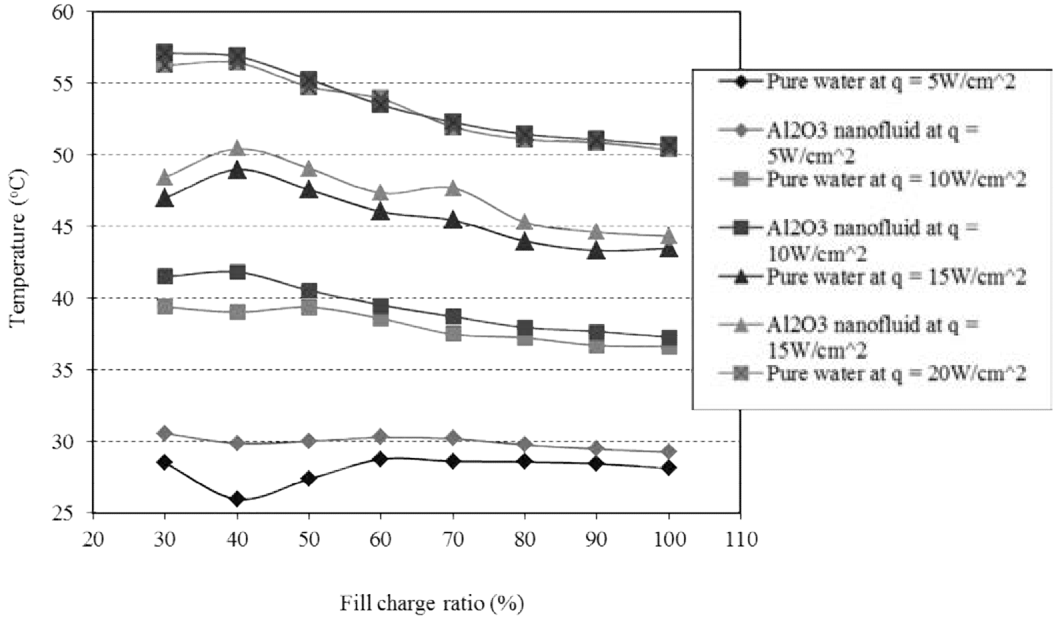

Fig.5 Mean temperature of the condenser section versus fill charge ratio with the use of pure water and Al_2O_3 nanofluid 0.1% Vol

3.2 Heat transfer characteristic of the self-oscillating heat pipe

Effective thermal conductivity k_{eff} of the heat pipe was calculated as follows:

$$Q = \mathrm{NA}q' = \mathrm{NA}k_{eff}\frac{T_H - T_C}{\mathrm{L}} \qquad (1)$$

$$k_{eff} = \frac{Q\mathrm{L}}{\mathrm{NA}(T_H - T_C)} \qquad (2)$$

Where, Q is total heat load (W), *q'* is the heat flux from the evaporator section to the condenser section (W/mK), L is the length from center of the evaporator section to center of the condenser section (m), that is the approximate distance between T_H measuring point and T_C measuring point. N is the number of tubes of the adiabatic section (N = 4). A is the flux area of the inner part of a tube in the adiabatic section (m^2).

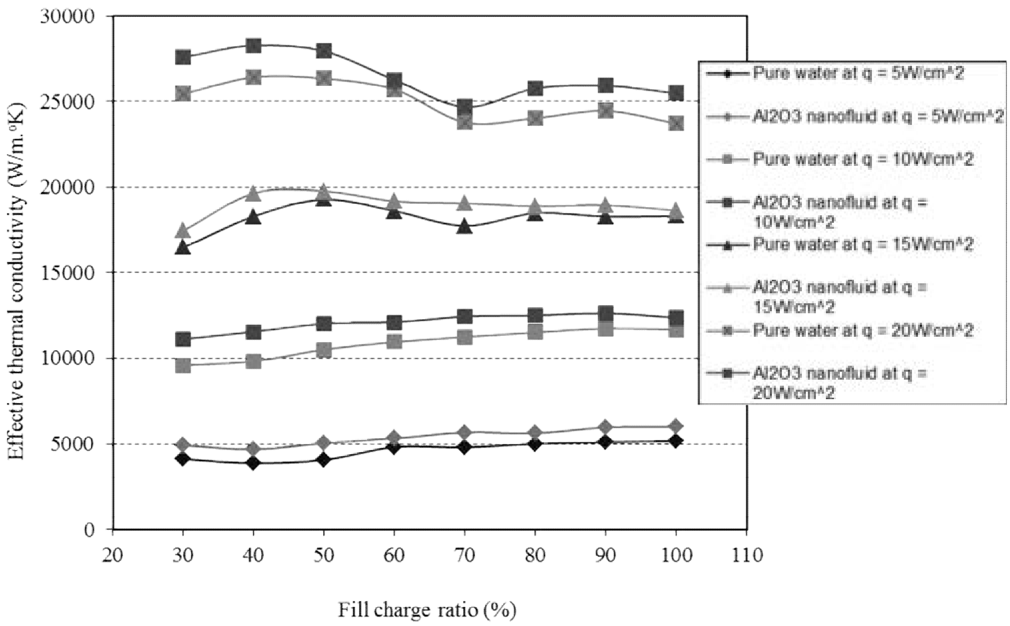

Fig.6 Effective thermal conductivity of the heat pipe
versus fill charge ratio with the use of pure water and nanofluid

Fig. 6 shows the variation of effective thermal conductivity k_{eff} as a function of fill charge ratio fcr of the heat pipe with the use of pure water and alumina nanofluid 0,1% volume fraction, respectively. As shown in Fig. 6, we can see that at 5W/cm^2 and 10W/cm^2 of heat flux, in both cases of working fluid, effective thermal conductivity of the heat pipe tends to increase when fill charge ratio increases, in other word, the higher the fill charge ratio is, the higher the effective thermal conductivity is. However, from 15W/cm^2 and over, the relationship between effective thermal conductivity of the heat pipe and fill charge ratio is different. Namely at 15W/cm^2 of heat flux, the effective thermal conductivity of the heat pipe still increases corresponding with the increase of fill charge ratio, but the maximum effective thermal conductivity occurs at 50% of fill charge ratio. At 20W/cm^2, the relationship between effective thermal conductivity of the heat pipe and fill charge ratio is inverse, the effective thermal conductivity of the heat pipe tends to decrease when the fill charge ratio increases, and the maximum effective thermal conductivity occurs at 40% of fill charge ratio. This can be explained that when heat flux applied to the evaporator section of the heat pipe increases and exceeds a certain value, a high amount of heat from the evaporator section is transferred through the wall of the heat pipe to the condenser section and makes it reaches high temperature even when it was being cooled by cooling water. In addition, with a high amount of working fluid inside the heat pipe f_{cr} = 100%, it yields too much vapor when working fluid evaporated and this causes lack of inner space in the heat pipe and condensation temperature of vapor will be increased. Therefore, heat transfer efficiency is decreased. In other words, high temperature at the condenser section combines with much vapor makes condensation performance decreases and this corresponds with the decrease of heat transfer performance.

Also from this figure, it is easy to see that with the same heat flux and fill charge ratio, the effective thermal conductivity of the heat pipe with the use of nanofluid is higher than that with the use of pure water. In other words, the heat transfer performance of the heat pipe is enhanced.

4. CONCLUSION

From the observation of the results in this study, the following conclusions are drawn:

With the conditions of the experiment

- With this type of heat pipe, from 30% to 100% of fill charge ratio at 10% intervals of working fluid, when applied low heat flux until 10W/cm2, the higher the fill charge ratio is, the higher the heat transfer performance is. When applied higher heat fluxes 15W/cm^2 and 20W/cm^2, the highest effective thermal conductivity of the multiple-heat pipe appears around 40% of fill charge ratio.
- This self-oscillating multi-heat pipe has capability increasing heat transfer performance corresponding with the increase of heat flux.
- The heat transfer performance of this self-oscillating multi-heat pipe is enhanced when working fluid – pure water is replaced by alumina (Al_2O_3) nanofluid 0.1%.

REFERENCES

A. Faghri,. 1995. Heat pipe science and technology, Taylor & Francis.

S.H. Noie,. 2005. Heat transfer characteristic of a two-phase closed thermosyphon, *Applied Thermal Engineering* 25 495 - 506.

Y.J. Park, H.K. Kang, C.J. Kim,. 2002. Heat transfer characteristic of a two-phase closed thermosyphon to the fill charge ratio, *International Journal of Heat and Mass Transfer* 45 4655-4661.

Wei Gue, Darin W. Nutter,. 2009. An experimental study of axial conduction through a thermosyphon pipe wall, *Applied Thermal Engineering* 29 3536 - 3541.

Choi, S.U.S.,. 1995. Enhancing thermal conductivity of fluids with nanoparticles, in Developments Applications of Non-Newtonian Flows, FED-vol. 231/MD-vol. 66, ASME: 99-105, edited by D.A. Siginer and H. P. Wang. New York.

J. A. Eastman, Stephen U. S. Choi, Shaoping Li, L. J. Thomson, and Shinpyo Lee,. 1996. Enhanced thermal conductivity through the development of nanofluids, *Proceedings of the Symposium on Nanophase and Nanocomposite Materials II*, Material Research Society, Bonton, MA, pp. 3-11.

S. Lee, Choi, S. U. S., S. Li, and J. A. Eastman,. 1999. Measuring thermal conductivity of fluids containing oxide nanoparticles, *Journal of Heat Transfer* 121 280 - 289.

Lee, S.P., and Choi, U.S., 1996. Application of metallic nanoparticles suspensions in advanced cooling system, in: Y. Kwon, D. Davis, H. Chung (Eds.), *Recent Advances in Solid/Structures and Application of Metallic Materials*, PVP-Vol.342/MD-Vol.72, The America Society of Mechanical Engineering, New York, pp. 227-234.

S. Torii, W.J. Yang,. 2009. Heat transfer augmentation of aqueous suspensions of nanodiamonds in turbulent pipe flow, *Journal of Heat Transfer* 131 043203-1-5

T.P. Teng, Y.H. Hung, T.C. Teng, H.E. Mo, H.G. Hsu,. 2010. The effect of alumina/water nanofluid particle size on thermal conductivity, *Applied Thermal Engineering* 30 2213-2218.

S.H. Noie, S. Zeinali Heris, M. Kahani, S.M. Nowee,. 2009. Heat transfer enhancement using Al2O3/water nanofluid in a two-phase closed thermosyphon, *International Journal of Heat and Fluid Flow* 30 700-705.

Earthquake behavior of reinforced concrete framed buildings on hill slopes

Ajay K SREERAMA[1] and Pradeep K RAMANCHARLA[2]
[1]Ph.D Student, Civil Engineering, IIIT Hyderabad, Gachibowli, Hyderabad-500032, India
ajay.s@research.iiit.ac.in
[2]Professor of Civil Engineering, Earthquake Engineering Research Centre, IIIT Hyderabad, Gachibowli, Hyderabad-500032, India
ramancharla@iiit.ac.in

ABSTRACT

Recent earthquakes, 18 Sep 2011, Sikkim earthquake, M6.9 and 1 May 2013 Doda earthquake, M5.8 produced two major effects, namely on buildings and on hill slopes. The maximum intensity of ground shaking experienced during these earthquakes was only about VI or less on the MSK scale. Considering the low intensity of ground shaking in the affected areas, the damage attributed was disproportionately higher. It is mainly due to high amplification in local site areas. In this regard, a research is carried out to understand the performance of buildings on hill slopes.

In this paper, the study of the behavior of a G+3 building on varying slope angles i.e., 15°, 30°, 45° and 60° is studied and compared with the same on the flat ground. Building is designed as per IS 456 and later subjected to earthquake loads. It was observed that as the slope angle is increasing, building is becoming stiffer. Two types of analyses were conducted viz., lateral load analysis and incremental dynamic analysis. It was observed from the initial results that the columns on the higher side of the slope i.e., short columns were subjected to more shear force then longer columns on the lower side. Finite element method is used to study the static behavior where as Applied Element Method (AEM) is used to perform incremental dynamic analysis.

Keywords: *hill-slopes, incremental dynamic analysis*

1. INTRODUCTION

North and northeastern parts of India have large scales of hilly terrain, which are categorized under seismic zone IV and V. In this region the construction of multistory RC framed buildings on hill slopes has a popular and pressing demand, due to its economic growth and rapid urbanization. This growth in construction activity is adding to tremendous increase in population density. While construction, it must be noted that Hill buildings are different from those in plains i.e., they are very irregular and unsymmetrical in horizontal and vertical planes, and torsionally coupled. Since there is scarcity of plain ground in hilly areas, it obligates the construction of buildings on slopes.

Recent earthquakes i.e., 18 Sep 2011, Sikkim earthquake (M6.9) and 1 May 2013 Doda earthquake(M5.8) produced two major effects, namely on buildings and on hill slopes. To perform well in an earthquake, a building should possess four main attributes i.e. simple and regular configuration, adequate lateral strength, stiffness and ductility (as per clause 7.1 of IS 1893-2002).

1.1. SEISMIC BEHAVIOUR OF BUILDINGS ON SLOPES IN INDIA

Shillong Plateau earthquake (M8.0) of 1897 and the Kangra earthquake (M7.8) of 1905, were the major of several devastating earthquakes to occur in northern India. An estimated of more than 375,000 population were killed in epicentral region, and over 100,000 buildings were destroyed by the earthquake. Similarly in recent earthquakes like Bihar-Nepal (1980), Uttarkashi (1991), Sikkim (2011), and Doda (2013) affected many buildings on hill slopes.

India having a great arc of mountains consisting of the Himalayas defines the northern Indian subcontinent. These were formed by the ongoing tectonic collision of the Indian and Eurasian plates where housing densities of approximately 62159.2 per Sq Km are around as per 2011 Indian census. Hence there is a need to study on the seismic safety and design of these structures on slopes.

Dynamic characteristics of hill buildings are significantly different from the buildings resting on flat topography, as these are irregular and unsymmetrical in both horizontal and vertical directions. The irregular variation of stiffness and mass in vertical as well as horizontal directions, results in centre of mass and centre of stiffness of a storey not coinciding with each other and not being on a vertical line for different floors. When subjected to lateral loads, these buildings are generally subjected to significant torsional response. Further, due to site conditions, buildings on hill slope are characterized by unequal column heights within a story, which results in drastic variation in stiffness of columns of the same storey. The short, stiff columns on uphill side attract much higher lateral forces and are prone to damage.

Figure 1: An aerial view of houses located on hill slopes in Sikkim

2. CASE STUDY AND ANALYSIS

A five different cases of G+3 buildings on varying slope angles i.e., 0°,15°, 30°, 45° and 60° are designed and analyzed as per IS 456 in SAP2000 as shown in Figure 2 and 3. The properties of the considered building configuration in the present study are summarized below.

Structural element sizes

Beams :	300 x 300 mm
Columns:	300 x 300 mm
Slab :	120 mm thick

Material properties

Grade of concrete:	M25
Grade of Steel reinforcement bars:	Fe 415

Loading

Live load :	3 kN/m^2
Floor finish load :	1 kN/m^2
Self-weight of slab :	3 kN/m^2

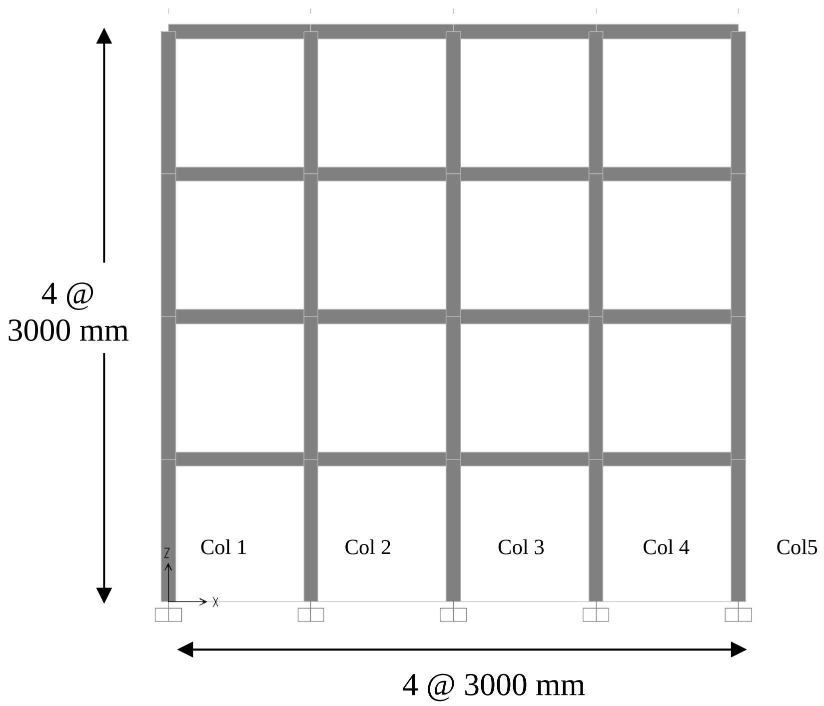

Figure 2: G+3 RC framed structure (Reference building)

The building has been subjected and analyzed for earthquake load i.e., N90E component of Northridge ground motion with a PGA of 0.565g and magnitude M6.7.

Table 1: Buildings considered for study: Details of 5 buildings

Building	Description	Number of bays (Both directions)	Bottom column lengths (m)				
			Col 1	Col 2	Col 3	Col 4	Col 5
A	G+3 Regular building (0°)	4	3	3	3	3	3
B	G+3 building on 15° slope	4	6.2	5.4	4.6	3.8	3
C	G+3 building on 30° slope	4	9.92	8.19	6.46	4.73	3
D	G+3 building on 45° slope	4	15	12	9	6	3
E	G+3 building on 60° slope	4	23.8	18.6	13.4	8.2	3

Two types of analyses were conducted viz., lateral load analysis and incremental dynamic analysis. It was observed from the initial results that the columns on the higher side of the slope i.e., short columns were subjected to more shear force then longer columns on the lower side. Finite element method is used to study the linear and non linear static and dynamic behavior of building on slopes, where as Applied element method is used for incremental dynamic analysis.

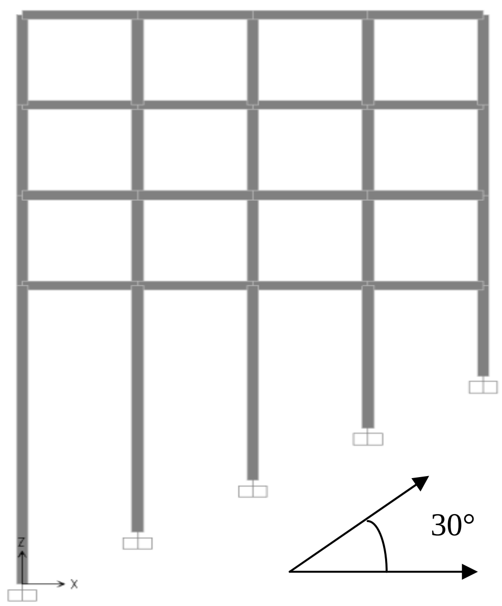

Figure 3: Model of Building on slope

3. RESULTS AND DISCUSSION

From the linear static analysis it is observed that the Shorter Columns is observed to take more loads since shorter columns are stiffer and hence has more stress carrying capacity. From Figure 4 column 1 is observed to have base reaction reduced to zero as slope angle increase because of long column effect.

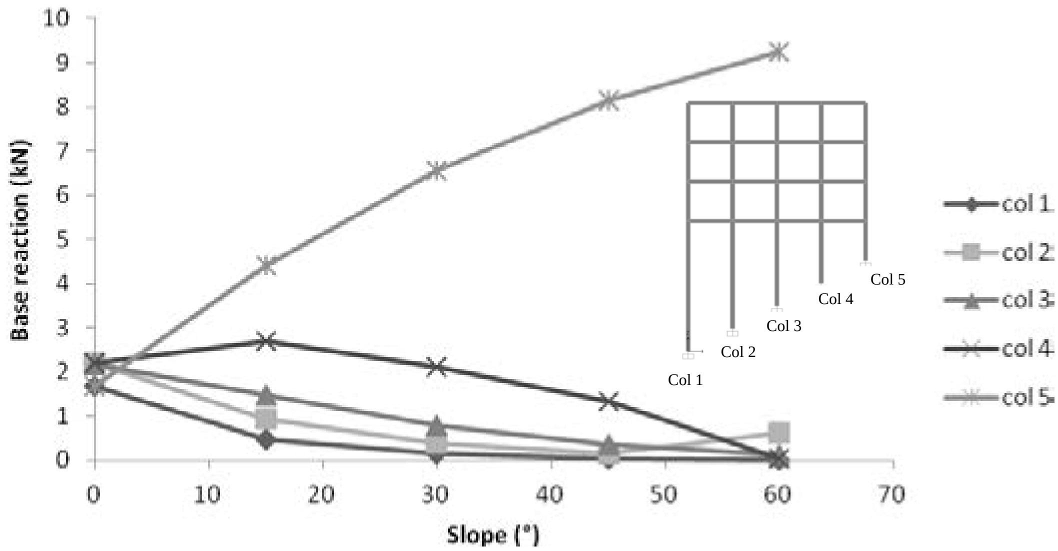

Figure 4: Base reaction Vs Slope

3.1. DYNAMIC CHARACTERISTICS OF BUILDING

An inertia force is caused due to the oscillation of building during an earthquake, where it is foremost for us to understand the mode of oscillation i.e., Natural period and deformed shape. Numerical results are used to study the dynamic behavior and the factors that influence it.

Table 2: Natural time period of Buildings on varied slope angles

	0°	***15°***	***30°***	***45°***	***60°***
T1	**0.724**	**0.881**	**0.994**	**1.0604**	**1.1545**
T2	**0.236**	**0.276**	**0.296**	**0.312**	**0.343**
T3	**0.1413**	**0.1544**	**0.159**	**0.162**	**0.1691**

From table 2, time period of buildings on slopes increase with increase in the slope angle. Since there is an increase in column length of the building the stiffness and mass of it is varying which alters the natural time period. We know that time period of structure is directly proportional to both mass and stiffness as below

$$T = \frac{2\pi}{\omega} \quad ; \quad \omega = \sqrt{\frac{k}{m}} \quad \Longrightarrow \quad T \,\alpha\, m \quad ; \quad T \,\alpha\, \frac{1}{k}$$

Stiffness influencing natural period:

Increasing the length of column because of building position on slope decreases the stiffness and increases mass of the structure. A study has been carried out on buildings A, B, C, D and E; where the top three storey of the building has same mass and stiffness, only the bottom portion of the building varies. It has been observed that due to the increase of column length the building becomes more flexible with less stiffness. Figure 5 shows the Stiffness degradation of whole structure as well as the effective stiffness of bottom storey of the structure with respect to the increase of slope.

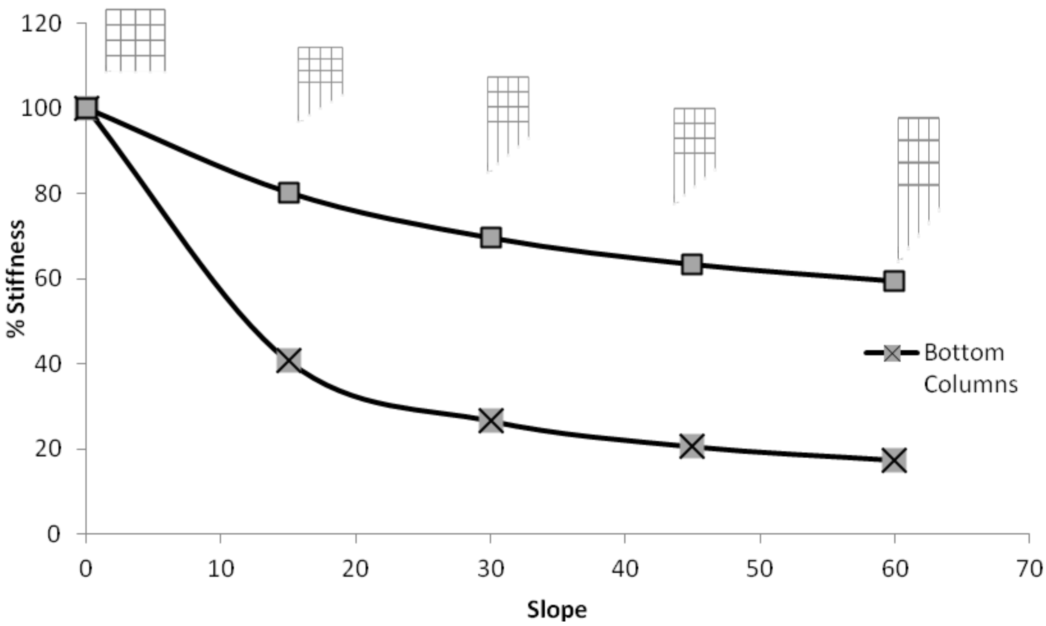

Figure 5: % Stiffness Vs Slope

Mass influencing Natural period:

An increase in mass of a building increass its natural period. Buildings B, C, D and E are with same paln size, column sizes but with different columns length at bottom (Figureure 6). The total seismic mass of the reference building A is 1055.12 kN while that in other buildings there is an increase in mass.

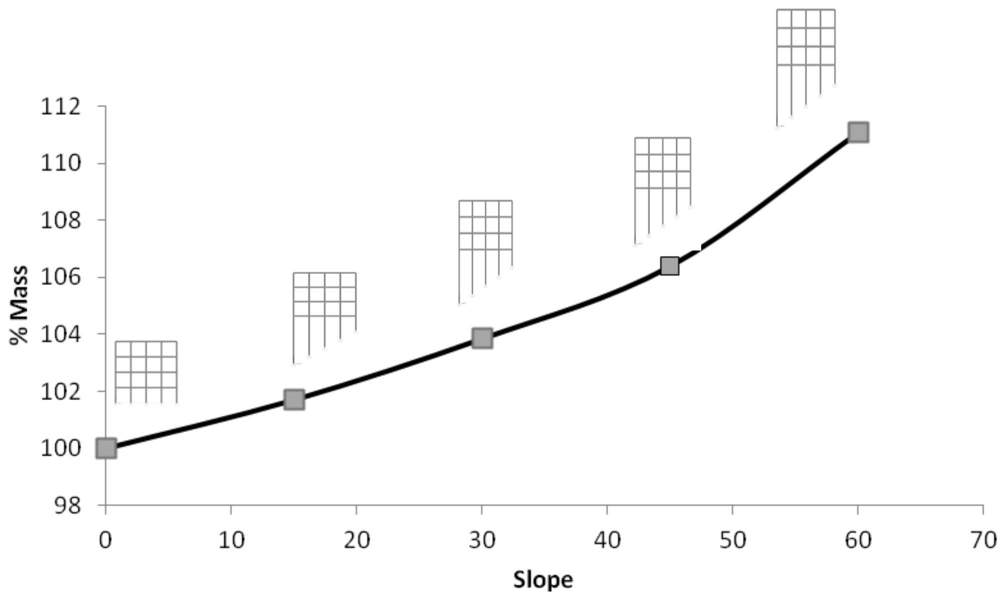

Figure 6: % Mass Vs Slope

3.2. TIME HISTORY ANALYSIS

The building has been analyzed for Northridge ground motion with a PGA of 0.565g and magnitude M6.7.

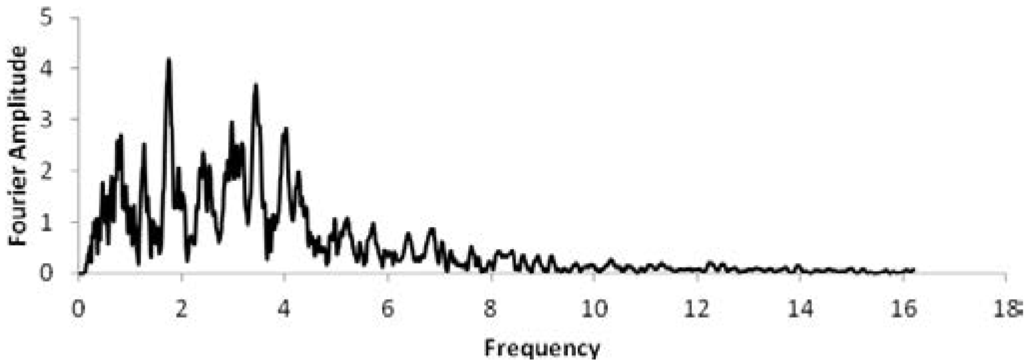

Figure 7: Fourier amplitude of Northridge ground motion

Figure 9 shows the evaluation results of the linear time history responses of the five buildings. Since the natural frequency of structure is resonating with the predominant frequency from Figure 8 we can observe the response of building on 60° and 30° slope is observed to have maximum displacement when compared to that of others. When observed the mass participation of the five buildings we can say the every structure is predominant in its first mode of vibration. It is also observed from below plot the storey drift of the building on 45° slope is very less when compared to that of other slope angles.

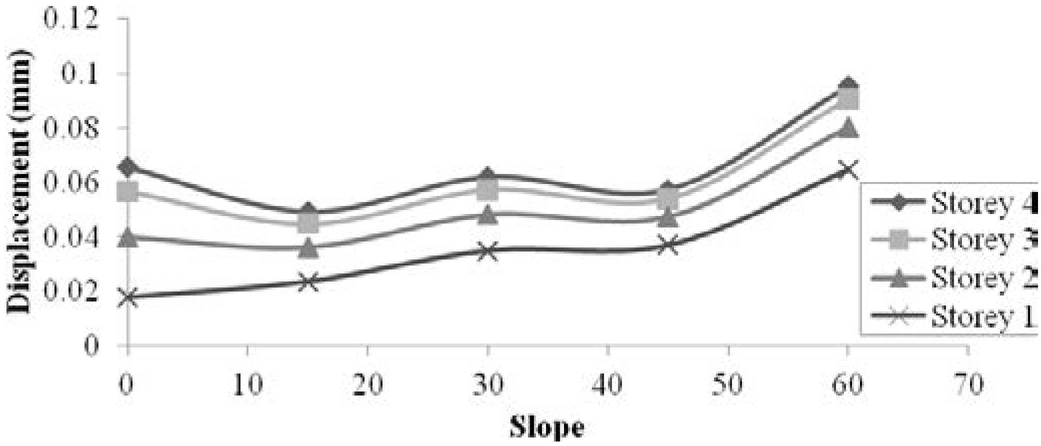

Figure 8: Maximum time history response of each storey for five cases

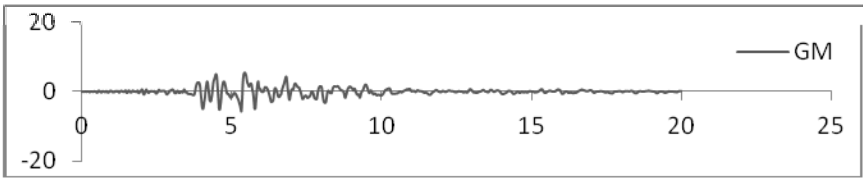

Figure 9(a): Northridge ground motion

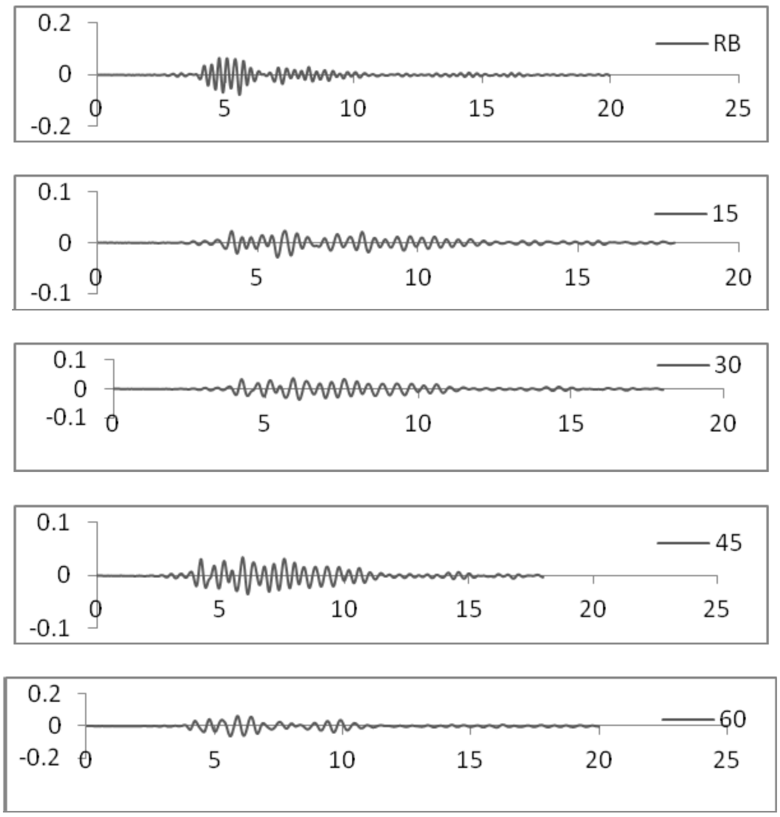

Figure 9 (b): Time history response of A, B, C, D and E buildings

3.3. PUSH OVER ANALYSIS

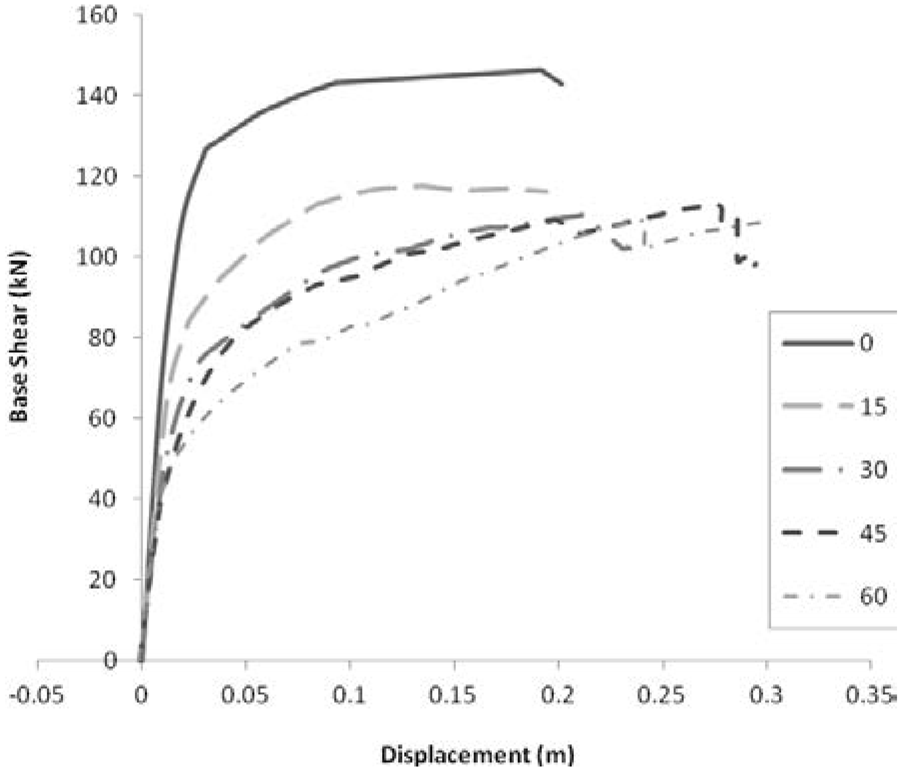

Figure 10: Pushover curves of A, B, C, D and E buildings

After designing and detailing the RC frame structure, a linear static pushover analysis is carried out for evaluating structurtal response.Figureure 10 shows the resulting capacity curves for the five cases. Initially they are linear where axial load is predominant but falls under inelastic range where the flexure and shear comes into picture. From Figure 10 the area under the pushover curve i.e. the capacity of building on flat surface is more than that of buildings on slopes.

PLASTIC HINGES MECHANISM

From Figure 11 we can easily observe the formation of hinge mechanism where as the slope increases the zone near the shoter coulmn is falling under E and D performance levels, which clearly indictaes the complete collapse of the structure. Comparision of Figureures b, c,d and e reveals that the pattern of forming hinges are quite similar. Plastic hinges formation starts with base columns of lower stories and end beams, then propagates to upper stories and continue with yielding of intermediate columns.

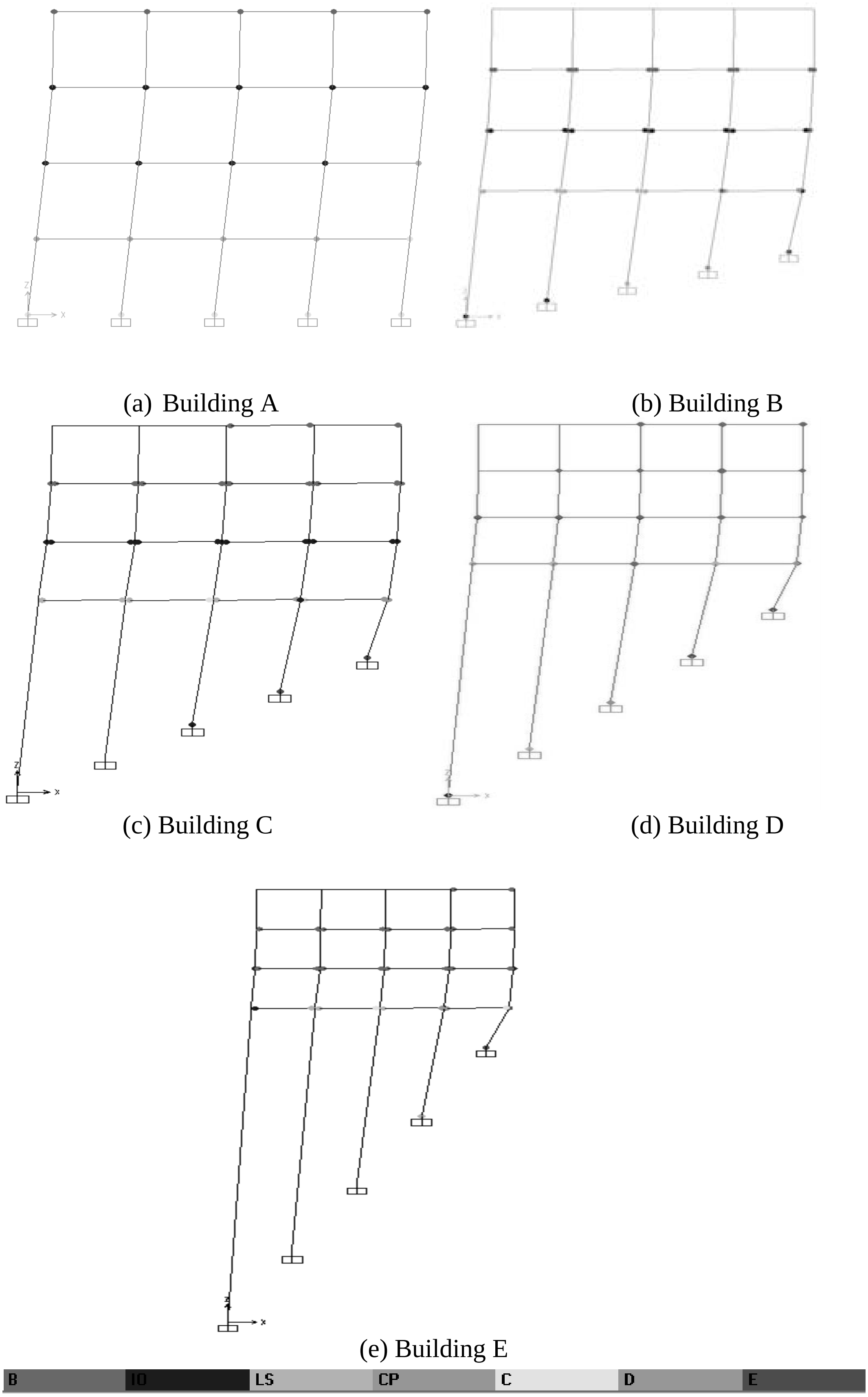

Figure 11: Hinge mechanism of A, B, C, D and E buildings

FRAGILITY CURVES

To undertstand the expected damage of the structures of varying time periods, fragility curves are plotted. Equation used to calculate the damage of the structure as explained below

$$Damage = \frac{E_i}{E_{max}}$$

E_{max} = Area under the pushover curve with line dropped parallel to initial stiffness at the end point.
E_i = Energy dissipated at every displacement (Area under the curve at every displacement with line dropped parallel to initial stiffness.

Conversion from Roof Displacement to Spectral Acceleration:

$$S_{di} = \frac{\Delta_{roof}}{PF_1 \times \emptyset_{1,roof}}$$

S_{di}: Spectral Displacement
Δ_{roof}: Roof displacement obtained from pushover curve
PF_1: Participation factors for the first natural mode of the structure
$\emptyset_{1,\, roof}$: Roof level amplitude of the first mode

$$S_{ai} = \frac{4\pi^2 S_{di}}{T^2 g}$$

T: Time Period of the structure
g: Acceleration due to gravity

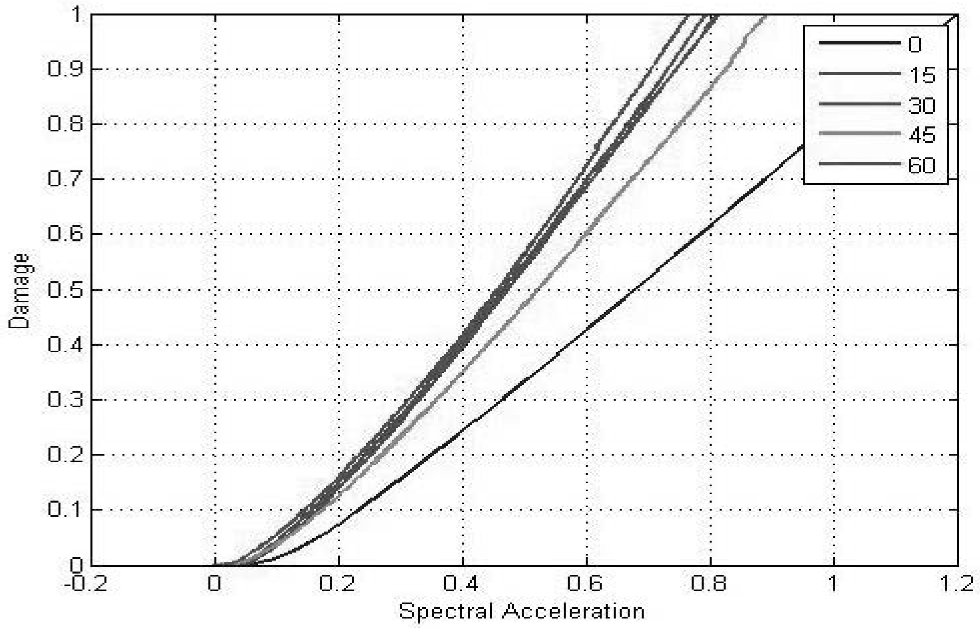

Figure 12: Fragility Curves

From Figure 12 we can observe that for a given ‘g’ value the expected damage is more in 15° and 30° slope buildings than building on falt surface. Whereas the damage of structure on 45° and 60° slope are less than 15° and 45° because of increase in column dimensions, but relatively the damage level is more in 60° than compared to that of 45° slope building.

3.4. INCREMENTAL DYNAMIC ANALYSIS

To understand and to estimate the structural performance thoroughly under seismic loads a method so called as Incremental dynamic analysis is performed on to the structures. It involves subjecting a structure to one or more ground motions scaled to multiples levels of intensity. The main advantage of IDA is that it addresses both demand and capacity of structure. In the present study Applied element method (AEM) is used to perform IDA.
Applied element method is a discrete method in which the elements are connected by pair of normal and shear springs which are distributed around the element edges. These springs represents the stresses and deformations of the studied element. The elements motion is rigid body motion and the internal deformations are taken by springs only. The general stiffness matrix components corresponding to each degree of freedom are determined by assuming unit displacement and the forces are at the centroid of each element. The element stiffness matrix size is 6x6.

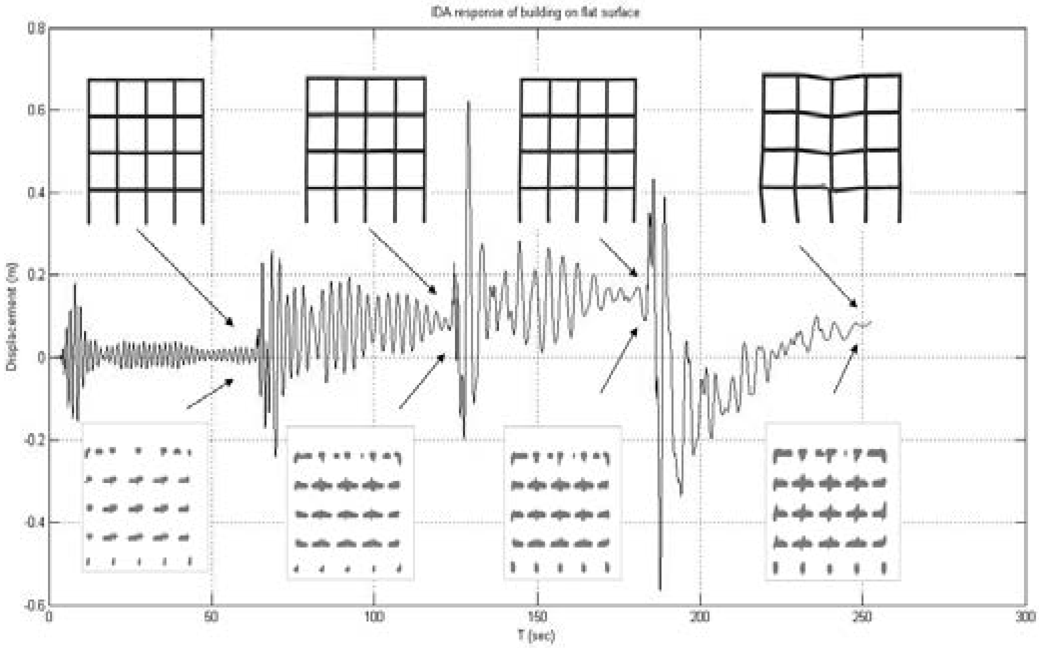

Figure 13(a): IDA response of the Building on flat surface with spring failure pattern

In present study Northridge ground motion is scaled to 4 levels i.e. up to 1g and applied incrementally on to the structures. From Figure 13 we can observe the response of the structure increases as the ‘g’ value is amplified. At the end of each ground motion the damage of structure and the spring’s failure pattern can be observed at the top and bottom of the plot. For building on 45° and 60° slope the structure is unstable.

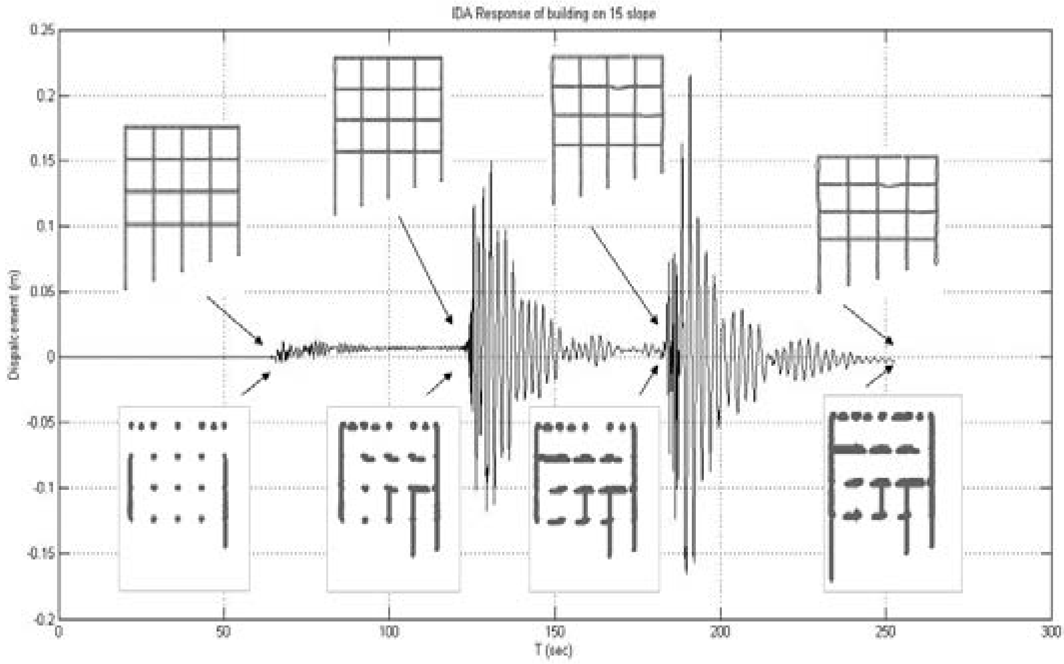

Figure 13(b): IDA response of the Building on 15° slope with spring failure pattern

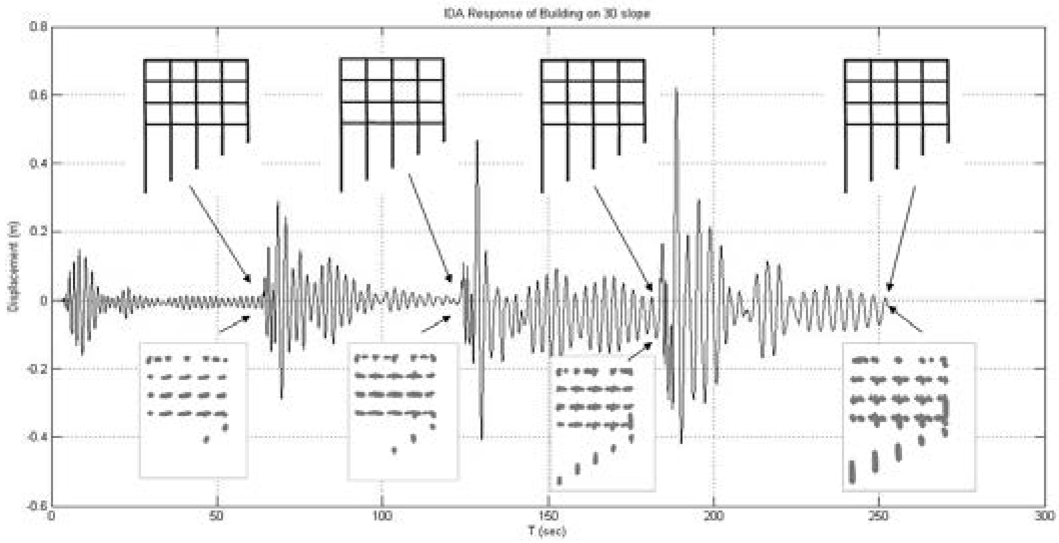

Figure 13(c): IDA response of the Building on 30° slope with spring failure pattern

4. CONCLUSIONS

The study clearly helps us to understand the significant difference between the seismic behaviors of building on slopes to building on flat surface. In summary, the natural period of building depends on the distribution of mass and stiffness along the building. As the slope angle increases, it is observed that the short column resist almost all the storey shear since other columns are flexible and tend to oscillate. A hinge mechanism is formed near the shorter column zone and is damaged earlier as the slope angle increases. From the fragility curve we can easily observe the damage of the structure is more when it is on steep angle. Major challenge which has to be focused further is considering together plan irregularity (i.e. Torsional effect) and vertical irregularity. It would be desirable to study more cases before reaching some definite conclusions about the behavior of reinforced concrete framed buildings on slopes.

REFERENCES

1. A.R.Vijaya Narayanan, Rupen Goswami and C.V.R. Murty., 15WCEE 2012 *Performance of RC Buildings along Hill Slopes of Himalayas during 2011 Sikkim Earthquake.*
2. Pandey A.D, Prabhat Kumar, Sharad Sharma., International Journal of Civil and Structural Engineering Volume 2, No 2, 2011 *Seismic soil-structure interaction of buildings on hill slopes.*
3. B.G. Birajdar, S.S. Nalawade., 13WCEE 2004 *Seismic analysis of buildings resting on sloping ground.*
4. ATC 40, Seismic evaluation and Retrofit of Concrete Buildings, Volume 1.
5. Nicholas A, Roger B., Current science, Vol.79, No.1, 2000., *A Note on the Kangra Ms=7.8 Earthquake of 4 April 1905.*
6. Dimitrios Vamvatsikos, C.Allin Cornell., *Incremental Dynamic Analysis,* Earthquake Engineering & Structural Dynamics 2002
7. Tagel-Din Hatem, Kimiro Meguro., *Applied Element Method for simulation of Nonlinear materials: Theory and application for RC structures*, Structural Eng./Earthquake Eng., JSCE, Vol 17,No.2,2000

Using surface roughness as a performance parameter for RC wastewater pipes

Rahul YADAV [1], Himanshu SINGH [2], Sunil SINHA [3] and Sudhir MISRA [4]

[1] Former, Graduate Student, Dept of CE, IIT Kanpur, India

[2] Final Year Student, Dept of CE IIT Kanpur, India

[3] Professor, Dept of CE, Virginia Tech, Blacksburg VA, USA

[4] Professor, Dept of CE, IIT Kanpur, India

sud@iitk.ac.in

ABSTRACT

Wastewater concrete pipelines constitute an important part of the underground infrastructure assets, and there is an urgent need to develop reliable tools and parameters to quantitatively understand and predict the performance of these pipes, which deteriorate under the action of wastewater, groundwater, etc.

Effort in this work was directed to study changes in the surface characteristics of concrete specimens drawn from normal RC wastewater pipes subjected to accelerated deterioration under the action of artificial sewage (biogenic sulfide). The water-cement ratio of the concrete was kept at two levels and the exposure media was prepared from sulfate reducing (SR) media with cow dung as the source for SR bacteria. The samples kept at room temperature in sealed plastic boxes, were removed at designated times for investigation and were studied visually before a more detailed investigation was carried out at a few locations.

Results from the preliminary studies suggest a definite possibility of using changes in roughness of RC pipes as an indicative parameter for forecasting their performance in the field, and, that (a) both the water cement ratio and exposure duration affected the surface characteristics of the concrete, (b) more changes in the surface roughness were found in cases when the water-cement ratio was higher, and, (c) samples drawn from concrete having a higher water-cement ratio had higher instances of 'tuberculation' on the surface.

Keywords: *Reinforced concrete, sewage, deterioration, surface roughness, infrastructure monitoring*

1. INTRODUCTION

"The Energy and Resources Institute in New Delhi has estimated that by 2047, waste generation in India's cities will increase five-fold to touch 260 million tonnes per year" - Acharya, 2012

With this kind of demand, there is a huge pressure on existing wastewater pipelines in urban areas and the Municipal Corporations face an infrastructure crisis requiring renewal of pipelines, which in most of the cases is beyond their capacity. A schematic variation of the present worth of replacement, repair and total costs is shown in Figure 1. It is clear that '*waiting till failure*' approach is economically not viable, as the optimal time to replace the pipe is when the total life cycle cost reaches its minimum, besides the fact that that approach has several other implications as well.

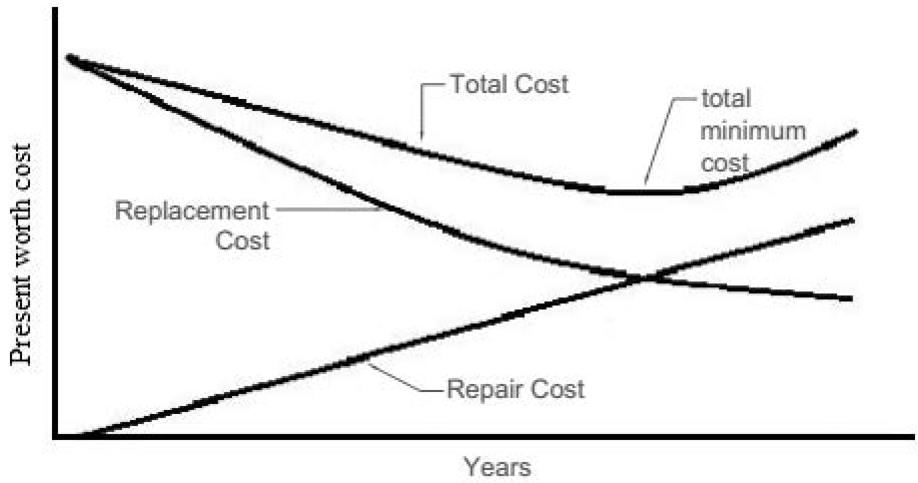

Figure 1: Economic Breakdown Even Analysis of a Pipeline

In order to tackle the demand for adequate maintenance of wastewater pipelines, a robust mechanism that assists in their condition evaluation and prediction, risk analysis, and renewal prioritization, is urgently needed. Monteny, et al., (2001) found that in many places in sewer pipes, sulfuric acid causes degradation of concrete. Hudon, et al. (2010) found that (a) bio-deterioration of concrete starts initially with pH decrease by carbon dioxide and hydrogen sulfide gases, which also react with cement paste, and, (b) microorganisms facilitate formation of sulfuric acid which attacks concrete. Ayoub, et al. (2004) conducted hydrogen sulfide assessment in cementitious sewer pipes and concrete culverts (more than 30 years old) in four major cities and found that only a negligible amount of sulfide was generated and also at a very slow rate.

2. BACKGROUND

In a wastewater RC pipe, a sulfur cycle is formed due to bacterial and chemical activity leading to the formation of sulfuric acid as can be seen in Figure 2, which is a schematic representation of the inside conditions. Sulfur is a substrate for many thiobacilli such as Thiobacillus thiooxidans, Thiobacillus neapolitanus, and Thiobacillus intermedius (Kelly, 1982; Hazeu, et al., 1988). In anaerobic conditions (due to long retention time or slow flow of the sewage), sulfate reducing bacteria, e.g., Desulfovibrio, reduce sulfur-compounds to H_2S, which may react with oxygen to precipitate elemental sulfur on the sewer wall (Vincke, 2009). The CO_3^{2-}, HCO^{3-} in the water or CO_2 in the air react with $Ca(OH)_2$ in the cement paste to generate calcite, a reaction that decreases the alkalinity of the cement paste and threatens decomposition of the calcium silicate hydrate (CSH) gel in the hydrated paste. The sulfate and carbonate erosion products react with the CSH gel in the presence of excess water to generate thaumasite $[Ca_3Si(OH)_6(CO_3)(SO_4).12H_2O]$ (Yang & Yang, 2012). Ultimately, the cement hydrates in the concrete structures are gradually broken down forming the erosion products of gypsum, ettringite, calcite and thaumasite.

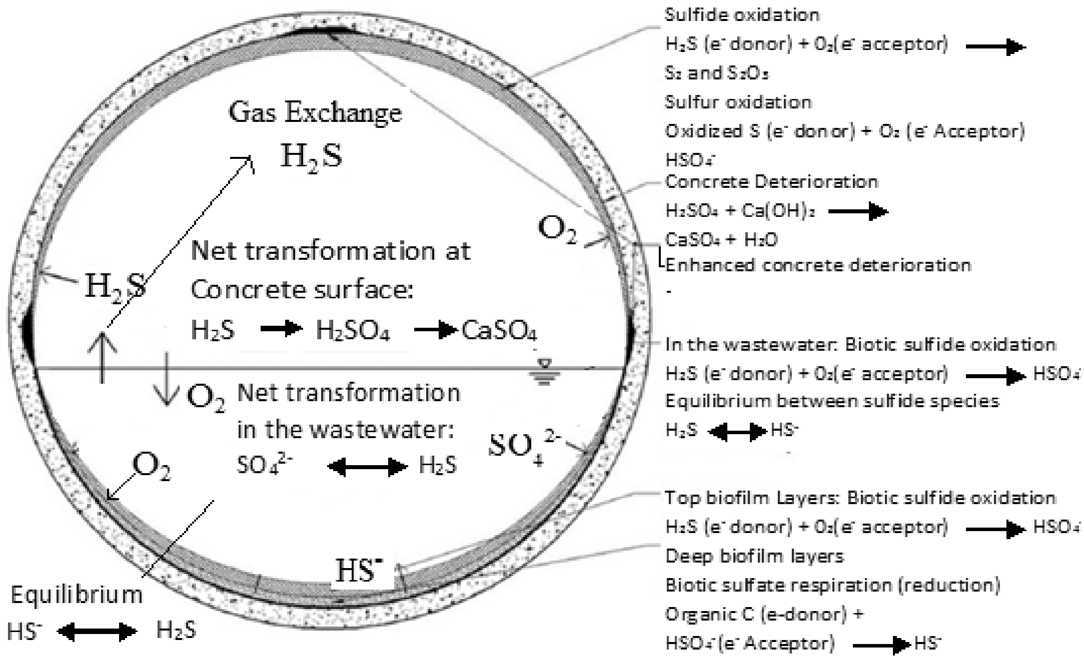

Figure 2: Schematic representation of processes in a sewer pipe
(Adapted from Hudon, et al., 2010)

3. EXPERIMENTAL DETAILS

3.1 Test programme

Experiments were carried out using concretes having two water-cement ratios (45% and 55%), with the changes in the specimens being recorded at 15, 30 and 90 days of exposure for 45% and 15, 30 and 45 days of exposure for 55%. The specimens were closely scrutinized visually and the roughness measured using surface profiling. Though chemical analysis using concrete powder drawn from the surface was also carried out, the results have not been reported here.

3.2 Preparation of concrete test specimens

Special effort was made to keep the effect of manufacturing method and workmanship to a minimum. The concrete specimens were drawn from pipes manufactured in a factory using the normally used material and methods, with only the proportions being decided according to the requirement of this research project and given in Table 1.

Table 1: Materials required to make the pipes

Materials	**Quantity (kg/per pipe)**	
	0.45 w/c ratio	**0.55 w/c ratio**
Cement Content	200	200
Coarse Aggregates (FM = 3.4)	546.12	546.12
Fine Aggregates (FM = 2.19)	303.60	303.60
Water Content	90 litres	110 litres
Chemical Admixture	1	1

The following steps were followed in obtaining the specimens used for testing:

a) *Casting and curing of pipes* – The concrete was mixed manually (as is the practice in the plant), and cast into 500mm long pipe segments conforming to Class NP3 (IS 458:2003) with internal diameter as 1000 mm having a wall thickness as 115 mm. The reinforcement in the pipes was kept in the middle of the wall. After feeding the concrete, the internal surface was finished with cement slurry, as per the usual practice. The pipes were cured in pond for 8 days before being transported to the laboratory, where they were left in air during which time the cores were drawn, etc.

b) *Drawing and slicing of cores:* Several cores (dia: 70 mm, length: 115 mm) were drawn from along the circumference of the pipes. These cores were then sliced using a diamond cutter into 20mm thick 'discs', to remove the cement finish layer and obtain specimens finally used for exposure. The process is schematically shown in Figure 3.

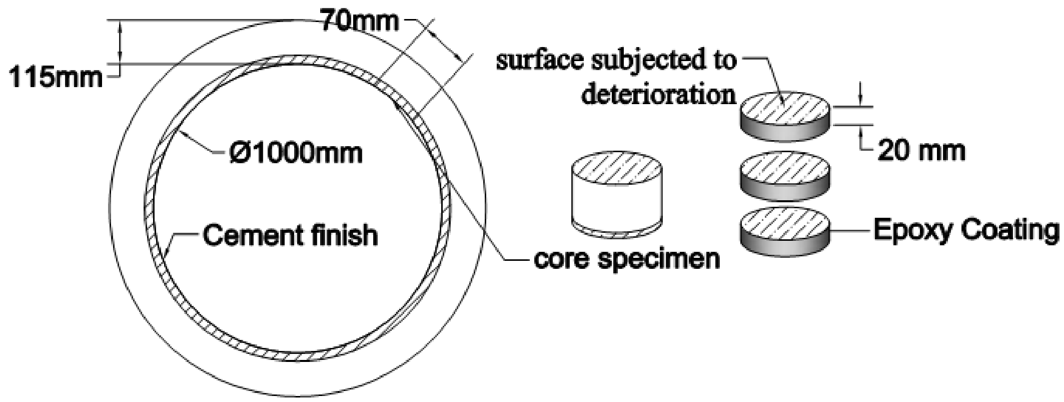

Figure 3: Schematic representation of process of obtaining samples

3.3 Exposure Media Used

Test samples were exposed to biogenic sulfide environment created using sulfate reducing media and sulfate reducing bacteria (SRB), sourced from cow dung, which was easily and freely available.

Table 2: Composition of sulfate reducing bacteria enrichment media

Ingredients	**gms/L**	**Ingredients**	**gms/L**
Part A		**Part B**	
Dipotassium phosphate	0.5	Ferric ammonium	0.392
Peptic digest of animal tissue	2	Sodium ascorbate	0.1
Beef extract	1	**Part C**	
Sodium sulfate	1.5	Sodium lactate	3.5
Magnesium sulfate heptahydrate	2	**Final pH (at 25°C) : 7.5±0.3**	
Calcium chloride	0.1		

a) *Details of SRB Media:* The sulfate reducing (SR) media used was from the manufacturer HiMedia Laboratories. The product code for media was M803, and it came in a triple pack with each designated as part A, B, and C. The composition of the media is shown Table 2.

b) *Preparation of the exposure media for the test specimens*: The procedure suggested by the SR media supplier was adopted in the study. For preparation of 1 litre of SR media, 7.1 grams of Part A was suspended in 900 ml distilled water, and then sterilized by autoclaving at 15 psi (121°C) for 15 minutes. Solution of Part B was prepared on the day of use by suspending 0.492 grams of Part B in 100 ml distilled water. It was then sterilized by filtration through a 0.45 µm membrane filter and this 100 ml solution was added aseptically to 900 ml Part A medium. Then 3.50g of Part C was separately sterilized by autoclaving at 15 psi (121°C) for 15 minutes and aseptically added to the mixture of Part A and B and thoroughly mixed. The complete medium was aseptically transferred to the sterile screw capped tubes. Finally it was purged with nitrogen gas for 20 minutes before pouring into the test boxes.

c) *Source of SR bacteria:* Fresh cow dung was used as the source of SRB (Shokes & Moller, 1999). Thus the media for exposure of the concrete specimens was prepared by mixing the SRB media with SR reducing bacteria.

3.4 Experimental Setup

The discs prepared from the concrete cores (See Figure 3) were immersed in the above exposure media to study the changes in the concrete undergoing accelerated deterioration under the action of (artificial) sewage – in the biogenic sulfide environment created using SR media and bacteria, as described above.
The setup was such that three discs could be placed in a test box, as shown in Figure 4. To prevent ingress of material from the lateral surface, it was effectively

sealed using an epoxy coating. Each box could hold three concrete discs in about 2 liters of SR media along with the SR bacteria, which was derived from about 100g of cow dung added to each box. The three concrete specimens in each box were tied to a glass fiber rod with the help of glass fiber cloth, which are chemically inert, and held in position during the whole exposure period. The boxes were sealed and maintained at ambient temperature (30°–35°C) under

Figure 4: Box used for tests showing concrete specimens held vertically and in position before addition of SR media and SR bacteria

anaerobic conditions. Five such boxes were used to house a total of 15 specimens for each of the water-cement ratios. Thus a total of ten test boxes were used.

3.5 Testing procedure

The boxes were opened only at the end of predetermined periods of exposure time when the concrete specimens were taken out for tests.

a) Numbering of specimens: Specimens made with water-cement ratios 45% and 55% were stored in separate boxes, and one box of each containing three 'discs' was opened at the end of each of the three exposure periods. Thus, boxes 45_1, 45_2 and 45_3, for specimens having a water-cement ratio of 45% were opened at the end of 15 days, 30 days and 90 days, respectively. Similarly boxes named 55_1, 55_2, and 55_3 were used to obtain specimens having a water-cement ratio of 55% at the end of 15 days, 30 days and 45 days, respectively. Suffices *a*, *b* and *c* have been added to the above to refer to the individual 'discs' drawn in each case.

b) Tests carried out: Specimens drawn at the end on an exposure period with lightly washed with tap water, before being carefully observed for changes. Finally spots were identified on the surface, where 'profiling' was carried out using a 3-D surface profiler (AEP Technology). The contact mode operation stylus tip diameter was 5 micron. The scanning frequency was selected to be 35 points per line with the scanning area of 1500*1500 microns as can be seen in Figure 5. Image obtained were processed using SPIP (Scanning Probe Image Processing)

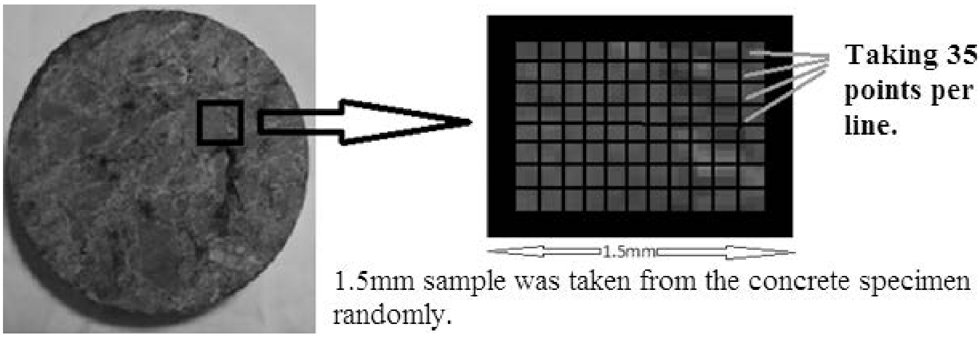

Figure 5: Selection of Scanning Area

<u>*c) Defining 'peak distance' and roughness numbers:*</u> Figure 6 shows a schematic representation of a roughened surface, with a certain profile. With the measurement of the 'depth' of the surface at different points, the *peak distance* is the maximum of such measurements and the *roughness number* is the average of the readings, as shown.

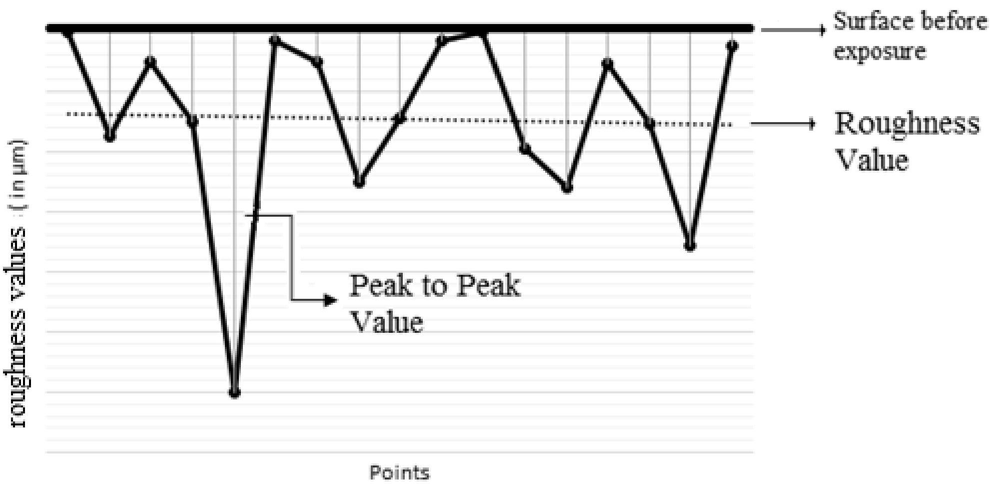

Figure 6: Calculating peak distance and roughness values

4. RESULTS AND DISCUSSION

4.1 Effect on pH of exposure media

The pH of the SR media was recorded initially and also at the time of opening of boxes at different times. The initial pH of all boxes was in the range of 7.26 to 7.34, which changed to slightly more acidic value depending on the duration of exposure and the water-cement ratio of the concrete specimens in the box (Yadav, 2013). This decrease can be attributed to the formation of acidic hydrogen sulfide, though only a marginal decrease in the pH is seen over the very brief period of exposure in this study and more data is required to be collected to substantiate the hypothesis.

4.2 Changes in roughness of concrete surface

Surface profiling at a few places on the mortar phase of the concrete was carried out in areas measuring 1.5 x 1.5 mm, and the results are discussed here in terms of the changes in the peak and average roughness values as defined above. The results are shown in Figures 6 and 7. The observations made from all the three discs which had been exposed for the same period are also shown in the figures. A photographic representation of the observations from the profilometer is given in Figure 8.

Though there is considerable variation in the observations, as can be seen in the Figures 6 and 7, which show the values obtained from chosen areas on all the three specimens (*a*, *b* and *c*, as explained in Section 3.5 above), it can still be stated that:

a) The parameters peak distance and the average roughness can be used as performance parameters to monitor the changes in the surface condition of a concrete pipe, as has been done here. They are capable of resolving a difference on account of parameters such as the water-cement ratio, and most importantly time. In other words, with sufficient data, a critical number can be defined for these parameters as a threshold before it may be advisable to actually change a pipe.

b) In the case of both parameters – peak distance and average roughness – there is an increasing trend with exposure period.

c) The increase in both parameters is greater in the case of concrete having a w/c = 55% compared to result in the case of concrete having a w/c =45%.

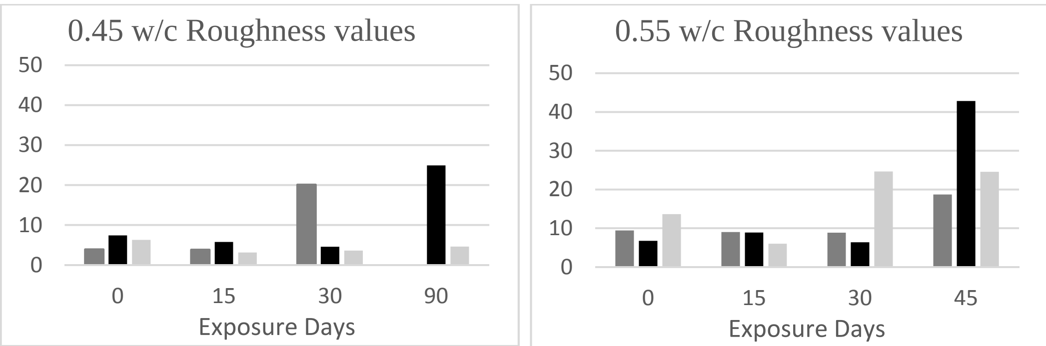

Figure 6: Variation of roughness values with exposure period

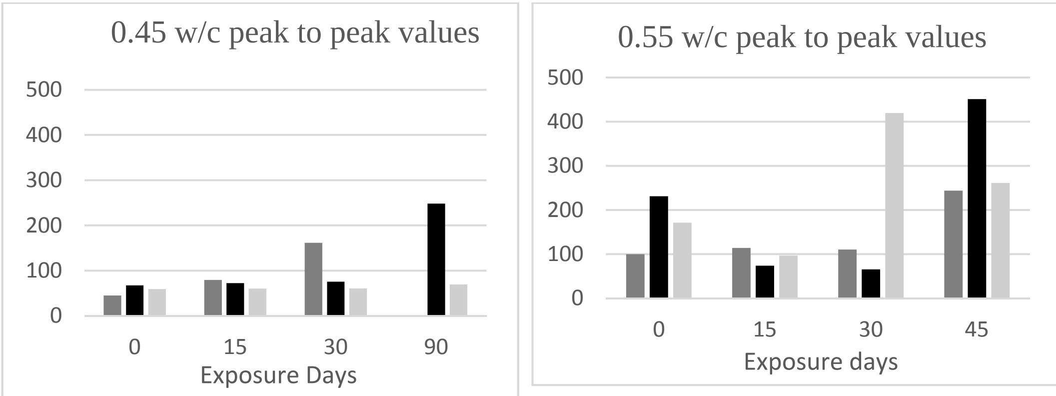

Figure 7: Variation of peak distance with exposure period

4.3 Visual observations of concrete samples

Visual observation of the concrete specimens in the course of the study showed that whereas there are no changes in the characteristics of the coarse aggregates, some sites in the mortar matrix could be identified, where 'nucleation' for further deterioration on account of attack by the sewage was taking place. Representative photographs of the concrete surfaces are given in Figure 8.

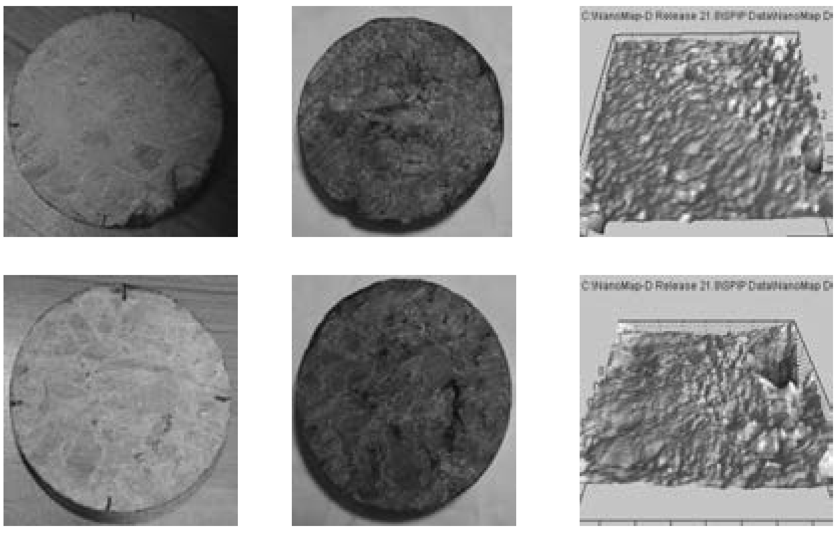

Figure 8: Changes in the roughness of the concrete surface of 45_2_c and 55_3_c; Surface Profile (as imaged from the surface profiling)

5. CONCLUDING REMARKS

Though only limited data has been obtained so far in the research directed at studying the possible use of changes in surface roughness as a parameter for deterioration of RC wastewater pipes, the following remarks can nonetheless be made:

a) The pH value of the SR media tends to decrease with increase in the exposure time.
b) Both, water-cement ratio and exposure duration, affect the surface characteristics of the concrete in the experiment.
c) The two parameter used in the study – peak to peak distance and roughness value can be used to characterize the change in roughness characteristics of the concrete. Both these parameters indicate an increase in the roughness values with (increase in) exposure time, with greater changes being identified in the case of concrete having a higher water-cement ratio

Further investigations however, need to be carried to relate remaining service life or the need to repair the deterioration of surface in term of roughness. In fact the problem can be effectively handled only when samples from the field are also tested for changes in these parameters over time. The present study also suffers from an important limitation in that there was no ‘flow’ of the media and therefore the erosion products could not be (continuously) removed from the system. This limitation is likely to significantly affect the changes in the pH (of the medium) and also formation of reaction products.

ACKNOWLEDGEMENT

The work reported in this paper was partly supported by the research grant under the Obama-Singh Knowledge Initiative administered by the Univeristy Grants Commission of India (Research Project No. UGC/CE/20120147 at IIT Kanpur). The support is gratefully acknowledged.

REFERENCES

Ayoub, G., Azar, N., Fadel, M. E. & Hamad, B., 2004. Assessment of hydrogen sulfide of cementitious sewer pipes: a case study. *Urban Water Journal,* 1(1), pp. 39-53.

Hazeu, W. et al., 1988. The production and utilization of intermediary elemental sulfur during the oxidation of reduced sulfur compounds by Thiobacillus ferrooxidans. *Archives of Microbiology,* 150(6), pp. 574-57

Hudon, E., Mirza, S. & Frigon, D., 2010. Biodeterioration of Concrete Sewer Pipes: State of the Art and Research Needs. *Journal of Pipeline Systems Engineering and Practice,* 2(2), pp. 42-52.

Acharya, K., August 1, 2012. “India Drowning in Waste, Experts Warn”, Inter Press Service news agency

Kelly, D., 1982. Biochemistry of the chemolithotrophic oxidation of inorganic sulfur. *Philosophical Transactions of the Royal Society of London. B, Biological Sciences,* 298(1093), pp. 499-528.

Monteny, J. et al., 2001. Chemical and microbiological tests to simulate sulfuric acid corrosion of polymer-modified concrete. *Cement and Concrete Research,* 31(9), pp. 1359-1365.

Shokes, T. E. & Moller, G., 1999. Removal of dissolved heavy metals from acid rock drainage using iron metal. *Environmental science \& technology*, 33(2), pp. 282-287.

Vincke, E., 2009. Biogenic sulfuric acid corrosion of concrete: microbial interaction, simulation and prevention.

Yadav, R., 2013, “Condition and Performance Assessment of urban drinking water and wastewater pipelines”, Thesis submitted to IIT Kanpur in partial fulfillment of requirements of M Tech degree

Yang, L. & Yang, L.,2012, “Erosion in Weak Sulfate Environment”, Journal of Civil Engineering and Architecture Concrete.

Capacity factors for implementing urban infrastructure projects in India

Yehyun AN[1] and Ralph HALL[2]
[1] Doctoral Candidate, School of Public and Intl. Affairs, Virginia Tech, USA
yehyun@vt.edu
[2] Assistant Professor, School of Public and Intl. Affairs, Virginia Tech, USA

ABSTRACT

Since the 1950s, Capacity Development (CD) has been one of the most important items on development agendas. The problem is that the concept has been included in development projects without due consideration to how it should be applied. The circumstance of CD for urban infrastructure projects in India is an example of an application of CD without sufficient review. Recognizing the shortage of urban infrastructure, the Government of India (GOI) launched Jawaharlal Nehru National Urban Renewal Mission (JNNURM) in 2005 to provide substantial central financial assistance to cities over a period of seven years. The GOI expected the JNNURM to reform institutions and strengthen human resource capability related to many areas of project delivery. During its implementation, however, the JNNURM has been confronted by problems relating to a lack of capacity. This paper reviews the capacity challenges related to the JNNURM program and considers the broader implications for urban infrastructure development in India. The paper 1) explores conceptual frameworks of CD by reviewing the existing literature, 2) finds operational elements of the concept applicable to empirical studies, and 3) determines capacity factors in accordance with the context of urban infrastructure in India.

Keywords: *capacity development, urban infrastructure, project implementation, JNNURM, India*

1. INTRODUCTION

It is estimated that the urban population in India will reach 600 million by 2030, which is nearly double the urban population of 377 million in 2011 (Planning Commission 2012). Along with rapid urban growth, socio-economic conditions in urban areas have changed significantly (MOUEPA and MOUD 2005). One approach adopted by the Government of India (GOI) to manage this rapid urbanization is the development of urban areas as an accelerator for inclusive economic development. The Jawaharlal Nehru National Urban Renewal Mission (JNNURM), established in December, 2005, was a first step in realizing this objective. This paper covers capacity development challenges related to the program with broader implications for urban infrastructure development in general. In the following section, this paper investigates Capacity Development (CD) frameworks provided by international organizations, and reviews the

JNNURM in terms of its stated objectives, evaluations, and CD interventions. Providing an overview of the JNNURM, this paper attempts to articulate the capacity issues related to urban infrastructure development in India. Considering the various features of CD, the identified capacity issues are classified into three capacity levels: enabling environment, organization/network, and individual/project. Lastly, this paper modifies the CD framework in accordance with the context of urban infrastructure development in India.

2. CAPACITY DEVELOPMENT

Capacity Development (CD) has its roots in Institution-Building, Institution-Strengthening, Human Resource Development, and New Institutionalism from the 1950s to 1990s. Each concept has its own objectives and emphasis. Human Resource Development focuses on the individual, Institution-Building and Institution-Strengthening approach capacity issues from the perspective of organizational learning and development, and New Institutionalism highlights the system in which organizations operate. CD considers the interdependencies between each of these levels and utilizes a multiple-level approach, which deals with specific interventions targeted at a given context. Thus, CD is an umbrella concept under which various approaches to development are subsumed (Kühl 2009).

The transition through these concepts has been accompanied by an evolution in the approach to development. Capital-focused development aid needed institutions to manage funds, which led to Institution-Building and Institution-Strengthening. Technical assistance and cooperation, which relied on knowledge transfer, required Human Resource Development in the recipient nations. In the 1980s, New Institutionalism emerged and emphasized a system approach, such as macro-economic policy and administration improvement.

The classification of capacity reflects its origin, which is derived by combining various concepts focusing on endogenous forces at different levels. Most literature uses hierarchical levels of capacity to specify capacity. In spite of minor differences in the naming of the levels, the levels can be divided into individual, organizational, and environmental levels. It is not possible to offer clear cut definitions for each of these levels (Pearson 2011). However, there are common components for each level.

The individual level usually refers to a person’s competencies, including skills and knowledge. It may also include motivations, attitudes, and personalities that can be affected by other higher levels. Second, components shared in an agency or broad networks of agencies—such as goals, structure, policies, behavioral norms, partnership, communications, incentive systems, etc.— belong to the organizational level. At this level, the benefits of the enabling environment are put into action when a collection of individuals come together (UNDP 2009). Lastly, the enabling environment contains elements at sub-national, national, regional, and global levels that are related to broad social systems. This level includes policies, laws, politics, social norms, cultures, and other important institutional/environmental factors that form settings where people and organizations function.

Capacity interventions should be designed to work within the context in which they will be deployed. Further, if capacity development initiatives are to achieve sustainable results, capacity needs to be considered not just at one level, but in terms of the linkages between levels and the complexity of the whole system (Pearson 2011). In other words, the levels are interrelated, and an intervention in one level may not bring the intended CD results.
Recognizing the lack of a common approach to CD, many development agencies have developed their own CD framework in order to facilitate a more systemic process of CD. Even though many differences exist between the frameworks of the development agencies, a common feature is that they follow an 'inputs–outputs–outcomes–impacts' model. The frameworks encourage the connection of changes in capacity and changes in development results by allowing capacity to be measured as both a means and as an end. Figure 1 presents the outputs-outcomes-impacts identified by WBI (World Bank Institute) and UNDP (United National Development Programme). Both agencies imply that changes in outputs and outcomes can be linked and promoted by specific CD activities. As the two frameworks show different components in each step, many agencies use analogous terms for different purposes or in different stages of CD. In other words, the applications of CD vary widely by different agencies. Consequently, the agencies have flexibility to apply the concept of CD depending on their focus.

	WBI	**UNDP**
Inputs ↓	Capacity Interventions ↓	Capacity Interventions ↓
Outputs ↓	**Leaning outcomes**: Raised awareness Enhanced skill Improved consensus & teamwork Fostered coalitions & networks Formulated policy & strategy Implemented strategy & plan ↓	**Change in Capacity Level across Core Issues**: Institutional arrangement Leadership Knowledge Accountability ↓
Outcomes ↓	**Capacity factors**: Conduciveness of sociopolitical environment Efficiency of policy instruments Effectiveness of organizational arrangements ↓	**Change in** Institutional performance Institutional stability Institutional adaptability ↓
Impacts	Local ownership, effectiveness, efficiency of resource use ↓ **Development Goals**	**Change in** people's well-being

Figure 1: Diagrams of Capacity Development Frameworks by WBI and UNDP

3. JAWAHARLAL NEHRU NATIONAL URBAN RENEWAL MISSION

In 2005, the Government of India (GOI) launched the Jawaharlal Nehru National Urban Renewal Mission (JNNURM) as a comprehensive package covering projects, reforms, and CD. In addition to construction projects, state governments and municipalities were required to implement reforms as a pre-requisite for assistance from central government. The JNNURM has seven mandatory state reform agendas, six municipal mandatory reform agendas, and ten optional reform agendas. These reforms are one of the key components emphasized by the GOI, and are closely related to the empowerment of local government for decentralization. As a comprehensive package, the JNNURM aimed to implement programs more efficiently through projects and maintain outcomes for long-run sustainability through reform(MOUEPA and MOUD 2005).

It is generally believed that the JNNURM has contributed to significant investments and improvements to the physical infrastructure of cities (Sivaramakrishnan 2011, p.xxv). According to the mid-term appraisal of the GOI, the program has been achieving its goals effectively. The Planning Commission (2011a) notes that, “the JNNURM has been effective in renewing focus on the urban sector across the country, and has helped initiate a comprehensive process of urban reforms within states and Urban Local Bodies (ULBs)”. Even though the JNNURM has been somewhat successful in terms of total number of sanctioned projects and size of allocated funds, many projects and reforms have remained incomplete. By 2012, only 172 (31 percent) of 551 sanctioned projects were completed. 65 percent of the reform agendas were realized, but depending on the state, the achievement rates vary from 33 percent to 90 percent.

In spite of the positive evaluation, during its implementation, the JNNURM has been challenged by issues related to a lack of capacity. For example, the mid-term appraisal notes that “many states and ULBs are facing significant shortages in financial, social, and governance capacity that limit their ability to steer urban development and create self-sustaining administrative units at the local level” (Planning Commission 2011a, p.390). The large gap of capacity has been recognized as an impediment of the program from the beginning, so the GOI earmarked 5 percent of the program budget to solve the problem when the program was designed. However, while the lack of capacity has received sufficient attention at the central government level, a large portion of the budget for CD at the local government level remains unspent.

In this regard, many initiatives for CD have been implemented under the JNNURM to fill the capacity gap by the GOI. The Indian Planning Commission (2011b) reviewed the capacity interventions undertaken by the GOI while creating the Twelfth Five Year Plan. They found the GOI’s interventions for CD through the program to be ad hoc. The commission found that insufficient attention was given to identifying ULBs’ demand for capacity interventions, resulting in a large gap between demand and supply of the capacity interventions. Further, the commission found that the capacity interventions were biased towards hard capacities such as technical skills and knowledge for development results.

4. IDENTIFYING CAPACITY FACTORS

As explained above, CD is a multi-dimensional concept, and requires a holistic approach at multiple levels of intervention. In order to investigate capacity in the urban infrastructure sector in India, the capacity gaps at each level need to be identified. In this section, the capacity factors in the context of the urban infrastructure sector in India are examined based on the literature of the JNNURM and expert interviews undertaken by the lead author in October, 2012, in India.

Twenty interviewees from different agencies including major international organizations and local governments participated in an individual interview, and discussed issues relating to infrastructure development in India. The interviews were a semi-structured, open-ended, and face-to-face, and the questions focused on the participant's experience, opinion, and knowledge on the following subjects: 1) Identification of capacity gaps for infrastructure development in India; 2) Status quo of current infrastructure development program; 3) Perspectives on sustainable infrastructure development in India; 4) Evaluation of capacity of the GOI including local governments for sustainable infrastructure development; and 5) Needs for an alternative capacity development program. The identified factors from these interviews are described at environment, organization, and individual levels.

4.1 Enabling Environment Level

This level includes factors related to sub-national and national systems which can encourage or discourage individuals and organizations to demonstrate their capacity.

Devolution of power to cities

Urban governance in India is described as muddled, ineffective, and nowhere near ready to face rapid urbanization (MGI 2010). Ineffective governance is closely related to the lack of capacity of local governments. CEPT University (2012) states that, "the challenge of urban capacity building is high, not only due to the number of staff needs to be trained, but also due to the complexity of institutional mechanism in city governance". Concerning the complexity of urban governance, many studies have referred to nonfulfillment of the 74th Constitutional Amendment Act (CAA). Municipal institutions in India, so-called ULBs, have a 300-year history (Vaidya 2009). Despite this history, the lack of legal frameworks for Local Self Government has created a weak structure for decentralization. In June 1993, the 74th CAA came into force to facilitate decentralization in India. The 74th CAA has accorded constitutional status to the ULBs to manage urban governance effectively. However, because devolution is a voluntary-based option, no state has fully devolved the functions to cities, and although the transfer has happened on paper, most decision-making power remains with the states (MGI 2010). Recognizing the need to facilitate the implementation of the 74th CAA, the central government included the fulfillment of the 74th CAA as a mandatory state reform agenda, and has provided incentives to those states achieving the reforms.

Most literature on the JNNURM (Sivaramakrishnan 2011, Planning Commission 2011b, Vaidya 2009, MGI 2010, Planning Commission 2012) argues that empowering ULBs through the devolution of functions, functionaries, and funds is critical to developing their capacity. In the mandatory state level reforms under the JNNRUM, there are five agendas related to empowering ULBs—the transfer of 12 scheduled functions, the constitution of District Planning Committee (DPC) and Metropolitan Planning Committee (MPC), the transfer of city planning, and management of water supply and sanitation. The achievement rates of the reforms related to the functions transferred vary depending on the state, and they can be considered as one of the enabling environment capacity factors.

Access to human resources

Lack of supply of qualified human resources can be a hindrance for CD. As the pool of human resources increases, local governments have more opportunities to employ qualified persons. However, in general, the urban sector in India is struggling with shortage of skilled manpower. For example, MGI (2010) notes that, "The Ministry of Urban Development (MOUD) estimated that India needs around 40,000 planners across its cities, while the number of registered planners is closer to 3,000". According to Gupta, Gupta, and Netzer (2009), in the construction industry, "70-80 percent of the existing workforce is untrained, which impacts the pace and quality of project implementation, and the situation is expected to worsen with infrastructure investments driving high growth in demand for skilled manpower". Hence, the human development level, that includes literacy and the presence of relevant educational institutions, can have an indirect influence on availability of qualified persons for implementation of the program.

Other environmental factors

The Enabling Environment level includes policies, laws, politics, social norms, cultures, etc. Since the JNNURM is a national program, its policies and laws are fixed. However, some environmental factors are different among states, and many experts insist that economic (e.g., Gross State Domestic Product), socio-cultural (corruption), and political factors (e.g., political alignment with the central government) can have influences on the enabling environment indirectly.

4.2 Organization/Network Level

In addition to the typical elements at the organizational level, the complexity of urban governance can be considered as one of the issues related to the expanded organizational network.

Institutional structure and involving agencies

In the current institutional structure under the JNNURM, there is considerable overlap in responsibility for the functions of policy making, regulation, and service provision (WB 2011), and there may exist fragmentation of responsibilities without any platform for coordination (MOUEPA and MOUD 2006). The situation relates to the project implementation and service delivery, and has a strong influence on the capacity of local governments. Sivaramakrishnan (2011) argues that project implementation was entrusted to parastatal agencies thereby "marginalizing the municipalities further".

In other words, due to the lack of capacity, the ULBs are not fully engaged in implementation of projects, but the service delivery should be provided by the

ULBs, "which often are not financially independent, client-oriented or professionally specialized" (WB 2011). This ineffective institutional structure often creates a vicious cycle, and weakens the capacity of the ULBs.

Organizational development strategy
There is a lack of organizational development strategies at the local government level in India. The lack of organizational development strategies leads to an absence of formal structures, comprehensive rules, staffing norms, procedures, job descriptions, pay scales, and the introduction of new technologies (Planning Commission 2011b). In addition, the absence of organizational systems results in deficiency in shared values amongst staff, commitment to vision, etc. Moreover, the lack of an organizational system can have a negative influence on capacities at other levels.

Financial viability
One of the main objectives of the JNNURM is to attract investment in urban infrastructure services. Hence, the JNNURM emphasizes local government's financing capabilities. As of September 2010, 36 ULBs were awarded an investment grade credit rating, but none of the 36 credit-rate-awarded cities have borrowed from the market (Sivaramakrishnan 2011). As a result, state governments and ULBs fell short of their required shares for projects. Thus, financial viability is closely related to the local governments' creditworthiness.

Partnership
In the JNNURM, communication channels with the private sector and civil society are not very effective (Planning Commission 2011b). The success of cities like Ahmedabad, Rajkot, and Surat, which have clearly reaped the benefits of partnerships at the city level for closing the critical information or knowledge gap, highlighted the greater needs for "Urban Partnerships" between the city administration and various other stakeholders including civil society, academia, research institutions, media, and private sector (CEPT University 2012).

Accountability
Accountability is one of the critical capacity factors identified by many studies, and most literature on the JNNURM puts emphasis on accountability for better project implementation and service delivery. From a CD perspective, the focus is on the interface between public service providers and its clients (UNDP 2009). In the case of the JNNURM, accountability between state governments as oversight bodies and ULBs as responsible bodies and between the ULBs as service providers and the public as a client can be critical to improving project delivery.

Other organizational factors
The organizational level includes internal structure, internal policies, procedures, behavioral norms, partnership, etc. One of the key capacity factors identified by the existing studies is leadership. In India, the recruitment, deployment, and retention system of government officials is not flexible, and is centralized. Thus, India's cities at the metropolitan and municipal levels do not have a single-point empowered leader with tenure to deliver against explicit mandates (MGI 2010). Hence, the organizations without leadership have less autonomy to pursue

customized policies. For this reason, whether a local government has empowered its mayor or not needs to be considered as a capacity factor at the organizational level.

4.3 Project/ Individual Level

An urban knowledge needs assessment study by CEPT University (2012) identified the knowledge gaps and barriers—such as a lack of good engineering skills and technical know-how, limited awareness, language barriers, poor computer literacy, over dependence on consultants, etc.—that can be connected with capacity at the individual level.

Skill and knowledge gaps
In the current context of rapid urbanization in India, there are many challenges in the urban sector, and the ULBs will require specialized knowledge and experiential learning to confront these challenges (Planning Commission 2011). "Unless the ULBs have skilled manpower to undertake the various additional tasks entrusted to them" (Vaidya 2009), the actual empowerment and reforms will not be achieved, and the projects under the JNNURM will face long-term sustainability challenges. Therefore, the skill and knowledge level of the officials in charge is considered a main capacity factor at the individual level.

Dependence on consultants / Outsourcing
The lack of capacity of local governments in some states causes over-dependency on consultants. When the JNNURM was launched, the ULBs were expected to lead the preparation of City Development Plans (CDPs) and Detailed Project Reports (DPRs). However, there were few states in which the ULBs could play a major role as a planning authority. Regarding this, Sivaramakrishnan (2011) notes that "in most cases, the municipalities did not understand or discuss the CDPs in the municipal councils but they were prevailed upon to adopt resolutions endorsing the CDP prepared so that projects could be submitted to the Centre and funds obtained" and "consultants were used in preparing or updating or even polishing up previously prepared project reports". The consultants from mega cities were more equipped with the methodology and techniques of CDP than ULBs, and there have been sufficient funds to hire the outside consultants. The availability of funds might have led to an over-dependence on outside consultants, which meant that ULBs were excluded from the planning process. Through the case of Patna Municipal Corporation, CEPT University (2012) notes that "over-dependence on consultant is blocking the city officials from engaging in information and knowledge hunting mode".

Other project factors
Some of the individual factors, such as soft skills, are difficult to measure and set up criteria to evaluate. However, characteristics of a project may have an influence on how individuals handle the project. For example, when projects are comparatively large, use new technology, and involve many stakeholders, the soft skills that manage the process and engage stakeholders are more critical than for small projects. The features of a project can be considered as an indirect capacity factor at the individual level.

4.4 Conceptual Framework

Integrating the identified capacity factors, this paper revises the existing CD frameworks (Figure 2). The modification is based on the following elements to reflect the Indian context:

1) General dimensions of capacity;
2) Identified capacity gaps by the GOI's documents and expert interviews;
3) Formulated CD strategy for JNNURM-II; and
4) Hidden factors which can have influences on CD interventions.

Similar to the existing WBI/UNDP frameworks, this conceptual framework follows the "input-output-outcomes-goal" model. The input is the CD interventions by the GOI, and the output is the changes caused by the CD interventions. The changes will have impacts on the outcomes such as the project's implementation, service delivery, and reform achievement. These outcomes are targeted at meeting the main objectives of the JNNURM.

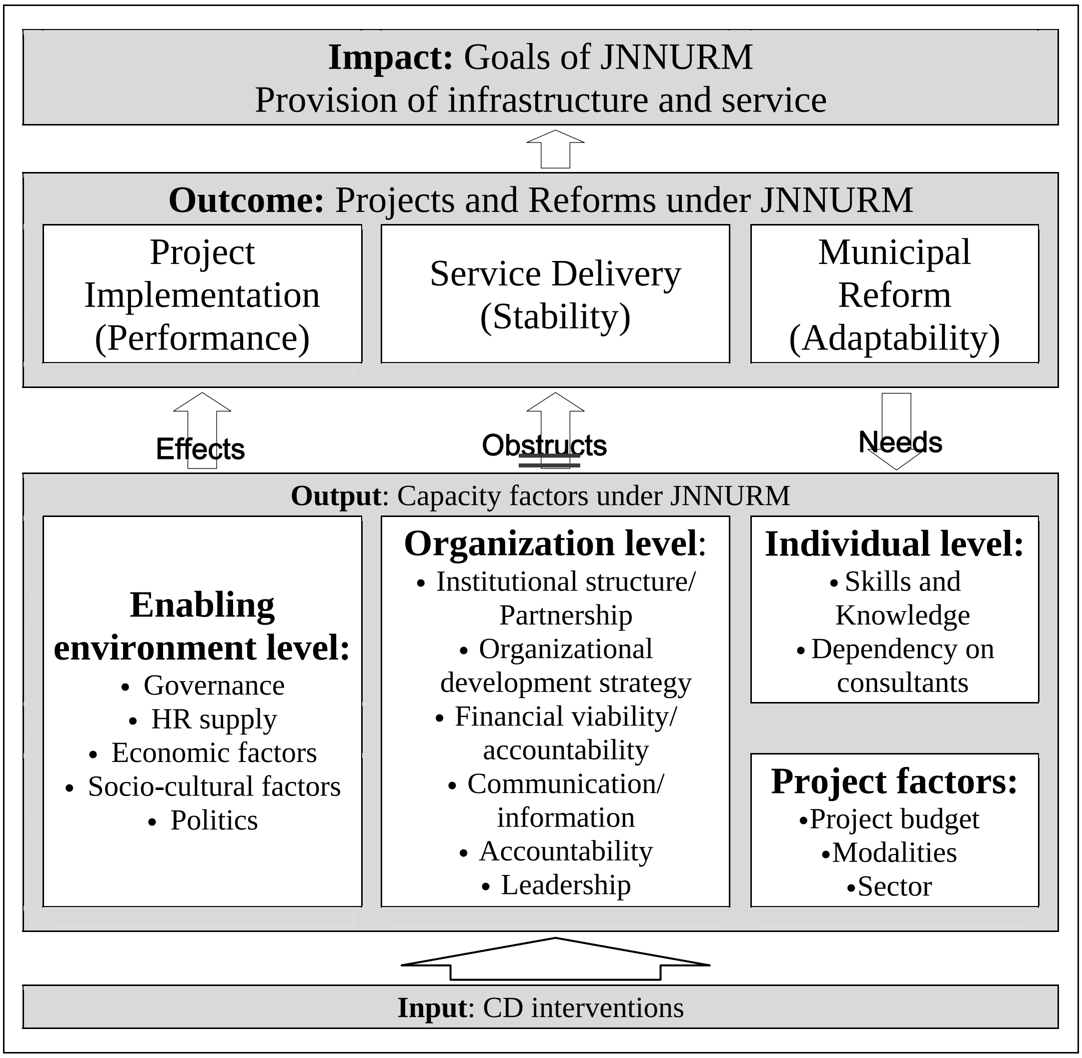

Figure 2: Capacity Development in the Context of Indian Urban Infrastructure

5. Conclusion

Many studies have identified the dimensions of capacity to clarify its operational meaning. As an umbrella concept, CD emerged from a multi-dimensional approach covering various levels of agency. By reviewing the existing literature and conducting expert interviews on the JNNURM, this paper presents a conceptual framework that considers CD at each of the three levels – i.e., enabling environment, organization, and individual. Operational factors for CD targeted at urban infrastructure development in India are presented.

The identified factors can individually and collectively have influences on project delivery and development goals. There have been many studies contributing theoretical discussions to CD, but few studies apply the theoretical discussions in empirical ways. In this regard, capacity factors should be examined empirically to confirm a positive impact on development goals. In addition, there are limited studies that attempt to evaluate a comprehensive CD approach based on multiple levels. Since the interaction between different levels is regarded as one of the key factors for CD, research studying how capacity factors at different levels affect development goals is needed. By empirically investigating the impact of capacity factors on project outcomes, better approaches to operationalizing CD can be developed.

REFERENCES

CEPT University. 2012. Urban Knowledge Needs Assessment. Ahmedabad, India: Centre for Environmental Planning and Technology University.

Gupta, Prashant, Rajat Gupta, and Thomas Netzer. 2009. Building India - Accelerating Infrastructure Projects. Mumbai, India: McKinsey and Company.

MGI. 2010. India's Urban Awakening: Building Inclusive Cities, Sustainaing Economic Growth. McKinsey Global Institute.

MOUEPA, and MOUD. 2005. Jawaharlal Nehru National Urban Renewal Mission: Brochure. Delhi, India: Ministry of Urban Employment and Poverty Alleviation/ Ministry of Urban Development.

MOUEPA, and MOUD. 2006. Jawaharlal Nehru National Urban Renewal Mission Toolkit. New Delhi, India: Ministry of Urban Employment and Poverty Alleviation/Ministry of Urban Development.

Planning Commission. 2011a. Mid-Term Appraisal of the Eleventh Five Year Plan 2007-2012. New Delhi, India: Planning Commission, Government of India.

Planning Commission. 2011b. Report of the working groups for the Twelfth Five Year Plan (2012-2017). In *Housing & Urban Development*: Planning Commission, Governmnet of India.

Planning Commission. 2012. Report of the Committee on JnNURM II: Clean bastis, safe communities and people's cities. Planning Commission, Government of India.

Sivaramakrishnan, K. C. 2011. *Re-visioning Indian cities : the urban renewal mission*. New Delhi, India; Thousand Oaks, Calif.: SAGE Publications.

UNDP. 2009. Capacity Development : A UNDP Primer. New York: United Nations Development Programme.

Vaidya, Chetan. 2009. Urban Issues, Reforms and Way forward in India. In *Working Paper*. New Delhi, India: Ministry of Finance, Government of India.
WB. 2011. INDIA: Capacity Building for Urban Development Project. In *PROJECT APPRAISAL DOCUMENT*. New Delhi, India: The World Bank.

Using GFRP for repair and rehabilitation of RC frames

AMARENDRA [1], Kunwar K BAJPAI [2], Sudhir MISRA [3] and Durgesh C RAI [4]
[1] Formerly Student, Dept of CE, MNIT, Allahabad, India
[2] Senior Scientific Officer, Dept of CE, IIT Kanpur, India
[3] Professor, Dept of CE, IIT Kanpur, India
[4] Professor, Dept of CE, IIT Kanpur, India
Email for correspondence: kunwar@iitk.ac.in

ABSTRACT

RC buildings are perhaps the most common type of building in urban areas across the world. In cases of being subjected to earthquake loads, these buildings are often damaged near the end of columns due to formation of plastic hinges, attributed to high bending moments at these regions. Hence, there is a need to develop a simple and efficient retrofitting technique to restore and possibly enhance the structural capacity of a damaged building.

Fiber reinforced polymers (FRPs) are emerging as very effective retrofitting materials due to their superior properties such as low weight and high strength and easy applicability. In the present experimental study, a damaged RC frame which was tested under cyclic loading (up to 4.5% drift level) in an earlier study was used and then retrofitted using glass fibre reinforced polymer (GFRP) fabrics repaired damaged portions using epoxy mortar. This 'repaired' frame was then again tested and its stiffness compared by forced vibration and load controlled slow cyclic tests (Stiffness of damaged RC frame: 1.0 kN/mm; Stiffness of FRP strengthened RC fame: 3.43 kN/mm). Further the displacement controlled reverse cyclic tests were repeated up to 4.5% drift level (as per ACI recommendations) on the FRP strengthened specimen. The test results indicates a marked increase in the performance levels compared to the original specimen tested up to same drift level.

Keywords: *Reinforced concrete frame, earthquake, damage, rehabilitation, GFRP, stiffness, lateral loading, hysteresis loops*

1. INTRODUCTION

Reinforced concrete buildings are most commonly used form of construction in recent times. RC buildings are generally analyzed such that moment resisting frames actions are developed in each member. Masonry infill walls are used in RC frame buildings partition walls and thus are considered as non structural elements and ignored in analysis and design of RC buildings. However, strength and stiffness of these members play a major role in determining the overall response of the building during an earthquake.

Now-a-days almost all the new construction is in the form of RC buildings, of which a large number have open ground story, making them vulnerable to earthquakes. So strengthening of buildings is needed to avoid damage and loss of life and property. Incidentally, there are few strengthening techniques available to improve seismic performance of buildings. Many of the existing strengthening techniques are costly and labor intensive, and often cause reduction in floor area capacity of the building. Moreover, most of them are not supported by analytical and experimental investigations.

2. OVERVIEW

Most of the existing structures are not designed as per seismic design provisions and have abundant deficiencies in their overall configuration. As a result, most of the RC frames are observed to have inherent deficiencies such as insufficient longitudinal reinforcement, transverse reinforcement, with wide spacing, open stirrups and hoops with 90-degree bend, inadequate lap splicing of longitudinal of longitudinal reinforcement etc (Bai and Hueste 2003). Such buildings are more prone to severe damages during an earthquake. Generally columns of a non ductile RC frame suffer more damage under earthquake shaking as compared to beams due to inadequate lateral load resistance capacities. Most common observed modes of column failure are in the form of premature shear failure, brittle crushing of unconfined concrete, reinforcement splice failure near potential plastic hinge region, shear cracking and column shortening.

Strengthening techniques used can be broadly classified into two groups. First aims at increasing strength and ductility of concrete section by enlarging their cross-section or by attaching the longitudinal steel plates. Second method aims at passive confinement to the concrete section due to additional elements to enhance strength and ductility. Presently the most common retrofitting techniques are concrete jacketing, steel jacketing and steel caging.

2.1 Concrete Jacketing

Concrete jacketing involves the encasement of RC columns with an additional layer of concrete and reinforcement cage. Concrete is poured in the formwork containing newly placed additional reinforcement around the column after the surface of the column has been roughened by trimming and chipping. In addition to strengthening columns, this technique is also used to upgrade the beams and beam-column joints of RC buildings. The construction procedure involves a) welding of the ends of the jacket stirrups and poured concrete jacket b) welding, ends of Jacket stirrups, dowel placement at the interface and a poured concrete jacket, and c) bent down bars connecting the jacket bars to the longitudinal bars of original column and a shortcrete jacket. Lateral strength of the columns was enhanced by jacketing even if there was no treatment at the interface of jacket and old concrete columns.

Concrete jacketing improves seismic resistance of the structural element (CEN, 2005). However, increase in the lateral stiffness of the strengthened structural system can attract more seismic forces (Wu et al., 2006). The main disadvantage of concrete jacketing is that it is labour intensive and causes reduction in usable floor area due to significant increase in size and self weight of jacketed column system. Ferro-cement jacket has been considered as an alternative to strengthen the RC columns of inadequate shear strength and ductility. Ductility of RC columns is increased by providing external confinement over the entire height. Ferro-cement jacketing with expanded meshes produce distributed fine shear cracking at large displacement ductility level.

2.2 Steel Jacketing

To improve the lateral strength, stiffness and ductility of deficient columns, steel-jacketing is the most common technique. In this method wrapping of steel plates, strips or bars in the transverse directions of column sections is done after removal of damaged concrete cover. The main advantage of steel jacketing over concrete jacketing are relatively less increase in the column section, speed of fabrication, lower cost and interruption of use of structure, and also relatively less increase in the stiffness.

Steel jackets can also be pre-stressed in the hoop direction to improve the concrete confinement in the columns. The pre-heated jackets are used prior to welding and left to shrink while cooling after welding. This technique provides the active and passive lateral pressure to overcome the lateral expansion of the concrete under compression. The uses of this technique are reported extensively for retrofitting of damaged columns in the past earthquakes (Wu et. al. 2006, Murty et. al. 2005).

The main disadvantage of steel jacketing are a) it is labour intensive b) very time consuming c) involves lot of investment and skill and, d) it cannot be used in those places which are prone to electric and magnetic radiations.

2.3 FRP Jacketing

Recently advanced composite materials made up of fiber-reinforced jackets formed by bonding the continuous carbon, glass, or other synthetic fibers, fiber sheets to wrap the concrete surface along with matrix materials such as epoxy, vinyl ester resins etc. The primary function of transversely continuous jackets is to provide passive confinement to concrete similar to steel. Based on comprehensive experimental studies, advanced composite material jackets have proven to be effective measure to repair and retrofit squat circular and rectangular columns with insufficient shear reinforcement (Haroun et al, 2003). Fiber reinforced composite jackets have shown superiority over steel jackets since they do not alter weight of the columns significantly.

3. EXPERIMENTAL DETAILS

3.1 Description of test RC Frame

The RC frame used in current study is a partially damaged 1:2.5 scale model of a prototype RC building (figure 1) which was tested for seismic performance using various strengthening schemes such as use of steel braces, strengthening of columns by means of external steel cage and energy dissipation device (aluminum shear yielding device) in an earlier study (Sahoo and Rai, 2008).

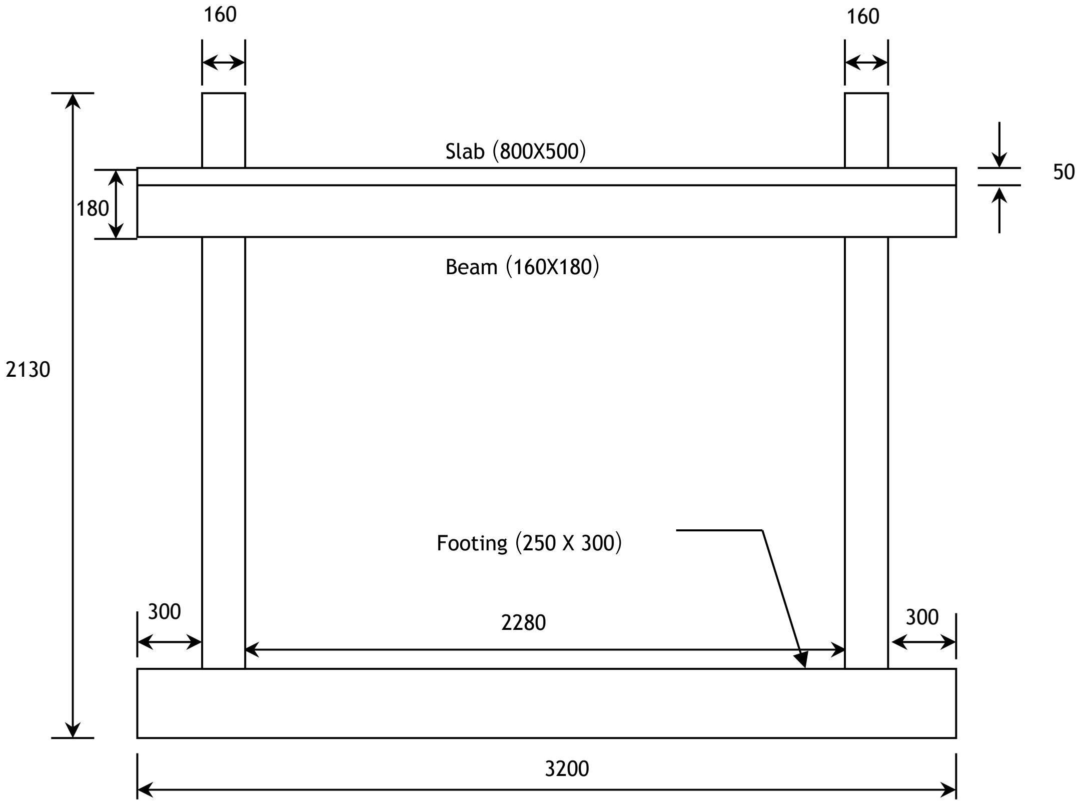

Figure 1: Dimensions of test frame

Properties of the frame under study

Excited mass (consisting of self weight of beam, slab and 1/3rd of mass of columns + imposed load) = 1905 Kg.

Dimensions of the column = 160mmX160mm

Longitudinal reinforcement = 4 numbers of 16mm diameter Fe-415 bars

Unconfined compressive strength of concrete = 35 MPa

Initial lateral stiffness = 7.8 KN/mm

Lateral Stiffness after partial damage =2.1 kN/mm

Final stiffness of the frame as reported = 1.00 KN/mm (after damage)

(Sahoo and Rai, 2008)

3.3 Strengthening Scheme

The RC frame used in the study was damaged considerably. It was repaired and retrofitted in three stages using epoxy, epoxy mortar and finally by means of FRP jacketing.

3.3.1 Use of Epoxy and Epoxy Mortar

Fine cracks in beams and columns were filled by low-viscosity epoxy SIKADUR-52 using injecting needle (figure 3) and allowed to cure for at least one day. The epoxy had a mix density of 1.14 kg/L and consisted of two parts A and B mixed in the ratio 8:1. Its viscosity at 30º is 250 CP. Its tensile strength is 34 MPa and compressive strength greater than 60 MPa after 14 days.

Figure 3: Epoxy Injection and repair using epoxy mortar

Major cracked and damaged concrete cover was removed first and then portions were repaired using epoxy mortar SIKADUR-31 and the damaged frame was brought back to its original dimensions. The epoxy mortar is a solvent free, thixotropic mortar based on the combination of epoxy resins and specially selected high strength fillers. It consists two parts A and B mixed in the ratio 2:1. The density of the mix is 1.85 kg/Ltr and compressive strength at 14 days equals to 60 MPa. A small form work was constructed so as to maintain the original dimensions of repaired columns.

3.3.3 Retrofitting using fiber-reinforced polymers

The main objective of retrofitting consists of strengthening the columns by confining the unconfined concrete by means of fiber reinforced composite jacketing. The standard provisions given in ACI 440-2R was used to calculate the number of layers of GFRP fabric required to bring back the confined compressive strength of cracked/damaged concrete equivalent to that of the unconfined compressive strength of initial concrete used in the construction original RC Frame.

The axial compressive strength of a normal weight concrete member confined with an FRP jacket can be calculated using formula (ACI 318-05)

$$\Phi P_n = 0.85\ \Phi\ [0.85\ f_c\ (A_g\text{-}A_{st}) + f_y \times A_{st}]$$

where,

$f_{c,as\text{-}built}$ = unconfined compressive strength of cracked concrete
$f_{c,target}$ = target unconfined compressive strength of concrete
f_{cc} = target confined compressive strength of concrete
f_l = Maximum confining pressure due to FRP Jacket
A_g = gross area of concrete
A_{st} = area of longitudinal reinforcement
f_y = yield strength of main reinforcement
Φ = constant =0.65
$f_{c,as\text{-}built}$ = 20 MPa
$f_{c,target}$ = 35 MPa
f_{cc} = 38.15 MPa
f_l = 14.63 MPa
Ψ_f = constant =0.95
Number of Plies = $[f_l \times (b^2 + h^2)2] / [\Psi_f \times 2 \times E_f \times t_f \times €_f]$

Property of GFRP used in the experimental program:
Bidirectional woven Fabric
Area density = 360 g/m^2
Volume fraction = 40%
Thickness per layer, t_f = 0.75mm
Ultimate tensile strength = 220 MPa
Modulus of elasticity, E_f = 19 GPa
Rupture strain, $€_f$ = 0.015
Number of layers of GFRP required = 8

The eight layers of GFRP were applied after initial repair of the damage columns by means of epoxy and epoxy mortar and allowing sufficient time for curing. First, a layer of SIKADUR 52 Epoxy was applied over the surface which was already cleaned off any loose mortar or dust remaining over it. Then the first layer of GFRP fabric was applied over it and another layer of epoxy was applied so as to complete impregnate the fibers completely. This layer was allowed to cure for a day, and following day remaining seven layers of GFRP sheets were applied providing sufficient time for curing.

Two layers of GFRP fabric were applied to the tension face of the beam because minor cracks were observed in the tension face of the beam.

3.4. Instrumentation and Test Set-up

The objective of this experimental investigation is to evaluate the linear elastic behavior of frames using the vibration and slow-cyclic tests. Thus, a test set-up (figure 4) was prepared which consisted of loading devices, reaction frame, and instrumentation consisting of various sensors and data acquisition system (Sahoo, and Rai 2008) to record load deformation data. Following are the details of the experimental test setup:

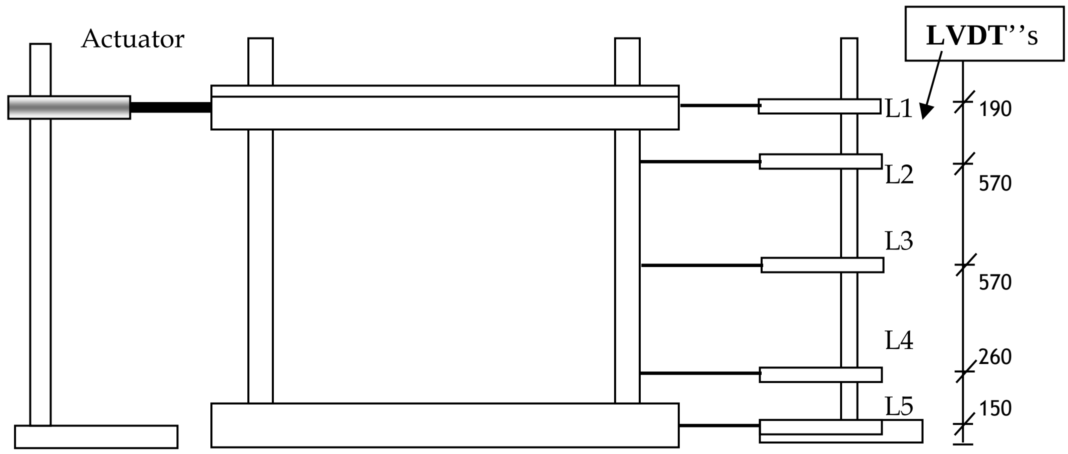

Figure 4: Schematics showing instrumentation and test setup

4. TEST RESULTS AND DISCUSSIONS

4.1 Force vibration test (Partially Damaged Frame)

The main objective of force vibration test was to determine the damp natural frequency of the frame. Natural frequency is considered as the frequency at which the maximum response of the frame is observed. The partially damaged test frame was subjected to the harmonic vibrations of varying frequencies by the electro-dynamic shaker placed at the center of the slab. The observed natural frequency was 2.75 Hz (equivalent to initial stiffness of 0.6 kN/mm) as shown in figure 5.

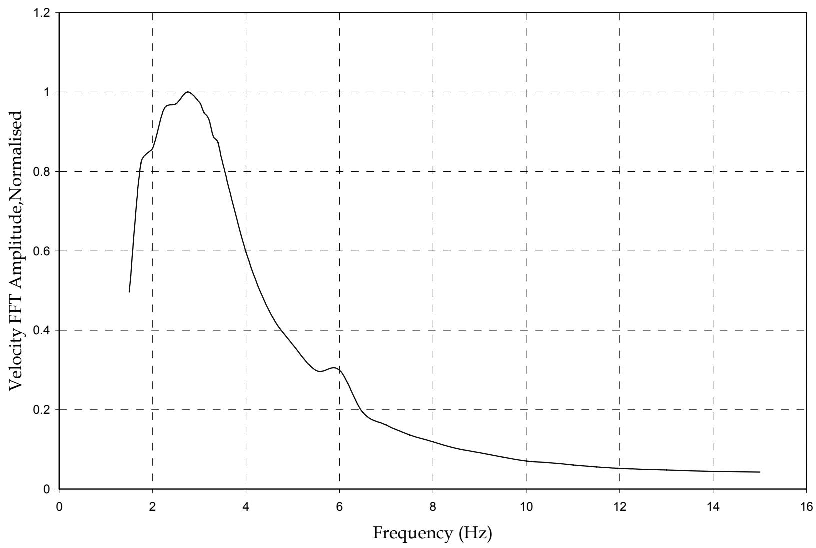

Figure 5: Frequency response of the partially damaged test frame

4.2 Evaluation of Frame Retrofitted with GFRP

4.2.1 Forced Vibration Test

After initial damage repair, the test frame was retrofitted using 8 layers of GFRP fabric as per calculations done using ACI 440-2R and allowed to cure for twenty four hours. First, a layer of SIKADUR 52 Epoxy was applied over the surface which was already cleaned off any loose mortar or dust remaining over it. Then the first layer of GFRP fabric was applied over it and another layer of epoxy was applied so as to complete impregnate the fibers completely. This layer was allowed to cure for a day, and following day remaining seven layers of GFRP sheets were applied providing sufficient time for curing. After curing the frame was tested under forced vibration test (figure 6) which yielded a significant improvement in stiffness. The natural frequency observed was 7.0 Hz and the stiffness calculated was 3.84 kN/mm.

4.2.2 Load-controlled slow-cyclic test

Load-controlled slow-cyclic test was carried out to determine the initial stiffness of the frame. The frame was subjected to a cyclic lateral load of 5kN in addition to constant gravity load of 18.7kN uniformly distributed over the slab. Figure 7 shows the lateral load-roof displacement response of the RC frame under cyclic loading. The peak displacement at roof of the frame was measured in push and pull direction of lateral loading of magnitude ±5kN. Initial lateral stiffness of the RC frame which was computed as the ratio of peak lateral load to lateral displacement was computed as 3.43 kN/mm, showing an increase of over 500% as compared to original damaged frame.

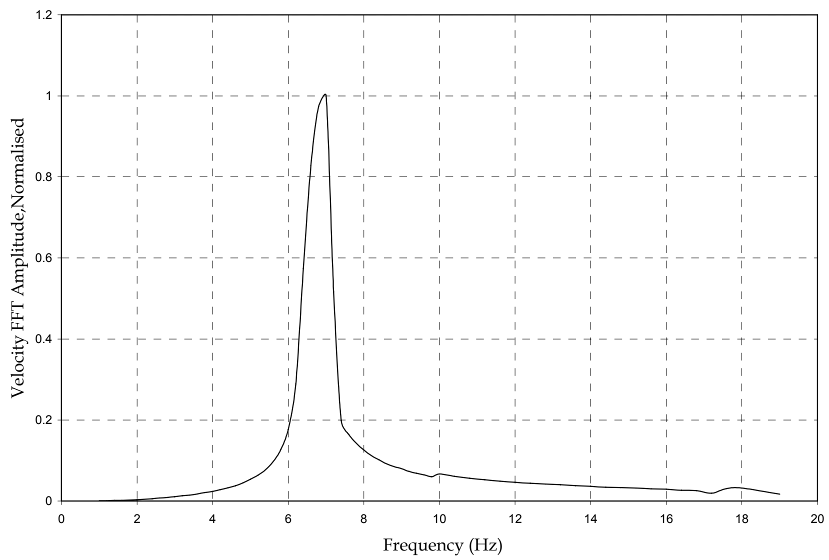

Figure 6: Frequency response of retrofitted Frame

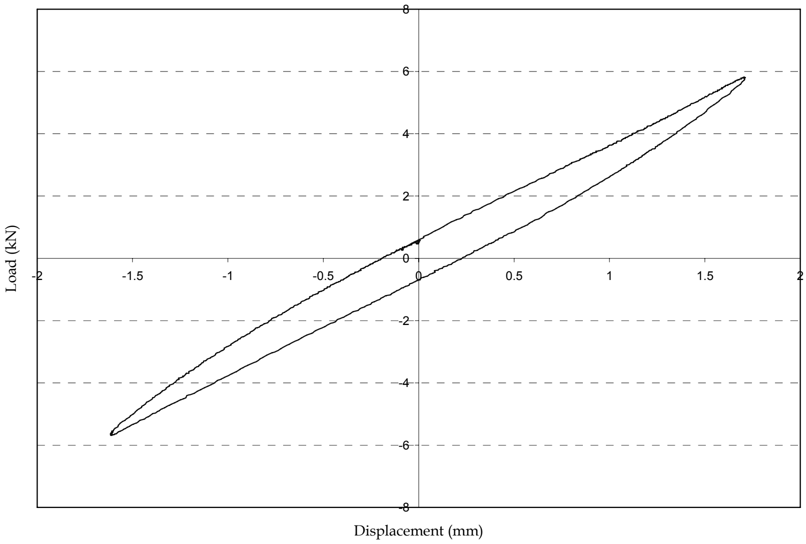

Figure 7: Load Displacement response of retrofitted Frame

4.3 Displacement controlled slow cyclic test

The strengthened RC frame was also subjected to displacement controlled slow cyclic test as per ACI recommendations [ACI 374.1-05] starting at different storey drift levels. The displacement history consisted of gradually increased storey drifts of 0.20%, 0.35%, 0.50%, 0.75%, 1.00%, 1.40%, 1.75%, 2.20%, 2.75%, 3.50% and 4.50%.Cyclic lateral load was applied to the RC beam of the frame in the form of a series of ramps at varied rate of loading such that the time required to complete the three cycles of each drift level was about five minutes.

Initially the fame was subjected to a storey drift of 0.20% and the response of the frame was recorded using LVDT’s. During the loading cycle for storey drift of 0.35% first cracking sound was observed, probably due to debonding of the layer of GFRP, however no major crack was observed in the column even at storey drift of 2.2%.Very gradual decrease in the value of stiffness was observed up to the storey drift of 2.2%, after which there was somewhat large decrease in the stiffness. At the storey drift level beyond 2.75%, continuous cracking sound was heard due to debonding of GFRP. Cracks also began to appear near ends of the column due to formation of plastic hinges.

The extent of damage in various storey drift is shown in Table 1, along with the test data of earlier study on the same frame (Sahoo & Rai,2008).

By comparing the values obtained from displacement controlled slow cyclic test with that of the earlier study [Sahoo and Rai,2008], a significant improvement in lateral load carrying capacity as well as lateral stiffness at various drift level varying from 0.20% to 4.5% has been observed . The hysteretic loops formed are also very stable without any sudden drop in stiffness of the frame up to 2.2% drift storey level.

TABLE 1: Test results

Storey drift (%)	Lateral disp. (mm)	Lateral Load, kN (Sahoo & Rai,2008) [% increase]	Lateral stiffness, kN/mm (Sahoo & Rai,2008) [% increase]	Observations
0.20	2.92	9.49(5.29)[**79.4]**	3.25(1.81)[**79.55**]	
0.25	3.72	11.83(6.56)[**80.33**]	3.18(1.76)[**80.68**]	
0.35	5.12	16.18(8.66)[**86.88**]	3.16(1.69)[**86.98**]	First cracking sound
0.50	7.43	22.14(11.77)[**88.10**]	2.98(1.58)[**88.60**]	
0.75	11.01	31.82(17.05)[**86.62**]	2.89(1.54)[**87.66**]	
1.00	14.71	38.83(22.69)[**71.13**]	2.64(1.54)[**71.42**]	
1.40	20.67	52.50(31.62)[**66.03**]	2.54(1.53)[**66.01**]	Cracks in joints
1.75	25.77	63.14(39.39)[**51.00**]	2.45(1.53)[**60.13**]	Debonding
2.20	32.38	75.45(49.97)[**50.99**]	2.33(1.54)[**51.03**]	Debonding
2.75	40.59	86.88(61.43)[**41.42**]	2.14(1.51)[**41.72**]	Debonding
3.5	51.62	88.27(69.20)[**24.66**]	1.71(1.34)[**27.61**]	Crack widening
4.5	66.35	89.2071.26[**25.17**]	1.34(1.07)[**25.23**]	Plastic hinges in column

5. CONCLUDING REMARKS

The performance of the partially damaged moment resisting frame was evaluated after GFRP retrofitting scheme by means of forced vibration test, load controlled slow cyclic test and finally by displacement controlled monotonic cyclic loading test. The results of the tests clearly shows that there was a significant improvement in the stiffness of the damaged frame from 0.6 kN/mm to 3.84 kN/mm, an increase of over 600%. There was also substantial improvement in the lateral strength of the frame. The displacement controlled slow cyclic tests also show that the RC frame retrofitted with GFRP fabric performed very well. No sudden drop in stiffness or load was observed in the specimen up to a storey drift of 2.2% which shows its excellent behavior considering the fact that the allowable storey drift of the moment resisting frames is considered as 1.5% for buildings of less than four storey and 2.0% for buildings of more than four storeys (IBC, 2000).

The load –displacement curve (figure 8) shows that that the hysteresis loops are stable without much pinching which is an indication of good retrofitting technique.

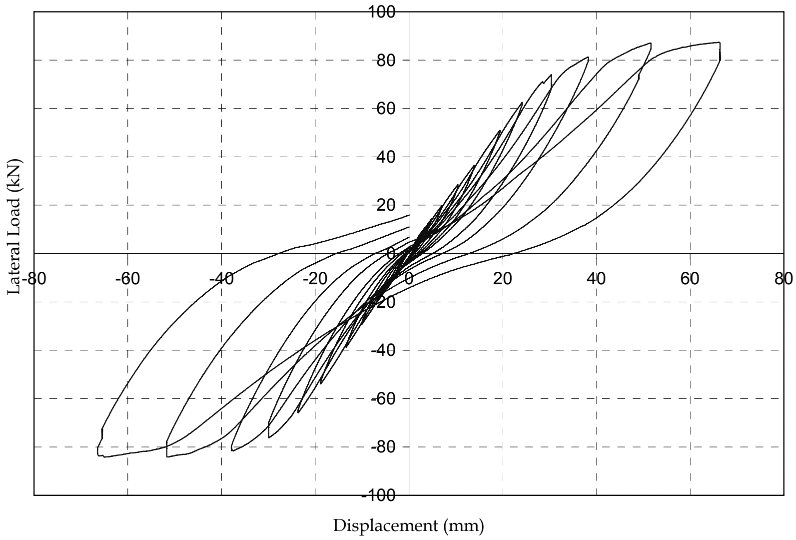

Figure 8: Load –displacement at various drift levels

REFERENCES

Bai,Jong-Wha and Hueste, M .B .(2003) "seismic Rehabilitation for Reinforced Concrete Building structures". *Consequence-Based Engineering Institute*, Final Report, Texas A&M university.

CEN.(2005)."Design of structures for earthquake Resistant Part 3: Assessment and retrofitting of buildings." Eurocode-8.

Wu,Y., Liu,T. and Oehlers,D.J.(2006) "Fundamental principles that govern Retrofitting of Reinforced Concrete Columns by Steel FRP Jacketing." *Advances in Structural Engineering*, Vol 9, No. 4, PP 507-533.

Murty C.V.R., Greene M., Jain S.K., Prasad N.P., and Mehta V.V. (2005) "*A Recovery Reconnaissance Report*" Earthquake Engineering Research Institute, Oakland, CA

Haroun.M A.Mosallam,A. S., Feng, M. Q. and Elsandedy,H.M (2003). "Experimental investigation of seismic repair and retrofit of bridge columns by composite jackets". *Journal of reinforced plastics and composites*, Volume 22, No 14.pp 1243-1268.

Sahoo, Dipti R. and Rai, Durgesh C.(2008), "Siesmic Strengtheningof Open-Ground-Storey RC Frame Using Steel –Caging And Aluminium Shear-Yielding Dampers*". IIT Kanpur.*

Savar building tragedy in Bangladesh: Way forward

Mehedi Ahmed ANSARY
Professor, Department of Civil Engineering,
BUET, Dhaka, Bangladesh
ansary@ce.buet.ac.bd

Naima RAHMAN
Research Planner, BNUS, Dhaka, Bangladesh
naima.rahman05@gmail.com

ABSTRACT

As garments industries have become the main source of foreign income of Bangladesh, many new factories have been established in Dhaka City. But due to lack of concern from authorities, this industry has become one of the highly risk working sector for workers. Garment industry has been experienced many fire accidents in the last decades taking life of many workers. But the recent accident of building collapse in Savar is the worst of all. This incident took lives of 1132 people and left many disabled. About 332 people are still missing according to their families. Six garments factories, one bank and many shops are going into debris within a few minutes without any shake from outside. In this study, the authors discuss the reason behind the accident, the role of authorities in search and rescue, overall co-ordination, rehabilitation and legal activities. The authors also recommend some measures to avoid this type of disaster in Bangladesh.

1. INTRODUCTION

1.1 Background

On 24 April at 9am, a nine-storey building collapsed in Savar, 25 kilometers north of the Bangladesh capital, Dhaka (see Figure 1). As of August, 1132 people died (CPD, 2013), 2438 people were rescued and were provided with immediate basic first aid or transferred to nearby hospitals for medical attention. The building housed several garment factories, a bank and several shops. The factories manufactured apparel for brands including Benetton, Bonmarché, Cato Fashions, the Children's Place, El Corte Ingles, Joe Fresh, Mango, Matalan, Primark and Wal-Mart. According to BGMEA (Bangladesh Garments Manufacturers and Exporters Association) 2800 workers of the 6 garment factories were in the building during the accident. But the actual number is around 3900 (CPD, 2013). Day before the incident, some cracks developed on some pillars and a few floors of the building following a jolt, causing panic among the people working there. They rushed out of the building and some even got injured in the process, said a number of garment workers and locals. The industrial police visited the building that day and asked the building authorities not to open the building. But the warnings and instructions were ignored. The shops and the bank on the lower floors immediately closed after cracks were discovered in the building. But workers of at least two garment factories at Rana Plaza were forced to join their workplaces following a false assurance on the building's safety from a local engineer, relatives of the victims alleged. As a result the deadliest garment-factory accident in the history of Bangladesh occurred which is also considered as the deadliest accidental structural failure in the modern world.

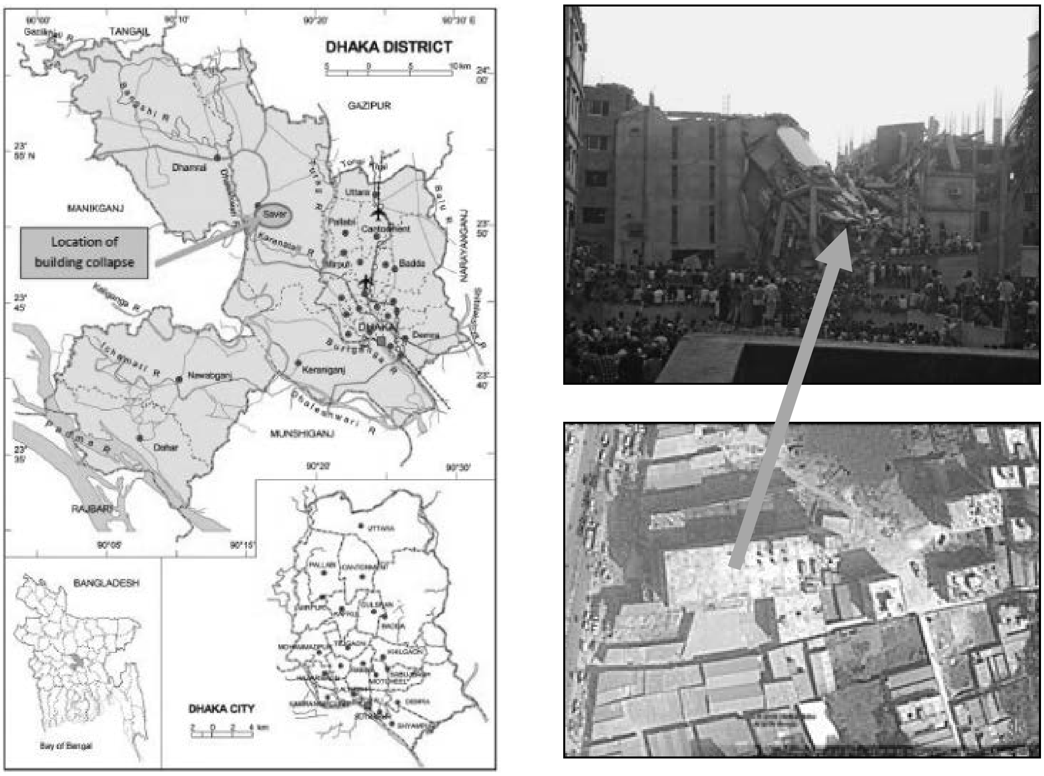

Figure 1. Location of the collapsed building

1.2 Purpose of the Study

The purpose of the study is to focus on overall scenario of the Savar tragedy. This article presents the search and rescue effort undertaken by different agencies in Bangladesh to rescue people from underneath the collapsed building and tries to explain the reasons behind the building collapse. Figure 2 shows the collapsed building.

Figure 2. The collapsed building

2. REASONS BEHIND THE BUILDING COLLAPSE

Rana Plaza was a 9-storied industrial building with a single basement. The local municipality gave the owner permission to construct a 5 storey commercial building with one basement in 2005 and later allowed the owner to extend it up to 9-storey, without considering the consequence of such action. The width of the building was around 25 m and length around 80 m. A typical grid of the building is 5.2 m by 8.2 m. The column sizes vary from 35 cm by 35 cm to 45 cm by 45 cm. The building was supported by pile foundation having 450 mm diameter and length of 18.3 m. Three main reasons can be attributed to the collapse of the structure: (i) Addition of four extra floors; (ii) Conversion of the building from commercial to industrial use and (iii) Placement of Power Generators at the higher floors. The steel grade used was 60 grade deformed bar and concrete strength was found around 3000 psi [see Figure 3].

Figure 3. (a) Broken samples collected from the building site and (b) Concrete cores collected from beams, columns and slabs of the collapsed building

2. SEARCH AND RESCUE OPERATIONS

2.1 Search and Rescue

Local Volunteers, volunteers of Bangladesh Red Crescent Society, personnel from Bangladesh Fire Service and Civil Defense, Bangladesh Armed Forces personnel, Border Guard Bangladesh and local police were involved in search, rescue and evacuation operation of trapped garment workers at Savar Building collapse site. On the day of incident, these organizations rescued 1762 people alive.

Figure 4. Search and rescue operation

The local people started rescue operation immediately after the incident. Then Bangladesh Army, Navy, Fire Service, BGB, Police and different volunteer teams joined in the rescue activities. Police and RAB are engaged to maintain law and order situation at the site. Rescue operation is continuing.1200 volunteer from Dhaka, Keraniganj and Narayanganj area (trained by Comprehensive disaster management Programme (CDMP) under Ministry of Disaster Management and Relief) are working in Rescue operation. To purchase rescue equipment instantly, MoDMR has given BDT 5,00,000 to Fire Service and Civil Defense. Figure 4 and 5 shows the acticity of people during Search and rescue operation

Figure 5. Search and rescue operation

More than 200 volunteers under the Department of Fire Service and Civil Defense (FSCD) who have received training under the previous DIPECHO VI Project implemented under the NARRI Consortium were immediately deployed after the incident and are working on location.

2.2 Overall Coordination

Armed Forces Division (AFD) of Bangladesh coordinated the search and rescue operation. Eman medical hospital played an important role for the injured victims by providing medical support. Fifteen Medical teams from Bangladesh Army, two from Navy, one from Air Force, one from BGB and ten teams from health department, the doctors and medical workers of local hospital and clinic are engaged for treatment of injured people.

2.3 Contribution of local volunteer

Some local people involved in search and rescue operation among them some died unexpectedly. Figure 6 shows the number of death and rescued alive from the day of accident to the day of last dead body found.

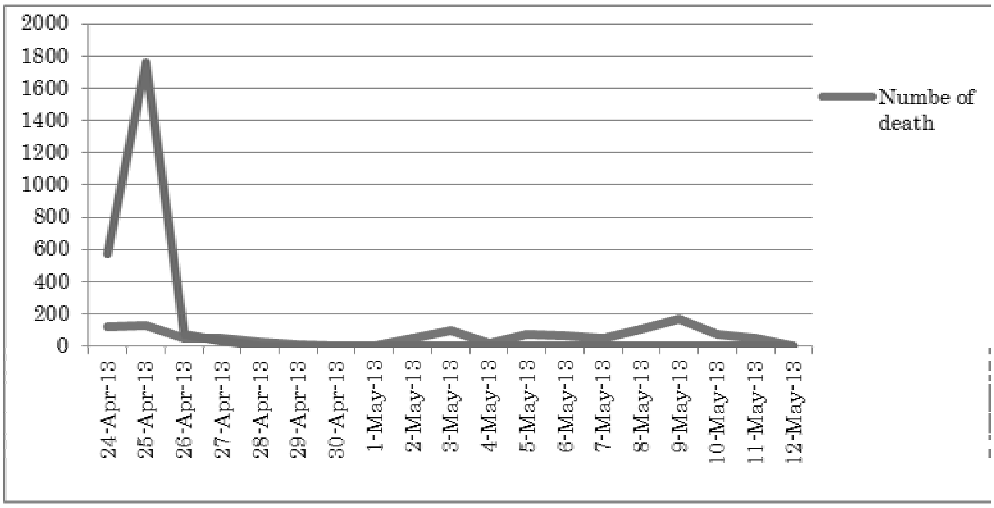

Figure 6. Number of death and rescued alive

From the day of accident, 574 people were rescued alive whereas 124 people were found dead. On the second day the highest number of people (1762) was saved alive. Alive people were found up to 4 days of the accident. But a woman named Reshma was found and rescued alive and almost unhurt under the rubble 17 days after the accident on 10 May. Dead bodies were found almost every day from 24 April to 12 May.

The Bangladesh Red Crescent Society was among the first responders on the scene. 100 trained volunteers are on the ground on a rotation providing search and rescue, basic first aid and safe drinking water. The organization also established a mobile medical team assisting the wounded. The Red Crescent Society ambulance service transported wounded people to various hospitals, and the organization also helped with the management of dead bodies. Restoration of Family Link (RFL) volunteers provided mobile phone services for the injured (see Figure 8) to connect with their families and relatives, and also compiled a list of the missing, injured and dead.

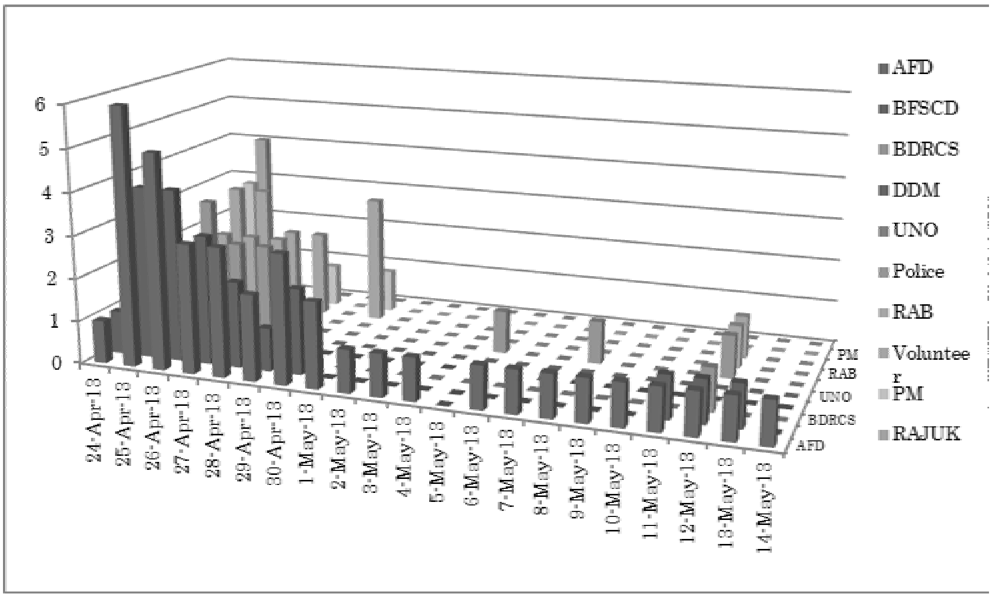

Figure 7. Number of key words in newspaper articles

Armed Forces Division (AFD) of Bangladesh engaged in the disaster management of the accident most as their name came in newspaper articles for 37 times. They appeared every day in newspaper from the day of accident to 14 May. Then come Bangladesh Fire Service and Civil Defence (BFSCD) with 20 times. Local volunteers contributed significantly with 15 times appearance in newspaper. The Department of Disaster Management (DDM) which is responsible for disaster management in the whole country appeared only 3 times in newspaper articles. The figure 7 shows the number of key words in newspaper articles from 24 April to14 May.

Figure 8. Some of the critically injured garments workers

3. MENTAL TRAUMA AND REHABILITATION

After the Savar tragedy, many victims and volunteers have been suffering from mental trauma of accident. One volunteer named Rubel committed suicide from the shock. Many of those who survived have lost their limbs, many have become paralyzed. Ironically, all those people are in their productive age and most of them are the only earning member of their family. With disability and deformity, it has become extremely difficult for them to get back to work again. But with long term rehabilitation support, they can lead a better life with acquiring productivity and mobility. After such traumatic experiences, nearly everyone will have the symptoms of stress and grief for the first month which is a natural grieving process. Some will still experience those symptoms and they cannot come to terms with what has happened and suffer Post Traumatic Stress Disorder (PTSD). Mental trauma can be solved by rehabilitation for a long time

4. NATIONAL VS. INTERNATIONAL RESPONSE

The Savar tragedy took limelight of both national and international media after the day of incident. Many international leaders including Pope, Secretary General of United Nations, ILO and international NGOs showed their deepest concern for the victims. The European Union (EU) has raised strong concern over labor conditions and declared appropriate action to encourage improvements in working conditions in Bangladeshi factories. Major western clothing retailers are squeezing Asian suppliers and a flawed approach to ensuring even basic working standards are fuelling conditions for tragedies like the Savar disaster.

United States of America suspended the Generalized System of Preferences (GSP) facilities on the entrance of Bangladeshi product into the US market after Savar tragedy considering the accident of Savar Rana Plaza, Tazrin Fashion, and unsolved case of murder of a trade union leader. They have also concerned about the safety, development of the standards of the laborers in Bangladesh as the biggest labor union of the USA, AFL-CIO has been convincing the government of USA to stop the GSP facilities for Bangladesh since 2007.

World Health Organization is going to provide more emergency drugs as per government request and has already provided blood transfusions sets, dressing and first aid materials along with emergency medicines to Savar Upazila Health Complex and Enam Medical College Hospital for the injured persons.

Islamic Relief, Bangladesh provided various equipments to support search and rescue to Fire Service and Civil Defense (FSCD). Action Aid, Bangladesh has provided emergency rescue equipment worth BDT 2,00,000 for FSCD’s rescue team and food worth BDT 50,000,00 for Urban Community Volunteers. Emergency medicine of BDT 10,000.00 is also supplied for injured people.

BDT 20000.00 has been provided to each deceased family. Total BDT 86,60,000 has been distributed to 433 families. Each injured person will get BDT 5000. BDT 47,15,000 has been distributed among 943 injured. BDT 4,00,00,000 has been allocated from MoDMR to DDM. DDM has allotted BDT 3,00,00,000 to District Administration for distribution.

The following graph shows the number of national and international articles on Savar tragedy in the Daily Star Bangladesh.

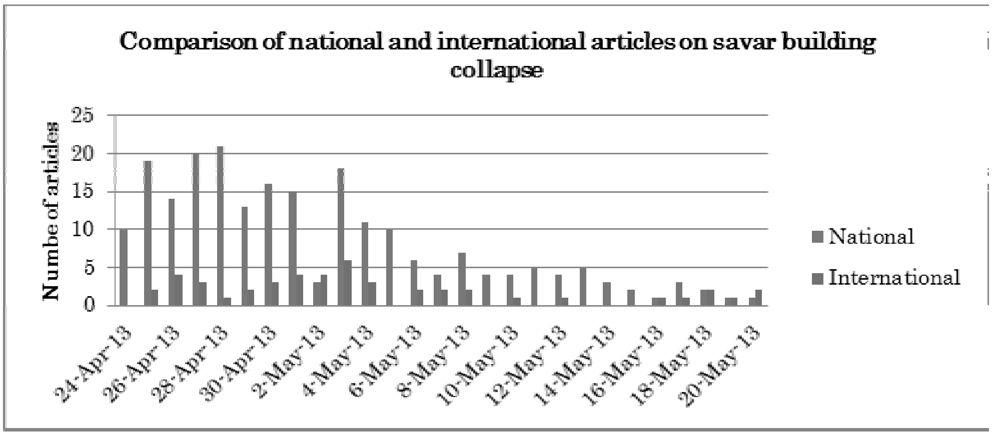

Figure 9. Comparison of national and international articles on savar building collapse

After the disaster, government of Bangladesh promised to give about $1,250 in cash and $19,000 in savings certificates to the families or relatives of died workers, but yet has provided about $1,250 to $5,000 to some 777 families. Nearly 300 bodies were not identified and claimed by families or relatives.

5. RECOMMENDATION

Bangladesh faced its worst human tragedy through Rana Plaza building collapse at Savar, Dhaka. In 1996 at Kalabagan, in 1997 at Khilgaon, in 2004 at Sakaribazar, in 2005 in Savar, in 2006 at Mahakhali, in 2010 at Hatirjheel and at Kathalbagan similar incidence occurred where altogether several hundred people were killed. Enforcement of Bangladesh National Building Code (BNBC) has become the top priority.

Immediately, we need to set up a Building Regulatory Authority (BRA) as prescribed in BNBC. BRA will aim to deliver: Better safeguards for consumers; Building industry transformation and Legislative reform. The Building Authority will work closely with four statutory bodies to provide industry leadership and will regulate building quality. The associated bodies will be the Building Advisory Council, Building Appeals Board, Building Practitioners Board and the Building Regulations Advisory Committee. The Authority and four bodies will

- Regulate Bangladesh’s building industry
- Administer the registration of a country’s building practitioners and monitor their conduct
- Advise the relevant Minister and the Government on building regulatory development
- Administer building legislation, the Building Act 1952 and Building Regulations 2008
- Resolve disputes and appeals arising from the Building Act

- Inform consumers about building and renovating
- Communicate changes that occur in building legislation
- Promote improved building standards nationally and internationally
- Provide comprehensive information on building activity
- Inform industry decision making through data and analysis
- Facilitate industry research
- Support the uptake of information technology and e-commerce
- Encourage sustainable and accessible building design, construction and use

The BRA will carry out these functions in consultation with a wide variety of stakeholders.

6. CONCLUSIONS

Many questions have already been raised about the future of the garments industry in Bangladesh after a number of accidents like Spectrum Garment Accident, Tazreen Fashion Disaster and the latest Savar Building Collapse. A large number of foreign buyers including Disney have decided not to buy clothes from Bangladesh because of the poor working condition in the garments industry. It may severely damage the social and economic future of Bangladesh in long term. The government, the leaders of the garments industry, the NGOs, and the civil society have to come forward in unity to increase the quality of working conditions and livelihood of the workers of this sector. The foreign buyers need assurance from the government that they will never again face this kind of disaster in Bangladesh.

REFERENCES

- BNUS field survey, 2013.
- Centre for Policy Dialogue (CPD), “Independent Monitoring Report”, August, 2013.
- The Daily Star. Accessed from 24 April to 25 May 2013.

Secular changes in people's consciousness regarding earthquake early warning -Based on national survey(2009-2012) in Japan-

Miho OHARA[1] and Atsushi TANAKA[2]
[1]Associate Professor, International Center for Urban Safety Engineering (ICUS), Institute of Industrial Science/ Interfaculty Initiative in Information Studies, The University of Tokyo, Japan
ohara@iis.u-tokyo.ac.jp
[2] Professor, Center for Integrated Disaster Information Research, Initiative in Information Studies the University of Tokyo, Japan

ABSTRACT

In Japan, earthquake early warnings (EEWs) have been broadcast to the general public since October 1, 2007. Issuance times of EEW increased drastically after the Great East Japan Earthquake, and citizens had much more frequent experience with EEWs. However, frequent missing and overlook of EEWs also occurred after the Great Japan East Earthquake, possibly adversely affecting the trustworthiness of EEWs.

This study analyzes secular changes in rates of recognition and reception experiences of EEW based on the regular disaster information survey from fiscal 2009 to 2012. It also analyzes awareness regarding EEW accuracy by comparing study results with EEW issuance history nationwide. Secular changes in the expectations of the general public regarding EEWs are also clarified.

As a result, the rates of recognition and reception experience of EEWs increased significantly after the Great East Japan Earthquake. It was confirmed that the rates of recognition and reception experience tend to rapidly increase when issuance times of EEWs increases. The both rates exceeded approximately 70% when the average issuance times exceeded roughly 10. The rate of responding "warnings should positively be issued in spite of the possibility of missing warnings" was as high as 85.6%. The decrease in the accuracy of EEWs did not clearly affect intention to use of EEWs. Meanwhile, reception experience leaded to positive intention to use.

As expectations for future EEW, needs for information about predicted intensity and time until ground motion arrives are increasing. Needs for information about "what to do specifically after EEW" are decreasing, suggesting a possibility of insufficient understanding for proper behaviors. Interest in behaviors when receiving EEWs should be enhanced especially in the regions where EEWs rarely issued.

Keywords: *Earthquake Early Warning, people's consciousness, Great East Japan Earthquake*

1. Introduction

Earthquake early warnings (EEWs), also known as alerts, have been issued to the general public since October 1, 2007, especially in regions with predicted intensity of 4 or more when predicted intensity of 5 lower or more is anticipated. According to records from the Japan Meteorological Agency (JMA) website, EEWs were issued 18 times before the March 11, 2011, Great East Japan Earthquake and 114 times from that date until the end of December 2012. Issuance times increased drastically after the March 2011 quake, and citizens had much more frequent experience with EEWs. Frequent missing and overlook of EEWs occurred after the Great Japan East Earthquake, possibly adversely affecting the trustworthiness of EEWs.
The University of Tokyo’s Center for Integrated Disaster Information Research (CIDIR) has annually conducted “regular survey on the degree of disaster information recognition and trends in disaster awareness” (hereafter, regular disaster information survey) since fiscal 2009. This paper analyzes secular changes in rates of recognition and reception experience related to EEWs by comparing results of 2012 with those since 2009. Issuance times and hit, missing, overlook rates of EEWs nationwide thus far are also calculated and calculation results are compared with those of regular disaster information survey to analyze regional differences among awareness of the general public concerning EEW accuracy. Expectations of EEWs are also analyzed.
EEWs include two types of warning; the one is the alerts for the general public receiving by TV or radio etc., the other is the alerts for advanced users receiving by special receiving devices. EEWs for advanced users are issued, as a rule, when “the amplitude of the P wave or S wave is 100 gal or more” and “the calculated magnitude is 3.5 or more or the maximum predicted intensity is 3 or more”. The EEW in this paper means the former one, the alerts for the general public.

2. Analysis of Rates of Recognition and Reception Experience with EEWs

2.1 Issuance Times of EEWs Nationwide

The JMA website gives detailed data on the EEWs issued, such as issuance date, location, and estimated magnitude. Based on this, Figure 1 shows EEW issuance times by month from October 2007 to December 2012. The highest numbers were 46 in March 2011, when the Great East Japan Earthquake occurred, and 26 in April 2011. Since then, issuance times have increased drastically due to aftershocks and induced earthquakes, although they decreased to 1–3 times a month after October 2011 and remained at that level thereafter. All issuances in March 2011 were after the great earthquake. EEWs are issued to approximately 200 prediction regions nationwide. Miyagi Prefecture, for example, is divided into north, central, and south regions. Average issuance by prefecture was calculated based on issuance for individual prediction regions as shown in Fig.2. The highest after the Great East Japan Earthquake was 56 times for Ibaraki Prefecture, 51 for Fukushima Prefecture, 33 for Tochigi Prefecture, 31 for Chiba Prefecture, and 28 for Miyagi Prefecture. Fukushima and Ibaraki Prefectures thus received more warnings than Iwate or Miyagi Prefectures where the damage from the concomitant tsunami was significant. For comparison, no warnings were issued until December 2012 to the prefectures of Kyoto, Osaka, Hyogo, Nara, Tottori Okayama, Yamaguchi, Tokushima, Kagawa, Ehime, Kochi, Fukuoka, Saga, Nagasaki, Kumamoto, Oita or Miyazaki Prefectures. No regions in the Shikoku district received warnings, either. The first EEW was issued on April 13, 2013, to the 10 prefectures of Kyoto, Osaka, Hyogo, Nara, Kagawa, Tokushima, Ehime, Kochi, Tottori, and Okayama when an earthquake hit Awaji Island in Hyogo Prefecture (Please note, that the scope of this paper does not include this in Fig. 2).

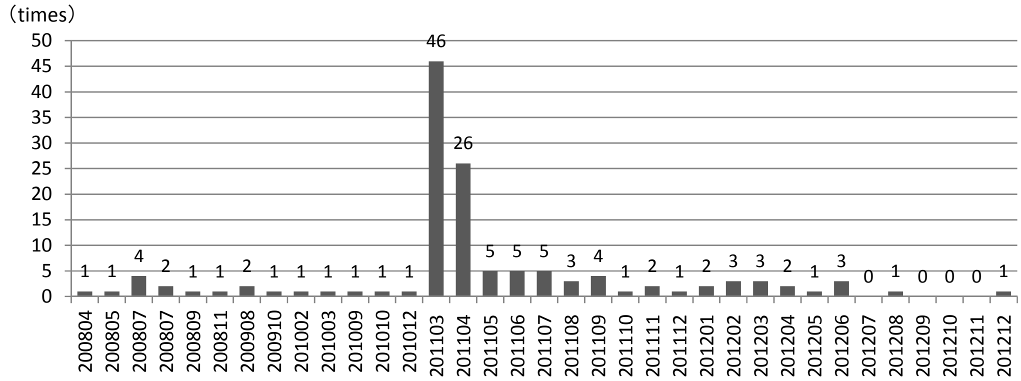

Figure 1: Issuances of EEWs from 2007 to 2012

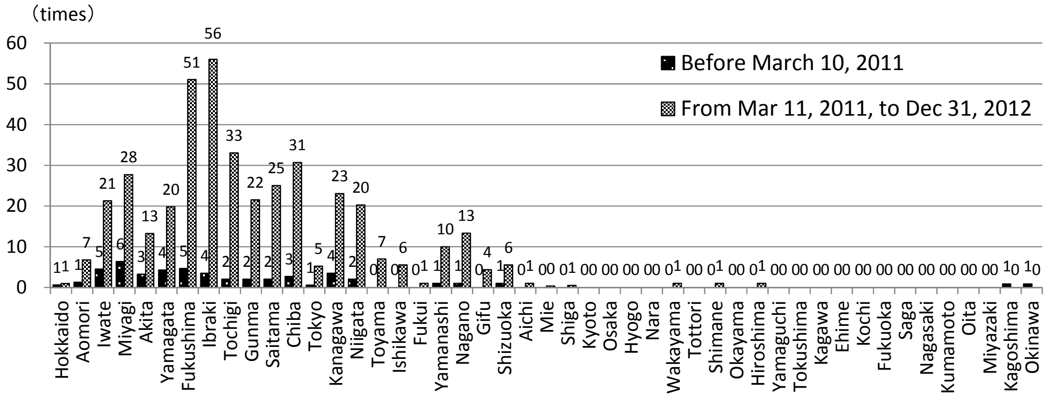

Figure 2: Average issuance of EEWs by prefecture

2.2 Overview of Regular Disaster Information Survey

The CIDIR, The University of Tokyo has annually conducted regular survey on recognition degree of disaster information and disaster awareness since fiscal 2009. The surveys were performed as follows.

- Research region: Entire Japan
- Research period: December of 2012, 2011, 2010, and 2009
- Research method: Internet questionnaire
- Research target: Males and females aged 20 to 69. Two-thousand people for 2009 and 2010 and 3000 people for 2011 and 2012. The sample number for each prefecture was distributed proportionally to the population composition ratios.

2.3 Secular Changes in Rates of Recognition and Reception Experience with EEWs

This section analyzes the secular changes in rates of recognition and reception experience of EEWs by comparing the results of the regular disaster information survey conducted in 2009-2012. The "recognition rate" is defined as a "rate of people who have heard of information." EEWs for the general public can be received by TV, radio, cell phones, and radio communications for disaster prevention and administration. Here, the "reception experience rate" is defined as a rate of people who have received EEWs by themselves by those means. The "recognition rate" is 56.1% in 2009 and 61.3% in 2010 before the March 2011 quake. The rate significantly increased to 79.3% as of December 2011 after the Great East Japan Earthquake, approximately 1.29 times compared to the figure in the previous fiscal year. This can be considered due to the effect of numerous EEWs issued after the March 2011 quake.

Figure 3 shows the age-based secular changes in rates of recognition and reception experience of the EEW. Here, the reception experience rate is shown only after 2010 because this item was not included in the survey in 2009. The recognition rate in 2009 and 2010 are highest for those who are in their 20's, while it increased from December 2011 after the Great East Japan Earthquake for all generations.

The reception experience rate is 27% on average for all generations in 2010 and 54.9% in December 2011 after the March 2011 quake, increasing approximately twofold. The reception experience rate decreased for all the generations in 2012. It is worrying that the memory of receiving numerous EEWs will fade and the consciousness about EEWs will diminish after the next fiscal year as time passes from the Great East Japan Earthquake.

Figure 4 shows the district-based secular changes in rates of recognition and reception experience of the EEW. The recognition rate exceeded 50 % in all the districts as of 2009. In 2009, the highest value of 61.9% is for Tohoku district, whereas the lowest of 50.5% is for Kyushu Okinawa district. In 2011 after the March 2011 quake, the highest value increased to 92.3% for Tohoku district and the lowest to 67.3% for Kyushu Okinawa district.

The results of district-based reception experience rate show a larger regional difference than those of recognition rate. The reception experience rate for Tohoku district is the highest in every year, increasing approximately 1.88 times from 47.3% in 2010 to 88.8% in 2011. The rate slightly decreased to 83.7% in 2012. In contrast, the rates for Hokkaido and Chubu district in 2012 are as low as approximately 40% and those for western Japan, Kinki, Chugoku, Kyushu, Okinawa districts are all approximately 20%. 13.0% for Shikoku district in 2012 is the lowest.

2.4 Analysis of Relationship Between Issuance Times per Region and Recognition Rate/ Reception Experience Rate of EEWs

Based on the results above, this section analyzes the relationship between average issuance times per prefecture and recognition rate/ reception experience rate of EEWs. Figure 6 plots the average issuance times of each prefecture from March

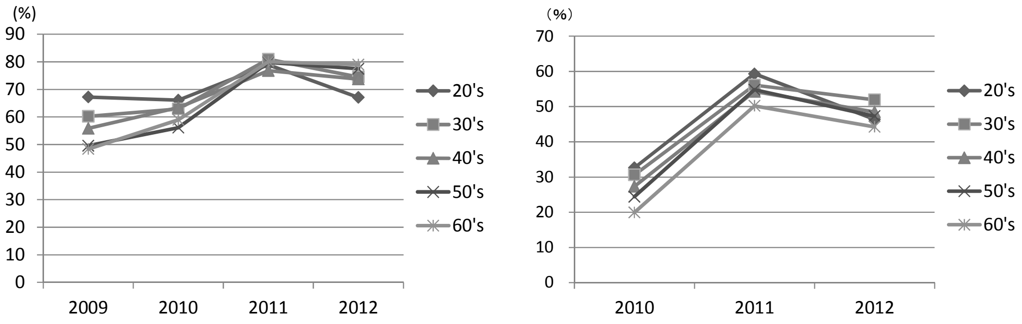

(a) Recognition rate (b) Reception experience rate

Figure 3: Age-based secular change in rates of recognition and reception experience of EEWs

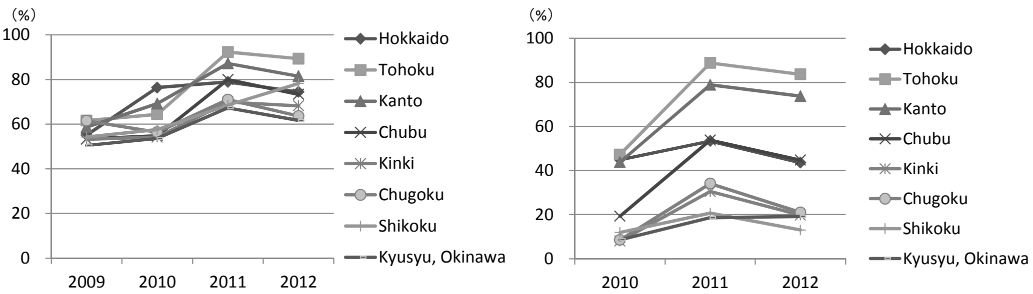

(a) Recognition rate (b) Reception experience rate

Figure 4: District-based secular change in rates of recognition and reception experience of EEWs

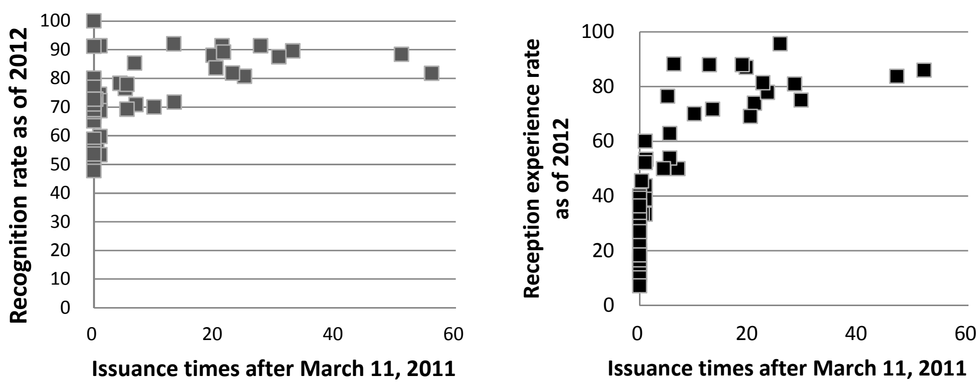

(a) Recognition rate (b) Reception experience rate

Figure 5: Relationship between issuance times and rate of recognition or reception experience of EEWs

11, 2011 to the end of December, 2012 (Fig. 2) against the recognition rate and the reception experience rate as of 2012. Each plot in the figure indicates individual values for each prefecture. When the average issuance times exceed 20, the recognition rate is approximately 80-90% and the reception experience rate is approximately 70% or more. In addition, when the average issuance times exceed 10, the rates of recognition and reception experience exceed approximately 70%.

It is confirmed that the rates of recognition and reception experience exponentially increase when the issuance times increase to a certain level. However, the rates of recognition and reception experience are not the highest for Ibaraki and Fukushima Prefectures, for which average issuance times are as considerably high as more than 50. The rates of recognition and reception experience per region are likely to differ depending on issuance time of a day, daytime or night. In the prefectures with the average issuance times of 0 or 1, the recognition rate ranges widely from 50 to 100%, while the reception recognition rate 10 to 60%. The recognition rate exceeds 50% for prefectures that have not received the warning. The issuance times are 0 and the reception experience rates are as low as slightly over 10% in Tokushima, Kochi, Ehime Prefectures in Shikoku district, and Fukuoka, Saga, Nagasaki, Oita, Kumamoto Prefectures in Kyushu district. Meanwhile, in Chugoku and Kinki districts, the issuance times are 0 or 1, but the reception experience rate dispersed from about 20% to 60%. If some TV program is being broadcasted nationwide when an EEW is issued, its warning message can be seen in regions that are not the target. This is thought to increase the reception experience rate for Kinki and Chugoku districts to which warnings were quite rarely issued.

3. Analysis of Awareness of General Public Concerning Accuracy of EEWs

Next, the awareness of the general public concerning the accuracy of EEWs is analyzed. The accuracy of EEWs for aftershocks and induced earthquakes after March 11, 2011 decreased due to the facts such that concurrent multiple earthquakes cannot be separated and the number of available seismometers decreased because of blackouts and disruption of communication lines. According to the press release of the JMA (2011), 70 warnings issued from 11 March to 28 April included many missing cases. At 17 earthquakes (24%), an EEW was issued to the regions whose observed seismic intensity was 2 or less by mistakes.
In addition, among 46 earthquakes with the observed maximum intensity of 5 lower or more, 20 cases (43%) were overlooked with no warnings although EEWs were issued to 26 cases (57%). They say these issues were partly resolved by the upgrade of software as of August 10, 2011. However, missing and overlook of EEWs may have affected motivation for use and recognition of usefulness regarding the warning.

3.1 Regional Trends in Accuracy Based on EEW Issuance History

This section discusses the regional trends in accuracy based on issuance history thus far. Here, trustworthiness of information offered by the JMA is focused on. The regional trends in accuracy of EEWs is analyzed by comparing EEWs issued to all or part of each prefecture with actually observed intensity, which is obtained in the intensity database of the JMA website. EEWs is issued to regions with predicted intensity of 4 or more when predicted intensity of 5 lower or more is anticipated in some regions. Ohara analyzed issuance history until the end of March, 2012 using a similar method. This paper includes comparison using the latest data, expanding the target period to the end of December, 2012.

Figure 6 aggregates hit, missing, overlook times of EEWs per prefecture before and after the great earthquake. It excludes prefectures to which EEWs was issued only once before and after the great earthquake. EEWs is issued to regions with predicted intensity of 4 or more when predicted intensity of 5 lower or more is anticipated in some regions. “Hit” warnings are therefore defined as those issued to all or part of a prefecture concerning an earthquake with observed intensity of 4 or more in the same prefecture when intensity of 5 lower or more is observed in any region in the country. “Missing A” warnings are defined as those issued to all or part of a prefecture when no earthquakes occur in the country. “Missing B” is the case in which a warning is issued to all or part of a prefecture when intensity of 4 or more is not measured in the same prefecture, but measured in other prefecture. The case of missing A is inferior to the case of missing B. “Overlook” warnings for a prefecture means the case in which EEWs is not issued when an earthquake with intensity of 5 lower or more is measured in any region in the country and intensity of 4 or more is also measured in the same prefecture.

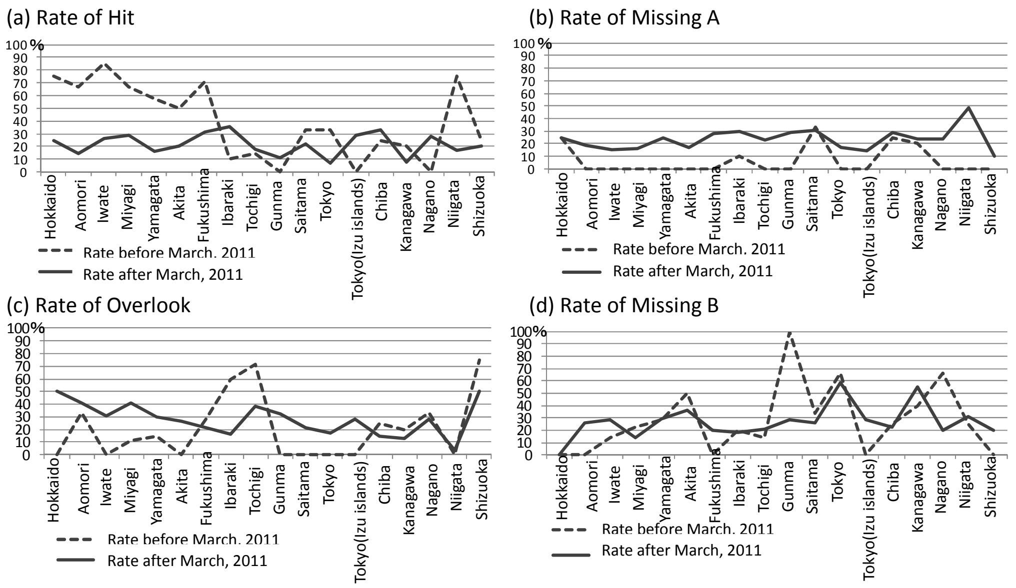

Figure 6: Rates of hit, missing, overlook by prefecture before and after the Main March 2011 quake

From the above, the rough tendency is that the hit rate decreased and overlook and missing A rate increased with no major difference in missing B rate in Hokkaido and Tohoku districts. The increase in the overlook rate in Iwate and Miyagi Prefectures is considered to be largely affected by the decrease in the number of seismometers available in the coastal area. In Ibaraki and Tochigi Prefectures, where EEWs were relatively frequently issued, the hit rate increased and overlook rate decreased after the great earthquake, indicating higher accuracy. The accuracy of Tokyo 23 wards and Tama area and Saitama Prefecture decreased with lower hit rate and higher overlook rate although they are far away from Tohoku district. In the regions with decreased accuracy after the Great East Earthquake, Intention to use and consciousness of usefulness regarding EEWs might presumably be decreased.

3.2 Intention to Use EEW

Considering the results in the previous section, the regular disaster information survey in December 2012 asked comments on whether EEWs should positively be issued in spite of possibility of missing warnings. 33.1% of the total responded “warnings should positively be issued in spite of possibility of missing warnings,” 52.5% responded “warnings should be issued in spite of possibility of missing warnings,” resulting in 85.6% of respondents accepting missing warnings.
Figure 7 shows the cross-aggregation results between the reception experience rate and intention to use considering missing warnings. As a result of chi-square test, a statistically-significant difference was confirmed when $p < 0.001$. 40% of those who have received EEWs responded “warnings should positively be issued in spite of possibility of missing warnings.” The reception experience is assumed to lead to positive intention to use. In order to study the effect of the decrease in accuracy of EEWs on motivation for use, figure 8 plots the decrease value of the hit rate after the great earthquake per prefecture against the rate of answering “warnings should positively be issued in spite of possibility of missing warnings” in the same prefecture. This figure indicates that the decrease in the hit rate do not directly cause intention to use EEWs to decline because there is no correlation between the two.

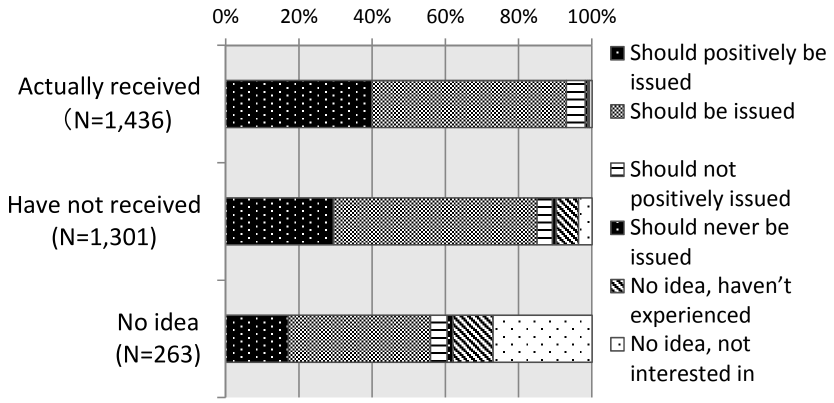

Figure 7: Reception experience and intention to use considering missing warnings

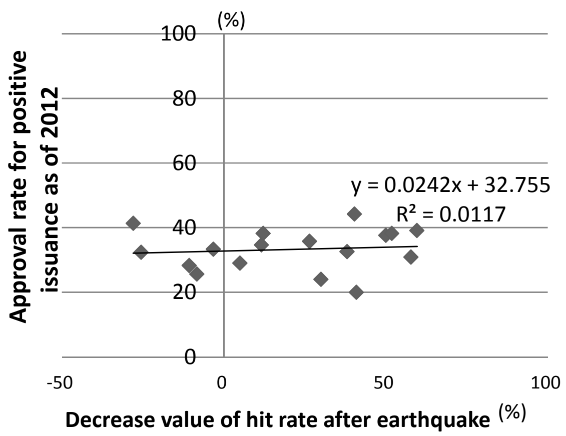

Figure 8: Relationship between decrease value of hit rate after the great earthquake and approval rate for positive issuance

4. Analysis of Expectations for EEWs

Finally, this section analyzes the secular changes in expectation for EEWs based on the results of the regular disaster information survey from 2010 to fiscal 2012. Figure 9 shows the answer rate of choices to the question "what should be done in order to make EEWs more easy to use?" The most popular answer in 2010 is "automatically turn on deactivated TV or radio to receive warnings" at 56.0%. However, the rate of this answer decreases together with "make warnings receivable by every kind of cell phones." This seems to be the effect of the recent increased rate of receiving the warnings using cell phones. The rates of "tell earthquake intensity" and "tell after how many seconds the shock will occur" increased from 2011 to 2012 after the Great East Japan Earthquake. The rate of "tell earthquake intensity" is the highest among all choices in 2012 at 55.6%. The motivation for more positively using EEWs enhanced after the March 2011 quake, resulting in desire to know predicted intensity and time until ground motion arrives. Currently, EEW for the general public don't tell predicted intensity or time until ground motion arrives, whereas EEW for advanced users inform of these information. It means interests in the information only for advanced users are increasing recently. Meanwhile, the rate of "want to know what to do specifically when receiving EEWs" decreased significantly from 41.8% in 2009 to 26.8% in 2012. It is possible that situations during earthquake disasters are more clearly imaged after the Great East Japan Earthquake but interest in proper behaviors is waning due to easy understanding. Nevertheless, this image is likely to include incorrect understanding for proper behaviors, so awareness for proper behaviors should continuously be raised. Interest in behaviors when receiving EEWs need be enhanced by means of training and materials of EEWs in regions to which EEW have rarely been issued so far and where the reception experience rate will fluctuate at a low level in the future, such as western Japan.

5. Conclusions

In this paper, the secular changes in the rates of recognition and reception experience of EEWs were analyzed by comparing the result of the regular disaster information survey from fiscal 2009 to 2012. In addition, the regional differences of the awareness of the general public regarding the accuracy of EEWs were analyzed by comparing issuance history of EEWs nationwide thus far with the results of the regular disaster information survey. Finally, the secular changes in expectations of citizens for EEWs were clarified. Major findings obtained are as follows.

- The rates of recognition and reception experience of EEWs increased significantly after the Great East Japan Earthquake.
- The recognition rate exceeded 50% as of 2009 in all districts, while the reception experience rate showed larger regional differences than the recognition rate. The reception experience rate in western Japan is as low as approximately 20%.
- It was confirmed that the rates of recognition and reception experience tend to rapidly increase when issuance times of EEWs increases. The both rates

exceeded approximately 70% when the average issuance times exceeded roughly 10.
- The rate of responding “warnings should positively be issued in spite of the possibility of missing warnings” was as high as 85.6%.
- The decrease in the accuracy of EEWs did not clearly affect intention to use of EEWs. Meanwhile, reception experience leaded to positive intention to use.
- Needs for information about predicted intensity and time until ground motion arrives are increasing for the future EEW. Needs for information about “what to do specifically after EEW“ is decreasing, suggesting a possibility of insufficient understanding for proper behaviors. Interest in behaviors when receiving EEWs should be enhanced in the regions where EEWs rarely issued.

Note that the analysis in Section 3 focuses on whether EEWs is issued or not to each prefecture. However, the relationship between whether or not EEWs was issued before the arrival of the main shock and the awareness of the general public cannot be analyzed due to the constraints of data. In addition, the relationship between the observed intensity in each prefecture and the awareness of the general public is not analyzed. Further analyses considering these points are required as future issues.

ACKNOWLEDGEMENT

Regular disaster information survey was conducted using donation for the course of cooperation between lifeline companies and mass medias at the CIDIR, for which the authors are deeply grateful.

REFERENCES

Japan Meteolological Agency, Earthquak Early Warning, ,
http://www. Jseisvol.kishou.go.jp/eq/EEW/kaisetsu/joho/

Japan Meteolological Agency, *Press Release: Issurance of Earthquak Early Warning after the Great East Japan Earthquake,* April 28, 2011.

Japan Meteolological Agency, *Press Release: Improvement of Earthquak Early Warning, Japan,* August 10, 2011.

Japan Meteolological Agency, *Search Engine of Intensity Database,*
http://www.seisvol.kishou.go.jp/eq/shindo db/

M. Ohara, K. Meguro, and A. Tanaka, “A study on Regional Tendency of Earthquake Early Warning Proveded to the Public in All Parts of Japan,” *Proceedings of the 32th JSCE Earthquake Engineering Symposium, Japan Sociery of Civil Engineers,* 2012.

Prediction on sediment related disaster through the satellite rainfall data

Yoshikazu SHIMIZU[1] , Toshio OKAZUMI[2], and Tadanori ISHIZUKA[3]
[1]Senior Researcher,
International Centre for Water Hazard and Risk Management under the auspices of UNESCO (ICHARM),
Public Works Research Institute (PWRI), Japan
shimizu@pwri.go.jp
[2]Chife Researcher, ICHARM, PWRI, Japan
[3]Chief Researcher, Volcano and debris-flow Research team, PWRI, Japan

ABSTRACT

In this study, the sediment-related disaster prediction method currently practiced in Japan was coupled with satellite rainfall data and applied to domestic large-scale sediment-related disasters. The study confirmed the feasibility of this integrated method.
In Asia, large-scale sediment-related disasters which can sweep away an entire settlement occur frequently. Leyte Island suffered from a huge landslide in 2004, and Typhoon Molakot in 2009 caused huge landslides in Taiwan. In the event of these sediment-related disasters, immediate responses by central and local governments are crucial in crisis management.
In developing countries, however, only limited rainfall information is available from regular and radar rain gauge networks. For this reason, the International Centre for Water Hazard and Risk Management (ICHARM) of the Public Works Research Institute has developed and has been disseminating the Integrated Flood Analysis System (IFAS) to establish flood warning and evacuation systems in developing countries with insufficient hydrological information.
This study confirmed that it is possible to deliver information on the risk level of sediment-related disasters such as slope failures and debris flows in addition to flood warning by IFAS. The prediction method tested in this study is expected to assist sparsely gauged areas in timely emergency responses to rainfall-induced natural disasters.

Keywords: *prediction, shallow landslide, debris flow, satellite rainfall, IFAS*

1. Introduction

In Japan, projects to control sediment and erosion (hereinafter “sabo”) have been implemented continuously since the late 1800s. These projects have contributed to prevention of sediment disasters by means of structural measures such as sabo dams. However, hazardous areas in which five houses or more are at immediate risk of sediment disaster amount to approximately 210,000, and in only about 20% of them have prevention measures been implemented. On top of this, there are approximately 520,000 areas where the risk of sediment disaster exists. Thus, taking infrastructure-based measures for all these disaster risk areas would require enormous amounts of time and cost.

Consequently, “non-structural measures”, i.e., prediction, forecast, and control measures when disasters occur, must be taken to save human lives.

2. Measures and policies on the prevention of sediment related disaster in Japan

In Japan, new residential areas have been developed in suburban areas, and such development leads to a yearly increase in the number of sediment disaster-prone areas. Thus, in addition to infrastructure-based approaches, such as construction to prevent sediment disasters, it is important to take activity-based measures, including identification of sediment disaster risk areas, establishment of warning and evaluation systems in risk areas, and control of the location of new housing in hazardous areas. The Sediment Disaster Countermeasures for Sediment Disaster-Prone Areas Act took effect on May 8, 2000, to implement these holistic approaches. The following are some of the measures listed in this law.

2.1 Implementation of basic surveys and designation of sediment disaster-prone areas

The measures listed below must be implemented to identify areas that are at risk of sediment disaster and establish a site-specific warning and evacuation system that are appropriate to cope with the characteristics of such disasters (e.g., they may occur suddenly without any signs, it may cause human damage, etc.) for individual locations.

1) Implementation of basic surveys

2) Designation of sediment disaster-prone areas and special sediment disaster-prone areas.

2.2 Establish the early warning system and regulation of land-use

The following measures must be implemented for sediment disaster-prone areas and high-risk sediment disaster-prone areas.

1) Disaster-prone area:
   Establishment of an early warning system
2) High-risk disaster-prone area:
   Permit system for certain development activities
   Structural regulations for buildings
   Recommendation of building relocation

3. Methodology of setting sediment related disaster warning and evacuation critical rainfall

Mayors of municipal governments are responsible for taking timely, appropriate response measures, such as calling for disaster prevention activities and issuing evacuation advisories to local residents, if the risk of sediment disaster due to heavy rainfall becomes dangerously high. To help mayors, the Sediment Disaster Warning and Evacuation Critical Rainfall (the Cooperative Proposal) has been developed jointly by the Sabo (Erosion and Sediment Control) Department of the River Bureau with the Information Division of the Meteorological Agency of the Ministry of Land, Infrastructure and Transport as judgment criteria. Mayors are advised to use the Cooperative Proposal to set “critical lines”.

Critical lines are set based on assessment of the risk of a sediment related disaster within a specified area based on rainfall. It is important to note that this assessment considers only rainfall, and does not consider local topography, geology, vegetation and other factors of individual locations.

3.1 Target phenomenon

The target phenomena are debris flows and concentrated cliff collapses. A concentrated cliff collapse is defined as “cliff collapses that occur within a specified range near the peak of a series of rains in a case where the soil-water index is at or above a specified value.”

3.2 Rainfall indices

A criterion is set by combining two indices: the short-term rainfall index and long-term rainfall index. The short-term rainfall index is defined as the 60-minute total rainfall; the long-term rainfall index as the soil-water index, which is an estimation of the retention status of fallen rainfall in soil (for a detailed explanation of the soil-water index, see Attachment 1, and obtain information provided as necessary from the regional meteorological observatory, etc.).

3.3 Setting procedure of Critical Line

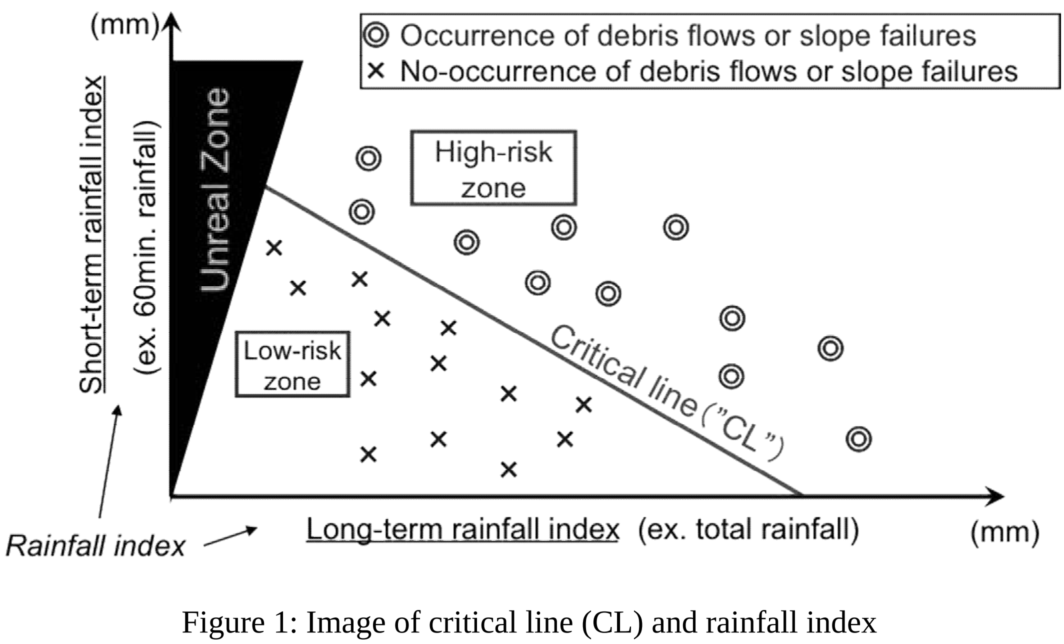

Figure 1: Image of critical line (CL) and rainfall index

The sediment disaster occurrence risk critical line (CL) is set as the boundary between two types of zones. The first type is called the “low-risk zone”, where the occurrence probability of rainfall that is unlikely to cause a sediment disaster is high. This probability is determined in reference to past rainfall that did not cause a sediment disaster (no-occurrence rainfall). The CL is set between a safe zone and a high sediment disaster risk zone in consideration of the occurrence probability and past records of sediment disasters as well as response measures, such as evacuation advisories, taken at the time.

3.4 Maintenance of Critical Line

Critical Line is revised as necessary based on new rainfall data and disaster data obtained after their establishment.

4. Prediction on sediment related disaster through the satellite rainfall data

In general, there are not enough rainfall gauge stations in developing countries. Therefore national and local governments have little information to determine the risk level of water induced disasters in their service areas.

In consideration of this situation, a feasibility study was conducted on the Japanese prediction methodology for sediment related disasters by using satellite based rainfall data.

4.1 Satellite based rainfall data

Table 1: Specification of satellite based rainfall data

Products	3B42RT	CMORPH	QMORPH	GSMaP
Providers	NASA/GSFC	NOAA/CPC		JAXA/EORC
Coverage	50N~50S	60N~60S	60N~60S	60N~60S
Spatial resolution	0.25°	0.25°	0.25°	0.1°
Time resolution	3 hours	3 hours	0.5 hour	1 hour
Delay	10 hours	15 hours	2.5 hours	4 hours
Datum	WGS			
Providing period	Mar. 2000 ~	Dec. 2002~	Recent 2days	Mar. 2000
Sensor	TRMM/TMI Aqua/AMSR-E AMUS-B DMSP/SSM/IIR	TRMM/TMI Aqua/AMSR-E AMUS-B DMSP/SSM/IIR		TRMM/TMI Aqua/AMSR-E AMUS-B DMSP/SSM/IIR ADEOS-II/AMSR

Table1 shows near-real-time satellite rainfall data products. The products have different space and time resolutions, using different sensors and algorisms. In this study, we used GSMaP provided by JAXA and 3B42RT by NASA.

4.2 Case study on prediction of sediment related disaster through the satellite rainfall data

In July 2009, a high-density sediment related disaster, or a debris flow, occurred in Hofu City of Yamaguchi Prefecture, Japan. This event was calculated by using the Japanese standard methodology such as like third section, and then analyzed for its feasibility.

4.2.1 Overview of phenomenon

Figure 2 shows hourly rainfall data and soil water index between the early June and the late August in 2009 at Manao hydrological station of MLIT, which is located near the disaster-hit area where many people were victimized.

The monthly rainfall reached 688mm in July 2009, exceeding July’s average rainfall of 294.9mm between 1981 and 2010. In addition, hourly rainfalls of over 30 mm were recorded before July 21, when multiple sediment disasters occurred, and the total rainfall between July 1 and July 20 reached 213 mm.

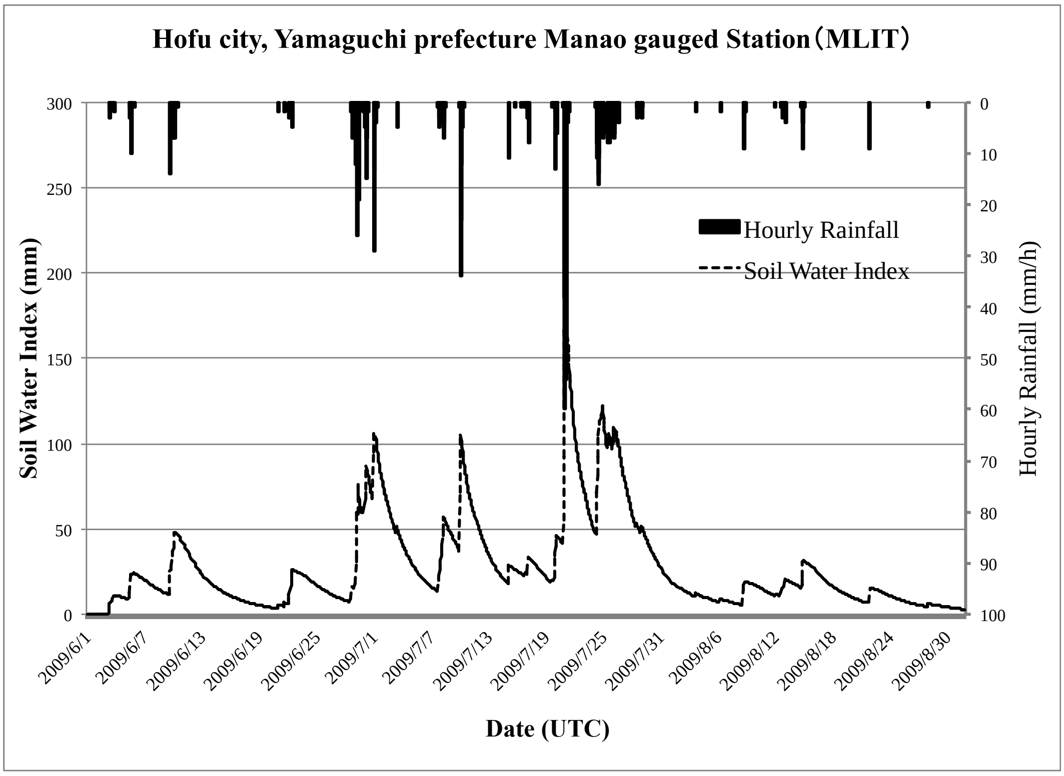

Figure 2: Rainfall data at Manao rain gauged station
（Jun 2009～Aug 2009）

4.2.2 Result of calculation of satellite rainfall data and compared ground based rainfall data’s

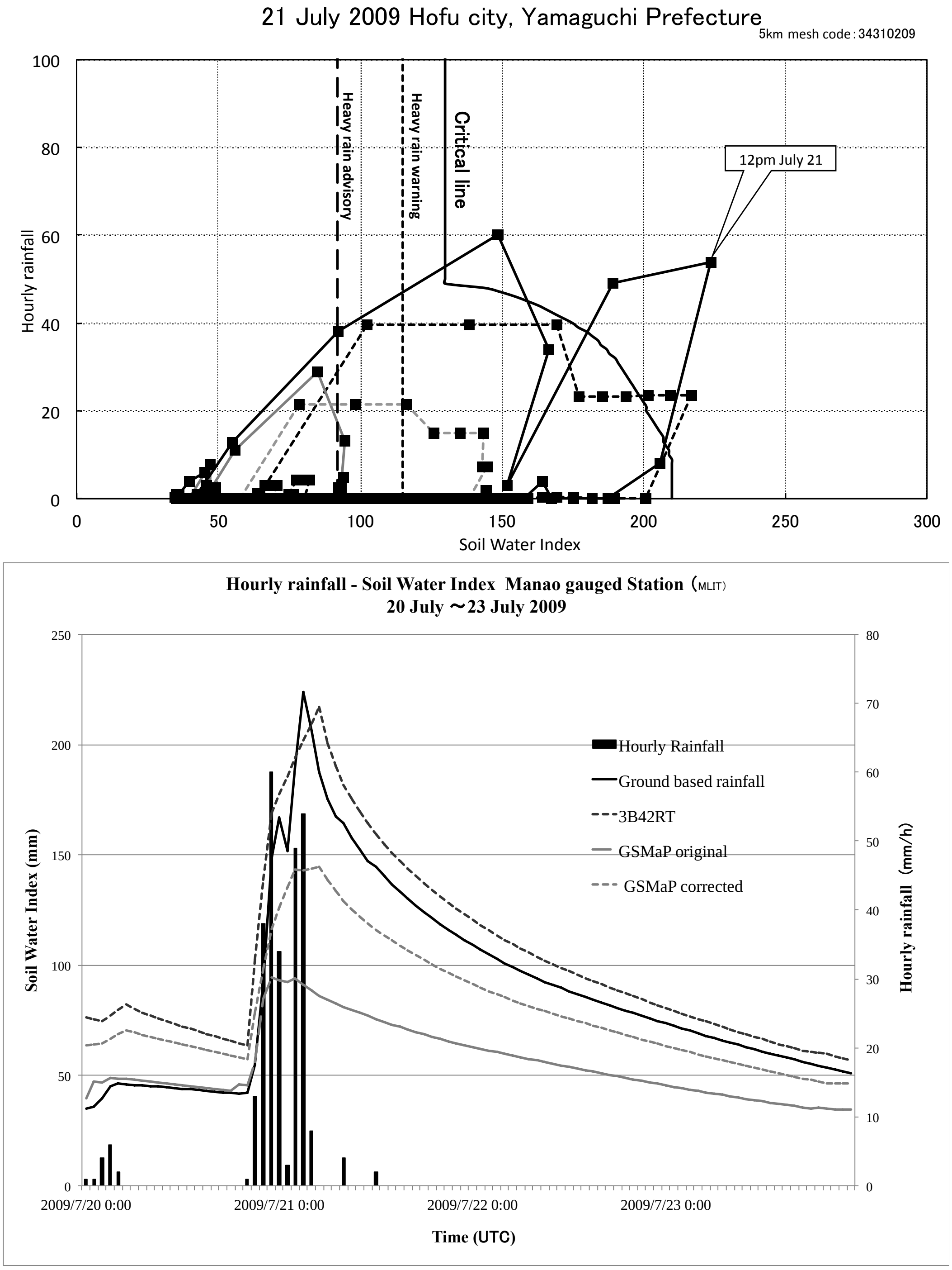

Figure 3: Comparing between ground based and satellite based rainfall data

Figure 3 shows sediment related disaster risk calculated based on the rainfall data between July 20 and July 23, 2009.

The upper graph of Figure 4 shows snake curves based on ground and satellite rainfall, and the lower graph shows hourly rainfall and soil water index. In both graphs, the thick solid line is ground based rainfall, the thick dashed line is

3B42RT satellite rainfall, the light solid line is GSMaP original rainfall, and the light dashed line is GSMaP corrected rainfall. Corrected GSMaP rainfall is average rainfall of the given hour and the hours before and after that in consideration of the movement of the rainfall area.

The snake curves from satellite rainfall data look relatively flatter than those from ground based rainfall data because of their underestimating tendency. On the other hand, in terms of soil water index, the curves from both types of data show a very similar temporal trend.

5. Conclusion

In this research, we have conducted a feasible study to compare grand based rainfall data with satellite based rainfall data for prediction of sediment related disasters, using a Japanese standard methodology.

As Figure 3 shows, hourly satellite based rainfall has an underestimating tendency compared with ground based rainfall data. In addition, due to time resolution and delay from real time, it was found not feasible to use satellite data for early warning systems though it may still be useful in risk management by central and local governments as information to facilitate crisis response by the public. As the Global Precipitation Measurement (GPM) Plan progresses, spatial resolution, time resolution and accuracy of rainfall data should be further improved and will be more effective in practical use.

We are planning to conduct longer term analysis and examine applicability to other regions in addition to studying when, where and how this methodology can be best used..

Reference

Osanai, N., Shimizu, T., et.al, Japanese early-warning for debris flows and slope failures using rainfall indices with Radial Basis Function Network, *Landslides*, Volume 7, Issue 3, 325-338

JAXA EORC, TRMM JAXA, *http://www.eorc.jaxa.jp/TRMM/index_e.htm*

Nishi, M., et.al, 2009, July 2009 northern Kyushu and Chugoku regional heavy rainfall induced sediment related disaster at Hofu city, Yamaguchi Prefecture, *Civil Engineering Journal*, Vol.51, No.9, 4-7 (in Japanese)

Okada, N., et al., 2001, Soil water index, *Weather*, vol.48, no.5, 349-356, (in Japanese) .

Effect of foreign government advisories on foreigners' post-disaster action after the 2011 Great East Japan Earthquake

Akiyuki KAWASAKI[1], Michael HENRY[2],
Ichigaki TAKIGAWA[3], and Kimiro MEGURO[4]
akiyuki@iis.u-tokyo.ac.jp
[1]Project associate professor, International Center for Urban Safety Engineering, Institute of Industrial Science, the University of Tokyo, Japan
[2]Assistant professor, Division of Field Engineering for the Environment, Faculty of Engineering, Hokkaido University, Japan
[3]Assistant professor, Creative Research Institute, Hokkaido University
[4]Professor and Director, International Center for Urban Safety Engineering, Institute of Industrial Science, the University of Tokyo, Japan

ABSTRACT

Immediately after the Great East Japan Earthquake, many foreign governments issued advisories to their citizens residing in Japan to relocate to the western part of the country or to leave Japan entirely, whereas other governments issued no advisory at all. The post-disaster response of many foreigners was to flee Japan, but it is not clear how much influence the government advisories had on this decision making or if other factors may have been involved. Through a questionnaire survey given to foreigners residing in the Kanto region at the time of the disaster, the relationship between the advisories issues by overseas governments and the behavior of foreigners residing in Japan was investigated in order to examine the differences among people who did and did not follow the recommendations of their government. Three sample groups were created based on the foreign governments' advisory level, and the effect on post-disaster action was examined and compared to other characteristics.

Keywords: *post-disaster action, relocation or evacuation advisory, foreigner, information*

1. INTRODUCTION

After the 2011 Great East Japan Earthquake disaster, many important issues arose with relation to the differences in the post-disaster response of foreign governments. Notably, some governments issued a variety of official advisories to their citizens residing in Japan, such as orders to evacuate areas around the Fukushima Daiichi nuclear power plant, recommendations to consider evacuation from eastern Japan (including Tokyo), and temporary travel restrictions on visiting specific areas of Japan or to travel to Japan in general. On the other hand, many countries did not issue any particular advisory.

What was the relationship between the advisories issued by foreign countries in response to the 2011 Great East Japan Earthquake disaster and the post-disaster evacuation action of their citizens? Similarly, what were the reasons why foreigners decided to remain in the Kanto region despite the recommendation of their home country's government to evacuate or relocate? To understand these relationships, an analysis of the results of a questionnaire survey taken of foreigners residing in the Kanto region of Japan at the time of the earthquake was carried out based on the advisory level of foreign governments around the world. First, the responses of foreign governments in the aftermath of the earthquake are organized and divided into three groups based on the level of their advisory. Next, the actual post-disaster actions, along with the timing and reason for those actions, of respondents are analyzed considering the government advisory level.

2. SUMMARY OF GOVERNMENT ADVISORIES

2.1 Temporary closure and relocation of embassies in Tokyo

As of March 23rd, 2011, the Japanese Ministry of Foreign Affairs (MOFA) reported that 25 countries had temporarily closed their embassies. In addition to the announced countries, it was reported that other countries such Thailand, France and Iraq also closed their embassy, resulting in closure of 29 out of the 150 embassies. In contrast to the embassies of Asian countries, which generally continued operations after the earthquake, a relatively large number of African countries closed their embassy. These embassies gradually resumed operations in Tokyo, with all of them returning to service by the end of May 2011.

2.2 Foreign government-issued advisories

A summary of the advisories issued by governments after the earthquake is shown in Tables 1 and 2. This information was collected from a variety of sources: MOFA (as of April 12th, 2011), major foreign media such as Reuters and ABC news, the websites of MOFA and embassies, and via direct inquiry to embassies. In this paper, the advisories are divided into four major categories: "evacuation from a specific area," such as from within x kilometers of the Fukushima Daiichi nuclear power plant; "leave Japan," including travel from eastern Japan; "travel restrictions to specific areas;" and "travel restriction to Japan," intended for citizens planning to visit Japan.

After the earthquake, a variety of notices and announcements were officially issued not only from embassies but also from government representatives such as prime ministers, foreign ministers, or ministers of foreign affairs. For the purpose of this paper, those notices and announcements related to evacuation or travel restrictions are all included as official advisories.

Table 1: Countries who advised leaving Japan

	Thailand	Hong Kong	Taiwan	Singapore	England	France	Italy	Switzerland	Austria	Netherlands	Portugal	Bulgaria	Denmark	Serbia	Australia
Evacuate from a specific area	○	○	○	○	○	○	○	○	○	○			○		○
Travel restrictions to specific areas	○			○	○	○	○			○					○
Evacuate from Japan	○	○	○		○[4]	○[1]	○	○[3]	○[2]	○[5]	○	○	○	○	○
Travel restriction to Japan					○[4]	○	○		○[2]	○[5]	○	○			

[1]Tokyo [2]Metropolitan area [3]Greater area of Tokyo and Yokohama [4]North of Tokyo [5]Kanto and areas north

Table 2: Countries who advised region-specific relocation in Japan

	China	S. Korea	Philippines	Malaysia	India	USA	Canada	Germany	Beglium	Norway	Sweden	Finland	Croatia	Hungary	Poland	Romania	Slovakia	Slovenia	Russia	Spain	New Zealand	Turkey
Evacuate from a specific area	○	○	○	○	○	○	○	○			○	○		○		○				○	○	○
Travel restrictions to specific areas	○						○						○			○			○		○	
Evacuate from Japan																						
Travel restriction to Japan	○	○ 4	○	○	○	○	○ 6	○	○	○	○ 1	○	○	○	○	○	○	○	○		○ 4	

[1]Tokyo [4]North of Tokyo [6]Tokyo and northern Honshu

2.3 Timing of advisory issuance

When examining the timing of advisory issuance, it can be seen that many countries responded promptly in the aftermath of the earthquake. On March 11th, the day of the earthquake, the National Tourism Administration of The People's Republic of China issued an advisory emphasizing that Chinese citizens should stay away from affected areas such as Fukushima Prefecture and Sendai City. The following day, a variety of countries – including South Korea, Taiwan, Hong Kong, Malaysia, Singapore, Canada, the United States, England, and France – issued various advisories for evacuation and restrictions on travel to Japan.

Those advisories – particularly those relating to travel restrictions – were eventually lifted or gradually relaxed. For example, Denmark lifted a voluntary ban on traveling near Tokyo on April 16th. On the following day, England removed Tokyo from its designated list of areas with a travel ban. Furthermore, on April 14th the United States lifted a travel warning to areas in Japan, excluding the area within an 80 kilometer radius of the Fukushima Daiichi nuclear power plant (which remained restricted), as the situation improved. However, some countries such as South Korea, Taiwan, Hong Kong, and Australia continued their travel restriction advisories until June.

Overall, it could be seen that while the issuance of advisories was concentrated in a short period immediately after the earthquake, the period until those advisories and restrictions were lifted or relaxed varied over a long period of several months, depending on the country.

3. SURVEY METHODOLOGY AND SAMPLE CATEGORIZATION

3.1 Survey contents and distribution

An online survey focusing on people in the Kanto region of Japan was carried out to understand the information collection behavior and post-disaster action after the 2011 Great East Japan Earthquake disaster. Complete details of the survey contents and distribution can be found in Kawasaki et al. (2012). The survey questions analyzed in this paper are summarized in Table 3.

Table 3: Selected survey contents analyzed in this paper

Theme	**Question contents**
Post-disaster action	Post-disaster action (remain in Kanto area, relocate to another area of Japan, or leave Japan)
	Timing of decision on post-disaster action
	Reason(s) for post-disaster action decision making*
Demographics	Nationality

** This question allowed for multiple responses*

3.2 Sample characteristics & categorization

A total of 1,357 responses were collected, of which 497 (36.6%) were from Japanese and 860 (63.4%) from foreigners representing 73 countries. Of the 860 responses from foreigners, 856 valid responses were identified: 492 from Asia, 24 from Oceania, 178 from Europe, 80 from North America, 52 from Central and South America, 12 from the Middle East, and 18 from Africa.

Based on the level of government advisories summarized in Tables 1 and 2, the sample of foreigners was categorized into three groups. After categorization

"Group 1" consists of 207 respondents from 13 countries whose governments issued the most cautious advisory; "Group 2" consists of 510 respondents from 30 countries whose government issued a less cautious advisory; and "Group 3" consists of 139 respondents from 29 countries whose government issued no specific advisory.

4. RESULTS AND DISCUSSION

4.1 Post-disaster evacuation or relocation action

The results of post-disaster action by government advisory level are shown in Figure 1. It could be seen that more cautious advisories lead to a greater number of respondents evacuating and vice versa. This result was statistically significant at a confidence level of 99%; that is, there appeared to be a correlation between the level of advisory and the post-disaster action.

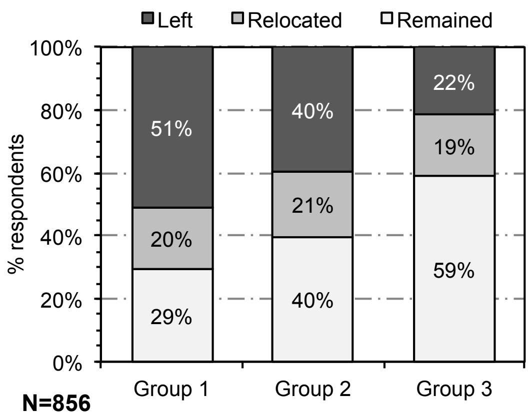

(χ^2=36.10427, *df*=4, *p*<.01)

Figure 1: Effect of government advisory on post-disaster action

In Group 1, which issued the most cautious advisory, 71% of respondents evacuated from the Kanto region; 51% of the total chose to leave Japan entirely whereas 20% relocated to another area in Japan. In Group 2, which advised only from specific areas such as the Tohoku region, a majority of the respondents (61%) evacuated from the Kanto region; 40% of the total chose to leave Japan entirely while 21% just relocated within Japan. In contrast to the other two groups, only 41% of Group 3 respondents decided to leave the Kanto region; 22% left Japan entirely and 19% evacuated to other regions.

When examining the differences between these groups, it can be seen that the percentage of respondents who evacuated Japan was considerably higher in Group 1 than in Group 3, while nearly double the percentage of respondents in Group 3 did not evacuate compared to Group 1. The results of Group 2 fell between those of Groups 1 and 3. This result indicates that the difference in government advisory exerted a certain level of influence on respondents' post-disaster action to relocate.

4.2 Timing of post-disaster action

To examine the effect of government advisory on the timing of post-disaster action, respondents who left Japan entirely or relocated to another area in Japan during the two weeks following the earthquake were extracted. The results are shown in Figure 2. From the chi-square test we can conclude that there is no statistically significant difference between the timing of post-disaster action and the distributions of the respondents who relocated and those who left for all three groups.

In Group 1, the cumulative percentage of respondents who made their decision to relocate within 1 to 3 days of the earthquake was 53%; over the same period, 54% of respondents decided to leave Japan. The cumulative value increased to 93% and 85% for relocation and leaving, respectively, when the time period reached 1 week. From these results, it can be observed that the majority of respondents made their decision to evacuate the Kanto region or Japan in a very short period of time after the earthquake.

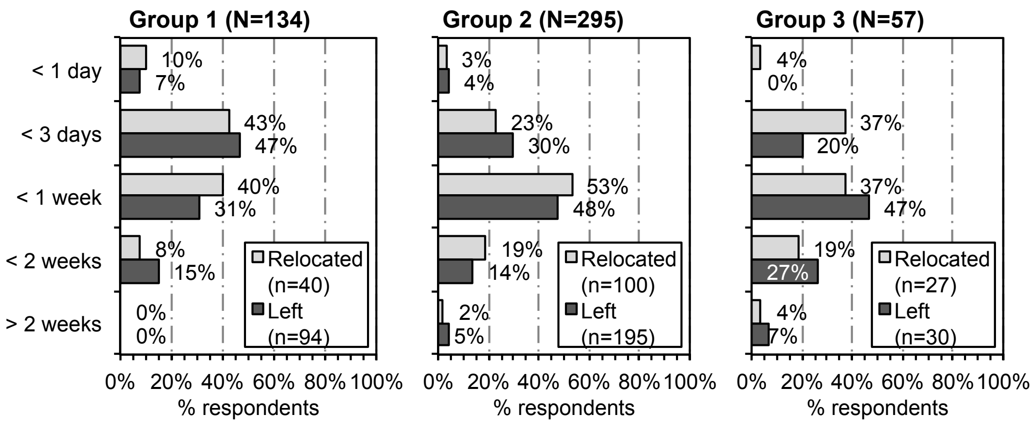

(χ^2=2.2457, df=3, p=0.523)   (χ^2=4.0251, df=4, p<0.4026)   (χ^2=3.5442, df=4, p=0.4712)

Figure 2: Effect of government advisory on timing of post-disaster action

In Group 2, the most-cited period for making the decision for post-disaster action was within 1 week (4 days to 1 week), as around half of the respondents decided to either leave the Kanto region (53%) or Japan (48%). The cumulative percentages at the time point were 79% for relocation and 82% for leaving Japan entirely.

In Group 3, the cumulative percentage of respondents who decided to relocate within Japan or evacuate the country entirely within 1 week were 78% and 67%, respectively. However, the total number of respondents in this group who decided to relocate or evacuate was much lower than the other two groups. The percentages of people who took their action within 2 weeks (between 1 and 2 weeks) or after more than two weeks were slightly higher than for Groups 1 and 2, which shows that the timing of decision making for respondents in Group 3 was slightly later than in the other two groups.

Overall, regardless of the countries' advisory level, it appeared that people made their decision at a very early time after the earthquake: the majority of respondents in Group 1 made their decision within 3 days, and even in Group 3 – where no specific advisory was issued – most respondents made their decision within 1 week. However, this question only focused on the timing of the respondents' decision-making, and does not clarify whether they acted upon that decision, whether they returned to the Kanto region later if they did, in fact, relocate or evacuate, nor does it clarify the timing of their return.

4.3 Reasons for post-disaster action

Figure 3 shows the reasons why respondents made their decision to leave Japan, relocate within Japan, or to remain in the Kanto area by government advisory level.

When examining Group 1, it can be seen that, among respondents who left Japan, the most-cited reason was "family request" (60%) followed by "personal decision" (51%). The third and fourth most-cited reasons were "concern for babies or children" (16%) and "government directive" (14%), but these are cited by 35% and 37% fewer respondents, respectively, compared to the second most-cited reason. Among respondents who remained in the Kanto region, the primary reason was "personal decision" (80%) followed by "job obligation" (54%). The percentage of respondents who cited these two reasons in this group was noticeably higher than for respondents who relocated to another area of Japan or left Japan entirely. For respondents who relocated within Japan, the results generally tended to fall between the percentages of the other two groups (left Japan or remained in the Kanto area).

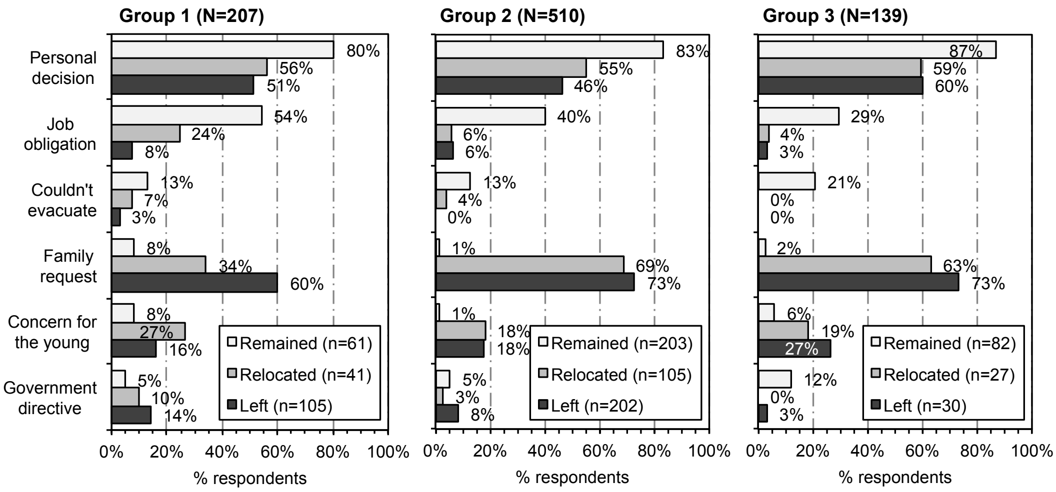

Figure 3: Effect of government advisory on reasons for post-disaster action

The results for Group 2 were similar to those of Group 1. The most-cited reason among both respondents who relocated to another of Japan and left Japan entirely was "family request" (69% and 73%, respectively). This was followed by "personal decision" (55% and 46%, respectively). Again, there was a large difference between the second and third most-cited reason for both groups: "concern for babies and children" (18% for both groups) was third and "government directive" (3% for respondents who relocated and 8% for respondents who left) was fourth. Among respondents who remained in the Kanto region, "personal decision" (83%) and "job obligation" (40%) were the most-cited reasons, following the pattern shown by Group 1.

In Group 3, the trend among respondents who relocated or left Japan was similar to that of Groups 1 and 2. The most-cited reasons were "family request" (63% and 73%, respectively), "personal decision" (59% and 60%, respectively), and "concern for babies or children" (19% and 27%, respectively). However, among respondents who elected to remain in the Kanto area, "personal decision" (87%) was the most-cited reason, followed by "job obligation" (29%).

Although, when comparing the results of each group, a general trend can be observed, it is difficult to fully clarify the true reason for the post-disaster action because the most-cited reason – regardless of the action – was "personal decision," the meaning of which will vary widely between individuals. Respondents from countries which issued more cautious advisories had a slightly higher tendency to cite "government directive" as their reason for post-disaster action. However, it was much less cited than "family request" or even "concern for babies or children." Furthermore, respondents who remained in Kanto despite their government's advisory to leave had a higher tendency to cite "job obligation."

Finally, for respondents who evacuated from Japan even though their government issued no specific advisory, "family request" was the most-cited reason and, understandably, they did not cite "government directive." In addition, "job obligation" was clearly another reason why these respondents chose to stay in the Kanto region.

5. CONCLUSION

This paper first gathered and sorted the previously undocumented information on the temporary closure and relocation of embassies in Tokyo and the advisories issued by foreign governments. Next, a combination of descriptive and statistical analyses were presented on how those advisories affected the post-disaster evacuation or relocation action of foreigners residing in the Kanto region of Japan. A clear relationship between the level of government advisory and post-disaster action was observed, as respondents from countries with more cautious advisories appeared more likely to leave or relocate. However, further analyses must consider these results together with the trend in other factors such as demographic characteristics. A comprehensive analysis examining all these factors will be very helpful in understanding the foreigner exodus phenomenon observed after the 2011 Great East Japan Earthquake disaster.

ACKNOWLEDGEMENT

This research was partially supported by the Japan Society for the Promotion of Science (Challenging Exploratory Research: "*Investigation on disaster* *information dissemination to foreigners after the great earthquake in Tokyo metropolitan area*”). In addition, the authors would like to express their gratitude to everyone who cooperated with and supported this investigation.

REFERENCES

Kawasaki, A., Henry, M., Meguro, K., 2012. Analysis of disaster information gathering behavior and language ability after the 2011 Tohoku Earthquake. *2012 New Technologies for Urban Safety of Mega Cities in Asia (ICUS Report 2012-03)*, Ulaanbaatar, Mongolia, 263-271.

Further modification and working stress design using K-stiffness method on soft and hard foundations

Sowarapan DUANGKHAE[1], Dennes T. BERGADO[2], Pankaj BARAL[3] and Barry T. OCAY[4]
[1] D. Eng. Graduate, Asian Institute of Technology, Thailand
[2] Professor, Asian Institute of Technology, Thailand
bergado@ait.ac.th, dbergado@gmail.com
[3] Research Assistant, Asian Institute of Technology, Thailand
[4] M .Eng. Graduate, Asian Institute of Technology, Thailand

ABSTRACT

In this paper, current design methods for internal stability design of geosynthetic and steel reinforced soil structures that are based on limit equilibrium concepts were compared with working stress K-stiffness method based on the data obtained from five full-scale reinforced embankments – two were constructed on hard ground and three on soft ground. A common element of this data set is that all the embankments were backfilled with cohesive-frictional soils. These embankments were reinforced with steel wire grids, metallic strips, hexagonal wire mesh and geogrid materials particularly polyester (PET), polypropylene (PP) and high density polyethylene (HDPE). Generally, the reinforcement loads predicted by AASHTO simplified method and FHWA structure stiffness method were consistently higher than those of working stress K-stiffness method and the measured reinforcement loads for all cases of embankments on hard and soft ground immediately after construction and at any periods after the completion of the embankment. Moreover, the load distribution factor, Dtmax, and the reinforcement load prediction approach for geogrid and hexagonal wire mesh reinforced embankments were also modified to be the same as both types of embankment showed the same behavior on the distribution and magnitude of reinforcement loads.

Keywords: *reinforced embankment, soft ground, hard ground, load distribution factor, limit equilibrium method and working stress method.*

1. INTRODUCTION

For the internal stability design of geosynthetic and steel reinforced soil walls, appropriate determinations of soil reinforcement loads and deformations are necessary. The predicted reinforcement loads impact the strength and spacing required for the reinforcement as well as the reinforcement length to resist pullout. Two limit equilibrium methods can be found in recent North American design specification to determine reinforcement loads: (i) the Tieback Wedge/Simplified

Method (AASHTO 2002), and (ii) the FHWA Structure Stiffness Method (Christopher et al. 1990). Current design methodologies uses limit equilibrium concepts to calculate reinforcement loads. K-stiffness methods, which is a novel working stress analytical method, as an original method (Allen et al, 2003) and modified method (Miyata and Bathurst, 2007b) have been proposed as alternatives of the conservative limit equilibrium methods. Tin et al. (2011) modified the K-stiffness method combining the effects of cohesion and settlements. The content of this paper is successful to validate the K-stiffness method for reinforced embankment on hard foundation and to compare the corresponding performance of reinforced embankments on soft foundation. Moreover, further modifications of K-stiffness method were made by investigating the effects of cohesion and settlement factors separately.

2. TEST EMBANKMENTS ON DMM IMPROVED SOFT FOUNDATION AND HARD FOUNDATION

2.1 Reinforced embankments on DMM improved soft foundation

The reinforced soil test embankment with 6m vertical height, 19 m length and 6 m width was erected at Wangnoi District of Ayuthaya province located 35 km north of AIT campus in Thailand (Lai et al. 2006 and Lai, 2009). The embankment was backfilled with silty sand material and reinforced with hexagonal wire mesh strips. Vertical precast concrete panel having a dimension of 1.5m x 1.5m x 0.15m per panel/element was utilized as facing material of the wall. The compressible foundation of the embankment was improved by DMM cement-clay piles using jet grouting pressure of 20MPa. Circular soil-cement piles of diameter 0.6m were placed at 1.5m spacing at the middle section and 2 m spacing at the edge portion of the embankment in square pattern. Immense field instrumentation program was employed to study the behavior and performance of the embankment and its foundation. The sectional view of the embankment and location of instrumentations are shown in Fig. 1. The foundation loads and settlements of the embankment at ground surface are plotted in Fig. 2.

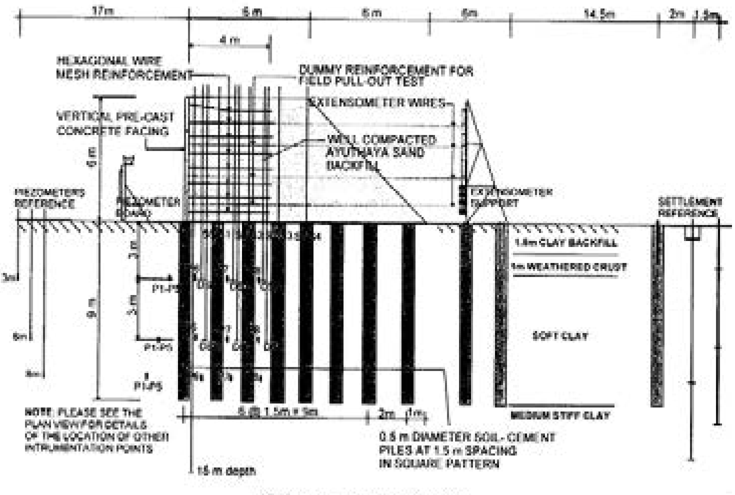

Figure 1: Full schematic diagram of the instrumentation program at test embankment (Lai, 2009; Lai et al, 2006)

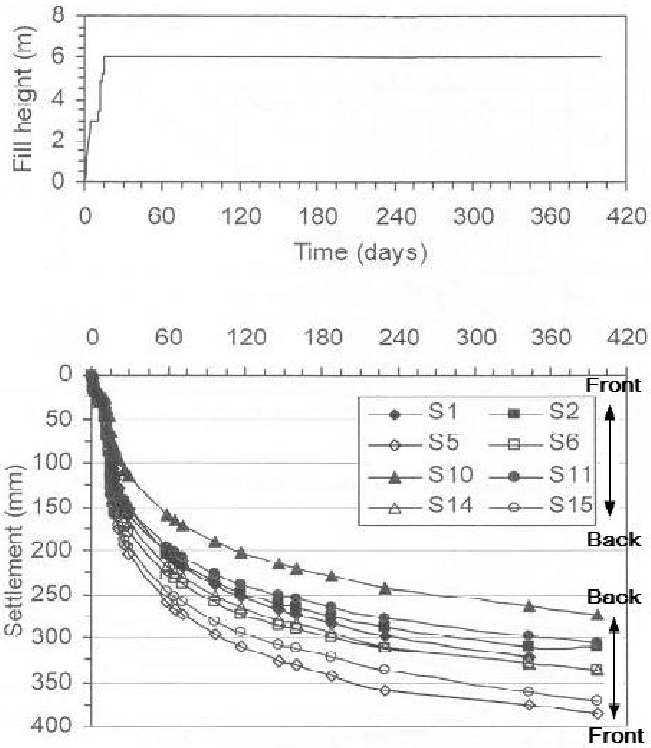

(Note: Solid symbols on piles
Hollow symbols on clay between piles)

Figure 2: Foundation loads and settlements with time on ground and on piles near the centre of embankment (Lai, 2009; Lai et al, 2006)

2.2 Reinforced embankment on hard Foundation

A full scale reinforced earth embankment was designed and constructed by Thailand Department of Highways (DOHs) and studied by Baral (2012). The construction site is near the Highway No.11 in Phitsanulok Thailand. The backfill soil consists of 50% lateritic soil and 50% silty sand with effective cohesion ranging from 5 to 20kPa and effective friction angle of 37 degrees measured from CU tension triaxial tests. The embankment consisted of reinforced soil slope (RSS) with 70 degrees from the horizontal with soil bags facing on one side. The other side consisted of mechanically stabilized earth wall (MSEW) with concrete panel facing. The RSS and MSEW test embankment were designed to 6 m of height, 15 m of width and 18 m of length. Three different types of polymeric geogrids reinforcement were installed, namely: polypropylene (PP), high density polyethylene (HDPE) and polyester (PET) on the reinforced soil slope (RSS) side. At the other side, the mechanically stabilized earth wall (MSEW) was constructed with two types of metallic reinforcements such as metallic strip (MS) and steel wire grid (SWG). The polymer and metallic reinforcements are shown in Fig. 3. The vertical spacing of the reinforcement layer was 0.5 m and the length was 5 m (Upper layers of metallic strip from layer 7 to layer 12 have 5.80 m length). The monitoring instruments are shown in Figs. 4 and 5 in plan and section views, respectively, consisting of inclinometers, strain gauges, piezometers, plate settlements and pressure cells. The metallic reinforcements consist of vibrating wire strain gauges while fiber optic was utilized in the polymer reinforcements. The hard foundation consists of interlayering of dense to very dense sand and very stiff to hard clay. The embankment was constructed to 6m in height for 125 days. Subsequently, a surcharge of 20 kPa (1.2 m thick) was added until 186 days after construction as shown in Fig. 5. The vertical settlements are plotted across the section with polyester (PET) and steel wire grid (SWG) reinforcements of the embankment as shown in Fig. 6. A sensitivity analysis varying the effective cohesion such as 5, 10 and 15 kPa were done, which indicated that 10 kPa confirmed the predictions.

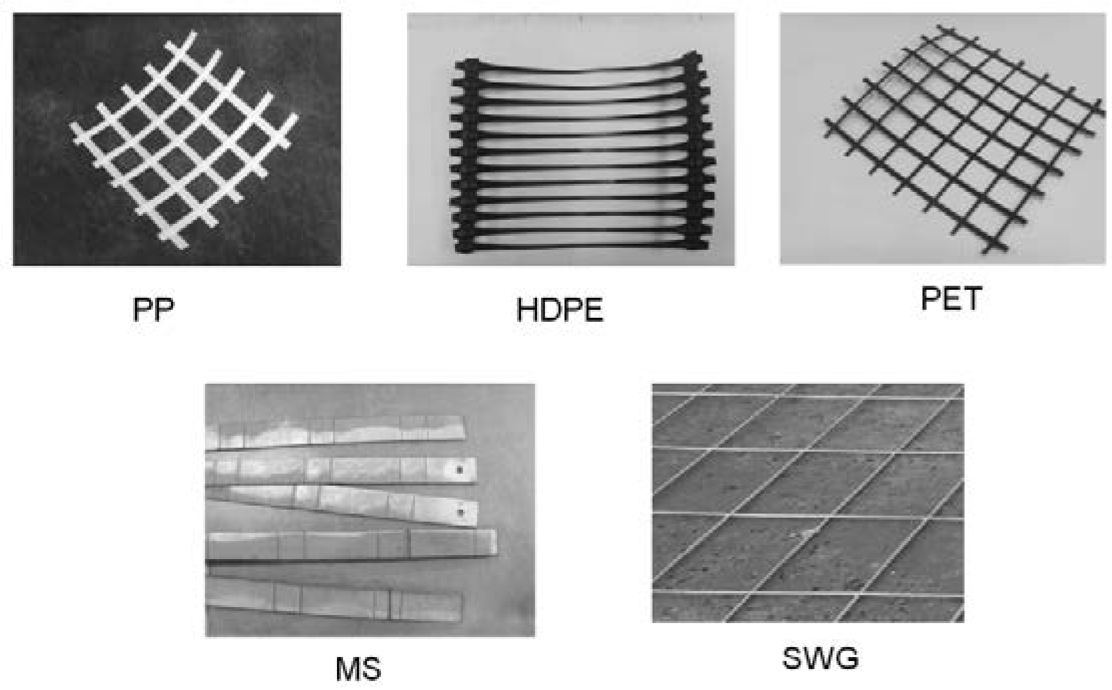

Figure 3: Polymer and metallic reinforcing materials

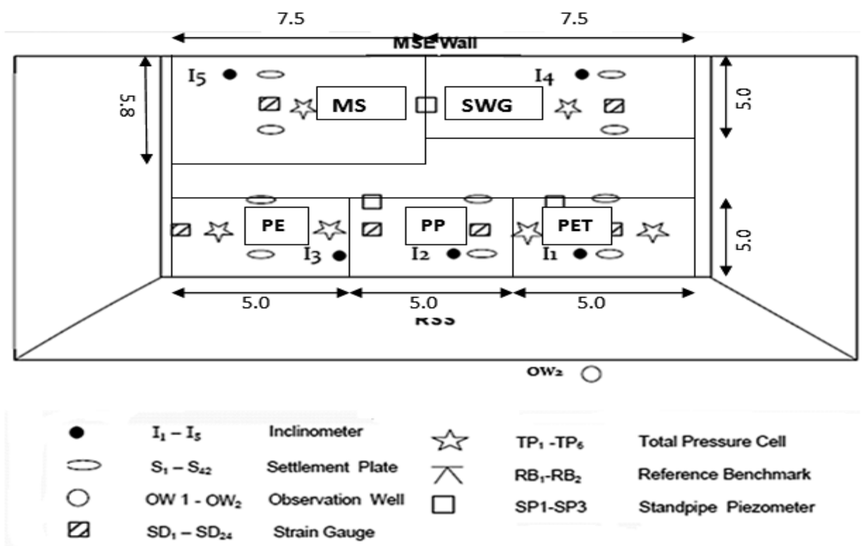

Figure 4: Plan of MSE wall/embankment

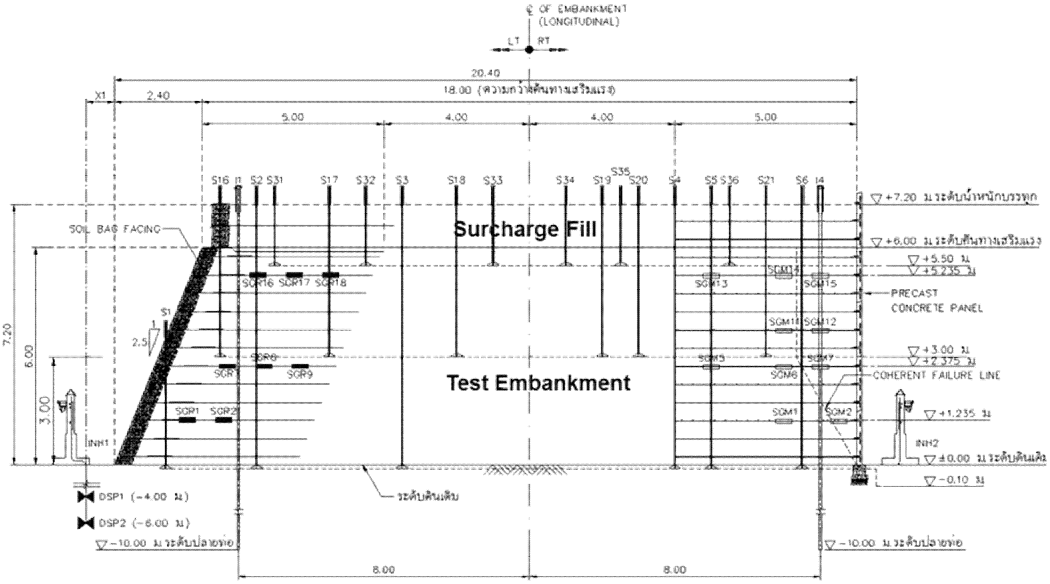

Figure 5: Cross section of MSE wall/embankment indicating the location of the monitoring instrument

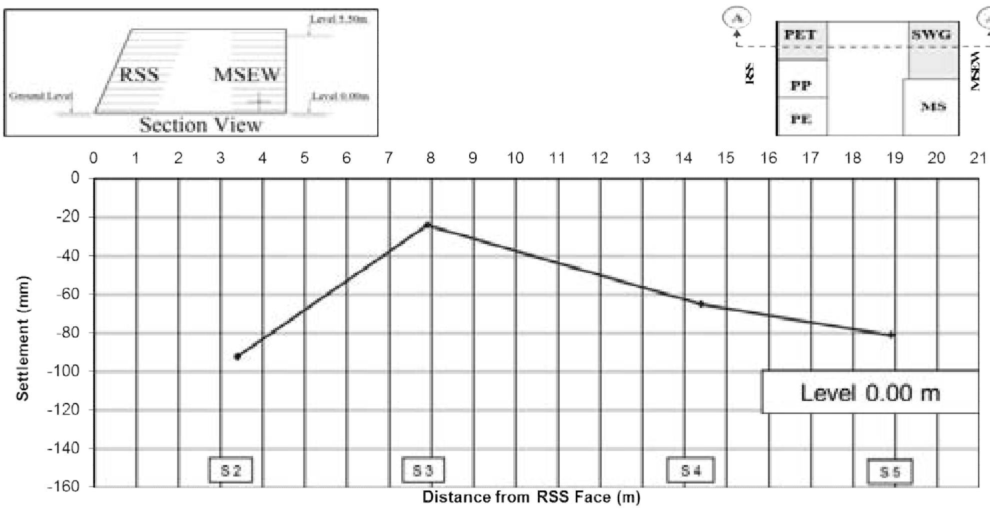

Figure 6 Compression profile of PET-SWG section at level 0.00m (bottom of embankment) at 186 days after construction.

3. PREVIOUS TEST EMBANKMENTS ON UNIMPROVED SOFT GROUND FOUNDATIONS

To validate the original and modified K-stiffness method, the data obtained previously from two test embankments constructed on unimproved soft Bangkok clay at AIT Campus were used by Tin (2009) and Tin et al. (2011). One embankment was reinforced with steel grids with three different backfill materials consisting of clayey sand (CS), lateritic soil (LS) and weathered clay (WC) as briefly described in section 3.1. The other was reinforced with two types of hexagonal reinforcement with silty sand backfill as briefly described in section 3.2. Details of this embankment were described by Tin (2009) and Tin et.al (2011).

3.1 Steel grid reinforced wall/embankment

Shivashankar (1991) and Bergado et al. (1991 a,b) noted the behavior of a welded wire wall with poor quality, cohesive-friction backfills on soft Bangkok clay. The wall with a vertical wire mesh facing had the height of 5.7 m, length of 14.64 m at the top and was divided into three sections along its length (Fig 7). The welded wire mats were 2.44 m wide and 5.0 m long and consisted of W4.5 x W3.5 (6.07 x 5.36 mm diameter) size bars with 6 x 9 in. (0.15 x 0.225 m) grid opening. There were seven mats instrumented with self-temperature compensating electrical resistant strain gauges for each section (Fig. 8). The vertical spacing between the reinforcement mats was 0.45 m. The backfill soil parameters as tabulated in Table 1 were deduced from CIU tests (Bergado et al, 1991a,b). The tensions in the reinforcement immediately after construction for the three types of backfills consisting of clayey sand, lateritic soil and weathered clay were similar. Figure 9 shows the typical values of reinforcement tension for clayey sand backfill. Moreover, the surface settlements were also observed as plotted in Fig. 10. The settlement profiles are also plotted at the bottom of Fig. 9. The soil profile of the embankment foundation consists of the uppermost 2.0 m thick weathered clay layer underlain by 6.0 m thick soft clay layer and followed by 6.0 m thick stiff clay layer. The strength and compressibility parameters are given in Bergado et al. (2000) and Bergado and Teerawattanasuk (2008).

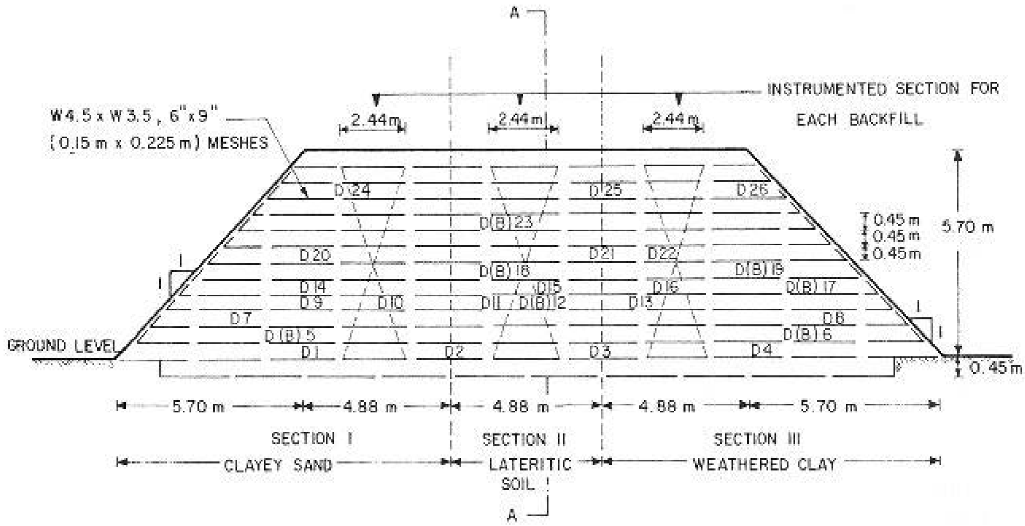

Figure 7: Front (longitudinal) section of the welded wire wall (Bergado et al., 1991 a,b)

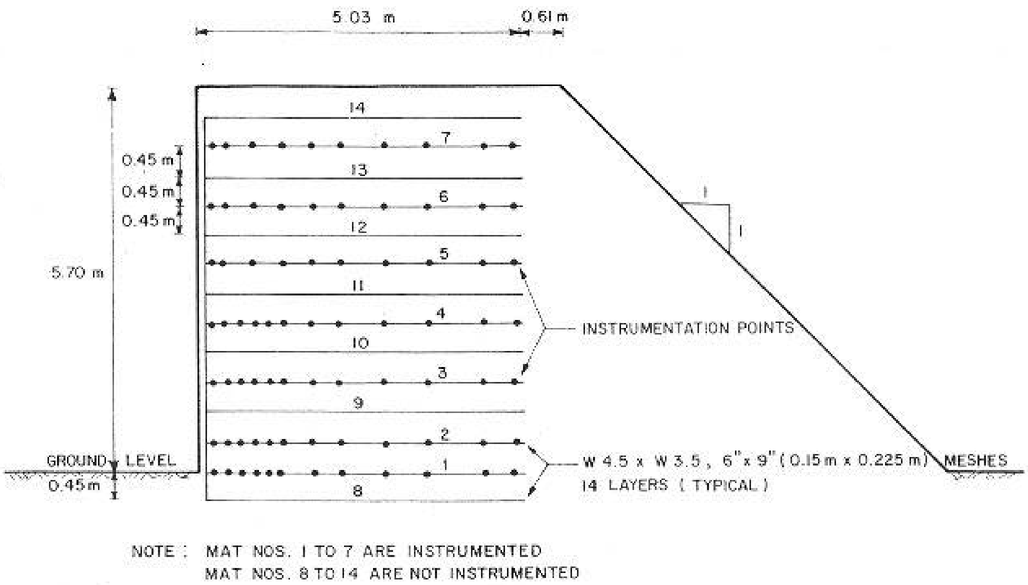

Figure 8: View of the welded wire wall along section A-A (Bergado et al., 1991). Note: mats 1 to 7 are instrumented; mats 8 to 14 are not instrumented.

Table 1: Parameters used to validate the data obtained from previous studies of MSE structures at AIT

	Shivashankar (1991) , Bergado et al. (1991)			Voottipruex (2000), Bergado et al. (2000)
	Fill material type			Reinforcement type
	Clayey sand	Lateritic soil	Weathered clay	PVC-coated wire mesh
Peak triaxial friction angle, $_{tx}$’ (degrees)	24	25.2	24	30
Cohesion *c’* (kN/m^2)	10	20	30	5
Unit weight of the soil (kN/m^3)	17	19.3	16.3	18
Height of the wall *H* (m)	5.7	5.7	5.7	6
Equivalent height of uniform surcharge pressure *S* (m)	0	0	0	0
Tributary area S_v (m)	0.45	0.45	0.45	0.5
Tensile stiffness J_i = $J_{2\%}$ (kN/m)	36000	36000	36000	1140

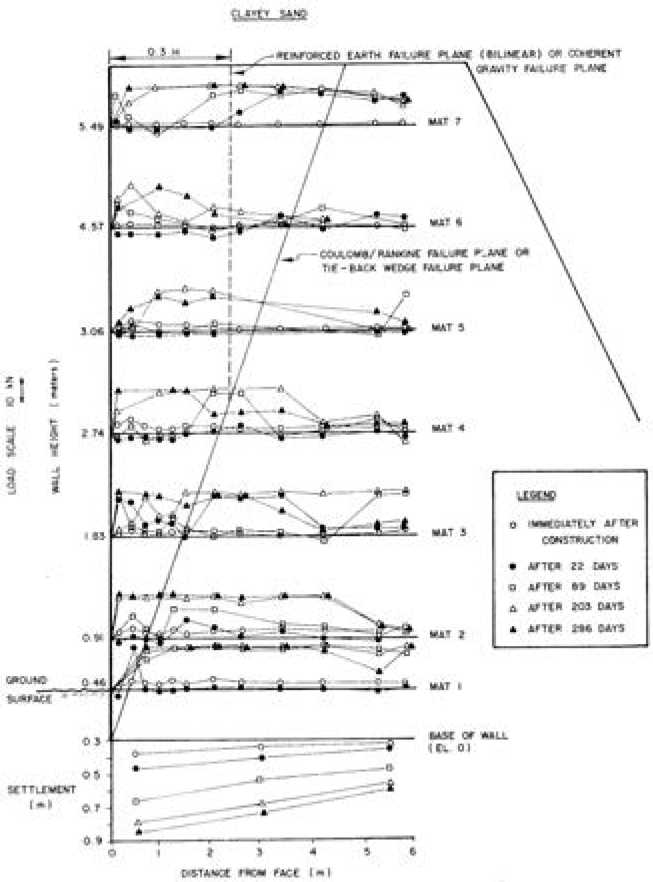

Figure 9: Variation of tensions in the longitudinal bars immediately after construction and for different periods after construction (clayey sand) (Bergado et al., 1991 a,b)

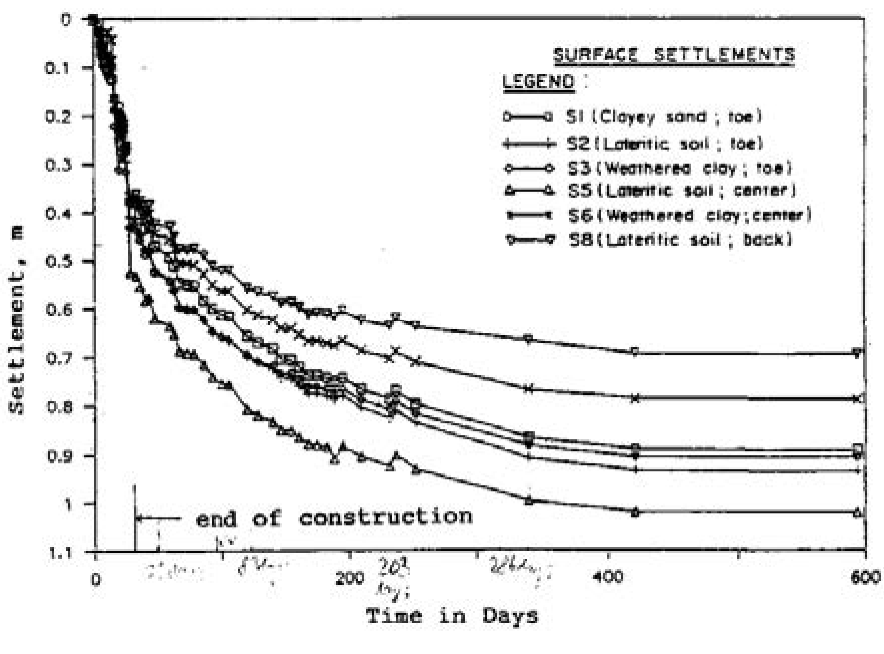

Figure 10: Observed surface settlements (Bergado et al., 1991a,b)

3.2 Hexagonal Wire Mesh Reinforced Wall

Voottipruex (2000) and Bergado et al (2000) investigated the behavior of full scale hexagonal wire grid reinforced embankment constructed in AIT campus with 6m height and 10 degree slope of gabion facing as shown in Fig. 11. The facing consisted of large rectangular wire baskets with 1m by 1m in cross section linked together and filled with rocks. Two types of hexagonal wire reinforcements, namely: zinc-coated and PVC-coated with different apertures, were used in two different sections along the length of the wall; and the vertical spacing between the reinforcement layers was 0.5 m. The silty sand backfill was found to have an effective internal friction angle of 30^o and effective cohesion intercept of 5 kPa as tabulated in Table 1 (Bergado et al., 2000; Bergado and Teerawattanasuk, 2008). The strength parameters were deduced from CIU triaxial tests with soil specimen compacted at maximum dry density (γ_{dmax}=18kN/m^3) and optimum moisture content (w=13%). The foundation subsoil layers were similar to the previously mentioned steel grid reinforced embankment. The tensions in the PVC-coated hexagonal wires with distance from the back face of the wall after construction are given in Fig. 12. In addition, the corresponding surface settlements were also observed for a period of 400 days as plotted in Fig. 13.

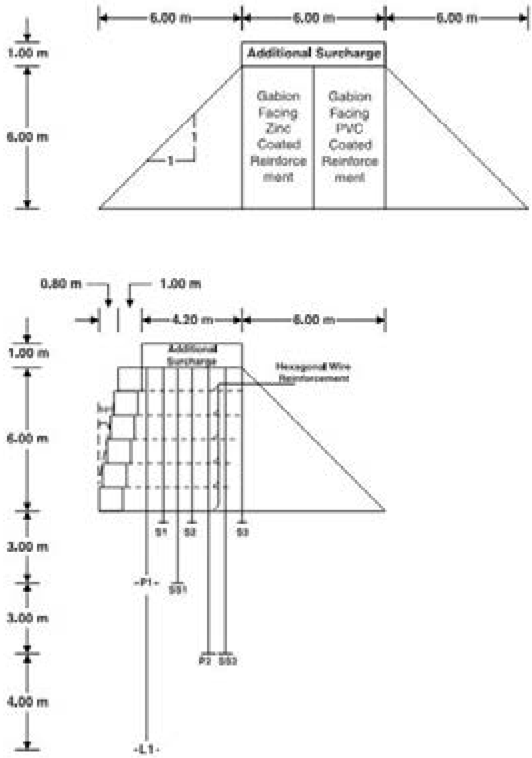

Figure 11 Front and section views of the hexagonal wire reinforced wall (Voottipruex, 2000)

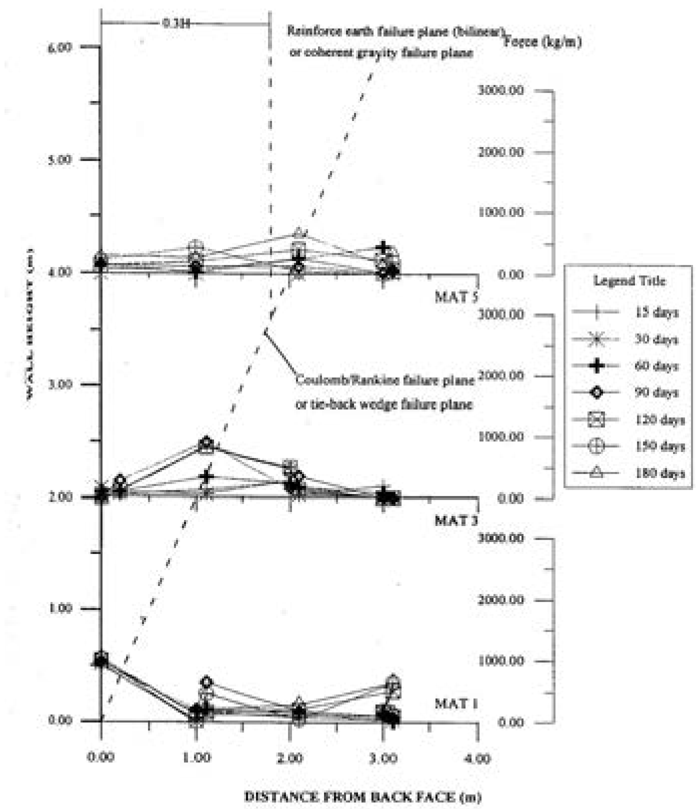

Figure 12: Reinforcement tension of PVC-coated wire mesh at different periods after construction (Voottipruex, 2000)

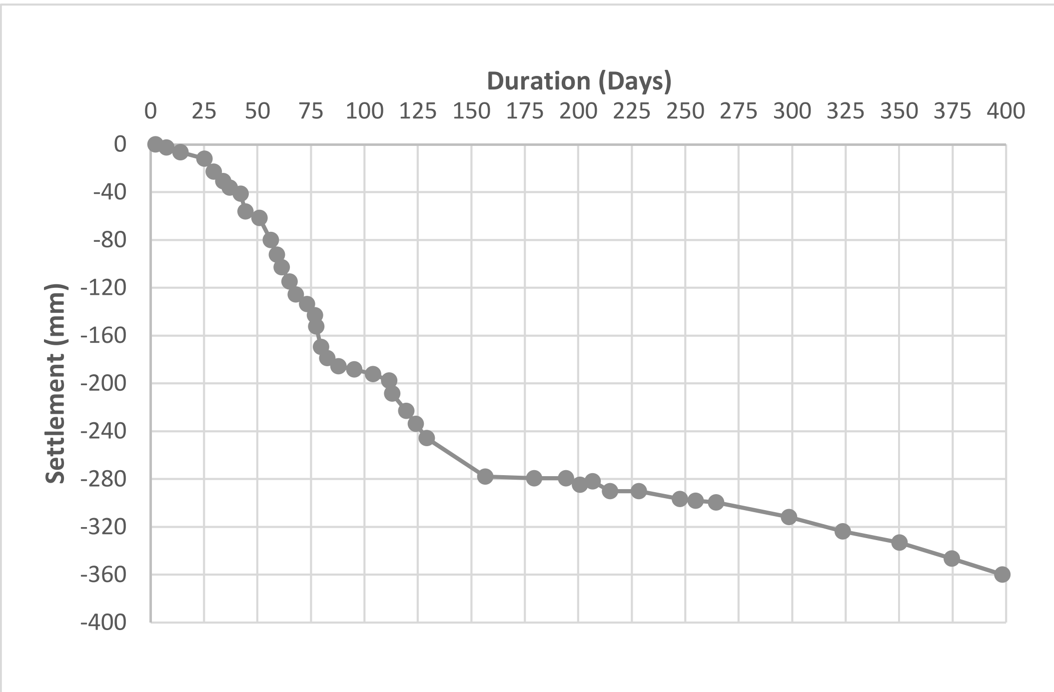

Figure 13: Observed ground surface settlement for embankment reinforced with PVC coated wire mesh (Voottipruex, 2000)

4. FURTHER MODIFICATION OF K-STIFFNESS METHOD FOR REINFORCED EMBANKMENT ON SOFT AND HARD GROUND

The contribution of consolidation settlements to the reinforced embankment in terms of distribution and magnitude of reinforcement loads as well as the lateral movement of the embankment facing were observed in the reinforced embankment case histories considered in this study. The embankments were evaluated for their performance immediately after construction and at different periods after completion of the embankment. Current design methods are not calibrated and evaluated for possible post-construction load increase. Thus, further modification of K-stiffness method to include settlement factor in addition to cohesion factor is proposed. The zinc-coated hexagonal wire mesh reinforced embankment section studied by Voottipruex (2000) were eliminated in the analysis because these embankments were judged poorly on the criterion set by Miyata and Bathurst (2007b) that the strain rates in the reinforcements should decrease as the time after the construction increases. The above statement is particularly applicable in this study for periods after the completion of the embankment when the ground has already attained considerable consolidation settlement. When the ground attains stability i.e. during the end of the primary consolidation of the foundation, the increase in strain rates of the reinforcements in the embankment should decrease.

The settlement factors, Φ_s, for the reinforced embankment case histories were back-calculated from the maximum measured reinforcement load in the embankment for each period after the construction. Subsequently, the back-calculated settlement factors were plotted against the normalized settlement ratio expressed as $S/\gamma H$ as shown in Fig. 18 for geogrid and hexagonal wire mesh, and metallic reinforcements, respectively. Considering the type of reinforcements used in the embankments and the range of values for the normalized settlement ratio, $S/\gamma H$, the settlement factor, Φ_s, is expressed as follows in Equations 1 and 2.

For geogrid and hexagonal wire mesh reinforced embankments:

For $S/\gamma H \leq 4.00$:

$$\Phi_s = 1.37(S/\gamma H) + 0.5 \quad (1)$$

For metallic reinforced embankments:

For $S/\gamma H > 4.00$:

$$\Phi_s = 0.076(S/\gamma H) + 2.00 \quad (2)$$

where Φs is the foundation settlement factor, S is the magnitude of foundation settlement at ground surface (mm) at any particular period, γ is the unit weight of backfill material (kN/m^3) and H is the height of the reinforced embankment.

As observed in Figs. 14 a,b to 17 a,b ,the maximum measured reinforcement loads in the embankment were generally found at the base of the reinforced soil embankment. Consequently, the load distribution factor, D_{tmax}, for geogrid and hexagonal wire mesh reinforced soil structure was further modified based on this observation. Subsequently, a uniform value of D_{tmax} equal to 1.0 was used starting from the normalized depth, $(z+S)/(H+S)$, value of 0.4 to the base of the reinforced soil structure where the normalized depth, $(z+S)/(H+S)$, value is equal to 1.0. The D_{tmax} for the metallic reinforced soil structure was not modified and the load distribution factor still applies. Finally, with the further modifications of the *K*-stiffness method, the maximum reinforcement load per unit width of the embankment is expressed in Equation 3.

$$T_{max} = ½\, K\, \gamma\, (H + S)\, S_v\, D_{tmax} \Phi_g \Phi_{local}\, \Phi_{fs} \Phi_{fb} \Phi_c \Phi_s \tag{3}$$

where the terms have been defined previously.

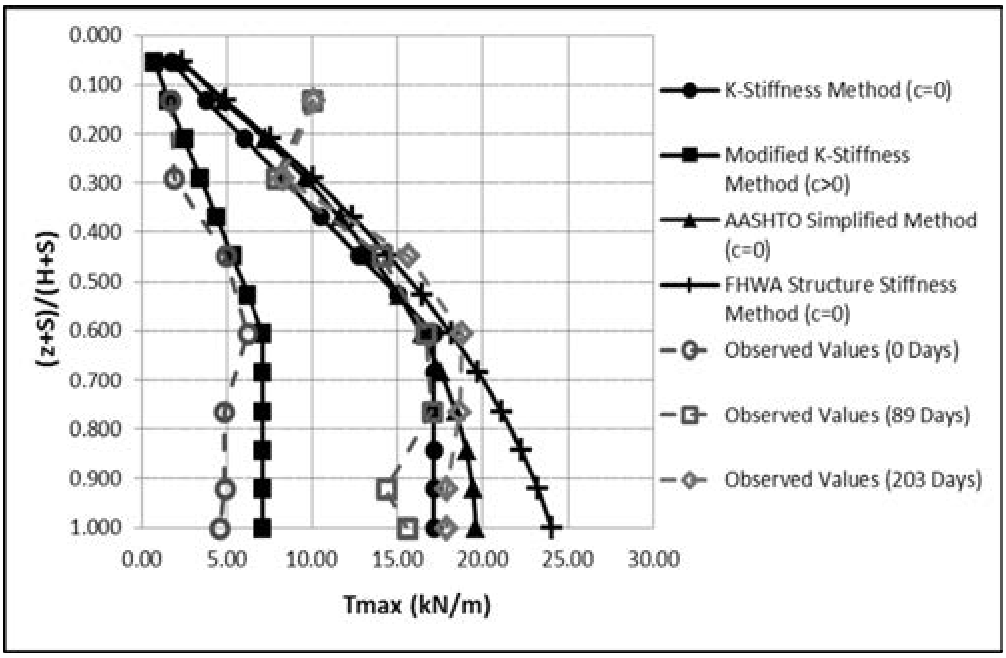

(a) Comparison of measured and predicted reinforcement load

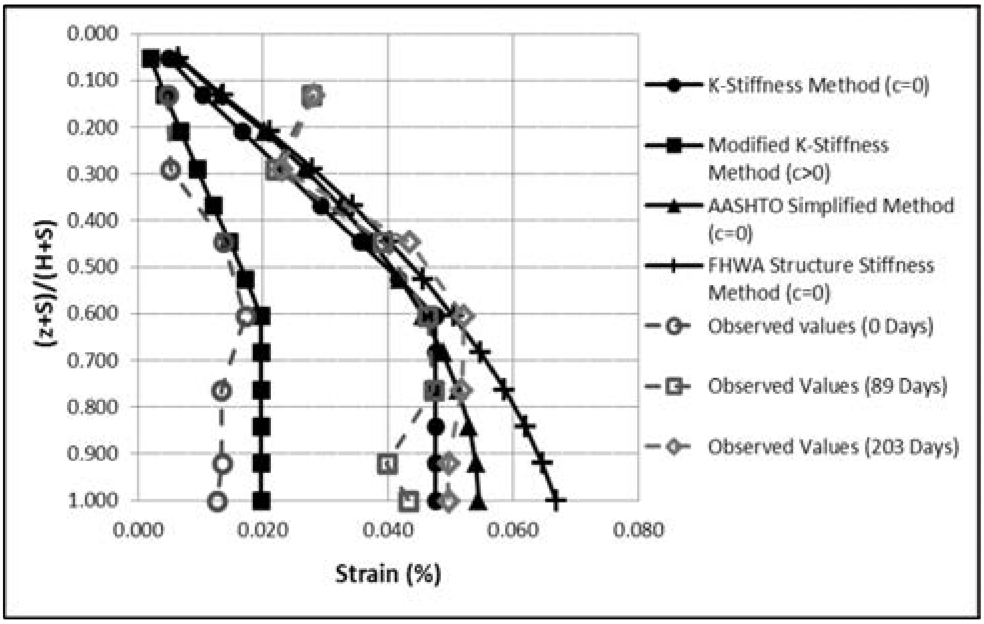

(b) Comparison of measured and predicted reinforcement strain

Figure14a,b: Measured and predicted reinforcement load and strain for SWG embankment with poor quality backfills (clayey sand) on soft ground (Shivashankar, 1991)

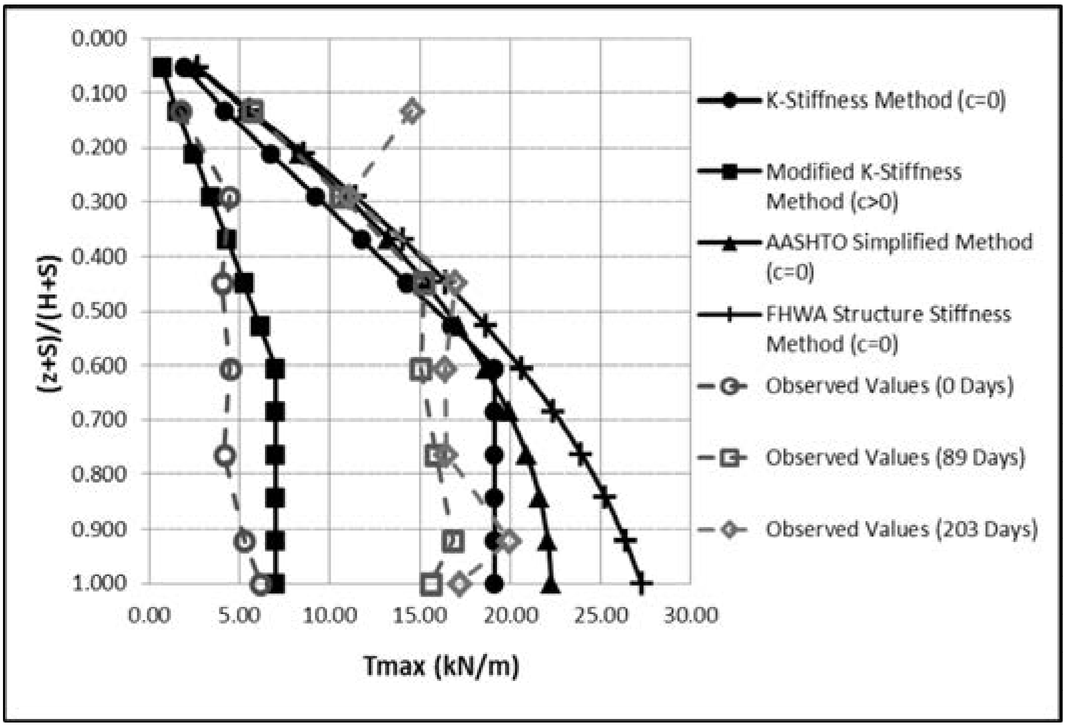

(a) Comparison of measured and predicted reinforcement load

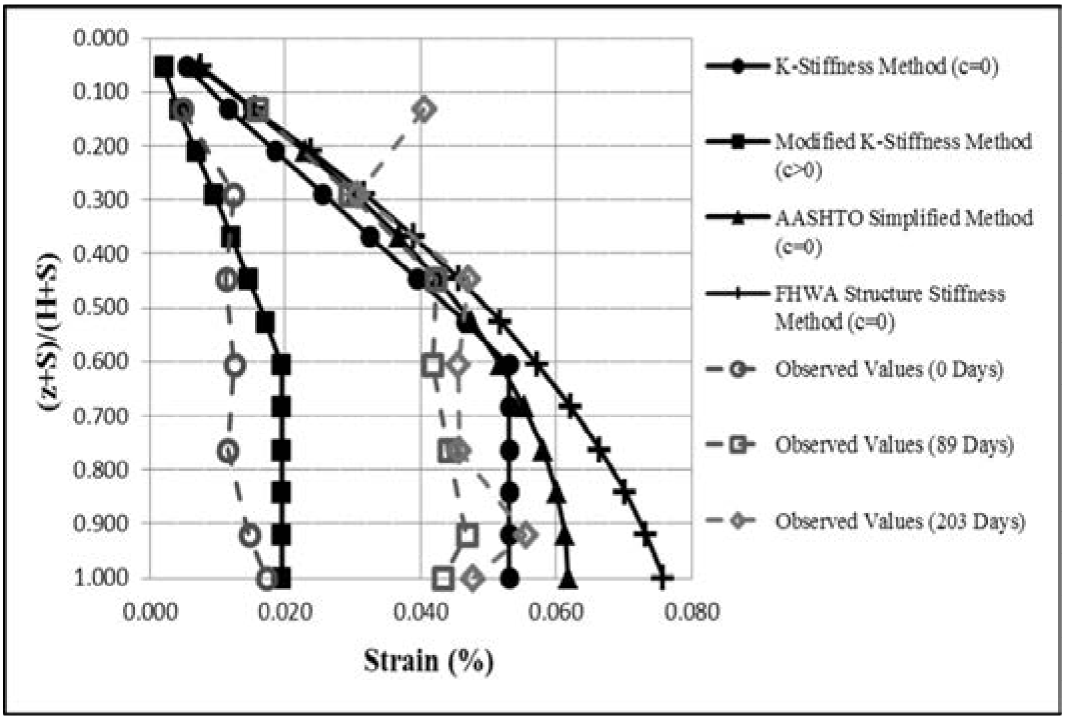

(b) Comparison of measured and predicted reinforcement strain

Figure 15 a,b: Measured and predicted reinforcement load and strain for SWG embankment with poor quality backfills (lateritic residual soil) on soft ground (Shivashankar, 1991)

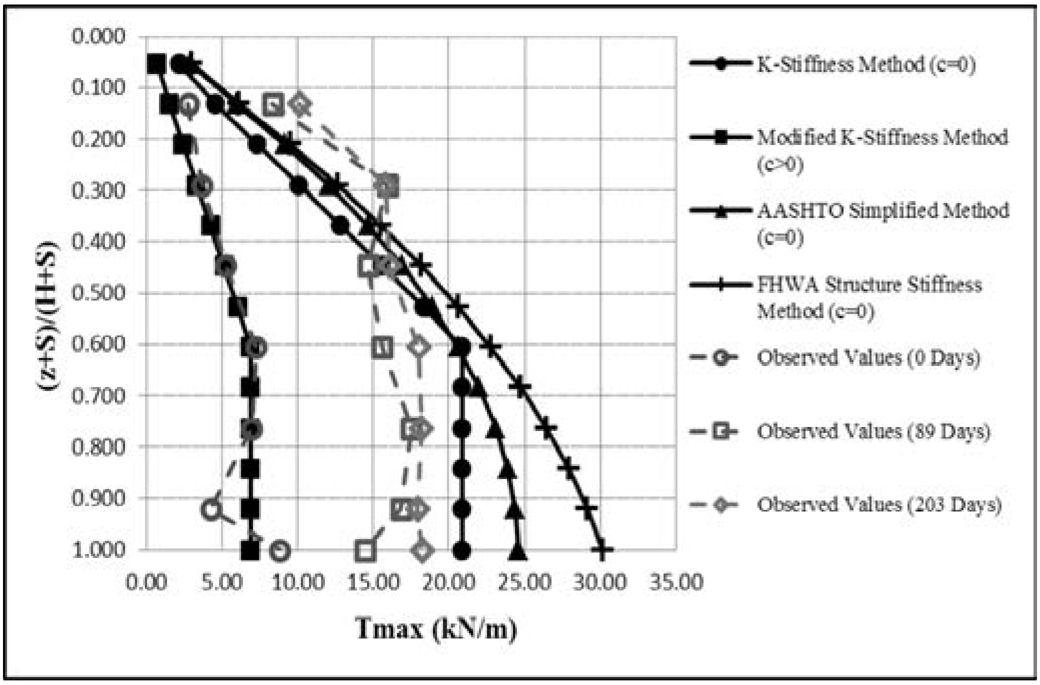

(a) Comparison of measured and predicted reinforcement load

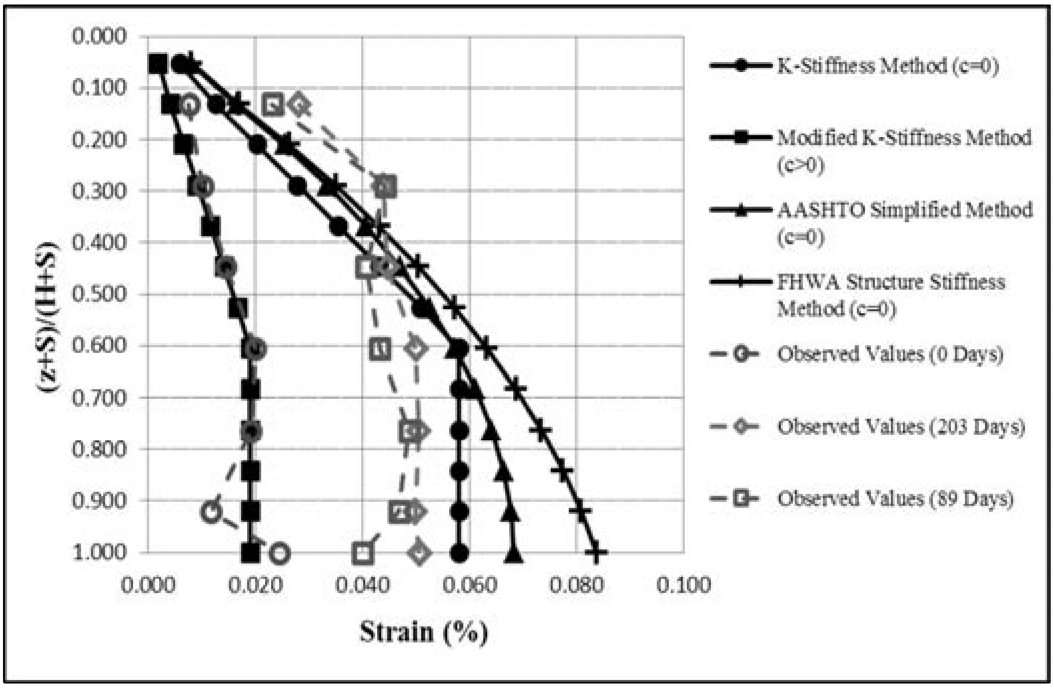

(b) Comparison of measured and predicted reinforcement strain

Figure 16a,b: Measured and predicted reinforcement load and strain for SWG embankment with poor quality backfills (weathered clay) on soft ground (Shivashankar, 1991)

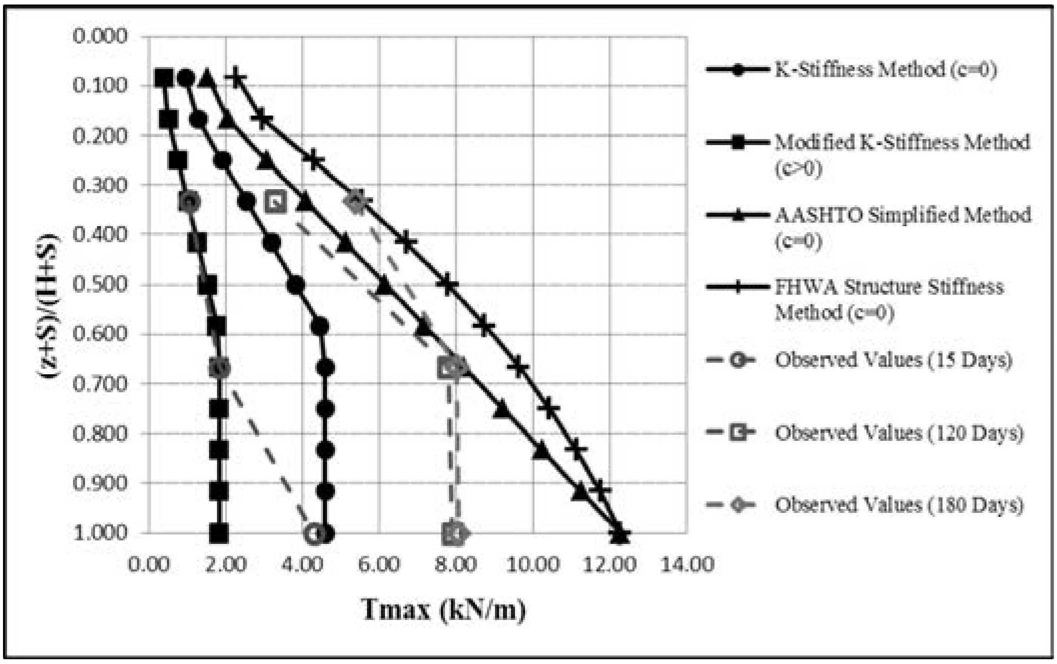

(a) Comparison of measured and predicted reinforcement load

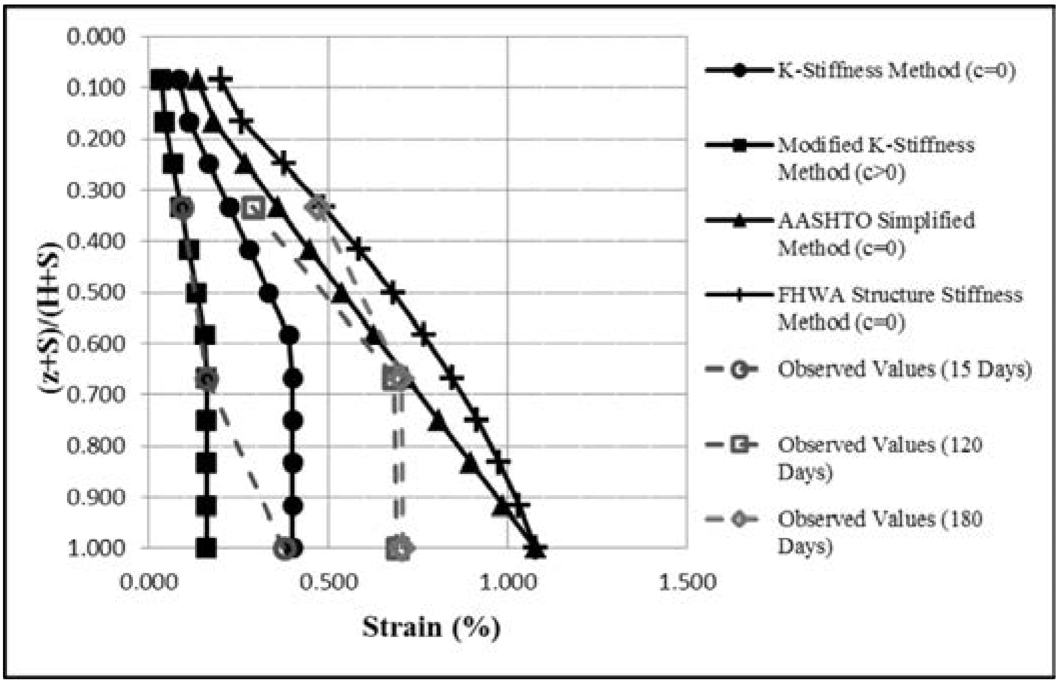

(b) Comparison of measured and predicted reinforcement strain

Figure 17 a,b: Measured and predicted reinforcement load and strain for HWM (PVC-coated) embankment on soft ground (Voottipruex, 2000)

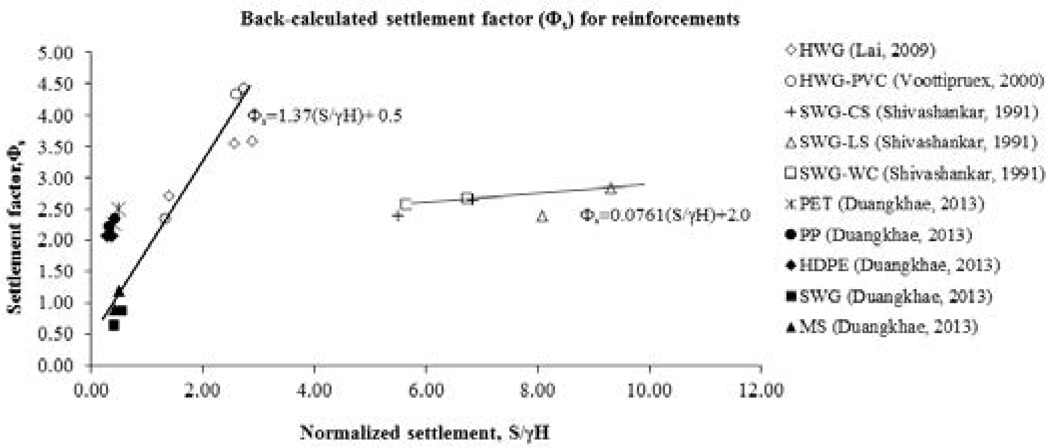

Figure 18: Back-calculated settlement factor, Φ_s for geogrid and hexagonal wire mesh (HWM) reinforcements and metallic strip reinforcements versus normalized settlement ratio, $S/\gamma H$

5. CONCLUSIONS

In this study, current reinforcement load prediction methods were presented and applied to assess the data obtained from four full-scale and fully instrumented reinforced embankments previously studied in AIT. Two of these reinforced embankments were constructed on hard ground while the rest were constructed on soft ground. These embankments were reinforced with steel wire grids, metallic strips, hexagonal wire mesh and geogrid materials particularly polyester (PET), polypropylene (PP) and high density polyethylene (HDPE). From the results of the analyses performed on the embankment case histories, the following conclusions were drawn:

1. The rate of increase in the magnitudes of the reinforcement load with respect to time was minimal for the embankments on hard ground but significant for the embankments on soft ground. The increase in the magnitude of the measured reinforcement loads especially at the base of the embankment is therefore proportional to increase in value of ground settlement.
2. Further modification of K-stiffness method was proposed by introducing a separate settlement factor, Φ_s, on the modified K-stiffness method in order to take into account the effect of foundation settlement on the magnitude and distribution of reinforcement load.

REFERENCES

AASHTO, 2002. Standard specifications for highway bridges. 17th Edition. American Association of State Highway and Transportation Officials (AASHTO), Washington, D.C., U.S.A.

Allen T.M., Bathurst R.J., Holtz R.D., Walters D. and Lee W.F., 2003. A new working stress method for prediction of reinforcement loads in geosynthetic walls. *Canadian Geotechnical Journal* 40: 976-994.

Bergado D.T. and Teerawattanasuk C., 2008. 2D and 3D numerical simulations of reinforced embankments on soft ground. *Geotextiles and Geomembranes* 26: 39-55.

Bergado D.T., Sampaco C.L., Shivashankar R. *et al.*, 1991a. Performance of welded wire wall with poor quality backfills on soft clay. In *ASCE GeotechnicalEngineering Congress,* Boulder, Colorado, U.S.A. pp. 909-922.

Bergado D.T., Shivashankar R., Sampaco C.L., Alfaro M.C. and Anderson L.R., 1991b. Behavior of welded-wire wall with poor quality cohesive-frictional backfills on soft Bangkok clay. *Canadian Geotechnical Journal* 28: 860-880.

Bergado D.T., Teerawattanasuk C., Youwai S. and Voottipruex P., 2000a. FE modeling of hexagonal wire reinforced embankment on soft clay. *Canadian Geotechnical Journal* 37: 1209-1226.

Lai Y.P., 2009. *Performance and Behavior of Full Scale Reinforced Soil Embankment/Wall on DMM Improved Foundation*. D. Eng. Dissertation No.GE-08-02, AIT, Bangkok, Thailand.

Lai Y.P., Bergado D.T., Lorenzo G.A. and Duangchan T., 2006. Full-scale reinforced embankment on deep jet mixing improved ground. *Ground Improvement* 10(4): 153-164.

Miyata Y. and Bathurst R.J., 2007a. Evaluation of K-stiffness method for vertical geosynthetic reinforced granular soil walls in Japan. *Soils and Foundations* 47(2): 319-335.

Miyata Y. and Bathurst R.J., 2007b. Development of the K-stiffness method for geosynthetic reinforced soil walls constructed with c-ϕ soils. *Canadian Geotechnical Journal* 44: 1391-1416.

Baral P., 2012. *Simulation and Back-analyses of Design Parameters of MSE wall/embankment on Hard Foundations using PLAXIS 3D Software.* M. Eng. Thesis No. GE-11-, AIT, Bangkok, Thailand.

Shivashankar R., 1991. *Behavior of Mechanically Stabilized Earth (MSE) Embankment with Poor Quality Backfills on Soft Clay Deposits, Including a Study of the Pullout Resistances.* D. Eng. Dissertation No. GT-90-03, AIT, Bangkok, Thailand

Tin N., 2009. *Factors Affecting The Kinked Steel Grid Reinforcement and Modification of K-Stiffness Method in MSE Structures on Soft Ground*. M. Eng. Thesis No.GE-08-03, AIT, Bangkok, Thailand.

Tin N , Bergado DT and Voottipruex P., 2011. Modification of K-stiffness method in MSE structures on soft ground. *Geosynthetic International* 18(5): 304-321.

Voottipruex P., 2000. *Interaction of Hexagonal Wire Reinforcement with Silty Sand Backfill Soil and Behavior of Full Scale Embankment Reinforced with Hexagonal Wire*. D. Eng. Dissertation No. GE-99-1, AIT, Bangkok, Thailand.

Survey of sub-surface cavities in the liquefied ground caused by the Great East Japan Earthquake

Ryoko SERA[1], Yutaka KOIKE[2] and Haruto NAKAMURA[2],
Reiko KUWANO[3] and Jiro KUWANO[4]
[1] Geo Search Co., Ltd., Japan
r-sera@geosearch.co.jp
[2]Geo Search Co. Ltd., Japan
[3]Professor, ICUS, IIS, The University of Tokyo, Japan
[4]Professor, GRIS, Saitama University, Japan

ABSTRACT

A ground penetration radar survey was conducted on the roads of Urayasu-city, Shinkiba-area and Narashino-city, all of which suffered damage caused by the ground liquefaction during the Great East Japan Earthquake. A large amount of fluidized sand, or sand boiling, was observed and a significant number of subsurface cavities were found in the liquefied ground. In this study, patterns of sub-surface cavities observed in the disaster areas are reported and characteristics of sub-surface cavities obtained by the survey are analyzed. It was found that cavities had a tendency to form near manholes and joints in the pavement. These cavities have a larger area, but are thinner compared to cavities normally observed in non-liquefied ground. Most of the cavities have been repaired by either grouting or open-cut method.

Keywords: *subsurface cavity, ground liquefaction, sand boiling, ground loosening*

1. GROUND LIQUEFACTION ALONG THE TOKYO BAY COASTAL AREA CAUSED BY THE GREAT EAST JAPAN EARTHQUAKE

The Great East Japan Earthquake of March 2011 (hereafter**,** “the Earthquake”) brought about disasters unprecedented in magnitude to the nation of Japan. Restoration work in the disaster area is still going on even after two years. The Earthquake played havoc in areas other than East Japan which was directly hit by the main quake and tsunami. The Japanese Geotechnical Society in its two reports [1) 2)] describe the ground foundation damage caused by the Earthquake as “extensive disasters that occurred in various locations covering a large geographical area outside of East Japan”.

Fig. 1: Subsurface cavity survey at a location where sand boiling and subsidence occurred

The most notable among these are ground liquefaction disasters. They occurred widely in reclaimed land sites along the coast of Tokyo Bay and in soft grounds along the lower stream of the Tone River. The ground liquefaction took its toll on the daily life of citizens by causing not only subsidence and tilting of stand-alone private residential houses, but also causing damage to the underground infrastructure. Sewer systems, for example, malfunctioned because of lifting, breaking, and clogging of sewer pipelines[3)], and cave-ins occurred on highways and roads as shown in Fig. 1.

2. STATE AND ANALYSIS OF SUBSURFACE CAVITY FORMATION IN LIQUEFIED GROUND AREAS

2.1 Location of subsurface cavities studied

This study was made based on data of 709 subsurface cavities which were confirmed through the inspection surveys covering a distance of 355km of paved roads. Fig. 2 shows the locations of subsurface cavities, and Table 1 shows a summary of the subsurface cavities studied.

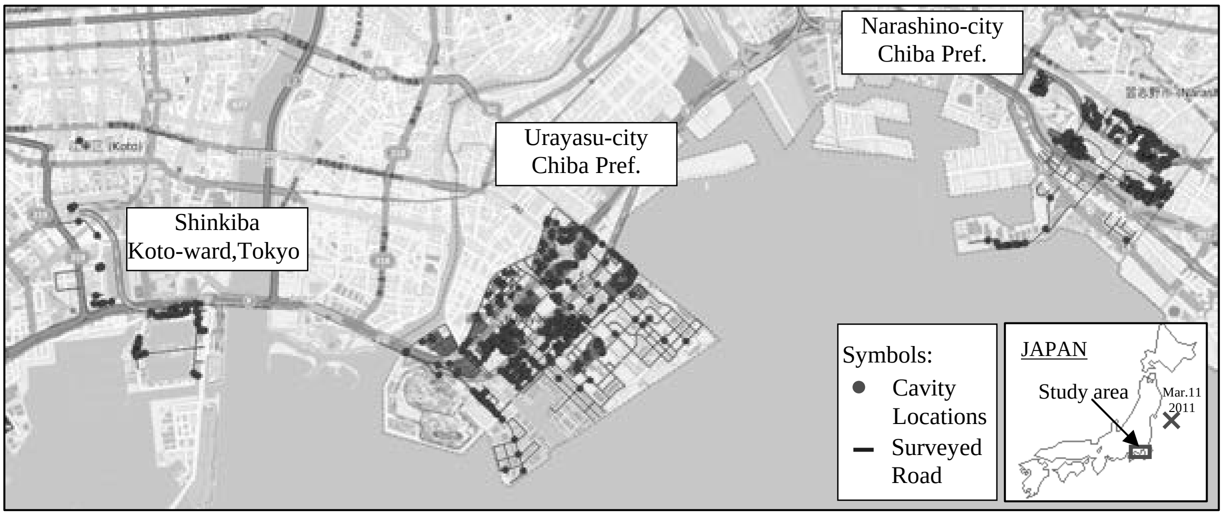

Fig. 2: Locations of subsurface cavities caused by ground liquefaction

Table 1: Summary of subsurface cavities studied

Municipality	**Subsurface Cavity Survey (Paved Roads)**			
	Survey Period	**Covered Distance (km)**		**Number of Cavities**
		Road	**Surveyed**	
Koto-ward	March 2011	5.75	47.78	54
Urayasu-city	April 2011-Aug 2012	136.28	307.23	528
Narashino-city	March- May2011	44.85	98.34	127
3 Municipalities in Total		142.03	355.01	709

2.2 Trend of subsurface liquefaction cavity formation

Cavities under roads are not only caused by ground liquefaction as described in this study, but also by natural disasters like earthquakes or localized heavy rains. There are other contributing factors under the normal situation as well, such as breakage of degraded underground pipelines. Subsurface cavities form when a void develops as soil particles or subbase materials wash away or settle due to consolidation for some reason. Cavities thus formed expand over time, and when the strength of the pavement exceeds its limit, a cave-in ultimately ensues. After frequent road cave-ins occurred in Tokyo in 1988, which became an object of social concern, regular subsurface cavity inspection surveys have been introduced on a nation-wide basis in Japan. Table 2 show a comparison between the liquefaction cavities covered in this study and normal cavities which are found with regular surveys.

Table 2: Comparison of cavities according to cause

		Normal Cavities	**Liquefaction Cavities**
Occurrence ratio		0.22 cavities/km	1.56 cavities/km
Average	Area	1.68 m^2	2.38 m^2
	Thickness	0.20 m	0.13 m
	Depth	0.38 m	0.37 m

2.2.1 Cavity occurrence ratio

Fig. 3 summarizes the cavity occurrence ratio based on 709 subsurface cavities which were confirmed in the areas that suffered ground liquefaction after the Earthquake. The cavity occurrence ratio is defined as the number of subsurface cavities found in 1km of survey distance. In the surveyed area, the occurrence ratio is 1.56 cavities/km. This is more than 7 times compared with the cavity occurrence ratio of 0.22 cavities/km [4)] of the regular inspection surveys conducted in the 12 government ordinance cities in Japan. The surveyed roads can be classified into 3 types, ‘arterial roads’, ‘sub-arterial roads’ and ‘community roads’. They differ in the number of buried objects that contribute to cavity formation, and they have a different pavement structure. The cavity occurrence ratios are 1.06 cavities/km for arterial roads, 1.30 cavities/km for sub-arterial roads, and 2.07 cavities/km for community roads.

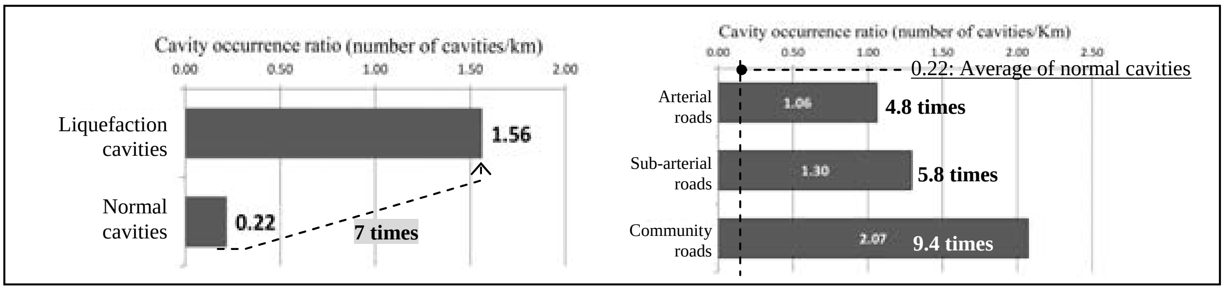

Fig. 3: Cavity occurrence ratio in ground liquefaction area (total area, according to road types)

2.2.2 Cavity area, thickness, and depth

Fig. 4 shows histograms of the liquefaction cavities area, thickness and depth. Additionally average and maximum values are shown.

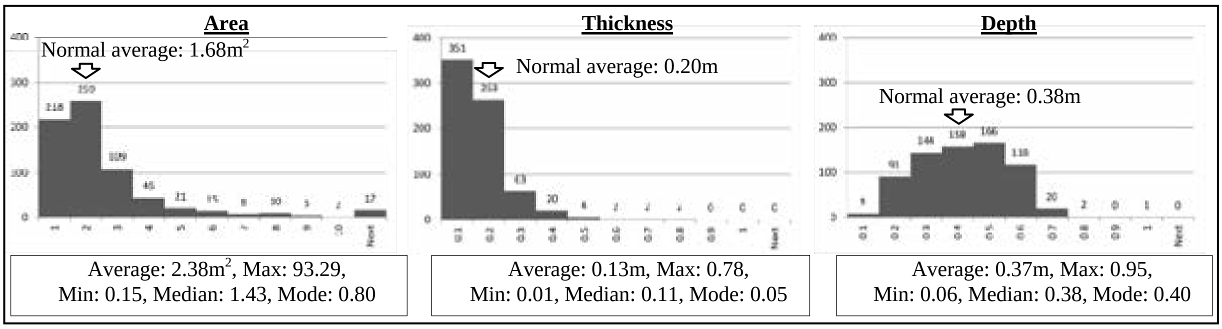

Fig. 4: Histograms of liquefaction cavities (Area, Thickness, Depth)

When compared with the average area of normal cavities, liquefaction cavities ($2.38m^2$) are larger. Furthermore the shape of the distribution histogram shows that more than 30% of the liquefaction cavities lie within the range of $1\text{-}2m^2$, and 17 cavities have an area larger than $10m^2$. This distorted distribution results in a rather large value for the average area. The average thickness is 0.13m and half of the cavities found had the thickness of less than 0.1m. If those cavities less than 0.2m in thickness were included, the number of cavities in this category exceeded 80% of the distribution. As a result, their average thickness is smaller than the average thickness of normal cavities. Regarding the depth of the liquefaction cavities, their average is equivalent to the average of normal cavities, which is close to the lower subbase depth. Furthermore the distribution was found to be approximately similar to the normal distribution. From this it was concluded that the cavity depth is not significantly different from the depth of normal cavities. The conclusion in this study is that liquefaction cavities tend to have larger area and smaller thickness.

2.3 Characteristics of liquefaction cavities

2.3.1 Large scale cavities

Analysis made in this study showed that liquefaction cavities tend to have larger areas and are thinner. Fig. 5 shows pictures of typical cavities (No. 1-4), and very thick cavities formed by liquefaction and damaged buried pipe and breakage of a manhole (No. 5, 6).

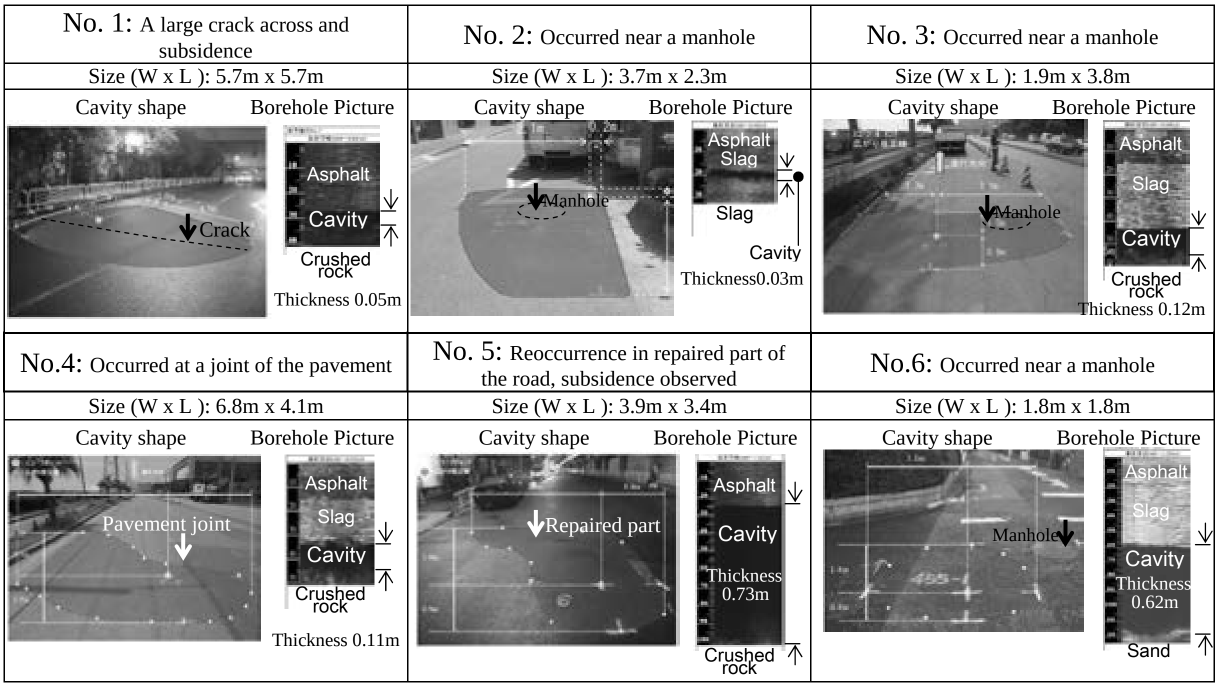

Fig. 5: Examples of large scale cavities

2.3.2 Strings of cavities

One of the characteristics of the liquefaction cavities covered in this study is the presence of “strings of cavities”, which are multiple cavities within a short distance. Although they form in very close proximity, each of those cavities in a string is an independent cavity. In fact, on the arterial roads, those strings of cavities occurred in the same traffic lane within a distance of 50-100m. Along the sub-arterial roads and community roads, such cavities were concentrated within a distance of 10-30m. In terms of a cavity occurrence ratio, this is equivalent to more than 100 cavities per km. Such cavities were found at locations where large-scale sand boiling occurred, or sometimes there were sewer mains directly under the traffic lane. Fig. 6 shows borehole pictures of cavities found in the arterial roads. All the cavities eroded the road subbase or base course materials in upward direction, and the bottom of these cavities is covered with fallen subbase materials or fallen sand, and also the bottom of these cavities is not consistently flat, the ground foundation underneath the pavement became undulated.

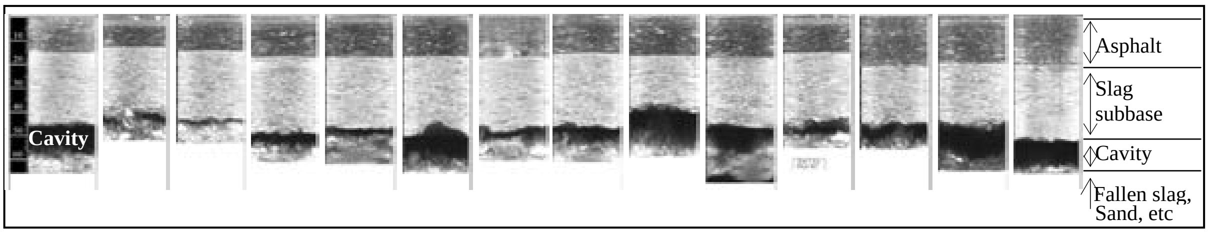

Fig. 6: Borehole pictures of a string of cavities in liquefied ground (14 cavities/100m)

2.4 Condition of the inside and bottom of liquefaction cavities

The result of a survey carried out more than one year after the Earthquake shows that there is sand ingress and groundwater inside many of the liquefaction cavities (Fig. 7). Although the groundwater level before the Earthquake was 1.5-3.0m[2)], the groundwater at the bottom of 26 cavities had not yet receded and the water level had been less than 1m (0.32-0.81m). Furthermore at the time of road restoration work, there were many pavement sections which showed soil ingress in what should have been the crushed rock layer, as shown in Fig. 7. These facts show that liquefaction sent a large volume of sand upwards, an example of which is shown in Fig. 8. The liquefaction at the time of the Earthquake left a strong mark on the road structure in a wide area. In addition, loose soil was confirmed at the bottom of many cavities. This condition indicates that the liquefaction brought about not only the sand ingress into the road subbase, but also structurally weakened the road beds in the affected areas.

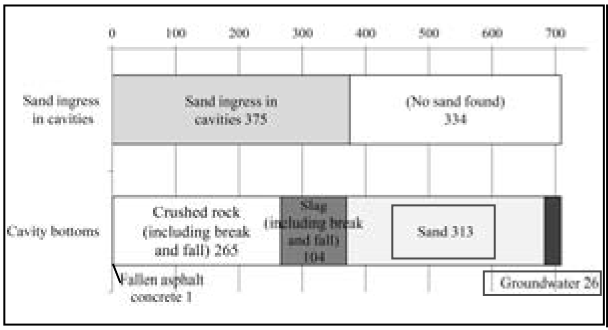

Fig. 7: Inside and bottom of liquefaction cavities

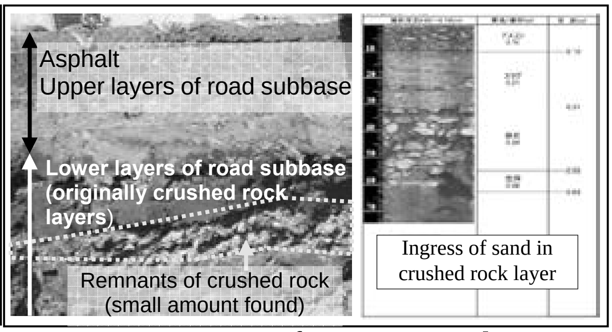

Fig. 8: Cross section of pavement under repair (left) and borehole picture (right)

2.5 Analysis of the spatial distribution of liquefaction cavities

2.5.1 Age of reclaimed land and cavity distribution

The studied areas are reclaimed land sites where dredged sea sand was used as land fill, but the work was performed at different times. Though the reclamation technique and ground improvement method were different depending on the location, it seems that reclamation work was carried out in two separate phases, before and after the legislative revision of reclamation regulations. According to Table 3, the location and characteristics of cavities found in the studied areas, the older the time of reclamation, that is, the older the time of community construction and burying of underground piping system, the higher the number of cavities. The number of cavities per ha is 5 times larger in older areas.

Table 3: Reclamation period and number of cavities

	Before 1974	After 1975(after revision of the reclamation regulation)
Number of Cavities	600 cavities	109 cavities
Reclaimed Area	1,214 ha	1,045 ha
Cavity Occurrence Ratio	0.49 cavities/ha	0.10 cavities/ha

2.5.2 Conditions around liquefaction cavities

In order to know what kind of local conditions influenced the formation of the 709 liquefaction cavities, detailed data of the local conditions for each cavity were collected in the inspection survey. The results confirmed that, in addition to those locations with large scale sand boiling and irregular road surface such as cave-ins, cavities formed under pavement joints, close to gaps around the peripherals of manholes, and around buried structures associated with drainage systems. Examples of cavities in areas where ground liquefaction was observed are shown in Fig. 9 and Fig. 10.

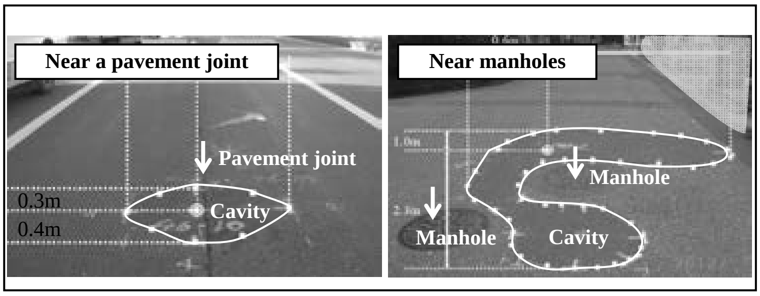

Fig. 9: Confirmed liquefaction cavities

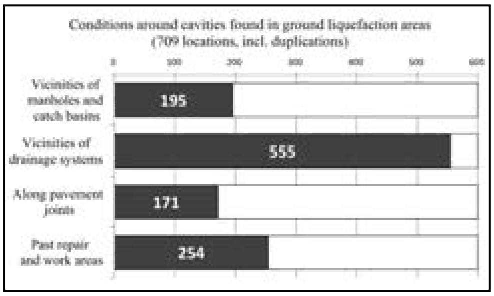

Fig. 10: Conditions around liquefaction cavities

2.6 Analysis of liquefaction cavities and subbase materials

As the surveyed locations were along Tokyo Bay coast, 524 (70 %) out of the total 709 cavities were found in locations where iron and steel slag was used as the lower subbase of the road structure. Slag is easy to obtain as byproduct of pig-iron and steel making process. The use of slag as subbase material, however, involves a risk of dilation. For this reason, in Japan, quality control of slag material is indispensable, and there is a JIS regulation especially for the use of slag as subbase material. For the use of slag in the lower layers of subbase, a modified CBR (California Bearing Ratio) is specified for various possible cases. In the studied areas it was inferred that the modified CBR value is the same as that of crushed rock or higher, and slag with a more than sufficient strength and thickness was used.

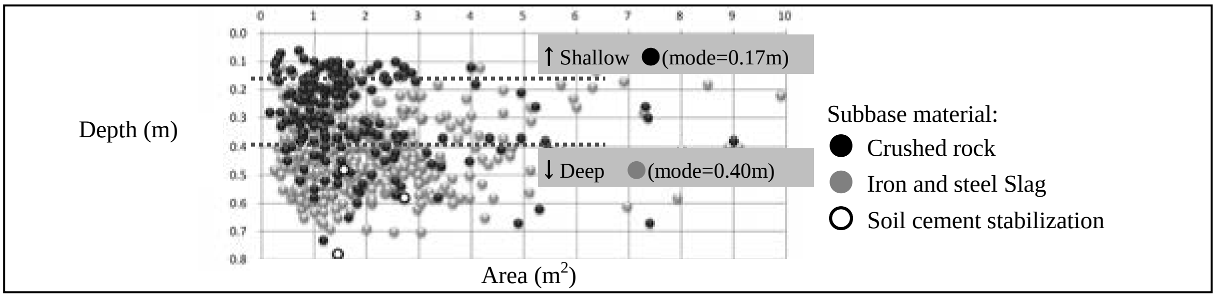

Fig. 11: Analysis of the relation between subbase material and cavity area

Fig. 11 shows the relation between the subbase material and the cavities area. The analysis result shows the mode value of the upper end of cavities found in crushed rock subbase is more than 0.1m shallower than those of the slag subbase. It is presumed that the strength intensified slag subbase prevented cavities under the pavement from migrating upwards because of the liquefaction. Furthermore, cavities found in cement stabilized locations (the cement stabilization is recognized to have the highest bearing strength) are larger than those in the case of the other two subbase materials, and the observed value shows there was no upward migration of cavities.

2.7 Cavity survey in a non-liquefied area

2.7.1 Outline of the survey

About two years after the Earthquake, a cavity inspection survey was conducted in Motomachi area of Urayasu-city where there was no liquefaction damage found, even though the area was located adjacent to where liquefaction damage occurred. The survey was conducted for the purpose of comparison of the site conditions and covered a distance of 10km. The survey revealed the possible existence of cavities in 17 locations. An open-cut inspection was conducted at one of the sites (a shallow cavity close to a manhole) to confirm the conditions of the cavity, followed by a penetration resistance test to measure the looseness of the soil on the cavity bottom.

2.7.2 Analysis result

Through a borehole inspection, a cavity was ascertained at the shallow depth of 0.14m in the crushed rock layer immediately under the pavement. The area of the cavity was 1.19m^2, the thickness was 0.34m, and the soil on the bottom was loose. The site inspection revealed a rain water drain, a trace of chemical grouting in the side wall of a sewer manhole, and noticeable loosening of the soil on the cavity bottom. The loose soil continued near as deep as the installed position of the sewer pipe. From these results, it is presumed that there could be one or more holes in the sewer pipe joints, and soil washed away these holes caused a cavity to form and loosened the soil on the cavity bottom. (Fig. 12)

Fig. 12 Result of open-cut inspection

2.8 Follow-up inspection of liquefaction cavities repaired using grout injection

2.8.1 Outline of inspection

The follow-up inspection was conducted using a borehole inspection in those locations of Narashino-city where liquefaction cavities were repaired using grout injection. The inspection was conducted in four locations; about one year after the grout injection took place. The grout material used was two-component fast curing cement.

2.8.2 Inspection of grouted cavities and their surroundings

No changes to the road condition, such as subsidence were noticed, and no new cavities were found. It was confirmed that there were no gaps or voids under the pavement. Only in No. 4 location, loose soil up to 0.34m in thickness was found in the sand layer at the cavity bottom, but the position of the grout material was confirmed to be at the same depth as the original cavity. Table 4 shows the comparison between borehole pictures taken before the grout injection and those taken one year later.

Table 4: Internal conditions of cavities repaired by grouting

		No.1	No.2	No.3	No.4
Borehole pictures Left: Before grouting Right: 1year after grouting		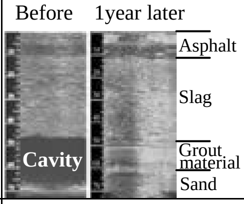	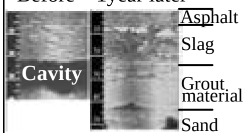	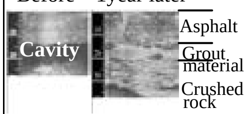	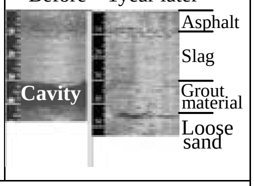
Survey Results	Grout material	Filling (No gap or void)			
	Bottom of cavity	No loosening			Loosening thickness:0.34m

2.8.3 Core sample study of grout material

Core samples show that the grout material was solidified in layers and there were unevenly colored layers, presumably because of unsatisfactory mixing of cement and curing agent (Fig. 13). A needle penetration test was used to measure uniaxial compressive strength under different condition: moistened, dry, and saturated (cured). It was ascertained that there was no problem in terms of compressive strength even though water is included. Through density measurements it was determined that there was no shrinkage or age related deterioration (Table 5).

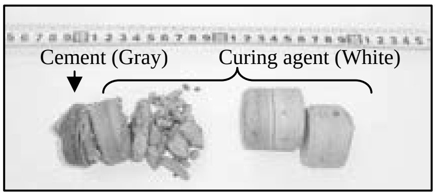

Fig. 13: No. 1 Core Sample

Table 5: Uniaxial compressive strength and density measurements

	$q_u$max	$q_u$min	$q_u$avg
Uniaxial compressive strength	24,143kN/m^2 (dry state)	379kN/$m^{2\,*}$ (cured state in water)	3,384kN/m^2
Density	0.6-1.5g/cm^3 (equivalent to the result of proportioning test of 1.2g/cm^3)		

Note:* Even at $q_u$min, the compressive strength is 3 times as high corresponding to CBR=6.

The core samples were broken easily by applying high pressure washing of 7.5MPa for about a minute. This indicates that there would be no difficulty in carrying out excavation in case repair is needed in the future. It was also confirmed that even in the unlikely case of grout material leaking into pipelines, it would be easy to remove the leaked grout material using high pressure washing.

2.9 Presumed mechanism of liquefaction cavity formation

The mechanism of liquefaction cavity formation is presumed to follow the process shown in Fig. 14. The process was deduced based on the field observation of the liquefaction cavities and analysis of cavity interiors as reported in this study, in addition to information from Kuwano's model tests[5)] simulating the formation of liquefaction cavities.

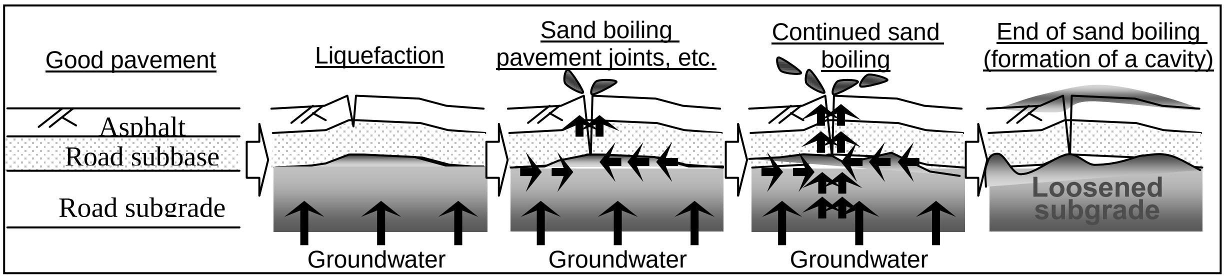

Fig. 14: Presumed mechanism of liquefaction cavity formation

3. PREVENTION OF SUBSIDENCE CAUSED BY LIQUEFACTION CAVITIES

Fig. 15 describes the knowledge obtained in the present study as to how the degree of safety (risk of subsidence or cave-ins) of roads relates to the progress of cavity formation under the road surface.

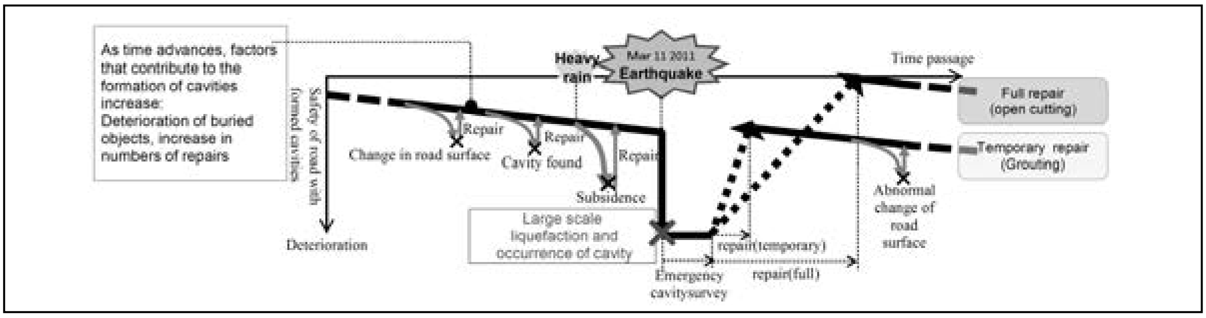

Fig. 15: Relation between the safety of the road and occurrence of subsurface cavities

It is necessary to consider proactive measures to prevent subsidence due to liquefaction cavities in two distinctive cases: one for normal times and the other immediately after earthquake disasters. In normal times, the main targets are those cavities which are yet to be repaired and cavities which were already repaired using grout injection. At the same time attention has to be paid to detect the possible spreading of loose soil around the cavities. Until cavities are repaired properly, constant attention has to be maintained by regular patrols, etc. Presently in Japan, the possible recurrence of large scale earthquakes is anticipated. It was confirmed by this study that the groundwater level in those areas where cavities formed still has not receded to less than GL-1m, and it is not expected that this will return to the previous safe level. Therefore, if a major earthquake occurs again in those areas, the recurrence of liquefaction is unavoidable. Especially along those arterial roads where strings of cavities were found, cavity inspection surveys to assure the safety of the roads will have to be conducted urgently after an earthquake before the start of emergency relief activities.

4. CONCLUSION

Research in this study focused on those cavities formed under the road surface due to liquefaction on an unprecedented scale. Traditionally, the formation of cavities under the roads is considered as one of the phenomena which occur because of age related deterioration of underground infrastructure. Accordingly, countermeasures were taken from the view point of maintenance and repair of road infrastructure. The liquefaction cavities caused by the Great East Japan Earthquake are clearly different from those cavities found during regular surveys. The following summarizes the findings of this study:

1. Liquefaction caused many cavities under the roads in a very short period of time. Sewer lines damaged by the Earthquake also caused cavities, whose formation spread out over a relatively longer period of more than a few months.
2. The cavity occurrence ratio in liquefied areas was 7 times larger than the normal condition. Many of these cavities were thin, had large areas, and eroded the road subbase leaving undulation at the cavity bottom.
3. Locations where many cavities formed coincided with large scale sand boiling, subsidence or cave-in of the road surface, and cavities were formed especially along pavement joints, around manholes where there were gaps, and around buried sewer line structures.

It is hoped that this study will serve as a basis of a practical guide for road administrators who have to carry out emergency countermeasures to prevent the formation of cavities under the similar situations when a large scale earthquake strikes in the future. By that time, solutions for the following issues will certainly be needed: standardized inspection surveys methods, selection of repair methods, and countermeasures to suppress cavity formation. We hope from the bottom of our heart that, in addition to this study, the precious experiences of many of those involved and the fruits of effectively executed measures will be systematically compiled to act as a road map.

ACKNOWLEDGMENTS

This study was carried out with grants provided by the project of The Japanese Geotechnical Society for investigation aimed at the improvement of geotechnical engineering for road management. Details are found in relevant reports listed in the References. Koto-ward of Tokyo, Urayasu-city, Chiba Pref., and Narashino-city, Chiba Pref., responded wholeheartedly.

REFERENCES

1) The Japanese Geotechnical Society., 2012. *Issues and Countermeasures of Foundation Disaster at the Time of Earthquake (Secondary) - Lessons Learned and Recommendations from The Great East Japan Earthquake 2011*, Page 119. (in Japanese)

2) The Ministry of Land, Infrastructure and Transport, Kanto Regional Development Bureau & The Japanese Geotechnical Society., 2011. *Report of Actual Conditions of Ground Liquefaction in the Kanto Region which due to the 2011 off the Pacific coast of Tohoku Earthquake,* Page 103. (in Japanese)

3) Tatsuhiko K, The Annual Technical Survey Report of Tokyo Bureau sewerage., 2012. *About Countermeasures against Liquefaction in Shinkiba (Pipe Line) caused by The Great East Japan Earthquake*., Page 65. (in Japanese)

4) Yutaka K, Ryoko S., 2012. *Study on the Occurrence of Liquefaction Cavities under Roads (Part I): Characteristics of the Formation of Liquefaction Cavities*, 47th Geotechnical Symposium, 1457-1458. (in Japanese)

5）Reiko K., 2013. *Model Tests Simulating Sub-surface Cavities Formed in the Liquefied Ground*, USMCA2013

Model tests simulating sub-surface cavities formed in the liquefied ground

Reiko KUWANO[1], Jiro KUWANO[2], Shinpei TAIRA[3], Mari SATO[4],
Ryoko SERA[5] and Yutaka KOIKE[5]
[1]Professor, ICUS, IIS, the University of Tokyo, Japan
kuwano@iis.u-tokyo.ac.jp
[2]Professor, GRIS, Saitama University, Japan
[3]Former student, Saitama University, Japan
[4]Graduate student, IIS, the University of Tokyo, Japan
[5]GEO SEARCH CO. LTD., Japan

ABSTRACT

Significant number of subsurface cavities was found in the liquefied ground after the Great East Japan earthquake. Using the results of the radar exploration conducted in Urayasu-city, Shinkiba-area and Narashino-city, all of those suffered from damage by the ground liquefaction, characteristics of sub-surface cavities are investigated. It was found that cavities tended to form near man-holes and joints in pavement. Size/shape of the cavities is larger and thinner compared to those of cavities observed in the non-liquefied ground.
A series of model tests was conducted in order to understand the mechanism of underground cavity formation when liquefaction occurs. Liquefaction and sand boiling was simulated in the model test. Sand grains initially moved horizontally and then vertically, causing disturbance and loosening in the ground. Gaps and voids near the ground surface were eventually generated at the location of the boiled sand. Penetration resistance of the model ground was measured after the test, indicating that the buried structure may have some effects on the extent of ground loosening around the structure.

Keywords: *subsurface cavity, liquefaction, boiled sand, ground loosening*

1. INTRODUCTION

A ground penetration radar survey was conducted on the roads of Urayasu-city, Shinkiba-area and Narashino-city, all of which suffered from damage caused by the ground liquefaction during the Great East Japan Earthquake. A large amount of fluidized sand, or sand boiling, was observed and a significant number of subsurface cavities were found in the liquefied ground. Sera et al (2013) reported patterns of sub-surface cavities observed in the disaster areas and characteristics of sub-surface cavities obtained by the survey are analyzed. It was found that cavities had a tendency to form near manholes and joints in the pavement. These cavities have a larger area, but are thinner compared to cavities normally observed in non-liquefied ground.

In this study, a series of model test was conducted to investigate the mechanism of sub-surface cavity formation. Penetration resistance was also measured to evaluate the ground loosening created around the cavities

2. TEST PROCEDURE

2.1 Apparatus

A model ground was prepared in a soil chamber of 30cm long, 8cm wide and 20cm high, as shown in Figure 1. Water was supplied from the bottom of the model ground. Hydraulic gradient of the water supply could be adjusted by the elevatable water tank connected to the bottom of the soil chamber. Surface of the model ground was covered by an acrylic lid having 2mm wide openings, from those boiling sand could be erupted. Water table was adjusted by the drainage at the side wall of the chamber.

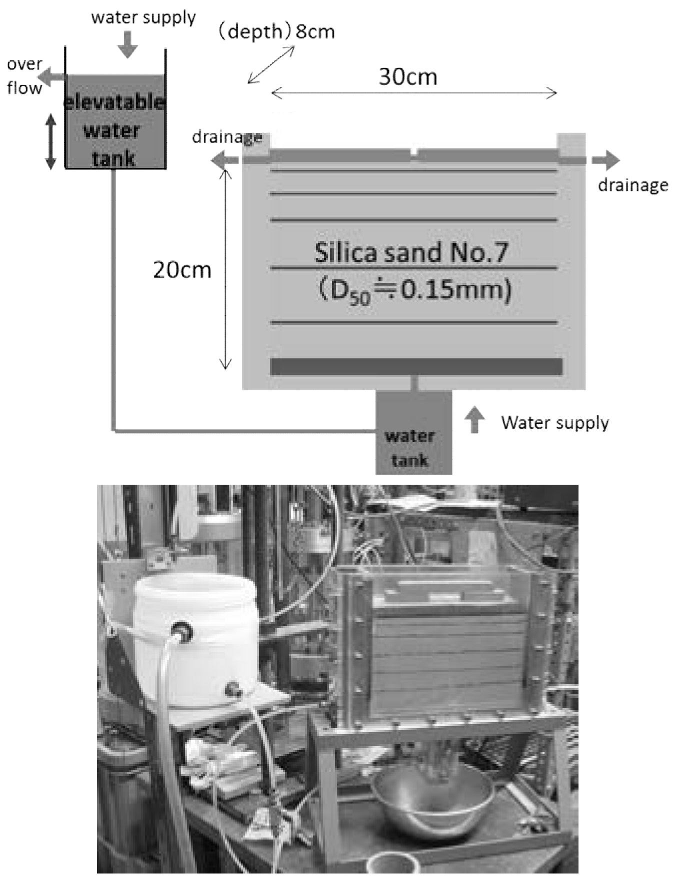

Figure 1. Photo and schematic figure of apparatus

2.2 Model ground

Silica sand No.7 was used for the material of the model ground. It has mean diameter of 0.15mm. Maximum and minimum void ratios are 1.24 and 0.74 respectively. Loose sand ground, relative density of approximately 75%, was prepared by the air-pluviation. The permeability of the ground was around 3.4 $\times 10^{-3}$cm/s. Colored sand was put on the surface and in front of the ground, as shown in Figure 2, for the observation of sand grains' movement.

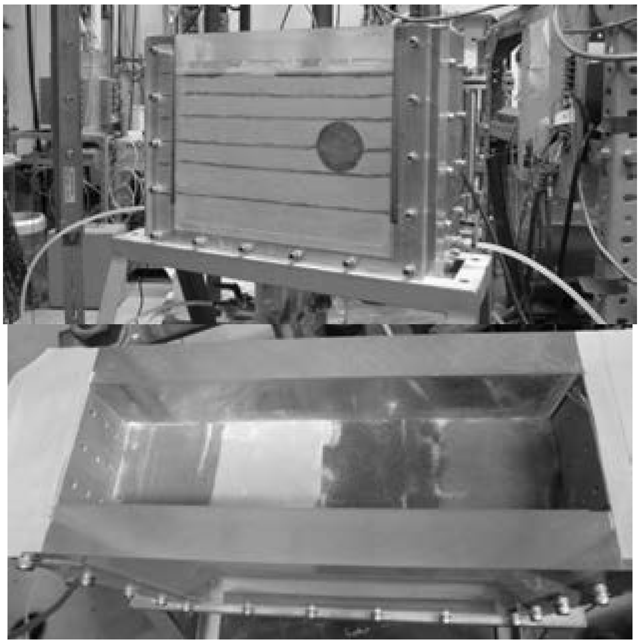

Figure 2. Set-up of model ground

2.3 Test procedure

Water was slowly penetrated and the model ground was saturated in advance. Then the water tank was elevated to apply additional hydraulic gradient to generate liquefaction in the ground. Sand grains lost effective stresses and upward seepage flow caused sand boiling from the opening in the lid. After the test, water in the model ground was drained for more than 24 hours and penetration resistance was measured at five locations using a 3mm diameter needle. In total, six tests were conducted as shown in Table 1.

Table 1: Test condition and sand boiling phenomena observed

Case No.	**Opening (x: cm)**	**Buried structure**		**Water table (z: cm)**	**Water head difference**	
		Shape, size	**Location (x, z)**		**at the beginning of sand boiling**	**when vertical movement of sand grains was identified**
0	x=0	-	-	z=-1.5	60cm	Not observed

		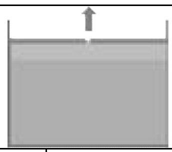				
1	x=0	-	-	z=0	30cm	90cm
		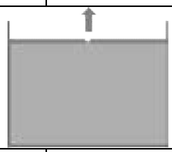				
2	x=0	Rectangular 2×10cm	(-1, -5)	z=0	35cm	Not observed
		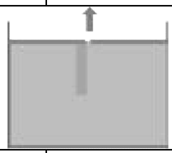				
3	x=0	Pipe ϕ6cm	(0,-9)	z=0	30cm	70cm
		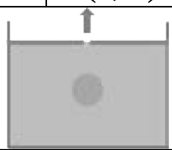				
4	x=0	Pipe ϕ6cm	(9,-9)	z=0	30cm	110cm
		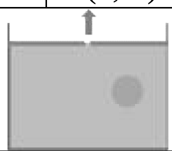				
5	x=±7.5	Pipe ϕ6cm	(0,-9)	z=0	55cm	Not observed
		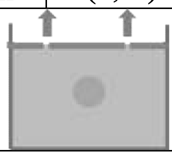				

3. TEST RESULTS

2.1 Sand boiling

Sand boiling was observed in all the test cases. Hydraulic gradient at the beginning of boiling, and at the moment when vertical movement of sand particles was identified is shown in Table 1. Although the drain lines were located at or below the surface, the drainage could not keep up with the supply of water. Therefore the water table at the beginning of sand boiling came to be above the ground surface. When the water head difference became larger than 30cm, sand boiling started in cases 1 to 4. Considering that the height of the model ground was 20cm, hydraulic gradient was 1.5, which exceeded critical hydraulic gradient. In case 1, the flow rate of water at the opening was measured to be 0.75cm/s, which approximately coincided with the value of flow rate calculated by the assumption of uniform water seepage from bottom.

After for a while from the beginning of sand boiling, it was observed that sand grains moved horizontally toward the opening in the gap between the lid and ground surface as shown in Figure 3. Further increasing hydraulic gradient caused vertical movement of sand grains. Especially when buried structure or pipe was located near the opening, water flow path seemed to concentrate around the buried structure, which often caused ground disturbance and loosening, as shown in Figure 4. At the end of the test, the surface of the ground became undulated as shown in Figure 5.

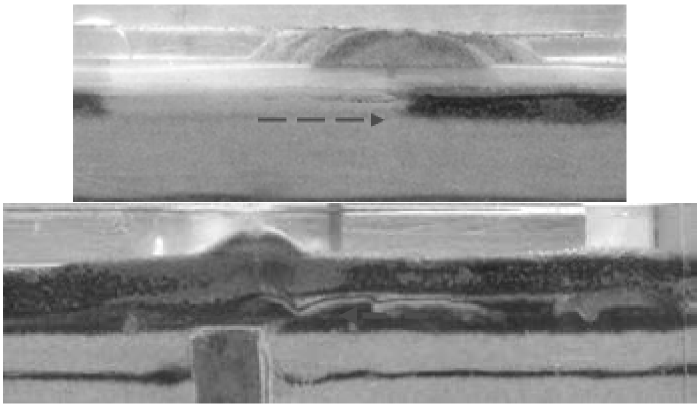

a) Case 1 (water head difference: 60cm) b) Case 2 (water head difference: 60cm)

Figure 3. Horizontal movement of sand particles

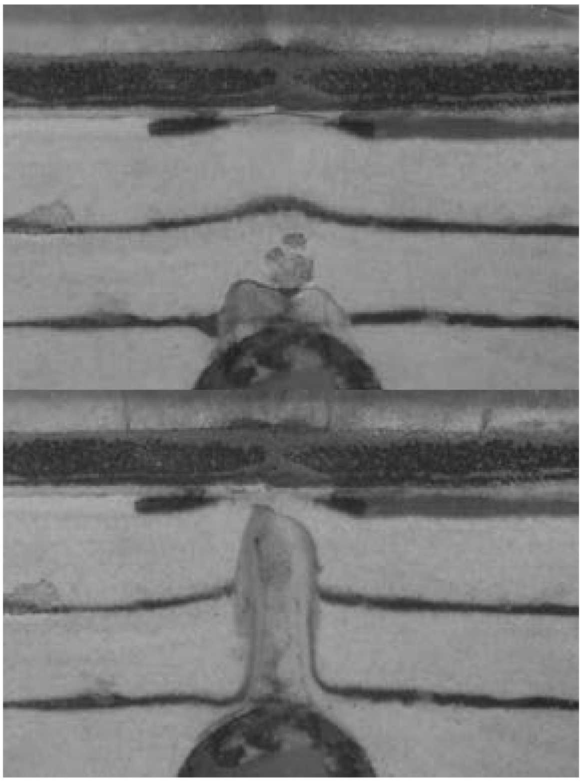

a) Case 3 (water head difference: 70cm) b) Case 3 (water head difference: 100cm)

Figure 4. Vertical movement of sand particles

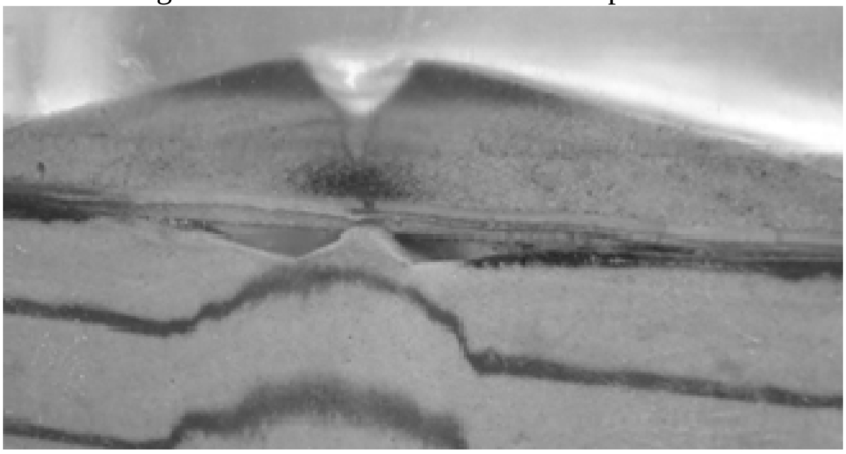

Figure 5. Undulated surface of the ground after the test (Case 4)

2.2 Ground disturbance and loosening around cavities

Figures 6 to 10 show the results of penetration test conducted after test cases 0, 2, 3, 4 and 5. For case 0, as shown in Figure 6, penetration resistance at all the locations showed similar results, indicating that the deep ground was not disturbed since the magnitude of sand boiling was small and only sand particles near the surface moved horizontally. In case large scale sand boiling occurred, especially when buried structure was located near the opening, there was significant reduction of penetration resistance.

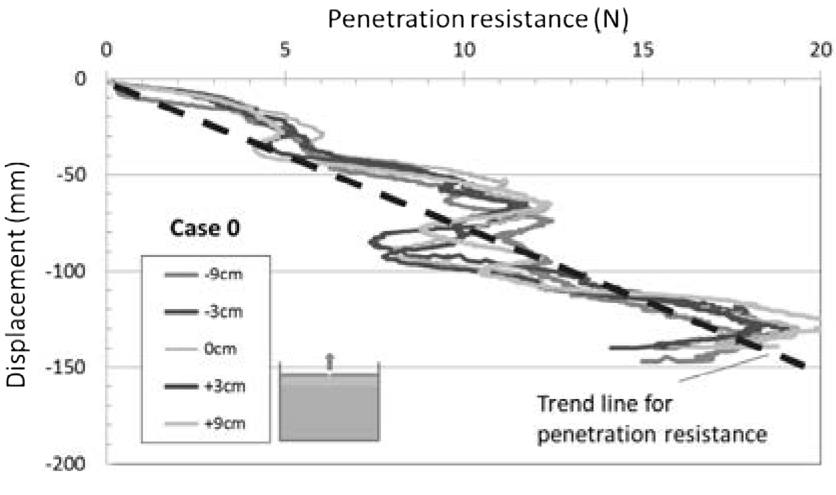

Figure 6. Penetration resistance after the test (Case 0)

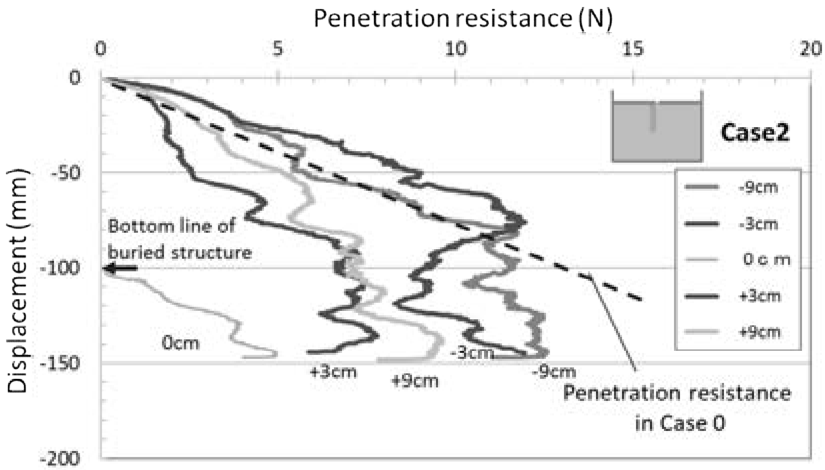

Figure 7. Penetration resistance after the test (Case 2)

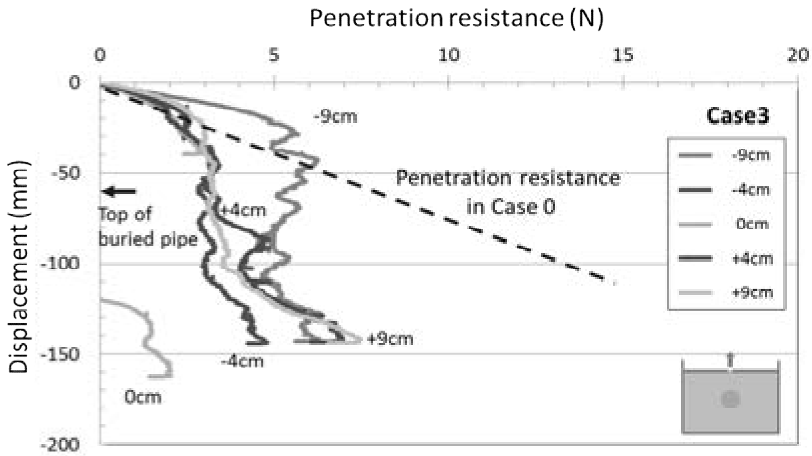

Figure 8. Penetration resistance after the test (Case 3)

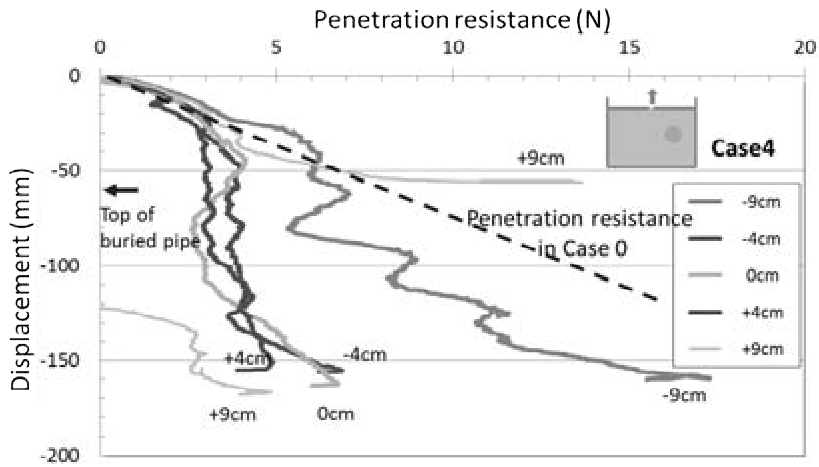

Figure 9. Penetration resistance after the test (Case 4)

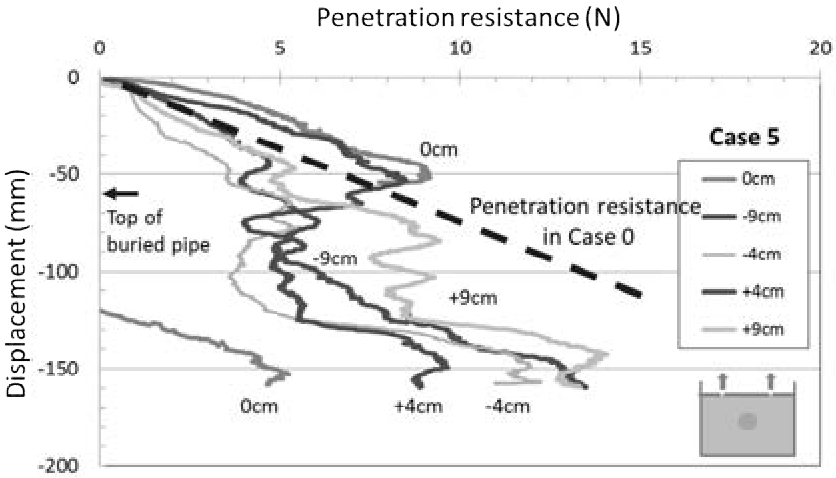

Figure 10. Penetration resistance after the test (Case 5)

3. CONCLUSIONS

A series of model tests was conducted to simulate liquefied ground under the pavement in order to investigate the effects of sand boiling on the formation of subsurface cavities. Following conclusions were drawn from the study.

- Horizontal movement of sand grains was observed in the early stage of sand boiling. When larger hydraulic gradient was applied, vertical movement of sand occurred.
- There was little disturbance in deep ground for the case of small scale sand boiling. In large scale sand boiling, especially when the some buried structures exist, deep ground may have loosening due to the disturbance cause by vertical sand movement along the water flow paths.
- In general, sub-surface cavities due to sand boiling locate near the surface and the bottom of the cavity tends to undulate. This feature was also confirmed in the field survey.

ACKNOWLEDGEMENT

This study was carried out with grants provided by the project of The Japanese Geotechnical Society for investigation aimed at the improvement of geotechnical engineering for road management.

REFERENCES

Sera, R., Koike, Y., Nakamura, H., Kuwano, R. and Kuwano, J., 2013. Survey of sub-surface cavities in the liquefied ground caused by the Great East Japan Earthquake, *Proc. 12th International symposium on new technologies for urban safety of mega cities in Asia, USMCA, Hanoi Vietnam, October 2013.*

Climate change effects in Chindwin River basin, Myanmar

Win Win ZIN[1] and Khin Than YU[2]
[1]Associate Professor, Civil Engineering Department,
Yangon Technological University, Myanmar
winwinzin@gmail.com
[2]Pro-rector, Yangon Technological University, Myanmar

ABSTRACT

This paper examines the possible effects of climate change on hydrological and meteorological variables in Chindwin river basin. These variables are important indicators of climate change. Chindwin river has the catchment area of 115,300 km^2. One of the commonly used tools for detecting changes in climatic and hydrologic time series is trend analysis. In this study, the Mann-Kendall non-parametric test, which is widely used to detect trends, was applied. The change per unit time was estimated by applying Sen's estimator of slope. Annual maximum rainfall at Minkin displayed a significant increasing trend. The application of a trend detection framework results in the identification of some significant trends in the annual minimum flow. Noteworthy was strong decreasing trend in the annual minimum flow of Kalaewa and Monywa. A noticeable increase in the monthly mean temperature was observed mostly in Mawlaik, Kalaewa and Monywa. It is important to investigate present and probable future climatic change patterns and their impacts on water resources so that appropriate adaptation strategies may be implemented.

Keywords: *climate change, trend analysis, non-parametric test, Mann-Kendall, Sen's slope*

1. INTRODUCTION

River systems have been changed in the global context as a result of both natural factors (climate change) and anthropogenic factors (land use change, river regulations, and water abstraction etc.) (Walling and Fang, 2003). The availability of long-term records of hydrological data enables identifying the presence of changes in the river systems and deciphering the possible influencing factors of the detected changes. The detection of changes in the long-term time series of hydrological data is of scientific and practical importance in the water resource management and is regarded as a permanent exercise with the continuously updated data (Kundzewicz, 2004).

Most water resources projects are designed and operated based on the historical pattern of water availability, quality and demand, assuming constantly climatic behaviour (Westmacott and Burn, 1997; Abdul Aziz and Burn, 2006). Precipitation, streamflow and evapotranspiration are important variables in

diagnosing climate change as well as revealing the eco-environmental response to climate change in regional scale. It is important to investigate present and probable future climatic change patterns and their impacts on water resources so that appropriate adaptation strategies may be implemented. Since the geomorphologic evolution of watershed is quite slow in comparison with climate change, the detectable changes in the hydrologic regimes of stable, unregulated watersheds may be considered as the reflection of changes in climate. Consequently hydrologic variables might be used as indicators to detect and monitor climate change (Kahya,2004). Analysing different hydrological and meteorological variables will indicate which variable is most affected by changes in the climate. Burn and Soulis (1992) suggest having a wide range of hydrologic variables to monitor since it is expected that climatic change will result in a diversity of environmental responses.
There are eleven different variables used in this study that are anticipated to be affected by climate change. Trend detection will be conducted in the monthly, seasonal and annual time series. The variables include the mean annual flow, mean monthly flow, extreme annual flow, mean seasonal flow, mean annual rainfall, mean monthly rainfall, annual maximum rainfall, annual total rainfall, mean seasonal rainfall and mean monthly temperature. Annually extreme variables, such as annual maximum and minimum values, are also to be examined. This paper examines the possible effects of climate change on hydrological and meteorological variables in Chindwin river basin. These variables are important indicators of climate change. One of the commonly used tools for detecting changes in climatic and hydrologic time series is trend analysis. In this study, the Mann-Kendall non-parametric test, which is widely used to detect trends, was applied. The change per unit time was estimated by applying Sen’s estimator of slope.

2. STUDY AREA

The Chindwin river is naturally configured with tremendous segments of rivulets, streamlets and tributaries and it could of course be ranked as the largest tributary of the Ayeyarwaddy river. The source of the entire river system approximately falls at 97.00 degree Eastern longitude and 26.50 degree Northern latitude. The basin is situated in North-West part of Myanmar and is covered with thick tropical forest. The Chindwin river has the catchment area of 115,300 km^2. The river course between Hkamti and the confluence has a gentler slope of 1:11,000, on the contrary, for the upstream of Hkamti with a steeper slope of 1:2300. There are only six rain gauge stations and five discharge gauge stations within the basin. Location of study area is shown in Figure 1.

Hydroclimatologists are concerned with analyzing time series by concentrating on differences in 30-year normals along the whole period of records. This is why the period of 30-year is assumed to be long enough for a valid mean statistic. It also amounts to describing hydroclimatic time series as non-stationary with local periods of stationary (Kite, 1991). Burn and Elnur (2002) stated that the selection of stations in a climate change research is substantial at the initial step and that a

minimum record length of 25 years ensures validity of the trend results statistically.
The length of data set in this study, mostly 46 years, suffices the minimum required length in searching evidence of climatic change in hydroclimatic time series. The majority of rainfall and streamflow records include observations of 46 years spanning from 1967 to 2012. The basin covers annual total rainfall from 760 mm in the south to about 3820 mm in the north. The majority of temperature records include observations of 38 years spanning from 1975 to 2012. Annual average temperature of basin is 25.7 °C. Land use types in the basin are closed forest, degraded forest, agricultural land, open land and water. The dominant land use type in the basin is closed forest. According to some researchers' results, it is seen that land use changes in the river basin.

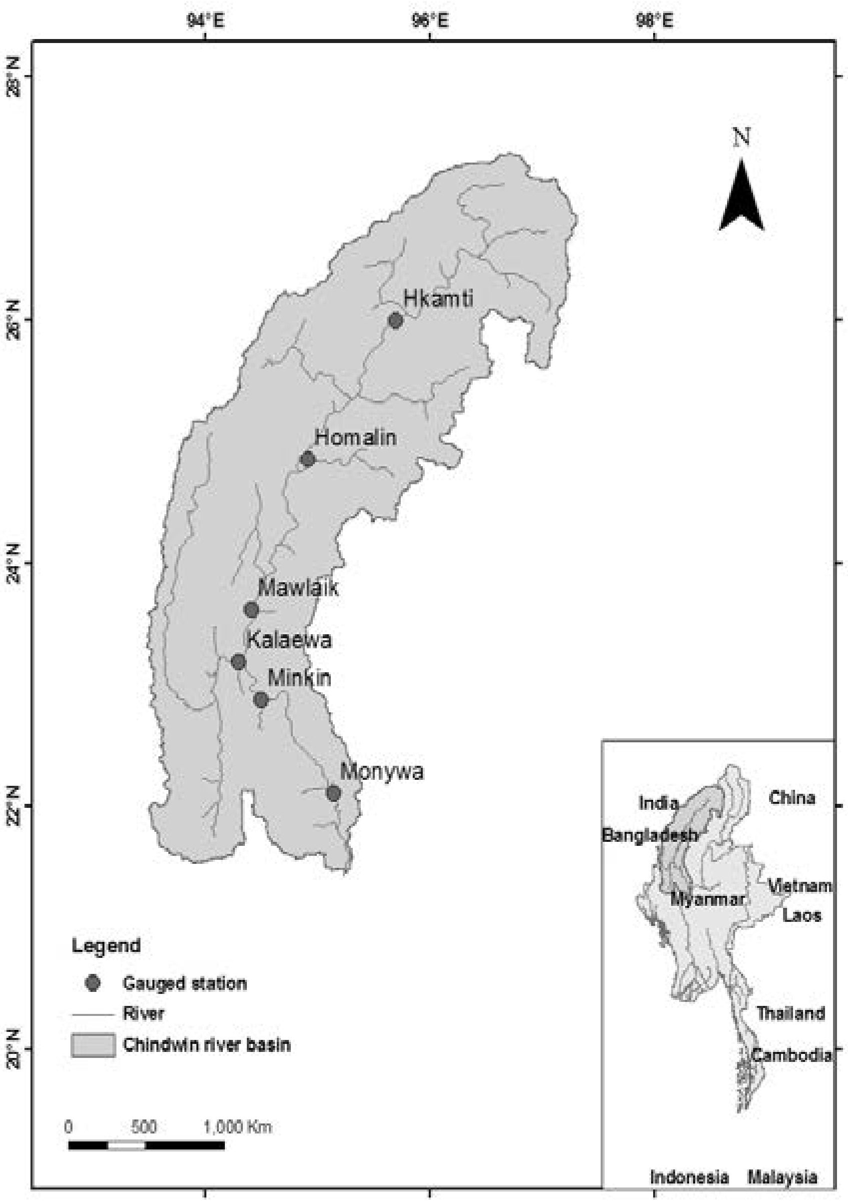

Figure 1: Location map of Chindwin river basin

3. METHODOLOGY

The detection of trends in measured time series data can be posed as a hypothesis testing problem in which the null hypothesis (H_o) is that there is no trend in the data, and the alternate hypothesis (H_1) is that there is a trend in the data. A number of parametric and non-parametric tests have been applied for trend detected. There are trend detection tests such as Mann-Kendall test, Spearman's Rho test, Sen's T test and linear regression test. One of the widely used in non-parametric tests for detecting trends in the time series is the Mann-Kendall test. In this study Mann-Kendall test was applied.

3.1 Serial correlation

The presence of serial correlation can complicate the identification of trends in that a positive serial correlation can increase the expected number of false positive outcomes for the Mann-Kendall test (von Storch and Navarra,1995). Several approaches have been suggested for removing the serial correlation from a data set prior to applying a trend test. The two common approaches are to pre-whiten the series or to 'prune' the data set to form a subset of observations that are sufficiently separated temporally to reduce the serial correlation.

The pre-whitening approach is adopted herein and involves calculating the serial correlation and removing the correlation if the calculated serial correlation is significant at 5% level. The pre-whitening is accomplished through

$$yp_t = y_{t+1} - r\, y_t \qquad (1)$$

where yp_t is the pre-whitened series value for time interval t, y_t is the original time series value for time interval t, and r is the estimated serial correlation coefficient.

3.2 Mann–Kendall test

The Mann–Kendall (MK) statistical test (Mann,1945; Kendall,1975) is a non-parametric approach for the monotonic trend. It has been widely used to assess the significance of trends in hydro-meteorological time series due to its robustness against nonnormally distributed, censored and missing data as well as its comparable power as parametric competitors (Helsel and Hirsch, 1992; Serrano et al., 1999; Yue et al., 2002).

This test has been widely used to test for randomness against trend in hydrology and climatology. It is a rank-based procedure, which is robust to the influence of extremes and good for use with skewed variables. According to this test, the null hypothesis H_0 states that the deseasonalized data ($x_1, . . ., x_n$) is a sample of n independent and identically distributed random variables. The alternative hypothesis H_1 of a two-sided test is that the distributions of x_k and x_j are not identical for all k, j ≤ n with k ≠ j. The test statistic S, which has mean zero and a variance computed by Equation (4), is calculated using Equations (2) and (3), and is asymptotically normal (Hirsch and Slack, 1984):

$$S = \sum_{k=1}^{n-1} \sum_{j=k+1}^{n} sgn(x_j - x_k) \qquad (2)$$

$$sgn(x_j - x_k) = \begin{Bmatrix} +1 \; if \; (x_j - x_k) > 0 \\ 0 \; if \; (x_j - x_k) = 0 \\ -1 \; if \; (x_j - x_k) < 0 \end{Bmatrix} \qquad (3)$$

$$Var(S) = [n(n-1)(2n+5) - \textstyle\sum_t t(t-1)(2t+5)]/18 \qquad (4)$$

The notation t is the extent of any given tie and $\sum_t$ denotes the summation over all ties. In cases where the sample size n > 10, the standard normal variate z is computed by using Equation (5) (Douglas *et al*., 2000).

$$Z = \begin{Bmatrix} \frac{S-1}{\sqrt{Var(S)}} \; if \; S > 0 \\ 0 \qquad if \; S = 0 \\ \frac{S+1}{\sqrt{Var\,(S)}} \; if \; S < 0 \end{Bmatrix} \qquad (5)$$

In a two-sided test for trend, H_0 should thus be accepted if $|z| \leq z\ \alpha/2$ at the α level of significance. A positive value of S indicates an ‘upward trend’; likewise, a negative value of S indicates ‘downward trend’. The significance level that indicates the trend’s strength.

3.3 Sen’s estimator

If a linear trend is present in a time series, then the true slope (change per unit time) can be estimated by using a simple non-parametric procedure developed by Sen (1968b). The slope estimates of N pairs of data are first computed by

$$Q_i = \frac{(x_j - x_k)}{(j-k)} \quad \text{for i = 1,……,N} \qquad (6)$$

where x_j and x_k are data values at times j and k (j > k) respectively. The median of these N values of Q_i is Sen’s estimator of slope. If N is odd, then Sen’s estimator is computed by $Q_{median} = Q_{(N+1)/2}$ and if N is even, then Sen’s estimator is computed by

$$Q_{median} = \frac{\left[Q_{N/2} + Q_{(N+2)/2}\right]}{2} \qquad (7)$$

The detected value of Q_{median} is tested by a two-sided test at the 100(1 -α)% confidence interval and the true slope may be obtained by the non-parametric test.

4. RESULTS AND DISCUSSION

4.1 Streamflow

It is seen that some significant negative trends in annual minimum streamflow. The largest negative trend was occurred in Kalaewa. There are no significant

trends detected in the annual maximum streamflow and annual average streamflow series. The mean monthly flow represents a further breakdown of mean annual flow analysis. Stations located in southern part of basin such as Kalaewa and Monywa display negative trends in monthly mean streamflow. Homalin located in northern part of basin displays positive trends, suggesting increase in monthly mean streamflow. In contrast, Hkamti and Mawlaik, in general, show no trends.
It is seen that monthly mean streamflow in Monywa for most months decreased, with the strongest decrease in summer and winter. The results of Mann-Kendall test with Sen's slope estimator for discharge time series of Homalin, Kalaewa and Monywa are summerised in Table 1, Table 2 and Table 3 respectively. In this study, the tested significance level α are 0.05,0.01 and 0.001.Figure 2 shows the results for the annual minimum daily flow for study period.

Table 1: Results of Mann-Kendall test with Sen's slope estimator for discharge time series for Homalin

Time series (m^3/s)	**Mann-Kendall test**			**Sen's slope estimator**		
	z	**trend**	**significance**	**Q**	**Q_{lower}**	**Q_{upper}**
Annual time series						
Mean	-	-		-3.72	-	11.5
Maximum	-	-		-38.60	-	29.6
Minimum	**3.0**	+	**	4.95	1.87	8.32
Monthly time series						
January	**2.4**	+	*	4.59	0.94	8.42
February	**2.1**	+	*	4.47	0.37	8.38
March	**2.1**	+	*	5.04	0.26	9.02
April	**1.9**	+	*	4.84	0.02	10.1
May	**2.3**	+	*	8.66	1.00	16.3
June	-	-		-11.79	-	28.7
July	-	-		-9.27	-	66.9
August	-	-		-30.54	-	25.7
September	-	-		-16.83	-	31.0
October	0.2	+		5.76	-	39.9
November	1.2	+		4.99	-2.44	12.3
December	**2.1**	+	*	4.75	0.63	8.67
Seasonal time series						
Summer-season	**3.0**	+	**	7.09	2.73	11.5
Rainy-season	-	-		-13.03	-	17.0
Winter -season	**2.0**	+	*	4.83	0.23	8.64

Data series with significant trends are shown in bold. Q_{lower} and Q_{upper} are slope confidence limits at the 95% confidence level.
* α = 0.05 level of significance
** α = 0.01 level of significance

*** α = 0.001 level of significance

Table 2: Results of Mann-Kendall test with Sen's slope estimator for discharge time series for Kalaewa

Time series (m^3/s)	Mann-Kendall test			Sen's slope estimator		
	z	trend	significance	Q	Q_{lower}	Q_{upper}
Annual time series						
Mean	0.0	+		0.58	-	14.8
Maximum	-	-		-70.00	-	23.1
Minimum	-	-	***	-4.43	-6.00	-2.67
Monthly time series						
January	-	-	*	-2.80	-5.54	-0.15
February	-	-	***	-3.24	-5.16	-1.43
March	-	-	**	-3.21	-5.59	-1.17
April	-	-	*	-3.67	-6.97	-0.83
May	0.0	+		0.26	-8.50	10.7
June	-	-		-1.27	-	43.7
July	0.2	+		12.79	-	93.8
August	-	-		-25.53	-	35.8
September	0.5	+		13.47	-	69.1
October	0.7	+		21.54	-	64.4
November	0.7	+		3.84	-	18.8
December	-	-		-2.94	-7.38	1.46
Seasonal time series						
Summer-season	-	-		-1.14	-5.06	3.09
Rainy-season	0.1	+		3.62	-	38.4
Winter -season	-	-		-0.91	-6.52	3.28

Table 3: Results of Mann-Kendall test with Sen's slope estimator for discharge time series for Monywa

Time series (m^3/s)	Mann-Kendall test			Sen's slope estimator		
	z	trend	significance	Q	Q_{lower}	Q_{upper}
Annual time series						
Mean	-	-		-9.21	-	6.29
Maximum	-	-		-5.81	-	103.
Minimum	-	-	**	-4.73	-7.57	-1.22
Monthly time series						
January	-	-	**	-6.62	-	-3.52
February	-	-	**	-5.25	-8.74	-1.86
March	-	-		-3.13	-6.90	0.31
April	-	-	*	-4.47	-8.92	-0.06

May	-	-		-2.33	-	7.48
June	-	-		-23.23	-	29.3
July	0.3	+		10.01	-	76.1
August	-	-		-28.86	-	20.9
September	-	-		-9.54	-	45.5
October	-	-		-26.06	-	36.1
November	-	-		-13.56	-	1.67
December	-	-	***	-9.10	-	-3.96
Seasonal time series						
Summer-season	-	-		-3.13	-9.15	2.33
Rainy-season	-	-		-4.63	-	27.3
Winter -season	-	-	**	-10.73	-	-4.42

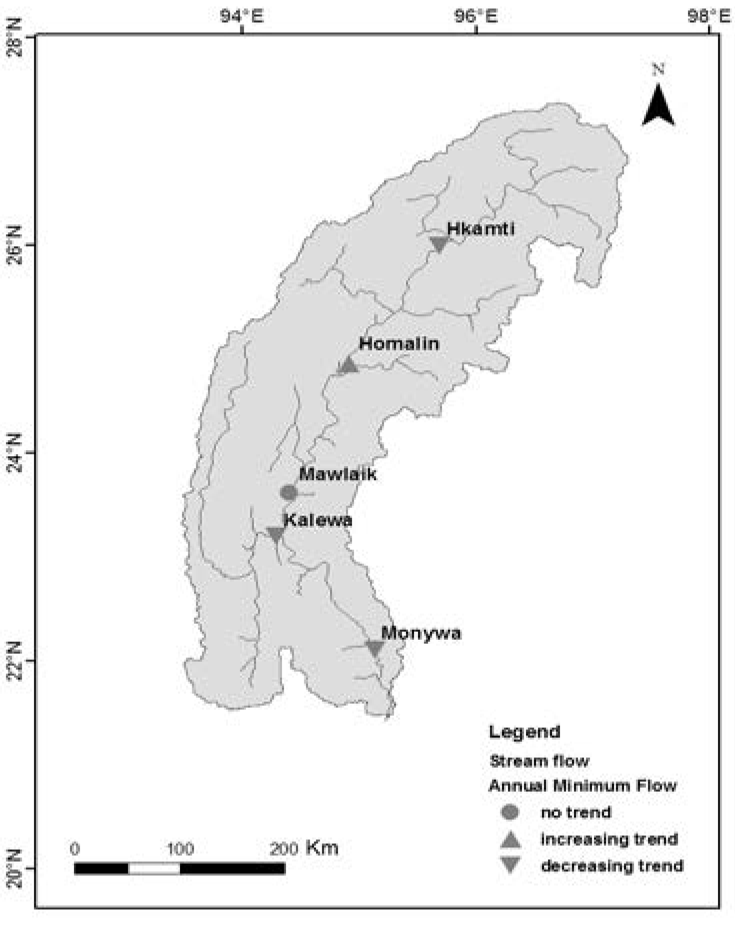

Figure 2: Trend results for annual minimum flow for the study period

4.2 Rainfall

Rainy season rainfall (from June to middle of October) accounted for about 85% of annual rainfall. The rainfall stations in Chindwin river basin displayed insignificant trends for annual total rainfall and annual average rainfall. Minkin station indicated increasing trend in annual maximum rainfall. There are no significant trends in most of the monthly rainfall time series in Hkamti, Homalin, Mawlaik, Kalaewa and Monywa. It is seen that some significant positive trends in monthly rainfall in Minkin.

4.3 Temperature

Geographically, the increasing trends of monthly mean temperature were concentrated in the southern regions of the river basin while the decreasing trends monthly mean temperature appeared primarily in the northern regions of the river basin.

5. CONCLUSION

The results of Mann-Kendall test showed some strong significant decreasing trends in the annual minimum flow. The application of trend detection technique to Chindwin river basin has resulted in the identification of significant trends of appearing in the southern parts of the river basin. The direction of trends of monthly flow is, in general, downward. The decrease in annual mean flow plays a dominant role in the determination of reservoir capacity and the reservoir management works afterward.

A noticeable increase in the monthly mean temperature was observed mostly in Mawlaik, Kalaewa and Monywa. Noteworthy was strong decreasing trend in the annual minimum flow of Kalaewa and Monywa. The timing of a hydrologic event was found to be influenced to the greatest extent by changes in temperature. The hydrologic variables would have decreasing flow trends and negative correlations with temperature.

It is important to investigate present and probable future climatic change patterns and their impacts on water resources so that appropriate adaptation strategies may be implemented. The trend attribution and the relation between the observed streamflow trends and climate change should be addressed in future studies with the inclusion of the influence of evapotranspiration variable. It may be concluded the climate change has caused the downward trends in streamflow in lower parts of Chindwin river basin.

REFERENCES

Abdul Aziz, O.I., and Burn, D.H., 2006. *Trends and variability in the hydrological regime of the Mackenzie River Basin*. J. Hydrol. 319, 282–294.

Burn, H.B., and Elnur, M.A.H., 2002. *Detection of hydrologic trends and variability.* Journal of Hydrology 255, 107–122.

Burn, D.H., and Soulis, E.D., 1992. *The use of hydrologic variables in detecting climatic change: possibilities for single station and regional analysis*. In: Kite, G.W., Harvey, K.D. (Eds.), Using hydrometric data to detect and monitor climatic change, Proceedings of NHRI Workshop No. 8, National Hydrology Research Institute, Saskatoon, Saskatchewan.

Douglas, E.M., Vogel, R.M., and Kroll, C.N., 2000. *Trends in floods and low flows in the United States: impact of spatial correlation*. Journal of Hydrology 240, 90–105.

Helsel, D.R., and Hirsch, R.M., 1992. *Statistical Methods in Water Resources*. Elsevier, Amsterdam.

Hirsch, R.M., and Slack, J.R., 1984. *A nonparametric trend test for seasonal data with serial dependence*. Water Resources Research 20 (6), 727–732.

Kahya, E., and Kalaycı, S., 2004.*Trend analysis of streamflow in Turkey.Journal of Hydrology*. 289,128-144.

Kendall, M.G., 1975. *Rank Correlation Methods*. Griffin, London, UK.

Kite, G., 1991. *Looking for evidence of climatic change in hydrometeorological time series*. Western Snow Conference, April 12–15, Washington to Alaska.

Kundzewicz, Z.W., 2004. *Searching for change in hydrological data*. Hydrological Sciences Journal 49, 3–6.

Liu, Q., Yang, Z.F., and Cui, B.S., 2008. *Spatial and temporal variability of annual precipitation during 1961–2006 in Yellow River Basin, China*. J. Hydrol. 361, 330–338

Mann, H.B., 1945. *Nonparametric tests against trend*. Econometrica 13, 245–259.

Sen, P.K., 1968b. *Estimates of the regression coefficient based on Kendall's tau*. Journal of American Statistical Association 39, 1379–1389.

Serrano, A., Mateos, V.L., and Garcia, J.A., 1999. *Trend analysis of monthly precipitation over the iberian peninsula for the period 1921–1995*. Physics and Chemistry of the Earth, Part B: Hydrology, Oceans and Atmosphere 24, 85–90.

Von Storch, H., and Navarra,A.,1995. *Analysis of climate variability*. Springer, New York.

Walling, D.E., and Fang, D., 2003. *Recent trends in the suspended sediment loads of the world's rivers*. Global and Planetary Change 39, 111–126.

Westmacott, J.R., and Burn, D.H., 1997. *Climate change effects on the hydrologic regime within the Churchill–Nelson River Basin*. J. Hydrol. 202 (1), 263–279.

Yue, S., Pilon, P., Phinney, B., and Cavadias, G., 2002. *The influence of autocorrelation on the ability to detect trend in hydrological series*. Hydrological Processes 16, 1807–1829.

Seismic stability of reinforced soil walls in the 2011 Tohoku Earthquake

Jiro KUWANO[1], Yoshihisa MIYATA[2] and Junichi KOSEKI[3]
[1] Professor, GRIS, Saitama University, Japan
jkuwano@mail.saitama-u.ac.jp
[2]Professor, Dept. of Civil and Environmental Eng., National Defense Academy, Japan
[3] Professor, IIS, the University of Tokyo, Japan

ABSTRACT
The 2011 off the Pacific coast of Tohoku Earthquake of Mw=9.0 with a huge source region of about 450km by 200km caused extensive damage of various structures. This paper briefly reviews the reinforced soil walls in Japan first. After discussing limit state levels of reinforced soil walls, the paper reports the summary of seismic performances of about 1600 walls in the 2011 Tohoku earthquake. It also reports some case histories on the reinforced soil walls which were subjected to the direct impact of the earthquake (shaking). Just less than 1% of the walls were seriously damaged but more than 90% of the walls did not show any serious damage. Repair works of the damaged reinforced soil walls are introduced as well.

Keywords: *reinforced soil wall, limit state, damage statistics, repair works*

1. INTRODUCTION

The 2011 off the Pacific coast of Tohoku Earthquake (The 2011 Tohoku Earthquake) of *M*w=9.0 with a huge source region of about 450 km by 200 km occurred on March 11, 2011 as shown in Figure 1 (USGS, 2012a). It is the largest earthquake ever recorded in Japan and the fourth largest in the world after 1900 (USGS, 2012b). Seismic motions observed in this earthquake are shown in Figure 2 (Yamanaka, 2011). As compared with the 1995 Hyogoken-Nanbu (Kobe) and the 2004 Chuetsu earthquakes, the 2011 earthquake has two main shocks with extremely long duration of vibration for more than two minutes. Because of the huge source region of the earthquake, the failure of the crust (energy discharge) did not take place at once but separately and gradually within the source region. It caused extensive damage of liquefaction in Tokyo and its surroundings. A

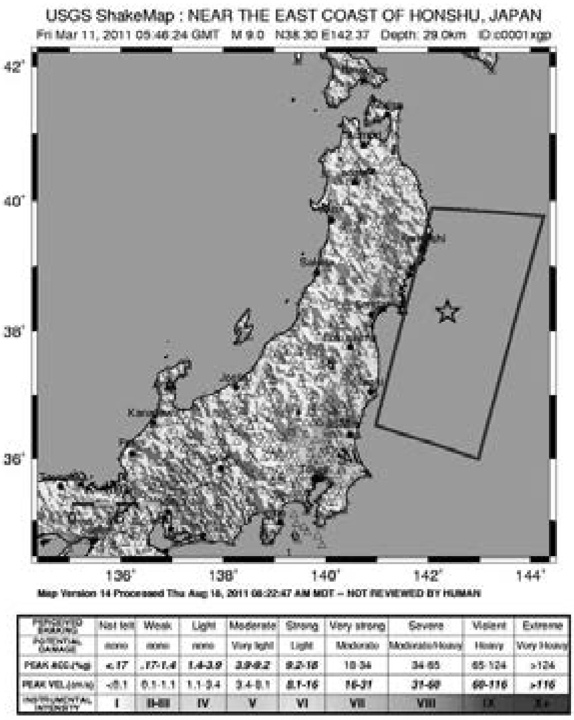

Figure 1: Source region and seismic intensity（USGS, 2012a)

lot of failures of slopes and embankments occurred in Tohoku and Kanto regions.

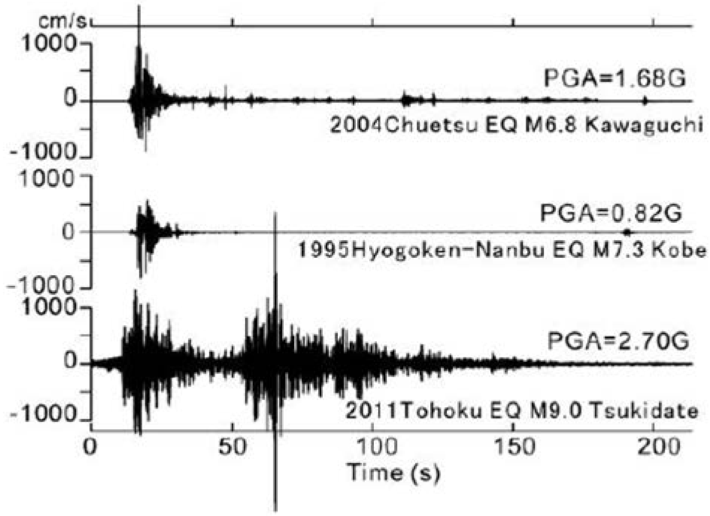

Figure 2: Observed seismic motion during recent earthquakes in Japan (Yamanaka, 2011)

Almost 20,000 people are dead or missing by the 2011 Tohoku earthquake. Tsunami was the most serious impact of the earthquake. Inundation height and run-up height were as high as about 40 m. It killed thousands of lives and caused extensive damage of various structures such as seawalls and bridges. Many seawalls and river dikes were washed out by the tsunami. However, many reinforced soil walls survived the tsunami impact, though they were partly or fully submerged.

There are numbers of reinforced soil walls in Tohoku region. Miyata (2012) reported the damage of the walls by the earthquake and summarized that just less than 1% of the walls were seriously damaged (some walls were damaged by the tsunami) but more than 90% of the walls did not show any damage.

This paper briefly reviews the reinforced soil walls in Japan first, then reports the summary of seismic performances of about 1600 walls in the 2011 Tohoku earthquake. It also reports some case histories on the reinforced soil walls which were subjected to the direct impact of the earthquake (shaking) and repair works for them.

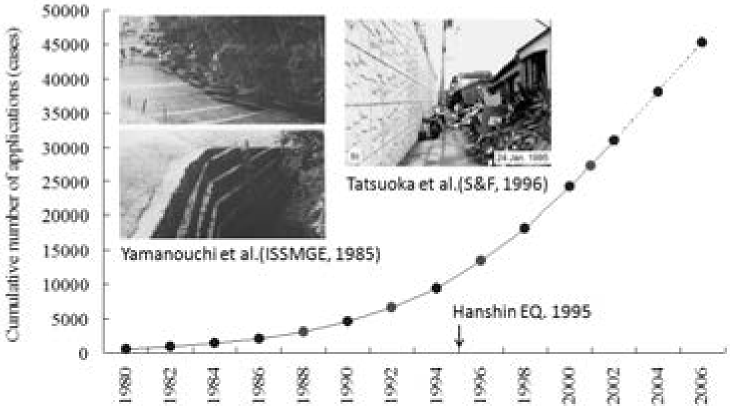

Figure 3: Diffusion of reinforced soil wall technology in Japan (Ochiai, 2007)

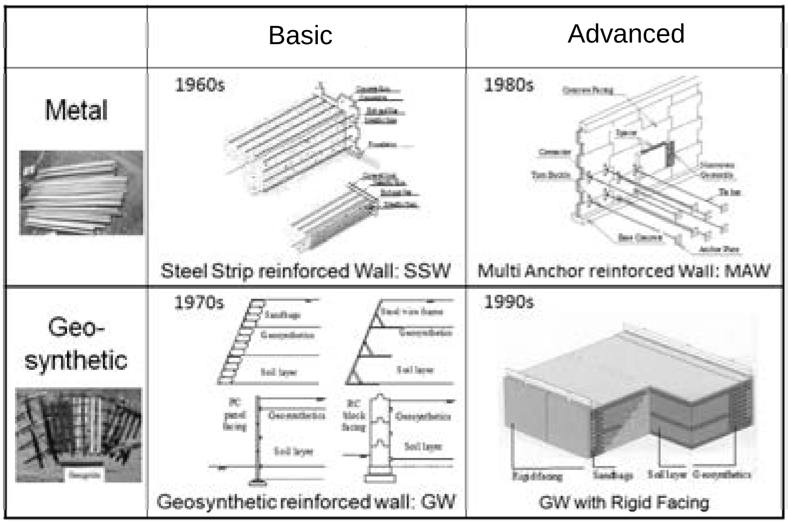

Figure 4: Reinforced soil wall technology in Japan (modified Miyata, 2012)

2. REINFORCED SOIL WALLS IN JAPAN

Application of reinforced soil walls in Japan begun in the 1970s and increased with time as shown in Figure 3 (Ochiai, 2007). Reinforced soil walls in Japan can be classified into four types by the reinforcement, metal or geosynthetics, and the development phase, basic and advanced, as summarized in Figure 4 (modified Miyata, 2012). They are a steel strip wall, a geosynthetic wall, a multi-anchor wall (Fukuoka et al., 1980) and a geosynthetic wall with full-height rigid facing (Tatsuoka et al., 1989). The right-hand picture (Tatsuoka et al., 1996) in Figure 3 indicates the survived reinforced soil wall with full-height facing and the seriously damaged adjacent houses in the 1995 Kobe earthquake (Great Hanshin earthquake). The performances of reinforced soil walls proved their high seismic resistance. Therefore, the application of this technology increased especially after the 1995 Kobe earthquake (Koseki et al., 2006).

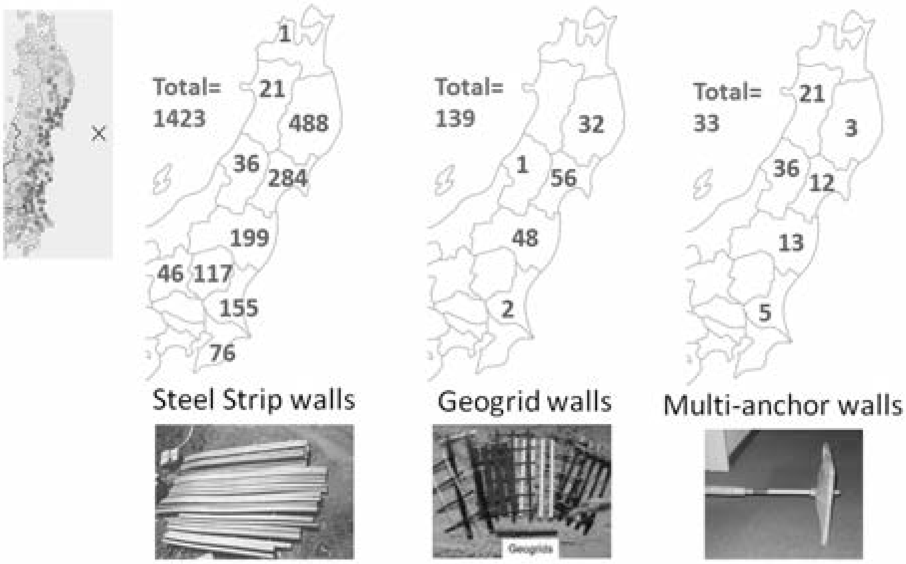

Figure 5: Site investigation of earthquake damage to reinforced soil wall in the 2011 Tohoku earthquake (Miyata, 2012)

Table 1: Damage statistics of reinforced soil wall in the 2011 Tohoku earthquake (Miyata, 2012)

	Steel strip walls	Geogrid walls	Multi-anchor walls
Ultimate limit state	0.3%	0.7%	0%
Restorability limit state	1.0%	4.3%	0%
Serviceability limit state	7.0%	0.7%	3.0%
No damage	91.7%	94.3%	97.0%

3. PERFORMANCE OF REINFORCED SOIL WALLS IN THE 2011 TOHOKU EARTHQUAKE

The 2011 Tohoku Earthquake is the largest earthquake ever recorded in Japan and the fourth largest in the world after 1900 (USGS, 2012b). Wide area in the Tohoku and Kanto regions were strongly shaken by the earthquake as shown in Figure 1 (USGS, 2012a). At some locations, very high accelerations of more than 1000 gal, or even more than 2000 gal at particular sites, were recorded. Large settlement, sliding failure, and collapsing of conventional type retaining wall of unreinforced soil structure, such as road and railway embankments, earth dams and housing sites, occurred by the earthquake.

With respect to the performances of reinforced soil walls, various teams went to the wall sites, where the JMA (Japan Meteorological Agency) seismic intensity scales were mostly greater than 5 upper. Although the current JMA scale is hard to be converted to the MMI (Modified Mercalli intensity) scale, the former JMA scale, I_{JMA}, was roughly connected with the MMA scale, I_{MM}, through the equation of I_{MM}=0.5+1.5I_{JMA}. If the sinusoidal seismic motion with a period of 1 second continues for a few seconds, I_{JMA} of 5 upper corresponds to about 100 gal. For I_{JMA} of 7, about 600 gal is necessary for a period of 1 second, however about 2700 gal for a period of 0.1 second (JMA, 2012). Figure 5 shows the number of investigated reinforced soil walls by prefecture in the Tohoku region for three types of walls, i.e. steel strip walls (Terre Armee), multi-anchor walls and geogrid walls.

The damage of reinforced soil walls can be classified into four levels, namely, ultimate limit state, restorability limit state, serviceability limit state, and no damage. Table 1 summarizes the damage statistics of investigated reinforced soil walls in the 2011 Tohoku earthquake. The ultimate limit state is only less than 1% of investigated walls for all the three types. More than 90% of the walls show no damage. It is to be mentioned that the 2011 Tohoku earthquake was so huge, and its aftershocks were also very strong. Such a strong seismic load was not considered in the design of reinforced soil walls. However, most of the walls showed very high seismic resistance in the earthquake. This implies that the actual seismic performance of reinforced soil walls is considerably higher than the design target.


Case 1: Ultimate limit state of a geogrid wall


Case 2: Ultimate limit state of a steel strip wall


Case 3: Restorability limit state

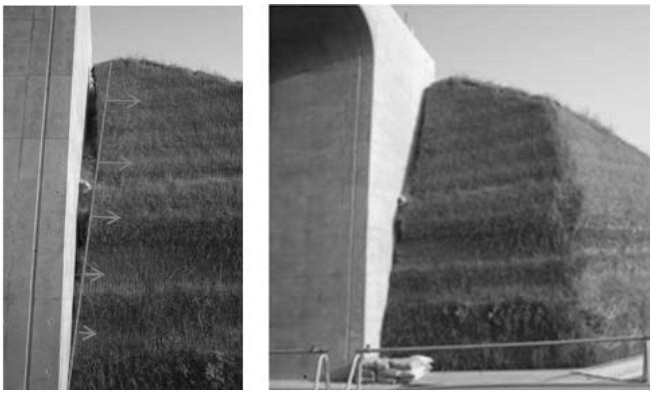
Case 4: Serviceability limit state of a geogrid wall


Case 5: Serviceability limit state of a wall with concrete facing panels

 

Case 6: collapsed embankment (left) and geogrid wall with no damage (right)
Figure 6: Performance of reinforced soil walls to the direct impact of seismic motion (Cases1: Kaneko and Kumagai, 2011; 2: courtesy of Dr. Otani, 3 to 6: JC-IGS Technical Committee)

4. PERFORMANCE OF REINFORCED SOIL WALLS TO THE DIRECT IMPACT OF SEISMIC MOTION

Some case studies of different level seismic performance of reinforced soil walls shown in Figure 6 are introduced in the followings.

4.1 Case 1: Ultimate limit state of a geogrid wall

A 5 m high geogrid reinforced wall with expanded metal mesh facing collapsed. Not only internal slippage but also connection failure was observed. This damage state can be classified into the “ultimate limit state.” The estimated seismic intensity was 6 lower at this location. The equivalent ground acceleration was estimated to be 300 gal. The site investigation indicated that this collapse was caused by the fact that the ground water level in this wall was very high because of the lack of a drainage system.

4.2 Case 2: Ultimate limit state of a steel strip wall

A 10 m high steel strip wall on the soft soil ground collapsed owing to the 7 m horizontal sliding of the foundation slope caused by seismic motion. The estimated JMS seismic intensity was 6 lower at this site. The equivalent ground acceleration estimated for the period of 0.5 sec was about 300 gal. The site investigation revealed that this slope failure occurred because the foundation soil was not sufficiently treated. Adequate ground improvement should have been carried out.

4.3 Case 3: Restorability limit state of a geogrid wall

A 5.4 m high geogrid reinforced wall with wire mesh facing was damaged. A considerable amount of horizontal deformation of the facing and a gap between the reinforced soil wall and the rigid reinforced concrete structure were observed.

This damage can be classified into the “restorability limit state” damage because the horizontal deformation was more than the allowable limit. The estimated seismic intensity was 6 lower at this location. The equivalent ground acceleration was estimated to be 300 gal. Further, the site investigation revealed that this damage could be attributed to the fact that the fill material had a considerable amount of fine contents and the ground water level in the wall was very high.

4.4 Case 4: Serviceability limit state of a geogrid wall

Although a gap between the geogrid reinforced soil wall and the concrete bridge abutment was found similar to the Case 3, the horizontal facing deformation was within the allowable limit and the damage of the wall was ranked as the “serviceability limit state”. This wall was repaired using soil nailing, soil cement, and vegetation technique, as shown in Figure 7.

4.5 Case 5: Serviceability limit state of a wall with concrete facing panels

A steel strip wall and a multi-anchor wall have concrete panel facing. After the earthquake, damage of the concrete panels was found at some points. This damage is categorized as the “serviceability limit state.” A repairing method for the damaged concrete panel has already been developed as shown in Figure 8. Only the damaged part in the panel was cut, and concrete milk was injected into the spot. Whole the panel can be replaced as well.

Figure 7: Repairing of differential deformation between geogrid reinforced wall and RC structure

Figure 8: Repairing of concrete panel facing of steel-reinforced soil wall

4.6 Case 6: No damage of a geogrid wall

A 5.4 m high geogrid reinforced wall with wire mesh facing was found to have no damage. This wall was constructed as a repair work of housing embankment failed due to heavy rain. However, an ordinary embankment without reinforcement failed due to the seismic motion in the slope beside the reinforced wall as seen in the figure. At this site, a strong seismic motion having the JMA seismic intensity of 6 lower seemed to act on both the structures. This is the case history which clearly indicates the high seismic resistance of a reinforced soil wall

5. SUMMARY

The 2011 off the Pacific coast of Tohoku Earthquake of Mw=9.0 caused extensive damage of various structures. Damage caused by tsunami was tremendous and a lot of lives were lost. Performance of reinforced soil walls in the 2011 Tohoku earthquake was reported in this paper. It was found through approximately 1600 site investigations that reinforced soil walls showed very high seismic resistance in the 2011 Tohoku earthquake. Just less than 1% of the walls were seriously damaged but more than 90% of the walls did not show any damage. Repair works of the damaged reinforced soil walls were introduced as well.

REFERENCES

Fukuoka, M., Imamura, Y., Kudoh, K., Naitoh, S. and Fukahori, T., 1980. Research on multi-anchor wall, *Proceedings of 15th Japanese Geotechnical Society Annual Meeting*, Hiroshima, Japan, 1525-1528 (in Japanese).

Japan Meteorological Agency, 2012. Seismic intensity and acceleration. http://www.seisvol. kishou.go.jp/eq/kyoshin/kaisetsu/comp.htm, viewed on September 11, 2012 (in Japanese).

Kaneko, K. and Kumagai, K., 2011. Damages of reinforced earth walls at Iwate area in the 2011 off the Pacific coast of Tohoku Earthquake and tsunami, *Geosynthetics Technical Information*, *JC-IGS*, 27 (2), 16-23 (in Japanese).

Koseki, J., Bathurst, R.J., Guler, E., Kuwano, J. and Maugeri, M., 2006. Seismic stability of reinforced soil walls, *Proceedings of the 8th International Conference on Geosynthetics*, Yokohama, Japan, 1, 51-77

Miyata, Y., 2012. Reinforced soil walls during recent earthquakes in Japan and geo-risk-based design. Keynote Lecture, *Second International Conference on Performance-Based Design in Earthquake Geotechnical Engineering*, May 28-30, 2012, Taormina, Italy, draft.

Ochiai, H., 2007. Earth reinforcement technique a role of new geotechnical solutions - memory of IS Kyushu, *Proceedings of the International Symposium on Earth Reinforcement*, *IS-Kyushu 2007*, Fukuoka, Japan, 1–23.

Tatsuoka, F. Tateyama, M. and Murata, O., 1989. Earth retaining wall with a short geotextile and a rigid facing, *Proceedings of the 12th ICSMFE*, Rio de Janeiro, 2, 1311-1314.

Tatsuoka, F., Tateyama, M. and Koseki, J., 1996. Performance of soil retaining walls for railway embankments, *Soils and Foundations*, *Special Issue for the 1995*

Hyogoken–Nambu Earthquake, 311-324.
US Geological Survey, 2012a. Magnitude 9.0 - Near the east coast of Honshu, Japan, http://earthquake.usgs.gov/earthquakes/eqinthenews/2011/usc0001xgp/, viewed on September 11, 2012.
US Geological Survey, 2012b. Magnitude 8 and Greater Earthquakes Since 1900, http://earthquake.usgs.gov/earthquakes/eqarchives/year/mag8/magnitude8_1900_mag.php, viewed on September 11, 2012.
Yamanaka, H., 2011. Strong motion characteristics and aftershock observations, *Center for Urban Earthquake Engineering (CUEE), Tokyo Institute of Technology Newsletter No.11 - 2011 Tohoku Pacific Earthquake.*

Ideal regional disaster management plan based on the experience from the 2011 Great East Japan Earthquake

Kimiro MEGURO
Professor, Director, ICUS, IIS, The University of Tokyo, Japan
meguro@iis.u-tokyo.ac.jp

ABSTRACT

At 14:26 (Japan local time) on March 11, 2011, gigantic earthquake with Mw 9.0, called Great East Japan Earthquake, occurred off the coast, approximately 70 km east of Miyagi Prefecture, Japan. The earthquake triggered powerful tsunami waves that reached heights of up to 40.5 m in Miyako City, Iwate Prefecture. Approximately twenty-thousand people were killed mainly due to Tsunami and over 100 thousand houses and buildings were completely collapsed. The number of municipalities in severely affected areas was over 240. In this paper, lessons learned from the disaster due to the 2011 Great East Japan Earthquake and the subsequent reconstruction process, issues and problems of the current regional disaster management plan are examined and the ideal regional disaster management plan and its implementation strategy are introduced. A comprehensive disaster management system is introduced based on three relief types (self-help effort, mutual assistance, and public support) and seven stages of disaster countermeasures (damage mitigation, preparedness, prediction & early warning, damage assessment, disaster response, recovery and reconstruction). Also, specific action plan with appropriate priorities is proposed.

Keywords: *disaster management plan, total disaster management, disaster life cycle, self-help effort, mutual assistance, and public support*

1. INTRODUCTION

In this paper, based on the lessons learned from the disaster and subsequent reconstruction process from the 2011 Great East Japan Earthquake and Tsunami disaster, issues and problems of the current regional disaster management plan are examined. In order to reduce the damage anticipated from Tokyo metropolitan earthquake and huge earthquakes along the Nankai Trough, the plan needs to be revised and the strategy for implementing ideal regional disaster management plan and specific action plan with appropriate priorities are introduced.

2. ISSUES OF THE REGIONAL DISASTER MANAGEMENT PLAN

2.1 Summary of regional disaster management plan

Within the legal system of the Disaster Countermeasures Basic Act enacted in 1961 in the wake of the damage caused by the Ise Bay typhoon of 1959, the regional disaster management plan is formulated by the local governments based on national basic disaster management plan prepared by the Central Disaster Management Council. It is positioned at the top of legal system and comprises of a comprehensive disaster management plan composed of damage estimation and plans for disaster prevention, response, recovery and reconstruction for each type of disaster.

2.2 Issues of Disaster Countermeasures Basic Act

The regional disaster management plan is determined by the municipalities and prefectures based on the national basic disaster management plan specified in the Disaster Countermeasures Basic Act, considering both social and natural environment of the region. Disaster Countermeasures Basic Act which provides the framework for regional disaster management plan specifies the policies and basic disaster response measures. It is intended to adjust the overall system and policies of disaster management organizations. Due to the nature of disaster management which is in close contact with the residents, the authority of the mayor of a municipality is enhanced. However, there are issues with this approach which have been pointed out for a long time and they were also recognized during the 2011 Great East Japan Earthquake and Tsunami Disaster. Five major issues pointed out are as follows:

1) Scale of disaster
   Strengthening of disaster response plan in case of a large-scale disaster over a wide area that exceeds the border between prefectures is needed.
2) Administrative coordination
   Administrative coordination among the adjacent municipalities, especially those under different prefectures, is difficult.
3) Resident participation
   The opportunity for the local residents and NPO/NGO staffs to participate in the planning phase is extremely low and the activity for publicizing disaster-related information is insufficient.
4) Principles in Disaster Relief Act or provision of public fund
   The disaster related laws are applied based on the scale of disaster however it is unfair considering at individual’s level.
5) Coordination among the responsible authorities
   While the Disaster Relief Act is under the jurisdiction of a Ministry of Health, Labor and Welfare, the Disaster Countermeasures Basic Act is under the Cabinet Office. Cooperative work between these two ministries is required in order to realize rapid and efficient disaster response.

2.3 Problems of regional disaster management plan

Facing the devastation beyond expectation caused by the Tsunami during the 2011 Great East Japan Earthquake, the administrative function of many municipalities has dropped drastically. Under such circumstances, could the existing regional disaster management plan function properly? Many of the existing plans do not reflect the natural and social environment that is unique to the region and that the way it is described is too abstract to follow at the time of disaster. The main problems are summarized into the following five points:

1) The request of help must come from the disaster affected municipalities to prefectures or adjacent municipalities during the large-scale disaster and the countermeasures for regional coordination including the national government is insufficient.
2) The current plan focuses on post-disaster countermeasures rather than on pre-disaster ones with an assumption that the work environment of the municipal officers is safe and unaffected by the disaster. It is necessary to prepare Business Continuity Plan based on the worst-case scenario.
3) There is a lack of regional cooperation and countermeasures involving the local actors including residents based on the idea of “total disaster management” and “public support, mutual assistance and self-help effort”.
4) There is a lack of understanding for a proper disaster management based on the disaster life cycle.
5) The countermeasures for recovery and reconstruction are poor.

In order to minimize the impact by the future big disaster, the problems described above must be solved and through reexamination of regional disaster management plan is the most urgent issue.

2.4 Problems with municipalities

What are the problems municipalities would face when formulating the regional disaster management plan? According to the surveys conducted to the prefectures and municipalities along the coast of Pacific Ocean along the Nankai Trough in February 2012, many of them have started to reexamine the regional disaster management plan and are recognizing the difficulty such as lack of man-power especially staff with special knowledge and skills in disaster management, and lack in budget, etc.

3. IDEAL REGIONAL DISASTER MANAGEMENT PLAN AND ITS IMPLEMENTATION STRATEGY

3.1 Vision for ideal regional disaster management plan

Based on the problems and issues discussed so far, the vision for ideal regional disaster management plan is stated below. This is aimed at the entire framework of the plan including all types of disasters.

The regional disaster prevention plan shall be on top of all disaster management measures of local public body and truly effective to mitigate the disaster. The plan must be comprehensive so that it is influential to all related planning such as urban planning. Its content shall include disaster prevention plan with clearly stated management plan to protect the lives and properties of all people and it shall be able to sustain its minimum function against mega-scale disaster based on agreements made with related agencies and residents.

3.2 Implementation strategy

In order to make truly effective regional disaster management plan, the following implementation strategy is proposed.

3.2.1 Structuring and practice for comprehensive management system for minimizing disaster impact

Comprehensive countermeasures can be broken down into seven stages as shown in Figure 1, starting with disaster mitigation, preparedness, prediction and early warning as a part of pre-disaster countermeasures and damage assessment, disaster response, recovery and reconstruction as a part of post-disaster countermeasures. All seven countermeasures combined is called "Disaster Life

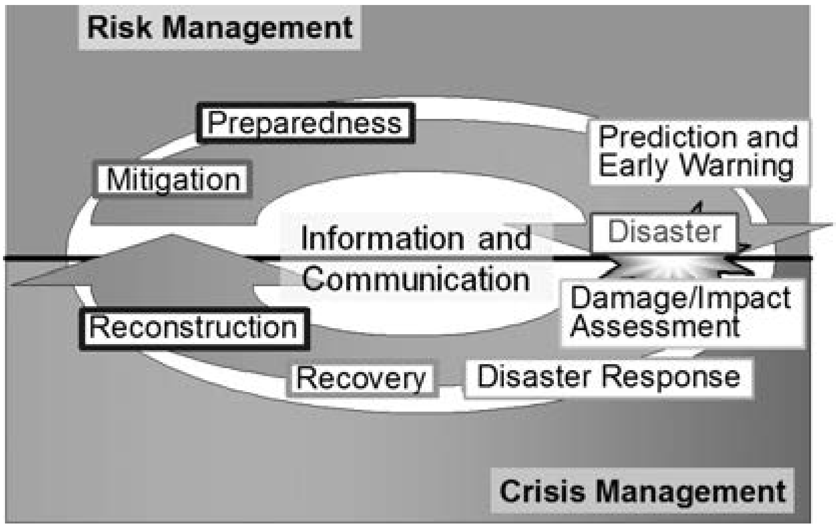

Figure 1: Total disaster management system for minimizing negative impact

Cycle" and information and communication play important role at all seven stages.

3.2.2 Disaster Countermeasure Matrix for Total Disaster Management

At all seven stages of disaster management, it is necessary to understand that the government is not the only actor in disaster management but the collaboration among local community and resident participation is vital. And it is necessary to act based on the idea that one must protect one's own life and recognize the three forms of relief effort described as public support (PS), mutual assistance (MA) and self-help effort (SE).

After the 1995 Kobe Earthquake, the importance of mutual assistance and self-help effort has been recognized, however during the 2011 Great East Japan Earthquake Disaster, private companies' involvement in mutual assistance and self-help effort was recognized as important, collaborating with the local people in action such as rescue and firefighting.
Disaster Countermeasure Matrix shown in Figure 2 represents the idea that in all

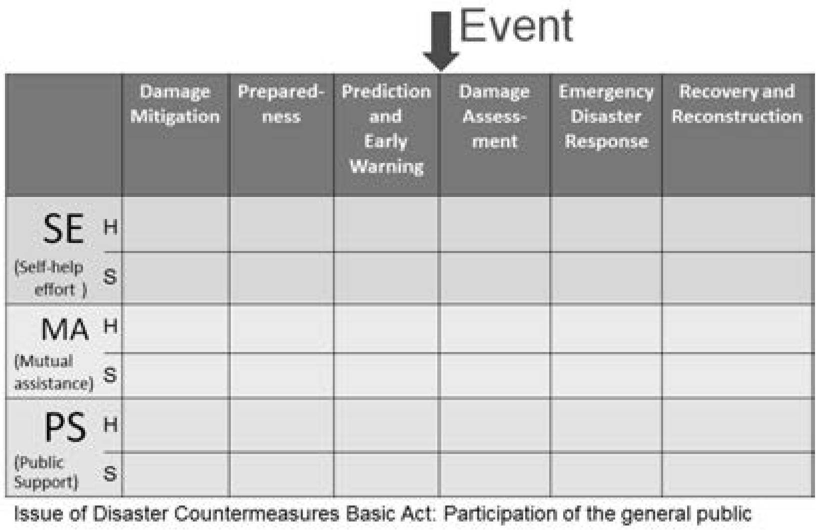

Figure 2: Disaster countermeasure matrix

seven stages, there are tasks for three types of relief effort – public support, mutual assistance and self-help effort. The countermeasure by three types of relief effort is often complementary to each other and it must be well-balanced. In other words, if the work is concentrated in public support part, the cost could be enormous while if each individual put an effort and cooperate with each other, it could be much more effective with less cost. Public support should promote mutual assistance and self-help effort rather than enhancing people's dependency to public support. In order to realize this situation, disclosure of information about the disaster risk to the general public becomes important.

3.2.3 Promotion method for comprehensive disaster management

In order to efficiently conduct disaster reduction countermeasures, it is important to make appropriate combinations of regional characteristics, target disaster types, available time and budget at each stage. Specific procedure is as follows (Figure 3). Local government offices should start by filling up the matrix with effective countermeasures. This approach can be applied not only for earthquake and tsunami but also for all other various types of disaster. However the contents will differ based on the type of hazard and thus Disaster Countermeasure Matrix for each type of disaster needs to be created and all necessary disaster matrixes should be integrated (Figure 4).

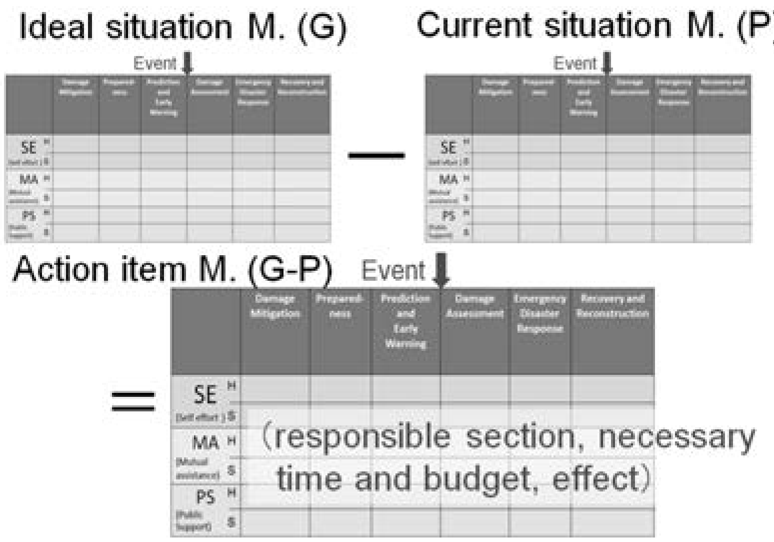

Figure 3: Making of action item matrix

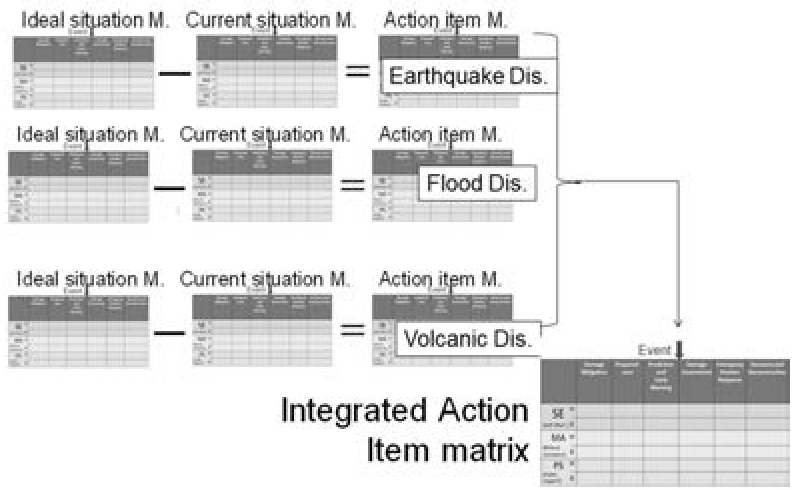

Figure 4: Making of integrated action item matrix

1) Describe specific countermeasures to achieve (G: goal) in order to implement the ideal regional disaster prevention plan as well as current situation (P: present) in Disaster Countermeasure Matrix (M).
2) The difference between the “Ideal situation M” and “Current situation M” indicate the “Action item M” that needs to be done.
3) Fill in the responsible section, necessary time & budget and effect into the “Action item M”. It is important to work this section together with site operators.
4) Examine available time and budget with the result of 3) and determine realistic countermeasures that can achieve maximum effect within the given condition. Combine the result and create project plan.
5) By practicing this process over several years, PDCA management cycle is put into practice and effective progress management is realized (Figure 5).

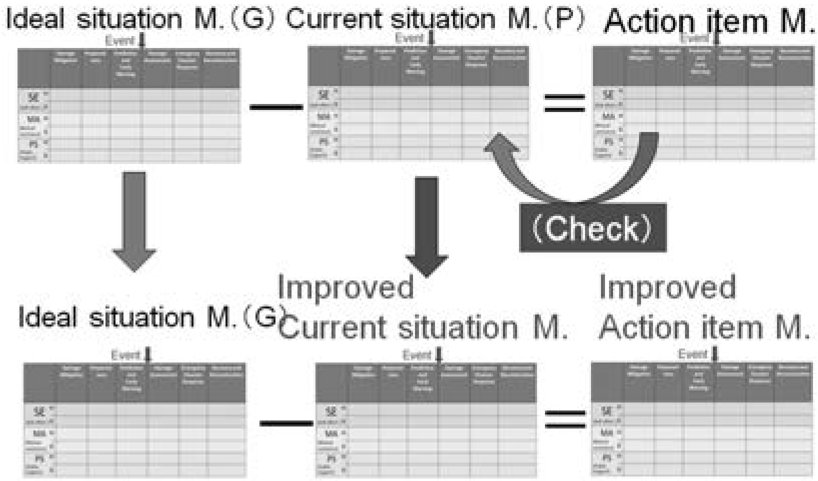

Figure 5: PDCA cycle of making action item matrix and its implementation

3.2.4 Relations among national, prefectural and city, town and village–level governments

According to the Disaster Countermeasures Basic Act, the mayor of the municipality, such as city, town, and village should have the first responsibility for disaster operation and response. Therefore, when they discuss the disaster management plan and countermeasures, they tend to consider hazard, which they can manage by themselves, as a scenario hazard. It was very difficult, or practically impossible for them to take a consideration of much larger-scale disaster that they could not manage and such that the local governments in

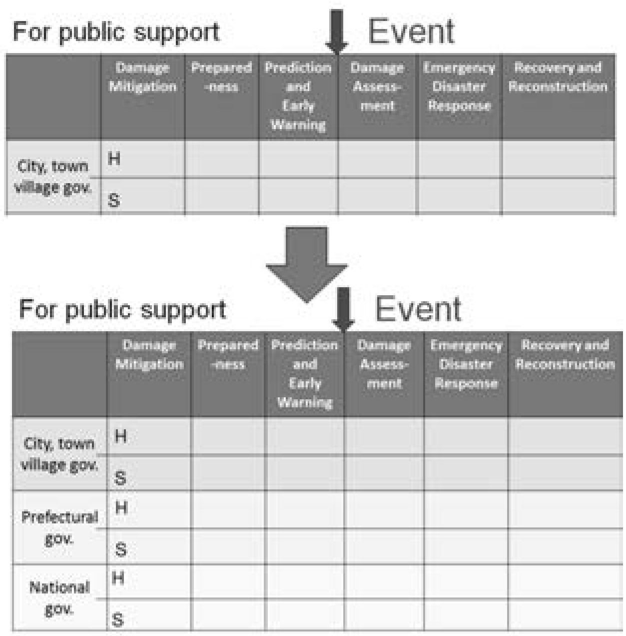

Figure 6: Three levels of players for public support

affected areas due to the 2011 Great East-Japan Earthquake faced. One of the main causes was that they put only them, municipality level government, in disaster countermeasure matrix when they discussed disaster management plan and countermeasures as shown in the upper figure in Figure 6. In order to solve this problem, they should put prefectural and national governments besides them in public support column, then, they can write what they cannot do in the columns of prefectural and national governments. While from the prefectural governments' viewpoint, they considered that what they should do in case of disaster was just waiting for requests from municipalities and respond them. But, prefectural governments can recognize that when the affected municipalities cannot respond because of too large disaster for the municipalities to manage, without waiting for requests from the affected the municipalities, prefectural governments should visit the affected sites and carry out operation and response of disaster instead of the affected municipalities. And also, when three-level governments fill all countermeasure items together that each government should do in the bottom matrix in Figure 6, they can recognize spontaneously duplications and/or gap among different governments.

4. CONCLUSION

In this paper, lessons learned from the disaster due to the 2011 Great East Japan Earthquake and Tsunami, and the subsequent reconstruction process, issues and problems of the current regional disaster management plan are examined and the ideal regional disaster management plan and its implementation strategy was introduced. A comprehensive disaster management system was examined based on three relief types (self-help effort, mutual assistance, and public support) and seven stages (damage mitigation, preparedness, prediction & early warning, damage assessment, disaster response, recovery and reconstruction) and a system to categorize seven countermeasures from each stakeholders and specific action plan with appropriate priorities were proposed.

ACKNOWLEDGEMENT

The author wishes to express his sincere gratitude to all the members of the special committee for regional disaster management plan established in Japan Society for Civil Engineers after the 2011 Great East Japan Earthquake.

Information collection and vulnerability of foreign students during the 2011 Tohoku Earthquake and 2011 Thai flood

Michael HENRY[1], Akiyuki KAWASAKI[2], and Kimiro MEGURO[3]
[1]Assistant professor, Division of Field Engineering for the Environment,
Faculty of Engineering, Hokkaido University, Japan
mwhenry@eng.hokudai.ac.jp
[2]Project associate professor, International Center for Urban Safety Engineering,
Institute of Industrial Science, the University of Tokyo, Japan
[3]Professor and Director, International Center for Urban Safety Engineering,
Institute of Industrial Science, the University of Tokyo, Japan

ABSTRACT

The number of students studying abroad is rising around the globe, and thus it is necessary to consider foreign students as a particularly vulnerable group and to clarify their vulnerability in disaster situations as well as understand how they collect disaster information. This paper briefly introduces two investigations on disaster information collection carried out after the 2011 Tohoku Earthquake and 2011 Thai flood, and analyzes the results focusing on the affected foreign students in each country. It was found that, in both disasters, foreign students were more vulnerable than foreigner non-students, as indicated by their greater tendency to leave Japan or to be affected by the flood waters in Thailand. Within the sample of foreign students in Japan there was a greater diversity of language levels which could be seen to have a large affect on what language the students used to access media. In general, however, the primary media modes were traditional Internet media and television. Conversely, in the case of the flood, most students were not skilled in the local Thai language so they relied almost entirely on English- or other-language media modes. The media they used was different than that used by comparable foreign students in Japan who were only skilled in English, with a much higher usage of social media and crisis mapping.

Keywords: *foreign students, language ability, Internet, social media, government directive, earthquake, flood*

1. INTRODUCTION

2011 was characterized by the occurrence of many large disasters, including the Great East Japan Earthquake disaster and the 2011 Chao Phraya River Flood in Thailand. One unique characteristic of these two disasters is that very large, dense, and diverse metropolitan areas were affected, both indirectly (Tokyo, Japan) and directly (Bangkok, Thailand).

During these disasters, people in the affected areas were dependent upon disaster-related information in order to keep abreast of the developing situation and to make decisions, such as whether to evacuate or not. However, due to the diversity of the populations in these areas, the disaster information-related needs of the affected people may have varied widely. In particular, Tokyo and the surrounding Kanto area is home to the largest population of foreigners in Japan; similarly, Bangkok is also home to a large population of foreigners, and a large number of foreign companies have industrial facilities in the area around the city.

While foreigners in disaster-affected areas represent a unique population group with different needs than the native population, foreign students are an even more unique and vulnerable group due to their special characteristics: that is, they have low economic resources but high educational level and high access to information resources. The OECD (2010) reported that there has been a steady increase in the number of students pursuing education outside their own country, as from 2000 to 20007 the number of international students doubled and reached more than 2 million worldwide. As this number increases, it becomes increasingly important to consider foreign students as a particularly vulnerable group in the event of a disaster due to cultural differences, separation from their families, their lack of familiarity with the local language, and so forth. Therefore, it is necessary to clarify their vulnerability in disaster situations as well as understand how they collect disaster information in order to consider their specific needs in disaster information dissemination systems.

In this paper, the results of two investigations on disaster information collection after the 2011 Tohoku Earthquake and 2011 Thai flood are presented focusing specifically on foreign students and analyzing their disaster information collection behavior considering language ability and vulnerability compared to non-students.

2. 2011 TOHOKU EARTHQUAKE

2.1 Survey methodology

An online survey focusing on people in the Kanto region of Japan was carried out to gather information on the information collection behavior and post-disaster action after the 2011 Tohoku Earthquake. The details of this survey are more fully summarized in Kawasaki et al. (2012), with Table 1 outlining the topics discussed in this paper.

Table 1: Selected survey contents (2011 Tohoku Earthquake)

Theme	**Question contents**
Vulnerability	Post-disaster action and reason for action
Information collection	Media modes utilized for disaster information collection*
Information difficulties	Difficulties experienced when collecting disaster information*

** These questions allowed for multiple responses*

2.2 Sample characteristics & categorization

The survey received 1,357 responses. Foreigners made up 63.1% (856) of the total, with responses from 73 different countries, and respondents who identified themselves as students made up 50.9% (436) of that number. Further details on the foreign respondents' demographics are available from Henry et al. (2011).

A previous study examining the relationship between language ability and information collection behavior found that foreign respondents with differing English and Japanese language abilities gathered information in distinctly different ways (Kawasaki et al., 2012). In order to explore this phenomenon for foreign students, the student sample was categorized based on their Japanese and English proficiency (Table 2). From these results, three distinct groups were extracted: those highly skilled in both Japanese and English (JPN+ENG), those highly skilled in English only (ENG only), and those highly skilled in Japanese only (JPN only). While these three groups represent the most extreme cases of language ability, it can be seen that a majority of foreign students' language abilities fall somewhere between these selected extremes.

Table 2: Language ability distribution of foreign students (N=436)

<table>
<tr><td colspan="2" rowspan="2"></td><td colspan="5">Japanese proficiency (speaking/listening)</td></tr>
<tr><td>Native</td><td>Advanced</td><td>Inter.</td><td>Basic</td><td>None</td></tr>
<tr><td rowspan="5">English proficiency</td><td>Native</td><td colspan="2" rowspan="2">JPN+ENG: 55 (12.6%)</td><td rowspan="2">66 (15.1%)</td><td colspan="2" rowspan="2">ENG only: 90 (20.6%)</td></tr>
<tr><td>Advanced</td></tr>
<tr><td>Intermediate</td><td colspan="2">57 (13.1%)</td><td>46 (10.6%)</td><td colspan="2">43 (9.9%)</td></tr>
<tr><td>Basic</td><td colspan="2" rowspan="2">JPN only: 34 (7.8%)</td><td rowspan="2">25 (5.7%)</td><td colspan="2" rowspan="2">6 (1.4%)</td></tr>
<tr><td>None</td></tr>
</table>

Note: 14 respondents (3.2%) did not provide their complete language ability information

The analysis of the post-disaster action and its associated reason was carried out comparing foreign students with non-students. Selected demographic characteristics of these two groups are summarized in Table 3. As may be expected, students tended to be younger and have lower annual income.

Table 3: Characteristics of foreign students and non-students in Japan (N=856)

Demographics		*Students (n=436)*		*Non-students (n=420)*	
		Freq.	**%**	**Freq.**	**%**
Age	**20-29**	336	77.1%	0	-
	30-39	90	20.6%	67	16.0%
	40-59	0	-	279	66.4%
	60 or higher	0	-	43	10.2%
	Other, no response	10	2.3%	31	7.4%
Annual income (10^6 JPY)	**< 1.95**	234	53.7%	56	13.3%
	1.95 to 6.95	2	0.5%	118	28.1%
	6.95 to 18	1	0.2%	29	6.9%
	18 <	2	0.5%	80	19.0%
	No response	197	45.2%	137	32.6%
Govt. adv.	**G1 (most cautious)**	78	17.9%	129	30.7%
	G2 (less cautious)	271	62.2%	239	56.9%
	G3 (no specific adv.)	87	20.0%	52	12.4%

This analysis also examined the effect of government advisory on post-disaster action. After the earthquake, foreign governments issued advisories of varying levels, from very cautious (Group 1: advising their citizens to leave Japan) to less cautious (Group 2: advising limiting travel to certain areas) to no specific advisory (Group 3). Based on their nationality, respondents could thus be classified into three groups depending on the advisory level of their home government (Kawasaki et al., 2013). The distributions of students and non-students by government advisory is also given in Table 3, where it can be seen that students appeared more likely than non-students to come from countries with either a less cautious advisory or no specific advisory at all.

2.3 Utilized media and information difficulties by language ability

The media modes utilized by foreign students are shown in Figure 1 and the average number of utilized modes are summarized in Table 4 by language ability. The most-used mode for foreign students skilled in both Japanese and English was Japanese television, followed by Japanese and English traditional internet media, which were all used by more than 60% of respondents. While Japanese was the dominant language for many modes, more respondents used other languages than Japanese or English when communicating interpersonally, whereas English was the most-used language for social media. This diversity of media usage is reflected in the average number of modes per respondent by language. For students skilled only in English, however, English traditional internet media was the most-used media mode, followed by English television and English social media. English was the most-used language across all modes, and other languages were generally more utilized than Japanese, as can be seen when looking at the average number of modes per respondent. The case of foreign students only skilled in Japanese, however, is the opposite of the previous group: English is barely used and Japanese-modes are dominant – particularly television and traditional internet media. Unlike students skilled in English, however, there is a greater usage of other language media.

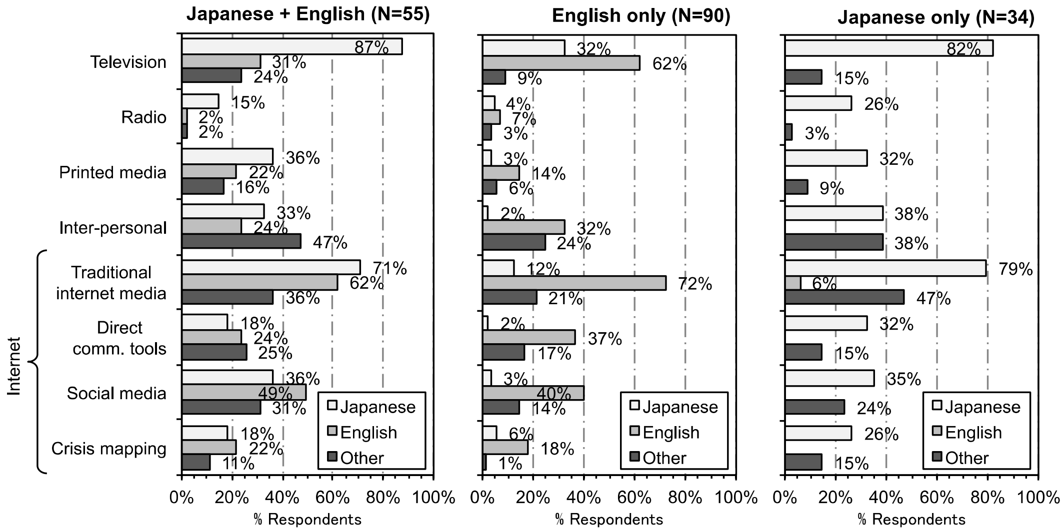

Figure 1: Utilized media of foreign students in Japan by language ability

Table 4: Average number of utilized media modes per respondent

Media mode language	*Language ability group*		
	Japanese+ English	**English only**	**Japanese only**
Japanese	3.15	0.66	3.53
English	2.35	2.82	0.06
Other	1.93	0.96	1.65

Figure 2 shows the various information difficulties of the foreign students by their language ability. Confused by conflicting and differing information was the most-cited reason regardless of language ability, with more than 70% of respondents in each group indicating they experienced that problem. A much larger disparity could be seen for the difficulty caused by inability to understand due to language ability: while 64% of students skilled only in English experienced this problem, only 11% of those skilled in both Japanese and English had the same difficulty. The inability to access information due to mobile congestion, power outage, etc. was also relatively highly cited among the three groups.

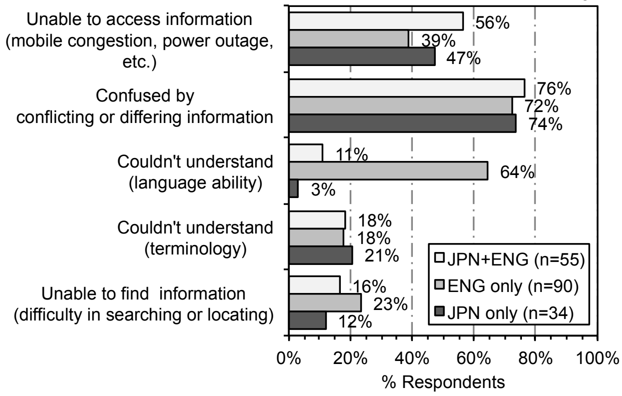

Figure 2: Information difficulties of foreign students in Japan by language ability

2.4 Post-disaster action by country directive

The vulnerability of foreign students in Japan was compared to that of non-students while examining the effect of government directive. The results for post-disaster action are given in Figure 3. It could be seen that the percentage of students who chose to leave Japan increased as the severity of the government directive increased, with 2.8 times more students from Group 1 countries leaving than from Group 3 countries (by percentage). Correspondingly, the ratio of students who chose to remain decreased as the advisory level increased, whereas there was only a small fluctuation in the percentage who merely relocated within Japan. Compared to students, non-students tended to leave Japan less, regardless of the advisory level, and also appeared less affected by the government advisory.

Figure 4 shows the reasons for post-disaster action. Among students who remained, the most-cited reason was personal decision, with little difference between the advisory levels. However, job obligation was cited by students from Group 1 countries more than twice as often as by students from other countries. For students who chose to relocate, family request was the most-cited reason, followed by personal decision. The government advisory level did not appear to have much effect on the reason for relocation, except among students who cited government directive or unable to leave as their reasons, for which the percentages were much higher for students from Group 1 countries. Finally, among students who left Japan entirely, the most-cited reason was again family request, followed by personal decision. In this case, however, students from Group 3 countries appeared more likely than students from other countries to cite personal reason as their motivation for leaving Japan.

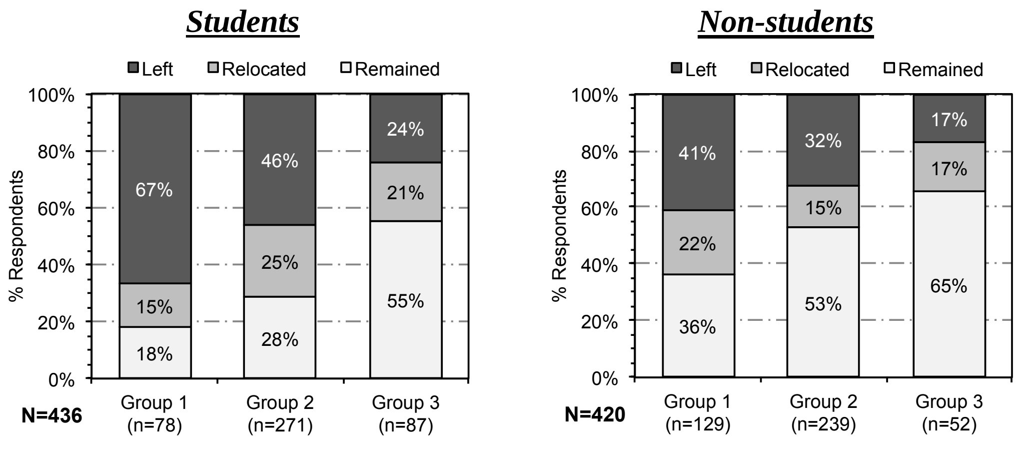

Figure 3: Post-disaster action of foreign students and non-students

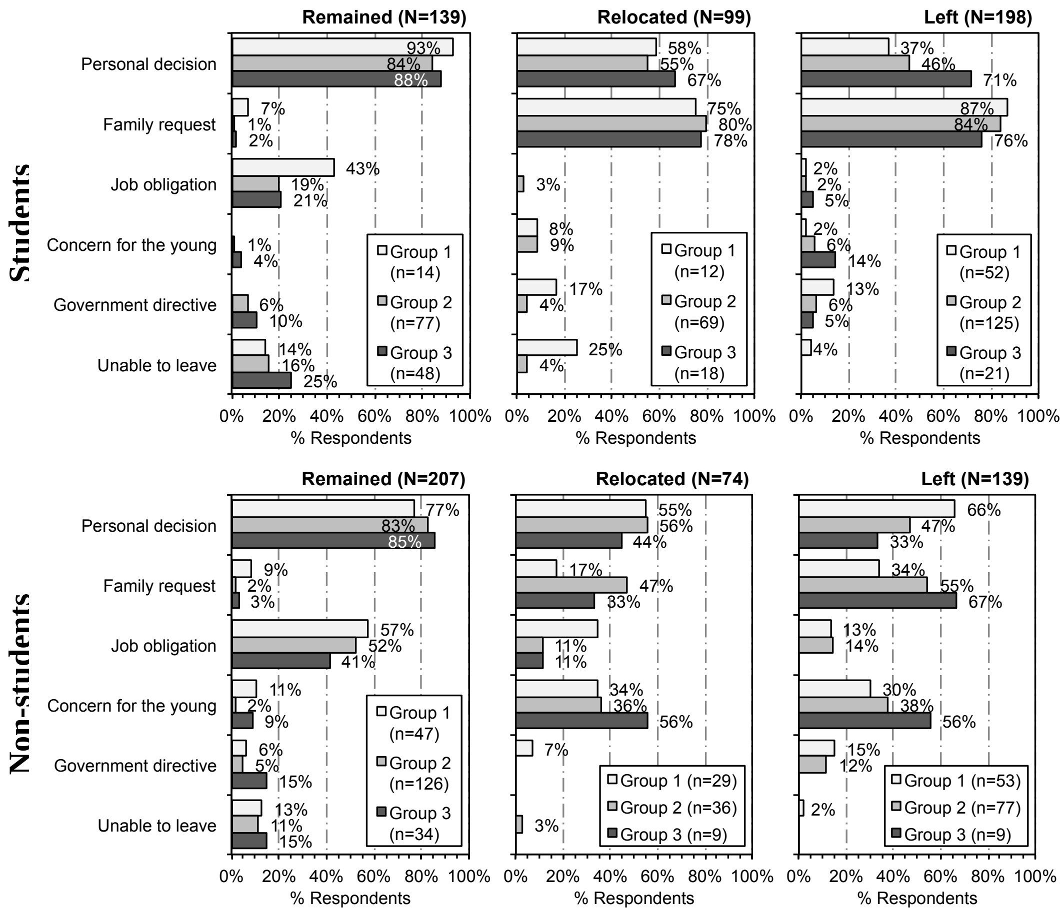

Figure 4: Reason for post-disaster action of foreign students and non-students

Compared to foreign students, non-students who remained more highly cited job obligation, with the percentage of respondents increasing slightly with an increase in the severity of the government directive. The responses of non-students who relocated or left Japan entirely, however, was markedly different from that of students: a greater percentage of non-students cited concern for the young and job obligation, whereas fewer non-students cited family request. Additionally, the government directive appeared to have a larger effect on non-students who chose to relocate or evacuate, particularly those who cited personal decision, family request, and concern for the young.

3. 2011 THAI FLOOD

3.1 Survey methodology

Data on information collection behavior and vulnerability were collected using a survey similar to that used for the investigation after the 2011 Tohoku Earthquake. Complete details of the survey contents and collection methodology are given in Henry et al. (2012), but the topics addressed in this paper are summarized in Table 5. Furthermore, unlike the prior investigation, the 2011 Thai flood survey was distributed via two methods: an anonymous online survey and a paper-based field survey which collected responses directly from people in the field.

Table 5: Selected survey contents (2011 Thai flood)

Theme	**Question contents**
Vulnerability	Situation of flooding and evacuation
Information collection	Media modes utilized for disaster information collection*
Information difficulties	Difficulties experienced when collecting disaster information*

** These questions allowed for multiple responses*

3.2 Sample characteristics and categorization

In total the survey received 975 responses, of which foreign respondents made up 21.5% (210 responses) representing 28 countries. Among these, 46.7% (98 people) identified themselves as students. A detailed overview of the foreign respondents' demographics can be found in Henry et al. (2012).

For understanding information collection behavior the students' language ability was first examined (Table 6). Unlike the case of the 2011 Tohoku Earthquake investigation, very few students were highly skilled in Thai and English and none were skilled in Thai only; furthermore, only 67 could be classified as highly skilled in English only. Therefore, for simplicity, the analysis of information collection was conducted without any categorization of the students.

The analysis of vulnerability was conducted by comparing foreign students to non-students. Table 7 shows that, compared to non-students, students tended to be younger, have much lower income, and live outside Bangkok.

Table 6: Language ability distribution of foreign students (N=98)

<table>
<tr><td colspan="2" rowspan="2"></td><td colspan="5">Thai proficiency (speaking/listening)</td></tr>
<tr><td>Native</td><td>Advanced</td><td>Inter.</td><td>Basic</td><td>None</td></tr>
<tr><td rowspan="5">English proficiency</td><td>Native</td><td colspan="2" rowspan="2">2 (2.0%)</td><td rowspan="2">2 (2.0%)</td><td colspan="2" rowspan="2">67 (68.4%)</td></tr>
<tr><td>Advanced</td></tr>
<tr><td>Intermediate</td><td colspan="2">2 (2.0%)</td><td>-</td><td colspan="2">23 (23.5%)</td></tr>
<tr><td>Basic</td><td colspan="2" rowspan="2">-</td><td rowspan="2">-</td><td colspan="2" rowspan="2">2 (2.0%)</td></tr>
<tr><td>None</td></tr>
</table>

Table 7: Characteristics of foreign students and non-students in Thailand (N=210)

Demographics		*Students (n=98)*		*Non-students (n=112)*	
		Freq.	**%**	**Freq.**	**%**
Age	**20-29**	70	71.4%	11	9.8%
	30-39	22	22.4%	42	37.5%
	40-59	2	2.0%	49	43.8%
	60 or higher	0	-	9	8.0%
	Other, no	4	4.1%	1	0.9%

	response				
Annual income (10^3 USD)	**Very low (<3.2)**	34	34.7%	26	23.2%
	Low (3.2 – 4.8)	6	6.1%	3	2.7%
	Middle (4.8 – 16)	4	4.1%	10	8.9%
	High (>16)	10	10.2%	58	51.8%
	No response	44	44.9%	15	13.4%
Living area	**Bangkok**	9	9.2%	71	63.4%
	Greater Bangkok	88	89.8%	30	26.8%
	Sub-central	1	1.0%	3	2.7%
	Other	0	-	8	7.1%

3.3 Utilized media and information difficulties

Figure 5 summarizes the media modes utilized by foreign students during the 2011 Thai flood. The most-utilized mode was crisis mapping at 64%, followed by direct communication tools (61%) and social media (51%), all of which were primarily utilized in English. Very little usage of Thai or other-language media could be observed. The foreign students used, on average, 3.01 different English media modes.

The information difficulties experienced by the foreign students are summarized in Figure 6. The two most-cited difficulties were being confused by conflicting or differing information and being misled or confused by rumors and/or exaggerated or false information, which were encountered by 70% and 67% of the respondents, respectively. The next highest difficulty was unable to understand information due to a lack of language comprehension, at just under 50%.

3.4 Situation of flooding and evacuation

In order to examine the vulnerability of foreign students during the 2011 Thai flood, two factors were examined: first, whether they were affected by the flood or not; and second, whether they chose to evacuate or not. In Figure 7, it can be seen that the percentage of students who were flooded was more than twice that of non-students. However, Figure 8 shows that students were more likely to have evacuated than non-students.

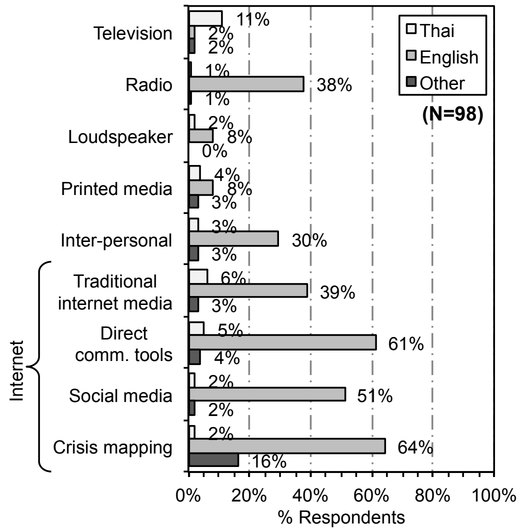

Figure 5: Utilized media of foreign students in Thailand

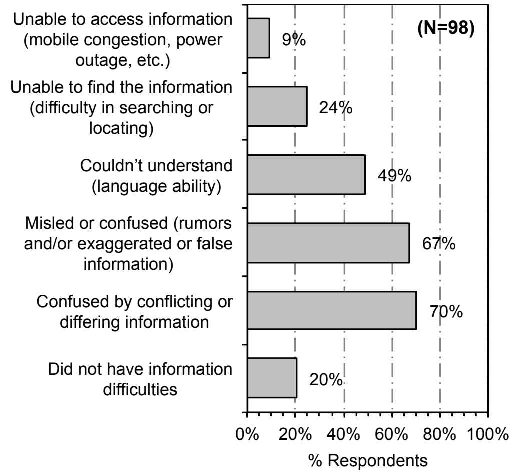

Figure 6: Information difficulties of foreign students in Thailand

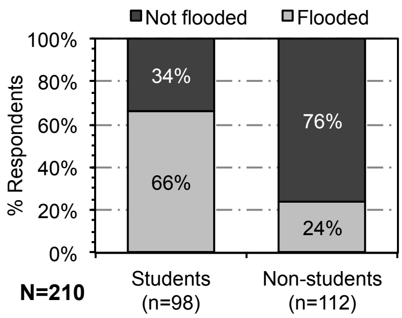

Figure 7: Flooding situation of foreign students and non-students

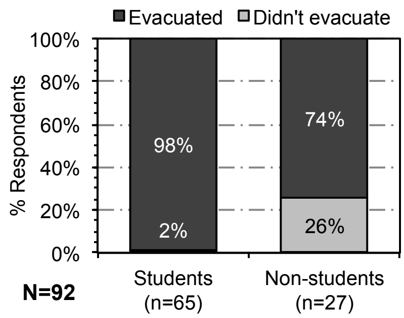

Figure 8: Evacuation action of foreign students and non-students
(for flooded respondents only)

4. DISCUSSION

4.1 Information collection

When examining the information collection, distinctly different behavior could be observed between the foreign students in Japan and Thailand. In the case of Japan, the language ability of foreign students was more diverse than that of foreign students in Thailand. While the media language was strongly affected by language ability, there was less of a difference in the utilized mode; the most-utilized modes were television and traditional internet media regardless of language ability. The most-cited information difficulty, confused by conflicting or differing information, was also similarly cited regardless of language ability; however, a large difference could be seen for the difficulty unable to understand due to language difficulties, which was very strongly cited by foreign students skilled only in English but barely noted by students with other language abilities.

The language ability of the Thai students was less diverse, with the majority of them being moderately to highly skilled in English. Comparing this group to the foreign students in Japan skilled only in English, it can be seen that the foreign students in Thailand utilized internet-based media much more and television much less than the students in Japan. In both cases, being confused by conflicting or differing information was the biggest difficult, but foreign students in Thailand had less of a tendency to cite language difficulties. This may be that, due to their usage of only English-language media modes, they did not have to deal with Thai-language information, whereas foreign students in Japan may have encountered more Japanese-language information in their information seeking.

4.2 Vulnerability

The analyses found that both the foreign students in Japan and in Thailand appeared to be more vulnerable to the effects of the respective disasters, but the reason for that vulnerability differs. In Japan, foreign students were more likely to relocate or leave Japan than non-students, and were also more affected by the government advisory level than non-students. When examining the reason for the relocation or evacuation, family request was much stronger for this group than for non-students, regardless of advisory level. These results suggest that disaster information dissemination not only in Japan but also in overseas countries may have a large effect on the post-disaster decision making of foreign students inside Japan due to the perception of foreign students' families of the severity of the disaster event as perceived from their home country.

On the other hand, the vulnerability of foreign students in Thailand may be closely related to their location of residence. It was found that students were more likely to have been flooded than non-students, but it could also be seen that students were more likely to live outside the Bangkok area than non-students. This may be due to the distribution of universities outside the city center as well as the concentration of wealthier foreigners in the city proper. Since the areas around Bangkok were more likely to be flooded, this would help explain why students were more vulnerable. However, among those respondents who were flooded, students were more likely to evacuate. In this instance, non-students may be more likely to have family or possessions which could have hindered evacuation compared to students, who are generally more mobile.

5. CONCLUSION

This paper found that foreign students are vulnerable to disasters in different ways than non-students and that, furthermore, even among foreign students the difference in language ability can strongly affect how those students gather their disaster information. The type of disaster or location where students are studying may also have an affect on this collection behavior and, certainly, on their vulnerability. Considering the trend towards greater globalization and the anticipated growth of foreign students into the future, disaster-prone countries with high numbers of foreign students should consider them as a particularly vulnerable group and prepare means to support them in the event of a disaster.

ACKNOWLEDGEMENT

This research was partially supported by the Japan Society for the Promotion of Science (Challenging Exploratory Research: "*Investigation on disaster information dissemination to foreigners after the great earthquake in the Tokyo metropolitan area*"). In addition, the authors would like to express their gratitude to everyone who cooperated with and supported these investigations.

REFERENCES

Kawasaki, A., Henry, M., Meguro, K., 2012. Analysis of disaster information gathering behavior and language ability after the 2011 Tohoku Earthquake. *2012 New Technologies for Urban Safety of Mega Cities in Asia (ICUS Report 2012-03)*, Ulaanbaatar, Mongolia, 263-271.

Kawasaki, A., Henry, M., Meguro, K. 2013. Advisories by foreign governments and the behavior of foreigners residing in Japan after the 2011 Great East Japan Earthquake. *Journal of the Institute of Social Safety Science*, submitted. (in Japanese)

Henry, M., Kawasaki, A., Meguro, K., 2011. Disaster information gathering behavior after the Tohoku Earthquake Part 2: Results of foreign respondents. *2011 New Technologies for Urban Safety of Mega Cities in Asia (ICUS Report 2011-02)*, Chiang Mai, Thailand, 149-161.

Henry, M., Kawasaki, A., Meguro, K., 2012. Disaster information collection by Thai and foreigners during the 2011 Thai flood. *2012 New Technologies for Urban Safety of Mega Cities in Asia (ICUS Report 2012-03)*, Ulaanbaatar, Mongolia, 43-54.

Organization for Economic Cooperation and Development (OECD), 2010. International Migration Outlook: SOPEMI 2010 English Summary. http://www.oecd.org/migration/mig/45612617.pdf (Accessed Sept. 13, 2013)

Risks from in-city construction works to urban inhabitants' safety in Hanoi: the city residents' perspective

NGUYEN Duy Cuong[1], MA Xuan Minh[2] and NGUYEN The Quan[3]
[1] Undergraduate student, University of Civil Engineering, Hanoi, Vietnam
[3] PhD, Vice Dean, Faculty of Construction Economics and Management, University of Civil Engineering, Hanoi, Vietnam
nguyenquan.nuce@gmail.com

ABSTRACT

In a growing city like Hanoi, there always are lots of construction works being carried out while the city is still in operation. The construction processes in those projects, if not being managed properly, can create risks that have negative impacts on urban inhabitants' safety, leading to accidents or a lower living quality of the city's residents which harms the city's sustainable development. This paper presents the results from a research into the safety risks from in-city on-going construction works in Hanoi. The paper lists out twenty four risks from the construction works to urban inhabitants' safety that are perceived by the surveys' participants. The risks are then classified into twelve categories with their causes and analyzed to measure their probability of occurrence and impact. It is concluded that "construction noise", "construction dust", and "construction waste" become the most significant causes to urban residents' safety. Urban inhabitants care much more about their living quality than life safety regarding safety risks the in-city projects may bring to them.

Keywords: *safety risk, urban inhabitants' safety, in-city construction works.*

1. INTRODUCTION

The development of a city can be seen in two major ways: new urban areas are built up next to the current cities and old construction works inside the city are destroyed for new construction. Some cities apply both of the ways: together with building up new urban areas in the surrounding green fields, there are lots of construction works being conducted in the city while the city is still in operation. According to Biddy (2009), cited by Spillane, Oydele et al (2011), an expansion of urban centers may not be seen very clearly and fast, they are being redeveloped from inside of the city. Being considered as one of the fastest developed cities in Vietnam, Hanoi has experienced similar situation with lots of projects being carried out in the inner city. Those construction works, more or less, influence the life safety and living quality of the city inhabitants. This paper will investigate the risks caused by construction activities to urban residents, under their perspective.

2. LITERATURE REVIEW

Risk can be defined as “an uncertain event or condition that, if it occurs, has a positive or negative effect on one or more project objectives such as scope, schedule, cost, and quality” (PMI 2012), p.310). When investigating a risk, it is necessary to look at two elements: the happening likelihood or probability, and the consequences or impacts if the risk happens (Cooper, Grey et al. 2005), p.3). The Merriam-Webster Dictionary defines safety as “freedom from harm or danger”, “the state of not being dangerous or harmful” (Merriam-Webster 2013). However, in construction, safety can also mean “health”, because safety and health are being managed together and in the same way (Holt 2008), p.3). Consequently, safety risk can be regarded as something that is likely to go wrong and harm the safety. Safety risk are related to accident, which is “an incident plus its consequences” or “an undesired event, which results in physical harm and/or property damage”, as well as to hazard – “the potential to interrupt or interfere with a process or person” (Holt 2008), p.3).

There have been a number of works in the literature writing about safety in construction projects. Researchers and practitioners in the field are concerned much about measuring accidents in construction (Ale, Bellamy et al. 2008), occupational health and safety (Rikhardsson 2006; Badri, Nadeau et al. 2012), developing and managing safety management systems of construction sites (Ismail, Doostdar et al. 2012), developing tools for safety risks analysis and prevention (Gangolells, Casals et al. 2010; Aminbakhsh, Gunduz et al. 2013), reviewing laws and regulations on safety in construction (Baxendale and Jones 2000). Some are concerned about the planning and management of construction processes in confined, narrow construction sites with regard to health and safety issues (Spillane, Oyedele et al. 2011). Others go for specific solutions for selected issues on the sites such as noise emission (Ballesteros, Fernández et al. 2010), motivation for safe work (Helander 1991), constructing road safety (Ma, Shao et al. 2011), etc. Regarding the impact of construction works in city to the city citizens, several works have been found from the literature, including the safety management in construction of tunnel in city (Ding, Zhang et al. 2014), risk from construction of adjacent buildings such as deep excavation (Shin, Kim et al. 2006; Abdel-rahman 2007), managing risk for pedestrian (Bilton 2012), etc. That is to say, there is very limited research having been done in terms of safety risk to city dwellers from in-city construction works.

3. THE RESEARCH APPROACH

As stated above, there are very limited references found in the literature relevant to the topic of risks from in-city construction works to urban inhabitants’ safety. Therefore, a combination of exploratory and descriptive approaches would be the most suitable research approach to be adopted for this study. A questionnaire was first designed for the purpose of data collection. 60 questionnaires then have been completed with face-to-face mode of interview. However, since the data collection process was very slow, the questionnaire was converted into an online survey using Google Form. 83 people have responded to the survey, but only 54 questionnaires are accepted to be used in the research, making it 114 completed questionnaires in total. Those additional questionnaires also add in several respondents who have been impacted by an on-going construction work inside the city in regularly passing by and/or working nearby.

Table 1: Categories of respondents

No	**Categories**	**No of respondents**	**%**
1	Age group		
1.1	Under 30	38	31.93%
1.2	30-39		
1.3	40-49	19	15.97%
1.4	50-59	21	17.65%
1.5	60+		
1.6	Not answer	14	11.76%
2	Sex		
2.1	Male	46	38.66%
2.2	Female	49	41.18%
2.3	Not answer	19	15.97%
3	Education		
3.1	Secondary and lower	29	24.37%
3.2	University graduate	50	42.02%
3.3	Post-graduate	5	4.20%
3.4	Not answer	30	25.21%
	Total	114	100.00

Table 1 presents the research sample using several categories. The data show that respondents are dispersed over a wide range in terms of age, sex and education. The sample includes all groups of people being classified by the aforementioned criteria. Since internet access is more popular to younger people than to the older, this explains the significantly bigger number of respondents from the age group of under 30 most of whom participated in the survey through responding to the online questionnaires.

Table 2: Type of construction works and their modes of impact to participants

No	**Categories**	**No of respondents**	**%**
1	Type of construction work		
1.1	Buildings	52	43.70%
1.2	Urban roads	27	22.69%
1.3	Bridges (overbridges)	27	22.69%
1.4	Tunnels, underground cellars etc.,	8	6.72%
2	Mode of impact		
2.1	Regularly passing by	39	32.77%
2.2	Living nearly	69	57.98%
2.3	Working nearly	6	5.04%
	Total	114	100.00

In terms of construction works that the survey participants have been impacted, they can be put into 4 large groups: (1) buildings, (2) urban roads, (3) bridges (overbridges), (4) tunnels, underground cellars and open trenches (Table 2). Among three modes that those construction works can have influence on urban citizens, the survey participants mentioned “living nearly” the most (57.98%), then “regularly passing by” (32.77%) (Table 2). Of course, there are lots of people who might be impacted by in-city construction works in more than a mode, yet the respondents were asked about the work that brings them the greatest impacts.

4. RESULTS AND DISCUSSIONS

The survey results show that the on-going construction works in Hanoi can have bad influences on urban inhabitants, and therefore, can create causes that bring risks to them. Table 3 presents the results of grouping the risks with regard to their causes, presenting the results in descending order in terms of the total number of being mentioned in the survey for the risk causes. Twelve causes have emerged from the survey, according to information provided by the respondents. Twenty-four risks then have been identified. Among them, “construction dust causing respiratory disease” becomes the most popular risk, being mentioned by 23.33% of the respondents. The next popular ones include “construction noise – causing insomnia or sleeping difficulties”, “construction noise – causing stress and inhibition”, “reduction of road areas – causing traffic jams”, “construction waste – causing hygienic problems for the environment and citizens’ health” and “falling materials – causing accidents to citizens” with the occurrence rates vary from 5.76% to 14.85% (see Table 3). That is to say, the risks identified harm the city residents in both their life safety and their living quality.

Table 3 also presents the risks in terms of their level of occurring probabilities and impact levels. Low probability of occurrence is scored 1 while high probability of occurrence is assigned a score of 3. Similarly, impact levels are assigned score from 1 to 3. Average scores for both the occurring probabilities and impact levels then are calculated. According to the results, the top five risks in terms of occurring probability are “construction dust - causing hygienic problem for the environment”, “construction dust - causing eye disease”, “construction waste - causing drainage system’s block leading to flooding”, “construction workers - causing social evil/crime surrounding the construction sites” and “construction noise - causing stress and inhibition” (risks coded 2.2, 2.3. 4.4, 11.2 and 1.2), but if their occurrences in the survey being taken into account, the top five change to “construction dust - causing respiratory disease”, “construction noise - causing insomnia or sleeping difficulties”, “construction noise - causing stress and inhibition”, “reduction of road areas - causing traffic jams” and “construction waste - causing hygienic problems for the environment and citizens’ health” (risks coded 2.1, 1.1, 1.2, 3.1 and 4.1). With regard to impact levels, the top five risks include “construction dust - causing eye disease”, “construction dust - causing hygienic problem for the environment”, “construction noise - causing stress and inhibition”, “reduction of road areas - causing traffic accidents”, “construction waste - causing drainage system’s block leading to flooding” and “construction workers on site - causing theft and burglary” (risks coded 2.3, 2.2, 1.2, 3.2, 4.4 and 11.1 – the last two have the same risk level). If their occurrences in the survey

Table 3: Risks categorized by causes and their occurrence in the survey, occurring probabilities and impact levels

No	Risk categorized by causes	Occurrences in the survey	%	Occurring probability				Impact level			
				Low 1	Average 2	High 3	Average score	Low 1	Average 2	High 3	Average score
1	*Construction noise*	*89*	*26.97%*								
1.1	causing insomnia or sleeping difficulties	49	14.85%	2	15	32	2.61	3	21	25	2.45
1.2	causing stress and inhibition	39	11.82%	1	9	29	2.72	2	10	27	2.64
1.3	causing working distraction	1	0.30%	0	1	0	2.00	0	1	0	2.00
2	*Construction dust*	*84*	*24.45%*								
2.1	causing respiratory disease	77	23.33%	1	32	44	2.56	7	25	45	2.49
2.2	causing hygienic problem for the environment	6	1.82%	0	0	6	3.00	0	1	5	2.83
2.3	causing eye disease	1	0.30%	0	0	1	3.00	0	0	1	3.00
3	*Reduction of road areas due to construction sites*	*45*	*13.64%*								
3.1	causing traffic jams	35	10.61%	5	23	7	2.06	8	19	8	2.00
3.2	causing traffic accidents	10	3.03%	0	8	2	2.20	0	4	6	2.60
4	*Construction waste*	*30*	*9.09%*								
4.1	causing hygienic problems for the environment and citizens' health	20	6.06%	1	8	11	2.50	1	12	7	2.30
4.2	causing traffic jams	5	1.52%	0	2	3	2.60	1	2	2	2.20
4.3	causing traffic accidents	2	0.61%	1	0	1	2.00	0	2	0	2.00
4.4	causing drainage system's block leading to flooding	2	0.61%	0	0	2	3.00	0	1	1	2.50
4.5	causing damage to	1	0.30%	0	1	0	2.00	0	1	0	2.00

No	Risk categorized by causes	Occurrences in the survey	%	Occurring probability				Impact level			
				Low 1	**Average 2**	**High 3**	**Average score**	**Low 1**	**Average 2**	**High 3**	**Average score**
	commuting vehicles										
5	*Road damage*	*22*	*6.67%*								
5.1	causing traffic jams	12	3.64%	8	4	0	1.33	0	8	4	2.33
5.2	causing traffic accidents	10	3.03%	4	6	0	1.60	0	6	4	2.40
6	*Falling materials*	*19*	*5.76%*								
6.1	causing accidents to citizens	19	5.76%	1	10	8	1	4	11	4	2.00
7	*Adjacent buildings' sinking and cracking*	*12*	*3.64%*								
7.1	harming safety of people next door	12	3.64%	3	9	0	1.75	1	5	6	2.42
8	*Broken and collapsed equipment*	*11*	*3.44%*								
8.1	causing accidents to citizens	11	3.33%	2	5	4	2.18	4	4	3	1.91
9	*Vibration due to construction activities*	*6*	*1.82%*								
9.1	causing damages to surrounding buildings	6	1.82%	0	2	4	2.67	3	1	2	1.83
10	*Lacking of lighting and signboards*	*4*	*1.21%*								
10.1	causing traffic accidents	4	1.21%	0	2	2	2.50	1	1	2	2.25
11	*Public disorder due to construction workers' coming to the site*	*4*	*1.21%*								
11.1	causing theft and burglary	2	0.61%	0	1	1	2.50	0	1	1	2.50
11.2	causing social evil/crime	2	0.61%	0	0	2	3.00	0	2	0	2.00

No	Risk categorized by causes	Occurrences in the survey	%	Occurring probability				Impact level			
				Low 1	**Average 2**	**High 3**	**Average score**	**Low 1**	**Average 2**	**High 3**	**Average score**
	surrounding the construction sites										
12	*Material trucks commuting*	*4*	*1.21%*								
12.1	causing traffic jams	2	0.61%	0	1	1	2.50	0	2	0	2.00
12.2	causing traffic accidents	2	0.61%	0	1	1	2.50	0	2	0	2.00
	Total	330	100%	29	140	161	2.40	35	142	153	2.36

is considered, the top five of risks in terms of impact level change to “construction dust - causing respiratory disease”, “construction noise - causing insomnia or sleeping difficulties”, “construction noise - causing stress and inhibition”, “reduction of road areas - causing traffic jams” and “construction waste - causing hygienic problems for the environment and citizens’ health” (risks coded 2.1, 1.1, 1.2, 3.1 and 4.1). It is noted that if we include the occurrence rates of the survey respondents in the calculation, the most significant risks do not change much. These are the risks that the respondents pay the greatest attention to because of their occurrence and impact.

In order to rate the perceived risks, each risk’s average occurring levels is multiplied with its impact level (Table 4). Top five of risks with the highest risk levels include “Construction dust - causing eye disease”, “construction dust - causing hygienic problem for the environment”, “construction waste - causing drainage system’s block leading to flooding”, “construction noise - causing stress and inhibition” and “construction noise - causing insomnia or sleeping difficulties” (2.3, 2.2, 4.4, 1.2 and 1.1). Integratedly, risk causes that may bring the highest risk (top five) are “construction noise”, “construction dust”, “construction workers’ coming to the site”, “construction waste” and “lack of lighting and signboards”. However, when taking into account the occurrence rates of the risks, they are “construction noise”, “construction dust”, “reduction of road areas”, “construction waste” and “road damage”. Apparently, noise, dust and waste are the most significant causes to risks to city dwellers from in-city construction works. Therefore, the greatest safety issues for urban inhabitants are related to their quality of life, not life safety. The omission of fatal and serious injuries from the risk list supports this conclusion.

Table 4: The risk levels of the perceived risks

No	**Risk categorized by causes**	**Occurring level**	**Impact level**	**Risk level**
1	*Construction noise*	2.53	2.65	6.70
1.1	causing insomnia or sleeping difficulties	2.45	2.61	6.40
1.2	causing stress and inhibition	2.64	2.72	7.18
1.3	causing working distraction	2.00	2.00	4.00
2	*Construction dust*	2.52	2.60	6.55
2.1	causing respiratory disease	2.49	2.56	6.38
2.2	causing hygienic problem for the environment	2.83	3.00	8.50
2.3	causing eye disease	3.00	3.00	9.00
3	*Reduction of road areas due to construction sites*	2.13	2.09	4.46
3.1	causing traffic jams	2.00	2.06	4.11
3.2	causing traffic accidents	2.60	2.20	5.72
4	*Construction waste*	2.27	2.50	5.67
4.1	causing hygienic problems for the environment and citizens’ health	2.30	2.50	5.75
4.2	causing traffic jams	2.20	2.60	5.72

No	Risk categorized by causes	Occurring level	Impact level	Risk level
4.3	causing traffic accidents	2.00	2.00	4.00
4.4	causing drainage system's block leading to flooding	2.50	3.00	7.50
4.5	causing damage to commuting vehicles	2.00	2.00	4.00
5	*Road damage*	2.36	1.45	3.44
5.1	causing traffic jams	2.33	1.33	3.11
5.2	causing traffic accidents	2.40	1.60	3.84
6	*Falling materials*	2.00	2.37	4.74
6.1	causing accidents to citizens	2.00	2.37	4.74
7	*Adjacent buildings' sinking and cracking*	2.42	1.75	4.23
7.1	harming safety of people next door	2.42	1.75	4.23
8	*Broken and collapsed equipment*	1.91	2.18	4.17
8.1	causing accidents to citizens	1.91	2.18	4.17
9	*Vibration due to construction activities*	1.83	2.67	4.89
9.1	causing damages to surrounding buildings	1.83	2.67	4.89
10	*Lacking of lighting and signboards*	2.25	2.50	5.63
10.1	causing traffic accidents	2.25	2.50	5.63
11	*Public disorder due to construction workers' coming to the site*	2.25	2.75	6.19
11.1	causing theft and burglary	2.50	2.50	6.25
11.2	causing social evil/crime surrounding the construction sites	2.00	3.00	6.00
12	*Material trucks commuting*	2.00	2.50	5.00
12.1	causing traffic jams	2.00	2.50	5.00
12.2	causing traffic accidents	2.00	2.50	5.00
	Total	2.36	2.40	5.66

5. CONCLUSIONS

The paper has presented results from an empirical survey in terms of risks created by construction activities in in-city projects in Hanoi. Emerging from the survey results, twelve risk causes which create twenty four risks have been categorized and then analyzed by their probability of occurrence and level of impact. Most of the significant risks only harm the respondents' living quality, not their life safety. Among the risks, repeated top five include "construction dust - causing eye disease", "construction dust - causing hygienic problem for the environment", "construction waste - causing drainage system's block leading to flooding" and "construction noise - causing stress and inhibition". Among the causes, noise, dust and waste are the most significant causes to risks to city dwellers due to in-city construction works, meaning life safety, more or less, has been ensured by the project executors, then urban inhabitants mostly consider their living quality as significantly important when considering in-city projects safety risks.

REFERENCES

Abdel-rahman, A. H. (2007). "Construction Risk Management of Deep Braced Excavations in Cairo." Australian Journal of Basic and Applied Sciences **1**(4): 506-518.

Ale, B. J., L. Bellamy, et al. (2008). "Accidents in the construction industry in the Netherlands: an analysis of accident reports using storybuilder." Reliability Engineering & System Safety **93**(10): 1523-1533.

Aminbakhsh, S., M. Gunduz, et al. (2013). "Safety risk assessment using analytic hierarchy process (AHP) during planning and budgeting of construction projects." Journal of Safety Research.

Badri, A., S. Nadeau, et al. (2012). "Proposal of a risk-factor-based analytical approach for integrating occupational health and safety into project risk evaluation." Accident Analysis & Prevention **48**: 223-234.

Ballesteros, M. J., M. D. Fernández, et al. (2010). "Noise emission evolution on construction sites. Measurement for controlling and assessing its impact on the people and on the environment." Building and Environment **45**(3): 711-717.

Baxendale, T. and O. Jones (2000). "Construction design and management safety regulations in practice—progress on implementation." International Journal of Project Management **18**(1): 33-40.

Bilton, P. (2012). Pedestrian Risk Management during Urban Construction projects. Australasian College of Road Safety Conference 2012, Sydney, New South Wales, Australia.

Cooper, D. F., S. Grey, et al. (2005). Project risk management guidelines: managing risk in large projects and complex procurements, John Wiley & Sons.

Ding, L., L. Zhang, et al. (2014). "Safety management in tunnel construction: Case study of Wuhan metro construction in China." Safety Science **62**: 8-15.

Gangolells, M., M. Casals, et al. (2010). "Mitigating construction safety risks using prevention through design." Journal of Safety Research **41**(2): 107-122.

Helander, M. G. (1991). "Safety hazards and motivation for safe work in the construction industry." International Journal of Industrial Ergonomics **8**(3): 205-223.

Holt, A. S. J. (2008). Principles of construction safety, Wiley. com.

Ismail, Z., S. Doostdar, et al. (2012). "Factors influencing the implementation of a safety management system for construction sites." Safety Science **50**(3): 418-423.

Ma, Z., C. Shao, et al. (2011). "Constructing road safety performance indicators using fuzzy delphi method and grey delphi method." Expert Systems with Applications **38**(3): 1509-1514.

Merriam-Webster (2013). "Merriam-Webster Dictionary." Retrieved 12 May, 2013, from http://www.merriam-webster.com/dictionary/safety.

PMI (2012). A guide to the Project management body of knowledge. Newtown Square, Pennsylvania, USA, Project Management Institute.

Rikhardsson, P. (2006). Accounting for Health and Safety Costs. Review and Comparison of Selected Methods. Sustainability accounting and reporting, Springer**:** 129-151.

Shin, H.-S., C.-Y. Kim, et al. (2006). "A new strategy for monitoring of adjacent structures to tunnel construction in urban area."

Spillane, J. P., L. O. Oyedele, et al. (2011). "Confined site construction: A qualitative investigation of critical issues affecting management of health and safety." Journal of Civil Engineering and Construction Technology **2**(7): 138-146.

Increasing community awareness of earthquake risk through children education: A case study of Dien Bien city in Vietnam

Thi Hong PHAM [1], Pennung WARNITCHAI[2], and Akiyuki KAWASAKI[3]
[1]Graduate student, Department of Disaster Preparedness Mitigation Management
Asian Institute of Technology (AIT), Thailand
[2]Coordinator and Associate Professor, Department of Disaster Preparedness Mitigation and Management, Asian Institute of Technology (AIT), Thailand
[3]Visiting Associate Professor, Asian Institute of Technology (AIT), Thailand

ABSTRACT

Raising awareness program plays an important role in mitigating earthquake damages. However, there are still existing challenges to successfully aware citizens about earthquake vulnerability and protection in urban areas. In this study, a new approach for conducting earthquake raising awareness programs in urban communities through children education was proposed. Two hypotheses were investigated: (1) if primary school children can learn earthquake mitigation, which includes complicated parts in class; (2) if children can transfer earthquake knowledge to parent in their family at home; and the exposure to this approach can help the parent living in urban communities improve their understanding of earthquake risk. In order to examine the hypothesis, an experiment using primary school children at age 10 to 12 and parent as participants was implemented. The result shows the statistically significant differences in students' pre and post test performance on earthquake knowledge test. It also showed children have ability to improve the parent's understanding of earthquake. Thus, the high effectiveness of the approach was proved. In this research, an earthquake concern survey was conduct to explore concern level of citizens about earthquake and factors effecting on their concern. The results of survey showed that, earthquake is highest concern of Dien Bien people and age, education, having earthquake experience effected on their concern.

Keywords*: Earthquake education, children education, children psychology, transforming knowledge, urban areas,*

1. INTRODUCTION

Big earthquakes happening continuously in the world are becoming dangerous threat of human being. Earthquake, depending on its magnitude and distance from the epicenter and location characteristics may cause a number of adverse effects including structural damages and non-structural damages. Logically, earthquake prediction is expected to help warning people from earthquake hit; however, short-term earthquake prediction have been studying but not all of them have good scientific explanation (CSEP, 2011), (Kirschvink, Joseph L, 2000), (Andrew Coburn, Robin Spence, 1992). Therefore, people used to rely on countermeasures to protec themselve from earthquake. Among of earthquake mitigation methodes, earthquake education is becoming more and more important method because it can find the answer for the hard question how to remind public about destructive damages of big earthquakes which have long return period comparing to human life. Earthquake education also creates the earthquake safety culture of a society (Parsizadeh, 2007).

The system, however, have not been adequately conducted in most coutries. Earthquake safety in school curriculumn focuses much on earth science which is not enough to promote risk awareness or action for earthquake protection (Wisner, 2006). Therefore, a good assessment of the role of parent in encourage earthquake knowledge among community need to be explored (Parsizadeh, 2007). Moreover, it was found that most of raising awareness activities are applied with high effectiveness in rural sides but in urban areas. A heterogeneous community in urban area with immigrant issues and low concern about campaigns activities would generate tensions in conducting awareness campaigns (Pelling, 2010).

This study explore the way to trainning public in city about earthquake risk protection through children education. Earthquake safety content including four parts: earthquake basis knowledge, preparedness for earthquake, response during and after earthquake, was prepared for children at age 10 to 12 year olds learning. Guidline teaching parent contact to their children and learn earthquake knowledge was provided for the parent.

Two of the issues raised in prevous studies are addressed here. First, could children at age from 10 to 12 learn earthquake safety which combines concent of earthquake science and earthquake protection drills? Second, did children can transfer what they learn in class to parent in their family at home? To our knowldege, no research exists checking the children’s abilities in transfering earthquake knowledge to parent in their family and teach them to protect adult from earthquake; therefore, the package including guiline and lectures should be developed as a tool to raising awareness earthquake safety in urban city.

2. EARTHQUAKE EDUCATION

Earthquake formal education in this study is defined as a systematic education model to educate about earthquake mitigation. This system is structured according to a given set of laws and presented in the curriculum as regards objectives, content and methodology.

Curricula teaching about earthquake risk is vary largely in approach and intensity in different countries. Iran has a nationwide earthquake safety education, for 16 million primary and secondary students (Ghafory-Ashtiany and Parsizadeh 2005) while Bangladesh, the country frequently suffered earthquakes set up disaster management chapters in the school curriculum but does not include earthquake education. In Japan, earthquake topics have been taught in the environment and disaster mitigation courses in 5 prefectures including Shizuok, Aichi, Wakayama, Osaka and Hyogo for total 1065 primary and secondary schools students (Shiwaku, 2007). In developing countries, earthquake integrating in school curriculum is limited.

Many teaching methods were applied accommodating with age of learners. Lectures based on drill exercise, earthquake simulators, lab experiment will employ most learning skills such as listening, writing, reporting and mapping for understanding and memorizing of children (Wisner, 2006). Tori Zobel, a teacher in the CleveHill Middle School proposed integrating earthquake education into elementary school curriculum by a whole language approach including such as art, math, music and science (Zobel, 1992). Lab experiment about dynamic movement of the building, a bench-scale shake table program earthquake engineering curriculum for undergraduate students (S.J. Dyke et al, 2000).

Non-formal earthquake education has been used in this research to describe the system that organized learning outside of the formal education with non – contiguous communication. This system includes training, drills and raising awareness activities. Learners from different responsibilities can participate in a variety of earthquake mitigation training courses such as teachers, staffs, pupils, authority, communities. Normally, basic knowledge about earthquake safety and earthquake preparedness in emergency case for individual safety and society safety are offered for community level and local government. Earthquake risk mitigation and preparedness plan are introduced to improve knowledge of the authorities according to following main issues: Earthquake safety basis; Emergency preparedness for individual safety and society safety; Preparedness plan; Rescue method, triage; Earthquake evacuation. Raising awareness activities also extended by linking with publications, demonstrations, simulations and exhibitions to remind public about destructive damage of earthquake.

4. METHODOLOGY

4.1 Survey of earthquake concern in Dien Bien city

Dien Bien is located in the Northern part of Vietnam where the active fault called Lai Chau – Dien Bien running through has caused significant damages to local people. According to scientists (Duong, 2010); (Thanh, 2007); (Phuong, 2011), Lai Chau- Dien Bien Phu fault is one of the active faults in Asia, therefore, Northern part of Vietnam especially Dien Bien city is the most vulnerable place to earthquake. Many small and medium earthquake happed in Dien Bien in the past. Earthquakes magnitude 6.7 recorded in 1983 ruined a large number of infrastructures and agricultural land of this area. Recently, number of earthquake is increasing, especially, earthquake M5.3 in 2001 damaged 2916 buildings, 58 office buildings and 264 schools in Dien Bien (Duong, 2010). Nowadays, Dien Bien has been suffered increasing number of earthquakes recently; therefore, citizens are expected to understand about earthquake risk in their living. However, until now, there is lack of awareness raising program for earthquake safety in this city; as the result, citizens still do not know how to protect themselves when an earthquake strikes.

To evaluate earthquake concern of people in the studying area, our research randomly chose 100 samples in the whole city. These respondents answered six questions in questionnaire about earthquake concern and their demand in the context of disaster mitigation. As our knowledge, no survey about earthquake disaster concern was conducted before in this city.

4.2 Earthquake mitigation teaching tool development

As noted earlier, the first step is to develop a teaching tool to educate children aged 10 to 12 about earthquake protection and mitigation in class.
The earthquake mitigation-teaching tool contains both earthquake training primary children in class and guideline for parent contacting and learning from children.

The first part of teaching content was designed to stimulate learning by allow children at age 10 to 12 can understand earthquake mitigation, which is complicated knowledge beyond their knowledge at primary level. The designer began by reviewing earthquake - teaching materials around the world and science knowledge at primary school level. The appropriated content of the earthquake training was selected with the purpose of helping primary students understanding and memorizing earthquake mitigation knowledge. It applied number of teaching methods including drawing, game, watching video, drills, which helped children enjoin in class better.

The second part of teaching tool was guideline handbook for parent contacting and learning from children was developed. The purpose of guideline is improving conversation between parent and their children focusing on what children learnt about earthquake in class. The study started to interview each parent to get information about their children's behavior and their free time to set up a appropriated guideline for each participant.

This tool can be used by teachers, volunteers, or disaster experts in term of raising earthquake awareness among community. Learning module with student learning objectives and activities is presented in bellowing table.

Table 1: Earthquake mitigation teaching tool development

Lecture	**Purpose of lecture**	**Materials**	**Activities of children**
What is an earthquake?	students understand: Structure of The earth; Internal and external forces; Cause of earthquake and type of	Fresh eggs, boiling eggs, orange Pens, color pencils, white	Drawing, watching videos and pictures; coloring their picture; observing and amazing

	movement Earthquake in Location	papers, rulers, Pictures, projectors,	
what are the effects of earthquakes	students understand: Special terms relating about earthquake risk: seismic wave, magnitude of earthquake, intensity of earthquake, hypocenter, epicenter of the earthquake What to expect during earthquake happen? (Student quake might see, feel, hear, during an earthquake) Damages of an earthquake might occur in communities in different intensity levels Other adverse damages of earthquake	Pens, color pencils, white papers, rulers, glues, scissors, Color pictures, projectors, video	play a matching game to recall their knowledge; Drawing, watching videos and pictures; observing and amazing
How to prepare for an earthquake?	Children would help their parents preparing for an earthquake through earthquake home plan Help students being aware with the risk place with earthquake in their houses Understanding what should be prepared in emergency kits will help them prepare the necessary for they won in emergency case	Picture, power point, Projector,	Coloring the pictures, identify the vulnerable place in room Working with their friend to share idea about earthquake plan watching the videos and pictures

	To understand the long-term preparation for an earthquake		
What to respond during earthquake?	After class, students know skills to behave when they meet earthquake in different situation.	Video, projector, pencils, papers	children enjoined to practical drills; therefore, they will not to be panic in emergency case Children watch video and design their own action Children have responded after learning Watching video to memorize
What to response in post earthquake?	After class, students know skills to behave in post earthquake	Video, projector, pencils, piece of papers	During class children watch videos and they fix their own wrong actions in post earthquake

4.3 Experimental design

An experimental prep-test and post-test research design was used. Several factors were taken into account in designing the experiment. Permission of experiment was signed by heard of primary school so that the main teachers helped to contact with parent and organized meeting. The researcher contacted directly to parent to access general situation of each family, which would help in writing earthquake learning guidance for parent.

93 children were randomly chosen in two primary schools, Thanh Luong primary school and Hanoi- Dien Bien primary school. These students were devised into three groups which were received different treatments in experiment process. For group 1, previous test were introduced to children participants. Children in group 1 were taught earthquake knowledge in the 5 hours (1 hour per day). After teaching, participants had to do post- test to check the knowledge improvement. Children in the second group enjoined class after testing knowledge. They also did post test after 5 class hours but they won't asked to share what they learnt in class to parent in their family. In control group, children did pre-test and post-test without class participation.

In this research, adult participation would be the parents or other family members of children who were willing to join to the experiment. For the adult groups, several socio-demographic variables that effect to children and parent communication were assessed. These included children age, parent' education and family size. Base on the information, researcher chose those parent frequently make conversations with children to participate in the experiment. Then researcher and the main teacher contact directly to parent in the group 1 to clear about purposes of the requirements. They were asked to read the guidance for contact to their children do homework with them. Parent in group and in group 2 and 3 were asked to answer question in earthquake exam before and after their children learning but they did not participated in learning.

4.4 Pre- and Post- examination evaluation

The pre- and post-examination are designed to measure the students' abilities of learning and transformation earthquake knowledge to parent in their family. Moreover, these tests also evaluated capability of parent in the new approach. The test consists 4 parts and associated questions. There are 3 questions were opened – ended, 2 multiple choice questions and 22 true or false question. There was 1 ranking question. Maximum score is 30 point. Higher scores indicated higher levels of earthquake awareness, while lower scores indicated lower levels of earthquake awareness knowledge.

The design allowed comparisons between groups and pre- and of post- test among groups. The main analysis is pair t-test checking the score difference in pre- and post-examination within group. Statistically significant paired differences indicate the students and parent in their family performed differently on the post-test. To examine how age, education and gender impact the test score of parent

To comply with regulation on research on human subjects, both children and parent were informed the nature of research. Only those students and parent indicated a willingness to be included in the study were included. Students and parent who did not complete research both pre and post-test were deleted from the list.

5. RESULT AND DISCOUSSION

5.1 How people in Dien Bien concern about earthquake?

Demographic information

Gender distribution: Many researchers found men and women have different social worries because of different responsibilities in society. In this survey, (64%) female responded which was much more than that of males (36%); therefore, the perception of the answers would be effected because of gender views

Age group: The human age might determine their experiences and knowledge about social problems. In Dien Bien, old people who are more than 60 year olds would have different perception about earthquake mitigation because they already experienced a lot of big earthquakes including a big earthquake in 1935 (M= 6.75), 1983 (M= 6.7) and earthquake in 2001 (M= 5.3). Those who are more than 30 year old suffered less big earthquake, some small earthquake including a damaged earthquake in 2001 with magnitude is 5.3. Young people who do not have experience about earthquake, so they might not respond to questions in the same as the older one.

In this survey, average of respondents 37.39 showed that most of the citizens have experiences about some small earthquakes especially big earthquake magnitude 5.3 in 2001. The standard deviation is age group distribution is 12.54 therefore, the information reflected ideas of citizens at a variety of ages.

Table 2: Summarizing results of earthquake concern survey in Dien Bien city (N = 100)

	Number of respondents	Percentage
Gender distribution		
male	36	36%
female	64	64%
Age group		
14 to 25	21	21%
26 to 54	71	71%
55+	8	8%
Educational level		
Primary school	2	2%
Secondary school	21	21%
High school	57	57%
Bachelor or higher	20	20%
Experience about earthquake		
Have earthquake experience	83	83%
No earthquake experience	17	17%
Need to understand earthquake		
need	69	69%
No need	31	31%

Educational level: Education is the process by which the knowledge, characteristic and behavior of respondents are formed and modified. Table 2 showed education level of respondents in Dien Bien city is also quite high with more than 70% of citizens graduated high school degree. These people were expected to have right access and concern about earthquake risk in their living area. Only 2% of samples was at primary school level and 21% of total respondents at secondary school level.

Disaster is the most worry of people in Dien Bien today

In life, people have to face with number of living problems including disaster, road accident, low income and diseases. Depending on different areas, one factor may be more or less important than others. In this survey, local people ranked their concerns among above problems according to weight from 1 (absolute don't worry) to 4 (very worry). The result showed that both disaster and low income received the highest worry from local people average points were 3.13 and 2.9

respectively with no significant difference in one-way ANOVA test between the Two (p value = 0.555> 0.05). The highest mean score was disaster which show how important role of disaster mitigation activities in this area. Disease factor and road accident got lower concern. There were no significant difference in mean score of two this factor (p value in one way ANOVA = 0.078>0.05).

Earthquake is the most concern of Dien Bien people among disasters
Storm, flood, earthquake and landslide are four types of disaster frequently happened in Dien Bien city. Local people ranked their concern about theses disasters according to different worry levels from 1 to 4. The result showed that, earthquake was most worry of people in the city (mean score = 3.89). After earthquake, storm was the second concern of local people in Dien Bien which also had significant difference from flooding (sig value = 0> 0.05_) and landslide (sig value = 0< 05).

In fact, respondents live in the city, where does not locate in the flash flooding root; therefore, this place rarely suffers from flash floods. Moreover, there are 5 lakes surrounding the city which can help people manage and reduce water flow and store water in the raining season. Concerning about storm worry in the city, the infrastructure including houses, road, and other constructions in the city are quite good to resist storm. Comparing to damage of other disasters, earthquake damage 2001 in Dien Bien happened in short time but caused huge damages, which easier to recall them their concern while responding the question.

Factors effect on local people need to understand earthquake
Success of earthquake mitigation programs at community strongly depends on the need to understand about earthquake of local people. As the result of research 69% of respondents did not want to understand earthquake mitigation even the percentage of people have earthquake experiment quite high, 81%.
A logistic regression test was utilized to find relation of earthquake educational need and age, having earthquake experiment of respondents. Result of the test demonstrated that it would predict “yes” answer success at 92% and predict “no” answer 32.3%. in general the model can predict the decide of local people about need or don’t need earthquake education successfully at 74%.

Table 3: Summarizing the result of checking logistic regression of relation between the earthquake educational need of respondents and factors education, age, having earthquake experiment

factors	**B**	**S.E.**	**Wald**	**Sig.**	**Exp(B)**
Education	.717	.357	4.039	.044	2.49
age	.044	.022	4.017	.045	1.045
Earthquake experience	1.423	.613	5.388	.020	4.150
Constant	-4.022	1.538	6.797	.009	.018

Results from table 2 shows that predictors age, education and “having earthquake experience” significant effect on earthquake educational need of local people with its sig value = 0.044, 0.45, 0.2 respectively < 0.05. The value of coefficients (Exp (B) from table 2 show there was positive relation between these predictor and the earthquake educational demand of local people. That is, the more local people got earthquake experience, high age and higher education the more they need and understand about earthquake. Among of three factors, the factor “having earthquake experience” significantly effects on demand of earthquake education of Dien Bien people.

Where does earthquake information mostly come from?

According to our research, television is the most popular source that provides earthquake risk information for studying the area. Other three sources such as newspaper, radio, and the internet received less concerned from local people. The result of analyzing SPSS also show that mean score of TV source is higher significantly than other sources (Sig value = 0.000). The finding suggests that, for remote area, television is the best way to raise awareness about earthquake risk

5.2 Can primary children learn earthquake mitigation?

The results of the paired t-test are given in the table 2 for each of four parts (basic earthquake knowledge, preparedness for earthquake, response during earthquake, response in post-earthquake) plus all question combination in test. Anpha level of 5% is assumed. For control group, none of the post- and pre-test score are statistically different (p value = 0.348).

All t-tests show significant differences between the post and pre-tests of students in group 1 (p value = 0.000) and group 2 (p value = 0.000) who participated in class. These significant differences indicate primary children can comprehend and learn as the earthquake mitigation-teaching tool applied. Result also shows that mean score in the post-examination of children group 1 with parent participation is 21.16 which is higher than that of children in group 2 without parent participation (the mean score =19.16). This finding may suggest that, adult participation would be one of the factors improve children learning disaster mitigation. Previous study also confirmed this finding by concluding that kids at 5 to 6 age can learn earthquake education better when they learn with their children (Gulay, 2010).

Table 4: pre-and post-test mean score associated with the null hypothesis of equality of pre- and post test score of students by T-test

score	Questions in different part				
	Total	Part 1 Basic EQ	Part 2 EQ preparedness	Part 3 Respond during EQ	Part 4 Respond in post EQ
Control group n = 31					
Post test mean	11.42	4.73	2.45	2.23	2.13
Pre-test mean	11.03	4.60	2.22	2.26	1.96
P -value	0.348	0.73	0.09	0.459	0.591

Group1 – parent participation (n = 31)					
Post test mean	21.16	6.9	3.45	6.39	3.45
Pre-test mean	8.13	3.06	1.39	2	1.67
P -value	0.00	0.000	0.000	0.000	0.000
Group 2 - non parent participation (n = 31)					
Post test mean	19.16	5.64	3.49	6.06	3.97
Pre-test mean	11.42	3.5	1.97	2.065	3.80
P -value	0.00	0.000	0.000	0.000	0.572

In all four parts, score of children in group 1and group 2 in post-test remarkably higher on the pre-test with p = 0.000. From table 2, ratio mean cores in posttest and maximum score in part 1 (6.9/7; 5.64/77) and in part 3 (6.39/7; 6.06/7) of children of group 1 and 2 were higher than that in the part 2 (3.45/7; 3.49/7) and part 4 (3.45/7; 3.97/7) . This illustrates that, the teaching tool have high effectiveness in training basic earthquake knowledge and response during earthquake. The reason for these successes would be, learners already have their own perception these issues in their past in the study area. Second, children may more concern about what to do during earthquake than other issues. Third, teaching material was good enough to teach people. Therefore, the teaching tool need to be more developed to provide earthquake knowledge for participants.

5.3 Can parent learn earthquake knowledge from their children?

As mentioned before, adult participants in this research were chose purposely with assume that most of them followed the guidance. Results from Two-way ANOVA analysis combining data of all adult participants in 3 groups showed that, gender, education and age did not have significant effected to score of parent' pretest with p value equal 0.08, 0.055 and 0.23 respectively.

According to table 4, while there was a significant difference in score of pre and post-test of parent in group1, non-difference could be found in that of parent group 2 and group 3. This result indicates those parent following the guideline and contact frequently to children would improve their earthquake knowledge.

Table 5: pre-and post-test mean score associated with the null hypothesis of equality of pre- and post test score of parent by T-test

score	Questions		
	Mean score	Std. Deviation	P value
Control group n = 31			
Post test mean	20.35	2.45	0.348
Pre-test mean	9.23	2.32	
Group1 – parent participation (n = 31)			
Post test mean	12.9	2.44	0.000
Pre-test mean	13.32	2.73	
Group 2 - non parent participation (n = 31)			

Post test mean	12.42	2.28	0.521
Pre-test mean	11.13	2.58	

To examine which factor have significant effects to posttest score of parent in group 1, two-way ANOVA showed that while education factor and age and education combination have significant effect on the score (p- education = 0.025, p age-education = 0.032) age factor, gender or combination of age, education and gender factor did not effect to the score. This means parent in family in different age, gender and education following the guidance can learn earthquake knowledge from student.

Concerning 4 parts in content of the teaching program, mean score of parent in part 3 was even better than that of children in part 3. That mean parent not only learnt from their children but also have their own experience from indigenous knowledge. Therefore, the most importance in training adult is raising awareness for them to get them involve in earthquake mitigation activities; from that, they can learn and achieve knowledge by themselves. In this case, children was one of the most important factors make them pay attention on earthquake mitigation activities. In looking beyond this study, this approach can be used effectively to raising awareness about earthquake protection in urban city.

6. CONCLUSIONS

While earthquake cannot be predicted accurately, raising awareness activities including formal and informal education is considered as one of the most important activities for Dien Bien city.

From the experiment, the findings indicated that the program carried out in urban city with children and adult participation was effective. Children at age 10 to 12 years-olds can learn earthquake mitigation and can transfer earthquake knowledge to their family members. Parent in urban city improved earthquake knowledge through learning from their children without effect of age, education and gender. In other words, the approach raising earthquake awareness for citizens through children education is effective.

The results of social concern survey in Dien Bien city showed that, local people are worry most disaster and income following these are other problems like disease and road accidents. Among disasters happened in city, earthquake is the most concern of citizens. People have experienced earthquake in the past recognized the importance of earthquake education while those who don’t have earthquake experience neglect that. The research found out that, the more local people having earthquake experienced getting older, having higher education, the more they need earthquake education. This survey also presented the limitation of disaster information sources in the city. Among number of information sources such as, TV, Internet, Newspaper, radio, Television is the most popular for them.

REFERENCES

Andrew Coburn, Robin Spence. (1992). *Earthquake protection.* New York: John Wiley & Sons.

Anh, D. N. (2010). Seismic Hazard of Territory of Viet Nam. Hanoi, Ha Noi, Viet Nam.

CSEP. (2011). *Independent Expert Panel on New Madrid Seismic Zone Earthquake Hazards.* New York: USGS.

Dinh, X. N. (1993). Vietnam systemartic strategy is begining to take shape. *Seismic Risk Management for Countries of the Asia Pacific Region* (p. 167). Bangkok, Thailand: WSSI (World Seismic Safety Initiative).

Gulay, H. (2010). An earthquake education program with parent participation for preschool children . *Educational Research and Review* , 624.

Izadkhah, Y. O. (2005). Toward resilient communities in developing countries through education of children for disaster preparedness. *Int. J. Emergency Management* , 138.

Kirschvink, Joseph L. (2000). Earthquake Prediction by Animals. *Evolution and Sensory Perception* , 312-323.

Parsizadeh, F. (2007). School Earthquake Safety education Present and Future. *First global Platform Intergrated Disaster Risk Management.* Geneva: United Nations.

Pelling, M. (2010). *Review and Systematization of Disaster Preparedness Experiences in Urban Areas in the Caribbean Region.* German: Oxfam.

Phuong, N. H. (2011). Eartquake - Tsunami assessment and Risk mitigation in Vietnam using GIS. Hanoi, Hanoi, Vietnam.

Phuong, N. H. (2012). Seismic Hazard Studies in Vietnam. *GEM semi- anual meeting.* Taipei, Taiwan: Institude of Geophysic.

Wisner, B. (2006). *Let Our Children Teach Us.* Bangalore, India: Book for Change.

Shiwaku, K. (2007). Disaster Education in Japan and Nepal. Kyoto, Kyoto, Japan.

Wisner, B. (2006). Let Our Children Teach Us. In *Let Our Children Teach Us* (p. 2). India: Books for Change

Zobel, T. (1992). *Intergrating Earthquake Education Into the Elementary School Curriculum: A Whole Language Approach.* Buffalo: National Center for Earthquake Engineering Research

Public housing after hurricane: Urban renewal or removal? The case study of Beaumont and Galveston, Texas, U.S.A.

Tho TRAN[1], Shannon VAN ZANDT[2], and Walter G. PEACOCK[3]
[1] PhD Student in Urban and Regional Sciences,
Department of Landscape Architecture and Urban Planning,
Texas A&M University, United States of America
ductho2211@neo.tamu.edu
[2] Associate Professor, Director of Center for Housing and Urban Development,
Texas A&M University, United States of America
[3] Professor, Director of the Hazard Reduction and Recovery Center,
Texas A&M University, United States of America

ABSTRACT

Decent housing is a goal for many people not only in the United States but elsewhere in the world. A house becomes the symbol of family spirit whether it is a single-family or multiple-family home. Public housing in the United States is housing of "last resort," for families whose incomes do not allow them to find housing in the private market. Yet, many studies focusing on public housing find a host of social issues plaguing these units. The US Government has initiated various programs to improve the quality of public housing as well as the living condition of local resident through agenda of Department of Housing and Urban Development (HUD). HOPE VI is one of the major programs that focuses on distressed public housing. This program funds local government and housing authority in order to revitalized or rebuild public housing. This program has been very successful in providing high-quality housing for public housing residents.

However, as any type of construction, housing usually received great damage when natural disaster happening. It can be partly damaged or completely destroyed due to the direct and indirect effects of disaster. Public housing, like most affordable housing, is often built in highly vulnerable areas, such as floodplains or other low-lying areas. When disasters such as hurricanes strike, housing located in these areas is likely to receive the greatest damage and recovery may be slower.

This study looks at the case study of public housing in Galveston and Beaumont after Hurricane Ike (2008) and Rita (2005). After Hurricane Rita in 2005, Beaumont has rebuilt some public housing developments with a HOPE VI grant awarded in 2007. These areas have successfully rebuilt through the cooperation of housing authority, local government, local residents, and developers. In contrast, Galveston could not reach agreement about the destiny of public housing after Hurricane Ike in 2008. This story becomes more serious when HUD announced that if Galveston cannot rebuild public housing in disaster area, they must refund the money to the Federal Government. These two cities provide a

comparative case study of the response and recovery of public housing after disaster, where on one successfully rebuilt while other did not.
By looking at the secondary data sources, this research analyzes the situation of these places in different period: before the Hurricane, when the Hurricane happened, and after the Hurricane. The paper will address the similarities as well as differences between two case studies in term of historical profile, demography, public housing program characteristics, damage, and recovery. Besides, economic change after hurricane approached is addressed. The housing situation will be further analyzed in Galveston to clearly show the obstacles in which this city coped with. Finally, the study will conclude by suggesting some implications for theory, housing policy, management, and further research.

Keywords: public housing, affordable housing, hazard management, response, recovery, hurricane, United States, Galveston, Beaumont, Texas.

1. INTRODUCTION

Decent housing is a goal of every family in the United States as well as elsewhere in the world. It can be appeared with different styles and layouts such as single-family home or multiple-family complex. After World War II, US government has released different Housing Acts through periods with the general purpose of bringing more housing opportunities for people. As one part of the working agenda, public housing had been placed as the center of social concentration. This type of social housings play important role in dealing with housing necessary of distressed families who are unable to purchase a house according to the private market. Public housing receives different support from the Federal government as well as agencies. There are several programs that greatly contributed to the development of public housing in the US such as Section 8, Community Development Block Grants (CDBG), HOPE VI, among others. Each program has their own features as well as requirements and supported objectives due to their mission. However, HOPE VI is a special program that is designed to support community to recovery after natural disaster such as hurricane, flooding, or earthquake.

Located in the large continent, the US has to face different types of natural disaster. Hurricane appears as one of the major threats that directly affect human life because of it devastated effects. Like other construction’s elements during the catastrophe, housing is vulnerable coping with the anger of nature. They are easily wiped out as well as destroyed partly or entirely due to the level of the hurricane. When it happen, public housing received more negative impacts due to its larger number of resident in compare with single family construction.

Based on the United States natural disaster risk map, Texas Gulf Coast is an area where hurricane visit frequently every year. Many coastal cities have been affected by the activities of hurricanes in the area. From those, Galveston and Beaumont are two places sharing the unhappy experiences with natural disaster. In 2005, hurricane Rita visited City of Beaumont on the way approaching Gulf Coast areas of the US. Rita had an impact on large area within multiple states including Florida, Louisiana, Mississippi, and Texas. According to the report, 25% of the trees in the city of Beaumont were uprooted by the hurricane. Together with that damage, an enormous number of houses and business had suffered damage by heavy wind as well as falling trees and debris in the air. Some areas did not have power for more than a month due to serious damage to city infrastructure.

Galveston is an barrier island on the south of Texas state. The City of Galveston is one of the high frequency place that hurricane approach each year in the US. In fall 2008, the major hurricane in the season namely Ike had visited Galveston. This hurricane last for more than a week and make huge damage for the City of Galveston. Hurricane Ike hit Galveston Island and damaged about 88% of the residential units. While the majority had minor damage, approximately 1,000 were substantially damaged. At that time, Galveston Housing Authority (GHA) was managing 990 units of public housing, including 356 units in two high rises for the elderly, 34 scattered sites, 20 new duplexes for the elderly, and 569 family units. According to the GHA's report, more than half of public housing stock was damaged beyond repair by the hurricane. Ike became the costliest hurricane in Texas history with the total damage approximately reach $29.5 billion dollars.

2. RESEARCH QUESTIONS

Both cities had received huge damages after storms left. There remains many works and efforts needed in order to bring normal life back to local areas. Besides all of the recovery processes, housing rebuild and recovery plays fundamental role that directly affect the residential and their family. This research focuses on the recovery issues of public housing where vulnerable population was waiting for external supports.

Housing recovery after hurricane is an inevitable part of revitalization process after disaster events. However, what happen in each place is different due to particular characteristics. Moreover, some processes happen with reverse direction with others. Those are the case of public housing after hurricane in Beaumont and Galveston, Texas. They share the same situation of being damage by devastated hurricanes. Housing stock in both cities has received negatively affected by storm while the shortage of affordable housing was their temporary problem. And, they both work in recovery process in order to rebuild public housing for low income people. However, the results of their efforts are totally different. Beaumont has rebuilt some public housing development with a HOPE VI grant awarded in 2007. These areas have successfully rebuilt through the cooperation of housing authority, local government, local residents, and developers. While Beaumont has a successful revitalization program with public housing after hurricane Rita, Galveston stuck in a debate about public housing's redevelopment plan. Housing authority in Galveston tried to create the most appropriate redevelopment plan for public housing while local community and some conservative city councilmen opposed bringing public housing back to the island. This story becomes more serious when Department of Housing and Urban Development (HUD) announced that if Galveston cannot rebuild public housing in disaster area, they must return the funding to the federal Government. These two cities provide a comparative case study of the rebuilding of public housing after disaster, where on one successfully rebuilt while other did not.

There are some questions have been raised through the study of both cities. Firstly, the overall change of demography in entire two cities is expected to find by looking at the data before and after hurricane. Secondly, the process of rebuilding public housing in each city might suggest the reason leading to redevelopment plan. In addition, by looking at closely at public housing area through various topics and data set, the author hopes to find quantitative evidences that support to what happen in both cities. The latter part of this paper will indicate two case studies with population data set in order to find the responses for above concerns.

3. METHODOLOGY

By looking at the secondary data sources, this research will address the similarities as well as differences between two case studies in term of demography, public housing program characteristics, damage, and recovery. Besides, economic change after hurricane approached is addressed. The housing situation will be further analyzed in Galveston to clearly show the obstacles in which this city coped with. Finally, the study will conclude by suggesting some implications for theory, housing policy, management, and further research.

3.1 Public Housing Areas Analysis

In order to observe the general picture in public housing areas as well as their fluctuations between 2000 and 2010, this study conducts equivalent analysis in a local level in terms of age groups, race, and housing characteristics. Gaining access to the location of each public housing development enables the author to precisely indicate in which block groups public housings were located. Then, census data for block group level in each city is accessed through U.S. Census Bureau web site. By adding up data of all block groups that contain public housing developments, the author analyzes basic trend as well as alteration of each topic in public housing areas from 2000 to 2010.

3.1.1 Races

Table 1 shows race data in public housing area in Beaumont. The Not Hispanic Black people took the largest share in total public housing population. In 2000, there were 5,900 people accounted for 70% people living there were Not Hispanic Black. This number increased to 6,107 people, equivalently to 73% of total population in 2010. Furthermore, Not Hispanic White is clearly perceived to be the group bearing the largest drop in in public housing population over this period. In 2010, they declined 607 people equivalent to 34.5% of their population in public housing neighborhood in 2000. In other hand, Galveston race has been shown some changes according to the Table 2. In contrast with Beaumont, Not Hispanic White in Galveston increased in this period from 963 people to 1,579 people while Not Hispanic Black decreased about 540 people represented 22% of their population in 2000. Although Not Hispanic Black remained the most populated group living in public housing, each city shows reverse direction of changing. While public housing areas in Beaumont increased from 70% to 74%, Galveston greatly decreased from 53% to 38% of total population living in public housing areas.

Table 1. Race in Public Housing Areas in Beaumont, TX

BEAUMONT, TX	Population 2000		Population 2010		Population Change	
	Count	Share	Count	Share	Count	Share
Not Hispanic White	1,760	21.02%	1,153	13.90%	-607	-34.5%
Not Hispanic Black	5,900	70.48%	6,107	73.63%	207	3.5%
Not Hispanic Others	230	2.75%	190	2.29%	-40	-17.4%
Hispanic or Latino	481	5.75%	844	10.18%	363	75.5%
Total Population:	8,371	100%	8,294	100%	(X)	(X)

Data Source: Census Bureau 2000, 2010

Table 2. Race in Public Housing Areas in Galveston, TX

GALVESTON, TX	Population 2000		Population 2010		Population Change	
	Count	Share	Count	Share	Count	Share
Not Hispanic White	963	20.69%	1,579	30.97%	616	64.0%
Not Hispanic Black	2,459	52.84%	1,919	37.63%	-540	-22.0%
Not Hispanic Others	71	1.53%	160	3.14%	89	125.4%
Hispanic or Latino	1,161	24.95%	1,441	28.26%	280	24.1%
Total Population:	4,654	100%	5,099	100%	(X)	(X)

Data Source: Census Bureau 2000, 2010

3.1.2 Housing Units

Table 3 and Table 4 show statistical data of housing characteristics in public housing in Beaumont and Galveston, TX. According to the data set, the number of owner occupied units in public housing areas of Beaumont reduced by 122 units from 1,511 in 2000 to 1,389 in 2010. At the same time, the renter occupied unit group only saw an increase of 25 units, which equaled to 1.5% of total rental occupied units in public housing area in 2000. More importantly, while the number of vacant units in Beaumont increased 145 units, the equivalent amount in Galveston was 520, approximately 136% of total vacant units in 2000 in public housing areas. Through Exhibit 6, a dramatically change in housing stock in Galveston has been depicted. Renter occupied unit dropped from 62% in 2000 to 45% in 2010 while vacant units increased from 16% to 34%. In Beaumont, there were stable trends except for a slight reduction in the number of owner occupied units.

Table 3. Housing Characteristics in Public Housing Areas in Beaumont, TX

BEAUMONT, TX	Units 2000		Units 2010		Change	
	Count	Share	Count	Share	Count	Share
Owner Occupied	1,511	43.4%	1,389	39.4%	-122	-8.1%
Renter Occupied	1,650	47.4%	1,675	47.5%	25	1.5%
Vacant	317	9.1%	462	13.1%	145	45.7%
Total	3,478	100.0%	3,526	100.0%	(X)	(X)

Data Source: Census Bureau 2000, 2010

Table 4. Housing Characteristics in Public Housing Areas in Galveston, TX

GALVESTON, TX	Units 2000		Units 2010		Change	
	Count	Share	Count	Share	Count	Share
Owner Occupied	516	21.6%	572	21.5%	56	10.9%
Renter Occupied	1,489	62.4%	1,186	44.6%	-303	-20.3%
Vacant	382	16.0%	902	33.9%	520	136.1%
Total	2,387	100%	2,660	100%	(X)	(X)

Data Source: Census Bureau 2000, 2010

3.2 Economic Analysis in Two Cities before and after Hurricanes

3.2.1 Job Earning Analysis

Table 5 and Table 6 show the statistical data about jobs respectively in 2004 and 2006, in Beaumont and Galveston. The category includes different monthly earning jobs such as low wage job, moderate wage job, and high wage job. In Beaumont, all of job categories increased from 2004 to 2006 with a total of about 4,047 jobs. Overall, high wage job experienced the fastest enhancement with more than 2,000 newly increased jobs while low and moderate-wage job shared the same improvement of more than 900 ones. Galveston experienced a different scenario after Hurricane Ike in 2008. Before that, moderate wage job group had the largest share with 40.9% while low wage job compromised only 27% of total jobs in Galveston in 2007. While both of these job groups reduced in 2009, high wage job slightly increased with 115 jobs equally 1.5% of total jobs in 2007. Low wage jobs in Galveston experienced a great lose after Hurricane Ike with more than 1,600 jobs. This reduction equals one quarter of low wage jobs in Galveston at the time of 2007. This decrease suggested the effect of Hurricane Ike as well as its damage towards the low income group in Galveston.

Table 5. Jobs in Beaumont, TX Before and After Hurricane Rita (2005)

BEAUMONT, TX	2004		2006		Change after Hurricane Rita (2005)	
Jobs by Earnings	Count	Share	Count	Share	Count	Share
$1,250 per month or less	14,863	32.2%	15,783	31.4%	920	6.2%
$1,251 to $3,333 per month	18,885	40.8%	19,871	39.5%	986	5.2%
More than $3,333 per month	12,465	27.0%	14,606	29.1%	2,141	17.2%
Total	46,213	100%	50,260	100%	4,047	(X)

Data Source: U.S. Census Bureau, OnTheMap Application at onthemap.ces.census.gov

Table 6. Jobs in Galveston, TX Before and After Hurricane Ike (2008)

GALVESTON, TX	2007		2009		Change after Hurricane Ike (2008)	
Jobs by Earnings	Count	Share	Count	Share	Count	Share
$1,250 per month or less	6,302	27.0%	4,682	23.0%	-1,620	-25.7%
$1,251 to $3,333 per month	9,557	40.9%	8,098	39.7%	-1,459	-15.3%
More than $3,333 per month	7,482	32.1%	7,597	37.3%	115	1.5%
Total	23,341	100%	20,377	100%	-2,964	(X)

Data Source: U.S. Census Bureau, OnTheMap Application at onthemap.ces.census.gov

3.2.2 Inflow – Outflow Analysis

One of the important features of economic flow analysis is the natural of movement in population in term of joining economic activities. Table 7 and Table 8 show the inflow and outflow of labor force in Beaumont and Galveston before and after disaster events. In Beaumont, the number of people living and working inside the city increased from 27,453 in 2004 to 29,768 in 2006. This phenomenon can be considered as an advantage of redevelopment projects that took place in Beaumont after Hurricane Rita. Clearly, it shows the advantage of urban renewal trend in this area where people can work and live inside the city. Together with the general trend of economic improvement, the number of people working in Beaumont but living outside greatly increased by 7,230 people, equally to 18.1% of the population before Hurricane Rita. Conversely, the number of Beaumont residents working outside marginally increased with approximately 1,732 people from 2004 to 2006.

Galveston shows a totally opposite trend in term of economic movements of the area. The number of people who lived and worked in Galveston declined more than 3,300, or more than a quarter of the previous figure obtained in 2007 before Ike. This trend might as well relate to the previous analysis of the decline in the low wage jobs in Galveston. More importantly, the author believes the issues of housing redevelopment processes greatly attributed to this trend in the Galveston area. In addition, the number of people working in Galveston but living outside as well as people living in Galveston but working outside both shared some minor changes. While the former group decreased by 725 people, the latter group increased by about 357 residents. These changes only equaled to 3.9% and 3.3% of total numbers in the same groups before Hurricane Ike approached Galveston.

Table 7. Work Movement Before and After Hurricane Rita (2005)

BEAUMONT, TX	2004		2006		Change after Hurricane Rita (2005)	
	Count	Share	Count	Share	Count	Share
Employed in Beaumont	67,366	100%	76,911	100%	9,545	(X)
Living in Beaumont	27,453	40.8%	29,768	38.7%	2,315	8.4%
Living Outside	39,913	59.2%	47,143	61.3%	7,230	18.1%
Living in the Beaumont	46,213	100%	50,260	100%	4,047	(X)
Employed in Beaumont	27,453	59.4%	29,768	59.2%	2,315	8.4%
Employed Outside	18,760	40.6%	20,492	40.8%	1,732	9.2%

Data Source: U.S. Census Bureau, OnTheMap Application at onthemap.ces.census.gov

Table 8. Work Movement Before and After Hurricane Ike (2008)

GALVESTON, TX	2007		2009		Change after Hurricane Ike (2008)	
	Count	Share	Count	Share	Count	Share
Employed in Galveston	30,853	100%	26,807	100%	-4,046	(X)
Living in Galveston	12,416	40.2%	9,095	33.9%	-3,321	-26.7%
Living Outside	18,437	59.8%	17,712	66.1%	-725	-3.9%
Living in Galveston	23,341	100%	20,377	100%	-2,964	(X)
Employed in Galveston	12,416	53.2%	9,095	44.6%	-3,321	-26.7%
Employed Outside	10,925	46.8%	11,282	55.4%	357	3.3%

Data Source: U.S. Census Bureau, OnTheMap Application at onthemap.ces.census.gov

3.3 Discussion

Natural disaster is unexpected event happening out of human control. However, with nowadays technology, we are able to predict as well as proactive with preparations in order to minimize the damage caused by natural disasters. Once they happen, the process of recovery plays a critical role in bringing people back to normal life. What happened in Beaumont and Galveston are regarded as two interesting stories. Both cities suffered from severe damages caused by some of the most devastated hurricanes in Texas history. Beaumont was not hit directly by Hurricane Katrina or Hurricane Rita as Galveston was, in the situation of Hurricane Ike. The impacts levels that hurricanes affected both cities varied according to their own features and their reactions to the events.

Beaumont was really an opportunity-catcher when wisely dealing with the situation of the city especially housing stock after Hurricane Rita dissipated. Although the public housing areas in Beaumont did not experience as huge damages as Galveston did, Beaumont still planned to rebuild the old public housing areas based on the nature of recovery processes after the disaster. The changes that Beaumont brought to ground for public housing areas as well as surrounding communities are considered as one of the most successful urban renewal achievements. They did not only achieve the goal of recovery after disaster but also turned this opportunity into a great catalyst for housing development. The success of Beaumont Public Housing redevelopment came from different elements. They had a clear plan with careful preparation, strongly support from the city as well as residents and most importantly, a great housing authority that understood the situation and knew how to realize the goal with flexible strategies as well as passionate willingness. This strong factor turned the hurricane into an opportunity for urban renewal that supported mixed-income developments.

Conversely, Galveston experienced a more depressing situation after Hurricane Ike. What happened in Galveston distressed every element of the whole redevelopment efforts. First and foremost, the public housing residents were the most distressed subjects since they lost everything because of the natural disaster. Many of them became the victims of hurricane damages which negatively affected their life, work, and properties. More seriously, they were unable to come back to their places because of others' opinions. This clearly was not fair with the most vulnerable group in population. In addition, what happened in Galveston after Hurricane Ike also affected local resident who were not public housing dweller. They had to spend their time and efforts in order to protect their opinions toward redevelopment of public housing. The author believes that many of them had to work extra hours as well as spend additional money for their debating. Besides the public housing resident group, the public authority was affected by the hurricane as well. These effects stand out-side the normal curriculum of recovery process. They are in the middle of two sides who shared reverse opinions towards public housing redevelopment after hurricane. These conflicts factored to the public authority's delay in recovery work. It not only affected the victims of hurricane but also the city in general since public works had been postponed due to deferred decisions. Last but not least, federal programs are another element that has been negatively affected by Hurricane Ike. They are forced to become involved in the debated of public housing in Galveston. In order to pursue the general goals of affordable housing and social equity, public programs needed to intervene with this debate. Clearly, if the problem had not been existed, the redevelopment processes would increase economic development as well as bring improvement for the island. One strong example is the case study of Beaumont, Texas. Therefore, Hurricane Ike was not only costly with regards to its damage on physical properties but also socially distressed for every side of the recovery processes.

3.4 Policy Implication

Beaumont and Galveston are two strong examples of the policy implication process. In Beaumont, the key of successfully redeveloping public housing after hurricane is the cooperation between each participant of recovery processes. Beaumont Housing Authority plays a crucial role in this collaboration. They reacted to the situation with adequate preparation as well as creative responses within their power. The damage of Beaumont did not get enough attention of federal agencies as it should because of the overwhelming attention drawn to New Orleans after Katrina. BHA was proactive in their responsibility in order to recall the support from federal agencies through many necessary actions by different groups. In addition, they took a wise move when collaborating with academic scholars and students from Department of Landscape Architecture and Urban Planning, Texas A&M University. This cooperation helped BHA effectively develop a comprehensive neighborhood revitalization plan to spur investment and redevelopment in public housing neighborhood. In addition, besides the innovation in financial solutions, BHA also developed an effective management mechanism that supported housing development. The public – private partnership also prove the successful result in supporting residents by abundant service from daily needs to professional skills as well as necessary consultancies.

In contrast, Galveston faced many issues related to policy implementation. After suffering from devastated damage from Hurricane Ike, Galveston could have accomplished this opportunity to redevelop housing stock and improve the spill-over effects of these developments as part of the urban renewal process. However, the cooperation between Galveston Housing Authority and City government proved an unsuccessful relationship when GHA could not get the support from residents as well as public authority despite of their great efforts. GHA is an example of housing authority who acts as a bridge that connects residents, public authority, and developers. In this case, the delay of redevelopment public housing negatively affected every party of this triangle. Therefore, Galveston could well be considered an example of ineffective policy implementation in relationship with housing recovery in post-disaster.

3.5 Practical Recommendations

Recommendation #1: Housing Authority should be more proactive with substantial preparations and innovative solutions.
Recommendation #2: Housing for low income population needs to be developed in mixed-income community in order to support the individual as well as family improvement.
Recommendation #3: Public-private partnership should be executed in any steps of the development as long as it shares the same goal of supporting community.
Recommendation #4: Collaboration between housing authority and academic experts or professional firms should be accessed as an effective way to conduct successful development for new project.

REFERENCES

Peacock, W. G., Zhang, Y. and Dash, N. 2005. *Single Family Housing Recovery after Hurricane Andrew in Miami-Dade County*. College Station, TX: Hazard Reduction & Recovery Center, Texas A&M University.

Schwartz, Alex F. 2010. *Housing Policy in the United States.* Second Edition. Routledge, New York

Van Zandt, Shannon, Edward Tarlton, June Martin, Dawn Jourdan, and Cecilia Giusti. 2012. *Magnolia Garden HOPE VI Evaluation*. College Station, TX: Center of Housing and Urban Development, Texas A&M University.

United States Census Bureau website: *www.census.gov*

Flood adaptive cities towards climate change adaption and urban development in Mekong Delta

Thu Trang LE
Lecturer, Faculty of Architecture and Urban Planning,
National University of Civil Engineering, Vietnam
Graduate student, Department of Urbanism,
Faculty of Architecture, Delft University of Technology, Netherlands
trangb16186@yahoo.com

ABSTRACT

Deltas are the magnetic regions to inhabit for half of the world's population because of their rich natural resources and strong economic potentials for agriculture, aquaculture, tourism, and port development (UN-Habitat, 2006). However, frequent floods, salt-water instruction, and freshwater scarcity are common challenges that put a large number of people living in the deltas at risks.

The Mekong Delta is considered as one of the largest delta in the world where is home for more seventeen millions people concentrating along the watercourses of rivers and canals. For a long time, local communities have traditionally adapted their lives to the presence of water. In the recent decades, water however has no longer plays the important roles in the social, economic and cultural activities of the citizens. As consequences of economic development and urban expansion, waterways have been replaced by roads and space for water in the delta-cities have been diminished. The city is losing its unique characteristic and inhabitants are facing more vulnerable to flooding. Therefore, finding innovative solutions to adapt to floods is crucial, especially in times of climate change. A new strategy is not only solely relying on technology of flood-defense but also has to combine water management with the urban development.

By using "Layer approach", this paper firstly determines the current problems of the Mekong Delta. Secondly, relevant strategies that can be visible the interaction between climate change adaption, water management and urban development of the Dutch delta are reviewed. Finally, the paper explores the possibility to apply these strategies in a case study of the Mekong Delta. We strongly argue that these flooding adaptive solutions can be useful for other delta-cities worldwide.

Keywords: *climate change, integrated strategy, water management, urban development, flood adaptive cities, the Mekong Delta*

1. INTRODUCTION

Deltas, where river flows into the sea, ocean, lake or reservoir, are the magnetic areas to inhabit for half of the world's population and also half of the world's urbanized areas (UN-Habitat, 2006) because of the most fertile land for agriculture and the most strategic locations for industrialization and urban development. Living close to the waterfront is now attracting a new stream of inhabitants, tourists, services and business to the cities. Since most of the large cities are located in delta region, an unintended side effect of the growth and the ensuing concentration of population is the increased challenge. The changing global climate recently puts additional pressure on this challenging situation.

How people deal with sea level rise, with erosion, with salinity intrusion, with subsidence and drought, and with the interactions between climate and urban areas?

Accommodating this question will involve the development of hydraulic infrastructure, such as: flood defenses, land reclamation, etc. In the Netherlands, answering this question is matter of survival. For a thousand year, the inhabitants built dikes to protect themselves and their properties against floods. After the devastating storm surge in 1953, Delta Works were created to keep the North Sea out of the estuaries and tidal inlets using dams, sluices and storm surge barriers (Delta program, 2012). The protection practices continue until the present day situation, however, the relation between Dutch people and water has changed: *'The main characteristics of the delta landscape in the past were the dynamic changes in water tables, the erratic and uncontrolled flooding and seepage and the vast, inaccessible stretches of low-lying land during winter inundations… This image has completely changed. Nowadays land is land, and water is water… Erratic changes in water tables are not allowed anymore'* (Nienhuis, 2008). Traditional approaches focus exclusively on the primary function: protection against flooding might not be efficient in the new challenge situation.

In the Mekong Delta region, people in the delta consider water dangers to be normal phenomenon and have generally adapted their lives to their presence. Thus, countries such as China, Vietnam and Thailand are known as some of the world's biggest exporters of rice (USDA, 2011). For hundred years, the water system including natural and manmade canals used for agriculture, irrigation, water transportation and military has been a foundation for other systems to be laid on (Shannon, 2009). However, in the last decades, as the rapid expansion of urban areas, road has replaced water to become the main economic, social and cultural life of the delta (Tayler, 2006). The canals are filled up and many flood plains are removed. Delta cities in this region are now separating from water and facing additional threats.

Therefore, sustainable development is crucial in deltas all over the world. This is not solely relying on technical solutions to fight against and control the delta environment, but a new approach that utilizes natural processes for water safety and sustainability for both the delta and its inhabitants. This approach is targeted at different disciplines: hydraulic engineering, urbanism and landscape architecture. Although there already exists a large body of knowledge on the characteristics and functioning of many deltas, most of this information is of a mono-disciplinary. There is relatively little knowledge that enables an overview of delta management in which these disciplines would be integrated. By using "Layer approach", this paper firstly determines the current problems of the Mekong Delta. Secondly, relevant strategies that can be visible the interaction between climate change adaption, water management and urban development of the Dutch delta are reviewed. Finally, the paper investigates the possibility to apply these strategies in a case study of the Mekong Delta.

2. LAYER APPROACH

Urbanized river deltas demonstrate different characteristics depending on their local climate, geographical condition, economic and political circumstances. Therefore not all deltas can easily be compared to other deltas. But many deltas have developed along the same patterns and have experienced the same problems as other deltas did at the same phase in their development. Delta cities all over the world, such as: New York, Rotterdam, Ho Chi Minh city, are the result of a long time interrelation between the nature and urban system. The natural complexity of the deltas, as the meeting of rivers and sea, with the complexity of urban pattern, as result of economic, cultural and social life creates unique areas with a double complexity (Meyer, 2009). Between these systems, infrastructure including waterways and roads play the key role in creating conditions for the development of the urban systems and influencing the nature system.

To provide insight in these complex systems, it is proposed to apply a simplified structure in the form of a "Layer model" (Figure 1) that is a component of three layers: the natural landscape (base layer), the infrastructural/ network layer (middle-layer) and the occupation layer (top-layer). This approach firstly was introduced by Ferdinand von Richthofen (1833-1905) to describe the chorological and topological relationships in the landscape. In the late sixties, Ian McHarg, a landscape architect, applied and developed it into 'layer cake model' for reasons of spatial analysis and planning in his seminal work: Design with Nature (McHarg, 1969). Recently, "Triple 3 layers approach", a more comprehensive planning and design oriented approach towards urban delta landscapes, was introduced by Meyer and Nijhuis (2010). This 'Layer model' presents a physical hierarchy in the sense that the layers enable and/ or constrain activities in another layer.

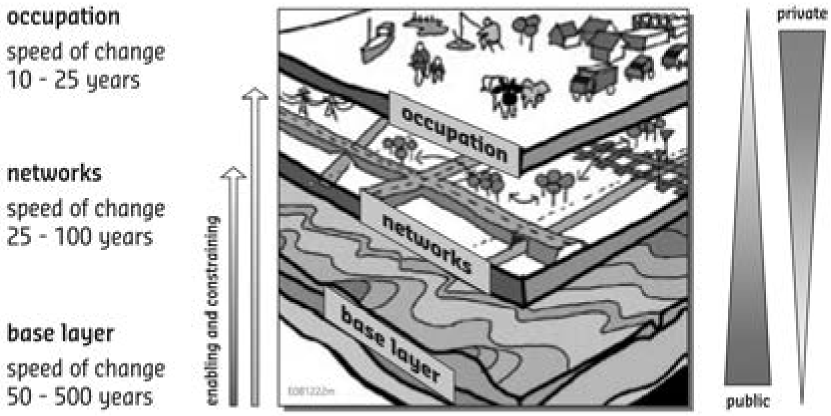

Figure 1. Layer model for planning of delta development

3. MEKONG DELTA AND ITS FORMATIVE LAYERS

3.1 Overview of the Mekong Delta

The Mekong River is the 7th longest river in Asia and 12th longest river in the world. Its estimated length is 4,350 km (2,703 mi), and it drains an area of 795,000 km2 (307,000 sq mi), discharging 475 km3 (114 cu mi) of water annually (MRC, 2010). Mekong River as the hydrological backbone of its basin travels 4200 km from its headwaters in the Tibetan plateau to China, Myanmar, Thailand, Laos, Cambodia and to its delta in Vietnam. The complexity of Mekong delta is ecologically shaped by water of the Mekong River, monsoon climate and tide of the South China Sea (Hans Dieter, E. and Simom, B, 2009). Annually, Mekong River carries 16 million tons of sediment. This sediment transport has created a fertile soil for agriculture production that provides food for approximately 60 million people living in riparian countries (Pham, 2011).

The Mekong River Delta, one of the largest deltas in the world, was formed by the deposition of sediments transported from the Mekong. Mekong delta is defined as a vast triangle plain, beginning at the downstream of Phnom Penh (Cambodia) (Pham, 2011). For two third the Mekong delta is situated in southern Vietnam and for one third in Cambodia. It is one of the most productive and intensively cultivated areas in Vietnam (known as 'Rice basket') and a priority area for economic development (Bucx, T., Marchand, M., Makaske, A., Van de Guchte, C., 2010). The Mekong Delta is a wave- and tide-dominated delta; as a result of meeting of the two branches of the Mekong River.

3.2 Natural landscape

Mekong Delta or "Cuu Long" Delta ("Cuu Long" refers to "Nine Dragon" in Vietnamese) is the region in south-western Vietnam where the Mekong River approaches and empties into the sea through a network of nine estuaries. The natural processes of erosion and sedimentation processes, which are influenced by sea current from both the South China Sea and Gulf of Thailand and annual flood condition, form complexity of the delta. A variety of delta landscape is displayed in this region: river landscape, floodplain and coastal landscape. Each of these natural landscapes is best suited for different land uses, such as: agriculture, recreation and urbanization.

3.3 Formation of infrastructure and occupation layer

Urbanization is the second step forming delta landscapes. *'Building deltaic cities in a manner that accommodates seasonal flooding by primarily urbanizing higher natural levees, leaving low-lying swamps and marshes undeveloped to store water, and strategically perforating riverfront levees balances urban requirements with deltaic processes'* (Campanella, 2010).

The Mekong Delta has only been occupied by the Vietnamese for about three centuries. Nevertheless, this short history has experienced a variety of changing regimes, warfare and revolution (Figure 2):

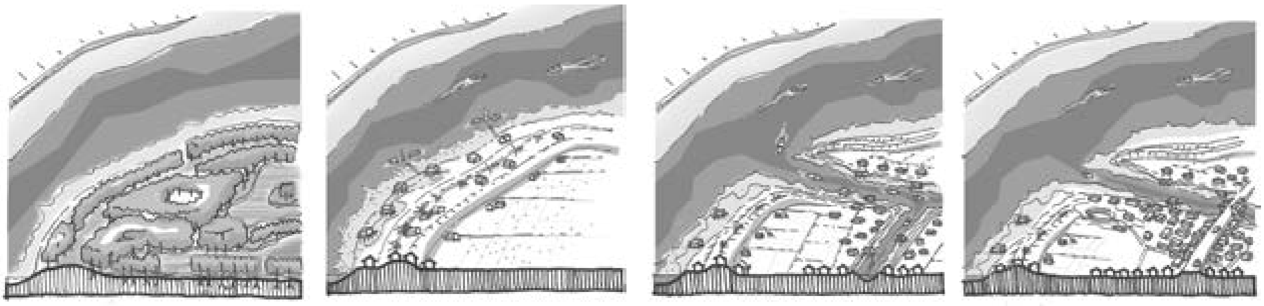

The Holocene landscape	Pre-colonial period	French colonial period	From American war to present

Figure 2. Development of urban pattern in the Mekong Delta

3.3.1 The Holocene landscape as a foundation

The high terraces of Mekong delta is believed to have formed as early as 1 million years ago (Gupta, 2008). The natural processes of sedimentation, change of sea level, tidal and current effects for approximately 8000 years created different delta landscapes in this region (Pham, 2011). According to Milton Osborne, a Southeast Asian historian, the delta was *'a largely waterlogged world of black mud and mangrove trees, bordered by thick tropical forests where the land rose away from the flooded plain'*.

Throughout thousands years, the natural process of sedimentation resulted in 'natural levees' of the river banks and other natural heights like river dunes, sandy ridges and barrier beaches that offered dry and safe land for the first urban settlements (Meyer, H.et al.2009).

3.3.2 Pre-colonial period-Nguyen dynasty (1802-1867): River city

The delta started to form its own landscape since the mid of 16th century when Nguyen Lords introduced a policy of land reclamation and breaking fresh ground to create villages (Pham, 2011). A large amount of inhabitants from the north and centre parts of Vietnam had come and reclaimed new lands. Therefore, the first type of settlement was created: villages around high ground areas along rivers (natural levees) and watercourses where the fresh water could be collected and the settlers could survive from flooding. At the same time, a system of canal and small ditches were built up for transportation and irrigation purposes. This process played an important role in transforming the uncultivated area of the delta into a fertile plain for wet paddy productions.

3.3.3 French colonial period: Canal city

The canalization process were introduced far later in the Mekong delta. Until the 19th century, canal systems were introduced and played a key role in the development of new urban form. Silt from digging these canals created high manmade levees for settlements. In these cities, waterways as rivers and canals were mainly transportation and goods exchanged routes. Moreover, they were also used for irrigation, drainage and fresh water supply purposes. Aware of the changing environment conditions, inhabitants in these cities developed adaptive strategies, often called "shaking hand with floods", that accepted rather than resist the potential catastrophic risk (Miller, 2006). These strategies resulted in a typical delta image with stilt houses, boat houses, floating markets, three sided canoes that are still visible in the current delta cities.

3.3.4 From American war to present: Cross-road city

Starting from the sixties, the system of land-based infrastructure and flood-control became a national concern for economic development. Settlements and cities developed at the meeting points of motor roads and waterways that are high and dry places in times of flooding. The road replaced the water as the domain of city and played a role in the embellishment of the city (Pham, 2011).

After a long history, cities in Mekong delta have always adapted with the dynamic changing environments. These adaptive processes resulted in different types of delta cities: river city, canal city and cross-road city.

3.4 Problems

For three hundred years, the Mekong Delta has become a water society where inhabitants in this region developed adaptive strategies, often called “shaking hand with floods”, that accepted rather than resist the potential catastrophic risk (Miller, 2006). Over twenty years after the introduction of “DOI MOI” policy (innovation), Mekong delta in Vietnam has experienced significant expansion of cities and rapid growth of population. The water cities are transforming into the road cities in which the role of water in the city structure is going to be neglected. Thus, the cities are losing its unique characteristic and inhabitants are facing more vulnerable to flooding. Furthermore, the consequences of human interventions into natural process have caused an essential change in the natural landscape (Meyer, H. and Nijhuis, S., 2011). The transformation from a natural dynamic water system in which people adapted to the forces of nature into an infrastructure system in which the forces of nature are attempted to be controlled, turns out to be more problematic (Figure 3).

Figure 3. Human interventions in the Mekong Delta

Finally, climate change will have a serve impact on the natural system of the delta and in the lives of those living in these areas, namely: flood events, storm surge, water scarcity, subsidence and salinization.

3.5 Can Tho City

Can Tho city is a suitable case to explore because of its experiences in urbanization and flood defense application. Can Tho is the fifth largest city in Vietnam and the largest city is Mekong delta. It is noted for its typical water based landscape with floating markets, rural canals and stilt houses along waterways. The city is located along the Southern benches of Hau River, the southern branch of Mekong River. Because of its advantages, Can Tho is striving to become a city of industry-trade-service and high-tech agriculture. The city maintained an average GDP growth rate of 16% per year for the 2006-2010 periods, and is expected to have a GDP growth rate of 17.1% for the 2011-2015 period and 18% for 2016-2020 period. On the other hand, its population has increased from 180,000 in 1979 (same population as Cao Lanh city nowadays) to approximately 1.2 million in 2011. By 2015, it is forecasted to rise to 1.5 million and 2.1 million in 2030 (Nedeco, 1993).

As the result, Can Tho had to transform to support the increasing population and economic development. City is becoming larger and denser. During 20 years, the urban areas have expanded double in size. The population growth led to the development of unplanned areas in the inner cities. This population movement promoted an increasing of risky settlements located on lands sensitive to flooding.

Historically, the system of canals inside the city worked as a sewage system that helps to drain off floodwater quickly to the rivers and store rainwater to other uses. This system, however, did not work anymore in the dense urban areas. Many of the waterways were polluted and cause health's problems. They were filled and replaced by underground drainage system that is not sufficient for the high rainfall in Mekong delta. As the consequence, in 2006 rainy season, more than 80 percent of the city was flooded, water level reached to 0.5 meters. The historic flood of 2000, in particular, destroyed many rice crops, aquaculture farms, housing and other infrastructure in the flooded areas. The local government's response to this disaster was to build a dyke system which should prevent such negative impacts and after 2004, dykes were constructed throughout the province. Although the new dyke system helped to reduce flood damages in whole of Can Tho city and the lower flooding areas such as Kien Giang, Hau Giang, Soc Trang, Tra Vinh provinces and secure agriculture in the flood protected areas, it also has disadvantages to other areas in various ways. It is one of the main causes leading to erosion, plant diseases, soil fertility decline and natural degradation in the protected flooding areas of the Mekong Delta (Tran Nhu Hoi 2005; Duong Van Nha 2006; Sarkkula et al 2008). Other negative impacts are changes in flow velocity and annual flooding levels with negative effects in both protected and non-protected flooding areas. Especially the high dyke system obstructs the fine-sediment flow into agricultural lands that causes a big conflict between Can Tho City with the whole region.

These consequences are not only coming from unstable urban development strategy or insufficient water management, but also from the lack of the integration between these two disciplines. Without interventions, other delta cities in Mekong Delta are predicted to develop in the same way and experience the same problems as Can Tho City does in recent years. Despite new techniques, however, the question then remains: *How to integrate urban planning and water management in the Mekong Delta?*

4. LESSONS LEARNT FROM THE NETHERLANDS

Today, most delta areas in the world are dealing with the increasing complexity and changing dynamics, because of two reasons: first, the changes in the natural dynamics of the delta due to climate change and human interventions, and second, the changes in the dynamics of land-use, dominated by urbanization, industrialization, port-development, agriculture and leisure/tourism (Meyer, H. and Nijhuis, S., 2011). Traditional approaches "protecting against flooding" or "building in nature" have not only separated nature from human and their urban development, but also damaged damaging to the nature system and human civilization. Therefore, these damage forces people to take a step back rethink about the problem, about their relationship with nature and understand intensely the natural landscape before impacting nature. ‘Man and nature are indivisible, and our survival and health are contingent upon an understanding of nature and processes’ (McHarg, 1969, p.27).

In the Netherlands, numerous long term planning studies and policies have been implemented. The new approach is no longer about “protecting against flooding” but instead respecting it and giving space for water and its natural landscape. Based on a clear understanding of the delta system, the Dutch attempt to plan their future with natural landscape, creating both healthy ecosystems and a safe country.

4.1 Room for the river

The process of urbanization in the Netherlands started from the 11th century that was based on agricultural exploitation of fertile soils. The Dutch landscape was soon transformed from a natural swamp of peat and clay into a number of “polders” surrounded by dikes and drained by a system of ditches, canals and locks (Meyer, H. and Nijhuis, S., 2011). Cities in these polders grew from the agricultural markets to the centres of regulation for the polder’s water system (Burke, 1960).

After disaster in 1953, the Delta committee was recognized to explore the cause of floods and asked to formulate an alternative approach on flood management in the Netherlands. A new flood control approach was constructed to design the flood defense system including: dams, sluices, locks, dikes, levees and storm surge barriers. Nowadays, the flood prone parts of the country are protected by more than 50 dike rings.

However, throughout a thousand years of protecting against flood, space for the rivers has become only more limited. Drivers of change put greater threats on the development of the country. So to make the Netherlands a safe, comfortable and pleasant place to live, trend has to be reversed. The answer lies in the plan to make more room for the river. As the Spatial Planning Key Decision, “Rooms for the River” (Ruimte voor de Rivier 2007) policy was proved by Dutch government in 2007. The policy outlines numerous designs to provide more space for the river and lower high water levels (Figure 4). These designs present an integrated spatial planning with the main objectives of flood protection, master landscaping and the improvement of overall environmental conditions.

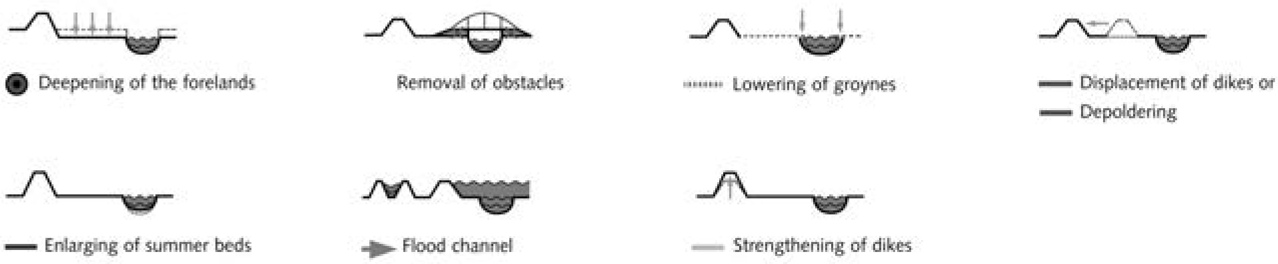

Figure 4. Measures of policy “Room for the River”

4.2. Multi-layer safety

Recent floods in Europe and hurricane Katrina have made the Dutch government realize that flood protection policy should be wider in scope than just prevention of floods. Therefore, in 2008, the Dutch Government developed a sustainable approach, multi-layer safety, that consists of three different layers. The first layer is about flood prevention with strong dikes, dunes and storm flood barriers. The second layer is sustainable, water proof and spatial planning. This layer aims at reducing victims and limiting the damage from possible flooding. The third layer is crisis management in case of flooding (Figure 5).

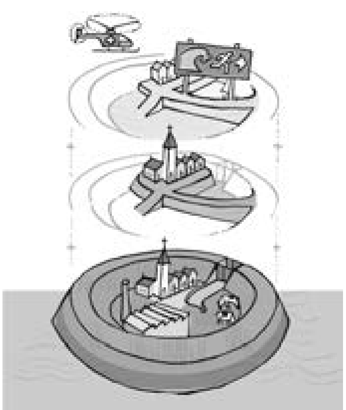

Figure 5. Model of multi-layer safety

While old policy was just based on prevention, the concept of multi-layer safety creates a more complex environment for flood protection. It requires the balance of roles and responsibilities of public authorities, private institutions and citizens. Thus, the effectiveness of appling this concept and the roles of different actors in this, have to be discovered in order to decide whether and how muliti-layer safety can be organized, coordinated and institutionalized (van den Heuvel, J. , Roovers, G.J. , Eijer,M.M).

5. CONCLUSION AND RECOMMENDATIONS

The Mekong Delta today is a product of different engineering decisions throughout three hundred year history. On one hand, agricultural production has developed successfully, and economic growth and urbanization has been very rapid. On the other hand, intensifying agriculture and large scale water control structures have challenged the natural landscape and social equity (Käkönen, 2008). The proposed strategy needs to create a new balance between safety, spatial quality, natural preservation and economic values that will benefit in all local, regional and international scales.

Achievements from “Room for the river” and “Multi-layer safety” in the Netherlands have marked a dramatic change in policy and thinking about water management. It showed that the protection paradigm has changed from “protecting against flooding” to “living with flooding” and towards a tendency of integrating water management and spatial planning. It can be seen as a suitable strategy to apply in the case of the Mekong Delta because:

- Indeed, water as the basic element in nature landscape of the delta, have become an indispensable element in the development of urban delta. The new strategy for the Mekong Delta requires a sustainable water management that can provide a sustainable use of floodwater, groundwater, surface water, waste water and drinking water. This water management combining with the green spaces, such as: parks and pedestrian paths functions as an attractive place for social interaction.

- Infrastructure layer as the middle layer connecting nature and urban landscape has achieved a lot of successes in creating safe conditions for human activities and urban development. Innovative infrastructure can design with more than just one purpose, that is aligned with natural process rather than traditionally working against them and that is adaptive to cope with changing conditions, such as: climate change and sea level rise (De Vriend, H.J. and Van Koningsveld, M., 2012). Especially when used in combination with the traditional approach, the new infrastructure system can lead to cheaper, more economic potential and more aesthetically appealing solutions.

- As a developing country, Vietnamese economy cannot support for large scale infrastructure and high cost flood control project. Using natural processes of the delta can help to make flood risk management more sustainable and cost-effective than hard, engineered defenses. As Ian Mcharg argued each of the natural landscapes is best suited for different land uses, spatial planning can work in a way that flood resistance zone, buffer zones and flood hazards zones are identified. For example, flood resistance zones are suitable for urban development, while in the buffer zones, space for future defense measures is reserved, other economic and recreation activities such as: ports, beaches and national park might be possible.

- In recent years, Vietnamese government has built many residential clusters and encouraged people to migrate to safer locations in order to avoid flood damages. However, this strategy received little attentions of the farmers who do not want to leave their farms. Therefore, the new strategy has to take into account providing inhabitants a safe and attractive living and working environment. It is targeted at different actors: government, developers, business owners, inhabitants…etc.

REFERENCES

Bucx, T., Marchand, M., Makaske, A., Van de Guchte, C. (2009). Comparative assessment of the vulnerability and resilience of 10 deltas– synthesis report. *Aquaterra 2009.* Amsterdam: Delta Alliance.

Campanella, R. (2010). Delta Urbanism: Lessons from New Orleans. In *New Orleans: New Orleans* (pp. 181-186). New Orleans: Amer Planning Assn.

De Vriend, H.J. and Van Koningsveld, M. (2012). *Building with nature: Thinking, acting and interacting differently*. Dordrecht, the Netherlands: EcoShape, Building with nature.

Gupta, A. (2008). The Mekong River: Morphology, Evolution, Management. In A. Gupta, *Large Rivers: Geomorphology and Management.* John Wiley & Sons Ltd.

Hans Dieter, E. and Simom, B. (2009). *Strategic group formation in the Mekong delta: the development of modern hydraulic society*. WISDOM, Department of Political and Cultural Change. Bonn: WISDOM.

McHarg. (1969). *Design with Nature.* New York: The Natural History Press .

Meyer, H. and Nijhuis, S. (2011). *Towards a typology of urbanizing deltas.* Department of Urbanism, Faculty of Architecture Delft University of Technology.

Meyer, H., Nijhuis, S., Pouderoijen, MT. (2009). A Tale of Two Urbanized Areas. In V. M. Meyer, *Dutch Dialogues: New Orleans-Netherlands. Common Challenges in Urbanized Deltas.* Amsterdam: SUN Publishers.

Miller, F. (2006). Environmental risk in water resource management in the Mekong Delta: a multiscale analysis. In T. a. Tvedt, *A history of water*. New York: I.B.Tauris.

MRC. (2010). *State of the Basin report.* Mekong River Commission. Vientiane, Laos: MRC.

Nedeco. (1993). *Master plan for the mekong delta in Vietnam: A perspective development of land and water resources.* Ho CHi Minh City, Vietnam: GOV.

Nienhuis, P. (2008). An ecological story on evolving human environmental relations coping with climate change and sea-level rise. In *Environmental history of the Rhine-Meuse Delta* (p. 550). Springer Verlag.

Pham, D. (2011). *Urbanized Mekong delta: A dialogue between water and land.*

Shannon, K. (2009). Landscape as Urban Structure: the Case of Cantho, Vietnam. In L. L. SCHWAB, *Landscape-Great Idea.* Vienna: ILA - Institute of Landscape Architecture.

Tayler, P. (2006). River into Roads: the terrestrialisation of a South - east Asian River Delta. In M. &. LEYBOURNE, *Water: histories, cultures, ecologies.* Melbourne: University of Western Australia Press.

UN-Habitat. (2006). *State of the Worlds Cities 2006/7:The Millennium Development Goals and Urban Sustainability: 30 Years of Shaping the Habita tAgenda*. Nairobi.

USDA. (2011). *United States Department of Agriculture*. Retrieved 2012, from http://www.usda.gov: http://www.usda.gov/wps/portal/usda/usdahome van den Heuvel, J. , Roovers, G.J. , Eijer,M.M. (n.d.). *Multi-layer cooperation in flood management: How to cooperate within flood management in public area's.*

Analysis on influencing factors of community participation in disaster countermeasures regarding land subsidence and climate change case study: North Jakarta (Indonesia) and Shinkoiwa Community, Katsushika City, Tokyo (Japan)

Maria Bernadet Karina Dewi [1], Takaaki KATO [2]
[1] Graduate student, ICUS, IIS, The University of Tokyo, Japan
dewi@iis.u-tokyo.ac.jp
[2]Associate Professor, ICUS, IIS, The University of Tokyo, Japan
kato-t@iis.u-tokyo.ac.jp

ABSTRACT

Both Shinkoiwa in Katsushika City and North of Jakarta have been facing land subsidence. Year by year the subsidence rate is increasing. Moreover, by the sea level projection as an impact of climate change, flood risk will be higher. Flood countermeasures should be approached not only by structural mitigation, but also social adaptation which involves community. Those can be implemented through preparedness and response activities. This paper aimed to analyze the required condition for successful process, and to find additional required condition for community based activity in disaster countermeasures. With case study of Shinkoiwa community in emerging community participation by experts and NPO, and community disaster risk reduction in Jakarta supported by NGO and professional urban planners group.

This paper analyzed the
Keywords: *climate change, land subsidence, community participation, support system*

1. INTRODUCTION

Land subsidence and climate risk are the background of this study. One impact of climate change is the rising sea level, which means increasing the inundation area of flood. Land subsidence will make the climate risk higher. Therefore, we need to adapt to climate change, including various layer and approach, from the policy making to the community based. Focus of this study is in adaptation measures in community based. As climate change continue gradually, adaptation measures needs continuity or sustainability.

This research aimed to understand the hazard and risk and its community participation for countermeasures, to clarify the required condition for successful process, and to find additional required condition.

2. BACKGROUND OF SHINKOIWA AND NORTH JAKARTA

The land subsidence rate in Jakarta is -0.5 to -17 cm/year, and in Shinkoiwa is -4 m in total. Climate projection for sea level rise is 0.35 m or 0.23 to 0.47 m per 100 years. (IPCC, 2007). It will increase the inundation level of flood. The 5 research areas have emerging community-based activity for flood countermeasures. There are 3 areas in North Jakarta supported by Indonesia Red Cross from 2007 to 2010, which are Muara Angke, Muara Baru, and Marunda; 1 area has been supported by Indonesia Association of Planners from 2012 to present named Kamal Muara (Refer to Figure 3). And the area in Shinkoiwa has been supported by experts and NPO A! Safety and Amenity Machidzukuri from 2006 to present.

2.1 Background of Shinkoiwa situation

Figure 1: Below sea-level area in Tokyo
(Kato, 2011)

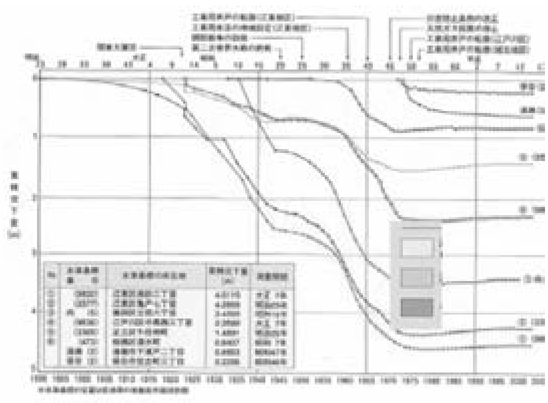

Figure 2: Ground subsidence due to industrialization
(Kato, 2011)

Katsushika city is located on the eastern part of Tokyo. With its below sea level geographic location, it has 31.5 km2 area under low tide sea level, 124.3 km2 area under high tide sea level (Kato, 2010). To control the tidal flood, several mitigation efforts have been done, such as super-high embankment constructed along urban river (MLIT, 2006). Local government has also established flood hazard map on the Arakawa River in 2007 (Katsushika City, 2007 in Kato, 2011). However, many countermeasures need to be taken into account, such as more evacuation space, and the mitigation during flood occurrence. Land subsidence has started since 1909, and became apparent from 1945 to 1958. It was caused by industrialization. The total subsidence is 4 meter.

Figure 3: The water level in Shinkoiwa, Katsushika City in case of flood (Kato, 2011)

2.2 Background of North Jakarta situation

The current situation of land subsidence in Jakarta has been increasing. As a metropolitan city located in the urban area, its urbanization contributes into ground water extraction. The groundwater extraction leads into increasing flood catchment area. The mitigation and preparedness activity itself is not enough. Utilizing community activity will give significant contribution towards disaster preparedness countermeasures. During 1982-1987, the subsidence was from 20 to 200 cm in several points in Jakarta (Abidin, et.al, 2009). And though GPS observation, in June 1997, there has been 7.5 cm to 32.8 cm subsidence within 4 years, depends on the local area where the points of measurement were located (Djaja, et.al, 2004). Generally, there has been approximate subsidence level of 1 to 15 cm per year, whereas in several locations reached 20-25 cm per year (Abidin, et.al, 2009).

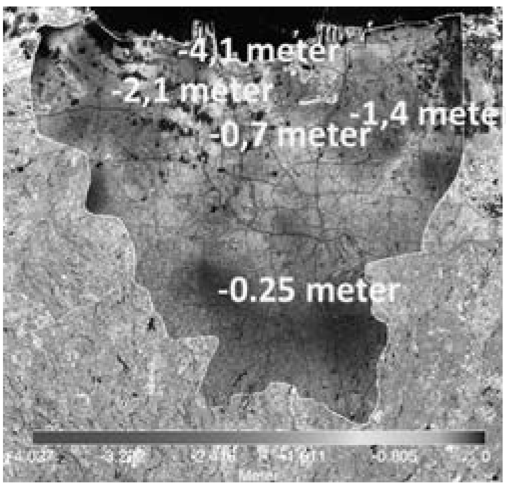

Figure 4: Subsidence map of Jakarta 1974-2010 by GPS:
Total subsidence -25 up to -400 cm ; rate -0.5 up to -17 cm/year (Andreas, et al, 2011)

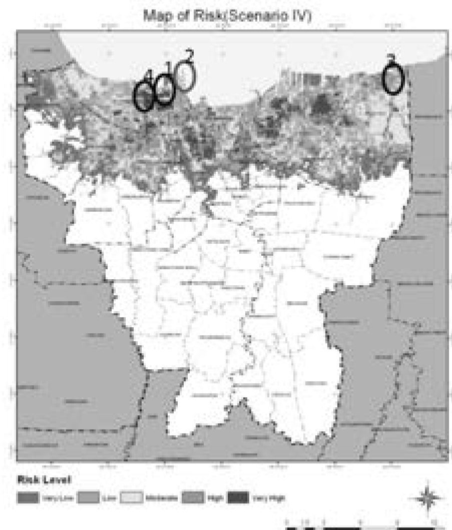

Figure 5: Simulation of flood considering the factors of tides, sea level rise, land subsidence, ENSO, and storm surge/tidal flood & exposure (Hadi, 2012)

Based on Andreas, et al (2011), due to land subsidence in the year 2010, there was 10.26% (66.355 x 106 m2) of Jakarta area below the sea level. This was following as before 1990, there was none of the area below sea level. And based on his prediction, in the year 2030, there will be 131.914 x 106 m2 or 20.41% of area will be located below sea level. A simulation consists of hazard elements such as tides (0.62), sea level rise (0.0057), land subsidence (0.001-0.035), ENSO (0.15), and storm surge (2.5) (Hadi, 2012). The worst case is predicted to occur on the northern part too, indicated by red and orange colour in figure 5.

3. FIELD INVESTIGATION

Field investigation in Shinkoiwa, Katsushika City was done through interview to the urban planning experts and participation in community activities towards disaster preparedness from November 2011 until April 2013. Field survey in North Jakarta was done in January and March 2013, covering the 4 area. It was done by interview to the support groups, community leaders, community members, and volunteers; also by participation in field investigation and survey by support group members in order to find flood evidence and infrastructure survey.

Training of using boat for evacuation (12-03-2012, 09-09-12)

Steering committee meeting for evacuation shelter (Nov 2012, Feb 2012)

Workshop of Tenzai Manabu-kun application to understand the flood risk (Mar 2013)

Figure 6: Field survey in Shinkoiwa (2011-2013)

Tidal flood due to improper sewage facilities

One of the reconstructed pump house

One of the water gate in Muara Angke

Inside the dike, people feel safe and not considering the risk they have.

A three storeys public facilities building which can be used for evacuation

Fish market as a significant economic activity of the local residents

Two storey houses

Neighbourhood union office where the second floor is used for evacuation

Figure 7: Field visit in North Jakarta (Muara Angke and Muara Baru), 2013

Field investigation was aimed to get the risk-hazard by community, and the countermeasures done by community, and the scheme and process of community based activity towards disaster countermeasures. The current hazard in North Jakarta is flood, caused by tide and rainfall, and in Shinkoiwa is flood and earthquake.

Support system by Red Cross to Muara Angke, Muara Baru, and Marunda was done in 2007 to 2010, with the activity as workshop, survey, disaster response and adaptation, and information dissemination. The objective of the support system is to achieve disaster preparedness and mitigation skills for community, and to have network amongst them for disaster response. Support system by Association of planners to Kamal Muara has been done in 2012 until present, within the activities of workshop, meetings survey, and technical support. The objective is to find current problem of hazard, propose guideline for better and safer neighbourhood, and empower community for disaster preparedness and response. Support by experts and NPO A! Safety and Amenity Machidzukuri has been done in 2006 until present, through workshops, stakeholders meeting, and disaster mitigation simulation. The objective is to understand the risk of natural hazard, get important key persons, and enabling sustainability of the activity.

4. ANALYSIS

The required condition for successful process has 3 findings:

First, focusing on definition of success by stakeholders (community leaders and support group) and the program achievement, all cases are successful. But considering the aspect of sustainability, 3 cases are successful: Muara Baru, Shinkoiwa, and Kamal Muara; and 2 unsuccessful cases: Muara Angke and Marunda. For the unsuccessful case, eventhough community has already understand the risk, but they feel that they have no risk at all, they began to think their ideal situation and do not have attention on disaster preparedness activities. In general for all case studies, the definition of successful is when community understand the risk, able to do the countermeasures, able to continue their effort, and able to make the effort sustainable for the future and attracts more participants.

Success is related with sustainability, because of the climate change and land subsidence risk. Climate change will give the risk of sea level rise. For example, as predicted by the IPCC, the prediction of sea level rate 2 mm/year in Jakarta (IPCC, 2007). With the continuing climate risk, the sea level rise will also higher. It is also influenced by the land subsidence level which is higher from time to time. While in period of 2010-2030 Heri predicted that with assumption of linear trend, no act on stopping ground water extraction, another addition maximum is -2.6 meter subsidence might happened in north of Jakarta (Heri, 2012). By increasing land subsidence and climate risk, the continuity of community participation is needed to tackle with the future disaster.

Area	Definition of success by support group	Definition of success by community leader	Achievement
Muara Angke and Marunda	- Coordination network for disaster response - Able to reduce the risk - Care about environment - Elementary school involves	-Understand when disaster happens - Emergency response - Evacuation route & evacuation space	-Understand when disaster happens - No continuity since 2010 - E. school involves
Muara Baru	- Coordination network for disaster response - Able to reduce the risk - Care about environment - Elementary school involves	-Evacuation route - Actively involved in disaster prevention - Report & voluntary work for damage of infra.	-Understand when disaster happens - Continue the efforts until present situation - E. school involves
Kamal Muara	-Propose the gov't for infrastructure project - 100% ideas from comm. - Creates adaptation plan as flood countermeasures	- When IAP can implement the ideas of community	-Aware of climate change - Can propose in the sub-district discussion - Aware on how to achieve their goal - Think abt. role sharing
Shinkoiwa	-Understand the risk of natural hazard - Get important key persons - Sustainability of the activity	-Sustainability of activity - Succeed to next generation - Get output of activity	-Understand the risk - Important key persons - Disaster response and evacuation drill - Many stakeholders and emerging young people

Table 1: Success definition and achieved goals

Support groups consists of several types, such as non-government organizations (NGOs), professional groups, and non-profit organizations (NPOs). They approach the community, who already has their own characteristics, history, and local knowledge. Those communities has been facing the risk and hazard by time. Thus the communities has its own countermeasures. The involvement of support agency into this system creates a new support approach and process, and renewed countermeasures.

Second, in order to be successful, this kind of process will be required: 1) Someone from the outside must inspire the community, 2) After inspiration from outside, keypersons emerge from inside, 3) Community starts to understand the natural hazard/risk precisely, 4) They need support system from outside, 5) Community starts to involve many people in the neighbourhood, and 6) Community starts to make the activity sustainable. Those 6 factors was obtained from the analysis in process of 4 cases.

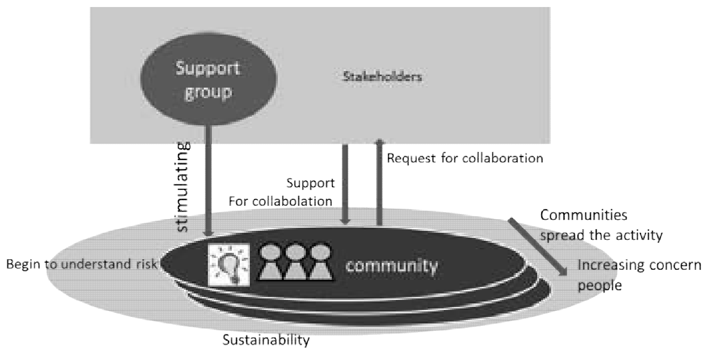

Figure 8: The six steps of successful process of community participation for disaster countermeasures

Third, analysis on timeline of support group corresponding to the factors of successful process. All 5 case studies corresponds to the six factors of success as shown by the graph below.

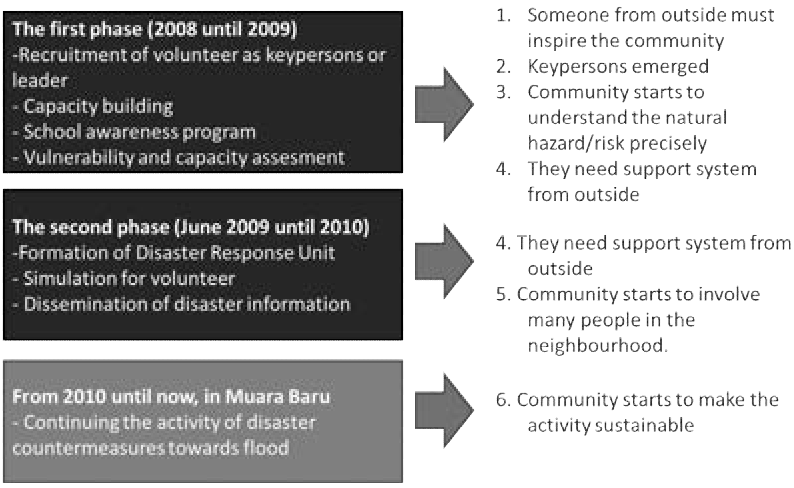

Figure 9a: Support by Indonesia Red Cross to Muara Angke, Muara Baru, and Marunda corresponds to the 6 factors of successful process

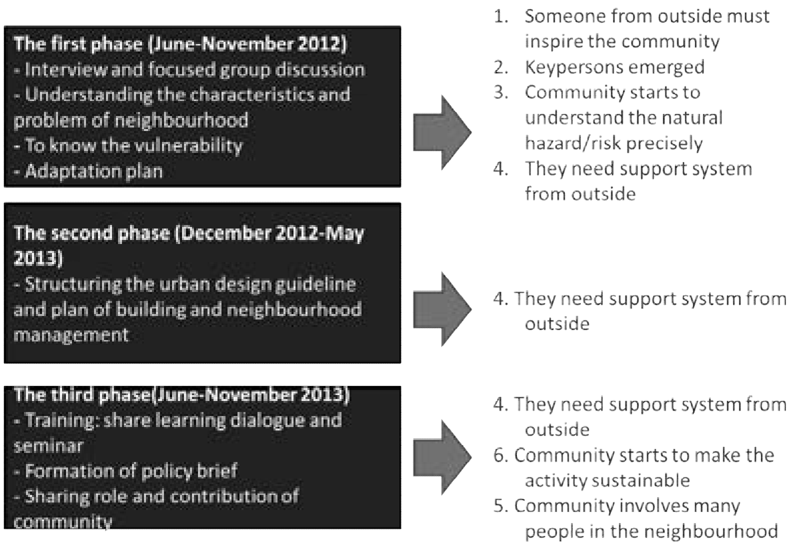

Figure 9b: Support by Indonesia Association of Planners to Kamal Muara community corresponds to the 6 factors of successful process

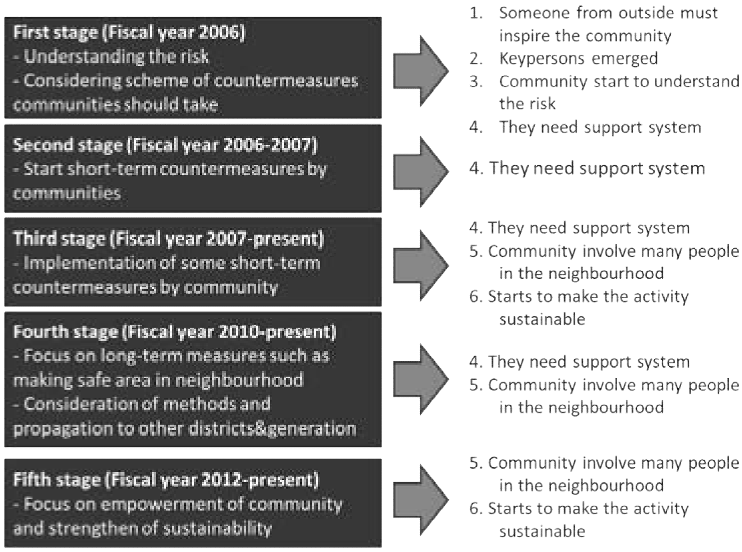

Figure 9c: Support by experts and NPO A! Safety and Machidzukuri to Shinkoiwa Community corresponds to the 6 factors of successful process

The additional required condition for successful process has 2 findings:
First, both physical and social countermeasures are influencing each other. Strong social countermeasures tend to make the community have stronger physical countermeasures. Somehow, it will make people feel safe, thus they have less activity on social countermeasures. So it is the space where support group can have role whether it will strengthen the social of physical countermeasures, by looking at the community characteristics and risk-hazard.

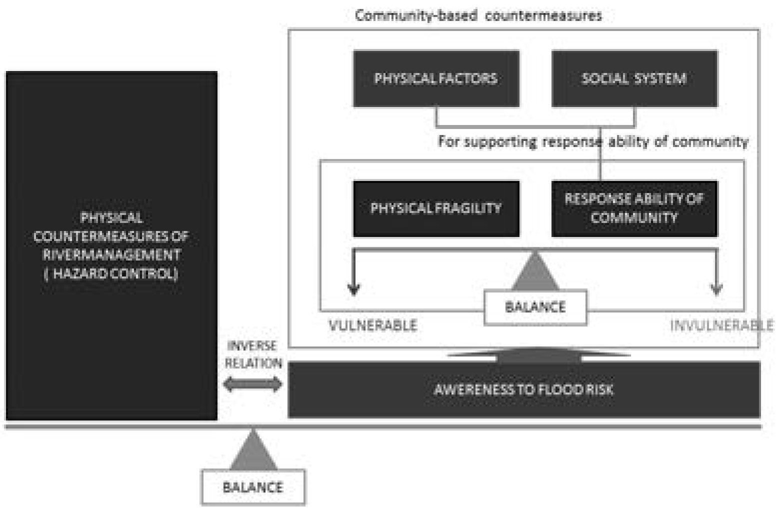

Figure 10: Balance of physical and social countermeasures

There are two kinds of countermeasures, which are hazard control and awareness to flood risk. Hazard control corresponds to physical facilities to control hazard, such as dike and sewer facilities. This kind of physical countermeasures makes the frequency of flood reduce, while at the same time it can make the awareness of citizen to flood risk decrease. Countermeasures in community level have two aspects, physical and social aspects. In social aspect it means that countermeasures related to organizational or planning matters such as disaster response plan and evacuation plan, and social system for confirmation of the safety by community members. Physical factors is one to support social system in a community such as construction of evacuation road and evacuation site. This kind of physical factors makes social system effective or should be combined with social system.

Balance between physical and social countermeasures is important to encourage people preparedness towards hazard, and because both physical and social countermeasures are influencing each other.

Second, the use of indigenous and local knowledge. As Shaw explained, due to exposure and proximity to hazardous conditions, a local population responds first even before assistance from aid-givers arrives at time of crisis (Shaw, 2012). Based on his explanation, there are several terminologies of indigenous and local knowledge, and the writer used in this is indigenous technical knowledge and community-based knowledge. Shaw said that indigenous technical knowledge is more framed on a technological perpective. It is related with traditional technical culture. In the case study, the technical knowledge can be indicated by the two storey houses of Bugis ethnic people who live in Kamal Muara, also *mizuya* house and in Shinkoiwa case study.

In Kamal Muara, there are only 10% of total are the traditional two storey wooden houses by newcomers from Bugis ethnic. This kind of house is adopted from people who are living in coastal area, thus it is responsive to flood. In Shinkoiwa there are *mizuya*, which means traditional 2 storey annex to a house which is located on elevated land. Basically people live on the first floor of main house. As it is built on the elevated land, the first floor can be protected against small flood. This type of houses only a few existing in Shinkoiwa. Because of modernization, this housing type was demolished. Then they changed for wooden and concrete houses.

Figure 11a: Traditional two storeys wooden houses by Bugis ethnic people in Kamal Muara

Figure 11a: *Mizuya* in Shinkoiwa

The community-based knowledge is explained as the knowledge that community get by interaction with other community members. This can be indicated by the heightening level of the house and the furniture for the community in North Jakarta. Therefore, all stakeholders should consider the advantage of indigenous and local knowledge in flood adaptation.

5. CONCLUSION

The required condition for successful process has 3 findings. First, focusing on definition of success by stakeholders (community leaders and support group) and the program achievement, all cases are successful. But considering the aspect of sustainability, 3 cases are successful: Muara Baru, Shinkoiwa, and Kamal Muara; and 2 unsuccessful cases: Muara Angke and Marunda. Second, in order to be successful, this kind of process will be required: 1) Someone from outside must inspire the community, 2) After inspiration from outside, keypersons emerge from inside, 3) Community starts to understand the natural hazard/risk precisely, 4) They need support system from outside, 5) Community starts to involve many people in the neighbourhood, and 6) Community starts to make the activity sustainable. Third, the timeline of support system corresponds to the 6 factors of successful community participation process, although all cases have different activities and approach.

The additional required condition has 2 findings. First, social and physical countermeasures are influencing each other, and should be in balance. Second, Community use the indigenous and local knowledge such as traditional housing in Kamal Muara and traditional structure called mizuya in Shinkoiwa. In community-based activity, stakeholders have to consider the advantage of indigenous and local knowledge.

REFERENCES

Abidin, et.al. (2009). *Land Subsidence and Urban Development in Jakarta (Indonesia)*

Andreas, et.al. (2011). *Jakarta Subsidence: More Info.* Jakarta Coastal Defense Strategy (JDCS) Study Team. Institute of Technology Bandung and Deltares-Delft Hydraulic. Second Atlas Workshop JDCS June 28th 2011.

Djaja, et.al. (2004). *Land Subsidence of Jakarta Metropolitan Area*

Hadi, Safwan. (2012). *Pemetaan Risiko sebagai Dasar Penanganan Dampak Perubahan Iklim di Kawasan Pesisir. Studi Kasus DKI-Jakarta*

Intergovernmental Panel on Climate Change (IPCC). (1997). *IPCC Fourth Assessment Report: Climate Change 2007.* http://www.ipcc.ch

Kato, Takaaki. (2011). *The Community-based Planning and Consideration of Countermeasures through Workshop in "Below-sea-level city" against Forthcoming Flood Disasters – Case in Katsushika City in Tokyo.* ICUS. Institute of Industrial Science, the University of Tokyo.

Ministry of Land , Infrastructure and Tranport (MLIT), Arakawa-Karyu River Office. (2006). *The Arakawa: River of the Metropolis – A comprehensive guide to the lower Arakawa.*

Shaw, Rajib. 2012. *Community, Environment and Disaster Risk Management Volume 10- Community-Based Disaster Risk Reduction.* Bingley: Emerald Group Publishing Limited.

Assessment of multi-hazard risk in mega cities in Japan

Tomofumi IKENAGA[1], and Miho OHARA[2]
[1] Undergraduate Student, Department of Civil Eng.,
The University of Tokyo, Japan
ikenaga@iis.u-tokyo.ac.jp
[2] Associate Professor International Center for Urban Safety Engineering (ICUS),
Institute of Industrial Science, The University of Tokyo, Japan

ABSTRACT

The 2011 Great East Japan Earthquake was historically huge disaster in Japan. However, it should not be overlooked that the possibility of such a big disaster was much lower than that of other disasters, which would cause less but still serious effect. This earthquake also taught us the necessity of considering various risk of natural hazards in addition to single hazard. It is necessary to identify where safer lands are considering multi-hazard risk and to plan better use of these safer lands.

This paper aims to integrate the risk of various disasters such as flood or landslide, earthquake disasters, etc. and analyze regional multi-hazard risk in mega cities in Japan. Moreover, the number of people exposed to the multi-hazard risk was analyzed. At first, existing hazard maps for various kinds of natural hazards were collected and overlaid on GIS database. As a result, the areas with or without hazards were identified. The correlation among different types of natural hazard in mega city was also analyzed. Then, the population who exposed to single or several hazards in mega city was assessed and regional vulnerability was evaluated. The land with no disaster risk should be recommended to be developed more in the future. On the other hand, in the area with high risk of several disasters, countermeasures just considering single kind of disaster are not sufficient, but considering complex disasters are necessary.

Keywords: *multi-hazard risk, population exposure, hazard map*

1. INTRODUCTION

The 2011 Great East Japan Earthquake was historically huge disaster in Japan. This earthquake taught us the importance of taking prepared measures for tsunami such as regular evacuation drills. But this does not just mean that the measures for tsunami are the most important than others. In spite of the big economic loss in the affected areas, some disasters have not got much attention specially if there are few deaths. In 2013 Japan had much longer rainy season in early summer. This abnormal weather caused unprecedented heavy rain bringing serious damage in some region, especially in Shimane and Yamaguchi. Fortunately this series of calamity did not kill many people, but it also shows the threat of strong rain in mega cities seems to be paid less attention than that of earthquake or tsunami. There are various kinds of natural disasters, and what is the important thing is to make fair comparison of these risks to formulate the best strategies for multi-hazard risk of disasters. Emotional anxiety about big disasters should not bring excessive investments for a particular hazard and cause lack of measures for another hazard, which does not attract much attention from society but probably cause serious damage.

The 2011 Great East Japan Earthquake also taught us the necessity of considering various risk of natural hazards in addition to single hazard. Many people living near the sea were killed by the tsunami regardless of the eagerness to decrease the risk of earthquake. It is necessary to identify where safer lands are considering multi-hazard risk and to plan better use of these safer lands.

This paper aims to integrate the risk of various disasters such as flood or landslide, earthquake disasters, and analyze regional multi-hazard risk of Japanese land. The correlation among different types of natural hazard in mega city was also analyzed. Then, the population who exposed to single or several hazards in mega city was assessed and regional vulnerability was evaluated.

2. METHODOLOGY

2.1 The definition of the risk area

In this paper, the risk area of single hazard is defined as follows. If the J-SHIS (Japan Seismic Hazard Information Station) suggests that the big earthquake which comes approximately once in one hundred years causes an earthquake with a seismic intensity of a lower 5 or greater on JMA scale, such area is regarded as the risk area of earthquake. And the risk area of inundation by river water and landslide is determined based on the hazard map published by prefectures or MLIT (Ministry of Land, Infrastructure, Transport and Tourism). The multi-hazard area is the area that has overlap of two or three dangerous areas. The risks of inundation inside a levee, high tides, tsunami, and volcanic eruption are not considered because of the difficulty on getting hazard maps in digital format.

2.2 Risk assessment

At first, existing hazard maps for various kinds of natural hazards were collected and overlaid on GIS database. As a result, the areas with or without hazards were identified. Then the risk of single or several hazards was assessed by calculating the size of risk area in each mega city and the population exposure, that is, the number of people living in there. The size was calculated by geometric operation, one of the functions of Arc GIS. In the evaluation of the population exposure, 1 kilometer mesh data of population in 2005 was used. With regard to each mesh, the size of the areas with hazards and the population exposure was assessed as follows (equation 1). Population exposure to hazards is calculated based on the ratio of risk area over total mesh area and the total population in the mesh.

$$P_h = P \times S_h / S \quad (1)$$

P_h: Population exposure in the mesh

P: All population in the mesh
S_h: Size of area with hazards in the mesh
S: Size of the mesh

After figuring out the size and population exposure of hazardous areas, mutual correlation between these two factors was depicted with a graph. If many people live densely in the area with several high risks, the area seems to have especially high vulnerability to natural disasters.

3. RESULTS

The risk was assessed in the three mega cities in Japan, Tokyo, Aichi, and Osaka. These cities are located in eastern, middle, and western area of Japan, and they have 13 million, 7.2 million, and 8.8 million people, respectively. There are 30 million people, a quarter of all population in Japan, in these three mega cities although their size is just 3% of the country. The results of overlaying hazard maps are shown in figures 1, 3 and 5. And figures 2, 4 and 6 show the rate of risk area to the whole prefectural area in terms of size and population.

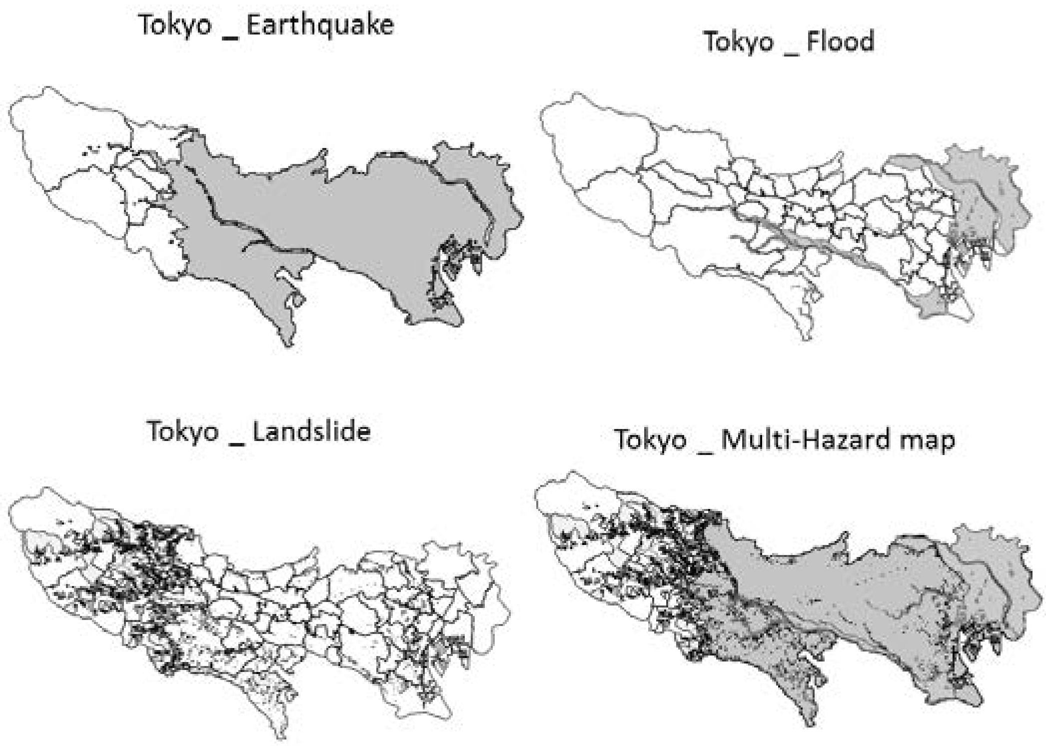

Figure 1: Hazard maps of Tokyo

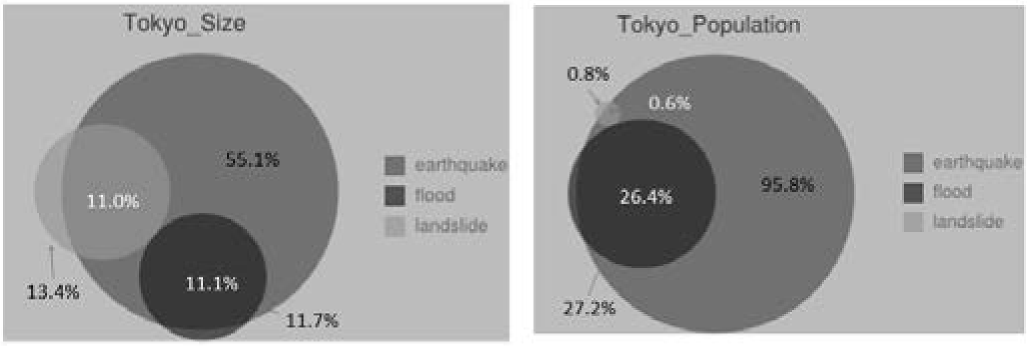

Figure 2: the rate of risk area in Tokyo

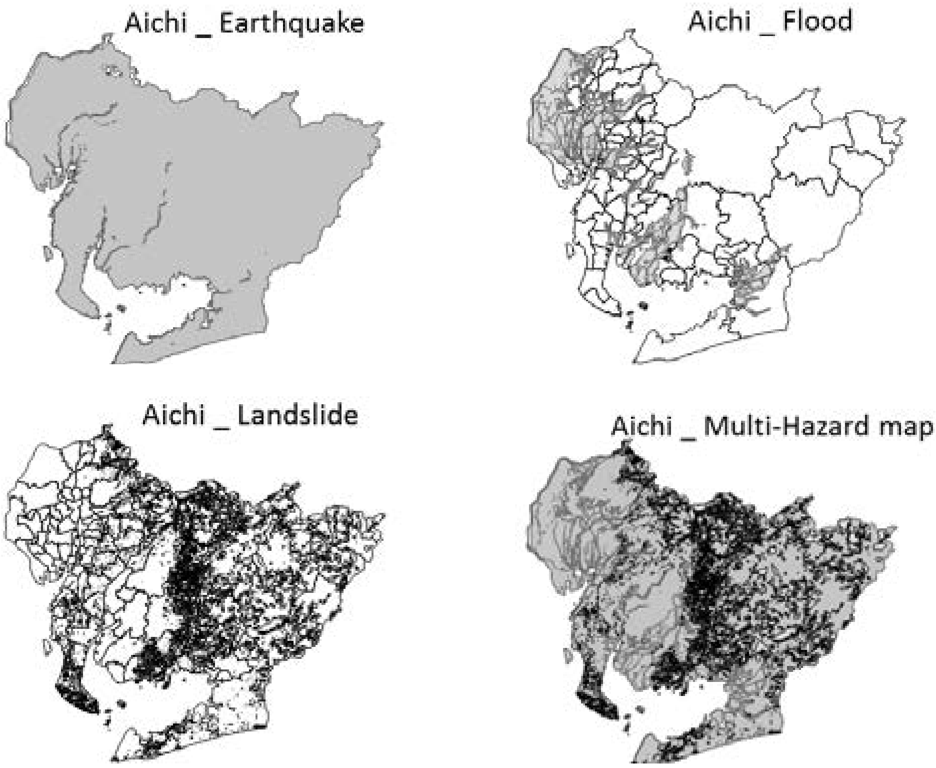

Figure 3: Hazard map of Aichi

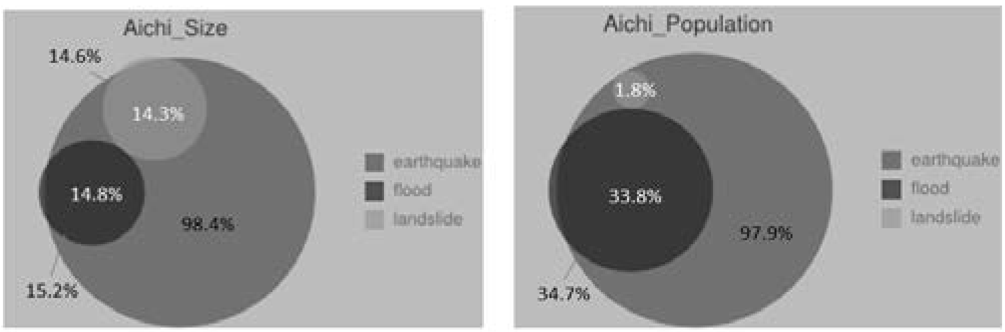

Figure 4: The rate of risk area in Aichi

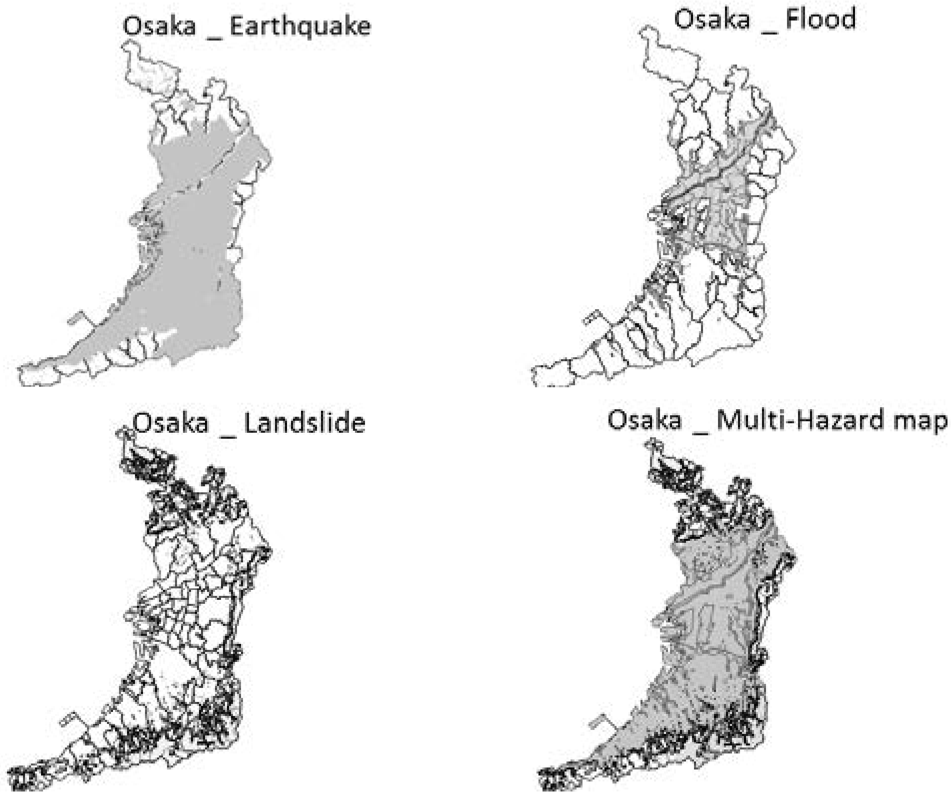

Figure 5: Hazard maps of Osaka

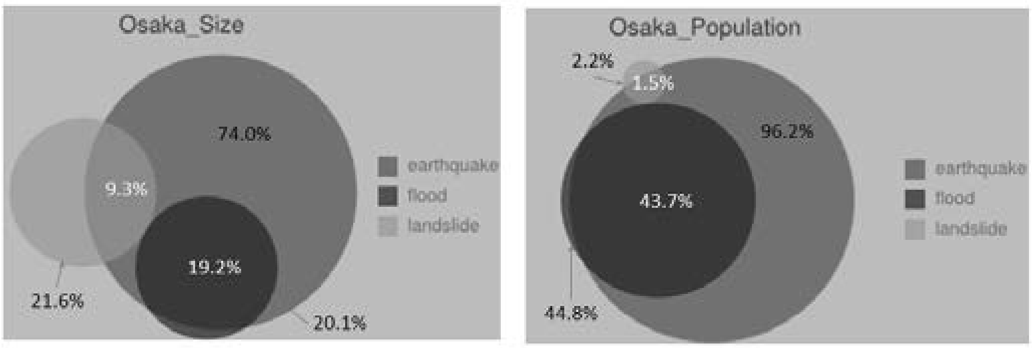

Figure 6: The rate of risk area in Osaka

These maps show almost all the lands have the risk of earthquake. And many people live densely with flood risk while few people live with the danger of landslide.

The flood risk area is located in the vicinity of a river or sea while that of landslide is near mountainous area, so these two areas has less overlap. But the large area with flood risk also has the high earthquake risk probably because of the soft soil condition with fluvial sedimentation.

It can be found that the proportion of those who live with multi-hazard risk to the whole population is roughly within a range from quarter to half.

4. CONCLUSIONS

In this paper, existing hazard maps for various kinds of natural hazards were collected and overlaid on GIS database. As a result, the areas with or without hazards were identified. The correlation among different types of natural hazard in mega city was also analyzed. Then, the population who exposed to single or several hazards in mega city was assessed and regional vulnerability was evaluated.

It is necessary to assess multi-hazard risk in the whole area of Japan although the assessment is confined to three mega cities in this paper. Evaluating the risk of all prefectures will make possible cluster analysis of them, which can be useful to understand the characteristics of disasters risk and formulate the best strategies for totally mitigating the threat of disasters. The risk of each single hazard should be classified according to the magnitude of disasters to analyze the risk in more detail.

REFERENCES

Nojima, N. 2004. Macroscopic assessment of seismic risk in Gifu prefecture in terms of population exposure to seismic intensity. Tono Research Institute of Earthquake Science, Gifu, 37-53.

J-SHIS (Japan Seismic Hazard Information Station).
http://www.j-shis.bosai.go.jp/en/

National Land Numerical Information download service.
http://nlftp.mlit.go.jp/ksj-e/index.html

Development of an innovative stormwater management framework toward building cities resilient to climate change in Vietnam

Duong Du BUI[1,2,*], Kieu Duy TRAN[1], Thanh Ngoc TONG[3], Tung Son NGUYEN[1]
[1]Hanoi University of National Resources and Environment (HUNRE), Vietnam
[2] NUSDeltares, National University of Singapore (NUS), Singapore
duongdubui@gmail.com; bui@hunre.edu.vn
[3]National Center of Water Resources Planning and Investigation, Vietnam (NAWAPI)

ABSTRACT

Frequent urban floods have remained as key challenges to various socio-economic activities and threaten sustainable development of many regions and countries around the world. Growing evidences show that traditional approaches of urban stormwater management in Vietnam, which mainly depend on engineering measures to immediately release stormwater to drainage system, have failed to manage recent urban floods, especially extreme floods due to climate change and rapid urbanization, and "wasted" rainwater resources. This study thus proposed an innovative approach, which is based on concepts of a traditional indigenous knowledge widely practiced in rural areas in Vietnam: Vuon-Garden, Ao-Pond, Chuong-Livestock (VAC). The proposed approach, namely VAC Infrastructure (VACI), deals with urban stormwater at sources, on pathways and at receptors with uses of various infrastructures related to concepts of VAC agricultural system. VACI is preliminarily examined with case study of Hanoi city. The findings showed that the proposed framework provides promising solutions toward building a livable city resilient to climate change because it helps to bring people closer to nature in cities where water, green, and biodiversity are enhanced. Though the proposed approach was initially developed at conceptual level, the findings provide useful foundation for developing a holistic framework which manages stormwater as "resource" rather than "waste" or "problem".

Keywords: *urban flooding, stormwater management, VAC system, city resilience, climate change, Hanoi*

1. INTRODUCTION

1.1 Current flood situation

In recent years, along with the erratic, extreme weather, sea level rise and changes in surface conditions caused by urbanization process, the frequency and severity level of floods have tended to increase (Tong, 2012, Bui, et al., 2010). According to statistics in the number of global disasters from the World Health Organization (EM-DAT, WHO), in the last 30 years, floods accounted for 33% of all natural disasters, and the number of people affected by flooding is about 52% of the total number of people affected by natural disasters (Figure 1). It is noticed that Asian regions most suffered from flooding in both aspects of the number of incidents and the level of damage (number of people affected), with over 50% of the total floods and 90% of the total number of people affected (Bui, et al., 2011).

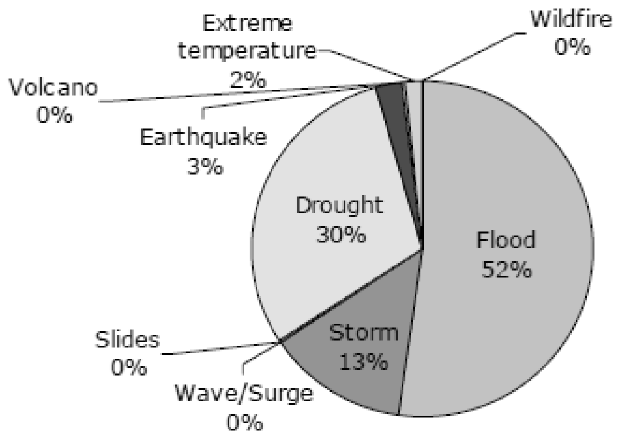

Figure 1: Numbers of people affected by climate-related natural disasters (1979-2008) (Bui, 2011)

Recently, the number of floods (Figure 2) and losses of life due to floods tend to rise and may continue to increase in the future. The main reasons are the high density of population in cities due to process of urbanization and the increasing of extreme weather events. Increasing trend in flood events and damages are clearly revealed in developing countries. According to the projection, the number of people affected by flooding will increase to approximately 2 billion by 2050 and the consequences are unpredictable in the future due to effects of climate change, sea level rise, global warming, urbanization, among others. [1].

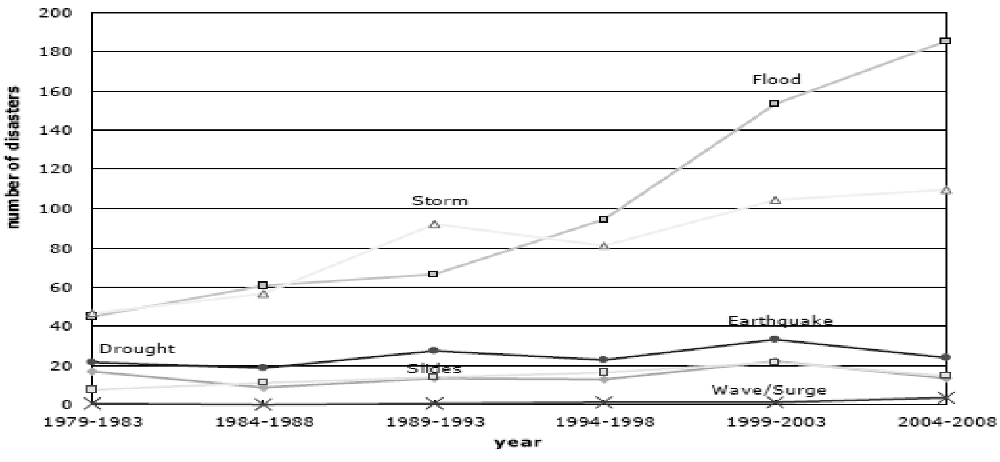

Figure 2: Global trends in numbers of natural disasters during the period of 1979-2008. (*Source: ICHARM, 2008 (Bui, 2011)).*

1.2 Impacts of urbanization on rainfall-runoff process

Among different types of floods, urban flooding likely occurs most frequently and can cause the most property damages and death toll. To be able to propose effective solutions for urban flooding, we should first understand the causes of urban flooding and the impacts of urbanization on floods. Typically, floods are the results of a synthesis process of three main driving factors: meteorological (rain, storm, snow ...), hydrological (humidity and soil permeability, river morphology...) and anthropogenic factors (land-use pattern, urbanization, deforestation ...). Depending on the dominance of each factor, flooding can have different characteristics. Generally, floods can be grouped into the several categories: local flooding, riverine flooding, flash flood…

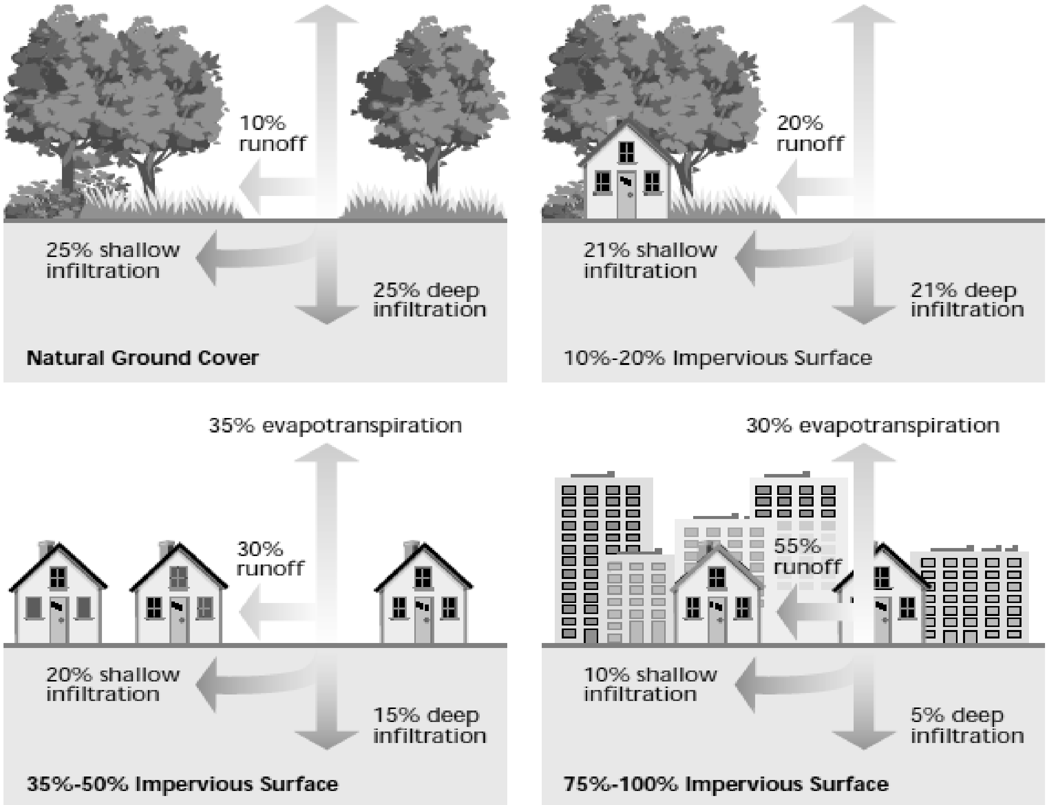

Figure 3: Conceptual diagram presenting effects of urbanization on rainfall-runoff process *Source: FISRWG, 1998*

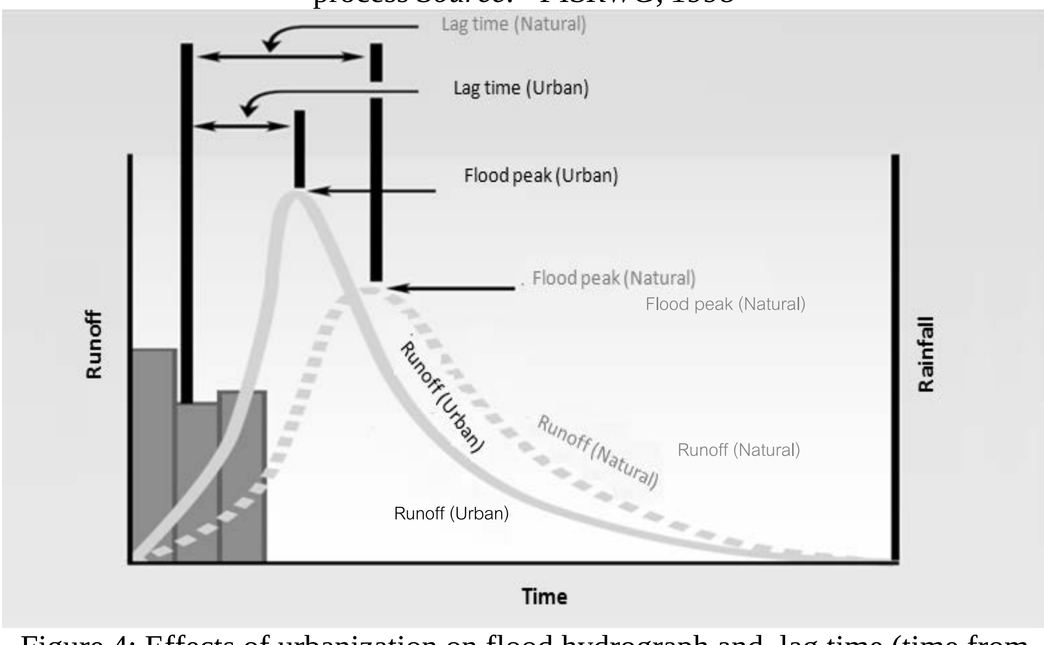

Figure 4: Effects of urbanization on flood hydrograph and lag time (time from rainfall peak to flood peak)

In urban areas, the decline of natural infiltration due to built-up areas has resulted in the generation of higher surface runoff flow in comparison to the natural watershed (Figure 3). Moreover, urbanization led to the reduction of lag time- the time from rainfall peak to flood peak (Figure 4) thus made the flooding faster and more difficult to cope with. In other words, urbanization would increase flood risks in both terms of occurrence and level of severity.

2. THE CONCEPT OF FLOOD RISK MANAGEMENT

Traditional approaches in flood management are primarily using structural solutions to achieve the goals of flood control. Practices and studies [3],[4],[6] showed that this method is difficult to implement and ineffective in cases of abnormal complex weather events, as well as to assess the damage caused by the floods in areas with different infrastructures and socio-economies conditions. Therefore, in recent years, new approach of "flood risk management", rather than a traditional approach of "flood crisis management" has been implemented, in which, we can take into account three factors: Hazard, Vulnerability and Exposure. This method has proven to be more flexible and more holistic than the old ones, especially in developing countries.

Figure 5: Proposed Urban Flood Risk Management based on the concept of Natural Disaster Risk Management by UNU (Bui, et al, 2010) &UN/ISDR)

What is Flood Risk Management?

As defined by the United Nations International Strategy for Disaster Reduction (UN/ISDR) and the United Nations University Institute for Sustainability and Peace (UNU-ISP), flood risk management concerns about four main factors:

- *Hazards:* The possibility, severity level and duration of floods;
- *Exposure:* Elements at risk when floods happen;
- *Vulnerability:* The population, social, economic and environmental factors;
- *Capacity*: Awareness, preparedness and ability to cope with floods.

As given by the above definition: Flood risk is proportional to three factors: hazards, exposure, vulnerability and inversely proportional to the ability to adapt (capacity). In context of urban flooding assessment and management, enhancing our "adaptive ability" also means that we reduce the "vulnerability" thus the definition of UNISDR can be shortened as described in the formula (1) and illustrated by Figure (5).

Flood Risk = *F (Flood hazard, Vulnerability, Exposure)* *(1)*

3. GROUPS OF KEY MEASURES

3.1 Measures for flood hazard reduction

3.1.1 The proposed conceptual framework

As discussed previously, the main difference between the an urban catchment and a natural one is the increasing of built-up areas resulting in the higher surface runoff and flood peaks in urban area. Therefore, promising solutions to reduce urban flood risks are to enhance more “natural” built elements while constructing infrastructure in urban areas in order to restore the natural rainfall-runoff process. This approach will increase the use of "natural" structures with characteristic of high permeability and ability of storing water such as water infiltration trench, ponds, artificial wetlands, artificial vegetation cover, environmental buffers, etc.,. to slow down the rainfall-runoff process and reduce the flood peaks thereby reduce flood risks. At the same time, proposed infrastructure also helps improving water quality, beatifying the landscape and the environment of urban area, increasing biodiversity in urban areas as well as the ability to adapt to climate change, with abnormal weather events and phenomenon of "heat islands" in urbanized areas.

In Vietnam, many cities have been struggled to solve the problems of urban flooding by using traditional approaches which focus more on improving the drainage system to drain stormwater as quickly as possible. Most of the rain water is not adequately treated before flowing into the flood conveyance systems (i.e. river, channel...), resulting in many environmental adverse consequences that affect people's health during the flood season. The practical evidences have shown that traditional approaches have many drawbacks, such as: the ineffectiveness of flood drainage, avoiding floods in certain areas but increasing floods in others, wasting valued rainwater, causing environmental pollutions, depletion of river flows in the dry season, etc.,.

Therefore, the key idea is to reduce urban flood risks by integratedly managing the entire rainfall-runoff process: at the **Sources**, on the **Pathway,** to the **Receptors** (Figure 6) with various environmental-friendly structural measures, such as: green roof, green wall, underground storages and infiltration systems, bio-treatments, bio-detentions, bio-swales, etc.,. Using this approach, we not only reduce flood risks (i.e. deduction of flood peak and volumes), but also retain and treat stormwater which would later be used to relief water supply stresses, increase groundwater recharges, maintain base flow in the rivers, improve habitat, increase biodiversity and create beautiful city landscape.

In that sense, a Vietnamese traditional knowledge, namely VAC that is widely practiced for poor families to be self-sustainable in rural regions, is highly appropriate and adoptable. Originally, VAC means *"Vuon-Garden, Ao-Pond, Chuong-Livestock"* which provides vital foods and water for family's daily needs (Figure 6). In the context of cities, VAC has its new meanings: Green-Water-Biodiversity, which are essential components shaping Livable and Sustainable Cities. With these VAC Infrastructures, so called “VACI”, urban area will be greener, cleaner, more beautiful, sustainable and harmonious with nature, where flowers and green (*Vuon-Garden*), water (*Ao-Pond*) and Biodiversity (*Chuong-Livestock*) will be will be the core components of a sustainable cities.

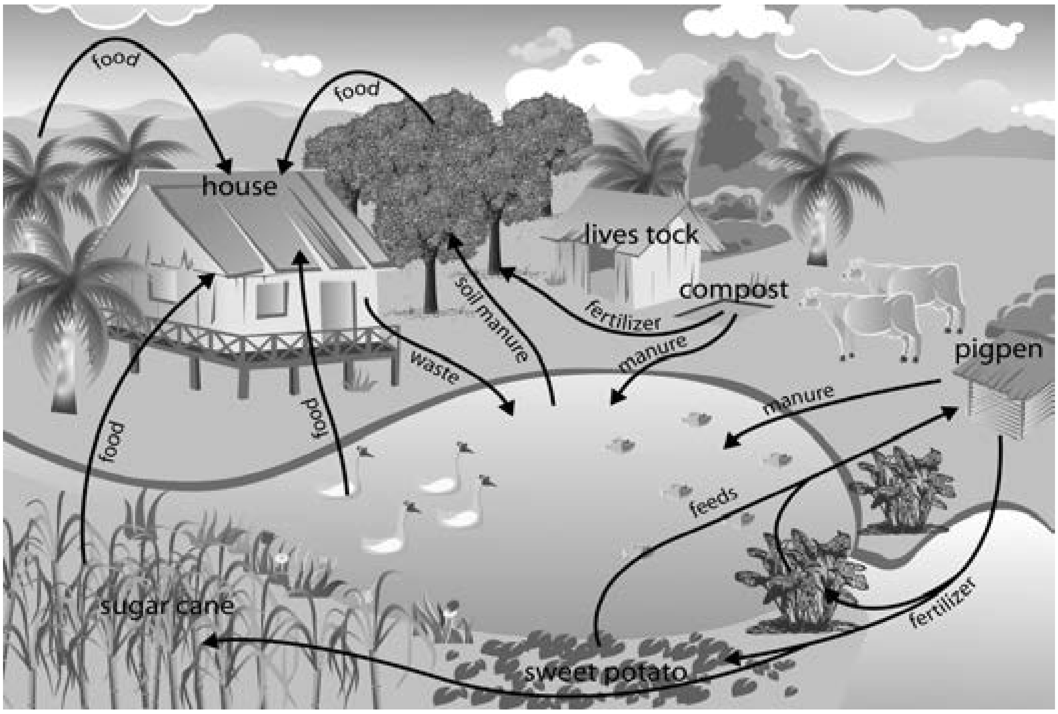

Figure 6: Simplified sketch of Vietnamese VAC Integrated farming system

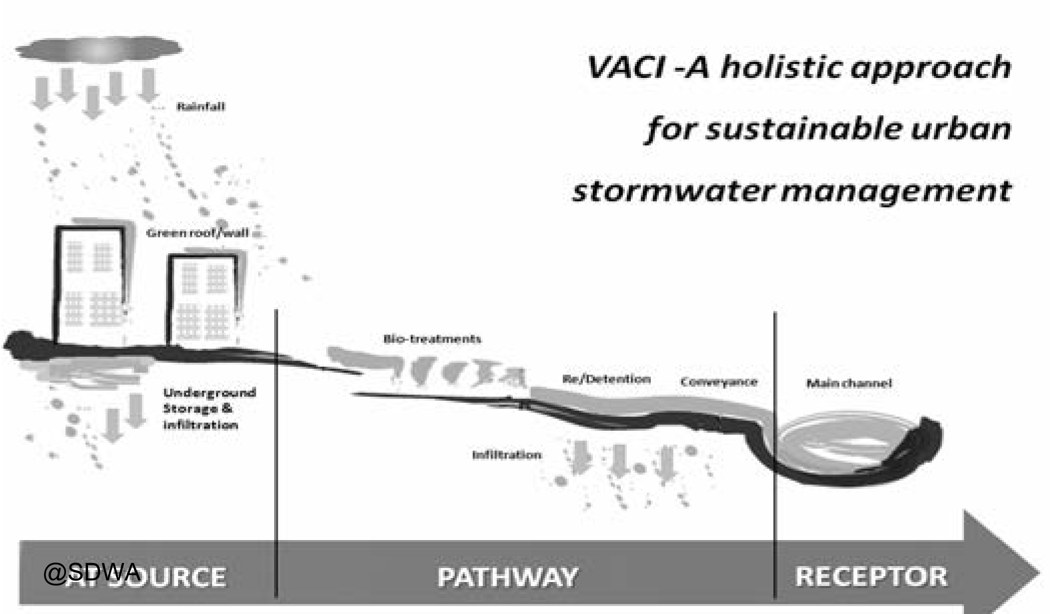

Figure 7: Proposed VACI framework for urban stormwater management

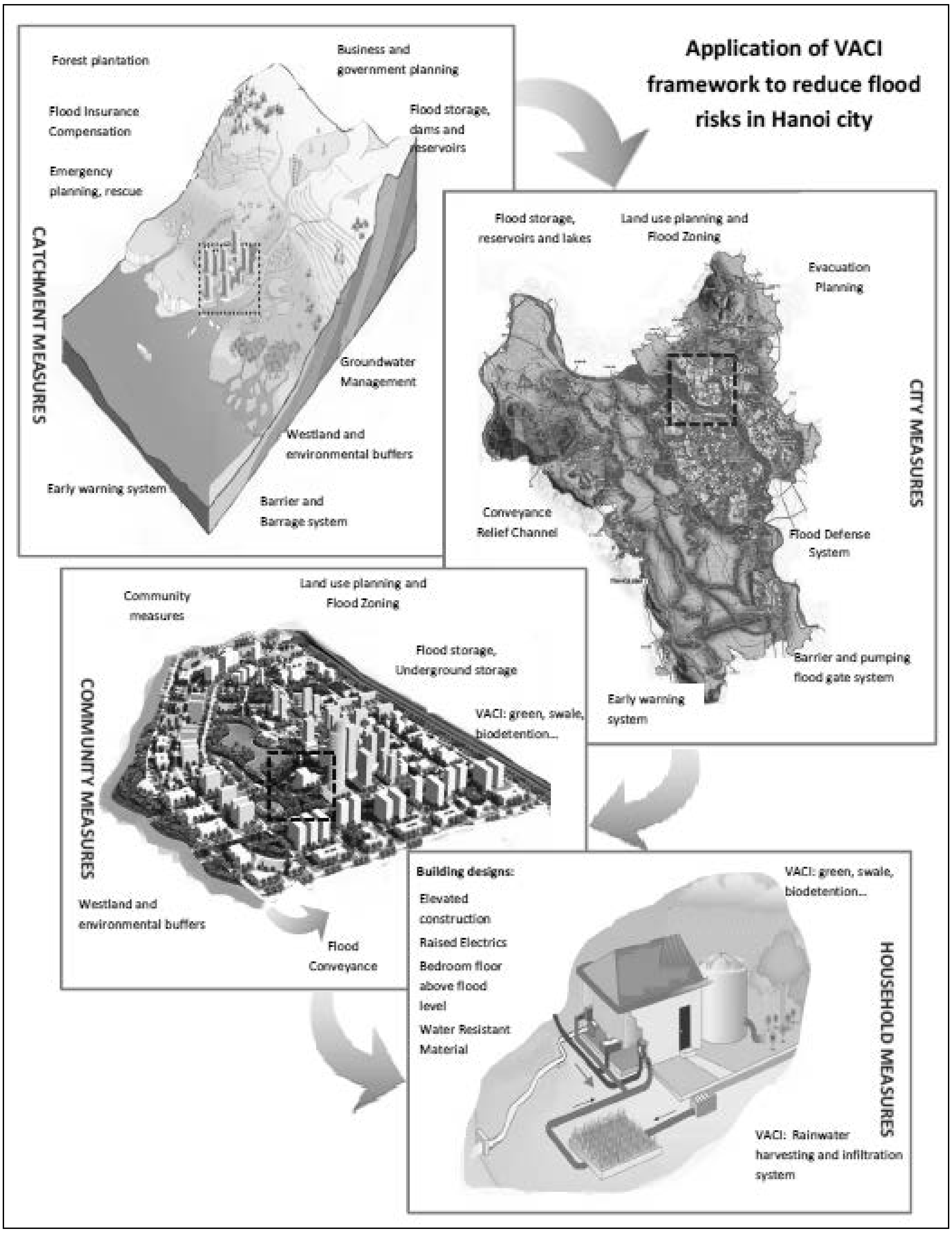

Figure 8: VACI framework in reducing urban flood risks: case study of Hanoi city. Illustrative figure adapted from urban flood risk management measures by A. K Jha, R. Bloch and J. Lamond, 2011.

3.1.2 Application of VACI framework to reduce flood risks in Hanoi city

Applying VACI stormwater management framework (Fig. 7) to given urban areas requires different specific measures to suit the local conditions of the areas. In this study, VACI framework is initially examined to Hanoi, the capital of Vietnam as a case study. As Hanoi located in the lowland of the Red River Delta, the risks of both internal flooding and external flooding caused by the Red River during flood season are very high. Flood risk management strategies for Hanoi thus must be developed from integrated and holistic perspectives which cover different scales: catchment, city, community and household scales as shown in Figure 8.
At each scale, specific solutions need flexible combinations between structural and non- structural measures and a right balance between short term and long term strategies to minimize the cost and maximize the effectiveness. For example, flood risk management strategies at catchment scale need a right mix between structural measures such as forest plantation, flood storages, dams and reservoirs, barrier and barrages systems, etc., and non- structural measures such as flood insurance, compensation, emergency planning, etc.,.

3.2 Solutions for increasing resilience/reducing vulnerability

Although the application of VACI strategies is promising and potential to reduce the flood risk in cities; it cannot guarantee the absolute avoidance from the flood risks, particularly in the context of erratic weather caused by climate change. Therefore, it is necessary to combine between risk management measures and the solutions that increase resilience/reduce vulnerability in order to minimize flood risks effectively. These types of solutions also need a flexible combination and right mix between structural measures (such as flood shelter, emergency assistance systems and evacuation routes) and non-structural measures (soft solutions). Non-structural measures can be divided into four main categories as followings:

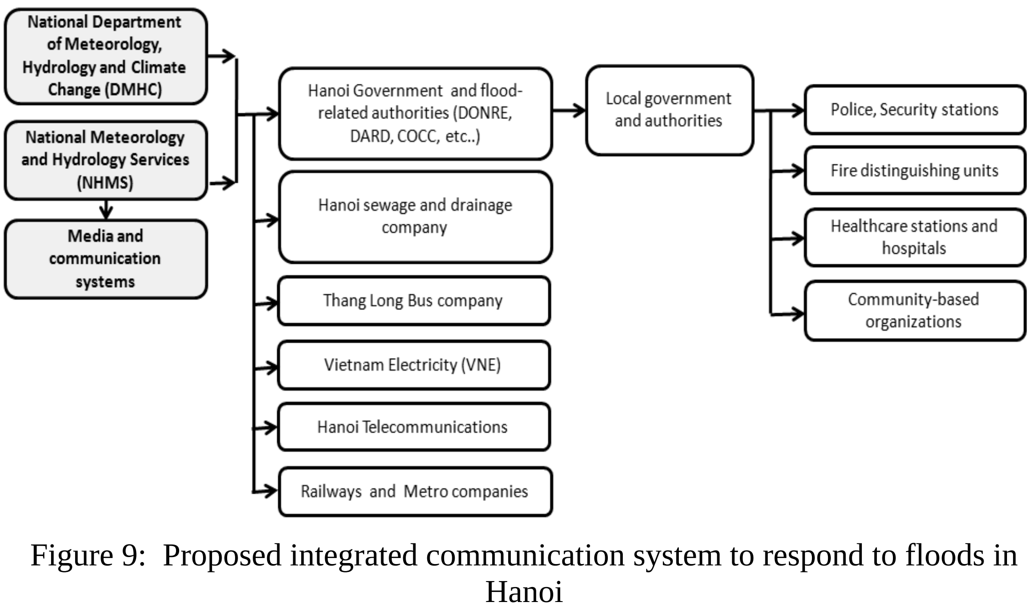

Figure 9: Proposed integrated communication system to respond to floods in Hanoi

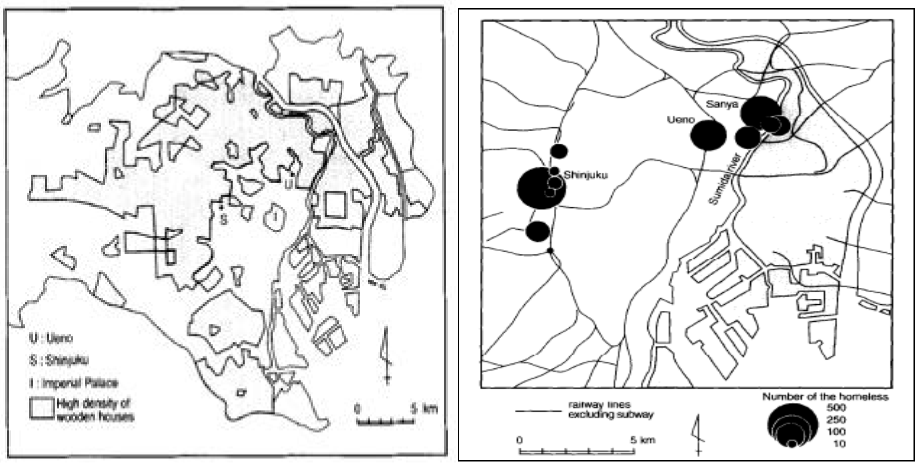

Figure 10: Spatial distribution of temporary wooden houses and homeless people in Tokyo

(Source: Takahashi, 1998)

- *(1) Raising public awareness and improving preparedness before flood events:* We need to implement educational programs, promote media to raise public awareness about the possibility of flood risks in their living areas and the extent of possible damage might occur, as well as the preparatory work to minimize damages caused by floods. Raising public awareness can be done in a number of ways, such as: using bulletin board in highly populated areas, posters, newspapers, meetings, presentations, TV/Radio, photo exhibitions, training courses, or integrating useful information related to floods into local social activities.
- *(2) Planning for emergency assistance during flood events:* implementation of rescue and evacuation plans, providing food, water and other basic needs (medicines, shelters...) play important roles in reducing flood damages when the floods is occurring. In addition, early warning systems and communication systems that help convey flooding information to people quickly and accurately is also very necessary. Figure 9 illustrates the proposed integrated communication system to respond effectively to the floods in Hanoi.
- *(3) Improving damage recovery after flood events:* During and after the flood events, the rapid deployment of remedial solutions, security, food, energy, sanitation, health care, financial assistance is necessary to help people quickly recover to daily life.
- *(4) Assessing vulnerability:* The comprehensive assessment of vulnerability, including economic, infrastructural, social and cultural aspects is necessary. When flooding occurs, vulnerable groups of people such as poor families, the elders, single people, homeless people, foreigners, etc.,. will bear higher risks to floods. Currently, the vulnerability in terms of culture, society, traditions is often improperly cared and not incorporated into practical flood risk management planning, though various researches have been highlighted the importance of these factors in reducing flood damages. For example, in Tokyo (*Takahashi, 1998*), in the 1970s, up to 70% of the elders (> 65 years old) lived with their children, but currently, this dropped to only about 32%. With people living in Tokyo, radio and TV are the only sources of information when disasters happen and most families are of only 1 or 2 people (higher risk than families of more people). Despite of the increasing in the number of foreigners in recent decades, all the forecasts, warning, guiding to shelters, evacuation… related to natural disasters remain entirely in the local language- Japanese. Takahashi (1998)

studied the relationship between disaster risk capabilities with social factors such as the distribution of temporary wooden houses and homeless people in Tokyo (Figure 10).

4. CONCLUSION

Annual flooding has caused serious damage to the economic and social activities, threatening the sustainable development of countries and territories around the world. The planning for strategic direction and implementation of the appropriate measures to prevent flooding damages in urban areas is the urgent but challenging tasks to many countries. Under the impacts of climate change and urbanization, the traditional methods to cope with flooding revealed many shortcomings especially with the recent floods. Therefore, a new approach based on the principles of risk management methods is proposed. This approach is primarily composed of two main groups of measures: measures of reducing the flooding hazards (i.e. reduction of flood occurrences and severity), and measures to increase resilience or reduce vulnerability. In this approach, we need to implement flexible combination between short-term and long-term solutions as well as between structural and non-structural measures. Solutions of reducing flood risk were studied within conditions of Hanoi, while the solutions of increasing resilience / reducing vulnerability are analyzed with illustrations from the actual data from the recent study conducted in the city of Tokyo. The results showed that in Hanoi, the solutions should be implemented comprehensively in different scales from river basins to residential households in order to reduce the risk of flooding effectively. Research in Tokyo has shown that comprehensive assessment of vulnerability, including culture, society, traditions ... also plays a very important role. The methodology developed in this research has opened a promising approach for a more holistic and flexible management of urban flooding.

ACKNOWLEDGEMENTS

This study was carried out as a part of the project “Improvement of Groundwater Protection in Vietnam-IPGVN” supported by Germany Government and the project “Hanoi inundation mapping in context of climate change”, financed by the Hanoi Metropolitan Government.

REFERENCES

Tong, N. T., et al., 2012. *Technical Report of the Hanoi’s Government-funded project “Hanoi inundation mapping”*, National Centre for Water Recourses Planning and Investigation (NAWAPI), 297 pages.

Tran, D. K., 2012. *Managing Extreme Floods in the Lam river basin, Vietnam*. PhD thesis, Water Resources University, 165 pages.

Bui, D. D., et al., 2010. *Understanding Flood Hazard, Vulnerability and Coping capacity in mega cities: Reflections from Tokyo*. The United Nations University Institute for Sustainability and Peace (UNU-ISP), 93 pages.

Bui, D. D., et al., 2011. *Technical guideline on water-related disaster management for drought (part IV)*. World Federation of Engineering Organizations - WFEO, 135 pages.

Federal Interagency Stream Restoration Working Group (FISRWG), 1998. *Stream Corridor Restoration: Principles, Processes, and Practices,* 653 pages.

The United Nations International Strategy for Disaster Reduction (UN-ISDR), 2009. *Terminology on Disaster Reduction,* 35 pages.

Takahashi, S. 1998. Social Geography and Disaster Vulnerability in Tokyo. *Applied Geography* 18 (1): 17-24.

Workshop to Produce an Information Kit on Farmer-proven. Integrated Agriculture-aquaculture Technologies (IIRR; 1992; 119 pages)

A. K Jha, R. Bloch and J. Lamond, 2011, *Cities and Flooding: A Guide to Integrated Urban Flood Risk Management for the 21st Century*, The World Bank, 637 pages.

Assessment of potential greenhouse gas emission of domestic solid waste treatment in Hanoi, Vietnam

Minh Giang HOANG
Lecturer, Department of Environmental Technology and Management, IESE,
National University of Civil Engineering, Vietnam
hmgiang83@gmail.com

ABSTRACT

Domestic waste in most of developing world cities including Hanoi have diseperately collected and primarily landfilled. It caused a large amount of greenhouse gas (GHG) emissions. This study aim to estimate and compare the amount of GHG emission from operating domestic solid waste treatment facilities in Hanoi city by using the IPCC 2006 method from various possible scenarios. In oder to use Tier 2 model of IPCC 2006 for GHG estimation, an analysis on current household solid waste management system of the city was obtained by using MFA approach. There was a reduced of around 70% of the amount of CH_4 emissions and up to 60% of total GHG saving ($CO_{2\text{-}eq}$) from avoiding organic waste to landfill as well as increasing material recovery through composting and recycling of household waste.

Keywords: waste treatment alternatives, GHG emission, household solid waste

1. INTRODUCTION

Climate change is a major international concern for modern society. Since the pre-industrial era, atmospheric concentrations of carbon dioxide (CO_2) have increased by 35% and methane (CH_4) concentrations have more than doubled (ISWA, 2010). Together with greenhouse gas mitigation strategies and technologies from main emitters according to the Intergovernmental Panel on Climate Change (IPCC) such as Energy sector; Industrial processes and product use sector (IPPU), Agriculture, forestry, and other land use sector (AFOLU) etc… Scientists all over the world has clearly taken on the commitment to make a contribution so that the waste sector may change its status at the global level – *from being a net greenhouse gas emitter to becoming a net GHG saver* (Savino, 2009).

Cities in developing countries, Hanoi included have unsorted solid waste collection system and landfill is the primary disposal method, which is a major source of GHG emissions from the waste sector (UNEP, 2010). Low efficiency of waste collection system leads to a great amount of household solid waste released to the environment. Solid waste is not separated at source resulted in lost opportunities for resource and energy recovery as well as treatment technology application. Moreover, contemporary practices of dealing with waste in Hanoi gave way to less environmentally friendly alternatives, such as the disposal of waste in riverbanks, empty space or open burning within urban areas. The current solid waste treatment facilities contributed a great amount of GHG emission, especially methane from sanitary landfill and it plays an important role of impact on global warming.

The 2006 IPPC (IPCC, 2006) provided a methodology for annual accounting of GHG emissions for the waste sector, defined by the IPCC, is different from how the waste management industry perceives itself (Gentil et al., 2009). Certainly, the reporting methodology of the IPCC waste sector identifies only the direct emissions of post-consumer waste management and recycling, intermediate waste facilities as well as waste transportation are excluded. The method is crucial in assessment of the potential of GHG emission/mitigation associated with all activities or sectors within a reporting country.

This study aimed to assess the impact of solid waste treatment practices, especially household waste towards GHG mitigation for the IPCC waste sector. Thus, the study proposes to use the 2006 IPCC method to evaluate greenhouse gas emission. A case study for Hanoi city in 2011 has been conducted under some possible scenarios, which are suitable for the current situation of the city. However, because of the complex waste management in the city, a material flow analysis (MFA), therefore, have carried out on household solid waste management system in order to obtain a database of waste stream for applying the Tier 2 model of 2006 IPCC guidelines.

2. METHODOLOGY

2.1 Research target area

The purpose of this study assessed the amount of GHG emission from solid waste treatment activities in Hanoi city, which had a great size of population of around 6,5 million in 2010. The number of urban residence accounted for 43%, while the number of peopel living in countryside is 3,8 million, 57,4% (HSO, 2011). The concerning target of the research was systematical an analysis of the household waste stream of the city in 2011 and calculation the directed greenhouse gases according to the 2006 IPCC guidelines such as CH_4 and N_2O, emitted from landfill and composting plant activities. The 3 main landfills and 3 composting facilities in Hanoi was taken into acount in this study including Nam Son, Xuan Son, Kieu Ki as well as Cau Dien, Kieu Ki, Seraphin respectively.

2.2 Scenarios description

In order to assess the potential contribution of GHG mitigation of solid waste management alternatives for Hanoi city. Some reasonable waste management scenarios were assumed with the priority of keep using temporary solid waste treatment technologies but improving collection efficiency and seperation at source application. Scenarios description was illustrated in Table 1.

Table 1. Scenarios description

Scenarios	Collection rate	Separation at source	Technologies description
HT (business as usual)	Urban area 95% Countryside 60%	Not separate at source	Landfilled without LFG recovery Composting
S1	100%.	Yes The percentage of recyclable waste recovered up to 80%.	Use current technologies: Landfilled without LFG recovery Composting 100% organic waste
S2	100%	Yes The percentage of recyclable waste recovered up to 80%.	LFG recovery: Landfill with LFG recovery with the rate of 20% of CH_4 recovered Composting 100% organic waste

2.3 Waste material flow analysis

2.3.1 Waste quantity and composition data

The data of household waste related to analysis in this study have been obtained from published report in 2011 of Hanoi urban environment one member limited company (URENCO, 2011) and National report on environment 2011: solid waste by Ministry of Natural Resource and Environment (MONRE, 2011). In addition, research data conducted by JICA was used in the study. The household waste generation and collection rate of urban area and countryside area of Hanoi in 2011 have been introduced in those reports above and also calculated in Table 2.

Table 2. Household waste generation and collection of Hanoi in 2011

Area	Collection rate (%)	Amount (t/d)
Waste generation in the whole city	-	6500
Waste generation in urban area	-	4100
Waste generation in countryside area	-	2400
Waste collected in urban area	95%	3895
Waste collected in countryside area	60%	1440
Total waste collected		5335

The household solid waste information including waste quantity and composition by physical categories of the city as well as landfills was provided by URENCO and MONRE, also calculated and summarized in Table 3.

Table 3. The composition of waste of the city and landfills in 2011

Composition	Urban Area		Countryside Area		Percent of whole the city (%)***	Percent of waste composition in LF			Waste moisture (%) ***
	Percent (%)*	Amount (t/d)	Percent (%)*	Amount (t/d)		Nam Sơn **	Xuân Sơn **	Kiêu Kị ****	
Paper [i]	4,85	198,85	2	48	3,80	6,53	5,38	5,47	57,63
Plastic [i]	4,02	164,82	2,05	49,2	3,29	13,57	8,35	11,89	53,91

Nylon [i]	8,48	347,68	5,35	128,4	7,32	-	-	-	53,91
Metal [i]	2,18	89,38	0,4	9,6	1,52	0,87	0,25	0,46	-
Organic waste	38,03	1559,23	56	1344	44,67	53,81	60,79	56,84	70,00
Rubber, leather	4,15	170,15	1,8	43,2	3,28	0,15	0,22	0,83	0,72
Textile	2,15	88,15	1,86	44,64	2,04	5,82	1,76	4,32	9,9
Wood	3,02	123,82	2,24	53,76	2,73	2,51	6,63	4,44	30,9
Glass	2,79	114,39	1,3	31,2	2,24	1,87	5,08	2,5	-
Ceramic	7,36	301,76	0,7	16,8	4,90	0,39	1,26	0,84	-
inert	22,74	932,34	12,2	292,8	18,85	14,31	9,46	12,14	-
Hazardous waste	0,23	9,43	14,1	338,4	5,35	0,17	0,82	0,27	-
Amount (t/d) **, ***		**4100**		**2400**	**6500**	**3468**	**227**	**118**	

(*) *Source: Report on Solid waste in 2011 of Hanoi URENCO (URENCO, 2011)*

(**) *Source: National report of environment 2011 – Solid waste (MONRE, 2011)*

(***) *Source: Report on solid waste management research in Vietnam 3/2011 (JICA, 2011)*

(****) *Calculated based on data of waste composition of some landfills in the northern Vietnam such as Nam Son, Xuan Son, Trang Cat, Dinh vu (MONRE, 2011)*

[i] *Type of recycle waste in private business and recycling villages*

According to URENCO, the amount of waste collected in 2011 was 5335 tons/day, meanwhile that of waste treated was only 3972 tons per day according to JICA (2011), accounted for 75%. It was possibly as a result of recycle activities through waste pickers and junk-man as well as low efficiency of waste collection activities. The two official household waste treatment methods in Hanoi currently are landfills and composting. In 2011, the total amount of organic waste treated in composting plants was 159 tons per day while that of house hold waste landfilled in Nam Son, Xuan Son and Kieu Ki was 3468, 227 and 118 tons per day respectively. The preferably recycled waste was collected through many activities of including mostly junk-shops and waste pickers on street as well as landfills. The percentage of waste recycled was at about 10% of total waste generation (MONRE, 2011), mainly recovered in some recycling villages which are private and small producers, as a result it was difficult to determine the amount of recycled waste exactly.

2.3.2 Waste stream calculation

The study was applied MFA approach to calculate the amount of waste recovered from landfills ($G_{tc\text{-}BCL}$), as following equations

$$G_{tc-BCL} = G_{tc} - 10\% x G_{ktg} - \left[\sum_i G_{tc,i} - \left(\sum_i G_i^{NS} + \sum_i G_i^{XS} + \sum_i G_i^{KK} \right) \right] \textit{(t/d)} \quad (1)$$

Where,

- G_{ktg}, the total amount of household waste was not collected *(t/d)*;
- $G_{tc,i}$, the total amount of recyclable waste generated within the city,

$$G_{tc,i} = r_i^{NT} \times G^{NT} + r_i^{NgT} \times G^{NgT} \quad \textit{(t/d)} \qquad (2)$$

+ r_i^{NT}, r_i^{NgT}, the percent of recyclable waste i generated in urban and countryside;

+ G^{NT}, G^{NgT}: the total amount of waste in urban and countryside was 4100 and 2400 t/d respectively;

- G_{tc}, the total amount of waste recycled of the city in 2011, accounted for 10% of the total generation (MONRE, 2011), $G_{tc} = 10\% \times 6500 = 650$ *(t/d)*;

- $G_i^{NS,XS,KK}$, the amount of recyclable waste i transported to Nam Son, Xuan Son and Kieu Ki landfills, $G_i^{NS,XS,KK} = G_{CL}^{NS,XS,KK} \times r_i^{NS,XS,KK}$ *(t/d)* (3)

+ $G_{CL}^{NS,XS,KK}$, the total amount of waste transported to Nam Son, Xuan Son, Kieu Ki landfills;

+ $r_i^{NS,XS,KK}$, the percent of recyclable waste type i such as paper, metal, plastic… transported to Nam Son, Xuan Son, Kieu Ki landfills;

- the term $\left[\sum_i G_{tc,i} - \left(\sum_i G_i^{NS} + \sum_i G_i^{XS} + \sum_i G_i^{KK}\right)\right]$ presented the amount of recyclable waste recovered outside landfills *(t/d)* (4)

The amount of recyclable waste type i landfilled was accounted as difference between amount of waste i transported to landfills and that of i recovered from landfills. An assumption is made that percentages of recyclable waste recovered from landfills including paper, metal, plastic and nylon are equal. The amount of other waste landfilled in 2011 was calculated by their percentages in table 2.

2.4 Estimation of GHG emission from treatment facilities

2.4.1 CH_4 emission from landfills

The study propose to use 2006 IPCC guideline – model Tier 2 (IPCC, 2006) for estimating methane emission from landfills. The input data of composition of waste landfilled was used are the results from waste material flow analysis as well as some defualt parameters suggested by IPCC (presented in Table 3). In order to calculate the direct CH_4 emitted from landfilling the amount of household solid waste in 2011, author assumed that landfills in Hanoi operated within 1 year and closured in the end of 2011 when completed the treatment for the waste of 2011.

The CH_4 emissions from solid waste disposal for a single year can be estimated using the general Equations 5. Part of the CH_4 generated is oxidized in the cover layer, or can be recovered for energy or flaring. The CH_4 actually emitted from the landfill will hence be smaller than the amount generated (IPCC, 2006).

$$L^{CL}_{CH_4} = \left[\sum_i (CH_{4-gen,i,T} - R_T)\right] \times (1 - OX_T) \text{ (thousand tons)} \quad (5)$$

Where:

$L^{CL}_{CH_4}$, CH emitted in year T, *(thousand tons);*

R_T, recovered CH_4 in year T *(thousand tons);*

T, inventory year ;

OX_T, oxidation factor in year T, *(fraction);*

Table 3. Default parameters used in IPCC model

	IPCC default	Used	Explaination
DOC (% wet waste)			*Degradable organic carbon (DOC) is the organic carbon in waste that is accessible to biochemical decomposition. The DOC in bulk waste is estimated based on the composition of waste and can be calculated from a weighted average of the degradable carbon content of various components (waste types) of the waste stream.*
Organic waste	0.08-0.20	**0.15**	
Paper	0.36-0.45	**0.4**	
Wood	0.39-0.46	**0.43**	
Textile	0.20-0.40	**0.24**	
DOC_f (%)		**0.5**	*Fraction of degradable organic carbon (DOC_f) is an estimate of the fraction of carbon that is ultimately degraded and released from landfill.*
K ($Year^{-1}$)			
Organic waste	0.17–0.7	**0.4**	*The reaction constant $k = ln(2)/t_{1/2}$, where $t_{1/2}$ is half-life-time, which depended on various factors including mostly climate conditions factors. With MAP>1000m, The climate of Vietnam is moist and wet tropical.*
Paper	0.06–0.085	**0.07**	
Wood	0.03–0.05	**0.035**	
Slowly degrading organic waste	0.15–0.2	**0.17**	
Delay time (month)		**6**	*Delay time should not be chosen more than 6 months according to IPCC suggestion.*
F		**0.5**	*Methane fraction in LFG*
Oxidation factor		**0**	
MCF		**0.6**	*Methane correction factor. With landfills in Hanoi, author chose as Semi-aerobic managed solid waste disposal sites*

2.4.2 GHGs emission from composting facilities

Composting is an aerobic process and a large fraction of the degradable organic carbon (DOC) in the waste material is converted into CO_2. CH_4 is formed in anaerobic sections of the compost, but it is oxidized to a large extent in the aerobic sections of the compost. This process also emitted N_2O and acounted for about from 0,5% (Beck-Friis et al., 2001) to 5% of total nitrogen in solid waste.Thus, according to 2006 IPCC guidelines, the study used default CH_4 and N_2O emission factor at about 4gCH_4 per 1 kg waste and 0,3gN_2O per 1 kg waste respectively.

2.4.3 Global warming potential

The Global warming potential (GWP) provides a metric for evaluating and comparing the potential climate change associated with emissions of different GHGs (Scheutz et al., 2009). The IPCC provides the GWP for a time horizon of 20, 100 and 500 years, but a time horizon of 100 years is employed most commonly (Forster, 2007). According to Fuglestvedt et al. (2001) the choice of time horizon depends on the policy objective. This study adopted the 100 years horizon with GWP of CH_4 and N_2O equal to 25 and 298 respectively suggested by Forster (2007) in order to determine the maximum change in climate.

3. RESULTS AND DISCUSSION

3.1 Waste material flow analysis

The amount of recyclable waste recovered outside landfills is determined by the equation 4 and it equal to 1036 – 780 = 256 tons per day, where 780 is amount of recyclable waste transported to landfills (in equation 3). Thus, the amount of recyclable waste recovered from landfills, determined by equation 1 is 277.5 tons per day.

Within landfills in Hanoi city, activities of waste recovery of waste pickers and junk-mans contributed an amount of 277.5 tons recyclable waste a day. In addition, debris material released from composting plants and recycle village of about 55.55 (35% mass of organic waste input) and 65 tons per day (10% mass of recycle waste input) respectively (MONRE, 2011), was landfilled likewise. Thus the actual total amount of waste landfilled daily was 3656 tons and the percentages of recycled paper, plastic and nylon, metal in Hanoi in 2011 was 36%, 53% and 79,64%. Figure 1 describes the waste material flow in 2011 of Hanoi and the table 4 illustrated waste stream information of comparative scenarios.

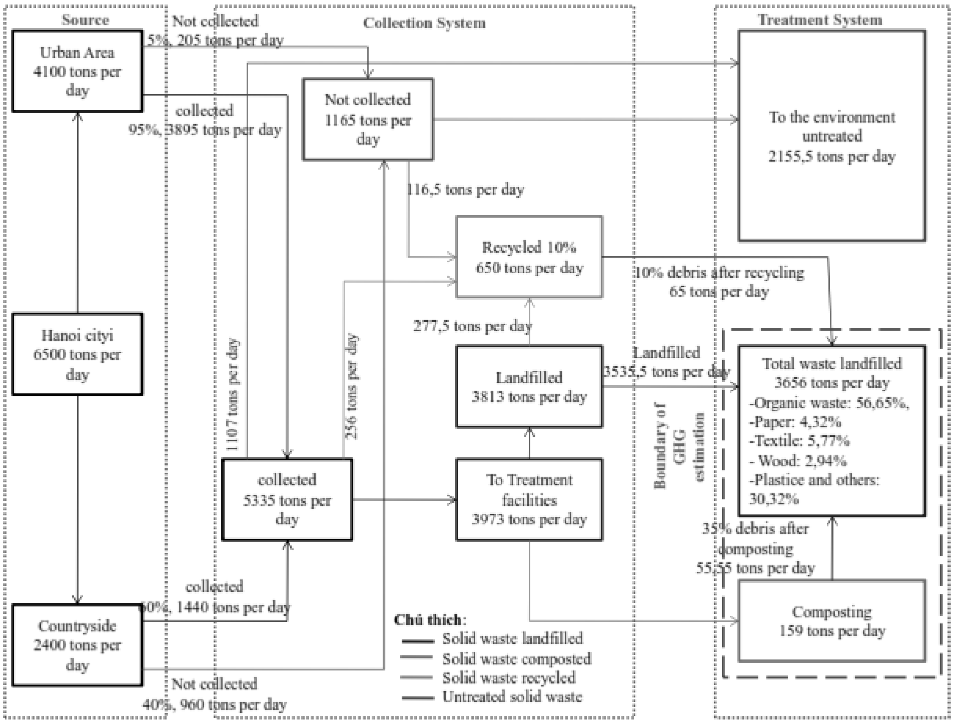

Figure 1. Waste material flow analysis in 2011 of Hanoi

Table 4. Waste material flow analysis for scenarios

Scenarios	Compost (tons/day)	Landfill (tons/day)	Percentage of different waste landfilled					Recycle (tons/day)	Untreated (tons/day)
			Organic	Paper	Textile	Wood	Others		
HT	159	3656	56,65%	4,32%	5,77%	2,94%	30,32%	650	2155,5
S1	2903	3141	0	1,57%	4,23%	5,65%	88,5%	829	0
S2	2903	3141	0	1,57%	4,23%	5,65%	88,5%	829	0

3.2 GHG emission from treatment facilities

3.2.1 CH_4 emission from landfills

Organic the waste, paper, wood and textile are the main sources of CH_4 emission in landfills. The figure 2 illustrated the potential quatity of CH_4 emissiom of above types of waste. Results showed that the capacity of CH_4 emission are different from various waste and organic waste contributed the largest propotion of 70%, followed by paper with the percentage of approximately 17%. The smallest contributer in landfill is wood accounted for about 14% of total CH_4 emitted from landfills.

The CH_4 emission factor waste presents the amount of CH_4 released per 1 ton of that kind of waste landfilled. That of textile and paper waste was very high at around 90 kg CH_4 per tom of waste treated. On the other hand, the CH_4 emission factor of organic waste was smallest though that is the largest source of CH_4 emission from landfills.

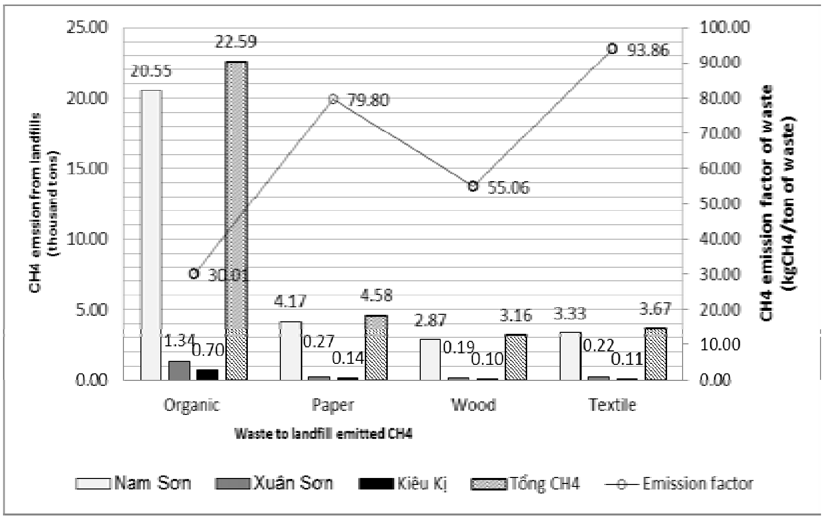

Figure 2. CH_4 emission from landfills of different materials

3.2.2 GHGs emission from composting plants

Results of CH_4 and N_2O emission from composting facilities and there GWP_{100} were summarized in the Table 5.

Table 5. Quantity of GHG emission from composting

GHG	Total organic waste, 2011	Emission factor	Amount	GWP_{100}
	(thousands ton)	(g/kg)	(tons)	(tons $CO_{2\ -eq}$)
CH_4	58,04	4	232,14	5803,5
N_2O	58,04	0,3	17,41	5188,33
Total GWP_{100}				**10 991,7**

3.2.3 Potential GHG emission and mitigation

The total potential amount of GHG emission from treatment of household solid waste generated in 2011 in Hanoi city is the sum of nearly 100 years of emission. As a result, the potential the total amount of GHG emission from treatment facilities in Hanoi was approximately 855 thousand tons $CO_{2\text{-eq}}$, landfills accounted for 99% and made a contribution of 845 thousand tons $CO_{2\text{-eq}}$.

The GHG emission of comparative scenarios S1 and S2 was 426 and 386 thousand tons $CO_{2\text{-eq}}$ respectively. It means these scenarios contributed to GHG emission mitigation which was calculated as a comparison between the GHG emission and the GHG of current status emission. Figure 3 presented the GHG emission of scenarios. It is shown that GHG emission reduction can reach up to about 60% when use scenarios S1 or S2. The results showed that scenario S2 was the most GHG emission mitigation practice due to applying LFG recovery technology.

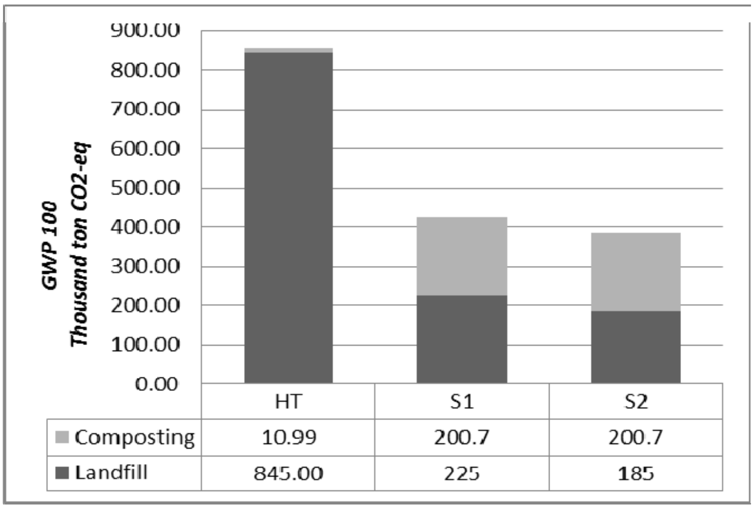

Figure 3. GHG emission and reduction

4. CONCLUSIONS

Result of waste flow analysis in 2011 of Hanoi showed that there were a great amount of waste untreated, 2100 tons per day. That reflected accurately the low efficient solid waste collection system of the city.

The result of this study also certified the importance of separation at source and recycling practices including composting in order to avoiding landfilling organic waste and others emitted CH4. Hargreaves et al. (2008) reported that organic waste composting had a potential as a beneficial recycling tool for waste management and treatment. Furthermore, this method reduced the volume of waste which goes to landfill and the production appropriated for applying agriculture fields as safety fertilizer as well as avoiding biogenic CO_2 emission by long time C storage in soil (Boldrin et al., 2009).

REFERENCES

Beck-Friis, B., Smars, S., Jönsson, H., Kirchmann, H. (2001) Gaseous emissions of carbon dioxide, ammonia and nitrous oxide from organic household waste in a compost reactor under different temperature regimes. Journal of agricultural engineering research 78, 423-430.

Boldrin, A., Andersen, J.K., Møller, J., Christensen, T.H., Favoino, E. (2009) Composting and compost utilization: accounting of greenhouse gases and global warming contributions. Waste Management & Research 27, 800-812.

Forster, P., V. Ramaswamy, P. Artaxo, T. Berntsen, R. Betts, D.W. Fahey, J. Haywood, J. Lean, D.C. Lowe, G. Myhre, J. Nganga, R. Prinn, G. Raga, M. Schulz and R. Van Dorland, (2007) Changes in Atmospheric Constituents and in Radiative Forcing, in: Solomon, S., D. Qin, M. Manning, Z. Chen, M. Marquis, K.B. Averyt, M.Tignor and H.L. Miller (Ed.), Climate Change 2007: The Physical Science Basis. Contribution of Working Group I to the Fourth Assessment Report of the Intergovernmental Panel on Climate Change. Cambridge University Press, Cambridge, United Kingdom and New York, NY, USA.

Fuglestvedt, J.S., Berntsen, T., Godal, O., Sausen, R., Shine, K.P., Skodvin, T. (2001) Assessing the metrics of climate change: current methods and future possibilities. Report/CICERO-Senter for klimaforskning.

Gentil, E., Christensen, T.H., Aoustin, E. (2009) Greenhouse Gas Accounting and Waste Management. Waste Management & Research 27, 696-706.

Hargreaves, J.C., Adl, M.S., Warman, P.R. (2008) A review of the use of composted municipal solid waste in agriculture. Agriculture, Ecosystems & Environment 123, 1-14.

HSO, (2011) Hanoi Statistical Year book 2010, in: Office, H.S. (Ed.). Statistic Publisher, Hanoi, Vietnam.

IPCC (2006) 2006 IPCC Guidelines for National Greenhouse Gas Inventories - Vol 5: Waste. IPCC National Greenhouse Gas Inventories Programme, Institute for Global Environmental Strategies (IGES), Hayama, Japan.

ISWA, (2010) ISWA White Paper: Waste and Climate Change, in: Gary Crawford, C.F., Jens Aage Hansen, Antonis Mavropoulos (Ed.). International Solid Waste Association, Vienna, Austria.

JICA, (2011) Report on solid waste management research in Vietnam 3/2011 Hanoi, Vietnam.

MONRE, (2011) Nationa Report on Environment 2011: Solid Waste, in: Environment, M.o.N.R.a. (Ed.). Ministry of Natural Resource and Environment, Hanoi, Vietnam.

Savino, A.A. (2009) Editorial. Waste Management & Research 27.

Scheutz, C., Kjeldsen, P., Gentil, E. (2009) Greenhouse gases, radiative forcing, global warming potential and waste management — an introduction. Waste Management & Research 27, 716-723.

UNEP (2010) Waste and Climate Change: Global trends and strategy framework UNEP, Osaka/Shiga.

URENCO, (2011) Solid Waste Report. Hanoi urban environment one member limited company, Hanoi, Vietnam.

Optimisation of indoor environmental quality and energy consumption within urban office buildings

Tran Ngoc QUANG
Department of Building Service Engineering and Built Environment
National University of Civil Engineering, Hanoi, Vietnam
tnq.qut@gmail.com

ABSTRACT

This paper summaries the author's PhD work, which has been conducted in Brisbane, a capital city of the State of Queensland, Australia. The research aimed to investigate particle characteristics and dynamics inside and around office buildings, together with their relationship to one another and the factors which affect them. Based on the above, a multi-component model, including indoor particle number (PN) model, was developed and applied to optimise indoor environmental quality and energy consumption in office buildings. The significant contributions of this study include: (i) an improved understanding of particle characteristics (particle number size distribution - PNSD and $PM_{2.5}$) around building envelopes under the influence of vehicle emissions and nucleation events; (ii) an improved understanding of indoor particle characteristics and dynamics inside mechanically ventilated office buildings; (iii) acknowledgement of the role of nucleation events in producing particles, and their influence on urban environment (this is the first time that the effect of new particle formation on the vertical profiles of particle concentrations around building envelopes and PN concentration inside office buildings has been identified and quantified); (iv) the first multi-component model consisting of indoor PN and CO_2 concentration, thermal comfort and energy usage, which can be applied to optimise HVAC systems in mechanically ventilated office buildings; and finally (iv) provision of scientific and practical information on which to base the selection, location and operation of filters and outdoor air intakes in a building's HVAC system, in order to optimise its operation, in terms of energy conservation and improvements in indoor environmental quality.

Keywords: *ultrafine particle, particle number (PN), particle number size distribution (PNSD), vehicle emission, nucleation event, multi-component model*

1. INTRODUCTION

In most urban environments, vehicle emissions and new particle formation are the dominant source of outdoor particles ((Perez et al., 2010; Pey et al., 2008; Shi et al., 2001; Shi and Harrison, 1999; Shi et al., 1999; Wahlina et al., 2001) and (Cheung et al., 2011; Cheung et al., 2012; Pey et al., 2009), respectively).

Ambient air quality legislation regulates airborne particulate matter, in terms of particle mass concentration, expressed as $PM_{2.5}$ and PM_{10} (mass concentrations of particles smaller than 2.5µm and 10µm respectively), and to date, these are also the most common parameters measured for research purposes. However, the majority of particles emitted by vehicles, in terms of number, belong to the ultrafine size range (UF < 0.1µm). UF particles contribute very little to $PM_{2.5}$ and PM10, however they contain the majority of toxins emitted by combustion sources. Epidemiological research has consistently shown an association between fine (< 2.5 µm; $PM_{2.5}$) particle concentrations and increases in both respiratory and cardiovascular morbidity and mortality (Davidson et al., 2005; Pope, 2000; Schwartz and Neas, 2000). The health effects of UF particles are less well understood, however recent research indicates that they may be equally or more detrimental than those of $PM_{2.5}$ and PM_{10} (Franck et al., 2011; Oberdorster, 2000).

Significant population growth and urbanisation has been experienced by most large cities in the world, including capital cities in Australia, where population growth was by 17% between 2001 and 2011, faster than the remainder of Australia (11%) (Statistics, 2011).New approaches to land and urban planning are needed in order to accommodate significant population growth, however such approaches, which include transit oriented urban development, can increase the number of public and residential developments located close to transport corridors. Given that outdoor particles can penetrate the building envelope via doors, windows, building structure leakages and mechanical ventilation systems, the exposure of building occupants to outdoor particles is on the rise.

In Australia, most public buildings are equipped with mechanical heating, ventilation and air conditioning systems. The function of these systems is to remove pollution generated indoors from the indoor environment, to filter outdoor air supplied to the building, and to provide the required thermal comfort conditions within the building. However, mechanical ventilation systems always require considerable amounts of energy to operate. Many efforts have been made to optimise building HVAC systems, however most studies have focused on indoor thermal comfort and energy consumption (e.g. Al-Sanea and Zedan (2008), Chowdhury et al. (2008), Freire et al. (2008), Taylor et al. (2008), Conceição et al. (2009)). Some studies also considered indoor air quality, but only indoor CO_2 concentration was taken into account (Atthajariyakul and Leephakpreeda, 2004; Congradac and Kulic, 2009; Kavgic et al., 2008; Mathews et al., 2001; Nassif et al., 2008; Wong et al., 2008a; Wong et al., 2008b).

An urban environment is characterised by the presence of a large number of roads, bordered on either side by buildings of various sizes. Changing building heights and small local structures in street canyons can generate very complex wind patterns and turbulence, which result in localised areas that experience low wind flow. Vehicle movement, together with wind induced turbulence and efficient mixing, can lead to inconsistencies in the vertical profile of particle concentrations around building envelopes, which has been reported regularly in scientific literature.

The contribution of outdoor and indoor particle sources to the concentration of indoor particle varies and depends on many factors, including the type of particle source, air exchange rate in the building and the type of filters used. Besides dominant outdoor sources in the urban environment consisting of vehicle emissions and new particle formation, printing and vacuum cleaning were recently reported as the main sources of indoor particles in office buildings. Ventilation systems that utilise filter media can reduce indoor particle levels which originated from both outdoor and indoor sources. However, information on the impact of such systems on indoor particle concentration, especially fine and UF particles in office buildings, is very limited.

Given that fine and UF particles are ubiquitous, emitted from both indoor and outdoor sources and can be toxic to human health, they could be considered just as, or even more dangerous than many other indoor pollutants. However, due to a lack of information regarding the characteristics and dynamics of particles in and around office buildings, fine and UF particle concentrations have yet to be considered in the optimisation of building HVAC systems.

The main goal of this research project was to develop a tool that will allow building designers and managers to maximise indoor environmental quality while minimising energy consumption to provide better indoor office environments in order to protect the health of building occupants within office buildings located in high outdoor particle concentration areas. The following specific objectives were implemented to achieve the study goal: (1) Assess the variation of PNSD, PN and $PM_{2.5}$ concentrations at the rooftop and street levels of three urban office buildings located close to busy roads in Brisbane, Australia; (2) Quantify vertical profiles of PNSD and $PM_{2.5}$ concentration around these buildings and analyse the influence of vehicle emissions and nucleation events on these vertical profiles; (3) Quantify and interpret differences between PNSD and $PM_{2.5}$ concentration at different levels around these buildings; (4) Determine indoor and outdoor particle concentrations in these buildings; (5) Quantify the in-situ efficiency of different filter types in these buildings; (6) Assess the impact of ventilation systems using these filters on indoor particle levels under the influence of different indoor and outdoor particle sources; (7) Adopt, validate, assess and apply an existing dynamic indoor particle number concentration model to evaluate their important factors affecting indoor particle levels; (8) Develop a multi-component model for the optimisation of indoor air quality, thermal comfort and energy consumption; and (9) Apply the multi-component model for assessing indoor air quality and energy usage in mechanically ventilated office buildings.

2. SUMMARY OF THE RESEARCH METHODS

The research was conducted in the subtropical city of Brisbane, which is the capital city of Queensland, Australia. Three urban office buildings, located close to busy roads with different terrains, heights, and mechanical ventilation systems, were selected.

Two sets of instruments including TSI 3934 Scanning Mobility Particle Sizer (SMPS), TSI 3781 Condensation Particle Counter (CPC), and TSI 8520 DustTrak aerosol monitor, were used to simultaneously measure PNSD, PN, and $PM_{2.5}$ concentrations, respectively at different levels surrounded building envelopes, and at upstream and downstream of central plant room filters at all three buildings.

At the same time, other set of instruments including TSI 3025 CPC, TSI 8520 DustTrak, and TSI 8552 QTrak, were used to measure indoor air quality, consisting of PN, $PM_{2.5}$, CO_2, CO, Temperature, and Relative Humidity, respectively.

Relevant meteorological parameters and traffic densities were obtained from the Queensland Bureau of Meteorology weather station located in Brisbane CBD and Queensland Department of Transportation, respectively.

An existing indoor particle concentration model was modified, validated to model indoor particle concentrations under different sources and ventilation scenarios.

An indoor CO_2 concentration model was also developed to integrate with the indoor particle concentration model to optimal outdoor ventilation rates.

Finally, an HVAC energy consumption model related to outdoor air ventilation was built up based on the optimal outdoor ventilation rates and optimal indoor thermal comfort.

All statistical analyses (correlation, regression, t-test, One-Way ANOVA, …) were conducted using SPSS for Window version 18 (SPSS Inc.). The 5% level was used to indicate statistical significance in all cases.

The detail description of the research methods is provided in the author’s journal papers (Quang et al., 2013a; Quang et al., 2012; Quang et al., 2013b).

3. SUMARY OF THE MAIN STUDY RESULTS AND DISCUSSION

In the first paper (Quang et al., 2012), the vertical profiles of particle concentrations around three office buildings in Brisbane were quantified and the influence of vehicle emissions and new particle formation were determined. The major findings of this work are summarised below.

As expected, vehicle emissions strongly influenced both PN and $PM_{2.5}$ concentrations at both street and roof levels, especially during rush-hours at all three buildings. Similarly, building topography, distance from the emission sources, and wind speed and direction also had an observed effect on particle concentrations at the three buildings.

On the other hand, new particle formation events were found to influence and contribute to increases in PN concentrations at both rooftop and street levels at all three buildings. However, the factors that contributed to the observed phenomena were different between buildings. For those buildings close to busy roads, the new particles were mainly formed from local vehicle emissions and therefore, the formation process was expected to depend mainly on local conditions, such as high condensable gas concentrations and solar radiation intensity, together with low pre-existing particle concentrations. Meanwhile, for buildings where the newly formed particles were blown in from the direction of a nearby industrial zone, new particle production was not the result of local sources but was strongly influenced by wind speed, wind direction and the origin of incoming air masses. Therefore, all of these factors need to be undertaken into consideration prior to modelling urban canyon particle profiles and concentrations, and a 'one-size-fits-all' approach is unlikely to be able to account for the specific determinants at each individual building. In addition, nucleation events are often studied in the context of their role as physical phenomena, and typically within the context of producing natural and anthropogenic aerosols that may affect climate change. This study has shown that the typically under-valued role of nucleation can produce particles that can affect large numbers of people, due to the high density and occupancy of urban office buildings and the fact that the vast majority of people's time is spent indoors.

The vertical profiles of $PM_{2.5}$ concentrations around building envelopes were found of decreasing concentrations with increasing height. However, vertical profiles of PNSD were building-specific and the rate of change with height was different at all three buildings. The results indicate that it is not only vehicle emissions that influence particle vertical profiles, but new particle formation as well, with both increases in particle number and a reduction in particle mass observed during nucleation events. These results serve to further define the specific effect of roadway proximity and nucleation formation on the vertical profiles of PN and $PM_{2.5}$ concentrations around building envelopes. Moreover, the highly building-specific nature of these profiles and factors affecting them, indicate that measurements should form the basis of any modelling or planning exercise prior to or after the construction of a new building. Such an approach, which is currently lacking for the most part, will ensure the greatest reliability. This has important implications for selecting appropriate sites for the air intakes of building HVAC systems, in order to minimise occupant exposure to combustion products and also to investigate how street-level exposures may be mitigated via improved design practices.

Correlations between PNSD and $PM_{2.5}$ were characterised by a significant variability and dependence on particle size fraction, measured height and particle emission sources. The linear correlations for the building envelopes, especially during rush-hours and nucleation events, varied fluctuated significantly. This indicates that it is not appropriate to use particle mass concentrations to infer PN concentrations when modelling vertical concentrations around the building envelope and at a street level. This finding, while not a novel observation, adds weight to the existing case for considering particle mass and number separately during any urban modelling or exposure assessment exercise.

In summary, vertical profiles of $PM_{2.5}$ concentration around building envelopes showed a consistent decrease in concentration with increasing distance from nearby streets. However, vertical profiles of PN size fraction concentrations were building-specific and its rate of change was inconsistent with height. These results were not unexpected, in view of the complex flow patterns around the building envelopes, as well as in the busway and street canyons that were proximate to some of the buildings. The results of simultaneous measurements indicated that it was not only vehicle emissions, but also new particle formation that influenced the vertical profiles of particle concentrations. Time series ratios of PN and $PM_{2.5}$ concentrations at street and rooftop levels showed clear diurnal variation, which suggests that it is impossible to generalise vertical profiles of particle concentrations for all buildings, and that there is a need to conduct measurements or model these vertical profiles for a specific case when planning building morphology and air intake locations. Furthermore, newly formed particles and building-scale variability should also be taken into account when modelling particle concentrations around the building envelope, and also for urban environments and the exposures that occur within them.

The results of this work serve to provide better insight into the impact of nucleation and local scale variability on particle concentrations, and will also help to better define particle behaviour and variability around building envelopes, which has implications for studies of both human exposure and particle dynamics.

The influence of ventilation and filtration on indoor particle concentration within office buildings located close to busy traffic areas was reported in the second paper (Quang et al., 2013a). The findings and their implications can be summarised accordingly.

The average indoor PN and $PM_{2.5}$ concentrations were (2.46 – 5.71) $\times 10^3$ p cm^{-3} and 5.2 – 6.81 µg m^{-3}, respectively, and the average outdoor PN and $PM_{2.5}$ concentrations were (8.94 – 17.4) $\times 10^3$ p cm^{-3} and 9.25 – 13.9 µg m^{-3}, respectively, for the three buildings. The significantly higher indoor and outdoor particle concentrations for Building A compared to Buildings B and C were due to the proximity of this building's air intakes to a strong outdoor particle source (i.e. busway). This suggests that the location of the HVAC system's outdoor air intakes can significantly reduce the impact of outdoor particles on indoor air.

The in-situ efficiency of deep bag (DB) filters ranged from 26.3 to 46.9% for the three buildings, while the efficiency of the electrostatic (ES) filter in Building C was 60.2% and the efficiency of the fan coil unit (FCU) filter in Building A was 21%. The results show that the efficiency of the DB filters was strongly affected by particle characteristics, in particular particle size and particle upstream concentration. The efficiency of the ES filter was lower than those tested in the laboratory, which could be due to the different operating conditions and upstream particle characteristics between the real-world and laboratory environments. However, this work only measured one ES filter in one office building and therefore, further investigations into in-situ ES filter efficiency under different conditions is recommended. Additionally, the overall filtration efficiency of the FCU filter was significantly lower than those applied in the central plant rooms. This result strongly suggests that a better filter needs to be used for the FCU, in order to clean outdoor air, if it contains high particle concentrations.

The I/O particle concentration ratios showed that mixing air filters not only prevent outdoor particles penetrating indoors, but they also reduce the impact of indoor particle sources on indoor particle concentrations. On the other hand, the utilisation of both outdoor and mixing air filters can significantly reduce and keep indoor particle concentration lower when compared to the use of only mixing air filters.

Based on the comparison of I/O particle concentration ratios and their I/O correlation during rush-hours, nucleation events and overall working-hours, the results indicate that indoor PN concentration was strongly influenced by outdoor PN concentration during rush-hours and nucleation events. Many studies have investigated new particle formation and its effect on regional environments or climate change, but they are yet to focus on indoor environments, especially office buildings. Once again, this work draws attention to the under-valued role of nucleation in generating particles that can penetrate inside buildings and affect large numbers of people, due to the high density and occupancy of urban office buildings.

A previously reported dynamic model for indoor PN concentration was modified, evaluated and applied to assess the influence of the filtration/ventilation systems on indoor particle levels under different indoor and outdoor particle source conditions. The results of the 24 h modelling indicated that the model performed very well when outdoor air was the main source of indoor particles, with less uncertainty for indoor source emissions, or when the ventilation system was turned off. These results also highlighted the fact that the filtration of both mixing air and outdoor air can significantly reduce indoor particle levels.

These findings provide scientific grounds for the selection and location of appropriate filters and air intakes in building HVAC systems, in order to minimise occupant exposure to high outdoor particle concentrations from combustion products and new particle formation. The results also serve to provide a better understanding of indoor particle dynamics and behaviours in office buildings, under different ventilation scenarios.

Based on the findings of the first and second papers, a multi-component model was developed, in order to optimise indoor environmental quality and energy consumption in mechanically ventilated office buildings located close to high outdoor PN concentrations originating from vehicle emissions and/or new particle formation (Quang et al., 2013b). Indoor PN and CO_2 concentrations, and energy usage were evaluated under different operation modes, for optimal indoor temperature settings (according to a survey of building occupant preferences) during summer and winter. It was found that indoor air quality and potential energy savings increased significantly when the ventilation system as operated according to optimal operation modes compared to the normal modes used during the summer and winter months. If combined with other building thermal load components, the model will become more comprehensive and highly effective for the simulation and operation of HVAC systems to maximise indoor air quality and minimise energy consumption within office buildings located close to busy traffic areas.

4. CONCLUSIONS

This is the first time that the influence of new particle formation on the particle concentrations around the building envelopes and inside the office buildings has been identified and quantified. This research developed the first multi-component model consisting of indoor PN and CO_2 concentrations, thermal comfort and energy usage, and it can be applied to optimise building HVAC systems. Overall, this study not only improves scientific understanding and knowledge regarding the characteristics and dynamics of particles around and inside office buildings, but also provides scientific and practical information for the design, upgrading and operation of HVAC systems in mechanically ventilated office buildings.

ACKNOWLEGEMENT

The author would like to express his sincere appreciation and gratitude to his principal supervisor, Professor Lidia Morawska, for her continuous advice, suggestions and encouragement throughout the course of this study. Without her close supervision, this study would have never come to fruition. The author expresses his profound gratitude to his co-supervisor, Dr Congrong He, for his constructive comments and valuable suggestions during the course of this research. The author is also grateful to the Queensland University of Technology (QUT) for providing a tuition fee waiver scholarship, together with the Vietnamese Government, the School of Physical and Chemical Sciences, QUT and the International Laboratory for Air Quality and Health - ILAQH, QUT for providing living allowance scholarships.

REFERENCES

Al-Sanea, S.A., Zedan, M.F., 2008. Optimized monthly-fixed thermostat-setting scheme for maximum energy-savings and thermal comfort in air-conditioned spaces. Applied Energy 85, 326-346.

Atthajariyakul, S., Leephakpreeda, T., 2004. Real-time determination of optimal indoor-air condition for thermal comfort, air quality and efficient energy usage. Energy and Buildings 36, 720-733.

Cheung, H.C., Morawska, L., Ristovski, Z.D., 2011. Observation of new particle formation in subtropical urban environment. Atmospheric Chemistry and Physics 11, 3823-3833.

Cheung, H.C., Morawska, L., Ristovski, Z.D., Wainwright, D., 2012. Influence of medium range transport of particles from nucleation burst on particle number concentration within the urban airshed. Atmospheric Chemistry and Physics 12, 4951-4962.

Chowdhury, A.A., Rasul, M.G., Khan, M.M.K., 2008. Thermal-comfort analysis and simulation for various low-energy cooling-technologies applied to an office building in a subtropical climate. Applied Energy 85, 449-462.

Conceição, E.Z.E., Lúcio, M.M.J.R., Ruano, A.E.B., Crispim, E.M., 2009. Development of a temperature control model used in HVAC systems in school spaces in Mediterranean climate. Building and Environment 44, 871-877.

Congradac, V., Kulic, F., 2009. HVAC system optimization with CO2 concentration control using genetic algorithms. Energy and Buildings 41, 571-577.

Davidson, C.I., Phalen, R.F., Solomon, P.A., 2005. Airborne particulate matter and human health: A review. Aerosol Science and Technology 39, 737-749.

Franck, U., Odeh, S., Wiedensohler, A., Wehner, B., Herbarth, O., 2011. The effect of particle size on cardiovascular disorders — The smaller the worse. Science of The Total Environment 409, 4217-4221.

Freire, R.Z., Oliveira, G.H.C., Mendes, N., 2008. Predictive controllers for thermal comfort optimization and energy savings. Energy and Buildings 40, 1353-1365.

Kavgic, M., Mumovic, D., Stevanovic, Z., Young, A., 2008. Analysis of thermal comfort and indoor air quality in a mechanically ventilated theatre. Energy and Buildings 40, 1334-1343.

Mathews, E.H., Botha, C.P., Arndt, D.C., Malan, A., 2001. HVAC control strategies to enhance comfort and minimise energy usage. Energy and Buildings 33, 853-863.

Nassif, N., Moujaes, S., Zaheeruddin, M., 2008. Self-tuning dynamic models of HVAC system components. Energy and Buildings 40, 1709-1720.

Oberdorster, G., 2000. Toxicology of ultrafine particles: in vivo study. Philos Trans R Soc London A 358, 2719-2740.

Perez, N., Pey, J., Cusack, M., Reche, C., Querol, X., Alastuey, A., Viana, M., 2010. Variability of Particle Number, Black Carbon, and PM(10), PM(2.5), and PM(1) Levels and Speciation: Influence of Road Traffic Emissions on Urban Air Quality. Aerosol Science and Technology 44, 487-499.

Pey, J., Querol, X., Alastuey, A., Rodriguez, S., Putaud, J.P., Van Dingenen, R., 2009. Source apportionment of urban fine and ultra-fine particle number concentration in a Western Mediterranean city. Atmospheric Environment 43, 4407-4415.

Pey, J., Rodriguez, S., Querol, X., Alastuey, A., Moreno, T., Putaud, J.P., Van Dingenen, R., 2008. Variations of urban aerosols in the western Mediterranean. Atmospheric Environment 42, 9052-9062.

Pope, C.A., 2000. Review: Epidemiological basis for particulate air pollution health standards. Aerosol Science and Technology 32, 4-14.

Quang, T., He, C., Morawska, L., Knibbs, L., 2013a. Influence of ventilation and filtration on indoor particle concentrations in urban office buildings. Atmospheric Environment 79, 41-52.

Quang, T., He, C., Morawska, L., Knibbs, L., Falk, M., 2012. Vertical particle concentration profiles around urban office buildings. Atmospheric Chemistry and Physics 12, 5017-5030.

Quang, T., He, C., Nibbs, L., Dear, R., Morawska, L., 2013b. Optimisation of indoor environmental quality and energy consumption within urban office buildings. Environmental Science & Technology - Submitted.

Schwartz, J., Neas, L.M., 2000. Fine particles are more strongly associated than coarse particles with acute respiratory health effects in schoolchildren. Epidemiology 11, 6-10.

Shi, J.P., Evans, D.E., Khan, A.A., Harrison, R.M., 2001. Sources and concentration of nanoparticles (<10 nm diameter) in the urban atmosphere. Atmospheric Environment 35, 1193-1202.

Shi, J.P., Harrison, R.M., 1999. Investigation of Ultrafine Particle Formation during Diesel Exhaust Dilution. Environmental Science & Technology 33, 3730-3736.

Shi, J.P., Khan, A.A., Harrison, R.M., 1999. Measurements of ultrafine particle concentration and size distribution in the urban atmosphere. The Science of The Total Environment 235, 51-64.

Statistics, A.B.o., 2011. Regional Population Growth, Australia, 2011. Australian Bureau of Statistics - http://www.abs.gov.au/.

Taylor, P., Fuller, R.J., Luther, M.B., 2008. Energy use and thermal comfort in a rammed earth office building. Energy and Buildings 40, 793-800.

Wahlina, P., Palmgren, F., Van Dingenen, R., 2001. Experimental studies of ultrafine particles in streets and the relationship to traffic. Atmospheric Environment 35, Supplement 1, S63-S69.

Wong, L.T., Mui, K.W., Chan, W.Y., 2008a. An energy impact assessment of ventilation for indoor airborne bacteria exposure risk in air-conditioned offices. Building and Environment 43, 1939-1944.

Wong, L.T., Mui, K.W., Hui, P.S., 2008b. A multivariate-logistic model for acceptance of indoor environmental quality (IEQ) in offices. Building and Environment 43, 1-6.

A basic study on future strategy for effective disaster information dissemination: Case study in Thailand

Niwat APICHARTBUTRA[1], Miho OHARA[2]

[1]Doctor Course Student, Department of Civil Engineering,
Graduate School of Engineering, the University of Tokyo, Japan
niwat-a@iis.u-tokyo.ac.jp
[2]Associate Professor, International Center for Urban Safety Engineering,
Institute of Industrial Science
The University of Tokyo, Japan
ohara@iis.u-tokyo.ac.jp

ABSTRACT

Information Dissemination is considered as one of the most important tools to disaster risk reduction; yet, if poorly managed, it can pose hindrances to disaster mitigation process. This paper examines disaster information dissemination system in Thailand. It intends to investigate how disaster-related information was disseminated during Thailand's most extensive inundation in 2011; and, attempts to draw recommendations. During the flood, the Thai government tried to establishment disaster information communication with the people. However, its attempt was not successful. This led to frustration of a majority of Thai people and, in turn, triggered a momentum of information flow in various forms and means of informal communication. In the latter part of this report strategies for effective disaster information dissemination are also proposed in a 3-tiered framework.

Keywords: *disaster information dissemination, Thailand flooding 2011*

1. INTRODUCTION

In July 2011, Thailand was hit severely by the build-up of waters brought by a 25% increase in average season rainfall. The inundation later spread through provinces of the Northern, North-Eastern and Central Thailand along the Mekhong and the Choa Phraya river basins and became the country's most extensive inundation in 70 years. The flood claimed more than 600 lives; and the World Bank (2011) estimated economic losses were at 45.7 billion USS. Due to the exorbitant lost, there were a number of evidence pointing that Thailand was unable to deliver effective disaster information to the people, which led to poor management of the flood and an urgency to develop a comprehensive framework to manage disaster. (Larnard and Sandman, 2011; Coben, 2011; Reuters, 2011; Bangkok Post, 2013)

Flood risk communication studies have been carried out extensively in the US and Europe as one of the most important tools to disaster risk reduction. (Cole T.W. and Fellows K.L, 2008; Tinker T.L. and Galloway, Jr. E.G., 2009; Bradford and O'Sullivan, 2011) In case of Thailand, however, there is a limited number of studies carried out in terms of flood disaster information dissemination during the worst flood in 2011. Therefore, this paper intends to investigate how disaster-related information was disseminated during Thailand's most extensive inundation in 2011. It focuses on disaster information dissemination in Thailand; and, attempts to draw recommendations. In this study, strategies for effective disaster information dissemination are also proposed.

2. THAILAND'S 2011 FLOOD DISASTER INFORMATION DISSEMINATION

To investigate disaster information dissemination during the 2011 flood, this report employs documentary research methodology and breaks lines of communication during Thailand's 2011 inundation into 2 periods using October 8, 2011, as the breakpoint because October 8, 2011, was when the Prime Minister of Thailand ordered a setup of Flood Relief Operations Centre (FROC) as the "one stop service" for flood-related matters including information and warning dissemination. The 2 periods comprises (1) Thailand's disaster information dissemination before October 8, 2011, and (2) Thailand's disaster information dissemination after October 8, 2011.

2.1 Thailand's disaster information dissemination before October 8, 2011

According to the National Disaster Prevention and Mitigation Plan B.E. 2553-2557 (2010-2014), Thailand's latest disaster prevention and mitigation scheme, general requirements have been introduced for effective disaster information dissemination. The following government agencies responsible for disaster information dissemination have to make notifications.

- Thai Metrological Department (TMD) and National Disaster Warning Center (NDWC) are responsible for close surveillances and warning at national level.
- Department of Disaster Prevention and Mitigation (DPM) receives warning information from TMD and NDWC and some relevant agencies and further disseminates warning information to the provincial government.
- Provincial government is responsible for the watch-out and dissemination of warning information at provincial level.
- District office is responsible for surveillance and dissemination of warning information at district level.
- Civil Defense Volunteer and warning information dissemination network are responsible for surveillance and dissemination of warning information at community level.

2.2 Thailand's disaster information dissemination after October 8, 2011

On October 8, 2011, the Prime Minister of Thailand set up the Flood Relief Operations Centre (FROC) in an effort to solve floods in a coherent and comprehensive manner. One of FROC main duties was to be the center of flood-related information to send out important information to people such as situation evaluation and warning. The Justice Minister was appointed to take charge FROC along with the Interior Ministry's Deputy Permanent Secretary. The Science and Technology Minister was put in charge of operations. The Transport Minister managed FROC's information and public relations. Governors of local entities were to follow FROC's orders in managing the floods in their respective localities and encouraged to set up provincial versions of FROC. The armed forces as well as other governmental agencies were to take orders from the Prime Minister's Office. Later in October 20, 2011, the Prime Minister invoked Section 31 of the 2007 (B.E. 2550) Disaster Prevention and Mitigation Act which gave the prime minister a single control to all officials.

In the setup day, FROC was assigned as the focal point to disseminate disaster information to people. Apart from regular announcement through mass media, FROC opted to send information in short messages (SMS) through mobile phone. It appointed the National Broadcasting and Telecommunications Commission (NBTC) to look after the task. NBTC summoned ad hoc cooperation with the 3 major mobile phone network carriers in Thailand, namely AIS, DTAC, and TRUE.

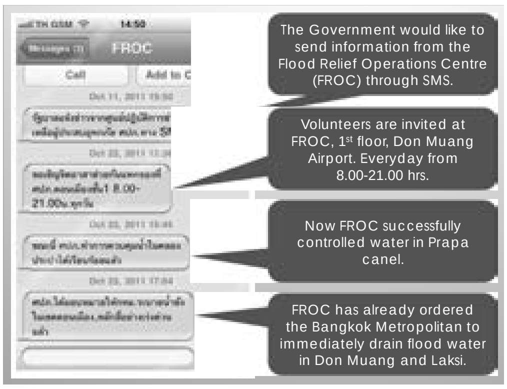

Table 1 : The 4 short messages sent by FROC

Unfortunately, FROC did not mount a united front in its management of the floods crisis and lost its credibility. (Chinchit, 2011) The FROC's chief often gave contradictory statements to the media, issued a false sense of confidence to the public and, most importantly, delivered irrelevant information that people did not really need. (Thairath, 2011) Its first SMS was released on October 11, 2011 and the last one was reported to be received on the October 23, 2011. Altogether, it was reported in Thairath newspaper (2011) that there were 4 messages sent by FROC and the people were not satisfied with the content of them because they did not serve the purpose of early warning and evacuation. Figure 1 shows the 4 messages with translation. On October 24, 2011, FROC officially announced that it had stopped sending SMS to the people by giving the reasons that "sending information via SMS messages is limited to 70 alphabets. The limitation would cause messages confusing and subjected to people's interpretation."

Matichon Newspaper (2011) reported that Assumption University's ABAC Poll Research Centre surveyed 415 people living in Bangkok and adjacent provinces in October 2011 regarding FROC's credibility. The survey revealed that nearly 90 percent of the respondents said they were confused by announcements from FROC. 87% said they did not trust information from FROC and 86% said FROC did not provide clear information as to whether their homes would be flooded. They gave average score of 3.36 out of 10.

Now FROC still exists but appears to be inactive under the Ministry of Natural Resources and Environment.

3. THAI GOVERNMENT AGENCIES RELATED TO FLOOD DISASTER DISSEMINATION

Apart from the aforementioned agencies, there are also a number of government agencies that routinely take part in disseminating flood information in Thailand. Some send warning and useful information directly to the people while some are in charge of information gathering, monitoring as well as issuing warning and useful information to concerned agencies. This part of the paper attempts to gather relevant agencies that disseminate disaster information particularly flood-related information to the people. Through an observation, there are 10 following agencies related to flood information dissemination in Thailand. Ones marked Ⓦ have warning systems.

1. Thai Meteorological Department (TMD) Ⓦ
2. National Disaster Warning Centre (NDWC) Ⓦ
3. Department of Disaster Prevention and Mitigation (DPM) Ⓦ
4. Department of Mineral Resource (DMR) Ⓦ
5. Department of Water Resources (DWR) Ⓦ
6. Department of National Park, Wildlife and Plant Conservation (DNP) Ⓦ
7. Royal Irrigation Department (RID) Ⓦ
8. Hydro and Agro Informatics Institute (HAII)
9. Electricity Generating Authority of Thailand (EGAT) Ⓦ
10. Bangkok Metropolitan Administration

All 10 agencies have established their own means to communicate with the people mostly through websites and some have certain system that issues warnings to (1) concerned agencies and/or (2) areas or people that might be at risk. Table 1 shows agencies that have warning systems, while Table 2 shows agencies that have monitoring function. To mention some, DPM and DMR have established a network of trained volunteers that can disseminate disaster information to the local people and collect information from the at-risk sites to send back to central authorities. DWR has developed early warning systems in local areas where sound alarm can be triggered after detecting dangerous level of rainfall.

Table 1 : Agencies that have warning systems			
	Agencies	Content of Information	Means of Warning
Issuing warnings to relevant agencies	Thai Meteorological Department (TMD)	Weather Forecast by weather radar and satellite picture	Disaster warning announcement, SMS
	Department of Disaster Prevention and Mitigation (DPM)	Disaster information received from relevant agencies	Disaster warning announcement, SMS
	Department of Mineral Resources (DMR)	Rainfall information, Geo-hazard and landslide information	Disaster warning announcement, SMS
	Royal Irrigation Department (RID)	River Water and Rainfall Information by rain gauging stations, Medium- and Large-sized Reservoir Water Level by Telemetering system	Disaster warning announcement
	Electricity Generating Authority of Thailand (EGAT)	Dam Water Level by Telemetering System	Disaster warning announcement
Issuing warning to people	Thai Meteorological Department (TMD)	Weather Forecast by weather radar and satellite picture	Mass media*
	National disaster warning center (NDWC)	Deep-ocean Assessment and Reporting of Tsunami (Dart), Landslide, Disaster information received from relevant agencies	Mass media, Mobile Phone Application (iOS & Android), Tsunami warning towers
	Department of Disaster Prevention and Mitigation (DPM)	Disaster information received from relevant agencies	Mass media, Mr.Warning**
	Department of Mineral Resources (DMR)	Geo-hazard and landslide, Heavy rain warning	Mass Media, SMS, Volunteer Network (13,857 volunteers in 39 provinces), Village warning tower
	Department of Water Resources (DWR)	Possibility of flood and landslide (in 1,587 at-risk villages)	Early Warning station at risk areas
	Department of National Park, Wildlife and Plant Conservation (DNP)	Forest flood and rainfall information by Rainfall Monitoring Stations in National Conservation Forests (1,034 stations)	Warning through Website
*Mass media means making a national broadcast through TV and Radio. **Mr.Warning is a network of trained community coordinators who give warning to people as well as monitor and send useful information back to central authorities.			

Table 2 : Monitoring Agencies

Agencies	Content of Information	Means of Communication
Thai Meteorological Department (TMD)	Rainfall Statistics, Weather Forecast by Weather Radar, Meteorological Satellite Picture, Dam Water Level Data Analysis, Meteorological Information, Storm Tracking	Website
Department of Mineral Resources (DMR)	Geo-hazard and landslide information, Rainfall information	Website
Department of Water Resources (DWR)	Water Level Monitoring by CCTV (27 sites), Main rivers' water level report by remote water-level gauging stations (114 stations), Flood and Water Information through Mekhala (Centre for Water Crisis)	Website
Department of National Park, Wildlife and Plant Conservation (DNP)	Rainfall Monitoring Stations in National Conservation Forests (1,034 stations)	Website
Royal Irrigation Department (RID)	River Water and Rainfall Information by rain gauging stations, Medium- and Large-sized Reservoir Water Level by Telemetering system	Website
Hydro and Agro Informatics Institute (HAII)	Information on rainfall and storm by Mini Telemetering System/Satellite/Radar	Website
Electricity Generating Authority of Thailand (EGAT)	Dam Water Level by Telemetering System	Website
Bangkok Metropolitan Administration	Rainfall Information by radar, water drainage monitored by Telemetering system	Website

4. FLOOD-RELATED INFORMAL COMMUNICATION

Since the government's attempt to deliver flood information to the people was not successful, frustration of a majority of Thai people was developed and, in turn, triggered a momentum of information in various forms and means of informal communication. One of the channels that Thai people favorably opted for getting information was through the Internet and social networks such as Facebook, Twitter, YouTube, and Weblog. There were statistics showing a sharp increase in messages shared through Twitter during flood disaster in Thailand from 1.5 million messages a day in normal time to about 2.2 million messages a day during the flood (Bangkok Biz, 2011).

Informal communication during the flood can be grouped into 3 following categories with some examples.

Category I Communication that have already existed before the flood and its function changed to disseminate flood information.

- Seub Nakhasathien, YouTube channel, normally served the purpose of promoting forest conservation. During the flood, Sasin Chalermlarp, Secretariat-General of the foundation, used the channel to broadcast his flood analysis. The number of accumulative viewers reached almost a million. The most popular VDO reached 450,000 viewers.
- Muang Ake community used its existing platform such as website and Facebook page to communicate with its inhabitants within the community during flood crisis. Its original function was to share general and administrative information.

Category II Communication that was created for flood purpose but now inactive

- Roosuflood (know and beat the flood) is a YouTube channel that have anime VDO concerning how to fight the flood. Some VDO reached more than 300,000 views. The last activity was May 2012.
- ThaiFightFlood, ThailandFlood2011 and NamKunHaiReepBok (when water rises, we tell) are Facebook account that updated news regarding flood. Their last activities were October and September 2012.

Category III Communication that was created for flood purpose and have functioned up till now.

- www.thaiflood.com and its Facebook and Twitter account were lunched during flood in 2010 and now continues to broadcast flood-related information. Now it has over 70,000 likes.
- Volunteers watchdog for Bangkok flood (in Thai) is Facebook account that created during the flood and still posts flood information.

Though social media has proven to be a popular and effective tool for sharing information, it can hinder response efforts especially when the information is incorrect, malicious, outdated, and inaccurate. In some cases, the location of the hazard or threat was inaccurately reported, or some requests for help were retransmitted repeatedly even after victims were rescued.

5. RECOMMENDATIONS FOR DISASTER INFORMATION DISSEMINATION IN THAILAND

The 2011 flood has led to the necessity that the government established a comprehensive framework for better management of flood disaster in the future. As a result, on 13 February 2012, the government issued the Regulations of the Office of the Prime Minister to improve flood and water prevention and mitigation by integrating work plans of relevant agencies and establishing a central unit that gives command on water management. This directed to the establishment of the Office of the National Water and Flood Management Policy (NWFMP), run by the National Water and Flood Management Policy Committee, chaired by the Prime Minister, with the hope to make comprehensive national water and flood management policy.

However, information communication and dissemination is one of the essential aspect determining whether or not Thailand is to achieve water and flood management. Some hindrances can pose threat to the credibility, and the government might not be able to achieve what it has hoped for. To avoid repeating the 2011 flood's history, strategies for effective disaster information dissemination are proposed in a 3-tiered framework; 1) decision making and warning issuance, 2) information dissemination, and 3) disaster preparation and risk reduction.

Tier I Decision making and warning issuance

- So far, there have been at least 2 government agencies whose duties are to disseminate flood-related information in times of crisis; for example, NDWC and FROC. As a result, there is possibility that Thai people will be confused over which agency they should listen to. Choosing only one agency is recommended to create a true single command to avoid redundancy and confusion.
- This single command must be focal for disaster-related matters. It must be the place where information from monitoring agencies is concentrated and processed, decision is made, and warning is issued.
- It is recommended that NDWC takes the leading role in disaster information dissemination as its objective was aimed to respond to any disaster that might occur in Thailand, unlike any other agencies in Thailand. Also, since its establishment in 2005, NDWC has gradually matured and developed a strong institution needed for disaster information dissemination especially in terms of relationship with other agencies, existing disaster-related technology, and ties with the people.

Tier II Information dissemination

- It is encouraged that the government should use as many and various channels as possible to deliver message to the people since the people are not homogenous and can be categorized in various groups like the handicapped, the flood-inexperienced, foreigners, and the elderly.
- The use of high-technology devices as a means to deliver information must be encouraged such as issuing warning through mobile phones, and sending useful information through websites and social network.
- However, an on-site information dissemination cannot be left out as it is very crucial to deliver information to the people who have no access to high-technology devices. It also help complete a 2-way communication as an on-site information officer can bring some input voiced by the people back to the command center, so that the government can supply accurate solutions.
- Since FROC's messages were reported that they were irrelevant information that people did not really need. The content of messages during flood disaster is recommended to focus on reporting current situation, issuing warning when needed, informing of an evacuation, and providing information regarding risk reduction and activities that help reduce risk.

Tier III Disaster preparation and risk reduction

- The government should also focus on the preparation. Disaster education and preparation should be continuous even though there is no coming disaster.
- Behavioral changes are more likely if they are self-motivated, rather than imposed, and it is likely that some people will have to hear the message coming at them from multiple directions before it has any impact. Therefore,

developing an awareness of current flood information sources such as websites, brochures, and flood campaigns offers potential for empowering individuals and communities to mitigate flood risk in an appropriate manner.

- Scope of content can be larger than that needed in times of disaster and stakeholders can be anyone in the society, from government agencies to parents, sidewalk posters to school teachers.
- Means of promoting information sources includes dissemination through mass media and circulation by post or through recognized access points such as train station, council officers, bus stops, universities, and libraries.

ACKNOWLEDGEMENT

This study was done as a part of the research project “Design of Disaster Information Dissemination system and Proposal of Technical Strategies for Supporting Asian Rural Communities” supported with Grants in Aid for Scientific Research by Japan Society for the Promotion of Science.

REFERENCES

Bangkok Biz, 2011. Thai Social Network Behaviour during Flood Crisis *(in Thai)*. October 26, 2011. Retrieve July 2013, from www.bangkokbiznews.com

Bangkok Post, 2013. Government shows its intractability. May 20, 2013. Retrieved July 2013, from http://www.bangkokpost.com/opinion/opinion/350880/government-shows-its-intractability.

Bradford, R.A., and O’Sullivan, J.J., 2011. Improving Communication Strategies for Effective Flood Risk Management. Unpublished paper for *National Hydrology Conference*. Retrieved July 2013, from http://www.opw.ie/hydrology/data/speeches/05%20-%20Bradford%20-%20Improving%20 Communication%20 strategies%20for%20effective%20flood%20risk%20management.pdf

Chingchit S, 2011. Thailand Flood: Not Enough to Destroy the Government. In *IPRIS Viewpoint*, Volume 78, December 2011.

Coben R., 2011. UN: Southeast Asian Floods Trigger Humanitarian Crisis. October 17, 2011. Retrieved July 2013, from http://www.voanews.com/content/thai-soldiers-rush-to-reinforce-bangkok-flood-walls-132036703/ 146797.html

Cole T.W., and Fellow K.L., 2008. Risk Communication Failure: A Case Study of New Orleans and Hurricane Katrina. In *Southern Communication Journal*, Volume 73, Issue 3, Page 211-228. Routledge, London.

Larnard J., and Sandman P. M., 2011. Over-Reassuring Thai Crisis Communication about the Great Flood: When “Restoring Trust” is too Much to Expect. Retrieved July 2013, from http://www.psandman.com/col/Thai-flood.htm

Matichon, 2011. ABAC Poll Revealed Majority Distrusted FROC and Evaluated 3.36 from 10. October 18, 2011. Retrieve July 2013, from http://www.matichon.co.th/news_detail.php?newsid=1318911293&grpid=03&catid=03

Reuters, 2011. Thai Govt Faces Lawsuit over Flood Crisis Handling. December 22, 2011. Retrieved July 2013, from http://www.trust.org/item/?map=thai-govt-faces-lawsuit-over-flood-crisis-handling/

Thairath, 2011. People unsatisfied: FROC SMS were useless *(in Thai)*. October 24, 2011. Retrieve July 2013, from http://www.thairath.co.th/content/tech/211564

Tinker L.T., and Galloway E.G., 2009. "How to communicate flood risks effectively" in Journal of Business Continuity & Emergency Planning. Volume 3. Number 3.

World Bank, 2011. The World Bank Supports Thailand's Post-Floods Recovery Effort. December 13, 2011. Retrieved July 2013, from http://www.worldbank.org /en/news/feature/2011/12/13/world-bank-supports-thailands-post-floods-recovery-effort

Analysis of initial disaster responses for disaster management stakeholders in emergency and recovery phase for sustainable disaster management system

Muneyoshi NUMADA[1] and Kimiro MEGURO[2]
[1] Research Associate, ICUS, IIS, The University of Tokyo, Japan
numa@iis.u-tokyo.ac.jp
[2] Professor, ICUS, IIS, The University of Tokyo, Japan

ABSTRACT

This research aims to develop a "Sustainable disaster/emergency management system" that enables "seamless transfer from ordinary times to emergency situations".
The system is a time-series disaster management system for that the disaster management stakeholders will no longer be confused by unexpected conditions. In ordinary times, vulnerable or weak points and problems are analyzed and solved. Just before a disaster occurs, emergency alert will be run. In after disaster phase, damages are accurately assessed and are responded accordingly.
To develop this system, it is necessary to make a "spatio-temporal disaster transition model". Because no such model exists today, many disaster management stakeholders have no idea what they should actually do or how their activities contribute to disaster reduction. When they all become aware of the meaning of their roles, effective disaster management cycle would be put into practice.
The key factor in developing effective spatio-temporal disaster transition model is to make accurate estimation ahead of time even from limited information, and then making the best response.
Needless to say, no matter how well we grasp the spatio-temporal transition, it is necessary that each stakeholder has the correct understanding of his/her assignment, or else appropriate disaster response will never be possible.
This paper focus on making and defining disaster response flows for each disaster management stakeholders by analyzing the responses during the Pacific coast of Tohoku earthquake on March 11, 2011. Yabuki town located in Fukushima prefecture is used for the case study of this analysis. The results show that the analyzed flow can clearly explain the role of each stakeholder to response in the emergency and recovery phase.

Keywords: *initial disaster response, disaster management stakeholders, sustainable disaster management system*

1. INTRODUCTION

At 14:46 JST (5:46 UTC) on March 11th, 2011, an earthquake of a moment magnitude 9.0, the largest earthquake ever recorded in Japan, struck off the shore of the Sanriku area in the Tohoku Region. The *"mega tsunami"* followed, deeply hitting indented coastal areas and bringing enormous and devastating damage to many cities and villages in the area. Damage by the "*mega tsunami"* was not only limited to buildings, but the resulting fires destroyed many communities, taking lives of thousands. Moreover, nuclear power plant (NPP) facilities suffered complicated and serious damage. This earthquake was later officially named *"The 2011 off the Pacific coast of Tohoku Earthquake"* by the Japan Meteorological Agency (JMA).

The Magnitude 9.0 "off the Pacific coast of Tohoku earthquake" on March 11, 2011, has caused extensive damage that still continues today. Although Japan had been recognized as one of the leading countries in disaster management, its poor level of risk management or numerous problems in disaster reduction were revealed by this unexpected and unprecedented disaster.

Throughout the centuries, Japan has suffered from natural disasters of many different kinds. And now that the country has entered a seismically active period, damage mitigation is addressed as the major national issue. The Great East Japan Earthquake has taught us the priceless value of safety and sustaining the quality of life.

As one of the solutions to minimize damage, we suggest a total disaster response cycle featuring measures on the following: pre-disaster damage prevention, damage reduction, disaster prediction, alert system, damage assessment, emergency response according to damage assessment, and smooth recovery/reconstruction. Current efforts by regions and organizations should be reviewed (in terms of hard/software and disaster response) while different kinds of hazard and its levels (in terms of intensity, extension and frequency) should also be taken into consideration. After a careful checkup, weak points are sorted out, prioritized under limitations of time and budget, and then starting from the weakest agenda, things move ahead for improvement. This process is the most effective and efficient way to change *"the way things are today"* into *"what they need to be in the future"*.

Our research aims to develop a ***"sustainable disaster/emergency management system"*** to accomplish the above-mentioned process. By following this system, problems will be sorted out accurately, improvements made at ordinary times, alert will be heightened before urgent danger, damage precisely assessed after disaster, and damage response conducted appropriately according to the assessments. It realizes ***"seamless transfer from ordinary times to emergency situations"***.

The biggest challenge lying ahead is to develop a ***"model which accurately estimates spatio-temporal disaster transition"***. Because no such model exists today, many disaster management stakeholders have no idea what they should actually do or how their activities contribute to disaster reduction. When they all become aware of the meaning of their roles, effective disaster management cycle

would be put into practice. The key factor in developing effective the spatio-temporal disaster transition model is to make accurate estimation ahead of time even from limited information, and then making the best response. Needless to say, no matter how well we grasp the spatio-temporal transition, it is essential that each stakeholder has the correct understanding of his/her assignment, or else appropriate disaster response will never be possible.
Effective initial responses in crisis management are important to reduce or minimize the impact of large-scale disasters such as the Great East Japan Earthquake for the prevention of secondary disasters and rescue.
However, it is difficult to operate initial disaster responses effectively for the disaster response headquarters just after the disasters under the condition of the limitation of human and product resources.

In order to solve these problems, there are the current researches such as standardization and system of disaster responses[1,2)].
This study analyze the patterning the kinds of disaster response, defining its flow and evaluating its amount of volume which are expected in advance to build effective the spatio-temporal disaster responses model. By understand these operations for each different actors or players, it will be possible to carry out disaster responses immediately under the condition of confused disaster phase.
This paper provides the case study that the initial responses of Yabuki town in Fukushima prefecture are analyzed during the 5days after the Tohoku earthquake to achieve the effective disaster system.

2. Analysis data

The analysis data in this paper is obtained from the staffs who worked for the disaster response immediately after the earthquake from 11th to 15th March for 5 days.
Table 1 shows the analysis data for a staff which are divided into six time sections for one day as the early morning, morning, daytime, afternoon, evening, night.
The around half numbers of staffs answered to that with the exception of the staffs who could not engage in disaster responses at the time and who have already left or retired after the earthquake (Figure 1). If the staffs transferred to the new department from the department at the disaster, we collected the data as that staffs belongs to previous department.

3. Analysis of disaster responses

3.1Time historical analysis

Table 2 shows the change of the time history of disaster emergency responses. The number inside of this table is the total number of working staffs during the time division. The vertical line is ordered from the higher total numbers of working staffs for a response category item.
According to this result, "food supply", "water supply", "damage investigation" and "evacuation management" are frequent in the order during the five days. 33

staffs worked for the damage investigation on March 11. Many staffs worked for the food supply from March 11.
The number of staffs gradually increased for the water supply and the most of the staffs worked for that on March 14. Because the water in the water tank on the roof of the government building was used up immediately after the disaster, it was necessary to supply water to the people. The water supply was carried out by the truck with water tank at the entrance of the government building.
For evacuation centers, in addition to the distribution of goods, the staffs walked around the all evacuation places to check the number of evacuee.
Due to the damage of JR (Japan railways), some passengers could not move on March 12. Yabuki town received the people who could not go home, and Yabuki town transferred the people to the Shinshirakwa station by the bus of town on the next day of the earthquake

Table 1: example for the analysis data (shown from 11th to 12th March)

	2013/3/11				2013/3/12					
	Immediately	Evening	Night	Midnight	Early morning	morning	Daytime	afternoon	Evening	Night
Division / Name	damage survey	damage survey	damage survey	damage survey	Food supply	Water supply	damage survey	Water supply	Water supply	Food supply

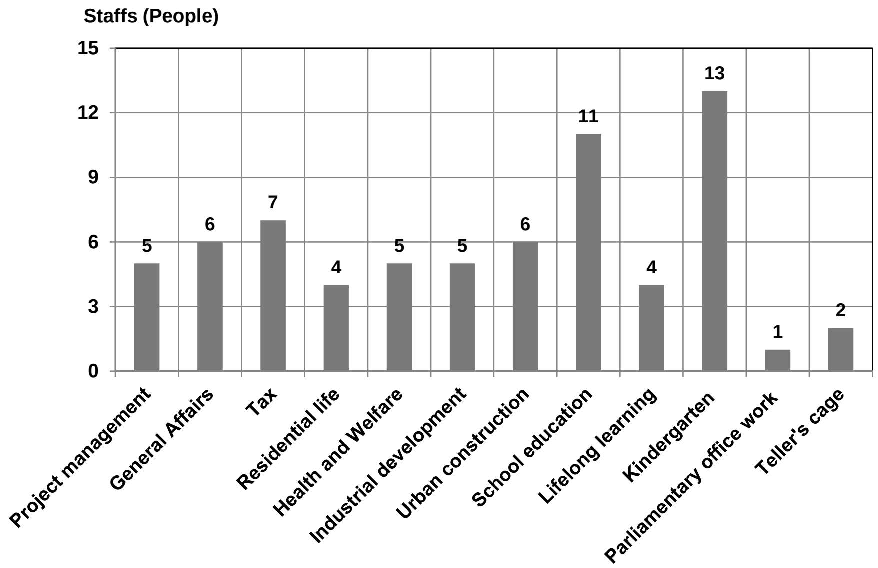

Figure 1: The number of respondents according to divisions

3.2 Analysis for each division

We analyzed the disaster responses for the each department of the town. Table 3 shows that all numbers of working staffs for the each department during 5 days totally. The number in the table describes the working load in each department that the total working people times the total working hours (people × working hours) assumed as 3 hours for each time sections.

Table 2: Time history of disaster response (unit: number of people)

Response items	2013/3/11				2013/3/12						2013/3/13						2013/3/14						2013/3/15						Sum
	Immediately	Evening	Night	Midnight	Early morning	morning	Daytime	afternoon	Evening	Night	Early morning	morning	Daytime	afternoon	Evening	Night	Early morning	morning	Daytime	afternoon	Evening	Night	Early morning	morning	Daytime	afternoon	Evening	Night	
Food supply		6	8	8	13	6	9	8	9	9	12	1	14	1	12	8	13	1	16	12	14	11	7	11	13	13	13	9	284
Water supply		1	1		3	6	3	7	12	3	6	12	9	16	11	7	9	2	17	18	16	14	8	16	14	14	11	7	261
Damage investigation	33	13	8	6	4	16	17	11	7	5	2	6	6	3	4	5	2	4	9	9	5	7	5	8	4	7	5	3	214
Evacuation	1	7	11	5	4	6	3	5	4	8	4	11	9	9	4	2	5	7	4	5	5	5	5	6	5	6	6	9	161
Information collecting	4	1	8	7	5	2	4	5	3	4	4	2	1	2	2	3	5	4	3	2	2	4	4	2	5	4	4	4	109
Goods supply		2	2		2	2	4	3	2			2	3	3	1		1	3	4	4	3	3	2	3	5	6	5	1	66
Emergency safety check of house		1	1		2	3	3	3	3	1	2	3	3	3	3	2		2	2	2	2	2	2	3	3	3	3	1	58
Meeting		1	1	2	3	2			5	1	4	2	2	1	8	1	3	1		1	7	1	2	4	1	1	2	1	57
Staying at home			6	1	5	4	3	2	4	4	2	4	4	4	5	4	1						1	1				2	57
Restoration		2			1	1	3	3	2	1	2	2	2	3	2	1	1	2	1	2	2	2	1	4	4	4	4	3	55
Others	5	2	3	2	3	3	2	1	2	4	4	1	1	2	1	2	4	1		1			2	1		1		2	50
Safety check	1	2	2		6	5	7	6	3	1	3	2	3	1	1		1		1				1		1				47
Office counter work	2										1	2	1	1			1	3	2	3	3	3	2	3	3	3	2		35
Traffic control	2	5	4	1	1	1	1	1	1	1	1	1	1	1	1		2	1	1	1	1		1	1	1	1	1		34
Disaster wireless system	1	1	1		2	1	1	1	1	1	1	1	1	1	1	1	1	1	1	1	1	1	1	1	1	1	1	1	28
Clearing up		1			1	2	2	4	3			4	2	2				1		1	1	1		1					26
A child's delivery	6	8	2																										16
Fire-fighting round		1	1		1	1	1	1	1	1	1	1	1	1	1	1													14
Disaster waste							1	1	1	1	1	1	1				1	1	1				1	1	1				13
Suffering certificate														1	1	1				1	1	1				1	1	1	9
Temporary house						1	1							1			1		1	1	1								7
Liaison and adjustment			1	1		2																			1	1	1		7
Acceptance wide-area support																				2	2	1		1					6
Evacuation guidance	4	1	1																										6
Parliamentary correspondence	1	1				1												2											5
Support disabled persons	1				1						1							1					1						5
Volunteer					1															1	1	1							4
Supply of food for school children								1	1						1			1											4
Information arrangement						1	1	1	1																				4
Installation of a temporary lavatory														1						1						1			3
Check a school road							1	1				1																	3
Victim unable to return home					1	1																							2
Defense				1																					1				2

Table 3: disaster response and division (unit: people times hours)

Division	Food supply	Water supply	Damage investigation	Evacuation	Information collecting	Goods supply	Emergency safety check of house	Meeting	Restoration	Safety check	Office counter work	Traffic control	Disaster wireless system	A child's delivery	Fire-fighting round	Disaster waste	Suffering certificate	Temporary house	Liaison and adjustment	Acceptance wide-area support	Evacuation guidance	Parliamentary correspondence	Support disabled persons	Volunteer	Supply of food for school children	Information arrangement	Installation of a temporary lavatory	Check a school road	Victim unable to return home	Defense	Sum
Project management	138	90	15	27	9	15	0	33	0	0	0	0	0	0	0	0	0	0	0	9	0	0	0	0	0	12	0	0	0	3	351
General Affairs	3	96	30	42	6	90	0	0	93	0	0	6	0	0	0	0	0	0	0	0	0	0	0	3	0	0	0	0	6	0	375
Tax	75	186	24	99	9	33	0	0	3	0	0	3	0	0	42	0	0	0	0	0	3	0	0	0	0	0	0	0	0	0	477
Residential life	81	6	6	0	3	0	36	0	0	0	30	3	84	0	0	39	27	0	6	0	0	0	0	0	0	0	0	0	0	0	321
Health and Welfare	39	45	3	129	6	21	0	3	0	6	48	0	0	0	0	0	0	0	15	0	3	0	15	9	0	0	0	0	0	0	342
Industrial development	21	123	84	24	24	0	0	0	0	0	0	18	0	0	0	0	0	0	0	0	0	0	0	0	0	0	0	0	0	3	297
Urban construction	0	0	183	0	0	0	138	0	18	6	0	72	0	0	0	0	0	21	0	0	0	0	0	0	0	0	0	0	0	0	438
School education	99	36	222	90	150	0	0	120	18	15	0	0	0	15	0	0	0	0	0	0	0	3	0	0	12	0	0	9	0	0	789
Lifelong learning	42	111	66	36	36	0	0	0	0	0	0	0	0	0	0	0	0	0	0	0	0	0	0	0	0	0	0	0	0	0	291
Kindergarten	234	75	9	36	84	39	0	9	3	114	3	0	0	33	0	0	0	0	0	9	12	0	0	0	0	0	9	0	0	0	669
Parliamentary office work	0	15	0	0	0	0	0	6	30	0	0	0	0	0	0	0	0	0	0	0	0	12	0	0	0	0	0	0	0	0	63
Teller's cage	120	0	0	0	0	0	0	0	0	0	24	0	0	0	0	0	0	0	0	0	0	0	0	0	0	0	0	0	0	0	144

For the project management division, "food supply (138 [people × time])" is the highest, "water supply (90 [human × time])" followed by it. As the management of "Conference" is the one of the role of the disaster response headquarters, this was controlled by the project management division. The "meeting" by the school education division means that they discussed about how to response to the students and restart the classes.
The project management division takes a role of the wide-area supports from the municipalities located in outside of damaged area (9 [human × time]) as well. Yabuki town were received the supports from Mitaka city, Towada city, Kawaminami city and the others.
The General Affairs Division mainly worked for "water supply", "goods supply", "Recovery". In addition, the operation of evacuation centers and the understanding of the number of the evacuees are managed.

The Tax Division mainly worked for water supply, operation of evacuation centers and food supply. The evacuation guidance shows that the division induced the people who came to the governmental building just after the earthquake.
The residential life division mainly worked for the community wireless system, food supply, building inspection survey, disposal of wastes, issuances of a victim's certificate.
With regard to the community wireless system, three kinds of those systems those of Yabuki town, volunteer fire group and Fukushima prefecture were used.
On March 11, information was provided to the people in every one hour, and then on March 12 the frequency of information was provided in every two hours.
Immediately after the disaster, information about severed road was send to the government from a volunteer fire group, and then the staff in the room of the community wireless system sends its information to the urban construction division. The room of the community wireless system played the role of the information hub in the town.
The Health and Welfare Division worked for care of evacuees and provide food in evacuation centers.
The Industrial Promotion Division conducted a damage survey and water supply mainly. For damage investigation, they checked the function of agricultural related facilities.
The Urban construction division conducted a damaged survey of infrastructures, recovery of infrastructures.
The School Education Division conducted a damage survey of school facilities, food supply, and operation of evacuation center.

4. Comparing the responses in the Great East Japan Earthquake and the regional disaster prevention plan

By comparing the responses in the Great East Japan Earthquake and the regional disaster prevention plan, we analyze the important view for rebuilding the regional disaster prevention plan.
Figure 2 shows the relationship between disaster responses in the Great East Japan Earthquake and the second chapter of emergency response of Yabuki town regional disaster prevention plan.

Table 4 shows the responses for classification of each division. In order to understand the working load for each division, we estimate those values by calculating the denominator that the total working hours each tissue was determined by dividing each task.
According to the Figure 2, "Gathering and transmission of Information in Section 3" was spent the most frequently. This is due to the damaged survey and safety confirmation by the School Education Division and the urban construction division (Table 4).
Food supply in Section 12", water supply in Section 13, operation of evacuation center in Section 6 and goods supply for daily necessities in Section 14.
Here we want focus on the responses those were not carried out in the earthquake such as "Section 7 rescue measures," "Section 8 emergency measures", "Section 15 Medical Measures", and "search dead bodies in Section 18 ", and some actions. This is because that the human damage was very slightly, those actions were not required such as emergency response or rescue in Yabuki town.

Figure 2: Comparing the responses in the Great East Japan Earthquake and the regional disaster prevention plan

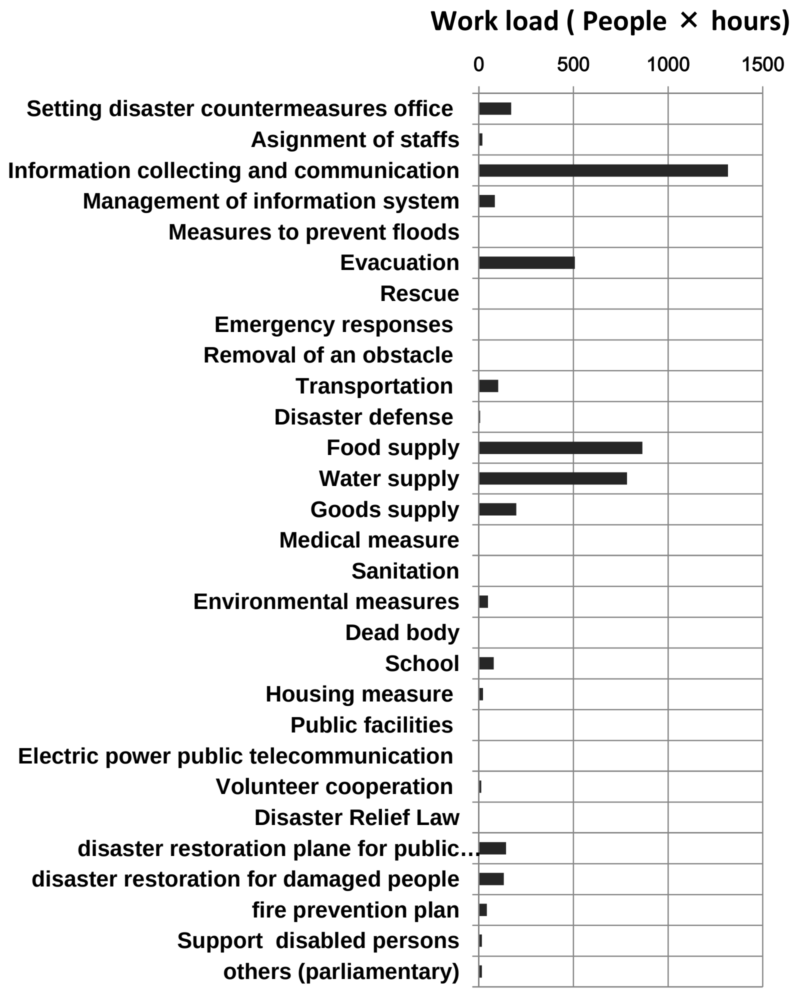

Table 4: Comparing the responses in the Great East Japan Earthquake and the regional disaster prevention plan in each division

Section	disaster responses/ Division	Project management	General Affairs	Tax	Residential life	Health and Welfare	Industrial development	Urban construction	School education	Lifelong learning	Kindergarten	Parliamentary office work	Teller's cage	Sum
Sec. 1	Setting disaster countermeasures office	33	0	0	0	3	0	0	120	0	9	6	0	171
Sec. 2	Asignment of staffs	9	0	0	0	0	0	0	0	0	9	0	0	18
Sec. 3	Information collecting and communication	36	36	33	51	30	108	327	387	102	207	0	0	1317
Sec. 4	Management of information system	0	0	0	84	0	0	0	0	0	0	0	0	84
Sec. 5	Measures to prevent floods	0	0	0	0	0	0	0	0	0	0	0	0	0
Sec. 6	Evacuation	27	48	102	0	132	24	0	90	36	48	0	0	507
Sec. 7	Rescue	0	0	0	0	0	0	0	0	0	0	0	0	0
Sec. 8	Emergency responses	0	0	0	0	0	0	0	0	0	0	0	0	0
Sec. 9	Removal of an obstacle	0	0	0	0	0	0	0	0	0	0	0	0	0
Sec. 10	Transportation	0	6	3	3	0	18	72	0	0	0	0	0	102
Sec. 11	Disaster defense	3	0	0	0	0	3	0	0	0	0	0	0	6
Sec. 12	Food supply	138	3	75	81	39	21	0	111	42	234	0	120	864
Sec. 13	Water supply	90	96	186	6	45	123	0	36	111	75	15	0	783
Sec. 14	Goods supply	15	90	33	0	21	0	0	0	0	39	0	0	198
Sec. 15	Medical measure	0	0	0	0	0	0	0	0	0	0	0	0	0
Sec. 16	Sanitation	0	0	0	0	0	0	0	0	0	0	0	0	0
Sec. 17	Environmental measures	0	0	0	39	0	0	0	0	0	9	0	0	48
Sec. 18	Dead body	0	0	0	0	0	0	0	0	0	0	0	0	0
Sec. 19	School	0	0	0	0	0	0	21	24	0	33	0	0	78
Sec. 20	Housing measure	0	21	0	0	0	0	0	0	0	0	0	0	21
Sec. 21	Public facilities	0	0	0	0	0	0	0	0	0	0	0	0	0
Sec. 22	Electric power public telecommunication	0	0	0	0	0	0	0	0	0	0	0	0	0
Sec. 23	Volunteer cooperation	0	3	0	0	9	0	0	0	0	0	0	0	12
Sec. 24	Disaster Relief Law	0	0	0	0	0	0	0	0	0	0	0	0	0
Other	disaster restoration plane for public facilities	0	72	3	0	0	0	18	18	0	3	30	0	144
Other	disaster restoration for damaged people	0	0	0	57	48	0	0	0	0	3	0	24	132
Other	fire prevention plan	0	0	42	0	0	0	0	0	0	0	0	0	42
Other	Support disabled persons	0	0	0	0	15	0	0	0	0	0	0	0	15
Other	others (parliamentary)	0	0	0	0	0	0	0	3	0	0	12	0	15

Thus, empirical knowledge on disaster medical responses were not accumulated based on experiences. However, as there are many medical facilities in Yabuki town, the cooperation with medical institutions is very important to take an effective disaster response in an aging society. The important things is to analyze what kinds of disaster responses experienced or not experienced, with following this results, it is necessary to build the regional disaster prevention plans

We found that many officials worked for the responses (food supply, water supply, and etc.) most of those are available not only government people.

The staffs belong to the management division such as the project management division or The Tax Division and etc. worked for those responses which everyone can do.

In order to perform disaster responses effectively with around 130 Yabuki town officials, all disaster responses need to be classified according to the level or characteristics of the responses.

Then, we can apply the responses in accordance with the characteristics.

In this paper, the disaster responses are divided into four types.

(1) the responses by everyone can work immediately after disaster such as such as management of the Volunteer Center etc., (2) the responses by government staff at first stage of disaster but gradually shifting to the other people such as food supply, water supply etc. (3) the responses by every government staff such as residents

support, issuance of certificate, etc., (4) the responses by government staff with a special skills such as restoration of infrastructure and lifelines, health issues etc.
It is important to make a category for each disaster response according to these kinds of types in a regional disaster prevention plan. Then we can understand what kinds of disaster responses are necessary by staffs with special skills or without those, and manage the limited resources effectively.

5. CONCLUSIONS

Our research aims to develop a ***"sustainable disaster/emergency management system"*** to accomplish the above-mentioned process. By following this system, problems will be sorted out accurately, improvements made at ordinary times, alert will be heightened before urgent danger, damage precisely assessed after disaster, and damage response conducted appropriately according to the assessments. It realizes ***"seamless transfer from ordinary times to emergency situations"***.
This study analyze the patterning the kinds of disaster response, defining its flow and evaluating its amount of volume which are expected in advance to build effective the spatio-temporal disaster responses model. By understand these operations for each different actors or players, it will be possible to carry out disaster responses immediately under the condition of confused disaster phase.
This paper provides the case study that the initial responses of Yabuki town in Fukushima prefecture are analyzed during the 5days after the Tohoku earthquake to achieve the effective disaster system.

AKCNOWLEDGEMENT

To write this paper, many staffs in Yabuki town support us. I describe here and appreciate deeply.

REFERENCE

1) IWASA Yuichi, HAYASHI Haruo and KONDO Tamiyo: Business Activity Analysis of the "Basic Plan for Disaster Prevention" for More Standardized Emergency Response, Institute of Social Safety Science (5), pp.193-202, 2003. (in Japanese)
2) Muneyoshi Numada, Shinya Kondo, Masashi Inoue, and Kimiro Meguro: Analysis of Description of Local Disaster Management Plan for Smooth and Effective Wide-Area Support System During Large-Scale Disaster, JDR (Journal of Disaster Research), Vol.7 No.2, pp. 147-159, 2012.

Planning tool for urban sustainable development management in Vietnam cities

NGUYEN THI THANH MAI
PhD. Head of Urban Infrastructure Planning (UIP), National University of Civil Engineering (NUCE), Ha noi
Maixaydung@yahoo.com

ABSTRACT:

Viet nam is one of the Asian countries where there has been a fast economic growth in recent years. Many challenges have emerged in urbanization process, such as the rapid increase of urban population and the continuing expansion of urban periphery. As result, agricultural land and open space have gradually been declined and replaced by buildings, roads with high density and increasingly numerous motobikes and autos. This causes the excessive consuming the natural energy and destruction of human living environment. The more seriousness is the deepened social cleavage and the urban poverty. It is clear that the traditional urban management tools is becoming out of date and not overtaking the growth demands of cities nowadays. So the question is that which is a effective management tool for local government to deal with the problems and challenges in urbanization, as well as to attain the objectives of sustainable development. In this article, the author focus on studying on planning methods utilized in urban development management. The assess and comparision between the traditional planning tool and new planning methods like CDS will indicate that we should change our mind on applying the new initiative in urban development management for the era of deep integration in global economy.

Keywords: *Urban management, Urban planning, Sustainable development.*

1. INTRODUCTION:

Like other cities in Asia, Vietnam cities have been in the process of rapid urbanization [1] under the context of globalization. The speed and scale of urbanization have profoundly impacted urban areas, especially in the biggest cities (Ha noi, Ho chi minh, Danang). The challenges that those cities face with is increasing population along with spatial extension on the urban periphery where local management capacity is still weak and lack of development control regulations. The impacts of urbanization process hence are narrowing the agricultural land and open space, declining the natural resources (river, lake,

[1] According to a MOC report in June 2013, Viet nam has 765 cities in which there are 2 largest cities at special rank (Ha noi and Ho chi minh), 13 cities at the first rank, 10 cities at the second rank, 53 cities at the third rank, 60 towns at the fourth rank and 627 towns at the fifth rank . Urbanization scale is 33%.

forest ecology, ...), pollutting air and bringing about accidents by using excessive private vehicles (cars, motorcycles), degrading the infrastructure and service system, creating an unbalance between economic growth and poverty that finally exacerbating social issues.

The international organizations suppose that the best choice for all fast-growing cities to deal with the challenges is implementing the targets of urban sustainable development. The World Bank refers to 5 criteria for urban sustainable development include economic growth bases on enhancing urban competitiveness; making good living conditions to gether with decreasing urban poverty, ensuring financial healthy and taking municipal governance relies on the strength of the social community.

However the question for leaders of Vietnam cities is which effective management tools could solve the problems and challenge in order to attain the targets of urban sustainable development. Meanwhile, it seems that the traditional planning methods for development management have not yet kept pace with the rapid changes of socio-economic growth in the cities.

Some international organizations have actively contributed their initiatives to find out the innovative management tools that could assist the municipalities to solve the urban challenge regarding land use management, infrastructure development, environment protection and community economic development. In particular, the City Development Strategy (CDS) tool proposed by the Cities alliance and its member organizations, including the World Bank, is considered as a new approach for municipality to overcome the disadvantages of traditional planning tool (Son [1]). CDS aims at integrative and multi-sectoral planning process by forsting the community participation with all their potential and enthusiasm.

The article below provides a review on traditional planning method being used in Vietnam today, after that compares with the CDS approach to conclude of the essential changes in applying the innovative planning tool on city development management aiming at sustainable socio-economic growth in the context of international integration.

2. TRADITIONAL PLANNING METHOD IN VIETNAM.

The current planning process in Viet nam is generally inherited from the prior reforms in the subsidized economy and has not changed much so far. Traditional planning method was profoundly affected by previously centralized planned economy and has been adjusted in order to agree with the demands of socialist-oriented market economy since 1986 (Quang, 2007).

2.1 Planning process: (diagram 1)

As regulation in Viet Nam, general development strategies were approved will be foundation to build socio-economic planning and sectoral plannings (such as transport, agriculture) which are concretized by middle term and short term development plans including groups of investment projects (Đạt, 2009)

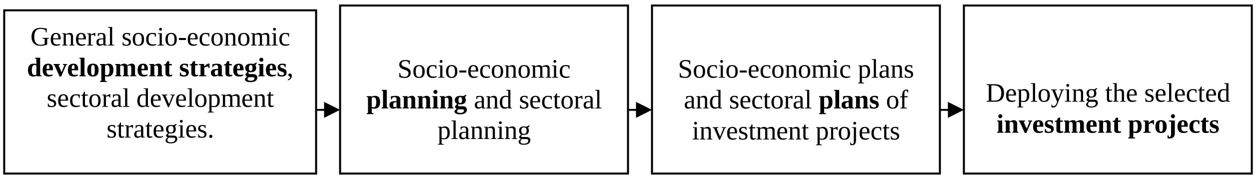

Diagram 1: General process on planning and implementing plans of investment projects in Viet nam

This process is implemented for most of socio-economic sectors as well as applied on the different territories that belong to administrative hierarchies from central to local levels (province, city, district). There is mutual relationship among the specialistic sectors and administrative levels in development management process (Achieve, 2009). In the sphere of city, the implementing process is a part of whole planning process and also comply with general principles.

Regarding the planning period, there are 3 types of basic planning: socio-economic development planning, sectoral development planning and (spatial) construction planning (diagram 2).

Socio-economic development planning leads the sectoral development plannings to implement comply with general missions in the direction of hamonized and balanced development among setors. While sectoral plannings stem from requirements of themselves will contribute their recommendations on completing the content of general socio-economic development planning (Viêm, 2009).

Approved plannings will be basis for proposing the socio-economic development plan and sectoral including a list of priority of investment projects. Likes this, those planning/plans will be implement at different territories belong to administrative hierarchies. The planning/plan at higher level will regulate the the planning/plan at lower level.

Construction planning is mentionned as creating physical environment where all socio-economic sectors can operate.

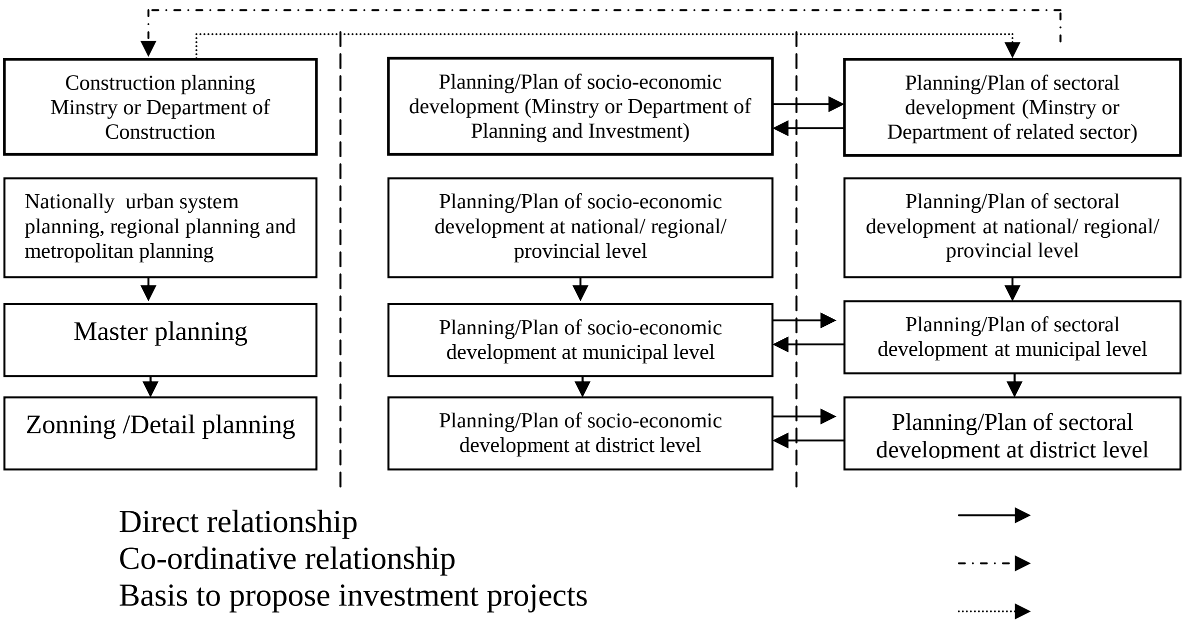

Diagram 2: Relationship among 3 types of basic planning, including socio-economic development planning, sectoral development planning and (spatial) construction planning

2.2 Master planning tool:

In Viet nam, construction planning (spatial planning) considered as an output of development planning process. It is impacted by 2 planning components, socio-economic planning and sectoral planning. The product of construction planning represented by the land use planning drawings These drawings will be basis to select a land for investment projects as well as to manage deploying the projects in practice. Besides this, there are more sectoral plannings be proposed by other ministries/departments, for example the transport development planning proposed by Ministry of Transportation, agricultural land use planning set up by Ministry of agriculture and rural development… It is obviously by this method there is issues of overlapping and unfitness among the sectoral plannings, even when there is presence of experts from varioius departments/ ministries to consult and to give opinions in construction planning.
Today the master planning tool is considered as old approach in making the construction planning. This method has a quite long history of thousands of years and was popularly utilized in the 60s, 70s in the socialist countries where centralized planned economy existed (Son, 2005). The master planning is supposed that get high technically and inflexible by its products are colourful drawings regulated through rigid standard system. The ideas of master planning is mainly decided by specialists like planners and architects who have responsibility to concretize the point of views of central government and municipal leaders by planning solutions. The participation of social community, such as residents, businesses and private economic sectors was recently regulated in the law of construction, however, it seems quite fomalistic and low effective. Therefore, land use planning formed by the traditional planning tool is considered as impractical and unadaptable with self-motivated market economy (Son, 2005).

2.3 Development plan on investment projects

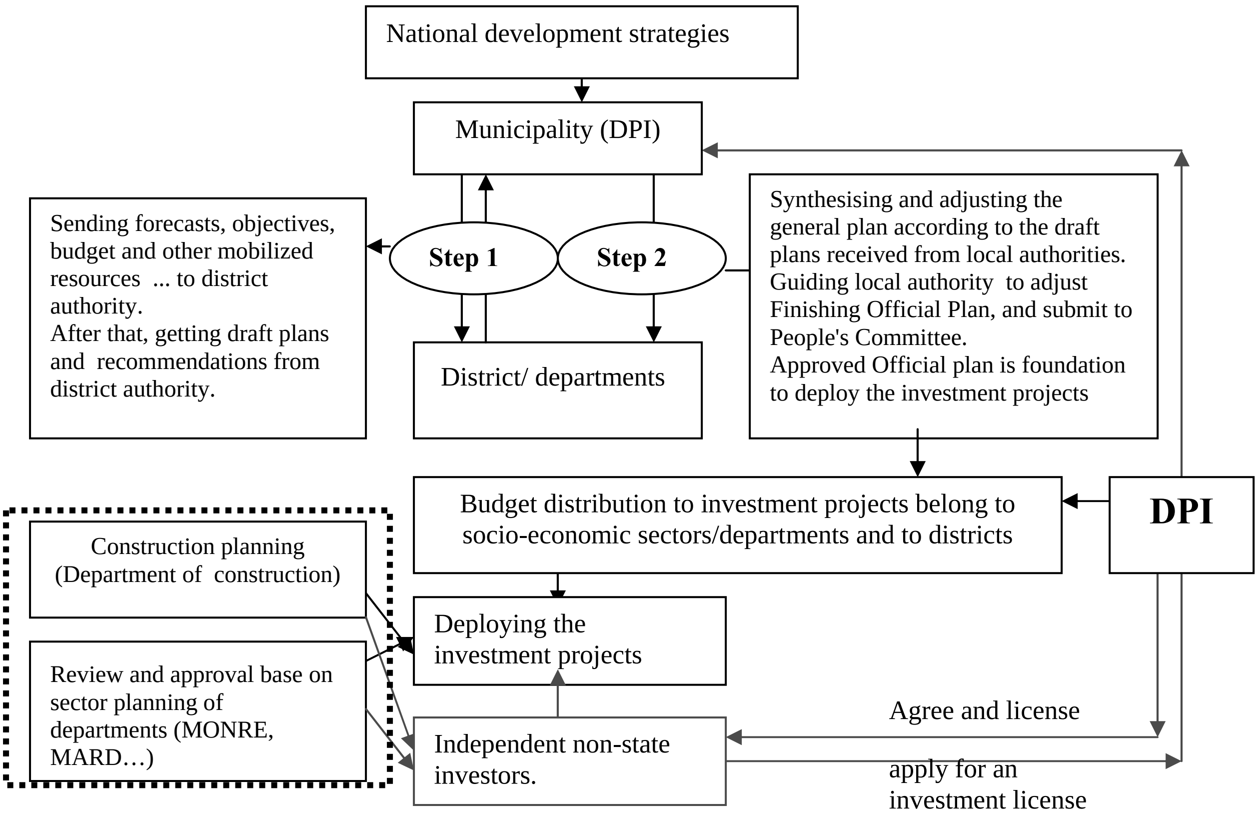

Diagram 3: Process of proposing plans on investment projects in Vietnam

Development plan on investment projects is proposed on the territorial units according to administrative management levels and in the socio-economic industries (ministries/departments). The process of proposing plan is carried out through 2 steps (Sơn, 2007, Đạt, 2009) (diagram 3) :

Step 1: Municipality (DPI) sends the forecasts, objectives, informs budget and mobilized resources... to the district authorities and departments. These units will build up draft plan of investment projects for themselves.

Step 2: Municipal agencies (DPI) synthesis and correct the general plan bases on recommendations mentionned in the draft plans of the district authorities/departments. After that municipal agencies guide the districts/departments to adjust their plan. An official plan will be complete and submit to People’s committee in order to have approval. Ratified official plan including a long list of priority of investment projects is basis to manage the construction activities in practice.

In theory, this process shows an unity amongs general plan of municipality and specific plans of districts/departments relied on two-dimension information from top-down to bottom-up, and vice versa. However in reality, the investment projects proposed by districts/departments just focus on particular benefits and demands of themselves without multi-sectoral coordination. The approved official plan does not represent for the benefits of all departments/sectors at once, as well as has not created yet a coordinative action plans between stakeholders. There is

a few opportunity for business representatives, the private sectors to participate and to contribute their oppinions in the making process. As results, it has not mobilized yet various financial resources out of state budget, particularly in the infrastructure development projects.
In the traditional planning method , *the role of municipality as an exclusive provider and market must comply with* (Alan coulhard, 2007).

3. CITY DEVELOPMENT STRATEGY (CDS):

3.1 CDS process:

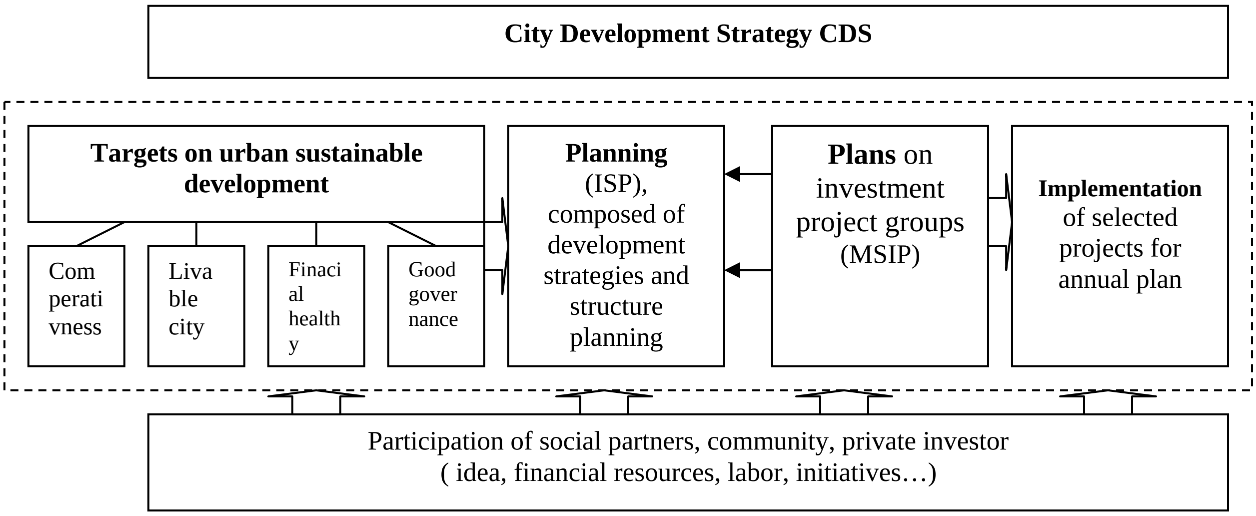

Diagram 4: General process of implementing CDS

CDS combines 2 phases (planning and proposing plan of investment projects) into one complete process in which the preferential mechanism is set up to encourage the community participation. There are 3 initiative tools applied in CDS implementation process:

- Integrated Strategic Planning (ISP)
- Multi-Sectoral Investment Plan (MSIP)
- Community participation (CP)

3.2 Integrated Strategic Planning (ISP):

Integrated Strategic Planning (ISP) covers 3 planning components such as socio-economic planning, spatial planning and environmental planning (land use planning, environment) (diagram 4). ISP promotes cooperation among the stakeholders including the state, social community, organizations and the private sector to mobilize resources and to coordinate in operation aims to planning targets of urban sustainable development. Outputs of ISP include the development strategies (Son, 2005) and structure planning which is an innovative planning can replace the traditional master planning.

Structure planning was formed in 1950 applied on new city planning in UK and popularly utilized in the 1970s. Structure planning does not regulate specific types of construction or rigid stadards on planning drawing. It prepares a long term development plan for land use and proposes the orientation of spatial structure development for the city future. Structure planning approach is conformably utilized to establish the city general planning. It permits easily adjusting at detail planning because of its flexibility (Son, 2005)

3.3 Multi-Sectoral Investment Plan – (MSIP)

ISP development strategies are important basis to establish the MSIP. These strategies will be translated into medium-term and long-term development plans including a long list of investment projects. MSIP process is deployed base on the principles of multi- sectoral coordination to propose priority of construction projects. Beside this, a capital investment program CIP also be annually done with preparation of the municipal budget each year for construction. (Dat, 2009)

3.4 Community Participation (CP)

Community participation approach is paid attention in performing CDS. The social community and stakeholders such as local government, businesses, residents ... by their commitment efforts to involve in the CDS implementation process, from the step of identifying existence, defining opportunities untill to propose a future vision and to find out the coordinative action plans aiming at a multi-sectoral and comprehensive strategies.
In summary, CDS is the integrated, multi-sectoral planning tool that assists effectively the authority to propose development strategies and investment plans. Spatial planning is a part of whole process, not a final output as it is in traditional planning process. Results of CDS represents an coodianative action program between stakeholders. It assigns concretely who, when and how to participate in implementation process. Hence CDS tool will bring a new way in urban development management, *the market orders and city as a provider (*Alan CoulHart, 2007).

4. CONCLUSIONS:

Thus, the CDS approach is as an initiative to assist the municipal authority to establish the development plan by encouraging the enthusiastic participation of community and promoting the close coordination between social-economic sectors. CDS is considered as effective tool to find out the actions aiming at the equitable growth and sustainable social development. It's time that the municipalities needs to change their inherent mind on deploying the city development planning by inserting the CDS approach into traditional methods.
Although the CDS has been studied by the international organizations in the cases of Ho Chi Minh, Ha Long, Hai Phong and Can Tho, it still considered as pilot tool. It has not yet been executed in reality for experts to draw experiences.
However, CDS tool want to go into our life and effectively utilized in practice, it is necessary to adjust the current management mechanism in order to create

favorable conditions for stakeholder participation and for collaboration between professional departments.

REFERENCES

Tien, Nguyen Hong, 2013. *Role of Ministries, Industries in drainage and sewerage management in Vietnam*, Conference on Role of Stakeholders in sewerage and Wastewater treatment Management, Ministry of Land, Infrastructure Transport and Tourism, Japan and MOC, Vietnam.

World bank, 2012. *Assessment on urbanization in Vietnam*, publish by WB.

Son, Nguyen Dang, 2005. *Toward swifting the planning method*, Publish House of Construction

Dat, Nghiem Xuan, 2009. *Multi-Sectoral Investment Plan*. Trainning course on capacity building for urban planners in VietNam, Modul 1, publish by Vietnam institute of Architecture, Urban and Rural Planning.

CoulHart, A., 2007. *Urban planning and management* , Training course on environment management, course material approved by World bank and MOC.

Quang, Nguyễn, 2007. *Changes on Planning method in Viet Nam*, Training course on environment management, course material approved by World bank and MOC.

Hai, Ngô Trung, 2009. *City Development Strategy in Hạ long city*, Trainning course on capacity building for urban planners in VietNam, Modul 1, publish by Vietnam institute of Architecture, Urban and Rural Planning.

Viem, Đo Duc, 2009. *Socio-economic planning, sectoral planning and construction planning in Vietnam*, Trainning course on capacity building for urban planners in VietNam, Modul 1, publish by Vietnam institute of Architecture, Urban and Rural Planning

Tuan, Hoang Ngoc, 2007. *Some challenges in building CDS in Hai phong city*, Training course on environment management, course material approved by World bank and MOC.

The integration approach for broad-scale land-use change prediction modelling

Anh Nguyet DANG[1] and Akiyuki KAWASAKI[2]

[1] Research Assistant, Regional Network Office for Urban Safety (RNUS) Asian Institute of Technology (AIT), Thailand.

dang@ait.ac.th

[2]Associate Professor, International Center for Urban Safety Engineering (ICUS) Institute of Industrial Science (IIS), the University of Tokyo, Japan.

ABSTRACT

The magnitude and pace of human intervention on land surface has markedly increased and become unpredicted. Half of the Earth's ice-free land surface has been transformed by humankind and most of the rest has been managed for human purposes over the past 10 millennia or so. Land-use change models have been developed to analyze the causes and consequences and assess the impacts of land-use change on ecosystems as well as supporting land-use planning and policy. At broad-scale, the complexity of land-use systems has called for a multidisciplinary analysis. However, there is a challenge of abstracting the interaction among a large number of multi-level factors to explain broad-scale land-use change processes. No single model is able to do so. Recently, a newer approach known as integrated models has been carried out with the promise of overcoming the limitation of single model application. In this study, the conceptual framework was introduced to facilitate integration approach in broad-scale land-use modeling. We do this by:(1) summarize the most important concepts and characteristics of broad- scale land-use models from previous studies, (2) discuss about the framework for modelling land-use change at broad-scale and (3) propose the application of this framework for land-use change for DakLak province, Vietnam. This work could be used for better understanding of the potential of integrated approach and provide scientific support for land-use planning and managements at broad-scale.

Key words: *land-use change model, broad-scale, integrated model*

1. INTRODUCTION

Most estimates suggest that half of the Earth's ice-free land surface has been transformed by humankind and most of the rest is managed for human purposes over the past 10 millennia or so (Global Land Project, 2005). However, the magnitude, scale and pace of human intervention on land surface has markedly increased and become unpredicted since the Industrial Revolution (Mimienium Ecosystem Assessment, 2005). There still exist confusion and misunderstandings of what is exactly meant “land-cover” change and “land-use” change (Agarwal et al., 2002; Verburg et al., 2006). Actually, the linkage between land-use and land-cover change is emphasized that the impacts of land-use change and their contribution to local and global change are mediated by land-cover changes (Turner et al., 1999). In other words, human intended land-use determinate the conversion of land-cover along with the natural land-cover change.

Land-use change put the negative impacts on the hydrological system, air quality, soil properties, ecosystem processes and function. These changes, ultimately, contribute to local, regional and global climate change through greenhouse gas fluxes and surface Aledo effect etc. Land-use change issues, in-turn, increase the vulnerability of people to climatic, economic or socio-political perturbations. Human have become ever more adept at appropriating and altering the land for human needs. Therefore, the way people use the land has become a source of widespread concern for the future of the world (Mohamed, 1999).

Questions of the causes and the consequences of land-use change have attracted interest among a wide variety of researchers (Lambin et al., 2003; Ronneberger, 2006). At first, most land-use change research was focused on land-cover conversions (e.g., deforestation, urbanization) by a simple comparison of successive land-cover maps (Irwin et al., 2001). However, land-use change is a complex process including a number of interactions between associated drivers and feedback from land-use change to these drivers (Pijanowski et al., 2005). The driver factors of land-use change are described in detail by Lambin et al (2003) including natural variability, economic and technological factors (e.g. rural income, agricultural productivity), demography (e.g. population growth, immigration), institution, culture and globalization related factors.

The complexity of land-use change process has called for the development of land-use change model over the last decades (Briassoulis, 2000; Parker et al., 2003; Pontius Jr et al., 2001; Turner et al., 1999; Veldkamp et al., 2001). It help for better understand of land-use dynamics, to develop hypotheses that can be tested empirically, and to make predictions and/or evaluate scenarios for land-use planning and policy (Müller, 2003; Verburg et al., 2004a; Verburg et al., 1999). In simple word, land-use change projection model have been developed to address why, how, when and where the changes occurred. The development of land-use change model may aim at one of the six main purposes: description, explanation, prediction, impact assessment, prescription and evaluation of land-use change process. However, the most important purpose of analysis land-use change is to predict future changes in land-use (Lambin et al., 2000; Veldkamp et al., 2001).

In this research, we aim at the appropriate framework for broad-scale land-use modeling (the term “broad-scale” will be explained in the next section). The reason is that modeling broad-scale land-use changes requires a robust method which is able to seize the complicated interactions among the factors as well as deal with the issue of data limitation. Review from the previous studies address that a large variety of concepts, approaches and techniques is already applied for broad-scale land-use change research. Nevertheless, there remains the issue of duplication within the land-use models. There are several models addressing similar systems often are developed independently. Hence, this has the advantage for our research of demonstrating a more organized modeling framework to avoid the competition and duplication between models. This framework is expected to be flexible and transparent to apply for different case studies. We also proposed the application of this framework to DakLak province in Vietnam. With the potential for economic development, recently, DakLak has witnessed the increase of population due to immigration from other provinces. The province has also attracted more domestic and foreign investment. As a result, DakLak is facing the intense changes in land-use especially for infrastructure and agriculture development. This calls for exploration of land-use model to support of sustainable development in Daklak.

2. DEVELOPMENT OF FRAMEWORK FOR BROAD-SCALE LAND-USE MODELING

2.1 Broad-scale definition

The term "scale" may cause confusion because it has different meanings across disciplines. Geographers define "scale" as the ratio of a distance on a map and that same distance in reality. Scientists from social sciences give opposite meanings to the terms "scale". To them, a large-scale study means it covers a large extent (correspond to small-scale maps of geographers), and a small-scale study is a detailed study covering a small area (are large scale, to use the geographer's term) (Agarwal et al., 2002). From literature of land-use model, we figure out that most models occupied the word "scale" as the extent of study area (Agarwal et al., 2002; Heistermann et al., 2006; Lagarias, 2012; Schaldach et al., 2011; Valbuena et al., 2010; Verburg et al., 2008). To avoid the confusion, instead of using the term "large-scale", we employ the term "broad -scale" which refers to the study area with large extent. The broad-scale model can be subnational, national, continental and global scale studies.

2.2 Reviews of broad-scale land-use models

Due to the variety of application purposes, each model was built to answer specific questions. In this section, we will discuss about the common characteristics as well as the methodological insights of representative models.
An inspection of the literature on broad-scale models reveals that, most of the time, these are integrated models. At large extent, the high level of aggregation of data obscures the variability of situations and relationships calls for multidisciplinary analysis. Therefore, no one model is capable of capturing the whole range of land use change's characteristic (Briassoulis, 2000; Lambin et al., 2000; Verburg et al., 2004a). Integrated model, based on combining elements of different modeling techniques, has been widely used because of its capacity to explicitly deals with temporal and spatial dynamics, and achieves a higher level of multidisciplinary approach (Michetti, 2012; Upadhyay et al., 2006; Verburg et al., 2009). Examples of such integrated land-use models include AGE, IMAGE, IMPACT, CLUE, IIASA LUC and LandSHIF etc.
These models present different dimension of integration. The CLUE model, one of the commonly used models, occupied the combination of different modeling techniques: geographic-based and statistical analysis (regression analysis). The

methodology of regression analysis, however, does not allow long-term projections, since the empirical relationships cannot necessarily be assumed constant over long time periods. Another issue is that the CLUE model is not able to reflect the macro-demand for land-use based on the given socio-economic scenario. In some cases, the objectives of the authorities are used as the input data of the land demands. In other researches, to solve the limitation of CLUE, some related models were introduced to calculate the land demands, for example GTAP (Global trade Analysis Project) (Luo et al., 2010).

Meanwhile, AGE, IMPACT, IMAGE, IIASA LUC and LandSHIF represent for the integrated model group in which the integration is defined as the combination of sub-model adopted from a wide range of disciplines. However, almost models of this group, are not specifically developed for land use studies. IAM for the Asian-Pacific region e.g. is designed to study impacts on the market and on greenhouse gas emissions of land-using sectors rather than on land-use change prediction (Matsuoka et al., 2001). The IMAGE, IMPACT models are specific for agriculture sector (Strengers et al., 2004). And LandSHIFT model has the purpose to provide a tool for assessment of environmental impacts of land-use change (Schaldach et al., 2011). Of these models, IIASA-LUC is currently the most fully integrated model. Although this model incorporates many sub-systems, interactions and feedbacks, it has become complex to operate and, above-all, difficult to parameterize due to the high data requirements for most countries (Fischer and Sun 2001). The other disadvantage of highly complex, integrated models is that the degree and type of integration often appears to be subjective based on the modelers disciplinary background (Agarwal et al., 2002). In some cases, highly aggregated assessments obscure the variability of geographic situations through the high aggregation level of the data, and cause an underestimation of the effects of land-use change for certain regions (Verburg et al., 1999).

Land-use models of regional, continental to global scale (broad-scale) require specific methodologies that are different from local scale approaches. They have to cope with data limitation for many variables and parameters, and for many regions of the world and face the challenges of abstracting local land-use decision-making to explain regional or global processes (Heistermann et al., 2006). This issue infuses appropriate frameworks that influence modeling, from data collection, to data analyses, to interpretation of results. The framework is a fully integrated approach, qualitative modelling allows a focus on the system as a whole.

2.3. Appropriate framework for broad-scale land-use modelling

A number of review papers characterized integrated models by modular components. Modularity might help facilitate modeling land-cover change by assigning a particular disciplinary aspect of the model to a separate module. We found the majority of the modular models tended to consider multiple disciplines. Judging from our review of the recent literatures, the integrated model framework is mostly the combination of demand module and allocation module, respectively (Heistermann et al., 2006; Schaldach et al., 2011; White et al., 2012). The demand module can be economic model purpose trend analysis, simple demand models (Kok et al., 2001) or complex multi-sectoral models are used

(Heistermann et al., 2006; Verburg et al., 2008). This module is used for markets and policies analysis and ultimately quantify demand and supply of land-intensive commodities. The geographic module is occupied for the actual allocation of land-use. The geographic module have been supported by the rapid improvement of remote sensing and GIS. This combination can help to utilize the strengths and minimize the weaknesses of individual model. For example, economic models can consistently address demand and supply of land use. Yet, they are limited in representing behavior of land use change. On the other hand, geographic models are strong in capturing the spatial determination of land use and in quantifying supply side constraints based on land resources. However, they lack the potential to treat the interplay between supply, demand and trade endogenously.

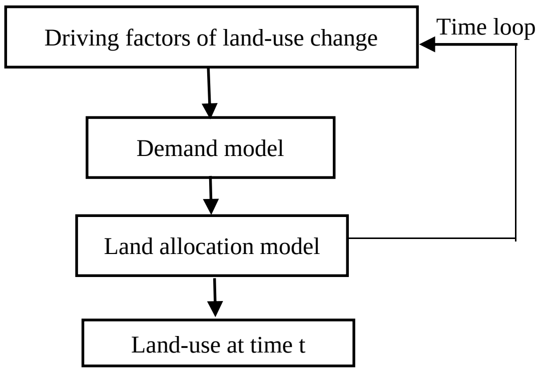

Figure 1: General framework for land-use prediction model at broad scale

3. PROPOSE LAND-USE MODELLING FRAME WORK FOR DAKLAK PROVINCE

DakLak has the largest forest area in Vietnam and been at the high risk under the development pressure. The main problem in DakLak is the increase of population, especially due to a high rate of immigration. Increasing population creates a growing demand for agricultural land and forest products, which leads to a degradation of forest quality and a decrease in forest cover. The emergence of the large-scale cultivation of coffee is also one the most prominent which led to a transformation of the rural economy in the recent history of DakLak and inducing massive land-use change and widespread deforestation.

Previously, some researches of land-use change were carried out in DakLak province and some other researches in the Mekong river region encompassed land-use change in Daklak in some extent. However, there has not been any comprehensive model for land-use change in DakLak. Some crucial problems still remain in the context of land-use change modeling for DakLak. Firstly, the previous studies pointed out the limitation of excluding economy and policy factors in land use change measurement. The research of Müller et al. (2004) put effort to examine the complexity of natural, social and economic issues in two district (Lak and Krong Bong) of Daklak, but only two factors, policy and technology, were taken into account.

The framework proposed in our research is expected to fill the gap in land-use research in DakLak in particular and Mekong river basin in general. The proposed integrated land-use model is the combination of System Dynamic Model and GIS-based Model for land-use change prediction at DakLak. It can contribute as the technical assistance for DakLak to address future land use change. From the model result, the researchers, policy makers and planners can gain initiative in their land use planning and management for sustainable development.

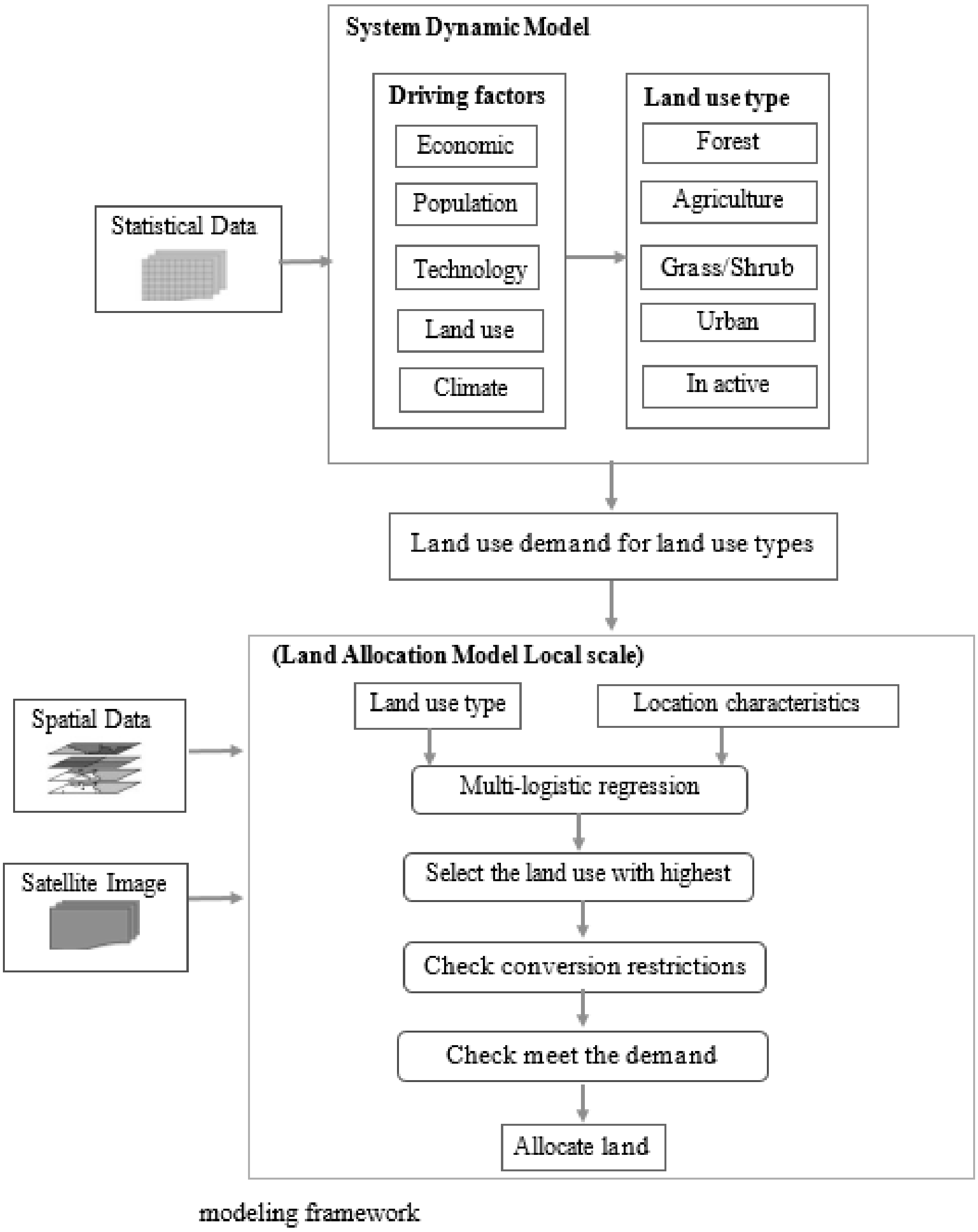

Figure 2: Land-use modeling framework

3.1. System Dynamic model for land-use demand

Land use is never static, but it is constantly changing in response to dynamic interaction between drivers and feedback from land-use change to these drivers (Lambin et al., 2003). Case studies show that not all drivers of land-use change and all levels of organization are equally important. The important step is how best to represent these drivers in a model. This requires linking dynamically the processes of land-use change to biophysical processes (Veldkamp et al., 2001). Once a systems model has been constructed, what-if scenarios can be explored more easily than with other modeling approaches that are not systems oriented.

The application of System Dynamic (SD) in land-use model was demonstrated in previous study. Patuxent Landscape Model (Voinov et al., 1999) was designed to simulate fundamental ecological processes on the watershed scale, in interaction with a component that predicts the land-use patterns. The research of Luo et al. (2010) described an integrated methodology in which the conversion of land use and its effect model (CLUE), a spatially explicit land use change model, has been combined with a system dynamic model (SD) to analyze land use dynamics at different scales. This application of combination of SD and CLUE suggests that this methodology have the ability to reflect the complex behavior of land use system at different scales to some extent and be a useful tool for analysis of complex land-use driving factors such as land-use policies and assessment of its impacts on land-use changes.

SD methodology is a simulation technique that models large-scale, complex social economic systems using stock and flows and explicitly including feedback loops. It attempts to understand how physical processes, information flows and managerial policies interact to create the dynamics of the variables of interest (Liu et al., 2013). System components can be described by a set of state variables (stocks or reservoir), such as population or crop production etc. These state variables are influenced by process (flow), such as the birth process or investment process etc. The converter play an important role in the system as a rate at which reservoir or stock contents changes.

Development of modeling tools allows us to build more sophisticated models. As for SD analysis, STELLA with good documented references is our selection. It provides a platform for dynamic modeling that has a very intuitive graphic user interface and can be used to develop from simple to very complex models. The structure of STELLA model on land use is drawn with the causality functions and feedback loop structure between number of socio-economic and policy.

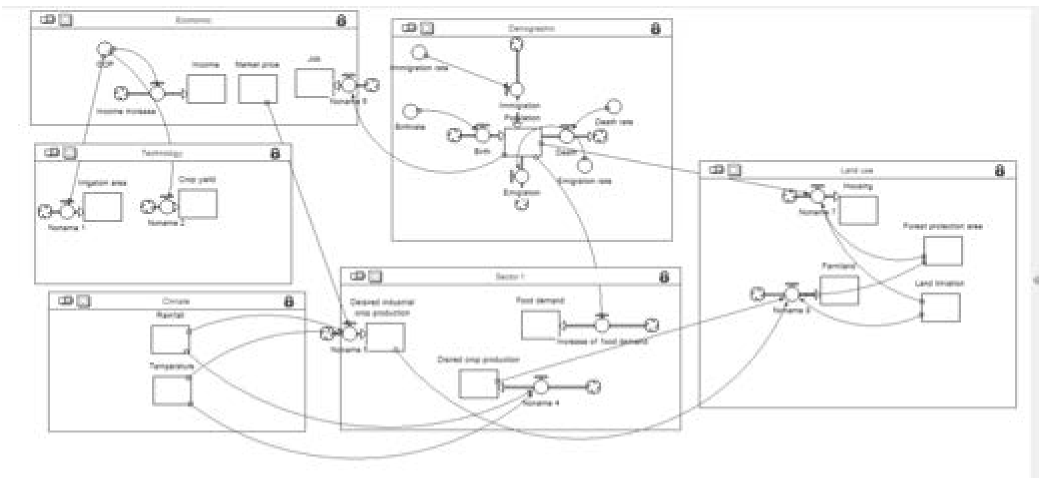

Figure 3: System Dynamic model for land-use demand in DakLak province

3.2. ArcGIS Model builder for allocation module

For the allocation module, the driving factors will bed translated into suitability or preference maps, which are a key component of the allocation. Such suitability maps can be created using theory or expert knowledge of the land-use system, empirical analyses or rules based on neighboring cells (Verburg et al., 2004b). Using this suitability and the magnitude of change, an allocation algorithm will then allocate the claims in the best suited areas. This allocation algorithm can be a simple cut-off value that selects the most suitable locations, but can also be a more sophisticated algorithm that takes the competition between different land uses into account (Verburg et al., 2006).
ArcGIS Model Builder is selected to open black box of other land allocation models. In Model Builder, the model is represented by a flux diagram in a graphic user interface that facilitates to create, visualize, edit, and execute geo-processing workflows. Model Builder is an easy-to-use application for creating and running workflows containing a sequence of tools. In addition, tools created with Model Builder can be used in Python scripting and integrated ArcGIS with other application.

4. CONCLUSION

Modeling involves making trade-offs between realism, precision and generality (Wainger et al., 2007). The more precisely a model captures a particular system, the less likely it can be applied to another area (generality). As for the demand module, the selection of factors and modeling the integration among factors depend on the practical socio-economic circumstance of DakLak. Therefore the model cannot directly applied to other study area. However, the research is expected to demonstrate the potential of the integrated framework for broad-scale land use modeling. The framework is designed in such a way that it is flexible in including other models and indicators if needed for a specific policy scenario application. Our further task will be done to complete the System Dynamic model as well as land use allocation module.

REFERENCE

Agarwal, C., Green, G. M., Grove, J. M., Evans, T. P., & Schweik, C. M. (2002). A review and assessment of land-use change models: dynamics of space, time, and human choice. *Gen. Tech. Rep, NE-297*(Newton Square, PA: U.S Department of Agriculture, Forest Service, Northeastern Research Station), 61.

Briassoulis, H. (2000). *Analysis of Land Use Change: Theoretical and Modeling Approaches* Retrieved from http://www.rri.wvu.edu/WebBook/Briassoulis/contents.htm 12 Feb 2012.

Global Land Project. (2005). Annual report. IGBP Report No. 53/IHDP Report No. 19.IGBP Secretariat, Stockholm.64.

Heistermann, M., Müller, C., & Ronneberger, K. (2006). Land in sight?: Achievements, deficits and potentials of continental to global scale land-use modeling. *Agriculture, Ecosystems & Environment, 114*(2–4), 141-158.

Irwin, E. G., & Geoghegan, J. (2001). Theory, data, methods: developing spatially explicit economic models of land use change. *Agriculture, Ecosystems & Environment, 85*(1–3), 7-24.

Kok, K., Farrow, A., Veldkamp, A., & Verburg, P. H. (2001). A method and application of multi-scale validation in spatial land use models. *Agriculture, Ecosystems & Environment, 85*(1–3), 223-238.

Lagarias, A. (2012). Urban sprawl simulation linking macro-scale processes to micro-dynamics through cellular automata, an application in Thessaloniki, Greece. *Applied Geography, 34*(0), 146-160.

Lambin, E. F., Geist, H. J., & Lepers, E. (2003). Dynamics of land-use and land-cover change in tropical regions. *Annual Review of Environment and Resources, 28*(1), 205-241.

Lambin, E. F., Rounsevell, M. D. A., & Geist, H. J. (2000). Are agricultural land-use models able to predict changes in land-use intensity? *Agriculture, Ecosystems & Environment, 82*(1–3), 321-331.

Liu, X., Ou, J., Li, X., & Ai, B. (2013). Combining system dynamics and hybrid particle swarm optimization for land use allocation. *Ecological Modelling, 257*(0), 11-24.

Luo, G., Yin, C., Chen, X., Xu, W., & Lu, L. (2010). Combining system dynamic model and CLUE-S model to improve land use scenario analyses at regional scale: A case study of Sangong watershed in Xinjiang, China. *Ecological Complexity, 7*(2), 198-207.

Matsuoka, Y., T. Morita, & M. Kainuma. (2001). Integrated Assessment Model of Climate Change: The AIM Approach. In T. Matsuno & H. Kida (Eds.), *Present and Future of Modeling Global Environmental Change: Toward Integrated Modeling* (pp. 339–361): Terrapub.

Michetti, M. (2012). Modelling Land Use, Land-Use Change, and Forestry in Climate Change: A Review of Major Approaches. *FEEM Working Paper No. 46.2012; CMCC Research Paper No. 133.*

Mimienium Ecosystem Assessment. (2005). Ecosystems and Huam Well-being:Sysnthesis. Island Press, Washington, DC.155.

Mohamed, A. A. (1999). *An integrated agro-economic and agro-ecological framework for land use planning and policy analysis.* (Proefschrift Wageningen Universiteit), [s.n.], [S.l.]. Retrieved from http://edepot.wur.nl/195739

Müller, D. (2003). *Land-use change in the Central Highlands of Vietnam: A spatial econometric model combining satellite imagery and village survey data.* (Doctoral thesis), Georg-August University of Göttingen. Retrieved from http://ediss.uni-goettingen.de/handle/11858/00-1735-0000-0006-AB5C-0

Müller, D., & Munroe, D. K. (2004). *Tradeoffs between rural development policies and forest protection: spatiallyexplicit modeling in the Central Highlands of Vietnam.* Paper presented at the American Agricultural Economics Association Annual Meeting, Denver, Colorado.

Parker, D. C., Manson, S. M., Janssen, M. A., Hoffmann, M. J., & Deadman, P. (2003). Multi-Agent Systems for the Simulation of Land-Use and Land-Cover Change: A Review. *Annals of the Association of American Geographers, 93*(2), 314-337.

Pijanowski, B. C., Pithadia, S., Shellito, B. A., & Alexandridis, K. (2005). Calibrating a neural network-based urban change model for two metropolitan areas of the Upper Midwest of the United States. *International Journal of Geographical Information Science, 19*(2), 197-215.

Pontius Jr, R. G., & Schneider, L. C. (2001). Land-cover change model validation by an ROC method for the Ipswich watershed, Massachusetts, USA. *Agriculture, Ecosystems & Environment, 85*(1–3), 239-248.

Ronneberger, K. E. (2006). *The global agricultural land use model KLUM : a coupling tool for integrated assessment.* (Doctor), University of Hamburg, Hamburg, Germany.

Schaldach, R., Alcamo, J., Koch, J., Kölking, C., Lapola, D. M., Schüngel, J., & Priess, J. A. (2011). An integrated approach to modelling land-use change on continental and global scales. *Environmental Modelling & Software, 26*(8), 1041-1051.

Strengers, B., Leemans, R., Eickhout, B., Vries, B., & Bouwman, L. (2004). The land-use projections and resulting emissions in the IPCC SRES scenarios scenarios as simulated by the IMAGE 2.2 model. *GeoJournal, 61*(4), 381-393.

Turner, B. L., Skole, D., Sanderson, S., Fischer, G., Fresco, L., & Leemans, R. (1999). Land-Use and Land-Cover Change; Scinece/Research Plan. HDP Report No.7.Stockholm and Geneva.

Upadhyay, T. P., Solberg, B., & Sankhayan, P. L. (2006). Use of models to analyse land-use changes, forest/soil degradation and carbon sequestration with special reference to Himalayan region: A review and analysis. *Forest Policy and Economics, 9*(4), 349-371.

Valbuena, D. F., Verburg, P. H., Bregt, A. K., & Ligtenberg, A. (2010). An agent-based approach to model land-use change at a regional scale. *Landscape Ecology, 25*(2), 185-199.

Veldkamp, A., & Lambin, E. F. (2001). Predicting land-use change. *Agriculture, Ecosystems & Environment, 85*(1–3), 1-6.

Verburg, P., Eickhout, B., & Meijl, H. (2008). A multi-scale, multi-model approach for analyzing the future dynamics of European land use. *The Annals of Regional Science, 42*(1), 57-77.

Verburg, P., Kok, K., Pontius, R., Jr., & Veldkamp, A. (2006). Modeling Land-Use and Land-Cover Change. In E. Lambin & H. Geist (Eds.), *Land-Use and Land-Cover Change* (pp. 117-135): Springer Berlin Heidelberg.

Verburg, P., & Overmars, K. (2009). Combining top-down and bottom-up dynamics in land use modeling: exploring the future of abandoned farmlands in Europe with the Dyna-CLUE model. *Landscape Ecology, 24*(9), 1167-1181.

Verburg, P., Schot, P., Dijst, M., & Veldkamp, A. (2004a). Land use change modelling: current practice and research priorities. *GeoJournal, 61*(4), 309-324.

Verburg, P. H., de Koning, G. H. J., Kok, K., Veldkamp, A., & Bouma, J. (1999). A spatial explicit allocation procedure for modelling the pattern of land use change based upon actual land use. *Ecological Modelling, 116*(1), 45-61.

Verburg, P. H., de Nijs, T. C. M., Ritsema van Eck, J., Visser, H., & de Jong, K. (2004b). A method to analyse neighbourhood characteristics of land use patterns. *Computers, Environment and Urban Systems, 28*(6), 667-690.

Voinov, A., Costanza, R., Wainger, L., Boumans, R., Villa, F., Maxwell, T., & Voinov, H. (1999). Patuxent landscape model: integrated ecological economic modeling of a watershed. *Environmental Modelling & Software, 14*(5), 473-491.

Wainger, L. A., Rayburn, J., & Price, E. W. (2007). Review of land use change models, Applicability to Projections of Future Energy Demand in the Southeast United States. Southeast Energy Futures Project Cambridge.

White, R., Uljee, I., & Engelen, G. (2012). Integrated modelling of population, employment and land-use change with a multiple activity-based variable grid cellular automaton. *International Journal of Geographical Information Science*, *26*(7), 1251-1280.

China's growing civil society for disaster response

Xiaoge XU[1], Koide OSAMU[2], and Takaaki KATO[3]
[1]Graduate Student School of Eng., The University of Tokyo, Japan
xuxiaoge@city.t.u-tokyo.ac.jp
[2]Professor, School of Eng., The University of Tokyo, Japan
[3] Associate Professor, ICUS, IIS, The University of Tokyo, Japan

ABSTRACT

Previous studies on civil society responding disaster suggest that, the disaster often present an opportunity for civil society organizations (CSOs). This article firstly examines the impact of the 2008 Wenchuan Earthquake on China's civil society as a background, points out that the disaster served as a turning point to push existing CSOs into the field of disaster response, and gave birth to a number of grassroots CSOs. Their participation in disaster relief and reconstruction work indicates the changing disaster management mode of China, which used to be monopolized by the state. Case study is used in the second section to illustrate the growth process of grassroots CSOs in the past five yeas, and their performance in the field of disaster response. The case study indicates that transparency and professionalism are two factors contribute to the growth of grassroots CSOs, while the cooperation between CSOs is still under dispute. Based on the findings and issues, the author argues that Chinese government should further relax its related regulation on CSOs to promote its self-sufficiency. Weak tie between the CSOs should be established as a sustainable mode for disaster response.

Keywords: *Disaster Response, Civil Society Organizations, China.*

1. INTRODUCTION

Previous studies suggest disasters brought changes to civil society in Japan (Shaw and Goda, 2004; Yatsuzuka, 2007), Turkey (Jalali, 2002; Kubicek, 2002), and India (Özerdem and Jacoby, 2005). On May 12th, 2008, Wenchuan Earthquake attacked Sichuan Province in West China, led to a death toll of nearly 70,000 (CNCDR and UNDP, 2009). Accompanying this tragedy was an unprecedented participation of volunteers and civil society organizations (CSOs) in disaster relief activities. Their participation changed the disaster relief mode of China, which used to be monopolized by government. Scholars regard the year of 2008 as the "First Year of Civil Society" (Xu, 2008; Gao and Yuan, 2008; Xiao, 2009), while other scholars hold an opinion that China is still on the way to civil society (Wang, 2009). However, the dispute exists in the abstract concept of *civil society*. Both of them admit that CSOs have made significant progress experiencing the earthquake. On the other hand, active roles of CSO responding disasters have been examined in Kobe Earthquake (Atumi, Sugiman, Mori and Yatsuzuka, 1995), Mozambique

Floods (Moore, Eng and Daniel, 2003) and Indian Ocean Tsunami (Kilby, 2008). In China, there are also many preliminary studies on CSOs' roles to response disaster (Gao and Yuan, 2008; Teets, 2009; Xiao, 2009; Zhu, Wang and Hu, 2009). However, most of these researches concentrate in 2008-2009, and focus on 2008 Earthquake. On April 20th, 2013, a 7.0 magnitude earthquake struck Sichuan again. The epicenter is located in Lushan, which is only about 200 kilometers away from Wenchuan. The author was in Sichuan at that time to attend the fifth anniversary forum of Wenchuan Earthquake, noticed that a number of CSO members who actively participated in 2008 relief contributed themselves in the affected areas again. Most of their organizations were born being touched by Wenchuan earthquake after 2008. Thus, how did these CSOs perform in the last disaster, and how did these CSOs develop during the past five years?

This paper aims make clear to the growth of China's CSOs, particularly in the field of disaster response, during 2008-2013. Method of multiple case studies is used for in-depth and multi-faceted explorations. The author interviewed CSOs, government officers, volunteers, and local victims from April to May in 2013. In order to be more objective, reports, news and other literature were also reviewed to collect more comprehensive data. The paper is divided into three major sections. In the first section, the impact of 2008 Wenchuan Earthquake on China's civil society is presented as a background. Secondly, multiple case studies are used to illustrate the growth of China's CSOs in the field of disaster response, by examining their establishment motivations, organizational structure, evolution process and activities in the past five years. The paper closes with a discussion of the issues and lessons based on findings.

2. IMPACT OF 2008 EARTHQUAKE ON CHINA'S CIVIL SOCIETY

It is necessary to define *civil society* firstly because the contemporary meaning of this term is contested. The definition of *civil society used* in this paper refers to the sphere of voluntary associations in which individuals engage in activities of public consequence, distinguished from the public activities of government, and from the private activities of markets. CSO refers to an organization which is self-governing, not profit distributing, and formed voluntarily by members, including NGOs, NPOs, volunteer organizations and foundations for the commonweal. One fact need be mentioned is that relation between government and CSO in China is closer than in Western countries. It is a consequence not only of unique social and political context, but also the CSOs' own understanding of their roles. Most CSO leaders do not see their objective in confronting government or protecting society from the state. Rather, they see the mission as fulfilling their citizen responsibility in collaborating with government (Edele, 2005). In addition, more and more government-organized NGOs (GONGOs) are detaching link from government in recent years. For example, *China Foundation for Poverty Alleviation (CFPA)* has sought to distance itself from its past identity as a GONGO, making efforts to professionalize and increase transparency and accountability. It is also famous for its consistent support on grassroots CSOs. Therefore, although the focus of this paper is the real grassroots CSOs, it is also impossible to exclude involvement of these transforming GONGOs in China's civil society.

CSO development in China has been quick. Economic reform process initiated in the late 1970s created the possibility for China's emerging civil society. Before the commencement of economic reforms in 1978, the provision of social services such as housing, health insurance, schools and pensions were all organized through state systems related mainly to work units, resulted in no living space for autonomous organizations. Since the 1980s, the government has been establishing GONGOs formally situated outside the state system in order to address social and environmental problems. At the same time, international NGOs (INGOs) began to enter China. The rapid economic growth led to emergence of a middle class with stronger economic level and higher education. They became the first generation organizing autonomous groups. The first real grassroots CSO *Friends of Nature* was set up in 1993. From then, more and more homegrown grassroots CSOs have been established. According to the official data from the Ministry of Civil Affairs (MOCA), at the end of 2007, China had almost 381,000 CSOs. The data only indicates the number of registered CSOs which had registered at MOCA, while a large number of unregistered CSOs are not included.

However, although the number is so huge, only few GONGOs and INGOs had participated in disaster relief before 2008 earthquake (refer to Table 1). There are various factors contribute to absence of grassroots CSOs such as: (1) Insufficient priority. The rapid economic development has led to a mass of social problems. Comparatively, CSOs had paid more attentions to the issues such as poverty and children, identified these issues as their missions, rather than disaster response. (2) Shortage of funds. Only two GONGOs, *Red Cross Society of China (RCSC)*, a nominally NGO but actually a part of the central government, and *China Charity Foundation (CCF)*, another agency affiliated with MOCA, had been permitted to receive donations and relief materials. Public foundations, most of which are GONGOs, may raise fund publicly in peacetime, while had been excluded to receive donations when disaster occurred until the enactment of *Administrative Measures for Disaster Relief Donations* on April 28, 2008. Most of grassroots CSOs had survived depending on the aid from INGOs, lacking of ability to carry out long-term activities in affected areas. (3) Political pressure. Although the *National Preparatory Plan for Disaster Relief and Emergency Response* issued by the State Council in 2006 had encouraged participation of CSOs nominally, there had been no approach available in practice. For example, in January 2008, when a snow disaster occurred, some grassroots CSOs located in Guangdong tried to participate in disaster relief, but refused by local government. Instead, the members were permitted to take actions in the name of individuals (Yu, 2010). Wang, the former director of MOCA disaster relief department, describes the characteristics of disaster management system in China as: "unified led by the Party and government, divided responded by each department, and managed at different administrative levels". From the interview of a local government officer in Sichuan, disaster relief "is the responsibility of government. The participation of other organizations outside the state system would disturb the social order." In summary, before 2008 earthquake, the disaster response used to be monopolized by the state in China.

Wenchuan Earthquake triggered changes from May 12th, 2008. After the disaster, outpour of citizens provided their aid and funds to the affected areas. They helped with health, sanitation, medical aid, food distribution, and security in days and months following the quake. Official data from MOCA indicates that more than 3,000,000 volunteers contributed their time and efforts in the disaster affected areas until the end of 2008; donations for emergency relief and post-disaster reconstruction achieved 76.7 billion Yuan, in which donation from the individual reached 45.8 billion Yuan. It is the first time that individual donation exceeding donations from the enterprises historically (Charity and Donation Information Center, 2009). The nationwide participation ignited CSOs' enthusiasm. According to an incomplete statistics survey, more than 264 CSOs have taken actions in disaster relief and reconstruction work (Zhu, Wang and Hu, 2009). They have carried out projects in the field of emergency rescue, health care, reconstruction of housing, livelihood support for residents, etc. Their behaviors are regarded as "the first exposition of the Chinese CSO sector" by a CSO leader.

The disaster also featured an unprecedented large-scale cooperation of CSOs. It is very significant because there had been almost no autonomous network and umbrella bodies due to legislative restrictions in the past. According to the report from NGO Research Center (2006), only a bit more than 6% of CSO stakeholders thought that CSOs were active in sharing information amongst each other; nearly 40% of stakeholders thought that Chinese CSOs had few or none cooperation with one another; nearly nobody thought they cooperate very well before 2006. Most of the CSOs began to choose cooperation in disaster relief because the devastating earthquake had made them recognize their limited capacity to address this severe damage. On May 13, a joint declaration sponsored by *Narada Foundation*, *CFPA* and *Friends of Nature* called on CSOs to unite to response disaster attracted 164 CSOs nationwide. A survey of 70 CSOs indicates that 58.6% of the respondents belong to an alliance with 3 or more than 3 CSOs (Wang, 2009). According to an incomplete statistics investigation, there were 19 CSO-networks formed after the earthquake (Zhu, Wang and Hu, 2009). One example is *Sichuan United Office for NGO Disaster Relief (SUND)*, which was set up on a few hours after the earthquake. Although it was closed on May 30, more than 100 organizations had joined using the internet. It had raised materials of 1.8 million and mobilized thousands of volunteers. Another network located in the disaster affected areas is *Sichuan 512 Voluntary Relief Service (SVRC)*, which was established on May 15 to united 34 NGOs, including 18 homegrown CSOs, 6 INGOs, 4 foundations, 3 volunteers associations and 3 internet-based associations. Different *SUND*, *SVRC* was restructured after the emergency period of 2008 earthquake. Until now, it has still played the active roles as a regional platform to share information and coordinate disaster relief efforts among local CSOs. There were also some CSO-networks located outside the affected areas helping to gather supplies donated by enterprises and transport them to Sichuan, such as *Xintuofeng Action*, a smaller network involving *One Foundation* and 4 NGOs located in Shanghai.

Moreover, the increasing need of victims could not be met only by governments, which had been also severely destroyed in the earthquake. The pressing shortage of relief personnel and resources led to the welcome attitude of national and local government. In addition to *RCSC* and *CCF*, 18 public foundations were permitted to receive donation after this disaster. Some public foundations such as *RCSC* and *China Youth Development Foundations*, and some private foundations such as

Narada Foundation, began to realize the importance of grassroots organizations' participation in disaster management after 2008 earthquake. On the one hand, these existing CSOs began to take actions in the following disasters; on the other hand, they have contributed to the birth of new-established CSOs providing them funds. Touched by 2008 earthquake, a number of grassroots organizations in the field of disaster response were established as stated in Table 1. For example, after the closure of *SUND*, one leader established *NGO Disaster Preparedness Center (NDPC)*. *Beichuan China Heart Association* is another CSO located in Sichuan evolved from an embryonic temporary association of volunteers after earthquake to deal with disaster relief. The influence is not only within Sichuan, but also brought impact on the regions outside affected areas: 2 volunteers worked in *SUND* went back to their hometown and established *Ying Team* located in Yunnan Province. *Will Gathering Disaster Mitigation Center* was also established in Guizhou Province by a volunteer experiencing 2008. In the next section, a case study of One Foundation is presented. One thing need to notice is that, the case study cannot represent all of these CSOs. Actually, within the limited space for CSOs in China, these CSOs must have their own unique advantages.

Table 1: Part of CSOs involving disaster response in China

<table>
<tr><th colspan="2">Type</th><th>Name</th><th>Founded Time*</th><th>Time into DR field</th></tr>
<tr><td colspan="2" rowspan="4">INGO</td><td>Oxfam</td><td>1991</td><td>1991</td></tr>
<tr><td>Tzuchi Foundation</td><td>1987</td><td>1991</td></tr>
<tr><td>Save the Children</td><td>1989</td><td>2008</td></tr>
<tr><td>Mercy Corps</td><td>2001</td><td>2008</td></tr>
<tr><td rowspan="5">GO-NGO</td><td rowspan="2">Agency</td><td>RCSC</td><td>1950</td><td>1987</td></tr>
<tr><td>CCF</td><td>1994</td><td>1998</td></tr>
<tr><td rowspan="4">Public foundation</td><td>CFPA</td><td>1989</td><td>2002</td></tr>
<tr><td>China Charities Aid Foundation for Children</td><td>1981</td><td>2008</td></tr>
<tr><td>China Youth Development Foundation</td><td>1989</td><td>2008</td></tr>
<tr><td rowspan="8">Grass-roots CSO</td><td>One Foundation</td><td>2007</td><td>2008</td></tr>
<tr><td rowspan="2">Private foundation</td><td>China Social Entrepreneur Foundation</td><td>2007</td><td>2008</td></tr>
<tr><td>Narada Foundation</td><td>2007</td><td>2008</td></tr>
<tr><td>National organization</td><td>Huaxia Commenweal Service Center</td><td>2010</td><td>2010</td></tr>
<tr><td rowspan="4">Regional organization</td><td>NDPC</td><td>2008</td><td>2008</td></tr>
<tr><td>Yixing Team</td><td>2008</td><td>2008</td></tr>
<tr><td>Will Gathering Disaster Mitigation Center</td><td>2008</td><td>2008</td></tr>
<tr><td>Beichuan China Heart Association</td><td>2008</td><td>2008</td></tr>
</table>

* For INGOs, the time indicates they began their activities in China Mainland.

3. CASE STUDY: GROWTH OF CSO RESPONDING DISASTER

As a case study, *One Foundation* is described in details in this section, while other CSOs cooperated with it such as *NDPC* will also be involved. Given the relative young age of these organizations, it may be too early to proclaim success or failure, while much can be learned by understanding their growth process during the past five years.

3.1 Establishment motivation

One Foundation was founded by international kung fu star Jet Li in 2007. The motivation to establish such an organization primarily involved in disaster relief activities is related to his own survivor experience in 2004 Indian Ocean Tsunami. On Dec 25th, 2004, he was in the Maldives and almost lost his children during an island vacation. Touched by this life-shaking experience, he announced his plans to start the *One Foundation* a few days later. The formula is very simple: one person + one Yuan per month = one big family. However, he did not quite know where to begin at that time (Li, 2008). The status of a public foundation is needed to be authorized to raise funds publicly, but it was difficult to register as a public foundation without any connection with the government at that time. Finally, he had to set up an attached special project under *RCSC* in 2007, named as the *Jet Li One Foundation Project* to share its right to raise funds publicly, and registered as a private foundation with the named of *Shanghai-based Jet Li One Public Welfare Foundation* to legitimize its legal entity in 2008.

3.2 Performance in Wenchuan Earthquake

The Wenchuan Earthquake is the first massive disaster *One Foundation* faced after its establishment. The identity under *RCSC* made it become the only grassroots organization to receive public donations after the disaster. Within 3 days, the donations had reached 60 million Yuan, excluding mountainous relief materials donated from enterprises and individuals. It was a challenging task for this young organization with 13 staffs totally, in which only 3 staffs in Shanghai office to manage the donations at that time. The shortage of personnel pushed it cooperate with 4 NGOs located in Shanghai on May 14th. Their united action was named as *Xintuofeng Action*. All of the information, such as lists of materials and receipted signed by local victims were open on the internet, and supervised by the public. The high transparency, different from the government and GONGOs in the past, earned *One Foundation* a growing reputation afterwards. According to its annual financial statement audited by Deloitte, the donations earmarked for Wenchuan Earthquake had reached 96,891,706 Yuan until the end of 2008. The abundant funds made it possible to carry out continued activities in the disaster affected areas for reconstruction. Until April 30th, 2011, three years after the earthquake, *One Foundation* had put about 108,021,201 Yuan into affected areas, including 42 projects covering education, poverty alleviation, community development, health care and many other fields. It claims more than 5 million people had been directly and indirectly benefited in its open report published on May 12, 2011.

The outstanding performance of *One Foundation* pushed it becomes the first grassroots public foundation without government backing. In December of 2010, *One Foundation* was eventually able to register as a public foundation in Shenzhen, where the registration regulation had been reformed and relaxed. Both of the identities before along with funds, projects and personnel were integrated to the *Shenzhen One Foundation Charity Fund*.

3.3 Current system for disaster response

The legal status as a public foundation further guarantees the abundant fund for rapid development. Two networks, *One Foundation* Rescue Alliance (OFRA) and *One Foundation* United Rescue (OFUR), as well as five Disaster Preparedness Warehouses (DPW) located in disaster-prone areas have been established as its main channels to response disasters during the past five years. OFRA was set up to unit 30 rescue volunteer teams on May 12th, 2009. It is an open system to welcome groups, as well as the individuals who are enthusiasts in outdoor sports. At present 163 voluntary rescue teams has joined; the number of volunteers (includes the member of teams and individuals) has reached nearly 5000.Another network, OFUR, was set up to unite 11 regional CSOs involving disaster response on Feb. 23rd, 2012, including NDPC and Yixing Team. OFUR is seeking to build a dynamic, interconnected response mechanism to carry out emergency disaster relief, reconstruction work and routine disaster prevention education. In the event of disaster, the local partner CSO establish a working platform and assume the responsibility of coordinating and providing services, while other partner agencies support operations and resources. Different from OFRA, members of OFUR are all in the forms of organizations. They participate in all the periods of disaster management cycle: response, recovery, mitigation and preparedness.

In the recent years, OFRA and OFUR have played their active roles in Sichuan, Qinghai, Guizhou, and Yunnan Province for earthquakes, mudslides, droughts, floods and other natural disasters. The network of regional teams guarantees the quick response for disaster. In the case of 2013 Lushan Earthquake, the leader of OFRA Sichuan Team was feeling the shakes and immediately organized local team for preparedness. 10 minutes after the quake, pioneering team departed to the affected areas and arrived 2 hours later. It is a disgrace for my profession if we cannot arrive the disaster affected areas within 24 hours." A member said. For reference, the response timeline is presented in Table 2. At the same time, OFUR partner proceeded to deliver relief materials from DPW in Sichuan, Guizhou and Shaanxi Province. The Emergency Response Plan was officially announced early morning 4 am, April 21st: Stage One for Rescue, with rescuing of lives and salvaging of materials as main focus in the first month after the disaster; Stage Two for Relief, the settlement of disaster victims within 4-8 weeks, ensuring the delivery of basic living necessities; Stage Three for Rebuilding, within 1-2 years after the disaster, providing psychosocial rehabilitation facilities and services for post-disaster children. Within 72 hours after the disaster, emergency rescue and transportation of the injured is the focus. During the two days after Lushan Earthquake, OFRA rescued 20 people serious injured, 56 people lightly injured, and transported more than 600 people injured. A total of 182 personnel was dispatched in the disaster area until April 27th.

Table 2: Quick response of OFRA after Lushan Earthquake on April 20, 2013

Time	**Events**
08:02	Earthquake occurred.
08:12	2 members departed as reconnaissance group.
10:05	The first two pioneer members arrived in affected areas, returned feedback to the headquarters and began rescue.
10:08	1st group, Sichuan rescue team, departed for affected areas with dogs and equipments.
10:30	2nd group, including 6 rescue teams from other provinces: Hebei, Henan, Guangxi, Beijing, Qinghai and Yunnan had been assembled, departed to the affected areas.
14:40	1st group arrived. Field command was set up.
16:40	Logistical support team for 1st group arrived.
22:45	Henan rescue team of the 2nd group arrived.

4. FINDINGS AND ISSUES

Characteristics of *One Foundation* are summarized as the following:

TRANSPERANCY Different from the government-backed public foundations, *One Foundation* has adopted its transparency mechanism from its establishment. All the public donations to *One Foundation* is hosted by *China Merchants Bank*, audited by *Deloitte*, and accounted by *KPMG*. List of relief materials, financial statements, procurement notices and invoices can be checked on its official website. The public has expressed distrust of GONGOs, using the checkbooks to vote for the bottom-up CSO over the government-backed *RCSC*. A recent survey by newspaper *China Youth Daily* reflects that 60% of interviewees expressed trust in NGO, while only 10% trusted GONGO. After 2013 Lushan Earthquake, One Foundation has received donations worth 28.5 million Yuan until May 12th, 2013.

PROFESSIONALISM OFRA members have outstanding capabilities in various fields such as diving, flying, carving, mountaineering, psychological counseling, cross-country driving, and radio communication and so on. Some of them hold the international rescue license, and have participated in international operations. Moreover, most of the member teams are equipped with professional tools including satellite phones, SUVs, rescue dogs and generators. The professionalism is also reflected in the procedure. Once a disaster occurs, members are assembled following an agreed process: in order to avoid unnecessary waste of personnel, the reconnaissance team is sent out as the pioneer firstly, while others are standby. The regional leader decides whether to send follow-up team according to the feedback from the reconnaissance team. In the case of Lushan Earthquake in 2013, the leader of Sichuan Team only sent two members for damage assessment at the beginning. The reconnaissance returned the message two hours after the quake, indicate that the situation is very serious. Then, the leader immediately sent the second team to the affected areas, followed up by the third.

LINKS WITH LOCAL CSOs Members of OFRA are distributed in 30 provinces, while members of OFUR are distributed in 11 provinces. The alliance is not only able to response the emergency events in each region, but also to coordinate the inter-provincial relief efforts. The network of local volunteers and organizations also guarantees its quick response for disaster. However, it is not easy to maintain these independent CSOs in the peacetime. Members of OFRA usually have their own jobs, and join in the actions of rescue voluntarily. They participated only the period of emergency rescue, while the connections in OFUR are tighter because the members of OFUR participated in all periods of disaster cycle. Although the CSOs have accumulated experience in disaster relief over the years, they are still facing problems such as insufficient staffs for community disaster preparedness training, lack of daily office expense. The leader of NDPC, who is the first person to come up with the idea of United Rescue, openly expressed his dissatisfaction to the media. “One Foundation hopes us to wear their uniforms in the disaster relief, but our organizations also need our own influence to develop ourselves. Funds received from only one foundation is not enough to maintain an organization. We have to find other foundations for cooperation.” The founder of Yixing Team also expressed his opinions as “Some foundations see local CSOs as merely a short-term instrument. They hope they can all on organizations to be effective in a disaster even without providing them with support on an ongoing basis.”

5. CONCLUSIONS AND DISCUSSIONS

The 2008 earthquake serves as a turning point for many existing CSOs to intake the disaster response to their main fields, and also offers opportunity for those grassroots organizations established in a bottom-up way. Case study indicates that transparency and professionalism should be the future direction for those powerful organizations, while its link with local organizations is still under disputation. Localized and community-based disaster prevention and disaster mitigation measures tend to provide the most effective and rapid disaster relief to response the more complicated natural disaster. The mode of CSO-network is a good vision for a sustainable development of disaster affected community, but realizing it still requires further considerations. Galaskiewicz (1985) argued while the hierarchical models of resource allocation and movement emphasize the power during inter-organizational transactions. Thus, to avoid the possible unequal connections among member organizations, the problems such as insufficient staff and shortage of funds have diminished the development of grassroots CSOs should be firstly addressed.

Chinese government encourages CSOs to participate in disaster response in many statements. However, there are not operational laws formulating mechanism and procedure on the participation of CSOs so far. Moreover, the regulation on public fund-rising is so strict even celebrities as well-connected as Jet Li, have a difficult time acquiring public foundation status. As the first step, government need further relax the regulation on public foundation to support these grassroots local CSOs. And then, when the local CSOs become self-sufficient and more independent, a organizational structure like OFRA with weak ties can be established to be more equal and effective.

REFERENCES

Charity and Donation Information Centre, 2009. *2008 Annual Report of Chinese Charitable Contributions*. Retrieved from http://www.mca.gov.cn

CNCDR, and UNDP, 2009. *The Research Report of the Sichuan Earthquake Emergency Relief.* Retrieved from http://ch.undp.org.cn/downloads/CPR/2.pdf

Edele, A., 2005. *Non-Governmental Organizations in China*. Centre for Applied Studies in International Negotiations, Geneva.

Gao, B., & Yuan, R. (editors), 2008. *The Blue Book on Chinese Civil Society Development.* Peking University Press, Beijing.

Galaskiewicz, J., 1985. Interorganizational relations. *Annual Review of Sociology*, 11, 281-304.

Jalali, R., 2002. Civil society and the state: Turkey after the earthquake. *Disasters*, 26, 120-139.

Kilby, P., 2008. The strength of networks: the local NGO response to the tsunami in India. *Disasters*, 32, 120-130.

Kubicek, P., 2002. The earthquake, civil society, and political change in Turkey: assessment and comparison with Eastern Europe. *Political Studies*, 50, 761-778.

Li, J., 2008. My turn: the tsunami that changed my life. *Newsweek*, 152 (14).

Moore, S., Eng, E., and Daniel, M., 2003. International NGOs and the roles of network centrality in humanitarian aid operations: a case study of coordination during the 2000 Mozambique floods. *Disasters*, 27, 305-318.

NGO Research Center of Tsinghua University, 2006. *A nascent civil society with a transforming environment*. CIVICUS civil society report, Beijing.

Özerdem A., and Jacoby T., 2005. *Disaster Management and Civil Society: earthquake relief in Japan, Turkey and India*. I.B.Tauris, London.

Shaw, R., and Goda, K., 2004. From disaster to sustainable civil society: the Kobe experience. *Disasters*, 28, 16-40.

Tweets, J., 2009. post-earthquake relief and reconstruction efforts: the emergence of civil society in China? *The China Quarterly*,198, 330-347.

Wang, M (editors), 2008. *Emerging Civil Society in China, 1978-2008*. Social Sciences Academic Press, Beijing

Wang, M (editors), 2009. *Reports on the Civil Society Action in Wenchuan Earthquake: China NGOs in Emergency Rescue*. Social Sciences Academic Press, Beijing.

Xiao, Y., 2009. *Wenchuan Earthquake Witnesses: the Growth of China's Civil Society*. Peking University Press, Beijing.

Xu, Y., 2008. The first year of Chinese civil society, *NPO Journal*, Vol 4, 1-5.

Yatsuzuka, I., 2007. Recording volunteer activities after the Great Hanshin Earthquake and their transition: their functions and possibilities from the viewpoint of social change. *The Japanese Journal of Experimental Social Psychology*, 47, 146-159.

Yu, X., 2010. *How Chinese Civil Society Organizations involved in Responding to Climate Disasters*. Friends of Nature, Beijing.

Zhu, J., Wang, C., and Hu, M., 2009. *Obligation, Action, and Cooperation: Case Studies on NGO's Participation in Wenchuan Earthquake Relief*. Peking University Press, Beijing.

Survey on current system for disseminating disaster early warning by cell phones in Japan

Takanori SAWARA[1], and Miho OHARA[2]
[1]Graduate Student, Graduate school of Eng., the University of Tokyo, Japan
sawara@iis.u-tokyo.ac.jp
[2]Associate Professor, International Center for Urban Safety Engineering (ICUS), Institute of Industrial Science, the University of Tokyo, Japan

ABSTRACT

Dissemination of disaster early warning to cell phone users is becoming more effective for disaster mitigation and preparedness as a lot of people are getting their own cell phones. In Japan, the ratio of the cell phone users exceeded more than 90-percent of the total population. Now, two kinds of systems for dissemination disaster early warning to cell phone users are popular in Japan. One is cell broadcast service called "Area-mail" that is provided by several cellular service providers to send e-mails informing disaster early warning to all the cell phone users in the high risk area. Under this system, earthquake early warning and tsunami warning are automatically sent to all the cell phone users. In addition, local disaster information such as evacuation counsels is also sent if local governments adopt this system. The other system is e-mail service by local governments that provide disaster warning or information to the people who registered their e-mail addresses through the website in advance.
This research aims to understand current situations of both systems for disseminating disaster early warning by cell phones in local area. A questionnaire surveys to the 33 local governments in Kanagawa Prefectures were conducted to know how both systems are used for information dissemination between governments and local residents. The survey revealed that both systems were widely adopted by many local governments in Kanagawa Prefectures. Their target disasters and criterion for sending warnings, frequency of their emergency and daily uses were verified. Especially, e-mail service with pre-registration by local governments was frequently used for various purposes such as disaster drills or sending information on normal events. Finally, issues to improve these systems were discussed based on the survey results.

Keywords: *information dissemination, disaster warning, cell phone*

1. INTRODUCTION

Dissemination of disaster early warning is effective for disaster mitigation and preparedness. In Japan, local governments have introduced many measures to disseminate disaster early warnings.

One of the major systems for disseminating disaster information is "disaster prevention administrative radio system." When a local government sends disaster information by the radio system, the information is disseminated instantly by loudspeakers and radio transmitters. Other measures to disseminating the information are local government official websites, official accounts in a social networking service such as twitter, community radio by the governments, official channels in cable TV, and data broadcasting system in local television companies. In addition, some local governments can disseminate the information to cell phones of local residents. Disseminating disaster early warning to cell phone users is becoming more effective. Two kinds of systems for disseminating information to cell phone users are becoming popular in local governments in Japan.
One is cell broadcast service called “Area-mail” that is provided by several cellular service providers to send e-mails informing disaster early warning to all the cell phone users in the high risk area. Under this system, earthquake early warnings and tsunami warnings are automatically sent to all the cell phone users without residents’ registering their e-mail address. In addition, local disaster information such as evacuation counsels is also sent if local governments adopt this system. To send local disaster information by this system, local governments send text messages to each cellular service providers.
The other system is e-mail service by local governments that provide disaster warning or information to the people who registered their e-mail addresses through the website in advance.
As local governments can decide the use of the two systems for cell phone users and the contents of the information, there are some differences among local governments to the use. This research aims to understand current situations and the difference between both systems.

2. METHODOLOGY

2.1 Outline of questionnaire procedures

To understand current situations of two systems for disseminating disaster information to cell phone users, a questionnaire survey to almost thirty three local governments in Kanagawa Prefectures were conducted to evaluate the efficiency of both systems for information dissemination between local governments and residents. The questionnaire was sent by fax to disaster prevention section or crisis management section in each local government’s office before the beginning of August 2013, and twenty two local governments answered.

2.2 Contents of the questionnaire

Table 1 provides the information of all questions on the questionnaire. At first, all available media to disseminate disaster information for local governments are asked in the questionnaire survey. If a local government has adopted either cell broadcast system or e-mail system with pre-registration by the local government, the current situation such as the contents of information sent by the systems, history, frequency of their usages, and problems of the systems which is recognized by the local governments was asked.

Table 1: Contents of the questionnaire

Current situations of information dissemination	All available media to disseminate disaster information
	The number of outside loudspeakers for disaster prevention administrative radio system
	The number of individual receivers in residents' houses for disaster prevention administration radio system
	Current situation of adopting the national early warning system which is called "J-ALERT"
Cell broadcast service	Adoption of the service by major cellular service providers
	Contents of disseminated information by the service
	Comparison of the use between disaster prevention administrative radio system and cell broadcast service
	Past use of the service during disasters
	Past use of the service for drills
	Problem of the service
	Common question asked by residents
E-mail service by local governments	Adoption of the service by the local governments
	The number of registered people
	Contents of disseminated information by the service
	Comparison of the use between disaster prevention administrative radio system and e-mail service
	Frequency of sending e-mail by the service
	Problem of the service

3. RESULTS

3.1 All available media for local governments

Based on the answers obtained from local governments in Kanagawa Prefecture, most of the local governments can use multiple media to disseminate disaster information. Table 2 provides the information regarding the media adopted by local governments. It shows that almost all the local governments use loudspeakers for disaster prevention administrative radio system and that information dissemination for cell phones is also commonly used by local governments.

Table 2: Available media for local governments (N=22)

Media	**Num. of local governments**	**Percentage**
Loudspeakers for disaster prevention administrative radio system	21	95.5%
E-mail system by local governments	20	90.9%

Official website of each governments	19	86.4%
Cell broadcast service	15	68.2%
Data broadcasting by local TV	12	54.5%
Community radio	10	45.5%
Social networking service (Twitter etc.)	9	40.9%
Cable TV	8	36.4%

In two systems for information dissemination for cell phone users, cell broadcast service is used by 68.2% of local governments, and e-mail system by local governments is used by 90.9% of local governments. Figure 1 shows which city uses two systems. Big cities such as Yokohama, Kawasaki, and Sagamihara tend to use both systems.

Figure 1: Available system for disseminating information to cell phones

3.2 Contents of disaster early warnings for cell phones

Survey revealed the difference of contents between the information sent by cell broadcast service and by e-mail system with pre-registration by local governments. Figure 2 shows the contents disseminated by the systems.
Information surrounded by red lines is urgent disaster early warnings disseminated by both systems. For example, many local governments use both systems to disseminate evacuation orders, evacuation advisory, Tokai Earthquake prediction information, and emergency warnings which are issued to alert people to the significant likelihood of catastrophic disasters. Missile information and sediment disaster bulletins which are issued at the high risk of sediment disaster are disseminated by both systems in many cities or towns. Since heavy rain warnings and flood warnings are frequently issued, less local governments disseminate the warnings by cell broadcast system.
Information surrounded by green lines is earthquake early warnings and tsunami warnings. Approximately forty percent of local governments disseminate these warnings by e-mail service, but these warnings are disseminated to all areas likely to be affected by earthquake or tsunami.
On the other hand, e-mail service by local governments is used for disseminating other kinds of information which is not urgent and not related to disaster such as

photochemical smog, crime, request for searching for person, fire, and public relations by governments. The information is surrounded by orange lines in the figure 2. The information is not disseminated by call broadcast service at all.

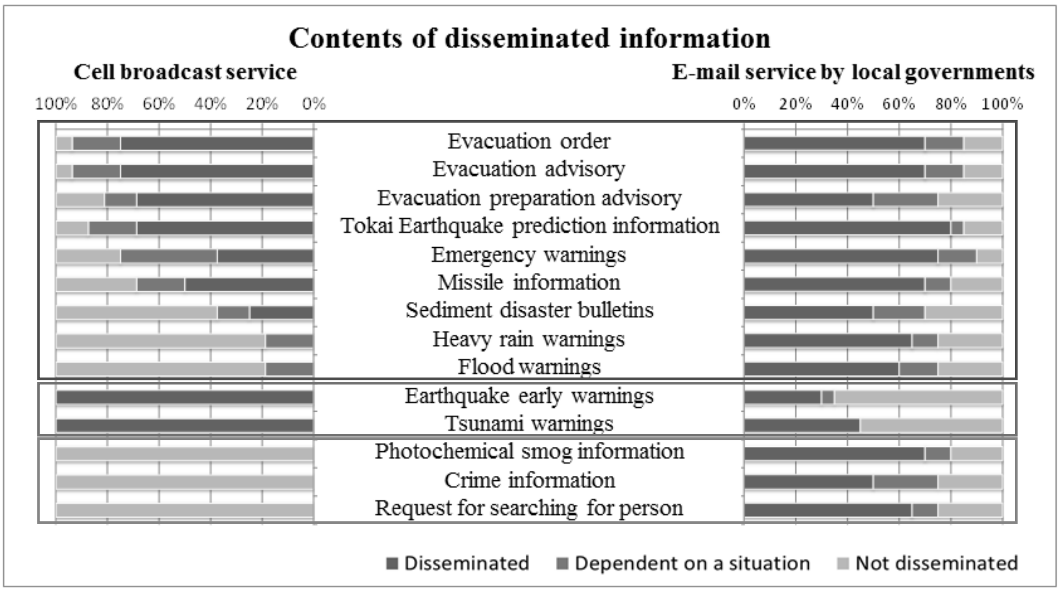

Figure 2: Contents of disseminated information

3.3 History and frequency of past use

Result of survey revealed that frequency of usage is completely different in two systems. Figure 3 shows how many times cell broadcast service was used by each local governments in the past. This service has been used only three times at most. Furthermore, more than a half of all the local governments which introduced the service have never used the service.

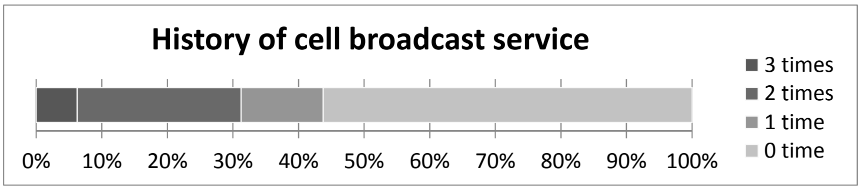

Figure 3: Number of times when cell broadcast service was used by each local government

On the other hand, e-mail service by local governments has been used more frequently than cell broadcast service. Most local governments introduced the system before the introduction of cell broadcasting service. Figure 4 shows the frequency of e-mail sent by e-mail service by local governments. This service is used at least once a month in almost all of local governments.

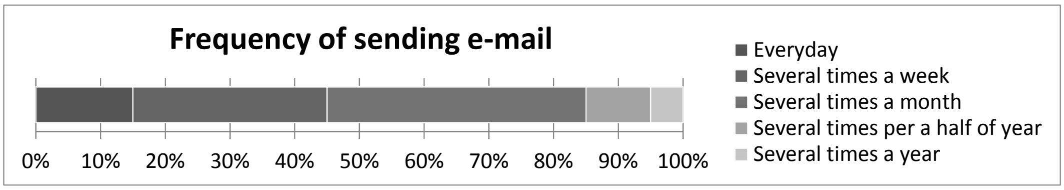

Figure 4: Frequency of e-mail sent through e-mail service by each local government

3.4 Problems in the two services

Survey has also elaborated the problems of the two systems which are considered by local governments, as shown in figure 5 and 6.

One of the most serious problems of cell broadcast service is a time-consuming work to send the same message to each cellular service provider. If a local government sends a message to cell phones by cell broadcast service via three cellular service providers, the staff has to send the same message three times to each cellular service provider. Another problem is that some cell phones cannot receive the information by the system. In addition, it may be difficult to disseminate information to elderly people because the ratio of elderly cell phone users is low. Another problem is that local governments cannot designate specific area at high risk. When a city decides to use the system for information dissemination, information will be disseminated in the whole city regardless of risk. For example, tsunami warning may be disseminated in mountainous area.

E-mail service by local governments has different problems. The most serious problem of this system is that the number of registered residents is limited. Based on the answers obtained from local governments, the average ratio of registered people to the total population of each city or town is 8.8 percent, although some registered people are not residents in the city or town. If urgent disaster early warnings are sent by the e-mail service, limited people will receive the warnings. Local governments cannot increase the number of registered residents easily because residents decide whether they register their e-mail address or not. Another problem is that it takes long time to send e-mail to all registered people. When lots of e-mail is sent at the same time, the e-mail will be likely to delay. In addition to it, the limitation of the office staff is also a problem. When members of staff in a local government's office are not enough such as night time, they cannot send e-mail to registered people.

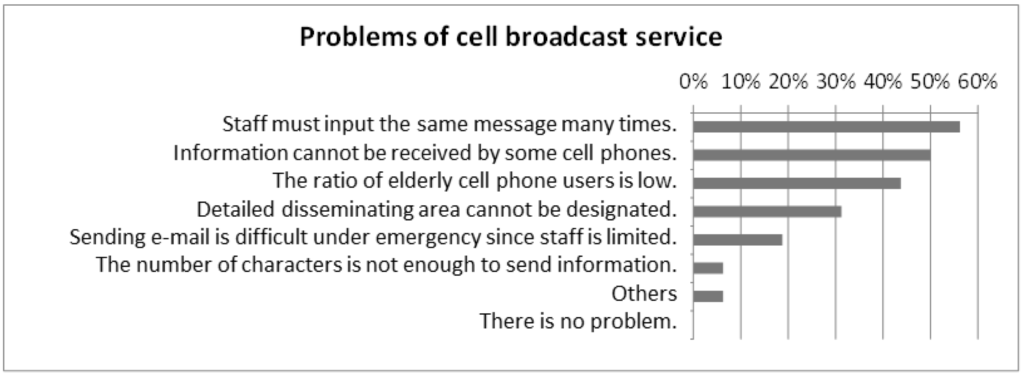

Figure 5: Problems of cell broadcast service

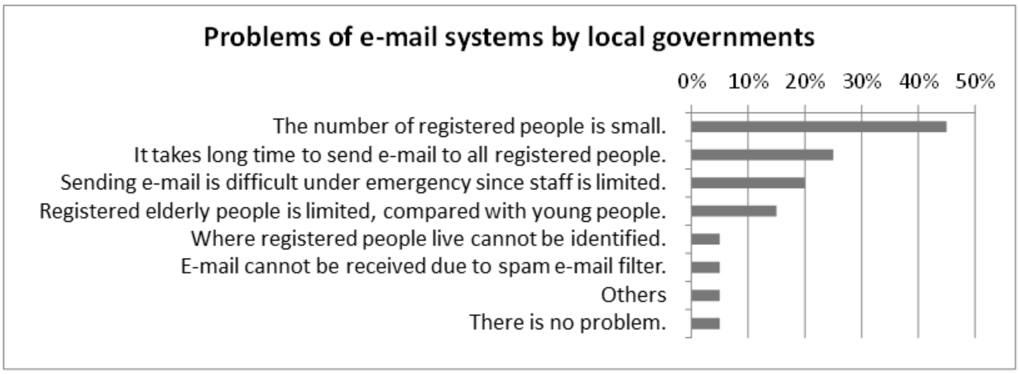

Figure 6: Problems of e-mail service by local governments

4. CONCLUSION

Current survey has revealed that both systems were widely adopted by many local governments in Kanagawa Prefectures. Their target disasters and criterion for sending warnings, frequency of their emergency and daily uses were verified. Especially, e-mail service with pre-registration by local governments was frequently used for various purposes such as disaster drills or sending information on normal events. Cell broadcast service is used only for urgent situations.
To improve these systems, cellular service providers should adapt new cell phone to cell broadcast service. Secondly, information disseminating area should be divided into small areas. In terms of local governments, cell broadcast service should be used more actively as a drill. This service has never been used in some cities or towns, so residents don’t understand the system. To improve e-mail service by local governments, an increase of registered residents is important. Public relations of this service should be done and the procedure of registration should be made more user friendly.

REFERENCE

Miho OHARA, Akiyuki KAWASAKI, Shinya KONDO, Atsushi TANAKA, 2012. A Survey on Information Dissemination by Area-mail during Storm Disaster due to Typhoon Talas in September 2011: Quick Report on Survey in Miki-cho, Kagawa Prefecture, *Seisan Kenkyu*, Vol 64, No 4, 553-556.
Japan meteorological agency, Weather, Climate & Earthquake Information, from: http://www.jma.go.jp/jma/indexe.html
NTT docomo Inc., 2013, the user policy for “Area-mail” service.
Fire disaster management agency, 2013. A guidance for developing disaster information dissemination method.

Assessing recovery: existing practices and evaluation measures

Yasmin BHATTACHARYA[1] and Takaaki KATO[2]
[1] Graduate Student, Department of Urban Engineering, the University of Tokyo, Japan,
yasmin@iis.u-tokyo.ac.jp
[2] Assistant Professor, ICUS, IIS, the University of Tokyo, Japan

ABSTRACT

Recovery is an essential part of the disaster cycle and perhaps the one that requires immense combined efforts from several parties, more so compared to other phases such as mitigation and preparedness measures. It is also an area which requires considerable study and contemplation due to its process and impacts being long-term. However, this is exactly where the complexity arises; recovery is also that much harder to study and define because of its long-term nature and impact. This paper is a literature review of the field of disaster studies in regards to recovery: when it emerged; how it was defined and conceptualized; and how it has developed to the present day. It will further focus on the aspect of 'quality' of recovery and provide perspectives on how recovery manuals and guidelines offer the assurance of quality in their approaches. Existing measures for assessing recovery are also discussed in brief and some future considerations for evaluating recovery are identified.

Keywords: *recovery, disasters, methodologies*

1. INTRODUCTION

The term "Recovery" is so often used and applied to so many contexts, that it is a major dilemma to try to define it let alone measure and evaluate it. Furthermore, a major obstacle in the field of recovery research is the long-term nature of recovery embedded within the broader context of regional development, which makes it even more difficult to track, measure and analyze.

This paper conducts a literature review on all of these aspects to understand the existing methods of analysis and the difficulties that arise when following manual-oriented approaches to recovery. Thus, it separates the ideologies from the realities and further aims to observe what have been highlighted as crucial to the methods of assessing recovery to give a foundation for future development of recovery assessment measures.

2. DEFINITION OF RECOVERY

Though most of the defined phases in the disaster cycle lack a specific definition (Neal 1997), ‘recovery’ is perhaps the most vaguely defined concept among them. As Neal (1997) notes, recovery research did not receive much attention in the early stages of disaster research and thus it is still in its nascent stages of development (with only about twenty years of history).

2.1 Sub-categories of Recovery

Although across literature, there are various usages of recovery, so far reviews have identified these major categories: reconstruction, restoration, rehabilitation, restitution, repopulation, redevelopment and recovery (Quarantelli 1999; Neal 1997; Aldrich 2012).

Overall differentiation of these categories as shown by Neal (1997) and Quarantelli (1999) are as follows: While ‘Reconstruction’ focuses exclusively on the rebuilding of the physical structures, ‘Rehabilitation’ considers more of the social aspects. Moreover, ‘Restoration’ has a stronger emphasis on bringing the society back to the pre-disaster status whether it be the physical or social structure. ‘Restitution’ implies legal actions to return to a former state of affairs, while ‘Repopulation’ is dependent on statistical data of human occupancy. Further to this, ‘Redevelopment’ stresses the facilitation of a *new* or *reformative* development as opposed to the restoration-oriented thinking, while ‘Recovery’ signifies bringing back the post-disaster situation to some level of acceptability which may or may not be the same as the pre-disaster level.

2.2 The Problem of Aim

Furthermore, while ‘prevention & mitigation’, ‘preparation’ and ‘response’ can still provide a clearer indication of what to aim for, the understanding of ‘recovery’ is troubled by its lack of direction. Its aim is an unidentifiable entity (because “there is no common solution” (Kato et al. 2013)) which is subject to constant criticisms by insiders and outsiders alike due to either their dissatisfaction or incomprehension. In addition, its complexity is furthered by the fact that it is a long-term process and therefore unable to be properly defined as a short-term project which is achievable and thus measureable.

3. EXISTING MEASUREMENTS OF RECOVERY

As mentioned previously, the measurement of recovery is immensely difficult due to the complexities involved as well as its long-term nature. Still, in looking at long-term recovery, some form of measurement is required to evaluate recovery. The following are some of the existing methods for evaluating the quality of recovery.

3.1 Housing Reconstruction

Monitoring housing reconstruction has been the most widely used measure of recovery. Physical reconstruction of infrastructure and housing appear to be most prominent because they are seen as the "key to revitalizing communities following major disasters" (Zhang & Peacock 2009), and provide a physical measure of permanent settlement population. Bolin and Stanford (1991) discuss recovery in terms of housing recovery arguing that that economic recovery and housing recovery are the precondition for psycho-social recovery of the victims. Similar discussion is also carried out by Peacock et al. (2007). Thus the level of housing restoration in a neighborhood has been directly related to the level and/or quality of recovery in many studies. In many cases, authorities also equate the reconstruction of housing with the end of population outflow from the region, and thus positive recovery from then on. Remote sensing is a frequently used method to observe this recovery process by the means of infrastructure and housing reconstruction (Vinci et al. 2011).

3.2 Domestic Assests Index

Bates and Peacock (2008: 3) carry out a cross-cultural, cross-disaster impact measure which "utilizes a conceptualization of living conditions and their relationship to household functioning." The basic idea revolves around measuring household recovery through observing the recovery of functionality necessary to carry out a household's routine activities. This is different from recovery measured in terms of physical reconstruction of houses at a community scale, because it considers recovery at a more micro level scale. It focuses on "domestic assets" (capital equipment used to perform normal household functions –i.e. stove, tables, light, etc.) acquired by a household over time and the need to *reaccumulate* those in the event of a disaster. It further considers how the introduction of housing recovery programs changes the processes through which the reaccumulation occurs and how this might affect the overall recovery process. This methodology allows for a novel way to measure recovery cross-culturally (without being hindered by the national development status i.e. allowing comparisons between a developing and a developed country).

3.3 Social Capital

Though Aldrich (2012)'s study is not directly related to measuring the quality of recovery, it measures the pace of post-disaster recovery in terms of social capital. He studies four different disasters which vary across time and scale: Tokyo Earthquake 1923; Kobe Earthquake 1995; Indian Ocean Tsunami 2004; and Hurricane Katrina 2005 to show that *"high levels of social capital –more than such commonly referenced factors as socioeconomic conditions, population density, amount of damage or aid –serve as the core engine of recovery"* (Aldrich 2012: 15). For measuring these recoveries, various data sets used include voter turnout rates, participation in political activities, involvement in communal festivals, connections to extralocal organizations and such.

While the above have highlighted the existing methods for evaluating recovery, they may not be the best method for evaluating the *quality* of recovery. For example, in the case of housing reconstruction, many problems may continue to persist within the social fabric which may not be easily visible as discussed by Wisner (2004) and Pais (2008). Moreover, for the case of Great East Japan Earthquake recovery, Nakabayashi (2012) states that the first aim of recovery in the current era of depopulation should be to restore the "human-ware" (referring to the restoration of jobs and means of livelihood), while the reconstruction of the urban spaces, urban facilities and houses, or in other words the "hard-ware" aspect, should be last.

The approach of measuring Domestic Assests Index is a useful one. However, this is limited to measuring the recovery on the household scale. While one is likely to relate this to the overall recovery of the region, this may not be ideal. There are other layers of recovery involved such as the recoveries of the organizations, social networks, psychological rehabilitation, etc., which may not be adequately addressed in this method.

Similarly, the application of social capital for measuring recovery pace may not be so easy in a case like New Zealand where aftershocks are still continuing and therefore slowing down the pace of recovery considerably (Wilson 2012). More in-depth consideration of interactions among the different levels of social entities and how social capital copes with reoccurring disasters in a short period of time may be necessary.

4. MYTHS AND REALITIES OF EXECUTING SUCCESSFUL RECOVERIES

This section focuses on few of the general methods and practices that are considered to enable a *good* recovery. Elements such as citizen participation, recovery speed and   are emphasized in several recovery manuals and guidelines (Natural Hazards Center 2005; Department of Homeland Security & Federal Emergency Management Agency 2005; Hyogo Prefectural Government 1995; Canterbury Earthquake Recovery Authority 2012; The Reconstruction Design Council in Response to the Great East Japan Earthquake 2011) but how well are they implemented? It aims to disentangle the mythical ideologies from the realities of recovery by discussing implementation difficulties and questioning orthodox ideas.

4.1 Citizen Participation = Successful Recovery

Citizen participation is no doubt important when it comes to recovery, and accordingly, almost all recovery manuals worldwide have incorporated 'public involvement' in their design for a successful recovery (Natural Hazards Center 2005; Department of Homeland Security & Federal Emergency Management Agency 2005; Hyogo Prefectural Government 1995; Canterbury Earthquake Recovery Authority 2012; The Reconstruction Design Council in Response to the Great East Japan Earthquake 2011). "Bottom-up" community based plans are hailed as successful representations of recovery, while "top-down" approaches are highly criticized. These are evident in the recovery stories of Kobe after the Great Hanshin Earthquake and New Orleans after Hurricane Katrina. For example, Kondo (2008) and Edgington (2010) note that the initial selection of targeted development areas in Kobe (the twenty-four Intensive Restoration Zones or *jūten fukkō chiiki*) within a two month period after the earthquake, met with intense resistance from the citizens due to its non-participatory nature. This led to the development of the "two stage planning process" where local governments would set the basic urban structure and local communities would be involved in the neighborhood-level rebuilding and planning (Kondo 2008). Likewise, the New Orleans early planning initiatives like the 'Bring New Orleans Back' plan (autumn 2005 – spring 2006) also met with widespread criticisms for not including participatory procedures, necessitating the formulation of new participatory plans such as the 'Lambert Plan' (summer 2006) and 'Unified New Orleans Planning' (autumn 2006 – spring 2007) (Barrios 2011).

Although the necessity of citizen participation is agreed upon by all researchers, its successful implementation remains an overwhelming task. How to adequately involve citizens? How frequently and to what extent? These are issues that need further deliberation. For example, Maki (2006, cited in Kondo 2008), observes that in the case of the Great Hanshin-Awaji Earthquake recovery "community participation in Kobe was limited to local level rebuilding planning, and did not encompass a citywide planning vision and goals for recovery" –indicating that local level community involvement may not be sufficient. In regards to the frequency of citizen participation, Kato et al. (2013) note that in the case of the Great East Japan Earthquake recovery, due to the deadlines set forth by the central government and the local municipalities' obligations to meet these deadlines, the public participation and consensus building has become limited. A similar case caused due to the "tension between simultaneous desires for speed and for deliberation" is also observed in recovery planning of New Orleans (Olshansky 2008). Moreover, as observed by Kondo (2008) and Barrios (2011), more than often, "citizen participation" just remains a term on recovery manuals while the rigid application of professional planners' knowledge that is without consideration of the cultural, political and historical particularity, prevails –thus "threatening the environmental sustainability and creates conditions of social marginalization".

The above shows a greater dilemma in the context of how to facilitate proper citizen participation. Clearer guidelines regarding the extent of citizen involvement and further assessment in regards to what is adequate and what is not is needed. And additionally, the co-relations between the time required for citizen-participation and its effect on the pace of overall recovery needs to be thought about. Perhaps a "total-management" system as suggested by Kato et al. (2013) need to be put in place.

4.2 Fast is Good?

In general, there exists a strong image of fast recovery being equated to successful recovery. The Japanese recovery system tends to be especially focused on this issue. For example, Hayashi (2007) notes that the infrastructure of Kobe was restored in two years while the economic and social recovery continued to be underway 13 years later. Likewise, China’s rapid recovery from the large-scale damage of the Sichuan Earthquake was completed in two and a half years astonishing the whole world (Kato et al. 2013). Accordingly, the slow recovery of New Orleans on the other hand, encountered severe criticisms by the public (Aldrich 2012; Barrios 2011; Olshansky 2008). The ongoing recovery from the Great East Japan Earthquake also puts emphasis on how to achieve a fast recovery (with the official recovery duration set to five years).

However, in recent times there have been some debate regarding whether a fast recovery is really ideal (Kato et al. 2013). For instance, Olshansky (2008) notes how haste can create chaos and problems: decisions often occur at a faster pace than people can absorb; planning processes may proceed even in the face of discord; time for citizen participation may be limited (noted above as well); and mistakes in planning efforts are likely to occur. In New Zealand, the ongoing aftershocks have forced authorities to realize the dangers of a recovery proceeding in haste. The Canterbury Earthquake Recovery Authority declares the following in their Recovery Strategy manual:

> *“Recovery activities need to be sequenced carefully to avoid bottlenecks and minimise frustrations. Although a fast recovery is desirable, going too fast can create further problems. It creates competition for resources between projects, drives up costs and creates pressure on existing services and facilities. It may also not produce the best outcomes in the long term. As the aftershocks are continuing, time is needed for the land to settle down or be remediated. It is important to obtain the right information, including scientific data, and take a considered approach to planning and developing robust solutions before implementing them.” (CERA 2012)*

Citing the cases of New Orleans and Canterbury recoveries, Kato et al. (2013) also suggest that perhaps recovery does not necessarily have to be ‘fast’ in developed countries, but rather it is necessary to have a clear identification of the short-term and long-term goals.

4.3 Resilient Recovery, an unachievable aim?

‘Resilience’ is the buzzword of today, at least in the field of disaster research. It too, like recovery, is an ambiguous concept with multiple definitions given by different researchers. Guo (2012) lists the chronology of the term’s use and incorporation into urban planning (presented in brief here): stemming from the field of ecological sciences, the term originally referred to the “time required for an ecosystem to return to an equilibrium or steady-state following a perturbation” (Holling 1973, cited in Guo 2012), which was modified in the context of disasters as the “capacity to adapt to stress from hazards and the ability to recovery quickly from their impacts” (Timmerman 1981, cited in Guo 2012). The term was further broadened by Pelling (2003, cited in Guo 2012) as the "capacity to adjust to threats and mitigate or avoid harm" –which also accommodated the need to consider and prepare against future potential disasters. An all-inclusive definition provided by Comfort et al. (2010) provides a clearer picture:

> *"Resilience is the capacity of a social system (e.g., an organization, city, or society) to proactively adapt to and recover from disturbances that are perceived within the system to fall outside the range of normal and expected disturbances."*

While defining a resilient system is one thing, recognizing one is an even bigger challenge as noted by Comfort et al. (2010). In terms of recovery, this requires the consideration of many factors, especially the *state of return* that resilience would need to accomplish as mentioned by (Comfort et al. 2010: 8). Although disaster research in recent years have put much emphasis on the resilience factor in recovery and highlighted the need to rebuild to a better standard than the pre-impact level not only in terms of infrastructure, but also through social means, the policy implementation of this remains to be seen. For example, Edgington (2010) notes that "until the Kobe catastrophe there had been a notable lack of interest in either personal recovery or the long-term revival of stricken urban areas after a disaster." Though, after the Kobe earthquake, there have been considerable debate among scholars regarding the insufficiencies of a system which only aims for restoration and physical infrastructure improvement (Ota et al. 2010; Aota et al. 2010), Kato et al. (2013) note that in the current Japanese Disaster Countermeasures Basic Act, still the term *fukko* (referring to "longer term recovery") is only used only once and even then it is used in conjunction with the more frequently used *fukkyu* (referring to "recovery to original state"). One reason of such lack of implementation may be due to the fact because restoration or rehabilitation enables the definition of a clear and measurable goal, while recovery that emphasizes "improvement of the previous state" is more ambiguous as well as being controversial (Ota et al. 2010).

Perhaps the same reason can be applied to the field of disaster research. The scope for increasing resilience (or improvement) is unlimited; there will always be something more that can be done. Thus constructing an evaluative criteria for recovery is difficult. In addition, recovery quality comparisons are also difficult to make because the achievable level of improvement may vary across regions or countries due to their economic situation, political climate, cultural acceptability, and other various issues. Furthermore, validating resilience is another difficult task: it would be easy if the disaster occurred routinely; the capability comparisons in dealing with the disaster could be easily studied. However, apart from the routinely occurring floods, disasters rarely occur at the same place with the same criteria. Thus, measuring the quality of improvement remains problematic and the policy aims of long-term recoveries end up being vague at best and non-existent at worst.

5. PITFALLS OF ASSESSING RECOVERY

This section will focus on the six points raised by Quarantelli (1999) as essential in assessing recovery and discuss what existing methods there are for evaluating successes or failures in recovery and whether these methods address the issues mentioned here. In brief, these are: 1) Goals of recovery; 2) Levels of recovery; 3) Size of the recovering unit; 4) Perspective on recovery; 5) Recovery from secondary or ripple effects of disasters; 6) Recovery from disasters differs from recovery from catastrophes.

1) In regards to the goals of recovery, unclear goals can invite miscommunication between those that are assisted and those that are assisting. This is especially evident in the consideration of what the end product of recovery is (i.e. the *state of return* mentioned in the previous section). Moreover, if a better standard than the pre-impact level is the goal, then how to measure the improvement is also a necessary consideration.

2) The levels of recovery refers to the fact that “the [recovery] process might not proceed at the same rate or in the same way at different levels of the social units involved” and thus any assessment of recovery has to specify what social level unit is being evaluated Quarantelli (1999). Furthermore, considerable research is still required to clarify the relationships between individuals, households, organizations, and community.

3) In extension to the above point, “the larger the social unit involved, the more likely there will be postimpact recovery” Quarantelli (1999). This refers to the fact that on a bigger scale considering overall community recovery, the (lack of) individual recoveries tend to appear insignificant, implying that smaller units have more recovery problems which can go unaddressed. Thus, it is necessary to recognize that the assessment of recovery will be affected by the size of the recovering social unit considered, with the larger ones more likely to recovery well.

4) Success or failure of recovery is also a matter that depends on the viewpoint of the actors involved (municipality, national government, or individuals). Quarantelli (1999) emphasizes that this may be dependent on prior experiences; and a higher level organization such as the government, which may have to deal with several disasters, would have a more realistic rather than idealistic conceptions of recovery.

5) There are secondary or “ripple effects” of a disaster which may tend to go unaddressed (for examples and details see Quarantelli 1999). Thus in assessing recovery it is necessary to take into account whether or not only direct effects but the wider ranging indirect consequences of the disaster have been dealt with in the recovery process.

6) It is necessary to understand that disasters are different to catastrophes. This important in the observation is that: community and regional level disaster there is typically a convergence of assistance from nearby community (Quarantelli, 1999). Yet the more a disaster encompasses nearby geographically contiguous areas, the less likely will those localities themselves impacted, be able to help in emergency relief or recovery activities. Thus, the larger the disaster, not only is there more likely to be greater short and long run needs, but there is less likely to be available certain kinds of nearby assistance that would be present in smaller type disasters. Thus, there

is need for different kinds of planning and managing for catastrophes compared with disasters.

6. CONCLUSION

This literature review has provided an overall survey in regards to the ongoing debate about the concept of recovery. Along with the multiple definitions of the term, some existing measures for assessment have been identified including the housing recovery measurement approach, domestic assets index and social capital, and their applicability discussed. Furthermore, by questioning the conventionally established views of what an ideal recovery consists of, the paper has highlighted the need to reconsider the means to address and assess recovery. And finally, it has highlighted the points raised by Quarantelli (1999) which can serve as a guideline for structuring recovery assessment studies. It is hoped that much needed further discussions will focus on these aspects and drive the development of future recovery assessment methods.

REFERENCES

Aota, R., Tsukui, S.,Yamasaki, E., Yamanaka, S. and Yamamoto, S. Special Feature: On the Draft of the Disaster Recovery and Rehabilitation Basic Act. *Studies in Disaster Recovery and Revitalization*. No.2, pp. 1-115, 2010 (in Japanese),http://ci.nii.ac.jp/naid/40017216647/en/ [accessed May 1, 2013]

Aldrich, D. P. 2012. *Building resilience: social capital in post-disaster recovery*. University of Chicago Press.

Barrios, R. 2011. Post-Katrina Neighbourhood Recovery Planning, in Dowty, Rachel A., and Barbara L. Allen, eds., *Dynamics of Disaster: Lessons on Risk, Response and Recovery*. EarthScan: 97-114.

Bates, F. L., & Peacock, W. G. 2008. *Living conditions, disasters and development: An approach to cross-cultural comparisons*. University of Georgia Press.

Bolin, R., & Stanford, L. 1991. Shelter, housing and recovery: a comparison of US disasters. *Disasters*, *15*(1), 24-34.

Canterbury Earthquake Recovery Authority. 2012. *Recovery Strategy for Greater Christchurch Mahere Haumanutanga o Waitaha.* Christchurch: Canterbury Earthquake Recovery Authority.

Comfort, L. K. (Ed.). 2010. *Designing resilience*. University of Pittsburgh Press.

Department of Homeland Security & Federal emergency management Agency. 2005. *Long-term recovery planning process: A self-help guide.* Washington, D.C. The Federal Emergency Management Agency.

Edgington, D. W. 2010. *Reconstructing Kobe: The Geography of Crisis and Opportunity*. UBC Press.

Guo, Y. 2012. Urban resilience in post-disaster reconstruction: Towards a resilient development in Sichuan, China. *International Journal of Disaster Risk Science*, Vol.3, No.1, pp. 45-55, 2012, http://link.springer.com/article/10.1007%2Fs13753-012-0006-2 [accessed May 1, 2013]

Hayashi, H. Long-term Recovery from Recent Disasters in Japan and the United

States. *Journal of Disaster Research* Vol.2, No.6. 413-418.

Hyogo Prefectural Government 1995. Hashin-Awaji Earthquake Recovery Plan https://web.pref.hyogo.lg.jp/wd33/wd33_000000043.html [accessed on August 2013]

Kato, T., Bhattacharya, Y. Sugata, H. Otagiri, R. 2013. The Six Principles of Recovery: A Guideline for Preparing for Future Disaster Recoveries. *Journal of Disaster Research* Vol.8, No.sp. 737-745.

Kondo, T. 2008. Planning for Post-disaster Recovery in New Orleans after Hurricane Katrina. *International Symposium on City Planning, Tokyo*. 2008.

Nakabayashi, I. 2012. How to Optimize the Urban Recovery After Earthquake Disaster –Preparedness for Recovery from the Next Tokyo Earthquake- *Journal of Disaster Research* Vol.7 No.2. 227-238.

Natural Hazards Center. 2005. *Holistic Disaster Recovery: Ideas for Building Sustainability After a natural Disaster*. Boulder, Colorado.

Neal, D. M. 1997. Reconsidering the phases of disasters. *International Journal of Mass Emergencies and Disasters*, *15*(2), 239-264.

Olshansky, R. B., Johnson, L. A., Horne, J., & Nee, B. 2008. Longer view: Planning for the rebuilding of New Orleans. *Journal of the American Planning Association*, *74*(3), 273-287.

Ota, T., Johnson,L., Maki, N. and Hayashi, H. Planning Process of Long-term Disaster Recovery Plan – a comparative study of planning process with Kobe and New Orleans. *Proceedings of Institute of Social Safety Science,* No.13, pp.335-345, 2010 (in Japanese).

Pais, J. F. 2008. Places as Recovery Machines: Vulnerability and Neighbourhood Change After Major Hurricanes. *Social Forces*, Vol.86.No.4., June 2008.

Peacock, W. G., Dash, N., & Zhang, Y. (2007). Sheltering and Housing Recovery Following Disaster*. In *Handbook of disaster research* (pp. 258-274). Springer New York.

Quarantelli, E. L. 1999. The disaster recovery process: What we know and do not know from research. *Preliminary Paper*. University of Delaware Disaster Research Center.

The Reconstruction Design Council in Response to the Great East Japan Earthquake 2011. Towards Reconstruction “Hope Beyond the Disaster” (Report to the Prime Minister).

Vicini, A., Bevington, J., Davidson, R., & Hill, A. 2011. Post-disaster Evaluation of Community-based Housing Recovery from Aerial Imagery. *Ninth International Workshop on Remote Sensing for Disaster Response*, Stanford, CA. 15-16 September 201.

Wilson, G.A. 2012. Community resilience, social memory and the post-2010 Christchurch (New Zealand) earthquakes. *Area.* Vol. 45 No. 2, pp. 207-215. Royal Geographical Society (with the Institute of British Geographers).

Wisner, B. (Ed.). 2004. *At risk: natural hazards, people's vulnerability and disasters*. Psychology Press.

Zhang, Y., & Peacock, W. G. 2009. Planning for housing recovery? Lessons learned from Hurricane Andrew. *Journal of the American Planning Association*,*76*(1), 5-24.

Study on earthquake early warnings provided to public/advanced users at the 2011 off the Pacific coast of Tohoku Earthquake

Ayaka NISHIGUCHI[1] and Miho OHARA[2]

[1] Master student, Department of Civil Engineering, The University of Tokyo, a-nishi@iis.u-tokyo.ac.jp
[2]Associate Professor, International Center for Urban Safety Engineering (ICUS), Institute of Industrial Science, The University of Tokyo, Japan

ABSTRACT

Japan has Earthquake Early Warning (EEW) system that provides prompt warnings before strong tremors arrive at an earthquake. EEWs include two types of warning; the one is the alerts for the general public receiving by TV or radio, cell phones etc., the other is the alerts for advanced users receiving by special receiving devices. The EEWs have a possibility to reduce physical and human loss due to a coming earthquake. EEW for advanced users includes more detailed information such as expected intensity or lead-time before the strong tremors although it needs a special receiving device. It can be more effective warning to reduce earthquake damage especially in the densely-populated or industrial area compared with the warnings for public users.
Japan experienced the 2011 off the Pacific coast of Tohoku Earthquake on March 11, 2011. At this earthquake, EEW was provided to the general public in the part of the shaken area. However, the areas where EEW for advanced users was provided are not clearly understood because the reception and use of the warning depends on the expected seismic intensity at the receiving location. Therefore, this research aims to understand the situation of EEW issuance both for the public and advanced users at the Tohoku Earthquake. The issuance times of the both warnings were plotted on the observed seismic wave data in several cities in the eastern Japan. Considering the population and industrial activity in these cities, the effects for reducing physical and human loss by the issuance of the both warnings were discussed.

Keywords: *Earthquake Early Warning, Disaster Reduction, the 2011 off the Pacific coast of Tohoku Earthquake*

1. INTRODUCTION

Japan has Earthquake Early Warning (EEW) system that provides prompt warnings before strong tremors arrive at an earthquake. EEWs include two types of warning; the one is the alerts for the general public receiving by TV or radio, cell phones etc., the other is the alerts for advanced users receiving by special receiving devices. EEW for the general public started since October 1, 2007 and it is provided especially to the regions with predicted intensity of 4 or more when predicted intensity of 5 lower or more is anticipated. On the other hand, EEW for advanced users includes more detailed information such as expected intensity or lead-time before the strong tremors although it needs special receiving devices. It is issued, as a rule, when “the amplitude of the P wave or S wave is 100 gal or more” and “the calculated magnitude is 3.5 or more or the maximum predicted intensity is 3 or more”. It can be more effective warning to reduce physical and human loss due to a coming earthquake especially in the densely-populated or industrial area, compared with the warnings for public users.

On March 11, 2011, Japan experienced “The 2011 off the Pacific coast of Tohoku Earthquake”. It occurred in the Pacific Ocean, and its hypocenter was 38°6’12”N, 142°51’26”E at a depth of 24km. Its magnitude (Mw) was 9.0 and maximum JMA seismic intensity was 7 (it is maximum lank of it). Figure 1 shows the distribution of observed JMA seismic intensity, showing the wide area in the eastern Japan was attacked by the strong tremors. The earthquake and great tsunami attacked the coastal area caused about 18,000 dead and missing people.

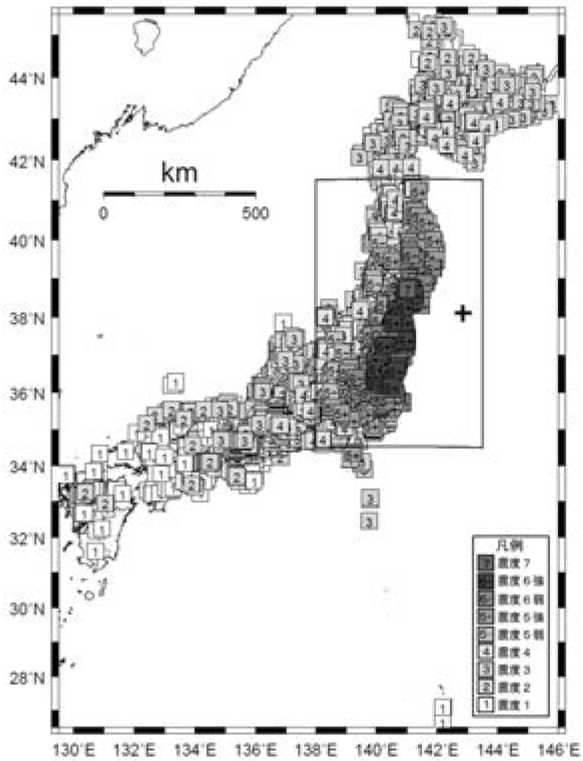

Figure 1 Distribution of observed JMA seismic intensity of the Tohoku Earthquake

At this earthquake, EEW was provided to the general public in the part of the shaken area. However, the areas where EEW for advanced users was provided are not clearly understood because the reception and use of the warning depends on the expected seismic intensity at the receiving location. Therefore, this research aims to understand the situation of EEW issuance both for the public and advanced users at the Tohoku Earthquake. The issuance times of the both warnings were plotted on the observed seismic wave data in several cities in the eastern Japan. Considering the population and industrial activity in these cities, the effects for reducing physical and human loss by the issuance of the both warnings were discussed.

2. EEW PROVIDED AT THE 2011 OFF THE PACIFIC COAST OF TOHOKU EARTHQUAKE

2.1 Mechanism of EEW

The mechanism of EEW is shown in Figure 2. The Japan Meteorological Agency (JMA) locates about 220 seismographs in Japan which are continuously

monitoring ground motion. When an earthquake occurs, seismometers near the epicenter detect seismic waves and the location of its hypocenter, magnitude is determined by the analysis of the obtained seismic wave data. As time passes, more seismometers can observe seismic wave and the accuracy of the estimated information increases. Then, the JMA repeatedly estimates every time when it receives new data from seismometers, and updates the warning information until the result becomes stable. Advanced users can get all the warnings from the first to the end of the estimation. It contains the information such as time of wave detection, the location of estimated hypocenter and epicenter, estimated magnitude. It is received with a special receiving device that can estimate additional information such as expected seismic intensity and expected arrival time of S-wave of the earthquake at the receiving location.
On the other hand, when more than two seismometers observe ground motion and the maximum seismic intensity is expected to exceed 5 lower, the warning is regarded as the one for the general public and provided to the regions with predicted intensity of 4 or more by TV, radio, cell phones. In this case, information such as seismic intensity and expected arrival time of S-wave is not provided.

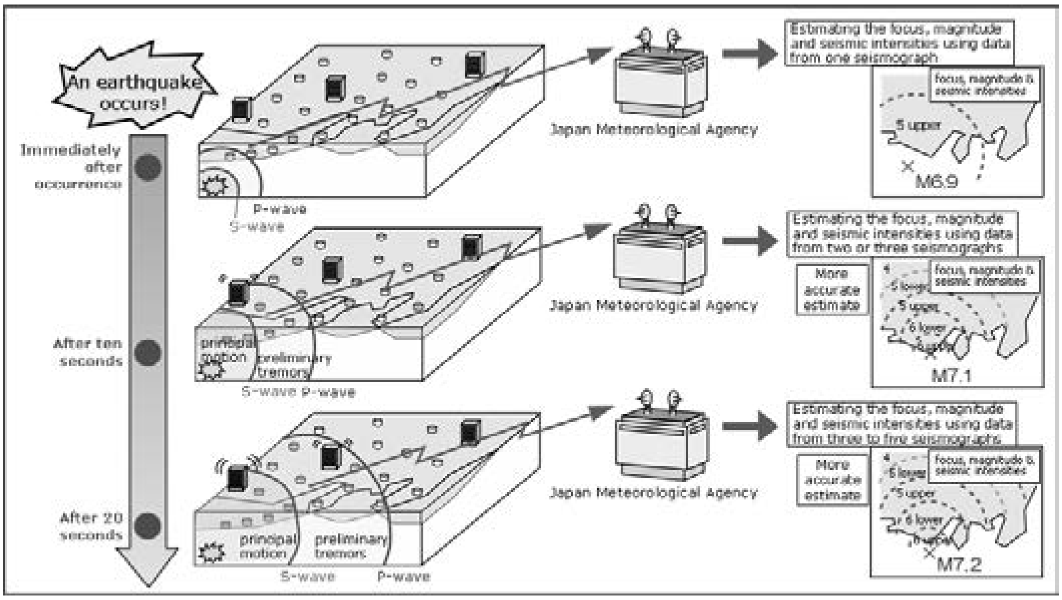

Figure 2 Mechanism of EEW system

2.2 EEWs provided at the 2011 off the Pacific coast of Tohoku Earthquake

EEWs issued at the 2011 off the Pacific coast of Tohoku Earthquake on March 11, 2011 are shown in Table 1. EEWs for advanced users were issued 15 times in total. The first announcement was issued at 14:46:45, after which the information of estimated hypocenter became accurate, and final announcement was issued at 14:48:36. The estimated magnitude was changed every time although the location of estimated hypocenter was not altered much. During the first four warnings, the magnitudes increased drastically. It is because the earlier warnings only use the limited number of observed seismic waves during very short time. In case of the Tohoku earthquake, the fault size was too huge to estimate the correct magnitude

using the limited number of wave observations. Then, the estimated magnitude was decided to be 8.1 finally at the 15th warnings, which caused underestimation of the magnitude compared to the real gigantic one.
The EEW provided for public users is the fourth warning that is highlighted in yellow color in table 1. Figure 3 shows the warning message actually broadcast for the general public on TV. It addressed only five prefecture names in Tohoku area, Miyagi, Iwate, Fukushima, Akita and Yamagata prefecture due to the underestimation of the magnitude mentioned above, whereas many people in other areas experienced strong tremors without receiving any EEW for public users.

Table1 : EEWs provided at the 2011 off the Pacific coast of Tohoku Earthquake

No.	Time of EEW Issuance	Time of EQ Occurrence	Expected Hypocenter			
			latitude	longitude	depth	magnitude
1	14:46:45	14:46:19	38.2N	142.7E	10 km	4.3
2	14:46:46	14:46:19	38.2N	142.7E	10 km	5.9
3	14:46:47	14:46:19	38.2N	142.7E	10 km	6.8
4	14:46:48	14:46:19	38.2N	142.7E	10 km	7.2
5	14:46:49	14:46:19	38.2N	142.7E	10 km	6.3
6	14:46:50	14:46:19	38.2N	142.7E	10 km	6.6
7	14:46:51	14:46:19	38.2N	142.7E	10 km	6.6
8	14:46:56	14:46:17	38.1N	142.9E	10 km	7.2
9	14:47:02	14:46:16	38.1N	142.9E	10 km	7.6
10	14:47:10	14:46:16	38.1N	142.9E	10 km	7.7
11	14:47:25	14:46:16	38.1N	142.9E	10 km	7.7
12	14:47:45	14:46:17	38.1N	142.9E	10 km	7.9
13	14:48:05	14:46:17	38.1N	142.9E	10 km	8.0
14	14:48:25	14:46:17	38.1N	142.9E	10 km	8.1
15	14:48:36	14:46:17	38.1N	142.9E	10 km	8.1

Figure 3 EEW for public users shown on TV at the Tohoku Earthquake

3. METHODOLOGY

At this earthquake, EEW was provided to the general public in the part of the shaken area as shown in figure 3. However, the areas where EEW for advanced users was provided are not clearly understood because the reception and use of the

warning depends on the expected seismic intensity at the receiving location. Therefore, this research aims to understand the situation of EEW issuance both for the public and advanced users at the Tohoku Earthquake.
At first, among the prefectures hit by strong tremors, 14 prefectures in the eastern Japan, Aomori, Iwate, Akita, Miyagi, Yamagata, Fukushima, Niigata, Ibaragi, Chiba, Gunma, Tochigi, Saitama, Tokyo and Kanagawa are selected. From these prefectures, 1 to 3 cities in each prefecture with the largest populations on the national census (2010) are selected.
Then, the issuance times of the both warnings are plotted on the observed seismic wave data in several cities in the eastern Japan. As the observed seismic wave data, K-NET data in the selected cities is used. K-NET is a nation-wide strong-motion seismograph network consisting of more than 1,000 observation stations operated by the National Research Institute for Earth Science and Disaster Prevention (NIED) . Authors downloaded acceleration records from the website. The estimated seismic intensity at each K-NET station is calculated using the location of K-NET and information of EEW shown in table 1 following the technical guideline of JMA. From this, the time when the estimated seismic intensity reached to the JMA intensity 3, 4, 5 lower is obtained and plotted on the K-NET data.
Finally, considering the population and industrial activity in these cities, the effect for reducing physical and human loss by the issuance of the both warnings were discussed. K-NET

4. EFFECT OF EEW ISSUANCE IN 19 CITIES

Table 2 is a list of 19 cities with large population that were selected based on the national census (2010) . The cities with the largest population in each prefecture and additional several cities which have more than 500,000 population were selected and colored with red in table 2. In case of Tokyo prefecture, many cities and wards have more than 500,000 people. So, the largest 2 cities were chosen.
Table 3 shows K-NET stations corresponded to 19 cities. Since the nearest K-NET to Setagaya-ku and Nerima-ku was the same, only one station for Tokyo was selected. In table 3, the observed instrument seismic intensity, JMA intensity and the expected seismic intensity for each city calculated by each EEW from the first to the fifteenth were shown. The instrument seismic intensity and JMA intensity scale has the relationship shown in table 4. The cells of expected seismic intensity in the table 3 were colored by this relationship.
Regarding the EEWs for public users, 5 cities in 5 prefectures (colored in red font in table 3) exceeded the criteria and received the warnings. From this, it is shown that there were many cities which were not received EEW for the general public although they experienced tremors with more than 5-lower in JMA intensity scale.
At the third or fourth EEW for advanced users, the expected seismic intensities are small with the JMA intensity 3(light blue in table 3) in almost all the cities. It is because of the underestimation of the magnitude. However, at the later EEWs, the expected seismic intensities increased to be around 4 and these colors changed to be green. As mentioned before, the EEW for public uses were the fourth warning. If an advanced user had set their criteria for receiving and using the warnings as the intensity 4, they could not use the warnings prior to the warnings for public use.

Table 2 : Selected 19 cities in large population in 14 prefectures

prefecture	population [people]		
	more than 1,000,000	more than 500,000	more than 250,000
AOMORI			Aomori, Hachinohe
IWATE			Morioka
AKITA			Akita
MIYAGI	Sendai		
YAMAGATA			Yamagata
FUKUSHIMA			Iwaki, Kooriyama,Fukushima
NIIGATA		Niigta	Nagaoka
IBARAGI			Mito
TOCHIGI		Utsunomiya	
GUNMA			Takasaki, Maebashi
SAITAMA	Saitama	Kawaguchi	Kawagoe,Tokorozawa, Koshigaya, Souka
CHIBA		Chiba, Funabshi	Matsudo,Ichikawa,Kashiwa,Ichihara
TOKYO		Setagaya, Nerima, Ota, Adachi, Edogawa, Hachioji, Suginami, Itabashi	Koto,Ktsushika,Machida,Shinagawa,Kita, Shinjuku,Nakano,Toshima,Meguro,Fuchu,Sumida
KANAGAWA	Yokohma, Kawasaki	Sagamihara	Yokosuka,Fujisawa,Hiratsuka

Table 4 : Observed and expected seismic intensities in 19 cities

City	K-net station	Observed intensity		Expected instrumental seismic intensity at the EEW announcement														
		JMA	instrumenta	1st	2nd	3rd	4th	5th	6th	7th	8th	9th	10th	11th	12th	13th	14th	15th
Aomori	AOM020	4	4.1	-0.22	1.40	2.34	2.78	1.81	2.12	2.12	2.67	3.14	3.26	3.26	3.51	3.64	3.77	3.77
Akita	AKT010	4	3.9	0.21	1.83	2.77	3.22	2.24	2.56	2.56	3.09	3.56	3.68	3.68	3.93	4.06	4.20	4.20
Morioka	IWT018	5-lower	4.8	0.41	2.03	2.98	3.42	2.44	2.76	2.76	3.29	3.76	3.88	3.88	4.14	4.28	4.42	4.42
Sendai	MYG013	6-upper	6.3	1.04	2.66	3.62	4.08	3.08	3.40	3.40	3.92	4.41	4.53	4.53	4.80	4.94	5.09	5.09
Yamagata	YMT010	4	4.2	0.40	2.02	2.97	3.42	2.44	2.76	2.76	3.29	3.77	3.89	3.89	4.15	4.29	4.43	4.43
Niigata	NIG010	4	3.9	-0.13	1.48	2.43	2.87	1.90	2.21	2.21	2.77	3.23	3.36	3.36	3.61	3.74	3.87	3.87
Iwaki	FKS011	5-upper	5.4	0.36	1.98	2.93	3.38	2.40	2.72	2.72	3.32	3.80	3.93	3.93	4.19	4.33	4.47	4.47
Utsunomiya	TCG007	5-lower	4.7	-0.17	1.45	2.39	2.83	1.86	2.18	2.18	2.78	2.78	3.25	3.25	3.62	3.75	3.89	3.89
Mito	IBR006	6-lower	5.8	-0.01	1.61	2.55	3.00	2.02	2.34	2.34	2.96	3.43	3.55	3.55	3.81	3.94	4.08	4.08
Takasaki	GNM013	5-lower	4.9	-0.75	0.87	1.81	2.25	1.28	1.59	1.59	2.20	2.66	2.78	2.78	3.03	3.16	3.29	3.29
Saitama	SIT010	5-upper	5.1	-0.44	1.18	2.12	2.56	1.59	1.91	1.91	2.53	2.99	3.11	3.11	3.36	3.49	3.62	3.62
Kawaguchi	SIT011	5-upper	5.0	-0.39	1.23	2.17	2.61	1.64	1.96	1.96	2.58	3.04	3.16	3.16	3.41	3.54	3.67	3.67
Funabashi	CHB028	5-upper	5.0	-0.44	1.18	2.12	2.56	1.59	1.91	1.91	2.54	3.00	3.12	3.12	3.37	3.50	3.64	3.64
Setagaya &Nerima	TKY007	5-lower	4.8	-0.46	1.05	2.10	2.54	1.57	1.88	1.88	2.51	2.97	3.09	3.09	3.34	3.47	3.60	3.60
Chiba	CHB009	5-upper	5.1	-0.21	1.41	2.35	2.79	1.82	2.14	2.14	2.77	3.24	3.36	3.36	3.61	3.74	3.87	3.87
Sagamihara	KNG008	4	4.4	-0.79	0.83	1.77	2.21	1.24	1.55	1.55	2.17	2.63	2.75	2.75	3.00	3.13	3.26	3.26
Kawasaki	KNG001	5-upper	5.1	-0.42	1.19	2.14	2.57	1.61	1.92	1.92	2.55	3.01	3.13	3.13	3.38	3.51	3.64	3.64
Yokohama	KNG002	5-upper	5.1	-0.24	1.37	2.31	2.75	1.79	2.10	2.10	2.73	3.19	3.31	3.31	3.56	3.69	3.82	3.82

$$[The\ expected\ lead - time\ until\ arrival\ of\ S - wave] = [(a)] - [(b)] \quad \text{---- (1)}$$

$$[(b)] = [(c)] - [(d)] \quad \text{---- (2)}$$

(a) Expected travel time of the S-wave (estimated according to JMA method)
(b) Elapsed time until publishing EEW from detecting of EQ
(c) The publish time of EEW (on Table1)
(d) The expected time of earthquake occurrence (on Table1)

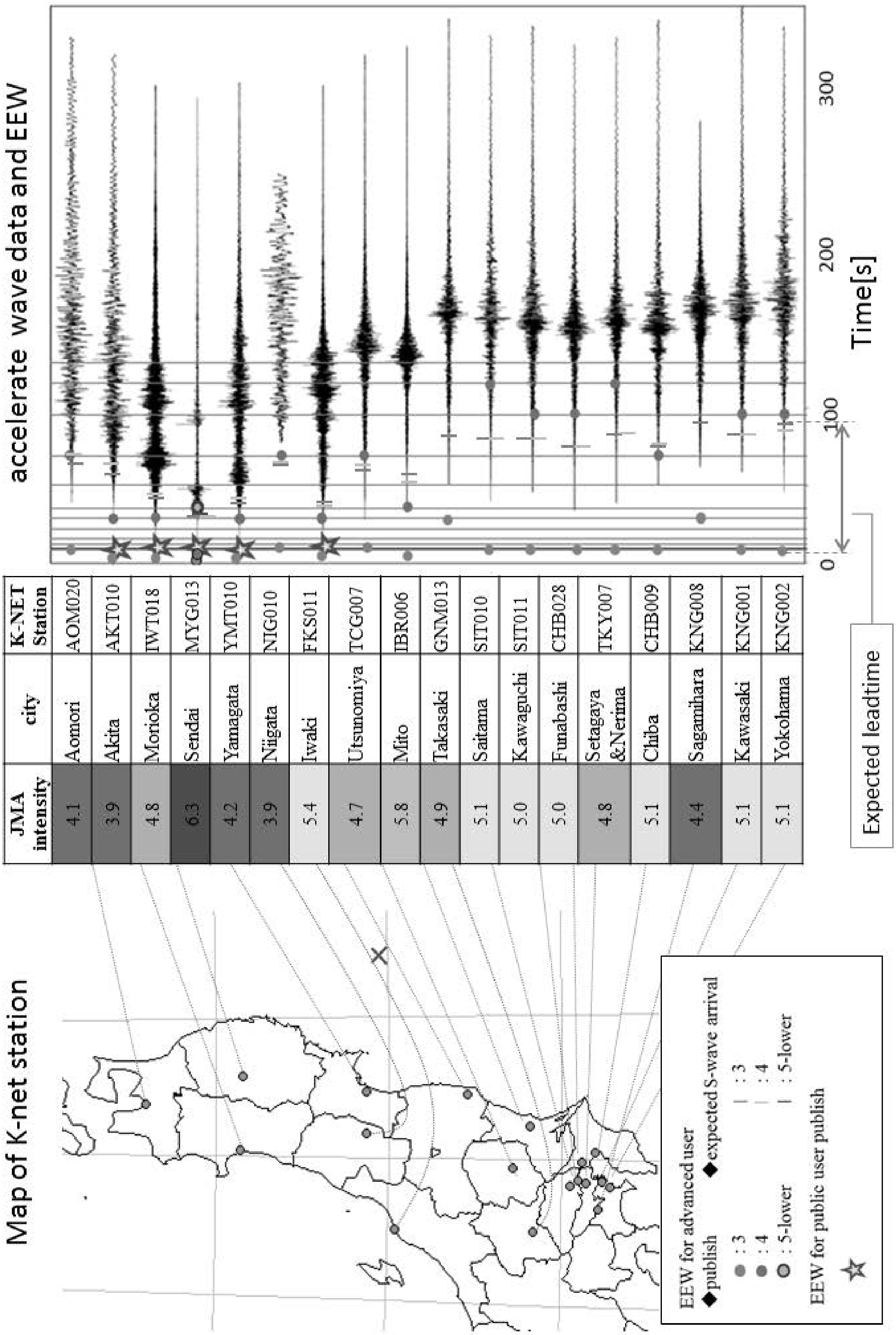

Figure 2 Map of K-NET stations and EEW issuance on observed seismic waves

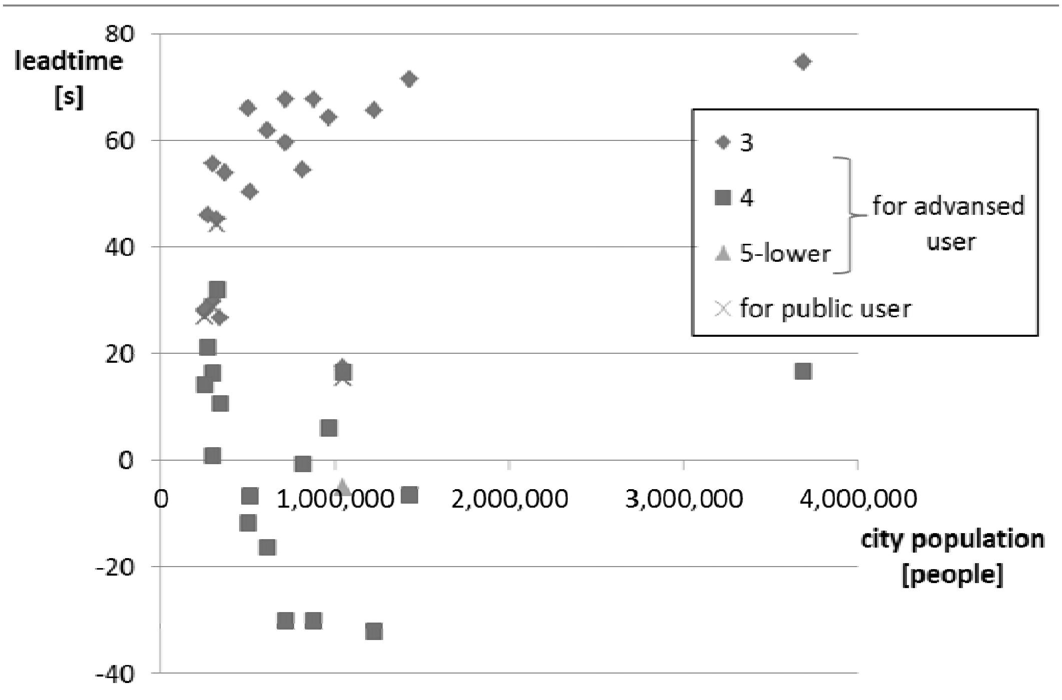

Figure 5 : Scatter diagram of population and lead-time in large population cities

Figure 4 is a map of K-NET station and EEW issuance on observed seismic wave. Regarding the EEW for advanced users, EEW issuance when they got EEWs with expected seismic intensities 3,4 and 5-lower was plotted. In addition, the expected lead-time before the arrival of S-wave by the EEW was calculated by the equation 1 and also plotted on figure 4. Here, lead-time doesn't include the time required for information transmission and calculation.

The red stars in figure 4 show the time when the city got EEW for the public users. The red stars mean that the EEW for public users in the 5 cities was successfully provided before the strong tremors. On the other hand, the cities without red stars could not get EEW for public users but EEW for advanced users.

JMA seismic	instrumental seismic intensity
0	under0.5
1	over0.5-under1.5
2	over1.5-under2.5
3	over2.5-under3.5
4	over3.5-under4.5
5-lower	over4.5-under5.0
5-upper	over5.0-under5.5
6-lower	over5.5-under6.0
6-upper	over6.0-under6.5
7	over6.5

Table 3 : Definition of JMA intensity

Figure 5 is a scatter diagram of population and lead-time in large population cities. It shows that many cities had more than 1 minute as the expected lead-time if they set their criteria for receiving EEW as intensity 3. But when they got an EEW of intensity 4 or 5-lower, some cities had minus lead-time and had been already suffered from initial tremors before getting EEW. The number of advanced users who had set the criteria for receiving EEW as intensity 3 might be small because intensity 3 is quite low compared with the public use case. From this, it is said that the effect of the EEWs for advanced users at this earthquake was limited.

On the other hand, due to the underestimation of the magnitude, real S-wave took more time for reaching at the each city than calculated by EEW. It might fortunately give more time for people to prepare for the coming shaking.

5. EFFECT OF EEW ISSUANCE IN INDUSTRIAL CITIES

In this chapter, the effect of EEW issuance in industrial cities was focused. Six cities with the largest population of industrial workers were selected based on academic census (2009). The issuance times of EEWs were calculated following the same methodology in the previous chapter. In table 5, the observed instrument seismic intensity, JMA intensity and the expected seismic intensity for each city calculated by each EEW from the first to the fifteenth were shown. Figure 6 is a scatter diagram of population and lead-time in these cities.

2 cities among 6 got both EEWs for the public and advanced users, although 4 cities only got EEWs for advanced users. All the cities got the EEW of intensity 3 and most of them had more than 40 seconds as lead-time before the strong tremors. When the expected intensity reached to intensity 5-lower, there was almost no lead-time before the shaking. It means that the industrial companies using advanced EEW could get lead-time for preparing for the shaking only if they had set their criteria for receiving EEW as intensity 3 or 4.

Table 5: Observed and expected seismic intensities in 6 industrial cities

City	K-net station	Observed intensity		Expected instrumental seismic intensity at the EEW announcement														
		JMA	instrumenta	1st	2nd	3rd	4th	5th	6th	7th	8th	9th	10th	11th	12th	13th	14th	15th
Hachinohe	AOM012	5-lower	4.9	-0.22	1.40	2.34	2.78	1.81	2.12	2.12	2.67	3.14	3.26	3.26	3.51	3.64	3.77	3.77
Kitakami	IWT012	6-lower	5.9	0.21	1.83	2.77	3.22	2.24	2.56	2.56	3.09	3.56	3.68	3.68	3.93	4.06	4.20	4.20
Ishinomaki	MYG010	6-lower	5.9	0.41	2.03	2.98	3.42	2.44	2.76	2.76	3.29	3.76	3.88	3.88	4.14	4.28	4.42	4.42
Hitachi	IBR003	6-upper	6.4	1.04	2.66	3.62	4.08	3.08	3.40	3.40	3.92	4.41	4.53	4.53	4.80	4.94	5.09	5.09
Oota	GNM011	5-upper	5.0	0.40	2.02	2.97	3.42	2.44	2.76	2.76	3.29	3.77	3.89	3.89	4.15	4.29	4.43	4.43
Minato	TKY007	5-lower	4.8	-0.13	1.48	2.43	2.87	1.90	2.21	2.21	2.77	3.23	3.36	3.36	3.61	3.74	3.87	3.87

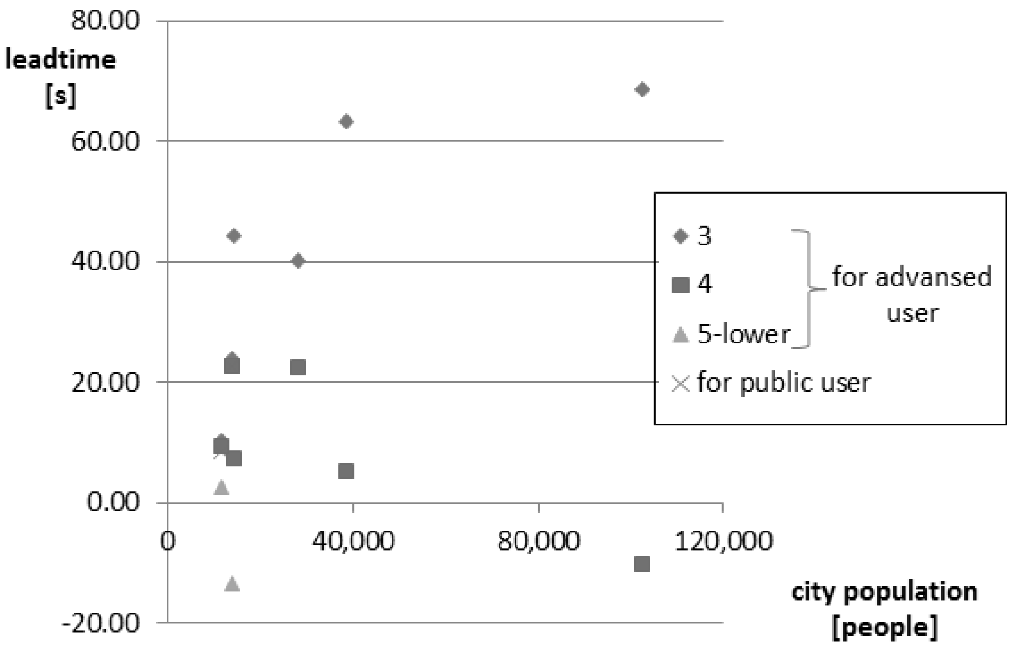

Figure 6: scatter diagram of population and lead-time in industrial cities

6. CONCLUSIONS

This research aimed to understand the situation of EEW issuance both for the public and advanced users at the 2011 off the Pacific coast of Tohoku Earthquake on March 11, 2011. The issuance times of the both warnings were plotted on the observed seismic wave data in several cities in the eastern Japan. Considering the population and industrial activity in these cities, the effects for reducing physical and human loss by the issuance of the both warnings were discussed.

All the targeted cities with large populations got EEW for the advanced users, although the number of the cities provided with the EEW for the public users was limited. Regarding EEW for advanced users, many cities with large populations had more than 1 minute as the expected lead-time if they set their criteria for receiving EEW as intensity 3. But when they got an EEW of intensity 4 or 5-lower, some cities had minus lead-time and had been already suffered from initial tremors before getting EEW. From this result, it is said that some of the public or advanced users of EEW could get much lead-time to prepare for the shaking, but unfortunately, these populations might be limited due to the underestimation of the magnitude of the Tohoku Earthquake in 2011.

As a future study, the effect of EEWs at the aftershocks had better be analyzed. Now, the technologies for source estimation are being improved based on the lessons from the Tohoku earthquake. It is expected that EEW could give more effect for reducing physical and human loss at the coming earthquakes.

ACKOWLEDGEMENT

We would like to thank Dr. Hiroshi TSURUOKA, Associate Professor of Earthquake Research Institute for providing the records of EEW and helping with several estimations. We also thank NIED for permitting the use of K-NET data.

REFERENCES

Japan Meteorological Agency, http://www.jma.go.jp/jma/en/Activities/eew.html

National Research Institute for Earth Science and Disaster Prevention (NIED), http://www.kyoshin.bosai.go.jp/

Statistics Bureau, Ministry of Internal Affairs and Communications, 2010 Population Census, 2010

Statistics Bureau, Ministry of Internal Affairs and Communications, 2009 Economic Census, 2009

Study on victim transportation planning considering street blockades
-Case study of expected Tokyo inland earthquake-

Fei JIANG[1], Miho OHARA[2]
[1]Master Course Student, Graduate School of Interdisciplinary Information Studies
The University of Tokyo, Japan
jiangfei@iis.u-tokyo.ac.jp
[2]Associate Professor, International Center for Urban Safety Engineering (ICUS),
Institute of Industrial Science, the University of Tokyo, Japan

ABSTRACT

Tokyo Metropolitan area has high risk of the Tokyo Inland Earthquake in the future. In case of the earthquake, disaster base hospitals have missions to accommodate seriously-injured victims and provide medical treatment for them. According to the lessons from past disasters, medical treatment within 72 hours after the disaster is essential to increase the possibility of saving the lives of victims. Rapid transportation of seriously-injured victims to disaster base hospitals and immediate medical treatment are very important to avoid their "Preventable Death".

In this research, effect of street blockades to transportation of seriously-injured victims to hospitals in case of the expected Tokyo Inland Earthquake was analyzed considering road network. The maximum transportable area where victims could be transported to some hospitals by car within certain time was identified using a software "ArcGIS Network Analyst". After the Kobe Earthquake in January 1995, road blockades due to the debris from collapsed buildings caused problems on medical transportation. This research simulated the effect of road blockades on maximum transportable area. As a result, almost all the areas in Tokyo Prefecture were accessible to disaster base hospitals within 10 minutes by car in normal situation. However, maximum transportable area drastically shrank when road blockades in case of disaster was considered. This analysis identified the areas where rapid transportation to the nearest disaster base hospitals was impossible in case of the earthquake. Increase in the number of disaster base hospitals or dispatch of medical treatment team with portable facilities such as DMAT (disaster medical assistance team) may be necessary in these areas.

Keywords: *Tokyo Inland Earthquake, seriously-injured victims, disaster base hospitals, transportation*

1. INTRODUCTION

It is believed that in the Tokyo Metropolitan Area, massive trench-type earthquakes with magnitudes of 8 or greater, such as the Great Kanto Earthquake (1923), will occur at intervals of 200-300 years. Additionally, it is presumed that several Tokyo Inland Earthquakes of magnitude 7 will occur prior to a magnitude 8 earthquake, and the imminent possibility in the first half of this century has been pointed out. Because of that, many types of Tokyo Inland Earthquakes are assumed by the cabinet office of Japanese government and Tokyo metropolitan government with various possible epicenters and the complicated mechanism of occurrence. According to the estimation of The Tokyo metropolitan government, the number of seriously-injured victims will be about 150 thousand in the earthquake with an epicenter in the northern part of Tokyo Bay (assumed scale of M7.3, 18p.m.). So, it is essential to provide the medical treatment within 72 hours after the disaster to increase the possibility of saving the lives of victims due to the lessons from past disasters. Rapid transportation of seriously-injured victims to disaster base hospitals and immediate medical treatment are very important to avoid their “Preventable Death”.

A disaster base hospital is responsible to accommodate seriously-injured victims whom the medical aid stations are not able to treat, based on the stations’ request (Tokyo metropolitan disaster base hospital installation management guidelines, 2003). A disaster base hospital is designated as huge hospitals with enough seismic strength of buildings. In Tokyo metropolitan area, there are 70 disaster base hospitals and 182 emergency hospitals, with an average number of beds of 574 and 158. Figure 1 shows the distribution of seriously-injured victims based on the occurrence of the earthquake with an epicenter in the northern part of Tokyo Bay (assumed scale of M7.3, 18p.m.). The darker the color is, the higher the number of the seriously-injured victims is. The circles with black dots are the disaster base hospitals and the empty circles are the emergency hospitals, where the size of the circles shows the number of beds. According to this figure, the eastern part of the Tokyo metropolitan area has more seriously-injured victims but has fewer disaster base hospitals.

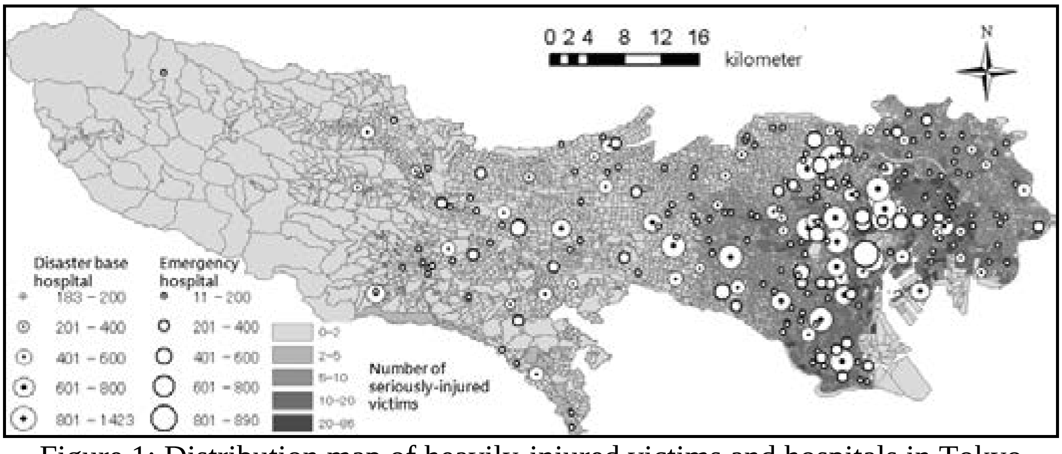

Figure 1: Distribution map of heavily-injured victims and hospitals in Tokyo

However, as figure 2 shows, the eastern part of the Tokyo metropolitan area is the most severe part according to building collapse. The debris may cause serious street blockades and traffic jams which could impede the speed of medical treatment and decrease the possibility of saving the lives of victims.

Figure 2: Distribution of the total collapse of buildings
(Assumption by Tokyo metropolitan government)

There are mainly two previous researches on the seriously-injured victims transported to disaster base hospitals. Ohara (2008) estimated the number of seriously-injured victims transported to disaster base hospitals and emergency hospitals using an entropy model. However, the direct distance between the location of the injury and the hospital has been used in calculations instead of the road network. Maruyama (2010) analyzed the level of function loss of disaster base hospitals. Road network and decrease of the speed of transportation due to the street blockades based on the intensity of earthquake were considered. However, it still needs some more detailed calculations on the effect of street blockades.

Based on the background and previous researches, this paper aims to consider the road network and the effects of street blockades on transportation to identify the areas where rapid transportation to the nearest disaster base hospitals are impossible in case of the expected Tokyo Inland Earthquake. This kind of analysis would become a basis to provide a plan for increasing number of disaster base hospitals by strengthening existing emergency hospitals or the dispatch of medical treatment teams with portable facilities such as DMAT (disaster medical assistance team) in these areas.

2. METHDOLOGY

To identify the areas where rapid transportation to the nearest disaster base hospitals is impossible, “ArcGIS Network Analyst” is a useful tool. It can be used to identify the maximum transportable area up to which victims could be transported to a specific hospital by car or on foot within a certain time. This section describes the outline of the methodology to analyze the traffic situation both in normal and disaster situations using “ArcGIS Network Analyst”.

2.1 Method of traffic simulation in normal situation

First, a hospital database was made based on the list of disaster base hospitals in Tokyo metropolitan area. Next, the map, hospitals and road network (Table 1) of Tokyo metropolitan area were plotted on GIS. The maximum transportable areas have been identified for time distance of 5 and 10 minutes traveled by car, using “ArcGIS Network Analyst”. Figure 3 and 4 show the maximum transportable areas within 5 minutes and 10 minutes, respectively. According to the Fire and Disaster Management Agency of Japan, the average time from the ambulance call to reach was 10.2 minutes (2012). Figure 4 shows the result that almost all the area in Tokyo Prefecture is accessible to disaster base hospitals within 10 minutes by car after an ambulance call.

<table>
<tr><td></td><td></td><td>1</td><td>2</td><td>3</td><td>4</td><td>0</td></tr>
<tr><td colspan="2">Code of Road Type</td><td>13m></td><td>13m-5.5m</td><td>5.5m-3m</td><td>3m<</td><td>Uninvestigated</td></tr>
<tr><td>National highway for high speed car</td><td>1</td><td colspan="2">80</td><td rowspan="2">20</td><td rowspan="2">10</td><td rowspan="9">2</td></tr>
<tr><td>Urban freeway</td><td>2</td><td colspan="2">60</td></tr>
<tr><td>General national highway (toll way)</td><td>3</td><td rowspan="7">30</td><td>20</td><td rowspan="5">12</td><td rowspan="5">7</td></tr>
<tr><td>Major local roads (prefectural road)</td><td>4</td><td rowspan="4">17</td></tr>
<tr><td>Major local roads (specified city road)</td><td>5</td></tr>
<tr><td>General prefectural roads</td><td>6</td></tr>
<tr><td>General city roads for specified city</td><td>7</td></tr>
<tr><td>Other roads</td><td>9</td><td rowspan="2">12</td><td rowspan="2">8</td><td rowspan="2">4</td></tr>
<tr><td>Uninvestigated</td><td>0</td></tr>
</table>

Table 1: Velocity table of roads in Tokyo metropolitan area

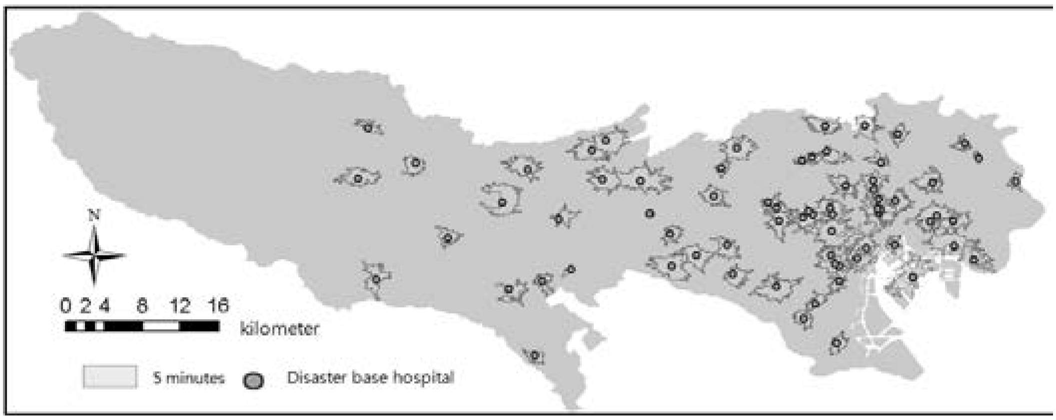

Figure 3: The maximum transportable areas
of disaster base hospitals in 5 minutes

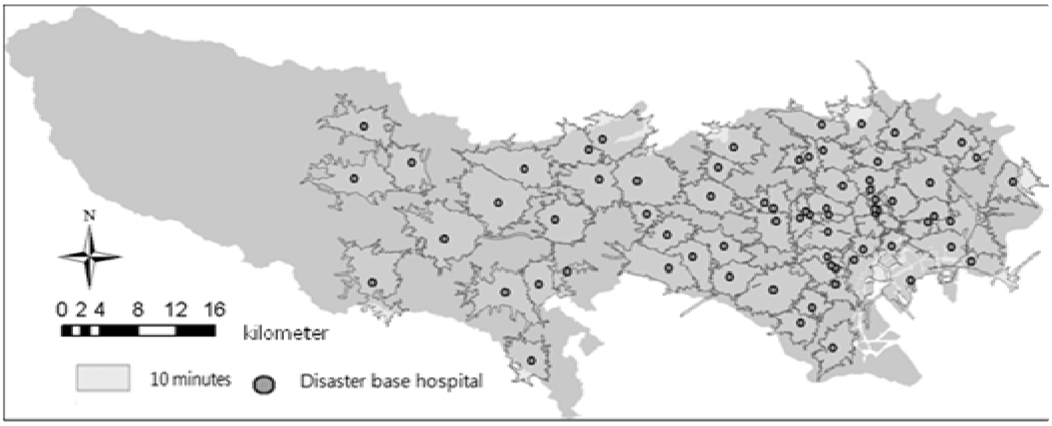

Figure 4: The maximum transportable areas
of disaster base hospitals in 10 minutes

2.2 Method of traffic simulation in disaster situation

The Method of traffic simulation in disaster situation is almost the same as that in normal situation except for the road network changes. Here, the effect of street blockades on transportation was considered. Figure 5 shows the flow of the method of traffic simulation in disaster situation.

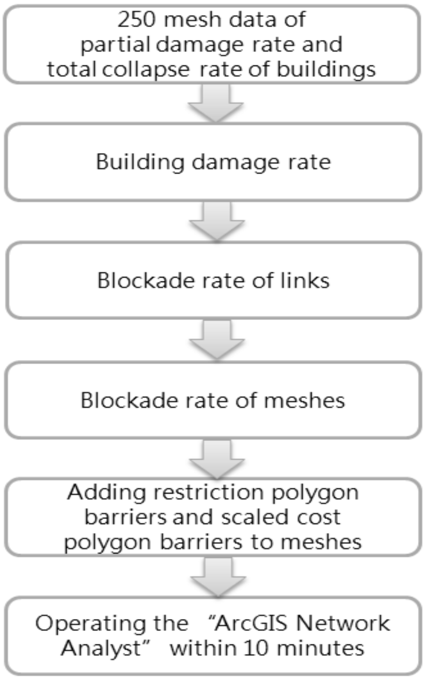

Figure 5: Flow of the method of traffic simulation in disaster situation

At first, using the 250 mesh data of expected partial damage rate and the total collapse rate of buildings in case of the earthquake with an epicenter in the

northern part of Tokyo Bay, building damage rates was calculated by the equation below:
Building Damage Rate = Total Collapse Rate + 1/2 Partial Damage Rate -----Eq.1

Next, the expected blockade rates of the links were calculated using building damage rate. Ieda (1997) surveyed the relationship between building damage and blockade rates in the affected district in Kobe City after the 1995 Kobe Earthquake. According to these survey results, equations based on the widths of roads were proposed by the Cabinet Office of Japanese Government for calculating blockade rates of links in the damage estimation of the Tokyo Inland Earthquake. In this research, the calculation using the equation based on the worst situation by Ieda's survey was defined as case 1, the equation used in the damage estimation of the Cabinet office as case 2 and the equation based on the best situation by Ieda's survey as case 3. In figure 6, case 1, 2 and 3 according to the widths of the roads are shown in red, green and orange lines, respectively.

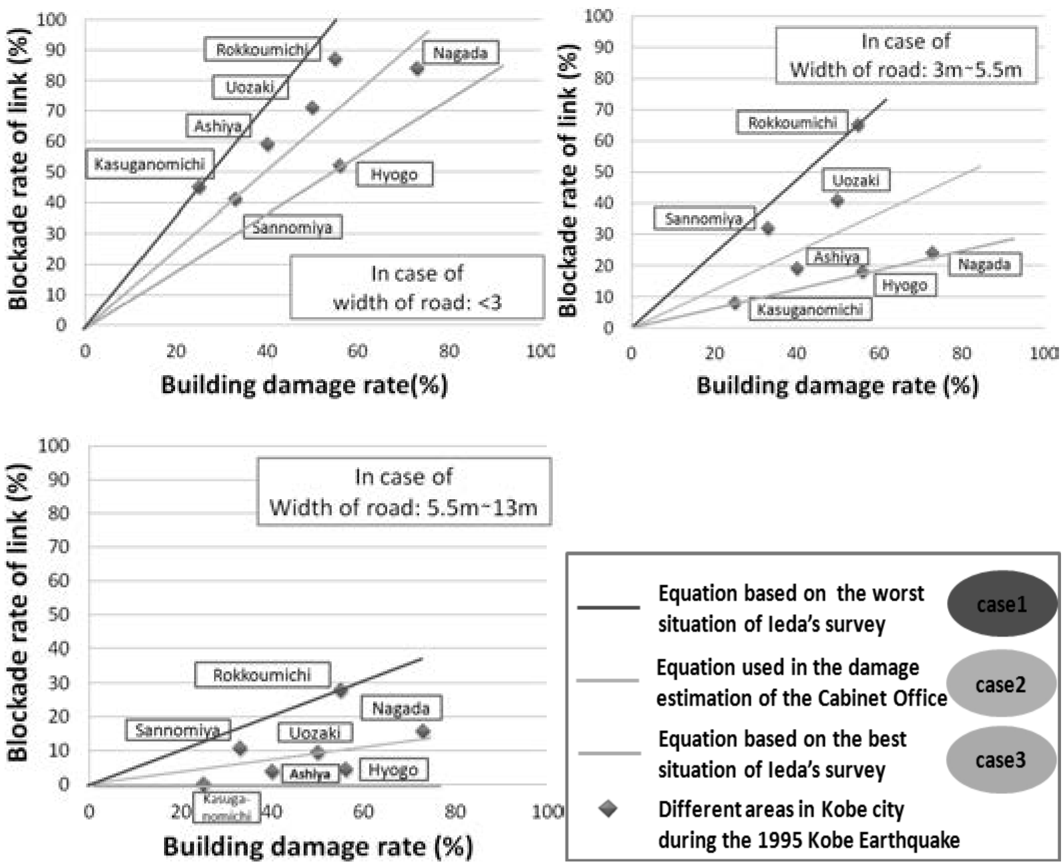

Figure 6: The relationship between building damage rate and blockade rate of link

Then, the blockade rates of the meshes were calculated by the blockade rates of the links using the equation below:

$$\text{Blockade Rate of Mesh} = \frac{\sum \text{length of road} * \text{blockade rate of link}}{\sum \text{length of road}} \quad \text{------ Eq.2}$$

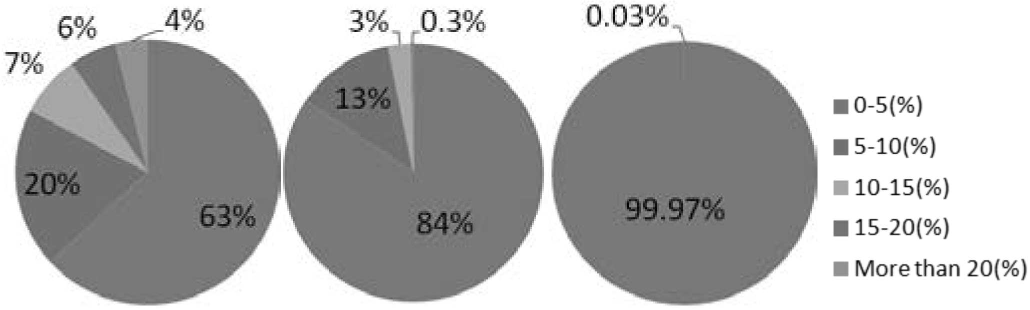

Case 1 Case 2 Case 3

Figure7: Distribution of blockade rates of meshes of case 1, case 2 and case 3

Based on the result of the blockade rates of the meshes of case 1, 2 and 3 shown in figure 7, restriction polygon barriers or scaled cost polygon barriers were added to the meshes. Figure 8 and 9 show examples of restriction polygon barrier and scaled cost polygon barrier, respectively. Barriers are feature classes in network analysis layers that restrict or alter impedances of the underlying edges and junctions of the associated network dataset. There are two types of polygon barriers; one type is restriction polygon barrier that prohibits travel anywhere the polygon intersects the network, and the other type is scaled cost polygon barrier that doesn't restrict travel on the edges and junctions it covers; rather, it scales the cost of traversing the covered edges and junctions by a factor you specify. For example, a factor of 2 would mean it is expected to take twice as long as normal.

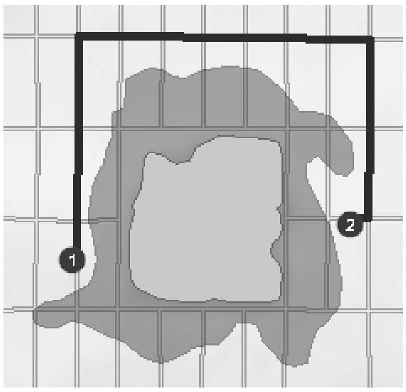

(Example)

Figure 8: Restriction polygon barrier

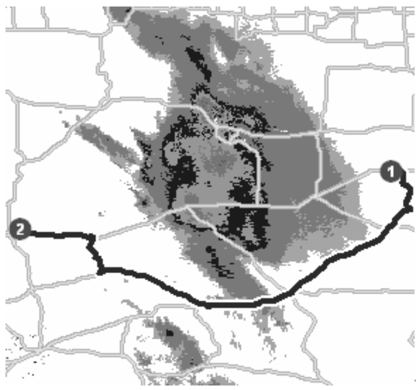

(Example)

Figure 9: Scaled cost polygon barrier

According to Hagita (2009), in the case of Hanshin-Awaji Earthquake, the running speed of Route 2 of the Kobe city fell down from 25 km/h of rush hours in normal situation to less than 3km/h at the day of the occurrence. Because the running speed fell down to almost 1/10 of the normal situation, a factor of 10 was adapted as scaled cost polygon barriers as shown in figure 10. Furthermore, according to Ieda's survey (1997), almost all the road users gave up using the

blockade links or areas which had been blocked with 20% or more. Based on this, restriction polygon barriers were added to the links with 20% or more blockades as shown in figure 10. According to the result of blockade rates of the meshes of case 1, 2 and 3, restriction polygon barriers were added in case 1.
Lastly, by operating the “ArcGIS Network Analyst” within 10 minutes based on the changes of the roads, the maximum transportable areas in disaster situation were identified.

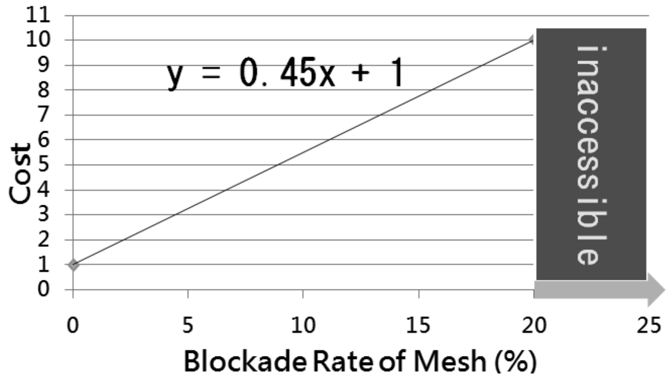

Figure 10: Relationship between cost and blockade rate of mesh

3. SIMULATION RESULTS

The result of inaccessible meshes of case 1 (Figure 11) shows that most of the inaccessible meshes were in the eastern part of Tokyo, which led to seven inaccessible hospitals and much shrank of maximum transportable areas (Figure 12) to the nearest hospitals compared with case 2 and case 3. Furthermore, compared with the normal situation, the maximum transportable areas also shrank seriously when road block in case disaster was considered. However, the maximum transportable areas could be expanded when transportation to disaster base hospitals and emergency hospitals were both considered as shown in figure 13.

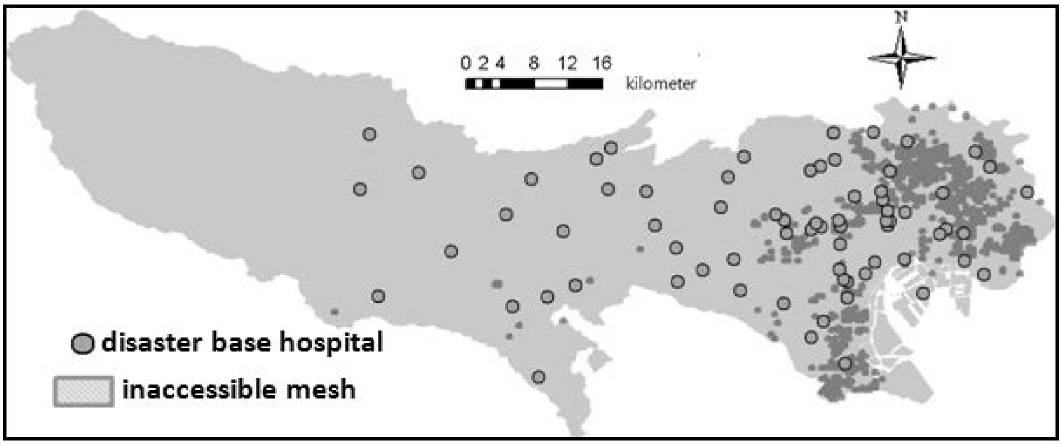

Figure11: Inaccessible meshes of case 1

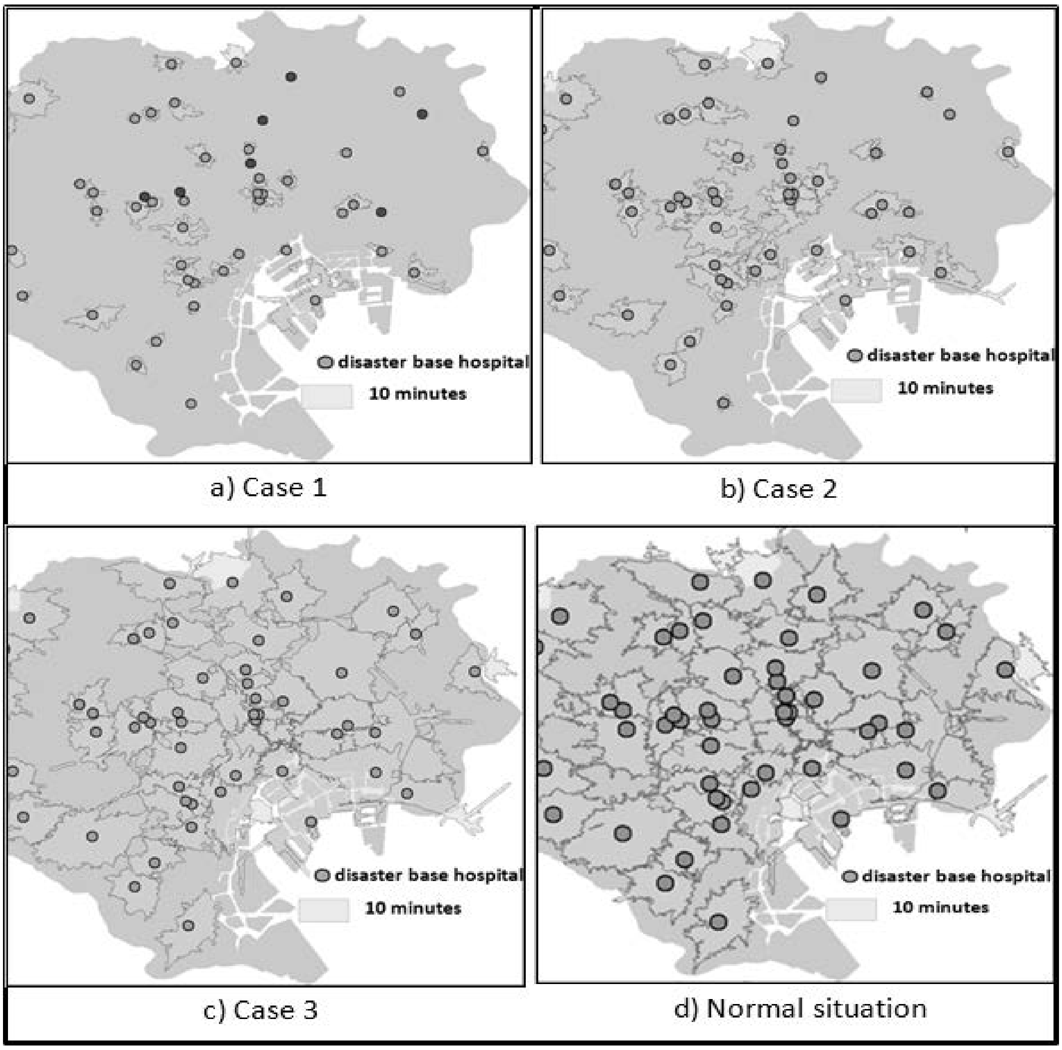

Figure12: Transportable areas of disaster base hospitals

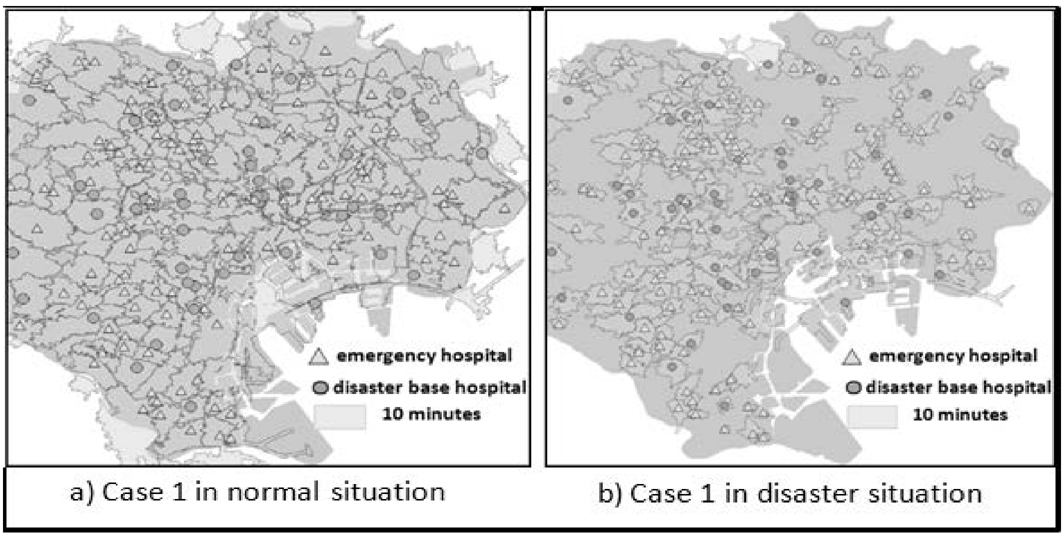

Figure13: Transportable areas of disaster base hospitals and emergency hospitals

4. CONCLUSION

This study simulated the effect of street blockades on the transportation of seriously-injured victims to hospitals using "ArcGIS Network Analyst" in case of the expected Tokyo Inland Earthquake. The simulation results showed that almost all the areas in Tokyo Prefecture were accessible to disaster base hospitals within 10 minutes by car in normal situation. However, maximum transportable area drastically shrank when road block in case of disaster was considered. This analysis identified that the rapid transportation of the eastern part of Tokyo metropolitan area to the nearest disaster base hospitals would be impossible in case of the earthquake.

According to this result, a series of countermeasures such as upgrading existing emergency hospitals as disaster base hospitals, increasing in the number of disaster base hospitals by new construction, preparation for accommodating victims rapidly in the hospitals in surrounding areas with little damage or dispatch of on-site medical treatment team with portable facilities such as DMAT (disaster medical assistance team) could be considered in those areas.

As future studies, various scenarios should be considered such as expanding the maximum transportable areas to within 30 minutes or 1 hour or changing the parameters of the scaled cost polygon barriers, etc. Additionally, transportation to the hospitals on foot should also be considered in the next steps.

REFERENCES

Tokyo Metropolitan Government, 2012. Damage Estimation of Tokyo Inland Earthquake.

Cabinet Office, Government of Japan, 2013. Damage Estimation of Nankai Through Earthquake

Ohara, M., Meguro, K.,2008. Estimation of the number of heavily injured victims transported to hospitals in case of expected Tokyo Inland Earthquake. *Industrial Research* vol. 60, No. 6, pp. 33-38.

Sho, L., Maruyama, Y., 2010. Analysis of wide area road network of disaster base hospitals in case of expected Tokyo Inland Earthquake, *proceedings of undergraduate's thesis*, Chiba University.

ArcGIS help 10.0: Restriction polygon barrier and scaled cost polygon barrier http://resources.arcgis.com/en/help/main/10.1/index.html#//004700000056000000

Ieda, H., Kaminishi, S., Inomata, I., Suzuki, I., 1997. Street Blockades in Hanshin Earthquake'95 and Its Influence on Disaster Relief Activities. *Doboku Gakkai* No.576/ IV-37, 69-82.

Kagita, K., Yamashiro, T., Hongo, K., 2009. Operating simulation of police rescue corps on the next Tokyo Metropolitan Earthquake. *National Research Institute of Police Science* Report 60 (1.2), pp. 30-36.

Solutions for a higher living quality for people in Hanoi's Old Quarter

Thi Hoai An LE[1] and Anh Quan PHUNG[2]
[1,2] Lecturers, Faculty of Construction Economics and Management,
National University of Civil Engineering, Vietnam
hoaian102@gmail.com

ABSTRACT

Locating in the centre of Hanoi, the Old Quarter (OQ) has been established thousands years ago and become one of the most significant heritages of this city. The paper first presents a set of indicators developed to be used in a survey for measuring aspects of living quality of Hanoi's Old Quarter inhabitants and their dwelling expectations. The result shows that people living in the Old Quarter have faced with so many problems that impact on the quality of their life such as unsecured life, environmental pollutions, cramped shelters, and infrastructure downgraded. It can be seen the main cause of this serious situation is overloaded population, so the key solution for the OQ is the decrease in population density. Therefore, 3 main groups of the inhabitants are indentified: (1) People compelled to move out; (2) Inhabitants want to change dwelling location; and (3) Residents keep staying in the OQ. Based on the three categories, the paper puts forward some recommendations for the government to support inhabitants in each group to improve their quality of lives in the Old Quarter. Moreover, the research notices a relationship between people's dwelling expectation and financial benefits that they gained when running a type of business in the OQ. The Government should take this relationship in account when considering and implementing further solutions.

Keywords: *old quarter, life quality improvement, dwelling expectations, reduce population density*

1. INTRODUCTION

Hanoi's Old Quarter (OQ) is located in the center of Hanoi. It is well-known because of the unique architectures and significant heritages in the area. The OQ was formed in Ly dynasty (in the 11th century) and it has become a heavily populated and the most bustling trading area since that time.

The OQ is recognized as a preserved area because it represents many historical and cultural heritages of the capital city and becomes one of the famous features of Hanoi's tourism. As in an old saying: "Birds of a feather flock together", people living nearby in the OQ often formed specific guilds trading and/or producing the same type of products. Thus, in the OQ, each street was addressed a name closely related to a particular traditional trading product, e.g. "Hang Muoi" (salt market) for the street selling salt, "Hang Manh" (curtain market) for the street selling bamboo curtains. Currently, Hanoi's OQ covers 100ha, including 10 wards of Hoan Kiem

District and up to 76 streets [MOC, 1995]. Over thousands years of development, the OQ has changed significantly. The infrastructure there has been downgraded while the population density is very high and seems to be increasing in the future. There are about 82.300 people per square kilometers, that it is classified in one of the most crowded areas in the country [Statistic, 2009]. Consequently, the OQ inhabitants are living in a lower level of living quality than people in others parts of Hanoi. Being aware of that serious problem, various agencies of the city and the national government have been trying to find out effective methods for the enhancement of life quality in the OQ. Unluckily, there are no solutions worked effectively so people there continues living in unfavorable conditions.

2. METHODOLOGY

The paper uses results from survey with respondents who include people living in the OQ, civil servants in the area and selected experts to determine the failure causes of previous living quality upgrade plans as well as to measure significant aspects of living quality of the OQ inhabitants and classify their dwelling expectations in the situation. A total of 52 factors were included in the questionnaire. The interviewees are requested to answer the questions according their own experience and feeling of life in the OQ. 57 results of the questionnaire were received back from plenty of age, occupation, house location, gender, and time of living in the OQ of interviewees. Collected data was transcribed, coded, and analyzed using SPSS software. Moreover, authors had met some experts and planning officer to interview for their expectations, as well as experience and current situation of implementing related OQ project.

3. CURRENT LIVING QUALITY STATUS OF THE OQ INHABITANTS

According to previous researches and the survey results, there are both advantages and disadvantages living in the OQ. Significant advantages include improving social status, experiencing diversity in cultural and spiritual activities, getting more opportunities in doing business and servicing tourists and being highly prioritized in selected government policies. Besides, narrow houses and environment pollution can be considered as major disadvantages of living in the OQ.

3.1 Advantages

- Improving social status: Because of specific history and culture, the OQ is recognized as the most centralization area and a pole status of Hanoi city [H.H.Phe, 2000]. The survey shows that the residents are very proud to be the residents of the OQ and they feel satisfactory with convenience of living in this area. There are 87% people live there stated that they are proud and very proud to be inhabitants of the OQ. In detail, the distance from their houses to some important facilities like schools, hospitals, administrative offices is short. Moreover, it is very convenient for their daily life activities because supermarkets, restaurants, shops, and entertainment places are located inside and around the OQ. In addition, the inhabitants said that living in the OQ gave them many priorities in getting jobs, borrowing capital from banks and obtaining school admission for children.

- Diversity in cultural and spiritual activities: Because of its 1000-year history with trading unions and villages, residents in the OQ experience a diverse environment in terms of united community, cultural and spiritual life. Firstly, one positive consequence of the living conditions in the quarter is that people tend to help each other even in small matters such as shopping, cooking meals and looking after one another's houses and children. Sharing a living space with many other family members, people must harmonize their individual personalities in order to live together happily as a united community. Secondly, Hanoi People Council organizes a lot of annual cultural and entertainment activities such as Flower festival, Fire-work, Mid-term festival which can enrich the spiritual life of the OQ inhabitants. Last but not least, there are many temples in the OQ to commemorate the founders of their trade or craft, for instance Lo Ren temple (blacksmith), Thuong temple, Kim Ngan temple (jewelery). This, thus they feel safe in soul and make them want to live there in long time.

- Advantages in doing business and providing tourism services: The OQ is a location that attracts tourists, especial foreign tourists, because of its unique features, millennial culture and history. As a result, traditional trading activities, souvenir shops, restaurants, hotels have been developed and have created job opportunities for people in the area. If a household has a house for rent they can earn much money from the status of their location.

- Get priorities in government policies: In order to preserve the OQ as a historical cultural heritage, on the 4th June 1999, Hanoi People's Committee issued the Tentative Regulations on Management of Construction, Preservation, and Restoration of Hanoi's OQ. Consequently, more priorities are given to the improvement of infrastructure in the OQ than in other areas in Hanoi. The Regulations also state that, in the near future, the drainage and sanitary system in the Old Quarter will be improved and rebuilt. The networks of electric wires and communication cables weaving above the streets in the Quarter will be replaced with underground systems. Recently, Ministry of Construction, being supported by experts from Toulouse city (France) has succeeded in the project of "Preservation, Renovation and Refurbishment apart of Ta Hien street" and the similar projects will be carried out in other streets in the OQ in the future.

3.2 Disadvantages

- Cramped living in narrow house: In the past, the most popular structure for houses in the OQ was the old type of house named "tube house". In this type of house, the structure nevertheless was deeply influenced by life style, old handicraft industrial production and old trading. The house was narrow in width and about tens of meters long. Sunlight entered the structure through open yards and courts, giving the house an open feeling and healthy atmosphere. On the ground floor of each house, there was a shop, and the back was used to produce goods and people lived there. The inner yard, kitchen and the back garden were used by both families.

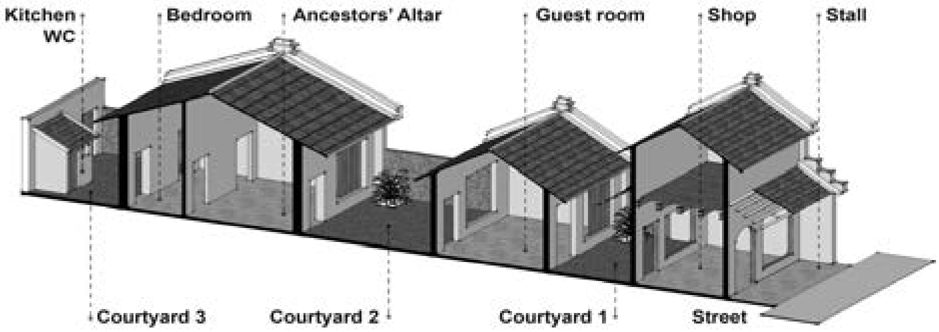

Figure 1: Typical architect of houses in the OQ in 1800s

When the next generations were born and grew up, the situation has changed dramatically. The number of people living in the house keeps increasing whereas the area of the house stays limited. Although they expanded living area by using open yards, courts and lane areas, the average area per person in the OQ is very small. In Hang Buom Street, there is a two-member family with a dad and a son living in an area of about 3m^2 (1.9mx1.2m) participated in the survey. According to the data collected from the survey, the average area per person in the OQ is 12.275m2/per person while the average figure for Hanoi is 21.5 m^2/person [Hanoi People Committee, 2013].

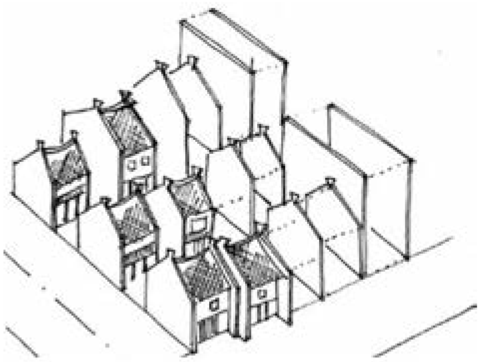

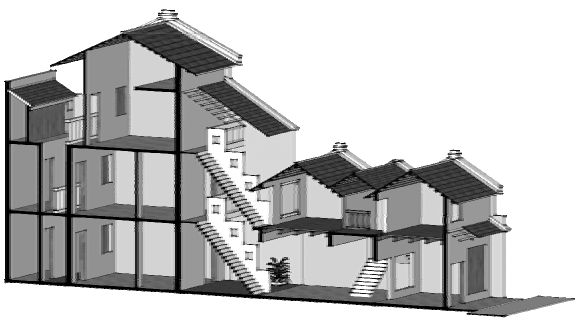

Figure 2: Revolution of old houses   Figure 3: A typical house in the OQ in 2000s

- Pollution in the living environment: Living in a small area and sharing a kitchen and a WC makes people unsatisfactory even in personal demands. For example, in the house No 44 at Hang Buom street, there are 3 families with up to 40 people sharing a water closet The water closet is old and shabby so that local people feel very inconvenient. In addition, the low graded sanitation system has bad influence on the surrounding environment. Lanes are often small and dark. Almost all of lanes in the surveyed area are just from 0.60 to 1.0 meter in width and always in insufficient lighting condition. Similarly, the buildings always lack natural light, natural wild, especial houses in inner lanes. Even worse, in the rainy seasons and especially after some terribly heavy rains, some streets, for instance Phung Hung, Ha Trung, Dinh Liet etc.., have been flooded polluting the area and may bring high risky diseases to the inhabitants. Furthermore, several respondents in the survey stated that they were unhappy due to the sound pollution from tourism activities, for example a night market at weekends in streets.

4. PROBLEMS IN THE ENHANCEMENT OF THE LIVING QUALITY IN THE OQ

The main cause of the problems mentioned above is the high population density in the OQ. Since 1998, Hanoi People committee has issued plans for moving people from the OQ to other parts of the city, and for improving living conditions. However, these previous plans were not successful as expected because of their low feasibility. In 9th January 2013, Hanoi issued Decision No 168/QĐ-UBND which approved the plan for moving people out of the OQ in order to attempt solving the problems for the majority of people living there. According to the literature reviews, expert judgment, and the survey result, the difficulties in moving inhabitants out from the OQ and in improving their living quality include:

- Problems related to perception change of the OQ inhabitants: For the residents, the advantage of their dwelling location as mentioned above is meaningful. Although they know their unsafe living status, they do not want to move out of the OQ. In the survey, 70.4% of the participants do not want to move out and only 1.9% of them want, but in the near future. They do not want to move because they worry if living conditions in the new place can be as convenient as in the OQ. People are afraid of losing their current job and having difficulties in applying new jobs in the new location. Besides, they enjoy interesting culture and living a spiritual life as well as with good neighborhoods and community relationship in the OQ.

- Problems of people who want to move houses: These people account for only 1.9% of the participants, yet most of them have financial problem. They do not have enough money to buy a new house while it is difficult for them to sell their current house in the OQ because of the tiny area (approximately 10m2)

- Problems with the authorities' actions: Because the OQ is a conservation area, any minor changes must be reviewed and approved before being executed. For the downgraded, crowded and old apartments in other areas of Hanoi, it is easy to demolish them, and then build new ones on the former ground with many more floors. However, this solution cannot be applied here. The height of buildings in the OQ is controlled by Hanoi Department of Planning and Architecture. Accordingly, all buildings are required not exceeding 3 floors (not counting the mezzanine in the 1st floor), the maximum height (from the ground to the top of the roof) is prohibited to exceed 12 meters. Moreover, as the budget for solving the problem is limited, authorities have insufficient source to implement expensive and complete solutions such as relocation allowance, housing subsidization for all householders in the OQ.

5. SET OF INDICATORS TO MEASURE THE LIVING QUALITY OF OQ RESIDENTS - RESULTS AND RELATIONS

5.1 Result of the survey

A special set of indicators was created in order to measure the current living quality of OQ residents. The measurement of indicators was based on the 5-point likert scale with code 1 to code 5. Code 1-5 mean strong disagree, disagree, neutral, agree and strong agree, respectively. This set of indicators based on 10 types of indicators of “The quality of Life indicators project” that New Zealand government was implementing in their country. There are 10 categories of indicators used to estimate the living quality of residents in Hanoi’s OQ.

Table 1: Indicators of the survey

No	Sectors	Indicators	Range of Means
1	Education	Short distance from house to school, quality of the education system, convenience in reaching extra education, effort of the government in developing education	3.52-4.2
2	Health care system	Effort of the government in preventing infections, distance from the house to the nearest health care center, quality of health care system	3.58-3.98
3	Safety and security	Sense of safety, safety for children and old people, frequency of accidents, criminal rates	3.98-4.73
4a	Housing and artificial environment	Satisfaction of: the living (area, house structure, equipment), population density, surrounding building, air quality, green rate, noise pollution	2.07-3.22
		Satisfaction of the services: Electricity, water supply, sewage system, garbage collection, vehicle parking	3.05-3.8
5	Traffic	Traffic jam, convenience, fluency, public transportation system	3.0 -3.58
6	Convenience of service and products	Convenience in reaching to markets, places of amusement, other services and products	3.26-4.19
7	Social connection	Harmony with neighbors, diversity in community activities	3.24-3.94
8	Civil and Political Rights	Strong voice to related policies, understand of current policies and plans	2.5 -3.06
9	Economic standard of living	Total income, total expense, comparison of living cost, financial trouble	1.93-2.84
10	Economic development	Running business in the house, total profit gained, difficulties in running business	2.61-4.07

- Education and health care system: The people in the OQ highly appreciate the health care system and preschool-primary education in this area. The median value of the all these variables achieved level 4/5 (Good).

- Safety and security: The inhabitants believe this is a very safe area to live. Over three-quarters of respondents agreed and strongly agreed that the sense of security; and safety for the elderly and children in this area is good. Accidents and criminals in this area is very low. Actually, people rarely have witnessed robbery or accident within recent 12 months.

- Housing and artificial environment: Contrary to the position of a status pole in Hanoi, the quality of housing in this area is rated in low levels. Indicators in section 4 of the table illustrate that people do not satisfy with their houses and surrounding buildings in terms of construction quality, and especially for noise pollution, which frequently occur day and night because of animated business activities. However, the quality of supporting services is good and meets almost demands of residents.

- Traffic in the area: Data in section 5 of table 1 demonstrates that the transportation system of people living here is relatively favorable. This convenience was created by the centralization of roads in this area, and great success of OQ scheme in arranging and distributing transport flows. Therefore, traffic jams have not occurred frequently in this region.

- Convenience of services and products: The people can be very favorable for shopping, eating, drinking and entertaining in this area. As this is a diverse area in terms of commercial products and services, people can easily buy all products they need without going far. Moreover, the OQ also focuses a big number of restaurants, markets and malls, small shops at acceptable prices.

- Social connection and Civil and Political Rights: With high average scores of indicators in section 7 of the table, people in this area represent a strong link among their neighbor community as the content of 3.1 in this paper. Besides, through the criteria in Section 8 of the table and the results of open-answer questions in the survey, people living here found their voice in terms of affecting politics and policy issue is in normal level. Besides, activity of announcement responded by local government seems not to work effectively.

- Economic development and Economic standard of living: It is easy to see that majority of local people are not pleased about their income. The result of the survey illustrated that 70.5% of asked households have total income under 700US$ per month. However, their monthly expenditure is quite high and it is expected to be more expensive than other regions (94.4% of respondents agreed with this statement). In addition, about one half of the asked households run a business in or nearby their house in order to take commercial advantage of the location. In fact, this is a good place to trade any kind of goods and products. Furthermore, there are not many difficulties with the local authorities as well as the people living around.

5.2 The relationship between the living quality and dwelling expectation

By analyzing data, hypotheses testing was carried out (with 5% accepted error) to find down the relationship of ordinal variables (indicators), the scale variables and nominal variables (which identified the decision whether or not to move out of OQ). There are several interesting findings:

- There is a relationship between owning a type of business in or nearby the house and dwelling related decision. Specifically, if residents run a business in their house, they trend to keep staying in that house. On the contrary, when local people cannot make profit by using their house, they rather choose to move out. The strength of this relationship is reflected by the value of the gamma coefficient, at a rate of 0.567. Error of this hypotheses testing is 3.8% (Lower than accepted rate of 5%).

- There are unrelated or weak relations between dwelling related decision and these variables in pairs: average living area per person; rated value of living quality (presented in the result table); number of years that they have been living there; and proudness to be an OQ resident.

6. SOLUTIONS OF IMPROVING LIVING QUALITY IN THE OQ

Through the investigation, it can be seen that the key solution to improve living quality in the OQ is successes in moving people out of the OQ project. And according analysis of the set of indicators, the research notices a relationship between people's dwelling expectation and financial benefits that they gained when running a type of business in the OQ. Good quality of life should satisfy people's desire for their own lives. Therefore, the Government should give priority to solve business problem or occupation opportunities for people who want to move out.

6.1 Solutions for business or occupation problem

Obviously, the people are afraid of losing their current jobs and having difficulties in applying new jobs in the new location, especially for households that run a business in the OQ area. Therefore, this problem must be considered in solutions. There are several ways to solve this: Initially, the government is supposed to give good business conditions for people after resettlement. In detail, 1st floor of apartment blocks in resettlement area need to be designed as series of shops to help the households continue their current business. Secondly, the authority could open skills training, vocation classes in accordance with the industries in nearby districts for resettlement people to help them having more work opportunities in the new relocated area. Besides, opening more factors for city establishment (like industry area, service and entertainment centre, and education system) must be implemented simultaneously to create employment. Moreover, the government should take sources of competitive advantage in account when researching and making city plans. Thirdly, the public transport system from new resettlement area to the center should be improved in terms of capacity, and service quality.

6.2 Classifying groups of inhabitants' expectations

"Divide and conquer" is always a good strategy. In order to resettle the inhabitants in the OQ, a realistic and feasible classification must be identified. Under particular conditions of the OQ, there are three groups of the residents:

- The 1st group includes the people living in the public or historical places like monument, campus of the school, state offices. Once their appearance in these places makes bad impact to public activity, they are forced to change dwelling as soon as possible. It is very easy to define household in that group by investigating public places in the area. For this group, they should be announced strictly about resettlement requirement. The priority policy will depend on their collaboration with the government.

- The 2nd group is people living in private area but willing to move out. The 2nd group can be identified by a simple survey of the local government. Preferential policies for this group could be priority of buying new house in the new resettlement areas, especially for households that currently living in small house (less than $5m^2$ per person). Other subsidized policies like relocating support, loaned with low interest rate from state banks will be considered.

- The 3rd group is largest. They are residents that do not want to change dwelling. For these households, if their residential area is so small, they should have priority to buy the area of the households in the 2nd group surrounding their houses. Authorities will play a mediating role to ensure purchase price is reasonable and reflected the true value of that area. The households must sign one commitment, in collaboration with the government in improving the living environment there like reconstructing toilets, and alleys.

6.3. Appropriated design solutions and attractive life in the resettlement.

Hanoi People's Committee is currently investing in Viet Hung urban area, which is located far from 6km to the city center to relocate people. This project is giving priority registration for people in 1st and 2nd groups. This urban area need to meet three requirements of architecture, community connection and living facilities. Firstly, the architecture solution in new settlements should retain the specific characteristic activities of the ancient OQ like traditional trade, food, and community. Architecture of buildings needs to be flexible with various apartments' area. It is required to be suitable with the financial condition of each household. In case of paying by installments, payment schedule need to be long enough and be flexible to help people in buying new houses. Secondly, community events, which is familiar with normal life in OQ could be organized to attract people living in new settlement are. For example, night markets, flea markets and other exciting activity like farmers market. Lastly, transportation system, infrastructure, and other facilities in resettlement are expected to meet requirement of the former residents; kindergartens, schools, and health care centers will be built in the resettlement area.

6.4. Solutions to improve the quality of life of residents staying in the OQ

After project of reducing population density succeeded, living quality of Hanoi's Old quarter will have precious opportunity to be improved. Therefore, the residents should support the local government in term of buying the houses of their former neighbour (who moved out) to increase living area. Moreover, they need to repair and restructure the current house to improving living quality under legal framework and preservation rules. A commitment might be made to change the situation and to force the residents to implement. Moreover, they ought to do their duty of preserving historical and cultural buildings in Hanoi's Old quarter. On the other hand, local government should give favourable conditions for these people to repair and reconstruct building under legal framework and preservation rules.

6.5. Using mass media to raise awareness of the people

It is a good suggestion for the authorities to organize community meeting to propagate of reducing population policies. These events will to make people realize the whole profit of the policies for all of them. In order to get effectiveness, they can use mass media to share experiences and stories of people who moved and have a better life after moving from the OQ. This solution based on trust of people on their former neighbors, it will encourage people living in difficult conditions in the OQ to have wise plans about their dwelling decision. Moreover, these meetings are good circumstance for people to raise their voice, as well as for authorities to collecting ideals.

7. CONCLUSION

The paper points out the practice of living quality in OQ. It also concentrates on an important factor of improving living quality: the decrease of population density. Basing on data analysis, OQ residents' choices of moving out or staying there depend on what economic benefits they gained from that house in the OQ. This must be the starting point for all solutions of the government in the future. According to the project of reducing population density in the OQ, which is implemented by Project Management Board of Hanoi's OQ, the objective of the scheme is reducing the population density of the area from 823 persons/ha (in 2010) down to 500 persons/ha (in 2020). The solutions in Section 4 are expected contributing to the success of the project, and provide a safer life, higher living quality for residents in that significant historical and cultural area of Hanoi.

REFERENCES

Figure 1: Vietnam Association of Architects, The golden age of Hanoi - ThangLong
Figure 2: www.toulouse-hanoi.org/english/co-operation-initiatives/architectural-and-urban-heritage/
Figure 3: Project of reducing population density in the OQ, Project Management Board of Hanoi's OQ, 2013
MOC, Decision 70, 1995. Ministry of Construction, Decision No 70/BXD/KT-QH dated on 30th May 1995 determined the scope of the Old Quarter.
Statistic, population census 2009. General statistics of Vietnam, The 2009 Population and Housing Census.
Hanoi People Committee, 2013. Hanoi House Development Program (2012-2020).
Hoàng Hữu Phê and Patrick Wakely 2000. Status, Quality and the Other Trade-Off: Towards a New Theory of Urban Residential Location, in Urban Studies, No. 1, Vol. 37, Taylor & Francis, England.
Quang Minh Nguyen, 2013. Social sustainability and public responsibility in Vietnam modern city development context with Hanoi as a case study.
Sustainable Built and Environment for Now and the Future. 79-85.

A study on post-disaster housing by analyzing the pattern between the regional characteristics and people's preference

Tomoko MATSUSHITA[1] and Kimiro MEGURO[2]
[1] Graduate Student, School of Eng., The University of Tokyo, Japan
matsu-t@iis.u-tokyo.ac.jp
[2] Professor, Director, ICUS, IIS, The University of Tokyo, Japan

ABSTRACT

Almost two and a half years after the 2011 Great East Japan Earthquake, approximately 290,000 people are still living in temporary housing. Local governments are preparing to provide lots for building new houses or units of public housing based on the surveys conducted of the affected people. The survey results were similar throughout the fourteen more severely damaged municipalities and certain patterns were observed. This paper will analyze the results of the surveys by recognizing correlations between the regional characteristics and peoples preferences. By extracting specific patterns found during the housing reconstruction process, this research aims to support policy makers at regional level by suggesting an analysis of their geographic as well as demographic characteristics to prepare for future disasters more effectively.

Keywords: *temporary housing, post-disaster housing, the 2011 Great East Japan Earthquake*

1. INTRODUCTION

1.1 Background

Almost two and a half years after the 2011 Great East Japan Earthquake, 95% of evacuated people still live in temporary housing (including hospitals, public housing, etc.) while 5% live with relatives and friends and total of approximately 290,000 people need to move out from their 'temporary housing' by specified time which is causing great anxiety for displaced people. The government's latest plan which is supposed to reflect people's choice will provide either apartment units or lots for building houses for approximately 130,000 people and it will take at least next 3 to 4 years to complete.

1.2 Issues

According to the latest government plan, 24,577 'post-disaster' public housing units will be newly provided while 53,537 'temporary' housing (constructed type only) have already been built and provided. This simply implies that 46% of the housing is provided twice with public fund as a part of relief measures. Even though this is merely the result of peoples preferences, it is wasteful in terms of the use of public fund, land, time, human resources and building materials. Buildable vacant land is scarce in the disaster-affected area and such precious land which could possibly be used for building the post disaster housing may be taken up by temporary housing. The data shows that in Iwate Prefecture, approximately 40% of the land used for temporary housing was privately owned and unlike other type of land such as school grounds or parks that cannot be occupied for a long time, privately owned land is negotiable to be used as future housing property. The construction of temporary housing was delayed partially due to lack of land and the same can happen for the post-disaster housing. Another serious problem is the future maintenance issue. A majority of future occupants at newly provided approximately 24,600 public housing are elderly and soon the local government will face a high rate of vacancy. The central government's policy is to provide housing as per people's request however the local government must take care of the consequences of its action. This issue is only one of many problems caused by the current policy for the post-disaster housing and a better and effective system is needed.

2. FINDINGS

2.1 Result of Survey

The surveys conducted at 14 severely damaged municipalities in Iwate and Miyagi Prefectures are selected for this analysis (see municipalities marked with * in Figure 1). In general, no significant differences amongst the municipalities were observed. However there were a number of observations made regarding the profile of respondents and people's preference.

2.1.1 Profile in general

More than half of the respondents to the surveys were aged over 60 years old and majority of the household was two-person. This tendency of aging and smaller household size is not surprising considering the prevailing conditions prior to the disaster. In terms of form of housing, a majority were homeowners before the disaster with an exception in Sendai-city where homeowners and tenants counted about the same. A majority of respondents wishes to live and own a house again.

2.1.2 Profile by preference of temporary housing

Respondents are living either in prefabricated / constructed type or apartment type of temporary housing. The survey revealed that those who live in the former tend to be elderly, smaller household, low employment rate, and wish to return to their previous neighborhood while those who live in the latter type of housing (apartment type) tend to be younger with higher employment rate and do not wish as strongly as the elderly to return to the previous neighborhood.

2.1.3 Profile by the age group

Younger respondents preferred to build or own their house while the elderly preferred to move into public housing. According to the survey result in Watari town, 90% of respondents in the 30's wish to build a house on their own while

72.5% of elderly respondents wished the same. This reflects the reality of the majority of elderly's economical condition.

2.1.4 Profile with time factor

The delay of housing provision affects people's decisions. In Kamaishi city, a group of researchers conducted surveys twice asking the same questions one year apart. The results indicated that as time passed 1) more people preferred to move into public housing (increased from 14% to 44%), 2) single-person households have increased (increased from 23% to 32%), and 3) households with residents over 65 years of age have increased (increased from 47% to 52%). The reason for increase in the number of people who wish to move into public housing can be that people obtained more information and became more realistic in making decisions. The increase of single-person and older household can be explained by familial separation. It is more convenient and sometimes necessary for young people to stay at apartment type housing while elderly tend to stay at constructed type that are normally built in groups. During the prolonged period of 'temporary life', the young and elderly who have different agenda and priorities in life may become separated and elderly-only household can be more prone to choose public housing that will increase the need for construction as a result.

3. ANALYSIS

3.1 Correlation between regional characteristics and people's preferences

The severely affected regions in Iwate and Miyagi Prefecture along the coast of the Pacific Ocean can be categorized into two types shown as GROUP A and GROUP B in the Figure 1. Group A includes 10 municipalities in Iwate and Miyagi and these municipalities have in common a deeply indented coastal geography and steep rise in elevation known as a rias coastline. GROUP B includes 11 municipalities in Southern Miyagi and is characterized by a straight coastline and flat low land in contrast to the rias coastline. Generally GROUP A can be regarded as 'rural' while GROUP B is closer to 'urban' (or suburban) environment.

Both groups have similar population structures and average number of household members which is driven by the national phenomena of decreasing birthrate and aging population. However, examining the two groups by various other factors such as property ownership and industry structure (shown in the Table 1) revealed distinguishing characteristics both in geographic parameters as well as in people's preferences for housing.

The government's housing reconstruction plan includes two main publicly funded housing projects requested by people. Residents can request a developed piece of land for building a house on their own or a housing unit in a post-disaster public housing development and this decision could be correlated to the regional characteristics. The result shows that in GROUP A, for both temporary housing and post-disaster housing, people tend to show preference for constructing a new structure as opposed to moving into an apartment unit. GROUP B on the other hand shows the opposite result with higher preference for apartment type.

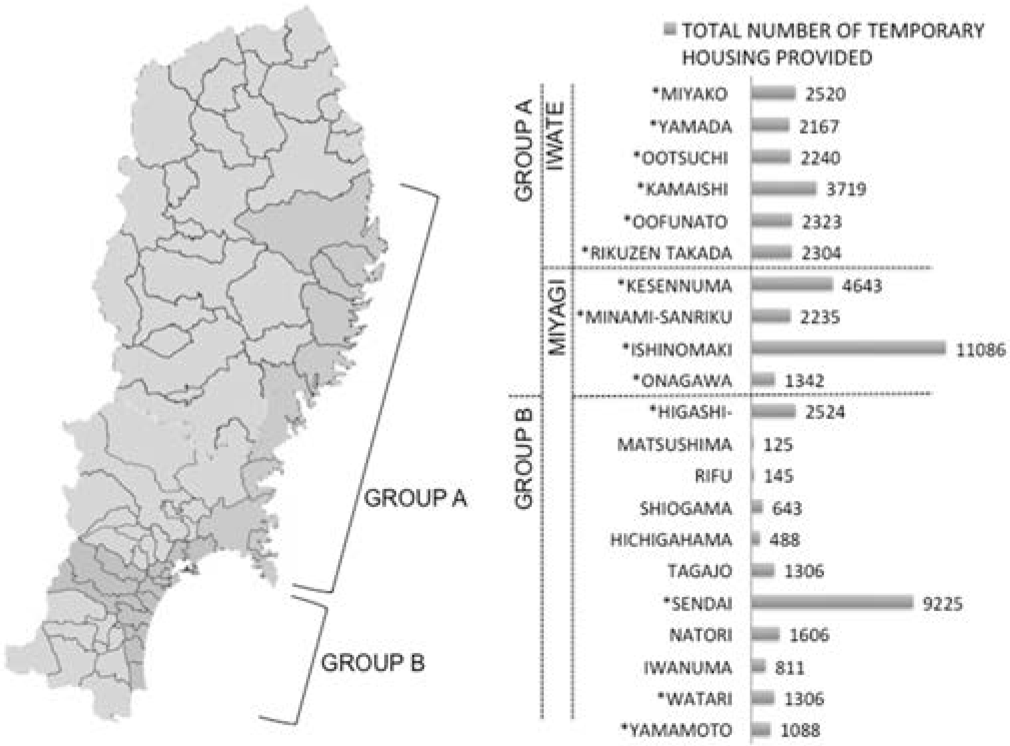

Figure 1: Map of affected municipalities of Iwate and Miyagi along the Pacific Coast and the number of temporary housing provided per municipality (the source: MLIT, Reconstruction Agency, Iwate and Miyagi)

Table 1: Regional characteristics and peoples' preferences regarding post-disaster housing categorized by GROUP A and GROUP B

Regional characteristics & people's choice	**GROUP A 'Rural'**	**GROUP B 'Urban'**
1) Age: 65 years old + (%)	32	23
2) Number of Household member (person)	2.5	2.7
3) Homeowners / Tenants (%)	80 / 20	73 / 27
4) Urban / Rural: Inhabitable land (%)	19	71
5) Industry Type: 1^{st} / 2^{nd} / 3^{rd} (%)	13 / 29 / 58	5 / 24 / 71
6) Temporary housing: Constructed /Apartment (%)	86 / 14	47 / 53
7) Post-disaster housing: Lot / Unit in Public housing (%)	56 / 44	33 / 67

3.2.1 Homeowners vs. Tenants: 3) in Table 1

Both GROUP A and B indicate a relatively high rate of homeowners, 80% and 73% respectively, compared to tenants, with GROUP A showing a slightly higher rate. A high rate of homeownership implies that there is a relatively small stock of apartments in the region and therefore the need for constructing housing is high. However when one looks at the rate for each municipality, Iwate Prefecture shows a high rate of homeowners overall while Sendai city and Tagajo city in Miyagi, which are both relatively urbanized, have an average of 52% rate of homeownership. In Iwate with an average of 82% ownership, 58% chose to build a new house on a lot provided by the government, while 42% chose to move into public housing. On the other hand, in the urbanized part of Miyagi with an average of 52% ownership, only 17% chose to build a new house while 83% chose public housing. This implies that homeowners tend to wish to build a house on a lot rather than moving into an apartment unit as a tenant.

The rate of homeownership is also closely related to people's work environment. People tend to settle when their work is inseparable from the land as in the 1st or 2nd industry such as fishing or processing. Thus high rate of homeownership can be translated as high rate of employment in primary and secondary industries.

3.2.2 Urban vs. Rural: 4) in Table 1

GROUP A suggests a low rate (19%) of inhabitable land while GROUP B indicates a much higher rate (71%). This is mainly due to the geographical condition and in GROUP B with a high rate of 'inhabitable land', there is a higher rate of people choosing apartment type of temporary housing as well as public housing for post-disaster housing. There is a higher need for apartment stock in the urban area naturally and this result confirms that people tend to choose the apartment type when there is a choice. This may lower the need for constructing temporary housing or public housing, however it can also scatter the original community which could undermine the effort of recovering the damaged community in the reconstruction process.

3.2.3 Industry Type: 5) in Table 1

According to the statistics taken before the 2011 Great East Japan Earthquake, the ratio of industry structure indicated that in GROUP A, 42% were engaged in the 1st and 2nd industry while in GROUP B the ratio was lower (29%). It may be said that the higher rate of 1st and 2nd industry implies peoples' willingness to own a house rather than renting a place.

4. CONCLUSION

By analyzing the correlation between the regional characteristics and people's preferences, the results of this study indicated certain patterns found in the process of housing reconstruction.

Even though the Disaster Relief Act sets the procedure for providing post-disaster housing universally at the national level, the result of this research indicated that people's decisions about housing can be preconceived to some degree by their regional characteristics. This suggests that policy making at a regional level rather than national level is necessary and effective. For example in the urban

region where people prefer to choose rental housing, finding appropriate land for constructing temporary housing is not so necessary. Rather than negotiating and preparing buildable land, it may be more effective for the local government to make arrangements with real estate industry. On the other hand, in rural areas, since people prefer constructing a house rather than renting it, it may be reasonable to plan and construct temporary housing with the intention of selling as public housing in the future at lower cost. This would help to ease the issue of "double" public funding by effectively eliminating the extra cost and time.
A correlation was identified by factors that are indicative of natural environment such as homeownership, the rate of inhabitable land or industry type. However there should be other factors that are more personal that influence people's preferences thus further research is required.

REFERENCES

Reconstruction Agency. 8.22.2013. *Total Number of Evacuees.*
Ministry of Land, Infrastructure, Transport and Tourism (MLIT). 4. 1. 2013. *Construction Situation of Temporary housing.*
MLIT. 2.4.2013. *Number of private rental housing leased as temporary housing.*
MLIT. 6.30.2013. *Housing Reconstruction Schedule.* <http://www.mlit.go.jp/toshi /toshi-hukkou-arkaibu.html> (accessed 8.2013)
Iwate prefecture. 2.7.2012. *Complete List of Temporary Housing Constructed in Iwate.* http://www.pref.iwate.jp/~hp0608/F_eizen/3rd/kasetsu.pdf (accessed 8.2013)
Rikuzentakata-city. *Residents Intention Survey 8-9.2012.*
Research group on Kamaishi-city. *Residents Intention Survey 7-8.2011.*
Research group on Kamaishi-city. *Residents Intention Survey 7.2012.*
Ofunato-city. *Residents Intention Survey. 4-5. 2012.*
Miyako-city. *Residents Intention Survey. 11-12.2013.*
Otsuchi-town. *Residents Intention Survey. 1.2012.*
Yamada-town. *Residents Intention Survey. 2.2012.*
Sendai-city. *Residents Intention Survey. 4.2012.*
Ishinomaki-city. *Residents Intention Survey. 2-3.2012.*
Kesennuma-city. *Residents Intention Survey. 7-8.2012.*
Higashi-Matsushima-city. *Residents Intention Survey. 2-3.2012.*
Watari-town. *Residents Intention Survey. 7.2012.*
Watari-town. *Residents Intention Survey. 10-11.2012.*
Yamamoto-town. *Residents Intention Survey. 6-8.2012.*
Onagawa-town. *Residents Intention Survey. 7-11.2012.*
Onagawa-town. *Residents Intention Survey. 7-8.2012.*
Minamisanriku-town. *Residents Intention Survey. 12.2011-1.2012.*
Ministry of Internal Affairs and Communications Statistics Bureau. 6.3. 2013. *Statistical Observations of Shi, Ku, Machi, Mura.* <http://www.e-stat.go.jp/SG1/ estat/List.do?bid=000001046053&cycode=0> (accessed 8.2013)

Proposed solutions to quality improvement and integrated operations of technical infrastructure systems for new urban areas in Vietnam

Ngoc Khoa HO[1], Hong Hai TRAN[2] and Nguyen Van Phuong PHAM[3]
[1]Phd, Faculty of Building and Industrial Construction,
National University of Civil Engineering, Vietnam
hnkhoa@yahoo.com
[2]Phd, Faculty of Building and Industrial Construction,
National University of Civil Engineering, Vietnam
[3]Msc, Faculty of Building and Industrial Construction,
National University of Civil Engineering, Vietnam

ABSTRACT

In recent years, in Vietnam, along with economic and population growth, the demand for housing and community living space have rapidly increased, leading to urbanization trend and the development of new urban areas and megacities. Technical infrastructure in urban areas is a basic system consisting of particular functional components that operate continuously during the whole service life of the areas. Construction of urban technical infrastructure therefore plays an important role. However, the majority of urban infrastructure project has faced various problems relating to quality and integrated operation, which can affect project investment efficiency negatively. The paper examined these issues and proposed solutions to improve the quality and ensure the integration of technical infrastructure systems in megacities' urban areas under Vietnamese conditions. Accordingly, the solutions could be applied in reality and contribute significantly to the enhancement of investment effectiveness for that kind of project.

Keywords: *Technical infrastructure, integration, new urban areas, megacities*

1. INTRODUCTION

In recent years, the world has witnessed unprecedented population growth in human history. The world population has been approximately 7 billion by 2013 and is expected to reach 10 billion by 2025 (Seitz, 2008). The world's population is becoming increasingly urban. There are many megacities with a population of over 10 million people have been formed. By 1950, the world counted two megacities, New York with 12,3 million and Tokyo with 11,3 million. After 60 years, there were 23 megacities, including 12 Asian megacities. The United Nations (2012) projected the number of Asian megacities will increase to 21 by 2025. Particularly, big cities such as Chongqing, Guangzhou, Jakarta, Lahore, and Shenzhen are predicted to reach 10 million people quickly. According to megacity definitions, Vietnam does not have any megacity; however, with rapid urbanization and population growth, it cannot be doubt that numerous cities are potential to become megacities in the future.

World Bank (2006) stated that urbanization is an indispensable trend and essential motivation for economic growth of nations. Urbanization and long-term development of an economy have a well-known positive relationship, driven by achievements from industrialization, commercialization, productivity improvement, employment opportunities, development of infrastructure and other facilities. Nations with higher levels of urbanization invariably have higher level of per capita income (World Bank, 2006).

Infrastructure is the heart of urbanization process. According to Le (2012), sustainable urbanization must proceed with the harmony of economic, social development, ecological protection, and appropriate infrastructure systems that create close connections between rural and urban areas. In particular, technical infrastructure is a key factor in order to achieve sustainability. Successful lessons of developed countries show that technical infrastructure built synchronously and modern is a material prerequisite for urban development. Sufficient technical infrastructure can help in improving living quality of urban residents, reducing poverty, narrowing gaps between developed and backward regions, and support economic growth (World Bank, 2006; Nagesh and Prabir, 2008).

World Bank (2006) recommended that during urbanization process, as a developing country, Vietnam should call for more investments in technical infrastructure development. In 2012, the Vietnamese Government highlighted that construction of urban infrastructure is one of the core investment areas in sustainable development strategy to 2020. During last 12 years, although the total investment for technical infrastructure projects accounted for 10% of GDP, urban cities have still faced many weaknesses of technical infrastructure systems (Nguyen, 2010). In Vietnam, urbanization took place early but in recent years, it has grown rapidly. Hoang (2013) identified that existing urban technical infrastructure has been showing poor quality, rapid degradation, and lack of integrated operation. Therefore, it is vitally important for finding out reliable solutions that could help ensure quality, integrated operation, stability, and sustainability of technical infrastructure components in new urban development projects as well as take into account the ability of connecting with other regions and enlarging spaces in response to urban development in the future.

This paper firstly will focus on examine the status of Vietnamese urban technical infrastructure. Difficulties and challenges arising from the implementation of infrastructure construction projects will be identified and analysed. The paper then will propose some solutions in order to improve quality, integration of urban technical infrastructure components, and enhance investment effectiveness of for that kind of project, towards sustainable urban development.

2. THE DEVELOPMENT AND CHARACTIRISTICS OF NEW URBAN AREAS IN VIETNAM

2.1 The status of urbanization process in Vietnam

In recent years, the pace of urbanization in Asia has become faster. Although urbanization in Asia had a relatively low starting point, it has taken place increasingly on a large scale compared to other regions. Asian Development Bank (2011) predicted that the process would continue to rise until 2050, in which the number of megacities as well as the size of cities will rise rapidly, including Hanoi and Ho Chi Minh City of Vietnam.

After the administrative boundary expansion by 2012, Hanoi's population reached to 6,87 million. Hanoi are about 7.1 million people and is expected to reach about 8,1 – 9,2 million by 2020 based on the fluctuation in population growth Urban spatial development of Hanoi is oriented towards the model of urban clusters including five satellite towns: Hoa Lac, Son Tay, Xuan Mai, Phu Xuyen and Soc Son. These towns and the centre are separated by green corridors, linked together by road belts and roads oriented to the central city, and belonged to the regional and national transport network (Vietnamese Government, 2011).

According to development strategies, Ho Chi Minh City will meet criteria for being a modern metropolis by 2020 (Ho Chi Minh City's Committee, 2012). The city's population will increase to approximately 10 million people by 2025. At the same time, there will be four new urban areas formed, namely Thu Thiem, Hiep Phuoc, Tay Bac, and Sai Gon Hi-Tech Park. Elevated railway system, railway for special purposes and highway bridges crossing Dong Nai, Sai Gon, and Nha Be rivers are expected to complete. Ho Chi Minh City Area will be constructed, including a nucleus (consisting of Ho Chi Minh City and some neighbourhoods) and five satellite towns for developing towards nearby provinces such as Dong Nai, Ba Ria – Vung Tau and Binh Duong. It is expected that population of Ho Chi Minh City Area will reach about 20 – 22 million by 2020.

Generally, urbanization process in Vietnam has increased rapidly, in particular the number of urban areas. Last century, there were about 600 urban areas, now this figure rises to more than 750, and is predict to reach 1000 by 2025 (Hoang, 2013). The urbanization rate is leading to rapid urban population growth whereas despite significant improvements, urban infrastructure systems are becoming unable to satisfy residents' requirements, and come under pressure increasingly. It is essential to take into account two answers for these problems, including: firstly, existing technical infrastructure is incapable of meeting the needs of urbanization growth; and secondly, technical infrastructure in new urban areas presents many limitations, for example, poor quality, lacks of operational integration and flexibility in association with the existing systems.

2.2 The development and characteristics of new urban areas in Vietnam

Vietnamese regulations define a new urban area as a part of city territory, with the high degree of integration of technical, social infrastructure, residential buildings and other service facilities. It may be either the expansion of an existing urban area or a completely new urban zone that has its own boundaries and determined functions in accordance with urban plans approved by the government. Its administrative boundaries belong to a province (Vietnamese Parliament, 2009).

The majority of new urban areas projects must comply with Construction Law, Decrees on investment and construction management, and other related legal documents. In fact, these documents are not brought up-to-date in order to be appropriate for rapid urbanization. Additionally, policies on land management, compensation and acquisition are not adequate. The level of construction and management is low. As a result, these projects have not been delivering successfully. The size and quality of technical infrastructure systems seem not to satisfy requirements of social infrastructure development and residents' demands. Most of urban projects are delayed frequently.

According to statistics made by Vietnamese Construction Ministry, the country currently has around 2,500 new urban projects that are mainly residential, office buildings and other properties. In Hanoi, there are more than 800 projects with an area of about 75,189 ha. Urbanized and residential areas account for nearly 390 projects with an area of 39,000 ha. Ho Chi Minh City counts about 1,400 projects with an area 4,490 ha. Meanwhile, Hai Phong City approves approximately 260 projects with the nearly 2,600 ha of land, and 100 projects have been implemented and generate approximately 700.000m2 contributing to the city's housing fund. Da Nang City invests in more than 120 projects of constructing new urban zones, offices, commercial and residential buildings with an area of about 2,300 ha. However, 19 provinces still do not have any urbanized area. There are main characteristics in urban development process found, as follows:

Regarding to customer focus, new urban zones primarily serve needs of those with high incomes while the main objective of urbanization strategies is to address demands of housing, living spaces for all different people groups, including those with low incomes. However, it seems that this objective is unlikely to achieve due to various reasons in terms of economic, social and custom issues.

Regarding to land acquisition, there are many problems causing a waste of time and money of all involved stakeholders. Their reasons mainly come from the lack of coordination among related authorities. Investigations for planning land acquisition are conducted slowly. Compensation for damages to residents' properties is not reasonable. In various projects, compensation process did not carry out overtly. Adjustment policies made by the government leading to a variance of compensation resulted in residents' claims and disagreements.

Regarding to urban design, master plans seem to be inappropriate. For example, urbanized areas mostly present inadequate layout of spaces. Low-rise buildings are situated alternately among tall buildings, or high-rise buildings are located mainly either along arterial roads or surrounding the boundary of urbanized areas. Master plans also do not take into account an idea of making a high-rise building complex become the highlight of an urban area. Approval process of architectural design always requires the harmony of architecture and climate and landscape of urbanized regions. However, in current practice, architecture of new urban areas is of poor quality with undefined and irrational styles, using many colours and boring box-shaped buildings. Urban designs show the lack of breakthrough ideas that can create different and original characteristics of a new urban zone. Besides, residential buildings account for the majority of a total urbanized area whereas the land area for social infrastructure, static traffic system, plants and trees, squares and lakes is limited.

Regarding to the quality of technical infrastructure and its operation, there are some serious problems. Due to the rapid development of new urban projects, infrastructure construction is of poor quality and lacks the consistency between new and existing systems. Drainage systems generally do not guarantee operational capacity as required. Flooding occurs frequently during the rainy season. In Hanoi, new urban areas such as Trung Hoa - Nhan Chinh, My Dinh, and Keangnam Complex, often face flooding after heavy rains, because of insufficient investment in drainage systems, lacks of integration and flexibility with existing systems and the nature of low-relief land areas. In many urban zones, wastewater treatment plants are putting pressure to meet defined requirements, causing the phenomenon of discharging wastewater directly into sewers, ponds and lakes. Consequently, the urban environment has been polluted, affecting the quality of residents' life adversely. "Dead pits" caused by local subsidence of urban transportation system due to poor quality of construction works are receiving negative feedback of the society. New urban zones are often located in suburbs. Therefore, excluding fence systems constructed, during site preparation investors have to face difficulties relating to traffic, water supply, and electricity. The handover of technical infrastructure components to clients do not provide enough all their operational relevant documents. Warranty and maintenance activities are not effective and efficient.

3. THE STATUS OF QUALITY AND INTEGRATION OF TECHNICAL INFRASTRUCTURE SYSTEMS IN NEW URBAN AREAS

Urban infrastructure consists of social and technical components. Social infrastructure are residential buildings; public service facilities for health care, culture, education, entertainment, sports, parks, commercial purposes and others; and buildings for urban administration works. Technical infrastructure includes the following items: transport system, surface water drainage system (drains, detention reservoirs, storm-water pump stations), sewage system (sewers, wastewater treatment plants), water supply system (water supply plants, pipelines, pump stations - tanks), power and gas supply system, lighting system, communication and telecommunication system, and tunnel engineering system (Choguill, 1996; Hardwicke, 2008; Vietnamese Construction Ministry, 2012). Technical infrastructure is defined as a system including particular functional components that are first built and operate continuously during the whole service life of an urban area. The quality and efficiency of technical infrastructure will be enhanced when all their components are integrated and linked closely.

The status of poor quality and integration of technical infrastructure of new urban areas in Vietnam comes from many perspectives at all stages of investment process, particularly management mechanism, legal documents, and problems in project planning and implementation. Owing to a diversity of scales, nature, investment capital, client requirement and duration, as well as impacts of a component upon others, technical infrastructure system needs to be managed strictly by stakeholders during and after investment process.

3.1 Management mechanism of government authorities

Inadequate legal documents: Although there are numerous legal documents about urban planning, construction investment and quality management, in fact, Vietnam still lacks a legal document system for technical infrastructure projects, which is holistic and comprehensive, in order to create favourable conditions for related authorities and parties involving in construction activities.

Lack of inspection and supervision during construction process of stakeholders who directly operate technical infrastructure components: After construction process, project products will be handed over to different local authorities to operate and manage in relation to their functions. For example, transportation authorities of urban zones are responsible for managing transportation systems. Nevertheless, during project implementation phase, the respective related authorities did not play a vital role in inspection and supervision works. Therefore, they do not fully comprehend the real status of project quality.

3.2 Problems in project planning phase

Poor quality of project planning: In various projects, detailed master plans of scale 1:2000 and 1:500 do not present clearly the predictability of motivations and opportunities supporting for development of urban zones, and do not consider variations of economic and social factors, especially urbanization and migration growth. Thus, many detailed master plans have to be adjusted, leading to a waste of time and money and affecting investment efficiency. Besides, urban planning is conducted by the Planning Institute (under the Department of Planning – Architecture of a city or province) based on client requirements. This department is also responsible for evaluation and approval of the scheme. Therefore, urban planning process is not transparent and effective.

Inappropriate capacity of consultants: To plan an urban development project requires many knowledgeable experts from different majors for example, finance, environment, technology and construction. Especially, the participation of companies, professionals with experience in infrastructure construction during the project planning and project evaluation phases is vitally important. However, many consultants, who do not have essential capacity and experience, are often involved in the projects because of bidding assignment or becoming the bidding winner by using the virtual profile. Data investigated in project planning are generally not reliable, and mostly replicated from other projects. Planning documents therefore do not meet defined requirements and affect project success seriously.

Limited predictability of socio-economic development growth of urbanized areas: Findings from investigations of economic and social factors (inflation, land and construction costs and urbanization rate) are initially not accurate and useful for project planning. The whole project particularly implementation phase thus will face challenges such as price fluctuations, inflation, cost overrun, policy adjustments, rapid urbanization, interest conflicts and land acquisition difficulties.

In fact, after handing over, many projects have not achieved economic efficiency as planned and deteriorated quickly.

Inadequate basic design of technical infrastructure: Basic design schemes are cursory and sketchy. They do not reflect in actual conditions and provide sufficient evidence in order to deploy next design steps. Many projects have to vary design solutions from basic schemes and calculate total investment capital again. While carrying out basic design, clients often do not have sufficient geological data because they are unable to conduct surveys in land areas without ownership. They therefore replicate other nearby projects' geological findings. Obviously, this phenomenon is the cause of inadequate basic design schemes.

3.3 Problems in surveys, engineering design and construction drawings

Poor quality of geological, topographical and hydrological surveys: In many infrastructure projects, surveys are not supervised and inspected closely, and neglect many important stages. Drilling data provided by surveying consultants largely do not meet basic requirements of design works. Meteorological and hydrological specifications are not studied and applied properly especially for drainage systems and detention reservoir projects.

Lack of inheritance and development of basic design schemes: Basic design scheme plays a key role in producing engineering and construction drawings. However, many projects do not comply with prime principles highlighted in basic designs such as technical specifications, sizes and boundary lines, therefore approval processe must lengthen to adjust and amend these documents.

Inappropriate indicators of technical infrastructure and project scale: During implementation stage, many projects are allowed to vary from the original scheme approved, by the increases in building density, the number of floors, plot ratio and urban population size. Meanwhile, specifications of technical infrastructure still depend on the original basic design, without any adjustment in accordance with these changes. Thus, urban technical infrastructure will become overloaded and cannot satisfy residents' demands.

Limited synchronization and integration of technical infrastructure components when designing: Owing to inadequate design led by clients' ineffective management, there are a plenty of significant adjustments in implementation phase that result in wastes of money and time. In fact, normally engineering design works are responsible by different consultants without discussion or coordination among them. The lack of integration of infrastructure components in engineering designs could cause serious omissions, considerable overlaps and project delays that affect project quality directly during construction phase.

3.4 Problems in construction phase

Improper land acquisition and construction schedule: In various projects, schedules of land acquisition and construction do not present any connection and consistency. Because of the complex nature of land acquisition, many clients cannot be active in deploying and controlling the schedule while construction schedule is prepared improperly. In some actual cases, construction phase must stop unexpectedly due to disagreements of those who are influenced directly by land acquisition; or construction equipment, machines and materials are gathered but there is not enough space at the site to place them because land acquisition does not finish.

Poor quality of construction works: There are serious problems in construction phase of urban infrastructure projects. Firstly, technical infrastructure system is designed in linear form with different altitudes and many intersecting points. Thus, the amount of earth works is considerable and affected directly by weather and hydrology factors. Secondly, despite undertaking construction works, a main contractor handovers their tasks to other subcontractors and get the variance of contract prices. This phenomenon could reduce the actual capital value and cause numerous difficulties in managing project quality. Thirdly, there is a variety of contractor and supervision consultant performing in the site at the same time. Their cooperation and communication seem to be limited; therefore, if there is any problem occurring and their works overlap others then it is difficult and takes time to solve. Another issue is that project management units do not have the appropriate capacity to control and monitor effectively construction activities.

Ineffective supervision: In infrastructure projects, supervision consultants often show the limitations of manpower and qualifications to achieve client satisfaction. Processes of checking, inspecting and approving construction works, equipment, machines and input materials are often undertaken cursorily with poor teamwork.

Limited connection with existing technical infrastructure: One of the most significant challenges in urban zones is that the new infrastructure built does not integrate with existing infrastructure systems nearby or beyond the urban area. In many urbanized zones, the integration of their technical infrastructure systems is paid more attention than others located beyond the boundary.

4. SOLUTIONS TO QUALITY AND INTEGRATION IMPROVEMENT OF TECHNICAL INFRASTRUCTURE SYSTEMS IN NEW URBAN AREAS

Based on the analysis of status and reasons for poor quality and limited integration of urban technical infrastructure systems in Vietnam, it can be seen that the management of authorities and clients, and the capacity of consultants and contractors play important roles. Accordingly, this study identifies two solution groups in order to help improve the effectiveness of urban infrastructure projects.

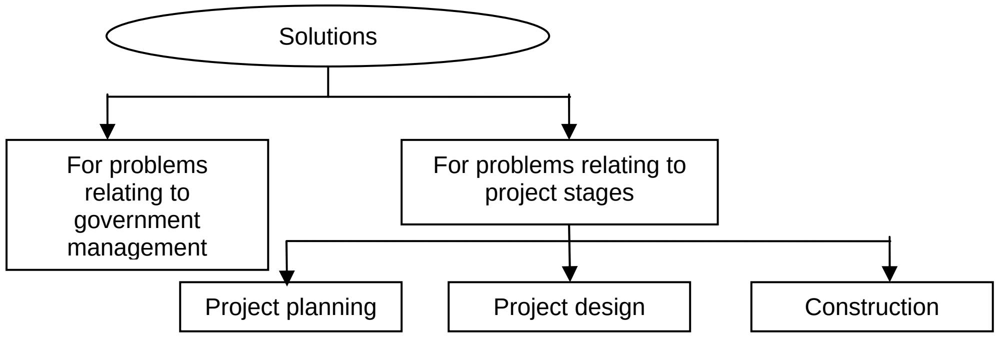

Figure 1: Solution groups for improvement of urban infrastructure systems

4.1 Solutions for problems relating to government management

It is vitally important to enhance the Vietnamese Government's role in urban planning, monitoring and controlling all project activities in order to improve quality and integration of technical infrastructure systems in new urban zones. This below figure presents three proposed solutions to handle with problems coming from ineffective management of the Government.

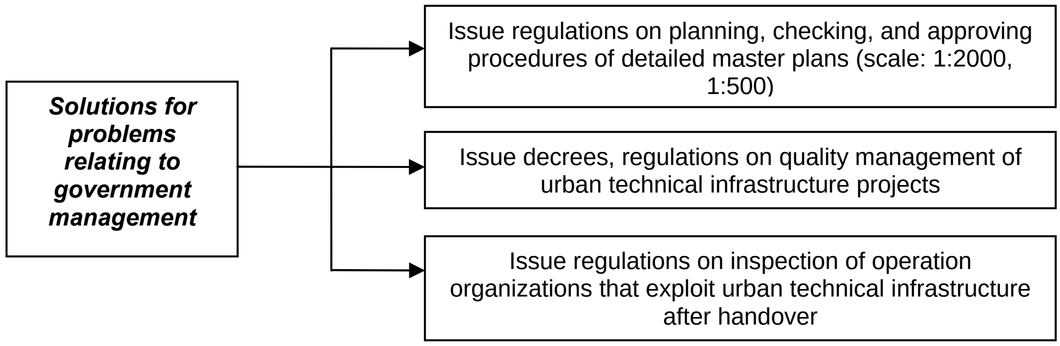

Figure 2: Solutions for problems relating to government management

4.2 Solutions for problems relating to project stages

There are four solutions proposed for project planning phase (shown in figure 3). The first solution concerns about how to improve quality of detailed master plans of scales 1:2000 and 1:500 and to reflect actual conditions of projects. Therefore, it is essential for clients in selecting appropriate consultants and the third party responsible for checking consultants' tasks and give advice prior to submission for approval. The second is to improve the predictability of economic-social development of urban zones. Clients should be allowed to be active in managing financial risks, land acquisition, interest conflicts led by changes in master plans and project schedule due to policy adjustments. Thirdly, the construction of urban technical infrastructure should be considered as an independent project and ensure that it will be deployed shortly in accordance with land acquisition schedule. This solution will enable clients to focus more on project management and quality improvement. Another solution is to improve the accuracy of basic design scheme that is vitally important for ensuring the efficiency of engineering and construction drawings in next project stage.

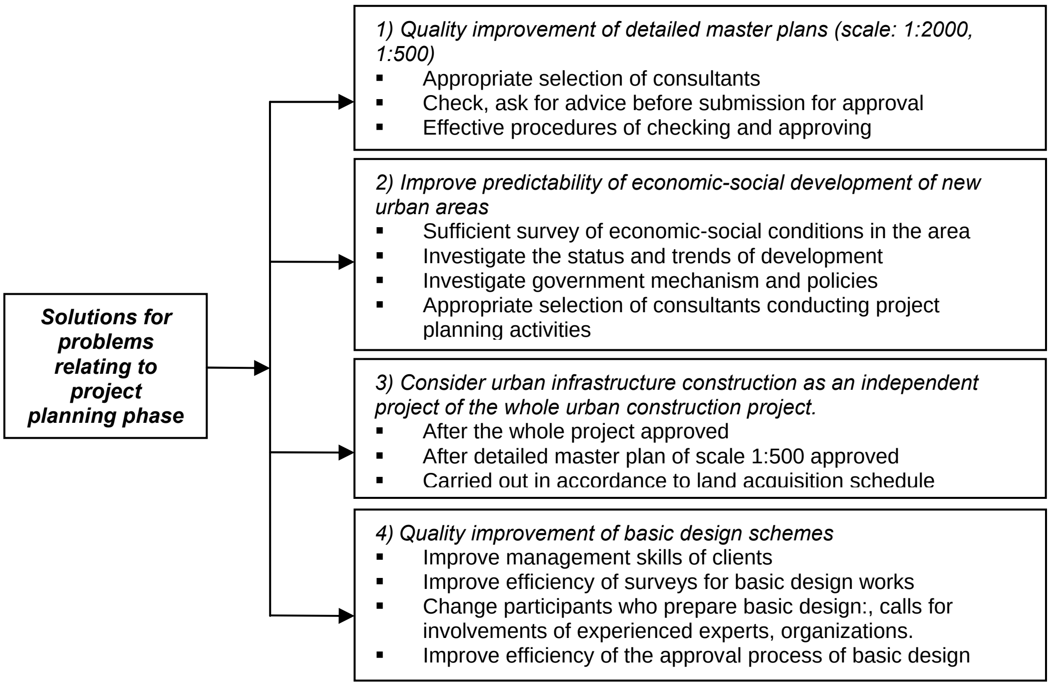

Figure 3: Solutions for problems relating to project planning phase

There are three solutions proposed for the production of engineering and construction drawings. The efficiency of surveys should be paid more attention to collect accurate and reliable data for preparing the drawings. The synchronization and integration of infrastructure components presented in design documents play considerable roles. They should inherit and develop from basic design scheme by selecting a general design-construction contractor and appropriate chief engineers. Additionally, to enhance the quality of approvals, the role of consultants who approve design documents and the compliance of approval procedure are essential.

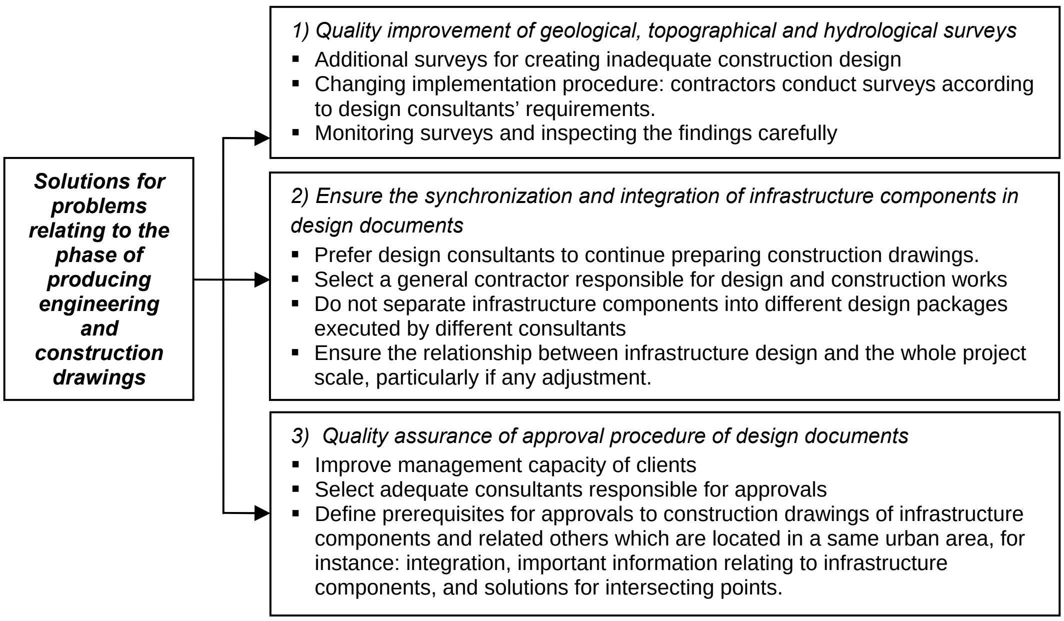

Figure 4: Solutions for problems relating to engineering and construction drawings

With regard to problems occurring in construction phase, there are four solutions identified. Firstly, it is essential for clients (or project management units) to become effective in managing projects by building a qualified manpower structure, applying appropriate management models and methods. Land acquisition completed on schedule is considered as a prerequisite for deploying construction works. To ensure construction quality, clients should prefer to select a general contractor to build all infrastructure components instead divided them into small packages with different subcontractors. Besides, the selection of a general supervision consultant for the whole project instead of employing various supervision organizations is more effective in ensuring the quality of construction works. The involvement in supervision activities of organizations responsible for operation of infrastructure systems should be obligated.

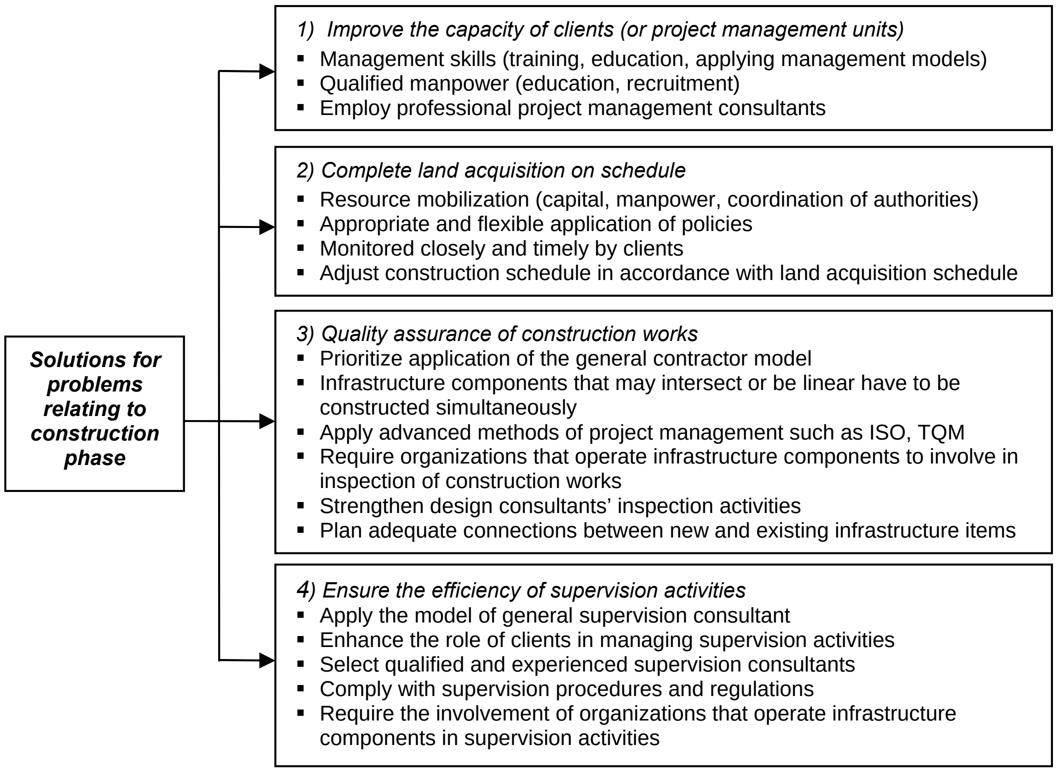

Figure 5: Solutions for problems relating to construction phase

5. CONCLUSIONS AND RECOMMENDATIONS

In Vietnam, urbanization growth has associated with the national strategies of industrialization and modernization. In recent years, urbanization has increased rapidly and begun to reveal a variety of limitations. The number of urbanized zones and the density of urban population have risen dramatically. These issues have led existing technical infrastructure systems become overloaded. Besides, although the government has paid considerable attention, limited integration and synchronization of technical infrastructure components have not been addressed yet. The main reasons identified include ineffective management of authorities, inappropriate basic design schemes and limited predictability of economic-social development of an urban area during project planning; inaccurate data collected from surveys, insufficient engineering and construction drawings, difficulties of land acquisition and poor quality of supervision activities.

Through the status of rapid urbanization and challenges of implementing technical infrastructure projects, it is assumed that Vietnamese urban areas have been facing unsustainable development. In order to strengthen the effectiveness of managing that kind of project, which contributes to the success of urban development strategies, it is important to apply multiple solutions. First solution group comprises the enhancement of Government role in urban planning, introduction of adequate legal documents and regulations on urban construction issues. Another group is to handle with issues during project planning, preparation of design documents and construction phase.

Economic – social development of the country in general and urbanized zones in particular, have a close relationship with sustainable technical infrastructure systems. Therefore, successful technical infrastructure project should be one of the most important national concerns that need to be focus. Further researches should be conducted to evaluate the effectiveness and ability of applying these proposed solutions in reality under Vietnamese conditions.

REFERENCES

Asian Development Bank, 2011. *Asia 2050: realizing the Asian Century.*

Choguill, C., 1996. Ten steps to sustainable infrastructure. *Habitat International*, 20(3), 389-404.

Hardwicke, L., 2008. Transition to smart, sustainable infrastructure. In P. W.

Ho Chi Minh City's Committee, 2012. *Master planning project of economic-social development of HCMC in 2020, vision to 2025.*

Hoang, C. L., 2013. Difficulties in urbanization process in Vietnam. *Journal of economy and forecast* 11.

Le, H. K., 2012. Urbanization and sustainability. *Journal of Vietnamese Architecture* 3, Hanoi.

Nagesh, K. and Prabir, D., 2008. *East Asian Infrastructure development in a comparative global perspective: an analysis of RIS infrastructure index.* ERIA research project report 2007-2, IDE-JETRO, Chiba, 7-28.

Newton (Editor), *Transitions: Pathway towards sustainable urban development in Australia*, CSIRO Publishing, Victoria, 599-608.

Nguyen, X. T., 2010. *Challenges of Infrastructure in Vietnam*. Phu Sy, Hanoi.

Seitz, J. L., 2008. *Global issues: An introduction*, 3rd Edition. Blackwell Publishing, Malden, Oxford, Victoria.

The United Nations, 2012. *World urbanization prospects: the 2011 revision.*

World Bank, 2006. *Vietnam's Infrastructure Challenges.*

Vietnamese Parliament, 2009. *Urban planning law.*

Vietnamese Construction Ministry, 2012. *National technical regulation on rules of classifications and grading of civil and industrial buildings and urban infrastructures.*

Vietnamese Government, 2011. *Decision No 1259/QĐ-TTG on approvals of Hanoi planning in 2030 and vision to 2050*.

Study on applicability of remote building damage assessment system for large-scale earthquake disasters - Focused on the photo upload system -

Makoto FUJIU[1], Miho OHARA[2] and Kimiro MEGURO[3]
[1] Project Researcher, Institute of Industrial Science,
The University of Tokyo, Japan
fujiu@iis.u-tokyo.ac.jp
[2] Associate Professor, International Center for Urban Safety Engineering (ICUS),
Institute of Industrial Science / Interfaculty Initiative in Information Studies,
The University of Tokyo, Japan
[3] Professor, International Center for Urban Safety Engineering (ICUS),
Institute of Industrial Science / Interfaculty Initiative in Information Studies,
The University of Tokyo, Japan

ABSTRACT

Building damage assessment is necessary for governments to issue the Victim Certificates for residents who suffered from housing damages. The process of assessment needs quickness, efficiency, accuracy, objectivity and fairness because the results of the assessment are used as the criteria for providing public monetary supports for rebuilding their livelihood. In order to solve the problems with building damage assessment in the past disasters, authors have proposed a new assessment system using photos of damaged houses taken by residents or volunteer fire corps in damaged area.

The proposed remote building damage assessment system consists of four sub-systems: photo uploading system used inside damaged area, remote assessment system for supporting experts such as registered inspectors outside damaged area, e-learning system for users and Web-GIS server located outside damaged area under cloud condition. Although the authors have already developed a prototype system, the evaluation of its effectiveness was not fully done. Then, in this research, operation trial was conducted in order to verify applicability of the developed photo upload system as a part of remote building damage assessment system. As a result, it became clear that the developed system have enough resolution to determine damage level of the houses.

Keywords: *earthquake disaster, building damage assessment, smartphone, IT*

1. INTRODUCTION

In Japan, several big earthquakes are expected to occur in the near future. A lot of structural damages due to these earthquakes will cause enormous needs for building damage assessment. Building damage assessment is necessary for governments to issue the Victim Certificates for residents who suffered housing damages. However, current number of human resources who are trained with the procedure of building damage assessment is not enough. The result of building damage assessment is used for issuing the victim certificate. Then, the building damage assessment during large-scale earthquake disaster requires some performances such as quickness, efficiency, accuracy, objectivity and fairness. The guidelines of general procedure for inspecting building damage and evaluating loss due to disasters were published by the Cabinet Office in 2001 and 2009. Tanaka (2008) pointed out various problems of building damage assessment such as inaccurate inspection, difficulty in quick inspection and lack of human resources with sufficient skill of assessment in past disasters.

Considering the future risk of big earthquakes, it is necessary to develop a new system which can correspond to next large-scale earthquake disaster. So far, Fujiu (2012) has proposed new remote system for building damage assessment using IT system and developed its prototype system. These systems have some features that can solve some problems pointed out at the past building damage assessments and execute building damage assessment with quickness, efficiency, accuracy, objectivity and fairness after a large-scale earthquake disaster. The proposed system consists of four sub-systems as shown in figure 1: photo uploading system used in damaged area, assessment system for supporting experts such as registered inspectors outside damaged area, e-learning system for users and Web-GIS cloud server located outside damaged area. Although the authors have already developed a prototype system, the evaluation of its effectiveness was not fully done. Then, in this research, authors conduct an operation trial to verify the usability and resolution of photos of the developed photo uploading system. This trial aims to verify applicability of photo upload system as a part of remote building damage assessment system.

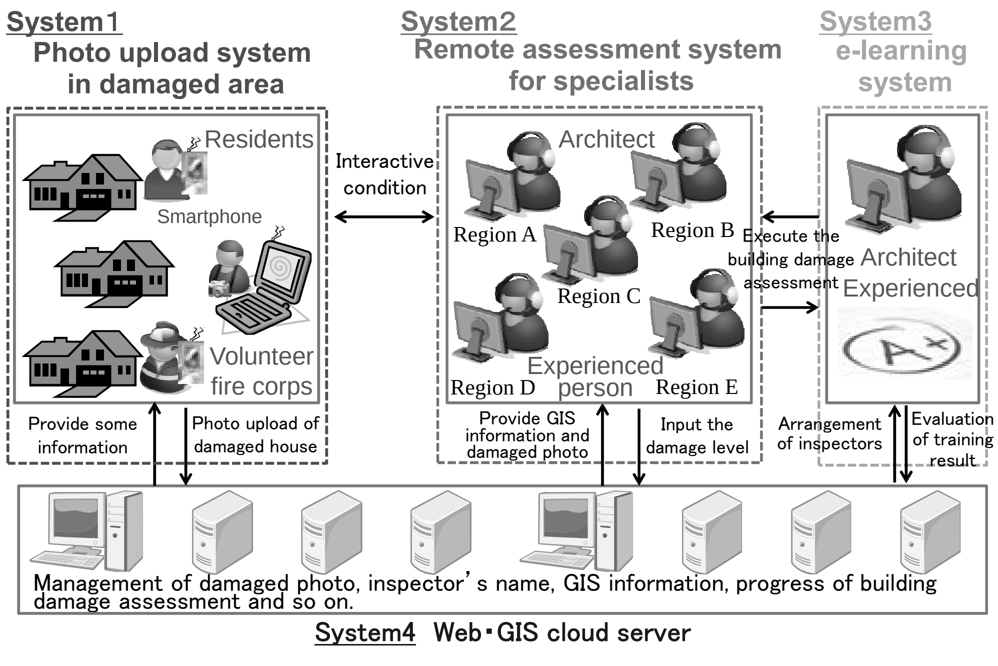

Figure 1: Concept of remote building damage assessment system

2. OUTLINE OF DEVELOPED PHOTO UPLOAD SYSTEM IN REMOTE BUILDING DAMAGE ASSESSMENT SYSTEM

2.1 Flow of building damage assessment

After the request from residents of damaged houses, building damage assessment is executed based on building damage assessment guideline, issued by Cabinet office in Japan. Figure 2 shows the flow of building damage assessment based on the guideline. The building damage assessment has three steps; the first one is the overview judgment which is the judgment of the building damage from the overview, the second one is the inclination judgment which is the measurement of the building inclination, and the third one is the building element judgment which is the measurement of the damage level and the damage area of roof, wall and foundation. In each step, the damage ratio is calculated based on the building damage level and the building damage area. When the damage ratio reaches the standard value in each step, the damage level is decided as major damage, major-moderate damage, moderate damage or minor damage.

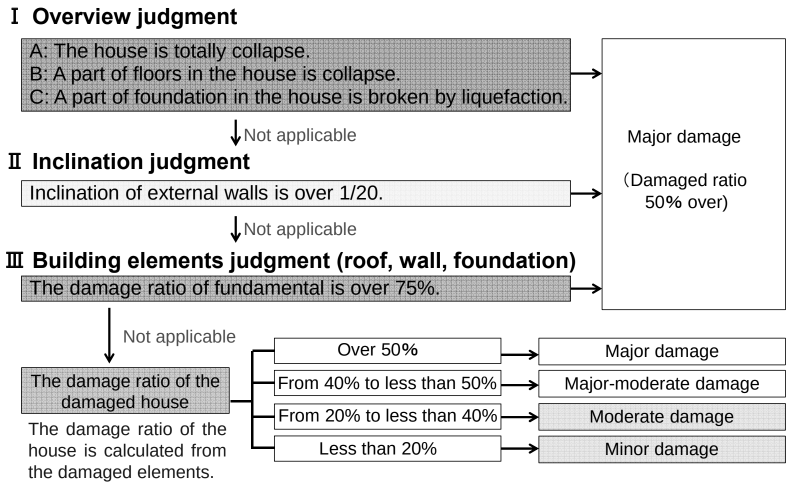

Figure 2: Flow of building damage assessment (Primary inspection)

Judgments of damage level and calculation method of damage area are explained in this paragraph as an example of damaged wall. Each damage level has a basic damage ratio. Figure 3 shows the relationship between damage level and basic damage ratio. The damaged wall has small and short crack as shown in Figure 3a, and the corresponding basic damage level is evaluated as 10%. The damaged wall has a long crack and small peeling off of the wall facade as shown in Figure 3b, and the corresponding basic damage level is evaluated as 25%. The damaged wall has a long crack and medium peeling off of the facade as shown in Figure 3c, and the corresponding basic damage level is evaluated as 50%. The damaged wall has peeling off of greater part of the exterior wall facade as shown in Figure 3d, and basic damage level is evaluated as 75%. The damaged wall has peeling off of almost the whole wall facade as shown in figure 3e, and the corresponding basic damage level is evaluated as 100%. The damaged area is calculated based on the decomposition method. The method is decomposition of the damaged wall to calculate the damaged area as shown in Figure 3f. The red dotted line shows the decomposition line of the damaged wall. If there is some damage in one part, the part is defined as a damaged part.

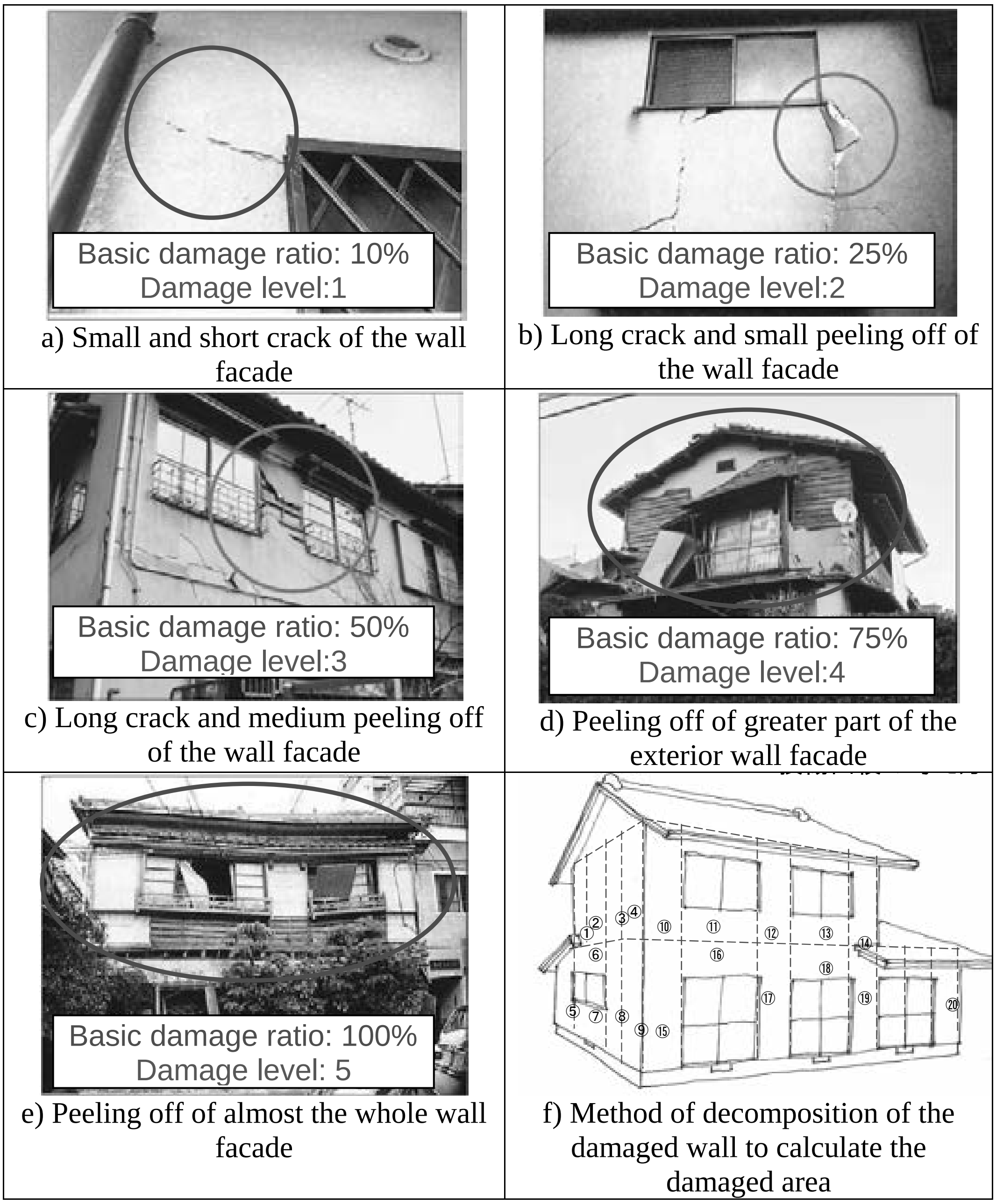

a) Small and short crack of the wall facade

b) Long crack and small peeling off of the wall facade

c) Long crack and medium peeling off of the wall facade

d) Peeling off of greater part of the exterior wall facade

e) Peeling off of almost the whole wall facade

f) Method of decomposition of the damaged wall to calculate the damaged area

Figure 3 Typical damage levels of walls

The damage ratio calculation has four steps: evaluation of basic damage ratio, calculation of damage ratio, calculation of sub total damage ratio and total damage ratio. The basic damage ratio is evaluated based on the damage level. The damage ratio is the value which is multiplied by basic damage level and damage area for each element, directions and damaged level as in equation (1). The sub total damaged ratio is calculated by summation of damage ratio for each element and directions as in equation (2). Finally, the total damage ratio is the value multiplied by sub total damage level and coefficient for each element as equation (3).

$$DR_{ij} = \sum_{i=1}^{n}\sum_{j=1}^{p}\sum_{k=1}^{q}\left(BDR_{ijk} \times DA_{ijk}\right) \tag{1}$$

$$STDR_{i} = \sum_{i=1}^{n}\sum_{j=1}^{p}\left(DR_{ij}\right) \tag{2}$$

$$TDR = \sum_{i=1}^{n}(STDR_{i} \times coefficient_{i}) \tag{3}$$

i:Element, j:Direction, k:Damage level
DR_{ij}: Damage ratio where i,j , BDR_{ijk} : Basic damage ratio where i,j,k
DA_{ijk} : Damaged area where i,j,k , $STDR_{i}$:Sub total damage ratio where i
TDR :Total damage ratio, $coefficient_{i}$: Element coefficient

2.2 DEVELOPMENT OF PHOTO UPLOAD SYSTEM

Here, the prototype of “Photo upload system in the damaged area” was developed. Photos of a damaged house are taken by residents or volunteer fire corps in the damaged area and uploaded to the server. This system was developed for mobile phones based on Android operating system which is installed in almost all the smart phones except iPhone. The photo upload application should be installed on each Android smart phone by the users who are residents or volunteer fire corps in the damaged area.

Flow of the photo upload system is shown in figure 4. Firstly, residents or volunteer fire corps as users input the basic information such as GPS information, address and owner name. Secondly, they upload some photos such as overview of the damaged house, inclination of the damaged house and the damaged point of roofs, walls and foundations. Finally, they confirm the input data and some photos.

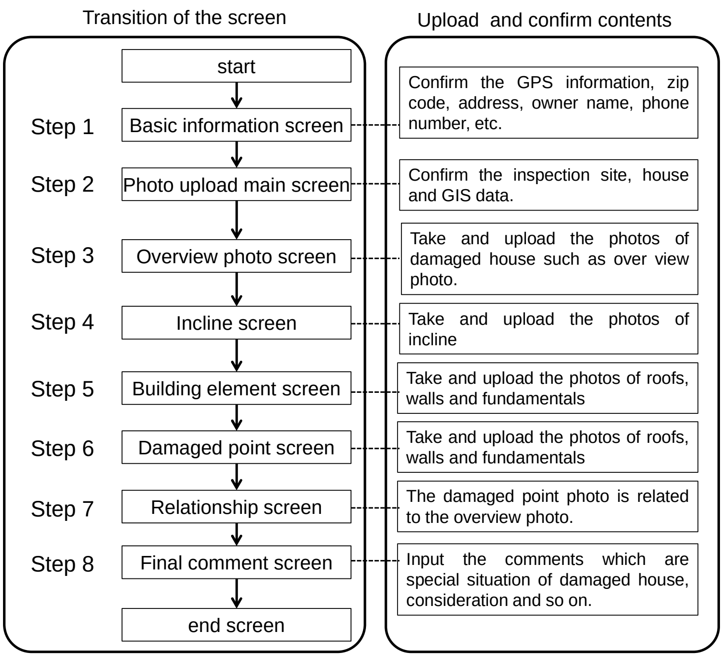

Figure 4 Flow of photo upload system

Method of completing photo upload in the damaged area using upload application is as follows: The users take some full view photos of a damaged house (entrance

side, opposite side of the entrance, left side of the entrance and right side of the entrance) and close-up view photos of the damaged points.
Figures 4 and 5 are the prototype system for primary inspection. After taking photos of a damaged house, residents or volunteer fire corps select some photos for uploading to each factor page. They should take pictures of the damaged house concerning three factors: overview, building inclination and building elements (roof, exterior walls and foundation). Further, they should relate the close-up views of the damaged points to the full views using touch screen functions. The red circle in prototype system shows damaged point which is related to overview photo. After taking some pictures, users need to upload them to an exclusive server in cloud condition using the upload application. Using this application makes it easier to select and upload photos which are taken by the users in the damaged area as smart phone has touch screen functions such as tap, drag, flick and pinch out/in operations.

Figure 5 Photo upload system
in the damaged area (wall upload)

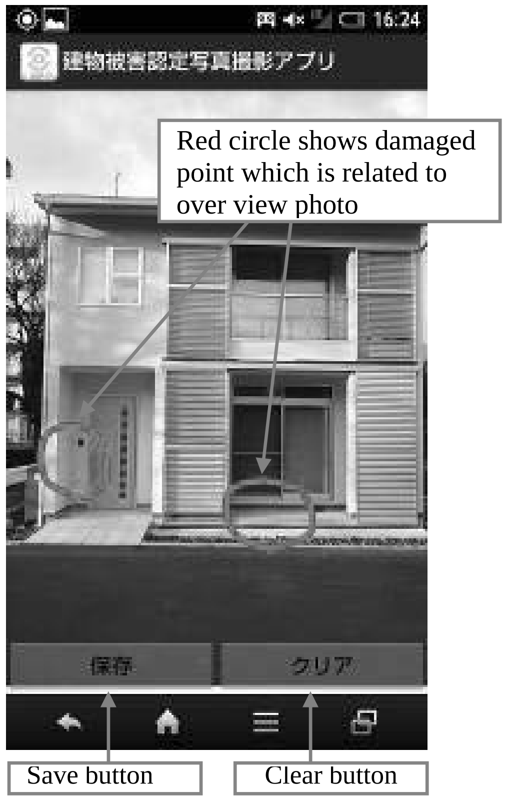

Figure 6 Photo upload system
in the damaged area (relationship)

Table 1 shows number of photos to be taken for remote assessment. The users take some pictures of damaged building such as overview photos, incline photos and close-up photos of damaged points. The overview and incline need 4 photos respectively. The close-up photos of damaged points depend on the number of damaged points of the building. Total number of required photos amounts to the sum of 4 overview photos, 4 incline photos and close-up photos of damaged points.

Table 1 Number of photos for remote assessment

Part		Points of taking picture	Number of photos
Overview photo		Four directions	Total 4 photos
Incline photo		Four directions	Total 4 photos
Element	Roof	Close-up photo *Number of damaged point	N_{roof}
	Wall	Close-up photo *Number of damaged point	N_{wall}
	Fundamental	Close-up photo *Number of damaged point	$N_{fund.}$
Total number of photos			$N_{roof} + N_{wall} + N_{fund.} + 8$

3. TRIALS OF PHOTO UPLOAD SYSTEM

3.1 EXAMPLE OF PHOTOS UPLOADED BY PHOTO UPLOAD SYSTEM

The authors tried to use photo upload system in Sendai city, Miyagi prefecture suffered from the 2011 off the Pacific coast of Tohoku Earthquake, on March 26, 2013. Some damaged houses are still remaining in Sendai city without repair, and 10 of the damaged buildings were selected as the sample. Figures 7 and 8 are the example of overview photos of damaged houses that are classified to be major damage, major moderate damage, moderate damage and minor damage, respectively. These photos implies that identification of major or moderate damage based on overview photos of a house is reratively easier compared with that of small damage. This suggests that additional close-up photos of damaged parts were especially important in case of small damage in order to achive the damage assessment accurately.

a) Major damage

b) Major moderate damage

Figure 7 Overview photos of damaged houses (1)

	
c) Moderate damage	d) Minor damage

Figure 8 Overview photos of damaged houses (2)

3.2 CONFIRMATION OF DAMAGE FROM PHOTOS

Figure 9 is four overview photos of a house classified as minor damage. These photos were taken from the four different directions. This house suffered from some damages due to the strong ground motions on b) the right side of the entrance and d) the left side of the entrance. However, these damages cannot be confirmed from the overview photo due to the limitation of photo resolution. Damages such as small cracks or peel off from the wall were difficult to be identified only by overview photos. In addition, these photos show that things surrounding a house such as plants, stone wall, etc. can be obstacles of the photos for assessment. Climate conditions such as too much sunlight or shadow might also reduce the quality of the photos for assessment. In these cases, close-up photos of the damaged points are especially important for accurate assessment. In our developed photo upload system, a function for users to add some comments with a photo was attached in case the photos don't have enough quality due to these reasons.

	
a) The entrance side	b) The right side of the entrance
	
c) The opposite side of the entrance side	d) The left side of the entrance

Figure 9 Four overview photos of a minor damage house

Figure 10 is the example of photos of both overview and close-up. By using additional close-up photos of damaged points, it become possible to identify the small damages of damage level 1 or level 2 such as small cracks and peel off from the wall. These photos are the example taken by a smart phone camera with the resolution of 1MB pixels. It was verified that both the overview photos and additional close-up photos are essential to enhance the accuracy of the assessment especially in case of small damage houses.

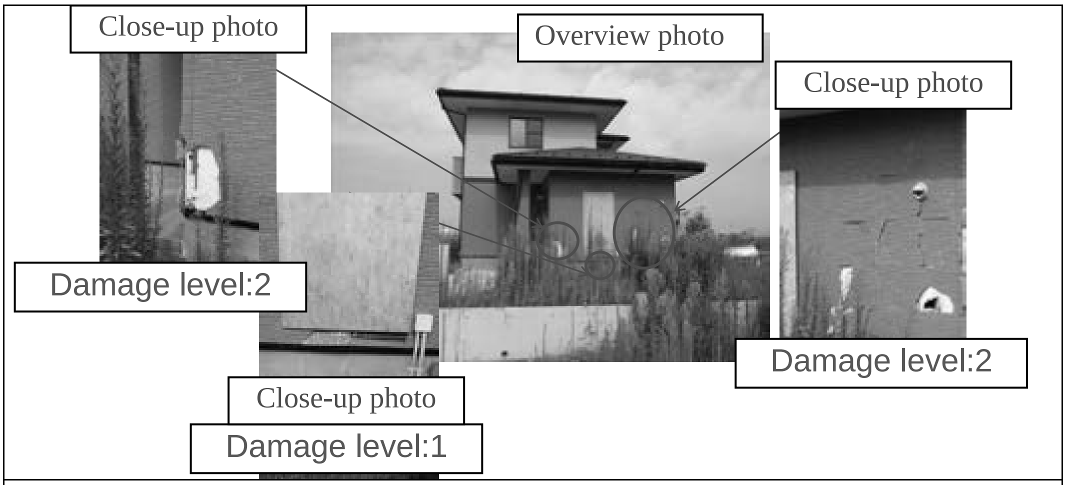

a) The right side of the entrance

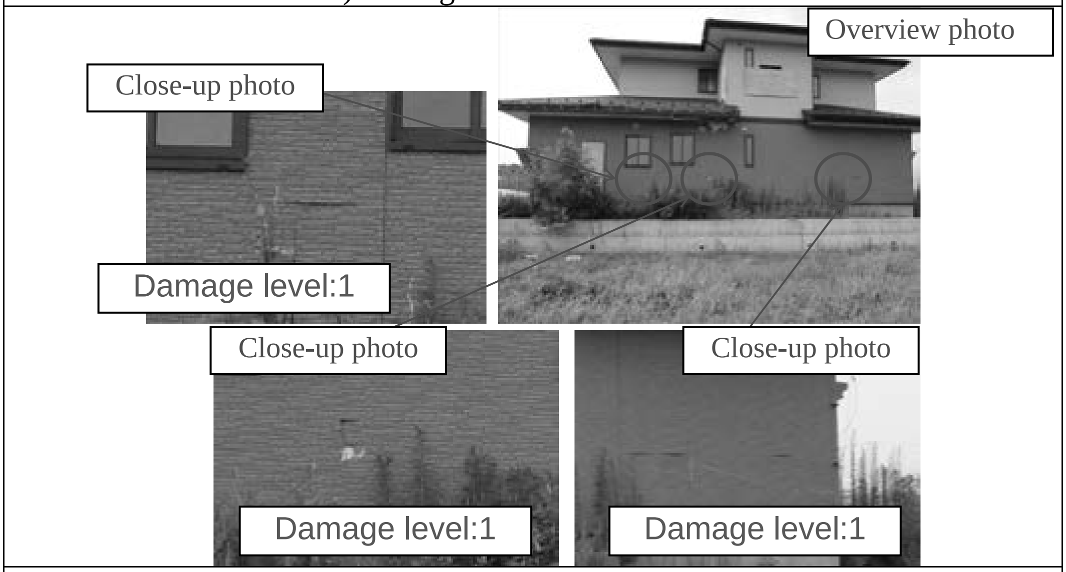

b) The opposite side of the entrance side

Figure 10 Photos of the some damages related to overview photos

According to the authors' verifications in previous research, the small damage such as cracks and peel off from the wall can be confirmed from photo which has over 1MB pixels. This photo upload system can change the resolution to 1MB pixels automatically. If the file size of a photo is very large, the photo taken by photo upload system cannot upload to cloud server due to the 3G/LTE line capacity. That point was also confirmed through this trial of photo upload system in the damaged area.

4. CONCLUSIONS

In this research, developed photo upload system as a part of remote building damage assessment system was used for trial in order to verify its applicability to the actual assessment. It became clear that big damage such as major damage and major moderate damage can be confirmed using overview photos. On the other hand, small damages such as minor damage might be difficult to be confirmed using only overview photos. In these cases, close-up photos of the damage points are necessary to identify the small damages accurately. From the trial, it was verified that damaged points of small damage with damage level 1 or 2 such as cracks and peel off from the wall can be confirmed from photo which has over 1MB pixels. However, in the actual damaged area, there might be many obstacles surroundings a damaged house such as plants, stone wall, etc, which reduce the quality of photos for assessment. Climate conditions such as too much sunlight or shadow can be another obstacles. Then, small damage in moderate damage and minor damage cannot be confirmed using overview photos. In our developed photo upload system, a function for users to add some comments with a photo was attached. In these cases, comments at taking photos can help the understandings of the photos of damaged houses. The education and training of these techniques to the users of photo upload system is essential.

As future study, we plan to conduct more practical operation tests with some local government staffs to evaluate the effectiveness of both photo upload system and remote assessment system using photos taken in the damaged area.

REFERENCES

Tanaka, S., 2008, *A Study on the Building Damage Assessment Processes for the 2007 Niigata Chuetsu Oki Earthquake Disaster : Kashiwazaki Case Study* , Proceedings of social Safety Science No.22, pp.35-38

Fujiu, M., Ohara, M., Meguro, K., 2012, *Development of remote building damage assessment system during large-scale earthquake disaster*, Proceedings of the 15th World Conference on Earthquake Engineering, CD-ROM, Lisbon, Portugal

Safe and sustainable energy use in tall residential buildings in Hanoi: Practices and orientation

Thuy An PHAM[1] and The Quan NGUYEN[2]
[1] Undergraduate student in class of 54KT6,
National University of Civil Engineering, Vietnam
thuyanpham91@gmail.com
[2] PhD, Vice Dean, Faculty of Construction Economics and Management,
National University of Civil Engineering, Vietnam

ABSTRACT

Hanoi is the city that has a highest rate of tall residential buildings at 16.64% among the whole country. Currently, the press and media keep reporting on unsafe cases in those tall residential buildings due to the use of different energy sources. This research has been done in order to investigate the current use of energy types provided in those tall buildings, the residents' assessment of safety level of each source, the practice of safety equipment use, their perception on design standards related to safety in energy provision system and the orientation of switching to new and more sustainable energy sources. The implications from the research results can be useful for real estate developers in their development projects as well as for Governmental authorities in issuing relevant policies, plans, standards, guidelines for sustainable construction in general and the use of safe and sustainable sources of energy in tall buildings in particular.

Keywords: *energy safety, tall residential buildings, apartment-buying decision, safety protection facilities, sustainable energy*

1. INTRODUCTION

Recently, residential buildings have proved to be an effective remedy for the complicated problem of providing accommodations for citizens in developing cities. Residential buildings have quickly predominated the real estate markets in Hanoi in particular and Vietnam in general. This type of accommodation helps authorities to take advantage of utilizing Hanoi's urban area which have the highest population density in Vietnam. According to the statistical figures issued by the Construction Ministry, the nationwide proportion of residential buildings in urban areas only accounts for 3.72 % of total living area and Hanoi have the highest residential-building percentage (16.64 %), followed by Ho Chi Minh city, Hai Phong and Da Nang (6.13%, 5.8%, 2.1 % respectively) (Linh Van 2011). Until 2012, there were over 5000 multi-storey buildings including 927 over-nine-storey buildings in Vietnam. All most all of the over-nine-storey buildings at the time were located in major cities, such as Ho Chi Minh City (440 buildings), Hanoi (368 buildings), Hai Phong (36 buildings), Quang Ninh (18 buildings), Thanh Hoa (13 buildings) (Lan

Huong 2012). As a result, more attention has been paid to the issue of safety related to energy using for citizens in tall residential buildings due to a series of factors such as structure quality, security and so forth. However, the number of conflagration in residential buildings in Hanoi is rising to an alarming rate. According to the Fire Protection Office, in the first 9 months in 2012 there were 15 fires in residential buildings nationwide (12 fires in Hanoi and the 3 others in Ho Chi Minh City) with 1 case due to electric weld, 9 cases due to electricity problem and 5 cases under investigation. Significant causes for fire are mainly associated with energy-supply issues created by unconformity in construction processes, occupants' lack of perception and sense of safety (Lan Huong 2012).

This paper looks into the practice of the utilize of safe and sustainable energy in tall residential buildings in Hanoi in order to investigate the related issues such as safety behavior and residents' choice for sustainable energy sources, which may be of interest for real estate developers as well as urban management authorities in Hanoi.

2. RESEARCH METHODOLODY

The research is based on a survey using face-to-face interviews with 175 respondents, who engage in the decision-making of buying their apartments. The survey respondents are selected across a spectrum of major districts of Hanoi including Hoang Mai, Hai Ba Trung, Cau Giay, Ha Dong, and Dong Da districts with convenient sampling method. They are at different age groups, education levels and levels of household income. Then, data collected was coded and analyzed with SPSS software. Table 1 below presents the survey sample in terms of age group, education and household income.

Table 1. Classifications of the survey participants

No	Classification criteria	Number	%
1	Age		
1.1	20-30 years	54	30.86
1.2	30-50 years	79	45.14
1.3	50-70 years	21	12.00
1.4	>70 years	3	1.71
1.5	Not answer	18	10.29
2	Education level		
2.1	High school	10	5.72
2.2	University/ college degree	120	68.57
2.3	Postgraduate degree	38	21.71
2.4	Others	7	4.00
3	Monthly household income		
3.1	5-10 mil	46	26.29
3.2	10-20 mil	75	42.86

No	Classification criteria	Number	%
3.3	20-30 mil	28	16.00
3.4	>40 mil	9	5.14
3.5	Not answer	17	9.71
	Total	175	100

As can be seen from the table, a large majority of survey respondents are 30-50 years old, accounting for 45.14%, and the proportion of people aged 20-30 is 30.86% whilst the percentage of the over-fifty-year-old respondents is 13.71% …. The number of graduates with at least one university qualification constitutes approximately 90.28 %. The figures reveals that tall building residents who are decision-makers in buying houses are mostly young and middle-aged with high education level. Nevertheless, income of a typical household is just above the average level of the country; nearly half of interviewed households earn 10-20 million VND per month. The average number of family members in a household is around 3.5 people, which means that each person is provided about 19.529 m2 for living.

3. DATA ANALYSIS AND DISCUSSIONS

3.1. The sources of energy used in tall buildings and their safety levels

It can be seen from the survey figures that every apartment is using energy from national electricity network. In detail, nearly two-thirds (61.7%) of the households use gas cylinders whereas the proportion of central gas system and solar energy are smaller, at 17.5% and 1.9% respectively. Meanwhile, 97.8 % of total households admitted that electricity is the major energy taking the highest power expenditure. Grid electricity predominates a powerful role in the total consumption, making a huge the demand for electricity in the city. It is predicted that the energy demand within the period of 2001 to 2020, with the average GDP of 7.1-7.2%-GDP growth, is 201 billion kWh and the demand in 2030 is estimated to reach 327 billion kWh. Whereas, maximum domestic energy supply is estimated to be at 165 billion kWh in 2020 and 208 billion kWh in 2030, leading to the shortage of 119 billion kWh (Minh Hanh 2006).

In order to measure the safety level of each source of energy, the survey respondents have been asked to score each source from 1 (the least safe) to 5 (the most safe). Sources of energy that have been included in the survey are grid electricity, gas vessels (cylinders), centre gas system, solar energy and nuclear energy. Table 2 presents the results generated from the respondents assessments using SPSS.

Table 2. Respondents' assessments on safety level of each source of energy

Safe assessment for type of energy						
		Grid electricity	Gas cylinders	Center gas system	Solar	Nuclear
N	Valid	160	160	156	155	154
	Missing	15	15	19	20	21
Mean		3,72	2,49	2,95	4,17	2,10

Solar energy has the highest score (4.168) which means it is considered as the safest source of energy. Electricity ranks second with 3.719, preceding central gas system and gas cylinders (2.949 and 2.488 respectively) and nuclear energy has the lowest credibility (2.097). It seems that the survey respondents less trust on nuclear energy since the media keeps reporting about accidents with nuclear power plants on over the world, such as Fukushima accident. According to the survey, evidently, consumers favor solar energy most. Nevertheless, this type of energy is not popular in Hanoi in particular and in Vietnam in general.

3.2. The use of safety equipment and firefighting equipment in the surveyed apartments

The survey results reveal that approximate 60.3% of the respondents' apartments being bought in the post-construction stage. A certain number of apartments have been bought during the construction of the buildings (17.3%) or resold by a previous owner (not the developer – 16.7%) (Table 3). Safety equipment in households, therefore, are inherited from the previous owners or provided by the developers as in design documents.

Table 3. Classification of respondents' apartment by purchasing time

No	Time of purchasing	Number of apartment	Percentage (%)
1	Before construction stage	9	5.14
2	In the construction stage	27	15.43
3	Post-construction stage	94	53.71
4	Buying from previous owner	26	14.86
5	Not answer	19	10.86
	Total	175	100%

The survey data point out that over a quarter (28.6 %) of the total participated households do not use any safety devices (like automatic fuse, gas-leaking alarm, smoke alarm), and the rest have installed at least one. Among the one that self-equipped safety devices, 27.5 % of households installed only one device, roughly 38.5 % of them have fixed over two fixtures and there are only 5.5 % having installed more than 3 safety devices.

In comparison to the use of safety devices in the participants' apartments, firefighting equipment (fire extinguishers) is more concerned by the majority of households, with up to 64.5% of apartments are fully equipped. Among the households' flats in the survey that have not been equipped with fire extinguisher devices, only 6.5% of the respondents don not have any intention of installing firefighting equipment while 23.7% of them do. As can be seen from the results above, there is an increasing awareness of safety among residents in terms of using energy sources in their apartments.

In order to analyze the effect of safety equipment in the buying decision of respondents for apartments, respondents were asked if they agreed to buy an apartment without their desired energy sources, yet the apartments were equipped with safety equipment. Up to 52.2 % respondents accept the apartment; 36.9% of them show a hesitation and only 10.8% of them refuse to buy since they doubt the equipment quality. Based on the above results, it can be concluded that safety devices in tall residential buildings catch customers' attention. Nonetheless, safety equipment provided in Hanoi market must be examined thoroughly, since they are not completely reliable (Bao Linh 2011).

3.3. Tall residential building citizens' knowledge about standards for design and construction of energy supply and firefighting system in residential buildings

When considering buying an apartment, up to 57 % of residents who participated in the survey pay no attention to the energy sources provided with the apartment; only 20.4% of them examine this issue. The survey results show that the energy sources provided with apartments do not influence the buying decision of a majority of respondents. There are 25 % of them do not pay attention to this factor when they can balance different factors such as price, convenience, area of the apartment. 42,4% of the participated citizens think that this factor only accounts for nearly 20% of their decision of choosing to buy a flat. Consequently, the survey part on the awareness of construction and design standards of energy provision system have brought up similar information. There are 57.2 % of citizens living in the surveyed apartments are not aware of these standards, 30.2% of them only know about their existence and there is only 11.9% of them knowing the contents while just 0,6% of them can understand the standards thoroughly. With an alarming of awareness of the standards like that, it is necessary to raise more attention of the tall residential buildings citizens on this issue.

In practice, a wide range of legal documents relevant to the issue have been published. The most important regulations include Decree 169/2003/NĐ-CP about electricity safety which indicates standards in generation, transferring and using electricity; Decision 51/2008/QD-BCT decision issued national technical regulations on safety in the storage, transport, use and disposal of industrial explosives; Vietnam Standard TCVN 6160 - 1996 - Fire Fighting building - Design requirements: This standard specifies the basic requirements for fire protection (PCCC) when designing new construction, renovation and expansion of the houses, tall residential buildings; Vietnam Regulation QCVN 06: 2010/BXD by the Institute for Construction Science and Technology compiled, Department of

Science, Technology and Environment browsers, the Ministry of Construction issued Circular No. 07/28 2010/TT-BXD in 7/2010 - National Technical Regulation on fire safety for houses and works; system of national standards for electrical safety as TCVN 7441 - LPG supply system in consumption - Requires design, installation and operation..... These have become guidelines for the designers and developers of tall buildings to do their development job, but have not been promoted enough to become popular to the potential residents.

3.4. Tall building residents' perspective on future sustainable energy sources

When being asked about their choice on future sustainable energy sources, participants came up with a wide range of ideas. Figure 1 shows the research results on the choice of the survey respondents in terms of future sustainable energy sources.

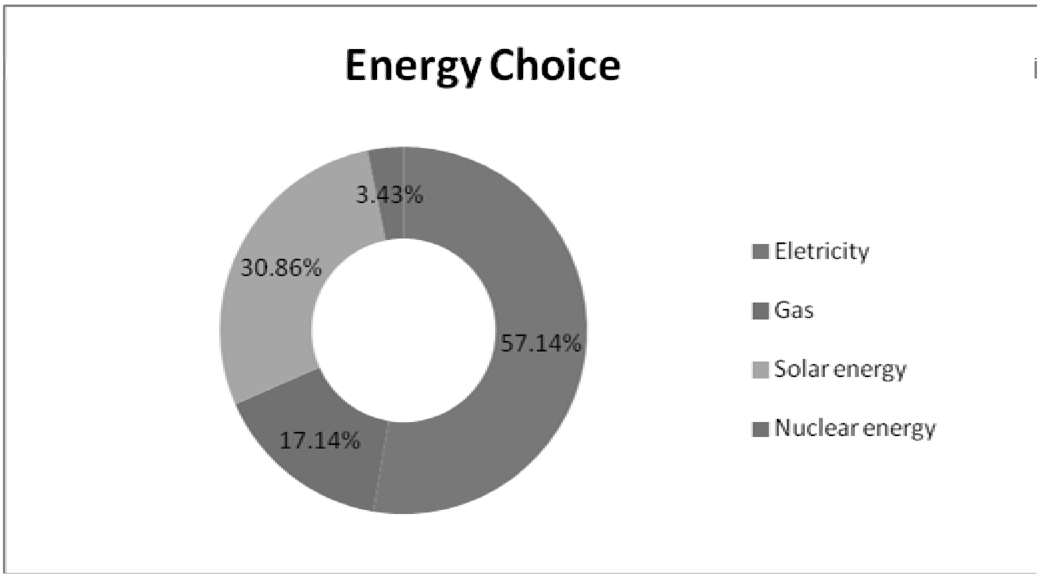

Figure 1. Choice for future sustainable energy sources

The data shows that electricity is still the most selected source of energy, even in the future. This fact raises the need of more investment into this type of power source.

Investigating residents' concern over sustainable energy, it is observed that only 2.5% of the survey respondents find it unnecessary but nearly a half (44.6%) of them will decide to switch on to the new source but need to make price consideration. The rest (52.9%) completely support new energy sources which are safe and environment-friendly. This fact indicate a good sign for investor in application of sustainable and renewable energy. On the other hand, installation and operation cost is an issue of broad concern.

The correlation between age and the concern for new energy source was tested with SPSS with testing results presented in Table 4. Age and the concern are supposedly not mutually related. After analyzing the collected data, the results are represented in the following table:

Table 4. Chi-Square Tests for the correlation between age
and concern for new energy source

Chi-Square Tests			
	Value	df	Asymp. Sig. (2-sided)
Pearson Chi-Square	5.899a	2	.052
Likelihood Ratio	6.328	2	.042
Linear-by-Linear Association	2.431	1	.119
N of Valid Cases	166		
a. 0 cells (,0%) have expected count less than 5. The minimum expected count is 10,41.			

Based on the calculation results, Sig = 5.2% <Pearson Chi-square = 5.899% to reject the initial assumption. It is then can be concluded that age and concern for new energy source have an interactive relationship with each other. To proceed to learn more about this relationship, an additional test was conducted. The symmetric measures are presented in Table 5.

Table 5. Symmetric Measures Results

Symmetric Measures					
		Value	Asymp. Std. Errora	Approx. Tb	Approx. Sig.
Ordinal by Ordinal	Gamma	-.190	.131	-1.424	.154
N of Valid Cases		166			
a. Not assuming the null hypothesis.					
b. Using the asymptotic standard error assuming the null hypothesis.					

It is noticed that the two quantities have an inverse correlation, which means residents having higher age have less desire to change the current energy sources than young people. However, due to limited number of samples, this relationship cannot be validated accurately.

4. CONCLUSIONS

The results of survey illustrates that grid electricity is the most popular energy resource used in the investigated household, but the solar energy is evaluated as the safest source of energy. This has contributed to the raising need of the country in more investment for this type of power. Residents of the tall residential building, especially the ones from young intellectual class, have increasingly considered safety issues as important in the use of energy sources. However, due to solar and other sustainable energy sources are not popularly used, citizens are timid in deciding to switch to these sustainable energy sources.

The survey respondents often purchase apartments when they have been not equipped with adequate safety facilities to guarantee their families' safety in using of energy whilst the fire safety equipment are more concerned. This is because of an enhancement in the society's perception of the risk of fire due to news and reports by the mass media and the availability of this type of equipment and their ease of installation in comparison to safety devices which must be installed during construction time. Nevertheless, still people are not really aware of their rights related to safety when buying apartments, since very few people in the survey know or care to the design standards related to safety of energy supply for tall buildings.

Since people in Vietnam in general and Hanoi in particular have raised interest in saving energy and developing sustainable sources of energy, as well as the rising awareness of city dwellers in sustainable development and the needs of sustainable buildings such as the ones that meet LOTUS standards, real estate developers need to pay more attention on alternatives of sustainable sources of energy to be used in their projects. Though some of them still think of the cost they have to bear when switching to a new source of energy that is more sustainable, most of the tall building residents in the research are ready to switch to a new and more sustainable energy source. The Government, however should be aware of this issue in developing plans and policies on sustainable construction in general and standards and guidelines for sustainable energy use in buildings in particular.

REFERENCES

Bao Linh (2011) Gas leaking sensor: Safe or unsafe?. An Ninh Thu Do Newspaper Online

Lan Huong (2012) Hanoi takes the lead in quantity of fire in tall buildings. Dan Tri Online

Linh Van (2011). Hanoi become a champion in terms of tall buildings. Dien Dan Doanh Nghiep Online Newspaper.

Minh Hanh (2006) One solution for the problem of electricity insufficiency. Dang Cong San Vietnam Online

Development of simulation exercise for emergency response headquarters focused on management by objectives

Shinya KONDO[1], Akiyuki KAWASAKI[2], Miho OHARA[3], Akira KODAKA[4] and Adisorn SUNTHARARUK[4]
[1] Chief Researcher, Disaster Reduction and Human Renovation Institution, Japan
kondo2@dri.ne.jp
[2] Project Associate Professor, ICUS, IIS, The University of Tokyo, Japan
[3] Associate Professor, ICUS, IIS, The University of Tokyo, Japan
[4] Loei Fund for Nature Conservation and Sustainable Development, Thailand

ABSTRACT

Our research group hopes to propose a disaster information system for improving local communities' disaster response ability in rural and agricultural mountainous areas where support from the national and local governments cannot be expected. A disaster information dissemination system is based on lessons and knowledge of disaster management accumulated in Japan, and this system is localized according to needs and current situation of each country.

Thailand has disaster risks everywhere in the country, including drought, flood, and landslide in the northeast, cyclone in the northwest, tsunami in the south coastal area, and flood in Bangkok city. The fast and wide transmission of disaster information by communications infrastructure is important for implementation of disaster mitigation measures. In the northeast, the economy has lagged behind compared with other regions, people become migrants in urban areas such as Bangkok, and education level is generally low. In such areas, it is considered that people could not use disaster information effectively, even if they can get disaster information.

In this paper, the authors organized the reality and problems of disaster information dissemination system in Loei province (Thailand) from the perspective of "planning and output of disaster information", "disaster information generation flow" and "disaster information distribution flow". Furthermore, issues and improvements of disaster information dissemination systems in Loei province were revealed in comparison with the case of disaster management for typhoon Talas of three municipalities in the southern part of Wakayama Prefecture from the view point of "multiplexing communication network" and "early evacuation before dark".

Keywords: *disaster information dissemination system, flood disaster, sediment disaster, localization, area-mail, rural and agricultural mountainous area*

Comparing benefits of hydropower development in two boundary systems in the Mekong

Seemanta Sharma BHAGABATI[a], Akiyuki KAWASAKI[a,b]
[a] Regional Network Office for Urban Safety, Asian Institute of Technology, Thailand.
E-mail: seemanta0605@gmail.com
[b] Institute of Industrial Sciences, The University of Tokyo, Japan

ABSTRACT

Hydropower dam development, although is a very promising source of energy, has enormous economic, environmental, and social impacts at a local, national, and trans-national level which may result to transboundary conflicts among the riparian countries. Past literature has suggested that the conflicts arising from hydropower development may be approached through benefit sharing. Selecting different sets of riparians (such as countries (Political boundary) and river sub-basins (Natural boundary)) within the same study area may lead to different benefit sharing system. While a lot of research has been done in the country aspect (political boundary), the natural boundary aspect has been left simply untouched. This study shows promising results of the natural boundary approach. The study attempts to investigate the difference in benefit sharing in the transboundary sub-basin, the Sekong, Sesan and Srepok (commonly known as 3S) sub basin, covering areas of Laos, Cambodia and Vietnam in the Mekong River Basin using a game theory approach. Two sets are defined, based on Political boundary (National boundaries) and based on Natural boundary (3S boundaries). A wide range of parameters such as energy production, irrigational benefits, flood control socio-economic costs etc. have been incorporated to define models and methodologies. This study then compares these two sets using the game theory concepts, such as core stability and incentive compatibility. Here we show that depending on the type of riparians chosen, the extent of benefit sharing changes. The results of the study will provide a basis for local policy decisions and regional planning in the Mekong River and beyond.

Keywords: *Mekong River Basin, 3S sub-basin, Hydropower development, Game Theory, Natural boundary, Political boundary, Optimization*

Optimization the use of rice husk ash to increase bearing capacity of difficult soil foundation for low cost housing in Semarang's Urban areas.

Silvia Fransisca Herina
Senior researcher
Research Institute for Human Settlements,
Ministry of Public Works, Indonesia
silvia_herina@yahoo.com

ABSTRACT

For any kind of Urban areas the need of housing is one of the important aspects. Often the imbalance in between high buildings demand and limited land trigger an increasing of land prices followed by the driving up of the using of unstable soils as ground foundation. For high rise building that condition is not a problem, because they will selecting foundation's type that is safe, but for low cost housing, the selection of a more secure foundation ,deep foundation for example, lead to more expensive consequences, and this is a constraint, because the foundation could be much more expensive than the building's cost.
Rice husk ash which had been a waste materials, content fairly high SiO2 (55 to 58%) which is one of the chemical elements essential in the formation of cement, if SiO2 mixed with lime (CaO) would produce a product cementation . Optimization of the composition of a mixture of local sand and in situ soil result in concreting effect which possible to increase bearing capacity of the soil, so that simple shallow foundations can be used to support building on it.

In addition to economic considerations, this research also consider the issue of environment friendly by reducing material waste. The case project is the ground foundation of low cost housing in expansive soils in Semarang, center of Java.

Keywords : rice husk ash, expansive soils, foundation, low cost housing

Scale effects on the shear strength of waste in coastal landfill sites

Nguyen Chau LAN[1], Toru INUI[2], Kazuki IKEDA[3]
and TakeshiKATSUMI[4]

[1] PhD, Faculty of Civil Engineering, University of Transport and Communications, Vietnam
nguyenlan1981@gmail.com

[2] Associate Professor, Gradual School of Global Environmental Studies, Kyoto University, Japan

[3] Former Graduate Student, Faculty of Engineering, Kyoto University, Japan.

[4] Professor, Gradual School of Global Environmental Studies, Kyoto University, Japan

ABSTRACT

In Japan, a significant volume of municipal solid waste incinerator ash (MSWIA), slag and soil are disposed in coastal landfill sites located in Tokyo and Osaka bay. Future reclamation of these final disposal sites is an important goal. Thus, it is relevant to understand the shear strength properties of the waste layers in coastal landfill sites to utilize the land after closure. However, the particle size distribution of the waste ranges from fine-grained to coarse-grained (gravel, glass, etc.) affecting the estimation of the shear strength properties of the waste sample in coastal landfill sites. There is no available research on the effects of oversize particle on the shear strength of waste samples in coastal landfill sites. Therefore, this paper presents the results of larger triaxial test (150 mm x 300 mm) for waste samples. In the large triaxial test, the pore water pressure generated is higher compared to the results obtained for small samples due to the longer dissipation time of pore water pressure. The smaller values of shear strength for large samples are also related to the crushability of large particle size. Thus, the frictional angle of large specimens is slightly smaller than that of small ones. Moreover, to calculate the stability of coastal landfill sites, if the strength parameters results from large triaxial test are used, the safety factor might decrease due to the lower of friction angle of large triaxial test and it would be more precise compared to the value obtained from a small triaxial test.

Keywords: *waste, ash, coastal landfill, large triaxial test, mechanical properties*

1. INTRODUCTION

In Japan, a significant volume of municipal solid waste incinerator ash (MSWIA), slag and soil are disposed in coastal landfill sites located in Tokyo and Osaka bay. Future reclamation of these final disposal sites is an important goal. Thus, it is relevant to understand the strength properties of the waste mixture layers in coastal landfill sites to utilize the land after closure. However, the particle size distribution of the waste mixture ranges from fine-grained to coarse-grained (gravel, glass, etc.) affecting the estimation of the strength properties of the waste mixture sample in coastal landfill sites. Generally, the strength properties of a sample material is investigated by a triaxial test. When triaxial tests are run, the maximum particle size of the samples must be less than one-sixth of the diameter of the specimen. Therefore the standard triaxial test, with a specimen of 50 mm in diameter, cannot be used if the diameter of the waste mixture sample is larger than 9.5 mm. Numerous research studies have attempted to increase the maximum particle size of the specimens tested by increasing the size of the testing apparatus in order to accurately measured the mechanical behavior of geomaterials (Hennes, 1952; Holtz & J., 1956). Previous studies have investigated the effect of large particles on shear strength of soil by using large triaxial test and reported that the increase in gravel content decreases the density and shear strength of the material (R. Fragaszy, Su, & Siddiqi, 1990; R. J. Fragaszy, Su, Siddiqi, & Ho, 1992). Kirkpatrick (1965) studied the Leighton Buzzard sand with uniform particle sizes using triaxial tests; the results showed a reduction in friction angle as the mean particle size increased while the porosity was kept constant. However, other researchers concluded that the shear strength of mixture (soil and gravel) increases with gravel content.

Direct shear test is another method that can be utilized to determine the shear strength. Hennes (1952) and Simoni and Houlsby (2006) used this method to test sand and gravel samples; the results showed that the addition of gravel to the mixture causes an increase in friction angle. However, Cerato and Lutenegger (2006) studied the scale effect of dir**ec**t shear tests on sands and observed a decreased in friction angle when the maximum particle size increased. Their study showed that the friction angle measured by direct shear testing depends on sample size and that the influence of sample size is also a function of sand type and relative density. They concluded that for dense sand, the friction angle measured by direct shear tests is reduced as the box size increases at a ratio of at least 1:50 between box width and particle size.

However, there is no available research on the effects of large particle on the shear strength of waste mixture samples in coastal landfill sites. Therefore, in this research, large-scale (150 mm x 300 mm) and small-scale (50 mm x 100 mm) triaxial tests were carried out on waste mixture samples to study the effect of specimen size on the shear strength of the samples. This paper deals with the effects of particle size and confining pressure on the shear strength of waste mixture samples.

2. MATERIAL AND METHODS

2.1. Material

The waste samples and the simulated water in coastal landfill site employed in this study were obtained from the coastal landfill site in Osaka Prefecture. The waste samples were collected before being disposed at the coastal landfill site. Approximately 200 kg of wet waste sample include incinerator ash; slag and surplus soil, etc. were collected and then dried in a room with an average temperature of 20^{o}C. For conducting small specimen, large pieces such as glasses or rocks were removed and the sample was sieved with 9.5mm opening sieve and set aside until use. For large specimen, all large pieces were used except pieces larger than19mm. The maximum diameter of waste mixture for small and large triaxial test is 9.5mm and 19 mm, respectively. Figure 1 shows the particle size distribution for small and large samples, determined according to JIS A1204. The specific gravity of the waste sample was 2.67.

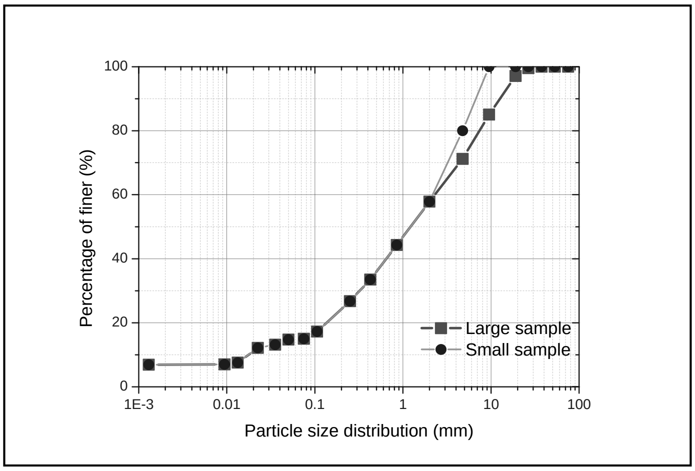

Figure 1: Particle size distribution of waste mixture samples for small and large triaxial tests

X-ray florescence Spectroscopy (XRF) was performed to determine the chemical composition of the waste samples. The chemical composition of the sample is shown in Table 1. The main components of the sample are CaO; Fe_2O_3 and SiO_2. The XRF shows that lime (CaO) is the main component of the sample (51.6 %).

Table 1 Chemical composition of waste sample (%)

CaO	**Fe_2O_3**	**SiO_2**	**Al_2O_3**	**TiO_2**	**SO_3**	**K_2O**	**ZnO**	**Cr_2O_3**	**MnO**	**CuO**
51.61	20.40	9.11	4.28	3.30	2.77	1.66	1.87	1.57	0.54	0.52

2.2. Methods

In this study, small specimens were prepared by compacting 5 layers of waste in to a split cylindrical mold (50 mm diameter and 100 mm in height) 80% of maximum dry density (1.28 g/cm^3) with optimum water content of 34.5% according to the value obtained from the Standard Proctor Compaction Test.

For large CU triaxial test, specimens were prepared by compacting 5 layers of waste mixture in to a split cylindrical mold (150 mm diameter and 300 mm in height) with the same maximum dry density and optimum water content as small specimens. In this test, D/d_{max}= 15/1.9= 7.89 (where D is diameter of specimen in large triaxial test and d_{max} is the maximum particle size of waste mixture).

Small and large CU triaxial tests were carried out on waste mixture specimens following the same procedure. These specimens were saturated by applying a vacuum procedure (Rad & Clough, 1984) to keep a constant confining pressure of 20 kPa. After reaching the final step (-70 kPa for cell pressure and -90 kPa for sample pressure) de-aired water was circulated into the specimen for 3 hours and then sample pressure and cell pressure were reduced to -20 kPa and 0 kPa respectively. Back pressure was increased step by step until it reached 240 kPa and cell pressure was 220 kPa. After that, pore pressure coefficient (B-value) was checked to have B-values larger than 0.95 and ensure that samples were fully saturated. The samples were consolidated with an effective confining pressure of 50, 100 and 150 kPa and sheared at a constant strain rate of 0.5%/min until 15% of axial strain was reached.

The target of conducting small and large samples in triaxial test is to consider the effect specimen size on shear strength of waste mixture is considered. It is crucial to estimate the shear strength of waste mixture in coastal landfill sites for future land utilization. The initial conditions for large and small triaxial test are shown in Table 2.

Table 2: Initial condition of waste mixture samples

Type of Triaxial test	**Confining pressure (kPa)**	**Dry density after consolidated (g/cm^3)**	**Void ratio e (after consolidated)**	**B value**	**D_{max} (mm)**
For small triaxial test	50	1.02	1.62	0.95	9.5
	100	1.02	1.62	0.95	
	150	1.02	1.62	0.95	
For large triaxial test	50	1.02	1.61	0.95	19
	100	1.03	1.56	0.95	
	150	1.06	1.53	0.95	

3. RESULT AND DISCUSSION

3.1. CU test for small triaxial test

Figure 2 shows the stress-strain curves for small samples. Generally, the deviator stress increases dramatically from 0 to 2 % of axial strain and reaches a peak after 6% of axial strain. After that the deviator stress reaches a constant value until 15% of axial strain. The stress-strain curves illustrate the strain hardening behavior of waste mixture samples.

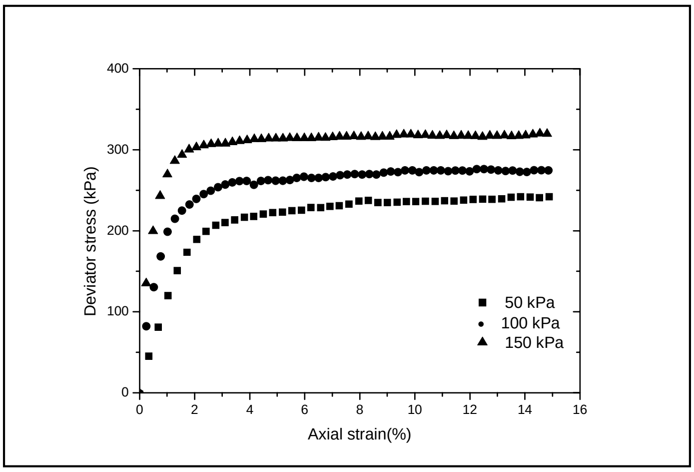

Figure 2: Stress-strain curves for small samples

Figure 3 shows the pore pressure results versus axial strain. For samples under a confining pressure of 50 kPa, the pore water pressure shows an increase trend at the initial stage until it reached a peak value of about 20kPa and then it is reduced steadily to nearly zero at 15% of axial strain. Pore water pressure generated in samples that sustained 100 kPa confining pressure, showed a similar trend than samples under 50 kPa but reaching a pore pressure peak value of about 50 kPa and then reducing steadily until reaching about 35 kPa. However, for samples under 150 kPa, pore water pressure increases and reaches a peak at 2% and then keeps a constant value until an axial strain of 15% is reached. The samples under initial conditions in small triaxial test showed a contractive behavior in shearing process due to the positive value of the pore water pressure when the axial strain increased from 0 to 15 %.

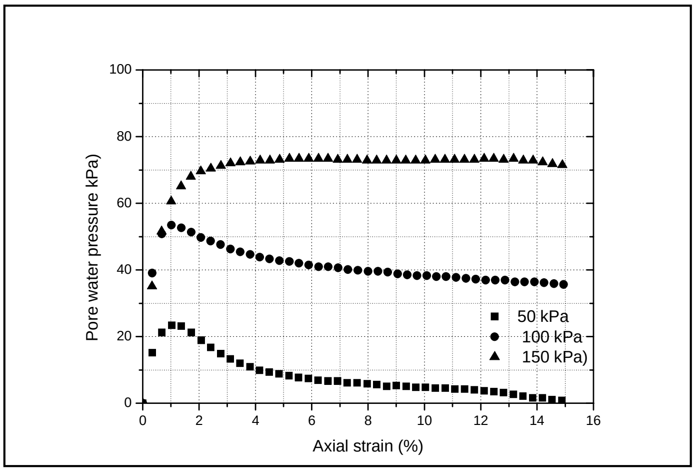

Figure 3: Pore pressure results versus axial strain for small triaxial test

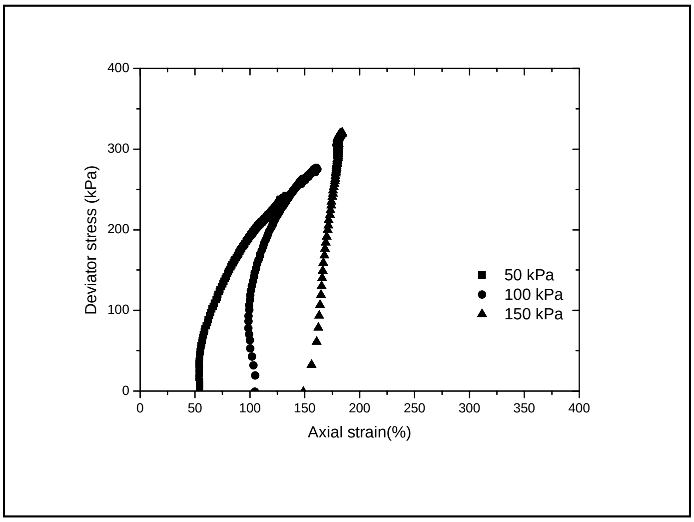

Figure 4: Stress paths for small triaxial test

The deviator stress (q) and the mean effective stress (p') are calculated by following Eqs. (1) and (2):

$$q = (\sigma'_1 - \sigma'_3 \quad (1)$$

$$p' = (\sigma'_1 + 2\sigma'_3)/3 \quad (2)$$

where σ'_1 and σ'_3 are the effective axial and confining stress. Fig. 4 shows the effective stress paths for samples in small triaxial test were plotted in a p'-q plane. In this figure, from the beginning, stress paths showed an increase of pore pressure with the stress path moving to the left until pore pressure reduces and the effective pressure increases moving the stress path into the right direction.

3.2. CU test for larger triaxial test

Figure 5 shows the stress-strain curves for large samples. The deviator stress increases dramatically from origin to reach a peak value at about 2% of axial strain. After that, the deviator stress decreases steadily until 15% of axial strain and the stress-strain curves illustrate the strain softening behavior of waste mixture samples. This behavior significantly change compare with the results for small samples.

Figure 6 shows the pore water pressure versus axial strain. For specimens that sustained 100 and 150 kPa of confining pressure, the pore water pressure increases dramatically from 0% to 2% of axial strain and from 2% to 15% it has a mild but steady increases. In the case of specimen that sustained 50 kPa of confining pressure, pore water pressure has a constant value from 2% to about 15% axial strain.

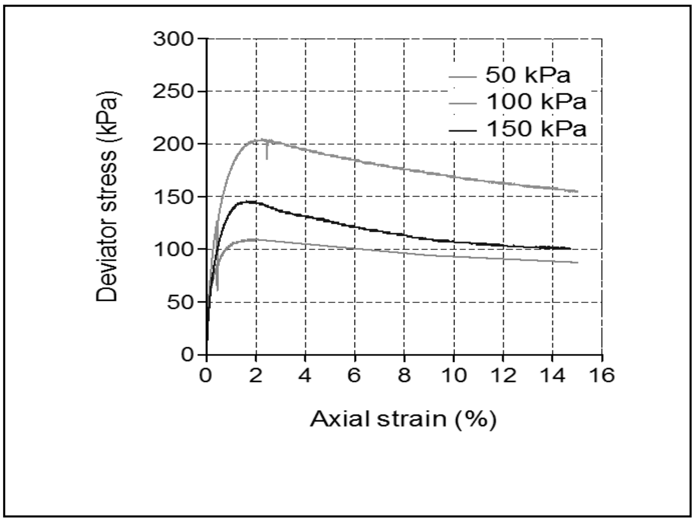

Figure 5: Stress-strain curves for large samples

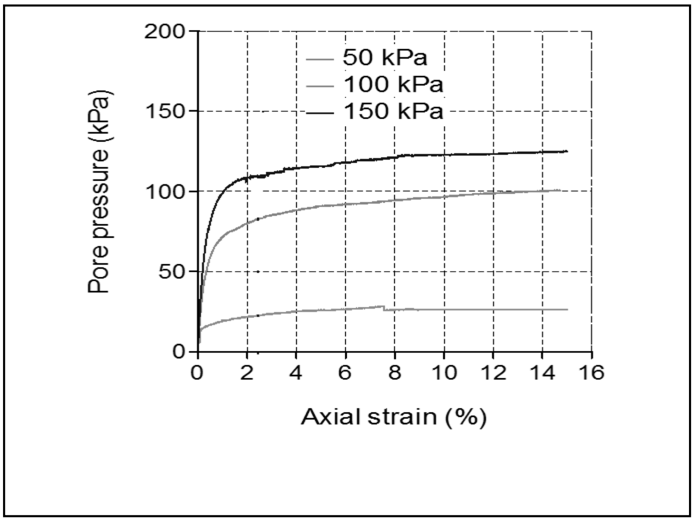

Figure 6: Pore pressure results versus axial strain for large triaxial test

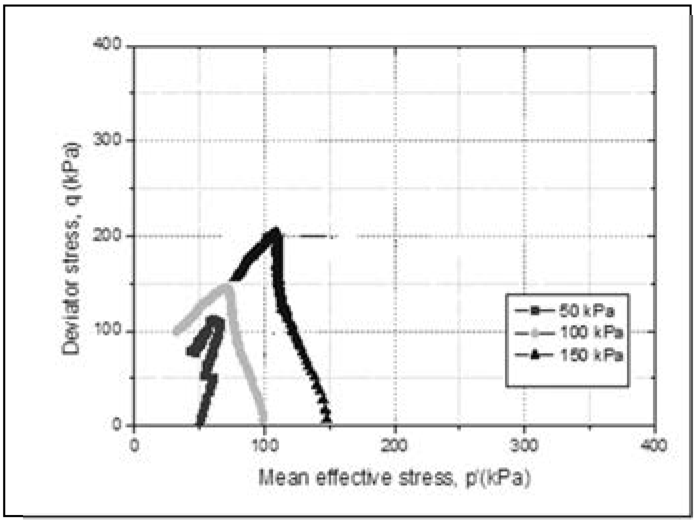

Figure 7: Stress paths for large triaxial test

Fig. 7 shows the effective stress paths for large triaxial test. In this figure it can be observed that from the beginning, stress paths moves to the right until the deviator stress reach a peak value and after that the deviator stress starts decreasing due to an increase in pore water pressure and moving the stress path into the right direction.

.

3.3 Effect of particle size on shear strength of waste mixture sample

In order to compare the peak strength envelopes and the shear strength parameters for large and small samples, the shear strength parameters are determined using a linear interpolation. Figure 8 shows the peak strength of small samples and large samples. The shear strength parameters-cohesion intercept *c*' and the angle of friction ϕ'- associated with these peak strength envelopes can be obtained using the following two equations:

$$\phi' = sin^{-1}\left(\frac{3M}{6+M}\right) \tag{3}$$

$$c' = f\left[\frac{3-\sin(\phi')}{6\,cos(\phi')}\right] \tag{4}$$

where *M* is the slope of peak strength envelope and *f* is the q-intercept of the peak strength envelopes in p'-q stress space.

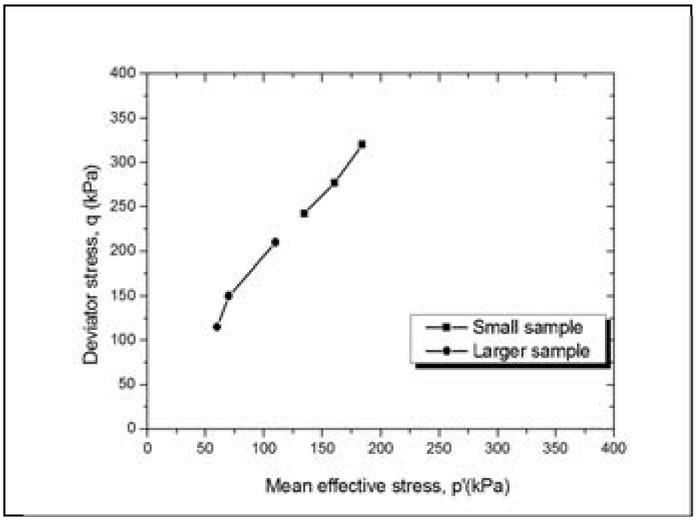

Figure 8: Peak strength envelopes of small samples and large samples

The cohesion and angle of friction obtained are 0 kPa, 46.7° for small sample, and 2.8 kPa, 44.78° for large sample, respectively. The direction of peak strength envelope for samples and larger samples is similar. Thus, the strength parameters results are almost no change. The most important reason for the change in shear strength is related to pore water pressure generated. In the large sample, due to large diameter of mixture waste and large specimen the pore water pressure generated are higher compare to those in small samples. The change in pore water pressure contributed to the change in shear strength of large sample compare with small samples. Thus, most important reason for the change in shear strength is related to pore water pressure generated. In the large sample, due its the large diameter, the pore water pressure generated is higher compare to the results obtained for small samples. The change in pore water pressure contributed to the increased in shear strength for large sample compare with small samples.

The differences in stress paths for small and large samples could be related to the crushability of the larger samples. The crushability of larger samples were observed, although the initial of dry density for small and large samples are the same but the void ratio were reduced in consolidated step for large samples compared with small samples. These results showed that the volume of large samples was reduced due to crushability. This behavior has been observed in a previous research conducted by Kokusho (2004). The two major factors governing the shear strength of granular materials are interlocking between particles and particle breakage. The interlocking between particles increases the shearing resistance, while the breakage of particles decreases the shear strength. In this test, the larger samples had larger breakage of particle and that lead to lower shear strength compare with results obtained from small samples. The results of this study show that as the size of particles increase, the shear strength of waste mixture decreases. These results are consistent with results presented by Kirkpatrick (1965); Fragaszy et al. (1990) and Kokusho et al. (2004).

4. CONCLUSION

Based on the experimental results, the following summarizes about the scale effects of specimens on the mechanical properties of waste mixture in coastal landfills:

1) In coastal landfill sites, the presence of large particles in waste mixture can change the results of triaxial test. It is necessary to estimate the change of shear strength if the waste mixture sample contains large particles. Thus, the comparison between small and large triaxial test is necessary to understand better the shear strength behavior and pore water generated from waste mixture samples. In this research, the particle size of the larger samples for large triaxial test 15cmx30cm is larger than 9.5mm. In the large triaxial test, the pore water pressure generated is higher compared to the results obtained for small samples due to the longer dissipation time of pore water pressure.
2) The value of shear strength obtained from the triaxial tests for large samples are smaller than with the results obtained for small samples due to the dissipation of pore water pressure that affect stress paths and that in turn reduce in the strength of large samples. The smaller of the shear strength for large samples are also related to the crushability of large particle size. Thus, the frictional angle of large specimens is slightly smaller than that of small ones. Therefore, in order to estimate the shear strength in the coastal landfill sites, it is suggested that the large triaxial test should be conducted due to large particle size of sample collected from the sites (23% of particle size larger than 9.5mm for the samples in Osaka coastal landfill sites). Moreover, for calculating the stability of coastal landfill sites, if we use the strength parameters results from large triaxial test, the safety factor will be lower due to the lower of friction angle of large triaxial test and it is more precise compare to the value of the small triaxial test.

REFERENCE

Cerato, A. B., and Lutenegger, A. J., 2006. Specimen size and scale effects of direct shear box tests of sands. Geotechnical Testing Journal, 29(6), 507-516.

Fragaszy, R., Su, W., and Siddiqi, F., 1990. Effects of oversize particles on the density of clean granular soils. Geotechnical Testing Journal 13(2), 106-114.

Fragaszy, R. J., Su, J., Siddiqi, F. H., and Ho, C. L., 1992. Modeling strength of sandy gravel. Journal of Geotechnical Engineering-ASCE, 118(6), 920-935.

Hennes, R. G., 1952. The strength of gravel in direct shear. ASTM special technical publication, STP 131, 51-62.

Holtz, W. G., and J., G. H., 1956. Triaxial shear tests on pervious gravelly soils. Journal of the Soil Mechanics and Foundation Division, 82, 1-22.

Kirkpatrick, W. M., 1965. Effect of grain size and grading on the shearing behavior of granular materials. Paper presented at the Proceedings of the sixth International Conference on Soil Mechanics and Foundation Engineering.

Rad, N. S., and Clough, G. W., 1984. New procedure for saturating sand specimens. Journal of Geotechnical Engineering-ASCE, 110(9), 1205-1218.

Simoni, A., and Houlsby, G. T., 2006. The direct shear strength and dilatancy of sand-gravel mixtures. Geotechnical and Geological Engineering, 24(3), 523-549.

Triaxial tests for elastic wave measurement with associated matric suction on unsaturated fine content sandy soil

Laxmi Prasad SUWAL[1], Reiko KUWANO[2], and Takeshi SATO[3]
[1] Project Researcher, ICUS, Institute of Industrial Science, The University of Tokyo
Suwal@iis.u-tokyo.ac.jp
[2] Associate Professor, Institute of Industrial Science, The University of Tokyo
kuwano@iis.u-tokyo.ac.jp
[3] Integrated Geotechnology Institute Ltd., Tokyo, Japan
tsato@iis.u-tokyo.ac.jp

ABSTRACT

Most of engineering infrastructures are constructed in shallow depth soil where moisture contents are being varied due to natural phenomena as well as human activities. The ground inevitably possesses variation of matric suction; sandy soils possess low suction in such shallow ground. In order to cope with the complex behaviour of sandy soil, the materials properties with associated suction variation are needed to evaluate. However there is still lacking of good tools for evaluating material`s properties of sandy soils; consisting of various degree of saturation with accounting matric suction and other elastic parameters. The triaxial apparatus enabling to measure elastic waves and matric suction, mainly low suction, was initially employed in this study. Triaxial tests were performed using natural sand; Edosaki sand, containing fines in various degree of saturation to be acquainted with elastic properties of sandy soil possessing low suction. Improved triaxial apparatus enabling to measure both elastic waves and matric suction was adopted. A specimen was prepared by tamping method with (5% - 15%) initial moisture content. The experiments were performed applying 50 kPa effective isotropic stresses. The elastic waves were measured in several moisture contents with monitoring the associated matric suction variation.

Keywords: Triaxial test, partially saturated soil, elastic wave, matric Suction

1. INTRODUCTION

Collapse of soil structures is generally known as the additional deformation within the short time period. So collapse is believed to be responsible to damage or fail of many kinds of infrastructures such as embankments, earthen dams, levee and buildings resting on not well compacted soil etc. Collapsing behavior consists of saturation process of unsaturated meta-stable soil. So, the theory of unsaturated soil is crucial for understanding this phenomenon. The mechanical behavior of a loosely deposited soil is strongly depends upon the amount of fines, volume mass of soils properties such as void ratio (e), water content (w) and degree of saturation (Sr.) (Fredlund and Morgenstern1977). Most of the infrastructures are constructed on shallow depth ground and the ground is generally composed by sandy soils like Edosaki sand. In this study, Edosaki sand was tested on the triaxial apparatus to evaluate collapse potential and elastic properties in unsaturated condition.

2. MATERIAL AND APPARATUS

2.1 Edosaki sand

It is natural sand of containing fines collected from the Ibaraki prefecture, Japan. Grains are mostly round with yellowish orange color. It is mostly used in earthen infrastructures as filling materials in japan. The photograph taken from optical microscope of the sample of Edosaki sand including gradation curve are shown in Figure 1

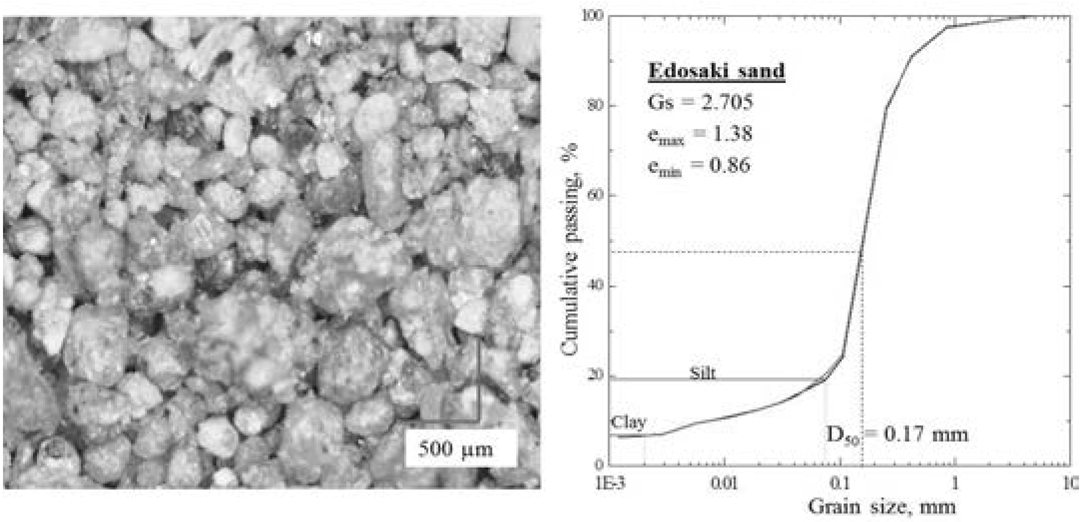

Figure1 Edosaki sand and its gradation curve

2.2 Apparatus and Transducers

Small size, gear driven and strain controlled triaxial apparatus was used for performing experiments. The axial loading system consists of an AC servomotor and a reduction gear system, electro-magnetic clutches and brakes. Experiments were precisely controlled by high speed computer. As shown in Figure 2, the specimen and other accessories were set up. The upper and lower tanks with load cell were hung to monitor the inflow and outflow of the water through the specimen. Local Deformation Transducer (LDT) as per Goto (1991) was employed for axial deformation of the specimen. A couple of LDT was attached on surface of the specimen. Clip gauge was used for radial deformation (strain) measurement. Three clip gauges were attached on the specimen. Recently developed technique for elastic wave measurement; disk transducer method and pressure membrane technique for suction measurement were merged in the modified triaxial testing apparatus enabling to acquire both elastic wave and matric suction on cyclindrical specimen, was employed. A pair of disk transducer, one in top cap and the other in pedestal, was encapsulated in the triaxial apparatus.

Micro-porous membrane (made of polyether sulfone, thickness: 140 µm, air entry value: 250 kPa) was utilized as a pressure membrane (Nishimura, 2010).

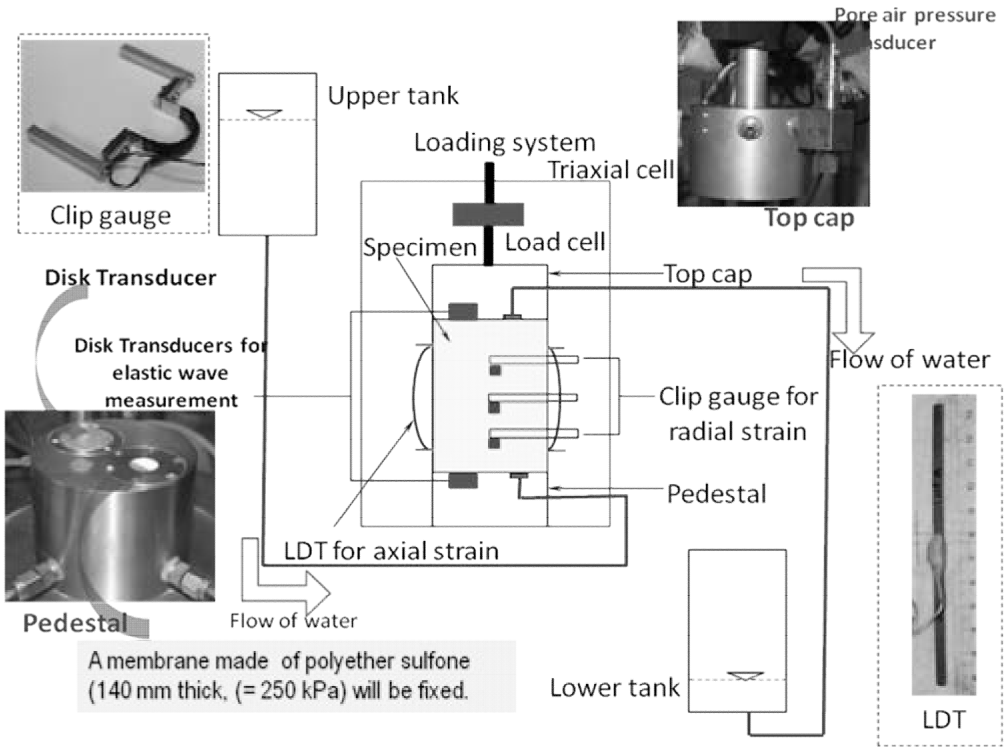

Figure2 Schematic plot of experimental set up

3. SPECIMEN PREPARATION AND TESTING PROCEDURE

3.1 Specimen preparation

This study had two motives; first, to study of the relevant deformation characteristics of sand containing fines due to first infiltration as well as successive infiltration within few hours. Second is to perform the test acquiring elastic wave velocities and matric suction on fine sandy soil. Former case was dealt with preparing the specimen having dimension 75 mm diameter by150 mm height. The total soil was divided in 15 parts and each part is compacted within 10 mm. Similarly, the specimen of 75 mm diameter and 75 mm height was prepared by tamping method for later case. The total soil was divided in 8 parts and each part is compacted within 10 mm. The specimen of 80 mm height was trimmed at the top by 5mm that generated a 75 mm heighted specimen on the pedestal.

3.2 Testing procedure

The tested materials were tamped at atmospheric pressure and around 25 kPa isotropic stresses (suction through top-cap and pedestal) were applied before removing the mold. With setting cell cover, the cell pressure was gradually increased up to 25 kPa with releasing suction at same rate. These all reflected that the specimen was prepared at isotropic stress state of 25 kPa. Then the stress level was raised to 50 kPa. Two test procedures were employed to achieve the aforementioned two goals. As schematically shown in Figure 3(a), the specimen was subjected in creep condition controlling constant stress state for sufficient time (nearly 12 – 18hrs). This creep stage is maintained for a long period to allow measuring the consolidation deformation precisely and to distinguish the deformation due to stress including creep with water induced collapse. A small-strain cyclic loading and elastic wave measurement by disk transducer were employed before starting wetting. The wetting of specimen was done by supplying water from upper tank. The water was fed through pedestal and drained out through top cap. To simulate the repeated infiltration condition in laboratory specimen, the input water was stopped after initiating to outflow of water and then allowed to deplete the water from the specimen through pedestal. For a sufficient time, the specimen was kept in depleting condition and again fed the water from bottom of the specimen. The strain and other parameters are measured during the whole processes.

The next proceduce was shown in Figure 3 (b). In this process, the specimen was subjected to constant stress state for sufficient time to maintain the stabilized matric suction.The specimen was subjected in the several water content condition by adding little amount of water and waited for stabilized matric suction. With getting the stabilized matric suction, elastic wave measurement was carried out.

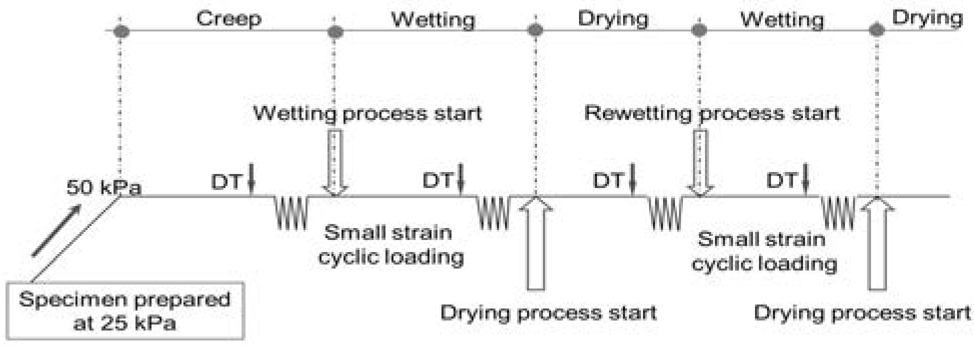

a. Water induced deformation measurement

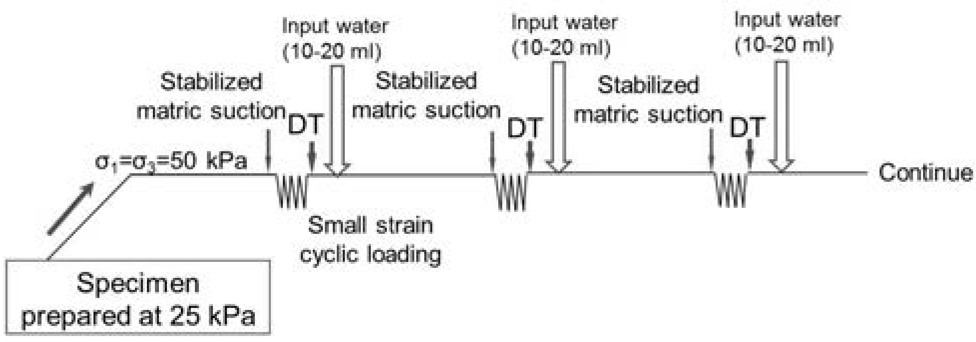

b. Matric suction and associated parameters measurement

Figure 3 Test procedure

4. TEST RESULT AND DISCUSSION

The list of the tests with the general information; size of specimens, initial density, initial void ratio and initial water content are given in the Table 1. The first series of tests were carried out on higher specimens (h= 150 mm) and second series were performed on shorter specimens (h = 75 mm).

Table 1: List of experiments on Edosaki sand

Experiment No.	Speicmen dimension	Initial dry unit weight	Relative density	Initial void ratio	Initial water content	Remarks
	mm x mm	gm/cm^3	%	e	%	
Edosaki-1	149.95 x Φ74.97	1.336	69.6	1.025	9.9	Isotropic
Edosaki-2	150.65 x Φ74.92	1.399	87.3	0.934	1.8	Isotropic
Edosaki-3	149.9 x Φ 74.64	1.304	60	1.074	2	Isotropic
Edosaki-4	150.85 x Φ 74.75	1.34	70.8	1.019	1.9	Isotropic
Edosaki-5	150.45 x Φ 74.55	1.386	83.8	0.952	4.5	Isotropic
Edosaki-6	151.25 x Φ 74.89	1.371	79.6	0.973	1.8	Anisotropic
Edosaki-7	149.45 x Φ 74.2	1.308	61.2	1.068	6.4	Isotropic
Edosaki-8*	74.85 x Φ 75.9	1.65	144.4	0.639	7.5	Isotropic
Edosaki-9**	76.25 x Φ 72.53	1.435	96.7	0.885	4	Isotropic
Edosaki-10	76.55 x Φ 74.5	1.307	60.9	1.07	9.4	Isotropic
Edosaki-11	76.05 x Φ 74.81	1.366	78.2	0.98	6.5	Isotropic
Edosaki-12	76.85 x Φ75.07	1.42	92.8	0.905	7.9	Isotropic

Note: *: densely compacted and **: reused specimen of Edosaki- 7

4.1 Water induced collapse (deformation)

The water infiltration process including repeated wetting was simulated in the laboratory allowing water to be stopped and supplied as shown in the testing sequence. The typical strain variations (axial, radial and volumetric) achieved on the test, Edosaki-1 was shown in Figure 4. In this figure, the elapse time of experiment is plotted in X-axis in hours (Hrs.) and strain variations are plotted in Y-axis in percentage (%). The axial, radial and volumetric strain increments are plotted in black, red and blue lines respectively. As shown in the figure, the strain increments are always found to be contractive and significant changes can be broadly separated into two parts. The initial variation was observed during stress spiking from 25 kPa e to 50 kPa. Behavior on creep was confirmed subjecting the specimen into the creep condition for approximately 12 -18 Hrs. During creep condition, slight changes in strains were observed.

The pre-eminent strain increments (both axial and radial direction) were observed while the water was passed inside the specimen. This is generally termed as the collapse during wetting. The water was stopped at time when just started to

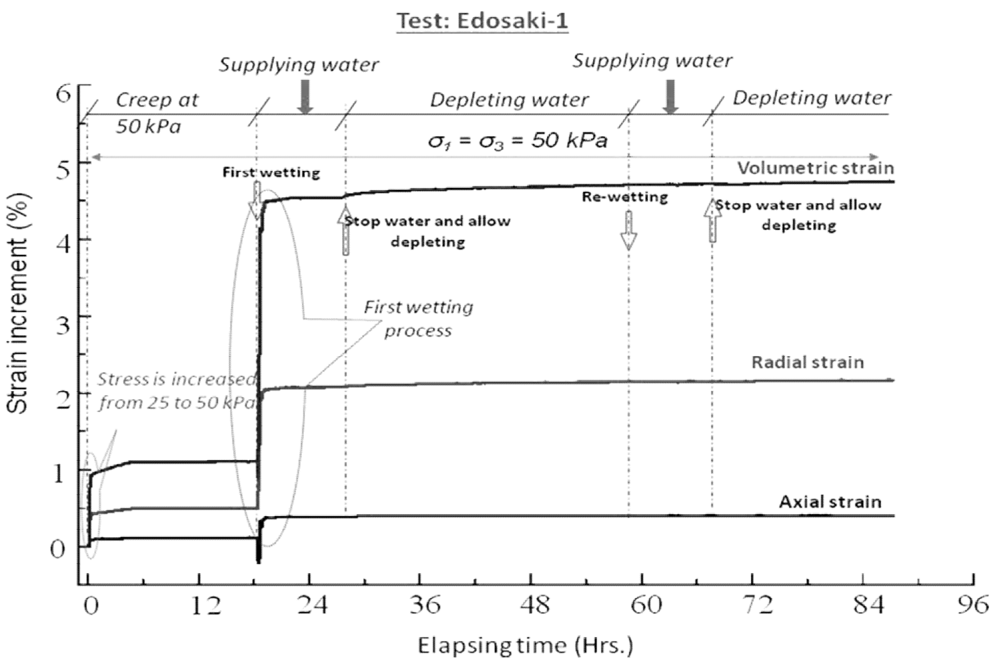

Figure 4 Typical strain variations obtained in time domain series

outflow through top of specimen. Then water was then allowed to be depleted from bottom of the specimen. After depletion, the specimen was again subjected into wetting process by supplying water as previous. The experiments were accomplished performing wetting and drying processes as prior described. The strain variations during all processes are monitored well in each case. It is noticed that the strain increments in first wetting process was paramount. The volumetric strain increments, calculated by axial and radial strains were plotted against the initial density in Figure 5. The water induced volumetric strain was confirmed to be nearly 7% at the loose state (ρ =1.3gm/cm^3 and ρ_{max} = 1.78gm/cm^3 by standard proctor test).

4.2 Matric suction and elastic wave velocity

The experiment was conducted in many steps by injecting a little water. Nearly 10 – 20 ml of water was poured into the specimen and waited in creep condition which tended to stabilize matric suction. The water was gradually added step by step and elastic waves were measured in each step. Degree of saturation and matric suction, for instance, as shown in Figure 6 were achieved. The apparent drop down of the matric suction was noticed at tiny water adding. It indicates that the matric suction is highly sensible to water content. However, the possibility of over-estimation was suspicious because the water content is locally increased in bottom. Erroneous in experiment was tried to reduced measuring the values on the shorter specimen (h = 75 mm). The results obtained on Edosaki sand are plotted in

Figure 7. The average trend line (red line in Figure 7), following to Fredlund and Xing, 1994, was drawn. This figure shows the variation trend of the matric suction of Edosaki sand and it possesses low range ofl matric suction (less than 100 kPa).

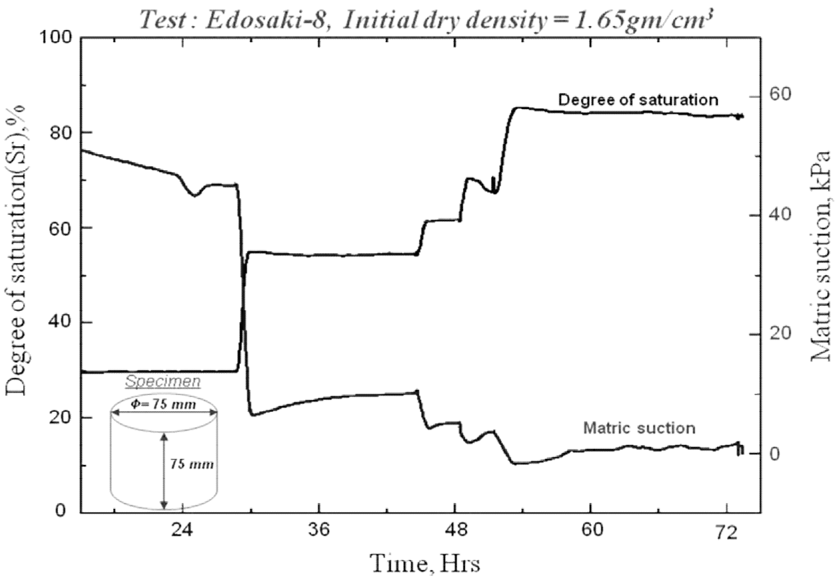

Figure 5 Volumetric strain increments obtained on Edosaki sand

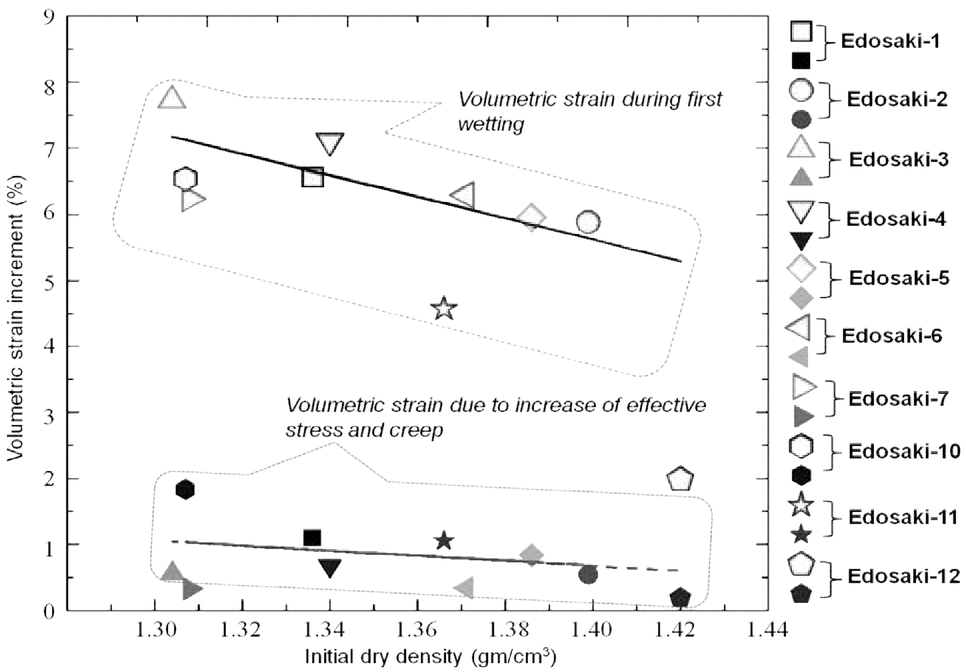

Figure 6 Degree of saturation and matric suction in time series

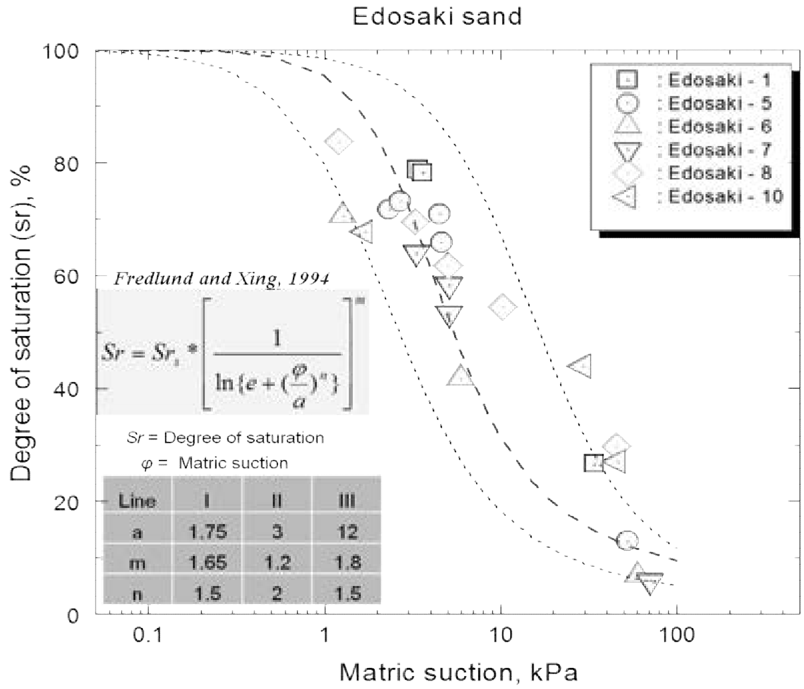

Figure7 Matric suction obtained on Edosaki sand

This study mainly focused on the unsaturated soil and its behavior. So, elastic waves, both P and S waves, were propagated each step. P and S waveforms achieved on the test: Edosaki – 8 at several moisture content conditions are traced on Figure 8 [right: P waveforms and left:S waveforms]. The input signals are shown in lowest row in volt and the outputs in increasing order of degree of saturation. The output signals are plotted in millivolt unit. The estimated points of arrival of received signal are pointed in the figure and it is seen that, with increasing degree of saturation, the travel time is getting longer. As compared to P wave, S waves are more sensitive to the moisture content. The travel time is noticed to be significantly changed with degree of saturation. Same trends were observed in all tests. Observing the waveforms obtained on the Edosaki sand, the amplitude of the received signals are found to be very small. However, the signals are enough to detect the arrival of the real signal. This is good evidence that shows the well performance of the disk transducer method in unsaturated as well as fine content sand.

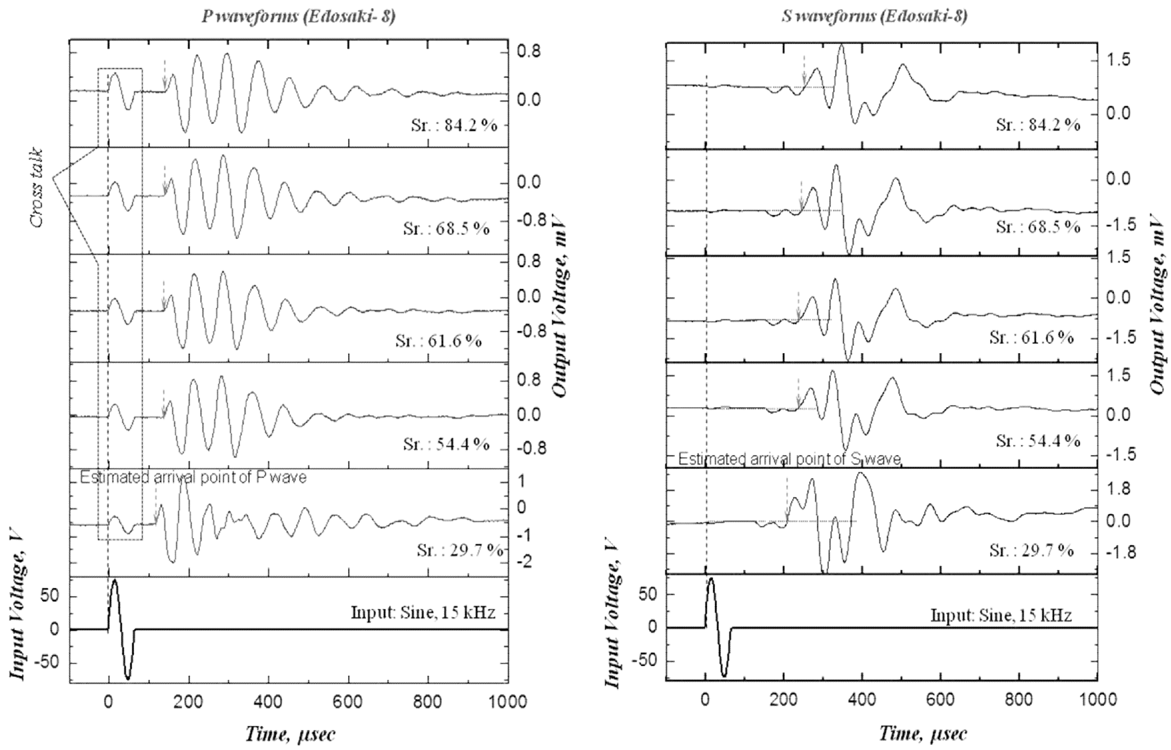

Figure8 P and S waveforms obtained on Edosaki sand specimen

The purpose of the performing test on the shorter specimen was to obtain the higher reliable data to interpret the relations among the matric suction, elastic wave velocities and water content or degree of saturation. The normalized P wave velocities obtained on four tests (Edosaki -8 to Edosaki 12) are plotted against the degree of saturation are given in Figure 9. Similarly S wave velocities obtained on those tests are drawn with respect to the degree of saturation in Figure 10. The normalized velocities; both P and S wave velocities, have found to not be concisely normalized. P wave velocity have shown two trend lines, one resulted by tests; Edosaki- 8 and Edosaki-12, another is resulted by tests; Edosaki – 10 and Edosaki-11. Normalized shear wave velocities are also found to be scattering in some extent.

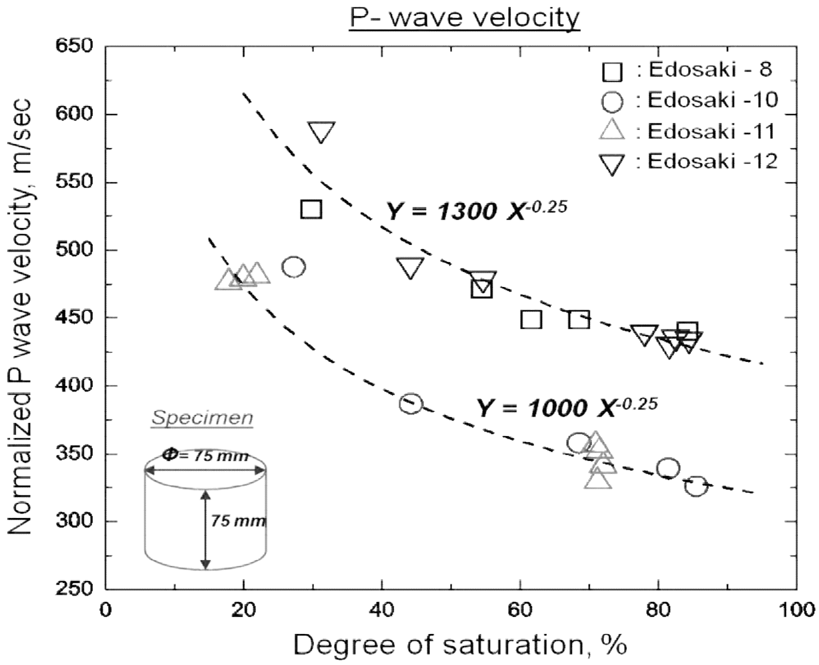

Figure 9 P wave velocity obtained on Edosaki sand

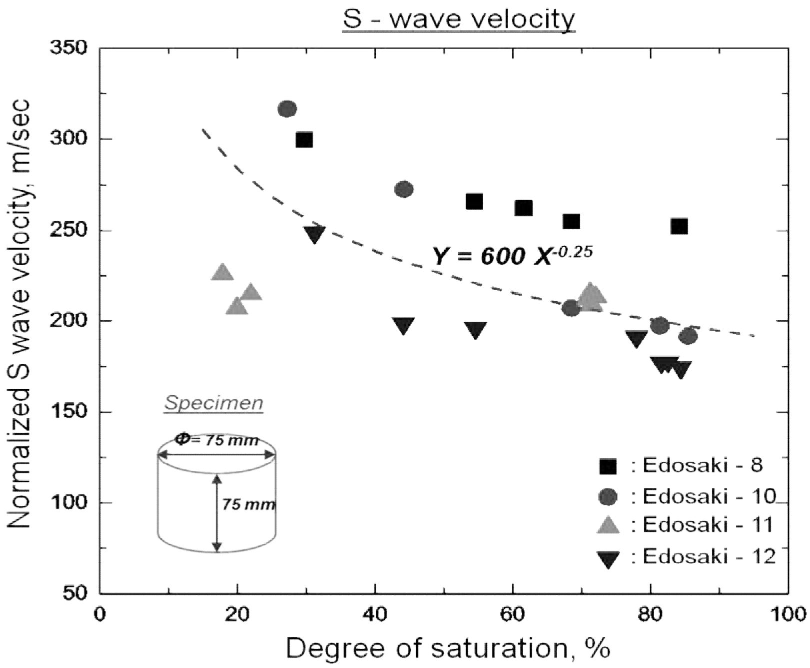

Figure 10 S wave velocity obtained on Edosaki sand

4. CONCLUSIONS

Edoasaki sand, fine content sand collected from the Ibaraki prefecture of Japan was tested to investigate the collapse behavior and mechanical properties. The findings on the experiments are summarized as;

- The strain variations due to water infiltration in edosaki sand reconstituted in the laboratory were measured by means of LDT and clip gauges on triaxial specimens. The collapse potential (volumetric strain) was observed to be varies in the ranges of 5 % - 7 %. These values are achieved on medium dense to loose specimens.

- The first wetting induced volumetric strain increment are confirmed to be the most significant and following repeated wetting and drying cycles are not much worthy.
- The matric suction activated in soil specimens of the Edosaki sand were evaluated on triaxial specimen. It is confirmed that Edosaki sand possesses a little matric suction (less than 100 kPa).
- Elastic wave measurement on the Edosaki sand specimens were performed in partially saturated conditions and its varying patterns were studies. The received waveforms at varying degree of saturation were shown. The changes in the elastic wave velocities were investigated.
- Elastic wave measurement technique by disk transducer showed its competency on unsaturated soil.

REFERENCES

Fredlund, D. G. and Xing, A., 1994. Equations for the soil-water characteristic curve, *Canadian Geotechnical Journal*, Vol. 31, pp.: 521 – 532

Fredlund, D.G., and Morgenstern, N. R. 1977. Stress state variables for unsaturated soils, *Journal of Geotechnical Engineering*, ASCE, 103(5):447-466

Goto, S., Tatsuoka, F., Shibuya, S., Kim Y-S.and Sato, T. 1991. A simple Guage for Local small strain Measurements in Laboratory. *Soil and Foundations*, 31(1):169-180

Nishimura, T., Koseki, J., Fredlund, D. G., and Rahardjo, H. 2010. Microporous Membrane Technology for Measurement of Soil-Water Characteristic Curve, *Geotechnical Testing Journal*, 35 (1): 1-8

Effect of permeability of dam body and foundation on free surface

Thi Dieu Chinh LUU
Lecturer, Water resources and Hydropower engineering Department,
National University of Civil Engineering, Vietnam
luuthidieuchinh@nuce.edu.vn

ABSTRACT

In the stability analysis of slopes, particularly those related to earth dams, it is necessary to estimate the location of the free surface or the phreatic surface. In this paper, the finite element method is used to investigate the effect of the permeability coefficients of the dam body and foundation on the free surface location. Then these results are used to analyze the stability of Buon Kuop embankment dam.

Keywords: *permeability, embankment, free surface, dam, stability*

1. INTRODUCTION

Seepage problem is one of the most important issues in design and construction of dams and hydraulic structures. Seepage problems can be categorized into confined and unconfined problems. First one refers to problems with known boundaries and the second one refers to problems with unknown boundaries. Seepage flow through the earth dams and groundwater seepage in unconfined aquifer are samples of unconfined seepage problems. In unconfined seepage problems determination the location of the free surface is the most important step in the solution. Free surface is the boundary of the saturated and unsaturated zones in the problem domain. (Ouria and Toufigh, 2009).

The slope stability and safety operation of earth dams are influenced greatly from seepage problem which is characterized by the location of the free surface (Huang, 1983). However the position of the free surface in earth dams cannot be determined easily. Thus, free surface detection has been studied by many researchers as a significant issue. (Mishra and Singh, 2005).

There are some methods to determine the free surface such as graphical flow net, application of the Dupuit theory (Cedergren, 1977; Harr, 1962). However, these methods only apply for the cases with simple boundary conditions; the real works often have the complicated boundary conditions which can be solved by using many numerical methods such as the routine finite difference method, the finite-volume method, the boundary-fitted coordinate transformation method, the finite element method, the numerical manifold method, the meshless method etc. (Bathe and Khoshgoftaar, 1979; Darbandi et al., 2007; Desai 1976; JIANG et al., 2010; Jie et al., 2004; Lam & Fredlund, 1984; Li, Ge & Jie, 2003; Zheng et al., 2005).

Normally, the permeability coefficient of dam body will be determined exactly by sampling the compacted soil of dam body and testing in laboratory (Nguyễn et al., 1978), therefore its reliability is high. Meanwhile the geology in the dam foundation is often very complicated including geology in the river-bed and two abutments in which the number of the geological survey bores are often limited, so it is difficult to determine the exact permeability coefficient of dam foundation.

In this paper, the Finite Element Method (FEM) is used to model a series of cases of earth dam with toe filter in which permeability coefficients of dam body (K_d) and foundation (K_f) are ranged within: K_f/K_d = 1÷50 times and K_d/K_f = 1÷50 times in order to survey the effect of permeability coefficients of dam body and foundation on free surface location.

2. PERMEABILITY ANALYSIS

2.1 Two-dimensional flow, stream function

Physically, all flow systems extend in three dimensions. However, in many problems the features of the groundwater motion are essentially planar, with the motion being substantially the same in parallel planes. For these problems we need concern ourselves with two-dimensional flow only, and thereby we are able to reduce considerably the work necessary to effect a solution. Fortunately, in civil engineering the vast majority of problems fall into this category.

Assuming the *y* axis as vertical (positive up) and the *x* axis as horizontal, *velocity potential* $\phi(x,y)$ will satisfy the Laplace's equation (1) and equation of continuity (2) as follows:

$$\nabla^2\phi = \frac{\partial^2\phi}{\partial x^2} + \frac{\partial^2\phi}{\partial y^2} = 0 \tag{1}$$

$$\frac{\partial u}{\partial x} + \frac{\partial v}{\partial y} = 0 \tag{2}$$

where *u*, *v* are the components of the seepage velocity in *x* axis and *y* axis respectively.

The *stream function* $\psi(x,y)$ also satisfies the equation of continuity and the Cauchy-Riemann equations and hence the equation of Laplace, (Harr, 1962).

$$\nabla^2\psi = \frac{\partial^2\psi}{\partial x^2} + \frac{\partial^2\psi}{\partial y^2} = 0 \tag{3}$$

The free surface is the upper streamline in the flow domain. It separates the saturated region of flow from the part of the soil body through which no flow occurs. The determination of its locus is one of the major objectives of groundwater investigations.

2.2 Increasing permeability coefficient of foundation, K_f/K_d = 1÷50

A series of calculations in case of earth dam with toe filter and $K_f \geq K_d$ are conducted and the changes in free surface are shown in Figure 1.

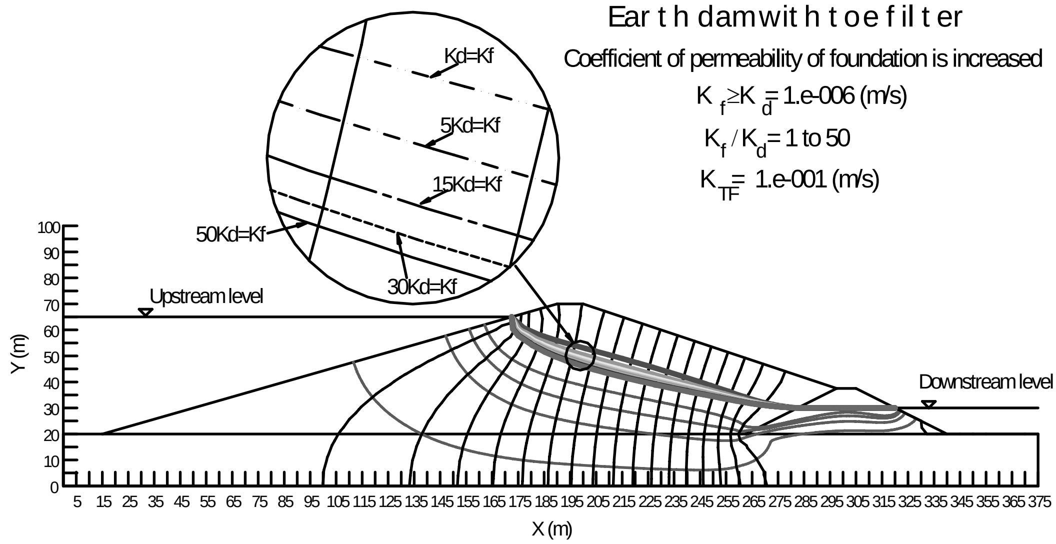

Figure 1: The free surface in case of earth dam with toe filter and $K_f \geq K_d$

The results show that when increasing the proportion of K_f/K_d = 1÷50, the free surface goes down according to the increase of permeability coefficient of K_f or the more permeability coefficient of K_f increases, the more free surface goes down.

2.3 Increasing permeability coefficient of dam body, K_d/K_f = 1÷50

A series of calculations in case of earth dam with toe filter and $K_d \geq K_f$ are conducted and the changes in free surface are shown in Figure 2.

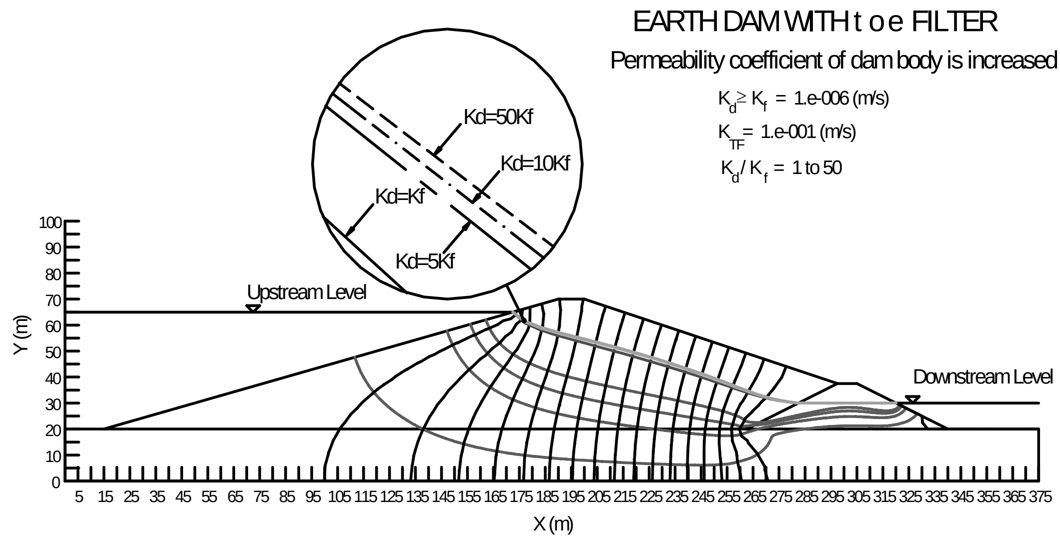

Figure 2: The free surface in case of earth dam with toe filter and $K_d \geq K_f$

The results show that when increasing the proportion of $K_d/K_f = 1 \div 50$, the free surface rises according to the increase of permeability coefficient of K_d or the more permeability coefficient of K_d increases, the more free surface rises.

3. Case study of Buon Koup earth dam

Earth dam seepage problem in the initial working time of the dam is the most important factor to consider. According to Vietnamese regulations, all the earth-rock dam of grade I to V must install the permeability monitoring equipment. It is necessary to analysis these data to evaluate the stability of dam.

Buon Kuop hydropower project which is the second largest in the Central Highland of Vietnam has an installed capacity of 280 (MW) and its electricity output is 1458.6 million kWh per year. Buon Kuop dam foundation is basalt rock, especially it has the porous basalt layers mixed with foam, and therefore the permeability of this layer is very complex. The installation of the monitoring equipment aimed to control the work of Buon Kuop dam.

It is considered the typical cross section 9-9 of the dam which includes the seepage observation holes: QTT9-1 (at crest dam of 415.5 (m)), QTT9-2 (at downstream slope elevation of 407.5 (m)) and QTT9-3 (at downstream slope elevation of 402.5 (m)). In the cross section 9-9, it is started to monitor the seepage holes from 25th February 2009 (at downstream water level of 397 (m)). The seepage monitoring data of the cross section 9-9 in dam-body showed that the seepage water level are pulled down much lower than the downstream water level (from 25-27 (m)), and the difference among the observation holes is not high which indicates that the earth-fill is consolidated and the observed free surface is suitable.

In this study the seepage of the Buon Kuop embankment dam body is numerically model by FEM. This analysis is numerically modeled by observational head piezometric data and it is compared between the predicted free surface and the observed free surface. As a result, it is showed that the observed free surface is much lower than the predicted free surface. The reason for this result is that Buon Koup dam foundation is porous basalt layers mixed with foam of which permeability coefficient is much larger than the permeability coefficient taken in the design stage. The free surface is dropped significantly and it is comply with permeability analysis in Figure 1. Then the comparison is shown in the Figure 3.

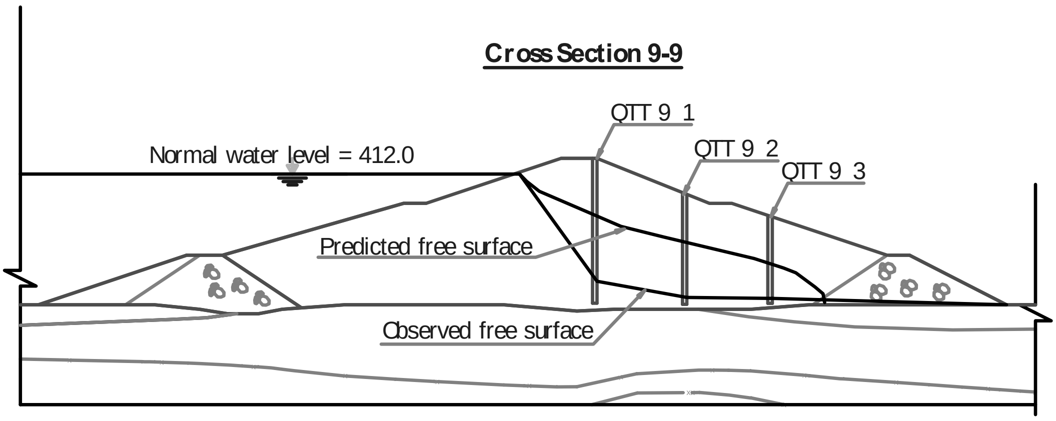

Figure 3: The predicted free surface and the observed free surface

In next step, the stability of dam in the cross section 9-9 is analyzed according to the locations of the predicted free surface and the observed free surface respectively.

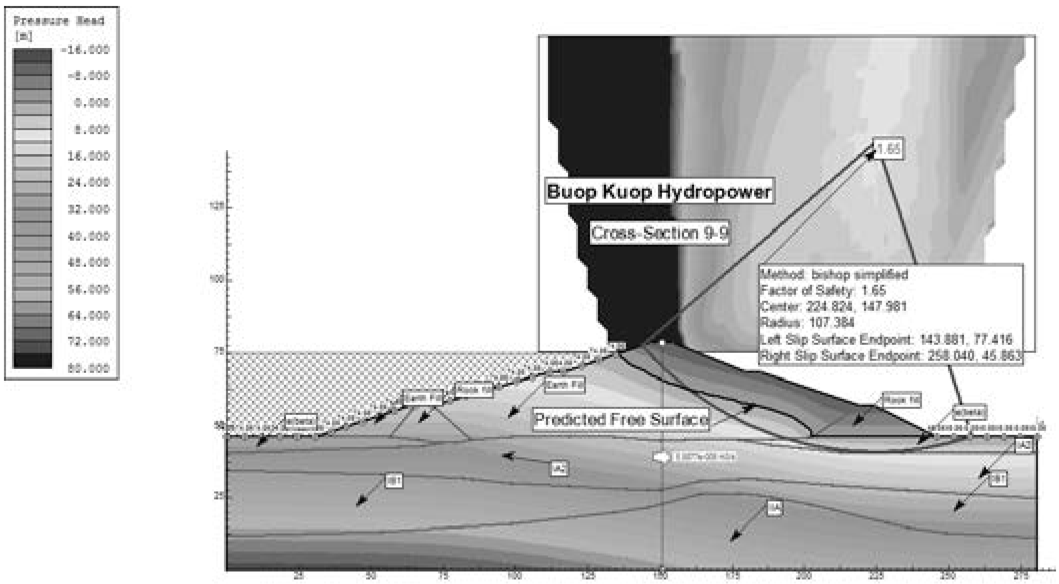

Figure 4: The stability analysis result of Cross section 9-9 according to the location of the predicted free surface; stability coefficient K = 1.65

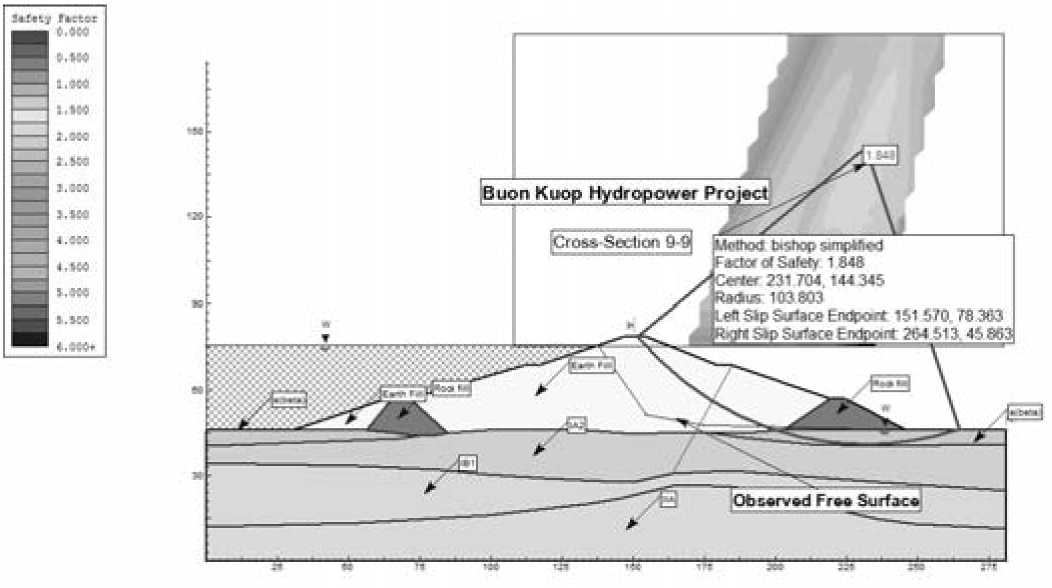

Figure 5: The stability analysis result of Cross section 9-9 according to the location of the observed free surface, stability coefficient K = 1.85

The stability analysis results as shown in Figure 4 and Figure 5 clearly illustrate that when the free surface goes down, the stability coefficient of dam increases.

On the other hand, it is obvious that when the permeability coefficient of dam foundation is too high such as the foundation of gravel, pebble, it is not necessary to layout the toe filters in dam body because the coefficient of permeability of foundation is nearly equivalent to the permeability coefficient of toe filters in design.

4. CONCLUSIONS AND RECOMMENDATIONS

In this study, FEM is used to analyze the case of earth dam with toe filter of which permeability coefficients of dam body (K_d) and foundation (K_f) are ranged within: K_f/K_d = 1÷50 times and K_d/K_f = 1÷50 times. The results show that due to the coupling effect of permeability coefficient of dam body and foundation, the location of free surface depends on the proportion of K_d/K_f. In addition, the more permeability coefficient of K_f increases, the more free surface goes down; and the more permeability coefficient of K_d increases, the more free surface rises.

Based on the analysis results of seepage observation data of Buon Kuop dam, it is recommended that in case of limitation of the geological survey in the river-bed and two abutments of dam foundation, the permeability coefficient of foundation in design calculation should have a smaller value bias in order to ensure safe operation of the dam.

REFERENCES

Bathe, K. J. and Khoshgoftaar, M. R., 1979. Finite element free surface seepage analysis without mesh iteration. *International Journal for Numerical and Analytical Methods in Geomechanics* 3, 13–22.

Cedergren, H. R., 1977. *Seepage Drainage and Flow Nets*. John Wiley, New York.

Darbandi, M., Torabi, S. O., Saadat, M., Daghighi, Y., and Jarrahbashi, D., 2007. A moving-mesh finite-volume method to solve free-surface seepage problem in arbitrary geometries. *International Journal for Numerical and Analytical Methods in Geomechanics* 31, 1609–1629.

Desai, C. S., 1976. Finite element residual schemes for unconfined flow. *International Journal for Numerical Methods in Engineering* 10, 1415–1418.

Harr, M. E., 1962. *Groundwater and Seepage*. Dover Civil and Mechanical Engineering Series, Dover.

Huang, Y., 1983. Phreatic Surfaces. *Stability Analysis of Earth Slopes*, Springer US, 40–51.

Jiang, Q., Deng, S., Zhou, C., and Lu, W., 2010. Modeling Unconfined Seepage Flow Using Three-Dimensional Numerical Manifold Method. *Journal of Hydrodynamics, Ser. B* 22, 554–561.

Jie, Y., Jie, G., Mao, Z., and Li, G., 2004. Seepage analysis based on boundary-fitted coordinate transformation method. *Computers and Geotechnics* 31, 279–283.

Lam, L., and Fredlund, D. G., 1984. Saturated-Unsaturated Transient Finite Element Seepage Model for Geotechnical Engineering. In Laible, J. P., Brebbia, C. A., Gray, W., and Pinder, G. (editors), *Finite Elements in Water Resources*, Springer Berlin Heidelberg, 113–122.

Li, G., Ge, J., and Jie, Y., 2003. Free surface seepage analysis based on the element-free method. *Mechanics Research Communications*, vol. 30, 9–19.

Mishra, G., and Singh, A., 2005. Seepage through a Levee. *International Journal of Geomechanics*, vol. 5, 74–79.

Nguyễn, C. C., Nguyễn, V. C., Lưu, C. Đ., and Hoàng, V. Q., 1978. *Thủy lực*, vol. 2, Đại học và Trung học chuyên nghiệp, Hà Nội.

Ouria, A., and Toufigh, M. M., 2009. Application of Nelder-Mead simplex method for unconfined seepage problems. *Applied Mathematical Modeling* 33, 3589–3598.

Zheng, H., Liu, D. F., Lee, C. F., and Tham, L. G., 2005. A new formulation of Signorini's type for seepage problems with free surfaces. *International Journal for Numerical Methods in Engineering*, vol. 64, 1–16.

Experimental application of biogrout to sand with fines

Tsubasa Sasaki[1] and Reiko Kuwano[2]
[1] Graduate student, Dept. of Civil Engineering, The University of Tokyo, Japan
tsubasas@iis.u-tokyo.ac.jp
[2] Professor, IIS, The University of Tokyo, Japan

ABSTRACT

Soil improvements with biogrout have the potential to mitigate geodisasters with minimal adverse consequences on the environment. However, applicability of this technique remains unaddressed for sand which contains fines. In this research, small specimens were prepared using two different sorts of sand, namely Toyoura sand and Edosaki sand, with only the latter containing fines, for the effect of the improvement on the sand with fines can be compared with that on the normal sand which has already proven to be suitable for biogrout. The specimen was injected with Biogrout containing Sporosarcina pasteurii (ATCC 11859), an ubiquitous microbial strain capable of mediating calcium carbonate precipitation, and urea-calcium ion medium, in order to induce calcium carbonate among the specimen, which binds soil particles together and increases the strength. The result showed that while the efficiency of calcium carbonate precipitation was almost 100 % for Toyoura sand and its strength doubled, that for Edosaki sand was merely about 40 % and there was not a distinct increase in its strength. These findings might indicate that the effectiveness of biogrout could be hindered for sand with certain levels of fines content.

Keywords: soil improvement, biogrout, microbe, sand with fines, calcium carbonate precipitation

1. INTRODUCTION

Biogrout has a great prospect of mitigating soil-related disasters such as liquefaction and landslides while presenting the minimal level of harsh effects on the environment. Biogrout normally means a solution containing specific microbes, urea and calcium sources; they work to solidify soil as follows. Firstly, the specific microbes produce urease enzymes, which decompose urea into ammonia and carbon dioxide. Then, the ammonia raises pH in the surrounding environment, helping the carbon dioxide to become carbonate ion. With the presence of ample calcium ion in addition to the carbonate ion, calcium carbonate precipitation happens near particle-particle contacts among soil, eventually reinforcing soil structures and increasing its strength.

Many pieces of existing research has already suggested that biogrout can be effective in improving the soil in terms of its undrained behaviors (DeJong et al. 2006), unconfined compressive strength (van Paassen et al., 2009) and confined compressive strength (Whiffin et al., 2007). However, all of these studies employed soils which contain no or marginal amount of fines (i.e. soil particles smaller than 75 μm in diameter), partly owning to the convenience provided by high permeability of these soils, with which biogrout can readily infiltrate and induce calcium carbonate precipitation.

Several studies have been carried out in an attempt to cement clay or sand with high levels of fines content using biogrout, and difficulties were experienced in most cases. Rebata-Landa (2007) applied biogrout to kaolinite clay, which resulted in no precipitation of calcium carbonate. In the same study, survivability of microbes was examined by putting them in soils with various grain sizes under a wide range of overburden stress, and it was found that in the soils whose d_{10} (i.e. 10 % of the soil particles by weight is smaller than this value in diameter) is less than 1 μm, microbes are not likely to survive for longer than 72 hours under the overburden stress levels equivalent to a depth of 1 m or deeper from the ground surface. Mortensen et al. (2011) employed a fine soil whose d_{10} was 2 μm and came up with a similar result, showing delayed and reduced precipitation of calcium carbonate.

Among the possible contributing factors to the reduced calcium carbonate precipitation in sand with fines are mechanical constraints which prevent a smooth transfer of microbes to the soil, giving rise to their entrapment, and low permeability which often causes delayed delivery of biogrout, leading to the precipitation before biogrout is disseminated throughout the target soil. Hence, in this study an experiment was carried out, where biogrout was infiltrated at an increased flow rate into the specimen comprising sand with or without fines, in an attempt to make calcium carbonate precipitation occur in a better way in terms of its efficiency and distribution.

2. MATERIALS AND METHODS

2.1 Biogrout Preparation

As was already mentioned, biogrout is often recognized as urea-calcium ion medium containing microbes capable of producing urease enzyme. However, it was anticipated that it would take long duration to infiltrate biogrout into the specimen of Edosaki sand, meaning calcium carbonate precipitation could occur before the specimen is saturated with biogrout. Hence, biogrout was separated into microbial solution and cementation solution; the former contained the microbes and the latter was constituted of urea-calcium ion medium.

2.1.1 Microbial Solution

Microbial solution was prepared by inoculating an arbitrary amount of Sporosarcina pasteurii (ATCC 11859), which had been cultivated on culture plates, into 0.13M Tris buffer at around pH 9.0 that also contained 20 g of yeast extract and 10 g of ammonium sulfate per 1 liter. Yeast extract and ammonium sulfate were put into separate flasks containing Tris buffer, and they were sterilized at 121 ^{o}C for 20min before mixing. The recipe for the culture plate is identical to that for microbial solution except 20 g of agar per liter being added to make it gelled. After the inoculation, the solution was incubated for 24 to 26 hours at 30 ^{o}C in order to let the microbes to augment up to a stationary phase.

2.1.2 Cementation Solution

Cementation solution mainly comprised urea and a calcium source; the former provides energy for the microbes and the latter is essential to induce calcium carbonate precipitation. Specifically, cementation solution employed in the experiment contained 30.03 g of urea, 73.507 g of calcium chloride bihydrate, 3 g of nutrient broth, 10 g of ammonium chloride and 2.12 g of sodium bicarbonate per liter of distilled water. Nutrient broth provides necessary nutrition for the microbes to augment, and ammonium chloride and sodium bicarbonate stabilize pH levels of the solution. Cementation solution was not sterilized prior to the injection to the specimen. All the chemicals used to prepare microbial and cementation solution were obtained from Wako Pure Chemical Industries, Ltd., Japan.

2.2 Specimen Preparation

The specimen of Toyoura sand (G_s = 2.656, e_{max} = 0.992, e_{min} = 0.632, d_{50} = 180 μm, F_c = 0 %) was prepared by water-pluviating the sand into a cylindrical plastic mold (ϕ50 mm×100 mm), aiming at a relative density of 90%. A filter paper was placed at the top and bottom of the sand column to prevent a loss of sand particles. As for the specimen of Edosaki sand (d_{50} = 156 μm, F_c = 17.5 %), the water-pluviation method was not applicable since Edosaki sand has high fines content and those fine particles were expected to be suspended in the water instead of being deposited with the larger particles, making it difficult to prepare a specimen with uniform grain size distribution. Hence, Edosaki sand had been compacted into the mold using a brass rod until its dry density was stabilized at 1.55 g/cm^3, and then a filter paper were put at the top and bottom of the column. Figure 1 shows the grain size distribution of Toyoura sand and Edosaki sand.

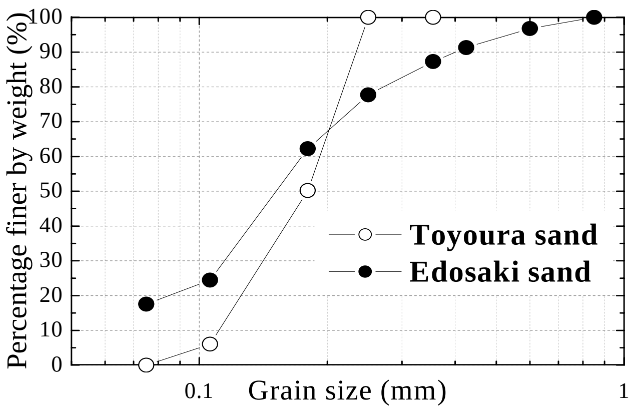

Figure 1: Grain size distribution of Toyoura sand and Edosaki sand

2.3 Test Procedures

2.3.1 Specimen Solidification with Biogrout

The specimen was fitted with an acrylic hollow cylinder at the top of the mold and a plastic tube at the bottom so that the infiltration of biogrout (i.e. microbial solution and cementation solution) from the top to the bottom would take place. The tube was connected to a small tank where negative pressure was applied to control the flow rate of biogrout (Figure 2), and microbial solution was transferred firstly to the specimen followed by cementation solution. Various levels of negative pressure were used, ranging from 0 kPa to -40 kPa, and the pressure was adjusted manually so that hydraulic gradient could be maintained when the water level declined as the infiltration proceeded. 90 ml of microbial solution and cementation solution were used for the solidification of a single specimen. Further details about test conditions for each specimen are summarized in Table 1. The infiltration was stopped while the top surface of the column was still slightly covered by the solution. The specimen was detached from the tank after the infiltration, and its top and bottom end were sealed properly in order to prevent drying of the sand. The specimen was retained for 20 hours after the infiltration of cementation solution had started, in order to let calcium carbonate precipitation develop. Then, distilled water was added from the top to cease the precipitation process and to wash out all the remaining chemical substances in the specimen.

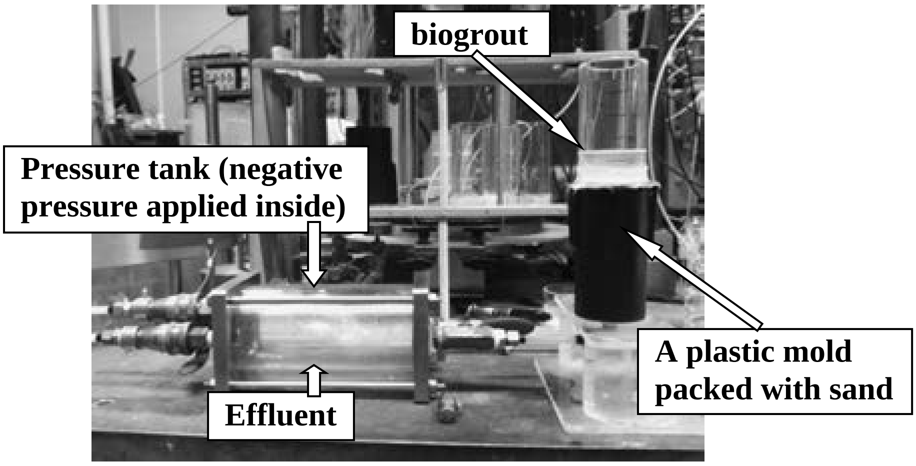

Figure 2: Infiltration of biogrout to the specimen

2.3.2 Measurement Procedures

The degree of cementation and its distribution were evaluated by needle penetration tests, in which the cemented sand column was pierced for a designated depth (e.g. 20 mm for Toyoura sand and 30 mm for Edosaki sand) from the top surface with a needle whose diameter was 3 mm. The resistance on the needle was recorded as it descended in the specimen at a speed of about 30 mm/min. After the first layer was done, it was excavated from the mold, and the next layer underwent the test. This had been repeated until the entire column was finished with the penetration test. In addition, the amount of precipitated calcium carbonate was estimated in two different ways; one was based on the concentration of calcium ion in the effluent of cementation solution ejected from the specimen (i.e. chemical efficiency), and the other is derived by comparing the weight difference of the specimen before and after the treatment (i.e. precipitation efficiency). The effluent was also examined to assess its pH level.

3. RESULTS AND DISCUSSION

The results of penetration tests are shown in Figure 3 and 4. Specifically, the results with the specimen of Toyoura sand are shown in Figure 3, and Figure 4 reveals those of Edosaki sand. Each symbol shown in the graphs (e.g. 1-a) corresponds to a combination of Test number and Column in Table 1.

Table 1 : Test conditions and results for each specimen

Test number	1					2				
Column	a	b	c	d	BM	a	b	c	d	BM
Material	Toyoura sand					Edosaki sand				
Relative density (%)	89.3	91.1	96.9	91.5	102.5	-	-	-	-	-
Dry density (g/cm^3)	1.59	1.60	1.62	1.60	1.64	1.55	1.55	1.55	1.55	1.55
Hydraulic gradient for MS	30	40	10	1	-	5	30	5	1	-
Duration of MS infiltration (min)	0.46	0.78	1.2	3.2	-	68	34	80	380	-
Hydraulic gradient for CS	1	1	1	1	-	5	5	5	1	-
Duration of CS infiltration (min)	5.8	6.8	7.0	4.6	-	93	112	95	-	-
Chemical efficiency (%)	96.5	97.3	98.1	97.0	-	12.7	27.6	0	38.6	-
Effluent pH	7.5	7.3	7.5	7.3	-	7.1	7.0	6.8	6.8	-

Note: MS = microbial solution; CS = cementation solution; BM = benchmark

In the case of the specimen of Toyoura sand, calcium carbonate precipitation successfully took place with high degrees of chemical efficiency; it was almost 100 % for all the treated specimens. The strength of the sand represented by penetration resistance is about twice as high as that of the benchmark result (i.e. no treatment with biogrout) at the end of each layer: as high as 40 N for the untreated benchmark specimen compared to up to 200 N for the solidified specimen with biogrout. In addition, it can be inferred that the quicker the infiltration of microbial solution was, the more uniform precipitation happened, since the relationships between penetration depth and resistance for different layers were more similar to each other as the duration of the infiltration was shortened. Note that the drop in penetration resistance near the end of the fifth layer is because of the outlet hole drilled at the bottom of the mold, which provided much less penetration resistance to the needle compared to the upper layers, so the decrease in the fifth layer can be ignored.

(a)

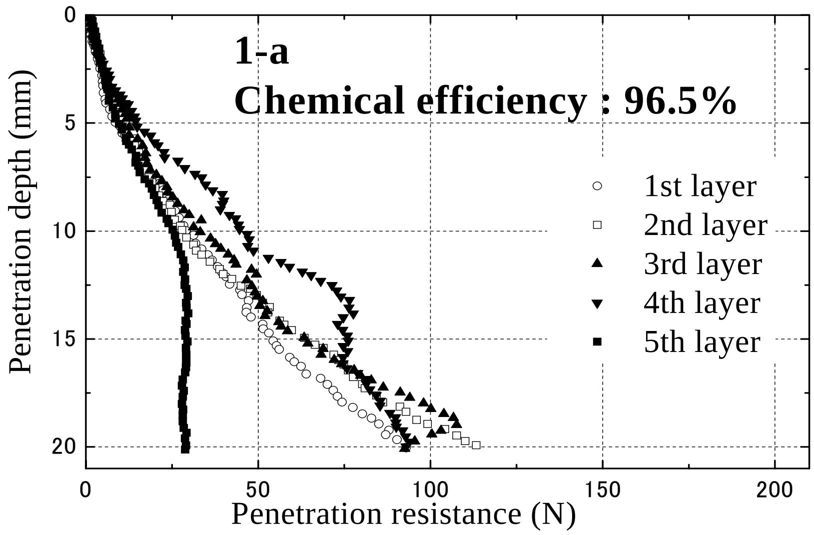
1-a
Chemical efficiency : 96.5%
1st layer
2nd layer
3rd layer
4th layer
5th layer
Penetration depth (mm)
Penetration resistance (N)
0
5
10
15
20
0
50
100
150
200

(b)

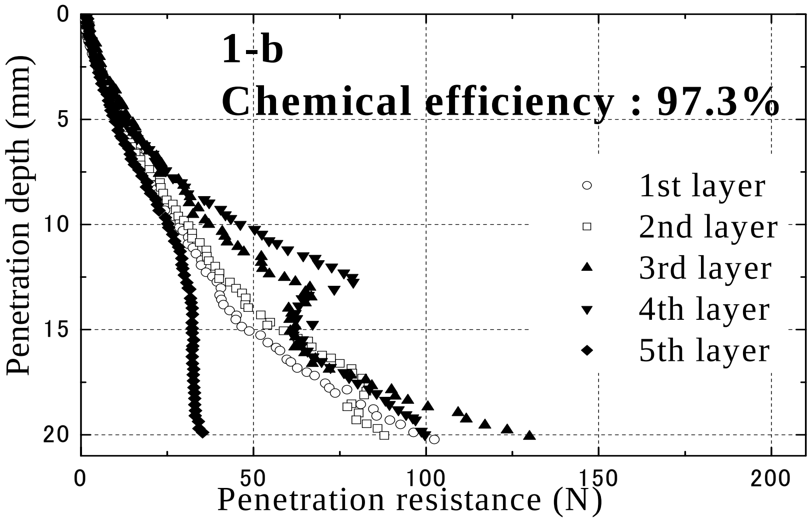
1-b
Chemical efficiency : 97.3%
1st layer
2nd layer
3rd layer
4th layer
5th layer
Penetration depth (mm)
Penetration resistance (N)
0
5
10
15
20
0
50
100
150
200

(c)

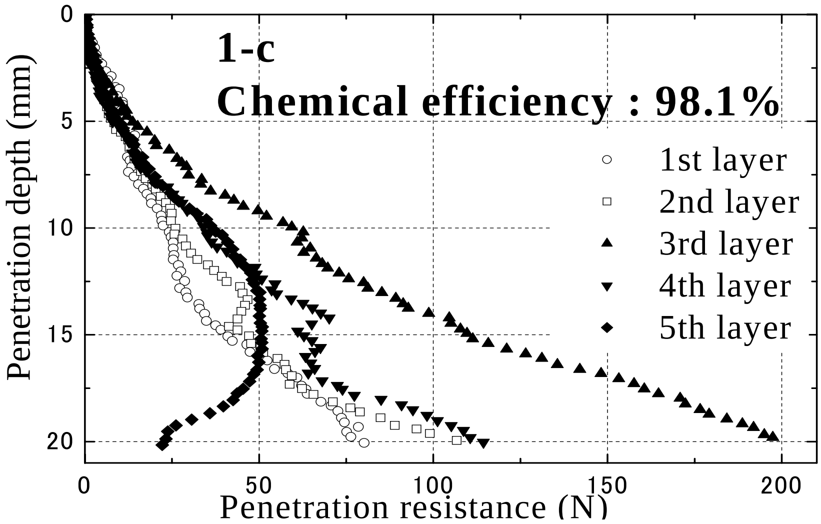
1-c
Chemical efficiency : 98.1%
1st layer
2nd layer
3rd layer
4th layer
5th layer
Penetration depth (mm)
Penetration resistance (N)
0
5
10
15
20
0
50
100
150
200

(d)

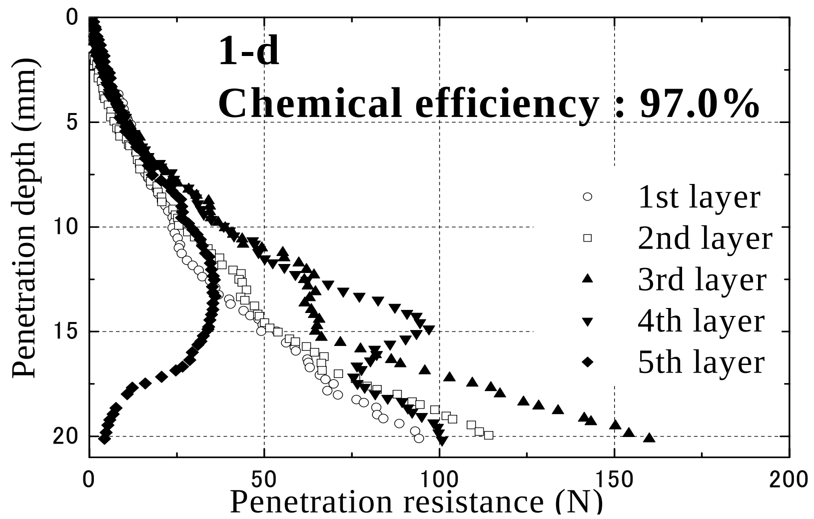

(e)

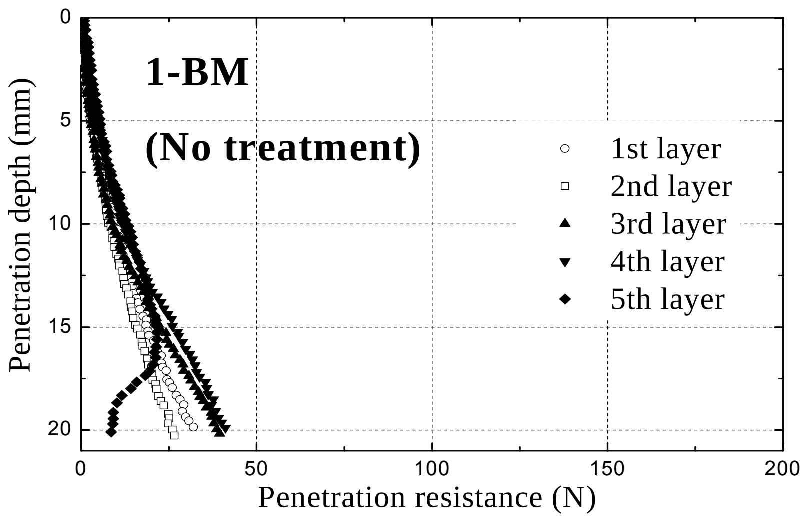

Figure 3: Result of penetration tests for the specimen of Toyoura sand; (a) ~ (d) solidified specimens with biogrout; (e) untreated specimen

(a)

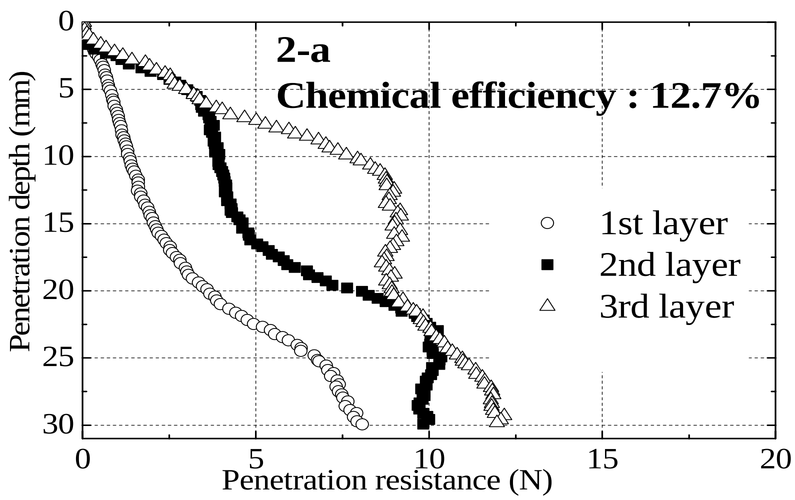

(b)

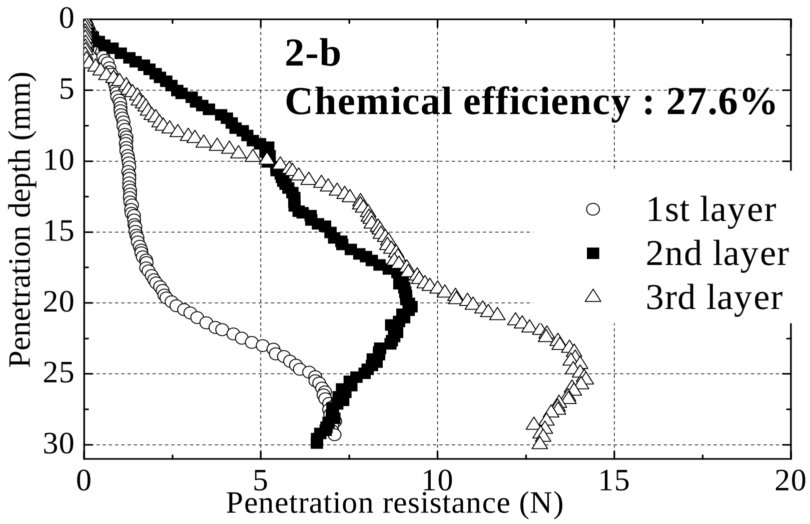
2-b
Chemical efficiency : 27.6%
1st layer
2nd layer
3rd layer
Penetration depth (mm)
Penetration resistance (N)
0
5
10
15
20
25
30
0
5
10
15
20

(c)

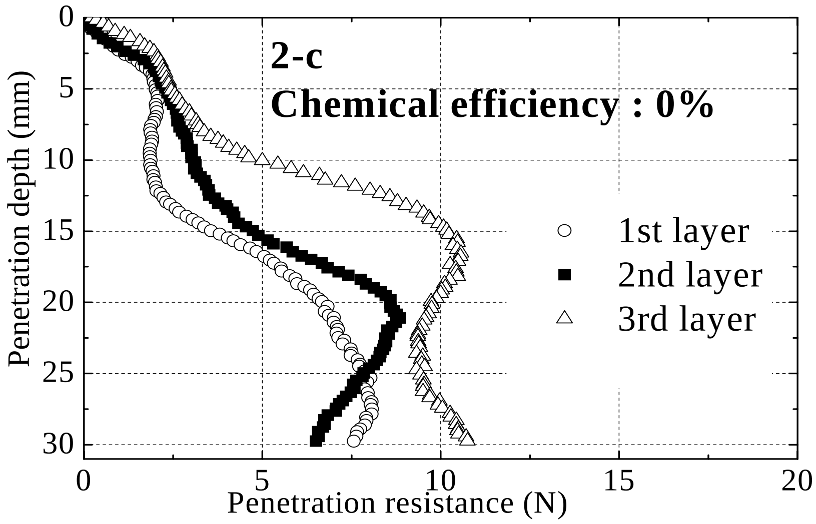
2-c
Chemical efficiency : 0%
1st layer
2nd layer
3rd layer
Penetration depth (mm)
Penetration resistance (N)
0
5
10
15
20
25
30
0
5
10
15
20

(d)

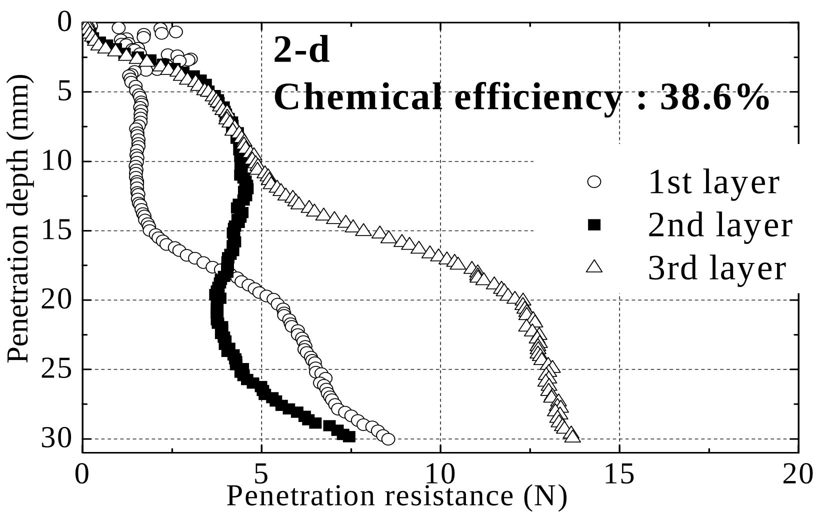
2-d
Chemical efficiency : 38.6%
1st layer
2nd layer
3rd layer
Penetration depth (mm)
Penetration resistance (N)
0
5
10
15
20
25
30
0
5
10
15
20

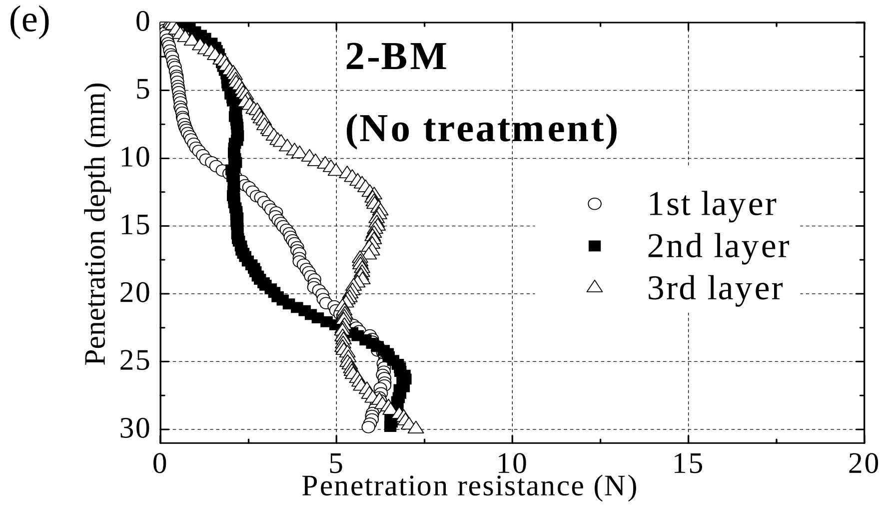

Figure 4: Result of penetration tests for the specimen of Edosaki sand;
(a) ~ (d) solidified specimens with biogrout; (e) untreated specimen

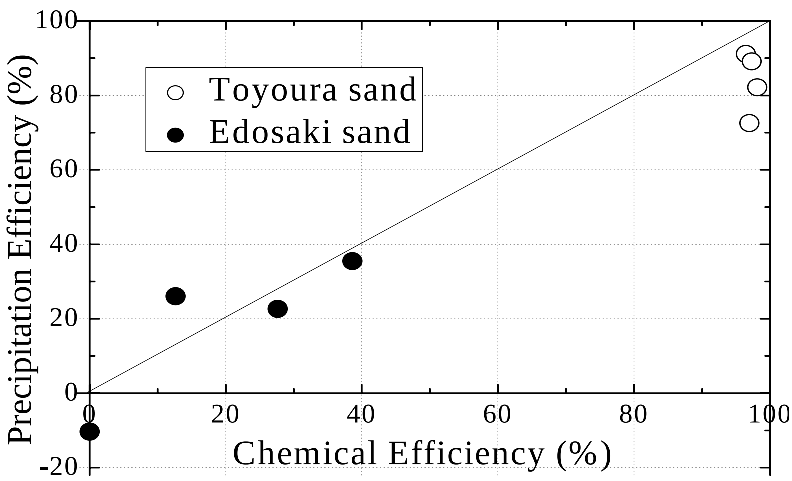

Figure 5: Correlation between chemical and precipitation efficiency

On the other hand, biogrout seemed ineffective in solidifying the specimen of Edosaki sand as the increase in penetration resistance was minimal compared to the benchmark result. Moreover, chemical efficiency was merely as high as about 40 % and no precipitation occurred in one of the specimens treated with biogrout. This tendency was further evidenced by the low pH levels in the effluent, which imply that there was not as successful microbial decomposition of urea in Edosaki sand as in Toyoura sand. Quicker transfer of biogrout by higher hydraulic gradient appeared meaningless in helping the distribution of the precipitation become more uniform in Edosaki sand as opposed to the case of Toyoura sand; the bottom layer saw the biggest increase in penetration resistance for most of the treated specimens regardless of test conditions, although usually precipitation of calcium carbonate (i.e. increase in the strength) tends to concentrate near the inlet of the specimen from which biogrout is infiltrated (Martinez et al. 2011, 2013, Mortensen et al. 2011, Whiffin et al. 2007, van Paassen et al. 2009). These results might suggest that microbes could not attach themselves on the surface of soil particles when microbial solution was infiltrated into the specimen and were washed out during the subsequent infiltration of cementation solution, leaving the residual microbes around the bottom of the specimen. Whether this was caused due to the presence of fines or other factors including effects of minerals in Edosaki sand needs to be investigated.

The correlation between precipitation efficiency and chemical efficiency is shown in Figure 5. It seems that the efficiency acquired by measuring the concentration of residual calcium ion in the effluent (i.e. chemical efficiency) yields similar values to the ones derived by comparing the weight difference of the specimen before and after the treatment (i.e. precipitation efficiency), indicating that chemical efficiency can be used as an alternative to estimate the amount of precipitated calcium carbonate in the soil.

4. CONCLUSIONS

In this study, biogrout was used to solidify the specimen of Toyoura sand and Edosaki sand, with only the latter having fines content. Even though Toyoura sand was readily cemented with calcium carbonate, with its strength almost doubled, Edosaki sand was precipitated with merely 40 % maximum possible amount of calcium carbonate, resulting in no distinct increase in the strength. The pH levels in the effluent also demonstrated this tendency; lower values were recorded for Edosaki sand, indicating that the microbes were not active enough to decompose all the urea molecules in biogrout. Potential causes for the reduced precipitation of calcium carbonate in Edosaki sand need to be investigated, in order to find a way to effectively solidify sand with fines using biogrout.

REFERENCES

Dejong, J.T., Fritzges, M.B. and Nüsslein, K. (2006):"Microbially induced cementation to control sand response to undrained shear", *J. Geotech. Geoenviron. Eng.*, 132, pp1381-1392

Martinez, B.C., DeJong, J.T., Ginn, T.R., Montoya, B.M., Barkouki, T.H., Hunt, C., Tanyu, B. and Major, D. (2013): "Experimental optimization of microbial-induced carbonate precipitation for soil improvement", *J. Geotech. Geoenviron. Eng.*, 139, pp587-598

Martinez, B.C., Barkouki, T.H., DeJong, J.T. and Ginn, T.R. (2011); "Upscaling of microbial induced calcite precipitation in 0.5m columns: experimental and modeling results", *Proc., ASCE Geo-Frontiers 2011 Conf.*, ASCE, Reston, VA., pp4049-4059

Mortensen, B.M., Haber, M.J., DeJong, J.T., Caslake, L.F. and Nelson, D.C. (2011): "Effects of environmental factors on microbial induced calcium carbonate precipitation", *Journal of Applied Microbiology*, 111, pp338-349

Rebata-Landa, V. (2007): *Microbial activity in sediments: effects on soil behavior*, Doctoral Dissertation, Georgia Institute of Technology, Atlanta, GA, U.S.A.

van Paassen, L.A., Harkes, M.P., van Zwieten, G.A., van der Zon, W.H., van der Star, W.R.L. and van Loosdrecht, M.C.M. (2009): "Scale up of BioGrout: a biological ground reinforcement method", *Proc., the 17th International Conference on Soil Mechanics and Geotechnical Engineering*, pp2328-2333

Whiffin, V.S., van Paassen, L.A. and Harkes, P.M. (2007): "Microbial carbonate precipitation as a soil improvement technique", *Geomicrobiology Journal*, 24, pp417-423

The deformation of flexible pipe buried in soil with different degree of compaction

Ngoc Duyen NGUYEN[1] and Reiko KUWANO[2]
[1]Master Student, ICUS, IIS, the University of Tokyo, Japan
duyen@iis.u-tokyo.ac.jp
[2] Professor, ICUS, IIS, The University of Tokyo, Japan

ABSTRACT

Flexible pipes have been utilized widespread in over the world for water, gas, sewage pipelines and many other purposes, especially in megacities. The need for studies on pipes becomes necessary for design and construction. One of important factors affecting its performance is the compaction of backfill around the pipe. Moreover the pipe's behavior under cyclic loading has not been fully investigated. A series of model tests with different degree of compaction has been conducted using the 32 sensor mounted pipe. It was found that with the better backfill compaction the lesser deformation the pipe showed. The study also clarifies the change in pipe deformation under the cyclic loading. The bending strain in the looser backfill compaction at the last cyclic loading is largely higher than the dense case, which further proves the importance of compaction work in practice. The performance of buried pipe when the backfill soil was improved only around the pipe was also studied.

Keywords: *flexible pipe, cyclic loading, deformation, density of backfill.*

1. INTRODUCTION

The urbanization and expanding the big cities in all over the world are the reasons for the large application of pipes such as water supply, sewage and many other purposes. Therefore, research for the influential factors on their lifespan plays an important role. Besides the subjective factors such as pipe stiffness (PS), site conditions, etc., backfill compaction and loading modes also significantly impact on pipe behavior. The role of compaction has been affirmed, however, the performance under the cyclic loading which is another form of traffic loading has not been fully investigated. A series of model tests with different degree of compaction under the cyclic loading has been conducted using the 32 sensor mounted pipe.
This paper presents the results of this series of experiments, which again confirm the critical effect of compaction to the buried pipe performance. Additionally, the behavior of buried pipe when backfill soil was improved only around the pipe was also studied. Under the same cyclic loading mode, the extent of deformation belongs to the pipe is clarified.

2. METHODOLOGY

2.1 Material

The material using for experiments is silica sand, the artificial standard sand for laboratory, which is fine-sized, uniformly graded sand. It is milky white in color with mostly well-rounded particles. Manufactured by grinding the natural rocks with specific strength, the silica sand has become a good substitute for the natural sands.

In this research, silica sand No. 7 was used. Figure 1 exhibits the grain size distribution curve.

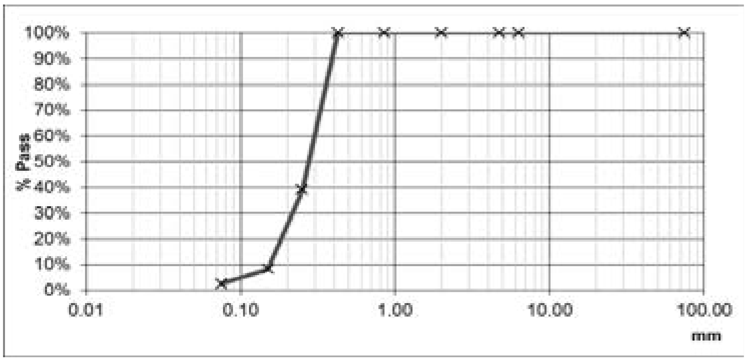

Figure 1: Grain size distribution curve of silica sand No. 7

2.2 Apparatus

2.2.1 Soil chamber

The experiments were all conducted in a large soil chamber having a dimension of 98 cm long, 40 cm wide and 80 cm high. The chamber which is made of transparent acrylic board is strong enough so that not to be deformed in the experiments.

2.2.2 Automated stress-controlled loading system

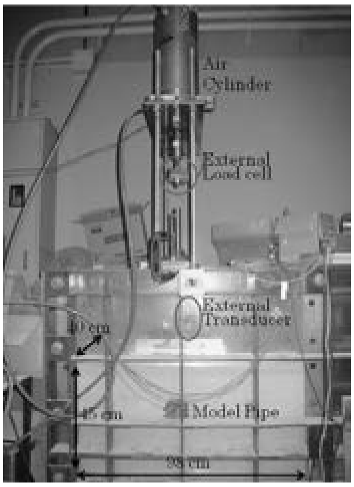

Figure 2: Soil chamber and loading system

The loading apparatus is automated stress-controlled loading system that consists of a bellofram cylinder, a pressure tank, E/P transducer, regulators and boosters. The air pressure is applied and amplified by control panel. Figure 2 shows the soil chamber and loading system.

2.2.3 Model Pipe

The model pipe is PVC pipe (VU125 – 140 mm diameter and 4.1 mm thick). In order to fully study the pipe behavior, the normal stress, shear stress and deformation of pipe were taken into account, which were derived from the sensors evenly attached on the pipe at different location. The sensor quantity is as in Table and theirs allocation is as Figure 3.

Table 1: The sensor quantity

Force	Quantity
Normal stress	08
Shear stress	08
Inner strain	08
Outer strain	08
Vertical displacement transducer	01
Horizontal displacement transducer	01

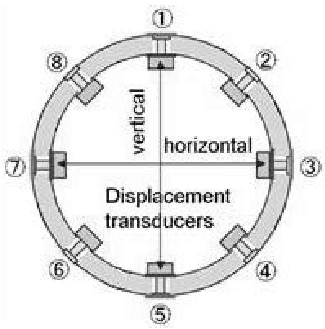

Figure 3: The sensor allocation

The two-way load cells have been utilized to measure the normal stress and shear stress; the strain gauges that attached directly to the pipe are used to measure the strain inner and outer of buried pipe. Figure 4 shows imagines of the two-way load cell and strain gauge that were used in these experiments.

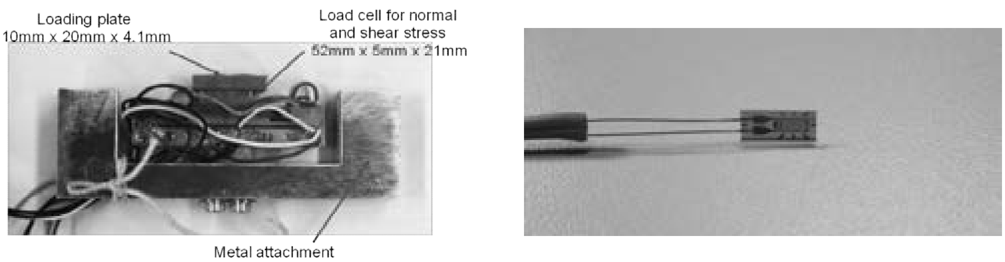

(a) (b)

Figure 4: Two-way load cell (a) and strain gauge (b)

2.3 Testing procedure

The experiments were all conducted in the soil chamber. To completely describe the interaction between backfill and pipe as well as the effect of different degree of compaction under the cyclic loading, the subsequences of the tests were the same except for the relative density of the initial backfill around the pipe: loose (Case 1), dense (Case 2) and improved backfill only around the pipe (Case 3). All the model grounds were prepared by the air pluviation method. The relative density for two states loose and dense is 33% and 89%, respectively. Figure 5 shows the experiment schematic of Case 1, Case 2 and Case 3.

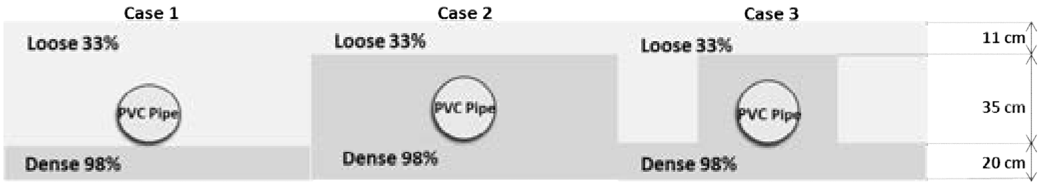

Figure 5: Experiment schematic

The pipe was placed on the 20 cm thickness of dense sand as the base. Then, the backfill of which relative density was controlled by the size of the hole in the metal plate was pouring into the soil chamber from the constant height. The footing plate made of high stiffness duralumin was placed onto the surface. Finally, the cyclic loading was applied.

Due to the high stiffness of soil chamber and footing plate, the model tests were all considered to be one-dimensional compression. A vertical pressure of 10 kPa was first applied, then a cyclic loading of 50 kPa following by 30 minutes creep. Each loading stage including cyclic loading and creep repeated 3 times.

3. RESULTS

3.1 Footing settlement

Under the cyclic loading, the ground surface tends to settle down. Its magnitude depends mainly on the compaction of backfill. Among three cases, Case 1 is predicted to have the largest displacement, following by Case 3 and Case 2. However, the disparity in magnitude of three cases needs clarifying.

The experiment results show the close coincidence with the expectation. Undergoing 50 kPa cyclic loading, the settlement magnitude of Case 1 is as twice as Case 2. However, Case 2 and Case 3 exhibit the similar movement. Figure 6 shows the relationship between displacement and vertical tress in three cases.

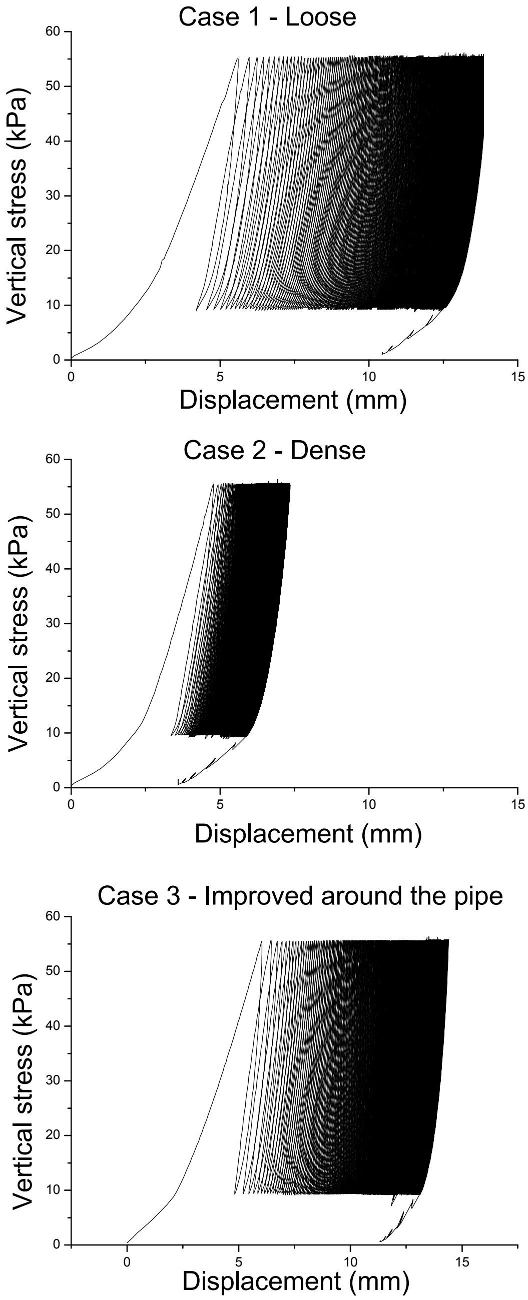

Figure 6: The relationship of vertical stress and displacement in three cases

In Case 3, there was no stable boundary between the dense and loose backfill around the pipe, which means when the model pipe was subjected to the cyclic loading, there was a shift in these two zones. This shift became larger when the pipe experienced three-stage cyclic loading, which reasons for why even when the pipe was improved by denser backfill around, the displacement is the same with Case 1.

3.2 Pipe deformation

Three cases of experiment investigated the reaction of buried pipe when cyclic loading applied in three stages for 100 cycles. The stress acting on the pipe in vertical and horizontal direction was plotted against the respective displacement of the pipe.

The Figure 7 shows the relationship in vertical displacement in dense and loose case. The normal stress was derived by LC1 and LC5 against the pipe's vertical displacement. It is clear that in Case 2 the displacement is critically smaller than in Case 1 not only in the magnitude of displacement but the normal stress as well. Moreover, the recorded data in LC1 and LC5 (approximately 150 kPa) exceeded the loading applied (60 kPa) causes wondering. The reason for this phenomenon can be explained by arching effects. Arching effect is stress redistribution by which stress is transferred a region of soil mass, which then subjected to lower stress. In loose backfill, the sand around the pipe is stronger than the other areas. That is the explanation when the model pipe undergoes the cyclic loading, these area support larger load than other zones.

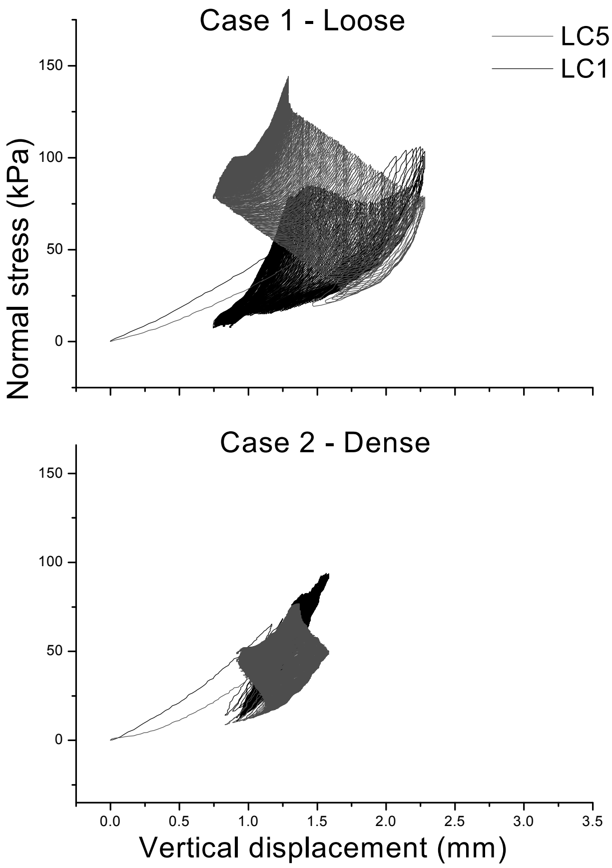

Figure 7: The relationship of vertical displacement and normal stress in Case 1 and Case 2

The influence of cyclic loading involving the direction is apparently different. In one-dimensional loading condition, especially the cyclic loading was vertically oriented; the magnitude of normal stress and displacement in lateral direction should be lesser than the other way. This expectation was proved when plotting the horizontal displacement against the normal stress (LC3 and LC7)

The Figure 8 presents the comparison in Case 1 and Case 2 in horizontal direction. In spite of the smaller magnitude than in vertical condition, the denser backfill still shows the lesser displacement and normal stress acting on the pipe.

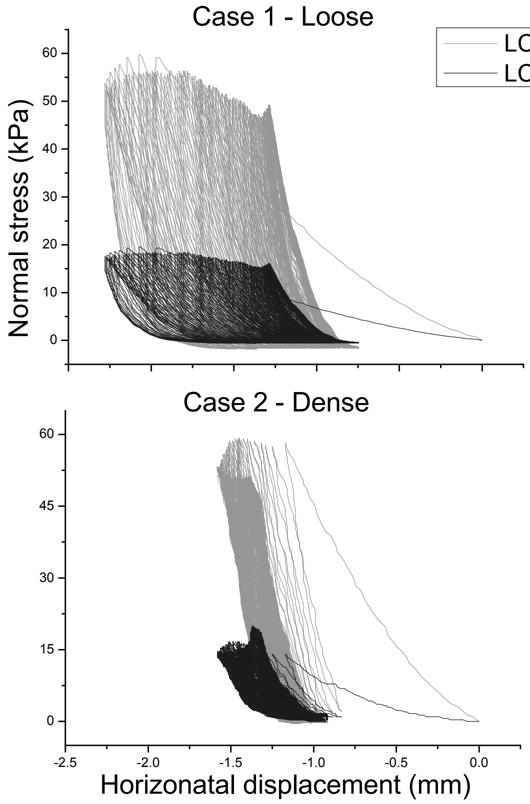

Figure 8: The relationship of horizontal displacement and normal stress in Case 1 and Case 2

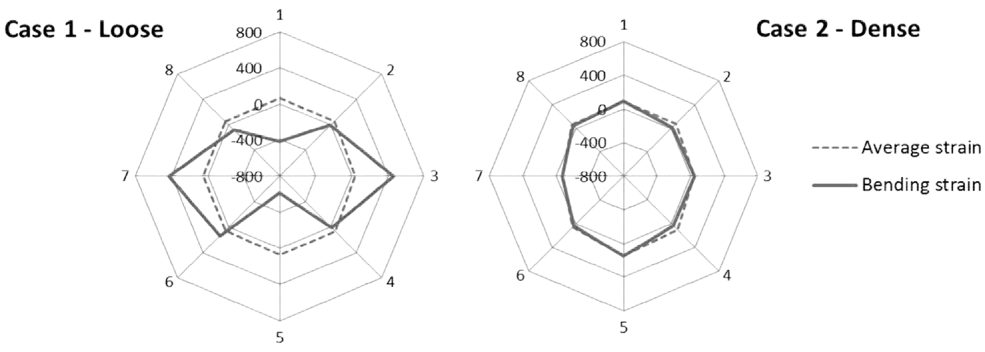

Figure 9: Bending strain in 100th cycle

Besides load-cells attached on the pipe, there are 16 strain gauges mounted inside and outside which reported the bending strain. Bending strain provides how much the pipe is bent by averaging the difference of inner and outer strain. Figure 9 shows the bending strain in Case 1 and Case 2 in the last cycle of loading.

Bending strain in the last 100th cycle in Case 1 is greatly larger than in Case 2, which means that in loose sand, the pipe is much easier to deform than in the dense case, while in Case 2 there is a slightly different in two parameters. The model pipe also has intention to deform in lateral direction, expressing in larger magnitude at location number 3 and 7. This result once again confirms the importance of the backfill compaction to the pipe behavior.

3.3 Effect of cyclic loading

The effect of cyclic loading is clarified by plotting the normal stress against the elapsing time. In loose backfill (Case 1) the vertical stress decreased, meanwhile the horizontal stress increases when raising the loading number. Reversely, for the denser backfill Case 2 expressed the same behavior with the slightly change in both vertical and horizontal stress. In another hand, for Case 3, the normal stress at locations except number 5 exhibited the same behavior with Case 2. At location 5, the normal stress increased gradually. Figure 10 presents the relationship of elapsing time and normal stress in all locations in three cases.

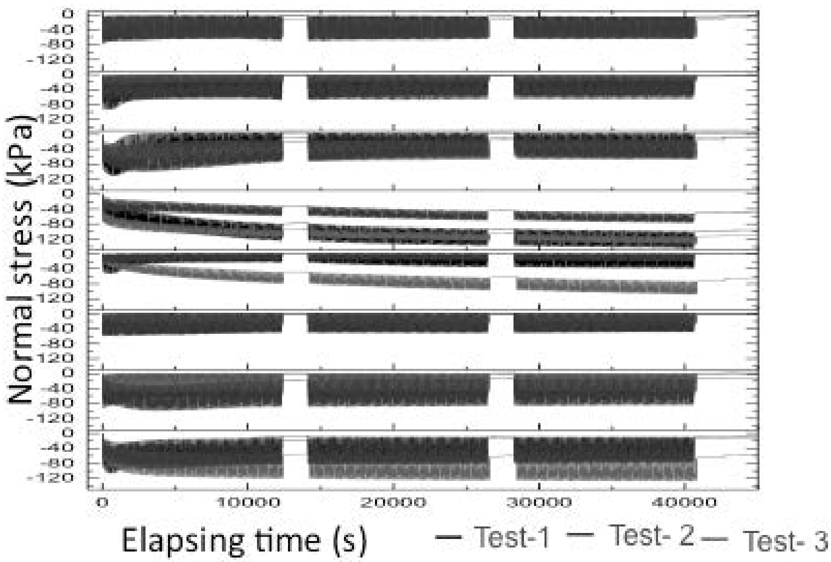

Figure 10: The relationship of elapsing time and normal stress

Due to the confinement in Case 2, normal stress according to elapsing time did not change much. However, as mentioned above, the Case 3 had no stable boundary, the movement of sand around the pipe also caused the increase in normal stress.

3. CONCLUSION

The results of a series of experiment achieved so far have confirmed the role of compaction to the pipe behavior.

1, The dense of backfill influence on the ground surface settlement as well as the displacement of the pipe subjected to different direction. The denser the backfill is compacted, the lesser the magnitude of settlement and deformation of buried pipe achieve.
2, The bending strain in the dense backfill is much smaller than in the loose case.
3, When the buried pipe experiences the cyclic loading, the normal stress acting in vertical orientation gradually reduces while horizontal normal stress increases progressively in loose backfill. On contrary, in dense backfill compaction the normal stress in both horizontal and vertical direction does not change much.
4, The buried pipe when the backfill soil is improved around shows the same behavior to the dense case, however because of the unstable boundary also the effect of cyclic loading, the settlement of footing surface is still large.

REFERENCES

Ko, Donghee, 2010. *Behavior of flexible liner in buried double-layered pipe by trenchless renewal*. Doctor Thesis, The University of Tokyo.
Clarke, N.W.B, 1968. *Buried pipelines – A manual of structural design and installation.* Maclaren And Sons London.
Plastic Pipe Institute. *Handbook of PE Pipe.* http://plasticpipe.org/publications/pe_handbook.html

Triaxial test for the evaluation of internal erosion

Mari SATO[1], Reiko KUWANO[2]

[1]Ph.D Student, Dept. of Civil Engineering,
Faculty of Engineering, the University of Tokyo, Japan
msato@iis.u-tokyo.ac.jp
[2] Professor, ICUS, IIS, the University of Tokyo, Japan

ABSTRACT

Internal erosion is the phenomenon washing fine particles out of the ground. It causes various ground disaster such as cave-in accidents and landslides, those are supposed to happen due to water penetration into the ground with rainfalls. Underground water penetration is sometimes concentrated at a certain area such as a boundary of fill and original ground, and surroundings of underground structures. Therefore it is considered that internal erosion repeatedly occurs peculiar areas with rainfalls, but influence of repetition of internal erosion on the mechanical properties of soil is not well understood.
In this research, new triaxial test apparatus was setup for the evaluation of the influence of internal erosion on the soil. A pedestal of the triaxial apparatus had small holes which allow soil particles outflow when applying high hydraulic gradient. In addition, soil stiffness was measured by cyclic loadings.

Keywords: *internal erosion, landslides, cave-in accident, triaxial test 1*

1. INTRODUCTION

Many ground disasters are caused by underground water flow[1)]. Water flow sometimes concentrates at the gaps between original fills and buried fills, where internal erosion happens. Internal erosion was a phenomena of soil particle loss inside the ground through water flow. Large amount of internal erosion caused collapse of the ground, which had been studied mainly about rock-fill dams. On the other hand, small amount of internal erosion had not been studied so much. It supposed to occur repeatedly by rainfall but the influence of small amount of internal erosion on the ground was not clarified.

In this study, triaxial test apparatus for internal erosion was installed for evaluating influence of internal erosion on soil stiffness and deformation.

2. TEST APPARATUS AND PROCEDURE

Schematically figure was shown in Figure 1 and picture was shown in Figure2. The bottom and upper plate of the apparatus had many holes as shown in Figure 3. Each hole’s diameter was 5mm. Soil specimen’s size was 160mm height and 75 mm diameter. 3 LDTs and 3 Clip gages were adapted.(Referring to Figure 4) LDT was for vertical displacement and Clip gage was for radial displacement. EDT was put outside the specimen, which was not accurate such as LDT and Clip gage but had longer ranges than those. The position of LDTs and Clip gages on the specimen was shown in Figure 4.

Test procedure was shown as below. First, mesh paper which was changed by the test conditions (Referring to chapter 2) was put on the bottom plate and below the upper plate. Then specimen was compacted under the optimum water content (around 14%). Specimen was kept on 25kPa confining compression stress putting by cell pressure, which was monitored by HCDPT. Inside the specimen was kept on atmospheric pressure. LDTs and Clip gages were fixed like Figure 4. After the specimen preparation, Water was infiltrated from an outside water tank, simulating the condition under the ground under water level. After water infiltration, 2 water tanks were connected to the specimen like Figure 1. One was connected to the top of the specimen and the other was connected to the bottom of the specimen. In this paper, one was called “upper water tank” and the other was called “bottom water tank”. -75kPa, negative pressure was put on the bottom tank for making downward water flow from upper tank to the bottom tank. Upper water tank was released to the atmospheric condition during the downward water flow. Load cell was put to each water tank, which the change of the weight of the tank was measured. Mesh paper controlled the amount of internal erosion by downward water flow. Weight of soil loss and turbidity of drained water was measured. Turbidimeter was 2100P, made by © Hach, which applied nupherometory method. Turbidity was represented by the unit “NTU”. Larger value meant water got cloudier. (Referring to Figure 5

After the downward water flow, the specimen was sheared with 0.06%/min with drained condition. During the test, 0.002% vertical strain of 11 times cyclic loading was carried out 3 times:1) after the preparation of the specimen 2) after the water infiltration 3) after the downward water flow to measure the Young’s Modulus and Poisson’s ratio.(Reffering to Figure 6)

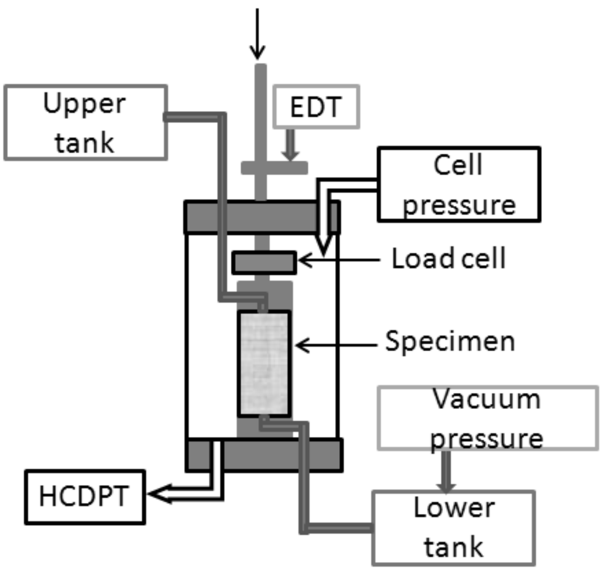

Figure 1. Schematic figure of test apparatus

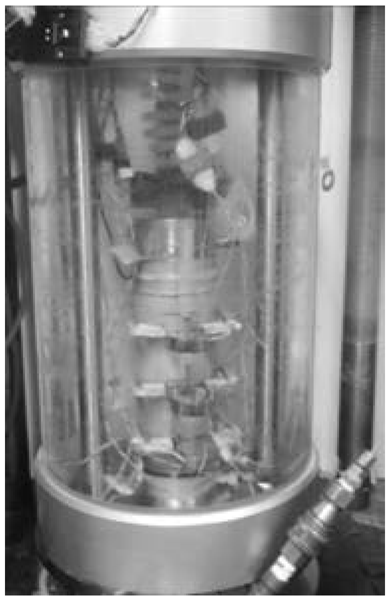

Figure 2. Photo of test apparatus

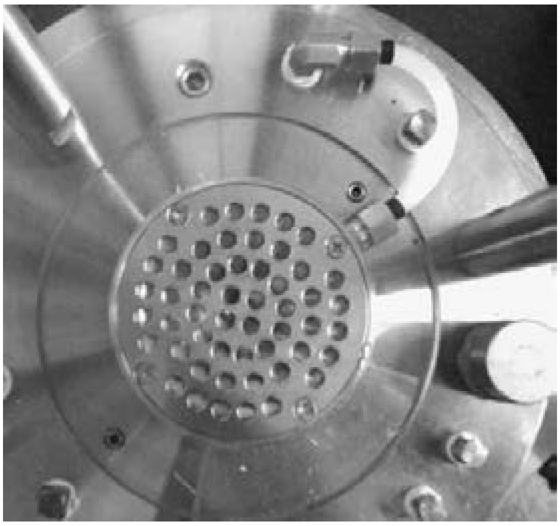

Figure 3 The bottom plate of test apparatus

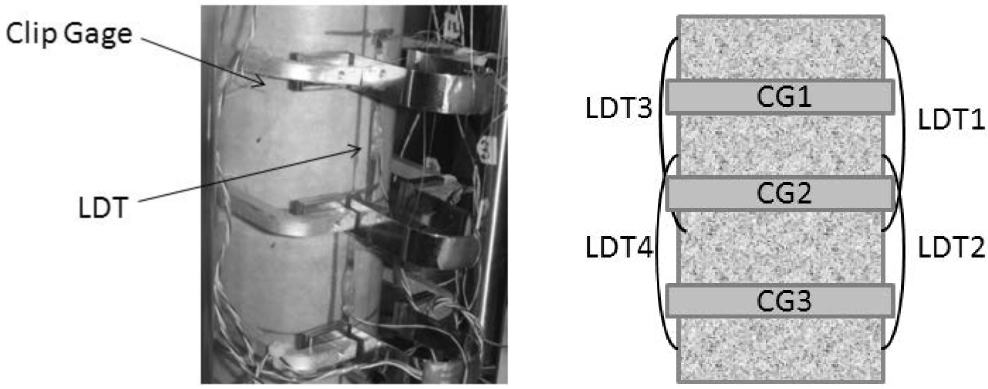

Figure 4. LDT and Clipgage (left: photo, right: position)

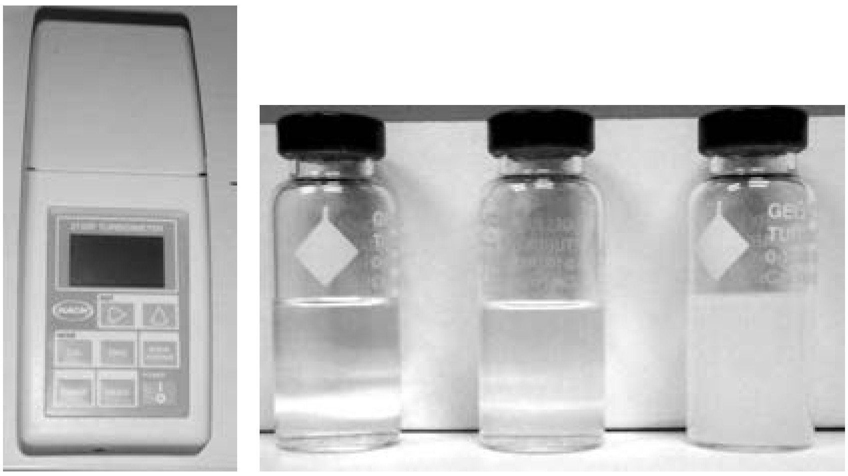

Figure 5. Turbidimeter(left) and sample cells(right)

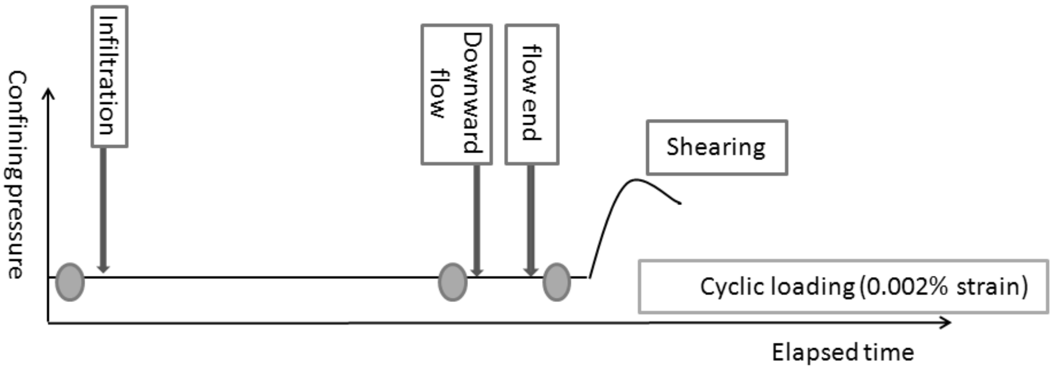

Figure 6 Schematic figure of test procedure

2. TEST CONDITIONS

All experimental conditions were shown in Table 1. Test material was Edosaki sand (ρ dmax=1.76g/cm^3 , W_{opt}=14.2%, ρ s=2.705g/cm^3, e_{min}= 0.868, e_{max} = 1.383) and particle size distribution of that was shown in Figure 7. From Figure 7, Edosaki sand was "unstable material" which was suggested by Kenny et al. (1985)[2)]. Dc (Compaction Degree) was a value before downward water flow, which was estimated from initial condition and deformation during water infiltration.

5 different kinds of mesh paper were applied; filter paper, cloth, 1mm mesh paper, 0.05mm mesh paper and holes of filter paper. Filter paper and cloth prevented almost all internal erosion. Especially filter paper prevented internal erosion completely. 1mm mesh paper and 0.05mm mesh paper caused some amount of erosion. The amount was larger in 1mm mesh. 0.05mm mesh paper only made fine particles' erosion. 2 holes were made in the filter paper mean "2holes". Each hole's size was 5mm diameter. This condition caused internal erosion easiest.

The amount of inflow water was changed in some test conditions. Twice and 5 times means twice or 5 times amount of water was flowed down as other test conditions' (around 1.5L)

Table 1. Test conditions

Code	Soil loss(%)	Turbidity	Soil loss	Dc
1mm212	0.18	580	Small	86.7%
0.05mm217	0.06	328	Small	85.8%
filterpaper227	0	1.92	Limited	85.8%
twice305	0.4	862	Small	85.5%
4times509	0.61	1265	Large	86.2%

rosi524	0	8.65	Limited	85.2%
1mm610	0.21	598	Small	83.8%
2holes619	0.993	1500	Large	85.2%
2holes630	0.873	1140.3	Large	84.9%
cloth703	0.03	141	Limited	85.3%
cloth708	0	53	Limited	86.4%

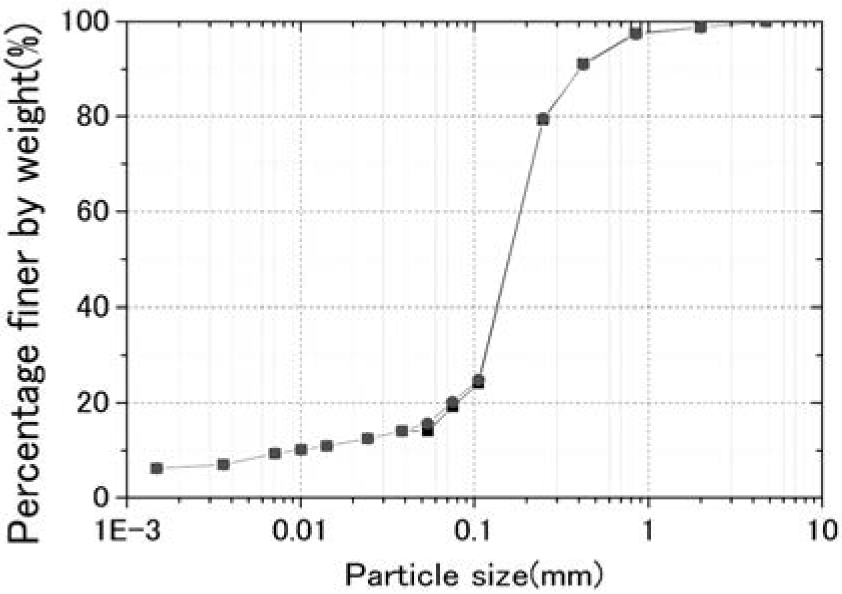

Figure 7. Particle size distribution of Edosaki sand

3. TEST RESULTS

3.1 Turbidity and weight of eroded soil

Turbidity and weight of eroded soil of all test conditions were shown in Table 1. In twice of 5 times test cases turbidity was the sum of each bottom tank's turbidity value. Weight of eroded soil was in dry condition. Test result was separated from 3 types depending on weight of eroded soil; limited (almost no) erosion case, small erosion case and large erosion case.

Relationships between turbidity and weight of eroded soil were shown in Figure 8. Weight of eroded soil was proportionate to turbidity, which was consent to Sato et al.(2012)[3)] mentioned.

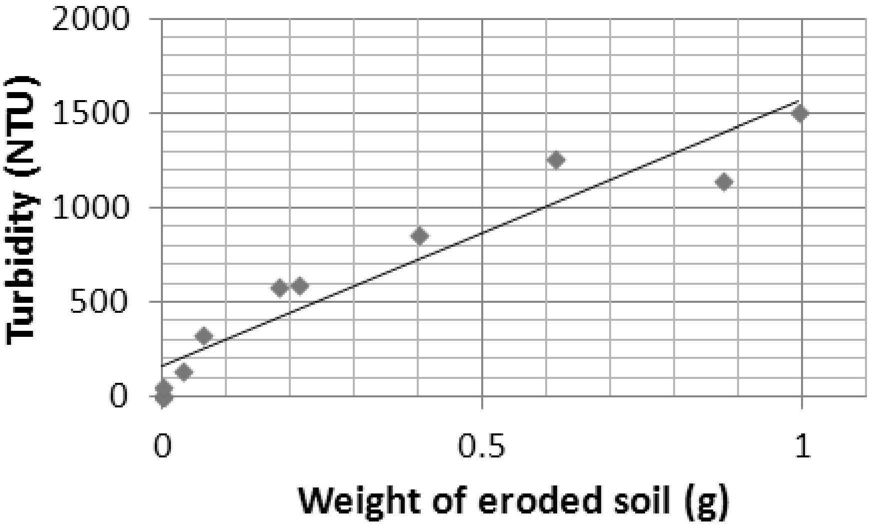

Figure 8. Relationships between weight of eroded soil and turbidity

3.2 Stress-Strain Curve

Stress-Strain curve of all test cases was revealed in Figure 9. For calculating of shear stress, cross-sectional area of the specimen was measured from Clipgages' data by around 5% of axial strain and then estimated from EDT's data (Poisson's ratio=0.2) Figure 9 revealed that residual stress was not so changed in all test conditions. On the other hand, large erosion case and limited erosion case of filter paper was compared in Figure 10. Figure 10 suggested that around 10% difference of peak stress. The reason why peak stress of cloth case was weaker than that of filter paper but one possibility was cloth was deformed during shearing.

Figure 12 represented relationships between turbidity and ratio of q at each peculiar small axial strain: 1%, 2%, 3%, 4% and 5%. Value 1 of Ratio of q was calculated from average q of filter paper test cases. From Figure 12, it was supposed that q decreased most due to increasing of turbidity in 1% axial strain. Then an relationships between turbidity and decreasing of ratio of q was stable from 2% to 4%. At 5%, Ratio of q didn't decreased so much by rise of turbidity. It was suggested that influence of erosion disappeared by increasing of shear stress. Finally influence vanished completely and residual stress were similar in all test conditions.

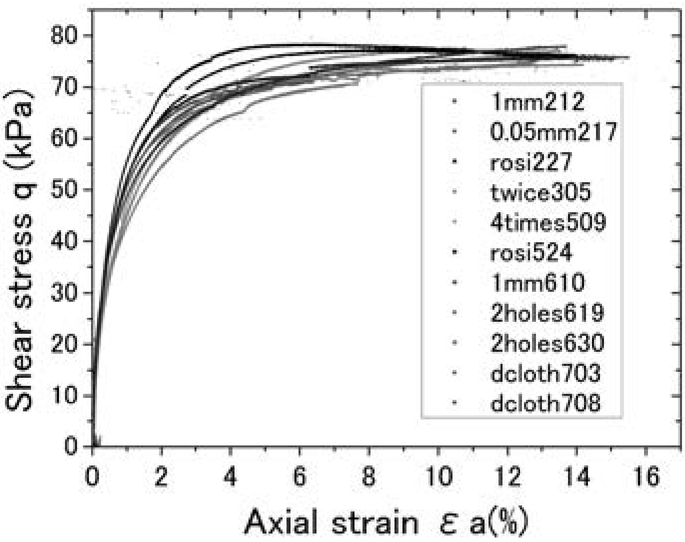

Figure 9. Stress-Strain curve of all test conditions

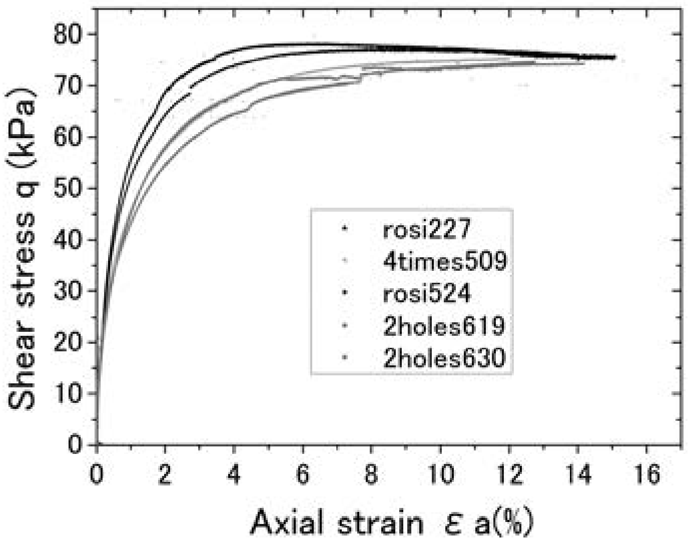

Figure 10. Details of Stress-Strain curve

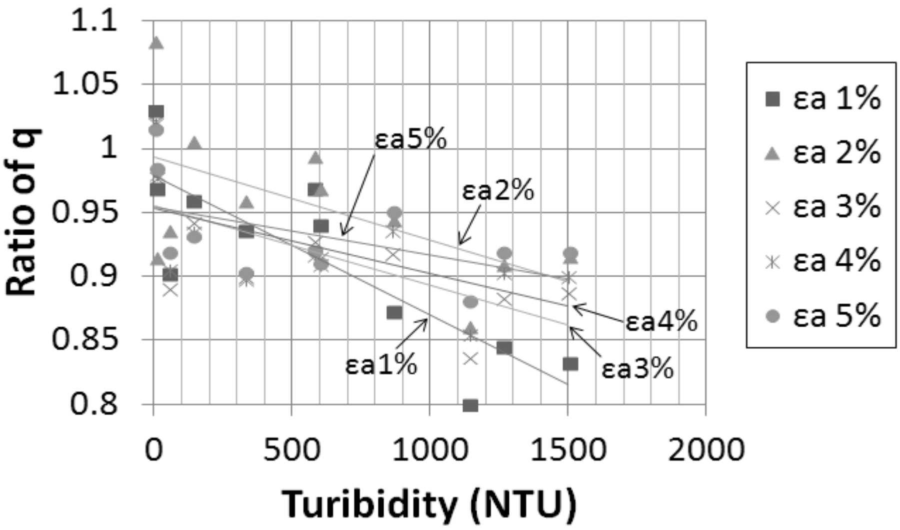

Figure 11. Turbidity and decreasing of shear stress

3.3 Young's Modulus and Poisson's Ratio

Young's modulus was calculated by Eq.1.

$$E = \frac{\Delta\sigma_1}{\Delta\varepsilon_{axial}} \qquad \text{Eq.1}$$

$\Delta\sigma_1$ = range of axial stress $\Delta\varepsilon_{axial}$ = range of axial strain

Axial stress was measured from the load cell and axial strain was measured from 4 LDTs during cyclic loading.

Poisson's ratio was calculated by Eq.2.

$$E = \frac{\Delta\varepsilon_{radial}}{\Delta\varepsilon_{axial}} \qquad \text{Eq.2}$$

Cyclic loading was repeated 11 times and 10th cycle was applied to calculate Young's Modulus and Poisson's Ratio.

Result of Young's Modulus was shown in Figure12. Vertical axis was a change ratio of Young's Modulus from previous condition. Limited erosion case was plotted in right of Figure 12. Small and large erosion cases were plotted in left of Figure 12. By comparing left and right of Figure12, it was suggested that decreasing tendency by water infiltration was similar in both cases. However, only small and large erosion test cases caused decreasing of Young's Modulus by downward water flow, which was influence of internal erosion.

Result of Poisson's ratio was shown in Figure 13. Clip gage's data had noises and not so accurate as LDT's. It was failed to get collects data of Clip gages in some test conditions. Poisson's ratio was not so changed during the test. The average value was around 0.2, which was applied for calculating σ (Referring to 3.2).

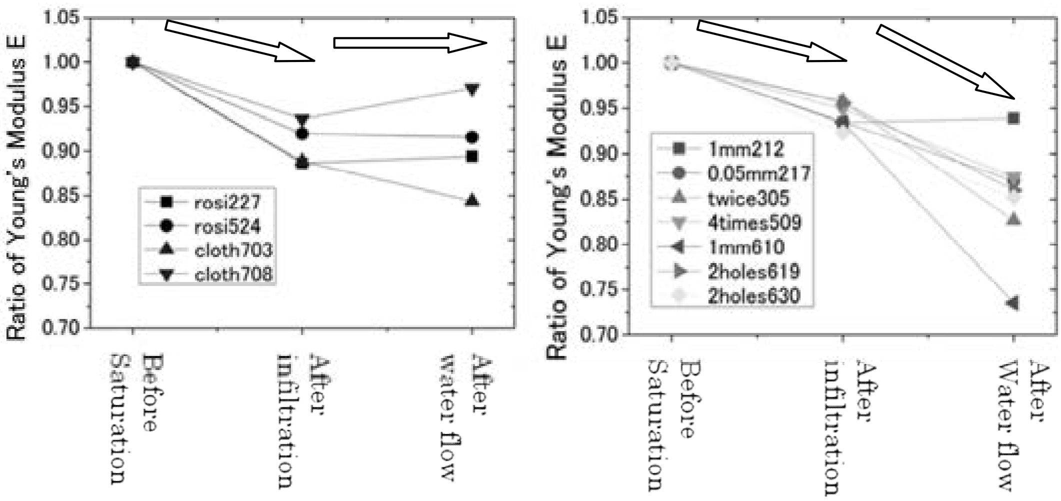

Figure 12. Change of Young's Modulus (right: limited erosion, left: small&large erosion)

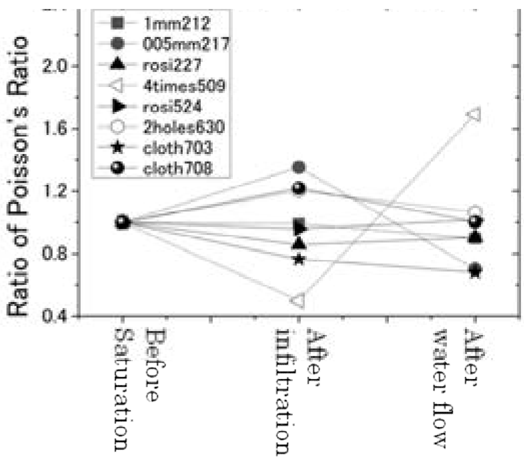

Figure 13. Change of Poission's Ratio

4. DISCUSSION AND CONCLUSION

- Erosion caused decreasing of mobilized deviator stress, which disappeared by increasing of axial strain. Probably because during shearing and consolidation, small voids created by internal erosion vanished as suggested by(Samanthi et al.(2011)[4].
- Young's modulus decreased by erosion but Poisson's ratio did not similarly change. It seemed to be affected by the direction of water flow.
- Maeda et al.(2012)[5] simulated effect of particle loss on soil stiffness by DEM. Tendency of the simulation was similar as our test result. They suggested small particle movement for long distance through connected voids in the ground was difficult. In this research, large holes at the bottom caused erosion easily. Therefore, large particles' unstable conditions and drainage changed particle structure inside the specimen. Then small particle moved out easily from the soil.
- For evaluating degree of erosion, turbidity of the drained water can be can be a good indicator..
- In the ground, repetition of small erosion maybe caused deterioration of the soil structure. If it has some loosened part or cracks like gaps of the buried structures (Sato et al.(2011)[6] and (2012)[7]) , water flow concentrate there and high water pressure may be generated, which made internal erosion easily and sometimes made soil pipes.

REFERENCES

1) Sato, M. & Kuwano, R. *Model Tests for the Evaluation of Formation and Expansion of a Cavity in the ground*. Proc. of the 7th International Conference on Physical Modelling in Geotechnics 2010. Zurich, June 2010, pp.581-586

2) Kenny,T.C.,Lau.D. (1985). Internal Stability of granular filters. Canadian Geotechnical Jornal Volume 22:215-225

3) Sato,M. and Kuwano,R. "Evaluation of internal erosion by turbidity of drained water", Proc. of 11th International Symposium on New Technologies for Urban Safety of Mega Cities in Asia, No.23, Ulaanbaatar, Mongolia, October 2012.

4) Renuka,S. & Kuwano,R. "Evaluation of ground loosening behavior and mechanical properties of loosened sand associated with underground cavities", master thesis of the Department of Civil Engineering, the University of Tokyo, September 2012

5) Maeda.K, Wood.D.M, and Kondo, A. Micro and macro modelling of internal erosion and scoring wih fine particle dynamics, Proc. of 6th International Conference on Scour and Erosion. 2012, Paris, France: ISCE-000197

6) Sato,M. and Kuwano,R. "Influence of Underground Structures on Cavity Formation", Proc. of 10th International Symposium on New Technologies for Urban Safety of Mega Cities in Asia, Session11-4, Chiang-Mai, Thailand, October 2011.

7) Sato,M. and Kuwano,R. "Influence of underground structures on cavity formation due to various conditions of water flow", Proc. of 2nd International Conference on Transportation Geotechnics, pp.617-622, Hokkaido, Japan ,September 2012.

A study of bored pile bearing capacities at some locations in Hanoi, Vietnam

Thuy Diep DUONG[1], Hung Quang PHAM[2], Hieu Duc KIM[3], Lam Thai GIANG[4]
[1] Master of Science, University of Civil Engineering, Hanoi, Vietnam
thuyxd0582@gmail.com
[2]Associate Professor, University of Civil Engineering, Hanoi, Vietnam
[3] Engineer, Geotechincal and Construction Engineering Institute, Hanoi, Vietnam
[4]Master of Science, University of Civil Engineering, Hanoi, Vietnam.

ABSTRACT

The paper presents test results of 06 bored/Barrette pile tests that installed strain gauges at three locations in Hanoi city. From the t-z and q-z curves obtained from the tests, the authors constructed the P-S curves of the piles. The estimated pile bearing capacity using the Davisson (1972) for each pile were then compared with the calculated ones using common equations for calculating bearing capacity of the pile from the soil profile. It is found that the bearing capacity calculated is much smaller than the one estimated from the test results. The paper also presents some suggestions for reasonable lengths of bored piles in gravel layer for different pile diameters and concrete grades at the three locations.

Keywords: *Bearing capacity, bored pile, Barrette pile, pile test, suitable length, Hanoi.*

1. INTRODUCTION

Thousands of bored and Barrette piles were built in Vietnam each year. In Hanoi, a bored/Barrette pile is normally designed with a length in the range from around 40 m to 80 m and pile toe is usually in the gravel or stone layer. Bored pile diameter is from 0.8 m to 2.5 m with allowable bearing capacity in the range from round 500 to 3,500 tons.

Figure 1. Three locations of the test piles in Hanoi city (Google, 2013)

When applying common equations in standards for calculating bored/Barrette pile bearing capacity in Hanoi city, toe bearing is around 30% to 60% bearing capacity of the pile. There is a fact that thick mud layers are usually found at toes of most cast-in-place piles. However, pile load test results show that most of designs are acceptable or even over design (Vu and Pham, 2010; Trinh, 2011; Bui and Nguyen, 2011). It means that the applied equations may not be appropriate for the soils in Hanoi city. Therefore, further study on the bearing capacity of bored/Barrette pile in Hanoi city is very necessary.

In this paper the author used load test results of 06 piles which used strain gauges along the piles in three locations (North Thang Long Urban area, Thanh Xuan District and Ha Dong District) to study the actual shaft and tip bearing capacity. In details, the author analyzed the test results to: 1) find the *(t-z)* curve knowing as the curve presents the relationship between the unit shaft friction versus the relative movement between the pile shaft and the soil and the (*p-z*) curve knowing as the curve presents the pile end bearing unit versus the pile toe movement; and 2) reconstructed the axial compression curve (*P – S*). The pile bearing capacities with different lengths and sizes are estimated from the *P-S* curves using Davisson (1972) method. Pile bearing capacity estimated is then compared with the pile bearing capacities calculated using some common equations in standards (Japaness standard; Meyerhoff, 1956 and FHWA, 2006). Also, a suggestion for reasonable lengths for different pile diameters and locations are presented.

2. THEORY

2.1 Construct the axial static load test curve (*P-S*)

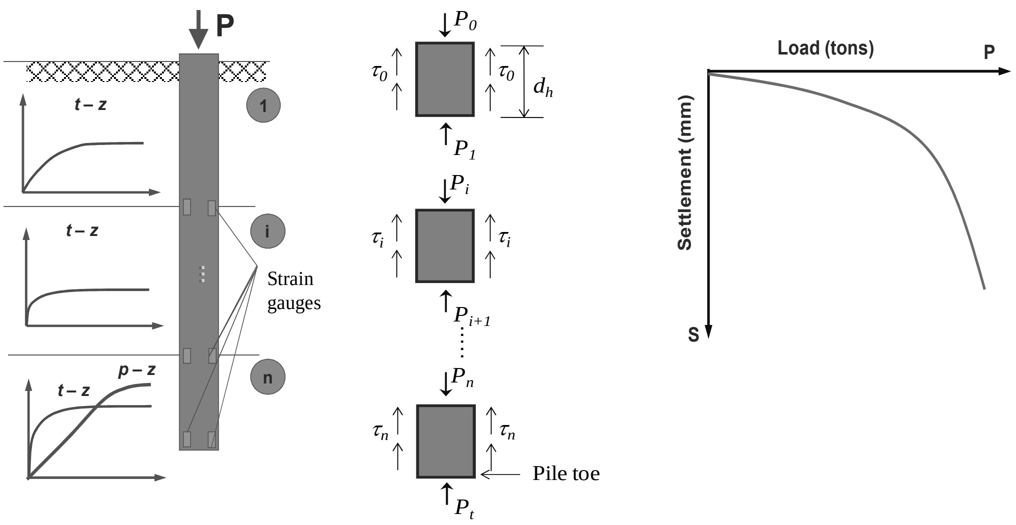

a) *t-z* and *p-z* curves of soil layers | b) Pile segment | c) *P-S* curve

Figure 2. Construction of the pile axial compression test curve (*P-S*)

From the static load test for bored pile with strain gauges installed, the *t-z* curves and *p-z* curves for soils could be obtained (Hayes and Simmonds, 2002; Vu and

Pham, 2010 and Duong et al., 2013). The *P-S* curve could be reconstructed from the *t-z* and *p-z* curve by dividing the pile into multiple small segments with a length of d_h. The load on top of the pile segment #*i* could be calculated as follows:

$$P_i = P_{i+1} + F_i \tag{1}$$

where: F_i = total shaft friction of the pile segment.

By assuming a small movement of the pile toe, S_0. From the *p-z*, the end bearing of the pile, P_t, could be calculated as follows:

$$P_t = p_t \,.\, A \tag{2}$$

where: p_t = unit end bearing resistance and A = pile cross section area.

Total shaft friction in a pile segment #*i* could be calculated as follows:

$$F_i = t_i.u.d_h \tag{3}$$

where: u = perimeter of the pile, d_h = length of the pile segment and t_i = unit shaft friction of the pile segment equivalent with the movement.

Elastic deformation, ΔS_i, of the pile segment #*i* could be calculated as follows:

$$\Delta S_i = (P_i+P_{i+1}).d_h/(2EA) \tag{4}$$

where: P_i and P_{i+1} are axial forces at the top and bottom of the pile segment, d_h = length of the pile segment, A = pile cross section area and E = elastic modulus of the pile material.

Using the above method to calculate the elastic deformation of pile and the axial force at the top of the pile, the *P-S* curve could be constructed.

2.2 Estimate the pile bearing capacity using Davisson (1972)

Davisson (1972) method is introduced in the Vietnamese standard and widely used for estimating pile bearing capacity. In this method, the ultimate pile bearing capacity is the load value that equivalents with the following pile settlement:

$$\Delta = \frac{PL}{EA} + 0.0038 + \frac{D}{120}(m) \tag{5}$$

where: P = pile load, L = pile length, A = pile cross section area, E = material elastic modulus, D = pile diameter.

2.3 Pile structure bearing capacity

In Vietnam, beside the Vietnamese standards, other international standards could be used with acceptance of the owner. In the Vietnamese standard TCXD 195-1997, the pile structure bearing capacity could be calculated as follows:

$$P = R_u.A_c + R_a.A_s \tag{6}$$

where: $R_u =$ strength of the concrete. For bored pile, $R_u = R/4.5$ but not over 60 kG/cm^2. $R_a =$ strength of steel (for rebar diameter less than 28 mm) and $R_a = R_c/1.5$ (for rebar lager than 28 mm) but not over 2,200 kG/cm^2. A_c = concrete area and A_s = steel area.

For the International Building Code (IBC-2009), the pile structure bearing capacity could be calculated as follows:

$$P = 0.25 f_c^{'}.A_c + 0.4 f_s.A_s \tag{6}$$

where: $f_c^{'} =$ strength of the concrete; $f_s =$ yield stress of the steel; $A_c =$ concrete area; $A_s =$ steel area.

2.4. Estimating the suitable length of piles

Based on the reconstructed *P-S* curve and the Davisson (1972) method as described above, bearing capacity of bored piles with different pile lengths and pile diameters at three locations in Hanoi were estimated. The authors suggested reasonable lengths for different bored pile diameters in the three locations by comparing pile bearing capacity estimated using the above method and the structure bearing capacity of the pile. The reasonable length is the length that bearing capacity of the structure is approximately equal to the bearing capacity estimated for the soil.

3. TESTING PROGRAM

3.1 Pile tests at North Thang Long area

a) Introduction

The first research location is in the North Thang Long urban area, Tay Ho district, Hanoi. The depth of the gravel layer is from -40 m compared with the ground surface. This area has 7 soil layers and gravel is the 7th layer with N-value from the SPT greater than 80. Detailed description of the soil profile is shown in Figure 3.

b) Description of the test piles

Two test piles in this area: 1) Barrette P1 with a size of 1.0 x 2.8 (m) and a length of 45 m; and 2) Bored pile P2 with diameter of 2.0 m and a length of 57.2 m. The Geokon model #4911 strain gauges were installed in both piles at 7 levels with from 2 to 4 gauges at each level (Loadtest, 2011). Locations of the strain gauges are presented in Figure 3.

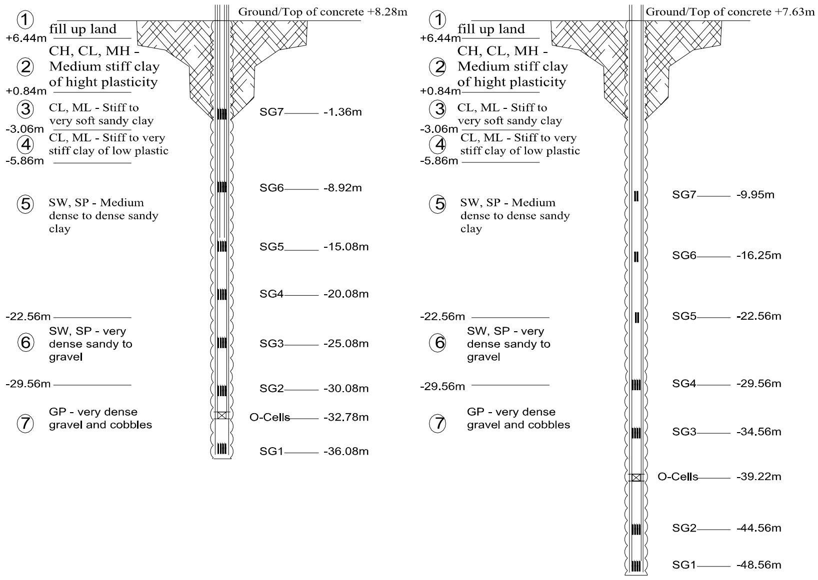

a) Barrette pile P1 b) Bored pile P2

Figure 3. Soil profile and strain gauges levels for test piles in North Thang Long urban area

c) Test results

Analyzing the test results, the *t-z* and *p-z* curves for each soil layer could be obtained and presented in Figures 4 and 5.

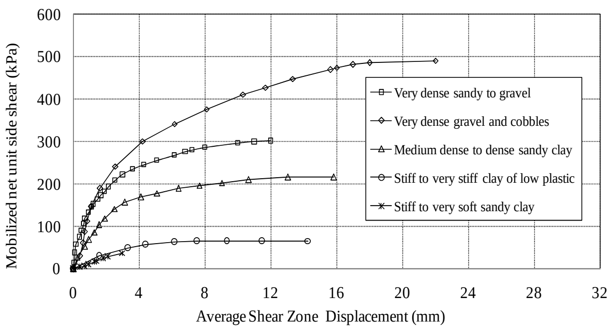

Figure 4. Mobilized unit shaft friction for soils at the North Thang Long urban area

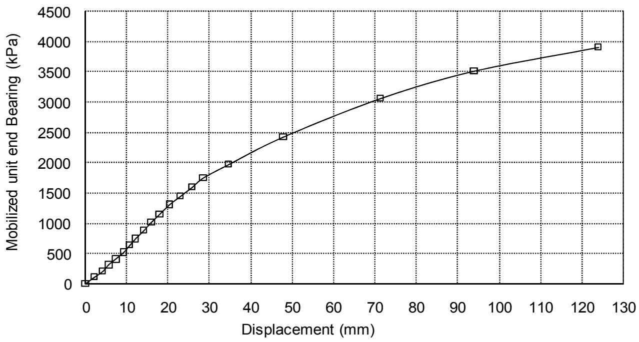

Figure 5. Mobilized end bearing for the gravel soil at the North Thang Long urban area (layer #7)

d) Estimating pile bearing capacities

From the *t-z* and *p-z* curves of soils at the testing location, the *P-S* curve is constructed. Using the Davisson (1972) method, the pile bearing capacity could be constructed (Figure 6).

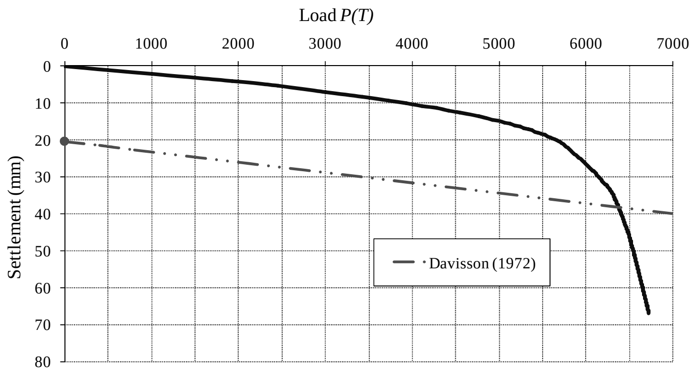

Figure 6. *P-S* curve and estimation of bearing capacity using Davisson method for a bored pile with diameter of 2.0 m and length of pile in the gravel layer is 4.0 m

By changing the diameter as well as the length of the pile in the gravel layer, corresponding pile bearing capacity could be obtained using the above method. Figures 7 to 9 present pile bearing capacities calculated using common equations based on the soil profile and estimated using Davisson (1972) methods for bored pile with diameter of 1.0, 1.5, and 2.0 (m) at various lengths in the gravel layer. In each figure, the structure pile bearing capacity is also presented for 1) Vietnamese standard (TCXD) and 2) International Building Code (IBC).

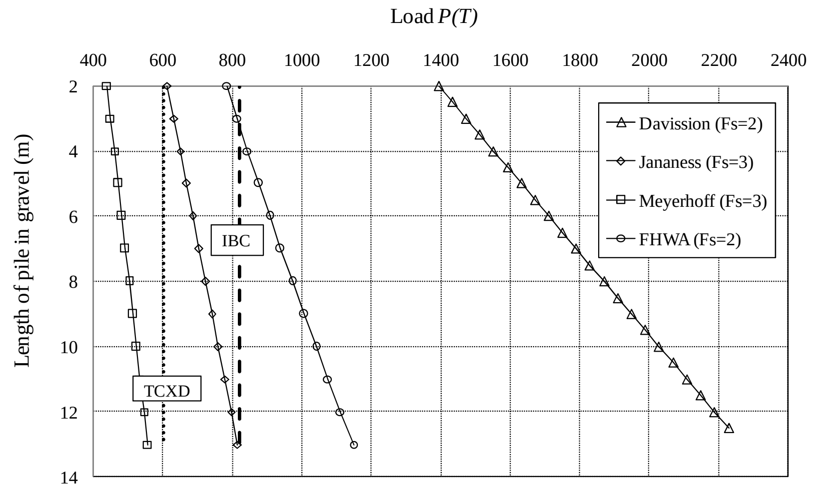

Figure 7. Comparison between the estimated bearing capacities using Davisson (1972) method and calculated values using soil profile for bored pile D1000 (diameter of 1.0 m at various depth in gravel layer)

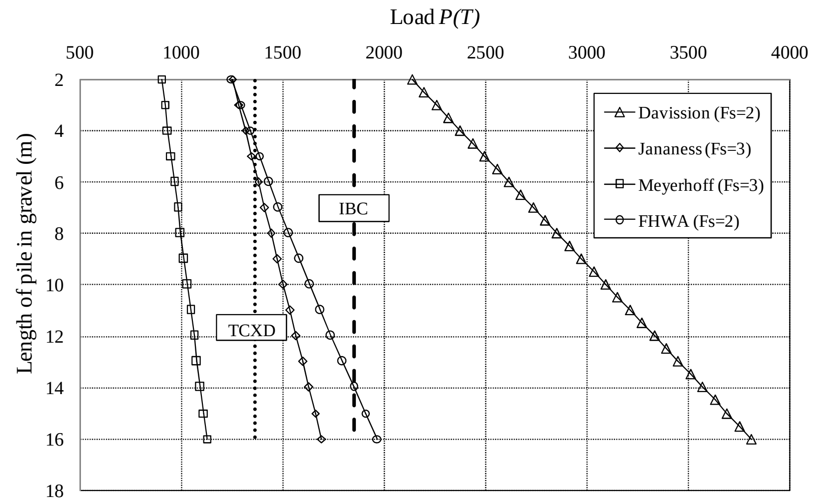

Figure 8. Comparison between the estimated bearing capacities using Davisson (1972) method and calculated values using soil profile for bored pile D1500 (diameter of 1.5 m at various depths in gravel layer)

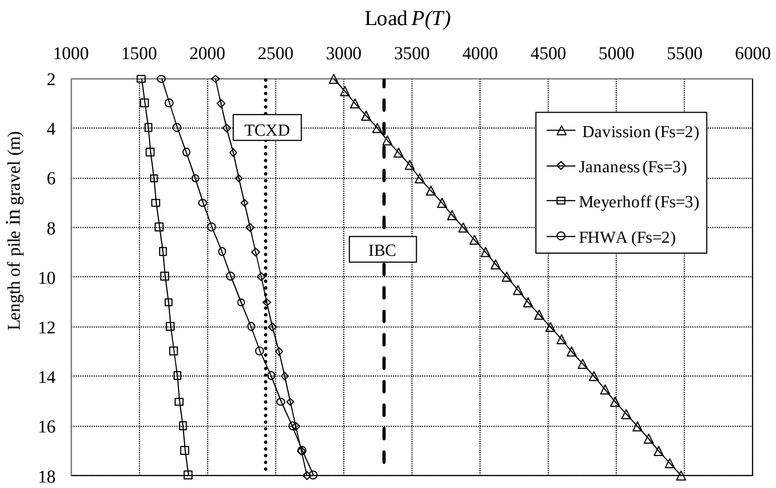

Figure 9. Comparison between the estimated bearing capacities using Davisson (1972) method and calculated values using soil profile for bored pile D2000 (diameter of 2.0 m at various depths in gravel layer)

Table 1. Reasonable length of pile in gravel layer for various pile diameters and concrete grades for North Thang Long area.

<table>
<tr><th rowspan="3">Pile structure bearing capacity</th><th rowspan="3">Factor of safety</th><th colspan="4">Pile D1000</th><th colspan="4">Pile D1500</th><th colspan="4">Pile D2000</th></tr>
<tr><th colspan="2">Concrete B40</th><th colspan="2">Concrete B45</th><th colspan="2">Concrete B40</th><th colspan="2">Concrete B45</th><th colspan="2">Concrete B40</th><th colspan="2">Concrete B45</th></tr>
<tr><th>P (T)</th><th>Ls (m)</th><th>P (T)</th><th>Ls (m)</th><th>P (T)</th><th>Ls (m)</th><th>P (T)</th><th>Ls (m)</th><th>P (T)</th><th>Ls (m)</th><th>P (T)</th><th>Ls (m)</th></tr>
<tr><td rowspan="2">IBC</td><td>Fs=2</td><td rowspan="2">745</td><td><2</td><td rowspan="2">822</td><td><2</td><td rowspan="2">1,668</td><td><2</td><td rowspan="2">1,843</td><td><2</td><td rowspan="2">2,984</td><td>3</td><td rowspan="2">3,295</td><td>4</td></tr>
<tr><td>Fs=3</td><td><2</td><td><2</td><td>5</td><td>7</td><td>11</td><td>14</td></tr>
<tr><td rowspan="2">TCVN</td><td>Fs=2</td><td rowspan="2">553</td><td><2</td><td rowspan="2">605</td><td><2</td><td rowspan="2">1,234</td><td><2</td><td rowspan="2">1,350</td><td><2</td><td rowspan="2">2,220</td><td><2</td><td rowspan="2">2,427</td><td>3</td></tr>
<tr><td>Fs=3</td><td><2</td><td><2</td><td>3</td><td>5</td><td>5</td><td>7</td></tr>
</table>

Note: *P is the pile structure bearing capacity determined using the two standards with assumption that the rebar area is 1.0% of the cross section.* F_s *is the factor of safety for pile bearing capacity determined using the Davisson (1972) method. Ls is the length of the pile in the gravel layer that results in the bearing capacity for soil structure is approximately equal to the one estimated using the Davisson (1972) method.*

3.2. Pile test at Thanh Xuan area

a) Introduction

The second pile test was at the Thanh Xuan district, Hanoi city. The gravel layer exists from the depth of -48 m from the ground surface. There are 18 soil layers and the 18th layer is the dense gravel with N-value from the SPT test is over 100. This layer appears to be very thick (Figure 10).

b) Description of the test pile

There are two test piles: 1) Barrette pile (TP3) with a size of 1.2 x7.0 (m) and a depth from -0.9 m to -50.45 m, and 2) Barrette T shape pile (TP4) with a size of

2.8mx4m and a depth from -0.9 m to -49.45 m. Each pile has 24 strain gauges installed at 4 levels (Figure 10).

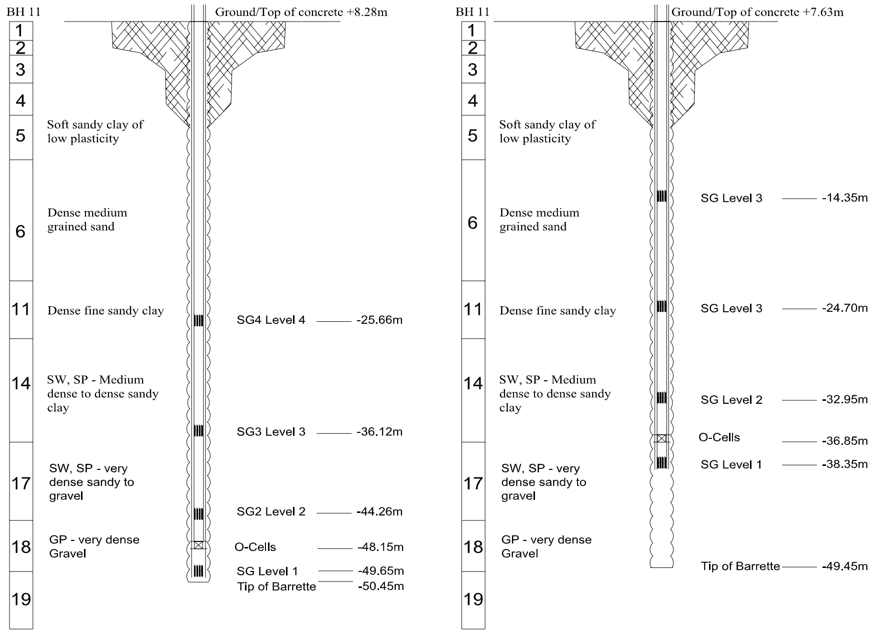

a) Barrette pile TP3 b) Barrette T-shape pile TP4

Figure 10. Soil profile and strain gauges levels for test piles in Thanh Xuan area

c) Test results and estimation of pile bearing capacity

The authors analyzed the test results as in the North Thang Long urban area (Loadtest, 2008). The pile bearing capacities calculated using common equations based on the soil profile and estimated using Davisson (1972) methods for bored pile with diameter of 1.0, 1.5, and 2.0 m with various lengths in the gravel layer are presented in Figures 11 to 13.

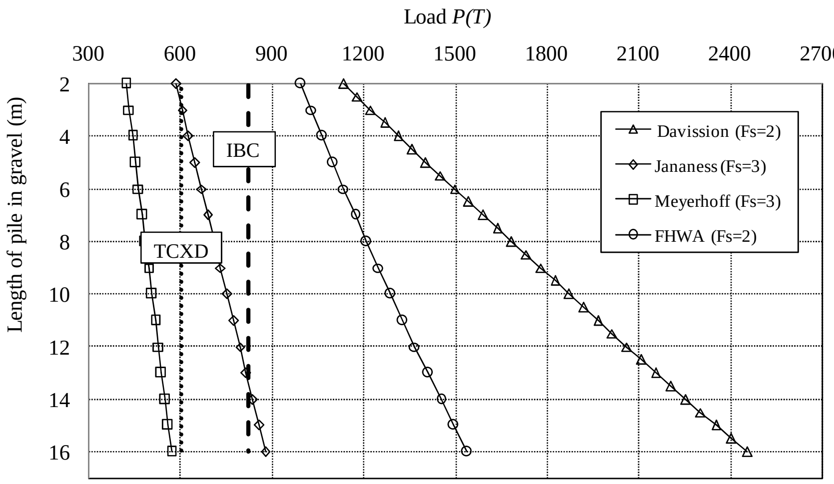

Figure 11. Comparison between the estimated bearing capacities using Davisson (1972) method and calculated values using soil profile for bored pile D1000 (diameter of 1.0 m at various depths in gravel layer)

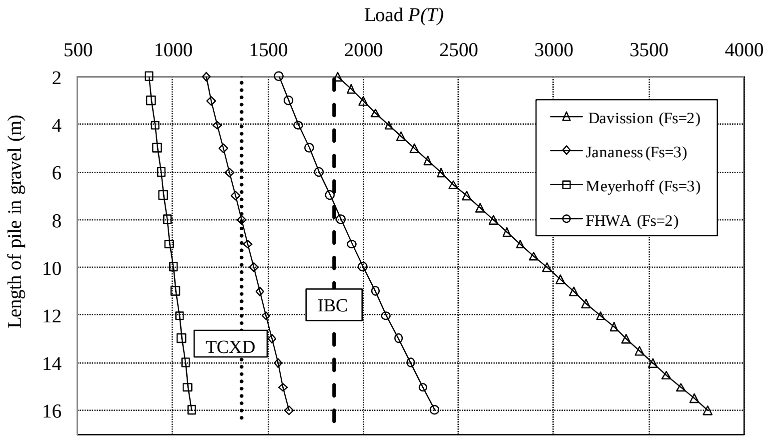

Figure 12. Comparison between the estimated bearing capacities using Davisson (1972) method and calculated values using soil profile for bored pile D1500 (diameter of 1.5 m at various depths in gravel layer)

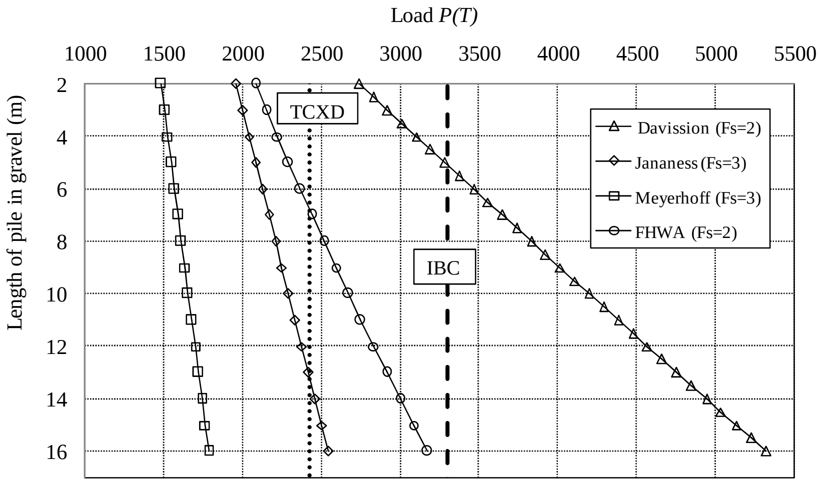

Figure 13. Comparison between the estimated bearing capacities using Davisson (1972) method and calculated values using soil profile for bored pile D2000 (diameter of 2.0 m at various depths in gravel layer)

Table 2. Reasonable length of pile in gravel layer for various pile diameters and concrete grades for Thanh Xuan area

Pile structure bearing capacity	Factor of safety	D1000				D1500				D2000			
		B40		B45		B40		B45		B40		B45	
		P (T)	Ls (m)	P (T)	Ls (m)	P (T)	Ls (m)	P (T)	Ls (m)	P (T)	Ls (m)	P (T)	Ls (m)
IBC	Fs=2	745	<2	822	<2	1,668	<2	1,843	<2	2,984	3.5	3,295	5.5
	Fs=3		<2		3		7		9		11.5		14
TCVN	Fs=2	553	<2	605	<2	1,234	<2	1,350	<2	2,220	<2	2,427	<2
	Fs=3		<2		<2		<2		3		5.5		7

Note: *P is the pile structure bearing capacity determined using the two standards with assumption that the rebar area is 1.0% of the cross section.* F_s *is the factor of safety for pile bearing capacity* *determined using the Davisson (1972) method. Ls is the length of the pile in the gravel layer that results in the bearing capacity for soil structure is approximately equal to the one estimated using the Davisson (1972) method.*

3.3 Pile test at Van Khe, Ha Dong area

a) Introduction

The third pile test location was at the Ha Dong district, Hanoi city. The gravel layer exists from the depth of -41 m from the ground surface. There are 7 soil layers and the 7th layer is gravel and coarse sand at very dense state with N-value from the SPT test is over 100. This layer appears to be very thick (Figure 13).

b) Description of test piles

There are two piles were tested at this location (Loadtest, 2009): 1) Bored pile TP5 having diameter of 1.5 m at the depth of -10.5 m to -66.55 m and 2) Bored pile TP6 having diameter of 2.0m from the depth of -9.1 m to -51.15 m (Figure 14)

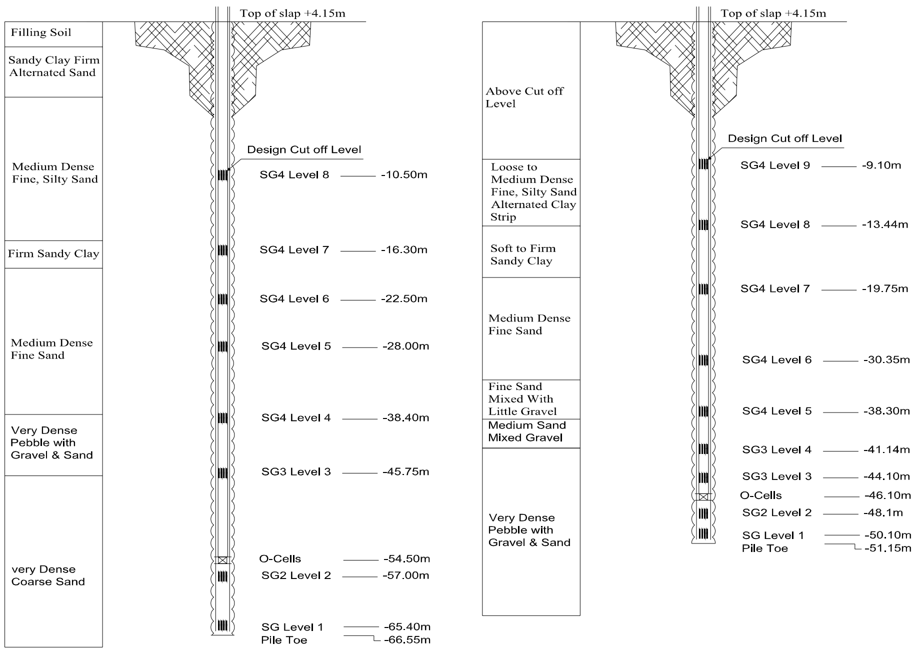

a) Bored pile TP5 b) Bored pile TP6

Figure 14. Soil profile and strain gauges levels for test piles in Ha Dong area

c) Test results and estimation of pile bearing capacity

Similar to the other pile test location, the pile bearing capacities calculated using common equations based on the soil profile and estimated using Davisson (1972) methods for bored pile with diameter of 1.0, 1.5, and 2.0 m at various depths in the gravel layer are presented in Figure 15.

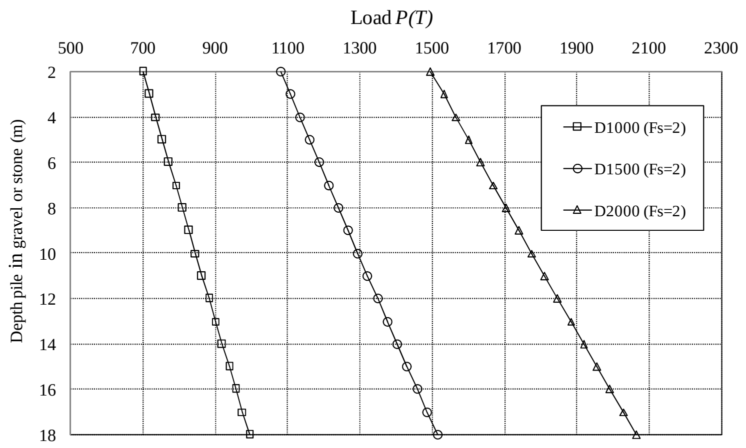

Figure 15. Estimated bearing capacities using Davisson (1972) method for bored pile D1000, D1500 and D2000 (diameter of 1.0; 1.5; 2.0 m at various depths in gravel layer)

Table 3. Reasonable length of pile in gravel layer for various pile diameters and concrete grades for Ha Dong area

Pile structure bearing capacity	Factor of safety	D1000				D1500				D2000			
		B30		B35		B30		B35		B30		B35	
		P (T)	Ls (m)	P (T)	Ls (m)	P (T)	Ls (m)	P (T)	Ls (m)	P (T)	Ls (m)	P (T)	Ls (m)
IBC	Fs=2	589	<2	667	<2	1,328	11.5	1,503	18	2,361	>20	2,672	>20
	Fs=2.5		4		9.5		>20		>20		>20		>20
TCVN	Fs=2	467	<2	510	<2	1,054	<2	1,151	5	1,873	13	2,046	18
	Fs=2.5		<2		<2		11		16		>20		>20

Note: *P is the pile structure bearing capacity determined using the two standards with assumption that the rebar area is 1.0% of the cross section.* F_s *is the factor of safety for pile bearing capacity determined using the Davisson (1972) method. Ls is the length of the pile in the gravel layer that results in the bearing capacity for soil structure is approximately equala to the one estimated using the Davisson (1972) method.*

3.4. Comments on the test results:

Pile bearing capacity is increased significantly when increasing the length of bored pile in the gravel layer in the all three locations. The calculation results showed that the pile bearing capacity calculated using some common equations are significantly less than the value estimated from the *P-S* curve using the Davisson (1972) method. By comparing the structure bearing capacity and the one estimated from the *P-S* curve, reasonable length of bore pile could be estimated as presented in the Tables 1 to 3.

For all three locations in Hanoi city, it was found that the length of bored pile D1000 in the gravel layer should be from 2.0 to 3.0 m. For the D1500 bored pile, the length of pile in the gravel layer should be from 3 to 9 m depending on the concrete grade as well as the selected factor of safety. For the D2000 pile, reasonable length of the pile in the gravel layer is in a range from 5 to over 20 m.

The test results also show that the soil profiles are quite different between the three locations.

4. CONCLUSIONS

Some conclusions could be drawn from the research as follows:

1. The test results of a pile load test that installed strain gauges could provide the useful information that could be used to: 1) estimate the shaft firction and end bearing capacity of the pile and 2) estimate bearing capacity of other bored piles with different diamaters and lengths at the same location.
2. The prediction of the pile bearing capacity using common equations are much less than the one estimated from the *P-S* curve using the Davisson (1972) method.
3. Resonable lengths of bored piles with different diamters in the three locations have been presented. These values could be used as references for future projects with an attempt to have cost-effective foundation designs.

REFERENCES

Bùi Đức Hải và Nguyễn Bảo Việt, 2011. *Thí nghiệm nén tĩnh cọc có kết hợp đo biến dạng dọc thân cọc - một phương pháp nâng cao độ chính xác khi xác định sức chịu tải của cọc khoan nhồi và cọc barrete ở Hà Nội*. Tạp chí Khoa học kỹ thuật Mỏ - Địa chất. Số 35 – 7/2011;

Dương Diệp Thúy, Phạm Quang Hưng và Kim Đức Hiếu, 2013. *So sánh sức kháng ma sát thành của cọc đổ tại chỗ giữa một số phương pháp tính thường dùng và kết quả thí nghiệm cho nền đất tại khu vực Bắc Thăng Long Hà Nội*. Hội thảo khoa học Hạ tầng giao thông Việt Nam với phát triển bền vững, TISDV 2013.

FHWA, 2006. *Design and Construction of pile foundation, U.S.* Department of Transportation, National Highway Institute, April 2006;

Hayes, J. and Simmonds, T., 2002. *Interpreting strain measurements from load tests in bored piles, Proceedings*, Ninth International Conference on Piling and Deep Foundations, DFI, Nice, France;

International Building Code (IBC), 2009;

Loadtest, 2008. *Report on Barrette pile load testing*, LTI-2612-1, Deep Foundation Testing, Equipment & Services.

Loadtest, 2008. *Report on Barrette pile load testing*, LTI-2612-2, Deep Foundation Testing, Equipment & Services;

Loadtest, 2009. *Report on drilled pile load testing (Osterberg method)*, LTI-2619-1, Deep Foundation Testing, Equipment & Services;

Loadtest (2009). *Report on drilled pile load testing (Osterberg method)*, LTI-2619-2, Deep Foundation Testing, Equipment & Services;

Loadtest, 2011. *Report on Barrette pile load testing*, LTI-2880-2, Deep Foundation Testing, Equipment & Services;

Loadtest, 2011. *Report on Bored pile load testing*, LTI-2895-1, Deep Foundation Testing, Equipment & Services;

TCXD 205:1998. *Móng cọc – Tiêu chuẩn thiết kế*, Nhà xuất bản xây dựng;

TCXD VN 269:2002. *Cọc – Phương pháp thí nghiệm bằng tải trọng tĩnh ép dọc* *trục*, Nhà xuất bản xây dựng;

Trịnh Việt Cường, 2011. *Một số kết quả bước đầu từ thí nghiệm nén tĩnh cọc có gắn thiết bị quan trắc tải trọng dọc thân cọc ở khu vực Hà Nội.* Tạp chí khoa học kỹ thuật Mỏ - Địa chất – Số 25- 7/2011;

Vũ Thanh Hải và Pham Quang Hưng, 2010. *Xác định sức kháng ma sát đơn vị dọc thân cọc qua thí nghiệm đo biến dạng dọc trục*. Tạp chí Xây dựng, Bộ xây dựng, số 7 năm 2010, trang 50-53.

A technique of image processing analysis recommended for research of laterally loaded pile using a system of X-ray CT scanner

Khoa Dang PHAM[1], Jun OTANI[2]
[1]Ph.D., National University of Civil Engineering, Ha Noi, Viet Nam
phamdangkhoa@nuce.edu.vn
[2]Professor, Kumamoto University, Japan

ABSTRACT

Geotechnical engineering researches are indispensable for Mega cities design in Asia. Especially, in study of laterally loaded pile, investigation of soil behavior is important for evaluating lateral bearing capacity of pile foundation.
The purpose of this research is to develop a technique of image processing analysis for simulating 3 dimensional (3-D) behavior of soil due to lateral pile loading using a system of X-ray CT scanner. Lateral pile loading tests were conducted with a soil box and a loading system. A large number of markers were setup as grids in the soil under the ground surface. After lateral loading was applied, CT scanning was conducted on the soil box. From all the CT images obtained containing images of cross sections of the markers, locations of all the markers after loading were determined. Thus, a simulation of 3-D movements of the markers in the soil was conducted. By connecting the centers of the markers at the stages before and after loading, the 3-D movements of the markers were obtained as vectors of the movement, and therefore, the soil behavior due to lateral pile loading was observed precisely in three dimensions.

Finally, 3-D behavior of soil due to lateral pile loading is quantitatively discussed.

Keywords*: mega city, image processing, laterally loaded pile, X-ray CT scanner.*

1. INTRODUCTION

Mega cities in Asia are known as big cities on the Earth with population excess of ten million people. Therefore, safety of mega cities is very important, especially in design of buildings' pile foundation.

In the field of research on laterally loaded pile, investigation of soil behavior is indispensable for evaluating lateral bearing capacity of pile foundation. A number of researches have been done so far on this topic. The pioneer work done by Broms (1974) obtained the ultimate lateral load applied to the pile head after discussing the behavior of pile and soil. Reese et al. (1974) also discussed the ultimate lateral soil resistance based on an assumption of 3-D failure pattern of soil. However, it is considered that those researches were proposed not concerned on the real interaction between pile and soil. Thus, precise investigation of actual behavior of soil due to lateral pile loading is necessary in order to make more quantitative design calculation.

An X-ray computed tomography (CT) method has been widely used in medical diagnoses based on the absorption of x-ray beam through materials. Recently, it has become an useful tool for investigating characteristics of soils in geotechnical engineering (Otani et al. 2000). Results of CT scanning can be realized as the change of density in the material. In this research, a technique of image processing analysis for simulating behavior of the soil due to laterally loaded pile using X-ray CT scanner is developed.

First of all, a model test apparatus, especially for X-ray CT, is introduced. By using this apparatus, a number of markers (plastic spheres with 2 mm diameter) are set up in the front of the model pile, where the failure of soil would occur, at three depths under the ground surface in the soil. Then, lateral pile loading test is carried out with three consecutive loading steps at the pile head. CT scanning is conducted continuously upward on the soil box from three initial depths of the markers, after each loading level. Thus, all images of cross sections of the markers after their movement in the failure zone of the soil are captured in the CT images. Based on these CT images, 3-D locations of the markers in the soil box are determined. Spheres with 2 mm diameter are drawn at those locations of the markers, and therefore 3-D images of the markers after loading are simulated. By connecting the centers of the drawn spheres corresponding to the stages before and after loading, the traces of the movements of the markers are obtained as vectors of movement. Hence, the soil behaviors inside the failure zone are visualized in three dimensions.

Finally, quantitative discussions are performed on the tendencies of 3-D movements of some of the markers.

2. SYSTEM OF X-RAY CT SANNER

The system of X-ray CT scanner used in this research is an industrial one. A photo of the scanner is shown in Figure 1 and its Diagram is shown in Figure 2.

Figure 1. A photo of the system of industrial X-ray CT scanner.

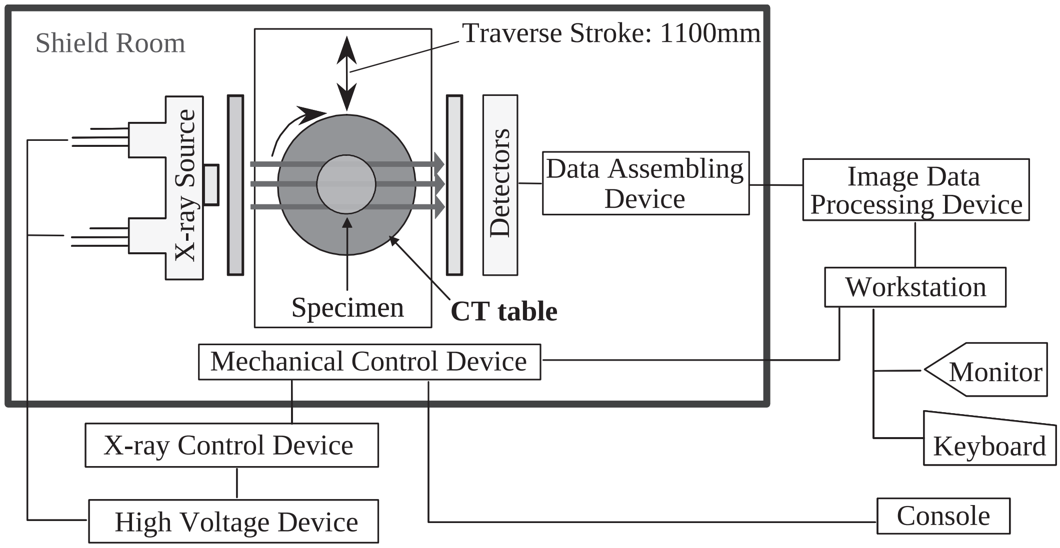

Figure 2. Diagram of the industrial X-ray CT scanner.

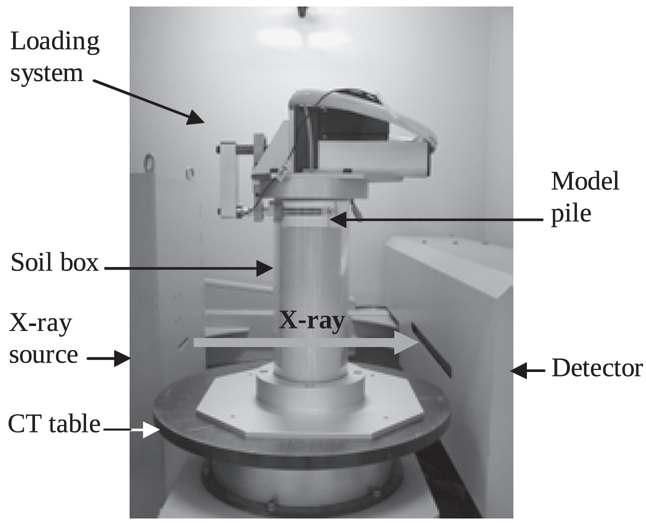

Figure 3. A photo of testing apparatus.

In this system, collimated x-ray is penetrated all around circumference of a specimen by rotating and translating of CT table. The detected data is assembled and cross sectional images are reconstructed using image data processing device by means of the filtered back-projection method. Then, the image is expressed on a monitor of workstation. By using all these cross sectional images around the circumference of the specimen, three dimensional images can be reconstructed.

3. TESTING APPARATUS FOR X-RAY CT

Figure 3 shows a photo of testing apparatus in this research, which is composed of a soil box and a loading sysem, placed in the system of industrial X-ray CT scanner (Pham et al. 2004). The lateral loads applied to the pile head would be conducted under the displacement control.

4. MATERIALS AND TESTING PROCEDURES

4.1 Materials

Toyoura sand was used as the model soil in this test with properties shown in Table 1. Properties of a model pile with rectangular cross section are shown in Table 2. For the purpose of simulating behavior of soil, a large number of markers (spheres) were placed in the soil. The marker with a diameter of 2 mm was made by plastic under consideration to be small enough and not to interfere with x-ray, either.

Table 1. Properties of Toyoura sand

Maximum dry density (t/m3)	1.66
Minimum dry density (t/m3)	1.34
Specific gravity	2.65
Relative density (%)	87.0 – 91.0

Table 2. Properties of model pile

Total length of pile (mm)	350
Length of pile in soil (mm)	330
Cross sectional dimension (mm)	20 x 2
Material	Aluminum

4.2 Testing procedures

In this test, the markers were placed at three depths under the ground surface in the soil. Figure 4 shows a plane view of setup of the markers in each depth, while Figure 5 shows those three depths at the soil box. Test procedures can be summarized as follows (7 steps):

(1) Model pile was fixed at the tip in the soil box;

(2) Sand was prepared into the soil box using multiple sieves to the depth of 70 mm under the ground surface;

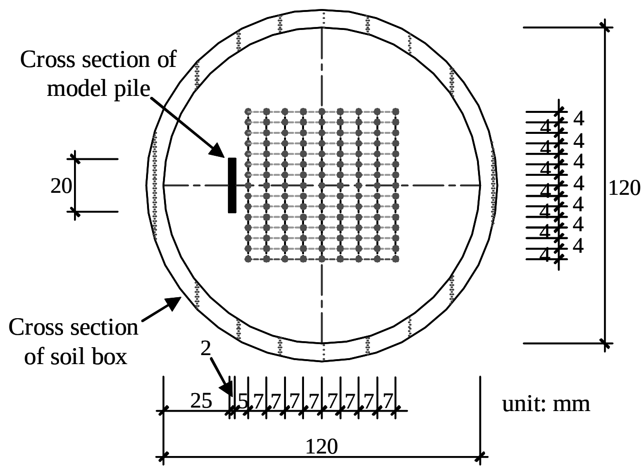

Figure 4. Plan view of marker setup.

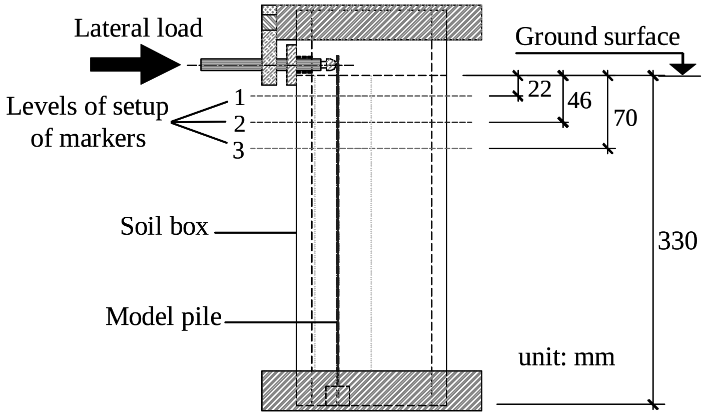

Figure 5. Three initial depths of markers.

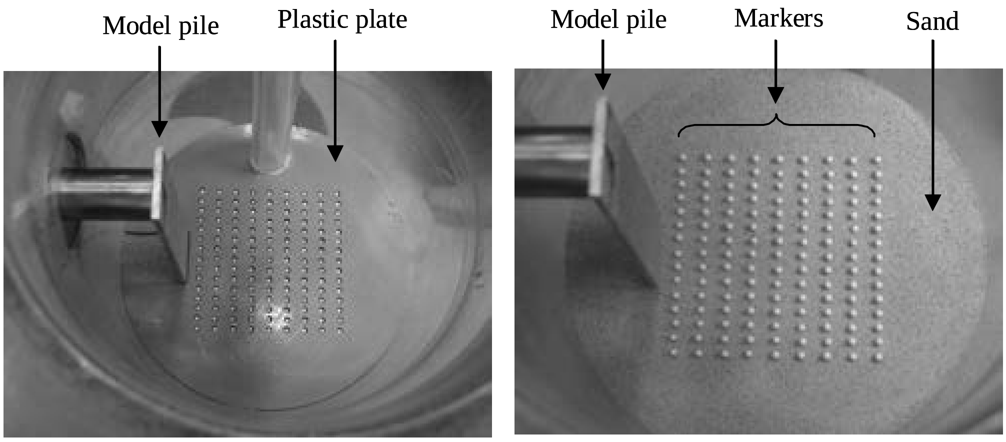

Figure 6. . Position device anf initial positions of markers.

(3) A plastic plate (position device) was used to set the initial positions of the markers at this depth, and shown in Figure 6;
(4) Steps (2) and (3) were conducted for the depths of 46 mm and 22 mm under the ground surface. After markers were installed at 22 mm depth, the sand was prepared until the level of the ground surface;
(5) Soil box was scanned at three depths of the setup of the markers. It is noted that the thickness of the x-ray was set to be 1 mm in all process of CT scanning in the test;
(6) Three consecutive loading steps corresponding to three displacements of the pile head of 5 mm, 10 mm and 15 mm, respectively, were conducted; and
(7) After each loading step, CT scanning was carried out on the soil box continuously upward from the depth of 70 mm.

5. RESULTS AND DISCUSSION

5.1 CT images

Figure 7 shows CT images along the pile depth of the model ground at the initial condition and after three loading levels. It is observed that cross sections of the markers are appeared as white circles in the CT images. The CT images at the initial condition show that all the markers were placed properly. In the CT images obtained after three loading steps, it is realized that the markers were spatially moved up from 22 mm depth. The relative dark color in these CT images is considered as the low density area or the failure zone of the soil due to lateral loading (Pham et al. 2004). It is interesting to observe that the areas of movements of the marker were inside the failure region of the soil. At the depths of 46 mm and 70 mm, it is seen that the markers were moved horizontally in the area of relative dark color. Thus it is considered here that the movements of the markers reflect the behavior of soil inside the failure zone.

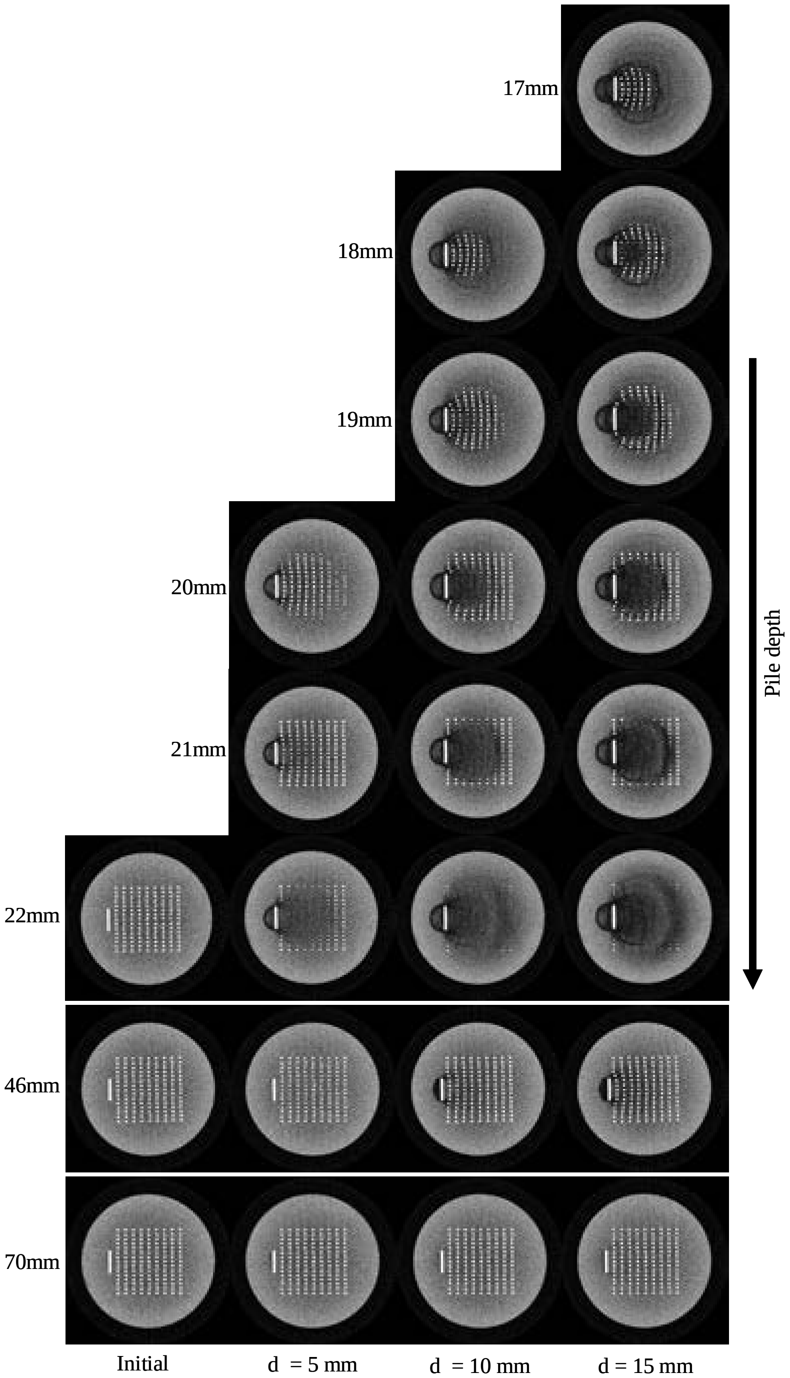

Figure 7. CT images at 8 depths under ground surface of initial condition and after three loading steps d = 5 mm, d = 10 mm, and d = 15 mm.

5.2 Visualization of 3-D behavior of the soil due to lateral pile loading

1) Technique of image processing analysis for simulating 3-D behavior of the soil:

(a) Depths of all the markers under the ground surface after their movements in each loading step are calculated from the CT images;

(b) Spheres with the same diameter of the markers (i.e. 2 mm) are drawn at positions of cross sections of the markers in the CT images (i.e. white circles). It is noted that the spheres are drawn in the way that their centers are coincided with the centers of the markers' cross sections. At this step, the depths of all the spheres are assigned as 0 mm;

(c) Depths of all the spheres under the ground surface then are changed according to those calculated in step (a); and

(d) Images of the 3-D movements of the markers or 3-D behavior of the soil are visualized.

2) Calculation of depths of the markers:

Figure 8 shows a large scale image of a marker, which is cut by an x-ray beam. It is noted in this figure that: (1) the thickness of this x-ray beam was 1 mm, and (2) cross section of a marker in the CT image is always appeared as a circle at the middle plane of the cutting x-ray beam.

The radius, R, of a marker is 2 mm. That of cross section of a marker in a CT image is measured to be r. Thus the distance, h, from the center of that marker to its cross section in the middle plane of the cutting x-ray beam is calculated as:

$$h = \sqrt{R^2 - r^2} \tag{1}$$

Therefore, the distance from the center of the marker to the ground surface, H_m, is calculated as:

$$H_m = H \pm h \tag{2}$$

where H is the distance from the middle plane to the ground surface. It is noted in Equation (2) that the depth, H, of the middle plane of a certain x-ray beam under the ground surface at the soil box is always availably known from the loading test.

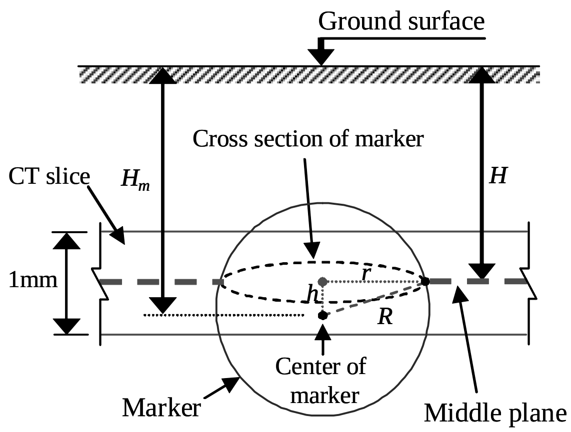

Figure 8. Large scale of a marker and an x-ray beam.

It is determined based on the setting on the CT scanner before carrying out process of scanning. The positive or negative sign in Equation (2) is taken depending on position of the middle plane, which is considered to be above or under the center of the marker.

3) Observation of 3-D behavior of the soil:

Figure 9 shows a 3-D simulating image of the markers at three depths in the initial condition and after three loading steps, including deformations of the model pile. It is realized that the markers at 22 mm depth were almost moved up totally. The markers near the model pile were moved obliquely from the initial positions. This can be explained as a slip up of the soil due to lateral pile loading. For the markers gradually far from the model pile, their movement tendencies were on upward direction. It may be due to the pressure of the lateral load at areas far from the pile could not exceed the natural soil pressure (at rest). It is seen that the markers lying on X-direction at the center line were mostly affected from the pressure of the lateral load. It is also observed in these figures the spatial increments of movements of the markers.

For the markers at 46 mm depth, they moved horizontally instead of upward after the first and second loading levels. These may be because the pressure of the weight of the upper soil of this level was relatively large compared to that of the lateral load. But after the third loading step, the markers were moved up.

For the markers at 70 mm depth, they were not moved after the first loading step because the pressure of the weight of the upper soil was relatively larger. After the second and third loading levels, they were only moved horizontally.

By connecting centers of the markers at the stages before and after loading, vectors of their movements or 3-D behavior of the soil inside the failure zone due to the lateral pile loading are indicated in Figure 10.

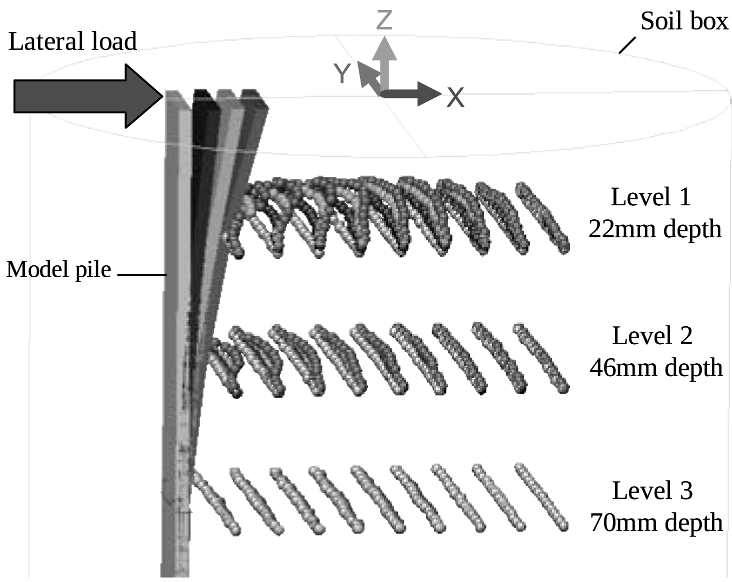

Figure 9. 3-D simulation of markers and model pile after three loading steps.

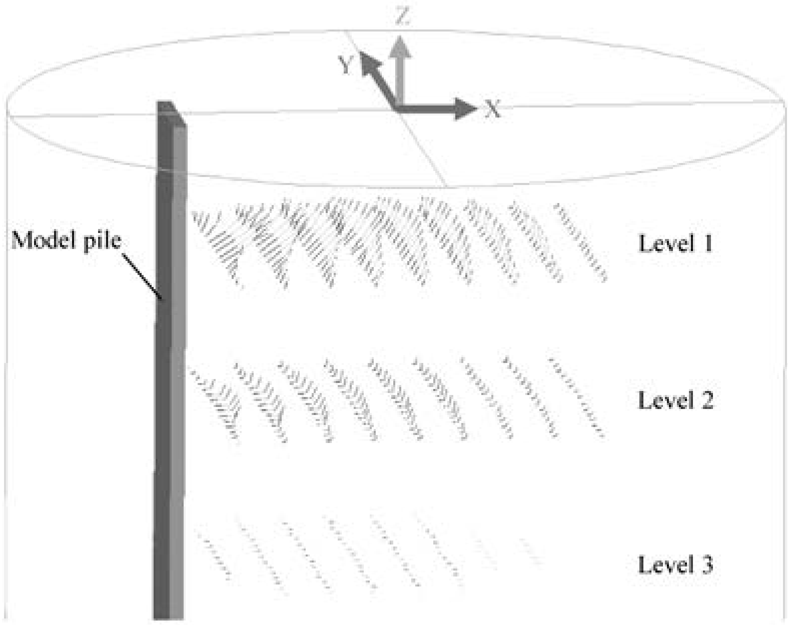

Figure 10. Vectors of movements of markers at three levels in soil box after three loading steps.

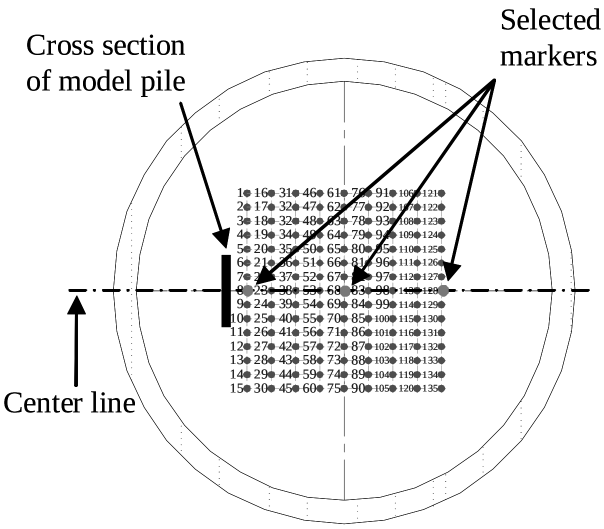

Figure 11. Plan view of numbered markers.

5.3 Quantitative discussion

Based on the vectors of the movement of the markers, quantitative evaluation on tendencies of the 3-D behavior of the soil could be conducted. In order to show that possibility, several typical markers at 22 mm depth were selected.

Figure 11 shows a plan view of numbered markers at 22 mm depth with the selected ones, which are those of numbers 8, 68 and 128 on the center line. Figure 12 shows a quantitative evaluation on tendencies of 3-D movements of these markers after three loading steps. It is noted in this figure that three vectors of the movement are drawn in their local coordinate systems of $O_8X_8Y_8Z_8$,

$O_{68}X_{68}Y_{68}Z_{68}$ and $O_{128}X_{128}Y_{128}Z_{128}$, which are congruent to the main coordinate system, OXYZ, shown in Figure 10.

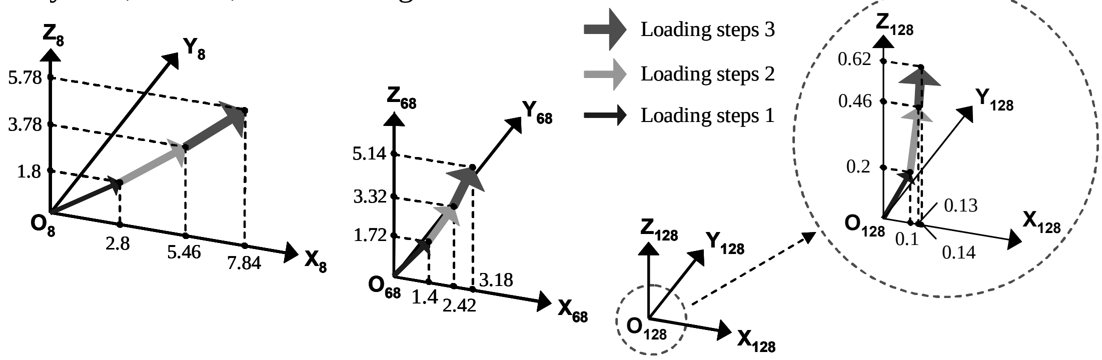

Figure 12. Tendencies of movement of markers number 8, 68 and 128.

In Figure 12, it is shown that when the loading is increased, the tendencies of the movement of these markers are those on upward direction. It is also realized from this figure that the marker number 8 is moved obliquely in the $X_8O_8Z_8$ plane when the loading is increased, but the tendency of movement of this marker becomes upward at large loading level.

Based on these typical results, it is shown that the technique developed herein for image processing analysis could be used for precise evaluation of soil behaviors inside the failure zone due to lateral pile loading.

6. CONCLUSIONS

A technique of image processing analysis for precise visualization of 3-D behavior of soil inside the failure zone due to lateral pile loading was developed. The results showed a possibility of this technique that could be applied for quantitative evaluation of soil behavior not only for laterally loaded pile but also for other field of study in geotechnical engineering, in order to improve safety for buildings' pile foundation of mega cities in Asia.

REFERENCES

Broms, B. B. 1964. *Lateral resistance of piles in cohesionless soils*, Proc. ASCE 90, SM (3): 27-63.

Otani, J., Mukunoki, T. and Obara, Y. 2000. *Application of X-ray CT method for characterization of failure in soils*, Soils and Foundations, 40(2): 111-118.

Pham, K. D., Sano, J. and Otani, J. 2004. *Development of new test apparatus for lateral pile loading using X-ray CT scanner*, Proc. Vietnam - Japan Joint Seminar on Geotechnics and Geoenvironment Engineering: 86-93.

Reese, L. C., Cox, W. R. & Koop, F. D. 1974. *Analysis of lat-erally loaded pile in sand*, Proc. Offshore Technology Con-ference, Houston, TX: OTC2080.

Assessment of urbanization impact to temperature, rainfall and flooding situation of Ha Noi city taken into account climate change

Vu Minh Cat,
Water Resources University,
Ha Noi, Viet Nam

ABSTRACT

Rain induced inundation is still serious in old city of Ha Noi although the drainage system has been being improved and upgraded gradually.
Rainfall data from 1960 till now show that annual rainfall trends to decrease 3 to 5%, but daily rainfall and shorter duration is increased about 10%. The urbanization is being occurred rapidly from city centre to outside that causes reducing some thousands hectares of agricultural land and lake and pond area is also decreased from 850 hectares to 550 hectares from 1990 till now. The main drainage rivers including To Lich, Lu, Set, Kim Nguu and some hundreds of canals, gutters from core city have been improved and canalized. However due to many reasons such as unacceptable dimension of drainage sluices, small cross section of drainage canals, sparse network of drainage, blocking up due to rubbish and waste materials etc. the inundated situation is occurred frequently, even rainfall seems to reduce.

Keywords: *Climate change, Rainfall regime, core area of Ha Noi, rain induced inundation, regulated lake*

1. INTRODUCTION

In 1954, area of Ha Noi is of 152km^2 and population of 53.000 inhabitants; in 1961 it was increased to 584km^2 in area and 91.000 peoples; in 1978, Vietnamese parliament decided to expand the capital into 2.136km^2 and 2.5 millions of inhabitants; in 1991, Ha Noi capital area was still of 924km^2 and more than 2 millions of people and in 2009, Hanoi was expanded with 3.325 km^2 and more than 6.4 millions inhabitants and becomes 17th ranking of world capitals in term of area.
Together with expansion of area, the urbanization in Ha Noi is occurred rapidly with many new living quarters, industrial areas and infrastructures and huge area of agricultural land is transformed into city. It means that ground surface is betonized and lake and rain water stored land is reduced significantly.
Natural rivers that can regulate water for the core area of Ha Noi are Nhue in the west and To Lich, Lu, Set and Kim Nguu. Now they are main drainage system and waste water for core area. However, the conveyance capacity is reduced significantly due to sedimentation and blocked seriously socio-economic activities.

Lake and pond area is also decreased from 850 hectares to 550 hectares from 1990 till now that is one of the reason to decrease rain regulated capacity and increased inundation.

With rapid urbanization, the meteo-hydrological parameters as temperature, rainfall are also changed quickly with higher rainfall intensity in rainy season, but drought also becomes more serious. With above reasons, inundated situation becomes seriously for core area of Ha Noi.

In this paper, the change of rainfall pattern and inundated situation is assessed and simulated for the core area of Ha Noi under the impact of urbanization and propose solutions to mitigate negative effects and gradually to improve city environment taken into climate change.

2. RESEARCH METHODOLOGY

In order to assess the inundated situation in core area of Ha Noi, the following methods are applied:

1. Based on observed data of meteo-hydrology, topography, inundated location, depth and duration and drainage system, the analysis and computation is carried out to assess and find out the inundated reasons for the core area of Ha Noi.
2. Application of Storm Water Management Model (SWMM) to simulate and quantitative assess inundated situation at core area with 2 rainfall events in November 1984 and November 2008. From simulated results, solutions to mitigate negative situation are proposed.

3. RESEARCH RESULTS AND DISCUSSION

3.1 Brief information of topography and existing drainage system of core area

As said above the study is carried out for the old Ha Noi city including 9 districts namely Ba Đinh, Hoan Kiem, Đong Đa, Tay Ho, Hai Ba Trung, Thanh Xuan, Cầu Giay, Hoang Mai and Tu Liem. Average ground elevation of area is of + 7 t0 + 8m, in which area having elevation greater than +8.00 is of 3,5 km^2 distributed mostly at Hoan Kiem district (narrow strip running from Yen Phu to river port of Ha Noi) and part of Ba Ding, Cau Giay districts along Hoang Hoa Tham, Buoi and dike from Tay Ho to Dong Mac. Elevation from +5 to +8 is of 50% and distributed mostly in south and southwest including low lying lands for agriculture, aquaculture and housing areas Lakes, ponds and natural rivers are located at the end of catchment with elevation lower than +5.00 in Dong Da, Thanh Xuan, Hai Ba Trung and Thanh tri districts.

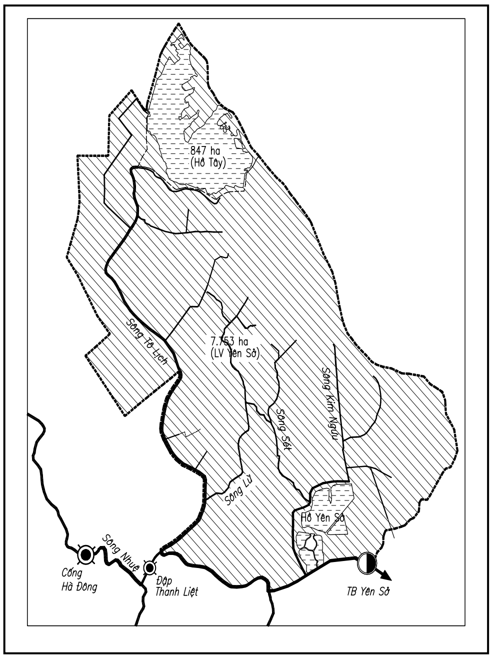

Figure 1: Study area

To lich, Lu, Set and Kim Nguu are main drainage system for the core area. It is shown in figure 1.
Waste and rain water from housing areas and streets is concentrated firstly into under ground sluices and then flowing to gutter and minor drainage canal just after the sluice lines and finally running to main 4 drainage rivers where water continues to flow the south. In case water level at downstream of Thinh Liet barrage is lower than +3.5m, it is opened and water is released into Nhue river and if water level there is greater than +3.5m, barrage is closed and water is flowing to Yen So lake through the canal of 7 km and pumped to Red river.

3.2 Development of infrastructures in surrounding core area

In current years, the infrastructures in Ha Noi are developed significantly to contribute socio– economic activities and serve citizen needs. Many transport roads are improved and constructed such as Hung Vuong avenue, national road 32, highway Phap Van – Cau Gie, ring road 3 Mai Dich – Phap Van etc. and many new urban areas are developed and expanded into west and southwest areas such as Linh Dam, Đai Kim, Dinh Cong, Tran Duy Hung, My Dinh Sport composite etc. However, existing drainage system is exposed many disadvantages and did not meet requirement if being considered in term of water drainage. When low-lying areas that are agricultural land or lakes are reduced then water body to store water temporarily before flowing to drainage system is also not existed that will cause more inundation in the core areas. In the other hand, the drainage system in the new developed sub-areas are not meet the requirement, so many new developed areas are also inundated in case of rainfall event is only less than 100 mm.

3.3 Rainfall regime changes due to climate change

In general, inundation in Ha Noi is mostly due to rainfall occurring in short duration (from hour to two days). Based on the recording data at Lang, Ha Noi from 1961 to 2010, the time series of daily and annual rainfall are constructed, then it shows that daily rainfall seems increasingly when annual rainfall is decreased. The increase of daily rainfall will impact strongly to drainage system and inundated situation will be more serious if drainage system is not improved accordingly.

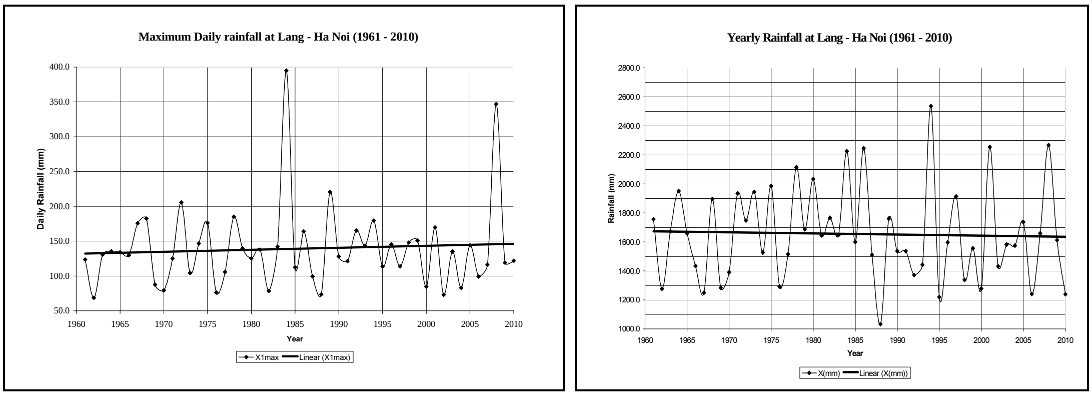

Figure 2: Time series of daily and annual rainfall at Lang, Ha Noi

Two typical rainfall events in November 1984 and November 2008 are considered for simulation of hydraulic regime and inundation in core areas.

Table 1: Hourly rainfall of 2 considered rainfall events

Time	XI/1984	XI/2008	Time	XI/1984	XI/2008
0-1	0.0	2.5	0-1	5.9	16.9
1-2	0.0	11.7	1-2	**126.5**	0.6
2-3	0.3	24.3	2-3	52.1	0.4
3-4	0.1	28.4	3-4	12.1	0.1
4-5	1.2	39.1	4-5	18.6	1.8
5-6	0.5	6.8	5-6	60.5	2.9
6-7	2.1	40.6	6-7	16.7	6.1
7-8	5.1	5.5	7-8	1.9	20.5
8-9	5.7	17.1	8-9	2.2	2.7
9-10	5.0	**68.8**	9-10	1.1	3.0
10-11	5.7	24.4	10-11	0.3	3.7
11-12	4.8	6.6	11-12	0.0	13.1
12-13	34.4	0.3	12-13	0.0	2.2
13-14	8.4	0.1	13-14	0.0	5.8
14-15	6.0	16.8	14-15	0.0	1.6
15-16	11.2	17.8	15-16	0.0	0.1
16-17	22.3	4.8	16-17	0.0	0.0
17-18	27.0	15.2	17-18	0.0	0.0
18-19	3.2	10.5	18-19	0.0	2.2
19-20	1.6	13.2	19-20	0.0	0.2
20-21	4.7	5.5	20-21	0.0	0.0
21-22	5.5	19.2	21-22	0.0	0.0
22-23	13.0	3.0	22-23	0.0	3.0
23-24	94.9	2.7	23-24	0.0	3.6
				560.4	**475.2**

3.4. Simulation of hydraulic regime and inundated situation in core areas

In order to assess the hydraulic regime and inundation situation, SWMM is used. The study area is schematized in model as figure 3 in which there are 60 sub-areas, 19 lakes, 104 nodes, 120 sluice lines, 12 barrages, 4 drainage river name To Lich, Lu, Set, Kim Nguu and drainage pumping station of Yen So.

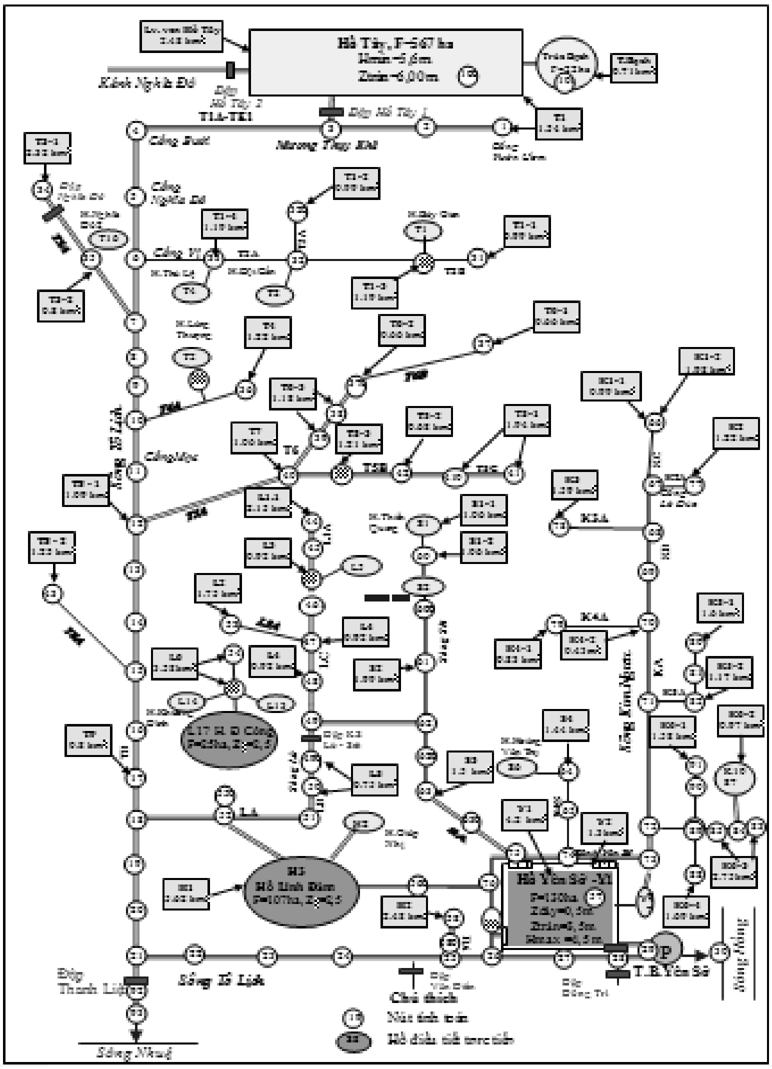

Figure 3: Schematization of drainage system in core area of Ha Noi

Logically the above drainage system will be worked as following when rainfall happens:

- Rain water at housing and sub-areas (being shown as yellow colour) will concentrate into sluice lines, later it flows to gutters and small canals connected directly to the sluice lines and finally flowing to main drainage rivers.
- 4 drainage rivers namely To Lich, Lu, Set and Kim Nguu are open channel to carry rain water from catchment to the end of system where water will release to Nhue river if water level downstream of Thanh Liet barrage is less than +3.50m. In case water level downstream of Thanh Liet is greater than +3.50m, rain water will flow through the canal to Yen So reservoir and finally pumped to Red river.
- It is also mentioned that in the system, there are 19 retention lakes that can store a part of rain water in it and will be released gradually when water level in drainage river is lowered.
- Yen So pumping station is included 5 normal pumps and 18 emergency pumps with total capacity of 90 m^3/s. When water level at suction tank is greater than +1.50m, the normal pump will start working and if water level is higher than +2.40m, pumping station will be connected to Yen So reservoir where rain water

will be concentrated there and emergency pumps start working. How many pumps are operated depending on quantity of rain water coming to reservoir. The whole system will be stopped when water level in suction tank is lower than +1.50m. Regulated procedure of pumping station is shown in figure 4.

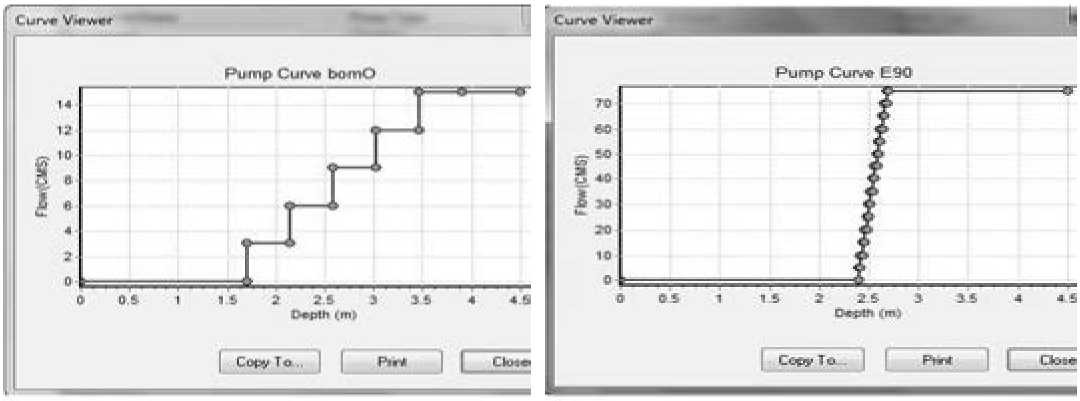

Figure 4a: Relationship between water depth and pumping discharge for norm Figure 4b: Relationship between water depth and emergency pump of

Figure 4: Working procedure of pumping station

Two rainfall events are used for simulation is shown in table 1.
In order to see the change of water level and inundated situation of the core areas, number locations in the scheme are extracted.

- Node 22 belongs to To Lich river in upper part of Thanh Liet barrage
- Node 49 is on Lu river around crossing point of Lu river and Truong Chinh street
- Node 62 is on Set river around crossing point between Set river and Nga Tu Vong street
- Node 68 belongs to Kim Nguu river at the section between Tran Khat Chan and Lac Trung streets
- Node 72 belongs to Kim Nguu around Mai Dong bridge area
- And Thu Le and Linh Dam lakes

Simulated results are summarized in table 2 and shown in the figure 5.

Table 2: Simulated results at nodes on the drainage system

TT	Node	River/lake	Duration (hrs) WL > +3.7		Peak water level (m)		GL (m)
			XI/1984	X/2008	XI/1984	X/2008	
01	22	To Lich	42	70	5.00	4.80	5.92
02	49	Lu	42	70	5.40	5.40	5.56
03	62	Set	50	81	5.25	5.25	5.95
04	68	Kim Ngu	45	75	6.00	5.50	5.95
05		Thu Le lake	45	70	5.15	6.00	7.80
06		Linh Dam	40	70	5.25	5.00	5.60

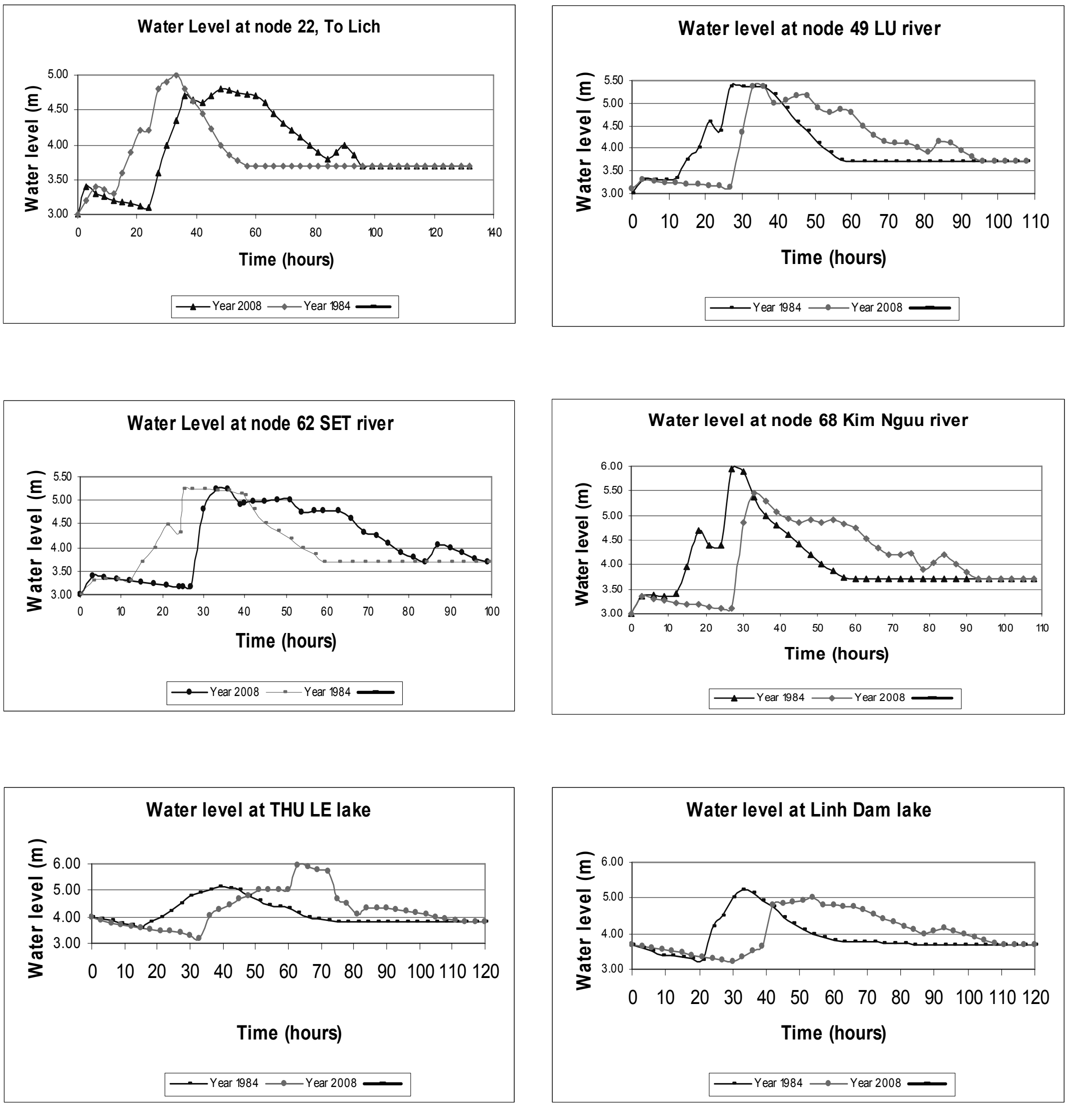

Figure 5: Simulated results at nodes in the drainage scheme

3.5. Discussion

- Rainfall patterns both quantity and distribution shape in November 1984 is more unfavorable than that in November 2008 in term of drainage. As recorded, maximum hourly rainfall in 1984 is of 126.5mm, when it was of 68.8mm in 2008. Similarly total rainfall in 3 continuous hours between 2 above events is of 190.7mm/110.4mm and 560.4/475.2mm for two days. But inundation in 1984 was lesser than that in 2008 in term of area, depth and duration
- Highest water level: As results summarized in table 2, maximum water level at nodes 22, 49, 62 and 68 seems to change litter bit at each point for both rain events. It means that although rainfall in 1984 is bigger, but the role of water regulation of lake, low-lying land around the city and large unconcretization of land in the city can reduce the inundation.

- Duration to keep high water level in drainage rivers (H > 3.70m): It is a great difference between 2 rainfall events. With rainfall event of 1984 the duration is only 42 to 50 hours, but it is of 70 to 80 hours for rain event of 2008. The same situation occurred at 2 studied lakes of Thu Le and Linh Dam. It can be explained that drainage rivers are good enough to convey water, but rain water is blocked at upper stages (gutters, small canals and sluice lines) to cause more inundation in the city and the longer time of releasing water to the main drainage rivers.

- As said above, ground elevation (GL) is decreased in the direction NW – SE and almost higher than maximum water level along the drainage rivers. But based on data reported by The Ha Noi drainage Company Ltd., with the rainfall event of around 100 mm then there are more 20 inundated locations permanently in which the inundated depth of 0.4 – 0.5m was existed at Le Duan, Pham Hung, Thai Ha, Thai Thinh, Quan Nhan, Nguyen Xien streets

From simulated results and observed data of Ha Noi Drainage Company Ltd., one can have conclusions as following:

- After rehabilitation, upgradation and new construction, 4 main drainage rivers and Yen So pumping station are good enough and they can drain perfectly with the rain event up to 310 mm in 2days if the drainage system is operated correctly.
- The serious inundation along the streets in core area can be explained as following:

1) The large reduction of retention lakes in the city

As stastical data of Ha Noi constructive Department, there are 111 lakes with total area of 1,165 hectares in which West lake is of 500 hectares (about 50%). In more than 20 year up to now starting in 1990, there are 21 lakes were disappeared with more than 300 hectares (or 36%). If seeing into existing lakes, one can find that due to unmanageable status water surface is encroached and reduced significantly in term of area and lake bottom is deposited as waste material from socio-economic activities and resulting that stored capacity of these lakes are gradually smaller. For this reason, the retention role of lake is disappeared and water is overflowed on the ground surface where are concretized mostly and inundated situation becomes more serious.

2) Narrowing agricultural land around the city due to urbanization

In 15 current years, some thousands hectares of agricultural and low-lying lands that can store much rain water is transformed into urban ones. Many new housing, industrial areas are constructed and transportation infrastructures are expanded in the west and south of core zone belonging Tu Liem, Dong Da, Thanh Xuan, Hoang Mai, Hai Ba Trung districts. It is one of the reasons to accelerate inundated situation in the city. If considering the drainage system in the new urban areas itself, we can say that it is behind the requirement.

3) On sluice network collecting directly rain water from house roofs and streets

Ha Noi is more flat and rain to cause inundation is more serious, but sluice network to collect directly rain water from house roofs and streets is not met requirement. It means that network is not dense enough and dimension of the sluice seem too small while they are deteriorated and blocked by raw rubbish, so rain water could not be transported through the sluice lines and it must be kept in the street to cause inundation.

4) On the minor canal system connected directly to sluice network

Logically rain water firstly is collected from the roofs and streets and transported through sluice network and latter water will transport to the minor canal system connected directly to sluice network before going to the main drainage rivers. The length of this minor system is of some hundred kilometers, located nearby the housing and subjected to all socio-economic activities. They are occupied illegally and cross section is narrowed many sections. Also all waster materials and rubbish are put in it, so water conveyable capacity through it is reduced significantly. At present, many minor canals are concretized and become close system, but with uncontrollable status, they may become dead in near future and drainage system of Ha Noi become worse.

CONCLUSIONS AND RECOMMENDATIONS

- Based on observed data, reports of rehabilitated, upgraded and new constructed projects of drainage network in Ha Noi and simulated technique, we can understand more clearly on drainage network and inundated situation in core zone of Ha Noi.

It is clearly that the main reasons to cause seriously inundation is

- To narrow the retention lakes due to illegal land occupation and put into it much waste materials and rubbish
- To transfer much low-lying and agricultural lands around core zone into urban ones
- The sluice and minor canal network is destroyed and deteriorated seriously due to uncontrollable activities, so they could not convey rain water to the main drainage rivers.
- Study realized that 4 main drainage rivers and Yen So pumping station are good enough to drain rain water with rain event of more than 310mm in 2 days. However, under the impact of climate change, rainfall in short period will be increasing, so it is needed to forecast these changes for the adaptation of drainage system in future.
- Study results are ideas for master plan of drainage system in particular and for design of whole infrastructures including electrical cables, water supply and even underground transportation system that will be developed in future.

REFERENCES

(1) Hoang Van Hue (2002). The drainage, Scientific and Technical Publishing House, Ha Noi.

(2) Lewis A. R. (2008). Storm Water Management Model, User’s Manual, Version 5.0. EPA.

(3) TCVN 7957:2008. The drainage – Network outside structures – Design standards.

(4) The number of drainage and waste water treatment projects for Ha Noi from 2002 till now.

Study on carbonation and pore structure of cementitous materials exposed to supercritical CO_2

Ryosuke HIRAI[1], Hikaru ISOZAKI[2], Shingo ASAMOTO[3]
[1] Graduate Student, Department of Civil & Environmental Engineering,
Saitama University, Japan
s12me119@mail.saitama-u.ac.jp
[2] Undergraduate Student, Department of Civil & Environmental Engineering,
Saitama University, Japan
[3] Associate Professor, Department of Civil & Environmental Engineering,
Saitama University, Japan

ABSTRACT

In this study, the carbonation progress of the cement paste in an injection well for a carbon capture and storage project is investigated. The hardened cement paste is exposed to supercritical CO_2 to examine the progress of the carbonation and the variation of the pore structure under the severe condition. The application of the cements such as Ordinary Portland and fly ash cement in civil engineering field to the well is also studied as well as the application of oil well cement in oil & gas field. In the case of oil well cement, when it is subjected to high temperature and high pressure, small amount of C_3A could prevent from cracking. On the other hand, many cracks on the surface of cement paste using Ordinary Portland cement occur and cement paste with fly ash has micro cracks on the surface under the severe condition. When oil well cement is used, the carbonation of C-S-H gel causes the increase of $CaCO_3$ amount in the paste, while Ordinary Portland cement and fly ash cement slightly increase the amount of $CaCO_3$ due to the C-S-H gel carbonation. It is inferred that C-S-H gel characteristics of oil well cement could be different from the others and lead to different precipitation of $CaCO_3$. It is experimentally found that the carbonation of C-S-H gel makes the pore structure coarse, especially pores of over 100 nm diameter in all cements. It is indicated that oil well cement is appropriate for the deeper well with higher temperature and pressure. Since the resistance of the carbonation under supercritical CO_2 is not significantly different among the cements. Cements other than oil well cement might be applied to the shallow injection well.

Keywords: *CO_2 capture and storage, carbonation, pore structure, supercritical CO_2, oil well cement*

1. INTRODUCTION

The reduction of the CO_2 emission is one of the most significant issues. As the countermeasure to the reduction, Carbon dioxide Capture and Storage (CCS) projects have been focused on as one of state-of-art technologies in recent years. In the projects, the CO_2 collected from factories is injected into a geological reservoir at deep underground through the well and stored in the reservoir for a long time in order to isolate the CO_2 to be reacted with the mineral as shown in Figure 1. The well is composed of a cement paste and a steel casing, and reaches over 1000 m depth. The well could have various deteriorations under the severe environment of deep underground such as high pressure, high temperature and high concentration of the injected CO_2. When the well is seriously deteriorated, the leakage of the CO_2 gas is likely to occur through the deteriorated sections. Figure 2 shows that the possible pathways of the CO_2 gas leakage, e.g. cracks in the deteriorated casting and cement paste, the interfaces between the casing/cement and cement/formation. The prevention of the leakage of the CO_2

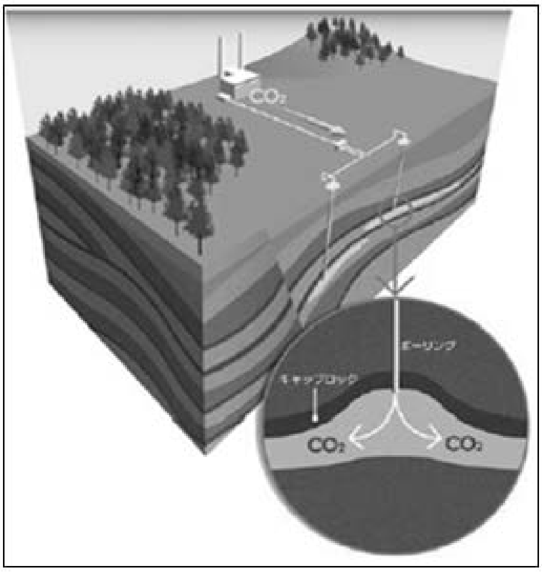

Figure 1: The overview of CCS projects

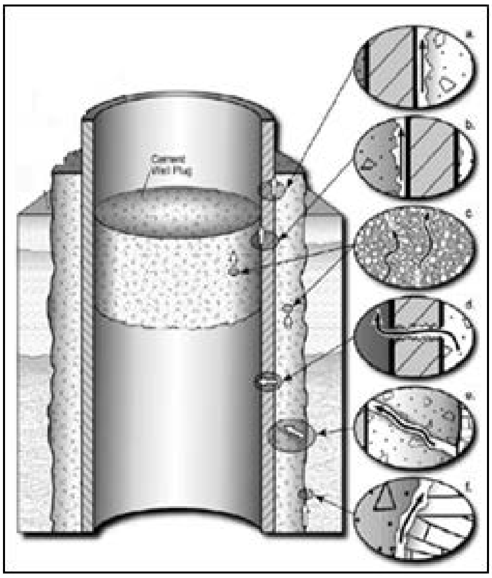

Figure 2: The cross section of the well and pathway of the CO_2 gas

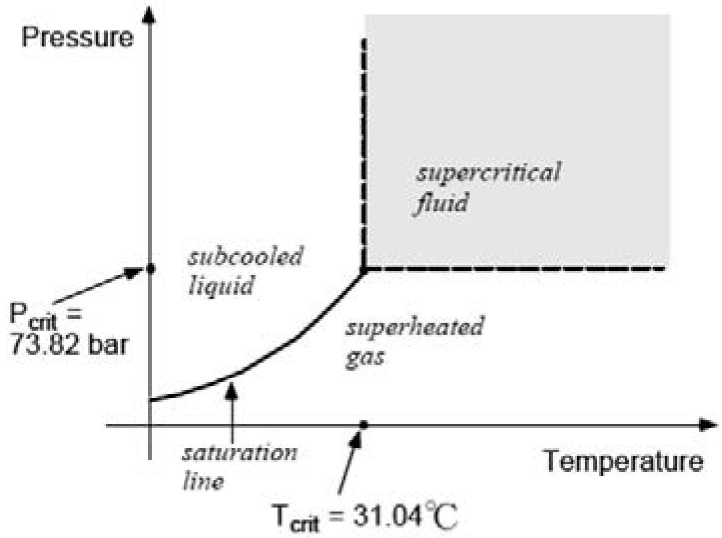

Figure 3: Phase change of the CO_2

gas stored in the reservoir is indispensable for CCS projects. The injected CO_2 could be changed into a supercritical state at deep underground (Figure 3) due to high temperature and pressure. Supercritical CO_2 is intermediate fluid with characteristics of both gas and liquid, and has high permeability. When the well is exposed to the supercritical CO_2, it is suggested that the deteriorations could be faster [1)] in comparison with the case of CO_2 gas or liquid However, the carbonation process of cement paste under supercritical CO_2 has not yet been clarified. For development of the technology, the integrity of the well should be inconsistently comprehended for the effective confinement of the CO_2 in the geology.

In this study, the authors focus on the hardened cement paste in the well and study the carbonation process under supercritical CO_2. In the experiment, cement pastes with oil well cement, Ordinary Portland cement and fly ash cement are exposed to the supercritical CO_2 under the severe condition assuming the actual environment at the deep underground. The applicability of each cement to the CCS well is examined. After the exposure, the phenolphthalein is transfused on the cutting surface and thermal analysis test are carried out in order to measure the carbonation depth. Mercury intrusion porosimetry test is also conducted to measure the change in the pore structure due to the carbonation.

2. EXPERIMENTAL PROGRAM

2.1 Materials

Three types of the cement were used in the experiment: oil well cement (OWC), Ordinary Portland cement (OPC) and the Ordinary Portland cement with 20 % replacement by fly ash (FA). Although the cement paste in the well generally has a water/binder ratio (W/B) of about 45 %, the W/B of the cement paste in the experiment was set to 55 % in order to promote the carbonation during a limited experimental period.

2.2 Experimental set-up

2.2.1 Supercritical CO_2 exposure

The specimen size of the cement paste was 100 mm x 50 mm cylinders. Specimens were cured under sealing until age of 7 days at 80 ℃. The curing temperature was determined assuming the environment of the underground at a depth of about 2000 m according to the temperature rise of 3 ℃/100 m with increase of the depth. After the curing, the upper and lower parts of about 25 mm in the specimens were cut (Figure 5) by the concrete cutter in order to prevent the effect of the bleeding. The cutting specimens were exposed to supercritical CO_2 in the vessel of supercritical CO_2 generator as given in Figure 4. Supercritical CO_2 was generated by setting the condition in the vessel to 80 ℃ at pressure of 10 MPa. The exposure periods were 1 day, 3 days and 7 days. Two specimens were prepared for each condition, thus, total 18 specimens were used.

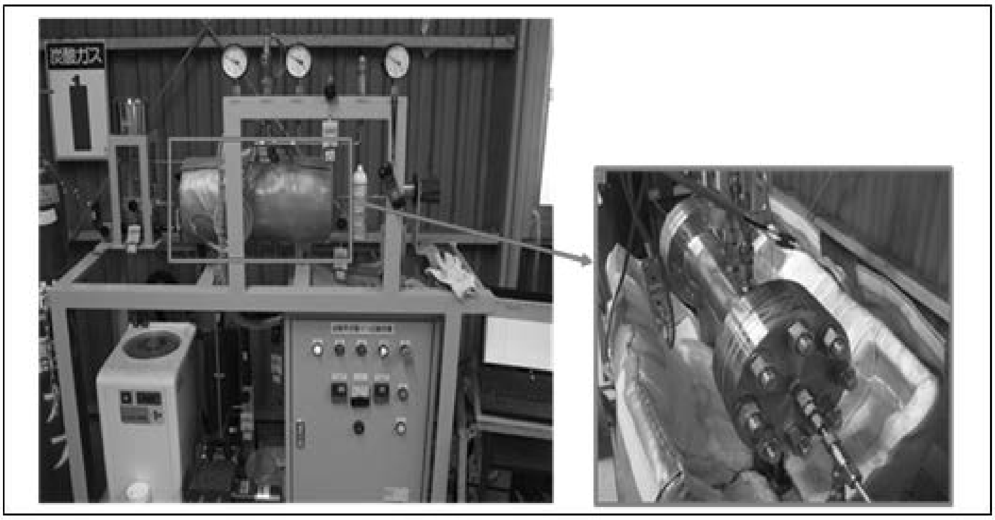

Figure 4: Supercritical CO_2 generator and vessel

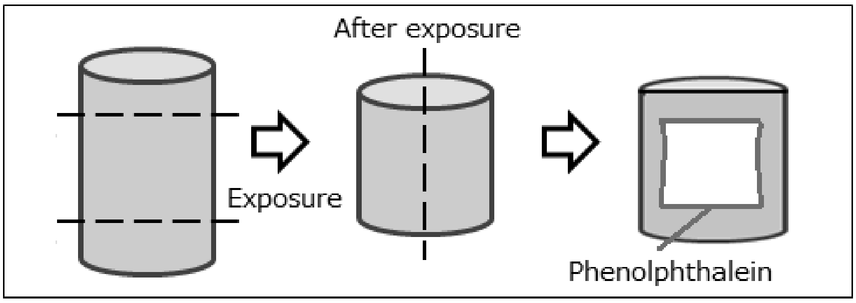

Figure 5: Cutting method of the specimens

2.2.2 Phenolphthalein indicator test and Thermal analysis test

After the exposure to supercritical CO_2, the solution of phenolphthalein was used to measure the carbonation depth of the specimen. The specimens after the exposure were cut vertically, and the 1 % phenolphthalein solution was splayed on the cross section to measure the noncolored depth due to the carbonation as shown in Figure 5. Also, thermal analysis test was conducted to measure the variation of hydration products due to the carbonation. The carbonation reaction in the cement paste is shown in equation 1.

$$Ca(OH)_2 + CO_2 \rightarrow CaCO_3 + H_2O \tag{1}$$

The same specimen as used in the phenolphthalein indicator test was used in thermal analysis test. The samples for the test were collected at the three points (0-5 mm, 10-15 mm, 20-25 mm) from the surface of the specimen exposed to supercritical CO_2 as shown in Figure 6. The collected samples were grinded into powder and set in TG-DTA thermal analysis test machine. The temperature was risen from room temperature to 100 ℃ with 10 ℃/min, and remained for 10 minutes to evaporate the liquid water in the sample as shown in Figure 7. Then, the temperature was risen to 1000 ℃ with the same temperature rise velocity. The amount of $Ca(OH)_2$ and $CaCO_3$ due to the dehydrogenation and decarbonized

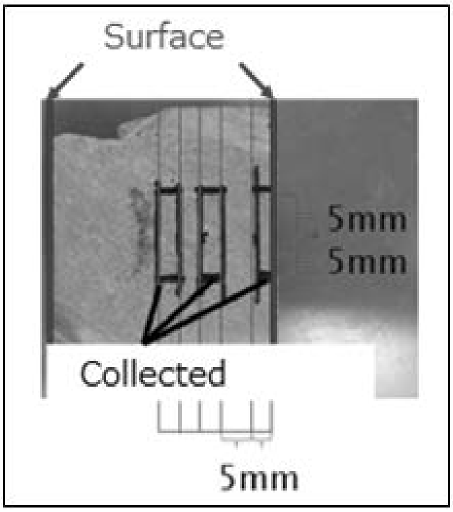

Figure 6: Sampling points

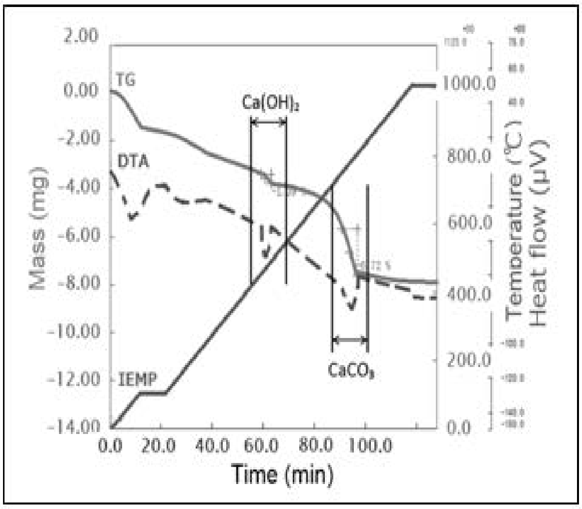

Figure 7: Result of DTA analysis

reaction were obtained by the mass loss based on the DTA information. Figure 7 represents that $Ca(OH)_2$ is dehydrated at 400-500 ℃ and $CaCO_3$ was decarbonized at 700-800 ℃ according to the endoergic peak by the DTA.

2.2.3 Mercury intrusion porosimetry test

The mercury intrusion porosimetry test was carried out in order to examine the change in the pore structure due to the carbonation under supercritical CO_2. After exposing for 1 day and 7 days, the samples were collected from the two points at 5 mm square area (0-5 mm, 20-25 mm from the exposure surface) in the same specimen as that for the thermal analysis test. The measurement was conducted after the vacuum freeze-drying for 24 hours. The pore distribution in the range from 3 nm diameter to 360 μm diameter was obtained assuming the cylindrical model which has 0.484 N/m of surface tension of the mercury and 130 degrees of contact angles.

3. EXPERIMENTAL RESULTS

3.1 Carbonation phenomena in supercritical CO_2 exposure test

3.1.1 Phenolphthalein indicator test

The experimental results of the phenolphthalein indicator test are shown in Figure 8. It was experimentally found that the red colorings by the phenolphthalein solution were heterogeneous in all cases, so that it was difficult to identify the carbonation depth. Especially, in the case of the OPC, micro cracks and destruction were observed in all specimens after the exposure, and the carbonation progress was irregularity. It is inferred that rapid drying under high temperature and high pressure could cause the cracking. In addition, C_3A included in Ordinary Portland cement could react rapidly during the curing and the exposure test at high temperature and results in the coarse pore structure[2), 3)] and the strength could decrease. On the other hand, the cracks were not observed in the case of the OWC. It is because a few C_3A and rich C_3S included in oil well cement could

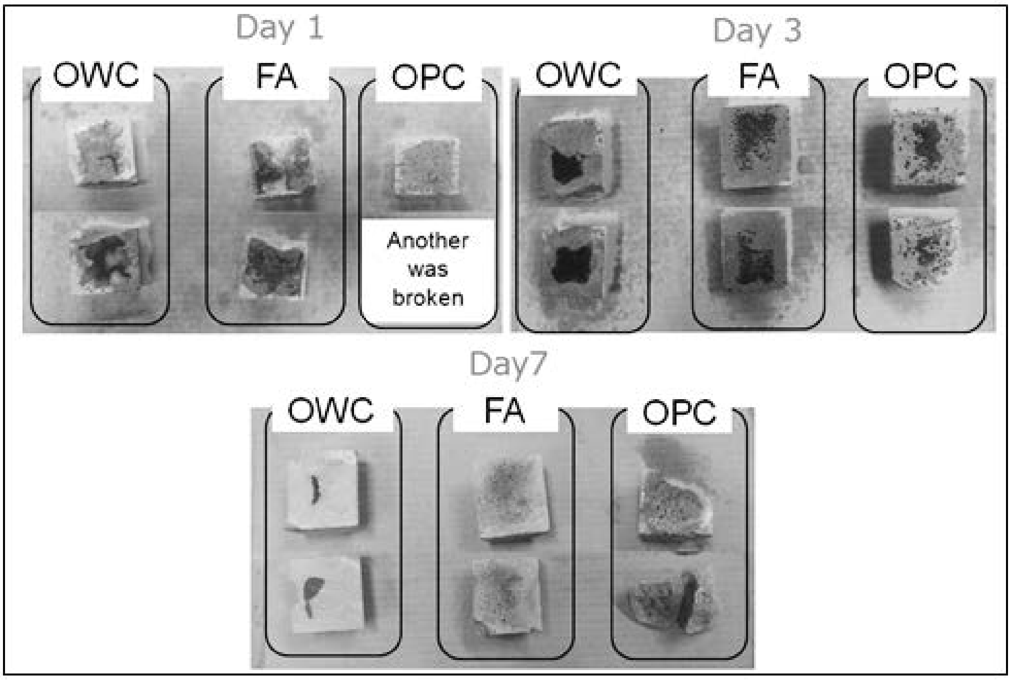

Figure 8: Result of the phenolphthalein indicator test after the supercritical CO_2 exposure test

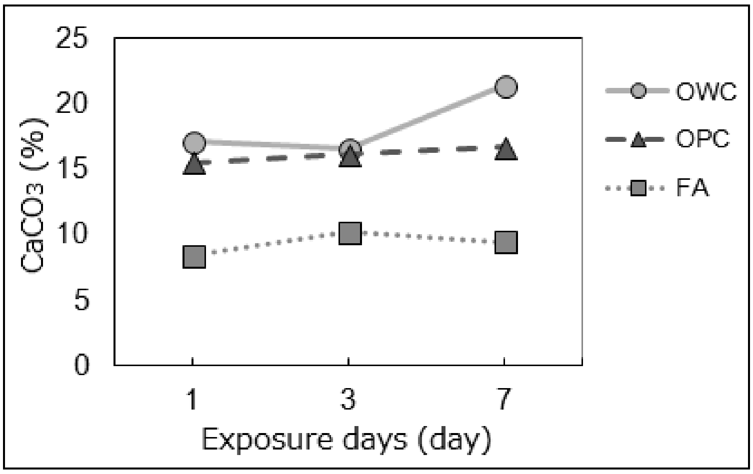

Figure 9: The amount of CaCO3
as exposure days at the 0-5 mm from the exposure surface

continuously develop the strength even under high temperature, so that the cracks were not observed visually. In the case of the FA, the pozzolanic reaction could be accelerated during the curing at high temperature and the strength was developed not to cause the observable cracks but micro cracks on the surface.

3.1.2 Thermal analysis test

The variation of the $CaCO_3$ content at the 0-5 mm from the exposure surface is shown in Figure 9. The $CaCO_3$ content 7 days after the exposure is increased in

Table 1: The amount of $Ca(OH)_2$ of the specimens cured with sealing under the room temperature for 26 days

Cement	OWC	FA	OPC
$Ca(OH)_2$ (%)	3.66	1.17	3.62

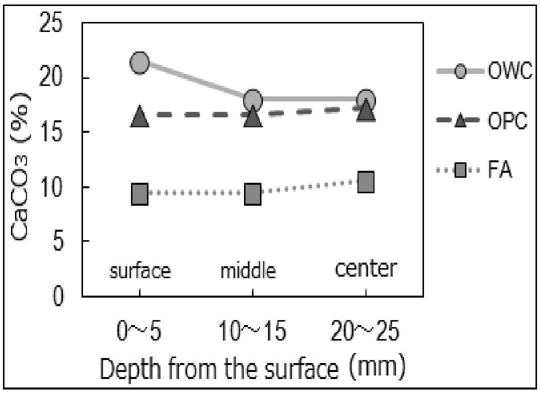

Figure 10: The amount of CaCO3 as the depth from the surface at the 7 day of the exposure

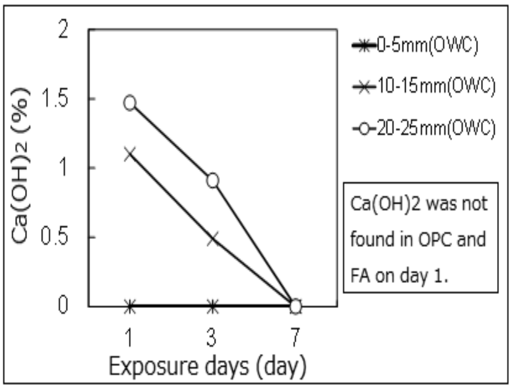

Figure 11: The amount of CaCO3 as the exposure days of the OWC

comparison with that 1 day after the exposure in all specimens. The $CaCO_3$ content in the OWC and OPC was almost the same and that of the FA was the smallest. The reason why the $CaCO_3$ content of the FA was the smallest is that $Ca(OH)_2$ could be used due to the pozzolanic reaction with the fly ash during the curing at high temperature and an initial amount of $Ca(OH)_2$ could decrease. Table 1 shows the amount of $Ca(OH)_2$ of each specimens cured under sealing at the room temperature for 26 days. Although it was different curing condition with the experiment, the amount of $Ca(OH)_2$ in the FA is less than the half of that in comparison with the OWC and OPC and the above hypothesis could be valid.

According to the result of phenolphthalein indicator test, as shown in Figure 8, the part of 0-5 mm (surface) were not colored in all specimens on 1 day after exposure. It is suggested that $Ca(OH)_2$ near the exposed surface could be carbonated. All $Ca(OH)_2$ at the surface are carbonated at 1 day after exposure as shown in Figure 11 but the amount of $CaCO_3$ still increase after that. When all $Ca(OH)_2$ are carbonated, it is anticipated that the main hydration products, C-S-H gel, is carbonated after the carbonation of all $Ca(OH)_2$ [4)] under severe conditions such as supercritical CO_2. The increase of $CaCO_3$ content at the surface after the 1 day of the exposure could be caused solely by the carbonation of C-S-H gel. However, the increase of $CaCO_3$ in the OWC was larger than those in the OPC and FA. It is speculated that the C-S-H gel in the cement paste of the OWC could be carbonated rapidly or the amount of the component in C-S-H gel which could generates $CaCO_3$ due to the carbonation could be large. Further detailed investigation such as the chemical analysis should be conducted near future.

Figure 10 shows the relationships between the amount of $CaCO_3$ and the depth from the surface at the 7 day of the exposure. The exposed surface (0-5 mm) of the OWC had rich $CaCO_3$ content, while the $CaCO_3$ content is smaller at the center (20-25 mm) because supercritical CO_2 will penetrate gradually from the surface into the inside of the specimen. On the other hand, the difference in $CaCO_3$ content at each depth from the surface was not found in the cases of the FA and OPC. The results are discussed from a view point of $Ca(OH)_2$ content.

The relationships between $Ca(OH)_2$ content and the exposed time of each specimens are shown in Figure 11. The figure shows that the remaining $Ca(OH)_2$ content is larger with the distance from the surface until the 3 day of the exposure and all $Ca(OH)_2$ disappeared at the 7 day of the exposure in the case of the OWC and all $Ca(OH)_2$ disappeared at the 1 day after the exposure in the cases of the OPC and FA according to the DTA information. Since the amount of $CaCO_3$ still increase after the disappearance of $Ca(OH)_2$, it is inferred that the carbonation could proceed to C-S-H gel even at the center. $CaCO_3$ content in the OWC at the center is smaller than that at the surface as shown in Figure 10 because the carbonation progress of C-S-H gel could be small at the center and the precipitation of $CaCO_3$ by the carbonation could be small while the carbonation of C-S-H gel is significant at the surface and large amount of $CaCO_3$ was precipitated, as shown in Figure 9.

On the other hand, however, $Ca(OH)_2$ was not found at all from the surface to the center in the cases of the FA and OPC even at one day after the exposure to the supercritical CO_2. It is hypothesized that all $Ca(OH)_2$ could be carbonated faster due to the penetration of supercritical CO_2 into the center though the cracks in the case of the OPC, and in the case of the FA, the initial $Ca(OH)_2$ content could be small because of the pozzolanic reaction and lead to faster carbonation of the $Ca(OH)_2$. Due to the rapid carbonation of the $Ca(OH)_2$, C-S-H gel in the FA and OPC could be also carbonated gradually from the surface to the center. As shown in Figure 10, although there was no difference in the amount of $CaCO_3$ between the surface and center, it is suggested that the increase of $CaCO_3$ due to the carbonation of C-S-H gel in the FA and OPC could be smaller than that in the OWC as mentioned above. Since the carbonation proceeded irregularly, especially in the case of the OPC, as shown in Figure 8, it could be plausible that the result could be varied if the collected points are different. Therefore, further studies with using more samples are necessary near future.

3.1.3 Analysis the variation of the pore distribution due to the mercury intrusion porosimetry test

The results of the variation of the pore distribution by the mercury intrusion porosimetry test are shown in Figure 12. The graphs on the left side in figure shows the pore distribution at the center at the 1 day and 7 day of the exposure, and the right side shows that at the center. At the surface, the distribution peak of pores with about 100 nm diameter at the 1 day of the exposure moves to the pore size of about 200 nm diameter at the 7 day of the exposure due to the carbonation in all specimens. It is inferred that the pore structure is coarser due to the carbonation of C-S-H gel and the volume of pores with diameter of over 100 nm could increase. It could be attributed to not coarsening gel pores and C-S-H gel layer with nanometer pore size but the discontinuous destruction of C-S-H gel chains because the micro pore with less than 10 nm diameter had no change according to the Figure 12.

In the case of center, the pores with diameter of about 100 nm are decreased and

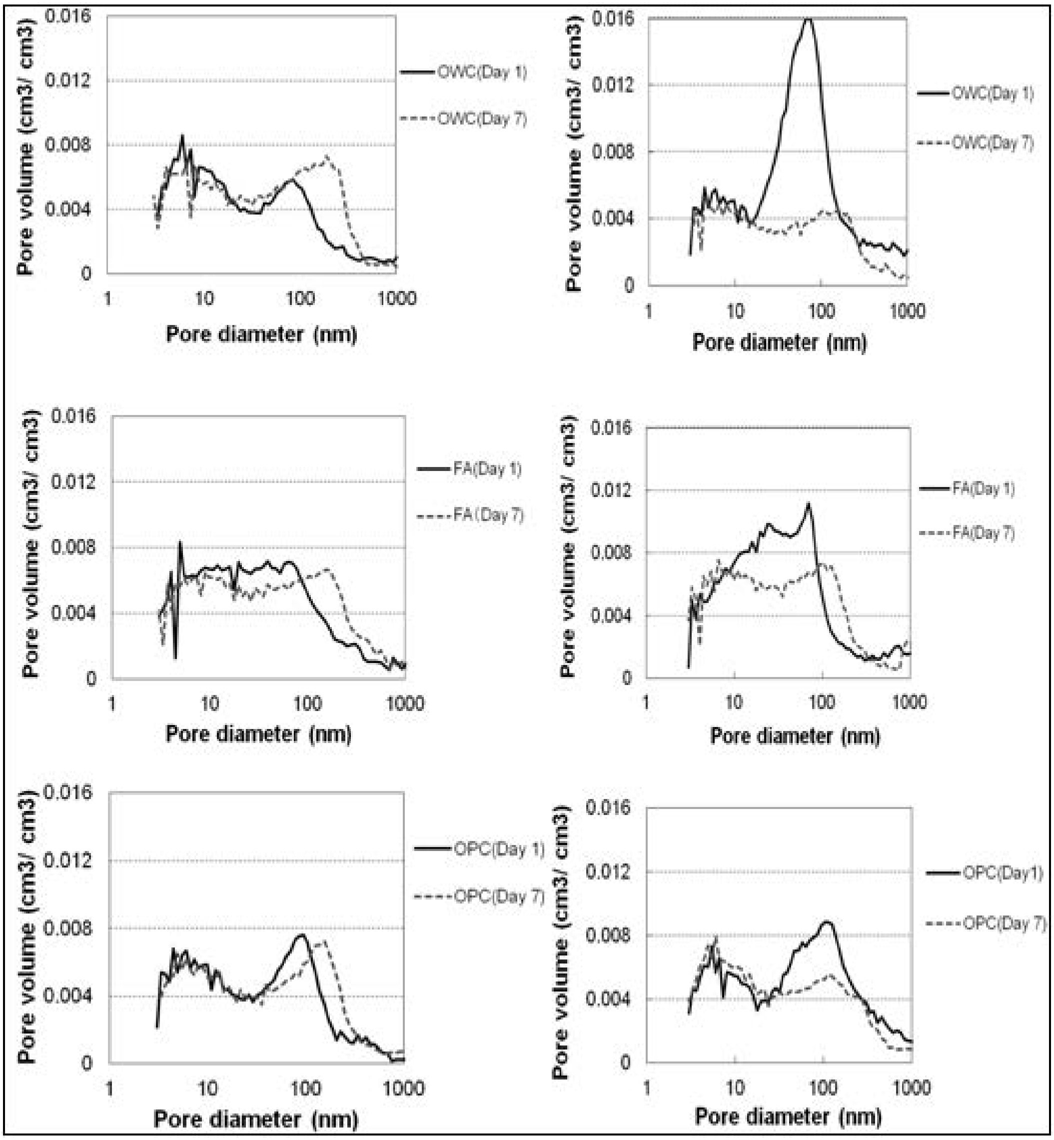

Figure 12: Pore distribution after exposure at the surface (left), and center (right)

fine pores with less than 10 nm diameter is not distinct. It is speculated that the slight carbonation of C-S-H gel could not cause the destruction of itself and the precipitation of the $CaCO_3$ could fill up the capillary pore spaces and make pore structure denser.

4. CONCLUSIONS

The conclusion in this study is summarized below.

(1) When the specimen is exposed to supercritical CO_2, it is difficult to identify the carbonation depth from the surface by the coloring of the phenolphthalein solution.
(2) If Ordinary Portland cement is used and exposed to supercritical CO_2 under high temperature and high pressure, the pore structure become coarser and strength decrease, and many cracks occur.
(3) In the case of using the FA, the amount of $CaCO_3$ generated by the carbonation of $Ca(OH)_2$ is small because $Ca(OH)_2$ could be used by the pozzolanic reaction during the curing and the initial amount of $Ca(OH)_2$ is small.
(4) If the specimen is exposed to the severe condition such as supercritical CO_2, it is suggested that the carbonation could proceed to not only $Ca(OH)_2$ but also C-S-H gel.
(5) When the specimen is exposed to supercritical CO_2 for 7 days, the pore structure become coarser at the surface and dense at the center.

REFERENCES

1) Preben Randhol, Karen Valencia, Ali Taghipour, Idar Akervoll, Inge Manfred Carlsen: Ensuring well integrity in connection with CO2 injection, SINTEF Petroleum Research, NO.936 882 331, 27 December, 2007

2) Sidney Mindess, J. Francis Young, David Darwin: Concrete Second Edition, Pearson Education, Inc, pp.41-43, 2003

3) H.F.W.Taylor: Cement chemistry 2nd edition, Thomas Telford Services Ltd, pp.346-348, 1997

4) Barbara G. Kutcko, Brian R. Straisar, David A. Dzombak, Gregory V. Lowry, Niels Thaulow: Degradation of Well Cement by CO2 under Geologic Sequestration Conditions, Environ. Sci. Technol. 41, pp.4787-4792, 2007

Effect of the application of surface penetrants on the mass transport properties of concrete

Nozomu SOMEYA[1] and Yoshitaka KATO[2]
[1]Doctoral Student, Department of Civil Engineering,
Graduate School of Science and Technology, Tokyo University of Science, Japan
j7613701@ed.tus.ac.jp
[2]Associate Professor, Department of Civil Engineering,
Faculty of Science and Technology, Tokyo University of Science, Japan

ABSTRACT

This paper presents an experimental study examining the effect of the application of silicate-type penetrants on the mass transport properties of concrete made with ordinary portland cement or ordinary portland cement incorporating fly ash. The penetrants were applied to water-cement ratio 0.55 and 0.60 specimens, and the mass transport properties (durability) were evaluated by the absorption rate and carbonation rate. To assist the hydration reaction of the penetrants, calcium hydroxide was utilized. Silicate-based penetrants were applied to the water-cement ratio 0.55 specimens and improved durability against carbonation. In addition, the application of calcium hydroxide to OPC was found to create good resistance against carbonation. Overall, the application of silicate-based surface penetrants was found to affect the depth of carbonation more than it assisted the hydration reaction.

Keywords: *silicate-based surface penetrants, improvement effect, carbonation*

1. INTRODUCTION

When the performance of a concrete structure is less than the required performance due to aging and deterioration, the performance needs to be restored through measures such as repair or reinforcement. Surface penetrants can improve the durability of concrete and delay the degradation of the structure. In addition, when applying penetrants at an early age for preventive maintenance, the progress of deterioration can be reduced from the beginning (JSCE, 2005). Silicate-based surface penetrants are one type of surface protection construction methods, and their application to the concrete surface can improve the durability of the concrete. The application of silicate-based surface penetrants has several benefits such as ease of maintenance and the ability to visually check the surface after application.

In past studies, it was found that the effect of silicate-based surface penetrants varies depending on the quality of the early-age concrete (Hirotake, 2010), and it was also shown that the penetrants could improve the durability of concrete containing micro-cracks and protect against carbonation. However, it is believed that the state of the concrete to which the penetrant will be applied is important, and the effect of application on the mass transport properties of concrete is unclear.

This paper presents an experimental study examining the effect of penetrants which were applied to early-age specimens. The study on early-age specimens examined the influence on hydration reaction and the difference due to application timing.

2. EXPERIMENTAL PROGRAM

2.1 Procedure

To understand the effect of application timing on the durability, penetrants were applied to specimens aged 7 and 14 days, after which the specimens were placed in a controlled environment (20ºC, R.H. 60%) for 4 weeks. The effectiveness of an additive (calcium hydroxide) for assisting the hydration reaction was also examined. Mass transport properties (durability) were then evaluated by the carbonation rate. The flow for the experiments on early-age specimens is shown in Figure 1

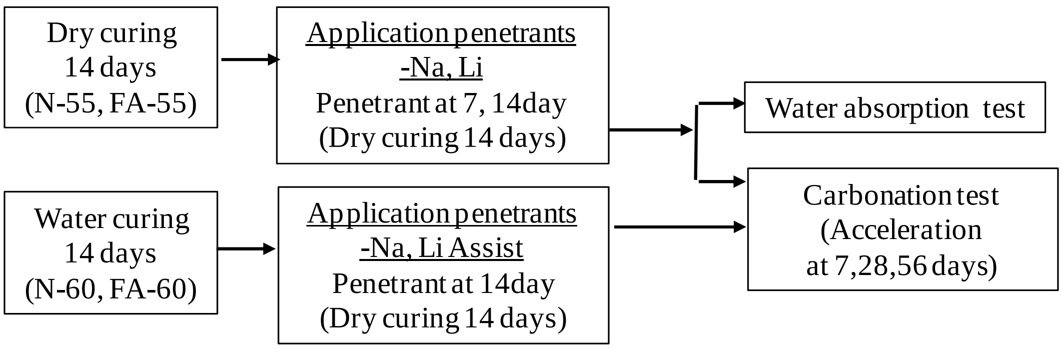

Figure 1: Flow of testing procedure

2.2 Material and specimens

Table 1 describes the two types of silicate-based surface penetrants and the calcium hydroxide additive, and the application method was carried out depending on the penetrant quality. Concrete was made with ordinary portland cement (density: 3.15g/cm^3, Blaine fineness: 3440cm^2/g) or ordinary portland cement incorporating fly ash (density: 2.28 g/cm^3, Blaine fineness: 3920cm^2/g, JIS A 6201 Ⅱ grade ash). The fine aggregate was river sand (density: 2.61 g/cm^3, fineness modulus: 2.91) while the coarse aggregate was crushed sandstone with G_{max} of 20mm (density: 2.73 g/cm^3, fineness modulus: 6.61).

The concrete mix proportions are shown in Table 2. The slump of fresh concrete was 10±2.5 cm and air content was 4.5±1.5%. The water-cement ratio was 0.55 and 0.60. The water absorption test was carried out on an area of 150×150×150 mm, and the carbonation rate test carried out on an area of 150×150×200 mm. Specimens were given a surface treatment to limit the number of mass transport surfaces. Table 3 shows the number of application sides and measurement area of the specimens, and an illustration of the specimens is shown in Figure 2.

Table 1: Description of the penetrants and the assisting additive

Code	Ingredient	Application quantity (g/m^2)
Na	Sodium silicates	120
Li	Lithium silicates	120
Assist	Calcium hydroxide	120

Table 2: Concrete mix proportions

Code	W/B (%)	s/a (%)	(kg/m^3)					
			W	C	F	S	G	AE
N-55	55	45	175	318	-	804	1016	C*0.002%
FA-55	55	46	175	318	107	698	1001	(C+F)*0.005%
N-60	60	45	175	318	-	804	1025	C*0.006%
FA-60	60	52	175	248	44	923	888	(C+F)*0.013%

Table 3: Details of specimen measurement areas

	Measurement area (mm)	Application surface
Water absorption test	150*150*150	2 opposing surfaces
Carbonation test	150*150*200	

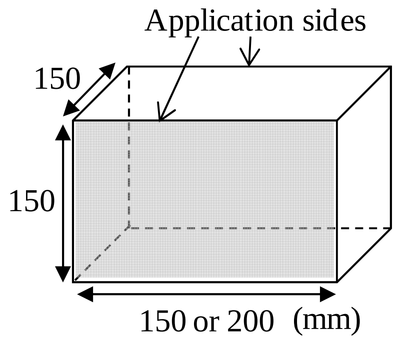

Figure 2: Illustration of test specimens showing application surfaces

2.3 Test methods

Water absorption test

The water absorption test was carried out according to JSCE-K 572-2012. The specimen was removed from the testing container seven days after the start of the test and the mass was measured (W_{ai}) after removing the surface water. Using this value the water absorption rate (W_a) was calculated using Equation (1). The reported absorption rate is the mean of three values.

$$W_a = (W_{ai} - W_{a0}) / W_{a0} \times 100 \quad (1)$$

where, W_a : absorption (%), W_{a0} : mass before the examination (g), W_{ai} : mass at the time of the measurement (g)

Carbonation test

The carbonation test was carried out according to JSCE-K 572-2012. The examination condition used a temperature of 20ºC, R.H. 60%, 5% CO_2 density, and the carbonation depth was measured after 7, 28 and 56 days. The carbonation depth was measured by applying phenolphthalein on the fracture surface, and the reported value was calculated as the mean of six data points, which were measured twice per specimen (the depth from two opposing sides).

Degree of hydration test

Degree of hydration was evaluated following the manual of the Japan Concrete Institute using the "degree of hydration test" (JCI, 2005). Specimens were prepared from mortar with a water-cement ratio of 0.55. Penetrants were applied to specimens at 3, 7 and 10 days, after which the specimens were placed in a controlled environment (20ºC, R.H. 60%) until 28 days. The degree of hydration was determined 28 days after casting.

$$Ma = ((M_i - M_0) / M_0) \times 100 \quad (2)$$

where, M_a: degree of hydration (%), M_i: mass after 105ºC drying (g), M_0: mass after 1000ºC drying (g)

3. RESULT AND DISCUSSION

3.1 Water absorption test

The results showed that the timing of the penetrant application at 7 days and 14 days affected the water absorption ratio (calculated as the ratio of the test result to the water absorption rate in the case that no penetrant was applied) as shown in Figure 3. N-55 experienced improved durability against water absorption, and the absorption ratio was lower when the penetrants were applied at 14 days than at 7 days. FA-55 specimens experienced improved durability against water absorption, and the absorption ratio was lower when the penetrants were applied at 7 days than at 14 days.

3.2 Carbonation test

Test results examining the carbonation ratio of concrete (56 days) are shown in Figure 4 and Figure 5. The carbonation ratio is calculated as the ratio of the case applying a penetrant to the case with no penetrant. As can be seen in Figure 4, the carbonation ratio for both N-55 and FA-55 became less than half the ratio of the standard specimen regardless of the application timing or type.

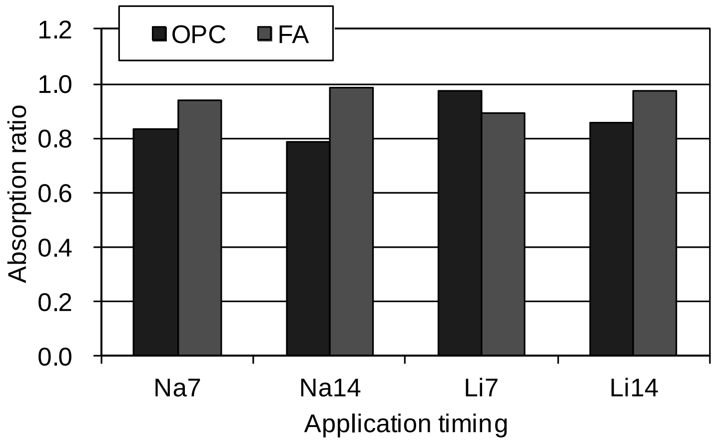

Figure 3: Water absorption ratio (N-55, FA-55)

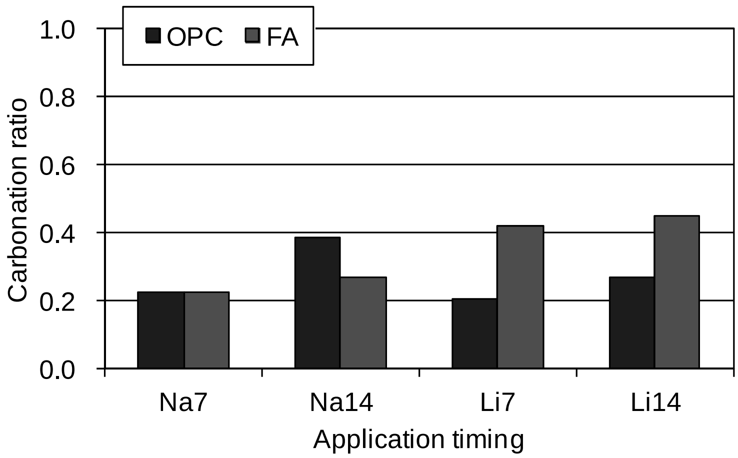

Figure 4: Carbonation ratio (N-55, FA-55)

Figure 5 shows the carbonation ratio results looking at different water-cement ratio and the effect of the assisting additive. In this figure, the experimental results shown for Na(Li)14 are the same as those given for N-55 and FA-55 in Figure 4. The results showed that, in the case of N-55 and N-60, the carbonation ratio of N-55 was half that of the standard specimen, whereas N-60 without the assisting additive was the same as that of the specimen with no penetrant. From this result it is thought that N-55 specimens with penetrants had improved resistance against carbonation due to an improvement in concrete surface quality. In the case of N-60 with calcium hydroxide applied, the ratio was around 80% of that when no penetrant was applied.

In the case of FA, the carbonation ratio was similar to that of specimens with no penetrant applied. As can be seen in Figure 5, the application of the silicate-based surface penetrant with calcium hydroxide did not improve concrete surface quality. In the FA specimens, calcium hydroxide may have been used up in the pozzolanic reaction, and thus the carbonation depth of FA specimens with the silicate-based surface penetrant and calcium hydroxide was not lower than that of OPC specimens.

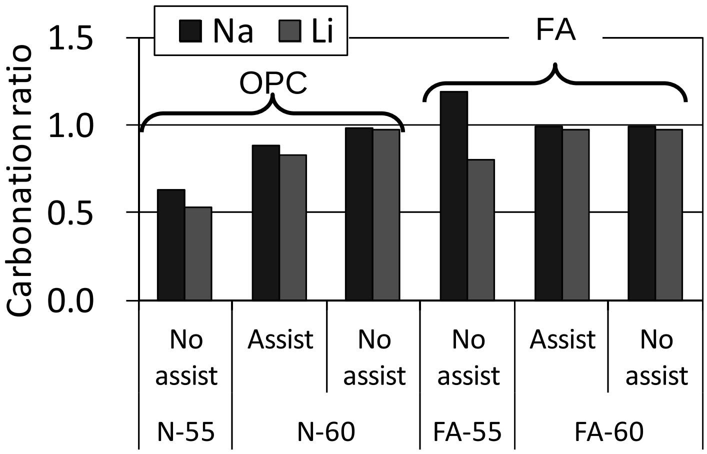

Figure 5: Carbonation ratio (N-55, N-60, FA-55, FA-60)

The relationship between carbonation depth and square root of time is shown in Figure 6 for N-55. In the case of no penetrant application a linear relationship can be seen. However, in the case of Na14, the data deviates from the linear relationship at around 40 days. Based on this result, it is possible that the carbonation depth exceeded the improvement depth. The improvement depth (Y) due to application of silicate-type penetrants can be calculated using Equation (3).

$$Y = (B_p / B_c) / H \tag{3}$$

where, Y: improvement depth ($\leq$ penetration depth) (mm), H: carbonation depth for no penetrant application (mm), B_C: carbonation rate for no penetrant application (mm/√day), B_P: carbonation rate for penetrant application (mm/√day)

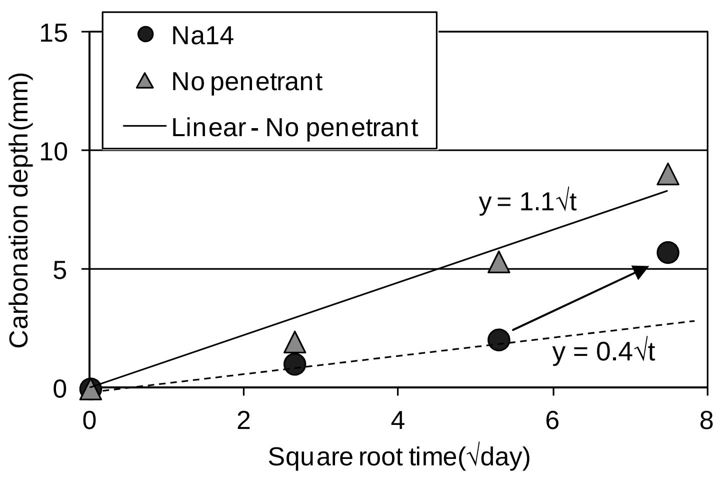

Figure 6: Progress of carbonation depth over time (N-55)

Improvement depth is shown in Table 4. The calculation could not be carried out for N-60 and FA-60 because the carbonation depth already exceeded the improvement depth. The results showed that the improvement depth became around 2 to 3 mm for N-55 and around 1 to 2 mm for FA-55. In the case of the sodium-type silicate application, the difference between concrete types appears to be large, whereas for lithium-type silicate the penetration depth is around the same for the two concrete types. In previous studies, the penetration depth was reported to be around 20 mm from the surface (Takayuki, 2011). Therefore, the affected depth found in this experiment was lower than that in previous studies.

Table 4: Improvement depth calculation result

Improvement depth (mm)		
	N-55	FA-55
Na7	3.2	0.9
Na14	3.2	1.0
Li7	1.8	2.0
Li14	2.2	1.9

3.3 Degree of hydration test

Based on the results in the previous sections, it can be understood that the effect of application timing on the water absorption ratio is different from the effect on the carbonation ratio. In order to understand this phenomenon, the degree of hydration test was conducted.

The hydration ratio results for the sodium-type silicate (N-55) are given in Figure 7. The hydration rate at 10 days is relatively higher than the standard material since the amount of calcium hydroxide is higher at 10 days compared to 3 and 7 days. From the water absorption rate and degree of hydration test results, it is believed that application of the sodium-type silicate penetrant at 14 days to the OPC specimen resulted in the greatest concrete surface improvement. Therefore, the water absorption ratio was improved because of the progress of the penetrant reaction. On the other hand, the carbonation ratio was not improved due to the consumption of hydroxide by the penetrant reaction.

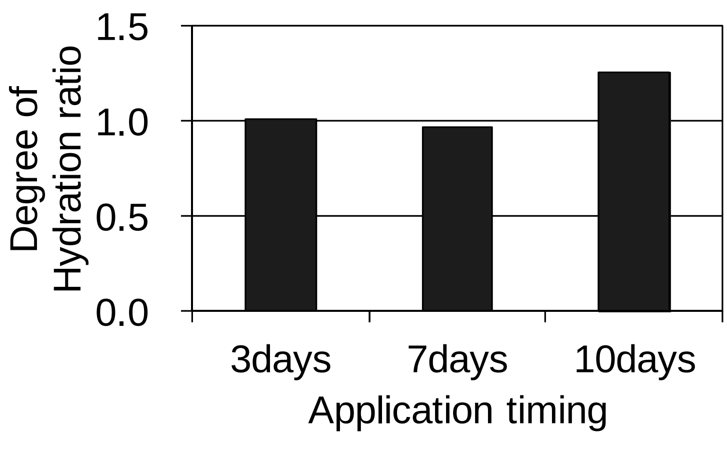

Figure 7: Hydration ratio for sodium-type silicate penetrant (N-55)

CONCLUSION

The effect of the application of silicate-based surface penetrants on the mass transport properties of concrete was experimentally examined. The results are summarized as follows.

1) When comparing OPC specimens with FA specimens, it could be seen that application was more effective at 14 days for OPC specimens but more effective for FA at 7 days.
2) Silicate-based surface penetrants were applied to the water-cement ratio 0.55 specimens and improved resistance against carbonation. In addition, the application of calcium hydroxide to OPC was found to create good resistance against carbonation.

REFERENCES

Hirotaka, H., Kouji, T., Toshinobu, Y. and Nao, S. (2010). "Fundamental Study on Performance and Difference of Various Surface Improvement Material." Proceeding of the Japan Concrete Institute, 48(5) 1619-1624. (in Japanese)

Japan Concrete Institute (JCI). (2000). *Examination and analysis manual of the concrete,* Study on long-term durability Committee of concrete. (in Japanese)

Japan Society of Civil Engineers (JSCE). (2005). *Recommendation for Concrete Repair and Surface Protection of Concrete Structures*, Concrete Library 119. (in Japanese)

Takayuki, S., Kouji, T., Toshinobu, Y. and Hirotaka, H. (2011). "Effects of surface improvement material on chloride panetration and neutralization." Proceeding of the Japan Concrete Institute, 33(1), 1625-1630. (in Japanese)

Torrent, R. (1992). "A two-chamber vacuum cell for measuring the coefficient of permeability to air the concrete cover on site." Proceeding of the Materials and Structures, 25, 358-365.

Influence of coexistent ions in seawater on the chloride permeability of concrete

Toshiya CHIBA[1], Katsuya MITA[2] and Yoshitaka KATO[3]
[1]Master student, Department of Civil Engineering,
Graduate School of Science and Technology, Tokyo University of Science, Japan
toshiya1350@gmail.com
[2]Assistant Professor, Department of Civil Engineering,
Faculty of Science and Technology, Tokyo University of Science, Japan
[3]Associate Professor, Department of Civil Engineering,
Faculty of Science and Technology, Tokyo University of Science, Japan

ABSTRACT

There has been considerable research on the penetration of chloride in concrete. However, most of these works focused on the permeation of only chloride ions in concrete, but the actual composition of seawater contains not only chloride but also different kinds of ions such as magnesium, calcium, potassium and sulfate, and concrete structures in marine environments are affected by all these types of ions. This study discusses the effects which various ions in seawater exert on the chloride permeability and diffusion in concrete through an experimental study in which we measured the salt concentration in concrete and depth of chloride penetration obtained using $AgNO_3$ solution spray method. The results showed that the sulfate ions, potassium ions and magnesium ions contained in seawater promote the penetration of chloride ions in concrete.

Keywords: *chloride ion, sulfate deterioration, diffusion coefficient, pore volume distribution*

1. INTRODUCTION

Concrete structures in marine environments suffer a variety of complex deterioration such as steel corrosion due to penetration of chloride ions from seawater, frost damage deterioration in cold climates and physical erosion caused by waves and tides. When further considering the chemical erosion of the hardened cement matrix, it is clear that sulfate salt and magnesium chloride erode concrete and affect the chloride permeability of concrete (Kumar, 2000).

The amount of salt contained in concrete is measured from crushed concrete samples following JCI-SC4. It has been confirmed that the analytical method can measure the chloride ion concentration with high accuracy, but it involves extensive labor, the analysis period is long, and the procedure is expensive, so it is difficult to measure the chloride ion concentration of many concrete samples. On the other hand, the $AgNO_3$ solution spray method is another means for measuring chloride ion penetration. With this method, the penetration depth can be immediately and visually measured.

With the $AgNO_3$ method, the depth of chloride penetration is measured by the use of a white silver chloride produced by the reaction between chloride ions contained in concrete and a sprayed aqueous silver nitrate solution (Nobuaki, 1990). However, there is little knowledge available on the quantitative chloride ion concentration at the boundary of the white discoloration. In addition, past studies only tested with immersion in salt water, and thus studies considering the effect of other ions in seawater are few. Given the above, it is important to experimentally investigate the effect of other ions in seawater on the $AgNO_3$ solution spray and quantitatively consider the applicability of the $AgNO_3$ solution spray in a real ocean environment using the measurement results of the potentiometric titration.

This study experimentally examined the penetration and spread of chloride ions contained in seawater via two methods: measurement of the depth of chloride ion penetration using the $AgNO_3$ solution spray method and analysis of the chloride ion content.

2. EXPERIMENTAL OUTLINE

2.1 Material and specimens

The cements used in this study were ordinary portland cement (symbol C, density 3.15 g/cm^3) and blast furnace cement Type B (symbol BS, density 3.04 g/cm^3). The aggregates used were Yamanashi Fujikawa river sand (symbol S, density 2.61 g/cm^3) and Chichibu (Saitama Prefecture) crushed stone (symbol G, density 2.72 g/cm^3). The mix proportions are shown in Table 1. The prepared specimens were rectangular columns (10 × 10 × 8.5 cm).

Table 1: Concrete mix proportions

Code	W/C(%)	s/a (%)	(kg/m^3)						
			W	C	BS	Gyp	S	G	Ad
OPC50	50	45	175	350	0	0	783	998	1.75
BS50	50(BS)	46	175	193	151	7	794	971	3.51

2.2 Experimental conditions

The specimens were demolded and cured for 28 days in water, then coated with epoxy resin except for the surface to be exposed to the immersion solution. Specimens were then immersed in either an NaCl aqueous solution or one of four mixed solutions for 56 and 91 days. The mixed solutions were made by dissolving sulfate-adjusted cations to concentrations based on seawater composition. The NaCl solution was mixed at 10% weight percent concentration. The types of sulfate dissolved were $MgSO_4$, $CaSO_4$, K_2SO_4 and Na_2SO_4 at percent concentrations of 0.61%, 0.38%, 0.21%, and 0.01%, respectively. The ion concentrations of the four mixed solutions are shown in Table 2.

Table 2: Ion concentrations in the mixed solutions

	Four kind of mixed solution (mol/l)			
	Mixed solution of $MgSO_4$	Mixed solution of $CaSO_4$	Mixed solution of K_2SO_4	Mixed solution of Na_2SO_4
Cl^-	1.71			
Na^+	1.71			
SO_4^{2-}	0.051	0.028	0.012	7.00×10^{-4}
Mg^+	0.051	0	0	0
Ca^{2+}	0	0.028	0	0
K^+	0	0	0.012	0

2.3 Potentiometric titration

The total chloride ion amount and soluble chloride ion amount contained in the concrete samples were measured by the potentiometric titration according to JCI-SC4. The soluble chloride ion was extracted with hot water at 50°C. The concrete samples were collected from mortar at varying distances from the exposure distance: 0-10 mm, 11-20 mm, 21-30 mm, 31-40 mm and 41-50 mm. The preparation method of the samples is shown in Figure 1.

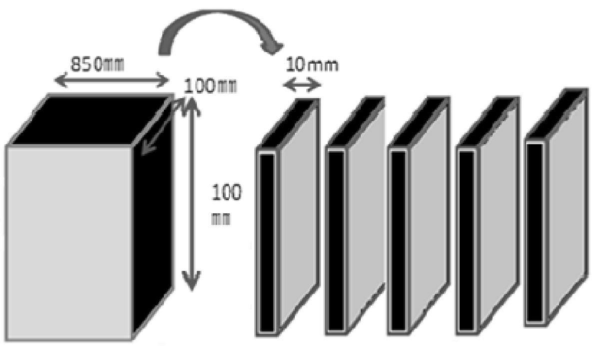

Figure 1: Sample preparation method

2.4 Pore diameter distribution measurement

Parts of mortar samples were used for measuring the pore size distribution by mercury intrusion porosimetry (MIP). The MIP specimens were collected from the sample surface and crushed to a size of 2.5-5 mm. They were then immersed in acetone to stop the hydration reaction, and the pore size distribution was measured after drying by the D-dry method.

2.5 $AgNO_3$ solution spray method

The $AgNO_3$ solution spray method was applied to measure the depth of chloride ion penetration. The specimen was split along its vertical axis and the cracked surface was sprayed with $AgNO_3$ aqueous solution (0.1mol/l). The penetration depth could then be measured as the depth of the white coloring of the silver chloride. This method measures the depth of the soluble chloride ions.

3. RESULTS AND DISCUSSION

3.1 Total chloride ion concentration

The measurement results of the total chloride ion concentration in OPC50 immersed for 91 days in each solution are shown in Figure 2. When looking at the the region of 0-10 mm, the chloride ion concentration increases in the order of potassium sulfate mixed solution, sodium sulfate mixed solution, magnesium sulfate mixed solution, NaCl aqueous solution, and calcium sulfate mixed solution. Figure 3 shows the measurement results for BS50 immersed 91 days. The amount of chloride ions for the potassium sulfate mixed solution and sodium sulfate mixed solution was high in the region of 0-10 mm. However, penetration of chloride ion after the region of 10-20 mm was not observed. Since the chloride ions are present in the region of 10-20 mm and 20-30 mm in OPC50, the inhibitory effect of blast furnace slag on chloride ion penetration was confirmed.

Using the chloride ion concentration distributions shown in Figure 2 and Figure 3, the apparent diffusion coefficient (D_a) and surface chloride ion concentration (C_0) from a theoretical solution of the Fick's diffusion equation under conditions of constant surface concentration were calculated. By using the result, the number of years until reaching the limit concentration (C_{lim}) for generating steel corrosion could be calculated, and compared with the ease of chloride ions penetration. The C_{lim} of OPC50 in this experiment was 1.9kg/m^3, following the 2012 JSCE Standard Specification for Concrete Structures, and the number of years leading up to the C_{lim} for 5 cm cover depth was calculated.

The results are shown in Table-3. The sulfate mixed solutions except for calcium sulfate mixed solution reached C_{lim} earlier than the NaCl aqueous solution. It is possible that sulfate, the main cause of sulfate deterioration in concrete, affected the salt permeability. In the case of sulfate mixed solutions, it is estimated that chloride ions easily penetrated into concrete due to sulfate deterioration, and resulted in subtle cracking and weakening that cannot be confirmed by visual observation (Yoshida, 2011). However, for calcium sulfate mixed solution, salt penetration was suppressed. This behavior may be due to differences in the elution amount of calcium ions from the concrete surface. According to Imoto (2004), the elution of calcium ions lowered the C/S of C-S-H in the concrete, leading to weak C-S-H with high void volume. It is thought that the calcium sulfate mixed solution suppressed the elution of calcium ions because, in calcium sulfate mixed solution, there are more calcium ions than in the other mixed solution and the difference in the concentration of calcium ions between the pore solution and soaking solution is small. The apparent diffusion coefficient of the specimens immersed in magnesium sulfate mixture was large, which may have led to the magnesium ion and sulfate ion, the main cause of sulfate deterioration in seawater, affecting the salt permeability of concrete. Due to the presence of magnesium ions, calcium sulfate and magnesium hydroxide are produced on the concrete surface, and lead to the formation of MSH and generation of ettringite (Yamaji, 2008). It is believed that the expansion pressure of ettringite leads to degradation, thus allowing easier penetration of chloride ions into concrete.

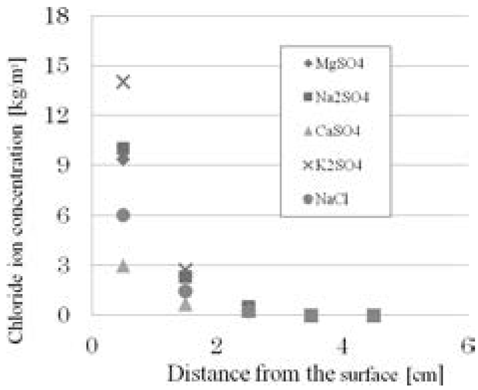

Figure 2: Total chloride ion concentration in OPC50

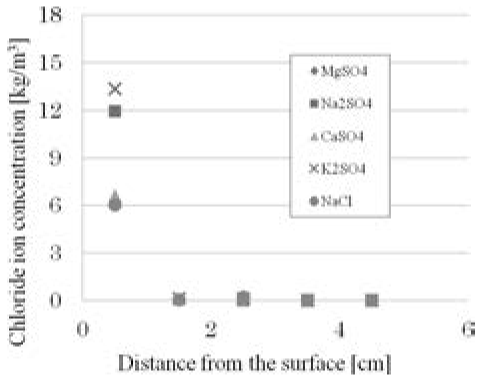

Figure 3: Total chloride ion concentration in BS50

Table 3: Diffusion coefficient, surface chloride ion concentration and the number of years leading up to the C_{lim}

Immersion solution type	Diffusion coefficient D_a （cm^2/year）	Surface chloride ion concentration C_0 （kg/m^3）	Time （year）
$MgSO_4$	2.3	14.5	2.3
Na_2SO_4	1.8	22.3	2.2
K_2SO_4	1.7	26.1	2.2
$CaSO_4$	1.7	4.7	10.0
NaCl	0.8	19.5	5.6

3.2 Pore diameter distribution

The cumulative pore volume distribution and differential pore volume distribution of OPC50 immersed NaCl aqueous solution and sulfate mixed solution are shown in Figure 4 and Figure 5.

The pore structure appears different depending on the immersion solution. For the pore diameter of 100 nm or less the cumulate intrusion decreases in the order of fresh water, NaCl aqueous solution, and sulfate mixed solution; that is, NaCl hydrate generated by sulfate deterioration. Therefore, in this study it is assumed that the filling of the pores was due to ettringite and gypsum. However, this is contrast to the effect of sulfate on the salt permeability obtained in Section 3.2, as densification of the pore structure should suppress the penetration of chloride ions.

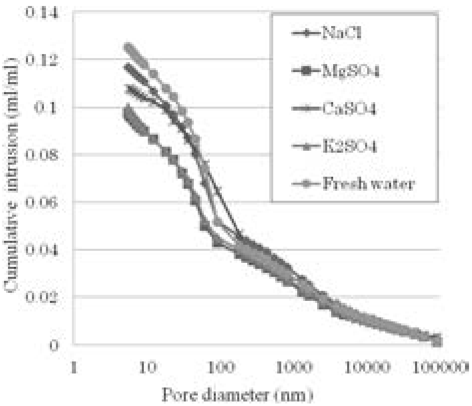

Figure 4: Cumulative pore volume distribution

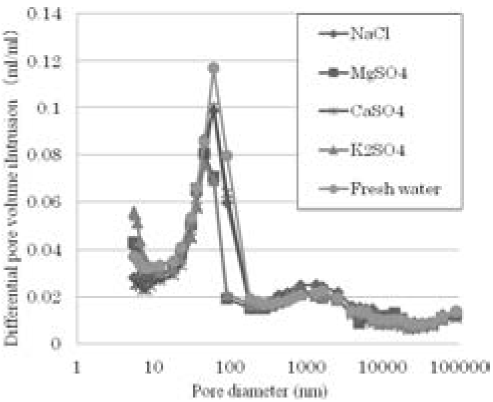

Figure 5: Differential pore volume distribution

3.3 Study on the $AgNO_3$ solution spray method

The measurement results of the chloride ion penetration depth using the $AgNO_3$ solution spray method are shown in Figure 6 and Figure 7. It can be clearly seen that blast furnace slag and immersion solution affected the chloride ion permeability in concrete. From these results, it can be said that concrete specimens with blast furnace slag had improved water tightness and were better shielded against chloride ion penetration. When comparing the depth of chloride ion penetration by the $AgNO_3$ solution spray method with the chloride ion concentration distribution shown in Section 3.1, there appears to be a difference in the effect of the solution species on the salt penetration. It was reported by Otsuki (1990) that concrete sprayed with the $AgNO_3$ solution became colored white due to reaction with the soluble chloride ions, and in the case of an $AgNO_3$ solution of 0.1 mol/L the amount of soluble chloride ion of the coloring limit is approximately 0.15% of the unit cement content. Therefore, based on the measurement results of the soluble chloride ion concentration, the concentration of color limit was determined.

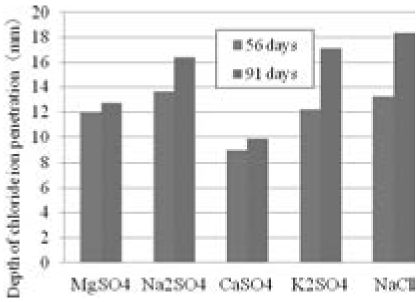

Figure 6: Depth of chloride ion penetration OPC50

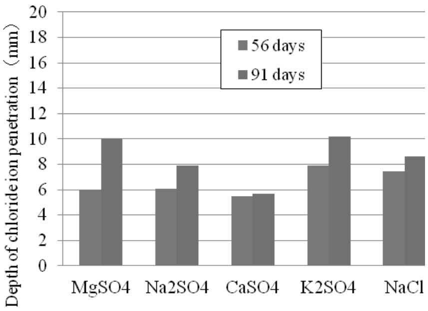

Figure 7: Depth of chloride ion penetration BS50

The relationship between the concentration color limits with soluble chloride ion concentration under immersion in an NaCl aqueous solution is shown in Figure 8. Then, assuming that C_b is the soluble chloride ion concentration at the color limit, the location where the soluble chloride ion concentration distribution (represented by the curved line in Figure 8) intersects the depth of chloride ion penetration (measured by the $AgNO_3$ solution spray method, shown as the vertical line) is considered to be C_b. Assuming C_a as the soluble chloride ion concentration in the color limits based on the study of Otsuki (1990), since the unit cement content of OPC50 is 350 kg/m^3, C_a could be calculated as 0.525 kg/m^3 and C_b then calculated as 1.81 kg/m^3. However, the measurement results does not match with the C_a obtained by Otsuki. In a similar manner, the C_b of the other immersion solutions were calculated along with the percentage of the unit cement content, as shown in Table 4. C_b is more than twice as large as C_a, and differed by immersion solution.

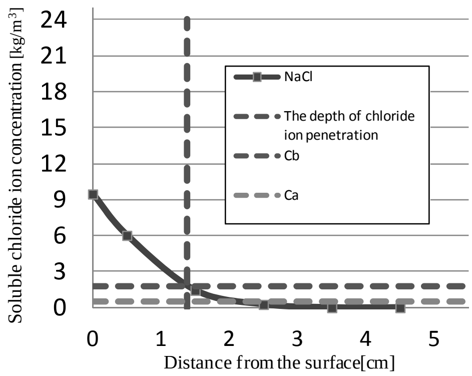

Figure 8: Relationship between the concentration color limits with soluble chloride ion concentration

Table 4: C_b and calculated percentage of unit cement content

	C_b [kg/m^3]	C_b/C_a	$C \times x$ [%]
Value obtained by Otsuki (1990)	0.525	1	0.15
$MgSO_4$	1.24	2.36	0.35
Na_2SO_4	1.06	2.02	0.30
$CaSO_4$	1.45	2.80	0.41
K_2SO_4	1.38	2.63	0.39
NaCl	1.81	3.45	0.51

4. CONCLUSIONS

The results of this study are summarized as follows.

- The penetration of salt is different from that of the NaCl aqueous solution and sulfate mixed solution, and it was found that the total chloride ion concentration in concrete exposed to potassium sulfate mixed solution, sodium sulfate mixed solution and magnesium sulfate mixed solution was large.

- From the pore size distribution measurements, exposure to the sulfate mixed solution may lead to a denser pore structure. However, densification of the pore structure is estimated to suppress the penetration of chloride ions, and so it is inconsistent that the total chloride ion concentration in the sulfate mixed solution was larger. In the future, it is necessary to consider the mass transfer of sulfate deterioration.
- From the calculation results of the soluble chloride ion concentration from the color limit of the $AgNO_3$ solution spray method, the soluble chloride concentration C_b at the color limit did not match the soluble chloride ion concentration of C_a referred to in previous studies.

REFERENCES

P. Kumar. (2000). “Concrete Microstructure, Properties, and Materials.” Gihoudo Shuppan. (in Japanese)

Otsuki, O. (1990). *Evaluation of the AgNO3 Solution Spray Method for Measurement of Chloride Penetration into Hardend Cementious Matrix Materials*, Technical Report No.42, Tokyo Institute of Technology.

Yoshida, N. (2011). *Deterioration of concrete due to crystal growth of sodium sulphate*, GBRC, Vol.36, No.3, pp.13-22.

Imoto, H. Japan Concrete Institute (JCI). (2004). *Leaching Property of Odinary Portland Cement Hardend Paste in Sodium Chloride Aqueous Solution,* Vol.26, No.1, pp.903-908.

Yamaji, T. Japan Concrete Institute (JCI). (2008). *Result of concrete quality in existing structures eposed under marine environment for long term*, Vol.30, No.1.

Kawaura, J. (2009). Japan Concrete Institute (JCI). *Analytical study of change the amount of pore regenerating ettringite by sulfate erosion,* Vol.31, No.1, pp.859-864.

Performance of crack self-healing concrete by development of semi-capsulation technique for functional effective ingredients

Vu Viet Hung[1], Toshiharu Kishi[2], Tae-Ho Ahn[3]
[1] Doctor candidate, the University of Tokyo, Japan
vhung@iis.u-tokyo.ac.jp
[2] Professor, IIS, the University of Tokyo, Japan
[3] Assocciate Professor, IIS, the University of Tokyo, Japan

ABSTRACT

In this study, concrete was designed with a crack healing capability, in which a crack of 0.2-0.4mm width could be self-healed by activating reactions between embedded granules and external water upon cracking. Trial of granules containing Portland cements & some specific self-healing additives manufactured by semi-capsulation technique was developed based on the basic design concept of self-healing materials (proposed by Ahn, 2008) and the granulation technique (proposed by Koide & Morita, 2010). Self-healing granules were added to the concrete mixture by partial replacement of sand. In this experiment, the capability of crack self-healing concrete was assessed by observing the time-dependent reduction of water leakage through a crack, the closing process of surface crack and chemical analysis of deposited products.
From the experimental investigation, it was concluded that the designed concrete possesses an excellent crack self-healing performance, in terms of recovery of water tightness property and crack closing process after cracking and long-term preservation of its capability by development of semi-capsulation technique for functional effective ingredients. Moreover, there is a promising possibility to broadly apply this concept to practice in order to improve the durability and functionality of civil infrastructures, such as water retaining and underground structures.

Keywords: *concrete, self-healing, granule, crack, semi-capsulation.*

1. INTRODUCTION

In structures subject to contact with water, such as water-retaining structures, tunnels or basements, crack appearance and water leakage are common phenomena. A penetrated crack causes a significant reduction in the durability, functionality/serviceability and aesthetics as well. In these structures, water tightness and durability are of paramount importance. There are several conventional methods to achieve the watertight property of concrete structures, for examples, application of waterproofing treatment on the surface (for newly constructed structures) or injection of filler material after cracking (for repaired structures), etc. However, it often increases the cost, lengthens construction period and also interferes with the normal service of the structure. Therefore, it inspires the possibility that; if concrete were designed with a sufficient healing capability, cracks in concrete can be self-healed to recover the water tightness property and improve the durability of concrete structures without human intervention.

In general, concrete/cementitious composite has a certain healing capacity (Edvardsen, 1999; Heide, 2005; Hirozo, 2012; etc.). Unfortunately, its capability is limited and uncertain in most circumstances (Reinharddt, 2003; etc). Recently, there are various approaches being developed to improve the healing ability of concrete. For instances, it can be listed as fiber reinforced *(*Lepech & Li 2009; etc.*)*; bacteria-based (Wiktor & Jonkers 2011; Wang 2012; etc.); polymer, epoxy or glue resin, etc. (Mihashi 2000; Kessler 2003; Joseph C. 2009; etc.).

Another approach introducing self-healing capability to concrete at a normal water/cement ratio was proposed by Ahn, 2008. Some specific mineral and chemical admixtures in terms of swelling, expansion and precipitation were added to concrete mixture in form of powder as partial cement replacement. Even though the self-healing performance was promising, there were some disadvantages in this approach, such as the reduction in workability and the self-healing efficiency due to further reactions between self-healing powder and mixing water. To overcome the above mentioned drawbacks, the self-healing granules having semi-capsulation effect, in which the inner material containing self-healing materials were coated by cement compound, were developed by Koide & Morita, 2010. Originally, this conventional granulation technique was widely used in the food/medicine industry. Therefore, the manufacturing cost was high. Moreover, due to immature technology and lack of design concepts at that moment, the performance of self-healing concrete containing granules was not so significant compared to the powder type approach. However, it is a preferable approach to introduce self-healing properties to concrete. Thus, it is necessary to develop a semi-capsulation technique for powder material.

2. OBJECTIVES

Based on its own advantages and high potential to improve the healing performance and manufacturing cost, self-healing granules having semi-capsulation effect were chosen as a research approach in this study. The objectives are to propose basic design concepts of granules having semi-capsulation effect, and to improve the self-healing performance of granules in concrete by enhancing the semi-capsulation technique with considerations of simple & cheap granule fabrication.

3. BASIC DESIGN CONCEPTS OF GRANULES HAVING SEMI-CAPSULATION EFFECT FOR POWDER MATERIAL

Even though the concept of self-healing granules having semi-capsulation effect was proposed by Koide & Morita, self-healing performance of concrete incorporating granules was not as good as expected in previous research. Firstly, it is thought to be due to the high strength of granules. As a result, when a crack penetrates into the concrete matrix, granules can not be broken as seen in Figure

1a. Secondly, the hardened condition of inner material in/after the granulation process or the surface of broken granules when contacting to water flow is believed to reduce the self-healing capacity (Figure 1b). Given this condition, even if granules are ruptured by crack penetration, the inside self-healing additives are thought to be difficult to dissipate into the crack surface and this restrains the healing capability.

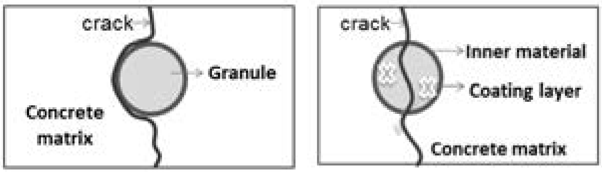

Figure 1: (a) Unbroken granule; (b) Hardened state of inner material

Based on the results obtained from the research of Koide & Morita (2010), it can be found that granules made by conventional granulation method do not fulfill the requirements of granules having semi-capsualtion effect. In order to achieve this, basic design concepts of granules for powder material are established in this paper, as follows:

3.1 Concept 1: Granule should have waterproofing property

A coating layer will be introduced to granule to render the surface impermeable to water. Even though the coating layer is made by cement compound, it is possible to control the water absorption of granule and further reactions between ingredients of granule and mixing water by producing an effective outer layer, which has good bonding property with concrete matrix, enough strength and thickness and watertightness property to protect inner material.

3.2 Concept 2: Granule containing inner self-healing material should be strong enough to preserve the healing capability from unexpected events during concrete mixing process and also should be weak enough to be cracked when necessary.

This means that an appropriate strength of inner material should be obtained. Being broken and released when needed is a very important aspect for granules to fulfill the semi-capsulation effect. The strength of granule, mainly contributed by the strength and thickness of the coating layer, should be strong enough to withstand the compaction/vibration effect while mixing and casting concrete. However, the outer layer also should not be too strong and thick as well. In addition, the inner material should be weak enough and easily released after rupture to ensure the spreading effect.

4. EXPERIMENTAL PROGRAM

4.1 Self-healing materials

Based on the basic design concepts mentioned-above, specific materials are chosen to manufacture self-healing granules as can be seen in Figure 2. Table 1 shows the ingredients of self-healing granule in percentage. In this trial, self-healing additives are composed of swelling, expansion and precipitation materials, based on the basic design concept of self-healing material (proposed by Ahn, 2008).

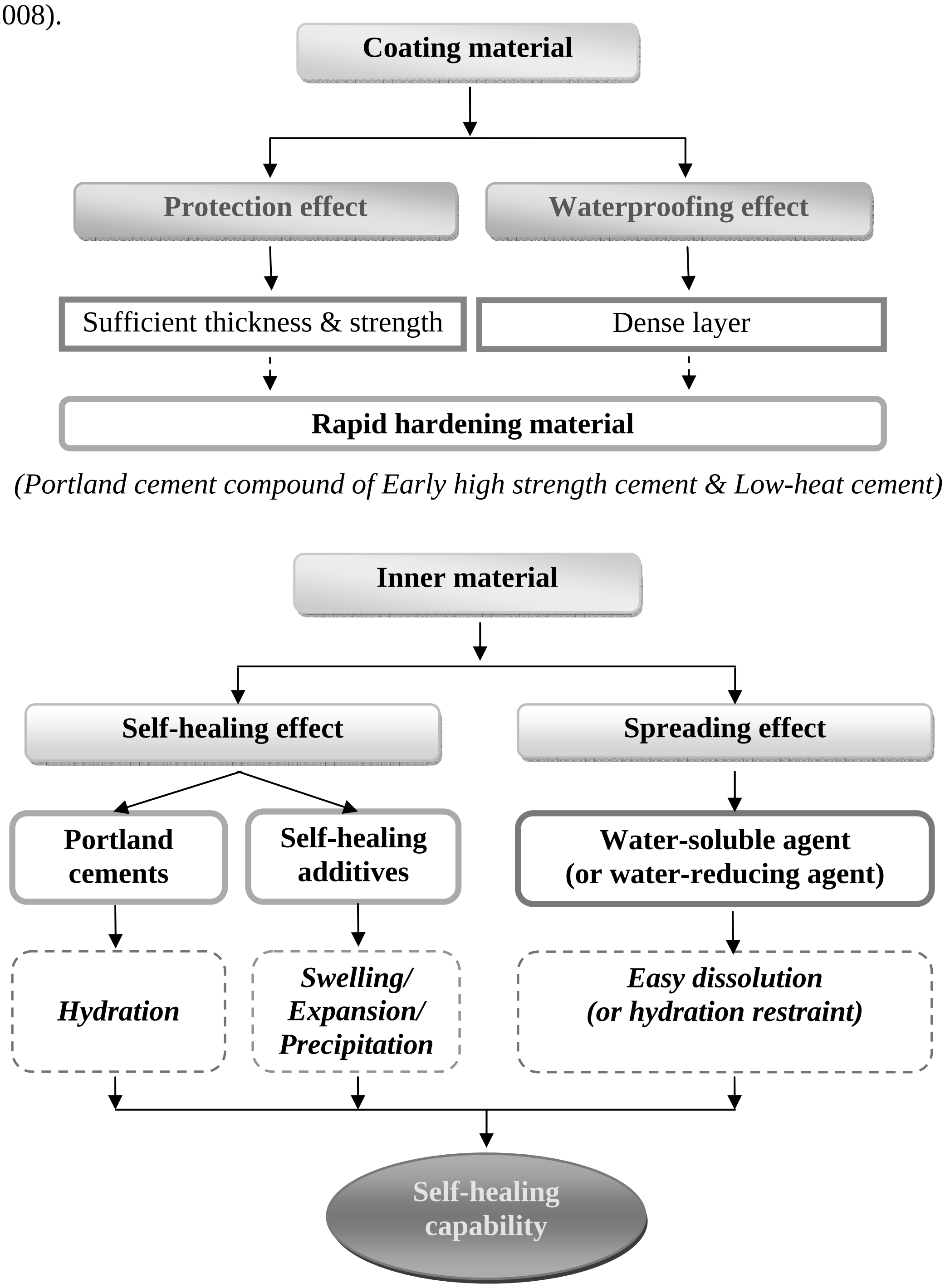

Figure 2 Strategies to select the materials of granule

Table 1: Ingredients of self-healing granule

Ingredients	Percentage [%]	
	Inner	Coating
Portland cements (HC&LC)	37.63	16.13
SHA & Water-soluble agent (water reducing agent)	37.63	-
Liquid	5.38	3.23

4.2 Semi-capsulation techniques

In this experiment, there is an effort to manufacture self-healing granules by using a typical concrete mixer in laboratory (drum mixer or roller mixer). Granules are made through a granulation process as following:

Firstly, the inner granule manufacture is prepared by gradually adding the self-healing powder and spraying the liquid in the drum mixer as seen in Figure 3. Due to this procedure, it is assumed that flocs of self-healing powder will be loose or weak (just pointed or small area of surface contact with each other) so that it is easier to be broken and diffuse out of the granule.

Secondly, a coating layer build-up is followed by continuously adding coating materials and spraying the liquid in the drum mixer. And then after curing in plastic boxes for a few days, pre-fabricated granules are steamed (Figure 3). Under the effect of steaming: high temperature & moisture, it is expected that a dense & hardened coating layer will be formed by the hydration products of cement compound. This layer will protect the weak inner material and also create a barrier that makes it difficult for water to pass through.

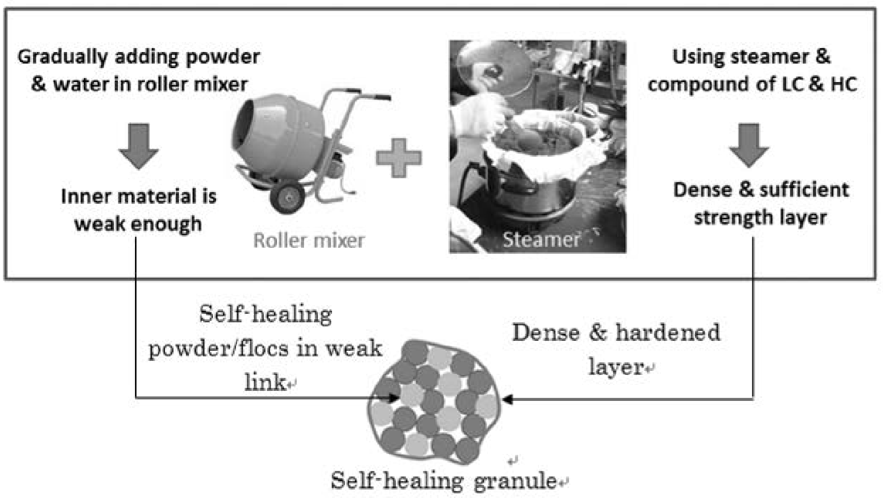

Figure 3: Granulation techniques

Typical sample and particle size distribution of self-healing granules also can be seen in Figure 4. From this figure, it can be found that about 80% of granules could pass the seive of 2.36mm. Therefore, it is expected that the distribution of granules in concrete matrix will be improved compared to past research. The smaller in size the granules are, the higher the possibility that a crack ruptures them, and the higher the healing capacity of concrete.

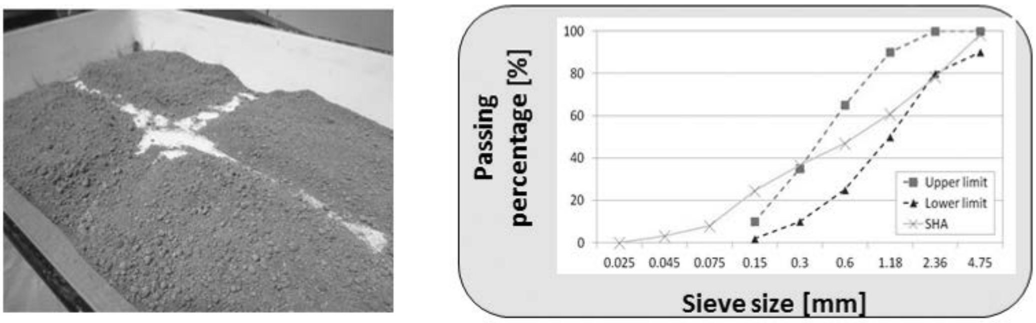

Figure 4: Typical sample & particle size distribution of granules

4.3 Experimental flow & techniques to verify self-healing performance

After fabrication in the laboratory, the granules were transported to a ready-mixed concrete plant for casting cylindrical concrete specimen (100mm diameter x 200mm height). Concrete was cast with a water/cement ratio of 49.6% and self-healing granules were incorporated as partial sand replacement at a dosage of 70 kg/m^3 of concrete (Table 2). After casting, concrete specimens were cured under three different regimes i.e regime one R1 (cured in water at 40^{o}C for one month-*short term range*), regime two R2 (cured in air at 20^{o}C, relative humidity of 60% for twelve months-*long term range*) and regime three R3 (cured in water at 40^{o}C for nine months and then in air at 20^{o}C, relative humidity of 60% for three months-*long term range*). The purpose was to investigate the self-healing performances of concrete incorporating granules with the elapsed time under different exposure conditions.

Table 2 **:** Mix proportion of self-healing concrete

W/C (%)	**s/a (%)**	**G_{max} (mm)**	**Air (%)**	**W**	**NC**	**SH Granule**	**S**	**G**
				kg/m^3				
49.6	51.3	20	4.5	175	353	70	830	869

(Note : W-water; NC-Ordinary Portland Cement; S-sand; G-gravel)

In this study, the water pass test, described by Morita (2010), was used to quantitatively evaluate the self-healing performance as water leakage control.
After curing, a penetrating crack was induced to the concrete specimen by applying tensile splitting load. The internal crack was controlled to around 0.2mm by the thickness of Teflon sheet, while the surface crack width was measured by microscope at three different spots. The average value of those spots was adopted as the surface crack width, ranging from 0.2-0.4mm (Figure 5a). In this expermient, a continuous water supply was conducted until 56 days to stimulate the chemical and other reactions in the crack (Figure 5b). It was assumed that once crack occurred, the embedded granules were broken. And when water flowed through the crack, not only did the self-healing materials get diffused into

crack surface but also the cement hydration products were dissolved in flowing water. Over time, the crack in concrete was healed & water leakage stopped, mainly due to the formation of new products.
The self-healing performance of concrete was evaluated by the water passing test, in which the water leakage through a crack under pressure of approximately eight centimeters water head and the crack closing process observed by microscope were measured periodically (Figure 5c). Moreover, analysis of chemical components of healing products precipitated at the crack was also conducted by Thermogravimetry-Differential Thermal Analysis (TG-DTA) and X-Ray Fluorescence (XRF).

(a) (b) (c)

Figure 5: (a) Surface crack width; (b) Exposure condition; (c) Water pass test

In order to observe the time dependent permeability of a cracked concrete, the water flow rate was measured and calculated by the formula (1), on the specific days until 56 days subjected to continuous water flow.

$$FR_i = \frac{V_{5\min,i}}{t} \tag{1}$$

where: FR_i-water flow rate on i days [cm^3/sec]; $V_{5min,i}$-volume of water flowing through a crack in five minutes on i days [cm^3]; t-period of testing, in this test t=300sec.
Furthermore, to assess quantitatively the decreasing flow rate with time, flow relative to initial flow was introduced as in formula (2):

$$RFR_i = \frac{FR_i}{FR_0} \tag{2}$$

where: RFR_i- relative flow rate on i days [%]; FR_i- water flow rate on i days [cm^3/sec]; FR_0- initial water flow rate on starting day of testing [cm^3/sec].

5. EXPERIMENTAL RESULTS & DISCUSSIONS

5.1 Result of water flow rate through a crack with time

The results showed that there was an insignificant difference of healing capability under three different curing regimes. The same tendency of reduction in water leakage and healing products deposited on the surface crack were observed with time even though the initial flow rates were relatively different (Figure 6). It could be seen that the water leakage after one day exposed to water flow was just about 10% of initial water flow and then after one week exposure, the water flow was almost stopped during the permeability test as clearly seen in Figure 6.

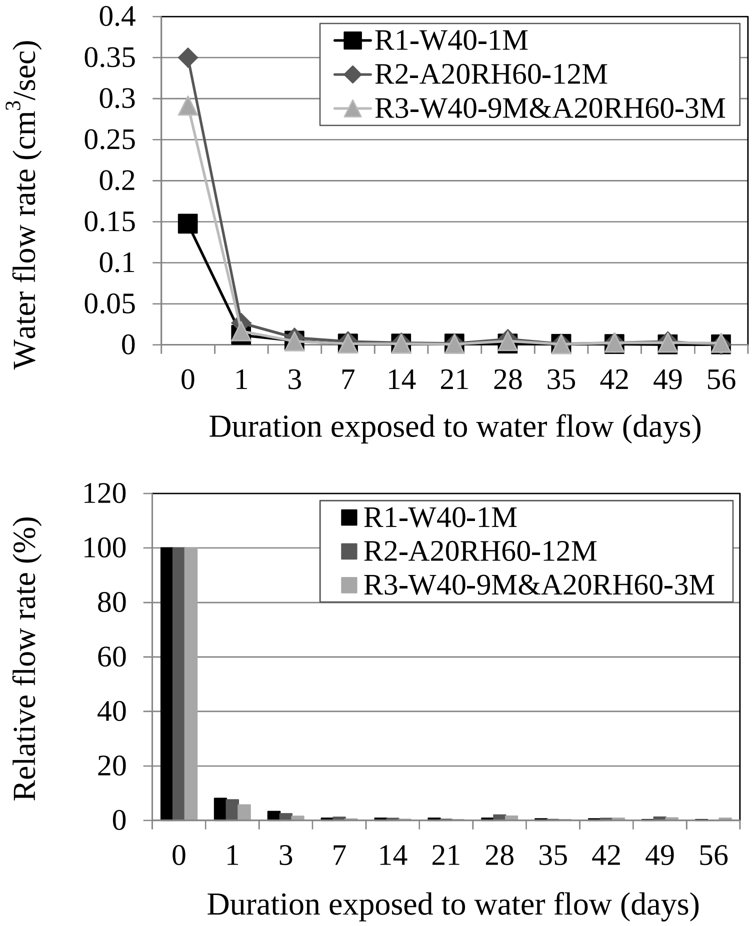

Figure 6: Water flow rate & relative flow rate with time

5.2 Result of crack-closing process at the bottom surface

Moreover, it was found that the crack closing process was mainly observed at the bottom of testing specimen by the substantial amount of white deposits forming at crack mouth (Figure 7). A possible reason was that under the effect of flowing water, there was a higher concentration of both calcium and carbonate ions, higher pH value of flowing water and also slower water flow rate at this area, facilitating the precipitation of calcite or other healing products.

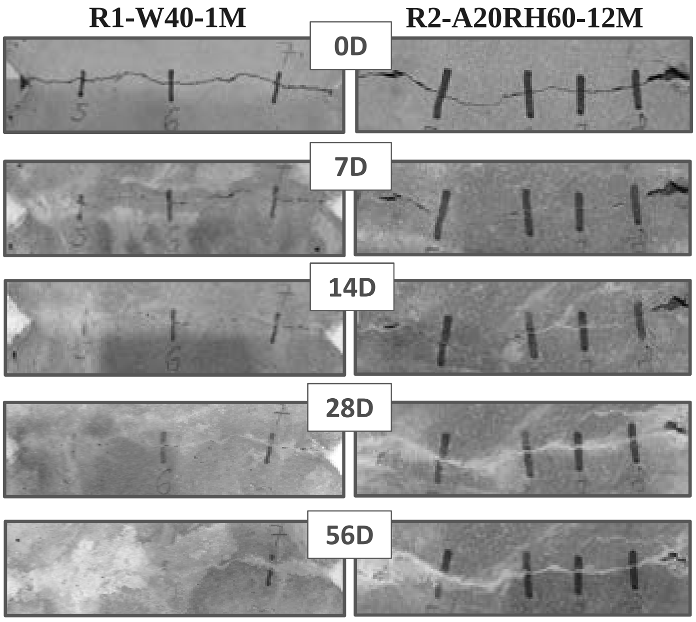

Figure 7: Crack closing process

5.3 Chemical analysis of deposited products at crack

After the water pass test at 56th day under continuous water supply, the specimens were kept in room conditions (T=20^{o}C & RH=60%) for a few days. The two halves of specimens were then split again by removing silicone rubber in order to observe the condition of inner crack surface. Moreover, healing products at the bottom of concrete specimen were examined to verify the chemical component by TG-DTA test. The result showed that the healing products at this zone were mainly composed of calcite as expected. Additionally, it was found that the healing products deposited on the surface of aggregate were mainly composed of calcium compounds based on the result of XRF test.

6. CONCLUSIONS & FURTHER RESEARCH

In this research, the normally used water/cement ratio concretes were designed with the self-healing capacity by incorporating the granules of Portland cements, other additives and a specific water-soluble agent (or also water-reducing agent), considered as a type of engineered self-healing approach. Especially, two basic design concepts for granules having semi-capsulation effect and improvement in terms of simple & cheap granule fabrication were proposed and established.
Based on the experimental results, it can be found that under certain laboratory conditions (static crack of 0.2-0.4mm, continuous water supply), concrete containing self-healing granules of functional effective ingredients is promising to maintain the self-healing ability of concrete, with respect to recovery of water tightness properties, for both short term and long term exposure. Crystalline healing products were gradually formed on the crack surface and thus significantly reduced or completely stopped the water leakage with time. This

approach may be suitable for self-healing of underground or water retaining structures where continuous water supply may be expected.
Furthermore, this approach showed a high potential to introduce self-healing concrete to the practical construction due to its feasibility in mass production of granules and concrete with considerations of simple & cheap manufacture. However, further research is needed to verify and confirm the roles of each ingredient of granule on its semi-capsulation effect. In order to apply this material in real structures, further test with different exposure conditions and types of structures should be performed, such as wet/dry conditions, high pressure water, water submersion, period of crack appearance and exposure to water, size or dimensions of specimen, crack pattern or crack initiation, etc.

REFERENCES

Ahn, T. H., 2008. Development of self-healing concrete incorporating geo-materials: A study on its mechanism and behavior in cracked concrete. Doctor thesis, the University of Tokyo, Japan.
Morita, S., Koide, T., Ahn, T.H., and Kishi, T., 2010. Evaluation of performance upgrade for the cracked self-healing concrete incorporating capsuled inorganic materials, *JCI-TC091A*, 183-190 (in Japanese).
Edvardsen, C., 1999. Water permeability and autogenous healing of cracks in concrete, *ACI*, 96(4), 448-454.
Heide, T. N., 2005. Crack healing in hydrating concrete, Msc-thesis, Delft University of Technology, The Netherlands.
Hirozo, M., and Tomoya, N., 2012. Development of engineered self-healing and self-repairing concrete –State- of –the- art Report, ACT, 10, 170-184.
Reinhardt, H. W., Jooss M., 2003. Permeability and self-healing of cracked concrete as a function of temperature and crack width, *Cement and Concrete Research*, 33(7), 981-985.
Yang, Y.Z, Lepech, M.D., Li, V.C., 2009. Autogeneous healing of engineered cementitious composites under wet-dry cycles, *Cement and Concrete Research* 39(5), 382-390.
Jonkers, H.M., Bacteria-based self-healing concrete, *Heron*, 56(1/2),1-12
Jonkers, H. M., Towards a sustainable bacterially mediated self-healing concrete, Delft University of Technology, the Netherlands.
Wiktor, V., 2011. Assessment of the crack healing capability in bacteria-based self-healing concrete, Conference on Self-healing materials, UK.
Wang, J., van Tittelboom, K., De Belie, N., Verstraete, W., 2012. Use if silica gel or polyurethane immobilized bacteria for self-healing concrete, *Construction and Building Materials*, 26, 532-540.
Mihashi, H., Kaneko, Y., Nishiwaki, T., Otsuka, K., 2000. Fundamental study on development of intelligent concrete characterized by self-healing capability for strength, *Transactions of the Japan Concrete Institute*, 22, 441-450.
Kessler, M.R., Sottos, N.R., White, S.R., 2003. Self-healing structural composite material, *Composites: Part A* 34, 743-753.
Joseph, C., Lark, R., Jefferson, T., Gardner, D., 2009. Potential application of self-healing materials in the construction industry, *A report for the Institution of Civil Engineeerers*, Cardiff university.

Response characteristics of R/C buildings considering impulsive force of tsunami drifting objects

Ho CHOI[1], Kazuto MATSUKAWA[2] and Yoshiaki NAKANO[3]
[1] Research Associate, Institute of Industrial Science, The University of Tokyo, Japan
choiho@iis.u-tokyo.ac.jp
[2] Research Associate, Institute of Industrial Science, The University of Tokyo, Japan
[3] Professor, Institute of Industrial Science, The University of Tokyo, Japan

ABSTRACT

After the 2011 Great East Japan Earthquake, the quantitative evaluation method of tsunami load and the design guideline for tsunami evacuation buildings were established in Japan. However, the impulsive force of drifting objects such as vessels and containers etc. due to tsunami is not taken into consideration in the guideline. Therefore, it is necessary to establish the quantitative evaluation method of the impulsive force and to investigate whether the force should be taken into account to the current design guideline for tsunami evacuation buildings.

In this paper, the response characteristics of R/C buildings considering the impulsive force of tsunami drifting objects are analytically and experimentally investigated. For this purpose, nonlinear analyses are conducted to evaluate the dynamic response of a six story R/C tsunami evacuation building, and collision experiments using 1/100 scale specimens are carried out to verify the validity of analytical results.

Keywords: *the 2011 Great East Japan Earthquake, tsunami evacuation building, impulsive force, drifting object, response characteristics*

1. INTRODUCTION

The 2011 Great East Japan Earthquake that occurred at 14:46 local time on March 11, 2011, had magnitude of 9.0 on the Richter Scale with the epicenter approximately 70 km east of the Oshika Peninsula in Miyagi Prefecture (38.322°N, 142.369°E, Depth: 32km). This earthquake triggered terrible tsunami waves which hit the coast of Japan and propagated around the Pacific Ocean, and this tsunami caused extensive and severe building damage such as pancake collapse, overturning, movement, tilting, sliding, and debris collision. Authors conducted tsunami damage investigations in Tohoku area (from Hachinohe city in Aomori Prefecture to Soma city in Fukushima Prefecture) from the beginning of April through the end of June, 2011.

After the 2011 Great East Japan Earthquake, the quantitative evaluation method of tsunami load and the design guideline for tsunami evacuation buildings were established in Japan. However, the impulsive force of drifting objects such as vessels and containers etc. due to tsunami as shown in Photo 1 is not taken into consideration in the guideline. Therefore, it is necessary to establish the quantitative evaluation method of the impulsive force and to investigate whether the force should be taken into account to the current design guideline for tsunami evacuation buildings.

In this paper, the response characteristics of R/C buildings considering the impulsive force of tsunami drifting objects are analytically and experimentally investigated. For this purpose, nonlinear analyses are conducted to evaluate the dynamic response of a six story R/C tsunami evacuation building, and collision experiments using 1/100 scale specimens are carried out to verify the validity of analytical results.

(a) Collapsed building due to collision   (b) Large vessel drifted by tsunami

Photo 1: Building damage due to collision of tsunami drifting object

2. BUILDING RESPONSE EVALUATION BY NONLINEAR ANALYSIS

2.1 Reference building and modeling for nonlinear response analysis

In this study, a six story apartment R/C building, which is a tsunami evacuation building designed as tsunami inundation depth *h*=10m and water depth coefficient *a*=2.0 (NILIM, 2012) as shown in Figure 1, is selected to analytically evaluate the response characteristics due to both of the tsunami load and the impulsive force of a tsunami drifting object.

The assumptions on nonlinear response analyses are as follows.

(1) The reference building is replaced as six degree of freedom model with single degree of freedom per one story as shown in Figure 2.
(2) The base shear coefficient *C* of this building is 1.15.
(3) The hysteretic characteristic of each story is employed Takeda model (Takeda, T. et al., 1970) having yielding drift angle of 1/200 rad. and stiffness degradation factor □ of 0.4 after yielding point.

(4) The well-known Newmark □ method is employed for numerical integration.
(5) The predominant period of this building is set as 0.26 second, and the weight per unit floor area is assumed as 14 N/mm^2.

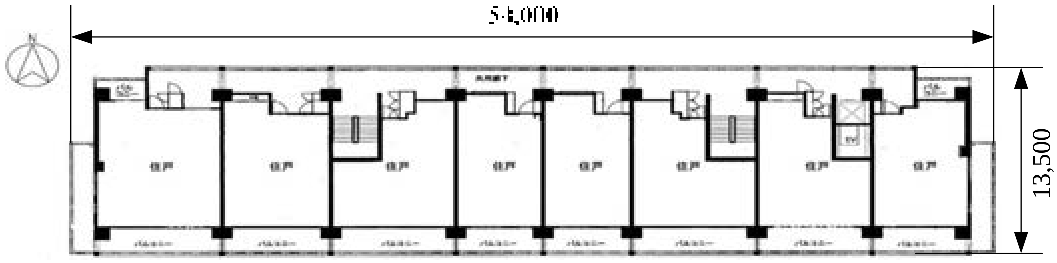

(a) Floor plan of first floor

(b) Elevation of sea side

Figure 1: Reference building

2.2 Estimation of tsunami load and impulsive force

As shown in Figure 2, overall tsunami load acting on the reference building is assumed a triangular shape with the height reaching the water depth coefficient *a* times of the design tsunami inundation depth *h* based on the Japanese guideline (NILIM, 2012), and the tsunami load acting on each floor is calculated by halves of story height of up-and-down story.

The debris collision force shown in Figure 2 is calculated by Mizutani equation shown in equation (1) (Mizutani, N. et al., 2007), and then the impulsive force can be computed by the product of the collision force F_m and the collision time d_t.

$$F_m = 2\rho\eta B_c V_x^2 + \frac{WV_x}{gd_t} \tag{1}$$

$$a = \sqrt{2}F_r \tag{2}$$

$$F_r = \frac{V}{\sqrt{gh}} \tag{3}$$

where,
F_m : Debris collision force (kN)
□ : Mass per unit volume of water (1.0 t/m^3)

□ : Tsunami run-up height (m, assumed as tsunami inundation height h (=9m) herein)
B_c : Width of tsunami drifting object (m)
V_x : Collision velocity (6.6 m/s, assumed as a half of tsunami flow velocity V (13.2 m/s) mentioned later)
W : Weight of tsunami drifting object (kN)
g : Gravity acceleration (9.8 m/s^2)
d_t : Collision time (s, assumed 10ms to 50ms (Mizutani, N. et al., 2007))
a : Water depth coefficient (=2.0 herein)
F_r : Froude number
V : Tsunami flow velocity (13.2 m/s, calculated by equation (2) and (3))

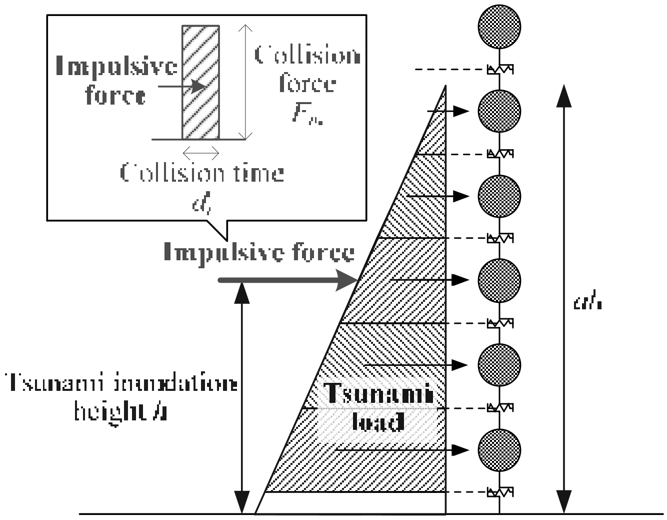

Figure 2: Schematic illustrations of tsunami load and impulsive force

2.3 Analysis parameters

Table 1 shows the parameters of this analysis. As shown in the Table, main parameter of Case 1 is the debris mass, and that of Case 2 is the collision time, respectively.

Table 1: Parameters of this analysis

	Debris mass (t)	**Collision time (s)**	**Collision velocity (m/s)**
Case 1	100	30	6.6
	200		
	300		
	400		
Case 2	200	10	6.6
		30	
		50	

2.4 Analysis results

2.4.1 Results of Case 1

Figure 3 shows the distribution of the ductility factor of each story according to increasing the mass of tsunami drifting objects. When only tsunami load is considered, the ductility factors of all stories are less than 1.0 of ductility factor. However, as the debris mass increases, the ductility factors of each story also increase, and yielding point is exceeded in more than 200*t* of the debris mass. This result means that it is occasionally necessary to take into account the influence of the collision of tsunami drifting objects at the time of the structural design of a tsunami evacuation building.

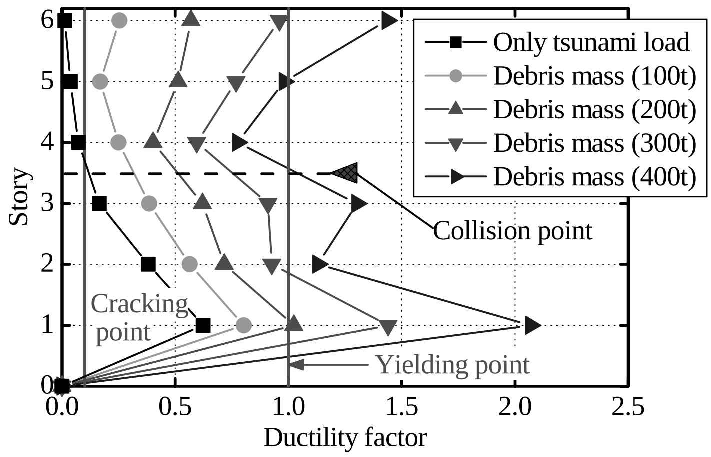

Figure 3: Ductility factor of each story according to increasing of debris mass

2.4.2 Results of Case 2

Figure 4 shows the distribution of the ductility factor of each story in accordance with changing the collision time. As shown in the figure, even if the collision time is changed, maximum ductility factors are almost the same. This result is caused by equation (1) employed in this analysis. Since the equation governs the second term, it can be briefly rewritten as equation (4). If the products of the debris mass m and the collision velocity V_x (i.e., the momentum) are the same as this case, the

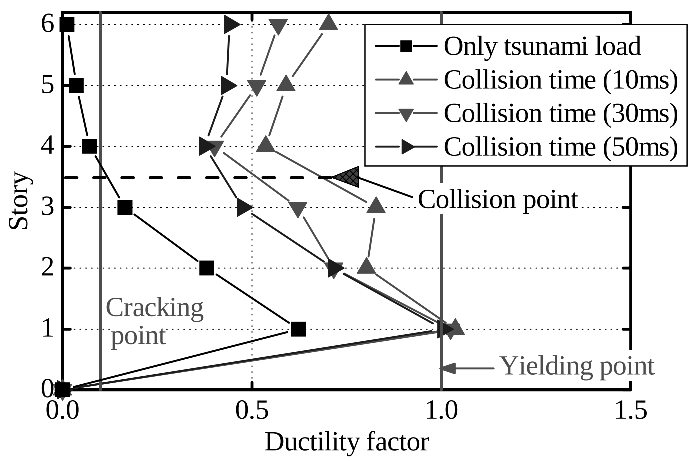

Figure 4: Ductility factor of each story according to changing collision time

collision time d_t and the collision force F_m serve as reciprocal relations as shown in equation (4). Therefore, the impulsive forces calculated by the product of the collision force and the collision time become the same, and eventually maximum ductility factors also become the same.

$$F_m d_t = mV_x \tag{4}$$

3. COLLISION EXPERIMENT USING SCALED MODEL

3.1 Outline of experiment and measurement system

In this study, 1/100-scale specimens which are model building designed by the reference building shown in Figure 1 and model tsunami drifting objects supposing vessels of 100 to 300 ton class are fabricated, and the collision tests are carried out to investigate the collision force and the collision time between model building and model tsunami drifting object. Figure 5 shows the schematic illustration of this experiment system. As shown in the figure, the model building fixed to linear slider run onto the model tsunami drifting object in this test.

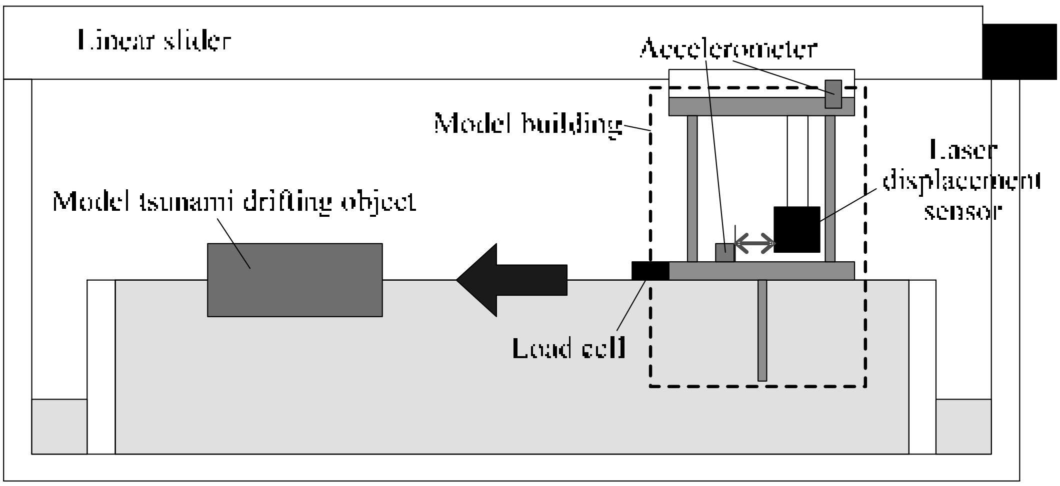

Figure 5: Schematic illustration of this experiment system

The maximum collision force F_m and the collision time d_t are calculated from the wave pattern obtained by the load cell installed the model building as shown in Figure 5. The relative lateral displacement of the model building is measured by the laser displacement sensor.

3.2 Experiment parameters

Table 2 shows the parameters of this experiment. As shown in the Table, main parameter of Case 1 is the debris mass, and that of Case 2 is the same momentum which is calculated by the product of the collision velocity and the debris mass, respectively.

Table 2: Experiment parameters

	Collision velocity(*mm*/*s*)	Debris mass (*g*)	Plate thickness (*mm*)
Case 1	200	100	0.5
		200	
		300	
Case 2	300	100	0.5
	150	200	
	100	300	

3.3 Experiment results

3.3.1 Results of Case 1

Figures 6(a) and 6(b) show the relationships between the collision force and the collision time, and the maximum collision displacement and the impulse force due to different mass of tsunami drifting object, respectively. As can be found in

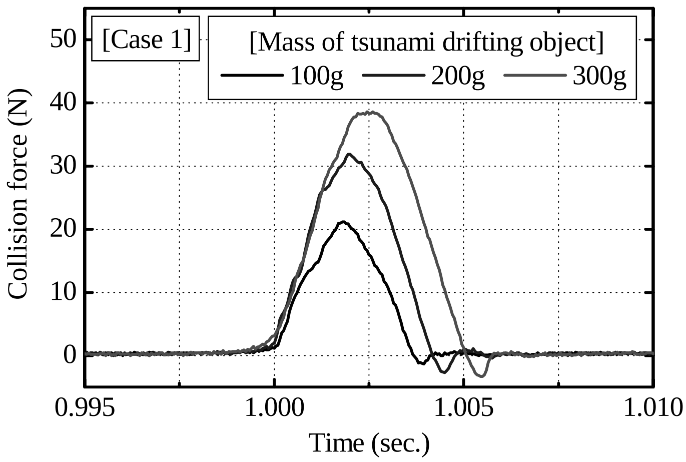

(a) Relation of collision force and collision time due to mass of drifting object

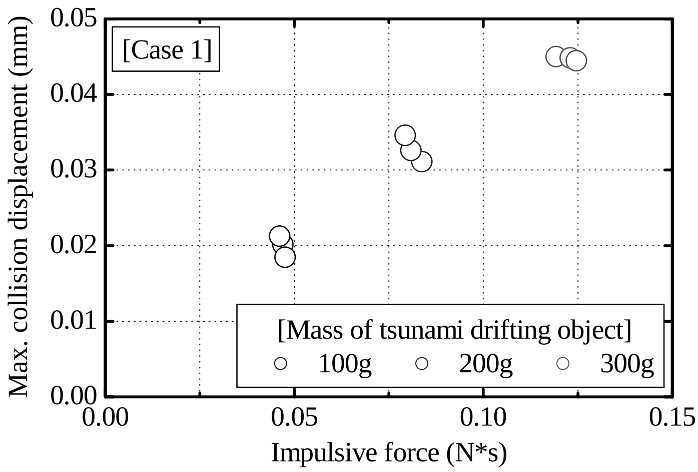

(b) Relation of collision displacement and impulsive force due to mass of drifting object

Figure 6: Results of Case 1

Figure 6(a), both of the collision force and the collision time quantitatively increase as the debris mass increases. Furthermore, the maximum collision displacement and impulsive force increase linearly together with increasing debris masses as shown in figure 6(b).

3.3.2 Results of Case 2

Figures 7(a) and 7(b) show the relations of the collision force and the collision time, and the maximum collision displacement and the impulsive force under same momentum, respectively. As the debris mass increases and the collision velocity decreases, the collision time increases and the collision force decreases as shown in Figure 7(a). However, the impulsive force and the collision displacement are almost the same under same momentum as shown in Figure 7(b).

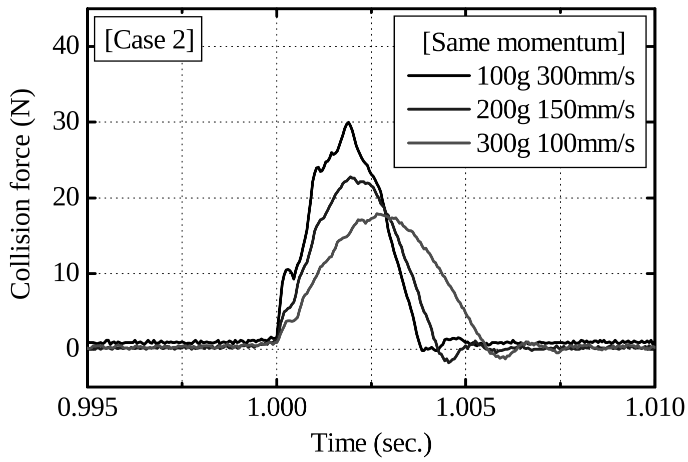

(a) Relation of collision force and collision time under same momentum

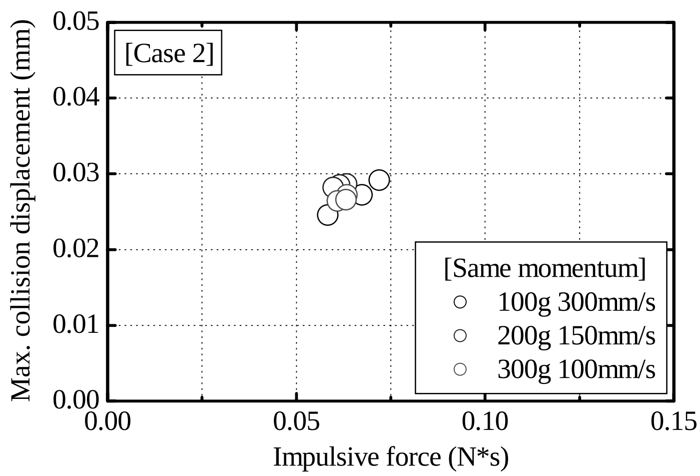

(b) Relation of collision displacement and impulsive force under same momentum

Figure 7: Results of Case 2

3.3.3 Relationship between impulsive force and momentum

In this section, the relationship between the momentum of the model tsunami drifting object and the impulsive force imposed the model building is investigated.

As shown in Figure 8, the impulsive forces calculated by the product of the collision force F_m and the collision time d_t shown in equation (4) are about 2 times of the momentums obtained by the product of the debris mass m and the collision velocity V_x. This result is different from the analysis result that the impulsive force is almost equal to the momentum as shown in equation (4) and Figure 4 in section 2.4.2. This can be explained from equation (7) obtained by equations (5) and (6) based on the law of conservation of momentum and the law of conservation of energy, respectively. As shown in equation (7), the velocity v_x’ of tsunami drifting object after the collision is 2 times of the velocity V_x of building before the collision when the value of □ is close to zero (M»m), while v_x’ is almost equal to V_x when □ is 1.0 (M=m). In this test, since the mass of the building is quite larger than that of tsunami drifting object, the impulsive force became twice the momentum as mentioned above.

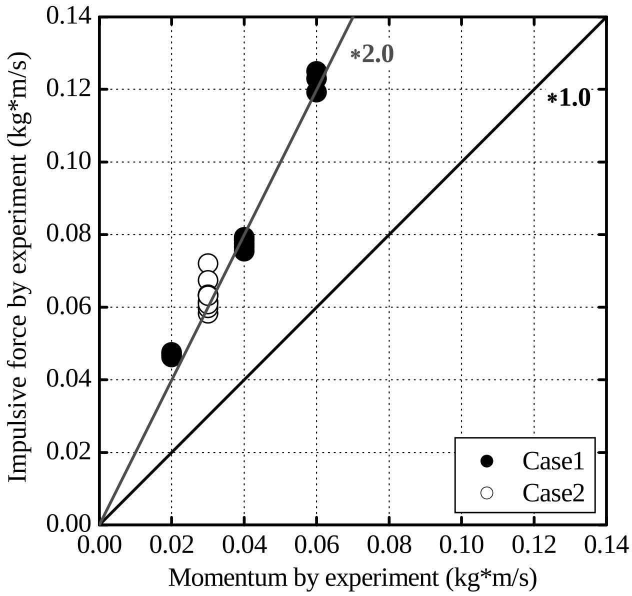

Figure 8: Relation of impulse force and momentum by experiment

$$MV_x + mv_x = MV_x{}' + mv_x{}' \tag{5}$$

$$\frac{1}{2}MV_x{}^2 + \frac{1}{2}mv_x{}^2 = \frac{1}{2}M\left(V_x{}'\right)^2 + \frac{1}{2}m\left(v_x{}'\right)^2 \tag{6}$$

$$v_x{}' = \frac{2}{1+\alpha}V_x \quad \left(\alpha = \frac{m}{M}\right) \tag{7}$$

where,

M, m : Mass of building and tsunami drifting object, respectively

V_x, v_x : Velocity of building and tsunami drifting object before collision, respectively (v is zero in this test)

V_x’, v_x’ : Velocity of building and tsunami drifting object after collision, respectively

□ : Ratio of mass of tsunami drifting object to mass of building

4. CONCLUSIONS

In order to investigate the response characteristics of R/C buildings due to collision force of tsunami drifting objects, nonlinear response analyses and simple collision tests are carried out. The major findings can be summarized as follows.

(1) As increasing of the mass of tsunami drifting object, both of the impulsive force and the maximum displacement of the building increased in both of the analyses and the tests.

(2) When the amount of the momentum is constant, the impulsive force and the maximum displacement of the building are constant in both of the analyses and the tests.

(3) When the mass of the building is quite larger than that of tsunami drifting object, the impulsive force became twice the momentum.

In future research, the collision tests for the value of □ which is the ratio between masses of building and tsunami drifting object will be carried out to establish the design procedure of a tsunami evacuation building considering the collision force.

REFERENCES

National Institute for Land and Infrastructure Management (NILIM), 2012. Practical Guide on Requirement for Structural Design of Tsunami Evacuation Buildings. *Technical note of NILIM*, No.673. (in Japanese)

Takeda, T., Sozen, A., and Nielsen, N.M., 1970. Reinforced Concrete Response to Simulated Earthquakes. *Journal of Structural Division*, *ASCE*, Vol.96:No.ST12, 2557-2573.

Yeom, G.S., Muzutani, N., Shiraishi, K., Usami, A., Miyajima, S., and Tomita, T., 2007. Study on Behavior of Drifting Containers due to Tsunami and Collision Forces. *Journal of Japan Society of Civil Engineers, Ser.B2 (Costal Engineering)*, *JSCE*, Vol.54, 851-855.

NIOM analysis of vertical array records observed in RC structure buildings

Yusuke ODA[1], Hidenori MOGI[2] and Hideji KAWAKAMI[3]
[1]Student, Saitama University, Japan
[2]Assoc. Professor, Civil & Environmental Engineering, Saitama University, Japan
[3]Professor, Geosphere Research Institute, Saitama University, Japan

ABSTRACT

In this research we conducted normalized input–output minimization (NIOM) analysis to investigate the S-wave velocities propagating on the two different RC buildings in Japan: (1) the 6th building of the Kashiwazaki-Kariwa Nuclear Power Plant in Niigata Prefecture, and (2) the Nagata high-rise building in Hyogo Prefecture. The 6th building of Kashiwazaki-Kariwa NPP sustained no damaged from the 2007 Chuetsu-oki earthquake while the Nagata high-rise building was reportedly damaged by the 1995 Hyogoken-Nanbu earthquake. The results of the records for the 6th building in the Kashiwazaki-Kariwa NPP before and after the 2007 earthquake shows no clear changes in the S-wave velocity that ranges from 800 m/s to 1100 m/s. Based on this, we concluded that there was no structural damage to the building caused by the strong ground motions. On the other hand, the results from the Nagata high-rise building show an abrupt decrease of the S-wave velocity from 200 m/s to 100 m/s for the B1F to 5F, and 150 m/s to 100 m/s for the 5F to 24F during the main shock of the 1995 earthquake. These results are consistent with the reported extent of damages to the building.

Keywords: *NIOM analysis, S-wave velocity, vertical array records, earthquake damage of RC building*

1. INTRODUCTION

The Niigata-ken Chuetsu-oki earthquake (16 July 2007, M 6.8) caused severe structural damage in Niigata Prefecture. Damage was also observed in the Tokyo Electric Power Company's (TEPCO) Kashiwazaki-Kariwa Nuclear Power Plant (NPP) located about 8.5 km from the fault rupture (TEPCO, 2008). And also the Hyogoken-Nanbu earthquake (17 January 1995, M 7.3) caused severe damage in Hyogo Prefecture. Damage was also observed in the Nagata high-rise building (Hayashi et al., 1997).

Kawakami and Haddadi (1998) developed normalized input–output minimization (NIOM) method to examine wave propagation velocity using vertical array records. In this study, using the NIOM method, we investigate the S-wave velocity in the two different RC building. With the consideration for structural damages in the buildings, we examine the validity of NIOM method.

2. Outline of the NIOM Method

This section describes the outline of NIOM method developed by Kawakami and Haddadi (1998). Let $H(\omega)$ be the transfer function of a system representing the relationship between two points in a vertical array where the waveforms are observed simultaneously. Then the output model of the system, $\mathrm{y(t)}$, for an arbitrary (real-valued) input model $\mathrm{x(t)}$ can be calculated by

$$\mathrm{Y(\omega) = H(\omega)X(\omega)} \tag{1}$$

where $\mathrm{X(\omega)}$ and $\mathrm{Y(\omega)}$ are the Fourier transforms of the input and output models $\mathrm{x(t)}$ and $\mathrm{y(t)}$, respectively. To get the simplified input and output models that satisfy equation (1), the following constraint is imposed on input $\mathrm{x(t)}$:

$$\mathrm{x(0)} = \frac{1}{\mathrm{N\Delta t}}\sum_{\mathrm{i=0}}^{\mathrm{N-1}}\mathrm{X(\omega_i)}\exp\left(\mathrm{j}\frac{2\pi \mathrm{im}}{\mathrm{N}}\right)|_{\mathrm{m=0}} = \frac{1}{\mathrm{N\Delta t}}\sum_{\mathrm{i=0}}^{\mathrm{N-1}}\mathrm{x(\omega_i)} = 1 \tag{2}$$

And the sum of the squared Fourier amplitude and its time derivatives are minimized subjected to the previously described constraint. Thus, the Lagrange multiplier method gives

$$\begin{aligned}\mathrm{L} \;=\; & \sum_{\mathrm{i=0}}^{\mathrm{N-1}}[|\mathrm{X(\omega_i)}|^2 + \mathrm{k}\omega_{\mathrm{i}}^2|\mathrm{X(\omega_i)}|^2 + |\mathrm{Y(\omega_i)}|^2 + \mathrm{k}\omega_{\mathrm{i}}^2|\mathrm{Y(\omega_i)}|^2] - \\ & \lambda\left\{\frac{1}{\mathrm{N\Delta t}}\sum_{\mathrm{i=0}}^{\mathrm{N-1}}\mathrm{X(\omega_i)} - 1\right\}\end{aligned} \tag{3}$$

where λ is the Lagrange multiplier, and k is the weighting constant for the time derivatives. Substituting equation (1) into equation (3) and minimizing the resulting equation yields,

$$\frac{\partial \mathrm{L}}{\partial \lambda} = \frac{\partial \mathrm{L}}{\partial \mathrm{X(\omega_i)}} = \frac{\partial \mathrm{L}}{\partial \mathrm{X^*(\omega_i)}} = 0, \qquad \left(\mathrm{i} = 0, \ldots\ldots, \frac{2}{N}\right), \tag{4}$$

Where $*$ denotes the complex conjugate. After minimization, the input model $\mathrm{X(\omega_i)}$ and output model $\mathrm{Y(\omega_i)}$ are obtained as follows:

$$\mathrm{X(\omega_i)} = \mathrm{N\Delta t}\frac{\frac{1}{(1+\mathrm{k}\omega_{\mathrm{i}}^2)(1+|\mathrm{H(\omega_i)}|^2)}}{\sum_{\mathrm{i=0}}^{\mathrm{N-1}}\frac{1}{(1+\mathrm{k}\omega_{\mathrm{i}}^2)(1+|\mathrm{H(\omega_i)}|^2)}} \tag{5}$$

$$\mathrm{Y(\omega_i) = H(\omega_i)X(\omega_i)} \tag{5}$$

The parameter k in equation (3) controls the contribution of high frequency components to L. That is, increasing the value of k decreases the contribution of high-frequency components. However, as the time lag time that results into a prominent peak in the output model is not affected much, the choice of the value of k is not so critical.

Lastly, the inverse Fourier transforms of the input model $\mathrm{X(\omega)}$ and output model $\mathrm{Y(\omega)}$ will give the simplified input model $\mathrm{x(t)}$ and $\mathrm{y(t)}$, in time domains. For the calculation of the inverse Fourier transform using fast Fourier transforms (FFT), the first half of the Fourier components of the models is calculated by equation (5), and the number of the Fourier components is increased by a factor of 16 by padding with trailing zeros to interpolate time intervals by 1/16. Then, the latter half of the Fourier components is set to the complex conjugates of the first half to get real-valued waveforms by FFT. As mentioned previously, the NIOM method is a simple input–output analysis technique in which the transfer function is calculated from two observations satisfying input x(t) at x(0) = 1. It is similar to a receiver function (Langston, 1989). In a receiver function, input x(t) should be assumed as a suitable pulse; however, in the NIOM method, the adjustment features are included to get simplified input and output waveforms.

3. The 6th building of the Kashiwazaki-Kariwa Nuclear Power Plant

Figure 1 shows the cross-sectional view of the 6th building of the Kashiwazaki-Kariwa Nuclear Power Plant and the location of seismometers. For this study, records from seismometers R66 and R67 are used (marked with circle in Figure 1). These two seismometers were equipped with three sensors in EW, NS and UD directions, respectively. The distance between seismometers R66 and R67 is 39.9 m.

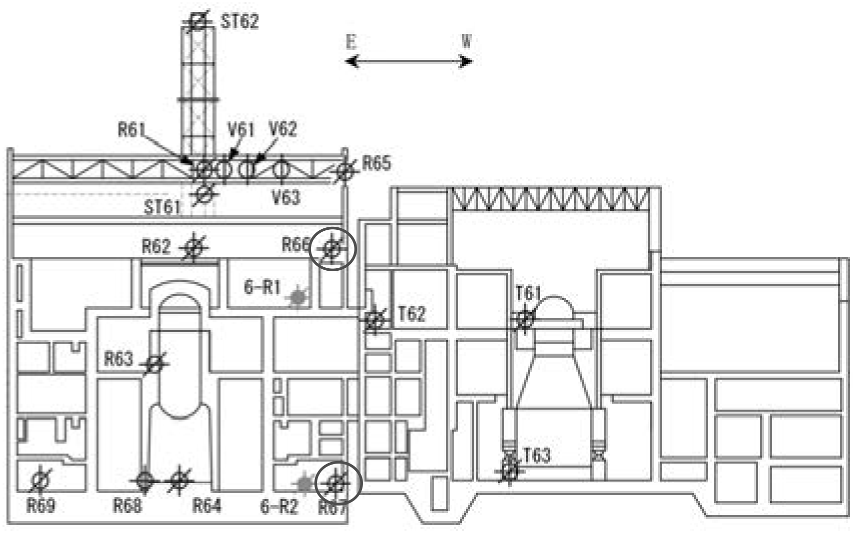

Figure 1: Cross-sectional view of the 6th building of the Kashiwazaki-Kariwa Nuclear Power Plant.

In NIOM analysis for the earthquakes that occurred before and after the Niigata-ken Chuetsu-oki earthquake, 10 sec time intervals of the principal motion in the S-wave part were analyzed. Figure 2(a) shows an example of observed waveform and Figure 2(b) shows the result of NIOM analysis. The earthquake accelerograms analyzed in this article are summarized in Table 1. Among these earthquakes, a through l1 (see Table 1) are aftershocks of the 2007 Niigata-ken Chuetsu-oki earthquake. Similarly, A to J are earthquakes that occurred before the Niigata-ken Chuetsu-oki earthquake and MS indicates mainshock of the Chuestu-oki earthquake. Mainshock of the Chuestu-oki earthquake records was not recorded at R66 and R67 seismometers. So we conducted NIOM analysis of the earthquakes that occurred before the Niigata-ken Chuetsu-oki earthquake and aftershocks of the 2007 Niigata-ken Chuetsu-oki earthquake. The earthquakes that occurred before the Niigata-ken Chuetsu-oki earthquake included that of occurred at Niigata and the rest off the coast of Noto penibshula. The epicenter location is shown in Figure 3.

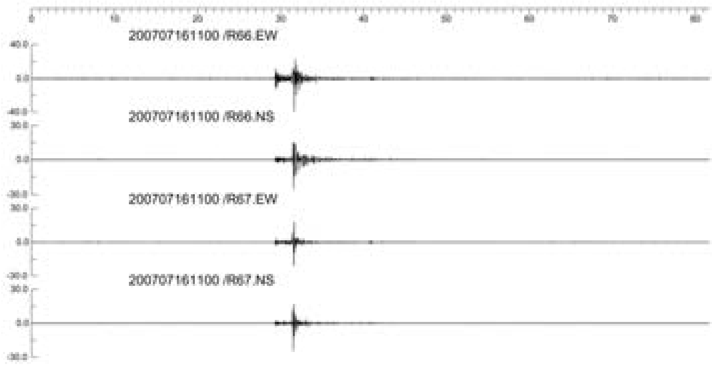

(a) Observed waveforms of aftershock of the Chuestu-oki earthquake on 16 July 2007 at 11:00, M3.7.

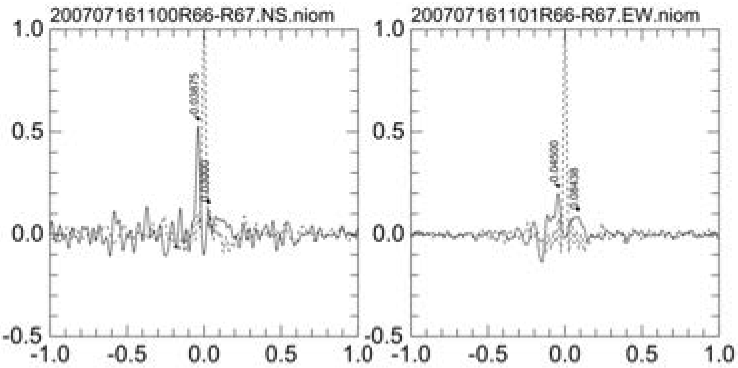

(b) Results of the NIOM analysis for the waveforms

Figure 2: Example waveforms and NIOM results

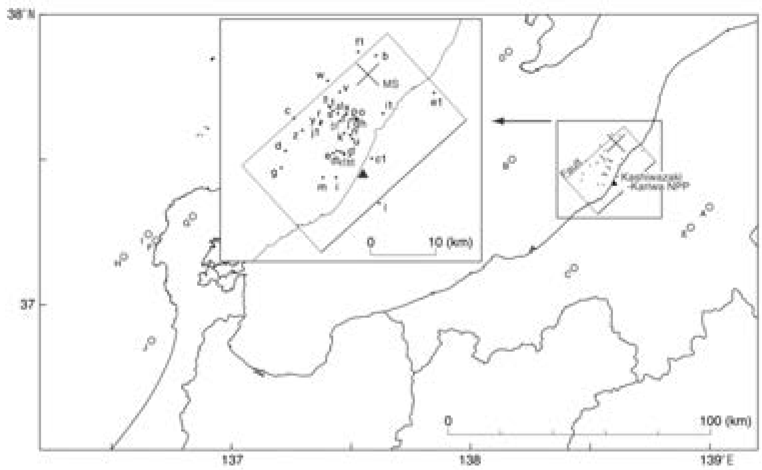

Figure 3: Location of epicenter for the NIOM analysis at the Kashiwazaki-Kariwa Nuclear Power Plant

Table 1: Source parameters of the earthquakes analyzed in this study

Date,time (JST)	Longitude	Latitude	Depth (km)	Epicenter distance (km)	Symbols for earthquake
2006/03/07 12:46	138 ° 59.9 '	37 ° 20.3 '	7.76	36	A
2006/03/14 12:01	138 ° 10.4 '	37 ° 30.1 '	274	39	B
2006/04/01 06:22	138 ° 26.0 '	37 ° 07.7 '	19.7	35	C
2006/12/26 05:17	138 ° 09.6 '	37 ° 52.4 '	14.46	64	D
2007/01/08 18:59	138 ° 55.2 '	37 ° 16.0 '	13.34	33	E
2007/03/25 09:41	136 ° 41.2 '	37 ° 13.2 '	10.7	171	F
2007/03/25 18:11	136 ° 50.4 '	37 ° 18.3 '	13.45	156	G
2007/03/26 14:46	136 ° 33.1	37 ° 09.9 '	8.62	184	H
2007/06/11 03:45	136 ° 39.2 '	37 ° 14.6 '	7	174	I
2007/06/22 03:34	136 ° 40.0 '	37 ° 55.7 '	8	182	J
2007/07/16 10:13	136 ° 60.8 '	37 ° 52.6 '	17	16	MS
2007/07/16 11:00	138 ° 33.9 '	37 ° 27.4 '	22	5	a
2007/07/16 11:01	138 ° 37.3 '	37 ° 35.0 '	20	19	b
2007/07/16 11:05	138 ° 29.1 '	37 ° 29.8 '	23	14	c
2007/07/16 11:12	138 ° 28.2 '	37 ° 27.1 '	24	12	d
2007/07/16 11:15	138 ° 33.0 '	37 ° 26.9 '	17	6	e
2007/07/16 11:20	138 ° 34.3 '	37 ° 30.1 '	20	10	f
2007/07/16 11:24	138 ° 27.8 '	37 ° 25.7 '	18	12	g
2007/07/16 11:25	138 ° 35.4	37 ° 29.8 '	20	9	h
2007/07/16 11:30	138 ° 33.3 '	37 ° 24.9 '	19	4	i
2007/07/16 11:35	138 ° 34.8 '	37 ° 29.7 '	12	9	j
2007/07/16 11:37	138 ° 33.7 '	37 ° 29.6 '	22	9	k
2007/07/16 11:43	138 ° 37.6 '	37 ° 22.8 '	26	5	l
2007/07/16 11:47	138 ° 32.0 '	37 ° 24.9 '	18	6	m
2007/07/16 11:50	138 ° 34.7 '	37 ° 28.4 '	19	7	n
2007/07/16 11:53	138 ° 35.5 '	37 ° 29.7 '	16	9	o
2007/07/16 11:56	138 ° 35.2 '	37 ° 29.8 '	17	9	p
2007/07/16 12:01	138 ° 35.3 '	37 ° 29.7 '	19	9	q
2007/07/16 12:04	138 ° 31.8 '	37 ° 29.6 '	21	11	r
2007/07/16 12:11	138 ° 33.0 '	37 ° 30.4 '	19	11	s
2007/07/16 12:20	138 ° 32.7 '	37 ° 30.7 '	20	12	t
2007/07/16 12:27	138 ° 34.9 '	37 ° 28.1 '	22	6	u
2007/07/16 12:29	138 ° 33.7 '	37 ° 32.0 '	17	13	v
2007/07/16 12:34	138 ° 32.5 '	37 ° 32.9 '	18	15	w
2007/07/16 12:37	138 ° 34.3 '	37 ° 30.2 '	18	10	x
2007/07/16 12:49	138 ° 31.8 '	37 ° 29.4 '	19	10	y
2007/07/16 12:59	138 ° 29.9 '	37 ° 28.8 '	20	11	z
2007/07/16 13:09	138 ° 33.5 '	37 ° 30.2 '	18	10	a1
2007/07/18 11:47	138 ° 34.1 '	37 ° 28.6 '	18	7	b1
2007/07/18 16:53	138 ° 36.9 '	37 ° 26.5 '	23	3	c1
2007/07/20 01:52	138 ° 33.4 '	37 ° 27.1 '	19	5	d1
2007/07/25 06:52	138 ° 43.2 '	37 ° 31.9 '	24	17	e1
2007/12/20 15:17	138 ° 35.5 '	37 ° 35.3 '	16	19	f1
2008/03/07 07:11	138 ° 34.1 '	37 ° 26.9 '	18	4	g1
2008/03/12 17:59	138 ° 34.1 '	37 ° 26.8 '	20	4	h1
2008/03/18 04:40	138 ° 38.0 '	37 ° 30.2 '	15	10	i1
2008/03/21 15:40	138 ° 31.7 '	37 ° 29.3 '	17	10	j1
2008/03/25 10:54	138 ° 33.8 '	37 ° 27.0 '	20	5	k1
2008/03/29 19:29	138 ° 32.6 '	37 ° 30.8 '	20	12	l1

Figure 4 shows temporal changes of the S-wave velocities between the R66 and R67 seismometers. Before and after the mainshock of the Chuetsu-oki earthquake, small changes in propagation velocity can be seen. Then we considered the shear modulus, given by

$$\mu = Vs^2 * \rho \,, \tag{6}$$

where, μ is the shear modulus, Vs is the S-wave velocity and ρ is the density. There is no changes in the shear modulus caused by the Chuets-oki earthquake of the Kashiwazaki-Kariwa Nuclear Power Plant's 6th building. This suggests that there was no damage of the building caused by the Chuetsu-oki earthquake. In this study, however, we obtained small changes in the value; not caused by the strong ground motion. Comparison of S-wave velocities for each components show that the NS component is larger than the EW component.

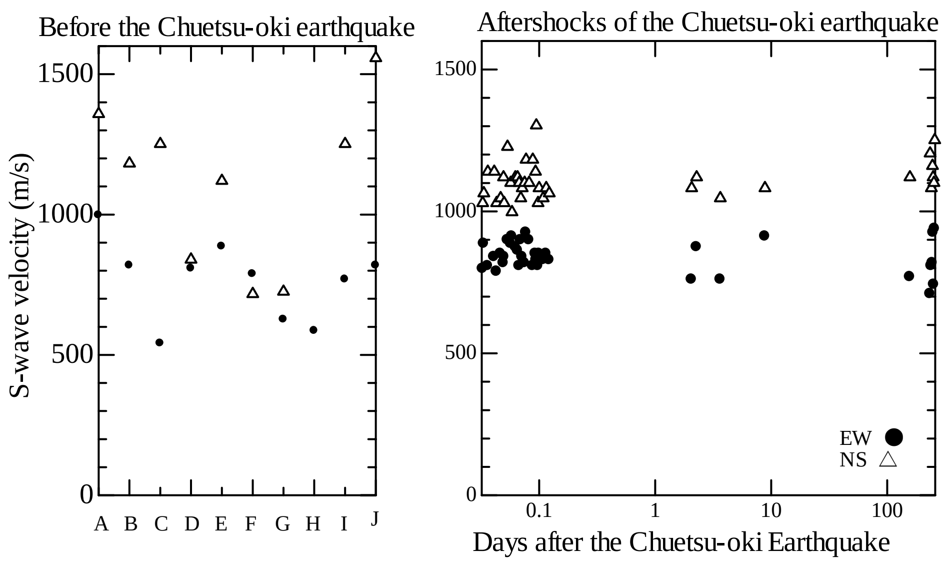

Figure 4: Temporal changes in the S-wave velocity between R66 to R67 seismometers at the Kashiwazaki-Kariwa Nuclear Power Plant 6th building estimated from the earthquake records before and after the Chuetsu-oki earthquake.

4 Nagata high-rise building

Figure 5 is the cross-sectional view of the Nagata high-rise building. As in the case of the Kashiwazaki-Kariwa Nuclear Power Plant's 6th building, seismometers recorded three components, i.e., EW, NS, and UD directions,. In this study, we use the seismometers located at 24F, 5F, and B1F. The distance between 24F and 5F is 54.4 m, while the distance between 5F and B1F is 24 m.

In NIOM analysis for the Hyogoken-nanbu earthquake, a moving window of 4.0-

sec duration was used from 4 to 37 sec at an increment of 1 sec. The epicenter and Nagata high-rise building location are shown in Figure 6. Figure 7(a) shows the observed waveforms of the Hyogoken-nanbu earthquake while (b) shows the result of NIOM analysis.

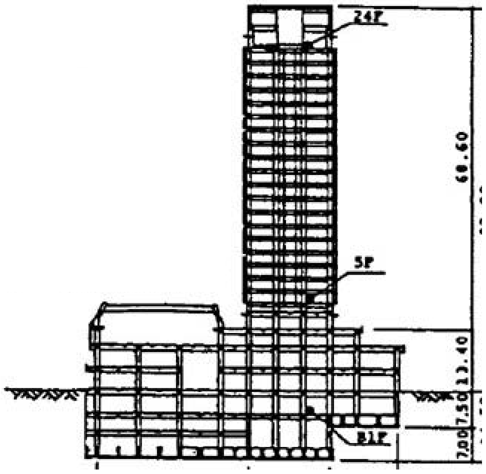

Figure 5: Cross-sectional view of the Nagata high-rise building (Hayashi et al., 1997)

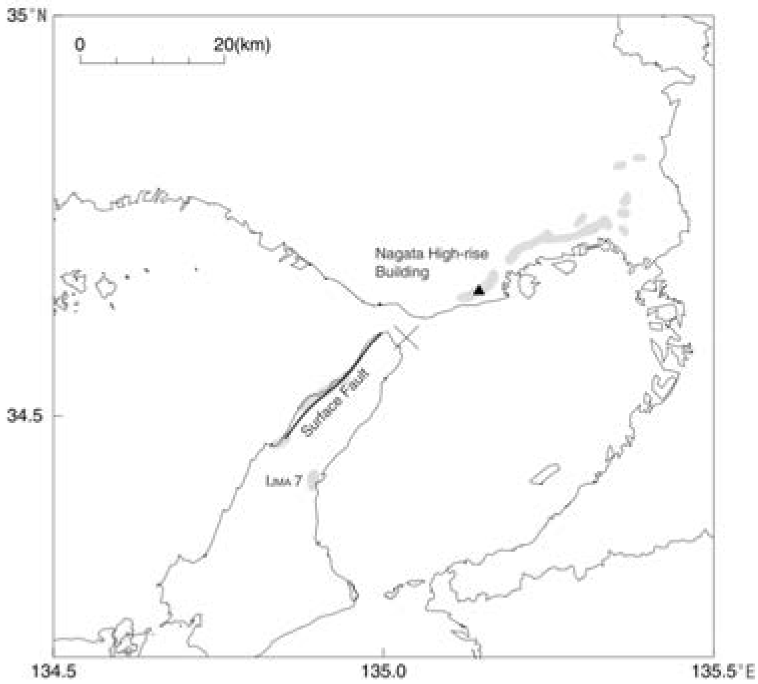

Figure 6: The epicenter of the 1995 Hyogoken-nanbu earthquake and the location of Nagata high-rise building

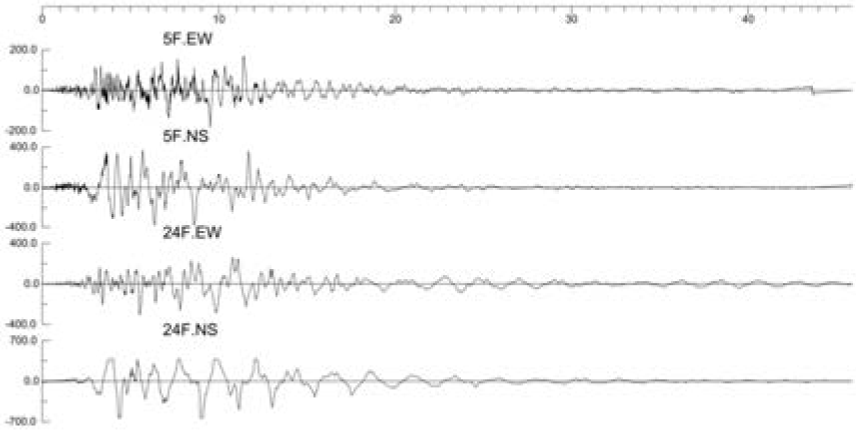

(a) Observed waveforms of Hyogoken-nanbu earthquake on 17 January 1995 at 05:46 (AIJ, 1996)

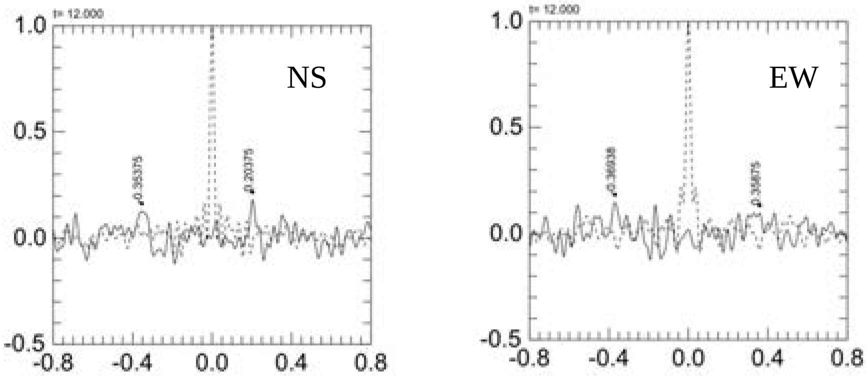

(b) Results of the NIOM analysis for the waveforms

Figure 7: Results for the Hyogoken-Nanbu earthquake record

Figure 8 shows the temporal changes in the S-wave velocities at the Nagata high-rise building estimated from the records of the Hyogoken-nanbu earthquake. Between the 5F and B1F, abrupt decrease in the S-wave velocities from 200 m/s to 100 m/s is seen. On the other hand, between the 24F and 5F, decrease in the S-wave velocities from 150 m/s to 100 m/s are observed. Decline of propagation speed is clearly seen in the lower part of the building than on the upper part of the building. This suggests that the damage of the lower part of the building was larger than the upper part of the building. In fact almost all the beams had shear failure near the opening of doorway and large shear cracks occurred in the walls (Hayashi et al., 1997). Comparison between this result and that of the Chuetsu-oki earthquake, decrease in the S-wave velocities was clearly observed for Nagata high-rise building.

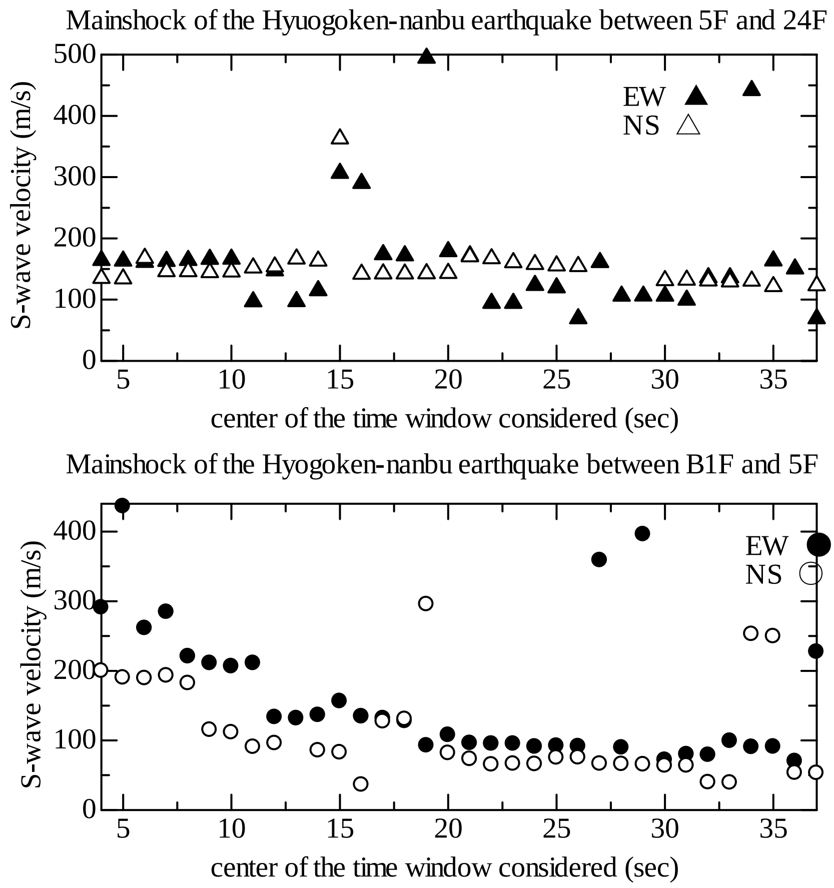

Figure 8: Temporal change of the S-wave velocities at Nagata high-rise building.

5 Conclusions

1. The S-wave velocities before and after the Chuestu-oki earthquake for the Kashiwazaki-Kariwa nuclear power plant's 6th building was almost the same. However, when the S-wave velocity of each component is compared, the NS component is larger than the EW component. S-wave velocity of the NS component is about 1100 m/s, while the EW component is about 800 m/s.
2. Decrease in the S-wave velocities during the mainshock of the Hyogoken-nanbu earthquake for 5F to B1F was observed. The S-wave velocities of the NS component fell from 200 m/s to 100 m/s. On the other hand, the S-wave velocities of the EW component fell from 300 m/s to 100 m/s.
3. A slight decrease in the S-wave velocities during the mainshock of the Hyogoken-nanbu earthquake for 24F to 5F was observed.
4. Based on conclusions 2 and 3, there is a clear indication that structural damage occurred in the Nagata high-rise building. And it is thought that the lower part of the building had serious damage.
5. Based on S-wave velocities estimated by the NIOM method, we confirmed that the 6th building of the Kashiwazaki-Kariwa Nuclear Power Plant suffered no damage.

REFERENCES

Mogi, H., Shrestha, S. M., Kawakami, H. and Okamura, S., 2010. Nonlinear Soil Behavior Observed at Vertical Array in the Kashiwazaki-Kariwa Nuclear Power Plant during the 2007 Niigata-ken Chuetsu-oki Earthquake. *Bulletin of the Seismological Society of America*, Vol. 100, No. 2, 762-775 (DOI: 10.1785/0120090091)

Hayashi, Y., Yasui, Y. and Yoshida, N., 1997. Effects of Soil-Structure Interaction in Heavily Damaged Zone during Hyogo-ken Nanbu Earthquake. *7th Dynamic interaction symposium of a structure and foundation: The aseismic designing method which considered the dynamic interaction,* Architectural Institute of Japan, 12-24.

Kawakami, H., and H. R. Haddadi., 1998. Modeling wave propagation by using normalized input–output minimization (NIOM), *Soil Dynamics and Earthquake Engineering.* Vol. 17, 117–126.

TEPCO, 2008. Accelerograms observed at the Kashiwazaki-Kariwa Nuclear Power Plant (revised version), DVD-ROM.

Architectural Institute of Japan (AIJ), 1996. Strong motion records observed during the 1995 Hyogoken-Nanbu earthquake (in Japanese).

Langston, C. A., 1979. Structure under Mount Rainier, Washington, inferred from teleseismic body waves, *Journal of Geophysical Research* 84, No. B9, 4749–4762.

Residual seismic capacity evaluation of RC frame with weak-beams based on energy absorption capacity

Chunri QUAN[1], Ho CHOI[2], Noriyuki TAKAHASHI[3], Yoshiaki NAKANO[4] and Kazuto MATSUKAWA[2]
[1]Graduate Student, Graduate School of Engineering, The University of Tokyo, Japan
quancr@iis.u-tokyo.ac.jp
[2]Research Associate, Institute of Industrial Science, The University of Tokyo, Japan
[3]Associate Professor, Faculty of Engineering, Tohoku University, Japan
[4]Professor, Institute of Industrial Science, The University of Tokyo, Japan

ABSTRACT

The objective of this study is to develop a method to evaluate residual seismic capacity of damaged RC frames with weak-beams after earthquakes. For this purpose, the residual seismic capacity ratio, which is defined as the ratio of residual energy absorption capacity to the initial (pre-earthquake) energy absorption capacity of an overall frame, is proposed for the weak-beam RC frames (detailed calculation method). Furthermore, a simplified calculation method for residual seismic capacity ratio is developed employing visual damage information such as maximum residual crack width of members.

In this paper, two evaluation methods, i.e. detailed and simplified methods, for residual seismic capacity of weak-beam RC frames mentioned above are applied to two test results. The relationships between the residual seismic capacity ratio and damage ratings such as slight, light, moderate, heavy and collapse are discussed and then the validity is confirmed based on the detailed calculation method. It is also revealed that the simplified calculation method can successfully evaluate the residual seismic capacity of weak-beam RC frames from the visual damage information based on the comparison results of detailed and simplified calculation methods.

Keywords: *residual seismic capacity evaluation, weak-beam RC frames, energy absorption capacity, residual seismic capacity ratio, damage rating*

1. INTRODUCTION

The major concern for damaged buildings after an earthquake is their safety to the aftershocks, and also quick damage inspections are needed. In the next stage following the quick damage inspections, a damage evaluation should be more precisely and quantitatively performed, to identify necessary actions required for the damaged buildings. For this purpose, the Guidelines for Post-Earthquake Damage Evaluation and Rehabilitation (JBDPA, 2001) originally developed in 1991 was revised in 2001 in Japan. In the guidelines, the damage classes of structural members should be classified first from the damage state. Then, a seismic capacity reduction factor η which is defined as the ratio of the absorbable hysteretic energy after an earthquake to the original absorbable energy of each structural member should be calculated corresponding to the damage classes of members. Considering the seismic capacity reduction factor η, a residual seismic capacity ratio index R which is defined as the ratio of post-earthquake seismic capacity to original capacity can be calculated. Finally, the damage of a building can be rated based on the damage rating criteria.

However, the current Japanese guidelines mentioned above mainly consider vertical members such as columns and walls. Since RC buildings with weak-beams are generally designed and constructed in recent years, the guidelines are often difficult to apply to those buildings. Accordingly, in this paper, a detailed calculation method of residual seismic capacity ratio index SI_{margin} is proposed for the weak-beam RC frames. Then, a simplified calculation method for the index SI_{margin} is developed employing visual damage information such as the maximum residual crack width of each structural member. Furthermore, the detailed and simplified methods proposed to calculate the index SI_{margin} are applied to two weak-beam RC specimens, and the relationships between the index SI_{margin} and damage rating are discussed and their validity is verified based on the detailed calculation method. The validity of the simplified calculation method is also confirmed based on the comparison results of the detailed and simplified calculation methods.

2. RESIDUAL SEISMIC CAPACITY EVALUATION METHOD

2.1 Detailed calculation method of index SI_{margin}

The basic concept of residual seismic capacity evaluation method for the weak-beam RC frames is illustrated in Figure 1.

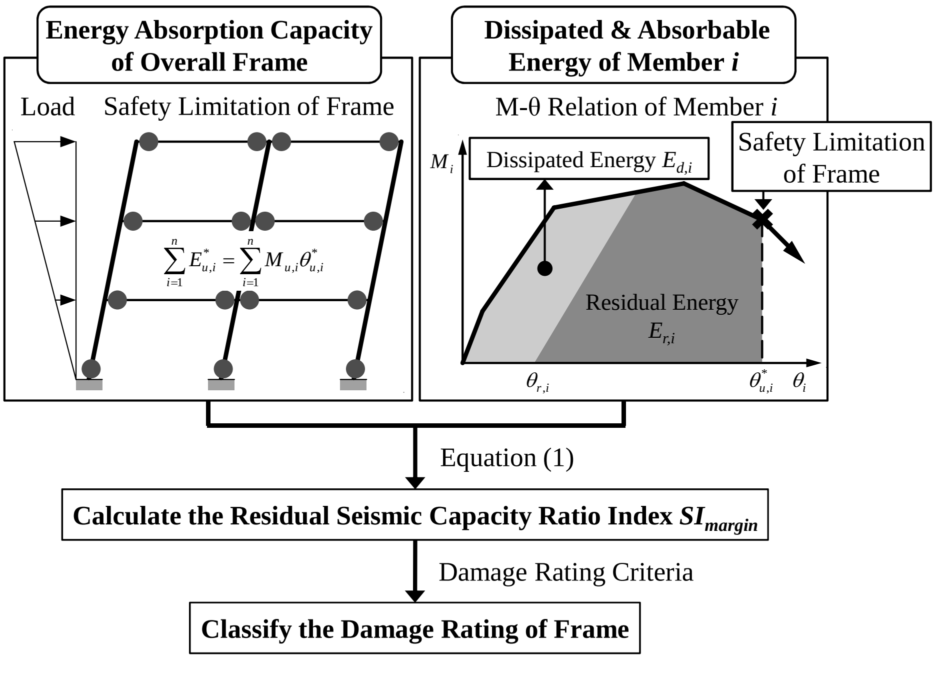

Figure 1: Basic concept of residual seismic capacity evaluation method

In this paper, the seismic capacity of building structure is evaluated based on the energy absorption capacity of overall frame considering the principle of virtual work. The energy absorption capacity of overall frame can be calculated as the total absorbable energy of structural members until the safety limitation of a frame, where this safety limitation is defined as the moment in which the maximum lateral strength of a frame deteriorates to its 80%. Then, the residual seismic capacity ratio index SI_{margin} of overall frame is defined as the ratio of total residual energy absorption capacity to the total initial energy absorption capacity of structural members as shown in Equation (1).

$$SI_{margin} = \left(\sum_{i=1}^{n} E_{r,i} \Big/ \sum_{i=1}^{n} E^{*}_{u,i} \right) \times 100 \ (\%) \qquad (1)$$

where, $\sum E^{*}_{u,i}$: total absorbable energy of structural members before earthquake, $\sum E_{r,i}$: total residual absorbable energy of structural members after earthquake

2.2 Definition of damage rating for weak-beam RC frames

In Japan, the damage ratings for weak-column RC buildings such as slight, light, moderate, heavy and collapse are generally classified from the state of observed damage of buildings as shown in Table 1 (AIJ, 1980).

Table 1: Definition of damage rating for weak-column RC buildings (AIJ, 1980)

Damage rating	Description of damage	Sketch
Slight	Slight or almost no damage on the columns and walls.	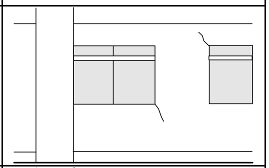
Light	Slight damage on the columns and shear walls, visible shear cracks on secondary walls.	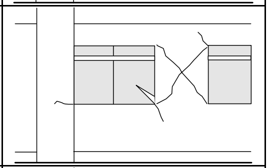
Moderate	Visible clear flexural and shear cracks on columns, visible shear cracks on shear walls, remarkable heavy damage on nonstructural members.	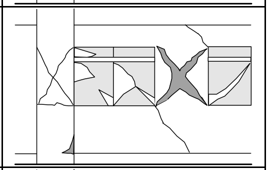
Heavy	Exposing and bucking of reinforcing bars on columns, considerable lateral strength deterioration of buildings with remarkable wide shear cracks on shear walls.	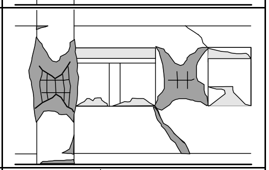
Collapse	Remarkable heavy damage on columns and shear walls, overall or partial collapse on buildings.	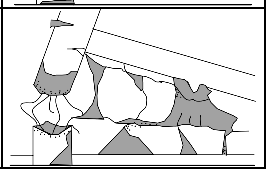

However, such a damage rating is not clearly defined for weak-beam RC buildings. Therefore, in this paper, the authors propose the criteria to define the damage rating of weak-beam RC frames through the engineering demand parameter (EDP) as shown in Table 2 and Figure 2.

Table 2: Damage rating criteria for weak-beam RC Frames

Damage rating	**Description of engineering demand parameter (EDP)**
No damage	
	Initial cracking of member
A	
	Initial yielding of member
B	
	Formation of yield mechanism
C	
	Maximum lateral strength of frame (P_{max})
D	
	80% of P_{max}
E	

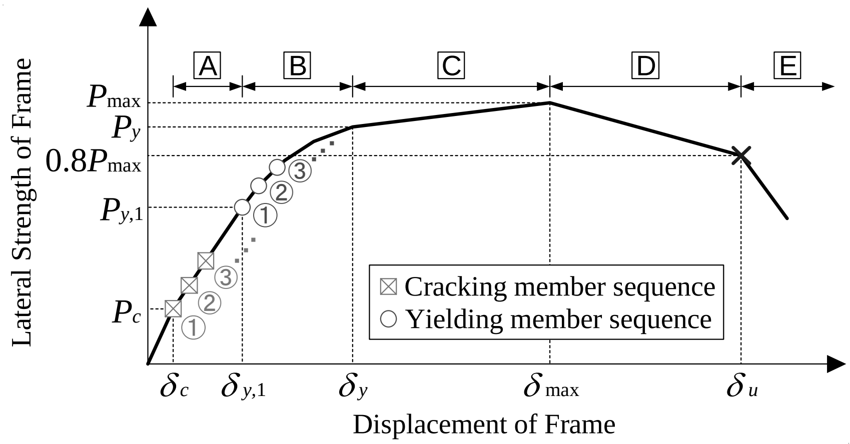

Figure 2: Conceptual diagram of damage rating

2.3 Application to weak-beam RC specimens

To discuss the relationships between the index SI_{margin} and damage ratings, in this section, the detailed calculation method for the index SI_{margin} is applied to the following two weak-beam RC specimens as shown in Figure 3, which illustrates the state of damage as well. 2SH-64 specimen is half-scale, two-bay, single-story bare frame specimen (IIS & HAEI, 2011) with load cell for each corner column. The lateral and vertical load carrying capacity of each column can be measured from the two load cells, and the load-deflection curve of each beam also can be illustrated from the difference of vertical load between the two columns which are connected with the end of the beam. 1SF specimen is full-scale, one by one-bay, single-story specimen, (BRI, 2011) with non-structural wall initially separated from the inner surface of the structural members by slit with width of 25mm. Since there is no load cell for this specimen, the lateral and vertical load carrying capacity of each member can not be measured.

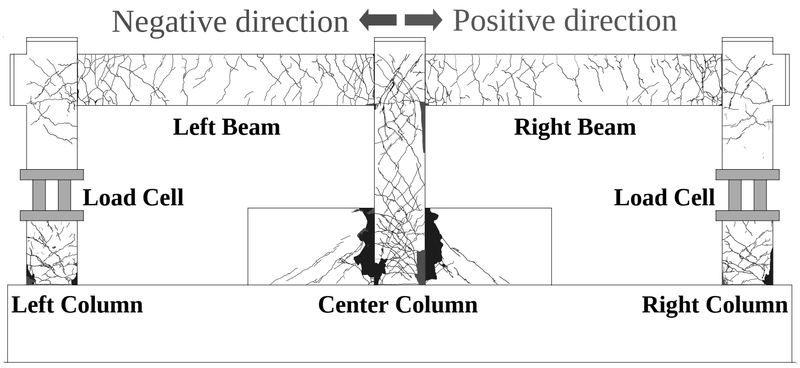

(a) Damage state of the 2SH-64 specimen at 3.03% drift angle

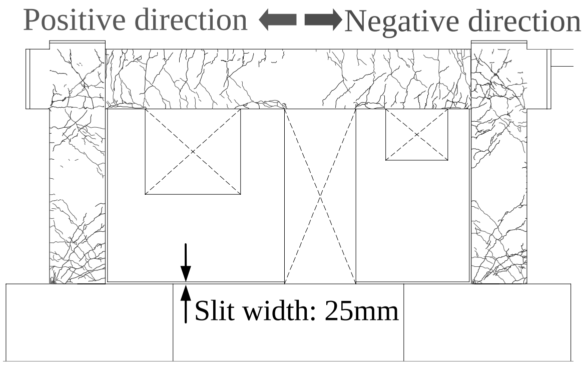

(b) Damage state of the 1SF specimen at 2% drift angle

Figure 3: Damage state of the two specimens

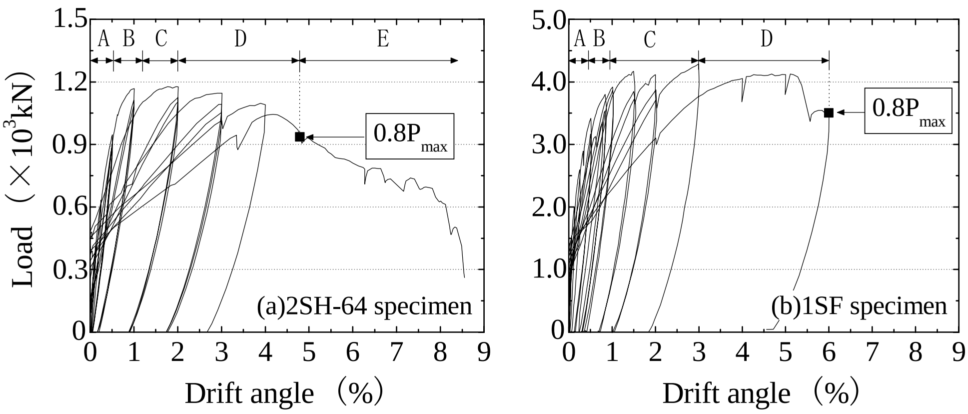

Figure 4: Load-drift angle relations of the two specimens

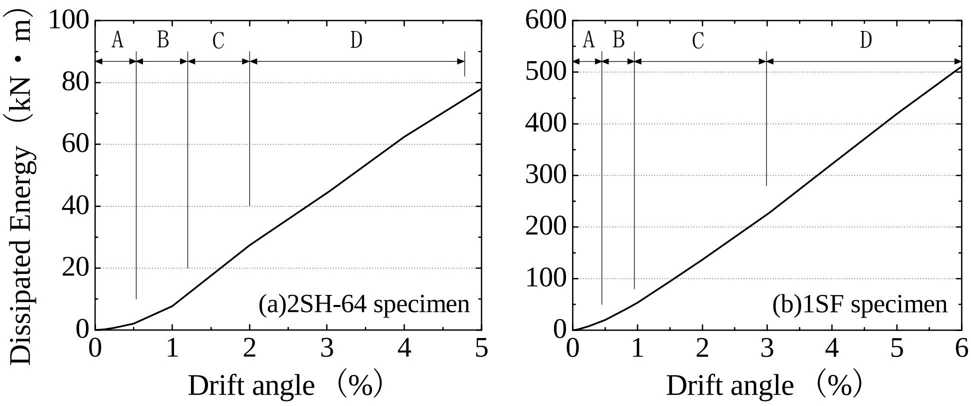

Figure 5: Dissipated energy-drift angle relations of the two specimens

2.3.1 Test results of two specimens

The load-drift angle relations of the two specimens are shown in Figure 4. Since the connection between the spandrel wall and the center column of the 2SH-64 specimen was compromised, the center column is damaged as flexible member. The load of the 1SF specimen was increased after the non-structural wall touched to the columns at 2% drift angle.

The relationships between the dissipated energy, which is calculated from the load-drift angle skeleton curves of specimens, and the drift angle of the two specimens are shown in Figure 5. The dissipated energy of the two specimens is increased gradually at the damage ratings A and B, then the dissipated energy is inversely proportional to the drift angle at the damage ratings C and D.

2.3.2 Relationships between index SI_{margin} and damage ratings

The index SI_{margin} of the two specimens, which is calculated by the detailed calculation method defined as Equation (1), is shown in Figure 6. The residual and initial energy absorption capacity of 2SH-64 specimen is calculated as the total residual and initial energy absorption capacity of structural members such as three columns and two beams. Since there is no load cell for 1SF specimen to measure the load carrying capacity of each member, the residual and initial energy absorption capacity of 1SF specimen are calculated from its load-drift angle skeleton curve. Then, the damage ratings of the two specimens are classified based on Table 2, and illustrated in Figure 6 with the index SI_{margin}.

The boundary values of the index SI_{margin} to define damage rating criteria are calculated for two specimens respectively from Figure 6, and shown in Table 3. As a result, the boundary values of the index SI_{margin} for the two specimens are similar to each other for damage rating classification points, and it can be considered that the damage rating criteria is valid for those two specimens.

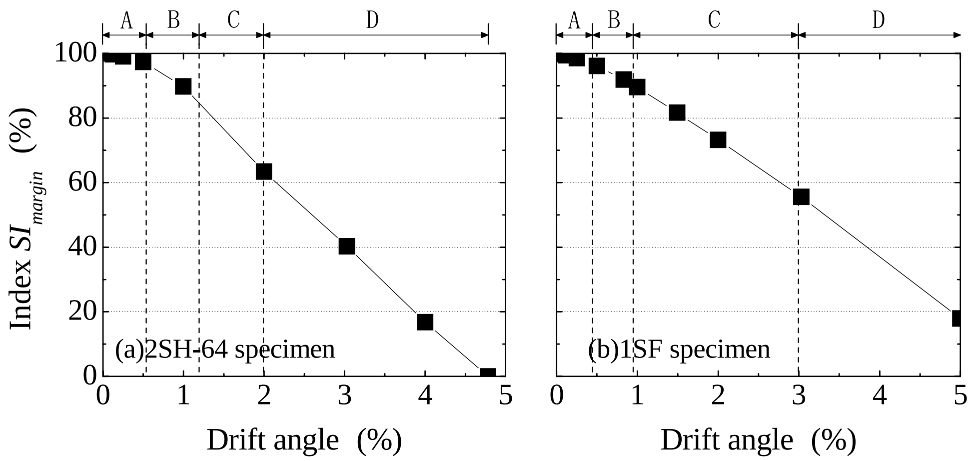

Figure 6: Index SI_{margin} of two specimens based on detailed calculation method

Table 3: Damage rating criteria of two specimens

Specimen	**Boundary Value of index SI_{margin}**		
	A-B	**B-C**	**C-D**
2SH-64 specimen	96%	84%	63%
1SF specimen	96%	90%	55%

3. SIMPLIFIED CALCULATION METHOD OF INDEX SI_{margin}

3.1 Flow of simplified calculation method

It is difficult to calculate the dissipated or absorbable energy of each structural member on-site. Therefore, in this chapter, a simplified calculation method for the index SI_{margin} is proposed considering factor η corresponding to visual damage information such as maximum residual crack width of each structural member. The basic concept of the simplified calculation method is shown in Figure 7.

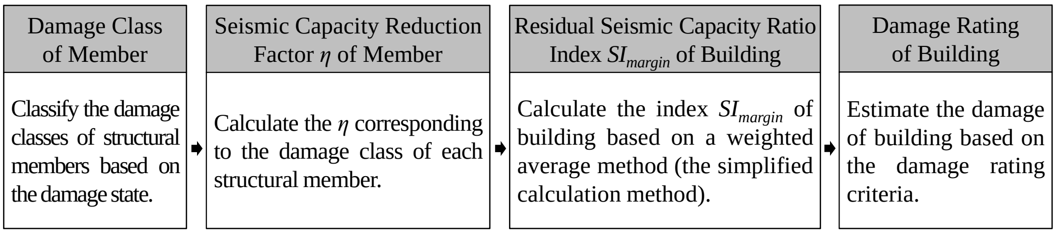

Figure 7: Basic concept of simplified calculation method

3.2 Damage class definition of RC beams

The damage classes of the columns and walls are originally defined based on the mechanical properties, such as yielding of tensile rebars (JBDPA, 2001). In order to classify the damage class easily on-site, the relationships between the damage class and visual damage information, such as maximum residual crack width, are defined as well (JBDPA, 2001).

Since such a damage class is not clearly defined for RC beams, in this paper, their damage classes are first defined by the mechanical properties, such as cracking, yielding of reinforcement and maximum shear strength, as shown in Figure 8. Then, the maximum residual crack widths according to the damage classes are calculated based on Figure 9, which is obtained from the 2SH-64 specimen test results. Considering the crack width of 1mm, which is widely used as boundary of the damage class in previous research, damage class Ⅱ of the RC beams is divided into Ⅱ$^-$ and Ⅱ$^+$, even though it is not governed by mechanical properties. The damage class definition for the RC beams is described in details as shown in Table 4.

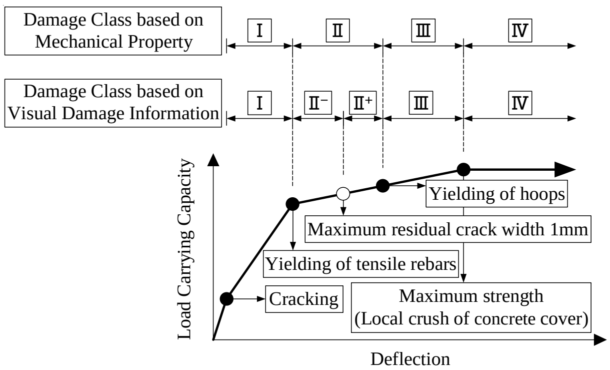

Figure 8: Damage class definition of RC beams based on mechanical property

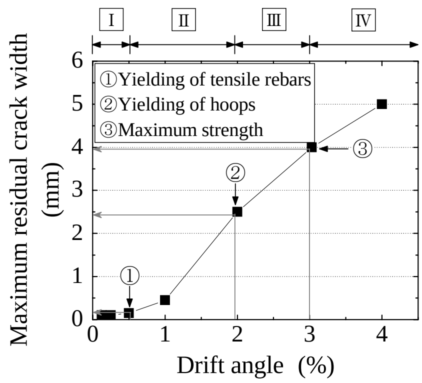

Figure 9: Relations of damage class and maximum residual crack width

Table 4: Damage class definition of RC beams

<table>
<tr><th>Damage class based on mechanical property</th><th>Detail of properties</th><th>Boundary value of w_{max}</th><th>Damage class based on visual damage information</th></tr>
<tr><td>I</td><td rowspan="2">Yielding of tensile rebars</td><td rowspan="2">w_{max}=0.2mm</td><td>I</td></tr>
<tr><td rowspan="4">II</td><td rowspan="2">II^{-}</td></tr>
<tr><td rowspan="2">-</td><td rowspan="2">w_{max}=1.0mm</td></tr>
<tr><td rowspan="2">II^{+}</td></tr>
<tr><td rowspan="2">Yielding of hoops</td><td rowspan="2">w_{max}>2.0mm</td></tr>
<tr><td rowspan="2">III</td><td rowspan="2">III</td></tr>
<tr><td rowspan="2">Maximum strength</td><td rowspan="2">w_{max}>4.0mm Local crush of concrete cover</td></tr>
<tr><td>IV</td><td>IV</td></tr>
</table>

w_{max}: maximum residual crack width

3.3 Seismic capacity reduction factor η of RC beams

The seismic capacity reduction factor η of a RC beam is calculated based on the previous method developed by BUNNO et al. in 2000. The factor η calculated from the load-deflection curve of left beam in 2SH-64 specimen, which is measured from the difference of vertical load between the left and center column, is shown in Figure 10. Also, the lower limit value of the factor η according to each damage class of the RC beams mentioned above is shown in Table 5.

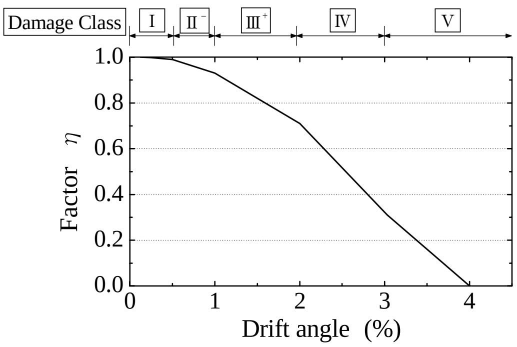

Figure 10: Calculation results of factor η (left beam of 2SH-64 specimen)

Table 5: Relationships between factor η and damage classes

Damage Class	Factor η
I	0.99
II^{-}	0.90
II^{+}	0.70
III	0.30
IV	0

3.4 Energy contribution coefficient α of structural members

The energy contribution coefficient α of a structural member, which means the energy absorption rate of the member for a building, is originally defined as the ratio of its dissipated energy to the dissipated energy of particular member. In this research, the particular member, which is also named critical member, is defined as the member that yields last. Since the dissipated energy of each structural member is difficult to grasp on-site, in this paper, the coefficient α of the member is defined as the ratio of its yield moment to the yield moment of the critical member. If the definition is valid, the coefficient α can be taken as a fixed value.
In order to compare these two methods mentioned above, the coefficient α of the different members is calculated based on the 2SH-64 specimen test results (left

column is taken as a critical member) as shown in Table 6. It can be found that the coefficient α calculated by these two methods is approximately equal to each other. As a result, the calculation method for coefficient α based on the yield moment of members is validated.
Since the center column of 2SH-64 specimen is damaged as flexible member due to the damage of the spandrel wall, the value of its coefficient α is taken as 1.0 in this paper. For the 1SF test specimen in that the beam is the critical member, the coefficient α of each column is taken as 1.39.

Table 6: Coefficient α of members for the 2SH-64 specimen

Member	**Coefficient α**	
	Based on dissipated energy	**Based on yield moment**
Right column	0.97	1.0
Right beam	0.63	0.65
Left beam	0.62	0.65

3.5 Definition of simplified calculation method for index SI_{margin}

According to the above results, the simplified calculation method of index SI_{margin} can be defined as Equation (2).

$$SI_{margin} = \frac{\sum_{k}(\alpha_k)\times\sum_{D=\mathrm{I}}^{\mathrm{V}}(\eta_{k,D}\cdot A_{k,D})}{\sum_{k}\alpha_k\cdot A_k}\times 100\ (\%) \tag{2}$$

where, k: type of the member (such as ductile/brittle column or beam), D: the damage class of member (0 through Ⅴ), α_k: the energy contribution coefficient of k type member, $\eta_{k,D}$: seismic capacity reduction factor of k type member having the damage class D, $A_{k,D}$: the number of k type members having the damage class D, A_k: the number of k type members.

4. COMPARISON BETWEEN DETAILED AND SIMPLIFIED CALCULATION METHOD OF INDEX SI_{margin}

In order to verify the validity of the simplified calculation method for the index SI_{margin}, the detailed and simplified methods are applied to the 2SH-64 specimen and 1SF specimen test results, and calculation results of the index SI_{margin} are compared as shown in Figure 11.
Figure 11(a) shows that the index SI_{margin} of the 2SH-64 specimen based on the detailed and simplified methods is approximately equal to each other. However, the index SI_{margin} of the 1SF specimen calculated by the simplified method as shown in Figure 11(b) is lower than the calculation result based on the detailed method. It can be considered that the simplified calculation method is not suitable for evaluating the effect of non-structural walls to the residual seismic capacity of overall frame. Therefore, it is necessary to propose an upgraded simplified calculation method for the index SI_{margin}, which will also consider the damage of non-structural walls in the further research.

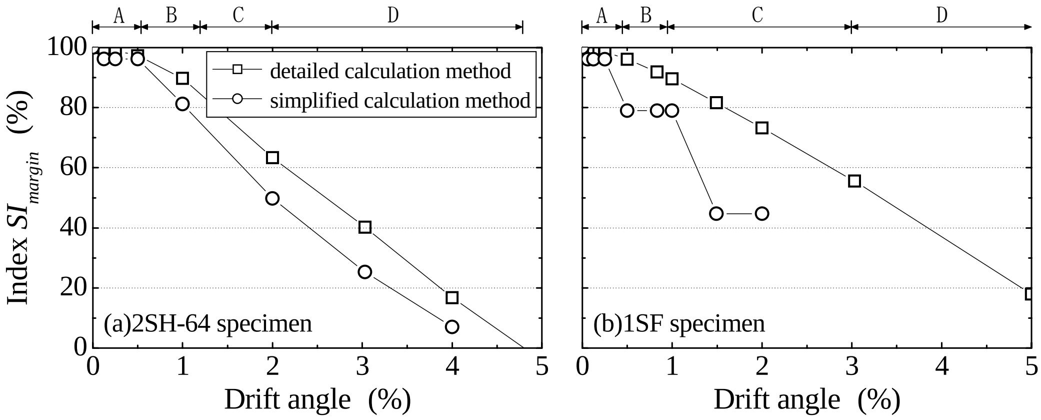

Figure 11: Detailed vs. simplified calculation method for index SI_{margin}

5. CONCLUSIONS

In this paper, a method which can evaluate the residual seismic capacity of weak-beam RC frames damaged by earthquakes is developed. The results can be summarized as follows:

(1) The boundary values of the index SI_{margin} classifying the damage ratings (From A to D) are calculated to define the damage rating criteria.
(2) The damage classes of RC beams are defined based on their mechanical properties. Then, the maximum residual crack width and the seismic capacity reduction factor η corresponding to the damage classes are calculated using the 2SH-64 specimen test results.
(3) The energy contribution coefficient α calculated by the dissipated energy ratio and calculated by yield moment ratio has almost the same value.
(4) The index SI_{margin} of the 2SH-64 specimen is similar when it is calculated based on the detailed and simplified calculation methods. However, the index SI_{margin} of the 1SF specimen is estimated to have smaller value for the simplified calculation method.

REFERENCES

The Japan Building Disaster Prevention Association (JBDPA), 1991 (revised in 2001). Guidelines for Post-earthquake Damage Evaluation and Rehabilitation. (in Japanese)
Architectural Institute of Japan (AIJ), 1980. Reconnaissance Report of the 1978 Miyagiken-Oki Earthquake. (in Japanese)
Institute of Industrial Science of the University of Tokyo and Horie Architecture Engineering Institute (IIS & HAEI), 2011. Test Results Report for Advancement of Seismic Evaluation Method. (in Japanese)
Building Research Institute (BRI), 2011. Proceedings of Development on New Structural Performance Evaluation System for Disaster Resilient Buildings. BRI Proceedings, No.20. (in Japanese)
BUNNO, M., MAEDA, M. and NAGATA M., 2000. A study of the damage level estimation of RC buildings based on residual seismic capacity of members. Proceedings of the Japan Concrete Institute, Vol.22, No.3, PP.1447-1452. (in Japanese)

Low temperature behavior and modeling of high damping rubber bearings

Tomoya MATSUMOTO[1], Yoshiaki OKUI[1], Dung Anh NGUYEN[1], Md. Shafquat HASAN[1], Kaho TAKAHASHI[2], Hiroshi MITAMURA[3], Takashi IMAI[4]
Department of Civil and Environmental Engineering, Saitama University, Japan
s13me127@mail.saitama-u.ac.jp
[2] Omiya branch office, East Japan Railway Company, Japan
[3] Civil Engineering Research Institute for Cold Region Sapporo, Japan
[4] Rubber Bearing Association, Japan

ABSTRACT

In Japan, high damping rubber bearings have been widely used as isolated devices since the Kobe Earthquake in 1995. The rubber bearings have various characteristics, such as temperature dependence, self-heating effect and, so on. Besides, in current Japanese Specifications of Highway Bridges, temperature effect on behavior of rubber bearings is not considered. In this paper, temperature increases in high damping rubber bearings under cyclic loading and their effects on seismic performance of a viaduct at low ambient temperatures are investigated. Experimental results of cyclic loading show that the temperature inside rubber bearings increase by approximately 27°C. Moreover the equivalent stiffness and the equivalent damping constant of rubber bearings are changing with increasing inside temperature. The equivalent stiffness at an ambient temperature of -20°C reported by Rubber Bearing Association in Japan is 2.19MPa. However, it is found that the equivalent stiffness at an inside temperature of -20°C is 3.76MPa. In this paper, nonlinear seismic response analysis with the bilinear model for low temperature is carried out.

Keywords: *high damping rubber bearings, temperature dependence, self-heating effect, seismic response, bilinear model.*

1. INTRODUCTION

1.1 Background

In recent years base isolation has become an increasingly applied to structural design technique for buildings and bridges in highly seismic areas. Various tapes types of base-isolation devices have been developed. Above all, high damping rubber bearings (HDRB) are widely applied to bridges. However, it is known that HDRBs have various characteristics, such as temperature dependence, self-heating effect and, so on. These characteristics may have adverse effects on the seismic performance of bridges with HDRBs, especially, in cold districts. The temperature effects on behavior of rubber bearings are not considered in seismic design based on current Japanese Specifications of Highway Bridges.

In this paper, the mechanical behavior of HDRB at low ambient temperatures are investigated with considering self-heating. Furthermore, the low temperature effect on the seismic performance of a viaduct is examined through nonlinear seismic response analysis.

2. Experiments under low temperature

2.1 Specimen and loading condition

In order to investigate the mechanical behavior of HDRB under low temperatures, cyclic loading tests at ambient temperatures of 23°C, -20°C, and -30°C were conducted, in which sinusoidal loading with a shear strain amplitude of 1.75 and 0.5Hz frequency was applied. The geometry and material properties of the specimens are given in Table 1 and illustrated in Fig. 1. The temperatures inside specimens were measured with thermocouples at the points shown in Fig. 2. The specimens were tested under shear deformation with an average constant vertical compressive stress of 6MPa.

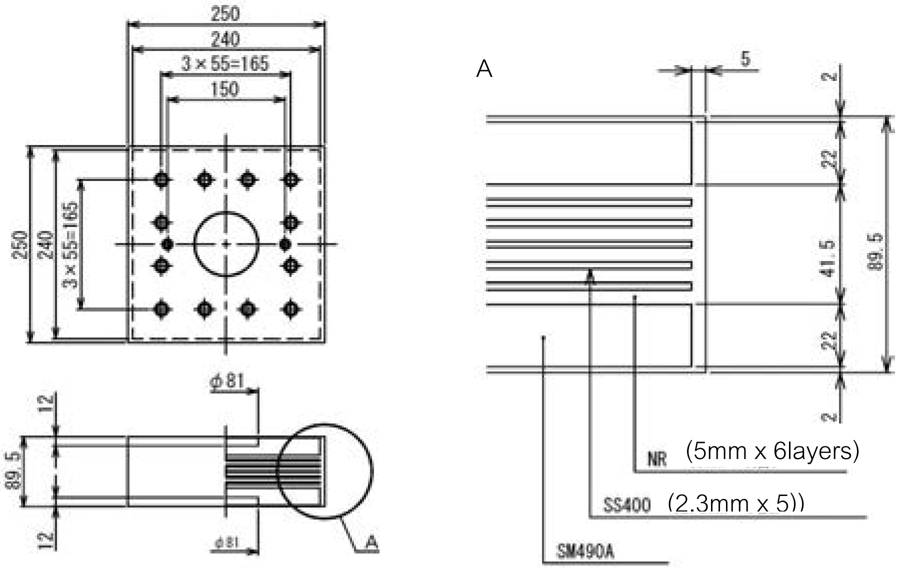

Figure 1: Dimensions of specimen [mm]

Table 1: Dimensions and material property of HDRB specimen

Particulars	Specifications
Cross-section [mm^2]	240×240
Number of rubber layers	6
Thickness of one rubber layer [mm]	5
Thickness of steel layer [mm]	2.3
Nominal shear Modulus [MPa]	1.2

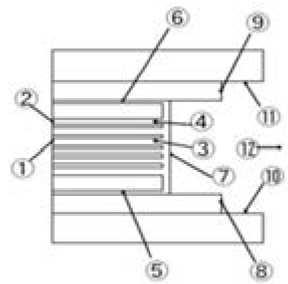

Figure 2: Measurements points of inside temperatures (Civil Engineering Research Institute for Cold Region, et al. 2009)

2.2 Experimental results and discussion

Figure 3 (a)-(c) illustrates the shear stress-strain relationships obtained from the sinusoidal loading tests at different ambient temperatures, and the corresponding temperature history inside the specimens are shown in Fig. 4 (a)-(c). The shear stress at low temperatures is larger than that at room temperature. The inside temperature rise at lower temperatures is larger than that at room temperature. Fig. 5 shows the stress-strain relationships obtained from a loading cycle at the same inside temperatures and different ambient temperatures. Although the stress-strain relationship in the first cycle of Fig. 5(a) is affected by the initial condition, HDRBs with the same inside temperature exhibit the identical stress-strain curve.

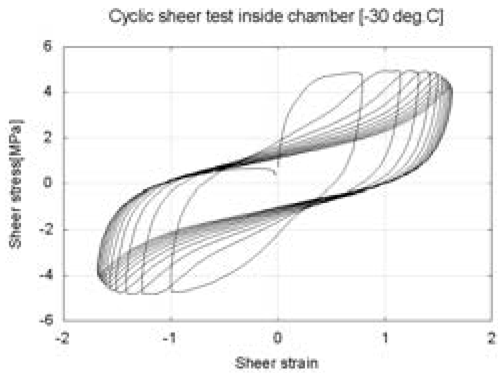

(a): -30°C ambient temperature

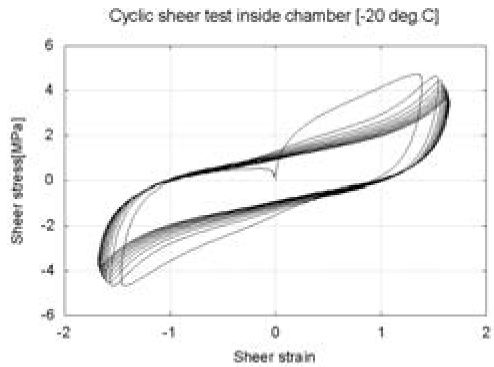

(b): -20°C ambient temperature

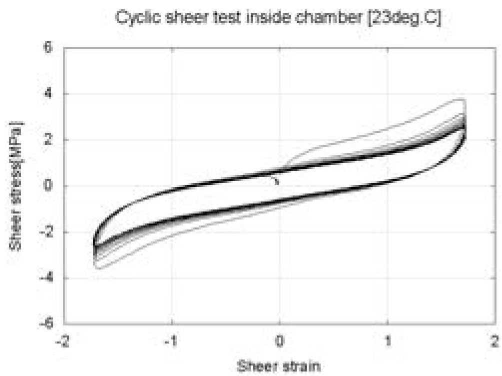

(c): 23°C ambient temperature

Figure 3: Stress-strain relationship

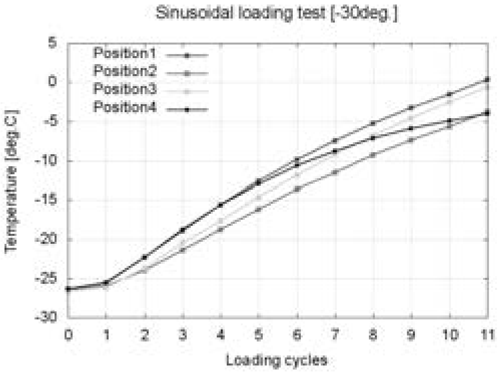

(a): Temperature history at -30°C ambient temperature

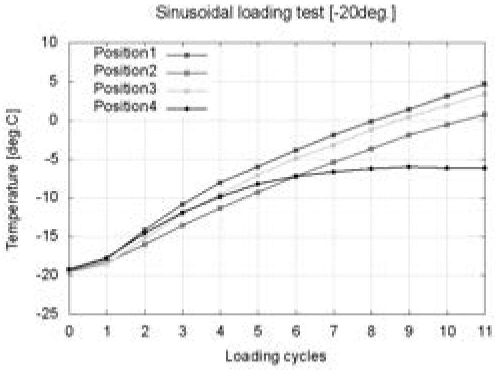

(b): Temperature history at -20°C ambient temperature

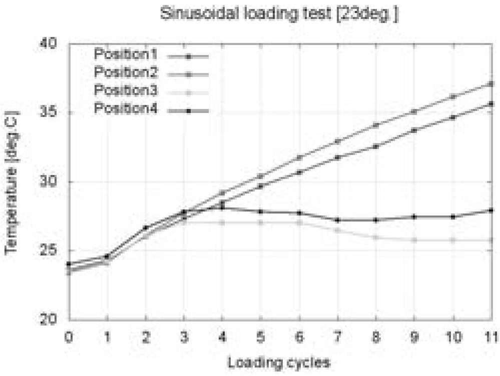

(c): Temperature history at 23°C ambient temperature

Figure 4: Inside temperature history

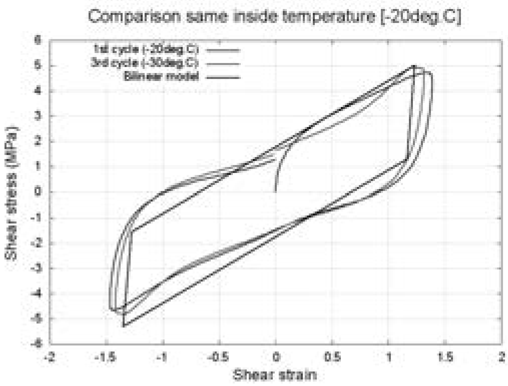

(a) -20°C inside temperature

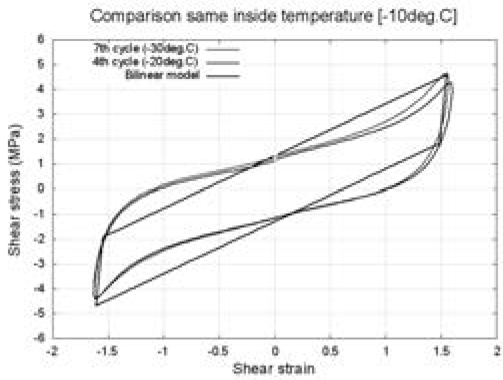

(b) -10°C inside temperature

Figure 5: Stress-strain relationship at the same inside temperatures and different ambient temperatures

In addition to the experimental results, the bilinear models for seismic design analysis are also plotted in Fig. 5. These bilinear models (Takahashi, 2009) are used in the subsequent nonlinear seismic response analysis of a viaduct.

3. Nonlinear seismic response analysis of a viaduct

3.1 Model viaduct and earthquake wave

Fig. 6 shows dimensions of a physical model of a viaduct. The model viaduct is a five-span continuous steel-concrete composite girder bridge isolated with HDRBs. The dimensions of this model bridge including HDRBs are determined by designing in accordance with Japanese Specifications of Highway Bridges (JSHB) (JRA, 2013) under the room temperature condition. Fig. 7 shows the analytical model of bridge system. The dimensions and material properties are shown in Table 2.

The superstructure is modeled with elastic beam elements. The concrete piers are modeled with elastic beam elements with a plastic hinge. Takaeda tri-linear model is used to express the nonlinear hysteresis behavior of the plastic hinge in each pier. The ground acceleration history used in the analysis is presented in Fig. 8, which is specified in JSHB for level-2 type-1 (1-1-2) earthquake.

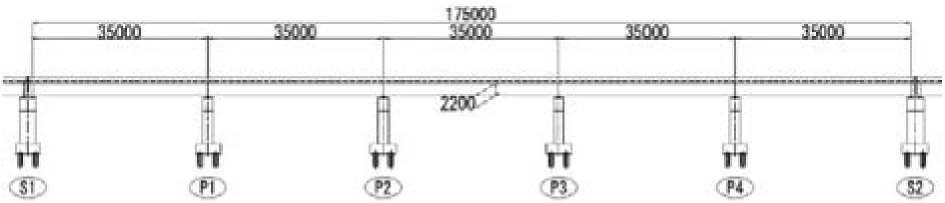

(a) Side view

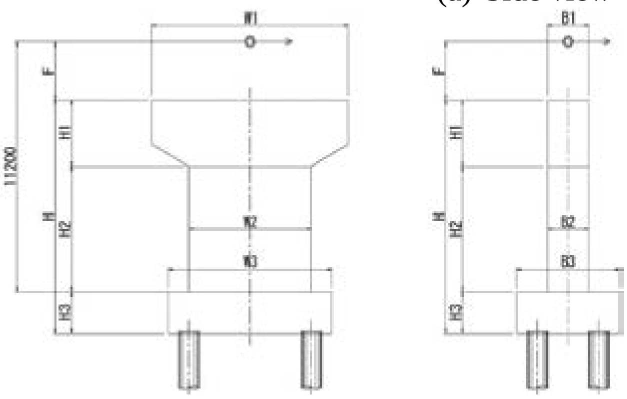

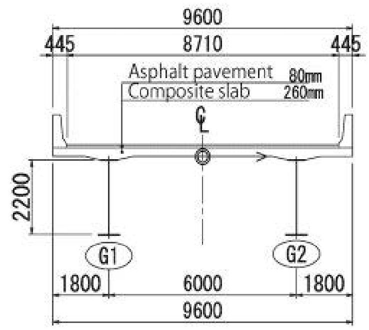

(c) Concrete brigdepier

(b) Cross section of superstructure

Figure 6: Model bridge for seismic analysis (Razzaq et al., 2012)

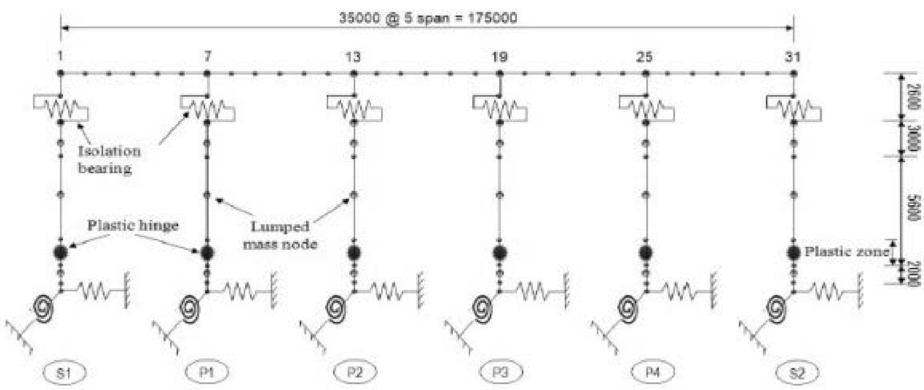

Figure 7: Analytical model of bridge (Razzaq et al., 2012)

Table 2: Geometric and material properties of the pier

Properties	Specifications	
	Pier S1 & S2	Pier P1 to P4
Cross-section of the pier cap [mm^2] B1 x W1	3300×9600	2000×9600
Cross-section of the pier body [mm^2] B2 x W2	3300×6000	2000×6000
Cross-section of the footing [mm^2] B3 x W3	5000×8000	5000×8000
Number of piles/pier	4	
Young's Modulus of concrete [MPa]	25000	
Young's Modulus of steel [MPa]	200000	

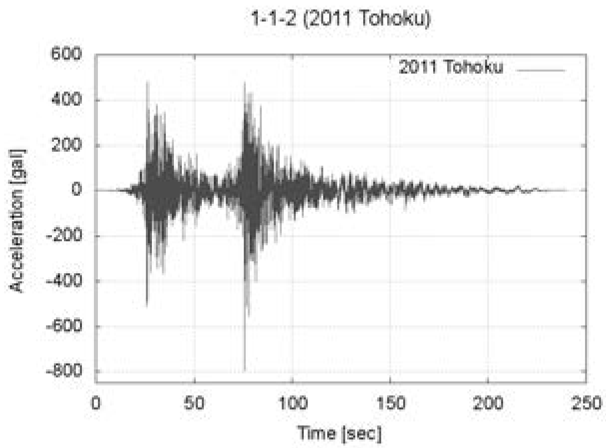

Figure 8: Typical ground acceleration history used in seismic response analysis

3.2 Analytical results

Fig. 9 shows the analytical results at -20°C as an example. Fig. 9(a) shows the stress-strain response of a HDRB, and Fig. 9(b) does the moment-rotation response of the plastic hinge of a pier.

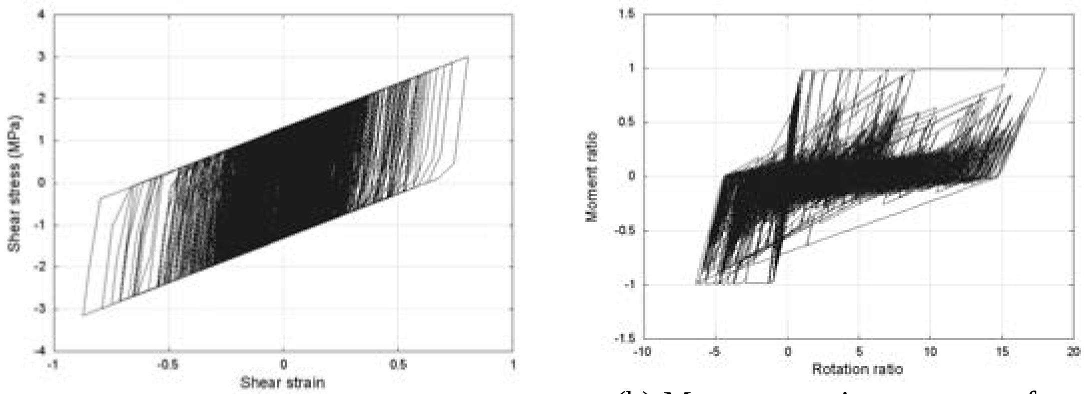

(a) Shear stress-strain response of HDRB

(b) Moment-rotation response of plastic hinge of pier

Figure 9: Seismic response of the Tohoku earthquake (1-1-2) (-20°C)

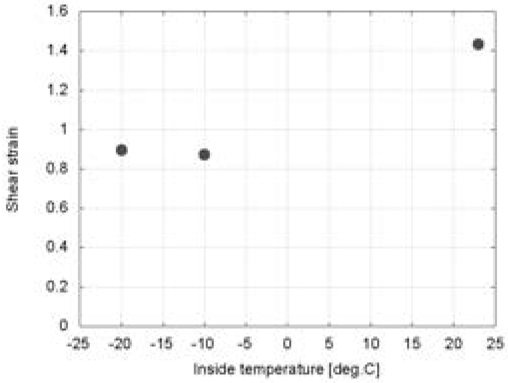

(a) Maximum shear strain

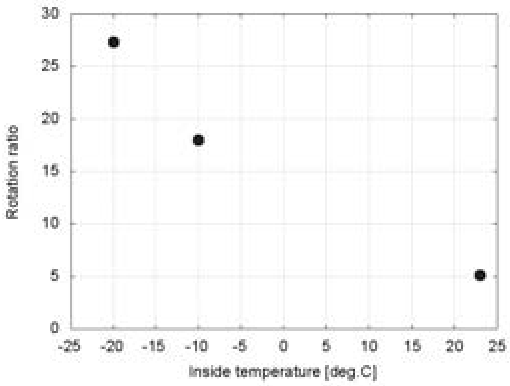

(b) Maximum rotation ratio

Figure 10: Comparison of maximum shear strain and rotation ratio among different inside temperatures

4. Summary

The experimental results of sinusoidal loading tests after several loading cycles are often used to identify a seismic design model of high damping rubber bearings, such as the bilinear model. The present cyclic loading test results of high damping rubber bearings at low ambient temperatures shows that the temperature rises inside the bearings due to cyclic loading attain to 27°C after 11 loading cycles at -30°C ambient temperature. The temperature rises inside the rubber bearings affect mechanical properties such as stiffness and equivalent damping, especially at low temperatures. The present results suggest that a design model of high damping bearings ignoring the self-heating may provide false seismic response, since the temperature rises under a seismic wave are considered to be not so large as those in a cyclic loading test. Finally, the nonlinear seismic response analysis of a viaduct based on the inside temperatures shows the maximum response of concrete piers at -10°C becomes 5 times larger than those at 23°C, which demonstrates the importance of considering temperature dependency of high damping rubber bearings at low temperatures.

REFERENCES

Japan Road Assocication, 2012. Specifications for Highway Bridges, Part V: Seismic Design. Maruzen, Tokyo.

Incorporated Administrative Agency Pubic Works Research Institute Civil Engineering Research Institute for Cold Region, Hokubu consultant Co. LTD, 2009. Report on seismic performance of bridges in cold district.

Razzaq, M. K., 2009. Seismic Response Prediction of Base Isolated Multi-Span Highway Bridge with Different Modeling Techniques for for Lead Rubber Bearings, *Satiama University Master thesis.*

Takahashi, K., 2012. Modeling of high damping rubber bearings at low temperatures, *Satiama University Graduation thesis.*

Razzaq, M. K., Okui, Y., Bhuiyan, A. R., Amin, A. F. M. S., Mitamura, H. Imai, T., 2012. Application of Rheology Modeling to Natural Rubber and Lead Rubber Bearings: A Simplified Model and Low Temperature Behavior, *Journal of Japan Society of Civil Engineerings*, Ser A1 (Structural Engineering and Earthquake Engineering (SE/EE)) Vol.68 No.3, 526-541.

The structural performance of traditional frames with through columns about townhouses in Japan

Hiromi SATO[1], Mikio KOSHIHARA[2] and Tatsuya MIYAKE[3]
[1] Research Associate, IIS, The University of Tokyo, Japan
Sato310@iis.u-tokyo.ac.jp
[2] Professor, IIS, The University of Tokyo, Japan
[3] President, Nihon System Sekkei Architects & Engineers Co., Japan

ABSTRACT

This paper presents a study of the structural performance of traditional timber townhouses in a historic town in Japan. The aim of this study was to clarify the structural performance of traditional timber frame with through columns in townhouses. The target area has many traditional timber townhouses built in from the late of 18th century to the early 20th century and these townhouses have few structural walls. In this study, static tests and seismic analysis of the frame with through columns were performed. As the results, it was clarified that the structural performance of the frame with through columns and the structural evaluation of the townhouses in this area was improved.

Keywords: *Traditional timber construction, Static lateral loading test, Static Analysis, Parametric study*

1. INTRODUCTION

Japan has a long history of earthquakes and timber structures in Japan have suffered great damage caused by strong earthquakes. Old traditional timber structures suffered especially heavy damage. Besides, many of historical towns in japan have many traditional timber buildings that construction method is same in each area. These traditional buildings often have insufficient earthquake-proof performance. However, if the structural evaluation is suitable for the characteristics of their construction, the technique of earthquake-proofing suitable for those buildings can be examined. Therefor it is important to clarify a suitable evaluation method in each historical area.

2. RESEARCH AREA

2.1 Sawara district

The research area of the present study is the Sawara district of Chiba Prefecture, which is located near Tokyo. The Sawara district is a historical town arranged on the riverside and contains traditional timber townhouse and storehouse with thick walls (Figure 1). They are built in from the late of 18th century to the early 20th century (The Sawara City, 2004). In townhouses in this area, the frontage direction of the first floor has few walls and the frames which consist of through columns.

Figure 1: View of the Sawara district

2.2 Previous earthquake disaster

On 11 March, 2011, timber structures suffered a great deal of damage due to the 2011 off the Pacific coast of Tohoku Earthquake. This earthquake destroyed or severely damaged 289 houses in the Katori city including the Sawara district. In the Sawara district, many falls of roofing tiles, collapse of mud walls, and foundation damage were observed.

2.3 Timber frame of through column

In the Sawara district, though the townhouses have few structural walls, they were constructed of many timber though columns. The column section of many of the through columns was larger than the jointed columns. The though columns have the horizontal load resistance from bending back of column (Figure 2) (Architectural Institute of Japan, 2013).

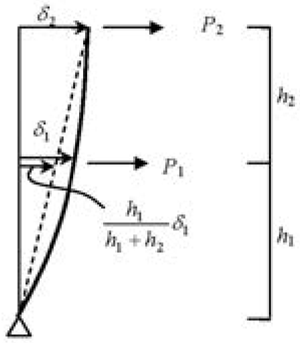

h_1 : height of the 1st floor
h_2 : height of the 2nd floor
δ_1 : displacement of the 1st floor
δ_2 : displacement of the 2nd floor
P_1 : load of the 1st floor
P_2 : load of the 2nd floor

Figure 2: Mechanism of bending back of though column

3. STATIC LATERAL LOADING TEST

3.1 Measurement plan

The static lateral loading test was performed (Figure 3) (H. Sato et al, 2010, 2012). The forces were applied by connecting the loading apparatus directly to the beam at the second floor level. The displacement and the strain of the columns were measured using 45 displacement transducers and strain gauges.

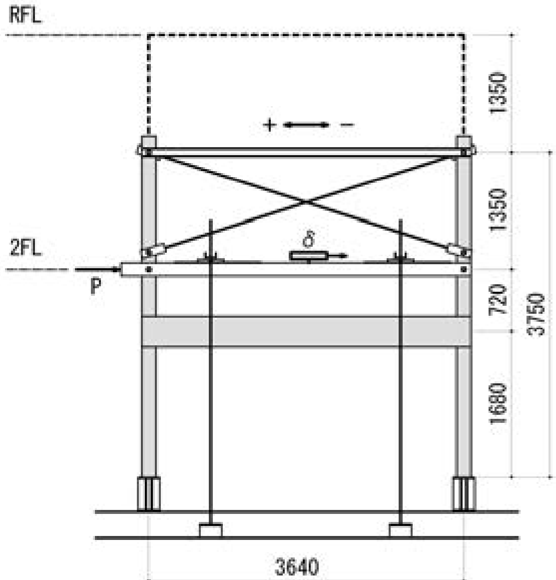

Figure 3: Loading apparatus (section)

3.2 Specimens

The static test was performed on specimens of three types in the through column (Table 1). The A series was improvement column section larger. The B series has original column section of existing townhouse in the Sawara district. The column of the C series change wood species to be stronger.

Table 1: Type of specimens

	A series	B series	C series
Column section	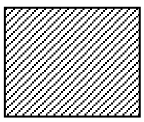	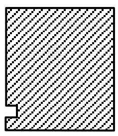	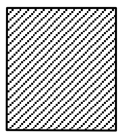
Wide*depth (mm)	180 * 150	150 * 165	150 *165
Young's modulus	1005 kN/cm^2	822 kN/cm^2	1162 kN/cm^2
Wood species	Japanese ceder	Japanese ceder	Zelkova
Explanation	Improvement column section for new build	Original column section of existing house	Change wood species (for new build)

3.3 Results of static test

3.3.1 Load-Displacement relationship

As a result, the maximum strength, stiffness and failure mode was observed (Table 2). The average of the maximum load ranged from 17.8 to 32.0 kN. The average of the secant stiffness at 1/30 rad ranged from 294.6 to 488.7 kN/rad. The strength and stiffness of the B series were smaller than other two. The strength of the C series has higher than others. About the stiffness, the A series was approximately equal the C series.

Table 2: The strength and the stiffness

		Maximum load (kN)		Stiffness (kN/rad.)	
			average		average
A	1	27.9	25.7	588.5	488.7
	2	22.1		456.4	
	3	27.2		421.0	
B	1	16.2	17.8	295.2	294.6
	2	17.9		272.5	
	3	19.4		316.0	
C	1	38.9	32.0	538.2	484.5
	2	28.0		453.2	
	3	29.2		462.1	

*stiffness is the secant stiffness at 1/30 rad.

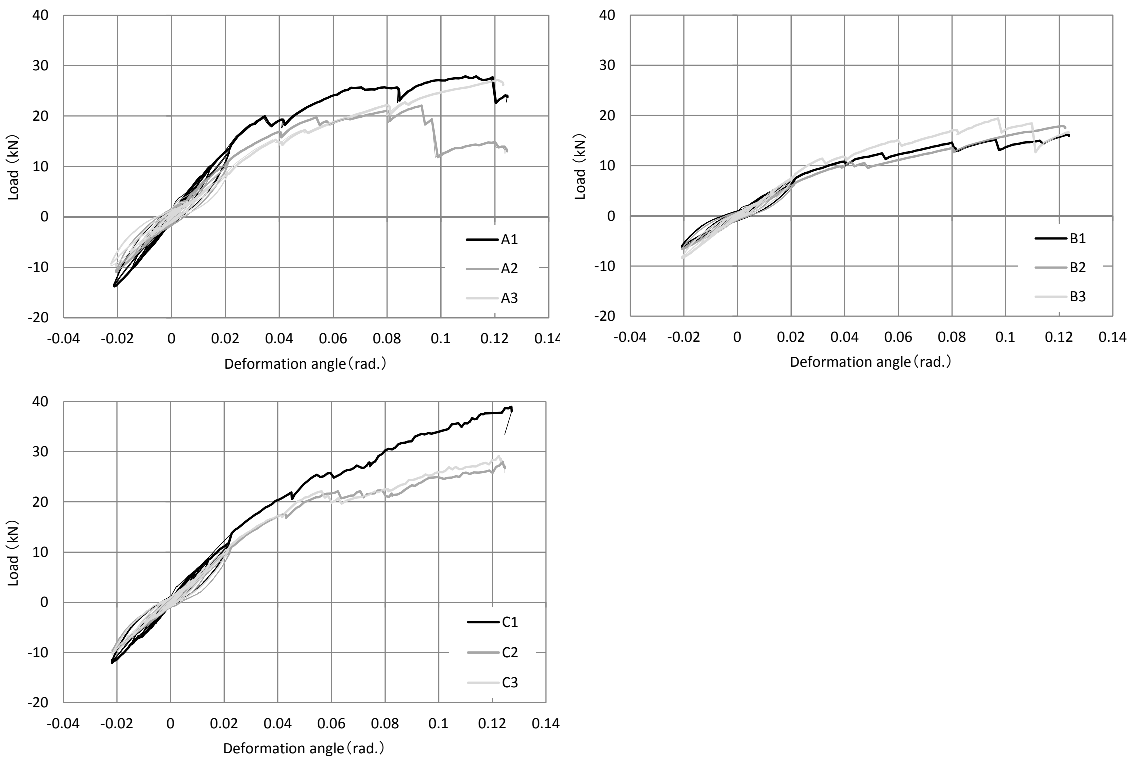

Figure 4: Load-Displacement relationship

3.3.2 Failure mode

In the all series, the displacement at first floor was ahead of the displacement at second floor (Table 5). Besides, the failure mode was different from each series (Table 3). The failure mode of the A and B series was often collapse of the through column. By contrast, the failure mode of the C series was collapse of the tenon joint; that was not brittle fracture.

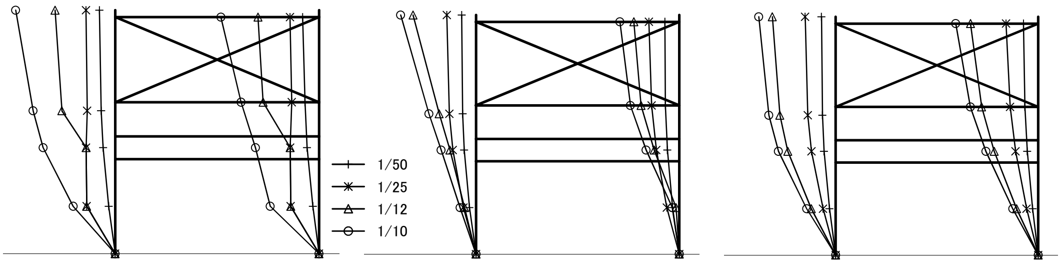

A series (A1) B series (B2) C series (C1)

Figure 5: Mode of deformation

Table 3 Failure mode

		Failure mode
A	1	Collapse of the column at the sashikamoi joint
	2	Collapse of the column at the 2nd floor level
	3	Collapse of top and bottom of the column
B	1	Collapse of the tenon joint
	2	Collapse of top of the column
	3	Collapse of the column at the sashikamoi joint
C	1	Collapse of the tenon joint
	2	Collapse of the tenon joint
	3	Collapse of the tenon joint

3.3.3 Wall ratio

The results of the static test were evaluated to effective wall quantity as other structural walls (Table 4) (The Japan Building Disaster Prevention, 2004). The wall ratio means the bearing strength per 1 meter and the wall quantity means the bearing strength per 1 frame in this study. The wall ratio of the frame with the timber through columns equals to approximately half the value of timber brace.

Table 4: Effective wall ratio

	A series	B series	C series
Wall ratio*	0.47	0.35	0.48
Wall quantity*	1.70	1.29	1.76

* Average of 3 specimens and consideration in unevenness

4. STATIC ANALYSIS

4.1 Model of analysis

The standard model of the analysis was based on the static test (Figure 6). The model consists of two through columns and beam. The horizontal load resistance elements were steel brace at the second floor as overall wall. The force carrying at second floor level was repeated as the static test. In this analysis, the parameters are the wall length (column span) and the opening pattern.

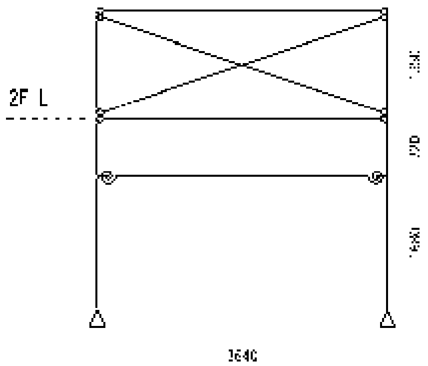

Figure 6: Analysis model (the standard model)

4.2 Results of analysis

The analyses were performed on the 9 models. The strength ratio was calculated based on the maximum strength of analysis (Table 5). As the wall length became to 1/2 or 1/4 times, the strength ratio became less than 1/2 or 1/4 times. The layout of the openings was not so effective on the strength of the frame.

Table 5: The results of the analysis (the ratio of the strength) [*1]

Second floor \ Length[*2]		1P	2P	4P
Brace[*3]		0.22	0.36	1.00
Opening[*4]				
1/2 length, in the center		-	-	0.27
1/2 length, in the end		-	0.23	0.37
Full Opening		0.09	0.07	0.48

[*1] the ratio is the each strength into the strength of the standard model
[*2] length is 910 mm per 1P
[*3] brace is the steal brace of the static test
[*4] the wall type is the same as the standard model

5. CONCLUSION

In this study, static test and analysis were performed on the traditional timber frame with through columns.

1) In the Sawara district, the traditional townhouse has few structural walls, therefore the frame of through columns is important as structural element.
2) As a result of the static test, the maximum load ranged from 17.8 to 32.0 kN. The secant stiffness at 1/30 rad ranged from 294.6 to 488.7 kN/rad. The failure modes were collapse of through column or tenon joint. The structural performance of the C series (Zelkova column) was higher than others.
3) As a result of the analysis, the wall length is very effective on the frame strength in this study. The difference of opening layout or column span were not became difference of the strength of the frame.

ACKNARIGEMENT

The authors express their appreciation to the members of the studies group of townhouse of the Sawara district, without whose help these experiment would not have succeeded.

REFERENCES

The Sawara City, 2004, Townscape of the Sawara district

Architectural Institute of Japan, 2013, Recommendation for structural calculation of traditional wood buildings by calculation of response and limit strength

The Japan Building Disaster Prevention Association, 2004, Seismic diagnosis and reinforcement of timber house

H. Sato and M. Koshihara, 2010, Horizontal load capacity of sashikamoi frame with through column, *Summaries of Technical Papers of Annual Meeting Architectural Institute of Japan*, C-1, 569-570

H. Sato, M. Koshihara and T. Miyake,2012, Horizontal load capacity of sashikamoi frame with through column Part 2 Effects of seismic performance of second floor on through column, *Summaries of Technical Papers of Annual Meeting Architectural Institute of Japan*, C-1, 461-462

Modeling and earthquake response analysis of traditional timber frames including Kumimono

Iuko TSUWA[1] and Mikio KOSHIHARA[2]
[1]Gradutate Student, Graduate School of Engineering,
the University of Tokyo, Japan
tsuwa@iis.u-tokyo.ac.jp
[2]Professor, Institute of Industrial Science,
the University of Tokyo, Japan

ABSTRACT

In building or renovating traditional timber structures such as temples and shrines in Japan, earthquake resistant design has been needed. However most of traditional timber structures are built based on the knowledge and experience of carpenters. The evaluation of seismic capacity for traditional timber structures from the view point of modern engineering is indispensable. The purpose of this paper is to quantitatively evaluate the seismic performance of traditional timber frames including Kumimono. In this paper, we constructed the spring model of seismic elements in three kinds of traditional timber frames including Kumimono based on shaking table test results. In addition, we conducted the earthquake response analysis with the models. The vibration characteristics of each frame are quantitatively compared based on both experimental and analytical results. The way of modeling of such traditional timber frames are discussed.

Keywords: *traditional timber structure, Kumimono, shaking table test, earthquake response analysis,*

1. INTRODUCTION

Earthquake resistant designed buildings are needed in building or renovating traditional timber structures such as temples and shrines in Japan. Therefore the quantitative evaluation of their structural behaviors from the view point of engineering is indispensable. When we build temples and shrines, column, mud wall, *Nuki* which is a tie beam extending from one pillar to another, and bracket complexes called *Kumimono* in Japanese which is a structural component between a column and roof, etc, are considered as structural elements. Each element has been researched and modeled experimentally and analytically. However it is not clear how each element contributes to the whole structural behavior. In this research, we performed shaking table tests with three kinds of traditional timber frames. They have different wall stiffness. Specimen 1 had no wall. Specimen 2 had mud wall which is the smallest stiffness in such traditional timber frame. In this time, we conducted shaking table tests about Specimen 3 including plywood wall as a wall with higher stiffness than Specimen 2. The aim of this research is to clarify the vibration characteristics of each element in a frame and the evaluation method of traditional timber frame including *Kumimono*. Based on the experimental results, we modeled each specimen with elastoplastic springs and performed the earthquake response analysis. The analysis results were compared with experimental ones.

2. EXPERIMENT

We performed shaking table tests two kinds of frame as presented at USMCA 2009 (Tsuwa et al, 2009). One frame, Specimen 1, was composed with column, *Nuki* and *Kumimono*. The other one, Specimen 2, was a frame added mud wall on Specimen 1. The details were shown in the paper in 2009. We conducted another shaking table test about Specimen 3 with a higher stiffness wall on Specimen 1. We explain the experimental outline and the results of Specimen 3 comparing with the results about Specimen 1 and 2.

2.1 Experimental method

The experimental method was shown in the Figure 2. The method was same as Specimen 1 and 2. The timber frame was a frame used in the tests of Specimen 1 and 2 because the frame was not destroyed. However we replaced dowels at column base with new ones because the dowels made shear deformation. In Specimen 3, we used plywood wall as a wall with higher stiffness than mud wall. We put the plywood walls between columns.

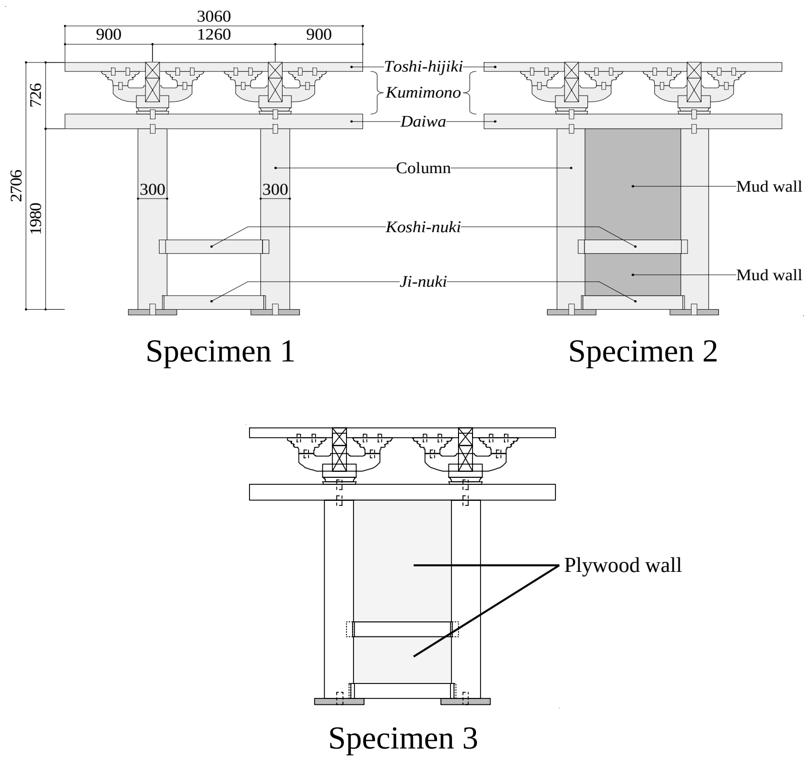

Figure 1: Specimens

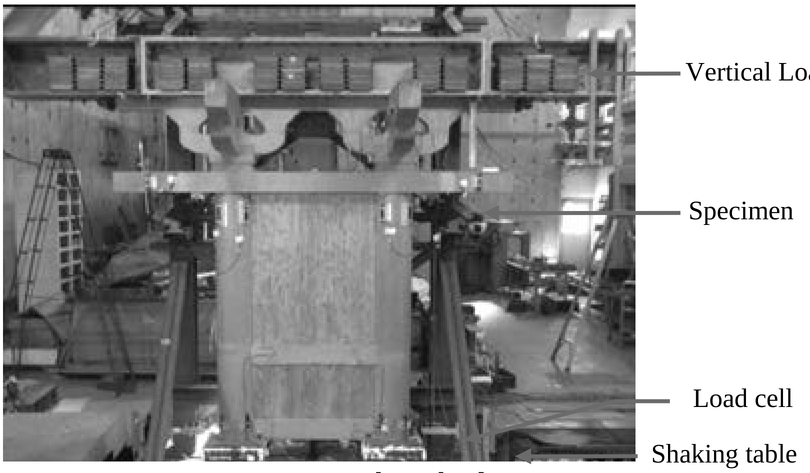

Figure 2: Experimental method

2.2 Experimental results

Figure 3 shows the relationship between shear force and horizontal displacement gotten by inputting BCJ-L2 100% of Specimen 3. Figure 4 shows the results from Specimen 1 and 2. In the result of Specimen 3, the load was decreased sharply after the maximum load. The behavior of the specimen was locking in BCJ-L2 100% test. Therefore the shear force of whole frame was decreased when a column base was going up.

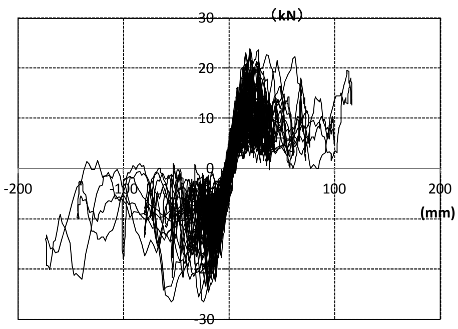

Figure 3: The relationship between load and displacement

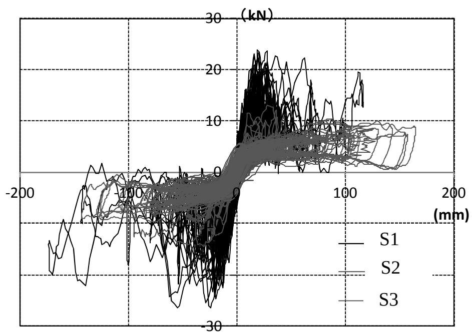

Figure 4: The relationship between load and displacement of bracket complexes

3. EARTHQUAKE RESPONSE ANALYSIS

3.1 Modeling of restoring-force characteristics

We conducted earthquake response analysis with the elastoplastic frame model. We considered springs as shown in Figure 5. The restoring-force characteristics of each structural element were modeled as follows.

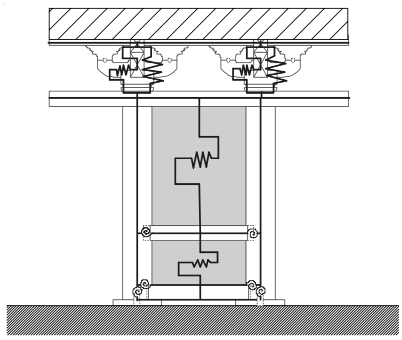

Figure 6: Analysis model

Column:

The restoring force characteristic of columns wss calculated with an equation provided by previous experiments and researches of Ban, 1942 and Kawai, 1992. The characteristic is shown in Figure 7. The hysteresis model was nonlinear elasticity.

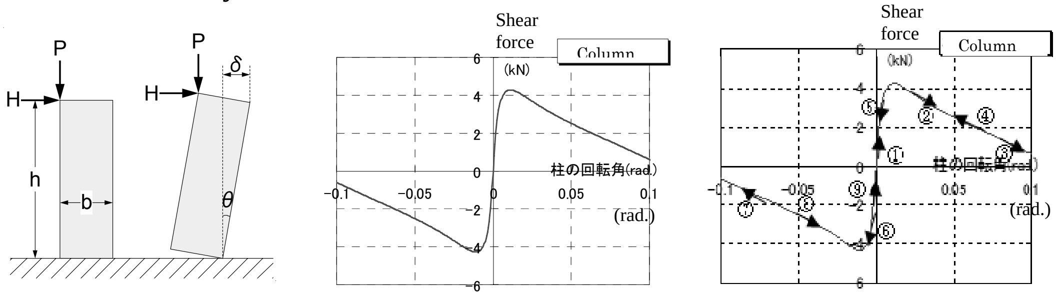

(a)Skelton curve *(b) Hysteresis model*

Figure 7: The restoring force characteristics of Column

The joints of a column and *Kosihnuki*:

The relationship of bending moment of column-*Koshinuki* joint was gotten from experiments in each specimen. On the base of experimental results, the skeleton curve of the restoring force characteristic was determined. The characteristic is shown in Figure 8. The skeleton curve was different with each specimen. We used a same frame in all tests. Therefore the compressive strains inclined to the grain occured repeatedly at column-*Koshinuki* joints. The resistance force of column-*Koshinuki* joint was decreased every specimen.

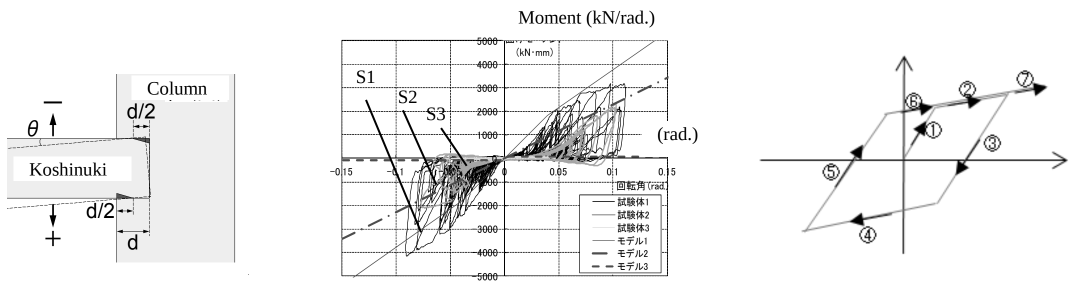

(a)Skelton curve *(b) Hysteresis model*

Figure 8: The restoring force characteristics of Koshi-nuki

The joints of columns and *Jinuki*:

The bending moment of column-*Jinuki* joint was defined by *Merikomi theory (*Inayama*, 1992),* because we did not get the experimental results like *Koshinuki*. The hysteresis model was same as *Koshinuki*.

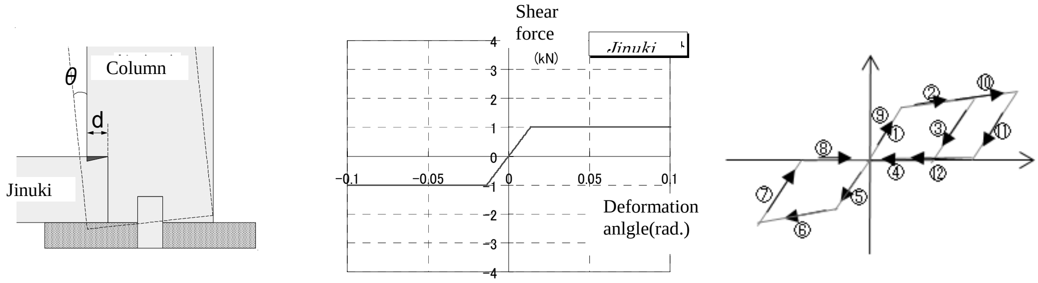

(a)Skelton curve *(b) Hysteresis model*

Figure 9: The restoring force characteristics of Jinuki

Kumimono:

Each relationship between load and displacement of *Kumimono* in all specimens was gotten as shown in Figure 10. The skeleton curve for analysis was defined such as red line. The hysteresis curve was bilinear model. The yield displacement was 2.6 mm. The yield load was 46.5 kN. The second stiffness was 0.4 times as high as the first one.

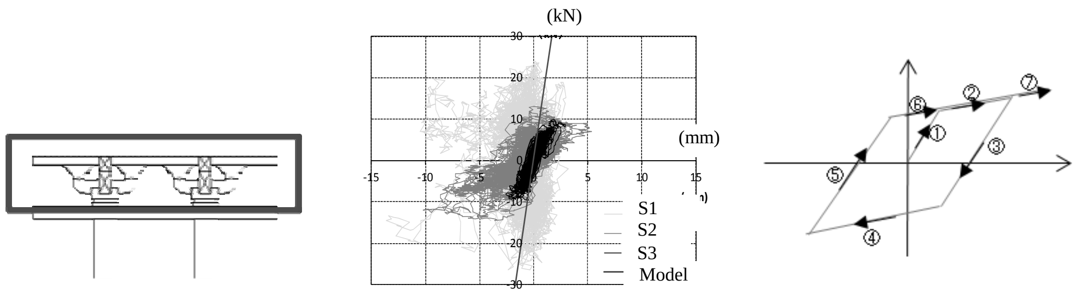

(a)Skelton curve *(b) Hysteresis model*

Figure 10: The restoring force characteristics of Kumimono

Mud wall:

The mud wall was destroyed during the test of BCJ-L2 100% in Specimen 2. Therefore the shear force of the whole specimen was decreased as shown in Figure 11. We defined the skeleton curve of mud wall from the experimental result. About each wall upper and lower *Koshinuki*, we defined each skeleton curve as shown in Figure 11.The shear force of the lower wall was zero at the deformation angle 0.03 rad. Both curves were bi-linear slip.

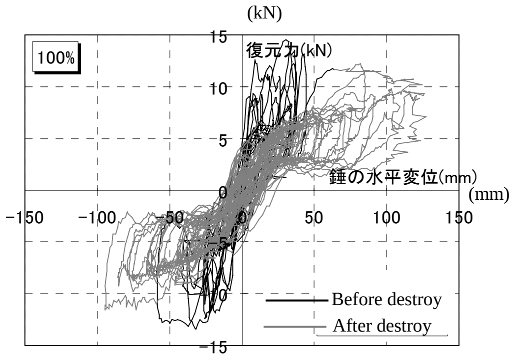

Figure 11: The restoring force characteristics of Mudwall

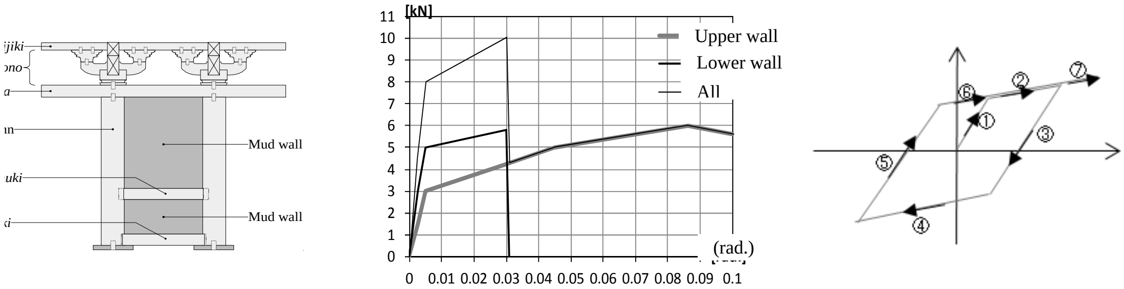

(a)Skelton curve *(b) Hysteresis model*

Figure 12: The restoring force characteristics of Kumimono

Plywood wall:

The restoring force characteristic of plywood wall was defined from the shear force of surface bars and nails as shown in Murakami et al, 2006. The skeleton curve was as shown in Figure 13.

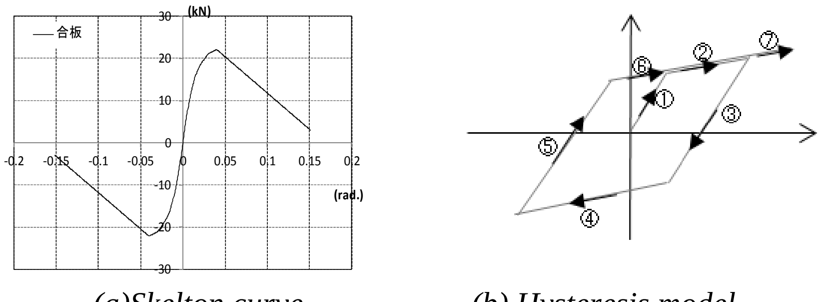

(a)Skelton curve *(b) Hysteresis model*

Figure 13: The restoring force characteristics of Plywood wall

The deformation characteristic of a specimen was different in each specimen as shown in Figure 14. In Specimen 1 and 2, the whole frame was shear deformation. On the other hand, locking deformation was seen in Specimen 3. Therfore, we evaluated a column base every specimen. We set an analysis condition as follows. A base column did not go up in Specimen 1 and 2. A base column went up in Specimen 3.

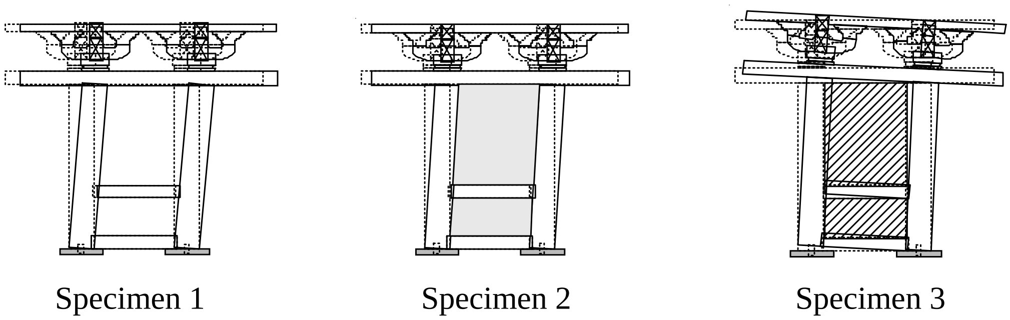

Figure 14: The characteristics of deformation

3.2 Analysis method

We used an improved analysis soft called wallstat ver2.0.1 (Nakagawa, 2006). Damping factor was 2.0 %. We analyzed about BJC-L2 100% which was the first maximum input wave.

3.3 Analysis results

The time history response wave until 60 sec is shown in Figure15. In all specimens, analysis results almost corresponded with experimental results. The difference between an experimental and analysis result in Specimen 3 was larger than one of Specimen 1 and 2. In the results of load-displacement relationship in Figure 16, almost same tendency was seen. In the result of specimen 3, the shear force was increased again after the deformation of 50 mm. The resistance force went up with the increasing deformation of a whole frame. It is possible because the compressive strain inclined to the grain was increased at the corner of wall. It can be seen that these results occurred because Specimen 3 was locking. It needs to reconsider the evaluation of behavior after locking.

4. CONCLUSIONS

In this paper, we conducted the earthquake response analysis of three kinds of specimen based on the experimental results. We made the frame model considered springs of column, the joint of column-batten, *Kumimono*, and wall. When the stiffness of walls was high like Specimen 3, it is possible that a whole frame is locking. In this case, it needs to consider it the base column of a frame goes up in an analysis. However the shear force of a frame was increased again after the force was decreased sharply. The analysis results were different with experimental results about this behavior of Specimen 3. We need to examine the evaluation of this phenomenon more.

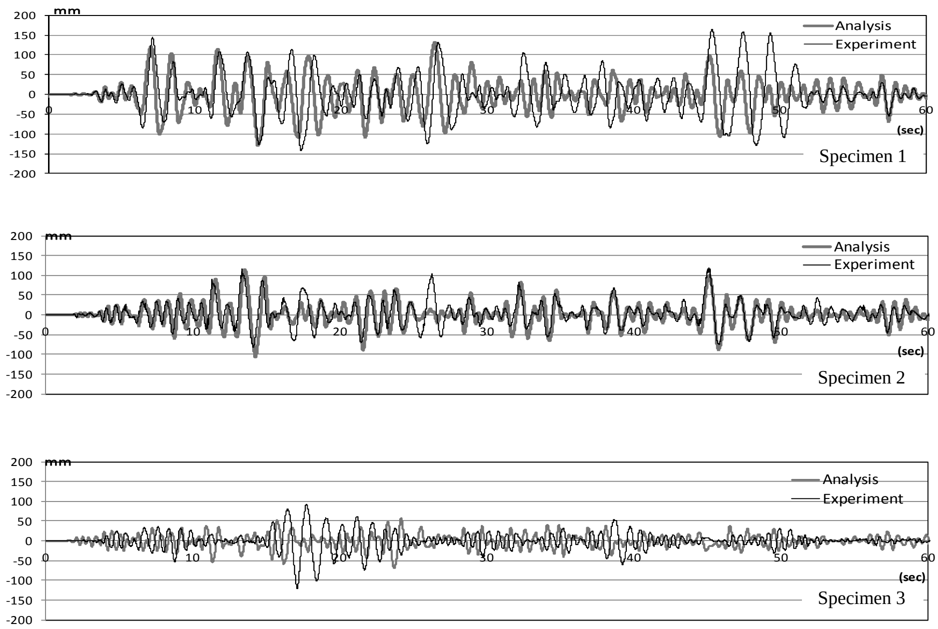

Figure 15: Time history response wave

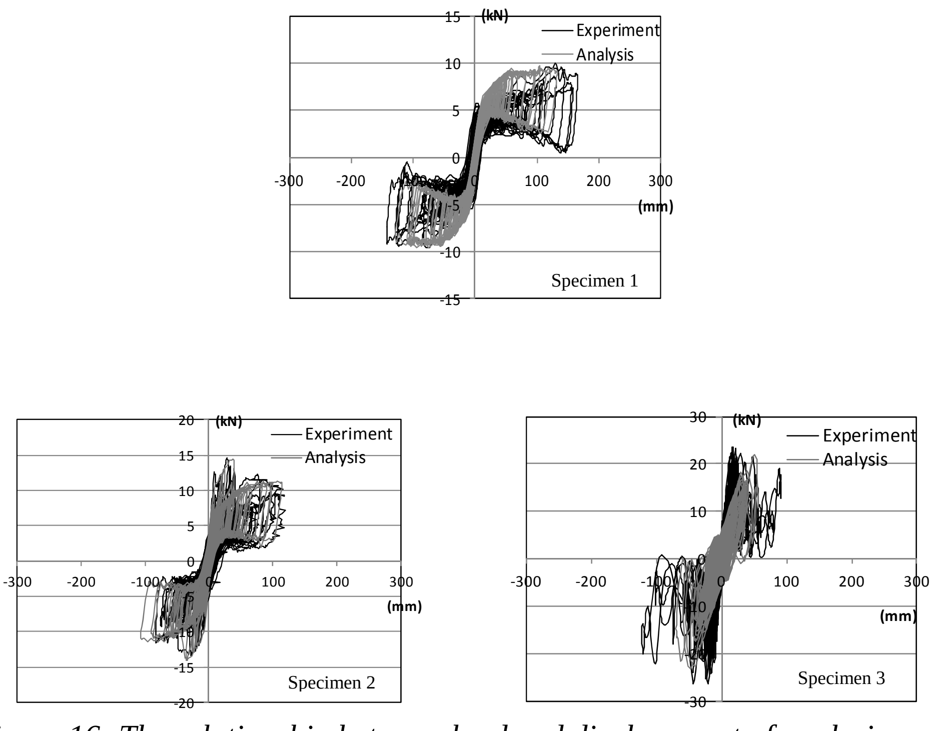

Figure 16: The relationship between load and displacement of analysis

REFERENCES

Tsuwa, I., Koshihara, M., 2009. Shaking table tests of traditional timber frames including Kumimono - Modeling of horizontal resistance force -, USMCA 2009

Tsuwa, I., Koshihara, M., 2011. A study on the effect of wall stiffness on the vibration characteristics of traditional timber frames including *Kumimono*, USMCA 2011

Ban, S., 1942. A study on the determination of the stability about main hall structures, Vol. 3: a mechanical study on the Japanese Traditional Frame, 1, the stability restoring force of a column. *Papers of annual meeting of Architectural Institute of Japan,* March, 252-258. (in Japanese).

Kawai, N., 1992. A study on the structural stability of traditional timber structures, *Report of the Building Center of Japan*, March. (in Japanese).

Inayama, M., 1991. The theory of compression perpendicular to the grain in wood and its application, Dissertation of the University of Tokyo. (in Japanese).

Murakami, M., Inayama, M., 2006. Formulae to predict the elastic and plastic behaviour of sheathed walls with any nailing aprangement pattern, *Journal of structural and construction engineering,* No.519, pp.87-94, (in Japanese).

Nakagawa, T., Ohta, M., et. al. 2010. "Collapsing process simulations of timber structures under dynamic loading III: Numerical simulations of the real size wooden houses", *Journal of Wood Science,* Vol.56, No.4, p.284-292

Kato, K., Tsuwa, I., and Koshihara, M., 2008. Shaking table tests of traditional timber frames including *Kumimono* Part 1 Experimental outline and results, *Summaries of technical papers of Annual Meeting Architectural Institute of Japan,* C-1, Structures III, pp.43-44 (in Japanese).

Tsuwa, I., Kato, K., and Koshihara, M., 2008. Shaking table tests of traditional timber frames including *Kumimono* Part 2 Modeling of horizontal resistance force and the analysis, *Summaries of technical papers of Annual Meeting Architectural Institute of Japan,* C-1, Structures III, pp.45-46 (in Japanese).

Tsuwa, I., and Koshihara, M., 2012. S Shaking Table Tests of Traditional Timber Frames including *Kumimono* Part 3 Effect of a wall stiffness on structural behavior, *Summaries of technical papers of Annual Meeting Architectural Institute of Japan,* Structures III, pp.425-426, (in Japanese).

Tsuwa, I., and Koshihara, M., 2013. S Shaking Table Tests of Traditional Timber Frames including *Kumimono* Part 4 Earthquake Response Analysis and Comparisons with Experimental Results, *Summaries of technical papers of Annual Meeting Architectural Institute of Japan*, Structures III, pp.467-468, (in Japanese).

Optimization of PP-band Mesh Connectivity for Cost and Time Effectiveness in Seismic Retrofitting of Masonry Structures

Adnan Mahmood DAR, Saleem M. UMAIR[2], Muneyoshi NUMADA[3], Kimiro MEGURO[4]
[1]Graduate Student, Department of Civil Engineering,
The University of Tokyo Japan
adnan@iis.u-tokyo.ac.jp
[2]PhD Student, Department of Civil Engineering,
The University of Tokyo Japan
mumair@iis.u-tokyo.ac.jp
[3]Research Associate, ICUS, Institute of Industrial Science,
The University of Tokyo, Japan
numa@iis.u-tokyo.ac.jp
[4]Professor and Director, ICUS, Institute of Industrial Science,
The University of Tokyo, Japan
meguro@iis.u-tokyo.ac.jp

ABSTRACT

Being common attraction for the people as economic viable solution for housing, unreinforced masonry (URM) construction has been economical and locally available in every part of the world with different types and form. Performance of URM masonry structures during different earthquake is still big question mark and has posed serious threats to human life in the past and future seismic disasters. The highest fatality rates during any earthquakes were always associated with masonry housing. Enhancing the performance of brick masonry in particular during the earthquake with material which will be cheap and having better performance during the earthquake have been dream of researcher and practicing engineer. The Polypropylene band (PP-band) retrofitting has been used for the retrofitting of masonry structures in many under developing countries. PP-band has been used as mesh on the walls with plaster coating. In the past behavior of PP-band is investigated during dynamic testing on small and full scale masonry houses. The PP-band applied on the masonry wall are connected at every intersection of the mesh. In the current research work an attempt was made by reducing the PP-band mesh connectivity for reaching the optimization in manner of time and cost for retrofitting of URM masonry structure. By varying these parameters we can propose a solution of PP-band retrofitting with less work force, price and duration by testing them in ¼ scale model on shake table test. Comparison of PP-band mesh performance having its connectivity at all points and with zero points has been made in damaged assessment of the structure.

Keywords: *Unreinforced Masonry, performance, retrofitting, brick masonry.*

1. INTRODUCTION & LITERATURE REVIEW

Masonry construction is the Popular and widely adopted in almost all continents of world. Economically affordable and locally available material for unreinforced masonry (URM) makes it attractive choice to adopt for housing purpose. Masonry construction poses serious life threats to human safety during the events of earthquake. Even though the human suffering during the earthquake cause huge problem for masonry housing but still new construction is far from stopping. The steps are required to overcome the problem of safety during earthquake with some techniques which are economical, locally available and socially acceptable.

The numbers of researcher are working on enhancing the performance of masonry retrofitting with different materials. In the past few years university of Tokyo research group working with PP-band (polypropylene) used as packing material in the cargo industry. The PP-band was utilized as retrofitting material for masonry construction has been developed by (Mayorca and Meguro, 2004). Many different aspects have been studied by Meguro Laboratory, Institute of Industrial Science, The University of Tokyo (Sathiparan, 2008).

Masonry with single story with regular brick has been common construction in the different part of the world. Masonry houses with stone, adobe and brick are common material adopted for construction of the house. The single story houses with PP-band mesh have been evaluated on the ¼ scale model with roof on Shake table test. The seismic performance for the PP-band retrofitted model has been enhanced in comparison to Non-retrofitted Model figure-1

a) Non retrofitted Model

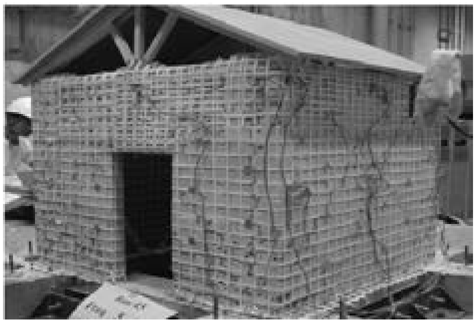

b) PP-band retrofitted Model

Figure-1 Condition of Model house at Frequency 5 Hz and Acceleration 0.4 g

2. RESEARCH OBJECTIVE

During the past research PP-band has been study to increase seismic performance which has been verified by number of researcher but connecting PP-band with PP-band welder and connecting all point is time consuming and requires extensive work time and cost. So there is need to investigate the reduced mesh connectivity for PP-band.

In this study we like to study the effect the PP-band mesh connectivity by varying them from all point of mesh connected with PP-band to non-connected in figure-2. We will keep the out-plane connectivity with wall and mesh pitch constant for both retrofitted houses. Three brick masonry model houses of ¼ scale with URM, PP-band mesh fully connected and non-connected were tested on shake table test by varying frequency and acceleration. By this study we can suggest reduction in connectivity of mesh and retrofitting time-cost.

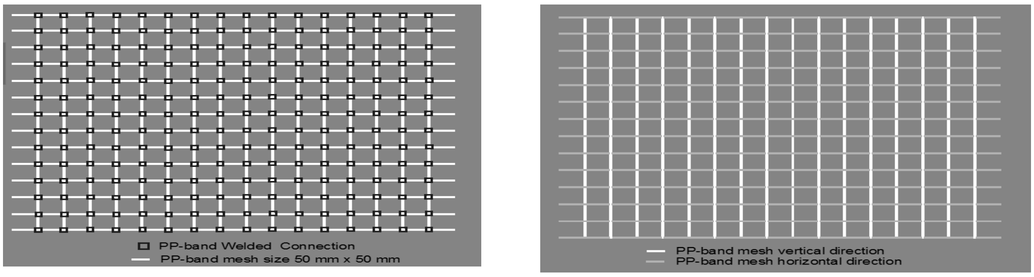

a) Fully connected Mesh b) Non Connected mesh

Figure-2 PP-band mesh connectivity for Model house

3. MATERIALS PROPERTIES

3.1 Masonry Properties

In making the model house the burnt bricks with 75 mm x 50 mm x 37.5 mm dimension and mortar from cement, sand, lime(1:7.9:20) with w/c 0.4 (water cement ratio). The thickness of mortar kept around 5 mm for masonry construction. After curing for 28 days and tested for material properties of masonry using the setup shown in figure-3.

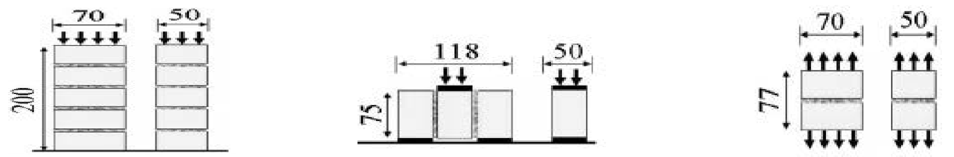

a) Compressive Strength b) Shear Strength c) Bond strength

Figure-3 Layout of material testing for masonry (unit: mm)

The effort was made replica of brick masonry in the developing countries and mechanical properties are shown in table-1.

Table-1 Mechanical Properties of Masonry

Property	*Fully Connected*	*Non-Connected*
Compressive Strength (Mpa)	13.60	13.45
Shear Strength (MPa)	0.021	0.018
Bond Strength (Mpa)	0.0028	0.0027

3.2 Polypropylene (PP) Properties

PP-band of size 6mm x 0.5 mm was used and thickness not uniform due to surface corrugation. Three band were tested under uniaxial tensile test and band fixed at one end and force applied from other end. The distance between two ends is 150 mm. The PP-band exhibit the 13 % axial strain, 6.80 GPa initial modulus and 1.98 GPa of final modulus.

4. CONSTRUCTION OF HOUSE MODEL

4.1 Shaking Table Description.

Shake table installed in IIS University of Tokyo have dimension of 1.5 m x 1.5 m having maximum weight of specimens of 2000 Kg. It has capability of controlling 6 degree of freedom, frequency ranging from 0.1 to 5 Hz and displacement ± 100 mm. Adopted house model with ¼ scale selected in keeping in mind the limitation of shake table.

4.2 Construction of House Model.

Concrete foundation were used for building the house and form erected initially. The base dimensions of the house were 930 mm x 930 mm and 720 mm height of the box shown in Figure-4(a). The 18 layer of brick with wall thickness 50 mm used with mortar having cement, sand, lime ratio as (1:7.9:20) with w/c as 0.4 (water cement ratio).Lintel were placed above the door and window having dimension were245 mm x 485 mm and 245 mm x 325 mm.

a) Construction of house b) Completed house

Figure-4 Phases of construction

The effort is made to make replica model similar to developing countries masonry houses in terms of strength. The straw were placed at bottom layer and after every fourth layer for Out of Plane connection of PP-band with brick wall. At the top layers cement bricks with bolt were placed along with brick in same mortar. The form work was removed after 7 days and sprinkled with water for same duration. The 28 days were given to house to gain strength. Wooden piece of 30mm x 50 mm are placed at top layer for providing level surface for placement of wooden roof truss Figure 4(b).

4.3 Retrofitting techniques.

Retrofitting scheme needs to be simple and easily employed by local people at site. Model with fully connected mesh was made by Cutting piece of PP-band (6m x 0.5mm) for horizontal and vertical length. The out of Plan connection was made with steel wire through the wall in figure-5(a). The horizontal piece at the bottom was attached outside and inside with ultra-sonic pulse welding device and then connected with out of plane connection. The vertical Piece was attached at pitch of 50 mm with bottom piece of PP-band as shown in figure-5(b). After attaching all the vertical pieces and then remaining horizontal pieces are placed at pitch of 50 mm. Then connected with out of plane for remaining connections. Around door and windows were warped for better holding of PP-band and mesh are connected at every intersection. Figure-5(c)

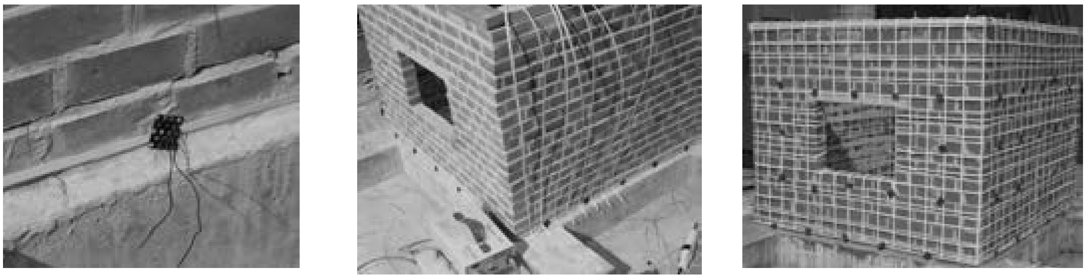

a) Out of plane connection with wall
b) Attaching vertical with horizontal PP-band
c) Fully connected PP-band mesh

Figure-5 Retrofitting Phases for Fully Connected House

Model house with non-connected PP-band is made by attaching horizontal piece inside and outside at bottom with out of plane connection shown in figure- 5(a). Attaching the vertical piece with bottom PP-band with pitch of mesh horizontally pitch 50 mm. Attaching horizontal plane by waving the horizontal PP-band as shown in figure-6(a). Connecting PP-band mesh at level of out of plane of connection to make have better grip. Attach remaining horizontal PP-band mesh inside and outside at pitch of vertical 50 mm. Warp the mesh around doors and windows opening as shown in Figure-6(c). The PP-band mesh is not connected with ultra-sonic welding device and only waving has been done to make the mesh.

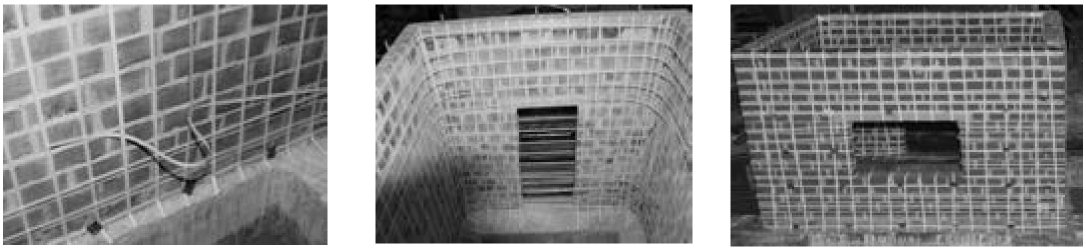

a) Waving for Horizontal PP-band
b) Inside View of house during retrofitting
c) Non Connected PP-band house

Figure-6 Retrofitting Phases for Non-connected PP-band House.

Retrofitting for both fully connected and non-connected house have been described in the table-2 explaining the two people have work on the retrofitting of the house. Retrofitting for fully connected 0.13 m^2/hrs whereas for non-connected 0.18 m^2/hrs.

Table-2 Time and Person for Retrofitting of Model House.

Model Name	**Time (hrs.)**	**Work (per.)**	**Retrofitting (m^2/hrs.)**
Fully Connected	20	2	0.13
Non-connected	14	2	0.18

per. - Working Persons
hrs. - Hours of Work

After the completion of retrofitting the houses was surfaced finished with mortar cement, sand, lime ratio as (1:7.9:20) with w/c as 0.4 (water cement ratio) and cured for 7 days. Wooden roof connected after surface finishes was hardened.

5. EXPERIMENTAL SETUP & LOADING SEQUENCE.

To study the global and local behavior of building during shaking accelerometer and laser are used to record the acceleration and displacement for the test. There were 24 one dimensional accelerometer attached to the specimen among which 13 in direction of shaking, 7 in transverse direction and 4 in vertical direction. There were total 5 laser attached among which 3 for top wall displacement, 1 for mid height and 1 for base level. The experimental can be seen from Figure-7. The measured data is recorded continuously at sample rate of 1/500 seconds in all the runs.

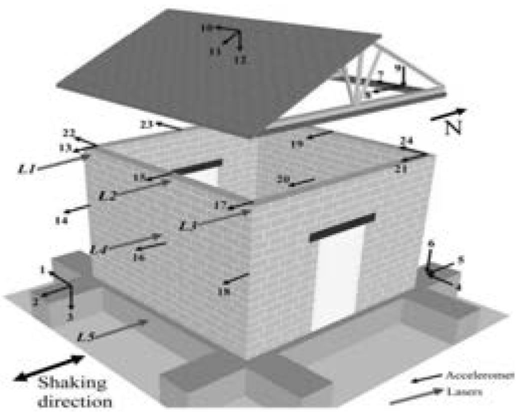

a) Location of Accelerometer and Laser b) Actual Setup for Experiment

Figure-6 Experimental Setup for Shake Table test

Simple Sinusoidal motions with frequency ranging from 2 Hz to 35 Hz by varying amplitude from 0.05 g to 1.4 g were applied to Model houses. The simple input shall be used because for numerical simulation model house. Loading sequence were given in the table-3 showing loading started from sweep motion and starting from 0.05 g amplitude varying frequency from 35 Hz to 2 Hz. The number of cycles were constant for all frequency Amplitude from 1.0 g higher frequency were ignored and lower frequency 5 Hz and 2 HZ have been used for testing. The number described in the table is the run number for dynamic loading applied.

Table-3 Loading Sequence

Amplitude	**Frequency**							
	2Hz	**5Hz**	**10Hz**	**15Hz**	**20Hz**	**25Hz**	**30Hz**	**35Hz**
Duration (sec)	**20.00**	**10.00**	**8.00**	**5.33**	**4.00**	**3.20**	**2.67**	**2.28**
1.2g		53						
1.2g	54	52						
1.0g		51						
0.8g	50	49	43	40	37	34	31	28
0.6g	48	45	42	39	36	33	30	27
0.4g	47	44	41	38	35	32	29	26
0.2g	46	25	24	23	22	21	20	19
0.1g	18	17	16	15	14	13	12	11
0.05g	10	09	08	07	06	05	04	03
sweep	01,02							

6. CRACK PATTERNS FOR MODEL HOUSES.

URM house there were no crack before Run-26(35 Hz and 0.4g) and diagonal cracks appear near openings and base of the house which further grows upon successive runs. Diagonal cracks appear on all the side opening which become prominent and visible after run 34(25 Hz and 0.8g). The cracks at the base are extend near diagonal cracks up-to Run-43(10 Hz and 0.8g). Furthermore, horizontal crack appear on the 6th layer from base and vertical crack extended from base at the run. House was partially separated near the opening top and showing large damage refer to figure-7 and finally house collapsed on run-44(5 Hz and o.4g).

Figure-7 URM Run-43 (5 Hz & 0.8g)

Fully connected PP-band house was not showing any significant damage before Run-28 (35 Hz and 0.8g) but cracks from top around opening have initiated. Small diagonal cracks appear after Run-32(25Hz and 0.4g) near openings. Run 37(20 Hz and 0.8g) there were diagonal cracks and horizontal crack at the base. Diagonal have been extended to base cracks Run-41(10Hz and 0.4g) and falling of plaster is also taking place. The cracks at this point were visible and prominent on the house. At Run-45(5Hz and 0.6g) out of plane crack were observed and condition of house was become worse. Run-51(5 Hz and 1.0g) the top part of near the opening has been damaged and plaster has fallen as shown in figure-8.The PP-band was broken at base and near openings, house is out of proportion. The Run-54(2Hz and 1.2g) was last on which house collapsed by detaching of PP-band from the base.

Figure-8 Fully Connected PP-band Run-51 (5 Hz & 1.0 g)

Non-connected PP-band house was not cracks before Run-27(35 Hz and 0.6g) and small cracks appear near the opening at this point. Run-28(35 Hz and 0.8 g) horizontal crack appear at the base. Cracks keep on extending near the opening for Run-33(25 Hz and 0.6 g). At Run-39 (15Hz and 0.6 g) there were horizontal and diagonal cracks on the house. Out of Plane cracks observed at Run-46(2 Hz and 0.2g) for the house. The cracks are prominent and visible at the point this point and plaster is falling from the crack parts of structure from the base. At Run-52(5Hz and 1.2 g) the mostly house was damaged at the base and remaining structure not showing damaged as shown in figure-9. The base suffered damaged due to the connection of PP-band at the base only. The house collapsed at the Run-54(2Hz and 1.2 g) similar to the fully connected PP-band house.

Figure-9 Non-Connected PP-band Run-52 (2 Hz & 1.2 g)

8. PERFORMANCE EVULATION.

Performance of the houses is evaluated on the basis of damaged level of the building during the earthquake. Different level of damages as lightly damaged, moderately damaged, partially collapsed, heavy damaged and collapse based on the European Macro-seismic Scale, EMS-98 combining the JMA intensity for the applied loading sequence.

URM has not shown any damage upto Run-25 (5 Hz and 0.2 g) and light structure damages were observed at up to Run-31(30 Hz and 0.8 g). After Run-34 (25 Hz and 0.8 g) diagonal cracks become prominent and visible and near Run-43(10 Hz and 0.8 g) was partially collapsed corresponding JMA 4.The URM house was collapsed at JMA5-. The performance of the URM can be seen from table-4 involving frequency and amplitude along with damaged category corresponding to different colors referring JMA intensity.

Table-4 Performance of URM house model with different JMA intensities

Acceleration (g)	Frequency (Hz)							
	2	5	10	15	20	25	30	35
1.4 g								
1.2								
1.0								
0.8			D4	D3	D3	D3	D1	D1
0.6			D4	D3	D3	D2	D1	D1
0.4		D5	D4	D3	D3	D2	D1	D0
0.2		D0	D0	D0	D0	D0	D0	D0
0.1	D0	D0	D0	D0	D0	D0	D0	D0
0.05	D0	D0	D0	D0	D0	D0	D0	D0

Index	JMA 0~4	JMA 5-	JMA 5+	JMA 6-	JMA 6+	JMA 7

DO: No damage
D1: Light Structure damage
D2: Moderate Structure damage
D3: Heavy structure damage
D4: Partially Collapsed
D5: Collapsed.

Fully connected PP-band was damage up-to Run-27(35 Hz and 0.8g) but light damaged after that slight cracks at the top opening. The house was moderate damaged up-to Run-43(10 Hz and 0.8g) equivalent to JMA 4 at which non-retrofitted house partially damaged at this stage. The structure showed partially damaged conditions which sustain large deformation and falling of plaster upto JMA 6+ but can give time to evacuate the building. The house collapsed at JMA 7 of Run-54(2 Hz and 1.2g) sustain shaking and finally collapsed by breaking of PP-band connection at the base. The performance of the PP-band fully connected can be seen from table-5 involving frequency and amplitude along with damaged category corresponding to different colors referring JMA intensity.

Non-connected PP-band has not shown any damage up-to Run-26(35 Hz and 0.4g) and lightly damaged to Run-30 (30 Hz and 0.6g).The model shows was

Table-5 Performance of Fully connected PP-band retrofitted model

Acceleration	Frequency (Hz)							
(g)	2	5	10	15	20	25	30	35
1.4		D4						
1.2	D5	D4						
1.0		D4						
0.8	D3	D3	D2	D2	D2	D2	D1	D1
0.6	D3	D3	D2	D2	D2	D2	D1	D0
0.4	D3	D3	D2	D2	D2	D2	D1	D0
0.2	D3	D0	D0	D0	D0	D0	D0	D0
0.1	D0	D0	D0	D0	D0	D0	D0	D0
0.05	D0	D0	D0	D0	D0	D0	D0	D0

Index	JMA 0~4	JMA 5-	JMA 5+	JMA 6-	JMA 6+	JMA 7

DO: No damage — D3: Heavy structure damage
D1: Light Structure damage — D4: Partially Collapsed
D2: Moderate Structure damage — D5: Collapsed.

moderately damaged up-to Run-43(10 Hz and 0.8g) and performance of fully connected and non-connected are in close relation to the one another and also giving better performance than URM. The house has been partially damaged on the JMA 6+ but collapsed at finally on Run-54(2 Hz and 1.2g) the base was damaged but has damaged but sustain almost same level of shaking to the fully connected PP-band. The performance of Non-connected PP-band model can be seen from the table-6 involving frequency and amplitude along with damaged category corresponding to different colors referring JMA intensity.

Table-6 Performance of Non-connected PP-band retrofitted model

Acceleration	Frequency (Hz)							
(g)	2	5	10	15	20	25	30	35
1.4		D4						
1.2	D5	D4						
1.0		D4						

0.8	D4	D3	D2	D2	D2	D2	D1	D1
0.6	D3	D3	D2	D2	D2	D2	D1	D1
0.4	D3	D3	D2	D2	D2	D2	D1	D0
0.2	D3	D0	D0	D0	D0	D0	D0	D0
0.1	D0	D0	D0	D0	D0	D0	D0	D0
0.05	D0	D0	D0	D0	D0	D0	D0	D0

Index	JMA 0~4	JMA 5-	JMA 5+	JMA 6-	JMA 6+	JMA 7

DO: No damage
D1: Light Structure damage
D2: Moderate Structure damage
D3: Heavy structure damage
D4: Partially Collapsed
D5: Collapsed.

9. CONCLUSION:

The brick masonry single story house with similar construction technique for PP-band retrofitting with fully connected and non-connected house have been made. The study gives appropriate solution for retrofitting with PP-band by which we can save the time and cost for house. URM house collapsed at JMA5- where as both retrofitted house were collapsed at JMA 7 showing better performance during sever ground shaking. Furthermore, retrofitted houses with fully connected and non-connected PP-band collapsed at JMA 7.

Although the performance during the dynamic test for fully and zero connectivity of PP-band gives similar damaged but non-connected is more damaged at the base. Thus life safety can be maintained with non-connected PP-band mesh and human casualties can be achieved during sever ground shaking. Thus we can Suggest that single story house having wooden Truss roof and surface finish can be retrofitted with non-connected PP-band mesh giving optimum seismic retrofitting solution in term of cost and time.

REFERENCES:

- Mayorca, P. and Meguro, K. (2004) Proposal of an Efficient Technique for Retrofitting Unreinforced Masonry Dwelling Proceedings on 13th World Conference on Earthquake Engineering, Vancouver, Canada

- Sathiparan, N. and Meguro, K. (2012). “Seismic behaviour of low earthquake-resistant arch shaped roof masonry houses retrofitted by PP-band meshes.” ASCE Practice Periodical on Structural Design and Construction. 17(2), 54-64.

- Saleem M. Umair (2013) “Seismic Retrofitting of Masonry structure using composite of Fibre Reinforced Polymer (FRP) and Polypropylene (PP)” Ph.D. Thesis, University of Tokyo.

- Grünthal, G., (ed.), (1998) "European Macro-seismic Scale 1998”, Volume 15, Luxembourg.

Monitoring system for Nguyen Van Troi - Tran Thi Ly stay cable bridge during construction and for service stage

NGUYEN Phuong Duy and TRAN Minh Phuong
VSL Vietnam Ltd.
duy.nguyenphuong@vsl.com

ABSTRACT

This paper briefly presents the monitoring system designed and installed for Nguyen Van Troi – Tran Thi Ly stay cable bridge during the construction and for service stage. Crossing the Han river in Da nang, Vietnam, the 731m long stay cable bridge has a main span of 230m and an inclined pylon with one plan of stay in main span and the twisting arrangement of back stays anchored symmetrically on each side of the bridge's abutment. The monitoring system designed and installed on the bridge consists of stay cable loadcells, pylon inclinometer, concrete temperature, concrete strain, wind intensity and direction. The monitoring data allows controlling the strains and movements developed in the structure in verifying with the design data. A portable accelerometer had been used to control indirectly the cables tension using the vibrating wire theory. The frequencies identified on the twisting back stay cables show a very good harmonious between two symmetric plans proving the convenient of the method. The cable tensions calculated through cable natural frequencies then compare with the loadcells data and the lift-off jacking forces. In neglecting both sag-extensibility and bending stiffness of the cables, a good correlation between lift-off jacking force, loadcells data and the tension forces calculated from cable frequencies had been observed for medium and long cables.

Keywords: *Stay cable bridge, monitoring system, cable tension, cable vibration*

1. INTRODUCTION

For modern bridge maintenance and management, a reliable monitoring system is of central important. The major objective of bridge monitoring system is to provide controls during construction stages but also to identify damages or deteriorations during exploitation.

Crossing the Han River, connecting the Hai Chau and Son Tra districts in Da Nang city, the new Nguyen Van Troi – Tran Thi Ly stay cable bridge is designed as a symbol of the beach and port city in the middle of Vietnam. The 12 degrees inclined pylon rising 145m height from the water level can be observed from any location of the city. The pylon supports one main span stay cable and twist symmetric back stay cable plans forming an interesting aesthetic aspect viewing from all direction.

Complicated structure and construction method raise the need to design and install a structural monitoring system for surveying the structural responses during the construction period but also extendable for bridge health monitoring during the service stage.

Figure 1: Nguyen Van Troi – Tran Thi Ly stay cable bridge

2. MONITORING SYSTEM REQUIREMENT

The design and installation of the monitoring system of Nguyen Van Troi – Tran Thi Ly bridge are for the following purposes:

- Providing the data for structural analysis and state asses through the structural response and behavior during the construction stages like stresses, deformation, temperature variation, tension and vibration of stay cable, pylon movement.
- Design verification by checking the design assumption to monitoring data such as wind direction and intensity, structural and ambient temperature variation, effect of gradient temperature of the bridge during the different construction stages. The stresses in the critical section are also assessed for design verification and construction control.
- For the service stage, the monitoring data is employed for assessing extent of damage/deterioration, evaluating the structural performance, response to unexpected accident or managing the traffic and bridge's normal operations.

3. MONITORING SYSTEM DESIGN AND DATA ASSESMENT

The structural monitoring system for Nguyen Van Troi – Tran Thi Ly stay cable bridge consists of:

- Monitoring the stresses variation in the critical section of concrete pylon and girder for the construction survey;
- Measuring and survey the movement of pylon during construction stages;
- Monitoring the temperature in the pylon, girder and stay cable;
- Monitoring wind intensity and direction;
- Measuring and monitoring the tensile forces on the stay cables by using a combination method (loadcells and vibration measurement);
- Vibration monitoring of the cables, girder and pylon by using the portable accelerator system;
- At the end of the construction period, a 3D movement monitoring system using the GNSS technology had been installed at the pylon top.

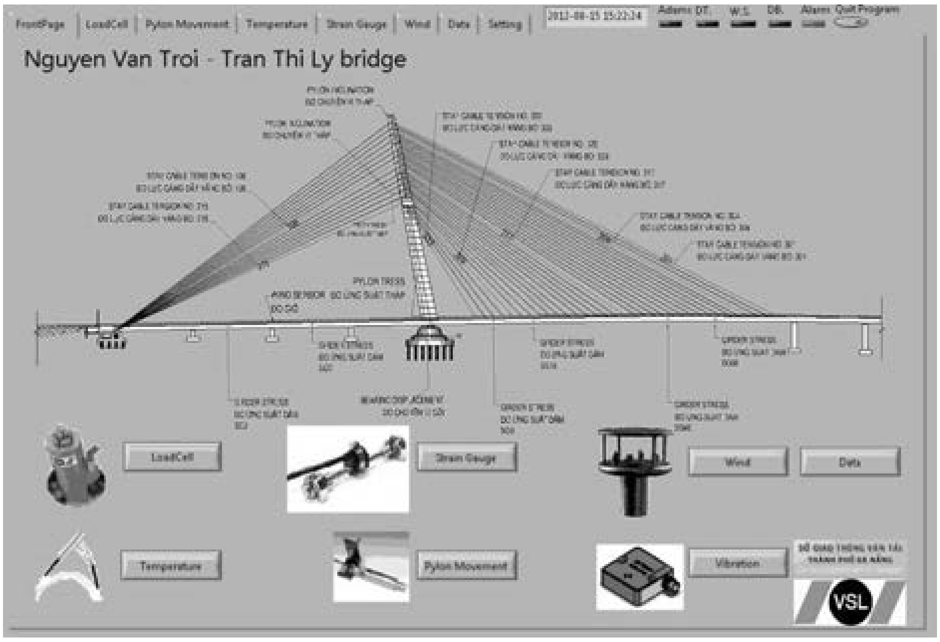

Figure 2: Data acquisition and analysis software interface

All the monitoring equipments have been configured to the data acquisition system and then transferring the data to the central computer installed on the bridge deck level assuring the continual data recorded and assessment. A data acquisition software had been developed specifically for Nguyen Van Troi – Tran Thi Ly bridge. The main function of the software is to acquire, record, analysis but also controlling the system and warning any measurement value reaching the critical range. The system is also designed to be able to extent for future needs.

4. CONCRETE STRESSES AND TEMPERATURE MONITORING

During the construction stages, stresses and temperature state in the concrete pylon and girder had been closely monitored and the data had been recorded for controlling the bridge structural response. The figure 3 shows the stresses state recorded for the period of September 2012 at pylon section PYS20. A good correlation between the measurement points on the section had been observed.

The stresses monitoring data allows to survey the construction method by comparing with the design values.

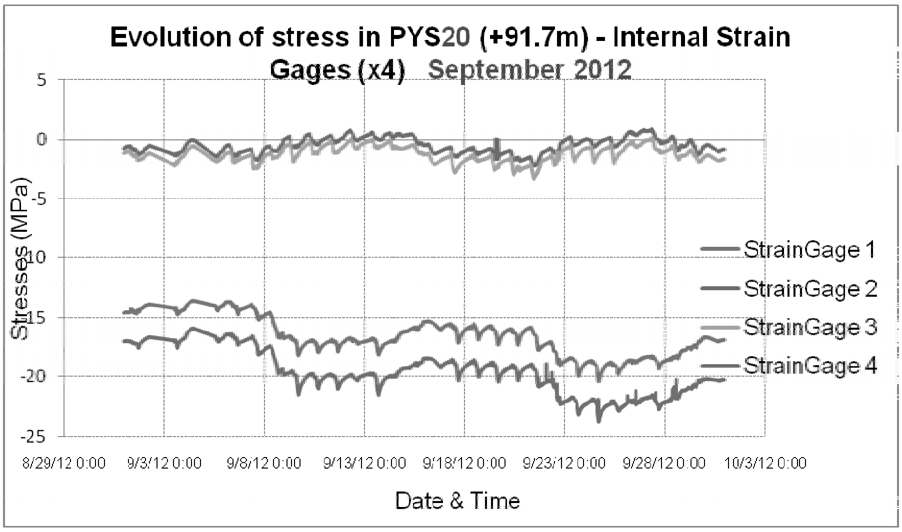

Figure 3: Pylon Stresses state monitoring data

5. STAY CABLE TENSILE FORCES MONITORING

Around the world and in Vietnam, there exist several techniques to assess the tensile forces in the stay cable. They are namely measurement of the force in a tensioning jack (lift-off), application of ring loadcell, topographic survey and elongation of the cable during tensioning and installation. In spite of their simple theoretical description, the practical application is highly complex and not always economically effective, accuracy or even applicable (Casas, 1994). A relatively simple, quick and inexpensive method of measuring cable forces in cable stay bridge is to use the vibrating wire theory in basing on the cable natural frequency (f), the mass (m) and the real length (L) by using the following formula:

$$T = 4mf^2L^2 \qquad (1)$$

This method had been successfully applied around the world to relatively short stay cable bridge cables with simple anchoring devices as well as to external pre-stressing cable (Demars and al., 1985). However, if the vibrating wire theory is applicable for determining the stay cable tensile forces, there is a linear correspondence between vibration modes and natural frequencies. The main assumptions of the theory are:

- The cable has a negligible flexural stiffness;
- There is no relative displacement of the point where the cable is anchored;
- The cable is inextensible. The transverse deflection of symmetrical modes does not generate additional tension in the cable.

For much longer stay cable length or the complicated anchorage devices, deviator, dumper, the determination accurately of the real vibrating length of the cable becoming very difficult (Kiska and al., 1991). On another hand, the actual vibrating behavior maybe deviated substantially from the vibrating wire theory. The determination of the lowest natural frequencies may have a big dispersion and then effect on the tensile force calculation (Robert and al., 1991)

Different methodology had been proposed in that circumstance to obtain accurate results of the stay cable tensile forces. The simplest one is to combine measurement techniques which compensates for the errors of one method with the results of another using the least-square minimization procedure. More complicated methodologies consists of taking into consideration the effect of stay cable flexural stiffness or extensible of the cable.

For measuring and monitoring the stay cable tensile force of the Nguyen Van Troi – Tran Thi Ly bridge, we adopted a combining method. The tensile forces were measuring by the vibration method in identifying the natural frequencies and indirectly calculated the forces. The results were then verified and calibrated by comparing with the monitoring data from seven loadcells pre-installed on the cables anchorages and the direct measurement of lift-off data.

The cable forces in cable stay is then calculated by using the following formula (Cunha and al., 1995):

$$T = 4mf_n^2L^2/(n^2g) \quad (2)$$

where T is the tensile force in the stay cable, f_n is the n^{th} natural frequency, L is the distance between two fixed ends of the cable and m is the mass of the cable per unit length.

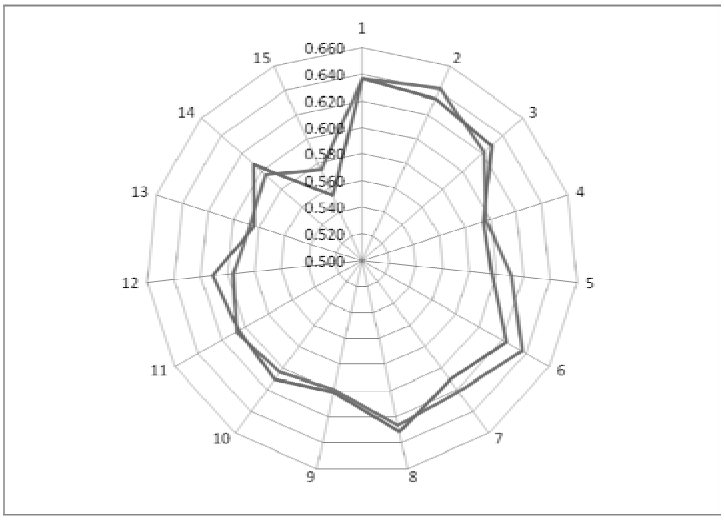

Figure 4: good harmonious frequencies between two symmetric plans of back stay

The natural frequencies identified on the twisting back stay cables at the end of construction are presented in the figure 4 and show a very good harmonious between two symmetric plans proving the convenient of the measurement method.

The calculated tensile forces are then compared with the lift-off data and the reading value from pre-installed loadcells for verifying the efficiency of the method (VSL VN, 2012). The figure 5 shows the tensile forces error between the direct lift-off measurement data and the indirect result using the vibrating wire calculation theory. In neglecting both sag-extensibility and bending stiffness of the cables, a good correlation between lift-off jacking force, loadcells data and the tension forces calculated from cable frequencies had been observed for both symmetric back stay cables. A maximum error of 4% is recorded for all back stay cables. Same error range had been recorded in comparing the calculated forces with the loadcell reading values.

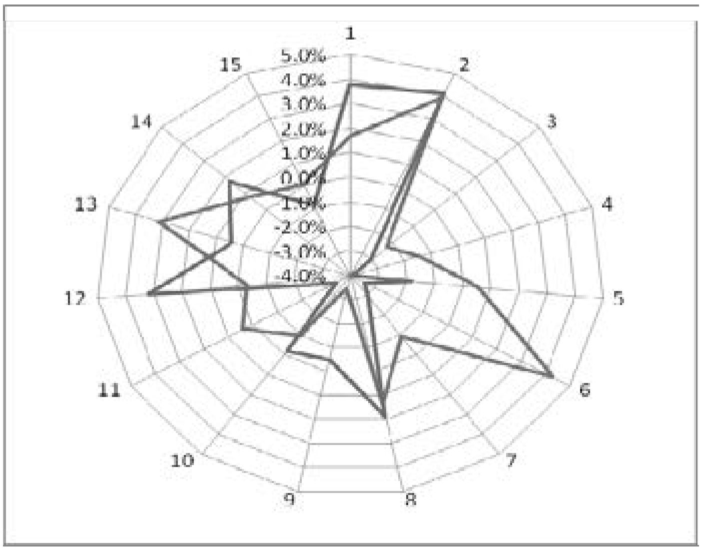

Figure 5: Error of the tensile forces between the direct and indirect method (twist plan of back stay 15 nos. each)

6. PYLON MOVEMENT MONITORING BY GNSS TECHNOLOGY

To manage bridges effectively, more needs to be done to access the day-to-day and long-term condition and behavior of in-service bridges, so that preventive measures can be taken, and deterioration rates can be better understood. Owning the advantages of high accuracy, all-weather condition and no requirements of inter-visibility between measuring points, the GNSS technology suits well this monitoring purpose fulfilling both static and dynamic measurement needs. This technology had been applied for the Nguyen Van Troi – Tran Thi Ly stay cable bridge for permanent 3D pylon movement monitoring.

The small network of GPS reference stations can be used very effectively for monitoring deformations and movements of man-made structures. For bridge structural monitoring, in order to monitor rapid, short-term movement and even vibrations, the raw data have to be streamed continuously at a high rate from the receivers to the control computer processes the baselines between the stations continuously. A software component running on the server can compute the baselines of the network continuously or at regular intervals to determine the positions (coordinates) of the monitoring points.

Figure 6: Rover antennas on top pylon and base station installation

For the bridge monitoring, reliable communication is vital for the efficient operation of GPS reference station and networks of stations. The reference station software running on the server has to control the receivers and download the data. In Nguyen Van Troi – Tran Thi Ly bridge, an optical fiber network had been adopted for RTK data transfer from base station and rover stations to the central computer. The figure 6 shows the reference station and the rover antenna installed on the top of pylon for permanent movement monitoring.

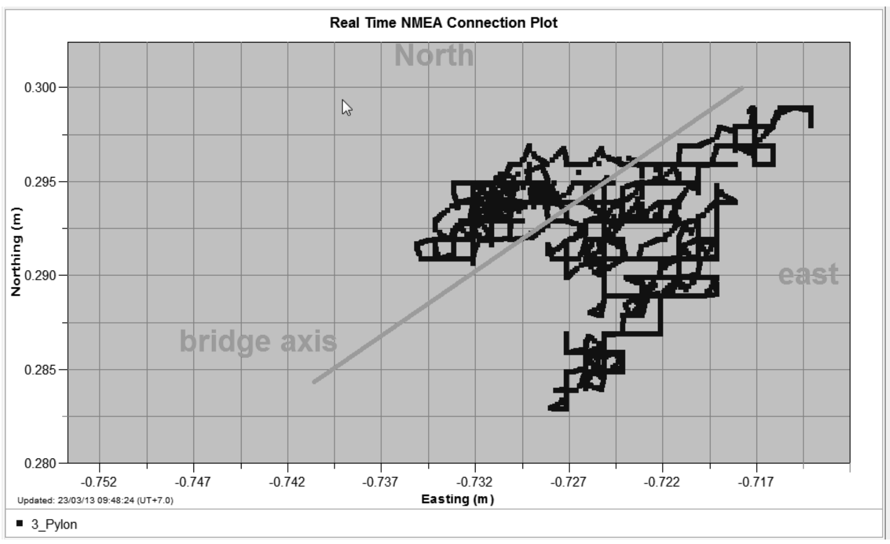

Figure 7: Real time movement of the top of pylon

The movement of the pylon had been calculated and an example of movement recording and displaying is showed on the figure 7.

7. CONCLUSION

The demand for bridge structural health monitoring is continually increased as engineers are continually challenged to provide and maintain a safe and efficient highway network. Considering as the only method to help engineer to understand completely the condition and behavior of the bridge structures, the structural monitoring is also considering as a traffic management strategy aids tool. The paper presents a monitoring system successfully designed and installed for Nguyen Van Troi – Tran Thi Ly stay cable bridge for construction survey and service stage assessment. The application of vibration method for measuring the stay cables forces proved the efficiency, the error recorded are less than 4% for all back stay cables in comparing with the lift-off data and loadcells monitoring data. The monitoring system is also proving the efficiency of the application of the GNSS technology for 3D pylon movement monitoring.

REFERENCES

Cunha, A. and Ceatano, E., 1997. “Dynamic measurements on stay cable of cable-stayed bridges using an interferometry laser system”. *Experimental Technique, 23(3): 38-43.*

Casas, J-M., 1994. “A combined method for measuring cable forces: the cable-stayed Alamillo Bridge, Spain”. *Structural Engineering International, Journal of the IABSE, Vol.4, No.4, pp.235-240.*

De Mars, P.: Hardy, D., 1985. “Mesure des efforts dans les structures a cables”. *Annales TP Belgique 6. Bruxelles. 1985, pp. 515-531.*

Kyska, R.; Koutny, V.; Rosko, P., 1991. “Tension Measurement in Cables of Cable-Stayed Bridges and in Free Cables”. *Proc. Of the Second Conf. on Traffic Effects on Structures and Environment, Zilina, Slovakia, April 1991. pp. 190-194.*

Irvine H.M., 1981. Cable Structures. MIT Press, 1981.

Robert, J.L.; Bruhat, D.; Gervais, J. P., 1991. “Mesure de la tension des cables par méthode vibratoire”. *Bulletin de Liaison des Laboratoires des Ponts et Chaussées, 173. Paris, 1991, pp. 109-114.*

VSL VN, 2012. “Report for Tensile forces measurement using vibration method on 12th Sept 2012”. *Nguyen Van Troi – Tran Thi Ly bridge project, Da Nang.*

Leica Geosystems, 2010. “GPS Reference Station and Networks – An introductory Guide”.

Practical evaluation method of collapse limit displacement based on seismic damage of structural members

Kazuto MATSUKAWA[1] and Masaki MAEDA[2]
[1] Research Associate, IIS, The University of Tokyo, Japan
mtkw@iis.u-tokyo.ac.jp
[2] Professor, Dept. of Architecture and Building Science, Tohoku University, Japan

ABSTRACT

Authors proposed an evaluation method of collapse limit displacement of RC structures based on its capacity curve and seismic response spectrum in past papers. In this paper, referring the method, more practical method to evaluate collapse limit displacement based on damaged members ratio (DMR) was developed. The DMR is briefly explained as ratio of number of severe damaged members and number of total members in a structure. Correlation of DMR and collapse limit displacement which calculated by proposed method in past papers was investigated by nonlinear static analysis for 20types of RC frame. At result, on average, these buildings suffered damage of DMR of 0.2 has 5% probability of collapse risk. This correlation was also investigated its validness by statistical analysis using a database of actual damaged buildings due to past earthquakes such as Tohoku EQ.2011, Kobe EQ.1995 and more. At result, it is found that damaged buildings less than DMR of 0.3 could avoid collapse in the earthquakes, therefore, a criteria for collapse prevention found in frame analysis mentioned above, DMR of 0.2 was conservative for the result of the statistical analysis.
DMR is index which is easy to calculate from result of frame analysis, therefore, structural engineers may be able to calculate collapse limit displacement practically by referring DMR of 0.2.

Keywords: *collapse assessment, shear failure*

1. INTRODUCTION

Due to huge earthquake, reinforced concrete structures might have collapse risk by shear failure of members. Shear failure may cause a total collapse of buildings because of rapid degradation of horizontal and axial capacity. In Japanese seismic code and design standards (AIJ.2004), such behavior in shear resistance has not been considered because of its complexity and unclearness. Therefore, safety limit state of buildings (maximum displacement point of buildings to prevent collapse) is generally taken at the first occurrence of shear failure of a structural member and it is often conservative comparing with actual collapse limit.
In addition, to know the collapse limit displacement is important because structural engineers will be possible to show the actual capacity of buildings to

owners. Therefore, collapse risk assessment has been a significant research topic and many kinds of research regarding collapse assessment were carried out. Haselton et.al (2011), the one of examples, are assessed collapse risk of buildings designed by referring ASCE 7 (ASCE 2002, 2005) and ACI 318 standards using Incremental Dynamic Analysis method (IDA method). In the IDA method, a ground motions were increasingly scaled and input until building collapse. However, IDA method requires extensive technical knowledge, high experience and lots of time to structural engineer, therefore, it may be difficult to use in structural design.

The authors proposed a method to evaluate collapse limit based on Capacity Spectrum Method (CSM) as a more practical method than IDA method (Matsukawa and Maeda, 2013). The accuracy of collapse limit displacement calculation by the CSM method was investigated by comparison with collapse limit displacement calculated IDA method using SDOF system. The results showed that collapse limit displacement by the CSM method corresponds with collapse limit displacement calculated by IDA method with errors within plus or minus 20 percent.

In this paper, relation of collapse displacement and damage of structural members was investigated by nonlinear frame analyses for several kinds of structures and by statistical analysis using database of actual damaged buildings. The aim of this research is to develop a more practical method to evaluate collapse limit displacement based on damages of structural members. The method will enable to evaluate collapse limit displacement without special computer analysis (by only static analysis) for structural engineers. And the method is also expected to develop more to apply in evaluation of residual seismic capacity of damaged buildings.

2. EXPLANATION ABOUT COLLAPSE LIMIT EVALUATION METHOD BASED CAPACITY SPECTRUM METHOD

2.1 Basic Methodology

In this chapter, evaluation method of collapse limit point against side-sway collapse (collapse when lateral displacement of building increase without bounds) based on CSM proposed in past paper (Matsukawa and Maeda, 2012) is explained. Key features of which are briefly summarized as follows:

1) Calculate Seismic Capacity Index (SCI) for equivalent SDOF system which is converted from frame model using results of its nonlinear static frame analysis.
2) Take the maximum SCI point of equivalent SDOF system as collapse limit.

SCI (Architectural Institute of Japan, 2004) is the ratio of ultimate spectral acceleration at each response point and standard spectral acceleration (5% damping) at period of the point as shown in Figure1, therefore, increment of SCI will roughly correspond with amplitude scale when IDA was carried out (see Figure2). As mentioned above, the maximum SCI point is taken as the collapse limit displacement in this method because that point means the maximum response point that building can prevent collapse when the maximum resistible scaled ground motion suffered.

The conceptual drawings about this method are shown in Figure3 (a)-(c). Response point will be found if ground motion (response spectrum) is much smaller than building capacity as shown in Figure3 (a). When larger ground motion suffered, response point will move and will get closer to the collapse displacement, then the response displacement reaches collapse displacement when ultimate ground motion that building prevent collapse was suffered (see Figure3 (b)). If spectral acceleration becomes larger or more, response point will not be found and building will collapse as shown in Figure 3 (c).

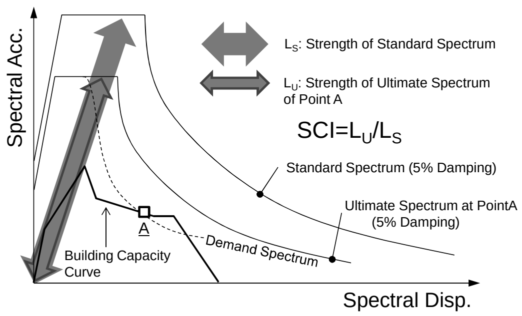

Figure : 1 General concept of SCI

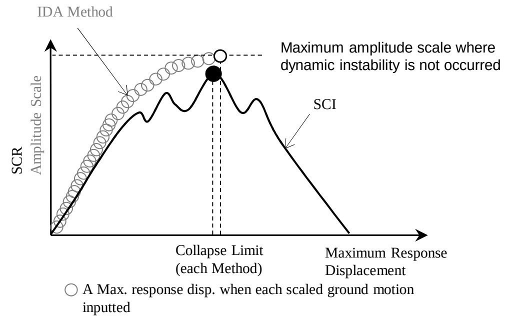

Figure 2 : Relation of SCI and amplitude scale of IDA

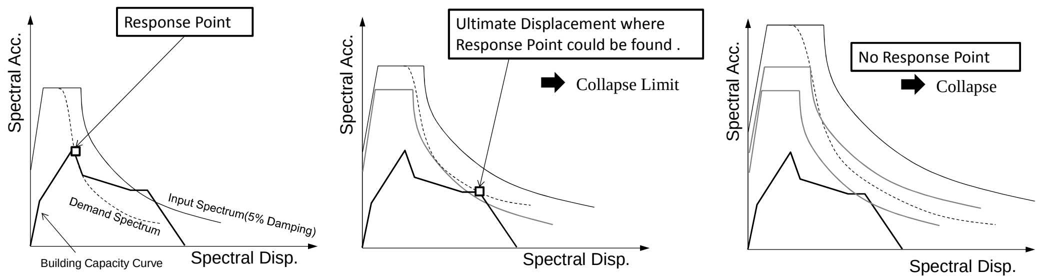

(a) (b) (c)

Figure 3 : Examples for relations of response spectrum and collapse

2.2 Analytical Models and Methodologies

2.2.1 Basic Models

Analytical models and methodologies are explained in this section to display calculation examples of the method mentioned above (and the results will be used in development more practical method based on damage of structural members in next chapter). The models of this research are 3stories and 6stories building models which have 4 bays and half beam with a roller support at both left and right side of each building model. Unit weight of each floor is assumed as 12kN/m^2. Drawing of basic modeling of the structures is shown in Figure4. Members composing each structure were converted as rod element models which have axial, shear and flexural spring, in addition, rigid zones exists at both end of the rod elements. As shown in Figure4, structures planed so that collapse by 1st story collapse mechanism will occur, therefore, elastic springs are applied for each spring of all members except for columns at 1st story. In addition, columns of 1st story are named from left to right as “Column A” to “Column E” (see Figure4).

2.2.2 Characteristics of Structures and Members

Columns at 1st story are applied several types of characteristics; F2, F3, F4, S3 and S6. Column characteristics named as F2, F3 and F4 are for flexural members and numbers after "F" means μ_{fu} which is mentioned later. Flexural members consist of an elastic shear spring, an elastic axial spring and inelastic flexural springs. 4-linear model is applied to the inelastic flexural springs and capacity degradation curve was assumed as strength reaches to 0kN when μ (plastic ratio: displacement divided by yield displacement) equal to μ_{fu}+2 (μ_{fu}: plastic ratio at capacity degradation start).

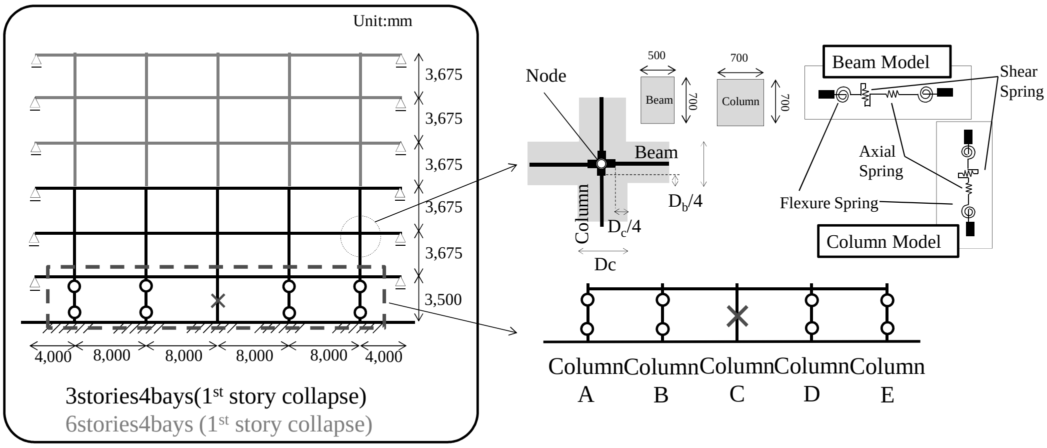

Figure 4 : Drawing of structure models and basic modeling of members

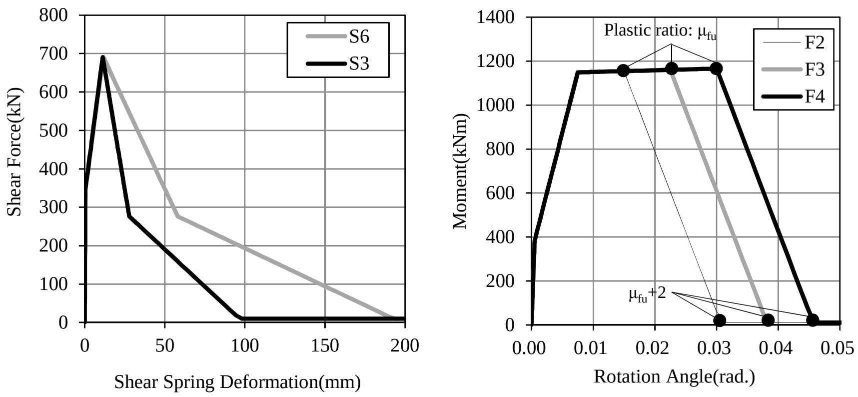

Figure 5 : Backbone characteristics of inelastic shear and flexural springs (for 3stories models)

Table1 : Application of column for each type of models

	type1	type2	type3	type4	type5	type6	type7	type8	type9	type10
ColumnA	F3	F3	F3	F3	F4	F4	F4	F4	F2	F4
ColumnB	F2	S3	F2	S6	F3	S3	F3	S6	F2	F4
ColumnC	S3	F2	S6	F2	S3	F3	S6	F3	S3	S3
ColumnD	F2	S3	F2	S6	F3	S3	F3	S6	F2	F4
ColumnE	F3	F3	F3	F3	F4	F4	F4	F4	F2	F4

Column characteristics S3 and S6 are for shear members, "3" and "6" are drift angle that strength reaches 0kN due to capacity degradation. Shear members have elastic flexural springs, an inelastic shear spring and an elastic axial spring. 4-

linear model is applied to the inelastic shear spring. Inelastic shear springs and flexural springs used in the analysis are shown in Figure5. Maximum strength of these inelastic springs is decided so that maximum strength summation of all 1st story columns corresponds 50% of total weight.

10 series of column type combination for each 3 and 6 story models are used in parametric study mentioned in next section. Table1 shows the combination, they are chosen so that many types of capacity curve will be obtained.

2.2.3 Analytical Procedure

Nonlinear static analysis (displacement-controlled pushover) was carried out so that displacement of each story at each analytical steps corresponds 1st vibration mode shape. After that, equivalent capacity curve was obtained by converting story shear –drift curve using EQ.(1) and (2).

$$S_a = Q_B \frac{\sum\left(m_j \cdot \delta_j^{\,2}\right)}{\sum\left(m_j \cdot \delta_j\right)^2} \qquad (1) \qquad\qquad S_d = \frac{\sum\left(m_j \cdot \delta_j^{\,2}\right)}{\sum\left(m_j \cdot \delta_j\right)} \qquad (2)$$

Where; Sa : spectral acceleration, Sd : spectral displacement, Q_B : base shear, m_j : mass at j^{th} floor, δ_j : j^{th} floor displacement from base.

12 observed ground motions in past earthquakes which consists of Elcentro 1940 wave (EW, NS), Kobe 1995 wave (EW, NS), Hachinohe 1968 (EW, NS), Ojiya 2004 (EW, NS) , Tohoku 1978 (EW, NS), Taft 1952 (EW,NS) were used to calculate response spectrum and were applied in collapse assessment. In addition, three response spectrums referred from Japanese Building Code (JBC, see Figure6) assuming each soil type as soil-type1 (solid), soil-type2 (Moderate) soil-type3 (soft) were also applied in this analysis.

Each model was evaluated collapse limit displacement for each response spectrum by the method explained in section 2.1. The number of combinations was 20 (types of 3 and 6 stories building) x 15 (Observed spectrum:12, JBC spectrum:3) equal to 300.

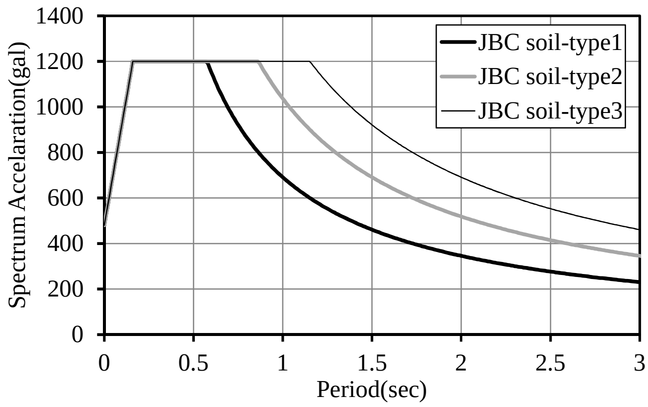

Figure 6 : Seismic response spectrum referred from JBC

In addition, dumping of each model is evaluated as weighted average dumping of each spring which is summation of viscous dumping (assuming 5% of initial viscous dumping) and hysteresis dumping. Hysteresis dumping of each inelastic spring is calculated by energy absorption and potential energy on hysteresis loop.

2.4 Analytical Result

2.4.1 Pushover Analysis

Examples of Pushover results are shown in Figure7. As mentioned above, first story collapse mechanism was generated in all cases.

2.4.2 Capacity curve of converted SDOF system and collapse limit

Figure8 shows examples of the calculation results for capacity curve of each equivalent SDOF system converted from the results of Pushover analysis by EQ.(1) and (2). Evaluated collapse limit points are also displayed in Figure8. Collapse limit points for JBC spectrum are conservative for results using response spectrum calculated by ground motion in past earthquake.

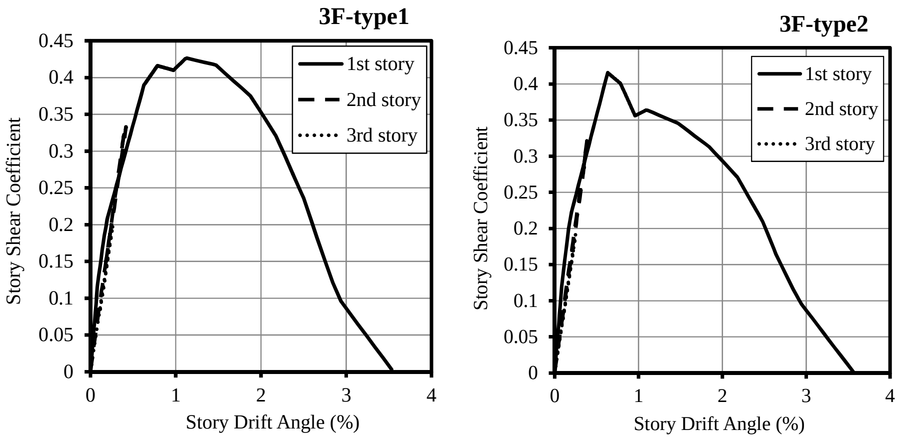

Figure 7 : Results of Pushover analysis (3stories model type1 and 2)

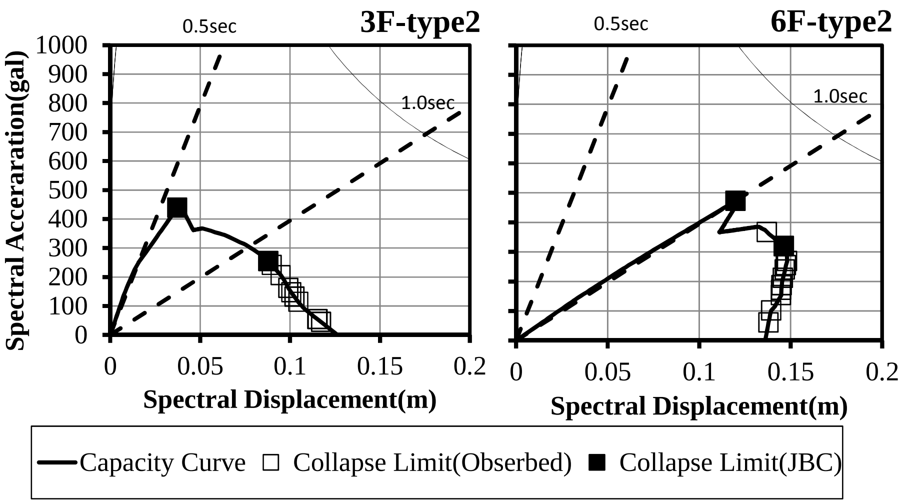

Figure 8 : Results of collapse assessment (3 and 6 stories model type2)

3. COLLAPSE LIMIT DISPLACEMENT AND DAMAGED MEMBERS RATIO

3.1 General Concept for relation of DMR and Collapse Limit Displacement

In this chapter, relation of structural damage of members in static analysis mentioned above and collapse limit displacement calculated previous chapter is investigated. A index of structural damage of members is called as Damaged Members Ratio (DMR) and is defined as Eq.(3) and (4).

$$DMR = \sum_{i=1}^{m} \lambda_i \qquad (3) \qquad\qquad \lambda_i = \frac{\alpha_i \cdot K_{\deg,i}}{\sum_{i=1}^{m} K_{\deg,i}} \qquad (4)$$

Where; λ_i : contribution factor showing that capacity degradation at plastic hinges and shear critical member (these are counted as damage part *i*) contribute capacity degradation of capacity curve of overall building, α_i : effectiveness factor; 0.5 for plastic hinges, 1.0 for shear critical members (these values are assumed in this paper and furthermore studies are needed to determine suitable values), $K_{deg,i}$: slope of capacity degradation curve of damage part *i*.

DMR is plainly explained as a weighted average of capacity degradation curve of each damage part $K_{deg,i}$, because past research (Matsukawa and Maeda, 2013) showed that collapse limit is dominantly decided by capacity degradation curve of equivalent SDOF system and response spectrum shape. DMR is used in correlation analysis to evaluate lower boundary (5% probability of collapse) of collapse limit as shown in Figure9.

From results for 240 of parametric analysis mentioned in previous chapter (analyses of JBC spectrum were omitted), DMR at collapse limit displacement for each model and each response spectrum were obtained. Figure10 shows one of calculation examples of DMR at every analytical step calculated based on pushover analysis mentioned in previous chapter and DMR at collapse limit is marked.

After that, cumulative frequency distribution curve that demonstrates cumulative frequency of collapse risk by DMR at collapse limit is constructed assuming it obeys beta distribution. As the result shown in Figure11, it is found that 5% probability of collapse corresponds 0.20 of DMR, in other words, buildings suffered damage equal to DMR of 0.2 have 5% of collapse risk. Although referring this curve enables to assess collapse risk from DMR as mentioned above and shown in Figure9, models or response spectrum used in this paper may have some bias, therefore, another approach is taken in this chapter using actual damaged building data.

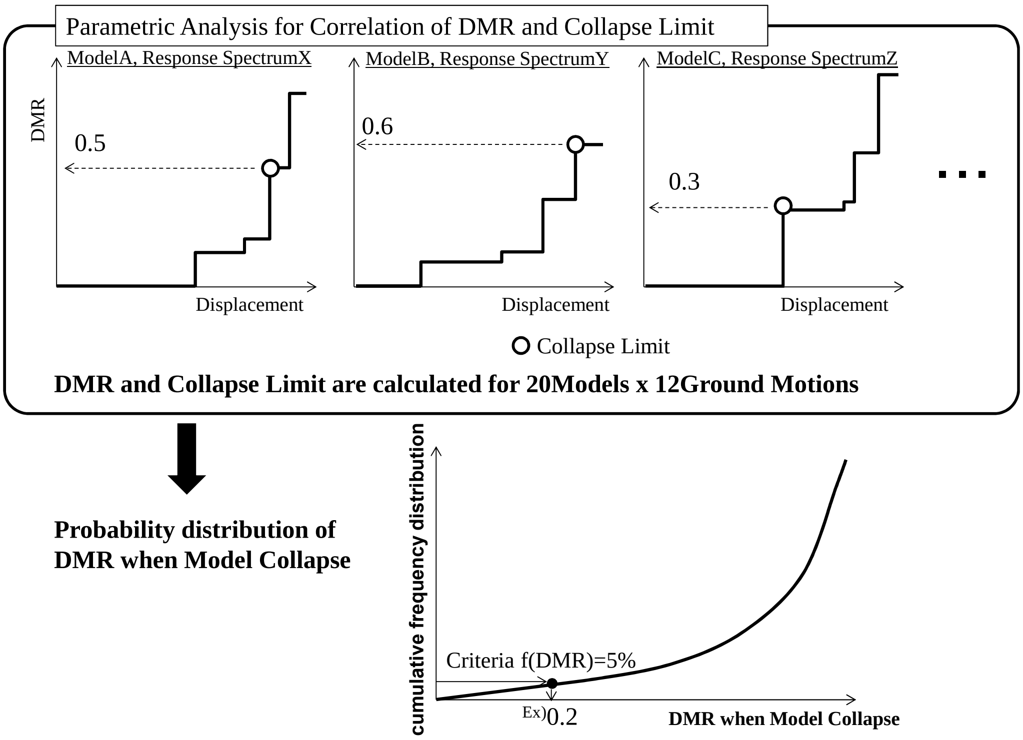

Figure 9 Conceptual drawing of DMR and collapse risk

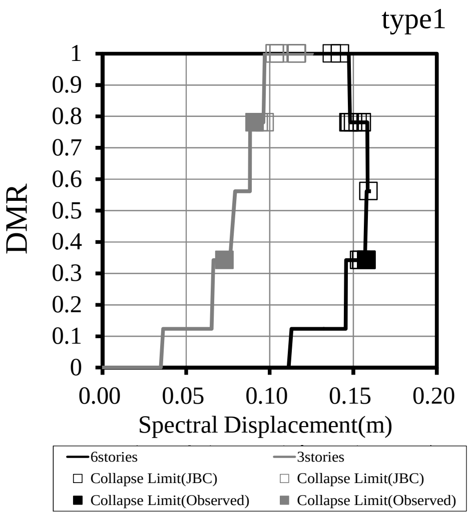

Figure 10 : Examples of DMR

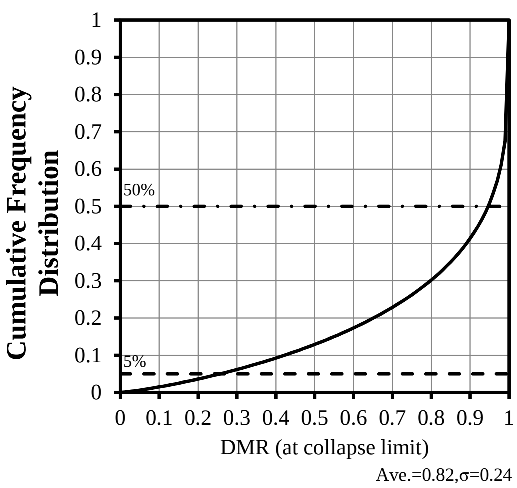

Figure 11 : Cumulative Frequency of DMR

3.2 Database of Damaged Buildings during Past Earthquake

The database was constructed from data of damaged Japanese RC school buildings in past earthquakes (e.g. Southern Hyogo Earthquake 1995, Mid-Niigata Earthquake 2004, Iwate-Miyagi Earthquake 2008 and Tohoku Earthquake 2011). Basic characteristics of the database components are shown in Figure12. In addition, the database consists of buildings classified damage level “heavy” and “collapse”.

In the database, damage class of each member inspected by the researchers are recorded and the damage class relates maximum response of members as shown in Figure13 (JBDPA, 2001).

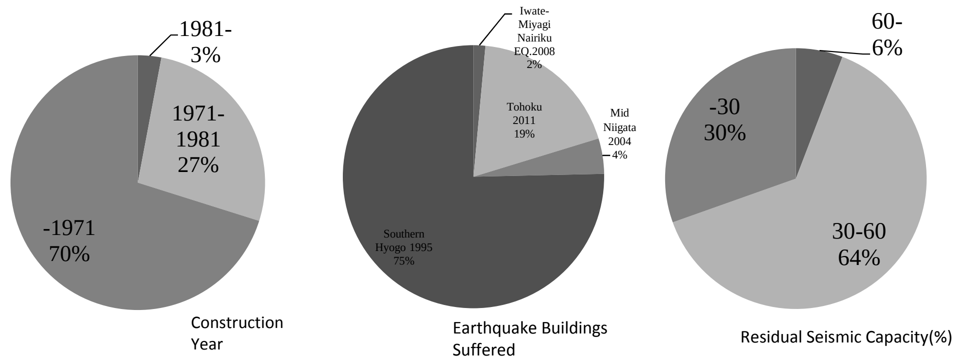

Figure 12 : Component ratios of the database

3.3 DMR at collapse limit

Relation of DMR and building damage level is shown in Figure14. The horizontal axis named as “Residual Seismic Capacity” is calculated capacity of damaged structures referring JBDPA Guideline (JBDPA, 2001). As shown in Figure14, collapsed buildings are pointed at region of DMR > 0.3 and the buildings pointed DMR < 0.3 could avoid collapse (although suffering “heavy” damage was not able to avoid).
From result mentioned previous section, 5% probability of collapse corresponded DMR of 0.2, therefore, the probability was conservative for analysis in this section.
Figure15 shows cumulative frequency distribution of both computational analysis and actual damage data. Computational curve calculated in chapter2 corresponds actual curve at DMR of lower value (DMR < 0.25) region and is conservative at DMR of higher value (DMR > 0.25) region. From these analyses, buildings possibly avoid collapse at displacement that DMR less than 0.2 although furthermore studies are needed.

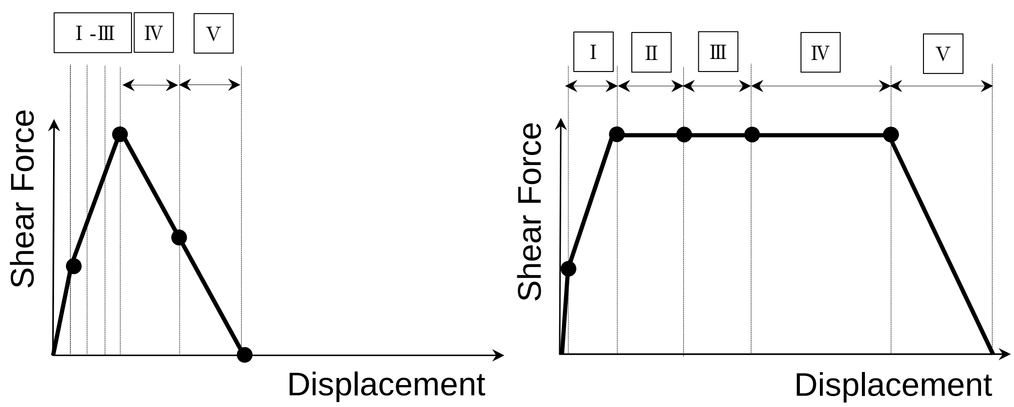

Figure 13 : Damage classification of shear (left) and flexural (right) members

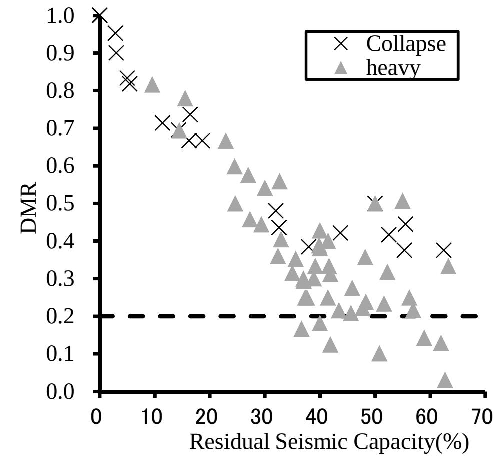

Figure14 DMR and actual damage

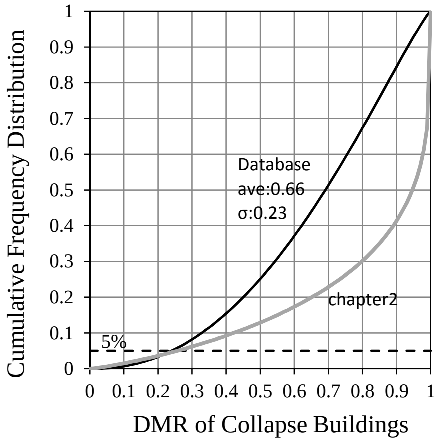

Figure15 Collapse risk based on DMR

4. CON CLUSION REMARKS

Contributions of this paper are shown in as follows;
1) Based on seismic response spectrum and capacity curve of models, evaluation methodology of collapse limit was explained. The method is practical approach to assess building collapse and assessment examples of 3 or 6 stories buildings were shown.
2) Damaged Members Ratio, the index of damage to structure was proposed. From pushover analysis of building models and statistical analysis of actual damaged building data, it is found that RC structures possibly can avoid collapse if structures suffered damage of DMR less than 0.2.

REFERENCES

Haselton, C. B., Liel, A. B. and Deierlein, G.G., 2011. Seismic Collapse Safety of Reinforced Concrete Buildings. I: Assessment of Ductile Moment Frames. *Journal of Structural Engineering.* 481-491.
Matsukawa, K. and Maeda, M. 2013. Methodology to Evaluate Collapse Limit State of R/C Frame Based on Seismic Response Spectrum, Journal of Structural And Construction Engineering. Architectural Institute of Japan. No.693. (Not Published but Accepted)
Architectural Institute of Japan, 2004. *Performance Evaluation of Earthquake Resistant Reinforced Concrete Buildings (Draft) (in Japanese)*, Japan
Japan Building Disaster Prevention Association, 2001. *Guidelines for Post-earthquake Damage Level Classification of Reinforced Concrete Building*. Japan

Ultra high performance concrete using a combination of silicafume and limestone in Vietnam

Nguyen Cong Thang [1], Nguyen Van Tuan[1], Pham Huu Hanh [1]

[1]Department of Building Materials, National University of Civil Engineering, 55 Giai Phong Road, Hanoi, Vietnam

ABSTRACT

Ultra-High Performance Concrete (UHPC) is considered to be one of major breakthroughs in concrete technology with superior quality, especially compressive strength greater than 150 MPa, high fluidity and durability properties. This opens a door for some new and very potential applications in construction industry such as thin shell structures, high rise-buildings, long span bridges, and construction in aggressive environments.

Regarding the material components, in general, a very high mount of cement, about 900-1000 kg/m^3 used to produce UHPC, will cause some disadvantages from the point of view of sustainable development. The use of mineral admixtures to replace cement is one of good ways to overcome this problem.

This paper presents the preliminary results of using a combination of silica fume and limestone powder in Vietnam as cement replacement material in making UHPC. The results show that this combination improves both the flow slump and compressive strength of UHPC. Additionally, a maximum amount of total cement replacement by this combination is also considered in this study. This is very important for the sustainable development of the construction industry.

1. INTRODUCTION

Ultra High Performance Concrete (UHPC) is a new class of concrete with high fluidity, high strength (over 150MPa), high flexual strength (using fiber), low permeability and high durability (AFGC-SETRA, 2002, Buitelaar, 2004). UHPC has been gained a strong interest in research and development from the early 1980s. Up to now, some potential applications of UHPC can be seen such as elements, girders, deck slabs, silos, etc in precast or repairing structures, or making columns with high load, nuclear waste tanks, etc.

UHPC, in general, is composed of cement, silica fume, quart sand (100-600µm) instead of the ordinary aggregate, water and superplasticizer. The high amount of cement in UHPC, about 900-1000 kg/m^3 (Richard and Cheyrezy, 1994) , in general, which impacts on global environment (Vooa and Fosterb, 2010, Turgut, 2007). Therefore, the use of the mineral admixture to replace cement in producing UHPC is feasible both technically, environmentally and economically.

In fact,some mineral admixtures such as ground granulated blast-furnace slag (GGBS), fly ash (FA), Metakaolin, Limestone (LS) have been being used to make normal concrete and even UHPCetc. Among these admixtures, LS is considered as a potential admixture in making UHPC with some advantages (Turgut, 2007, Heikal et al., 2000), i.e. not only reducing cost of UHPC production but also decreasing amount of cement which result in reducing the CO_2 emission and the use of natural resources. In addition, the finer limestone can improve the packing density of system and can densify the transition zone between cement paste and aggregates. The addition of limestone will improve workability of UHPC mixtures and help to disperse cement particles and to enhance the crystalline nucleation, thus promote the hydration of cement and increase compressive strength of UHPC.

This paper presents the exprimental results of using limestone in combination with or without silica fume on properties of UHPC at difference curing regimes. The limestone replacement content is studied from 5 to 20% by weight of binder (cement, silica fume and limestone). Two curing conditions, normal treatment (27±2^{o}C, RH>95%) and heat treatment (90±5^{o}C, RH>95%), are considered in this study.

2. MATERIALS AND METHODS

2.1 Materials

The materials used in this study were Portland cement PC40 (according to Vietnamese standard) with particle size of 14µm, condensed silica fume (SF), limestone (LS), and polycarboxylate based superplasticizer with 30% solid content by weight. The SF has an amorphous SiO_2 content of 92.3% and its mean particle size is about 0.15µm. The particle size distribution and the mean particle size of materials in this study were determined by laser diffraction. Quart sand with a particle size of 600µm. Limestone (LS) with a particle size of 5µm. Oxide compositions of the cement, silica fume and limestone used in this study are shown in Table 1. The particle size distribution of these materials is shown in Figure 1.

Table 1. The chemical composition of limestone, Cement and Silica fume

No	Chemical properties	Units	Contents, %		
			Cement	SF	LS
1	SiO_2	%	20.30	92.3	0.70
2	Fe_2O_3	%	5.05	1.91	
3	Al_2O_3	%	3.51	0.86	0.02
4	CaO	%	62.81	0.32	97.27
5	MgO	%	3.02	0.85	0.55
6	Na_2O	%	-	0.38	0.10
7	K_2O	%	-	1.22	
8	SO_3	%	2.00	0.30	0.10
9	LOI	%	1.41	-	0.92

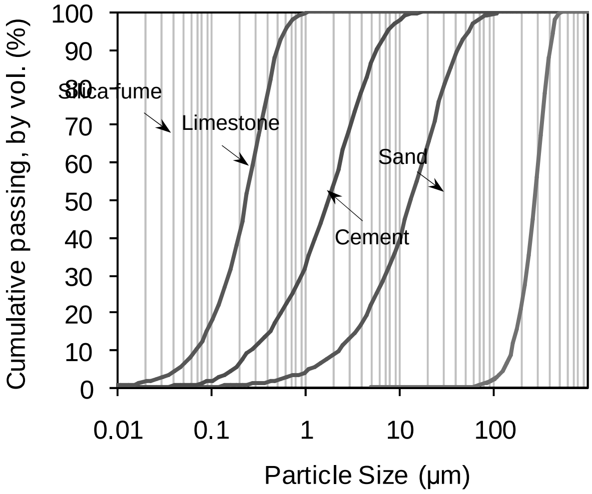

Figure 1. Particle size distribution of materials used in this study determined by laser diffraction

2.2 Methods

The workability of mixtures was determined by means of flow table test. The flow measurements were adjusted between 210 and 230 mm (according to BS 4551-1:1998) by changing the superplasticizer content.
Mixtures were cast into the 50mm×50mm×50mm cubes for the compression test.

3. MIX DESIGN AND MIXING PROCEDURE OF UHPC

3.1 Packing density

Optimization of granular mixture is one of the key issues in the UHPC mix design. The optimization of granular mixtures in this study was predicted by using the packing model developed by Larrard and Sedran (Larrard and Sedran, 1994), with the compaction index of 12.5 (Jones et al., 2002). The granular mixture was considered as a ternary system of sand, cement and admixture (silica fume and limestone) in which the SF content was fixed at 10% by weight of binder (cement, limestone and silica fume). The LS content was replaced about 0-20% by weght of binder. Thus, the granular mixtures are considered as a binary system of sand and binder.

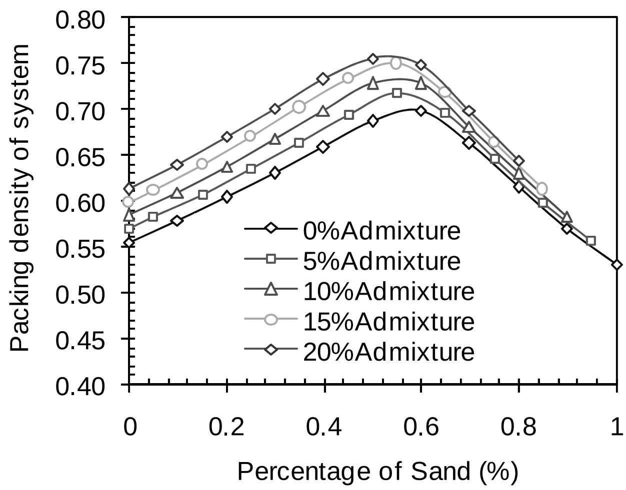

Figure 2: Packing density of system of sand – cement – silica fume - limestone, Binder herein is the mixture of cement, silica fume and limestone; 10%SF is fixed

The optimized packing of this ternary system was achieved at sand / (sand + binder) ratio of 0.5 and the content of LS about 20% by weight of binder.

3.2. UHPC compositions

Based on the results of the optimized packing density of granular mixtures, UHPC mixtures were designed with a sand / (sand + binder) ratio of 0.5. The water to binder (w/b) ratio of the mixtures was fixed at 0.18 by weight of the binder. The mix composition of UHPC was prepared as shown in Table 2

Table 2: UHPC compositions used in this study

No	Amount of binder (kg)	w/b ratio (by weight)	Sand/binder ratio (by weight)	SF, (% by weight)	LS, (% by weight)	Amount of superplasticizer (% by weight of binder)
1	1122	0.18	1	0	0	0
2	1119	0.18	1	0	5.0	0.9
3	1116	0.18	1	0	10	0.85
4	1112	0.18	1	0	15	0.75
5	1109	0.18	1	0	20	0.7
6	1102	0.18	1	10	5.0	0.7
7	1099	0.18	1	10	10	0.65
8	1096	0.18	1	10	15	0.6
9	1093	0.18	1	10	20	0.55

3.3. Mixing, workability and curing conditions of UHPC

UHPC was mixed in a Habart mixter (20 litre). The mixing procedure was shown in Figure 4.

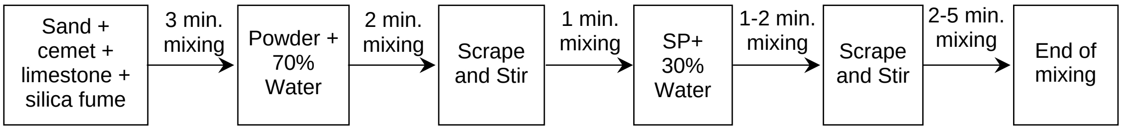

Figure 3: Mixing procedure for UHPC

Mixtures were cast into the 50mm×50mm×50mm cubes for the compression test and kept in moulds at temperature of 20°C, 95% relative humidity (RH) for 24 hours. After demoulding, samples were stored at two different conditions

(1) Normal treatment (at 20°C and 100% RH) until testing

(2) Steam-cured (at 90±5^{o}C and 95% relative humidity) for 48 hours, after that, continuous treating at at 20°C and 100% RH until testing.

Compressive strength of samples was tested at the age of 3,7, 28 and 90 days.

4. RESULTS AND DISCUSSION

4.1 Workability of UHPC mixtures

The amount of superplasticizer used in the mixtures for achieving the average flow diameter from 210 to 230mm, is presented in Figure 4. It can be seen that with the cement replacement percentage from 0 to 20%, the addition of LS decreases workability of mixtures. This was explained by the spherical shape of LS particles, which act as a lubricant. The effect of LS to workability of UHPC, mean particle of LS is 5µm , which is smaller than that of the cement particle size. Therefore, the LS will fill the empty space in the system and release water from pores, it means that, the free water is increased and thus improving the workability.

On the other hand, the range of particle size of LS between of the ranges of cement and silica fume (Figure 1), therefore the combination of LS and SF can make the mixture denser compared to the mixture without LS and SF (Figure 3).

The combination of 10% SF and LS improve the workability of UHPC mixtures. This was explained by the spherical shape of SF particles, in which the “ball bearing effect” caused by these particles will reduce the dry friction between cement particles, and thus improve the workability of UHPC mixtures.

From this result, it raises the idea that LS may be used to combine with SF to increase the workability of UHPC mixtures. Indeed, the amounts of superplasticizer of the LS mixtures reduce with addition of 10% SF. Moreover, the maximum amount of cement replacement by the combination of LS and SF can be increased to 30%.

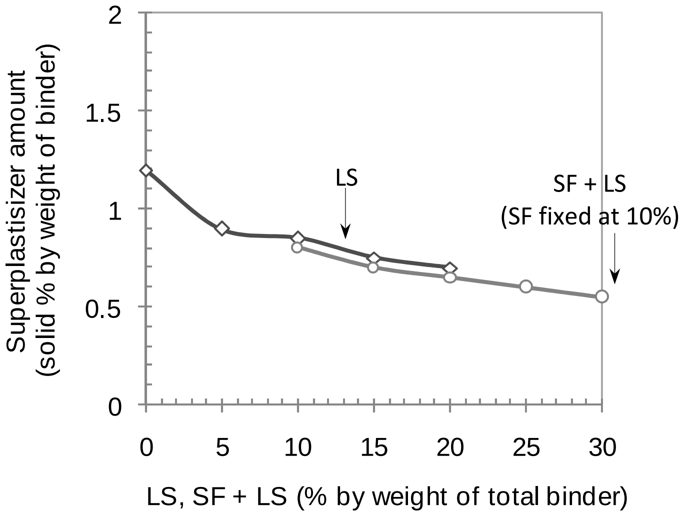

Figure 4: Amount of superplasticizer of UHPC mixtures and %LS, %(SF+LS) for achieving a constant flow value of mixtures between 210 and 230 mm, w/b = 0.18

4.2. The effect of LS on compressive strength of UHPC

The effect of LS on compressive strength of UHPC was investigated (Figure 6). It can be seen that the compressive strength of UHPC increases with the addition of LS. The highest compressive strength of the LS samples was achieved with using 10% LS, 137MPa and 155.3MPa with normal treatment and steam-cured, respectively. This result is significant higher than that of the control sample containing 0%LS. Although the compressive strength of the LS sample decreased with an increase of the LS replacement.

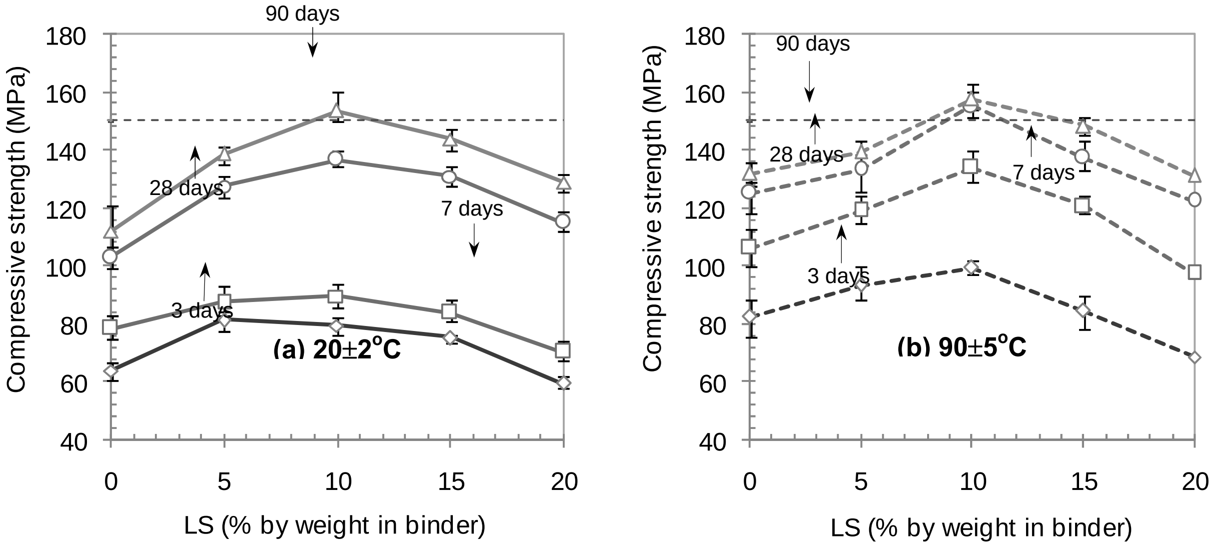

Hình 5: Effect of LS on compressive strength of UHPC

w/b = 0.18, (a) 20±2^{o}C, (b) 90±5^{o}C

Devolopment of the compressive strength with the addition of LS was shown in Figure 7. UHPC The addition of 5% and 10% LS and cured at 20^{o}C inscrease in compressive strength at early age. Especially, after 28 days had a very high compressive strength but did not match that at 90 days. This was explained, the replacement of cement by limestone strongly improves the workability of UHPC mixtures. In addition, limes improves to disperse cement particles and create the crystalline nucleation to promote the hydration of cement which increses the compressive strength at early age.

The 90^{o}C speciments can be seen achieved higher compressive strength at early age but this decreases more slowly at later (90 days). The speciments at 90 days is not much higher than that at 28 days. The effect of LS on the compressive strength is investigated. At LS contain at 5% and 10% by weight the compressive strength increases initially but decreases afterward when LS increases (Figure 7).

The highest compressive strength of the LS samples was attained with 10% LS replacement under 20^{o}C and 90^{o}C curing. Therefore, the LS content of 10% was considered as a maximum cement replacement value.

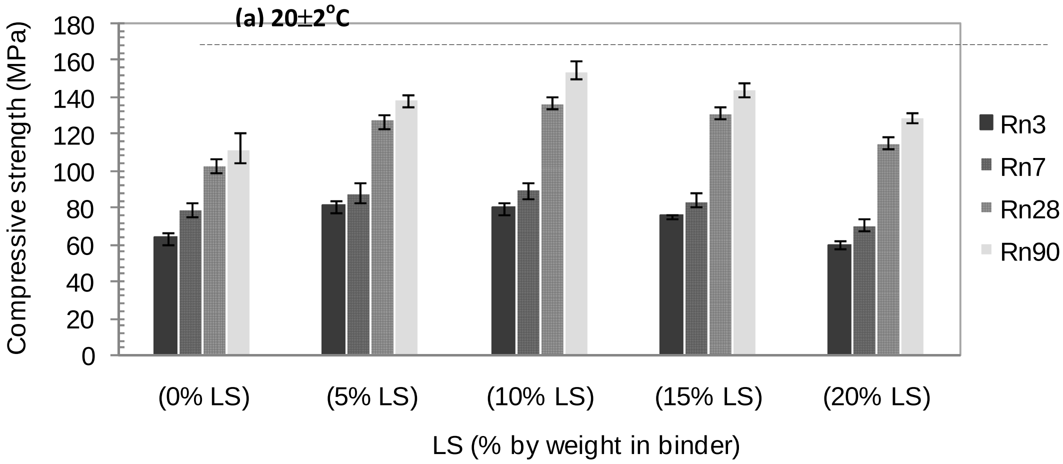

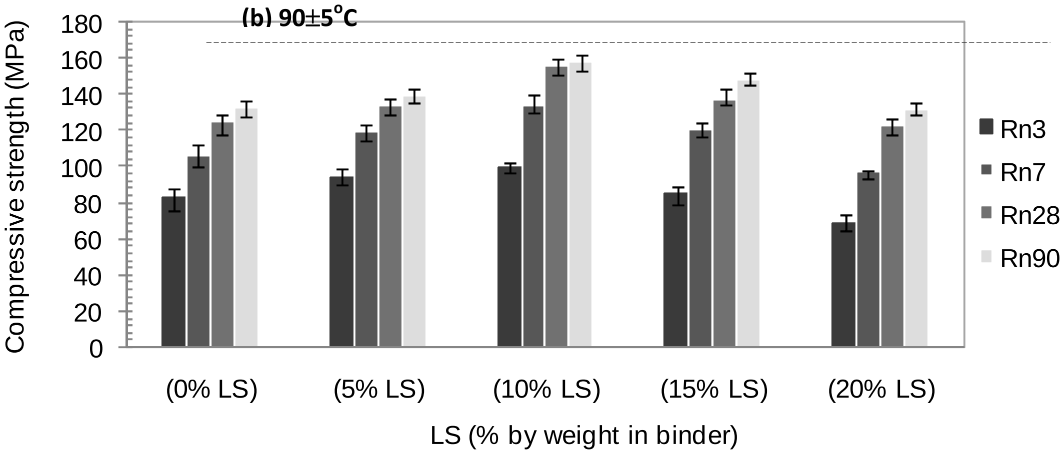

Figure 6: Devolopment of the compressive strength of UHPC over time, w/b = 0.18, (a) 20±2^{o}C, (b) 90±5^{o}C

4.3. Effect of combination of limestone and silica fume on compressive strength of UHPC

The previous work (Thang et al., 2012) shows that, the amount of SF was at 10% which was the most improvement not only workability but also compressive strength. Therefore, the content of SF was fixed at 10% by weight of binder in this research. The effect of combination of LS and SF on the 3, 7, 28, 90 day workability and compressive strength of UHPC was studied with LS contents in the range from 5 to 20% and with a SF content fixed at 10%. The result is depicted in Figure 8, 9.

The results show that, the combination of LS and SF improves not only workability but also compressive strength of UHPC mixture. Compared to the LS samples, the compressive strength of combination LS and SF is higher at the same contents.

It is clear that combined with 10% SF, the highest compressive strength of the combination LS and SF samples was attained with 10% LS replacement which was 153 MPa and 157 MPa under 20^{o}C and 90^{o}C curing, respectively. Under 90^{o}C curing, the LS replacement can be possibly increased to 15%. the compressive strength of all samples is in excess of 150 MPa. Therefore, when 10% SF was used, the total cement replacement by using a blend of LS and SF can reach to 25%. This is very important for the sustainable development of the construction industry.

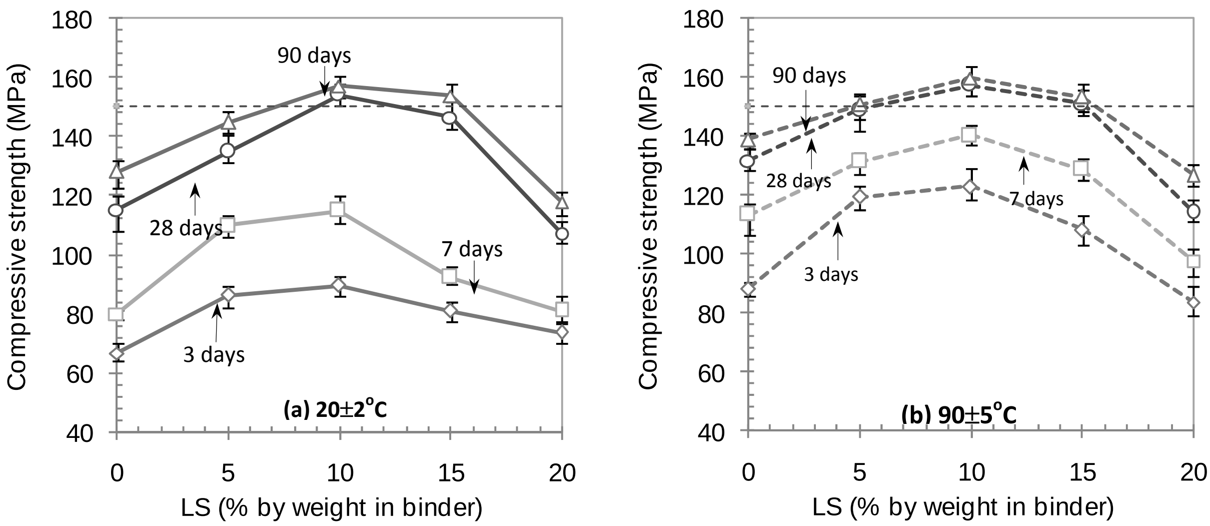

Figure 7: Effect of LS on compressive strength of UHPC, 10%SF was fixed, w/b = 0.18, (a) 20±2^{o}C, (b) 90±5^{o}C

Figure 9 shows the development of the compressive strength on the 3, 7, 28, 90 day of UHPC using combination LS and SF under 20^{o}C and 90^{o}C curing. The compressive strength at 20^{o}C curing increased slowly at early age but faster strength gain at 90 day which did not match that of the 90^{o}C cured specimens. From observation of the rate of increase in strength it seems unlikely that the strength of the 20^{o}C cured specimens would reach that of the 90^{o}C cured specimens at later ages. However, the compressive strengths of 20^{o}C cured UHPC is in excess of 150 MPa at 90 day.

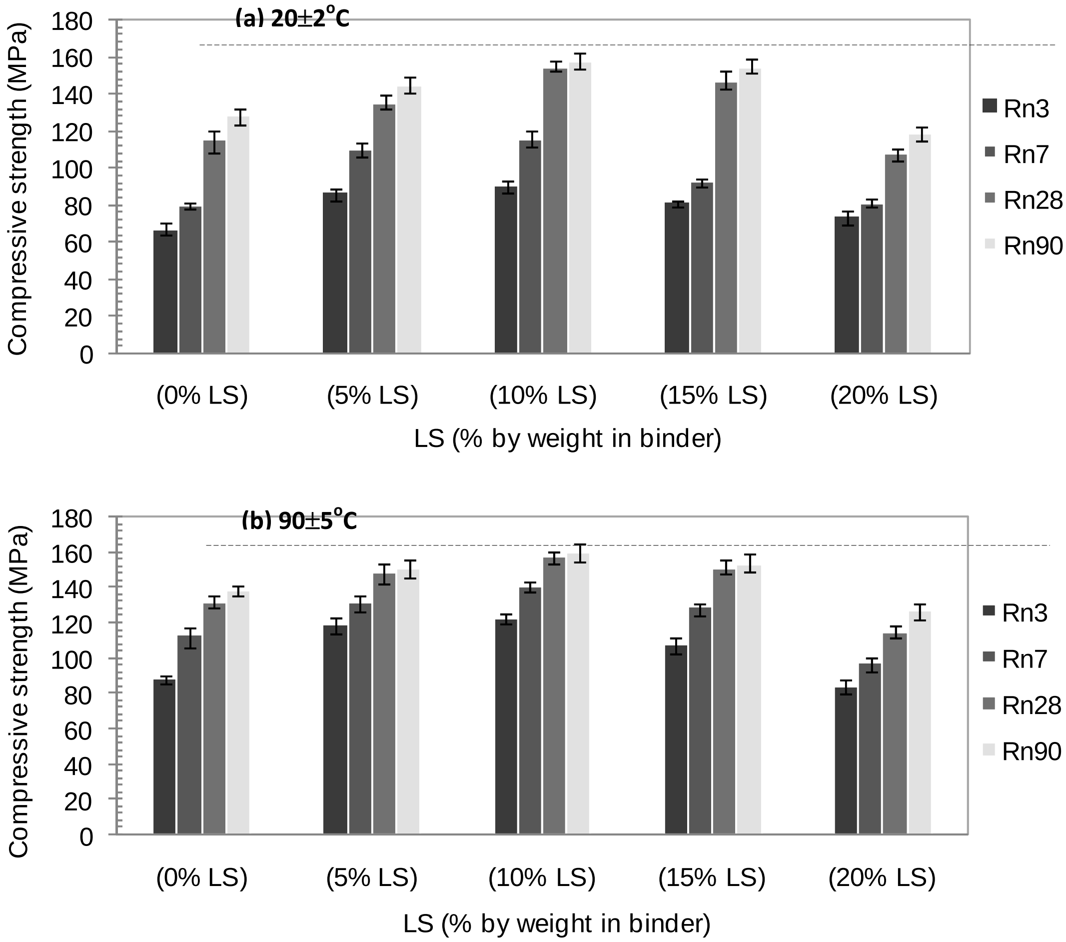

Figure 8: Devolopment of the compressive strength of UHPC over time, SF was fixed at 10%, w/b = 0.18, (a) 20±2^{o}C, (b) 90±5^{o}C

5. CONCLUSIONS

This paper presents the possibility of using LS in combination with and without SF to produce UHPC in order to get the benefits regarding costs, sustainability. Following conclusions can be drawn:

- Limestone can be used to replace cement to produce UHPC without decreasing the compressive strength.

- The addition of LS strongly improves the workability of UHPC mixture. The highest compressive strength of the LS samples was attained with 10% LS replacement under 20^{o}C and 90^{o}C which was 137MPa and 155.3MPa, respectively.

- LS in combination with SF improves not only workability but also compressive strength, the maximum of total cement replacement percentage to 25%, in which the percentage of LS replacement was 15%. The highest compressive strength of the LS samples was attained with 10% LS replacement under 20^{o}C and 90^{o}C which was 153MPa and 157MPa, respectively.

REFERENCES

AFGC-SETRA 2002. *Ultra High Performance Fibre-Reinforced Concretes,* Paris, France, Interim Recmmendations, AFGC publication.

BUITELAAR, P. 2004. Ultra High Performance Concrete: Developments and Applications during 25 years. *International Symposium on UHPC, Kassel, Germany*.

HEIKAL, M., EL-DIDAMONY, H. & MORSY, M. S. 2000. Limestone-filled pozzolanic cement. *CEMENT and CONCRETE RESEARCH*, 7.

JONES, M., ZHENG, L. & NEWLANDS, M. 2002. Comparison of particle packing models for proportioning concrete constitutents for minimum voids ratio. *Materials and Structures*, 35**,** 301-309.

LARRARD, F. D. & SEDRAN, T. 1994. Optimization of ultra-high-performance concrete by the use of a packing model. *Cement and Concrete Research,* 24**,** 997-1009.

RICHARD, P. & CHEYREZY, M. H. 1994. "Reactive Power concretes with high ductility and 200-800 MPa compressive strength." in Mehta, P.K. (ED). *Concrete Technology: Past, Present and Future, Proceedings of the V. Mohan Malhotra Symposium***,** ACI SP 144-24, 507-518. Detroit: Victoria Wieczorek.

THANG, N. C., TUAN, N. V. & HANH, P. H. 2012. Research on production of Ultra-High Performance Concrete using materials available in Vietnam. *Review of Ministry of Construction***,** 71-74.

TURGUT, P. 2007. Cement composites with limestone dust and different grades of wood sawdust. *Building and Environment***,** 7.

VOOA, Y. L. & FOSTERB, S. J. 2010. Characteristics of ultra-high performance 'ductile' concrete and its impact on sustainable construction. *The IES Journal Part A: Civil & Structural Engineering,* 3**,** 168–187.

Analytical and experimental study for seismic design of a typical bridge pier according to Vietnamese earthquake design code

PHAM Hoang Kien
Lecturer, ICE, the University of Transport and Communications, Vietnam
phkien@utc.edu.vn

ABSTRACT

Lying in the tectonical position of the Indochina and southern China micro-plates' boundary, Vietnam is supposed to be in the low to moderate earthquake region in the world. In the past, some historical earthquakes with large magnitudes of 5.0 to 6.8 Richte' scales were recorded in northern Vietnam such as earthquakes at Dien Bien (1935, M =6.8 and 2001, M = 5.3), earthquakes at Luc Yen (1953, 1954, M = 5.4), earthquake at Tuan Giao (1983, M = 6.7). Nowaday, seismic design is the compulsory issue when designing bridge and building structures in Vietnam. In this paper, firstly, a brief overview of seismic activities and design methodology stated in earthquake design code in Vietnam is presented. Then the dynamic analyses using fiber element model and the experimental study using shaking table test for a typical bridge pier are carried out. In these studies, due to the lack of strong ground motion records in Vietnam, the earthquake time-history used in non-linear dynamic analysis and shaking table test is the artificially generated time-history which fits to design response spectrum in Vietnamese earthquake design code. Through studies, the evaluations on results obtained by different design methods (response spectrum method and non-linear time-history method) are performed. It is found that the dynamic analysis using fiber model could simulate the experimental bridge pier behavior well.

Keywords: *earthquake disaster, Vietnamese earthquake design code, fiber element model, shaking table test*

1. INTRODUCTION

Vietnam is tectonically located in the position of the Indochina and southern China micro-plates' boundary, and it has been classified as low to moderate earthquake region in the world. Most of the main faults in Vietnam are strike-slip type; it remains tectonically active as shown by the occurrence of moderate earthquakes in the country and adjacent areas. In the research project named "Research and Forecasting Earthquakes and Ground Movements in Vietnam", which was implemented by the Vietnam Institute of Geophysics (*VIG,2005*), it is found that from 114 AD to 2003 AD Vietnam, either by measurement or by studying the historical archives, recorded 1645 earthquakes with magnitude (M) of 3.0 to 6.8 Richter's scale. In the past, Vietnam had been considered as a safe country with respect to earthquake disaster. However, recent earthquakes in the North and the South of the country made the government and society pay more attention to earthquake hazard risk. If large earthquakes occur in urban areas such as Hanoi and Ho Chi Minh city, the damages and losses may possibly be much more than those caused by typhoons or floods. Seismic design is now the compulsory issue when designing bridge and building structures in Vietnam. In this paper, the following contents are studied: (i) seismic activities in Vietnam; (ii) design methodology in Vietnamese earthquake design code; (iii) dynamic analyses using fiber element model and experimental study using shaking table test for a typical bridge pier. Due to the lack of strong ground motion records in Vietnam, the earthquake time-history used in non-linear dynamic analysis and shaking table test is the artificially generated time-history which fits to design response spectrum in Vietnamese earthquake design code.

2. SEISMIC ACTIVITIES IN VIETNAM

Results of a research project of the Vietnam Institute of Geophysics (*VIG, 2005*) showed that in the 20th century Vietnam had two earthquakes with intensity I0 = 8 ÷ 9 (MSK-64) and magnitude (M) of 6.5 ÷ 7 of Richter's scale, 15 earthquakes with I0 = 7 and M = 5 ÷ 5.9, and more than 100 earthquakes with I0 = 6 ÷ 7 and M = 4.5 ÷ 4.9. Seismic research by the VIG has also established a zoning map for maximum credible earthquakes in Vietnam (Figure 1).

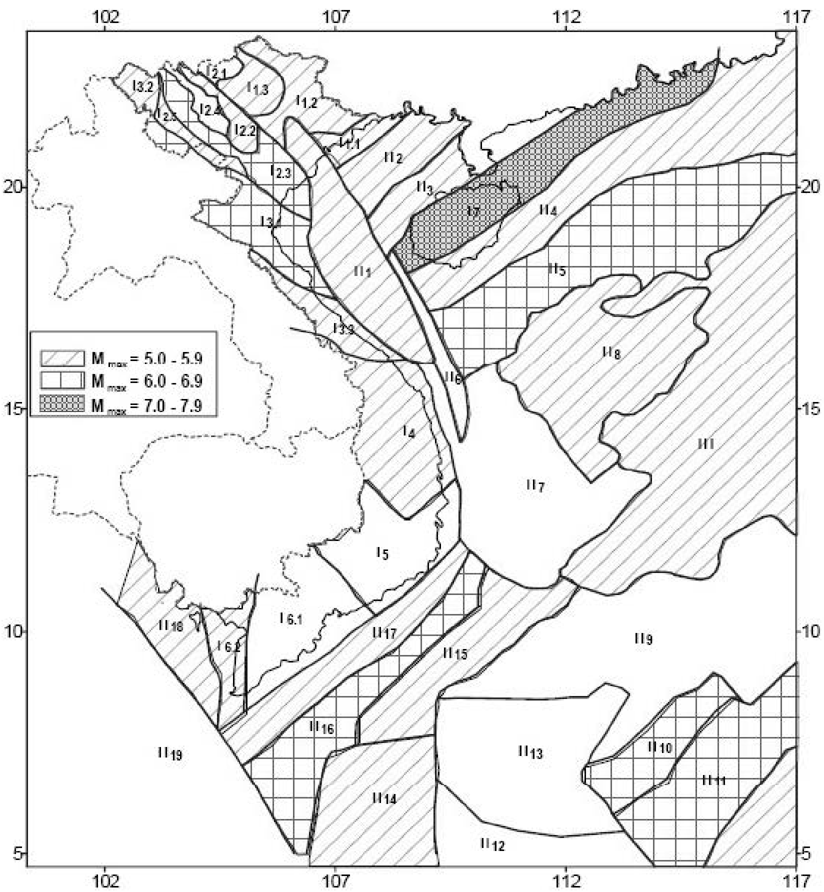

Figure 1: Maximum credible earthquakes in Vietnam (Cao, 2006)

From 1900 to 2001 strong earthquakes were recorded in the North of Vietnam, also in the Hanoi area. Two strongest earthquake were the Dien Bien earthquake (1935, M = 6.8) and Tuan Giao earthquake (1983, M = 6.7). All these earthquakes occurred in the Northwest of Vietnam, close to Chinese Yunan province and Laos. Many houses suffered damage and collapse during these two strong earthquakes.
On 19 February 2001, a strong earthquake with recorded magnitude (M) of 5.3 of Richter's scale and intensity (I0) of 7 ÷ 8 had occurred in Dien Bien Phu area (the epicenter in Nam Oun (Laos), about 15 km from Dien Bien Phu city). There were hundreds of aftershocks of which the strongest had magnitude up to 4.9. The earthquake caused destruction of building and constructions in the area of thousands square kilometers. There were 130 houses damaged and needed to be reconstructed, 1044 houses needed to be strengthened or retrofitted, 2044 houses slightly damaged and 4 people injured.
South of Vietnam is the region where the seismic activities were considered very low and the effects of earthquakes on structures were not needed to be considered. Therefore, when the earthquakes occurred in this region in August and November 2005, it surprised many scientists. These two earthquakes (with M = 4.6 and I0 =5 occurred on 5 August 2005 and with M = 5.5 occurred on 8 November 2005) could possibly be the strongest earthquakes in the South of Vietnam. It is said that, these seismic activities, both in the North and the South of Vietnam, made the government and society pay more attention to earthquake hazard risk. At present time, Vietnamese Seismological Network is established and it can monitor the seismic events of magnitude larger than 3.0 in the territory of Vietnam. Figure 2 shows the time history of the Dien Bien earthquake (2001) recorded at Dien Bien station.

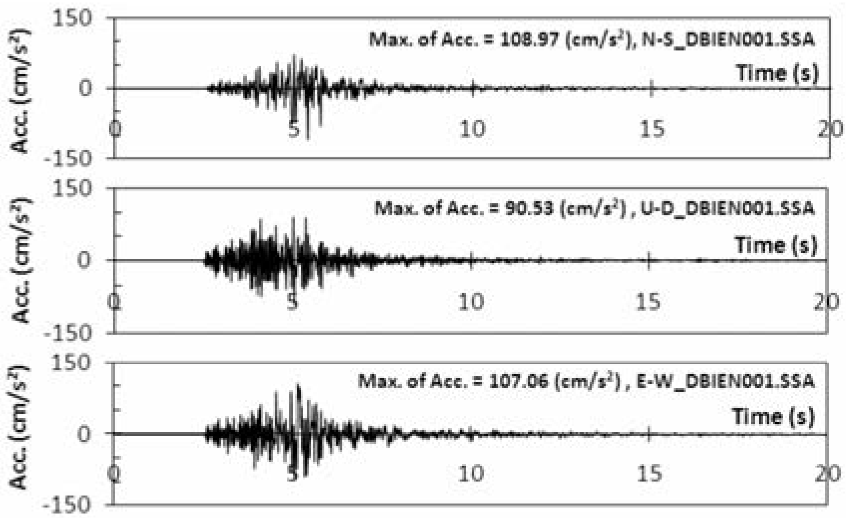

Figure 2: Time history of the Dien Bien earthquake (2001) recorded at Dien Bien station (DBV-21°23.38'N, 103°01.10'E).

3. METHODOLOGY IN VIETNAMESE EARTHQUAKE DESIGN CODE

The specification for bridge design in Vietnam (named as *22TCN 272-05*) is based on the *AASHTO LRFD 1998*. Seismic design is only a part of *22TCN 272-05*.

Vietnam also has an earthquake-resistant design specification mainly applied for building structures (named as *TCXDVN 375-2006*), which is based on the *EUROCODE 8*. The object of study in this paper is bridge pier so seismic design methodology in *22TCN 272-05* will be introduced.

3.1 Seismic design in *22TCN 272-05*

3.1.1 Seismic performance zones

22TCN 272-05 requires that each bridge shall be assigned to one of the three seismic zones with corresponding acceleration coefficient as shown in Table 1.

Table 1: Seismic zones

Acceleration coefficient	Seismic zone	MSK - 64 class
A ≤ 0.09	1	Class ≤ 6.5
0.09 < A ≤ 0.19	2	6.5 < Class ≤ 7.5
0.19 < A < 0.29	3	7.5 < Class ≤ 8

3.1.2 Elastic seismic response coefficient

The elastic seismic response coefficient, C_{sm} for the mth mode of vibration shall be taken as:

$$C_{sm} = \frac{1.2AS}{T_m^{2/3}} \leq 2.5A \qquad (1)$$

where:

T_m = period of vibration of the m th mode (s)

A = acceleration coefficient

S = site coefficient

The determination of the period of vibration, T_m, should be based on the nominal, unfactored mass of the component or structure. For soil profiles III and IV, and for modes other than the fundamental mode that have periods less than 0.3s, C_{sm} shall be taken as:

$$C_{sm} = A(0.8 + 4.0\, T_m) \qquad (2)$$

If the period of vibration for any mode exceeds 4.0 s, the value of C_{sm} for that mode shall be taken as:

$$C_{sm} = \frac{3AS}{T_m^{4/3}} \qquad (3)$$

An example of elastic seismic response coefficient is shown in Figure 3.

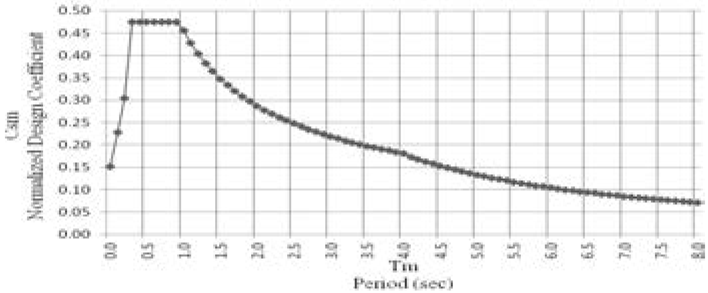

Figure 3: Example of elastic seismic response coefficient

3.1.3 Seismic design methodology

(1) Selection of design method

For multispan structures, the minimum analysis requirements are specified as shown in Table 2 in which:

*	=	no seismic analysis required
UL	=	uniform load elastic method
SM	=	single-mode elastic method
MM	=	multimode elastic method
TH	=	time history method

Table 2: Minimum analysis requirements for seismic effects

Seismic Zone	Single-Span Bridges	Multispan Bridges					
		Other Bridges		Essential Bridges		Critical Bridges	
		regular	irregular	regular	irregular	regular	irregular
1	No seismic analysis required	*	*	*	*	*	*
2		SM/ UL	SM	SM/ UL	MM	MM	MM
3		SM/ UL	MM	MM	MM	MM	TH

(2) Single-Mode Methods of Analysis

Either of the two single-mode methods of analysis specified herein may be used where appropriate.

- Single-Mode Spectral Method

The single-mode method of spectral analysis shall be based on the fundamental mode of vibration in either the longitudinal or transverse direction. This mode shape may be found by applying a uniform horizontal load to the structure and calculating the corresponding deformed shape. The natural period may be calculated by equating the maximum potential and kinetic energies associated with the fundamental mode shape. The amplitude of the displaced shape may be found from the elastic seismic response coefficient, C_{sm}, and the corresponding spectral displacement. This amplitude shall be used to determine force effects.

- Uniform Load Method

The uniform load method shall be based on the fundamental mode of vibration in either the longitudinal or transverse direction. The period of this mode of vibration shall be taken as that of an equivalent single mass-spring oscillator. The stiffness of this equivalent spring shall be calculated using the maximum displacement that occurs when an arbitrary uniform lateral load is applied to the bridge. The elastic seismic response coefficient, C_{sm}, shall be used to calculate the equivalent uniform seismic load from which seismic force effects are found.

(3) Multimode Spectral Method

The multimode spectral analysis method shall be used for bridges in which coupling occurs in more than one of the three coordinate directions within each mode of vibration. As a minimum, linear dynamic analysis using a three-dimensional model shall be used to represent the structure. The number of modes included in the analysis should be at least three times the number of spans in the model. The elastic seismic response spectrum shall be used for each mode. The member forces and displacements may be estimated by combining the respective response quantities (moment, force, displacement, or relative displacement) from the individual modes by the Complete Quadratic Combination (CQC) method.

(4) Time-History Method

Any step-by-step time-history method of analysis used for either elastic or inelastic analysis shall satisfy the requirements. The sensitivity of the numerical solution to the size of the time step used for the analysis shall be determined. A sensitivity study shall also be carried out to investigate the effects of variations in assumed material hysteretic properties. The time histories of input acceleration used to describe the earthquake loads shall be selected in consultation with the Owner. Unless otherwise directed, five spectrum-compatible time histories shall be used when site-specific time histories are not available. The spectrum used to generate these five time histories shall be the same as that used for the modal methods.

4. TIME HISTORY ANALYSIS AND SHAKING TABLE TEST FOR A BRIDGE PIER

4.1 Test specimen

Figure 4 shows the specimen tested in this study. This is a 1/8-scale model. The column diameter is 375 mm, and the height from the bottom of the column to the center of gravity of the top mass is 1400 mm, resulting in an effective aspect ratio of 3.7. Steel plates that idealize the inertia mass and dead load from superstructure are firmly integrated at the top of specimen. The inertia mass is 1,300 kg. The specimen is reinforced longitudinally with 8 of 18-mm diameter deformed bars (D18). Hoop reinforcement of 6-mm diameter deformed bars (D6) is used to confine the concrete core, spaced at a 100-mm pitch. The D10 and D6 bars have yield strengths of 400 MPa. The strength of concrete was 30 MPa.

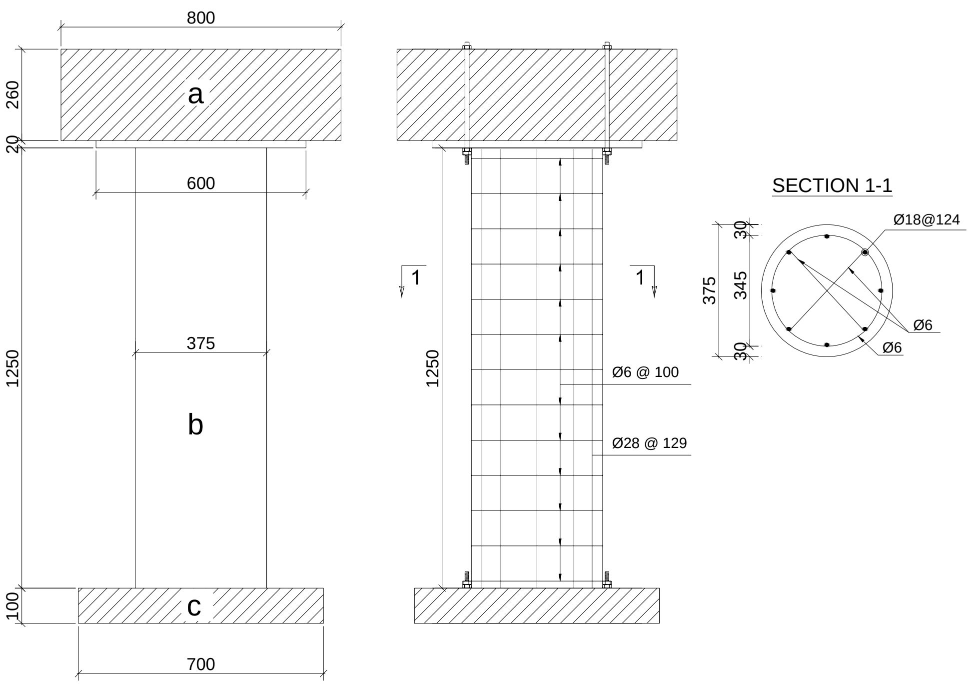

Figure 4: Test specimen

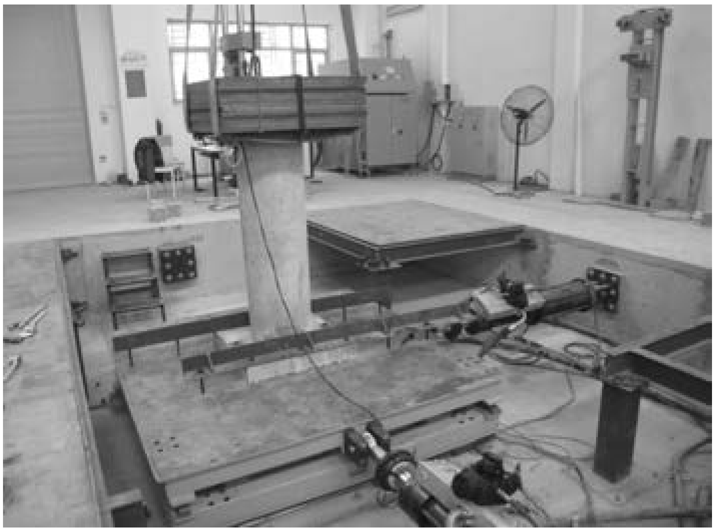

Figure 5: Test set up

4.2 Input ground motion

Due to the lack of strong ground motion records in Vietnam, the earthquake time-history used in shaking table test is the artificially generated time-history which fits to design response spectrum in *22TCN 272-05* (Figure 3). Basic input ground motion used in test is shown in Figure 6.

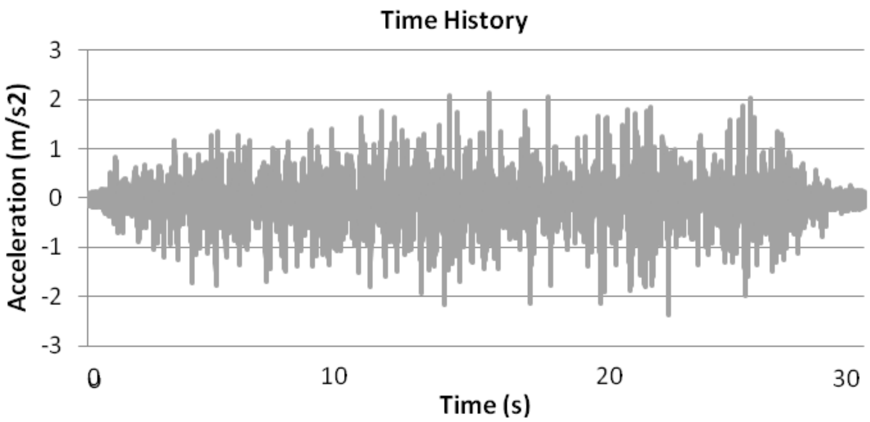

Figure 6: Basic input ground motion used in shaking table test

4.3 Analysis using fiber element model

Figure 7 shows the fiber model used in analytical simulation. Fiber model discretizes and analyzes the section of a beam element into fibers, which only deform axially. When a fiber model is used, the moment-curvature relationship of a section can be rather accurately traced, based on the assumption of the stress-strain relationship of the fiber material and the distribution pattern of sectional deformation. Especially, it has the advantage of considering the movement of neutral axis due to axial force. On the other hand, a skeleton curve based hysteresis model has a limitation of accurately representing the true behavior because some behaviors of a beam element under repeated loads have been idealized. In a fiber model, the status of fibers is assessed by axial deformations corresponding to the axial and bending deformations of the fibers. The axial force and bending moments of the section are then calculated from the stress of each fiber. The properties of nonlinear behavior of a section in a fiber model are defined by the stress-strain relationship of nonlinear fibers.

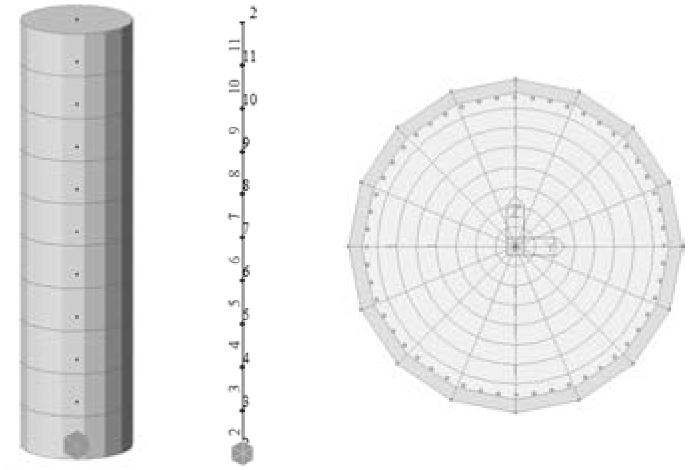

Figure 7: Structure model in analytical simulation

4.4 Dynamic response of the selected bridge pier

Figure 8 shows dynamic acceleration and displacement response at the top mass. The results of both analytical simulation and shaking table test are presented at the same figure. The input ground motion used in this analysis and shaking table test has amplitude 2 times larger than the basic one shown in Figure 6.
Shaking table tests were performed at University of Transport and Communications, Hanoi, Vietnam. Shaking table of University of Transport and Communications is the second one installed in Vietnam. The tests presented in this study are one of the first shaking table tests implemented in Vietnam. Comparing the results, it is found that the dynamic analysis using fiber model could simulate the experimental bridge pier behavior well.

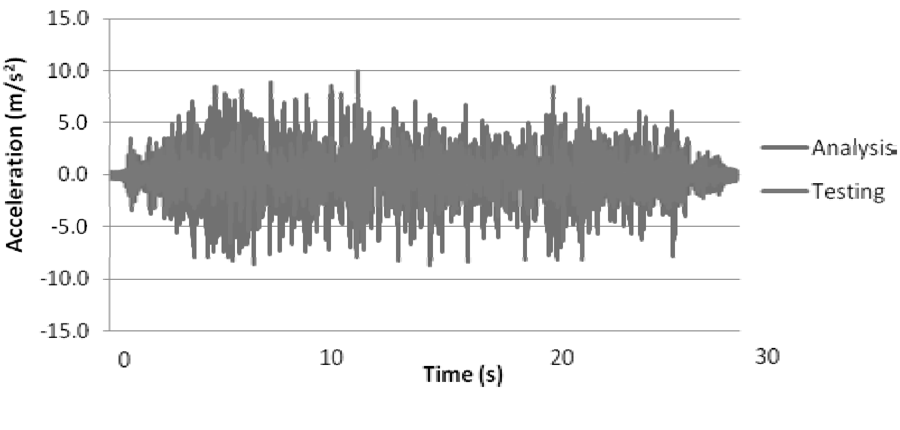

(a) Acceleration response at the top mass

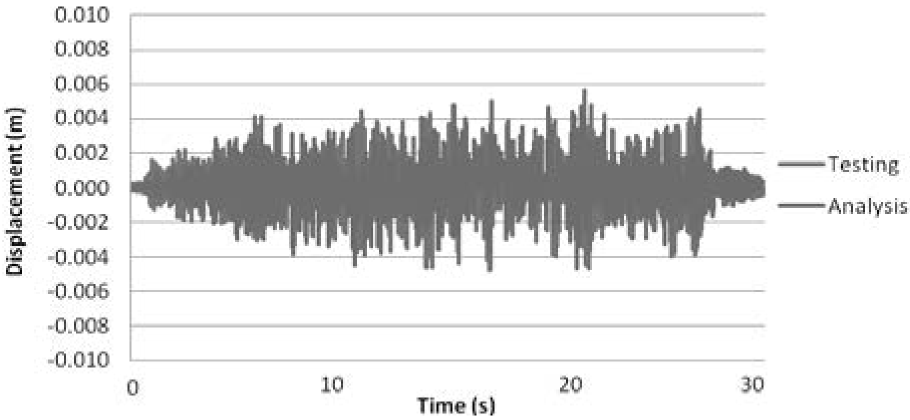

(b) Displacement response at the top mass

5. CONCLUSIONS

In this study, firstly, a brief overview of seismic activities in Vietnam is summarized and seismic design methodology in Vietnamese design code is presented. Then to investigate the dynamic response of a typical reinforced concrete bridge pier, an earthquake simulation test and dynamic analyses are conducted. Below are the conclusions determined from this study:

(1) Vietnam had been considered as a safe country with respect to earthquake disaster. However, recent earthquakes in the North and even in the South made the government and society pay more attention to earthquake hazard risk.
(2) If large earthquakes occur in urban areas such as Hanoi and Ho Chi Minh city, the damages and losses may possibly be much more than those caused by typhoons or floods.
(3) For a typical reinforced concrete bridge pier, generally, seismic design is not the critical one which decides bridge pier design.
(4) The dynamic analysis using fiber model could simulate the experimental bridge pier behavior well.
(5) Experimental test using shaking table should be further conducted in Vietnam to utilize the test equipments for earthquake hazard risk management.

ACKNOWLEDGEMENT

Supports for this research were provided by the Ministry of Education and Training (MOET, Vietnam) and the University of Transport and Communications (UTC, Hanoi, Vietnam). The author extends his appreciation to MOET for financial support, and to UTC for allowing using shaking table test equipment of the University.

REFERENCES

22TCN 272-05, 2005. *Specification for Bridge Design.* Ministry of Transport of Vietnam, Vietnam.

AASHTO LRFD, 1998. *Load and resistance factor design (LRFD) specifications for highway bridges*. Washington (DC): American Association of State Highway and Transportation Officials (AASHTO).

Ali, M. S., Mohammad, J. and Bashir, A., 2012. Experimental Seismic Performance Evaluation of Bridge Piers Constructed In Low Grade Concrete. *Journal of Mechanical and Civil Engineering,* Volume 3, Issue 6, 36-41

Clough, R.W. and Penzien, J., 2003. *Dynamics of Structures*, Third Edition, Computers & Structures, Inc.

Hung, T. V., 2012. *Study on Earthquake Ground Motion Prediction and its Application to Structural Response of Bridge in Vietnam*. Doctor dissertation, Waseda University, 163 pages, Japan.

Kawashima, K. and Unjoh, S., 2004. Seismic design of highway bridges. *Journal of Japan Association for Earthquake Engineering, Vol.4, No.3 (Special Issue)*, 174-183.

Ngo, T.D., Nguyen, M.D. and Nguyen, D.B., 2008. A review of the Current Vietnamese Earthquake Design Code. *Special Issue of the Electronic Journal of Structural Engineering (EJSE): Earthquake Engineering in the low and moderate seismic regions of Southeast Asia and Australia*, 32-41.

Phuong, N.H., 1991. Probabilistic assessment of earthquake hazard in Vietnam based on seismotectonic regionalization. *Tectonophysics,* Vol. 198(1), 81-93.

Sakai, J. and Unjoh, S., 2006. Earthquake simulation test of circular reinforced concrete bridge column under multidirectional seismic excitation. *Earthquake engineering and engineering vibration*, Vol. 5, No. 1, 103-110.

VIG, 2005. *Research and Forecasting Earthquakes and Ground Movements in Vietnam* (Researched by Vietnam Institute of Geophysics, Chairman - Prof. Nguyen Dinh Xuyen), Hanoi, Vietnam (in Vietnamese).

Influence of climate change to loads and actions to buildings

NGUYEN Vo Thong
Associate Professor, Vietnam Institute for Building Science and Technology (IBST), Vietnam
thongnguyenvo@gmail.com

ABSTRACT

Global Climate Change being happened increase natural effects: temperature, typhoons, floods, droughts, earthquakes, tsunamis in more severe, frequent, intensity occurrences. This paper presents influence of climate change to loads and actions to buildings.

Keywords: *Loads, actions, climate change.*

1. INTRODUCTION

From recent studies, climate change have occurred in the world and effected to all nations and life in the earth. Climate change has resulted in more severe and/or frequent occurrences of natural disasters, especially cyclonic storms, floods and droughts becoming more extreme. Viet Nam is likely to be one of the several countries most adversely affected by climate change. This paper presents the influence of climate change to loads and actions to buildings.

2. CAUSES AND PREDICTIONS OF CLIMATE CHANGE IN THE WORLD AND IN VIET NAM

2.1 Causes of climate change

Climate change is a significant and lasting change in the statistical distribution of weather patterns over periods ranging from decades to millions of years (Ministry of Resources and Environment, 2009). It may be a change in average weather conditions, or in the distribution of weather around the average conditions (i.e., more or fewer extreme weather events). Climate change is caused by factors that include oceanic processes (such as oceanic circulation), biotic processes, variations in solar radiation received by Earth, plate tectonics and volcanic eruptions, and human-induced alterations of the natural world; these latter effects are currently causing global warming. Climate change in the during period XX century to now was paid attention by people. Some recent studies showed that naturally occurring green house gases such as CO_2 and CH_4 are main reason for climate change, especially the industrialization in the world from 1950 and consumption, relating to fossil fuel use such as coal, oil, cement production, deforestation, increasing the number of cattle (increasing amount of CH_4) and exploitation under water territory with peat coal.

2.2 Some climate change projections in the world and in Viet Nam

The main phenomenon of climate change is global warming and associated sea level rise. According to the 4th report of Intergovernmental Panel on Climate Change (IPCC) in 2007 (IPCC, 2007), The 100-year linear trend (1906-2005) of 0.74 [0.56 to 0.92]°C is larger than the corresponding trend of 0.6 [0.4 to 0.8]°C (1901-2000). The linear warming trend over the 50 years from 1956 to 2005 (0.13 [0.10 to 0.16]°C per decade) is nearly twice that for the 100 years from 1906 to 2005 (Figure 1).

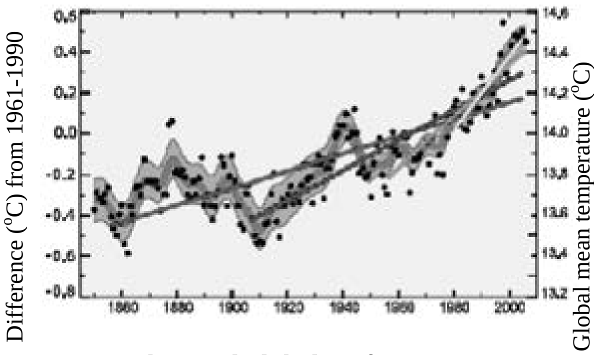

Figure 1: Observed global surface temperature anomaly during period the 1860-2000

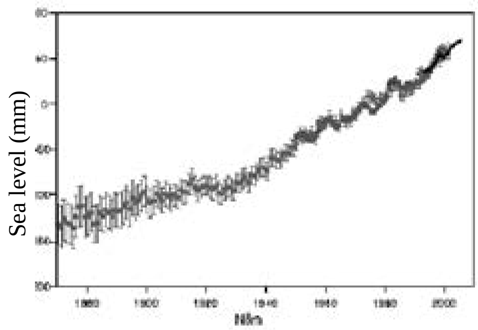

Figure 2: Observed global mean sea level anomaly during period the 1860-2000

The increasing of temperature causes the ice in Earth's North and South Poles melting to increase sea level. Data from TOPEX/POSEIDON satellite show that during period the 1993-2003 sea level rose by between 3,1 mm - 0,7 mm per year (Figure 2), faster than period the 1961-1993 (IPCC, 2007).

During the last 50 years, Viet Nam’s annual average surface temperature has increased by approximately 0.7^{o}C. The average temperatures in 2007 in Ha Noi, Da Nang, Ho Chi Minh are higher 0,8^{o}C ÷ 1,3^{o}C, 0,4^{o}C ÷ 0,5^{o}C than that of the decades 1931-1940 and 1991- 2000, respectively. Sea level in Cua Ong and Hon Dau increased about 20 cm. In the last two decades, the number of cold fronts crossing Viet Nam decreased, for example there were only 15-16 cold fronts (56% average number of several years) in 1994 and 2007. A strange phenomenon of climate there are several and long lasted very cold fronts, last 38 days in January and February of 2008. Average number of rainy days in year in Ha Noi decreased in decade 1981-1990 and is half (15 days per year) in the last ten years. At the same time, the number of typhoons with higher intensity, typhoon track move to south lattices, typhoon season is likely to end later and there are typhoons with strange track. After typhoons, floods, landslides often happen. Changes of natural conditions from climate change caused many influences of climate change to loads and actions to buildings.

3. INFLUENCES OF CLIMATE CHANGE TO LOADS AND ACTIONS TO BUILDINGS

3.1 Effects of temperature

According to the medium emission scenario, to the end of 21st decade, average temperature may increase to 2.6^{0}C in the North West, 2.5^{0}C in the North East, 2,4^{0}C in the North Delta, 2.8^{0}C in the North Central, 1.9^{0}C in the South Central, 1.6^{0}C in the Central Highlands and 2.0^{0}C in the South compared to average values of decade 1980-1999 (Ministry of Resources and Environment, 2009). The irregularity of the increasing of average temperature happen on regions. North Central has the highest increasing in temperature, and then turns to the North West, the North East, the North Delta, the South Central, the South and the Central Highlands (Table 1).

Table 1: Projections of average increase in temperature (^{0}C) during period the 1980-1999 in the medium emission scenario

Region	Year								
	2020	2030	2040	2050	2060	2070	2080	2090	2100
North West	0.5	0.7	1.0	1.3	1.6	1.9	2.1	2.4	2.6
North East	0.5	0.7	1.0	1.2	1.6	1.8	2.1	2.3	2.5
North Delta	0.5	0.7	0.9	1.2	1.5	1.8	2.0	2.2	2.4
North Central	0.5	0.8	1.1	1.5	1.8	2.1	2.4	2.6	2.8
South Central	0.4	0.5	0.7	0.9	1.2	1.4	1.6	1.8	1.9
Central Highlands	0.3	0.5	0.6	0.8	1.1	1.2	1.4	1.5	1.6
South	0.4	0.6	0.8	1.0	1.3	1.6	1.8	1.9	2.0

Beside the increase of temperature, hot summer and coldness are also stronger. Temperatures reaching peak in hot summers have an increasing trend and temperatures of cold winters have the decreasing trend (Table 2). Area of region affected hottest summer and coldest winter extend to South direction. The durations of hottest summer and coldest winter last longer. Phenomenon of ice and snow appeared in Sa Pa, Lang Son and high land areas in the North has a increasing trend.

If consider the annual increasing of temperature according to the medium emission scenario effects of temperature to structures increase higher than data in QCVN 02:2009/BXD (Table 3).

From data in Tables 1, 2 and 3, climate change affect to effects of temperature to buildings. When to design buildings, especially temperature-sensitive buildings it is need to consider unfavorable effects of temperature because of climate change to stress behavior, deformation and reasonable design solutions. Besides, stipulations relating data and effects outdoor temperature: Natural Physical & Climatic Data for Construction (QCVN 02:2009/BXD, 2009), length and width of thermal slot of structural types: concrete, reinforced concrete structures (TCVN 5574:2012, 2012) and steel structures (TCVN 5575:2012, 2012)... will need suitable studies and revisions.

Table 2: Hottest summers and coldest winters have the increasing trend intensity and duration

Hottest summer					**Coldest winter**				
Year	Location	Temperature (^{0}C)	Duration (day)	Note	Year	Region	Temperature (^{0}C)	Duration (day)	Note
1983	Ha Noi	40.4	-	Measured in weather tent	2/1968	Sa Pa	< 0	26	Ice and snow
6/2010	Lang	40.7	10		2/1989	Sa Pa	< 0	28	Ice and snow
	Son Tay	40			1973		-3		Ice and snow
	Tinh Gia	40.2			2/2008	Sa Pa	-2	38	Ice and snow
	Quy Hop	40.7				Mau Son	-5		Ice and snow
	Con Cuong	40.8				Ha Noi	7		-
4/2012	Ha Noi	40	13		1/2011	Mau Son	-1,9	18	Ice and snow
	Hoa Binh	42				Ha Noi	8		-

Table 3: Average increasing of temperature compared with data of QCVN 02:2009/BXD

Location	**Temperature**									
	Average temperature	**Increasing with time (%)**								
		2020	2030	2040	2050	2060	2070	2080	2090	2100
Dien Bien	22^{0}C	2.27	3.18	4.55	5.91	7.27	8.64	9.55	10.91	11.82
Ha Long	23.1^{0}C	2.16	3.03	4.33	5.19	6.93	7.79	9.09	9.96	10.82
Ha Noi	23.6^{0}C	2.12	2.97	3.81	5.08	6.36	7.63	8.47	9.32	10.17
Vinh	23.9^{0}C	2.09	3.35	4.60	6.28	7.53	8.79	10.04	10.88	11.72
Nha Trang	26.6^{0}C	1.50	1.88	2.63	3.38	4.51	5.26	6.02	6.77	7.14
Buon Me Thuot	23.6^{0}C	1.27	2.12	2.54	3.39	4.66	5.08	5.3	6.36	6.78
Ho Chi Minh	27.4^{0}C	1.46	2.19	2.92	3.65	4.74	5.84	6.57	6.93	7.30

3.2 Effects of strong winds

Formally, typhoons hit Vietnam the North in August, the Central in October and the South in December. Recently, typhoons occur lately and are gradually moving south. Climate change creates the increasing of sea temperature, warm water area extending to high latitudes of Pacific Ocean. As the result, typhoons occur more frequently in the Northwestern Pacific Ocean. wherefore number of typhoons hitting Viet Nam will increase. Wind speed and period of typhoons also increase.
Many strong wind phenomena (squall, tornado or downburst) with high intensity last longer and not follow normal rules. Formally, whirlwinds often occur in midland region but now they occur in big cities, cause many damages of human and properties.
The changes of typhoons and whirlwinds because of climate change are needed to research to help revision work of effects of wind loading in Vietnam Standard TCVN 2737-1995. Firstly, wind region map revised from updated data makes a

safety assurance to buildings and recommendations of building design under strong wind phenomena (squall, tornado or downburst).

a) Thai Nguyen (1 Sep 2011) b) Bac Kan (8 Aug 2012)

Figure 3: Damages by whirlwinds

3.3 Effects of strong floods and flash floods

Flood is an overflow of water that submerges land, which is normally lower and sunken area. Strong floods on rivers change slowly and often occur in large area and longer. Flash floods with sudden and violent behavior change fast and occur in narrow area and affected area is smaller than that of river flood. If heavy rain occurs, water is stopped by barriers such as stones and trees until water amount destroy barrier and run off very fast, sweep away soil, trees and other barriers. Normally flash floods occur rapidly in period from three hours to six hours.

Flood is a very dangerous hydrologic phenomenon, especially flash flood (Figure 4). It has a violent damage and become a natural disaster, for example the flash flood in Lai Chau city in 1998 destroyed whole Muong Lay village and area of city. Flash floods often occur in mountainous areas where have high mountains with valleys, low streams and rivers.

Flash floods are classified three types:

- Flash floods occur due to local rain, especially in natural basin (almost no effect from human);
- Flash floods occur due to heavy rain in basins strongly affected by economic activities from human to cause instability and non-equilibrium of basin ecology (change top layer, stream condition, volume or characteristics of basin...);
- Flash floods occur due to failure of dams and other hydraulic structures.

Climate change modifies precipitation in areas, increasing in the rainy season and decreasing in the dry season. Flash floods occur more frequently and have higher intensity because natural environment are destroyed. In 2007, from the beginning of October to 15 November, Central had five big floods, caused 155 death-toll, 13 missing persons, 147 injured persons, loss in facilities and farm produce up to 4,434 billion VND.

Loads and actions of floods, flash floods to buildings, roads, bridges, and drains... are large. Therefore, there is a need of planning for areas with floods and flash floods. When design structures for flood and flash flood resistance it needs to consider and collect updated data relating to flash floods (dykes, dams, water barriers, water reservoir...) and study to revise data relating to floods and flash floods in Natural Physical & Climatic Data for Construction suitability.

Table 4: Some flash floods during period the 1990 - 2005

No	Date	Affected region	River, stream	Rainfall	Loss	
					People (Dead/ Injured)	In-cash (billion VND)
1	16/6/1990	Krong Bong, Ging Son, Lak, Đac Lac	4 small lakes destroyed	370	22	3,4
2	27/6/1990	Lai Chau town	Nam Lay stream	233	104/200	22
3	27/7/199	Son La town	Nam La and Nam Pan streams	403	42	26
4	23/7/1998	Muong Lay, Lai Chau	Nam Lay stream	187	34	18
5	17/8/1990	Lai Chau	-	258	89	21
6	29-30/7/1999	Ham Tan, Binh Thuan	Dinh river	300	27	187
7	3/10/2000	Nam Coong, Sin Ho Lai Chau	-	138	39	2
8	19-20/9/2002	Huong Son, Ha Tinh	Ngan Pho river	500-700	53/111	824
9	18-19/7/2004	Du Gia, Yen Minh, Ha Giang	-	200 - 300	45/16	50
10	27-28/9/2005	Van Chan, Yen Bai	-	233	50/8	162

a) Flash flood dated 27 Sep 2005 in Yen Bai caused 42 people dead or missing

b) Flash flood dated 26 June 2011 in Tuong Duong (Nghe An) caused several hundreds of house inundated, many houses and a suspension bridge swept

Figure 4: Flash floods in Yen Bai and Nghe An

3.4 Corrosion effects

Corrosion effects by climate change to building structures maybe direct effect of sea air and sea water or acid rain. According to research by (Ministry of Resources and Environment, 2009), up to end of 21st century, sea water level may rise up to 1m (Table 5) compare to period from 1980-1999. At that time, if there is no plan to built sea dyke and embankment, forty thousand square kilometer of Vietnam’ coast plain will be flooded. Especially, in Mekong delta area, about 38% of area will be submerged, 90% of area will become salinity (Ministry of

Resources and Environment, 2009). Structures in these areas will be directly affected by sea air and sea water.

Table 5: Sea water level up compared to period 1980 ÷ 1999

Scene	Years								
	2020	**2030**	**2040**	**2050**	**2060**	**2070**	**2080**	**2090**	**2100**
Low	11	17	23	28	35	42	50	57	65
Medium	12	17	23	30	37	46	54	64	75
High	12	17	24	33	44	57	71	86	100

The cause of acid rain is the increasing of sulfur and nitro oxide in the atmosphere from natural and artificial actions. When it rains, under the action of solar radiation, these oxides react with water in the atmosphere to create acids such as H_2SO_4, HNO_3 (Figure 5a).

a) b) c)

Figure 5: Acid rain and corrosion effects to structures

These acid drops when fall down to structures will corrode them. For example, Capitol Building in Ottawa was heavily damaged because the volume of SO_2 in the air is too high (Figure 5b); statue was corroded by acid rain (Figure 5c); Silver bridge at Ohio river (USA) was collapsed because anchor of suspended cable was corroded by acid rain, caused 46 death-toll (Figure 6).

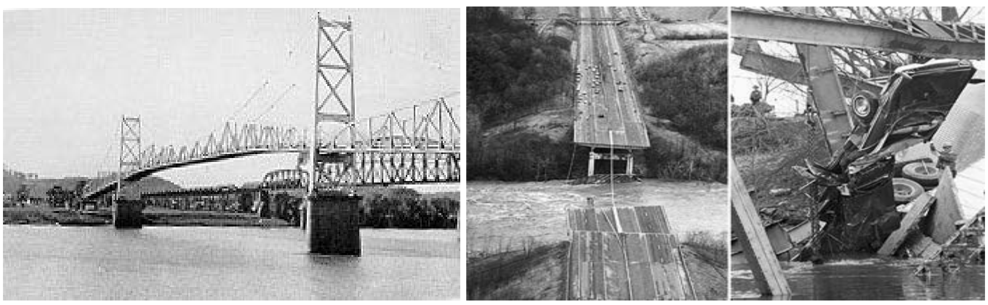

a) b)

Figure 6: Silver bridge over Ohio river before collapsed (a) and after collapsed (b) due to corrosion of suspended cable by acid rain

From above matters, it is necessary to research, plan areas maybe directly affected by corrosion when sea level increases and simultaneously compile design guidelines about preservation and maintenance for structures suffered from corrosion caused by climate change.

3.5 Effect of sea waves and pressure by increasing of sea level

Sea wave may be caused by wind, storm, or earthquake under the sea. Sea wave directly affect to the structures offshore and at the coast line. Damage caused by wave is very large, especially tsunami (Figures 7 and 8). Climate change makes the sea level increase so that effects from water pressure, sea wave to structures, especially dyke, embankment, bride, port, salinity protect system…, increase. There are some structures such as dike, embankment, bride, port were constructed but did not consider the possibility of sea level increasing, hence usage time and effectiveness were affected. Therefore, sea level increasing matter must be studied in order to propose measures to overcome for existing and newly-built structures at the coast line area.

Figure 7: Tsunami in Japan

Figure 8: Effect of Nock-ten tropical cyclone in Do Son, 30 July 2011

3.6 Earthquake and tsunami

Researches by Australia National University shows that, earthquakes occurred recently resulted from global warming phenomenon. According to these researches, Climate change in long period may change the structure of the earth crust, create forces affecting movement of tectonics. Earthquake will occur when the pressure at the boundary of tectonics reach threshold level.

Vietnam is located at the South-East part of Eurasia plate, between Indian plate, Philippines plate and Australian plate. Vietnam is not located at the boundary of these plates; therefore it is not vulnerable to earthquake compared to other countries in the area such as Indonesia, Philippines, Malaysia. However, on the territory of Vietnam, there are several active faults such as Lai Chau - Dien Bien fault, Song Ma Fault, Son La fault, Hong river fault, Ca river fault , 109^0-110^0 longitude fault…(Figure 9) (Le and et al., 2011),. Therefore, global tectonic change caused by sea level increasing may affect to these faults and wake up earthquakes. In addition, Viet Nam also suffers from earthquakes from out of territory, especially effect of tsunami. According to researches of Viet Nam Institute of Geophysics (Le and et al., 2011), earthquakes in the aera of East Sea and nearby may cause tsunami to Viet Nam coast line includes: 1) Ryukyu – Taiwan, 2) Manila subduction zone, 3) Sulu sea, 4) Celebes sea, 5 và 6) Ban Đa

sea, 7) North of East Sea, 8) Palawan and 9) West of East Sea. Among them, Manila subduction zone is considered highest vulnerability (Figure 10).
Follow scenarios calculated by the Ministry of Resources and Environment, if an earthquake with magnitude of 8.3 Richter occur at the Manila subduction zone, it may cause a tsunami with the height of wave up to 6.2 m at Quang Ngai and 2.1m at Nha Trang. If an earthquake with magnitude of 8.3 Richter occur at the same location, it may cause a tsunami with the height of wave up to 10.6 m at Quang Ngai and 5 m at Nha Trang, and the time for tsunami to travel from Manila subduction zone to Viet Nam coast line is about 2 hours (Le and et al., 2011).

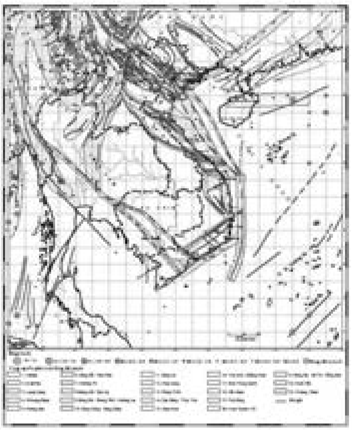

Figure 9: Seismic map for territory of Vietnam and nearby area.

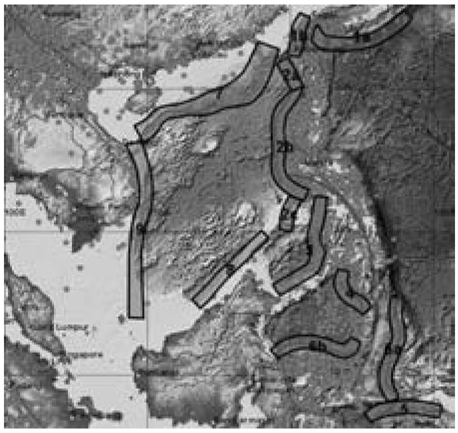

Figure 10: Sources of earthquake and tsunami may affect coast line and offshore islands of Viet Nam

From above results, it can be seen that climate change can affect to earthquake and tsunami action to structures in Viet Nam. Therefore, it is necessary to have studies to evaluate and forecast earthquake and tsunami vulnerability caused by sea level increasing. These data's are the base to revise or reestablish seismic zoning map in QCVN 02:2009/BXD and seismic design standard TCVN 9386:2012.

4. CONCLUSIONS

Climate change have been affecting to loads and actions to buildings. The clearest manifestations are effects of outdoor temperature, typhoons, whirlwinds, floods, corrosions, water waves, sea level rises, earthquakes and tsunamis.
Temperature-sensitive buildings need to consider unfavorable effects of temperature because of climate change to stress behavior, deformation and reasonable design solutions. Besides, stipulations relating data and effects outdoor temperature: Natural Physical & Climatic Data for Construction (QCVN 02:2009/BXD, 2009), length and width of thermal slot of structural types: concrete, reinforced concrete structures (TCVN 5574:2005, 2012) and steel structures (TCVN 5575:2012, 2012)... will need suitable studies and revisions.
The changes of typhoons and whirlwinds because of climate change are needed to research to help revision work of effects of wind loading in Vietnam Standard

TCVN 2737-1995. Firstly, wind region map revised from updated data makes a safety assurance to buildings and recommendations of building design under strong wind phenomena (squall, tornado or downburst).
There is a need of planning for areas with floods and flash floods. When design structures for flood and flash flood resistance it needs to consider and collect updated data relating to flash floods (dykes, dams, water barriers, water reservoir...) and study to revise data relating to floods and flash floods in Natural Physical & Climatic Data for Construction suitability.
From above matters, it is necessary to research, plan areas maybe directly affected by corrosion when sea level increases and simultaneously compile design guidelines about preservation and maintenance for structures suffered from corrosion caused by climate change.
Climate change makes the sea level increase so that effects from water pressure, sea wave to structures, especially dike, embankment, bride, port, salinity protect system…, increase. These unfavorable results must be studied in order to propose measures to overcome for existing and newly-built structures at the coast line area. Especially, large structures with long life time such as “live together with flood” structures at the Mekong delta, North-South sea embankment must be carefully studied so that structures are built today can be used for next generations.
Climate change can affect to earthquake and tsunami action to structures in Viet Nam. Therefore, it is necessary to have studies to evaluate and forecast earthquake and tsunami vulnerability caused by sea level increasing. These data’s are the base to revise or reestablish seismic zoning map in QCVN 02:2009/BXD and seismic design standard TCVN 9386:2012.

REFERENCES

IPCC, 2007. *The 4th assessment report of the Intergovernmental Panel on Climate change.*
Le Huy Minh and Nguyen Hong Phuong, 2011. *Vulnerability of earthquake and tsunami in Viet Nam*.
Ministry of Resources and Environment, 2009. *Scenarios for climate change and sea level increasing for Viet Nam*.
QCVN 02:2009/BXD, 2009. *National Building Code – Natural data for Construction Activities.*
TCVN 9386:2012, 2012. *Design of structures for earthquake resistance*.
TCVN 5575:2012, 2012. *Steel structures – Design standard.*
TCVN 5574:2012, 2012. *Concrete and reinforced concrete structures – Design standard.*
TCVN 2737:1995, 1995. *Loads ands actions-Design standard*.

Test methods for evaluation of sulfate resistance of limestone powder replacing cement mortars

Ittiporn SIRISAWAT[1], Warangkana SAENGSOY[2], Lalita BAINGAM[1],
Pitisan KRAMMART[3] and Somnuk TANGTERMSIRIKUL[4]
[1]Graduate Student, School of Civil Engineering and Technology,
Sirindhorn International Institute of Technology, Thammasat University, Thailand
ittiporn@g.swu.ac.th
[2]Researcher, Construction and Maintenance Technology Research Center,
Sirindhorn International Institute of Technology, Thammasat University, Thailand
[3]Assistant Professor, Department of Civil Engineering,
Rajamangala University of Technology Thanyaburi, Thailand
[4]Professor, School of Civil Engineering and Technology,
Sirindhorn International Institute of Technology, Thammasat University, Thailand

ABSTRACT

This study is aimed to indicate the inadequacies of the presently used methods for testing sulfate resistance of cementitious systems, especially when tested in magnesium sulfate solution, and propose proper laboratory tests for evaluating the sulfate resistance of mortars with various types of binders. The test methods involved immersion of mortar specimens in 33,800 ppm of sodium sulfate ($N\underline{S}$) and magnesium sulfate ($M\underline{S}$) solutions. The resistance of mortars with different binders to sulfate attack is determined by applying several test methods. Results of an investigation on sulfate resistance of ordinary Portland cement and limestone powder replacing cement mortars, which were tested by the test methods of weight loss, expansion, strength reduction, volume loss, and visual inspection with image processing technique, are presented. It was observed that for $N\underline{S}$ solution, expansion test is appropriate for performance evaluation of all ordinary Portland cement and limestone powder replacing cement mortars. In case of $M\underline{S}$ solution, both expansion and weight loss or volume loss or image processing technique are considered suitable to test limestone powder replacing cement mortars.

Keywords: *sulfate resistance, limestone powder, expansion, weight loss, image processing technique*

1. INTRODUCTION

Sulfate attack on concrete is a culmination of a series of reactions that occur in the presence of sulfate ions (mainly sodium and magnesium sulfate). Sulfate attack manifests itself in the form of loss in strength, expansion, surface spalling, mass loss, and eventually disintegration (Tikalsky and Carrasquillo, 1989). Many laboratory tests were established to evaluate the sulfate resistance of concrete. Although some of these methods have been adopted as standard test method by standards organizations or they have become national codes, many test methods are still not appropriate for some cases and being modified. Tests of the sulfate resistance are usually performed by the determination of expansion of mortar bars such as ASTM C452 and ASTM C1012. However, in magnesium sulfate environment, different mechanisms can affect the concrete differently. Test methods of ASTM may be good only to evaluate volume instability due to mainly ettringite formation. Krammart and Tangtermsirikul (2004) suggested that the appropriate test methods for magnesium sulfate environment should also include the strength reduction or weight loss test. There are currently no universally accepted methods for testing overall sulfate resistance of concrete.

This study is aimed to identify the inadequacies of the presently used methods for testing sulfate resistance of cementitious systems, and to propose proper laboratory tests for evaluating the sulfate resistance of mortars made from OPC1 and OPC5 cements and limestone powder replacing cements. The relative resistance of mortars made from different binders to sulfate attack is determined by applying several test methods such as expansion, weight loss, strength reduction, volume loss, and visual inspection with image processing technique.

2. MATERIALS AND MIX PROPORTIONS

Ordinary Portland cement type 1 (OPC1), ordinary Portland cement type 5 (OPC5), and limestone powder (LP) were used as materials in the experiment. LP with mean particle size of 3.2 micron was provided by Surint Omya Chemical (Thailand). The chemical compositions of materials used are given in Table 1. The mortar mixtures were made with a ratio by volume of sand to binder of 2.75. Water to binder ratio was controlled at 0.40 and 0.55. LP replacement percentages were 10 and 20% by mass of the total powder materials. The mix proportions were systematically designated as shown in Table 2.

Mortar cube specimens (50x50x50 mm) and mortar bar specimens (25x25x285 mm) were prepared in accordance with ASTM C109 and ASTM C1012, respectively. Immediately, after casting, the molds were covered with plastic sheets and the specimens were demolded at one day of age. After demolding, all bars and cube specimens were stored in a plastic tank of saturated limewater for 28 days and then exposed to the sulfate solutions. Sodium sulfate ($N\underline{S}$) used in this study contained 50g of $N\underline{S}$ dissolved in 1.0 liter of solution (SO_4^{2-} of 33,800 ppm or 5% by weight of solution) whereas 42.36g of magnesium sulfate ($M\underline{S}$) was used to prepare the magnesium sulfate solution in order to obtain the same concentration of SO_4^{2-} as that of the $N\underline{S}$ solution. The solutions were mixed 24 hours before use, and stored at a constant temperature of 30±2 ^oC. Volume ratio of sulfate solution to specimens in a storage container was approximately 4 to 1. The solutions were replaced every two months of exposure.

The measurements of expansion, weight loss, strength reduction, volume loss, and visual inspection with image processing technique of mortar specimens were conducted. Microscopic examinations were conducted on pastes with water to binder ratio of 0.40 for all mix proportions. The investigation included Thermogravimetric Analysis (TGA), Mercury Intrusion Porosimetry (MIP), X-Ray Diffraction (XRD) and Scanning Electron Microscopy with Back-Scatter Electron Mode (SEM/BSE with EDX analysis).

Table 1: Chemical compositions and physical properties of binders

Chemical Compositions (%)	OPC 1	OPC 5	LP
SiO_2	19.51	21.87	0.46
Al_2O_3	4.97	3.87	0.06
Fe_2O_3	3.78	4.34	0.03
CaO	65.38	64.56	55.25
MgO	1.08	1.11	0.37
SO_3	2.16	2.08	< 0.01
Na_2O	< 0.01	< 0.01	< 0.01
K_2O	0.47	0.24	0.01
TiO_2	0.25	0.21	< 0.01
P_2O_5	0.07	0.05	0.01
Free CaO	1.00	0.76	-
LOI	2.27	1.59	43.79
Physical Properties			
Specific Gravity	3.12	3.18	2.79
Blain fineness (cm^2/g)	3,550	3,830	8,840
Mean diameter (μm)	15.41	14.43	3.23

Table 2: Mix proportions of the tested mortar specimens

Mix	Mix Designation	Cement Type	Mix proportion (ratio by weight)			
			Cement	LP	Water	Sand
1	M1-0.40	OPC 1	1.0	-	0.40	2.75
2	M1 90 LP10-0.40	OPC 1	0.9	0.1	0.40	2.75
3	M1 80 LP20-0.40	OPC 1	0.8	0.2	0.40	2.75
4	M5-0.40	OPC 5	1.0	-	0.40	2.75
5	M1-0.55	OPC 1	1.0	-	0.55	2.75
6	M1 90 LP10-0.55	OPC 1	0.9	0.1	0.55	2.75
7	M1 80 LP20-0.55	OPC 1	0.8	0.2	0.55	2.75
8	M5-0.55	OPC 5	1.0	-	0.55	2.75

3. TEST PROCEDURES

In this investigation, the measurements of expansion, weight loss, strength reduction, volume loss, and visual inspection with image processing technique of mortar specimens were conducted.

3.1 Expansion measurement

The expansion was measured on mortar bar specimens according to ASTM C1012. The initial length of the specimens was measured after 28 days of curing in saturated lime water. Subsequently, they were placed in the sulfate solution and the length change was measured at the end of every 8 weeks of exposure. An expansion value was obtained from the average of three specimens.

3.2 Weight loss measurement

The weight loss was determined on the mortar cube specimens and computed as the difference between initial weight of the specimen after 28-day immersion in water and weight of the specimen after immersion in sulfate solutions, compared in % of the initial weight.

3.3 Strength reduction measurement

Strength reduction was calculated based on the compressive strength of mortar cube specimens immersed in water compared to the compressive strength of mortar cube specimens exposed in sulfate solution, in % of the strength immersed in water.

3.4 Volume loss measurement

Volume loss, a new conceptual test, is introduced to help predict the surface damage of concrete at early submersion ages. Usually, to be able to judge and compare the degree of damage, long term submersion periods are required while at early submersion ages, interpretation cannot be done. At the same time of weight loss measurement, the mortar cube specimens were measured for volume loss by a water displacement method. The volume of specimens was obtained by weighting the specimens in air and in water. The difference in weights of specimens could then be used to calculate the volume of specimens. A buoyancy balance weighting was used to measure the apparent immersed weight.

3.5 Surface area loss measurement by image processing technique

Determination severity of the mortar cube specimens in M$\underline{S}$ solution (surface deterioration) was evaluated by visual inspection. To bring the judgment of different observers into agreement, and to avoid variation in judgment from time to time, the image processing technique was developed by adopting Saengsoy and Tangtermsirikul (2010) previous work. The cube mortar samples were brought to take photos of their faces with sufficient resolution. The image size and quality of the photographs were adjusted for the sake of easiness to identify the damage boundaries of the specimen as shown in Fig. 1. The areas of the damage boundaries of the specimen were determined by computer software. The average surface areas of six faces of each specimen were determined. The surface area loss of cube specimens was calculated from the average of surface area of two specimens. The surface area loss of each specimen was obtained from

$$\text{Surface area loss (SAL), \%} = [(Sa_i - Sa_t) / (Sa_i)] \times 100 \qquad (1)$$

where Sa_t is surface area of the specimen after immersion in the sulfate solution and Sa_i is surface area of the specimen after 28-day immersion in saturated lime water before being exposed to sulfate solution.

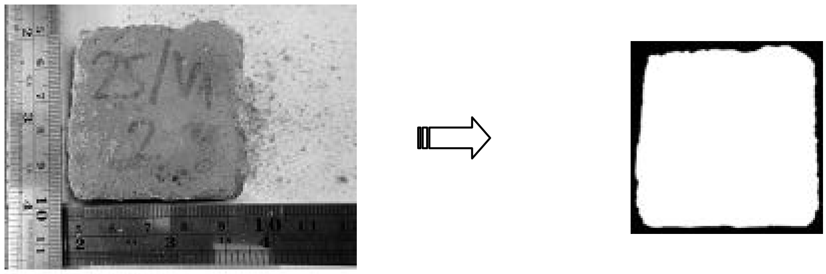

(a) Image of a specimen (b) Damage boundaries of a specimen

Figure 1: Determination of damage area of specimen

4. RESULTS AND DISCUSSION

4.1 Exposure in Na_2SO_4 solution

4.1.1 Expansion Results

Relationships between the expansion and period of immersion in N<u>S</u> solution of OPC and blended cement mortar bar specimens with w/b of 0.40 and 0.55 are shown in Fig. 2. These data indicated that, for specimens placed in N<u>S</u> solution, the expansion of OPC1 cement mortar was, as generally known, higher than that of OPC5 cement specimen. Smaller quantity of C_3A of OPC 5 cement (1.7%) than that of OPC1 (5.5%) leads to less amount of ettringite. At higher w/b (0.55), the effect of composition of cement becomes more significant. For the specimens made from limestone powder replacing cement, the expansion of 10% LP replacing cement (M1 90LP10) mortar bar specimen was significantly larger than that of 20% LP replacing cement (M1 80LP20) mortar bar specimen but still lower than that of the OPC1 mortar. This is partly because of lower $Ca(OH)_2$ (CH) when comparing between the amount of CH in LP replacing cement specimens (P1 90LP10, P1 80LP20) and that of the OPC1 specimen (P1). Amount of $Ca(OH)_2$ at the age of 91 days by TGA analysis of OPC1 paste (P1), P1 90LP10, and P1 80LP20 were 18.1%, 16.5%, and 14.8%, respectively. The incorporation of limestone also reduces the amount of C_3A in the LP replacing cement.

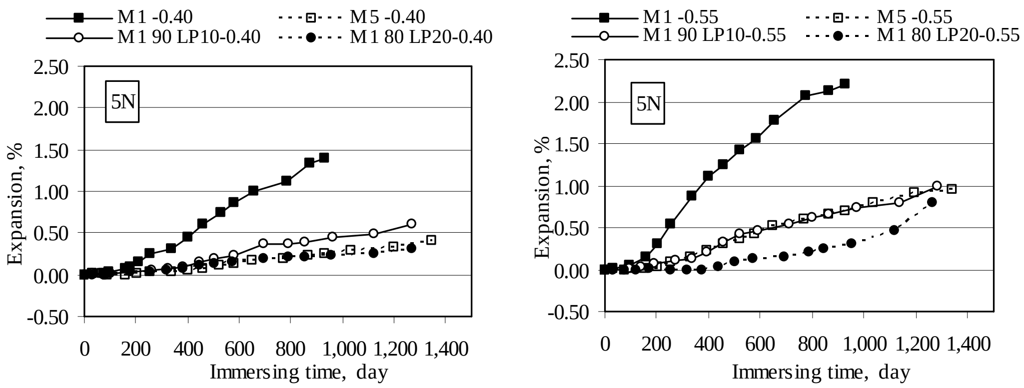

(a) w/b = 0.40 (b) w/b = 0.55

Figure 2: Relationship between expansion and period of immersion in N<u>S</u> solution of OPC and LP replacing cement mortars with w/b of 0.40 and 0.55

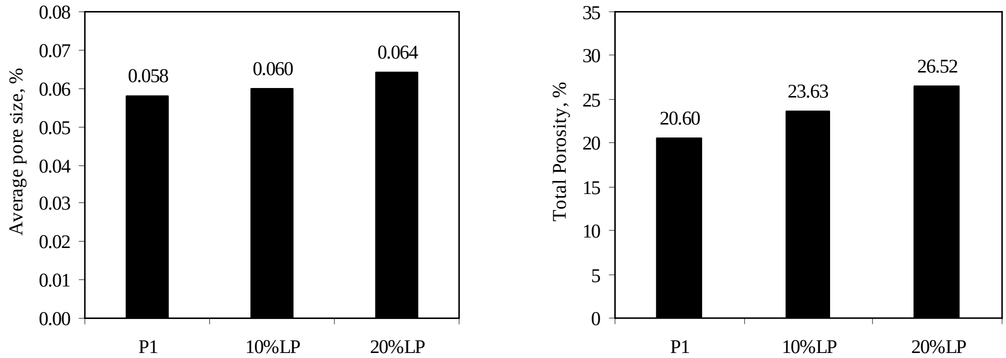

(a) Average pore size (b) Total porosity

Figure 3: Average pore size and total porosity at the age of 91 days by MIP analysis of LP replacing cement pastes

From Fig. 3, the average pore size and total porosity of 10% and 20% LP replacing cement paste were higher than that of OPC1 It is observed that the expansion of the LP replacing cement specimens was less than that of OPC1 specimens. It can be concluded that the more content of LP, the larger size of pore in cement matrix. This would be increased an available space of the cement matrix for ettringite accommodation (Fig. 4), as presented by a good behavior in less expansion due to Na_2SO_4 attack.

4.1.2 Weight Loss Results

Fig. 5 presents the effect of type and content of binders on weight loss of mortar cube specimens with w/b of 0.55 immersed in N$\underline{S}$ solutions for 1,300 days. It is obvious from this figure that no significant weight loss in each mixture was demonstrated. Almost all specimens in N$\underline{S}$ solution still gained weight or had very low weight loss although the test period had reached 1,300 days. These results do not provide any useful information for evaluation of N$\underline{S}$ resistance as the mechanism of N$\underline{S}$ attack is mainly the ettringite formation which results in expansion rather than weight loss (Al-Amoudi, 1995).

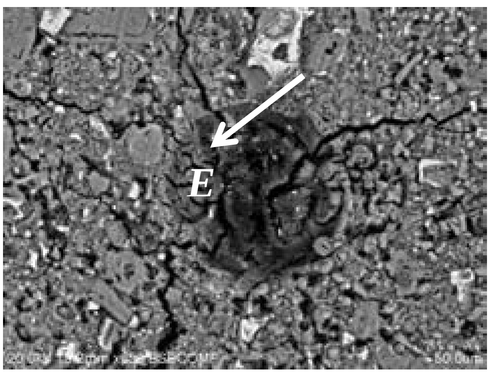

Figure 4: SEM image of LP replacing cement paste showing formation of ettringite in void

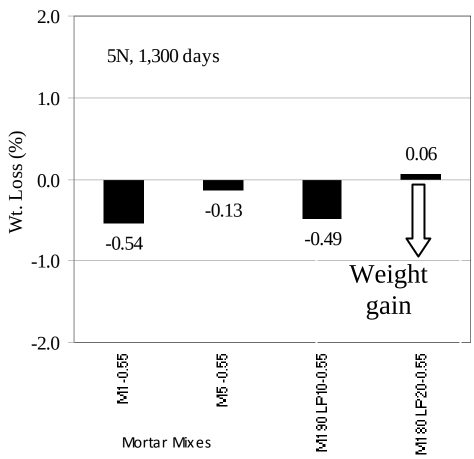

Figure 5: Weight loss in N$\underline{S}$ solution of mortar cube specimens with w/b of 0.55 at 1,300 days of immersion

4.2 Exposure in $MgSO_4$ solution

4.2.1 Expansion Results

Fig. 6 shows the comparison of expansion in M$\underline{S}$ and N$\underline{S}$ solutions of LP replacing cement mortars. The figures show that the expansion in M$\underline{S}$ solution of these specimens was higher than that in N$\underline{S}$ solutions when compared at the same immersion period. This is contrast to the behaviors of other types of binder system that usually produce larger expansion in N$\underline{S}$ solution than in M$\underline{S}$ solution. This is because M$\underline{S}$ solution decreases the pH of the system. For the system with LP, there occurred dissolution of $CaCO_3$ from the limestone powder that contributed to gypsum formation (Irassar et. al., 2003) and then increases expansion of the specimens (see Eqs. (2) to (5)).

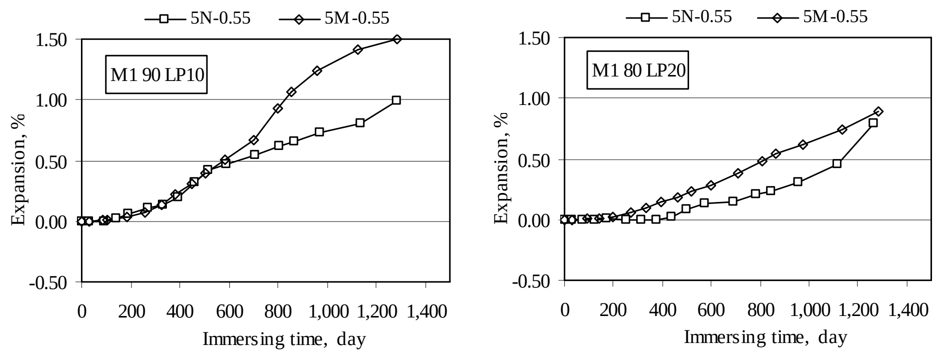

(a) 10% replacement (b) 20% replacement

Figure 6: Effect of type of sulfate on expansion of LP replacing cement mortars with w/b of 0.55

4.2.2 Weight Loss Results

For M$\underline{S}$ solution, relationships between the weight loss and period of immersion of LP replacing cement mortar cube specimens is shown in Fig. 7. These data indicated that, for specimens placed in M$\underline{S}$ solution, LP replacing cement specimens showed equivalent in weight loss to that of the OPC5. In addition, the LP replacing cement with 20% LP gave smaller weight loss than the LP replacing cement with 10% LP.

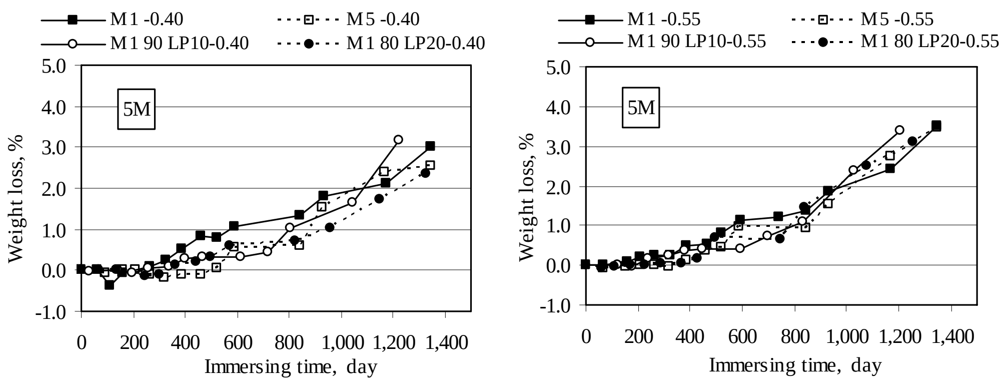

(a) w/b = 0.40 (b) w/b = 0.55

Figure 7: Relationship between the weight loss and period of immersion in M$\underline{S}$ solution of OPC and LP replacing cement mortars

For system with limestone powder, the solubility of $CaCO_3$ is a function of the pH value. The MS attack is found to decrease the pH with higher dissolution of $CaCO_3$ as shown in Eq. (2) which contributes to gypsum formation as in Eq. (3). The products which are magnesite in Eq. (4) and dolomite in Eq. (5), agreed with Lee's work (2007), can be formed in specimens with LP exposed to MS solution. Formation of gypsum, magnesite, and dolomite results in less weight loss and less severe surface etching of the LP blended cement. The formation of magnesite and dolomite by MS attack determined by the XRD analysis was confirmed in Fig. 8. It was found that more amounts of magnesite and dolomite presented in LP cement paste specimens than in the OPC specimens. Another reason was that the precipitation layer of calcite was found on the exposed surface of the LP cement paste as shown by SEM image in Fig. 9. This layer helped delaying the ingress of magnesium ions into the paste.

Dissolving of $CaCO_3$ $$CaCO_3(s) \longrightarrow Ca^{2+} + CO_3^{2-} \quad (2)$$

Gypsum formation $$Ca^{2+} + SO_4^{2-} + 2H_2O \longrightarrow CaSO_4 \cdot 2H_2O \quad (3)$$

Magnesite formation $$Mg^{2+} + CO_3^{2-} \longrightarrow MgCO_3 \quad (4)$$

Dolomite formation $$CaCO_3 + Mg^{2+} \longrightarrow Ca[Mg(CO_3)_2] \quad (5)$$

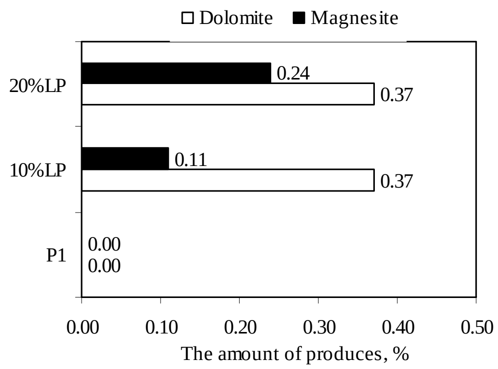

Figure 8: Amount of magnesite and dolomite by XRD analysis

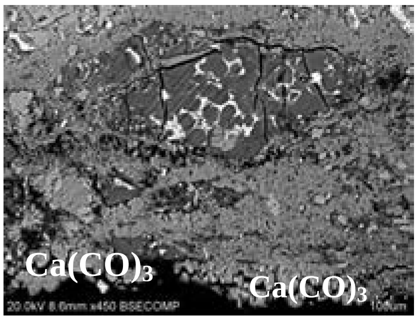

Figure 9: SEM photograph of LP cement paste showing the external layer consisted calcium carbonate

4.2.3 Strength Reduction Results

Figure 10 shows results of the strength reduction of mortar cube specimens with w/b of 0.55 made from various types of binder at 600 days of exposure in MS solution. For mortar cube specimens replaced in MS solution, the strength reduction of LP replacing cement mortars was lower than those of Type 1 and Type 5 control cement mortars. The trend of change of the strength reduction and weight loss performance is similar in such a way that strength reduction of mortar cube specimens increased along with the weight loss. However, a problem of compressive strength test for sulfate resistance evaluation is that it requires large number of specimens throughout the test period since the tested specimens can not be reused. In addition since damages occur on all surfaces, it is difficult to prepare surfaces for compression test and also to estimate the actual cross sectional area for compressive strength calculation

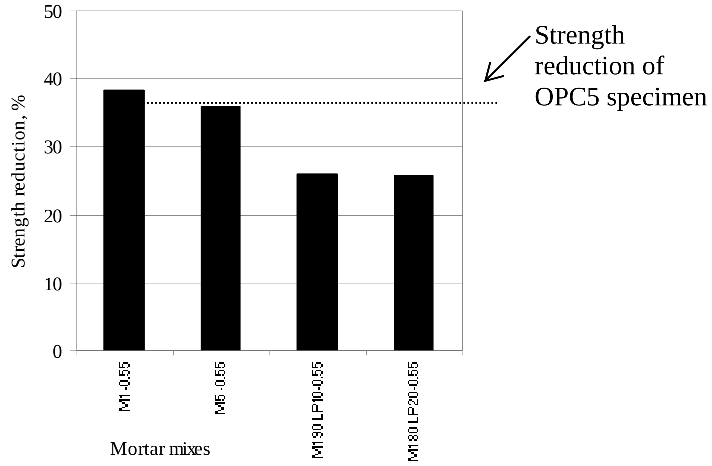

Figure 10: Strength reduction results of mortar cube specimens with w/b of 0.55 at 600 days of exposure in MS solution

4.2.4 Volume Loss Results

The test results of volume loss and weight loss of mortar cube specimens made from two cement types and replacing cements with limestone powder having w/b of 0.40 and 0.55, exposed in MS solution are shown in Fig. 11. In MS solution, the trend of change of the two performances was similar. That was to say when the weight loss of mortar cubic bar specimens increased, the volume loss also increased. It is noted that the volume loss can be measured at the earlier test age of submersion than the weight loss that the values of % volume loss are generally much larger than those of the weight loss. For prolonged test, the weight loss measurement is still recommended to be used to assess the sulfate resistance because it is easier to perform when compared to the volume loss.

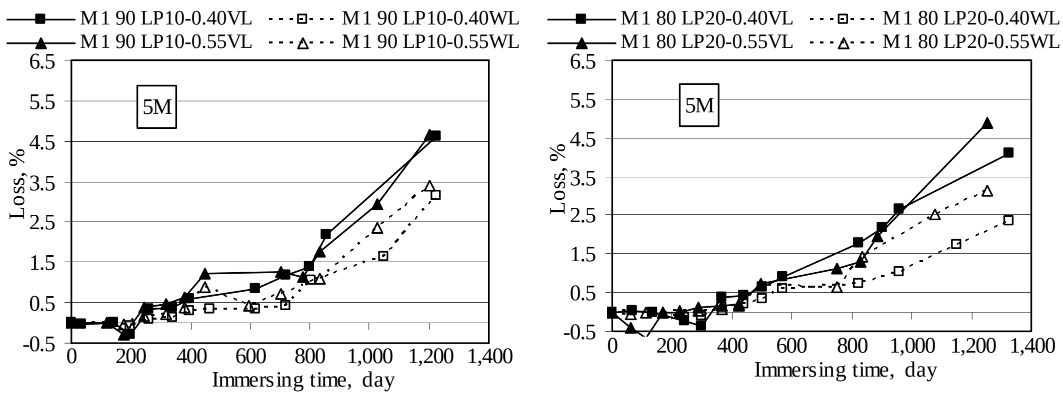

(a) 10% LP replacing cement (b) 20% LP replacing cement

Figure 11: Volume loss & weight loss of mortar cube specimens made from LP replacing cements with w/b of 0.40 and 0.55 of exposure in MS solution

4.2.5 Visual Inspection Results

Fig. 12 shows the relationship between the surface area loss (SAL) and period of immersion of OPC1, OPC5 and LP replacing cement mortar cube specimens with w/b of 0.55 immersed in MS solution. This figure indicated that the LP replacing cement mortar cube specimens performed relatively well after 1,360 days, with excellent performance at a SAL lower than 10%. On the other hand, SAL of OPC1 and OPC5 cement mortar cube specimens was the highest which was similar to the case of weight loss results as mentioned before.

The results from Fig. 13 supported the use of visual inspection with image processing technique as a method to assess the surface deterioration type of sulfate attack. Visual inspection has provided a much earlier indication of the deterioration than the weight loss test. At early submersion ages, all specimens recorded increases in weight as presented in Fig. 13 but the visual inspection with image processing technique could indicate surface deterioration at the SAL up to 1%. It was also observed that specimens with high SAL value, more than 1% loss at the age of 240 days showed very low weight loss at the same exposure period of 240 days (Fig. 13(a)), however they showed high weight loss in long term period (Fig. 13(b)) and the two values, SAL at 240 days and % weight loss at long term, had good correlation. Therefore, visual inspection with image processing technique was very useful as it is possible to evaluate the surface deterioration type of sulfate attack at the earlier period.

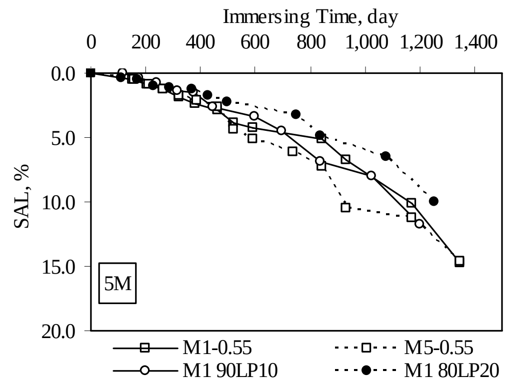

Figure 12: Relationship between the SAL and period of immersion in M<u>S</u> solution of mortar cube specimens with w/b of 0.55

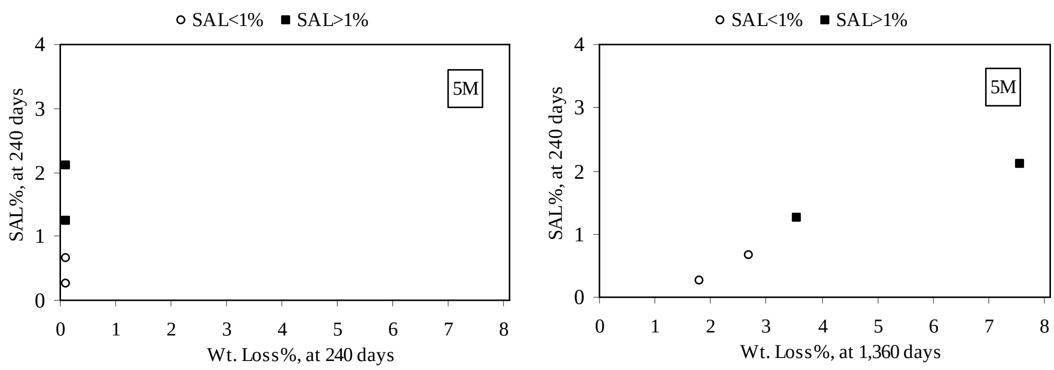

(a) 240 days (b) 1,360 days

Figure 13: Relationship between the SAL at 240 days and weight loss at 2 exposure periods (240 days and 1,360 days) of immersion in M<u>S</u> solution of specimens

Also, the choice of degradation measurement may lead to different conclusions due to the multiple mechanisms of deterioration. Often a combination of multiple relevant indicators will be necessary. Therefore, only one method of measurement may not be sufficient to characterise the degradation. Weight loss, for instance, may be well used when no secondary products precipitate, otherwise it may be the result of a combination of several phenomena. It is therefore more beneficial to use image processing technique to investigate the M$\underline{S}$ resistance of the specimen, for the surface deterioration type.

5. PROPOSED RECOMMENDATIONS FOR SELECTING TEST METHOD FOR SULFATE RESISTANCE EVALUATION

From the obtained results of expansion and weight loss, it could be seen that in case of N$\underline{S}$ solution, expansion test is appropriate for performance evaluation of ordinary Portland cement and LP replacing cement mortars. In case of M$\underline{S}$ solution, the relationship between expansion and weight loss of mortar specimens in M$\underline{S}$ solution, is directly proportional for LP replacing cement mortars. Therefore, for OPC and LP replacing cement specimens immersed in M$\underline{S}$ solution, the suitable tests should be both weight loss or volume loss or image processing technique and expansion. Based on the results of this study, the recommendations for selecting laboratory test method for sulfate resistance evaluation of cement and LP replacing cement are proposed in Table 3.

Table 3: Proposed recommendations for selecting test method for sulfate resistance evaluation

Type of sulfate solution	**Binder types**	**Recommendation for laboratory test method**
Sodium Sulfate	OPC and LP replacing cement	Expansion
Magnesium Sulfate	OPC and LP replacing cement	Weight loss *or* Image processing technique *and* Expansion

6. CONCLUSIONS

The study on sulfate resistance of mortars made from limestone powder replacing cements indicated that the limestone powder replacing cement had advantages over OPC1 cement in N$\underline{S}$ solution since it is less susceptible to the expansion due to higher porosity which increased available spaces for ettringite deposition. Weight loss measurement does not provide any useful information for evaluation of N$\underline{S}$ resistance as the mechanism of N$\underline{S}$ attack is mainly the ettringite formation which results in expansion rather than weight loss. For mortars containing limestone powder in M$\underline{S}$ solution, the M$\underline{S}$ decreased the system's pH. There occurred higher dissolution of $CaCO_3$ from the limestone powder which contributed to more gypsum formation as well as resulted in formation of magnesite and dolomite which mitigated the conversion of C-S-H to M-S-H and then resulted in less weight loss and less severe surface etching of the specimens.

For surface deterioration type in MS solution, the weight loss of specimens exposed to sulfate at early ages does not provide clear evaluation results of the sulfate resistance due to long period of weight gain while the strength reduction method requires large amount of specimens and difficult to prepare the damaged surface for the test. Visual inspection with image processing technique is useful to be applied to observe the deterioration of specimens at early submersion ages. The results obtained from the image processing technique also have good correlation with the long term deterioration.
It was proposed that for specimens immersed NS solution, expansion test is appropriate for performance evaluation of ordinary Portland cement and LP replacing cement mortar bar specimens. In case of MS solution, both expansion and weight loss or volume loss or image processing technique are considered suitable to test LP replacing cement mortars.

ACKNOWLEDGEMENT

This research was supported by the research funds from Srinakharinwirot University, Siam Research & Innovation Co Ltd., and Construction and Maintenance Technology Research Center (CONTEC) of Sirindhorn International Institute of Technology, Thammasat University. The research is also partially supported by the Higher Education Research Promotion and National Research University Project of Thailand, Office of the Higher Education Commission, and National Science and Technology Development Agency (NSTDA).

REFERENCES

Al-Amoudi, O.S.B., 1995. Performance of 15 reinforced concretes in magnesium-sodium sulphate environments, *Construction and Building Materials*, Vol. 9, No.3, pp. 149-158.

Irassar, E.F., Bonavetti, V.L., Gonzalez, M., 2003. Microstructural study of sulfate attack on ordinary and limestone Portland cements at ambient temperature, *Cement and Concrete Research*, Vol.33, pp.31-41.

Krammart, P. and Tangtermsirikul S., 2004. Expansion, strength reduction and weight loss of fly ash concrete in sulfate solution, *AJSTD* Vol.21 Issue 4, pp. 373-390.

Lee, S., 2007. Performance deterioration of Portland cement matrix due to magnesium sulfate attack, *KSCE Journal of Civil Engineering*, Vol.11, pp.157-163.

Saengsoy, W., and Tangtermsirikul, S., 2010. Determination of Mix Proportion of Hardened Concrete containing Fly Ash with Different Characteristics, *Proceedings of 4th ACF International Conference*, Taipei, Taiwan, Tue-S4.1-05.

Tikalsky, P.J., and Carrasquillo, R.L., 1989. The effects of fly ash on the sulfate resistance of concrete, *Research Report 481-5*, Center for Transport Research, The University of Texas at Austin, Austin, Texas, USA, 317 pages.

Hanoi towards 2030 - Substance flow analysis supporting the planning process

Viet Anh NGUYEN[1], Jan-Olof DRANGERT[2], Manh Khai NGUYEN[3], Thi Ha NGUYEN[4], Hans Bertil WITTGREN[5] and Celeste ZIMMERMANN[6]
[1] Associate Professor and Vice Director, Institute of Environmental Science and Engineering (IESE), Hanoi University of Civil Engineering, Vietnam.
vietanhctn@gmail.com
[2] Associate Professor and Managing Director, Vatema AB, Stockholm, Sweden
[3] Associate Professor and Vice Dean, Faculty of Environmental Science, Hanoi University of Science,
Vietnam
[4] Associate Professor and Head of Department, Environmental Technology Department,
Hanoi University of Science, Vietnam
[5] Associate Professor and Project Manager, Urban Water Management AB, Linköping, Sweden
[6] Master of Science, Division of Water and Environmental Studies, Linköping University, Sweden

ABSTRACT

Vietnam is rapidly urbanizing and Hanoi is becoming a megacity. The current population of Greater Hanoi, 6.6 million, is expected to increase by almost 50 % until 2030. Challenges faced by the city in terms of, e.g., water and wastewater management, food and energy supply, as well as social infrastructure, are typical for developing cities. The Master Plan of Hanoi city to 2030, with a vision to 2050, has just been completed (2011). It is therefore the right time to conduct a study on sustainable development solutions for the city, so as to propose efficient preparation of detailed sector development plans. In the present study, substance flow analysis of the crucial plant nutrient of phosphorus, and of organic "waste" (measured as COD), is employed to analyze the outcome of different scenario assumptions concerning, e.g., population increase and development of new satellite cities, changes in food habits, and different technologies for management of organic waste products. Furthermore, the database with associated flow calculations, supplemented with a user interface, is intended as a decision support tool. This project has scanned what options there may be for a sustainable Hanoi and the outcomes can be fed into the decision making process for the city development at various levels.

Keywords: *decision support tool, organic matter, phosphorus, substance flow analysis, scenario.*

1. INTRODUCTION

Limited global resources and increasing emissions push planners and societies to develop more sustainable cities. Phosphorus (P) is an essential nutrient for plant growth and food security, and it requires a holistic system approach to coordinate P-flows between urban and rural areas. Agriculture dominates the ecological footprints of phosphorus use and misuse, while urban demands from changing diets and detergents impact flows and emissions to the environment.

In this article the future of phosphorus flows in the Greater Hanoi area in Vietnam is analyzed from two perspectives. The linear flows with little or no recovery and recycling of urban nutrients in agriculture and, alternatively, short loop flows where most P-containing matter is recovered and brought back to soils for food production. Both scenarios build on estimates in the ‘Master Plan of Hanoi city to 2030, with a vision to 2050’ (Ministry of Construction - MOC, 2011). A preliminary survey shows that P flows in Greater Hanoi is dominated by pig and rice production and detergents. These three flows are singled out for the analysis of some scenarios.

2. MATERIALS & METHODS

As defined by Brunner and Rechberger (2004), Material Flow Analysis (MFA) is ‘a systematic assessment of the flows and stocks of materials within a system defined is space and time’. In industrialized countries it has been used to help identify and respond to emerging environmental problems (Montangero and Belevi, 2008), however it is also being increasingly applied in developing countries, particularly in the context of environmental sanitation.

2.1 System definition

The system boundary of this study is the geographical limits of Greater Hanoi, and the substances in focus are phosphorus and COD. This is an extension of the work done by Montangero in central Hanoi (Montangero, 2007). The work published in this paper is limited to the results regarding phosphorus (P).

In MFA, processes are physical or conceptual spaces in which substances are transformed, transported or stored. In this study, 19 different processes were defined, and each was assigned a number from 1 to 25 (Table 1). As we modeled the numbering system after Montangero (2007) and some of the processes were not used in our system, some numbers are left blank. Additionally, some processes were further divided into sub-processes, which are indicated by a lower case letter following the process number.

Table 1: List of processes and sub-processes used in the study

Process	Description
1	Inhabitants
2	On-site sanitation (a. Septic tank; b. Biogas latrine; c. Pit latrine; d. Single or double vault latrine; e. Bucket latrine; f. Open defecation; g. Urine diversion; h. Blackwater diversion)
3	Combined sewerage & drainage
4	Solid waste collection (a. Food waste collection; b. Sludge collection; c. Excreta collection; d. Urine collection; e. Blackwater collection and dewatering)

5	Water supply
6	Goods Exchange
7	Industry (a. Brewery; b. Distillery; c. Dairy; d. Bakery; e. Slaughterhouse)
8	Handicraft industry (a. Cassava & arrowroot processing; b. Rice vermicelli production)
9	(Not in use)
10	Composting
11	Waste site (a. Landfill; b. Open dump)
12	Livestock (a. Pig; b. Poultry; c. Cattle; d. Buffalo)
13	Aquaculture (a. Fish pond)
14	Crop (a. Rice; b. Maize; c. Vegetables; d. Soybean; e. Sweet potato; f. Fruit)
15	Surface water
16	Soil/Groundwater
17	Atmosphere
18 - 22	(Not in use)
23	Wastewater treatment plant
24	Biogas plant
25	Hazardous waste collection

2.2 Data Collection

The vast amount of data assembled for this study was collected in a variety of ways including interviews, observations, local documents and literature searches, and communication with experts. Most of the data is current (2009-2012) but some data, particularly with respect to the P content of different products, may be older. Due to the quantity of data assembled, it is not possible to cite references for every data point included in the database given the limited space of this publication.

Interviews and observations were the first stage of data collection. A total of 4 field studies were conducted; 3 in villages and 1 in an urban ward. Students at Hanoi University of Natural Sciences and Hanoi University of Civil Engineering composed questionnaires in Vietnamese and the local ward or village leader took them to various families to conduct the interviews. Local experts were also consulted in some instances. Some information was also made available via village reports and local industrial information since each commune submits an annual report and the industries issue yearly production figures. When information was required that could not be obtained locally through an interview or a local source, literature searches were conducted. The top priority was finding data from Hanoi or other nearby provinces, but if that was not available, figures were taken for Vietnam, South East Asia, or the world, in that order of preference. Ultimately the data from the various sources were combined to create a single database with separate information for the rural, urban and industrial sectors of Greater Hanoi.

2.3 Data management

Parameters are the raw data used for calculations. See Table 2 for examples. The parameters are given identifying names in the following pattern:

y_name: y = a symbol indicating the class of parameter; name = a short description of the parameter.

or, where applicable, **y_P_name** (where P indicates it is specific to phosphorus).

Table 2: Samples of the various classes of parameters

Parameter	**Description**	**Parameter Class**
n_inhabitants	Number of inhabitants	Number (n)
a_market	Market area	Area (a)
f_faecalsludge	Reported faecal sludge emptying factor	Frequency (f)
m_P_greywater	P load in greywater	Mass flow (m)
m'_SWbakery	Solid waste generation from bakery	Rate of mass change (m')
q_rain	Rain	Volumetric flow (q)
q'_WWslaughter housepig	Wastewater generation rate from pig slaughterhouses	Rate of volumetric change (q')
c_P_groundwater	Concentration of P in groundwater	Concentration (c)
r_fattener_pigs	Ratio between fatteners and total number of pigs	Ratio (r)

The *mass flows* of the substance(s) to and from each process are calculated by using relevant parameters. The following notation was used to represent the mass flow of substances between processes:

P*i-ii* (where P= phosphorus, *i*= the initial process, and *ii*= the receiving process)

For example P1-12a would represent the flow of phosphorus from process 1 to process 12a.

Parameters are used to write *system equations* for the mass flow variables. For example:

P1-12a = m_domesticFW * r_livestock_FW * c_P_domesticFW

multiplies the amount of domestic food waste (kg cap^{-1} yr^{-1}) with the ratio fed to livestock (-) and the P content in food (g P kg^{-1}) to obtain the P flow in food waste given to pigs (g P cap^{-1} yr^{-1}).

Once the mass flows are known, the stock change rate of a given substance in each process can be determined by finding the difference between the sum of the inputs and the outputs. In this study the following notation is used to represent the stock rate of change:

$$dM(Xi)/dt = \Sigma_{inputs} - \Sigma_{outputs}$$ (where X=the substance and *i*= the process).

For example, dM(P1)/dt would represent the stock change of phosphorus in process 1.

The database was constantly refined as questions or evidence of missing data emerged. Flows were re-considered and the system altered to be more representative of Greater Hanoi as new information came to light. If there seemed to be problems with the calculations the relevant data was reassessed at a new literature search was conducted to ensure appropriate data was used. Due to the wide scope of the project, specific uncertainties for each calculation were not determined. In the interest of simplicity the guideline of an acceptability of 10 % error in stock changes (Brunner & Rechberger, 2004) was taken as a reference point.

2.4 Visualization and user interface

The software STAN (Vienna University of Technology, 2012) was used to visualize the results. Weighted arrows are used to indicate the amount of mass in each flow. Diagrams were created for each process individually, as well as representations of larger parts of the system comprised of several processes.

To facilitate user interaction with the database, a user interface was constructed. This allowed the user to vary the values of selected parameters to observe the effects on the system. The interface is in a rudimentary form, but is continually being improved with the hope that it can serve as a resource for city planners and policy makers.

3. RESULTS

The results presented below concern phosphorus (P) flows in Greater Hanoi (GH) related to a 2010 population of 6 617 900 inhabitants (HSO, 2011), and a projected population of 9 135 500 inhabitants in 2030 (MOC, 2011). Focus is on the large P flows associated with inhabitants' consumption of rice, pork and detergents. The 'waste' flows associated with these processes serve as planning support for future improved P management in GH.

First, assumptions and results for the 'Present situation' are presented, and then assumptions regarding two scenarios, 'Scenario 2030 Master Plan Linear' and 'Scenario 2030 Master Plan Loops'. Both these scenarios involve an almost 50 % increase in population. Finally, the 'Present situation' and the two 'Scenarios 2030' are compared in terms of P flows.

3.1 Present situation

Current rice and pork consumption amounts to 137 kg and 24 kg cap^{-1} yr^{-1} respectively (VDD & UNICEF, 2011; The Pig Site, 2010), with a decreasing trend for rice and an increasing trend for pork that mirrors the enhanced economic development in Vietnam. Together with detergents, these two food items account for 66 % of the P use by GH inhabitants (Figure 1, ‘1. Inhabitants’). Other food items taken together account for 34 % and include fish and seafood, other red meat (excluding pork), poultry meat, vegetables, fruits, other cereals (excluding rice), tubers, milk, eggs, and miscellaneous food items. Among these, ‘fish and seafood’ account for the largest fraction (9 %), and, like pork, have an increasing consumption trend. The improved human nutritional status in Vietnam is reflected in the amount of protein that has increased from 45 g (1991) to 72 cap^{-1} d^{-1} (2008), and thereof from animal origin from 10 g to 27 g cap^{-1} d^{-1} in the same period (FAO, 2013).

More than 90 % of urban inhabitants, and between 50 and 60 % of rural inhabitants, have flush toilets connected to septic tanks (Nguyen V. A. et al., 2011). In urban and peri-urban districts, these septic tanks are mostly connected to the city sewer (WSP, 2012). Only blackwater enters the septic tanks, which seems to be a remnant from earlier direct collection of excreta. Greywater is usually discharged directly to sewers or waterways. Besides flush toilets, pit latrines or double vault latrines are the most common solutions in rural areas.

Today, three wastewater treatment plants treat 7 % of the effluent coming from core city area, while the remainder is discharged to waterways. Septic tanks are desludged on average only every 6th year. Only 10 % of collected sludge is collected by the urban environment company (URENCO) and brought to the landfill or composted (Nguyen V. A. et al., 2011). The remainder is collected by other service providers who usually discharge the sludge illegally to fish farms, landfills, or waterways, due to a lack of treatment infrastructure and poor inspection. New high-rise office and apartment building connect their blackwater to big septic tanks in the ground. Septic tank effluent and greywater is discharged into combined sewer, not being treated in most of cases. Much of the polluted effluent is used for irrigation in downstream areas. In the core city, 97 % of the over hundred lakes are eutrophic, of which 68 % are hyper-eutrophic (Hoang T. T. H. et al., 2012).

Pig production and rice farming dominate P flows in agriculture. Farmers in the Red River Delta typically grow three crops per year, spring rice from February to June, summer rice from June to September, and a winter crop (often maize) from October to January. The potential land area for growing winter crops is about 60 % of the rice area, but only 40 % of the rice area is currently cultivated with winter crops (Tran T. S. et al., 2004). Good lowland farmers routinely produce 15 to 18 tonnes of grain per ha each year in a system that is traditionally community-based, very labor-intensive, and involving much recycling of nutrients (Bray 1998). Farms are small, 0.1 – 0.5 ha and the population exceeds 2 000 people per km^2 in several provinces. Rice is mainly for local consumption (about 80 %). The area planted with rice has remained about the same since a few decades, while a substantial increase in yields is due to improved fertilization and expansion of irrigated areas from 65 % to 75 % of rice fields (1990 to 2000) (Tran T. S. et al., 2004). Most other crops such as tubers, vegetables, maize etc. has also experienced substantial increases in productivity (FAO, 2013).

The flow chart in Figure 1 is a simplified system that accounts for the main flows and connects urban and rural flows within GH.

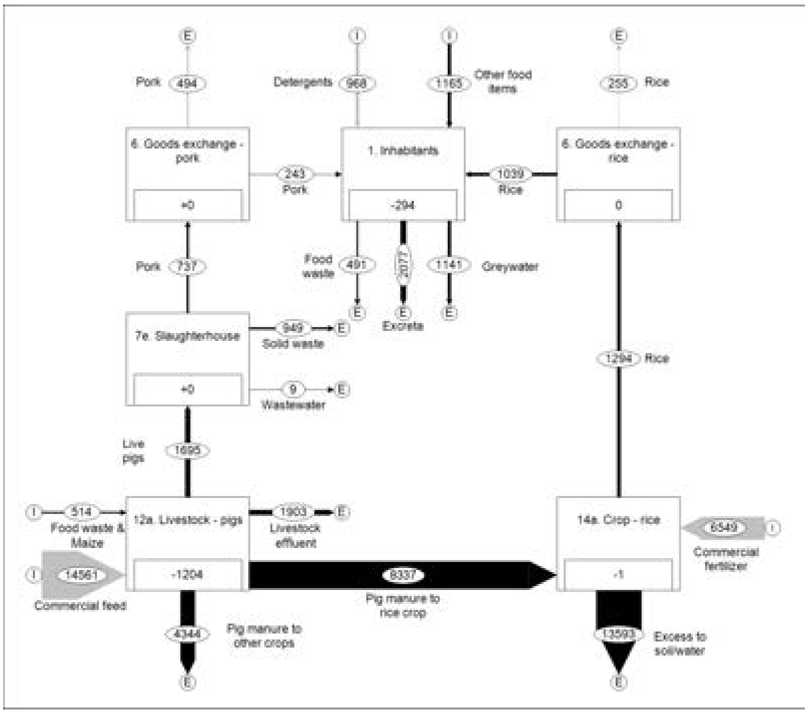

Figure 1: Current important phosphorus flows (ton P yr^{-1}) in Greater Hanoi

In Fig. 1, ‘I’ and ‘E’ represent import and export. Black arrows represent flows mainly within GH. Grey arrows represent import flows to and export flows from the GH area. Numbers given at the bottom of process boxes show ‘sum of input - sum of output’. If it is ‘0’, an unknown flow has been calculated as a difference between known input and output flows, i. e., Out 2 (unknown) = In 1 (known) + In 2 (known) – Out 1 (known). In two process boxes, ‘1. Inhabitants’ and ‘12a. Livestock - pigs’, inputs and outputs have been calculated independently.

The total feed need for pigs (input to ‘12a. Livestock - pigs’) is calculated from data regarding sows with piglets and fatteners. Eighty per cent of the food waste from rural inhabitants, and 20 % of the food waste from urban inhabitants (a total of 267 ton P yr^{-1}) is assumed to be given to pigs. All maize produced in GH is assumed to be used as pig feed (247 ton P yr^{-1}). The remaining required feed is covered by import of commercial feed.

Of all pig manure, 66 % is applied on rice fields according to the ratio between paddy rice area and total crop area (HSO, 2011). This results in an average application of 40 kg P ha^{-1} yr^{-1} to a paddy rice area of 204 662 ha in GH (HSO, 2011). This amount of manure is in line with observations from the Red River Delta, where farmers harvest two rice crops per year and apply 20-25 kg P ha^{-1} $crop^{-1}$ (Tran T. S. et al., 2004). The authors also report that 32 kg P ha^{-1} of commercial fertilizers are applied annually. These figures are used to calculate input to ‘14a. Crop - rice’.

It is assumed that about 1/3 of the pig manure is first used for biogas production prior to applying the slurry on crops (the biogas process is not shown in Figure 1). The assumption is that no P loss occurs in the biogas process. Therefore, potential losses will appear in the flow ‘Excess to soil/water’ from the ‘14a. Crop - rice’ process. This unknown flow is calculated as the difference between the known other flows to and from the process.

Based on Swedish figures that the slaughter-weight of fatteners is 73.7 % of the live weight, and that pork meat is 59 % of the slaughter-weight (Carlsson et al., 2009) gives that 737 ton P yr^{-1} is contained in pork meat. The P content of solid waste from ‘7e. Slaughterhouse’ is calculated as the difference between known flows.

The (net) export of pork from GH is calculated as the difference between the production of pork from ‘7e. Slaughterhouse’ and the input of pork for consumption to ‘1. Inhabitants’.

The P flow with rice from ‘14a. Crop - rice’ to ‘6. Goods exchange - rice’ is calculated given a total rice yield of 1 125 016 ton yr^{-1} (HSO, 2011), which corresponds to 5.5 ton ha^{-1} yr^{-1}, and assuming a P content in rice (excluding bran) of 1.15 g P kg^{-1} (USDA, 2012). Export (net) of rice is calculated in the same way as pork export.

The P flow with food waste from ‘1. Inhabitants’ is calculated from an annual generation of 37 kg cap^{-1} yr^{-1} (Co Loa Commune People’s Committee, 2009; Co Loa Interview, 2011-10-11) and a P content of 2 g P kg^{-1} (Diaz et al., 1996). For excreta and greywater, P loads are assumed to be 0.86 g P cap^{-1} d^{-1} (Nguyen V. A., 2007) and 0.4 g P cap^{-1} d^{-1} (Büsser, 2006), respectively.

3.2 Scenario 2030 - Master Plan with linear P flows to water bodies and landfills

The assumptions of the Master Plan 2030 deal with population increase, pattern of new suburbs, full coverage of water and sanitation, etc. No goals for sustainability or environmental issues are provided. Therefore, this scenario calculation takes into account an anticipated population increase of 42 % from 2010 to 9.14 million inhabitants 2030 (Prime Minister Decision 1239/QD-Ttg, 2011). As a result, other factors vary accordingly: a 42 % increase in all flows in and out from the process ‘1. Inhabitants’, and associated changes in import to/export from ‘6. Goods exchange’. For rice, the population increase result in that some import will be required to meet demand. In reality, such import may be avoided by increased productivity and/or increased area for paddy rice cultivation. For pork, production remains higher than local consumption, and there is still capacity to export pork meat from GH.

3.3 Scenario 2030 – P loops to recover and apply P on agricultural soils

This scenario is derived from the following desired functional criteria: no P in detergents, all organic solid waste generated in Greater Hanoi to be segregated, composted or digested to biogas, and the residues applied to farmland. The available nutrients in human excreta are used for cereal production. No eutrophication of rivers and lakes, and reduced import of commercial fertilizers.

In the ‘Scenario 2030 - Master Plan Loops’ the same population size as in the previous scenario is assumed. Pork consumption per capita is assumed to double from 24 to 48 kg cap^{-1} yr^{-1}, and rice consumption to decrease with the same amount, from 137 to 113 kg cap^{-1} yr^{-1}. For pork, this corresponds to an annual increase in consumption by 3.5 %, and for rice an annual decrease by 1 %. In the past 10-year period, both the consumption increase for pork and the decrease for rice have been larger, so the above assumption may be considered conservative. Detergents will be phosphate-free. Furthermore, P-rich waste flows will be recycled: (i) human excreta to arable land after proper treatment for hygienic purposes; (ii) solid waste from slaughterhouses to arable land, probably as a slurry after biogas production, and; (iii) food waste will continue to be recycled as pig feed, as is currently common in rural areas, but, in the context of increasing urbanization, also be used for biogas production and the resulting slurry recycled to arable land.

3.4 Comparison of Present situation and the two scenarios for 2030

The calculations of flows in the two scenarios are presented in Table 3, and builds on the flow chart in Figure 1. The figures in the column ‘Present situation’ repeats the data in Figure 1. The column ‘Scenario 2030 – Master Plan Linear’ presents revised data due to the population increase.

The column ‘Scenario 2030 – Master Plan Loop’ presents data resulting from recycling measures and changed diet. The total input of P to ‘1. Inhabitants’ will decrease primarily due to the phasing out of P in detergents, and consequently the P flow with greywater will decrease dramatically. The P flows associated with food waste and excreta will increase somewhat, since the P-content of pork is higher than that of rice. However, even without changes in pork production, the increased consumption still allow for some export, and the decrease in rice consumption results in that no import is be needed.

The demand of P inputs for rice production is shown in the lower four rows of Table 3. The loops scenario can reduce demand for commercial fertilizers by about 4 300 ton P yr^{-1}. in comparison with the linear scenario. This reduction is possible thanks to recycled P from food waste (336 ton P yr^{-1}) and human excreta (3 026 ton P yr^{-1}) from ‘Inhabitants’ and waste from slaughterhouses (949 ton P yr^{-1}) can replace imported commercial fertilizers.

Table 3: Comparison of P flows for the present situation and the two scenarios for 2030 (ton P yr^{-1}).

P flows	Present situation	Scenario 2030 - MP Linear	Scenario 2030 - MP Loops
Inhabitants – In			
Pork	243	345	691
Rice	1 039	1 476	1 219

Detergents	968	1 374	0
Other food	1 165	1 654	1 654
Inhabitants – Out			
Food waste	491	698	715
Excreta	2 077	2 951	3 026
Greywater	1 141	1 621	246
Goods exchange, pork – Out			
Pork (to Inhabitants)	243	345	691
Pork (Export)	494	392	47
Slaughterhouse – Out			
Solid waste	949	949	949
Livestock, pigs – In			
Food waste	267	379	379
Goods exchange, rice – In			
Rice (Import)	0	182	0
Goods exchange, rice – Out			
Rice (to Inhabitants)	1 039	1 476	1 219
Rice (Export)	255	0	74
Crop, rice – In			
Commercial fertilizer (Import)	6 549	6 549	2 238
Biogas slurry (from Inhabitants, Food waste)	0	0	336*
Excreta (from Inhabitants)	0	0	3 026
Biogas slurry (from Slaughterhouse, Solid waste)	0	0	949

* The difference between total generation of food waste, 715 ton P yr^{-1}, and food waste fed to pigs, 379 ton P yr^{-1}.

A further 1 374 ton P yr^{-1} can be saved by using P-free detergents. The loops scenario represents a win-win situation with reduced nutrient pollution of surface and groundwater by discharges of P from wastewater outlets and landfills. This environmental debt in the case of linear flows is a hidden cost in today´s discussion, but must be included in a sustainability calculation.

In addition to those savings it is reasonable to assume that increased food efficiency in pig production and better P management in crop production can decrease the two largest P flows in Figure 1: import of commercial feed and the excess of P to soil/water, where the latter is probably lost to water to a large degree.

4. DISCUSSIONS

Up to now, trends to manage P-containing matter in urban flows have become more and more linear. Previous recycling of P-rich human excreta and food waste to enrich agricultural soils has been replaced by waste discharges to water bodies and landfills. The huge increase in use of P in agriculture has been met by imported commercial fertilizers and animal feed. The previously strong nutrient link between urban and rural areas in Greater Hanoi is fading away.

Anticipated global scarcity of virgin P and nutrients more generally points to the need to reduce wastage and increase recycling (Cordell et al., 2009). A ban on P in detergents will reduce demand in GH by more than 1 000 ton P yr^{-1}, which is of the same magnitude as 20 % of the imported commercial fertilizers in 2010. The detergent manufacturers can easily introduce alternative washing compounds, e.g., polycarboxylates as have been done in other countries (EU, 2012). A great benefit is that eutrophication of water bodies will be reduced when there is less P in the greywater fraction.

The population increase requires new homes to be constructed, and these could be affordably built to facilitate recovery of nutrients. The infrastructure could be designed to transfer recovered P to farmland. Retrofitting existing houses would take longer and gradually be achieved as retrofitting is due anyway. The economic value of P, and more so of nitrogen, in the now wasted nutrient resources can pay for the transport of recovered nutrients to farmland (Jönsson et al., 2012).

By sorting food and other organic waste and turn it to compost material, recycling human waste and slaughterhouse waste to farmland, and banning P in detergents, some 5 700 ton P yr^{-1} can be saved in 2030. Thereby, toxic emissions from producing mined P and transport it to Vietnam will be reduced accordingly (Wissa, 2006).

The potential option to save on P by not shifting to a diet with more meat and dairy products would require other policy measures. Firstly, a shift requires that consumers have the information that meat and milk are P-inefficient methods to access building blocks for the human body. Secondly, the environmental costs accruing from leakages are high. Such negative factors must be balanced with positive aspects such as improved status and time-saving through access to easy-to-prepare meat-based food.

This article has presented some examples of calculations that can be made based on the decision support tool currently under construction. Work will proceed by completing the data base concerning both P and COD, and by development of a user interface to allow user-friendly access to calculation of different scenarios.

ACKNOWLEDGEMENT

The Paper was prepared based on the study results under the Sida PDC project coded AKT-2010-071: Contributions towards more equitable and sustainable South Asian Cities - The case of Hanoi towards 2030. Contributions to the study were made by the paper authors, and the other team members including Karin Tonderski, Nguyen Thi Anh Tuyet, Do Hong Anh, Nguyen Phuong Thao, Nguyen Tuan Linh, Bui Thi Thuy, Hoang Minh Trang, Ngo Van Anh, Nguyen Minh Phuong, Pham Hoang Giang, Nguyen Phuong Hong. Special thanks are delivered to all research team members, leaders and staff of related organizations who were involved in the study, providing valuable expertise and information.

REFERENCES

Bray, F., 1998. A stable landscape? Social and cultural sustainability in Asian rice systems. In: Dowling, N. G., Greenfield, S. M., Fischer, K. S. (editors). *Sustainability of rice in the global food system*. Pacific Basin Study Center & International Rice Research Institute (IRRI), Davis (California, USA) & Manila (Philippines), pp. 45-66.

Brunner, P. H. and Rechberger, H., 2004. *Practical Handbook of Material Flow Analysis*. Lewis Publishers, CRC Press LLC, Boca Raton (Florida, USA).

Büsser, S., 2006. *Characteristics of domestic wastewater flows in urban and peri-urban households in Vietnam*. ETHZ Practical Training Report. Eawag: Swiss Federal Institute of Aquatic Science and Technology & Sandec: Department of Water and Sanitation in Developing Countries, Duebendorf (Switzerland).

Carlsson, B., Sonesson, U., Cederberg, C. and Sund, V., 2009. *Livscykelanalys (LCA) av svenskt ekologiskt griskött (Life Cycle Analysis of Swedish Organic Pig Meat)*. SIK Report No. 798, SIK - the Swedish Institute for Food and Biotechnology, Gothenburg (Sweden). In Swedish.

Co Loa Commune People's Committee, 2009. *Annual report of Co Loa commune*. In Vietnamese.

Cordell, D., Drangert, J.-O. and White, S., 2009. The story of phosphorus: Global food security and food for thought. *Global Environmental Change*, 19, 292–305.

Diaz, L. F., Savage, G. M., Eggerth, L. L. and Golucke, C.G., 1996. *Solid waste management for economically developing countries*. International Solid Waste Association & CalRecovery Inc., Concord (California, USA).

EU, 2012. Regulation (EU) No 259/2012 of the European parliament and of the council of 14 March 2012 amending Regulation (EC) No 648/2004 as regards the use of phosphates and other phosphorus compounds in consumer laundry detergents and consumer automatic dishwasher detergents. *Official Journal of the European Union* 30.3.2012.

FAO, 2013. *FAO Annual Report 2013*. Food and Agricultural Organization. Rome (Italy).

HSO (Hanoi Statistical Office), 2011. *Hanoi Statistical Yearbook 2010*. Hanoi Statistical Office, Hanoi (Vietnam).

Hoang Thi Thu Huong, Ly Bich Thuy, Pham Thu Phuong and Doan Thi Thai Yen, 2012. Eutrophication in the lakes of Hanoi discovered by water quality index and chlorophyll-A indicator. *Journal of Science and Technology (Vietnam Academy of Science and Technology)*, Vol. 50, No. 1 C.

Jönsson, H., Hallin, S., Bishop, K., Gren, I.-M., Jensen, E. S., Rockström, J., Vinnerås, B., Bergkvist, G., Strid, I. and Kvarnström, E., 2012. Många skäl att återvinna mer fosfor (Several reasons to recover more phosphorus). *Dagens Nyheter*, 2012-08-03. In Swedish.

Prime Minister’s Decision 1239/QD-Ttg, dated 26 July 2011. *Decision on approval of General Master Plan for construction of Hanoi Capital to 2030, , and with the vision to 2050* (in Vietnamese).

Montangero, A., 2007. *Material Flow Analysis: A tool to assess material flows for environmental sanitation planning in developing countries*. Eawag: Swiss Federal Institute of Aquatic Science and Technology & Sandec: Department of Water and Sanitation in Developing Countries, Duebendorf (Switzerland).

Montangero, A. & Belevi, H., 2008. An approach to optimise nutrient management in environmental sanitation systems despite limited data. *Journal of Environmental Management*, 88, 1538–1551.

Nguyen Viet Anh, 2007. *Be tu hoai & be tu hoai cai tien (Septic tank and improved septic tank)*. Construction Publishing House, Hanoi (Vietnam). In Vietnamese.

Nguyen Viet Anh, Nguyen Hong Sam, Dinh Dang Hai, Nguyen Phuoc Dan, Bui Xuan Thanh, 2011. *Landscape Analysis and Business Model Assessment in Fecal Sludge Management: Extraction & Transportation Models in Vietnam.* Study report. For the Bill and Melinda Gates Foundation, USA.

Tran Thuc Son, Nguyen Van Chien, Vu Thi Kim Thoa, Dobermann, A. and Witt, C., 2004. Site-specific nutrient management in irrigated rice systems of the Red River Delta of Vietnam. In: Dobermann, A., Witt, C. and Dawe, D. (editors) *Increasing Productivity of Intensive Rice Systems Through Site-Specific Nutrient Management*. Science Publishers, Inc. & International Rice Research Institute (IRRI), Enfield (New Hampshire, USA) & Los Baños (Philippines), pp. 217-242.

The Pig Site, 2010. *Viet Nam - Growth in Pork Meat Consumption Leads to Opportunities for US Exporters*. Available <http://www.thepigsite.com/articles/3208/viet-nam-growth-in-pork-meat-consumption-leads-to-opportUnities-for-us-exporters> [Accessed 16 April, 2013].

USDA (U.S. Department of Agriculture, Agricultural Research Service), 2012. *USDA National Nutrient Database for Standard Reference, Release 25*. Available: <http://www.ars.usda.gov/ba/bhnrc/ndl> [Accessed 16 April, 2013].

VDD & UNICEF (Vien Dinh Duong & United Nations Children's Fund), 2011. *A review of the nutrition situation in Vietnam 2009-2010*. Medical Publishing House, Hanoi (Vietnam).

Vienna University of Technology, 2012. *STAN (subSTance flow ANalysis) software*. Available: <http://www.stan2web.net> [Accessed 16 April, 2013].

Wissa, A. E. Z., 2006. *Phosphogypsum disposal and the environment*. Ardaman & Associates Inc., Orlando (Florida, USA). Available: <http://www.fipr.state.fl.us/pondwatercd/phosphogypsum_disposal.htm> [Accessed 31 August, 2013].

WSP (Water and Sanitation Programme), 2012. *Economic Assessment of Sanitation Interventions in Vietnam. A six-country study conducted in Cambodia, China, Indonesia, Lao PDR, the Philippines and Vietnam under the Economics of Sanitation Initiative (ESI).* Water and Sanitation Programme (WSP) Technical Report, Washington DC (USA).

Comparisons nitrogen removal capacities by anammox process using different biomass carriers

TRAN Thi Hien Hoa[1], LUONG Ngoc Khanh[2], and Kenji FURUKAWA[3]
[1]National University of Civil Engineering (NUCE)
thhoadhxd@yahoo.com
[2] Vietnam Water And Environment Investment Corporation (VIWASEEN)
[3]Furukawa Consulting Company for Water Environment (FCW)

ABSTRACT

The using of biomass carriers is preferred for the cultivation of slowly growing anammox sludge. In this study, three types of PVA (polyvinyl alcohol) gel-bead, MC (malt ceramic) and PE (polyethylene) sponge were selected as biomass carriers for anammox sludge and applied in different reactors. The objective of this study is to compare the nitrogen removal capabilities of anammox process using PVA, MC and PE sponge as different biomass carriers. PVA gel-bead biomass carrier was used in a fluidized-bed reactor (FBR) (called PVA reactor). MC materials with two different sizes of d=3-5 mm and d=10-15 mm were applied in two fixed-bed reactors (called MC1 and MC2 reactors). PE sponge material was selected in fixed-bed reactor (called PE sponge reactor). PVA reactor was operated for 617 days with maximum removal rates of ammonium and total nitrogen were 1.5 and 3.0 kg N/m^3/day, respectively. MC1 and MC2 reactors were implemented for 368 days and 280 days, respectively. The T-N removal rates of MC1 were increased stepwise from 0.6 to 3.1 kg N/m^3/day from the days 187 to 315 while the T-N removal rate of MC2 obtained similarly to the results of MC1 with 0.7 to 3.1 kg N/m^3/day from the days 146 to 230. PE sponge reactor was operated continuously and T-N removal rate of 2.8 kg N/m^3/day was obtained after 240days of operation. In addition, T-N removal rate of 2 kg N/m^3/day was obtained after short operational time of 140 days for PE sponge reactor, in comparisons with the T-N removal rate of 2 kg N/m^3/day for PVA reactor, MC1 and MC2 over longer operational time of 546 days, 265 days and 185 days, respectively.

Keywords: *anammox, biomass carrier, malt ceramic, MC, polyvinyl alcohol, PVA gel beads, polyethylene, PE sponge, fixed-bed reactor, fluidized-bed reactor, FBR, NH_4-N, NO_2-N, T-N.*

1. INTRODUCTION

The traditional nitrification and denitrification processes for nitrogen removal has been researched widely. However, more economical considerations using shortcuts in the nitrification-denitrification process, i.e., <u>An</u>aerobic <u>Amm</u>onium

Oxidation (anammox), was much attention. This new process is combined with the nitritation step, the remaining ammonium and the converted nitrite from nitritation will be oxidized to dinitrogen gas under anoxic conditions with nitrite as the electron acceptor (Mulder A. *et al.*, 1995; Strous M. *et al.*, 1999a). This autotrophic process allows over 50% of the oxygen to be saved and no organic carbon source is needed (Jetten M. S. M. *et al.*, 1999). The anammox process can contribute significantly to the nitrogen removal from wastewater with low carbon content (Van de Graaf A. A. *et al.*, 1996**)**. In addition, the sludge production was negligible (Fux C. *et al.*, 2002). Therefore, anammox process is a promising and low-cost alternative of removing nitrogen from wastewater (Strous M. *et al.*, 1997a; Strous M. *et al.*, 1997b; Van de Graaf A. A. *et al.*, 1995).
The stoichiometry of the anammox reaction was determined based on mass balance over anammox enrichment cultures, as follows (Strous, M. *et al.*, 1998):

$$NH_4^+ + 1.32\ NO_2^- + 0.066\ HCO_3^- + 0.13H^+ \rightarrow$$
$$1.02\ N_2 + 0.26\ NO_3^- + 0.066\ CH_2O_{0.5}N_{0.15} + 2.03\ H_2O \quad (1)$$

The slow grow rate of anammox bacteria with a doubling time of around 11 days (Strous, M. *et al.*, 1998) required long cultivation for getting enough amount of anammox sludge. Consequently, the application of different carrier material using anammox process is a challenge and the study about the appropriate materials is paid much attention.
In this study, the first experiment was set-up by using PVA-gel beads as biomass carriers for anammox sludge in FBR (called PVA reactor). PVA-gel beads have porous microstructure that allows for microorganisms to penetrate and colonize throughout the gel material, thus providing favorable conditions for retention and cultivation of slowly growing anaerobic microorganisms (Rouse J.D. *et al.*, 2005). An upflow column reactor using non-woven biomass carrier (Furukawa K. *et al.*, 2002; Furukawa K. *et al.*, 2003; Rouse J.D. *et al.*, 2003) and packed-bed reactor using PVA gel beads(Rouse J.D. *et al.*, 2005) were established. However, influent medium for these reactors was not mixed completely. Therefore, anammox bacteria are inhibited easily by high nitrite concentration (more than 0.1 g N/L) (Strous, M. *et al.*, 1999b) at bottom of reactor. Consequently, the new fluidized bed reactor (FBR) was designed to mix substrate completely by recycling wastewater to dilute the influent medium and overcome inhibition for anammox bacteria at bottom of reactor. In addition, the surface area of PVA-gel beads is contacted better in fluidized-bed condition than in packed-bed condition and good release nitrogen gas. In the second experiment, MC materials with two different sizes of d=3-5 mm and d=10-15 mm were applied in two fixed-bed reactors (size of d=3-5 mm called MC1 reactor; size of d=10-15 mm called MC2 reactor) of the same configuration. MC is produced from beer barley husk and beer dregs. The raw material of the beer dregs is dried and molded in to cylindrical shapes, which are carbonized and crushed to different sizes. In addition, manufacturing process of MC material does not require chemicals. Therefore, MC material is natural product and low cost which is possible to reduce nitrogen removal cost. PE sponge is also effective biomass carrier material with the large pore diameter. Hence, PE sponge was selected as biomass carrier in a fixed-bed reactor (called PE sponge reactor) for nitrogen removal by the anammox process in the third experiment. The objective of this study is to compare the nitrogen removal capacities by anammox process using polyvinyl alcohol (PVA) gel beads, malt ceramics (MC) and polyethylene (PE) sponge as different biomass carriers.

2. MATERIALS AND METHODS

2.1 Experimental set-up in laboratory scale

The designed parameters and scheme diagrams for 4 reactors using PVA, MC and PE sponge are shown in Table 1 and Fig. 1, respectively.

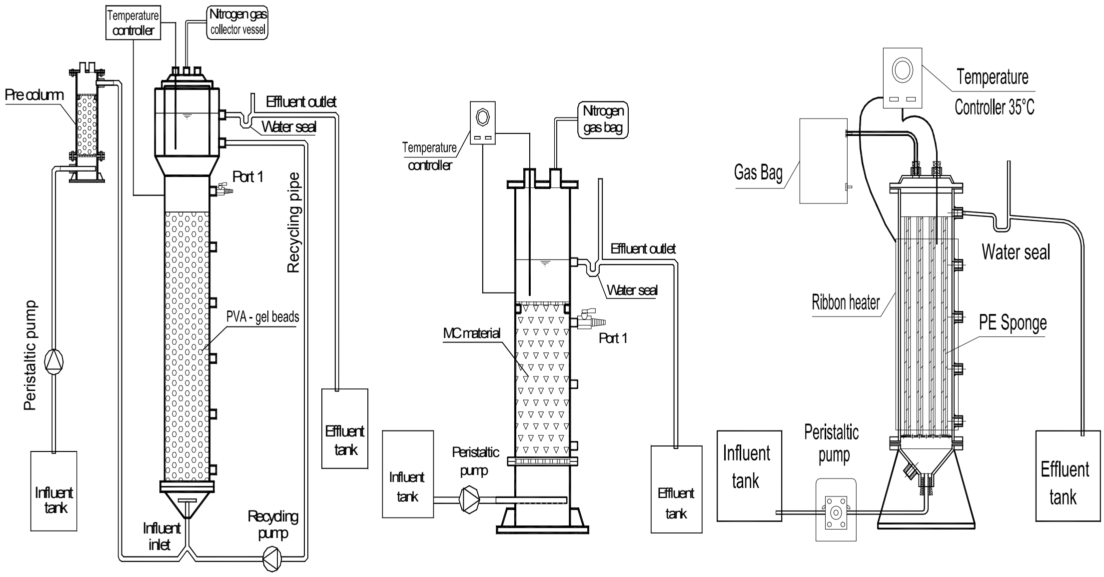

Figure 1: Schematic diagram of the reactors with differrent biomass carrier materials

Table 1: Designed parameters for 4 reactors

Parameters	**PVA reactor**	**MC1 and MC2 reactors**	**PE sponge reactor**
Type of reactor	Fluidized-bed	Fixed-bed	Fixed-bed
Total reactor volume (L)	4.06	1.62	2.90
Reaction zone volume (L)	2.15	0.65	2.60
Clarification zone volume (L)	1.4	0.34	-
Free zone volume (L)	0.51	0.31	0.30
Diameter of reactor (cm)	7.4	7.1	9.0
Height of reaction zone (cm)	50.0	16.5	41.0

2.2 Physical characteristics of different biomass carriers

Table 2: Physical characteristics of PVA-gel, MC and PE sponge

Characteristics	**PVA gel**	**MC**	**PE sponge**
Shape	Sphere	Grain	sheet
Pore diameter	10 – 20 µm	2.17×10^{-3} µm	1060 µm
Size	3.5-4 mm	3-5 mm; 10-15 mm	10 mm (thickness)
Porosity	90%	-	96%
Specific gravity	1.025 $g.cm^{-3}$	1.96 $g.cm^{-3}$	0.995$g.cm^{-3}$
Material	Polyvinyl alcohol	Charcoal	polyethylene

Polyvinyl alcohol (PVA) gel beads

PVA-gel beads Diameter is 4 mm (Fig. 2a). They are hydrophilic and have a porous diameter of 10 to 20 μm in (Fig. 2b).

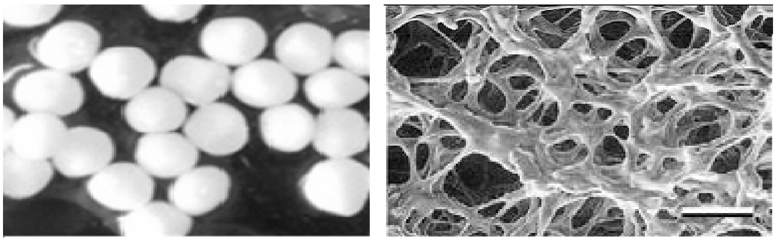

Figure 2: PVA-gel bead.
a. Origianl PVA-gel bead; b. Environmental Scanning Electron Micrograph (ESEM) of microstructure on the surface of an original PVA-gel bead. Bar indicates 10 μm

Malt ceramic (MC)

Two different sizes of MC material were 3-5 mm and 10-15 mm as shown in Fig. 3. This material has a porous microstructure with an average porous diameter of 2.17 x 10^{-3} μm.

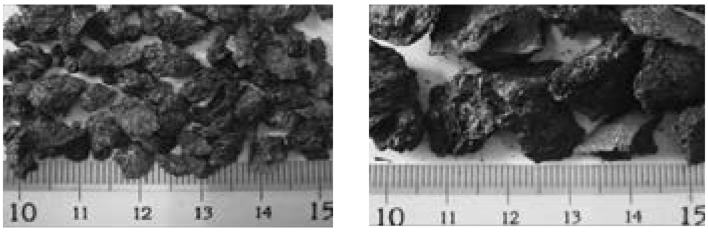

Figure 3: Malt ceramic. a. Size of 3-5 mm; b. Size

Polyethylene (PE) sponge

PE sponge material is shown in Fig. 4a with average porous diameter of 1060 μm. PE sponge material is soft hence it is supported by frame as shown in Fig. 3b.

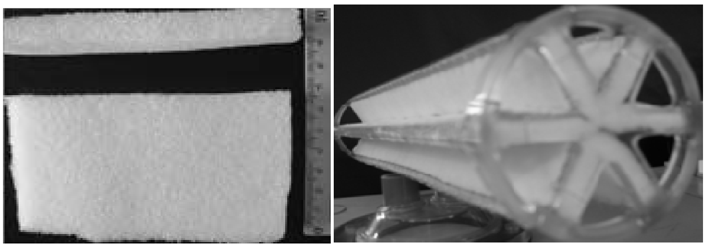

Figure 4: PE sponge material.
a. Original PE sponge material; b PE sponge material frame

As shown in Table 2, the porosities and other physical characteristics of these biomass carriers are very different. The pore diameter and porosity of PE sponge material are largest and highest in comparisons with the porous diameter and porosity of PVA gel and MC materials. Only PVA gel could be fluidized in water owing to light specific gravity and sphere shape. MC is cheap material because MC is utilized and carbonized from the beer dregs and manufacturing process does not require chemicals. Therefore, this one is cheap material in comparisons with PVA gel and PE sponge.

2.3 Seed sludge

The cultivated PVA-gel beads used for the PVA reactor originated from a anammox packed-bed reactor. Total volume of PVA-gel beads was 0.8 L in phase 1 which included 0.7 L of cultivated PVA-gel beads and 0.1 L of new PVA-gel beads. In phase 2, 0.2 L of cultivated PVA-gel beads were added for a total PVA-gel volume of 1 L. For MC1 and MC2 reactors, 0.65 g of anammox sludge taken from a nonwoven reactor was seed sludge in each reactor. For PE sponge reactor, 1.2 g of anammox sludge taken from the nonwoven reactor was also seed sludge.

2.4 Synthetic wastewater

Synthetic wastewater was prepared by adding ammonium and nitrite in the forms of $(NH_4)_2SO_4$ and $NaNO_2$, respectively to the mineral medium. Tap water originating groundwater was used for the preparation of this synthetic wastewater.

Table 4: Composition of synthetic wastewater

Composition	**Concentration**
$(NH_4)_2SO_4$ (mgN/L)	Variable (25-300)
$NaNO_2$ (mgN/L)	Variable (25-300)
$KHCO_3$ (mg/L)	125.1
KH_2PO_4 (mg/L)	54.4
$FeSO_4.7H_2O$ (mg/L)	9
EDTA (mg/L)	5
Trace element solution I (mg/L): $CaCl_2.2H_2O$ 700, $MgSO_4.7H_2O$ 500	
Trace element solution II (mg/L): $CuSO_4.5H_2O$ 0.25, $ZnSO_4$ $.7H_2O$ 0.43, $CoCl_2.6H_2O$ 0.24, $MnCl_2.4H_2O$ 0.99, $NaMoO_4.2H_2O$ 0.22, $NiCl_2.6H_2O$ 0.19, $NaSeO_4.10H_20$ 0.11, H_3BO_4 0.014	

2.5 Operational conditions for 4 reactors using PVA, MC and PE sponge as biomass carriers

Influents for 4 reactors using PVA, MC and PE sponge as biomass carriers were fed in up-flow mode using a peristaltic pump (Eyela Co., Ltd., Tokyo). The reactor temperatures were maintained at 33^oC to 35^oC, controlled thermostatically with an external ribbon-heating element. Dark conditions were maintained using black vinyl sheet enclosures. Small styrafoam balls were placed in the feed storage tank to retard oxygen transfer to the synthetic wastewater. In addition, purging with nitrogen gas was used on a daily basis to keep dissolved oxygen levels in the influent below 0.5 mg/L. Influent pH levels were 7.2 to 7.5 without adjustment.

Table 5: Operational parameters for 4 reactors using PVA, MC and PE sponge as biomass carriers

Parameters	**PVA reactor**	**MC1 and MC2 reactors**	**PE sponge reactor**
HRT (h)	16- 3	12 - 3	24 - 4
Flow rate (L/d)	3.2 - 17.2	1.3 - 5.2	2.6 - 15.6
Influent NH_4-N/NO_2-N concentration (mg N/L)	25-300/25-300	25-275/25-275	30-200/30-200

2.6 Chemical analyses

Ammonium concentrations were measured by the phenate method using ortho-phenylphenol as a substitute for liquid phenol (Kanda J., 1995). In accordance with Standard Methods (APHA, AWWA, WEF, 1995), nitrite concentrations were estimated by the colorimetric method (4500-NO_2^- B) and nitrate by the UV spectrophotometric screening method (4500-NO_3^- B). Nitrite was determined to have an interfering response in the nitrate UV screening method of 25% of the nitrate response on a nitrogen weight basis, thus results were corrected by calculation. Levels of pH were measured by using a Mettler Toledo-320 pH meter and DO was measured by using a DO meter (D-55, Horiba).

3. RESULTS AND DISCUSSION

3.1 Influent and effluent T-N concentrations and T-N removal efficiencies for 4 reactors using PVA, MC and PE sponge as biomass carriers

Figs. 2 and Fig. 3 present the changes in influent and effluent T-N concentrations and T-N removal efficiencies for 4 reactors using PVA, MC and PE sponge as biomass carriers.

For PVA reactor, throughout phase 1 (the first 364 days) influent and effluent T-N concentrations were 300-600 mg/L and 50-150 mg/L except during system upsets, respectively. Average T-N removal efficiencies were about 77%. In phase 2 from day 365 to day 564, average T-N removal efficiencies were about 75%. In phase 2 from day 565 to 617, T-N removal efficiencies were about 70% with influent T-N concentrations ranged between 550-500 mg/L and effluent T-N concentrations were high from 120 and 200 mg/L. These data were lower than results in phase 1 and the initial period of phase 2 due to the short HRTs of 3.5 and 3 h.

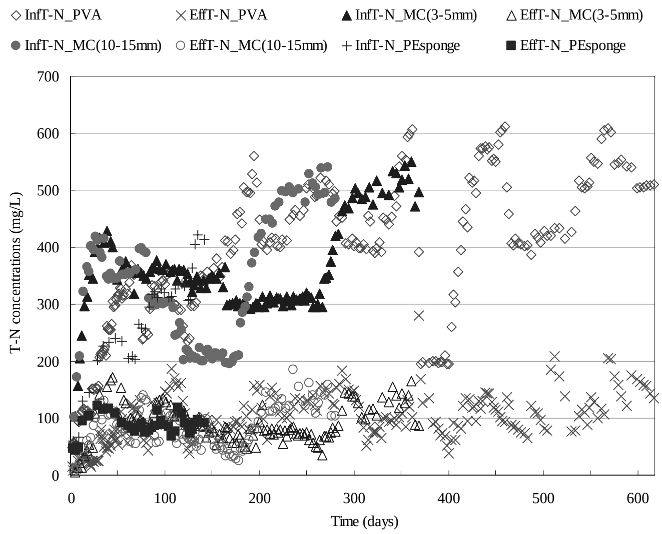

Figure 2: Changes in influent and effluent T-N concentrations for different reactors

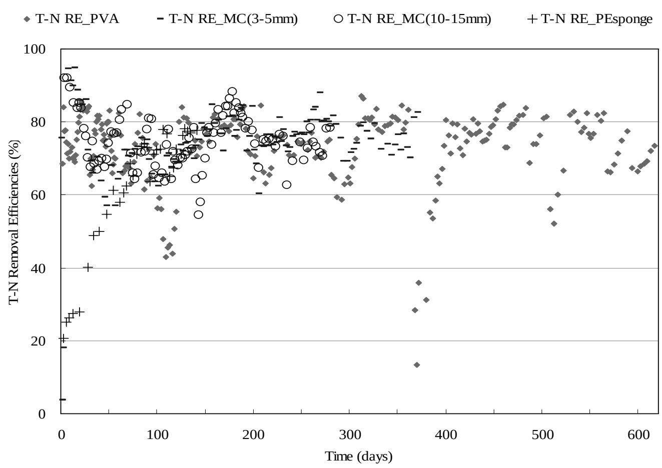

Figure 3: Changes in T-N removal efficiencies for different reactors

For MC1 and MC2 reactors, influent T-N concentrations were changed from 100 mg N/L to 500 mg N/L. With HRT of 12 h and influent T-N concentrations of 100-400 mg/L, average T-N removal efficiencies of MC1 reactor were 73% with effluent T-N concentrations of 10-175 mg/L in the first 163 days and average T-N removal efficiencies of MC2 reactor were higher of 87% with effluent T-N concentrations of 10-140 mg/L in the first only 23 days. With HRT of 10 h to 3.5 h and influent T-N concentrations of 300 mg/L, average T-N removal efficiencies of MC1 reactor were 76% (next 100 days) with effluent T-N concentrations of 40-90 mg/L. With HRT of 10 h to 3.5 h and influent T-N concentrations of 350-200 mg/L, average T-N removal efficiencies of MC2 reactor were 74% (next 150 day) with effluent T-N concentrations of 40-120 mg/L. With HRT of 3h and influent T-N concentrations of 200-450 mg N/L, average T-N removal efficiencies of MC1 reactor and MC 2 reactor were similarly of 78% (35 days) and 79% (40 days), respectively. However, with HRT of 3h and influent T-N concentrations of 500-550 mg/L, the average T-N removal efficiencies of the both MC1 and MC2 reactors were lower of 74% (69 days) and 73% (67 days) than before. The reason was due to the high influent T-N concentrations under short HRT of 3 h.

For PE sponge reactor, influent T-N concentrations were increased from 60 to 300 mg/L, effluent T-N concentrations were very high with 80-120 mg/L and average T-N removal efficiencies were low of 38% and 67% due to co-existing phenomenon of nitrification and anammox processes. During the next periods, influent T-N concentrations were increased from 300 to 400 mg/L and T-N effluent concentrations were from 70 to 120 mg/L. The average T-N removal efficiencies were higher of 72% and 74% than previous time owing to anammox process has dominated in comparisons with nitrification process.

Therefore, the average T-N removal efficiencies for 4 reactors using PVA, MC and PE sponge as biomass carriers were about of 73 to 80%.

3.2 T-N removal rates for 4 reactors using PVA, MC and PE sponge as biomass carriers

Changes in T-N removal rates for 4 reactors using PVA, MC and PE sponge as biomass carriers are shown in Fig. 4.

For PVA reactor, T-N removal rates increased from 0.27 to 1.35 kg N/m^3/day during 244 days of operation in phase 1. The highest T-N removal rate of 3.0 kg N/m^3/day was obtained after long time more than 550 days.

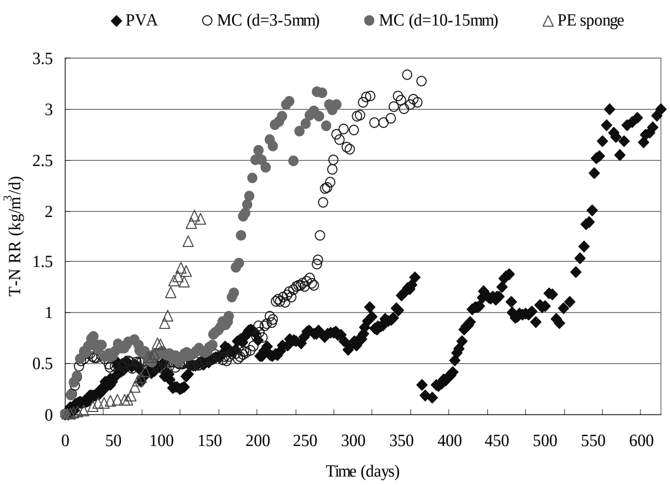

Figure 4: Changes in T-N removal rates for different reactors

For MC1 and MC2 reactors, T-N removal rates of MC1 reactor were around 0.5 – 0.6 kg N/m^3/day during initial 186 days of operation and T-N removal rates of MC2 reactor were around 0.5 – 0.7 kg N/m^3/day during a shorter time of operation of 145 days. Then, T-N removal rates of MC1 reactor were increased stepwise from 0.6 to 3.1 kg N/m^3/day in the next 129 days of operation. The T-N removal rates of MC2 reactor show the similar results of MC1 reactor and increased stepwise from 0.7 to 3.1 kg N/m^3/day in the next 85 days of operation. The high T-N removal rates obtained showed that the anammox bacteria grew actively in the anammox reactors using MC as biomass carrier.

For PE sponge reactor, T-N removal rates increased quickly from 0.1 to 0.6 kg N/m^3/day. T-N removal rates of 2 kg N/m^3/day was obtained after 5 months of operation. This PE sponge reactor is continuing in operation to obtain higher T-N removal rates.

The T-N removal rates for MC1 and MC2 reactors obtained similar results of 3.1 kg N/m^3/day over shorter time of 315 days and 230 days, respectively, in comparisons with the T-N removal rate for PVA reactor of 3 kg N/m^3/day over longer time of 564 days. In addition, T-N removal rate of 2 kg N/m^3/day was obtained in short operational time of 140 days for PE sponge reactor, in comparisons with the T-N removal rate of 2 kg N/m^3/day for PVA reactor, MC1 and MC2 reactors over longer time of 546 days, 265 days and 185 days, respectively owing to the largest porous diameter of PE sponge material. PVA reactor was operated with longer time due to the mechanic problems. On the other hand, operation of MC1 and MC2 reactors and PE sponge reactor are simpler and easier than operation of PVA – fluidized-bed reactor. However, the fluidized-bed reactor could reduce substrate inhibitions by complete mixing using a high recycle flow rate. This substrate inhibition will be the big problem for the operation of the fixed-bed reactors.

3.3 Ratios of T-N removal, NO_2-N removal and NO_3-N production rates to NH_4-N removal rates for 4 reactors using PVA, MC and PE sponge as biomass carriers

Ratios of T-N removal, NO_2-N removal and NO_3-N production rates to NH_4-N removal rates for 4 reactors using PVA, MC and PE sponge as biomass carriers are shown in Table 6. These values were similar to the stoichiometry value of the anammox reaction. The ratios of PVA reactor over phase 2, MC2 reactor and PE sponge reactor over phase 4 were closer to the theoretical ratios in comparisons with the ratios of PVA reactor over phase 1, MC1 reactor and PE sponge reactor over phase 3. Consequently, the anammox activities in PVA reactor over phase 2, MC2 reactor and PE sponge reactor over phase 4 were considered better than PVA reactor over phase 1, MC1 reactor and PE sponge reactor over phase 3.

Table 6: Reaction ratios of NO_2-N removal, NO_3-N production and T-N removal rates to NH_4-N removal rates for 4 reactors using PVA, MC and PE sponge as biomass carriers

Reactors	**Period of the operational time**	**NO_2-N/ NH_4-N**	**NO_3-N/ NH_4-N**	**T-N/ NH_4-N**
Theoretical ratios		**1.32**	**0.26**	**2.06**
PVA reactor	Phase 1 (days 120-364)	1.12	0.22	1.91
	Phase 2 (days 365-617)	1.18	0.21	1.96
MC1 Reactor	368 days	1.15	0.17	1.98
MC2 Reactor	280 days	1.2	0.17	2.03
PE sponge reactor	Phase 3 (days 90-111)	1.19	0.3	1.88
	Phase 4 (days 112-141)	1.23	0.24	1.99

3.4 Possible applications

With above experimental results, anammox process using PVA, MC and PE sponge materials as biomass carriers in the FBR and the fixed-bed reactors will be suitable for NH_4-N removal from wastewater containing high NH_4-N such as livestock farms, sites of aquaculture and agriculture, food and brewery processing industries, landfill leachate, etc. However, these wastewaters always contain high concentration of organic matter. Therefore, it is necessary to make clear whether PVA, MC and PE sponge materials can tolerate high organic carbon concentrations in anammox process.

4 CONCLUSIONS

With same operational conditions such as temperature, influent pH, influent DO, T-N removal efficiencies for 4 reactors using PVA, MC and PE sponge as biomass carriers were about of 73-80%. Influent T-N concentrations should be not too high (not higher than 550-600 mg/L for PVA reactor, and not higher than 500-550 mg/L for MC1 and MC2 reactors under too short HRTs (less than 3 h). Conversely, when T-N concentrations are higher than 550-600 mg/L for PVA reactor and 500-550 mg/L for MC1 and MC2 reactors, HRTs should be increased to more than 3 h. PE sponge reactor is operating to realize which level of T-N concentrations will be properly under short HRT. The T-N removal rates for MC1 and MC2 reactors obtained similar results of 3.1 kg N/m^3/day over shorter operational time of 315 days and 230 days, respectively, in comparisons with the T-N removal rate for PVA reactor of 3 kg N/m^3/day was obtained after long operational time of 564 days. In addition, T-N removal rate of 2 kg N/m^3/day was obtained after short operational time of 140 days for PE sponge reactor, in comparisons with the T-N removal rate of 2 kg N/m^3/day for PVA reactor, MC1 and MC2 reactors over longer operational time of 546 days, 265 days and 185 days, respectively owing to the largest porous diameter of PE sponge material. PVA reactor was operated with longer time due to the mechanic problems. Furthermore, operation of MC1 and MC2 reactors and PE sponge reactor are simpler and easier than operation of PVA – FBR. However, the FBR could reduce substrate inhibitions by complete mixing using a high recycle flow rate.
Anammox process using PVA, MC and PE sponge materials as biomass carriers in the FBR and the fixed-bed reactors will be suitable for NH_4-N removal from wastewater containing high NH_4-N. However, it is necessary to investigate whether PVA, MC and PE sponge materials can operate under high organic carbon concentrations in anammox process, because these wastewaters always contain high concentration of organic matter.

REFERENCES

APHA, AWWA, WEF, 1995: *Standard methods for the examination of water and wastewater*. 19th edition, American Public Health Association, Washington, D.C.
Christian Fux, Marc Boehler, Philipp Huber, Irene Brunner and Hansruedi

Siegrist, 2002. Biological treatment of ammonium-rich wastewater by partial nitritation and subsequent anaerobic ammonium oxidation (anammox) in a pilot plant. *Journal of Biotechnology* 99, 295-306.
Furukawa K., Rouse J.D., Imajo U., Nakamura K. and Ishida H., 2002. Anaerobic oxidation of ammonium confirmed in continuous flow treatment using a novel nonwoven biomass carrier. *Jpn. J. Wat. Treat. Biol.* 38, 87-94.
Furukawa K., Rouse J.D., Yoshida N. and Hatanaka H., 2003. Mass cultivation of anaerobic ammonium-oxidizing sludge using a novel nonwoven biomass carrier. *J. Chem. Eng. Jpn.* 36, 1163-1169.
Jetten M. S. M., Strous M., Van de Pas-Schoonen K. T., Schalk J., Van Dongen U.G.J.M., Van de Graaf A. A., Logemann S., Muyzer G., Van Loosdrecht M. C.M., Kuenen J. G., 1999. The anaerobic oxidation of ammonium. *FEMS Microbiol Rev.*22, 421-37.
Kanda J., 1995. Determination of ammonium in seawater based on the indophenol reaction with O-phenylphenol (OPP). *Water Research* 29, 2746-2750.
Mulder A., Graaf A. A. van de, Robertson L. A and Kuenen J. G., 1995. Anaerobic ammonium oxidation discovered in a denitrifying fluidized bed reactor. *FEMS Microbiol. Ecol.* 16, 177-184.
Rouse J.D., Fujii T., Sugino H., Tran H., and Furukawa K., 2005. PVA-gel beads as a biomass carrier for anaerobic oxidation of ammonium in a packed-bed reactor, CD-ROM. *Proceedings of 5th International Exhibition and Conference on Environmental Technology*. Heleco ’05.
Rouse. J.D., Yoshida N., Hatanaka H., Imajo U. and Furukawa K., 2003. Continuous treatment studies of anaerobic oxidation of ammonium using a nonwoven biomass carrier. *Jpn. J. Wat. Treat. Biol.* 39, 33-41.
Strous, M., Fuerst, J.A., Kramer, E.H.M., Logemann, S. M., Muyzer, G., van de Pas-Schoonen, K.T., Webb, R., Kuenen, J.G., and Jetten, M.S.M., 1999. Missing lithotroph identified as new planctomycete. *Nature* 400, 446-449.
Strous, M., Heijinen, J.J., Knenen, J.G., and Jetten, M. S. M., 1998. The sequencing batch reactor as a powerful tool for the study of slowly growing anaerobic ammonium-oxidizing microorganisms. *Appl. Microbiol. Biotechnol.* 50, 589 - 596.
Strous, M., Kuenen, J.G. and Jetten, M.S.M., 1999. Key physiology of anaerobic ammonium oxidation. *Appl. Environ. Microbiol.* 65, 3248-3250.
Strous M, Van Gerven E, Kuenen JG, Jetten M. S. M., 1997. Effects of aerobic and micro-aerobic conditions on anaerobic ammonium oxidizing (anammox) sludge. *Appl Enviro. Microbiol.* 63, 2446 – 8.
Strous M., Van Gerven E., Zheng P., Gijs Kuenen J. and Jetten M. S. M., 1997. Ammonium removal from concentrated waste streams with the anaerobic ammonium oxidation (Anammox) process in different reactor configurations. *Water Research* 31, 1955-1962.
Van de Graaf A. A., De Bruijn P., Robertson L. A., Jetten M. S. M., Kuenen J. G., 1996. Autotrophic growth of anaerobic ammonium-oxidizing micro-organisms in a fluidized bed reactor. *Microbiology* 142, 2187-2196.
Van de Graaf A.A., Mulder A., De Bruijn P., Jetten M.S.M., Robertson L.A. and Kuenen J.G., 1995. Anaerobic oxidation of ammonium is a biologically mediated process. *Appl. Environ. Micorobiol.* 61, 1246–1251.

Investigation of residential water end-use in urban areas of Hanoi

Huyen T.T. DANG[1] and Nga T.V. TRAN[1]
[1]Water Supply and Sanitation Department,
Institute of Environmental Science and Engineering,
University of Civil Engineering, Vietnam.
Email: huyendangctn@gmail.com

ABSTRACT

Most of water supply master plans and water investment projects in Hanoi and other cities have used national water demand criteria that was built based on experience and reference from elsewhere. The purpose of this research was therefore to investigate the real water consumption in Hanoi megacity and initially focus on residential areas. In this study, the micro-component data from household related to different water activities such as toilet flushing, kitchen, laundry, bathing and others including vehicle washing, gardening, etc., were collected via in-person interview and flow measurement. Results from nearly 180 household survey within two months (July and August 2013) in nine (09) Hanoi central districts showed the average consumption was 24.8 L/p/d for toilet, 15.17 L/p/d for laundry, 52.86 L/p/d for bathroom, 36.5 L/p/d for kitchen and 5.13 L/p/d for other water uses (house cleaning, fish pool, vehicle washing and gardening). The total daily water use of urban residence was averagely 134 L/cap/day. This number was much lower than the current criteria of 165 - 200 L/cap/day for megacities. The study would be a formal evidence for revision of national technical standard on urban water demand in near future.

Keywords: *Water consumption, end-users, survey, national criteria revision, urban areas*

1. INTRODUCTION

Estimation of water demand is very important step in water supply development projects. This requires understanding of water demand criteria for that area. At macro view, selection of appropriate water demand is crucial for optimization of water service infrastructure planning.

Studies of residential water end use (RWEU) began as early as 1990s in USA and Australia where the water saving was crucial due to severe droughts in these countries (Mayer, 1999; Roberts, 2005). In Australia, they even published a residential end-use measurement guidebook to guide how to design, sample and select proper technology (Giurco, 2008). Over 20 years, there have been thousands of studies worldwide to address the current and future water demand in their countries such as China, New Zealands, United Kingdom, Canada, Israel, etc. Looking into the basic water demand worldwide, it is shown that this value varies country by country (Human Development report, 2006). This report clearly showed the dependence of water use on economic condition, i.e., water consumption decreased from European countries and USA (100-600 L/cap/day) to Asian countries (100 - 200 L/cap/day) and then African countries (less than 100 L/cap/day). The water demand also varies city by city, for example, average daily water use in Australia ranges from as little as 100 litres per person in some coastal areas to more than 800 litres per person in the dry inland areas. Many factors affect residential water demand. Both empirical investigations and analytical studies of industrialized countries suggest such determinants as policy variables (i.e. water price or water rate) household economic variables (income); physical features and technological variables (i.e. water amenities and metering, or water-saving plumbing fixtures); environmental variables (i.e. temperature and precipitation); and demographic variables (i.e. household size and attitudinal variables) (Zhang and Brown, 2005). Figure 1 depicts clearly the dependence of water use on economic condition, i.e., water consumption decreased from European countries and USA to Asian countries and then African countries.

In Vietnam, determination of residential water demand for designing water supply systems is mostly based on the National technical criteria TCXDVN 33:2006. These criteria were referred from international and national designing experience, but not based on real data. According to TCXDVN 33:2006 criteria, the water demand varies depending on types of cities (megacities, big cities, medium or small cities, etc), urban or peri-urban.

Table 1. Residential water demand criteria

Type of city	Subjects	Water demand Criteria for 2010 (L/cap/day)	Water demand Criteria for 2020 (L/cap/day)
Megacities, category I cities, resorts, tourism places	Urban Peri-urban	165 120	200 150
Category II cities and category III cities	Urban Peri urban	120 80	150 100
Category IV cities and category V cities and rural areas		60	100

Note: Megacities or Special cities: >5mi. cap; Category I cities: >1mil. cap (central cities) or > 500 thousand cap. (provincial cities); Category II cities: >800 thousand cap (central cities) or > 300 thousand cap. (provincial cities); Category III cities: >150 thousand cap.; Category IV cities: >50 thousand cap.; Category V cities:>4 thousand cap. (Source: Vietnam Urbanization Review, 2011).

There have been not many studies on residential water demand in Vietnam. The first one was done in 2006 by Japan Society for the Promotion of Science and there was another study in 2010 by Japan Science and Technology (JST). According to the first survey of 21 urban households (HHs) and 17 peri-urban HHs in 2006, the water consumptions were reported as high as 170 L/cap/d and 92 L/cap/d for urban and peri-urban Hanoi respectively (Busser et al, 2006). While results from 2-month survey at 200 households in peri-urban Hanoi showed that the average consumption was about 70 L/cap/day (Otaki et al., 2012). It is worth noting that Hanoi is classified as Special city. Given the time of study, the current Vietnam criteria for urban Hanoi are sort of close, but the criteria for peri-urban is too high compared with the research results. It can be seen that the first study was conducted with very limited number of HHs and did not cover all districts of Hanoi. For better understanding of residential end-use water consumption, it encourages to have another study at bigger scale to somehow confirm the result. Besides, little is known about which determinants (water price, water amenities, climate or people awareness, etc) affect Hanoians the most in water use.

The objective of this paper was therefore to (1) investigate the end-use water consumption in urban Hanoi at a larger scale; (2) understand better how water is used by end users (i.e. for bathing, cooking, toilet or washing, etc.); (3) compare with the current criteria to see if it is relevant, and finally (4) demonstrate the relationship of water use and social and economic determinants.

2. METHODOLOGY

The study focuses on the behaviors of households that affect their water use and consumption. "Residential water consumption", in the context of this survey, refers to the water from both household faucets that are used for toilet flushing, cooking, bathing, laundry and similar purposes, such as flower watering or car washing (Zhang and Brown, 2005). The survey also elicited the consumer’s opinions on present water supply in order to understand quality of the service delivered.

2.1. Sample size

It is clearly that the more number of samples, the more accuracy and confidence the result can achieve. However, the choice of how many sample is often a compromise between the cost and the required level of statistical significance. In this study, a total targeted random sample of 173 households was selected in urban Hanoi.

2.2. Sample selection

Initially the sample selection aimed to base on income or household style as referred to some previous studies (Roberts, 2005; Zhang and Brown, 2005). According to Roberts's study, higher income households are often responsible for a higher proportion of peak demand use. In other speaking, the actions of high use households are more important than those of low use households, thus, they decided to deliberately sample 50% of high use households, 25% of low use households and the rest for middle use ones. In Zhang and Brown study, the stratified random sample was selected based on the proportions of housing types (high rise, low rise buildings, or individual houses) in Beijing that they estimated. However, official statistics of housing types or income are not available in Hanoi. One understandable reason is that Hanoi is still in transition process with changes year by year. Only the population density statistic is known. Therefore the number of households was selected depending on population density. As the focus for this study is urban Hanoi area, the samples were randomly selected from 9 central districts: Ba Dinh, Hai Ba Trung, Hoan Kiem, Dong Da, Cau Giay, Thanh Xuan, Hoang Mai, Long Bien and Tay Ho districts (Table 2).

Table 2. Sample selection

Districts	Population density* (persons/km^2)	Number of surveyed HHs
Ba Dinh	24,502	23
Hoan Kiem	27,851	20
Tay Ho	5,443	12
Long Bien	3,758	5
Cau Giay	18,741	19
Dong Da	37,160	23
Hai Ba Trung	30,805	24
Hoang mai	8,175	21
Thanh Xuan	24,555	26
Total		173

**Source: http://vi.wikipedia.org/wiki/To chuc hanh chinh tai ha noi, 2009)*

2.3. Survey method

The survey involved household visits 173 houses during July and August 2013, identified appliances by inspection, measured appliance flowrates and gathered extensive data on usage behavior (i.e., water bill). Individual household was asked to provide information by answering 33 questions covering four aspects: (1) household housing condition; (2) household socio data (age, gender, occupancy); (3) household water amenities and facilities; and (4) household water use behavior and perception.

3. RESULTS AND DISCUSSION

3.1. Characteristics of households and survey areas

Number of persons/household (HH)

The majority (57%) of surveyed houses have less than 5 members in a HH. This reflects the typical modern family in Vietnam in general and Hanoi in particular. HHs (>10 persons) with three generations or with multi families is not so common now in Hanoi.

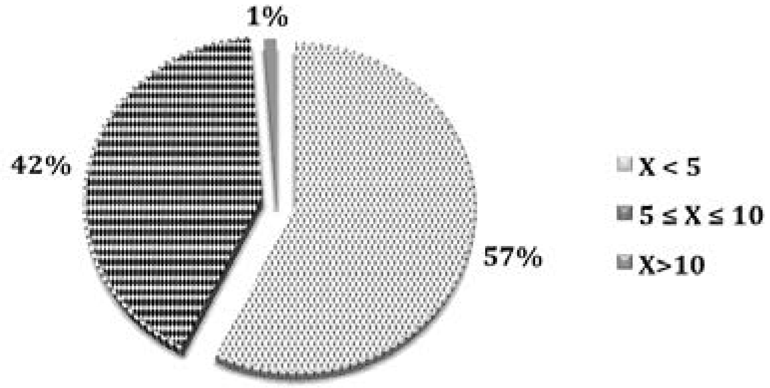

Figure 1: Number of person/household (X)

Types of houses

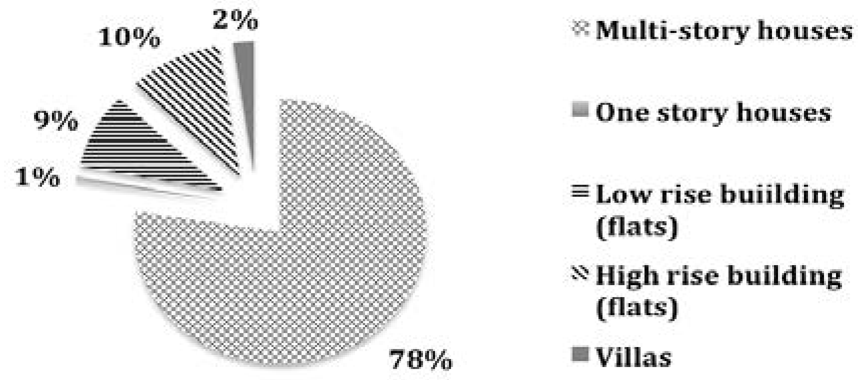

Figure 2: Surveyed housing typologies

The multi-story house refers to single house (or un-detached townhouse with courtyard or without courtyard) with 2 - 5 stories. One story house is the most simple and oldest house structure. This type of house is not common nowadays in such a megacity as Hanoi. They often are re-constructed to accommodate more people or become house-for-rent. Low-rise building refers to old residential blocks constructed between 1960 - 1980 in Hanoi. They often have max 5 stories, each story has 5-10 flats. High rise buildings refers to recently-built residential blocks which were built within the last 15 years, mostly developed in Hoang Mai and Cau Giay districts. Each building has more than 10 stories and number of flats varies depending on the size of building. Villas account for only about 2% of surveyed HHs. This type of house is also not very common since the land areas required large, at least 200 m^2/HH.

Multi-story houses

High rise buildings

Low rise buildings

One story (single story) houses

Villas

Figure 3: Images of Hanoi housing typologies

It is interesting that the randomly selected HHs for survey seems to reflect the observed housing typology distribution in Hanoi. In which, multi-story houses are most common types of houses in Hanoi (78%), followed by newly-built high-rise building flats (10%), and then low-rise building flats (9%). Villas and is not so popular and one-story houses are not our target in this survey.

3.2. Average water consumption

Figure 4 presents the average water consumption in 9 districts. The average water use varied from 120 L/cap/day to 143 L/cap/day. It is worth noting that most of Long Bien district was used to be sub-urban area, therefore, the living standard is not so as high as the urban districts, so does the water consumption.

On the other hands, as many rich people moves to Cau Giay or Hoang Mai to live in new residential areas, the houses are bigger and more modern. Water amenities are also more fancy and so does the water consumption. In Tay Ho district, the water consumption is relatively high since people here use well water (which is free of charge) quite often as the second water source.

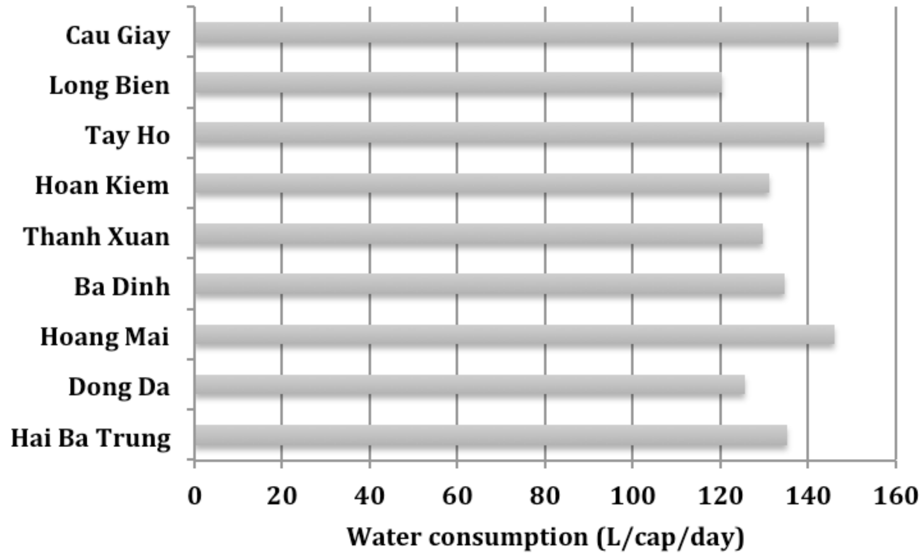

Figure 4. Average water consumption per person per day in 9 districts

The average water use was found about 134 L/person/day. This was lower than the figure of 170 L/person/day discovered by the Japanese research group in 2006. Compared to Vietnam water consumption criteria for Special city like Hanoi of 165-200 L/cap/day for period of 2010-2020 (TCXDVN 33:2006) and the designed value in Water Supply Masterplan for Hanoi toward 2020 of 160-180 L/cap/day, this result was also lower than that range. This source of data would be a base and real evidence for water supply system design and management in Vietnam.

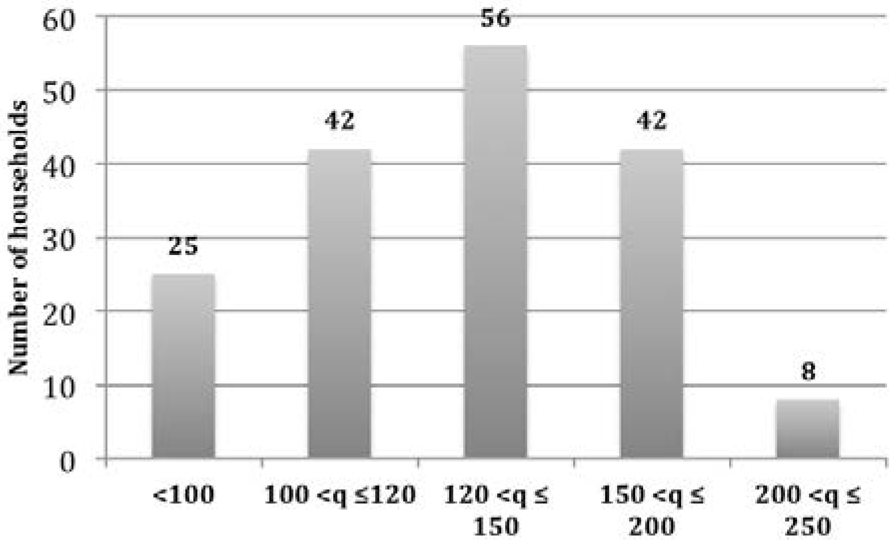

Figure 5. Average residential water consumption distribution (*q: water consumption - L/cap/day)*

Look into the breakdown of water consumption, the amount of water use for bathroom accounts for the most and quite significant, followed by those for kitchen and for toilet. This pattern is quite similar with those found in previous studies in other cities but at different absolute values (Prathapar et al., 2005; Friedler 2004).

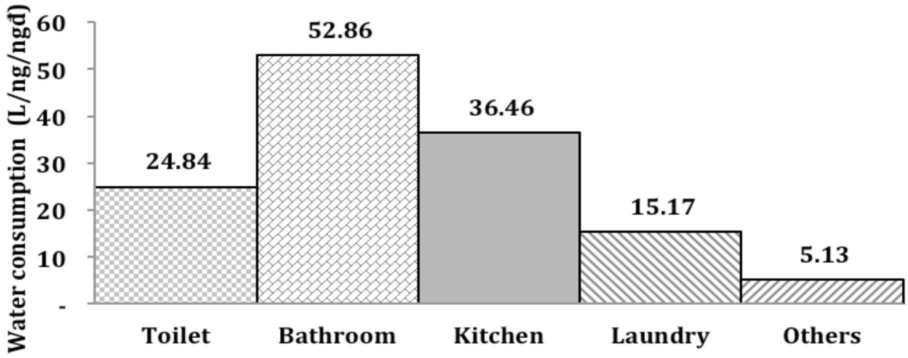

Figure 6. Breakdown of residential water consumption

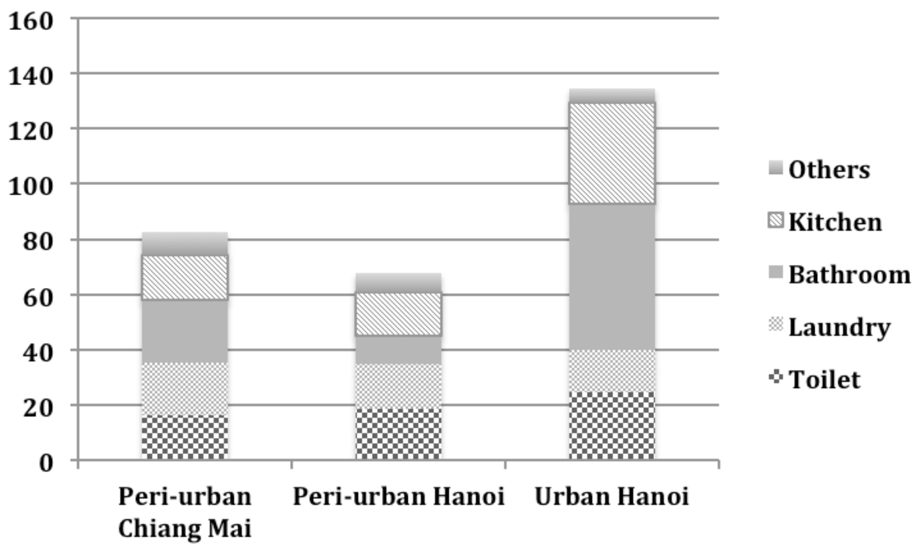

Figure 7. Micro-component residential water consumption in Hanoi and Chiang Mai (Otaki et al., 2012; Otaki et al., 2013)

Compared with Otaki's result (2013) which also has done in Hanoi, this study shows a bit higher values. It is because they conducted survey mostly in peri-urban Hanoi while this study was done in urban Hanoi. Micro-component residential water consumption in Hanoi and Chiang Mai seemed similar, except for laundry use. While compared between peri-urban Hanoi and peri-urban Chiang Mai, the difference was for bathroom use.

3.3. Impact factors on residential water consumption per capita per day

Type of house

The high-rise flats are more modern and larger than the low-rise flats which are smaller and were built 30-50 years ago. It was found that the water consumption increases with following order: low-rise building flats (136 L/cap/d) < multi-story houses (136.5 L/cap/day) < high-rise building flats (154 L/cap/day). Evidence can be seen that the water used for house cleaning in multi-story houses or in high rise building flats would be than for low rise ones due to large living and cleaning areas. Other explanation may lie in the living condition. High-rise buildings are those recently built which attract many high-income residents. High-income people often have higher living standard. Due to larger space, they use more water amenities and/or more fancy ones. Therefore, their water use is significantly higher.

Water availability (water quality, water sufficient or insufficient supply)
More than 80% of HHs reported no complains about water quality and quantities. Nevertheless, water interruption for few hours can occur once every few months due to power saving plan or construction. It would say if the water availability were limited, the water consumption would be lower. The high water use from this study proves that water shortage is not a common issue in Hanoi city.

In house water leakage
Based on the survey, there was not much water leakage from water amenities reported. Only a few cases were found, related to improper close of tap faucet, leak of pump hose and leak from old toilet spray hose. Once a while there was reported leakage event related to failure of water heaters due to hot water pipe rusty.
In general, HH water leakage is also not a common issue. They often fix once water amenity is leaked since it impacts directly their water bills.

Others (frequent guests, non-permanent residents)
Compared with the measured data and billed water use, there is about 15% difference. This could be due to either subjective reasons such as inaccuracy measurement of water amenities, and responders' insufficient information, or due to objective reasons such as staying of non-permanent residents, use of another water sources or water penetration from HH's underground water reservoirs. The objective causes are usually hard to control. However that difference of 15% is understandable and within accepted range.
About 6% of surveyed HHs uses wells water. Therefore that fraction is not included in average billed water consumption. HHs using dual water sources mostly located in Ho Tay (West lake) and Long Bien districts where the fresh water supply is constrained and wells water level is highly available.

4. CONCLUSIONS

Household survey in 9 districts of Hanoi was conducted to investigate the residential water demand. Here are some of our key findings:
- Households in urban Hanoi consumed much less water per capita than previously found in 2006's study (134 L/cap/day compared with 170 L/cap/day). It could be due to many reasons, however, some of them to be recognized are the increase of awareness of water saving; application of water-saving devices (for

examples two-button toilets in stead of one-button ones), impact of water price, etc. This data was lower the current standard for residential water consumption design of 165-200 L/cap/day.
- Water consumption increases with following order: low-rise building flats < multi-story houses < high-rise building flats. In addition, there was slightly variation on water consumption among 9 districts. Long Bien district was used to be sub-urban area, therefore, the living standard is not so as high as the urban districts. In Tay Ho district, use of well water is quite common as second water source.
- Household water use and consumption in Hanoi were predominantly indoor uses, due to housing and climate conditions.
- Most families in Hanoi were satisfactory with their current municipal water service and not concerned with the billing system
- The amount of water use for bathroom accounts for the most and quite significant, followed by those for kitchen and for toilet. This pattern is quite similar with those found in previous studies.
- Many factors impact on water use among surveyed households. However, there were no clear dominant determinants to explain the variation in household water use.

REFERENCE

Barrett, Greg; Wallace, Margaret. 2009. Characteristics of Australian urban residential water users: implications for water demand management and whole of the system water accounting framework. *Water policy*, Volume: 11 Issue: 4 Pages: 413-426

Busser S., Pham T.N., Antoine M., Nguyen V.A. 2006. Characteristics and quantities of domestic wastewater in urban and peri-urban households in Hanoi, *Annual Report of FY*-The Core University Program between Japan Society for the Promotion of Science (JSPS) and Vietnamese Academy of Science and Technology (VAST), P.395-P.397

Friedler, E., 2004. Quality of individual domestic grey water streams and its implication for onsite treatment and reuse possibilities. *Environmental Technology*, 25(9): 997-1008

Giurco, D., Carrard, N., McFallan, S., Nalbantoglu, M., Inman, M., Thornton, N. and White, S. 2008. Residential end-use measurement Guidebook: a guide to study design, sampling and technology. Prepared by the *Institute for Sustainable Futures*, UTS and CSIRO for the Smart Water Fund, Victoria.

Grafton R. Q., Ward M.B., To H., Kompas, T. 2011. Determinants of residential water consumption: Evidence and analysis from a 10-country household survey. *Water resources research*, Volume: 47

Zhang H. H., Brown D. F., 2005. Understanding urban residential water use in Beijing and Tianjin, China. *Habitat International*, 29, 469–491.

Jacobs H. E. 2007. The first reported correlation between end-use estimates of residential water demand and measured use in South Africa. *Water SA*, 33-4, 549-558

Otaki Y., M. Otaki, P. N. Bao, T. T. V. Nga and T. Aramaki, 2013. Micro-component survey of residential water consumption in Hanoi, *Water Science & Technology: Water Supply*, 13.2, 469-478.

Otaki Y., Otaki M., Ping L., 2012. The survey on the consumption of domestic water use in Hanoi and its analytical results, Proceedings, *The 2nd Climate Change and Urban Water Systems-Workshop for Adaptation and Better Management*, Hanoi, Vietnam, March 5-7th, 2012.

Roberts P., 2005. Residential End Use Research to support Demand management and forcasting, *Vicwater Conference.*

Mayer P. W., DeOreo W. B., Opitz E. M., Kiefer J. C., Davis W. Y., and Dziegielewski B., Olaf Nelson J.,1999. Residential End uses of water, *AWWA Research foundation.*

Prathapar S.A., Jamrah A., M., Ahmed S. Adawi Al, Sidairi S. Al, Harassi A. Al, 2005. Overcoming constraints in treated greywater reuse in Oman, *Desalination* 186, 177–186.

Sharon L. H., Scott T. Y., Larissa L., Anthony J. B. 2009. Household Water Consumption in an Arid City: Affluence, Affordance, and Attitudes, *Society & Natural Resources: An International Journal*, Volume 22, Issue 8, pages 691-709

Vietnam Urbanization Review. 2011. *Technical Assistance Report*, World bank.

Pollution and eutrophication control in urban lakes

Ha D. TRAN[1] and Huyen T.T. DANG[2]
[1] Assoc. Prof., PhD, Water Supply and Sanitation Division,
[2]PhD, Water Supply and Sanitation Division,
Institute of Environmental Science and Engineering,
Hanoi University of Civil Engineering, Vietnam
E.mai: tranducha53@gmail.com; hatd@nuce.edu.vn

ABSTRACT

In Vietnam, urban lakes are often considered as an urban ecological framework and play vital roles in municipal infrastructure system. However, many of them are in danger of having high level of eutrophication due to the disposal of un-treated wastewater and rainwater run-off. The lakes' water quality has degraded over the years because of algae explosion, organic re-pollution and unstable dissolved oxygen. Environmental experts from Hanoi University of Civil Engineering have proposed a series of solutions during the implementation of municipal drainage and sewerage and sanitation projects. Among them are separation of wastewater from discharging into the lakes, oxygen enrichment, aqua plant development, flow re-arrangement, etc. Those solutions have helped improve water quality, reduce pollution and eutrophication in some lakes in Hanoi, Haiphong, Danang and other megacities.

Keywords: *Urban lakes, pollution control, eutrophication, control solutions, megacities.*

1. INTRODUCTION

Vietnam currently has about 765 cities with different scales as of end of 2012 (Ministry of Construction, 2012). The urban residential areas and economic centers of Vietnam are mostly located in large river deltas, coastal areas or wherever have great sources of surface water such as channels and lakes. The flows through urban channels and lakes form ecological framework, creating water sources for domestic supply, manufacture and other urban activities. On the other hand, many urban cities are located in low land; therefore, the inner channels or lakes play an important role in drainage, rainwater regulation and wastewater reception. The urban drainage system is often designed as in Figure 1.

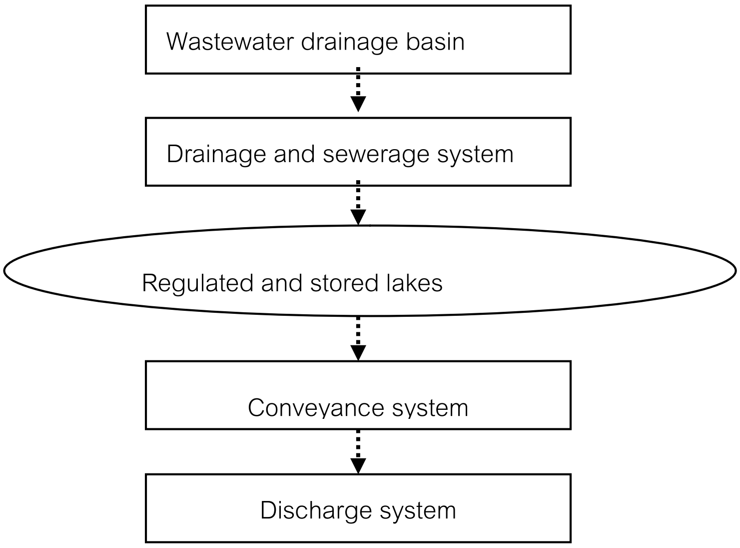

Figure 1. Diagram of urban drainage system

The density of drainage channels and lakes in Vietnam's urban cities is relatively high, about 10-15% of total urban area. The inner lakes' areas are ranging from several hectares to hundreds of hectares. They are divided into four function groups as below:

- Group 1 including lakes used for tourism, water sport and rain water regulation for the surrounding areas. The water quality of these lakes complies with Type A- National technical criteria QCVN 08:2008/BTNMT, for instances, West lake, Hoan Kiem Lake...in Hanoi city.

- Group 2 including lakes for water entertainment and rain water regulation for surroundings. They can be also used for fish raising. The water quality of these lakes complies with Type B- National technical criteria QCVN 08:2008/BTNMT, for instances, Goong lake in Vinh city, Tam Bac lake in Hai phong city, Thien Quang lake and Bay Mau lake in Hanoi, etc.

- Group 3 including ones for relaxing, entertainment of residential areas; regulating storm water for surroundings, and receiving treated wastewater. These lakes are often used for fish raising such as Giang Vo lake in Hanoi, Binh Minh lake in Hai Duong province, etc. Again, the water quality should meet the requirement of National technical criteria QCVN 08:2008/BTNMT-Type B.

- Group 4 are storage and regulated lakes for big areas or many basins in the city. They can receive treated wastewater, be used for fish and other aquatic animals raising. They are often the largest receiving lakes in the city such as Yen So lake (Hanoi), Au Thuyen lake (Hai Duong), Kenh Gia lake (Nam Dinh), etc. The water quality should meet the requirement of National technical criteria QCVN 08:2008/BTNMT-Type B.

Urban channels and lakes are often connected with each other through a united system, creating an urban ecological framework. Lakes are usually connected into a chain (system) such as Giang Vo lake-Ngoc Khanh lake-Thanh Cong lake-Dong Da lake-To Lich river chain; Giam lake-Van Chuong lake-Trung Tu-Lu river in Hanoi; An Bien lake - Mam Tom lake - Thien Nga lake - Dong Khe channel in

Hai Phong; Hao Thanh lake- Binh Minh lake - Bach Dang lake - Ke Sat river in Hai Duong, etc...to receive and regulate rainwater runoff and wastewater.

2. CURRENT POLLUTION AND EUTROPHICATION IN URBAN LAKES

Urbanization is the main factor causing water quality changes in urban lakes and rivers. In addition, the untreated wastewater disposal is the main reason that makes urban lakes more and more contaminated. Even though, under tropical climate condition, the ability of self-cleaning of these lakes is significant, the frequent reception of untreated and overloaded wastewater makes it impossible for self-cleanning process, resulting in severe pollution in urban lakes. The evidence can be seen most clearly in Hanoi, Hai Phong, Da Nang, Hue, Nam Dinh, Hai Duong and other large cities where the number of centralized wastewater treatment plants have not met the demand.

The monitoring data of the urban lakes in the past few years has showed that some parameters such as BOD_5, COD, NH_4-N, Coliform, etc did not meet the requirement of national technical criteria QCVN 08:2008/BTNMT-type B. Figure 2 depicts the BOD fluctuation with years in West lake (floating restaurant) and Bay Mau lake (in the middle of lake), Hanoi.

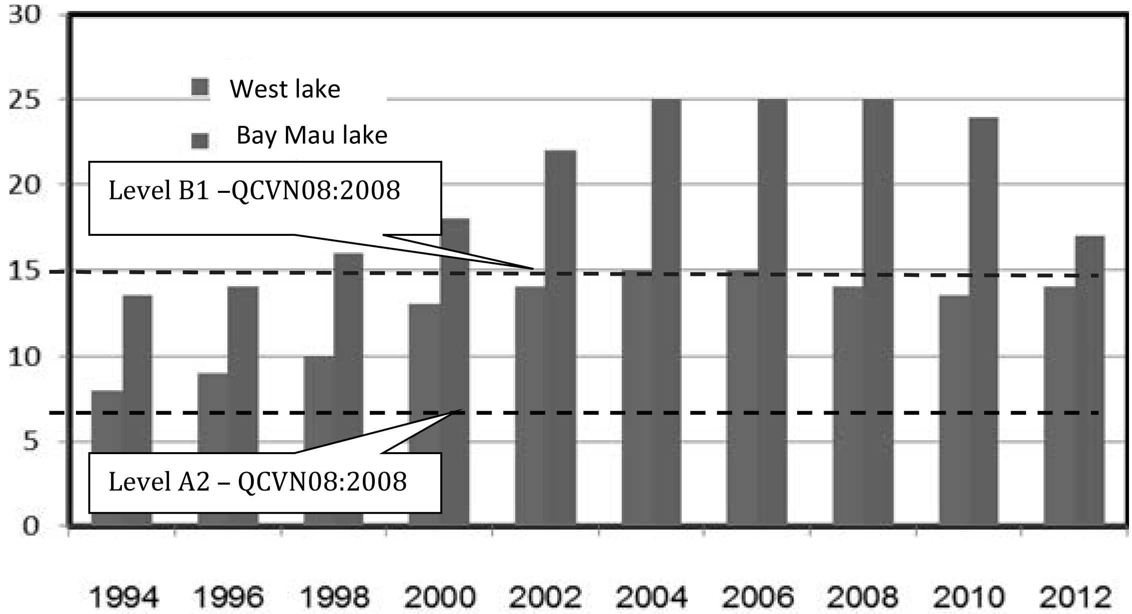

Figure 2. BOD fluctuation in West lake and Bay Mau (Hanoi), monitored by Institute of Environmental Science and Engineering (IESE) from 1994-2012

The channels and lakes which receiving untreated wastewater are all contaminated with 2-70 times higher than allowable values for all parameters. These lakes are contaminated at α - β mezoxaprobe level. The sediment at the bottom of lakes contains significant organic matters and heavy metals, which contributes to lake pollution and flow constraint.

In municipal wastewater, the normal N:P ratio is 4:1, however in natural lakes, the concentration of P is often much lower due to settling, transformation, digestion by aqua plants, etc, thus the N:P ratio can be up to 21. Table 1 presents the relation of N and P in a couple of urban lakes in the North of Vietnam, reported by IESE, University of Civil Engineering in 2009 (Tran, 2009).

Table 1. N and P concentrations in urban lakes in the North of Vietnam.

No	Name of Lake	Depth H, m	TN, mg/L	TP, mg/L	N:P ratio
1	Tinh Tam lake (Hue)	1.5	3.25	0.17	19.11
2	An Bien (Hai Phong)	2.9	3.19	0.15	21.2
3	Bay Mau lake (Hanoi)	3.0	5.19	0.24	21.6
4	West lake (Hanoi)		1.62	0.08	20.2
5	Goong lake (Vinh)	2.5	4.21	0.20	21.05

Usually, the N:P ratio depends on types of lakes, their depth, surface loading of P and N, etc. According to Vollenweider (1980) and Downing (1992), when N:P ratio was greater than 12, TP would be used as indicator of eutrophication. Due to receiving significant amount of rainwater and wastewater with high P loading, almost urban lakes in Northern provinces are in danger of eutrophication (Tran, 2009). The biological capability is often quite high (20-30g O_2/m^2-ngày), causing "blooming" in the lakes. This phenomenon leads to the reduction of surface oxygen and increase of water turbidity. The relationship between Hanoi urban lakes and eutrophication-causing factors is illustrated in below empirical formulas:

- *Phospho and chlorophyll a relationship:*

$$\text{Log(Chl. a)} = 0,69 \log (C_p) +2.58 \tag{1}$$

Where: Chl.a –chlorophyill a concentration, ∓g/L;

C_P- TP concentration in the lake, mg/L.

- *Chlorophyll a and Secchi-disk transparency relationship:*

$$S=6.4\ (\text{Chl.a})^{-0.473} \tag{2}$$

Where: S - *Secchi-disk transparency*, m.

- *Oxygen demand in lake bottom:*

$$D=0.086\ Cp^{0.478} \tag{3}$$

Where: D- Oxygen demand in lake bottom, g of O/m^2.d;

C_P- TP concentration, ∓g/L.

- *Relationship of orthophosphate and color:*

$$C=15,6.e^{0.577P} \tag{4}$$

Where: C- color, Pt-Co;

P- concentration of PO_4^{3-}, mg/L.

The above results proved that the relationship between chlorophyll a and P concentrations was often presented in a logarit relation. The chlorophyll a concentration greatly depended on P concentration and N:P ratio. This was consistent with findings in the studies of Dillon and Rigler (1974), Rast and Lee (1978). The linear relationship between P loading rate and other water parameters were also the same as some previous studies (Vollenweider and Kerekes, 1980).

Together with eutrophication was the outbreak of such algeas as *Cyanophyta, Chlorococcales, Centiric Diatoms*, *Euglenophyta, etc.* According Tran (2006), the toxic algeas have invaded Hanoi lakes with concentration of 50-100mcg/L, and about 2-3 mil of cells/L. They even reached 16-18 mil of *Microcystis* toxic algea cells per L in some urban lakes such as Giang Vo, Thanh Cong, Thanh Nhan, Hoan Kiem lakes, etc.

One of the challenges we are facing is the number and area of urban lakes as well other surface water sources have been decreasing due to illegal occupancy, leveling for housing development or waste dumping, etc. Based on IESE's survey data, the urban surface water areas have been reduced from 10-50% in the past 10 years. The uneven and sometimes over-controlled precipitation has caused overloaded infrastructure and led to pollution potentials. This mostly due to the fact that the management of urban lakes has not been focused and unified.

3. MITIGATION METHODS FOR EUTROPHICATION AND WATER IMPROVEMENT IN URBAN LAKES

Tran (2010) has studied and summarised several methods for control and mitigation of eutrophication and pollution in urban lakes. This section will discuss in details the four key solutions.

3.1. Reduction of untreated wastewater discharge into the lakes

Minimizing the disposal of wastewater into lakes is one of the best options to improve the lake water quality. Since most of the current sewerage and drainage systems in Hanoi and other cities are combined system, the best solution is to construct combined sewer overflows and interceptors around the lakes. By doing this, the wastewater will not be discharged into lakes, but collected and delivered to centralized wastewater treatment plants. This solution has been applying in West lake and Truc Bach lake in Hanoi. The principle is illustrated in Figure 3.

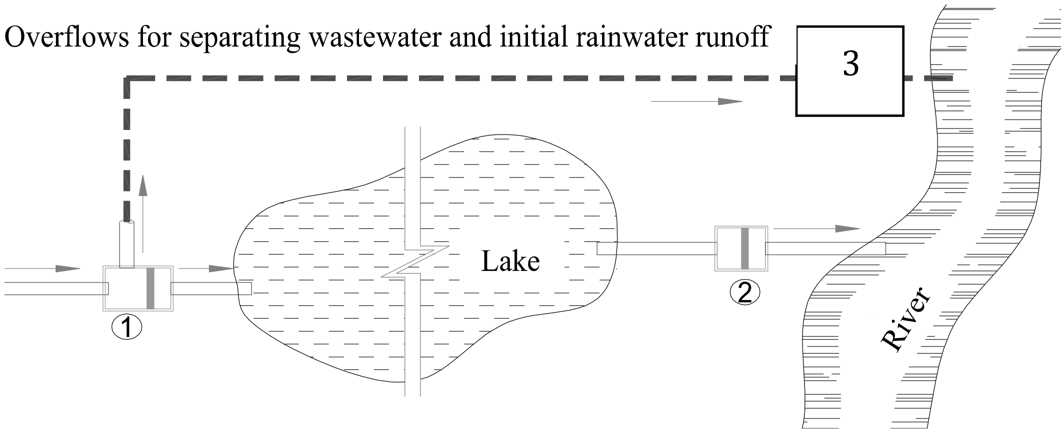

Figure 3. Diagram of controlling the wastewater and initial rainwater from discharging into the lakes

Note: (1) Combined sewer Overflows for wastewater and initial rainwater runoff; (2) Flap gate; (3) Wastewater treatment plant

3.2. Promotion of self-cleaning process

Self-cleaning process is a complex of natural processes including hydrodynamics, biology, chemistry, physics, etc inside contaminated lakes in order to recover to original status (components and characteristics). This means, the contaminants in discharged wastewater are further treated in the lakes.
Self-cleaning involves in two basic processes: dilution of wastewater and the receiver and metabolism of contaminants with time. Thus, there are some techniques that could be used to mitigate the "blooming" and reduce pollution as follows:

- Application of foutains, water turbins, water games (canoeing, pedalos, etc). The fountains can actually increase architure view and improve micro-climate in the surroundings.
- Combination with water animals raising or Phytoplankton to increase dissolved oxygen.

The above techniques can be enhanced by artificial aeration. The main principle is to provide more oxygen to microoganisms so that they can disgest organic matters in the wastewater. The oxidation within the lake is mainly self-oxidation, however, it is supported with a series of other reactions for lake water recovery. Currently, there are many types of artificial aeration; among them are dynamics, hydrodynamics, air blowing or other mixing, aerating processes.

Figure 4. Application of overflow weirs and foutains for oxygen enrichment in urban lakes

In urban lakes, the bottom water is often oxygen poor and nutrient rich due to settling and sedimentation disturbance. Thus, it is critical to supply of oxygen and reduction of nutrient to bottom water. To solve the problem, the most common practice is to pump the bottom water to a wetland and the treated water with lower organic and nutrient matters will be circulated to the lakes. Besides, it is recommended to use flora and fauna system to remove contaminants based on the metabolism via food chains. In water, algea and aquatic plants absorb nutrients (N, P) and C to growth mass and create the basic capacity of water environment. Aquarium plants play a vital role in subtracting organic matters, nutrients and heavy metals (Tran V. Quang, 2010). It is the lake water characteristics that decide types of aquarium plants used. This is a high effective, cheap, easy-to-conduct solution. On the other hand, it improves the attraction of urban lakes, which are usually a good place for entertainment.

Figure 5. Aquarium plants (left) and constructed wetland (right) for self-cleaning process in urban lakes

3.3. Enhancement of lake management

In order to apply appropriately methods for urban lake management, it is necessary to classify them based on their function. This would help determine authority responsibility levels and avoid complexity in management, which are happening in many local areas in Vietnam. For instance, the main function of inner lakes is to regulate rainwater runoff and flooding control, while for those locating at the beginning of drainage basin with limited capacity of regulation, they should be used mainly for entertainment.

The strategy of lake management can be outlined as followings:

- Close management of land use in lake surroundings;
- Preparation of detailed regulations on management and reclamation of water;
- Development of rehabilitation projects for existing urban lakes;
- Establishment of environmental control system around the lakes;
- Establishment of punishment procedures for lake violation activity.

3.4. Improvement of people's awareness on water resource protection

Besides the above technical methods for reducing eutrophication in urban lakes, it is vital to socialize the management and water protection activities to change the people behaviors and make people think of doing it as their responsibility, duties and benefits.

The basic concept of socialization is to build hygiene living habits and avoid pollution-causing manufactures. In addition, people should be educated so that they understand the importance of lakes and rivers in their lives, as a result make them involved in environmental protection in general and urban lakes protection in particular.

CONCLUSIONS

Urban lakes really play vital roles in urban activities. Nevertheless, many of them are in danger of pollution and eutrophication. So as to ensure their functions in rainwater regulation and environmental landscaping, it is necessary to apply integrated solutions including employing appropriate technologies and enhancing community education.

REFERENCE

Dillon, P. J., and F. H. Rigler. 1974. The phosphorus-chlorophyll relationship in lakes. *Limnol. Oceanogr*. 19: 767-773.

Downing JA, McCauley E. 1992. The nitrogen:phosphorus relationship in lakes. *Limnol. Oceanogr*.37: 936-945

Rast, W. and Lee, G. F. 1978. Summary analysis of the North American (US portion) OECD eutrophication project: nutrient loading-lake response relationships and trophic state indices, USEPA, EPA-600j3-78-008. Corvallis Experimental Research Laboratory, Corvallis, Oregon.

Tran D. H., 2009. *Protection and Management of Water resources Book*, Science and Technique Publisher.

Tran D. H., 2010. *Complex solutions for urban lakes improvement*, Institute of Environmental Science and Engineering, University of Civil Engineering.

Tran D.H., 2006. Evaluation of water quality fluctuation of five rehabilitated lakes and proposal of treatment solutions, *Hanoi Science research report* (Mã số: 01C-09/06-2005-1).

Tran V. Quang. 2010. Rehabilitation of urban lakes by eco techniques. *Proceedings, 2nd International Conference on Environment and Resources,* Hochiminh city, 2-3/11/2010.

Vollenweider, R.A. and Kerekes J.J. 1980. Background and summary results of the OECD cooperative program on eutrophication. *Proceedings of the International Symposium on Inland Waters and Lake Restoration. U.S. Environmental Protection Agency*. EPA 440/5-81-010, pages 25-36.

Introducing speed humps as a countermeasure for enhancing traffic safety in urban residential areas: Some insights from experiments in Japan

Do Duy DINH[1], Aya KOJIMA[2]
and Hisashi KUBOTA[3]
[1] Lecturer, Department of Highway and Traffic Engineering,
National University of Civil Engineering, Vietnam
doduydinh@yahoo.com
[2] Assistant Professor, Graduate School of Science and Engineering,
Saitama University, Japan
[3] Professor, Graduate School of Science and Engineering,
Saitama University, Japan

ABSTRACT

During the last decade, Japan has experienced an increasing trend in the percentage of accidents occurring on residential areas over all road accidents. This fact suggests that dealing with traffic safety issues on neighborhood streets is a promising area for enhancing the safety of urban cities in general. While excessive vehicle speed is the main traffic safety concern of the local streets, speed humps have been known as an effective tool to solve this speeding problem. Despite the safety benefits, speed humps have not been commonly used in Asian countries unlike North American and European counterparts. Meanwhile, a very limited experience in using the device from Asian areas has been reported. This paper, therefore, is to present some preliminary results of several hump experiments in Japan. A sinusoidal mobile hump (FLEXITEC) was developed and deployed on a number of residential streets. The results proved that the developed humps can effectively reduce vehicle speeds and generate an acceptable level of noise and vibration. The effectiveness of speed humps ranged at different intervals was also evaluated based on the viewpoint of noise and vibration as well as the effect of speed reduction. While the safety effects of setting humps on local streets have been proven elsewhere, the present paper provides helpful knowledge for practitioners on introducing humps as a safety countermeasure for traffic safety issues in Asian cities. .

Keywords: *traffic safety; traffic calming; speed humps; residential street.*

1. INTRODUCTION

During the last decade, Japan has been sustaining a decreasing trend in the number of traffic fatalities. According Traffic Bureau, National Police Agency, the total number of deaths by traffic accidents dropped by nearly a half from 8326 fatalities in the year 2002 to 4612 fatalities in 2011. With respect to the road type, the percentages of accidents occurred on residential roads with road width of 5.5 m or less amongst all accidents increased to 25.7% in the year 2007 and the figure has been almost no change until now. This fact suggests that dealing with traffic safety issues on neighborhood streets in Japan is a promising area for enhancing the overall traffic safety as well as the safety of urban cities in general.

A number of studies have been proven the strong relationship between vehicle speeds and road crashes. Meanwhile excessive vehicle speed is often deemed as the main traffic safety concern of the local areas. In Japan, a lot of efforts have been made to reduce neighborhood traffic problems. Most residential streets are operated at a speed limit of 30 km/h to favor for protecting vulnerable street users. In addition, some engineering interventions such as speed signs, road marking, pavement coloring etc has been widely used. However, these measures seem to be insufficient to solve the traffic safety issues in residential areas. As an illustration, speeding is a serious problem on local streets and most people often exceed speed limits while driving on these areas (Dinh and Kubota, 2013).

Speed humps have been known as traffic calming devices that can be used to effectively reduce speeding problems. Previous research has documented the safety benefits of traffic calming including speed hump installation. For example, Zein et al. (1997) reported that traffic calming reduced collision frequency by 40%, vehicle insurance claims by 38%, and fatalities from one to zero. Despite safety benefits, and while speed hump has been widely deployed in North American and Europeans areas, the devices has been still very rare in many Asian countries such as Japan.

It should be noted that speed hump may generate some side-effects such as noise and vibration. It should be much considered in case of Japan where people are often nervous about noise and vibration caused by this device. Even in countries where speed humps are popular, the noise and vibration have become serious issues (Harris et al., 1999; Lahrmann and Mathiasen, 1992). To obtain a sustainable development of urban infrastructure, it is important to solve the side-effect issues of speed hump installation. As a response to this, from 1990 several researches to reduce noise and vibration of speed humps were conducted and the studies found that the "sinusoidal" shape is the best from the viewpoint of noise and vibration as well as passenger's comfort (Sayer et al., 1999).

Up to date there has been still very limited experience in using speed humps from Asian areas. This paper, therefore, is to present some preliminary results of several hump experiments in Japan under several research projects conducted by the Urban Transportation Group of the Laboratory of Design and Planning, Saitama University, Japan (i.e., Kojima et al., 2011; Dinh et al., 2013). In this study, a sinusoidal mobile hump (FLEXITEC) was developed and experimentally deployed on a number of residential streets. During the experiments, traffic surveys were conducted to figure out the effects of humps on reducing vehicle speeds. Social surveys regarding many facets of the hump installation were also administered to residents who are living on the affected areas in order to find out public opinions on the matter.

2. HUMP DEVELOPMENTS

In 2000, the Urban Transportation Group of the Laboratory of Design and Planning, Saitama University, Japan have developed "sinusoidal mobile hump named as FLEXITEC" by using rubber made by Nippon liner Co., Ltd under a cooperation project with the company. A lot of experiments were made during the hump development process to figure out the best shape of hump, its size, and its suitable materials considering speed-reducing effectiveness and possible side-effects such as noise and vibration. Two final models of hump (FLEXITEC) were selected as shown in Figure 1. FLEXITEC is a “mobile” hump because its configuration consists of 1m square units that facilitates the installation process as illustrated in Figure 2.

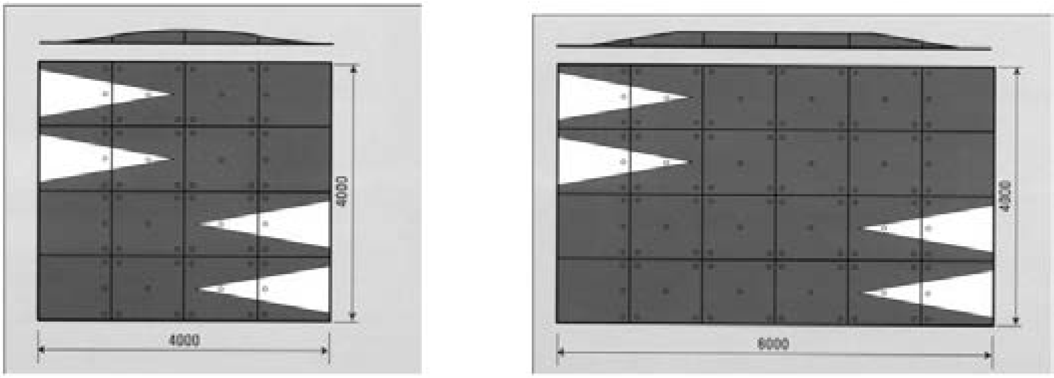

(4m-wide/4m-length/ 10cm-height)
Bow-shape

(4m-wide/6m-length with 2m flat/10cm-height)
Flat-top

Figure 1: Sinusoidal mobile hump (FLEXITEC)

Figure 2: Preparation of experiment

Figure 3: Introducing hump in front of non-signal intersection

The research group has proven that, FLEXITEC can effectively reduce vehicle speeds while generating little side-effects. Regarding noise, FLEXITEC can even reduce noise of the site because the noise produced by vehicle engine is significantly lower due to the speed reduction while the hump itself makes little noise due to its sinusoidal shape and rubber material. It has been also proven that FLEXITEC installed in front of non-signal intersections (see Figure 3) can dramatically reduce traffic accidents possibly by waking drivers to adapt their speeds.

3. SINGLE SPEED HUMP EXPERIMENTS

This section reported the effects of hump on reducing vehicle speeds when there is only one hump installed on a relatively long street section. The target is to find out drivers' speed choice behavior on the sections right before and right after the hump-setting zone.

3.1 Experimental settings

For this studying purpose, two street sections were selected, both located on urban areas of Minami-Hatogaya, Kawaguchi city, Japan. These sections are one-way traffic with a speed limit of 30 km/h. On the traffic moving direction, these sections are adjacent to a river embankment with limited accesses on the right hand side and residential neighborhoods on the left.

Excessive speeds are very serious on the streets that may cause unsafe for residents nearby. To reduce vehicle speeds, two humps were installed on these streets, one hump for each street section. Figure 4 shows the sketch of the study street sections and the location of humps.

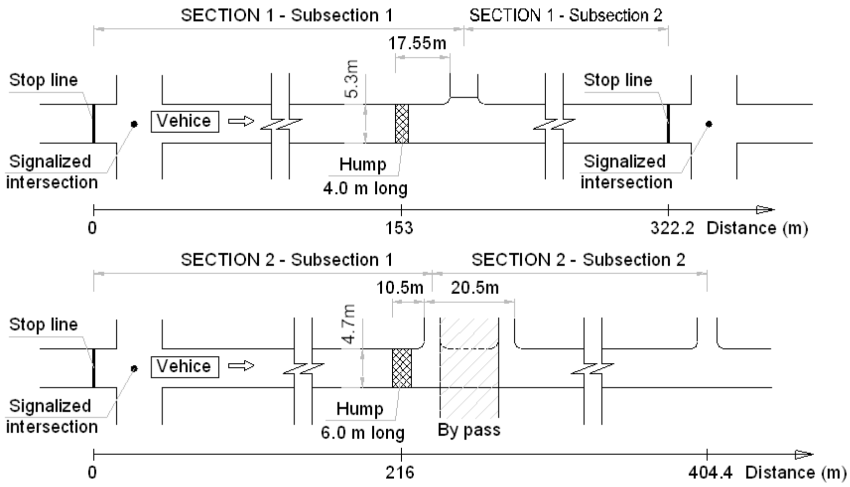

Figure 4: Sketch of selected street sections for single-hump experiments

Speed profiles were recorded for individual vehicles by using STALKER ATS radar guns connected to a laptop on the field. Vehicle speeds were measured both before and during the humps experiment. At least 75 speed profiles were recorded for each situation.

3.2 Results of single-hump experiments

Figure 5 presents the speed profiles for each street section while several speed indicators are shown on Table 1.

Table 1: Descriptive statistics of speed indicators

Indicators	Before experiment		During experiment		Mean speed reduction (km/h)	Mean speed reduction (%)
	Vmean	V85th	Vmean	V85th		
Section 1						
Maximum speed within subsection 1	44.63	50.33	42.60	47.07	2.03	4.56
Maximum speed within subsection 2	47.55	53.32	45.04	51.23	2.50	5.26
Speed at hump location	37.80	43.17	23.60	36.08	14.20	37.58
Section 2						
Maximum speed within subsection 1	49.65	55.83	42.93	47.59	6.72	13.54
Maximum speed within subsection 2	50.15	58.04	46.03	52.74	4.12	8.21
Speed at hump location	49.07	55.29	19.47	26.55	29.59	60.32

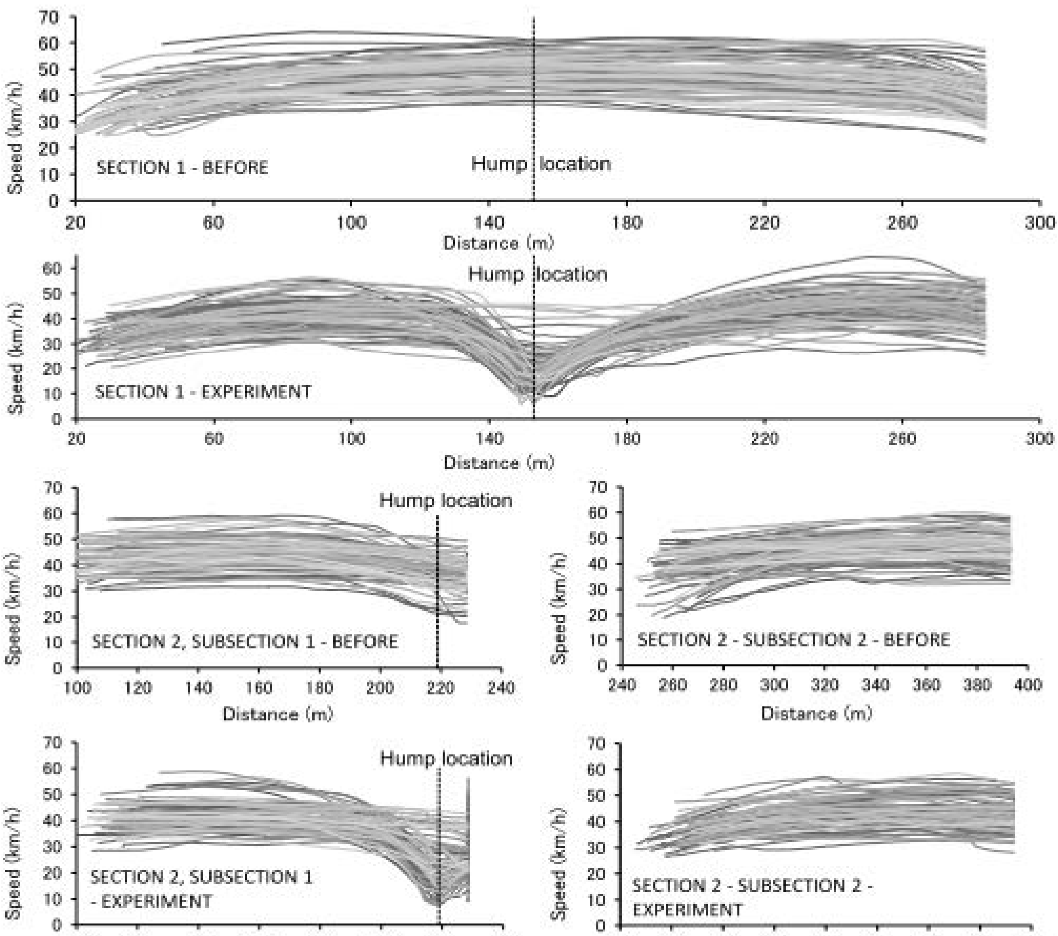

Figure 5: Speed profiles before and during hump experiments

The data showed that all mean speeds measured under the experiment are significantly lower than those measured before the experiment at the 95% level. Mean speeds at hump locations dropped rapidly after hump installation from 37.8 km/h to 23.6 km/h for Section 1 and from 49.07 km/h to 19.4 for Section 2. However, a part of drivers still exceeded 30 km/h when passing the humps. Mean speeds within the subsections before hump locations had a reduction of 2.03 km/h (4.56%) and 6.72 km/h (13.54%) for Section 1 and Section 2 respectively. The impact on mean speeds of the subsections after humps location seems to be smaller with only a decrease of 2.5 km/h (5.26%) for Section 1 and 4.12 km/h (8.21%) for Section 2 under the experiment. On average, drivers need a distance of about 30 m to decelerate from a speed of 40 km/h to the speeds at the hump location. Also, the acceleration rate after passing the hump is very high with only a necessary acceleration distance of less than 20 m to reach the speed of 30 km/h for Section 2.

The findings suggest that if the remaining length of the subsections before and after hump locations is large (more than 150 m as those under the current study), necessary measures should be considered to ensure the targeted speed reduction. Attention should be also paid at the high deceleration/acceleration rate occurred before/after hump location.

4. MULTIPLE SPEED HUMPS RANGED AT DIFFERENT INTERVALS

As illustrated in *Section 3*, a single hump is often insufficient to make drivers to keep lower speeds than the speed limit (i.e., a speed limit of 30 km/h applied for most residential streets in Japan) over the road section especially in cases the section length is relatively long. For such cases, it is necessary to install a series of humps with appropriate intervals. This section aims at finding the appropriate interval of ranged speed humps from the viewpoint of noise and vibration as well as the effect of speed reduction through the field experiments.

To find out the appropriate interval between humps, driving speeds were investigated on a study street with humps ranged at four different intervals including: 30m, 40 m, 60 m, and 100 m. The experiment was implemented along the Kokubunji Koko Higashi Dori street running north-south in Kokubunji city, Tokyo, Japan. It is a 3.6-meter wide and 600-meter long one way street: the direction of the one-way regulation is southward. During peak hours, as many as 500 cars per hour use the street as an alternate route. Most of these cars run at speeds over the legal limit of 20 km per hour. Thus, pedestrians and cyclists using the street are exposed to the dangerous situation and the residents living along the street suffer from the noise and vibration brought about by through traffic.

In order to solve those traffic problems, speed humps were experimentally installed on the street. The experimental period was for 4 weeks during October and November in 2006. Four speed humps were successively placed and the intervals between the humps were changed every 1 week: 30m, 40m, 60m, and 100m. The hump that was located at the north end was fixed throughout the experiment and other three humps were moved.

Before conducting the social experiment, there was a worry that drivers who do not know about speed humps run through the humps at high speeds and make loud noises. To avoid such situation, two kinds of humps, trapezoidal and sine curved humps, were used. Trapezoidal humps have comparably less impacts on motor vehicle occupants and make less noise than sine curved humps. One trapezoidal hump was put on the north end and three sine curbed humps were placed next to the trapezoidal hump. It was intended that drivers who experienced speed humps for the first time could learn the role of humps by the trapezoidal hump at first.

We conducted traffic surveys during the experiment and resident attitude survey after the experiment to evaluate ranged speed humps at four different intervals. In the traffic surveys, we measured vehicle speed, noise, and vibration during morning peak hours. In the attitude survey, we investigated how residents like the humps and how they thought about noise and vibration during the experiment. The following subsections describe the results of the surveys.

4.1 Results of Traffic Surveys

4.1.1 Vehicle speeds

As mentioned above, in the four-week experiment, the intervals of four humps were changed every week. We measured traffic speed at each interval, and before and after the experiment with the target of 150 vehicles for each situation. Targets were vehicles that traveling at free flow speed: it means that we choose vehicles not in congestions and not being influenced by other cars, cyclists, and pedestrians. Figure 6 shows block speed of vehicles from the trapezoidal hump located at the north end to the next hump. It displays the average, 85 percentile, the maximum, and the minimum speed for each interval, and before and after experiment. Before and after the experiment, the average vehicle speed is around 40km/h. All the average speeds measured in the experiment period are significantly slower than the average speed measured after the experiment at the 95% level. It suggests that the installation of ranged humps is effective at all the four intervals. However, the graph also indicates that the speed down effect decreases as the intervals become longer.

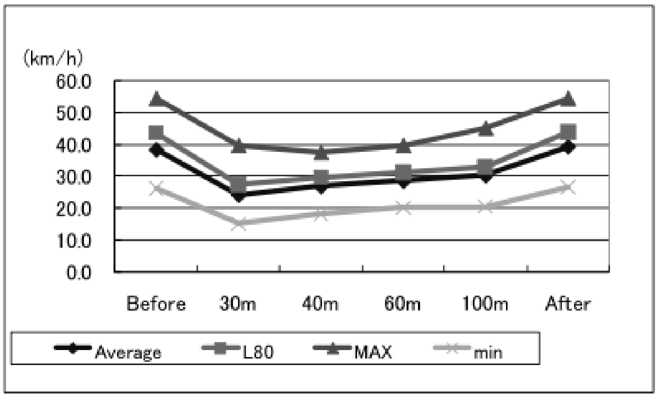

Figure 6: Speeds at different intervals

4.1.2 Noise

We measured noise produced by passing vehicles. The observation points are installation positions of humps and middle points of each hump. Figure 7 shows average momentary value of noise measured when cars run through each observation points. Comparing the average value of the subject street, 72.7dB, the noise at the locations of humps and middle points of each hump is lower. At the middle points, comparably high value of noise was observed than at the installation points of humps. Reacceleration of vehicles after passing humps may influence the result. There is no significant difference in noise values depending on the interval of ranged humps.

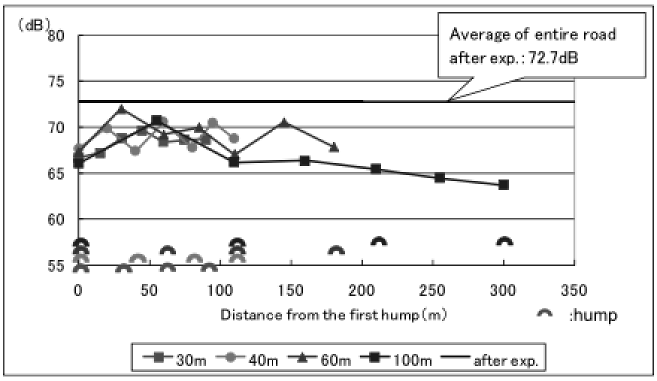

Figure 7: Average momentary value of noise at different intervals

4.1.3 Vibration

We observed vibration generated by cars at the same points where noise was measured. Figure 8 displays average momentary value of vibration measured when cars run through each observation points. Contrary to noise, the value of vibration is higher at the middle points of each hump than at the locations of humps. The value of vibration observed at the midway between humps is higher than the average value on the subject road measured after the experiment. However, the value of vibration does not exceed the environmental limit in Japan. So it is thought that the vibration generated during the experiment period does not influence the neighborhood. There is no significant difference in vibration values depending on the interval of ranged humps as in the case of noise.

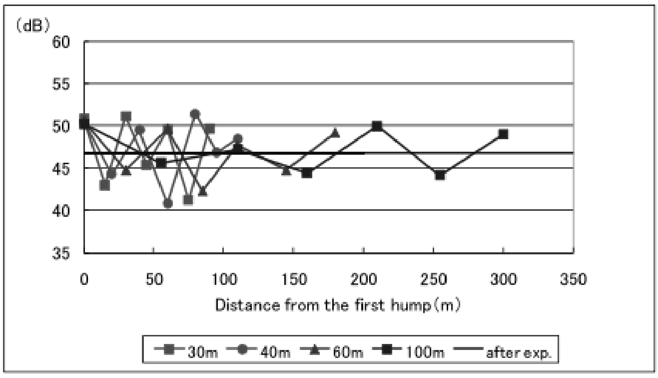

Figure 8: Average momentary value of vibration at different intervals

4.2 Results of Attitude Survey to Residents

As aforementioned, an attitude survey was conducted to understand residents' attitude toward hump installation. The survey method used a questionnaire, and the targets were heads of the households in the affected areas. The questionnaire was distributed by having it dropped into each mailbox by laboratory students, and it was collected by mail using a postage free envelope. After the time limit of the collection, a follow-up survey was conducted for the heads of households who did not reply. Out of 353 questionnaires administered, 179 questionnaires return accounted for 50.7%.

The data showed that, in general residents living in the neighborhood seem to support the hump installation. 73.0 % respondents in the questionnaire survey believed that the number of vehicles that slow down short of the humps "increased" or "somewhat increased". Regarding the traffic safety effects, the percentages of people who thought that the safety of the road was "improved" or "somewhat improved" are 50.0% and 56.5% for the stand point of pedestrian and car driver respectively. As to safety for cyclist, the figure is 37.5%. The rate for cyclist is comparably lower than the former two modes possibly because cyclists may have thought that the installation of humps make the part of roadway for cycling is narrower. Furthermore, for the question “How do you like installing humps on the road?”, 64.6% of respondents answered “good” or “somewhat good” while only less than 20% had a negative response.

The side-effects of hump installation may be largest to the residents who are living along the subject road where humps were placed. Taking account this, an analysis was conducted based on the sample including only people whose house is along the road. The sample size for this analysis is 18.

The data indicates that people living along the road recognized the slow down effect of hump because up to 88.9% believed that the number of vehicle slowing down their driving speeds “increased” or “somewhat increased”. However, on the other hand, the number of residents who thought noise and vibration became big during the experiment is large among the residents living along the road: 44.4% of them answered the noise increased during the experiment, and 50.0% of them answered that the vibration increased during the experiment. The noise and vibration concerns may be a possible reason for the negative evaluation to hump installation regarding the group of people living along the road. Only 27.8% of the respondents answered “good” or “somewhat good” to the question “How do you like installing humps on the road?”. The value is significantly lower than that of the whole respondents. This result and the former results indicate that although the residents living along the subject road highly evaluate the ability of humps to make the road safe, they are anxious about noise and vibration problems and had a negative impression of the installation of the humps.

4.3 Summary of the Experiment and Challenges

It is a big contradiction that residents along the road where humps were installed complained about problem of noise whereas observed noise level is low enough. Judging from free comments in questionnaire survey, the cause seems "re-acceleration" after passing the humps. By analyzing the result of this experiment, we have formulated a hypothesis about the reason of "re-acceleration" that intervals of humps are too long and they promote drivers to re-accelerate as a result.

5. EFFECTIVENESS OF HUMPS RANGED AT 20 M

Based on the lessons from the experiment in Kokubunji city, another experiment was conducted in 2009. This time, the intervals of the humps are purposely set at about 20m. It is expected that the 20m interval keeps drivers not to reaccelerate their vehicles. The experiment was implemented in Bunkyo-ward in Tokyo, Japan. The subject road is the ward road No.839, which is 4.5m width, 300m long one-way road. On the road, four humps were placed considering the road conditions that resulted in three intervals as 19m, 24m, and 29m.

A speed survey was conducted both before and during the experiment. The results provided in Table 2 showed that vehicle speeds decreased significantly after hump installation.

Table 2: Speeds of vehicles before and during experiment

Speed indicators (km/h)	Before experiment (N = 99)	During experiment (N = 126)
Average	22	14
Maximum	40	27
85% percentile	30	19

Noise was also measured with the results provided in Figure 9. As can be seen in the figure, the level of noise were restrained in the whole section where the humps were placed because the 20m intervals prevented vehicles from terrible reacceleration after passing hump locations.

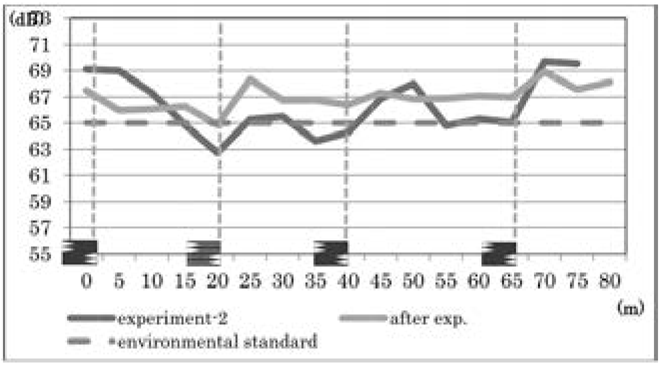

Figure 9: Momentary value of noise

Similar to the experiment in Kokubunji city, a questionnaire survey was again conducted to residents living in the affected areas. Regarding the noise issues, only 11.9% of respondents claimed that the noise made them “annoyed” or “somewhat annoyed”. As for the question with regards to whether humps should be permanently installed on the street, 59.4% of the people living along the subject street answered “agree”, “agree with reservations”, or “accept”. The results suggest that humps ranged at 20m intervals did not have too big noise problems and the most residents accept the impact.

6. CONCLUSIONS

This study has made an attempt to investigate some technical issues regarding setting humps on urban residential streets. Through the number of experiments, it was found that the developed sinusoidal humps can effectively reduce vehicle speeds while generate little noise and vibration when cars pass over.

In case there is only a single hump installed on a relatively long street section, although the mean speeds can reduce significantly to around 20 km/h at the hump locations, drivers often re-accelerate quickly afterward. The acceleration rate after passing the hump is very high with only a necessary acceleration distance of less than 20 m to reach the speed of 30 km/h. Drivers also sharply decelerate their speeds before reaching the hump location. On average, drivers need a distance of about 30 m to reduce from a speed of 40 km/h to the speed at the hump location.

This paper also aimed at finding appropriate interval between humps when a series of humps are installed on a street section. The appropriate interval was judged from the view point of noise and vibration as well as the effect of speed reduction through experimental installations. Regarding the interval, it was found that 60m-inerval can reduce speed to a speed of less than 30km/h in all over the road section. The first experiment conducted in Kokubunji city, Tokyo seemed successful judging from observed data. However, residents along the experiment street complained noise problems in any cases of experiment. Cause of the noise was not the shock of traffic passing through humps but the re-acceleration of cars after passing humps. In the second experiment conducted in Bunkyo-ward, Tokyo, the intervals between humps were reduced to 20m to make drivers to "give up" re-accelerating. Judging from the result of the questionnaire survey and noise observation, 20m-interval could control re-acceleration to the extent that residents along the road are acceptable.

Although the present research has made efforts on understanding drivers' speed choice behaviors on hump-installed streets in Japan and some related issues, there is still a lot of works that should be done before humps can effectively introduce widely to urban cities for traffic safety preventions. For example, further studies should focus on the safety effects of humps as well as the cost-benefit of the hump installations.

REFERENCES

Dinh, D.D., and Kubota, H., 2013. Profile-Speed Data-Based Models to Estimate Operating Speeds for Urban Residential Streets with a 30 km/h Speed Limit. *IATSS Research* 36, 115-122.

Dinh, D.D., Kojima, A., and Kubota, H., 2013. Reducing Vehicle Speed on Residential Streets: A Single-Hump Experiment. *Paper for JSCE 15th International Summer Symposium*, Japan Society of Civil Engineers, Chiba, September 2013.

Harris, J.I., Stait, R.E., Abbott, P.G., and Watts, G.R., 1999. Traffic calming: Vehicle generated noise and ground-borne vibration alongside Sinusoidal, Round-Top and Flat-top Road Humps, TRL Report 416.

Kojima, A., Kubota, H., Yoshida, M., Ichihara, S., and Yoshida, S:, 2011. Effectiveness of speed humps ranged at different intervals considering roadside environment including vehicle speed, noise and vibration, *Journal of the Eastern Asia Society for Transportation Studies*, 9, 1913-1924.

Lahrmann, H., and Mathiasen, P., 1992. Bumpudformning (Hump Design), Dansk Vejtidsskrift Nr9, 16-22.

Sayer, I.A., Nicholls, D.A., and Layfield, R.E., 1999. Traffic calming: Passenger and rider discomfort at Sinusoidal, Round-top and Flat-top humps a track trial at TRL, TRL Report 417.

Traffic Bureau, National Traffic Agency. Traffic Accident Statistics. (in Japanese).

Zein, S., Geddes, E., Hemsing, S., and Johnson, M., 1997. Safety Benefits of Traffic Calming, *Transportation Research Record* 1578, National Research Council, Washington, D.C., 3-10.

Some research on air quality of Ulaanbaatar City (Mongolia) in wintertime

O.Enkh-Uyanga[1], P.Chimedtseren[2] , G.Solongo[3]
[1-]Department of Chemistry , Ulaanbaatar school, National University of Mongolia
[2]- Disaster research institute under the NEMA
[3-]Pulmonary department of 3th policlinic Ulaanbaatar
ouyanga2001@yahoo.co.uk

ABSTRACT

Ulaanbaatar, the capital city of Mongolia is subject to high air particulate matter pollution episodes during winter. The process of urbanization which had accelerated in Mongolia in mid 1990-s of the capital contributed to the rapid growth of the capital which population is 1.1 million people while the total of the country is 2.8million (2011) [1]

The air pollution is visibly worse in the wintertime. Some sources of air pollution in Ulaanbaatar are four thermal power plants, about 200 small and medium sized heating boilers, 168000 traditional gers (traditional nomadic dwelling), wooden houses and 130000 automobiles. In these areas, the only source of heating are fueled by coal and wood. Annual average burned consumption of coal is 5.9million ton and wood is 237,2 thousand ton in Ulaanbaatar.[2]

We shown that , annual average particulate matter concentrations PM_{10}, SO_2, CO_2 comparative indices by last 5 year.

Research background: Pollutant substances including alien elements with dust, mistiness, toxic gas derived from burning, especially sulfuric gas derived from coal burning, nitric acid, carbon monoxide, carbonic acid, ammonia, ozone, hydro sulfur, formaldehyde, heavy metals, mercury, lead, arsenic and cadmium are regularly released from manufacturing, human activities and vehicles in the air in external surrounding of civilized areas.

In recent years, above chemical substance acetone amount in the air is a lot higher than the norm due to high amount of smoke in our capital city. Therefore, the population of the city often suffers from respiratory and cardiovascular illnesses and cancer due to the consequence of air pollution. We have conducted this research and defined content of pollutant substances including sulfuric anhydride, nitric acid, dust, carbonic acid in the air on the basis of air quality report of Ulaanbaatar between 2007 and 2012.

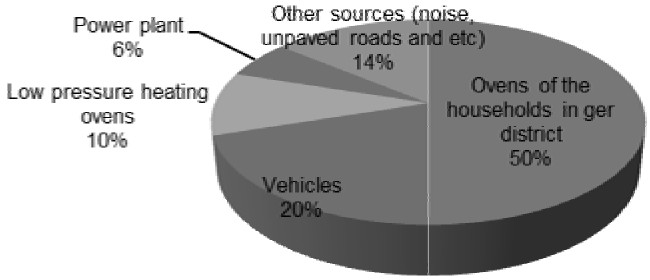

Graph 1. Air pollution factors in Ulaanbaatar

Research result: As the result of comparative study for air quality of 4 indicators of the statistical year based on air quality report of 2007-2012, amount of chemical substances having adverse impact on respiratory and other organs and systems is 1.5 to 5 times than the norm.

Amount of SO_2 in the air content *table.1*

Year	2007	2008	2009	2010	2011	2012
Content (mkg/m^3) SO2	11	15	18	27	31	30
Content SO_2 of air quality standard	10	10	10	10	10	10

As seen from the above table 1, SO_2 amount in the air is 2.5 to 3 times higher than allowed amount of 10 mkg/m^3. Amount of SO_2 in the air content of 2011 and 2012 is 30mkg/m^3 which is a lot higher than that of previous year's average amount.

As seen from the above table 2, amount of NO_2 in the air is 0.2 to 0.6 times higher than allowed amount in air quality standard of 40-50mkg/m^3. Amount of NO_2 in the air content of 2011 and 2012 is a lot higher than that of previous year's average amount.

Amount of NO_2 in the air content, Ulaanbaatar *table.2*

Year	2007	2008	2009	2010	2011	2012
Content (mkg/m^3) NO2	37	31	28	35	43	44
Content NO_2 of air quality standard	40	40	40	40	40	40

Research result shows that NO_2 amount in wintertime is 4 to 5 times higher than allowed amount. Spring and autumn time amount is approximately 40-50mkg/m^3 which is 1.5 to twice higher than the allowed amount. The result of measurement conducted in most polluted areas of Ulaanbaatar shows that yearly average of PM_{10} amount is 20 to 100 times higher than the international and Mongolian air quality standard. Generally, dust substance amount in major cities is lower than 40mkg/m^3. As seen from the above table 3, dust amount in the air of Ulaanbaatar is 3 to 5 times higher than the standard and there is a tendency to increase in recent years.

Content PM_{10} in the air, Ulaanbaatar table 3

Year	2010	2011	2012
Content PM10 of in the air content	148	230	259
Content standard of PM 10 in air quality	50	50	50

The above graph shows that smoke amount increasing in wintertime increases yearly average dust amount in the air to the maximum. O_3 amount in the air has been determined in our country since 2011. The research result shows that ozone amount does not reach allowed standard. For example, ozone amount in 2012 is 4 to 5 times lower than standard.

Conclusion:

1. Amount of SO_2 in the air of Ulaanbaatar which has adverse impact to respiratory organs 2.5 to 3 times higher, amount of NO_2 is 0.2 to 0.6 times higher, dust or PM_{10} amount is 3 to 5 times higher and ozone amount is 4 to 5 times lower than the allowed standard amount.
2. Amount of above chemical substance acetone in the air is high in winter and autumn. The lowest ozone amount is in winter.
3. The result of measurement conducted in most polluted areas of Ulaanbaatar shows that yearly average of PM_{10} amount is 20 to 100 times higher than the international and Mongolian air quality standard

Reference materials:

1. Capacity Development project for Air pollution control in Ulaanbaatar city Mongolia. 2011
2. www.tsag-agaar.mn
3. http://www.therestorationresource.com

Investigating future yield and adaptation measures in rice production under climate change scenarios in Quang Nam province, Vietnam

Trang BUI THI THU[1], Sangam SHRESTHA[2]
[1]Lecturer, Hanoi University of Natural Resources and Environmental, Vietnam
[1]Graduate Student, WEM, SET, Asian Institute of Technology (AIT), Thailand
thutrang.hunre@gmail.com
[2]Assistant Professor, WEM, SET, Asian Institute of Technology (AIT), Thailand

ABSTRACT

In recent years, climate change has become a biggest problem in developing countries all over the world, especially in Vietnam. Global climate change may affect the yield of rice crop in the future. This study analyses the impacts of climate change on rice production and adaptation in Nui Thanh district, one coastal district of central Vietnam where there are many natural disasters hit annually. This study pursue to seek following queries including forecast future rainfall, temperature and rice yield, and analyze adaptation measures to improve rice production under different climate change scenarios in Nui Thanh district, Quang Nam province, Vietnam. The study was based on firstly identification of the problem in the study area followed by collection of secondary data collection on weather, soil characteristics and crop management. Then the downscaling model was used to predict the temperature and precipitation of the study area in the future by A2 and B2 scenarios. The crop Aquacrop model was used to simulate the yield response with the outputs of the SDSM. After that, the impact of climate change scenarios on rice yield was analyzed. Lastly, the evaluation for adaptation measure to improve rice production under climate change based on water management was determined.

Keywords: *climate change, Aquacrop; investigating future yield; adaptation measures; climate change scenarios; Nui Thanh district; Quang Nam province, Vietnam.*

1. INTRODUCTION

Vietnam has long seashore, large population and economic activities in coastal zone and heavy base on agriculture, forestry and natural resources (Tran Duc Vien, 2011). Agriculture plays an important role in economy of Vietnam nation, especially in rural areas. As many developing countries, agriculture sector of Vietnam largely depends on weather conditions. Precipitation plays an important role in supplication water source to crops directly. Annual average rainfall of Vietnam is more than 2,000mm in which monsoon rainfall occupies about 70% of total annual (Tran Duc Vien, 2011). At recent years, in the Central and Southern Vietnam, the the frequency of flood has increased significantly, special in rainy season. But most of other regions in country, the drought came due to decrease of rainfall in dry season (Thuc, Tran, 2010). Rice has long been Vietnam's traditional food crop and the country's export product. It is about 99.9 percent of Vietnam population eats rice as their main meal. Paddy is grown on 53 percent of the agricultural land in Vietnam, and it represents 64 percent of the sown area crop with 60 percent of labor in rural area. Rice has recently become the second largest export, accounting for 10 percent of total value. Vietnam had successful transformed itself from a chronic rice importer to one of the three largest rice exporters in the world. Nonetheless, climate change directly affected precipitation and temperature, with rise in temperatures leading to water deficit and foods in the future, changing soil moisture status and pest and disease incidence (Chinvanno, 2010).

Parry et al. (2004) analysed the global consequences to crop yields, production, and risk of hunger of linked socio-economic and climate scenarios. Potential impacts of climate change are estimated for climate change scenarios developed from the HadCM3 global climate model under the Intergovernmental Panel on Climate Change Special Report on Emissions Scenarios (SRES) A1FI, A2, B1, and B2. Projected changes in yield are calculated using transfer functions derived from crop model simulations with observed climate data and projected climate change scenarios. Tao and Zhang (2010) cited the highest benefits were obtained from the development of new crop varieties that are temperature and have high thermal requirements. Based on simulations, at North China Plain (NCP) it was found that for the high temperature sensitive varieties, early planting of the crop is the effective option for reducing the yield loss from climate change in the region. Also it was concluded that for high temperature tolerant varieties, late planting is a good adaption option moreover the spatial analysis shows the relative contributions of adaptation options should be region and variety of crop specific as the adaptation varies geographically and crop variety.

Reidsma et al. (2010) analysed the adaptation of farmers and regions in Europe to the prevailing climate change, climate variability and climatic conditions in the last decade. The research concludes that, the impacts on the crop yields cannot be translated to the impacts on the farmers' income, since farmers adapt by changing the crop rotations and inputs and the incomes are also dependent on the subsidies by the government. Secondly, the observed impacts of climate change on the spatial variability on the yield and income is lower in warmer climates as compared to temporal variability in climate in the places where there is heterogeneity in the crops grown. Thirdly climate change and variability impacts are dependent on the farm characteristics (e.g. size, intensity and land use) which have ultimate influence on adaptation and management. As different farm types adapts differently, hence a larger diversity in the farm types reduces the impacts of the climate variability at a regional level. Finally from the study, they concluded that the yield and the farmers' income in the future is mainly dependent on the adaptation practices being followed which can reduce the potential impacts of climate change. Farmers continuously adapt to changes, which affects the current situation as well as future impacts. Geerts (2010) used AquaCrop to derive deficit irrigation (DI) schedules. In this study, they use the AquaCrop model to simulate crop development for long series of historical climate data. Subsequently they carry out a frequency analysis on the simulated intermediate biomass levels at the start of the critical growth stage, during which irrigation will be applied. From the start of the critical growth stage onwards, they simulate dry weather conditions and derive optimal frequencies (time interval of a fixed net application depth) of irrigation to avoid drought stress during the sensitive growth stages and to guarantee maximum water productivity. By summarizing these results in easy readable charts, they become appropriate for policy, extension and farmer level use. If applied to other crops and regions, the presented methodology can be an illustrative decision support tool for sustainable agriculture based on DI.

Climate change severe affects to the crops yield and finally to ramp up poverty in Vietnam. Therefore, it is necessary to seek the solutions to adapt to climate change, special for famer life and their agriculture production. The frame of this paper focus finding out impacts of climate change on rice production in Nui Thanh district of Quang Nam province in center of Viet Nam. The area often have tremendous catastrophically natural hazard by flood and typhoon. The main objective of this research was to forecast future rainfall, temperature and rice yield, and analyze adaptation measures to improve rice production under different climate change. The specific objectives are: to forecast rainfall, temperature on the future in the study area under climate change condition; to predict crop yield in future under climate change scenarios; to evaluate adaptation measures to improve rice production under climate change based on water management.

2. MATERIALS AND METHODS

2.1 Study area

The research was conducted in Nui Thanh district to typify for a coastal sub-region in order to understanding the impacts of climate change on rice production. Nui Thanh is the last district to the southward of the province and is adjacent to Quang Ngai province. With diverse topography: coastal zone, plain zone and mountainous zone, Nui Thanh is hard hit by storm, drought in the coastal area, flood in mountainous area, plain area. The hazards robbed the life and a lot of property in this district in the past years. Nui Thanh is assessed as one of the most serious damaged district by the hazard of Quang Nam province. Special, the important criteria for choice of study site are as follows: The high rate of population cultivates agriculture as major livelihood; not only storm and food but also the study site is affected by other irregular climate factors, such as temperature, rainfall.

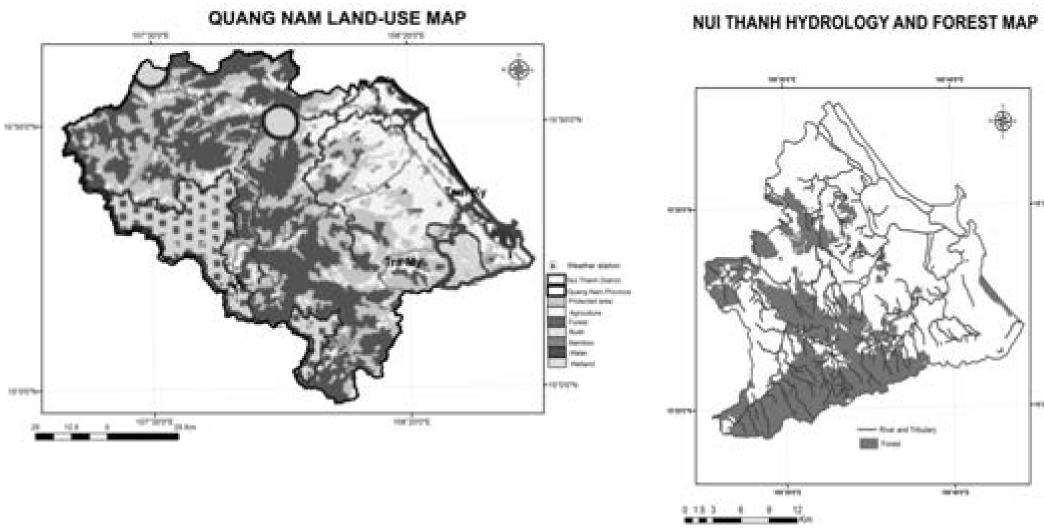

Figure 2.1: Quang Nam land use map and Nui Thanh hydrology and forest map

2.2 Climate data

The climate data were collected from Vietnam meteorological Department, with the Tra My and Tam Ky stations (the weather stations nearest Nui Thanh), where the experiments are performed. The data consists of daily weather data including rainfall, maximum and minimum temperature (from year 1961 to 2000), average monthly weather data including rainfall, maximum temperature, minimum temperature, sunshine hours, wind speed and relative humidity (from year 2000 to 2010).

2.3 Future climate scenarios

The future climate scenarios was downloaded from the Global Climate Model HadCM3 (Hadley Centre Coupled Model, version 3) developed by Met Office Hadley Centre, England. (Website: http://www.cccsn.ec.gc.ca/?page=sdsm). The high resolution data was developed considering the world growth forced by level of atmospheric CO2 concentration according to IPCC SRES A2 scenario (which is one of the most pessimistic projections) and B2 (another pessimistic projection but population growth rate lower than A2). Then the data was downscaled to the regional level by using SDSM (Statistical Downscaling Model) for the study area. The downscaled data for the period of 2014-2040, 2041-2070 and 2071- 2090 was used for the grid which falls nearest to the study area.

2.4 Future climate scenarios

The data of rice crop was collected from Quang Nam Department of Agriculture and Rural Development and Agriculture Division under Nui Thanh District People's Committee as secondary sources. The data included major rice varieties, transplanting date, density of plants, flowering date (anthesis date), senescence date, maturity date, and method of sowing, irrigated schedule and the rice yields. The information data is about two majors' rice varieties grown in the Quang Nam province: CH207 and TBR1 for period 2001-2010. The researcher assumed that the treatment and organic manures was provided full in the field. Other side, field surveys of smallholder farmers was conducted in three communes: Tam Hoa, Tam Hiep and Tam Xuan II about one month. 30 smallholder farmers were randomly selected from three communes and interview by trained assessors on a set of questions designed in a questionnaire. The questions were aimed to obtain information on the: indigenous farming practices, variety preferences and attitude to forwards modification of traditional farming method and crop varieties.

2.5 Soil properties data

The information about physical and chemical properties of the soil is collected from Quang Nam state land and development section. The data required are soil texture, pH, phosphorous, nitrogen, carbon and carbon exchange capacity.

2.6 Model

2.6.1 Downscaling of GCM data by SDSM

The general principle of downscaling is to relate large scale predictor variables to sub-grid or station level climate variable. This study used the statistical downscaling (SD) method to transfer large scale GCM grid data to local scale station data which are required to feed hydrological models for the simulation of future scenarios of climate change impact. The statistical downscaling model (SDSM) version 4.2.9 developed by Wilby et al. (2000) is use in this study. This model used the principle of developing multiple linear regression transfer functions between large-scale predictors and local climate variables (predictand) and these transfer functions were used for downscaling future climate predicted by GCMs. This study used the period of 1961-1990 as the base period for model calibration and validation. This period taken because most of the GCMs provide their projected climatic data starting from 1961 and in most of the study region observed climatic data are also available for this period. While using the modeled climate results for scenario construction, the base line serves as reference period from which the future changes are calculated. Downscaling with SDSM includes of four main steps: screening of large scale climatic variables (predictors), calibration of transfer functions, validation of downscaling model and scenario generation generation.

2.6.2 ETo calculator

The weather data required by AquaCrop model are daily values of minimum and maximum air temperature, reference crop evapotranspiration (ETo), rainfall and mean annual carbon dioxide concentration (CO2). ETo was estimated using ETo calculator using the daily maximum and minimum temperature, wind speed at 2 m above ground surface, solar radiation and mean relative humidity (RH). The weather parameters were collected from automatic weather station located at a distance of 13 m above sea level.

2.6.3 Calibration and Validation of Aquacrop model

Calibration or fine tuning of the AquaCrop model was run after preparing the input data files consist of meteorological data, precipitation, evapotranspiration, irrigation, plant and soil information from the field experiment during 2001 to 2010 for two crop seasons. The model calibration was conducted by changing the model parameters and based on best matching between the output and observed data. The simulating value of model predicted the output the yield, biomass and canopy cover (CC) which used to compare with measured yield and biomass of the experimental plot. The difference between the model predicted and experimental data was minimized by using trial and error approach in which one specific input variable was chosen as the reference variable at a time and adjusting only those parameters that were known to influence the reference variable the most. The procedure is repeated to arrive at the closest match between the model simulated and observed value of the experiment for each treatment combination. In this study, the winter crop was performed based on rainfed. However, the irrigated experiments were performed on the summer crop. In some cases such as upper and lower thresholds for canopy expansion, upper threshold for stomata closure and canopy senescence stress the recommended default value by model guidelines, was considered.

3. RESULTS AND DISCUSSION

3.1 Projection of future climate

3.1.1 Projection of future temperature

In this part, the SDSM was used to project the change in maximum and minimum temperature in three periods: 2014-2040, 2041-2070 and 2071-2090 relative to base period 1961-1990. The results show that the highest rise in maximum temperature will be 3.69°C and the lowest rise will be 0.93°C by period 2014-2040 according to scenario A2. The scenario B2 indicates lower rate of rise with average value of 1.85°C relative to baseline period. The highest rise in minimum temperature will be 1.72°C by period 2071-2090 and the lowest rise will be 0.35°C by period 2014-2040 according to scenario A2. The highest rise in minimum temperature will be 1.29°C by period 2071-2090 and the lowest rise will be 0.39°C by period 2014-2040 according to scenario B2. The average change in maximum and minimum temperature for SRES A2 and B2 scenarios are presented in figure 3.1.

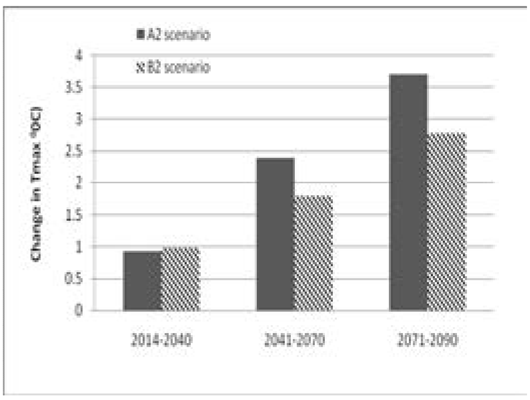

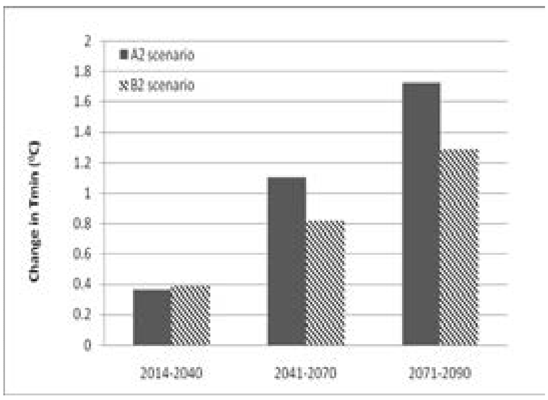

Figure 3.1: The changing in the average annual of maximum and minimum temperature

The average of monthly maximum temperature and minimum temperature for three future periods compared to baseline period with A2 and B2 scenarios are showed in figure 3.2. The temperature presents considerably most similar trends for two scenarios.

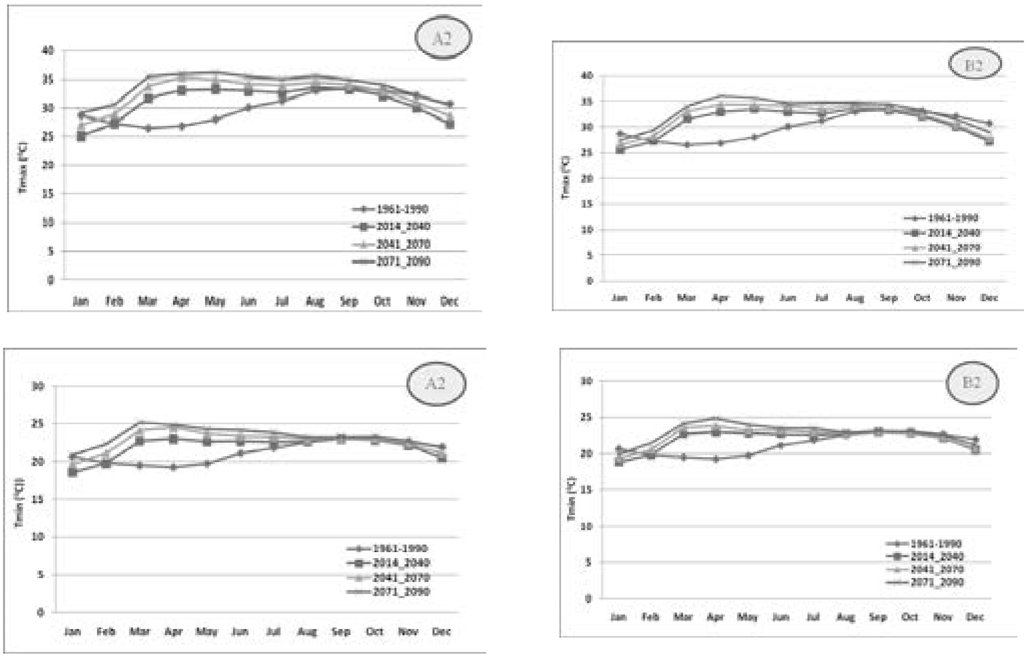

Figure 3.2: Monthly Tmax and Tmin average for 30 years interval for A2 and B2

3.1.2 Projection of future precipitation

In this part, the SDSM was used to project the precipitation in three periods: 2014-2040, 2041-2070 and 2071-2090 relative to base period 1961-1990. Figure 3.3 shows the relative changes in the precipitation for the study area projected for A2 and B2 scenarios for periods 2014-2040, 2041-2070 and 2071-2090 as compare to baseline period of 1961-1990. Scenario A2 shows increase in average annual precipitation by 0.66, 5.51 and 9.75% respectively for periods 2014-2040, 2041-2070 and 2071-2090. Scenario B2 has slightly higher increase rate on periods 2014-2040 and 2071-2090, there are about of 1.83 and 5.62%. But it is lower increase than scenario A2 in period 2041-2070, it is about 3.47 %.

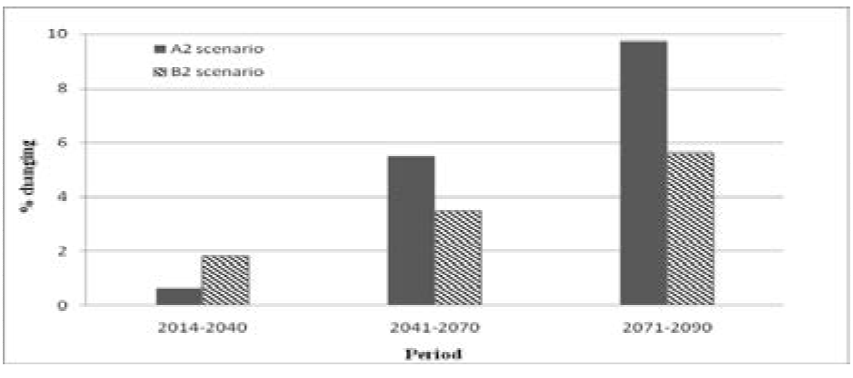

Figure 3.3: The changing in the average annual of precipitation for A2 and B2

The projected precipitation does not show any fixed trend for both scenarios. There is wide variation at temporal and spatial scale throughout the basin. The figure 3.4 shows the changing in monthly precipitation for the study area projected for A2 and B2 scenarios for periods 2014-2040, 2041-2070 and 2071-2090 compared to baseline period of 1961-1990. Scenario A2 and scenario B2 are most the same the trend. Those figures show decrease of precipitation during most of rainy season and increase during dry season. The precipitation strong decreases on January and April which is about 44.41 to 57.90%. The precipitation higher increases on June, it is over 150%. But the total precipitation of June is not very high; therefore the amount of changing is not too large. From the % changing in there figures, it is impress that the impact of climate change is very serious on the end of XXI century.

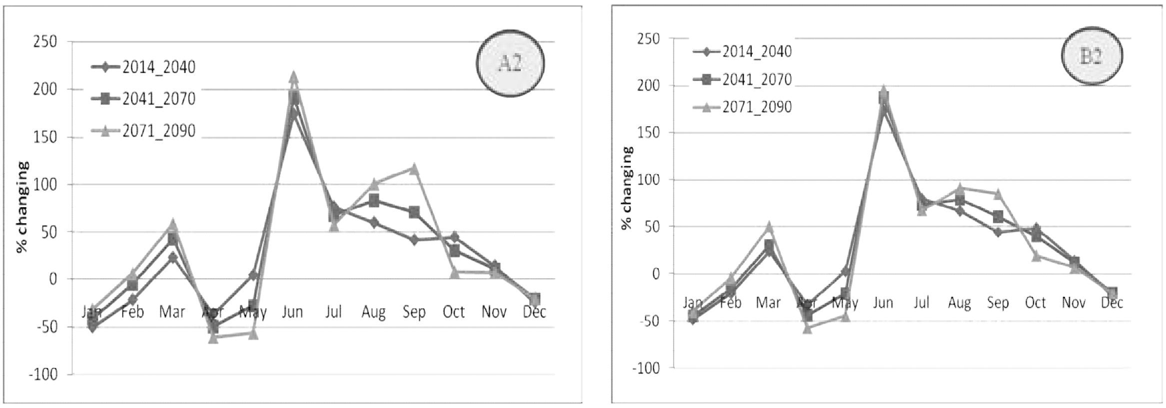

Figure 3.4: Variation in change of precipitation for A2 and B2 scenarios compared to the baseline period (1961-1990)

3.2 Forecast the yield in future period by using Aquacrop model

The rainy season in the northern delta usually begins in May-June and end on October-November. In the central province, rainy season come later, the large amount of rainfall usually during time of November-December. From the output of SDSM for the future climate, the precipitation higher increases on June to September, but the total rainfall during that time is not high, other case, the total rainfall is high during the months from October to March, but the future precipitation decrease on December, January, February, April and May. Therefore, the researcher recognized that there would be difference trend impact to future yield between the crop cycle Winter-Spring and Summer-Autumn. That why, the simulation of yield have done for two crop seasons to discover the impact of climate change to the yield.

The figure 3.5 presents the percentage change in rice for A2 and B2 scenarios for 2014-2040, 2041-2040 and 2071-2090 relative to 2001-2010 simulated by Aquacrop model during winter crop and summer crop.

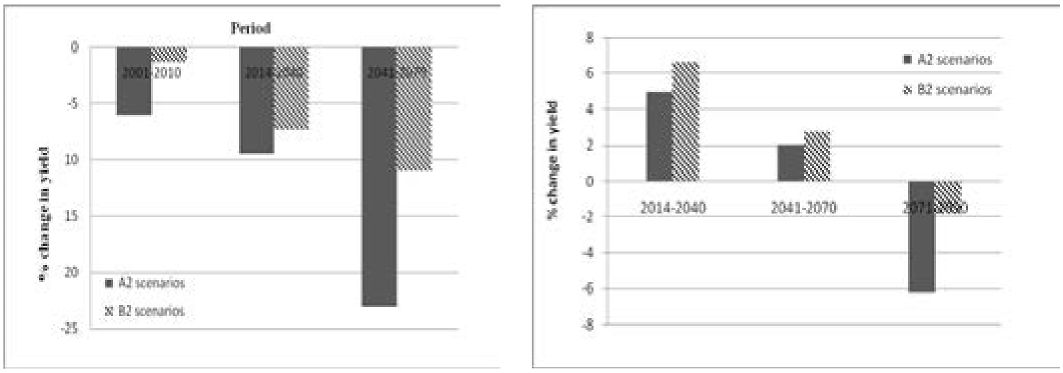

Figure 3.5: Percentage change in rice yields with A2 and B2 scenarios for periods 2014-2040, 2041-2040 and 2071-2090 relative to 1961-1990 during
(a) Winter crop and (b) Summer crop

For winter crop, with rainfed when calibration Aquacrop model, all of future periods the yield will reduce. The yield significantly decreases during period 2071-2090 with both A2 and B2 scenarios. The reason of forecasted yield reduces significantly from the baseline period this may be due to the effect of the reduced rainfall and the stress due to increased temperature during flowering. Similarly the biomass also shows a reducing trend for both scenarios.The yield simulated by Aquacrop express a decline 5.97 to 23.05 and 1.29 to 10.96 percent compared to the yield of the baseline period for A2 and B2 scenarios respectively. Therefore, for winter crop season, farmer should supplementary irrigation water applied using furrow method for three times at 10 days interval starting, flowering and grain filling to reach the optimum yield in the future periods.

For the summer crop, with baseline period 2001-2010, the model calibrated for irrigated crop. However, the rainfall significant increase on this season in the future. Therefore, the water available will be enough for crop for some periods. Then, the yield increase about 5% and 6.67 % for period 2014-2040, 2% and 2.78 % for 2041-2070 with A2 and B2 scenarios respectively. The yield will reduce 1.83% and 6.26% for 2071-2090 with A2 and B2 scenarios respectively. During period 2001-2010, to obtain the high yield or do not lose yield rice, the farmer had to supplement irrigation water. However, the output of SDSM for future climate changes scenarios. The rainfall will increase starting from June until September. This is the period of summer crop rice crop. Therefore, the additional irrigation for rice in the forecast period is increased. So the model can calibration for rainfed yield in the future period without additional water, which is perfectly consistent with the results predicted by SDSM model.

3.3 Agricultural adaptation measures

3.3.1 Impacts of supplementary irrigation on rice yield

Supplementary irrigation water applied using furrow method in incremental amount of 20mmm, 40mm, 40mm, 80mm and 100mm. Each irrigation level was applied four times at 20 days interval starting, 20 days before flowering date to coincide with the critical stages of rice growth, flowering and grain filling. The figure below explains the percentage change in yield under supplementary 20, 40, 60, 80 and 100mm for 4 applications as compared to rainfed crop (for winter crop) and irrigated crop (for summer crop) under A2 scenario. The results shows that for all future periods, in winter crop, the optimum amount of supplementary irrigation are about 400mm in four applications and this would increase the yield by 24.13% in 2014-2040, by 27.45% in 2041-2070 and by 42.1% in 2071-2090. For the summer crop season, the optimum amount of supplementary irrigation is about 320mm and this would increase the yield by 2.32% in 2014-2040, by 2.48% in 2041-2070 and by 2.52% in 2071-2090. The application for irrigation water in summer crop does not increase the yields significantly because of this season has fairly enough rainfall. The result shows there are good relative with the output of SDSM model.

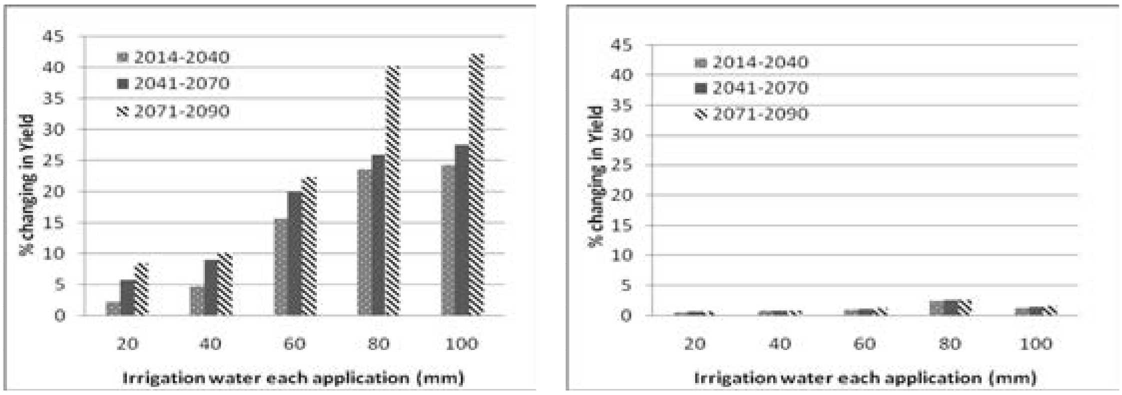

(a) rainfed (b) irrigation

Figure 3.6: Impact of supplemental irrigation on rice for A2 scenario
(a) Winter crop (rainfed) and (b) Summer crop (irrigation)

The figure 3.7 below explains the percentage change in yield under supplementary 20, 40, 60, 80 and 100 mm for 4 applications as compared to rainfed crop (for winter crop) and irrigated crop (for summer crop) under B2 scenario. The results show that for all future periods, in winter crop, the optimum amount of supplementary irrigation is about 400mm in four applications and this would increase the yield by 20.13 % in 2014-2040, by 30.45 % in 2041-2070 and by 32.81% in 2071-2090. For the summer crop season, the optimum amount of supplementary irrigation is about 320mm and this would increase the yield by 2.28 % in 2014-2040, by 2.35% in 2041-2070 and by 2.48% in 2071-2090. The application for irrigation water in summer crop does not increase the yields significantly because of this season has fairly enough rainfall. The result shows there are good relative with the output of SDSM model.

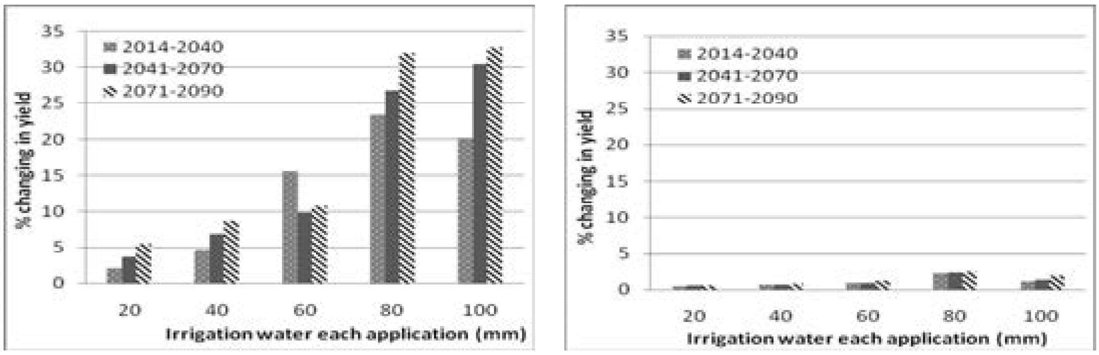

(a) rainfed (b) irrigation

Figure 3.7: Impact of supplemental irrigation on rice for B2 scenario
(a) Winter crop and (b) Summer crop

3.3.2 Impact of changing sowing date on rice yield

In this section, the date for transplanting was changed with different dates to determine which date is best to gain the optimum yield. The simulations were run with the dates around one week, two week, three weeks… compared with the current transplanting date. Figure 3.8 shows the percentage change in yield with different transplanting dates for CH207 and TBR1 with A2 scenario. For winter crop, the result shows that the transplanting date of 25th February is the optimum for future period, which can increase the yield up to 18.14%, 19.87% and 20.43% for 2014-2040, 2041-2070 and 2071-2090 respectively. Probably this due to the reason that, the precipitation is decreased during December to January, then if the transplanting is during this time the yield would reduce. From the second week of February, the rainfall increase, it is better to transplanting from 10th -30th February. For summer crop, the result shows that the transplanting date of 11st June is the optimum for period 2014-2040 and 2041-2070, which can increase the yield up to 27.78% and 26.43% respectively. With period 2071-2090, the optimum is 18th June, which can increase the yield up to 24.86%. Then, for summer crop, it is better to transplanting from 3rd – 18th of June.

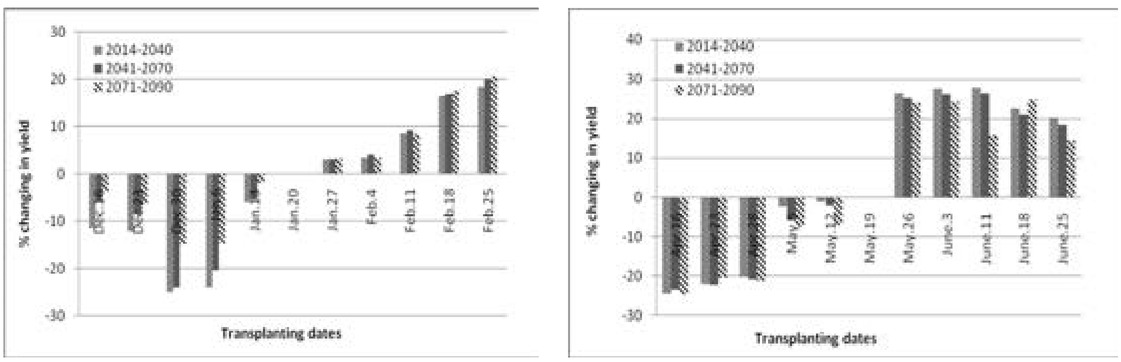

Figure 3.8: Percentage change in yield with different dates for A2 scenario (Jan 20th and Mar 19th are current planting date): (a) Winter crop and (b) Summer crop

With B2 scenario, for winter crop, the result shows that the transplanting date of 25th February is the optimum for future period, which can increase the yield up to 20.34%, 14.37% and 22.94% for 2014-2040, 2041-2070 and 2071-2090 respectively. Probably this due to the reason that, the precipitation is decreased during December to January, then if the transplanting is during this time the yield would reduce. From the second week of February, the rainfall increase, it is better to transplanting from 10^{th} -30^{th} February. For summer crop, the result shows that the transplanting date of 11^{st} June is the optimum for period 2014-2040 and 2071-2090, which can increase the yield up to 26.72% and 22.86% respectively. With period 2041-2070, the optimum is 3^{rd} June, which can increase the yield up to 26.18%. Then, for summer crop, it is better to transplanting from 26^{th} May to11^{th} June. Figure 3.9 shows the percentage change in yield with different transplanting dates for CH207 and TBR1 with B2 scenario.

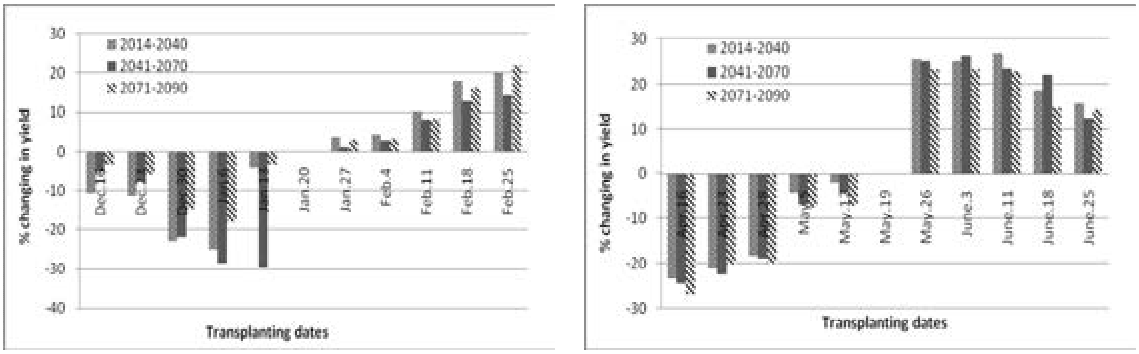

Figure 3.9: Percentage change in yield with different dates for B2 scenario (Jan 20^{th} and Mar 19^{th} are current planting date): (a) Winter crop and (b) Summer crop

4. CONCLUSIONS

In this paper the impact of climate change on paddy irrigation required and volumetric irrigation water demand have been presented. The results from the present study conclude that:

1. Downscaling with SDSM model has well estimated, then the simulated weather data downscaled by SDSM from the GCM HadCM3 had a good agreement with observed data. Therefore, the future scenarios weather data by HadCM3 can acceptable. Aquacrop model and the ETo calculator (Evapotranspiration from reference surface) performed satisfactorily in the study.

2. The minimum temperature will increase about 0.35^0C, 1.10^0C and 1.72^0C in periods 2014-2040, 2041-2070 and 2071-2090 respectively with A2 scenario; and increase about 0.39^0C, 0.81^0C and 1.29^0C in periods 2014-2040, 2041-2070 and 1971-2090 respectively for B2 scenario to compare with the period minimum temperature is 21.6^0C. In case of maximum temperature, for A2 scenario, the base period temperature is 30.110C which will increase 0.93^0C (in period 2014-2040), 2.38^0C (in period 2041-2070) and 3.69^0C (in period 2071-2090) in the future; and for B2 scenario, the maximum temperature increased 0.98^0C (in period 2014-2040), 1.79^0C (in period 2041-2070) and 2.78^0C (in period 2071-2090).

3. The annual precipitation may increase from 0.66% to 9.75% for A2 scenario and from 1.83% to 5.62% for B2 scenario. The precipitation will be decrease during rainy season and increase from mid of dry season.

4. When using Aquacrop for winter crop by rainfed calibrate. For all of future period the yield will reduce. The yield significantly decreases during period 2071-2090 with both A2 and B2 scenarios. The yield simulated by Aquacrop express a decline 5.97 to 23.05 and 1.29 to 10.96% compared to the yield of the baseline period for A2 and B2 scenarios respectively. With summer crop, for baseline period 2001-2010, the model calibrated for irrigated crop. However, the rainfall significant increase on this season in the future. Therefore, the water available will be enough for crop for some periods. Then, the yield increase about 5% and 6.67% for period 2014-2040, 2% and 2.78% for 2041-2070 with A2 and B2 scenarios respectively. The yield will reduce 1.83% and 6.26% for 2071-2090 with A2 and B2 scenarios respectively.

5. For winter crop, optimum of supplementary irrigation is at 400mm which would increase the yield about 24.13% to 42.1% with A2 scenario and about 20.13% to 32.81% with B2 scenario. The application for irrigation water in summer crop does not increase the yields significantly, the optimum amount of supplementary irrigation is about 320mm and this would increase the yield by 2.32% to 2.52% with A2 scenario and 2.28% to 2.48% with B2 scenario.

6. Changing the transplanting dates can increase the yield to higher extent under climate change scenarios. The yield obtains higher if transplanting during 10th-30th February for winter crop, and from 26th May to 18th June for summer crop.

ACKNOWLEDGE

This work was supported by Information and communication technologies (ICTs) project, The International Development Research Centre (IDRC), Ottawa, Canada.

REFERENCES

Chinvanno, S.,2010. Climate change adaptation as a development strategy: Amajor challenge for Southest Asian Countries. Southeast Asia START Regional Center, Chulalongkon University, Thailand.

Geerts, S., Raes, G., and Garcia, M., 2010. Using Aquacrop to derive deficit irrigation schedules. Agricultural Water Management.

Parry, M. L., Rosenzweig, C., Iglesias, A., Livermore, M., Fischer, G., 2004. Effects of climate change on global food production under SRES emissions and socio-economic scenarios. Global Environmental Change 14 (2004) 53–67.

Reidsma, P., Ewert, F., Lansink, A. O., Leemans, R., 2010. Adaptation to climate change and climate variability in European agriculture: The importance of farm level responses, *European Journal of Agronomy*, 32: 91-102.

Tao, F., Zhao, Z., 2010. Adaptation of maize production to climate change in North China Plain: Quantify the relative contributions of adaptation options. *European Journal of Agronomy*, 33: 103-116.

Thuc, Tran., 2010. Impacts of climate change on water resources in the Huong River basin and adaptation measures. VNU Journal of Science, Earth Sciences 26 (2010) 210-217.

Anaerobic submerged membrance bioreactor (AnMBR) for decentralized municipal wastewater treatment in Vietnam conditions

T. T. V Nga*, Vu Duc Canh*, M. Kobayashi**, and S. Wakahara**
* Institute of Environmental Science and Engineering, National University of Civil Engineering, 55 Giai Phong Road, Hanoi, Vietnam
** Water & Environmental Innovative Research Laboratory, Kubota Corporation. Hama 1-chome, Amagasaki-City, Hyogo Prefecture, Japan. 661-8567.
Corresponding author: nga.tran.vn@gmail.com

ABSTRACT

The study aims to investigate the application of anaerobic processes coupled with membrane filtration for the treatment of municipal wastewater at Vietnam tropical climate conditions. A laboratory-scale anaerobic membrane bioreactors (AnMBR) was run treating domestic wastewater in Hanoi city. The reactor is treating wastewater collected on-site at a condominium with COD level of 300-600mg/l, BOD: 180-350mg/l, NH_4-N: 40-85 mg/L. The reactor has been operated at different hydraulic retention times (48 hours, 36 hours, 24 hours and 12 hours) for a period of about 335 days (from June 2012 to May 2013) at ambient room temperatures ranging from 10-39°C. The removal of the total suspended solid, the soluble chemical oxygen demand and the biochemical oxygen demand were very good (100% for TSS, 78-95% for COD, and 80-88% for BOD). The AnMBR system achieved less than 85 mg /l of COD and less than 30 mg/L BOD in the effluent with organic loading rate from 0.28 - 2 kg COD/m^3.day. The biomass accumulated reached 10 - 12 g MLVSS/L in the last month of the operation period. Biogas production with the rate continuously increased with the increase of the loading rate in AnMBR. The average content of the biogas in methane reached 53-60% during the last month of operation period. Further, it is worthwhile noting that although the researchers observed little difference in removal efficiency for TSS, COD and BOD at the lower temperature, a significant decrease in methane gas production was observed. The results imply physical retention of organics by the MF membrane played a significant role in achieving good and stable performance at wide range of temperatures. It suggests that AnMBR could achieve the good and stable efficiency in the treatment of lower strength wastewaters at temperatures below 15°C in winter time.

Keywords: *Anaerobic membrane bioreactors, domestic wastewater, tropical climate, Ha Noi City.*

1. INTRODUCTION

Anaerobic treatments, which are commonly applied to highloaded wastewaters (sludge digestion and industrial wastewater treatment), have the following main benefits compared to aerobic treatments: minimum sludge production due to the low biomass yield of anaerobic organisms, low energy demand since no aeration is required, and biogas production that can be used to fulfil process energy requirements (Ho and Sung, 2010). Most of high-rate anaerobic processes, such as up-flow anaerobic sludge blanket (UASB), expanded granular sludge blanket (EGSB), and anaerobic filter are based on the attached growth systems. UASB and EGSB have had wide applications in the treatment of industrial and municipal wastewaters (Sutton et al., 2004).

Besides, over the last decade, the potential of the anaerobic processes as a treatment technology for low strength domestic wastewater has been evaluated. Nevertheless, domestic wastewater is quite complex due to the presence of fatty compounds, proteins, detergents, heavy metals and other toxic compounds. These characteristics impose limitations to the anaerobic process in respect to COD removal efficiency and also in terms of maximum organic and hydraulic loading rates to be applied. However, maintaining a long sludge retention time (SRT) is one of the challenges of anaerobic treatment processes due to the slow growth rate of anaerobic microorganisms. Therefore, the key to successful high-rate anaerobic technology is to decouple hydraulic retention time (HRT) and SRT in order not only to maintain high sludge concentration in the system but also to decrease reactor size.

Membrane–coupled anaerobic bioreactors have been applied as one alternative to the conventional anaerobic digestion process. A typical AnMBR system include: a anaeronic reactor which play a role as a digestor and memberbane modules which can either submerge or place outside of the reactor. It can retain all of the biomass in the reactor more effectively without any fear of sludge washout irrespective of short HRT. In addition, AnMBR could produce superior effluent quality in terms of suspended solids, chemical oxygen demand (COD) and pathogen count, and there is a possibility of reuse and recycling of the treated effluent for non-potable purposes. Previous studies elucidated the potential of AnMBR for the treatment of low strength wastewater at ambient temperature (Ho et al., 2007).

The objective of this project is to study the performance of an AMBR for the treatment of low strength wastewater like municipal wastewater in Hanoi. The focus was to transform the municipal wastewater into different valuable streams such as biogas (energy). The second purpose of this work is to investigate the optimum operation parameters while minimize backwashing or chemical cleaning of the membrane modules.

2. METHODOLOGY

2.1. Laboratory experiment set up

A laboratory-scale anaerobic membrane bioreactors AnMBR with 5L of working volume were run ambient temperature. The anaerobic reactors were equipped with biogas collection system and a blower for keeping the sludge in the suspension and membrane scouring effect using gas generated from the system. Other equipments are the transmembrane pressure sensor and a data logger, and level sensors to control permeate flow rate. The AnMBRs were coupled to a flat sheet, polyvinylidene fluoride (PVDF) with nominal pore size of 0.4µm and total filtration surface area of 0.09 m^2 (supplied by KUBOTA Cooperation, Japan).

Feed water for the reactor was taken from the equalization tank placed at the basements of Sky Tower condiminium (Address: 88 Lang Ha street). The raw wastewater have evarage COD content of 250-570 mg/L; BOD 90-290 mg/L, T-N: 25-170 mg/L, NH4-N: 22-152 mg/L. Seeding sludge (1.5 g/L) was obtained from the mesophilic anaerobic digester in Yen So municipal wastewater treatment plant. The AnMBR system hase been operated for more than 350 days at different hydraulic retention times. The average hydraulic retention times for the entire system were 48 hours, 36 hours, 25 hours and 12 hours. The membrane flux was maintained at 0.03, 0.08, 0.12, and 0.24 m^3/m^2.day, respectively. The organic loading rate was therefore 0.31, 0.54, 0.95, and 1.68 kgCOD/m^3.day accordingly.

There was no sludge withdrawal except for the analysis and SMA test with frequency of one time per week. No chemical cleaning was attempted during the entire experiment.

2.2. Sampling and Analysis

DO, pH, temperature of feed, feed and permeat (effluent) flowrate in aerobic tank were measured daily by portable meters. Wastewaters and mixed liquor were also sampled on times per week and analyzed for chemical oxygen demand (COD), Biological Oxygen Demand (BOD) total nitrogen (T-N), ammonia nitrogen (NH_4-N), dissolved oxygen (DO), Mixed Liquor Suspended Solid (MLSS) and Mixed Liquor Volatile Suspended Solid (MLVSS), Volatile fatty acids (VFA). The concentrations of COD, T-N, NH_4-N, MLSS and MLVSS were analysed following Standrd Method (APHA 2003) and HACH methods with the appropriate kits and a DR 2800 Spectrophotometer (HACH Company, USA). A wet-test gas meter was used to measure biogas. Gas composition and methane gas was analyzed using Test kit GAC25 (Japan). In addition, methanogenic activities were measured in duplicate for suspended and attached using 250 ml serum bottles containing acetic acids as a sole substrate.

3. RESULTS AND DISCUSSION

3.1. AnMBR performance at ambient temperature

The reactor has been operated at different hydraulic retention times (48 hours, 36 hours, 24 hours and 12 hours) for a period of about 335 days (from June 2012 to May 2013) at ambient room temperatures ranging from 10-39°C. Seeding sludge was obtained from the anaerobic digester in Yen So municipal wastewater treatment plant. Since it have been in operation for a couple of month, the MLSS concentration of the sludge is still low, ranging from 1200-1500 mg/L. The resuls show that the sludge concentration have been increased steadily when increasing of feed flow rate over experimental period and reached 10,000-12,000 mg/L at the end of the Phase 4 with the HRT is of 12 hours accordingly. It also indicates no sludge washout in the system.

Although pH in the AnMBR system was not controlled, the pH levels in the reactor did not affect anaerobic degradation of organics. VFAs profiles indicates that acetic acid was the predominant VFA in the reactor. Propionic and butyric acid were not detected.

3.2 Efficiency of the AnMBR in removing wastewater pollutants

Biological removal rate was calculated by the difference between influent COD and mixed liquor COD divided by the influent COD, while physical removal rate was the difference between the total COD removal rate and the biological removal rate. The concentration of COD in feed and permeat, removal efficiency are shown in **Figure 1**. COD in the feed water varied from less than 200 mg/L to about 570 mg/L. With this range of COD values, the feed water could still bbe classified as low strength wastewater. The removal rate for COD was stable and high after day 120 with COD in permeat is less thang 100 mg/L. Thenafter, throughout the operation at different hydraulic retention times, the COD removal rates remained stable.. BOD concentration in the permeat water is also stable and less than 30 mg/L, indicating AnMBR system effective in the treatment of organic matter. The good removal efficiency for COD (78-95%) and BOD (80-88%) could be achieved which meet the domiestic discharge standards into the environment (QCVN 14:2008 /MONRE, source type B).

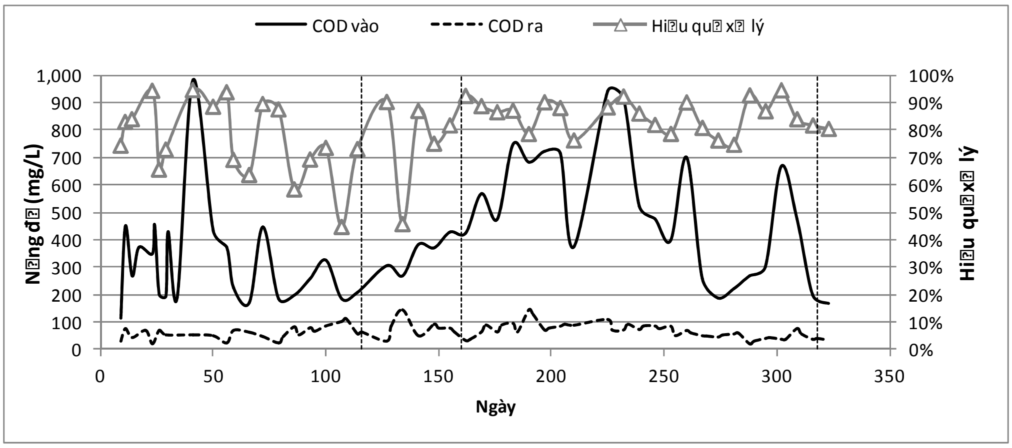

Figure 1. COD profiles in feed and permeat and removal efficiency in AnMBR system

The change in the ammonium concentratio in feed and permeat during operation is shown in **Figure 2**. Raw wastewater in the apartment building have high ammonium concentrations, ranging from about 20 -152 mg/ L. Ammonium concentration in permeat lso showed similar bands in anaerobic conditions, the ammonium is the main nitrogen component and sustainable existence. It also shows AnMBR system is ineffective in treating nitrogen counponds in wastewater to achieve the curent discharge requirements, highlighing the the need of further processes to reduce its residual nitrogen levels to meet stringent Vietnamese wastewater discharge standards

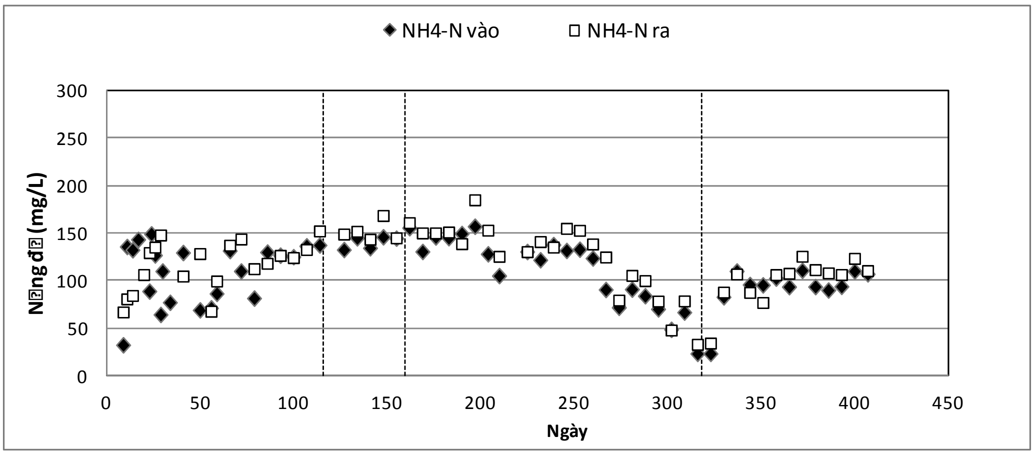

Figure 2. NH_4- profiles in feed and permeat; and removal efficiency in AnMBR system

3.2. Biogas volume

Biogas volume is collected and measured daily. Experimental results showed the amount of gas significantly increased when hydraullic residence time in the system AnMBR reduced from 36 to 25 hours, hence the average organic load increased from 0:53 to about 1.6 kg COD/m^3.day accordingly (**Figure 3**). The methane ratio have been incereading and reached 60 -70% of the total amount of biogas from day 180th , i.e when the system switches to 25 hour retention time. Experimental results also show that average methane yield achieved 0.24 L

CH_4/gCOD. This value is only about 60% compared with values calculated theoretically at 20oC (0.34 LCH_4/gCOD decomposed), showing a majority of methane is lost. The gas leakage control activities have been tightly controlled in the system so the only reason could be possibly the gas dissolved in the water and have been wash out of the reactor with permeat through the membrane. This observation also coincides with findings from the previous studies (Ho and Sung, 2010). The loss of methane, especially when large-scale implementation, not only to loss of biogas resources, but also bring negatively impact the greeenhouse gases emissions. This issue should be further investigated to control leakage of dissovled biogas in the system.

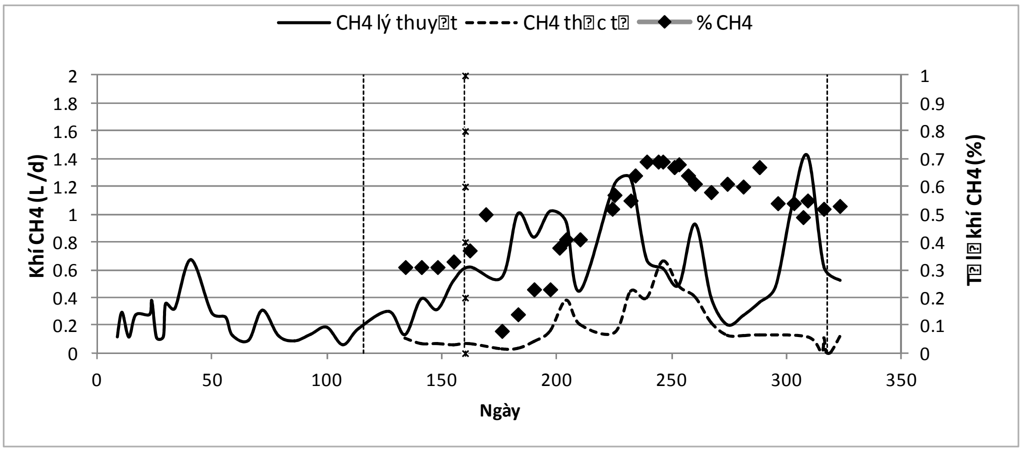

Figure 3. Lượng khí sinh học tích lũy trong suốt thời gian vận hành mô hình, và tỷ lệ khí mê tan trong khí sinh học

It was observed that the methanogenic activity of suspended sludge increased with time in this study. This implies that the active microorganisms are likely to be suspended growth rather than attached growth in AnMBR system. The other reason could be the propensity of microorganisms to be suspended or attached. Methanogenic bacteria had a higher tendency to grow in anaerobic fluidized bed reactor than in a chemostat reactor (Araki and Harada, 1994). The environmental conditions on the cake layer may not be favorable for attached growth due to the shear force by cross flow.

CONCLUSION

A laboratory-scale anaerobic membrane bioreactor system (AnMBR) was run over the couse of one year to investifage the efficiency in treating domestic wastewater in Hanoi. Results showed that at different hydraulic retention time and organic loading, high and stable removal efficiency of organic matter COD (80-90%) and suspended solid TSS (95-98%) were achieved. Nitrogen content (TN, NH_4-N) in the treated water was almost familiar with untreated sewage, suggesting anaerobic processed coupled with membrane filtration does not remove nitrogen. In order to meet the stringent discharge consent

(QCVN14:2008/MONRE or QCVN40:2011/BTNMT), the permeat from AnMBR system needs to be undergone a further treatment for nitrogen removal. The results show that AnMBR technology is suitable for treating domestic wastewater in Vietnam condition. Treated wastewaters were of good quality and fit with WHO guidelines for agricultural reuse. In addition, AnMBR bring small footprint advantadge which is very applicable in small urban areas and having difficulties in sludge treatment.

This study was conducted under the research project financed by Vietnam Minitry of Education and Trainning (B2012-03-03)

REFERENCES

1. Araki, N., Harada, H., 1994. Population dynamics of methanogenic biofilm consortium during a start-up period of anaerobic fluidized bed reactor. Water Sci. Technol. **29**, 361–368.

2. Baek, S.H., Pagilla, K.R., 2006. Aerobic and anaerobic membrane bioreactors for municipal wastewater treatment. Water Environ. Res. **78**, 133–140.

3. Ho J. Khanal, S.K. Sung, S., 2007. Anaerobic membrane bioreactor for treatment of synthetic municipal wastewater at ambient temperature. Water Sci. Technol. **55**, 79–86.

4. Jaeho Ho and Shihwu S. Methanogenic activities in anaerobic membrane bioreactors (AnMBR) treating synthetic municipal wastewater. Bioresource Technology **101** (2010) 2191-2196

5. Munariatis I. D. and Grigoropoulos S. G. - Low-strength wastewater treatment using an anaerobic baffled reactor” Water Environment Research, **74** (2002) 170-177.

6. Sutton P.M., Bérubé P., and Hall E.R. - Membrane Bioreactors for Anaerobic Treatment of Wastewaters. Final report- WERF Project 02-CTS-4 (2004). Water Environment Research Foundation.

HAN-sense: A solution for traffic air pollution monitoring in hanoi city using wireless sensor networks

Phong Thanh BUI, Thieu Nga PHAM, Quang Duc LE, Nguyet Thi THAI, Thuy Duong LE, Dang Hai HOANG[1], Thorsten STRUFE[2]
Hanoi University of Civil Engineering, Information Technology Faculty, Vietnam
[1] Ministry of Information and Communications, Vietnam
[2] TU Darmstadt, Germany

ABSTRACT

The rapid growing of air pollution is one of the most challenging problems for a large capital city like Hanoi today. Among various pollution sources, the exhaust gas from traffic system is the main cause of pollution. In order to help the city authorities monitor air pollution, as well as to have early accurate warning about urban environment hazard, a solution for urban-scale environment monitoring is necessary. This paper presents our developed system, called HAN-Sense system, which collects and visualizes traffic pollution data in Hanoi city. First, we introduce the design of HAN-Sense based on a sensor network using ZigBee wireless communication to collect the pollution data and briefly present our proposed method for data transfer to a monitoring center. Second, we describe how our monitoring center processes and visualizes measurement data to make it available online on a map-based web application. Finally, we present some result for pollution monitoring in an urban district of Hanoi city.

Keywords: *Wireless sensor networks, pollution data monitoring, data collection and forwarding, sensor calibration, data clustering and visualization.*

1. INTRODUCTION

In urban areas, traffic is the largest source of pollution. According to statistics of the Ministry of Transport of Vietnam in 2010, air pollution in urban areas due to traffic activities is about 70%. Hanoi, the capital of Vietnam, is the second largest city and most crowded city with high population of approximate 8 millions. High traffic density is due to the growing urbanization and the continuous increment of private vehicles, including mostly motorcycles. The air pollution generated by traffic is becoming one of the most challenging problems that directly affect life quality of citizens. The impact of air pollution is serious for peoples who daily get into traffic jam on their motorbike without any protection. Urban-scale environment monitoring is necessary to provide measured pollution data for further analysis to distinguish different pollution factors, for giving warnings and corresponding countermeasures such as city planning, green plants, vehicle emission control, etc.

Pollution measurements are usually carried out using a number of static high-precision sensors. While this cannot cover large areas, simulations are used to calculate pollution maps. This is both time consuming and expensive, and systematically unable to provide real-time results with sufficient resolution in both space and time. However, achieving real-time data is actually needed to allow any useful warning system. Wireless sensor networks (WSN) technologies have been widely adopted for environment monitoring (Khedol, 2010). Potential applications were proposed to monitor urban environment with a set of parameters such as noise, traffic density, temperature, air quality and exhaust gas concentration etc. These applications enable governments to build up such smart cities that allow detecting and controlling environment hazard (Wener, 2006). Although emergent communication technologies have been proposed, they have not been adequately applied in this area. There are several issues that should be further investigate for effective implementations including choice of network topology for the monitoring area with limited number of sensors, impact of wireless channels, etc. On the other hand, processing and visualizing dataset collected from WSNs is a further important part of the whole pollution monitoring system. For data processing and data visualization, several issues should be addressed including sensor calibration for accurate measurements, evaluation of typical datasets for each monitoring location, processing method, quality of visualization on a map.

This paper presents a solution for urban-scale pollution monitoring system called HAN-Sense to collect and visualize traffic-generated pollution in Hanoi city. HAN-Sense is based on a Wireless Sensor Network (WSN) using ZigBee technology and a method for data transfer from sensors to a monitoring center. Moreover, HAN-Sense enables data pre-processing, sensor calibration, data clustering and representation for online visualization on a map. Since Hanoi is a very large city, we select an urban district with high traffic density for our pilot project. The paper is organized as follows. Section 2 presents motivation and related works. Section 3 outlines the design of HAN-Sense and the method of data forwarding. Section 4 presents the issue of sensor data conversion and sensor calibration. Section 5 focuses on data processing and visualization. Section 6 presents our pilot project and finally, Section 7 concludes the paper.

2. MOTIVATION AND RELATED WORKS

A WSN consists of a large number of sensor nodes, which are densely deployed in the environment. A WSN node contains one or more sensors for collecting different environment parameters and several modules for processing and wireless communications. WSN using IEEE 802.15.4 (ZigBee) standards have gained prominence in recent years for environmental monitoring applications such as traffic-generated pollution monitoring. However, how to collect pollution data in a wide area only with a limited number of WSN nodes is remaining a practical question due to the characteristics of mobile wireless environment and specific pollution monitoring requirements. A practical solution for pollution monitoring in a big city requires several issues to be solved.

A number of research projects tried to investigate various aspects of WSN applications for pollution monitoring (e.g. Da-Sense, Rescatame, PermaSemse, OpenSense). Da-Sense proposed NoiseMap using a real-time noise sensing application and a Web-based map for displaying noise density over Darmstadt city. Rescatame is a smart city project developed in Salamanca, Spain for pollution monitoring and sustainable management of traffic. The PermaSense project aims to gather environmental data on high-mountain permafrost in the Swiss Alps. The OpenSense Zurich project is an emergent project for monitoring air pollution aiming to increase public awareness of urban air pollution and to involve general public into environmental monitoring. In general, these projects use sensors mounted on trams and public buses to record air pollution and transmit data to a server, either via a base station or 3G/GPRS. Several challenging issues have been addressed including on-the-fly-calibration of sensors, calibration accuracy, measurement accuracy, detection and filtering of systematic and transient sensor errors, area coverage problem, routing selection. The most drawbacks of low-cost sensors are their limited accuracy and resolution. Thus, the sensors require frequently recalibration in order to provide precise pollution recordings and to increase sensing accuracy.

3. DESIGN OF HAN-SENSE SYSTEM

Our HAN-Sense system for air traffic pollution monitoring consists of one server, one base-station and a number of sensors. The sensors collect data from environment and transmit them to the base station. Data from the base-station will be transferred to, processed and visualized in the server. A problem is how to collect data on the main roads in a large area with a limited number of sensors.

We solved the above problem by means of moving sensors on closed trajectories. These trajectories are thoroughfares with concentrated traffic. Sensors can transmit data only in a short distance (less than 100m) and the server needs to receive data for processing after a certain period of time (e.g. 1 hour). Due to these constraints, remote sensors cannot transmit data directly to the base-station. Data should be transferred through intermediate sensors, which act as dynamic bridges to forward data towards the base station gradually.

With this in mind, we designed our sensor network as follows. We divide the monitoring area by N trajectories. We require that at least one trajectory should be in the coverage of the base station. Moreover, any two trajectories should have at least one overlapping road distance, so that WSN nodes are enable to transmit data to each other. For collecting traffic pollution data, we use WSN nodes equipped with various sensors. WSN nodes will move on these predefined trajectories. Each WSN node will be assigned a level and a weight. The level of each sensor is determined as follows. If a sensor moves on trajectories in the base-station's coverage, its level is equal 1. If a sensor is in the coverage of another sensor, its level is equal to the level of the sensor it meets plus 1. If a sensor meets many sensors, its level is equal the smallest level of sensors it meets plus 1. Sensors will frequently update their levels trending towards level improvement (lower level, level decreases as the sensor closes to the center, level=1 is the closest to the center). Weight of each sensor is determined as follows. Initial value of weight is K, where K is a sufficiently large number. If a sensor successfully sent data to another sensor or the base-station, its weight increases by K. If a sensor successfully receives data from another sensor, its weight decreases by 1. If the weight becomes negative (<0), the level of this sensor needs to be reset to the level from beginning. This is the flexibility of the proposed method, helps to change the level of a sensor, when it does not perform his duty as a bridge for receiving and forwarding data, since negative weight means this sensor was not able to forward data, but only received data after a long time (depending on K). The levels of sensors will be updated as follows.

$$L_i = \begin{cases} 1 & \text{if } i \text{ sees the base station} \\ L_{\min} + 1 & \text{if } L_i = -1 \;\&\; L_{\min} \ge 0 \quad or \quad L_i \ge L_{\min} \\ -1 & \text{if } W_i < 0 \end{cases} \tag{1}$$

Where L_i is the current level of node i, W_i is the current weight of node i, L_{min} is the minimum level of n neighbor nodes, $L_{\min} = \min_{j \in n} \{L_j\}$.

Level and weight are the important parameters for data forwarding, since data is only forwarded from a WSN node with higher level to the one with lower level. If a WSN node sees many WSN nodes having the same level, it will send data to the node with higher weight. Our proposed method is called Adaptive Forwarding Protocol.

4. DATA PRE-PROCESSING

4.1 Converting the read data

Sensor is a device for sensing various information and converts them into electrical signals. There are many different types of sensors such as temperature sensors, gas sensors, optical sensors, infrared sensors, etc. For traffic air pollution, following typical sensors can be chosen: Carbon Monoxide (CO), Carbon Dioxide (CO_2), Methane (CH_4), Isobutane (C_4H_{10}), Nitrogen Dioxide (NO_2), Ozone (O_3), Volatile Organic Compounds (VOC's). Figure 1a shows a CO sensor mounted on a WSN device (Libelium). Multiple sensors may be integrated into a WSN node that enables to set up parameters for each type of sensors. Measured values are output voltages of sensors, whereas parameters for displaying gas concentration are *ppm* (parts per millions). Thus, we must convert sensor output voltages to *ppm*. We use the following equal for conversion (Libelium):

$$R_S = \frac{V_C . R_L}{V_{out}} - R_L \quad \text{or} \quad \frac{R_S}{R_L} = \frac{V_c}{V_{out}} - 1 \tag{2}$$

Where R_s is the sensor's output resistance, V_c is its power, V_{out} is the output voltage measurement and R_L the load resistance. From measured V_{out}, we calculate R_s (or R_s/R_L). Based on conversion graph provided by the manufacturer, we get the conversion formula. For linear graph of V_{out} and gas concentration, we use the following formula:

$$\log(y) = m\log(x) + b \quad \text{or} \quad y = x^m 10^b \tag{3}$$

Where $y = R_s/R_L$, x = gas concentration (*ppm*), *m* and *b* are coefficients that will be calculated based on two points on the graph.

However, the graph is not always linear, e.g. for O_3 gas concentration (Figure 1b). For nonlinear graph, a small change of V_{out} will result in a major change of the gas concentration.

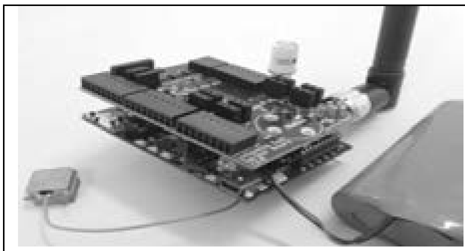

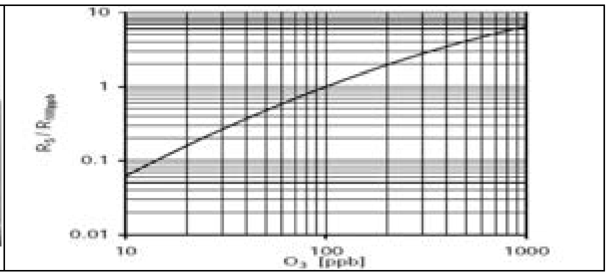

Figure 1a: A WSN node with sensors. Figure 1b: Graph of sensitivity O_3 sensor

The conversion performs by two steps: Graph digitizer and Regression. At the first step, a graph (in form of BMP, GIF, JPEG, PNG or XPM) is converted into digital data. We use Windig tool (Windig) for this conversion. At the second step, we use a Curve Fitting tool (MatLab) to get regression relationship of digitalized graph data. Possible regression models are linear regression, polynominal regression and other nonlinear regressions. To evaluate the appropriateness of the regression model, we rely on the assessment of parameters R^2 and SSE in fitting functions. The best-fit approximation of the points in the dataset has been extracted from the graph is the one with SSE close to 0 and R^2 close to 1.

With dataset received after Graph digitizer, we use Curve Fitting tool for linear regression with the function $x=0.00664y+ 0.2213$ as illustrated in Figure 2a. We get SSE=0.9012 and R^2= 0.985. If we use quardratic regression (Figure 2b), we get SSE = 0.03232, and R^2= 0.9995. The quadratic curve is better fit than the linear regression. The conversion formula is: $x = -0.000003316y^2 + 0.009712y - 0.01193$. The third-degree regression will approximate better (R^2=1), but with more complexity. Thus, we used quadratic regression.

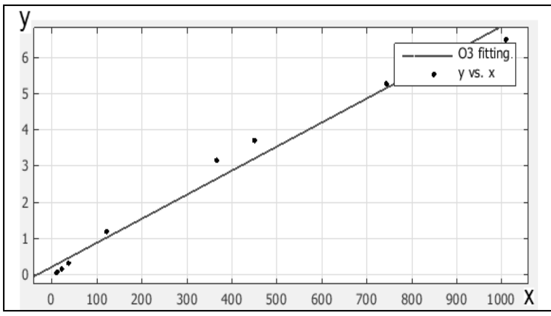

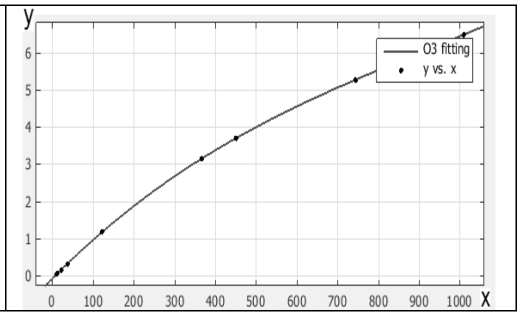

Figure 2a: Linear regression. Figure 2b: Quadratic regression

4.2 Sensor Calibration

We use low-cost sensors for our implementation, which have small size and are suitable to install on public transport vehicle. However, the main drawbacks of low-cost sensors are their limited accuracy, low stability and poor selectivity. There is a deviation of measured values of the same sensor types at the same location, thus, collected dataset may be unreliable. We should calibrate sensors to provide approximate values for the same measurement at the same location. Calibration process is carried out by modifying values of appropriate parameters for each sensor. Certain parameters can be used for calibration, e.g. the Load Resistance (LR) parameter for Carbon Monoxide sensors TGS2442 provided by Figaro company (Figaro, 2007).

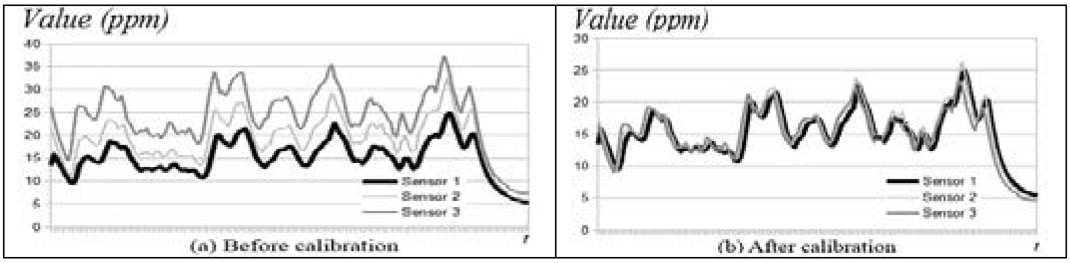

Figure 3: Calibration for three sensors using load resistance (LR)

Figure 3 illustrates the calibration for three sensors using LR parameters. We collect data in term of voltage and use the same LR parameters for three sensors to calculate the gas concentration values (*ppm* value). As depicted in Figure 3b, data values of sensor 2 and sensor 3 are adjusted by modifying the LR parameter to the values of sensor 1, approximately. In general, we do measurements with all deployed sensors in the same time interval and the same environment condition in order to calculate the average measured value. We determine the LR parameter for each sensor so that the deviation of measured value and the calculated average is less than a given threshold. Using this calibration method, the deviation can be evaluated by the mean absolute error.

5. DATA PROCESSING AND VISUALIZATION

5.1 Data Clustering

Raw measured data may be incomplete, incorrect or unreliable due to several reasons such as GPS position information missing, error-prone data transmission. For further analysis, measured data should be processed. As mentioned in Section 2, data objects may be complex for a location. For online visualization on map, there is a need to evaluate typical measurement value for each location in a certain period of time. Thus, we propose a clustering method for grouping similar data objects into the same group of data. Each data point in measured dataset consists of spatial attributes (latitude, longitude), timestamp, and gas concentration value. The clustering method, therefore, should consider both the density of data objects as well as the spatial limitation of each group.

According to (Kaufman, 1990) two basic clustering algorithms can be used, namely partitioning and hierarchical. Hierarchical algorithm creates a hierarchical tree, called *dendrogram*, in which each node is a subset of dataset (a cluster) and every leaf only has one instance. Partitioning algorithm creates a partition with *k* clusters from *n-instance* dataset. The most popular partitioning algorithm is K-means (Miller, 2009), which seams to be a better choice for large dataset in comparison with hierarchical algorithms. Thus, we decided to use K-Means for our data clustering. However, it is difficult to determine *k*, particularly for very large spatial dataset. Inappropriate choice may result in a poor partition. Moreover, if we set a limit for cluster's radius, then finding an appropriate *k* is more difficult. To this end, we propose an algorithm called Limited-Distance-K-means based on K-means, in order to determine parameter *k* and initial clusters that have radius less than a given distance value with an acceptable computational complexity. This Limited-Distance-K-means algorithm includes two stages. First, we create set *S* of *k* initial clusters. Second, we make adjustment to set *S* to remove unnecessary cluster with a modified K-means algorithm. After the first stage of algorithm, number of cluster can be large because of arbitrarily choosing instance from dataset. Subsequent instance tends to be selected into new cluster. Therefore, we can make clustering more effectively by modifying K-means algorithm to remove a cluster if all of its instance can be assigned to the other clusters.

5.2 Data Visualization

For online visualization, we organize measured data into sets of data points, where each point represents a pollution level in a certain location with latitude, longitude and measurement time. Each data point will be a colored cell on a map. The cells may be dense on traffic roads or sparse on the other areas depending on the dataset. In order to represent pollution independently of density of data points, hexagonal grid is used to divide the entire monitoring area into hexagonal cells. Cells in a hexagonal grid are aligned along three axes rather than just two in a rectangular grid. Thus, the outlines of groups of cells in a hexagonal grid can form more varied, less rectilinear shapes than groups of cells in a rectangular grid (Birch, 2007). Moreover, hexagon shape is closer in shape to circle than square. This characteristic is useful when determining how to get value point for applying interpolation. Instead of to determine which data points inside hexagonal cell, we just need to find data points inside the circumcircle of hexagonal cell.

For determining value of each cell, we apply Inverse Distance Weighted interpolation method (Donald, 1968). The inverse distance weighted procedure is versatile, and is fairly accurate under a wide range of conditions for visualizing pollution data. Value of target point is can be interpolated by observations in the following equation:

$$p(x_0) = \frac{\sum_{i=1}^{n} \frac{1}{d_i^{\alpha}} p(x_i)}{\sum_{i=1}^{n} \frac{1}{d_i^{\alpha}}} \tag{4}$$

Where $p(x_0)$ is the interpolation value, d_i is the distance from known point x_i to the unknown point x_0, α is power parameter, n is the total number of known points used in interpolation. The choice of power parameter α is arbitrary, but the most popular choice is 2. With each hexagon cell, we assume the value of cell is value of center point of cell. If we connect center point of each cell to center points of all neighbor cells, we can construct a triangular grid from hexagon grid (Figure 4). Hence, calculating values of hexagon cells turns into interpolating grid points on triangular grid. In order to interpolate value for grid point x_0, we need to determine set of data points surrounding x_0 involved in the interpolation. Denote r is the max distance from a data point x_i to x_0, we determine $r = d \times l$, where l is the spread level. For online visualization of measured data on map, we developed a website using Google Map service. Figure 5 shows pollution levels on a map region with different values of d and spread level l.

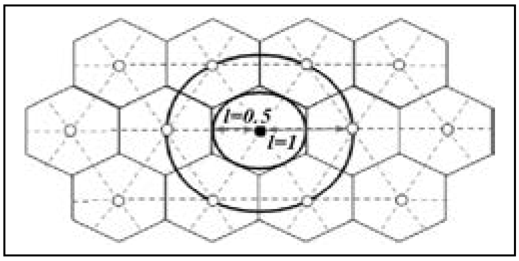

Figure 4: Determination of radius r by parameter l

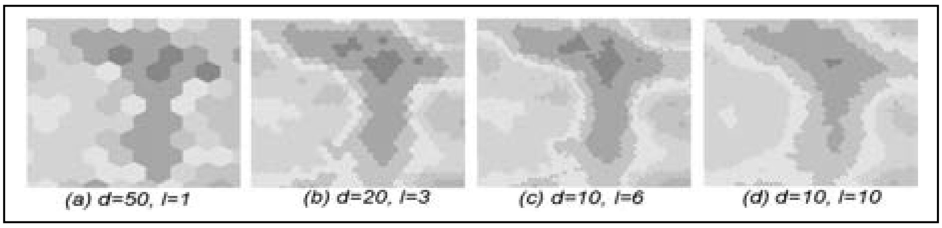

Figure 5: Visual effects by changing d and l

6. THE PILOT PROJECT

This Section presents the implementation results of HAN-Sense system for air traffic pollution monitoring in an urban district of Hanoi city. Hai Ba Trung is one of the two districts of Hanoi city that have highest traffic density. There are more than seventy-five thousands of resident families in which each own has at least two motorbikes. Besides, many personal vehicles come from other regions since Hai Ba Trung district has a complex of a garment industry park, two river ports and three largest universities including Hanoi University of Science and Technology, University of Civil Engineering and National University of Economics. Recently, high traffic density in this district is said to cause severe air pollution that makes a serious impact on local resident. At intersections that frequently have traffic congestion, exhaust emissions are usually very high. Therefore, we choose streets with large traffic density to set up a pilot project.

The HAN-Sense system was tested using a ZigBee mesh network consisting of a Meshlium base station and 8 Waspmotes (Libelium). These Waspmotes act as WSN nodes, moving on 8 trajectories in order to cover Hai Ba Trung district with an area of about 14.6 km2 (Figure 6a). The trajectories have been designed so that each mote can meet at least one other mote in an enough time to be able to send the data and two of the trajectories have some parts, on which Waspmotes can meet the Meshlium. Each mote runs on a trajectory and is numbered according to the trajectory number. We choose to measure CO gas concentration, since CO is a typical exhaust gas generated from traffic. CO is also classified as toxic gas that can seriously damage people health. During measurement time, each sensor is attached on a volunteer motorcycle running at the speed of 10 km per hour. Measurement value is captured from CO sensor for every 30 seconds, and then stored on local storage. The Carbon Monoxide TGS 2442 sensor is mounted on Waspmote, which is a compact, versatile and high mobility device, developed by Libelium. Parameters of each sensor are chosen to ensure the mean absolute error from the standard sensor must not exceed 1.5 *ppm* threshold.

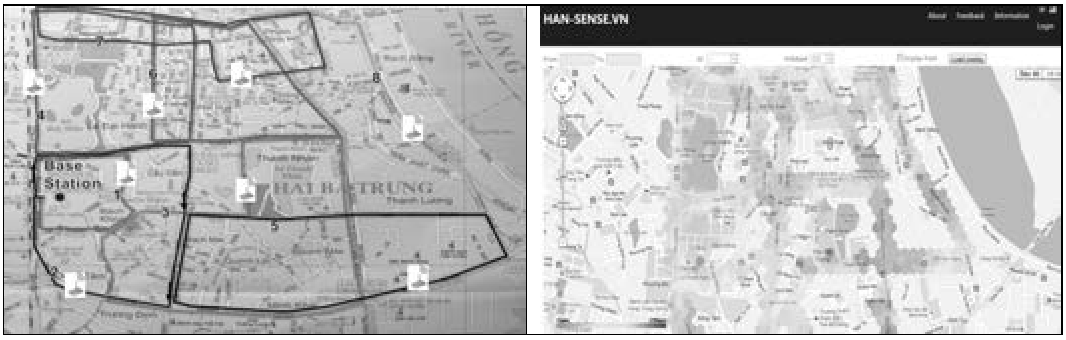

Figure 6a: Implementation with 8 trajectories. Figure 6b: Pollution data on map

Every hour, our server receives thousands of measurement records of data. We applied a Limited-Distance-K-means algorithm for clustering data and we could find out typical values for each location every hour using this algorithm. The locations are separated from each other by a distance of radius about 50m. Graph in Figure 7a shows the difference of CO concentration levels at different times, particularly in comparison with peak hour. Graph in Figure 7b indicates the difference of concentration measured at different positions along a street. Levels of CO gas at intersections, which are represented by point 1, 2, 3 in Figure 7b, are significantly higher than those at other position.

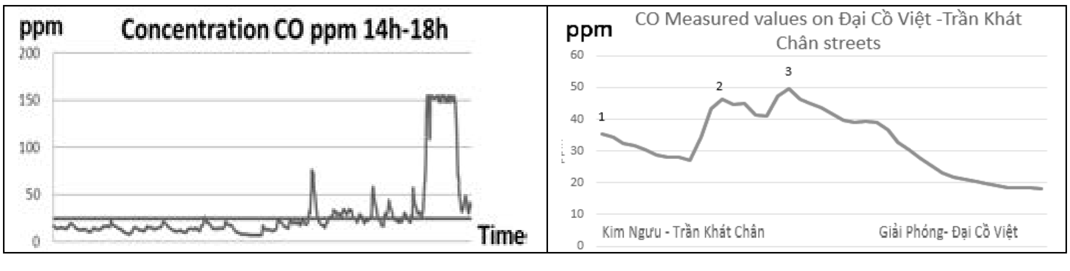

Figure 7: CO Concentration at different times (a) and different positions (b)

Measurement data collected from all 23 streets on 8 routes have been processed and visualized on an online map available at http://han-sense.vn (Figure 6b). The level of pollution, explicitly based on CO concentration, is represented by a range of colors on map in which each color matches with a certain value of concentration. User will be able to choose options that display measurement data by a certain time period, as well as by type of gas. Currently, we only measure CO concentration but we plan to measure more exhaust gases in the future. Providing measurement data on a public website does help user have more useful information about air traffic pollution.

7. CONCLUSION

The paper presented our HAN-Sense system for air traffic pollution monitoring. We described the design of HAN-Sense based on a WSN using ZigBee technology to collect pollution data and an adaptive data forwarding method to transmit data to the server. We addressed several issues such as data conversion from voltages to *ppm*, sensor calibration, data processing and online visualization of pollution data on a map. We implemented and tested our proposed system using a ZigBee network with one Meshlium base-station and eight WSN nodes to monitor an urban district of Hanoi City.

We would like to thank the Alexander von Humboldt Foundation (Germany) for the supports to this research work.

REFERENCES

Birch, C.P., Sander, P.O., Beecham, J.A., 2007. *Rectangular and hexagonal grids used for observation, experiment and simulation in ecology*. Ecological modelling 206 (2007), p.347–359.

Da-Sense, 2011. *Monitoring system for Smart cities*. Project of TU Darmstadt, Germany. http://www.da-sense.de.

Donald, S., 1968. *A two-dimensional interpolation function for irregularly-spaced data*. Proceedings of ACM National Conference. p. 517–524.

Figaro, 2007. Technical Information for Carbon Monoxide Sensors. Figaro Company. http://www.figarosensor.com/details.html.

Francesco, M., Das, S., 2011. Data Collection in Wireless Sensor Networks with Mobile Elements: A Survey. Journal ACM Trans. on Sensor Networks, Vol.8, Iss. 1, Aug.2011, NY, USA.

Kaufman, L., Rousseeuw, P.J., 1990. *Finding Groups in Data-An Introduction to Cluster Analysis*. John Willey & Sons, p.37-38.

Khedol, K. K., Perseedoss, R., Mungur, A., 2010. *Wireless sensor Network Air pollution Monitoring system*. International journal of wireless and mobile networks, Vol.2, No.2.

Libelium, *Waspmote datasheet version v.4.2*, Libelium Technical Doc., 4/2013.

Matlab, http://www.mathworks.com/products/curvefitting/.

Miller, H.J., Han, J. (Editor), 2009. *Geographic Data Mining and Knowledge Discovery*, 2nd Edition, Chapman & Hall/CRC Data Mining and Knowledge Discovery Series), p.156-157, 170-173.

OpenSense. *Open sensor networks for air quality monitoring*. Project of ETH Zurich and EPF Lausanne. http://data.opensense.ethz.ch

PermaSense, 2009. *PermaDAQ: A scientific instrument for precision sensing and data recovery in environmental extremes*. Internl. Conference on Sensor Networks

(IPSN), IEEE Computer Society, pp.265-276.
Rescatame, 2012. *Pervasive Air-Quality Sensors Network for an Environmental Sustainable Urban Traffic Management*. project report.
Shah,K., Francesco,M., Anastasi,G., Kumar,M.,2011. A Framework for Resource-Aware Data Accumulation in Sparse WSNs. Computer Communications, Vol.34, Issue 17, Nov. 2011, pp. 2094–2103.
Wener, A.G., Lorincz, K., Ruiz, M., Marcillo, O., Johnson, J., Lees, J., Walsh, M., 2006. *Deploying a wireless sensor network on an active volcano, Data-Driven Applications in Sensor Networks*. IEEE Internet Computing (Special Issue), March/April 2006.
Windig, http://www.unige.ch/sciences/chifi/cpb/windig.html.

Towards sustainable transportation through introduction of eco-drive management system for vehicle fuel efficiency

Dinh Van HIEP [1], Manabu OHNO [2], Yosui SEKI [3]

[1,] *PhD. Director, Institute of Planning and Transportation Engineering, National University of Civil Engineering, Room 208, Laboratory Building, No. 55, Giaiphong str., Hanoi, Vietnam*

hiepdv@ipte.com.vn

[2,3] *ALMEC Corporation, 1-19-14 Aobadai,*

ABSTRACT:

Sustainable transport development is a key factor for supporting economic development and growth, and facilitating the exchange of goods. However, rapidly increasing emissions of carbon dioxide from the transport sector, particularly in urban areas, is a major challenge to sustainable development in developing countries. In order to reduce CO_2 emission of automobiles, promotion of ecodriving is considered being effective. Ecodriving is a well-established, affordable and simple behavioral change intervention, which could reduce fuel consumption between 5 to 25% according to different situations. In this paper, Eco-drive Management System (EMS) was first introduced through a case study in Vietnam. The findings may help to realize the effectiveness of eco-drive toward sustainable transportation in Vietnam as well as to promote the countermeasures for the global warming issue. In addition, some major issues have been discussed for further studies of ecodriving and for introduction of fuel efficient vehicles.

Keywords: *GHG emissions, Sustainable transportation, Fuel efficiency, Fuel consumption, Eco-drive management system, Vietnam.*

1. INTRODUCTION

Sustainable transport development is a key factor for supporting economic development and growth, and facilitating the exchange of goods. At the same time, transport industry and vehicle are major emitters of gaseous and particulate pollution in urban areas which have serious health effects, including respiratory and cardiovascular diseases. The transport sector remains one of the main sources of CO_2 emissions from 10 – 25% in most countries (EEA, 2008; Timilsina and Shrestha, 2009). Ecodriving is a well-established, affordable and simple behavioural change intervention, which could reduce fuel consumption between 10 to 20% (Barth and Boriboonsomsin, 2009). Ecodriving attempts to change drivers' behaviour through advice such as driving more smoothly by anticipating changes in the traffic, shifting gear sooner, operating the vehicle within an optimum range of engine revolutions or with operating speed range, avoiding jerky braking/acceleration and avoiding traffic congestion. Many countries have promoted ecodriving in "Green Transport" as a key element of national strategies to reduce CO_2 emissions (ECODRIVEN, 2009; JAPE, 2012) towards sustainable development.

Ecodriving strategies can be classified more specifically. Driver training and advice can be called static ecodriving with limited feedback. Next, ecodriving based on instantaneous vehicle performance display fuel economy in real-time, with a growing number of such devices used in vehicles today. Finally, dynamic ecodriving adds to instantaneous performance with real-time advice or feedback, such as speed management suggestions based on roadway geometries or congestion. CE-CERT (2011) has recently conducted dynamic ecodriving studies on highways and arterials and found significant reductions in fuel use (13% reduction on highways, 12% reduction on arterials) and CO_2 emissions (12% on highways, 14% on arterials), while maintaining similar travel times. However, ecodriving research in Vietnam has never been studies so far.

Given the merit of ecodriving towards sustainable transportation, the objective of this paper is to introduce Eco-drive Management System (EMS) in order to reduce vehicle fuel consumption as well CO_2 emission through a case study in Vietnam. In the following sections, eco-driving along with EMS is first presented, then overview of transport situation and CO_2 emission from transport sector in Vietnam, which is followed by a case study demonstrating the introduction of EMS in Vietnam. Taxi vehicles are employed in the study with different traffic situations in center and suburban areas of Hanoi city.

2. ECO-DRIVE MANAGEMENT SYSTEM

2.1 Overview of Ecodriving

Ecodriving consists of changing driving behavior to maximize the fuel economy of existing cars and trucks while minimizing carbon emissions. It is a modified way of driving that is best suited for modern engine technology, taking into account various driving conditions. Ecodriving research and programs can take on many forms, ranging from providing basic advice such as anticipating changes in traffic, smoother acceleration and braking, and proper vehicle maintenance, all the way to receiving real-time information on how to drive in current traffic conditions, or what route to take. Ecodriving offers numerous benefits, including greenhouse gas (GHG) emissions reductions, fuel cost savings, as well as greater safety and comfort. Fuel reduction through applying ecodriving can be obtained up to 20 or 25% in most studies (Rakotonirainy et al., 2012; ECCJ, 2012). Figures 1 and 2 present driving patterns a long with the benefit of ecodriving according to driving patterns in different stages below.

1. When starting and accelerating: accelerate taking around 5 seconds to reach 20km/h then conduct further acceleration smoothly.
2. When driving: drive while watching in front and maintain a wide space from the car in front to prevent changes in speed.
3. When decelerating and stopping: remove your foot from the accelerator early and endeavour to drive stably.
4. When stopped: engage neutral gear and use the side brake. If possible, eliminate idling by stopping the engine.

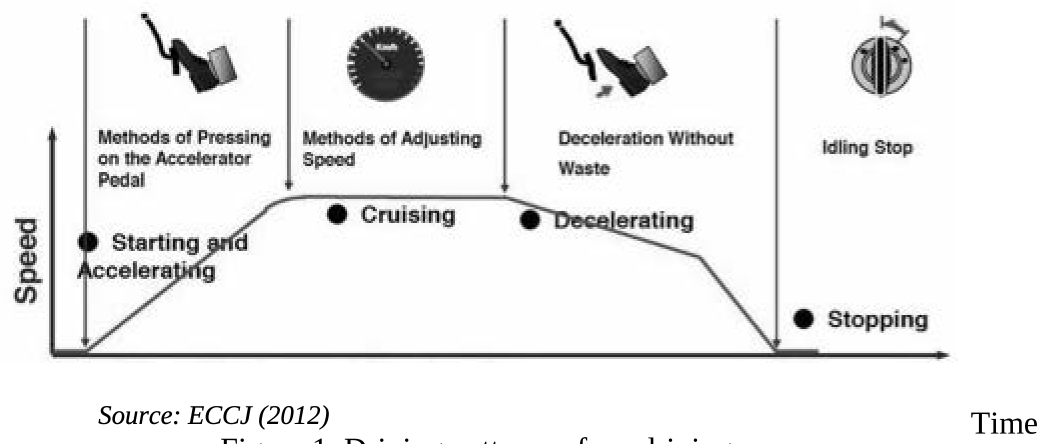

Source: ECCJ (2012)

Figure 1. Driving patterns of ecodriving

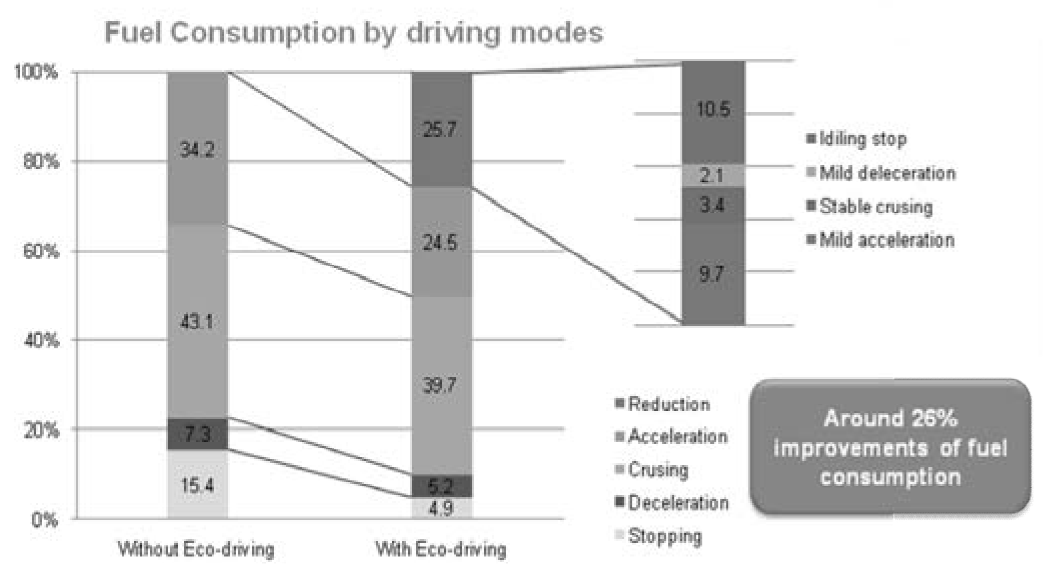

Source: ECCJ (2012)

Figure 2. Effects of ecodriving according to driving patterns

2.2 Eco-drive Management System

Eco-drive management system (EMS) is used for evaluating effectiveness of ecodriving and for dynamic ecodriving to display instantaneous performance with real-time advice or feedback. EMS application on smart-phone are used to collect and display the fuel consumption (FC) and other drive situation data (DSD) in real time. Using popular smart-phone as the EMS device offers inexpensive and effective eco-drive to vehicle users in developing countries. The On Board Diagnosis II (OBD2) (as a Bluetooth device) is installed in a connecter in the car. The data scanned in the connecter are transmitted to smart-phone by Bluetooth (wireless). Smart-phone used in EMS is an application of Android smart-phone with a EMS software developed by ISHIDA R&D. The EMS device help driver to practice eco-drive by in real time displaying the drive situation and notice for sudden acceleration or braking by alarm sound, including instantaneous fuel consumption, average fuel consumption, acceleration, GPS location, Eco-drive diagnosis point. The total of 55 types of data will be displayed and collected through EMS as shown in Figure 3.

a) OBD2 scanner

b) EMS device (Smartphone)

c) FC and DSD performance

Figure 3. Outline of EMS device

3. VEHICLE TREND AND TRANSPORT CARBON EMISSION IN VIETNAM

3.1 Vehicle Registration in Vietnam

Vietnam is one of the countries which is using motorcycle as a primary vehicle. The number of registered motorcycle has significantly increased within 10 years. According to statistics by Ministry of Transportation (MOT) from 2005-2011, the number of motorcycle is increased up to 2.05 times as shown in Figures 4. In the end of 2010, newly-registered cars account for 4% of registered vehicles, newly-registered motorcycles account for 96%. However, the number of car registration significantly increased in major cities such as Hanoi and HCMC during recent years. Before the year of 2006, a number of registered cars in Hanoi slowly increases, but from 2007 to present registered cars are rapidly increasing because the price of car gets closer to people’s affordability, even though total various tax is accounted for more than 200%. The fast growth of registered car in Hanoi is shown in Figures 5. Hanoi is one of the two cities (i.e., Hanoi and HCM cities) in Vietnam with the largest number of registered car, to the end of 2010, the number of registered car is 380,000 cars accounting for 1/6 of cars in nationwide.

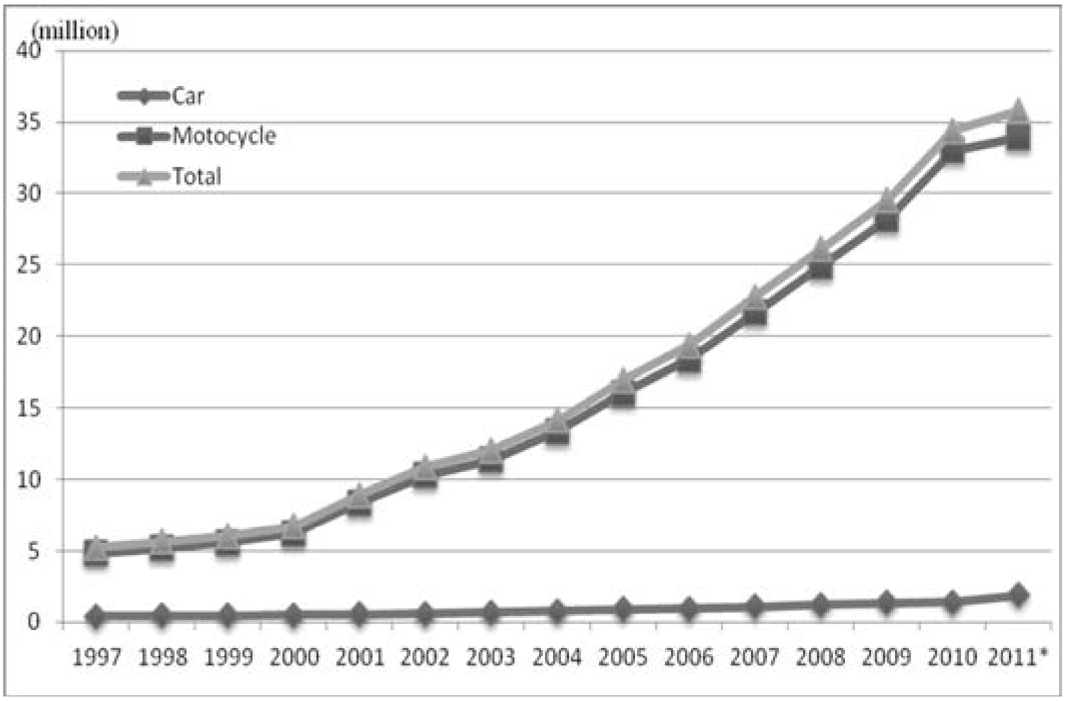

Source: The National Safety Traffic Committee, 2009; Ministry of Transportation, 2012.

Figure 4. Vehicle registration number in Vietnam

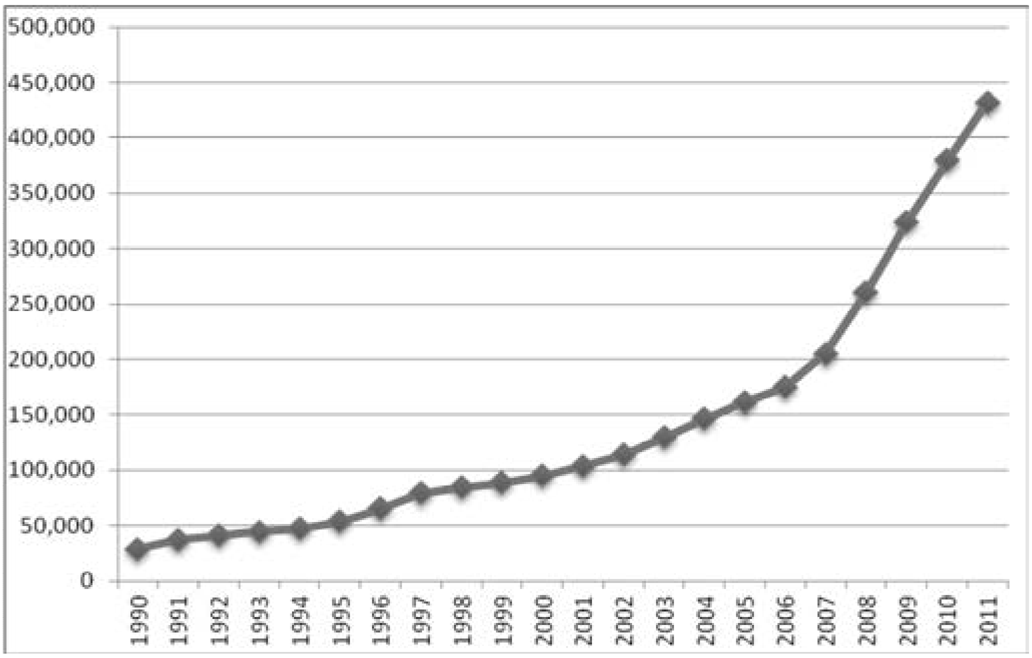

Source: Hanoi Traffic Police, 2011

Figure 5. Number of registered car in Hanoi

3.2 Carbon Emissions from Transport Sector in Vietnam

Rapidly increasing emissions of carbon dioxide from the transport sector, particularly in urban areas, is a major challenge to sustainable development in developing countries. The World Bank (Timilsina and Shrestha, 2009) has analyzed the CO_2 emissions growth of transport sector in selected developing Asian countries during 1980–2005. Figure 6 shows the trend of transport sector CO_2 emissions of selected countries in Asia. The transport sector remains one of the main sources of CO_2 emissions in most countries in Asia, while rising incomes a long with higher levels of car ownership (Webster et al, 1986a,b) and greater trip rates/distances (Schäfer, 2000) has resulted significant increase of CO_2 emissions in transport sector in these countries.

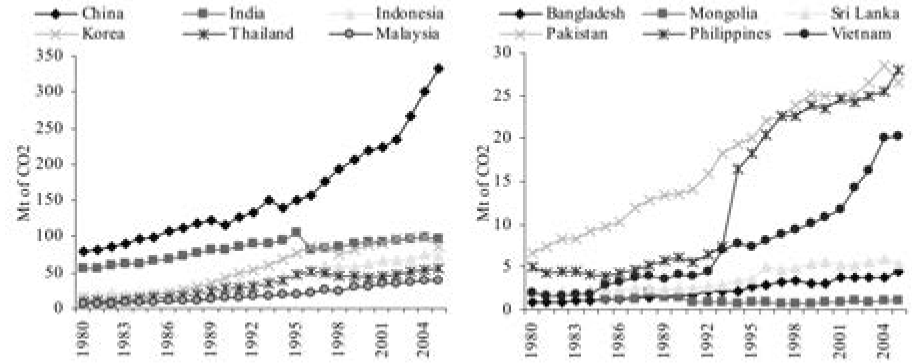

Source: IEA (2007)

Figure 6. Trend of transport sector CO_2 remissions in Asia

National CO_2 emissions in Vietnam have increased from 14 million tons in 1980 to 80 million tons in 2005, while the transport sector's share of those emissions has almost doubled from 14% to 25% as indicated in Table 1. In 2005, looking at different transportation modes, road transport accounted for the bulk of CO_2 emissions with 91.95%; other modes were air (2.5%), water (4.8%), and rail (0.8%) as illustrated in Figure 7. Therefore, any attempt to address climate change in Asia must pay attention to transport sector emissions, especially for road transport.

Table 1. CO_2 emission mix by sector

Country	1980					2005				
	Total	Power	Indus-try	Trans-port	Other	Total	Power	Indus-try	Trans-port	Other
	(Mt of CO_2)	(%)	(%)	(%)	(%)	(Mt of CO_2)	(%)	(%)	(%)	(%)
Bangladesh	7	21	41	14	24	36	35	29	12	24
China	1,403	20	51	6	23	5,060	48	37	7	9
India	292	26	39	19	16	1,147	52	30	8	10
Indonesia	69	10	39	26	26	341	28	39	22	11
Korea	122	20	32	12	37	449	35	31	19	15
Malaysia	23	32	34	28	6	138	33	35	28	3
Mongolia[#]	12	48	25	11	16	10	70	8	12	10
Pakistan	26	16	37	25	22	118	30	37	22	11
Philippines	32	27	39	15	18	76	37	19	37	7
Sri Lanka	4	8	22	55	16	12	28	16	45	11
Thailand	34	33	23	28	16	214	30	37	26	7
Vietnam	14	24	36	14	26	80	24	37	25	14

Source: IEA (2007)

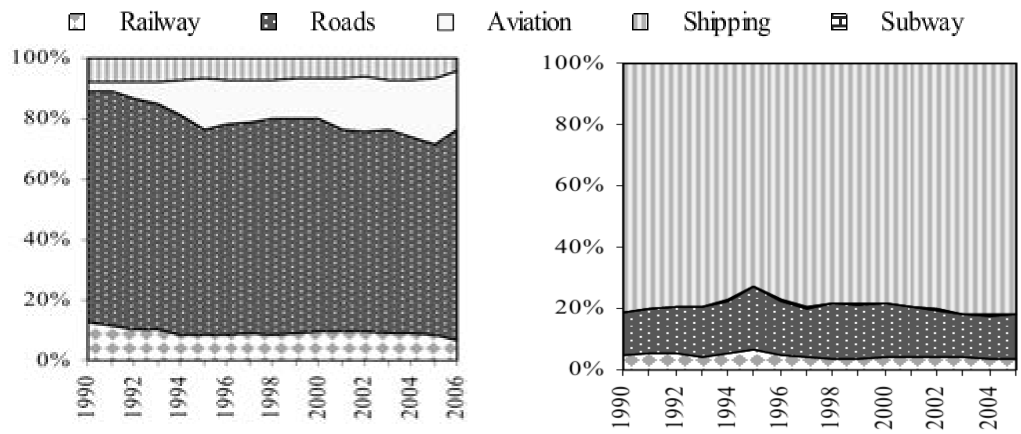

a) Modal mix for passenger transport b) Modal mix for freight transport

Source: IEA (2007)

Figure 7. Modal mix for passenger and freight transport in Vietnam

The analysis splits the annual emissions growth into components representing economic development; population growth; shifts in transportation modes; and changes in fuel mix, emission coefficients, and transportation energy intensity (which is the ratio of total fuel consumption for transportation in an economy to its gross domestic product). The World Bank study finds that of the six factors considered, three—economic development, population growth, and transportation energy intensity—are responsible for driving up transport sector CO_2 emissions in Vietnam. Transportation energy efficiency is the ratio of total fuel consumption for transportation in an economy to its gross domestic product. This value has slowly started to decline in Vietnam starting in about 1996, i.e., fuel consumption for transportation has declined per unit of economic output. However, of the 11 countries in southeast Asia for which data are presented, Vietnam has the second highest transportation energy inefficiency, trailing only Malaysia (Figure 8a). In effect, the high inefficiency of fuel consumption relative to economic output in Vietnam contributes to its rapid growth in CO_2 emissions from the transport sector as clearly presented in Figure 8b.

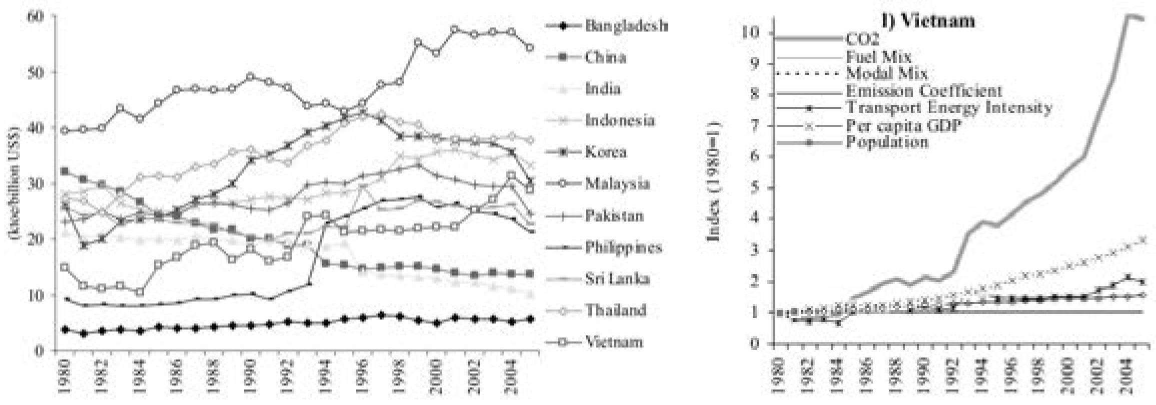

a) Transportation energy intensity in selected Asian countries (1980-2005)

b) Transport sector CO_2 emissions growth and driving factors in Vietnam

Source: IEA (2007)

Figure 8. Transportation energy intensity and transport sector CO_2 emissions growth

4. CASE STUDY

4.1 General Information

Road transport has been recently developed rapidly due to the economic development in Vietnam. As a result, emissions of carbon dioxide from the road transport causes a major challenge to sustainable development for the country. Realizing this problem, ecodriving employed EMS has been considered as an advanced low-carbon technology through a the Bilateral Offset Credit Mechanism (BOCM) in order to achieve reduction of GHG emissions. Japan Global Environment Centre Foundation (GEC, 2012) has firstly introduced a project of improvement vehicle fuel efficiency through application of EMS for taxies in Hanoi. The implementing procedure for the project is shown in Figure 9. The case study of this paper is to employ main input data and result from GEC's project for its analysis and discussion as in following sections.

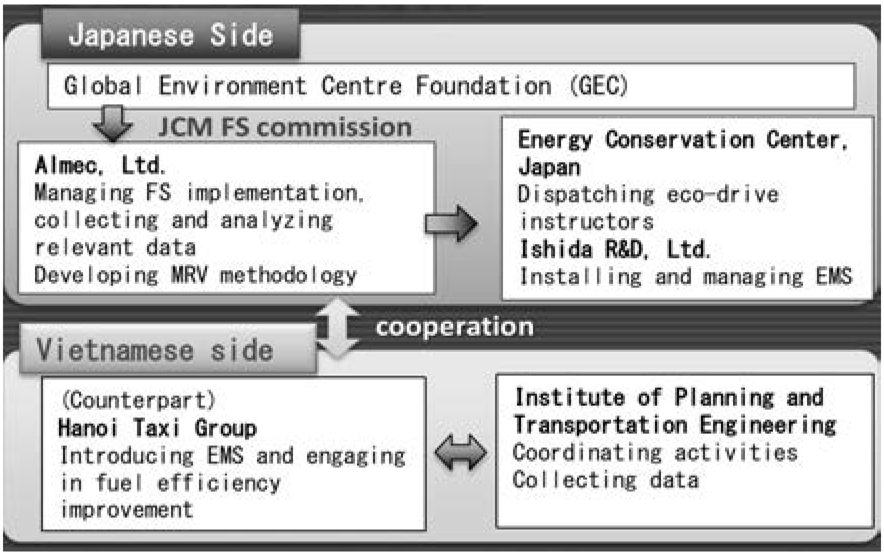

Source: GEC, 2012

Figure 9. Organizational chart for project implementation

4.2 Study Routes

Two routes, in city centre and suburban areas, will be used for training and field observation of ecodriving study as illustrated in Figure 10. Table 2 shows different traffic situations in these two areas in terms of average travel speed and average fuel efficiency which was collected and analysed by using EMS device with GPS driving trace.

Table 2. Average travel speed and average fuel efficiency

Item	Unit	Centre	Suburban
Traffic situation	-	Congested	Uncongested
Average travel speed	km/h	15.6	29.2
Average fuel efficiency	litter/100km	6.7	5.2

Centre area (4km) Suburban area (4km)

Figure 10.Routes of the case study

4.2 Selected Vehicle Type

Taxi operators have been rapidly increased with accelerating urbanization and motorization in big cities such as Hanoi and HCMC due the lack of adequate public transport means. Figure 11 illustrates the increasing trend of taxi number in Hanoi city in recent years. The number of taxi slowly increases in Hanoi from 2,000 cabs in 2003 to 2,600 cabs in 2006 equivalent to 200 cars per year in average. However, up to November 2007, the number of taxi was significantly doubled from 5,000 cabs to 9,000 cabs in 2008. In a short time from the end of 2009 to April 2010, the number of taxi cabs increases sharply from 12,000 up to 14,000. The growth rate is still maintained until now, the number of taxi cabs in Hanoi is 15,000 in March 2011 and 17,500 in April 2012. Figure 12 shows the list of taxi brands and taxi businesses in Hanoi, total of 114 registered companies, and the average number of taxi cabs in each taxi company. Taxi Group is presented as a biggest company with a larger number of taxi cabs, responsible for about 63% of total taxi cabs operating in Hanoi city. Given the fact, the study select Taxi Group for the case study with the vehicle of 4-seat Toyota Vios as the most popular vehicle in Hanoi's taxi operators.

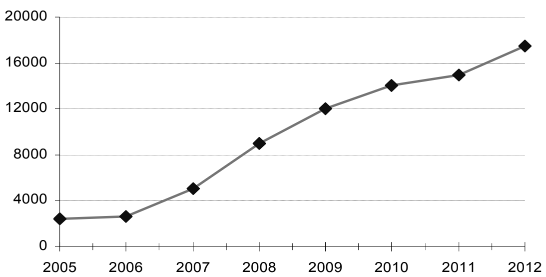

Source: ALMEC-IPTE (2012)

Figure 11. Growth of registered taxi in Hanoi

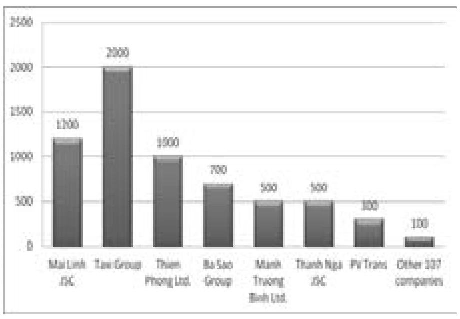

Source: ALMEC-IPTE (2012)

Figure 12. Number of cabs in each company

4.3 Analysis Procedure

The procedure for the study will be the following stages: (1) collection and analysis of the taxi operation data before the EMS introduction; (2) collection and analysis of the taxi operation data after installing EMS devices into studied cabs; (3) carrying out Eco-Drive Training Program based on the Japanese know-how; (5) implementing eco-drive in practice and collecting fuel consumption as well carbon emission; and (6) estimating for vehicle fuel efficiency and carbon emission reduction. Figure 13 shows the procedure of the eco-drive study.

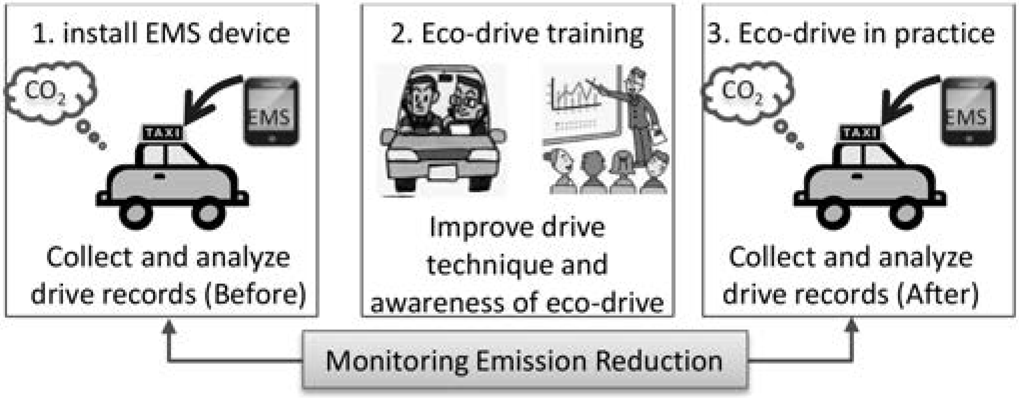

Figure 13. Procedure of the eco-drive study

5. ANALYSIS RESULTS AND DISCUSSIONS

5.1 Analysis Results

A designated course was cruised twice by taxi drivers, once in the normal manner (without project activity) and once in the eco drive mode. Number of participants is 6 and 16 for city center and suburban areas, respectively. The driving experience in city center is more than suburban area (due to the difficult driving in congested traffic in Hanoi center) which is 5.4 and 4.5 years in average respectively. The driving performance was recorded for comparative analysis as example illustrated in Figure 14. In the suburban course, cruising was without interruptions of traffic congestion while in inner city course the cruising was in traffic congestion mixed with other automobiles and motor cycles. After collecting data and carrying out analysis, average fuel reductions are obtained about 6.0% and 2.0% in suburban and inner city courses, respectively. Figure 15 shows the comparative data analysis of fuel consumption in the normal and eco-drive modes (GEC, 2012).

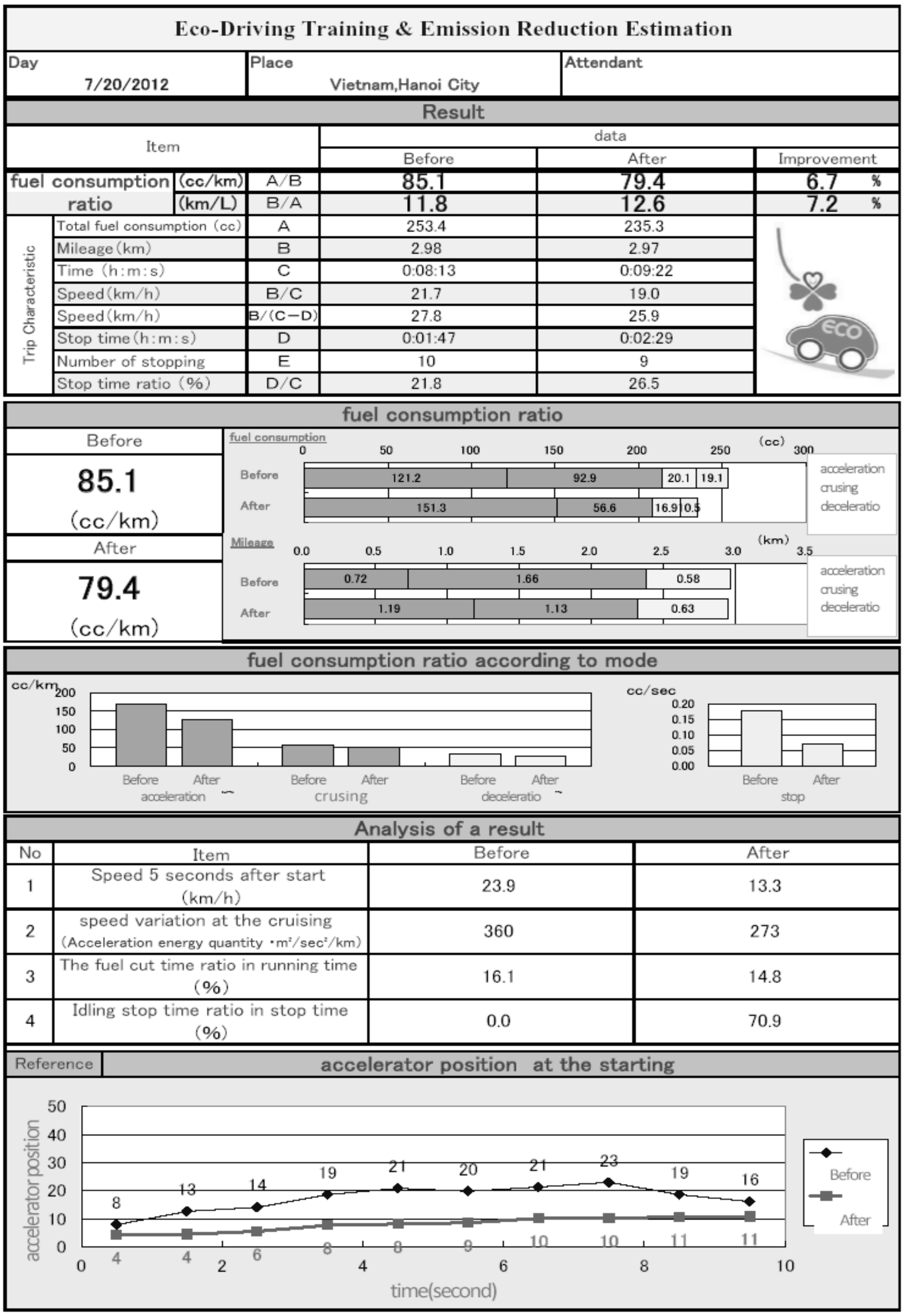

Eco-Driving Training & Emission Reduction Estimation

Day	Place	Attendant
7/20/2012	Vietnam,Hanoi City	

Result

Item			Before	After	Improvement
fuel consumption ratio	(cc/km)	A/B	85.1	79.4	6.7 %
	(km/L)	B/A	11.8	12.6	7.2 %
Trip Characteristic	Total fuel consumption (cc)	A	253.4	235.3	
	Mileage (km)	B	2.98	2.97	
	Time (h:m:s)	C	0:08:13	0:09:22	
	Speed (km/h)	B/C	21.7	19.0	
	Speed (km/h)	B/(C−D)	27.8	25.9	
	Stop time (h:m:s)	D	0:01:47	0:02:29	
	Number of stopping	E	10	9	
	Stop time ratio (%)	D/C	21.8	26.5	

fuel consumption ratio

Before	After
85.1 (cc/km)	79.4 (cc/km)

Analysis of a result

No	Item	Before	After
1	Speed 5 seconds after start (km/h)	23.9	13.3
2	speed variation at the cruising (Acceleration energy quantity ・m²/sec²/km)	360	273
3	The fuel cut time ratio in running time (%)	16.1	14.8
4	Idling stop time ratio in stop time (%)	0.0	70.9

Figure 14. Comparative analysis record before and after applying eco-drive mode

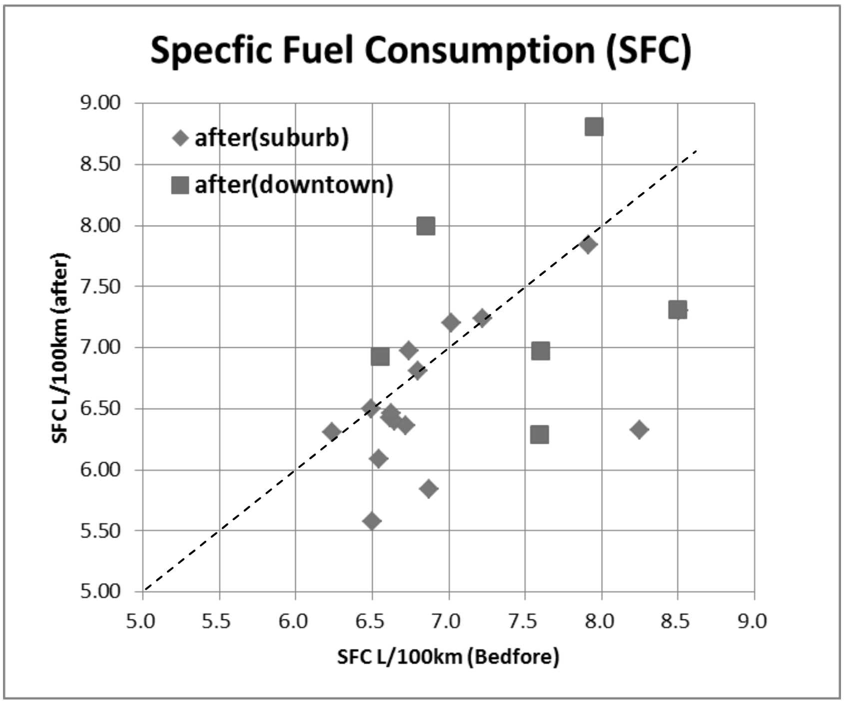

Figure 15. Fuel consumption analysis before and after applying eco-drive mode

5.2 Discussion of Eco-drive Issues

The aggregated average fuel reduction obtained in the study is not high as expected as well in comparison with other studies (e.g. ECODRIVEN, 2009; MRPI, 2011; Rakotonirainy et al., 2012; ECCJ, 2012). Furthermore, there is a significantly difference between city center and suburban areas. Main reasons have been primarily observed from the study, i.e. traffic situation, driving environment such as an inference of traffic flow by motorcycles, personal motivation, driver experience, vehicle quality. In the following, some major remained issues for further consideration are overviewed:

- When driving in a crowded urban area, it can be difficult to maintain a steady speed (e.g. keeping rolling in traffic) with a high gear, and safety should be prioritized by adopting a low speed although it is not fuel efficient. This matter is one of reasons that ecodriving is not so effective in city center of Hanoi where traffic is heavily congested.
- An experienced driver may understand easily that the best compromise depends on the situation, but it should be noted that driving habits learned by experience could also hard to change. Therefore, during a short time of training in this study, it is difficult for experienced drivers to change their habits and follow ecodriving technique exactly.
- Most drivers had an immediate fuel consumption improvement that was stable over time but some tended to fall back into their original driving style. Eco-driving style is difficult to turn into driving habit as it is dependent to the driving situation such as traffic, environment and personal motivations (Dogan et al., 2011). It points out that training is one of important ways to constantly improve driver skills related to ecodriving

technique. In Vietnam, ecodriving as a new introduction and its guideline should be added into instruction of driving license.

- Time saving is an issue when considering eco-driving (Dogan et al., 2011). CE-CERT (2011) has recently conducted dynamic ecodriving studies on highways and arterials and found significant reductions in fuel use, while maintaining similar travel times. However, further studies need for differently cultural, technical, and educational barriers inhibiting the adoption of eco-driving practices in order to promote ecodriving.
- Open research questions and challenges include providing drivers with dynamic traffic information through limited infrastructure, incentivizing manufacturers to install ecodriving feedback devices into automobiles, and further analyzing driver behavior and distraction. Ecological Driving Assistance Systems (EDAS) and Intelligent Speed Adaptation (ISA) will become a standard part of future driving assistance systems. The heterogeneity of vehicles, the complexity of the driving task and variability of driving style will require simple advices through the use of aggregated indicators to safety and ecology.

5. CONCLUSIONS

The study has implemented the eco-drive training program and thereby established the procedure from the preparation of the curriculum and the text to the implementation of training in Vietnam. The study has ascertained the positive effect of the eco drive activities on vehicle fuel efficiency improvement. The findings have shown that the average fuel reduction are about 6.0% and 2.0% in suburban and inner city courses, respectively. Although the reduction results are not so high, it shows a potential for introducing ecodriving as a friendly environmental technique to road transport system towards GHG improvement. Furthermore, the study carried out in a short time and limited areas as well not considering various factors effecting the eco-drive measure. Therefore, it need to further study to find the effective measure of introducing eco-drive into Vietnam according to its different traffic situations, driving environment, personal motivation, driver experience, vehicle quality and types (including trucks and buses). Other issues need to be simultaneously considered along with ecodriving such as safety, travel time, relationship between fuel consumption and emission that gaining optimal benefits. Continuous actions should be put on ecodriving on both training, practice and operating management strategies in Vietnam to achieve a goal of CO_2 reducion as well sustainable transportation, as referring to Japanese experience when its 2010 goal of reducing CO_2 emissions by 31 million tons below 2001 levels by encouraging drivers to use their vehicles more efficiently through Eco-driving (Transport America, 2010). Given merits of available advanced technologies, fuel efficient vehicles such as hybrid cars proposes a promising alternative which integrated safety and ecology driving assistance, i.e. Ecological Driving Assistance Systems (EDAS) and Intelligent Speed Adaptation (ISA).

ACKNOWLEDGEMENTS

The authors would like to express acknowledgement to Japan Global Environment Centre Foundation (GEC), Japan Energy Conservation Center (JECC), Department of Environment of Ministry of Transport (MOT)-Vietnam, Hanoi Taxi Group (HTG), ALMEC Corporation-Japan, Institute of Planning and Transportation Engineering (IPTE)-Vietnam, Ishida R&D-Japan for their cooperation and providing materials for the study.

REFERENCES

ALMEC-IPTE (2012). Final Report of Data Collection and Analysis for the Study of Eco-Drive under BOCM in Hanoi. ALMEC Corporation-Japan & Institute of Planning and Transportation Engineering (IPTE)-Vietnam.

Barth M., Boriboonsomsin K. (2009), Energy and Emissions Impacts of a Freeway-based Dynamic Eco-driving System, *Transportation Research Part D*: 14(6). The Interaction of Environmental and Traffic Safety Policies, 400-410.

CE-CERT (2011). Dynamic Ecodriving. Center for Environmental Research and Technology. Berkeley, CA.

Dogan E.B, Steg L., Delhomme P. (2011). The Influence of Multiple Goals on Driving Behavior: the Case of Safety, Time Saving, and Fuel Saving. *Accident Analysis Prevention*.

IEA (2007). Database Vol. 2007. International Energy Agency (IEA). Paris, France.

ECODRIVEN (2009). ECODRIVEN Campaign and Catalogue for European Eco-driving & Traffic Safety Campaigns – Intelligent Energy Europe (ecodrive.org).

ECCJ (2012). Ecodriving Guidelines. Energy Conservation Centre in Japan. Tokyo, Japan.

EEA (2008). Energy and Environment Report 2008, European Environment Agency, Copenhagen, Denmark.

JAPE (2012). Japan Association for Promotion of Eco-drive. Tokyo, Japan.

GEC (2012). Final Report of Improvement of Vehicle Fuel Efficiency through Introduction of Eco-Drive Management System(EMS). *Feasibility Study Program on Bilateral Offset Credit Mechanism (BOCM)*. Global Environment Centre Foundation (GEC)-Japan; ALMEC Corporation-Japan & Institute of Planning and Transportation Engineering (IPTE) - Vietnam.

MRPI (2011). Final Report of the Proceedings, *UC-MRPI 2011 Eco-driving Workshop*, Claremont Hotel, Berkeley, CA

Rakotonirainy, A., Haworth, N., Saint-Pierre, G. (2011). Research Issues in Eco-driving. Queensland University of Technology and French Institute in science and technology of transport.

Schäfer, A. (2000). Regularities in Travel Demand: an International Perspective. *Journal of Transportation and Statistics*, 1–31.

Shaheen, S.A. (2011). Eco-driving Research at Transportation Sustainability Research Center (TSRC*). Final Report of the Proceedings of the UC-MRPI 2011 Eco-driving Workshop*, Claremont Hotel, Berkeley, CA

Timilsina, G.R., Shrestha, A. (2009). Why Have CO_2 Emissions Increased in the Transport Sector in Asia? Underlying Factors and Policy Options. *Policy Research Working Papers 5098*. The World Bank, Washinton D.C.

Transport America (2010). Smart Mobility for a 21st Century America Strategies for Maximizing Technology to Minimize Congestion, Reduce Emissions and Increase Efficiency – Transportation America, *ITS America*, US.

Webster, F.V., Bly, P.H., Johnson, R.H., Dasgupta, M., (1986a). Part 1: Urbanization, Household Travel, and Car Ownership. *Transport Reviews*, 6 (1), 49-86.

Webster, F.V., Bly, P.H., Johnson, R.H., Dasgupta, M., (1986b). Part 2: Public Transport and Future Patterns of Travel. *Transport Reviews*, 6 (2), 129-172.

Compressive strength of ordinary and bridge high performance steel plates: Proposal of nominal design value and corresponding partial safety factor

Viet Duc DANG[1], Yoshiaki OKUI[2]
[1]Engineer, Institute of Transportation Science and Technology, Hanoi, Vietnam
dangviet.duc@gmail.com
[2]Professor, Dep. of Civil and Environmental Eng., Saitama University,
Saitama, Japan
okui@mail.saitama-u.ac.jp

ABSTRACT

The current Japanese design equation for load-carrying capacity of compressive steel plates is examined for four conventional steel grades and new bridge high performance steel grades SBHS500 and SBHS700. The analysis results of FEM plate models with initial imperfections show that the current Japanese design specification is un-conservative within the range 0.5<R<0.75 and over-conservative in the range R>0.8, where R is the slenderness parameter. Statistical distribution of the normalized compressive strength is obtained by means of Monte Carlo simulation in combination with the response surface which is obtained from sufficient number of FEM plate model analyses. Both initial deflection displacement and residual stress are considered as sources of variability. The mean values of normalized compressive strength in this study are similar to those obtained from experimental tests (Fukumoto and Itoh, 1984). The standard deviation of the current study exhibits about half of the experimental results (Fukumoto and Itoh, 1984) within the practical range 0.6<R<1.2. For the nominal strength is set to be equal to compressive strength mean value, the maximum partial safety factor results in 1.11, 1.13, and 1.16 corresponding to non-exceedance probabilities of compressive strength equal to 5.0, 3.0, and 1.0%, respectively.

Keywords: *bridge high performance steels, compressive strength, residual stress, initial deflection, local buckling.*

1. INTRODUCTION

Box columns and box plate girders consisting of unstiffened steel plates are widely used in bridge structures. The local buckling strength of the steel plates frequently governs the load-carrying capacity of these structural elements.
The current compressive strength design equation for unstiffened plates in Japanese Specifications for Highway Bridge (JSHB) version 2002 has been originally proposed in JSHB (1980). This equation was based on experimental

data for normal steel with yield strengths mainly less than 450 MPa. The bridge high performance steels, which poses high yield strength and good weldability, have been standardized since 2008 as SBHS500 and SBHS700 in Japanese Industrial Standard (JIS) (2008). However, SBHS steels exhibit different inelastic behaviour from conventional steels, such as almost no yield plateau and greater yield-to-tensile strength ratio. Hence, it is necessary to examine the applicability of the current compressive strength design equation of JSHB to steel plates with new steel grades.

Regarding the compressive strength design equation of JSHB, Usami and Fukumoto (1989), Usami (1993), and Kitada et al. (2002) show that the design equation is un-conservative within the range 0.5<R<0.75 (intermediate range) and over-conservative in the range R>0.8 (slender range), in which R is the slenderness parameter. However, Usami and Fukumoto (1989) and Usami (1993) consider only the normal (SM490Y) steel plates and they employed the perfectly elstoplastic assumption for modeling the inelastic behavior of steel material.

For theses reasons, the compressive strength design equation of JSHB need to be examined and developed for SBHS steel grades. However all the referred studies were based on the deterministic method. The recent design specifications trend towards the partial safety factor method (ISO 2394, 1998), in which a safety factor separates into individual causes, such as the variability on material property and the confidence of strength prediction method. The partial safety factor method with probability-based partial factors has been employed in Eurocode (CEN, 2004 and CEN, 1994) and AASHTO (AASHTO, 2007) as well. In order to determine the safety factors and the nominal compressive strength, statistical information, such as the mean value and standard distribution of the compressive strength, is necessary. Komatsu and Nara (1983) carried out a number of FE analyses of steel plates with considering initial deflection based on collected measurement data from actual steel bridges to obtain the mean value and standard deviation of compressive strength. However, this study considered only residual stress $\square_{rc}/\square_{y}$=0.3 as a deterministic quantity, where $\square_{rc}$ is the compressive residual stress. Fukumoto and Itoh (1984) proposed the mean (M) and mean minus twice standard deviation (M-2S) curves of the compressive strength on the basis of a database on single plate and box column compression test data. The M and M-2S curves also show that the current JSHB design equation for steel plates under compression is un-conservative within intermediate range and over-conservative in slender range. Fukumoto and Itoh (1984) also reported the statistical distribution of residual stress and initial deflection. However, this study also considered the steel plates with initial deflection W_0/b > 1/150, where W_0 and b are the maximum initial deflection and plate width, respectively.

This paper intends to examine the current JSHB design equation of steel plate compressive strength for normal and SBHS steels, and to evaluate the mean and standard deviation of compressive strength.

2. EXAMINATION OF JSHB DESIGN EQUATION

2.1 Plate properties

Four normal steel grades SM400, SM490, SM490Y, SM570 and two bridge high performance steel SBHS500, SBHS700 are considered in the current study. Figure 1 shows yield strengths and slenderness parameters *R* considered in the FE analyses, where *R* is defined by

$$R = \frac{b}{t}\sqrt{\frac{\sigma_y}{E}\cdot\frac{12(1-\mu^2)}{\pi^2 k}} \tag{1}$$

where *b*, *t*, $\square_y$, *E*, $\square$, and *k*=4.0 stand for the plate width, thickness, yield strength, elastic modulus, poison ratio, and buckling coefficient, respectively. The aspect ratio of all steel plates is assigned to equation 1.

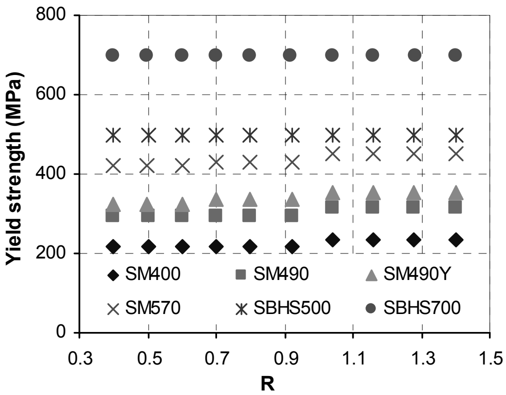

Figure 1: Slenderness parameter and yield strength in FE analyses

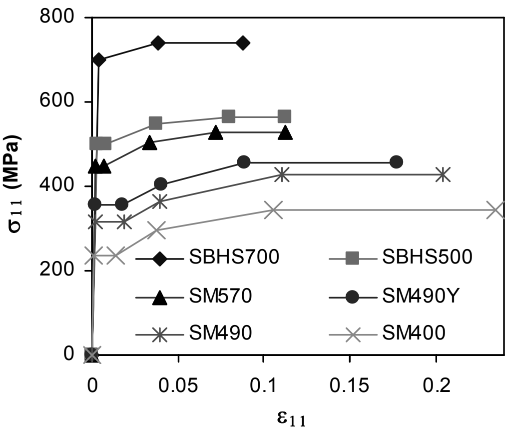

Figure 2: Idealized stress-strain relations of steel grades considered in current study

2.2 FEM model

Nonlinear FE analysis considering both material and geometric nonlinearity is conducted. Prandtl-Reuss equation is employed to model the steel plasticity. The idealized uniaxial stress-strain relationships used in the numerical analyses are shown in figure 2.

Regarding the boundary condition, all four edges of a plate model are assigned as simple supports. Figure 3 shows the distributions of residual stress and initial deflection assumed in the FE analysis. The probabilistic distributions of residual stress and initial deflection are based on measurement data reported in Fukumoto and Itoh (1984).

The displacement control method is used to apply the compressive stress. ABAQUS S4R shell elements are used for plate FE model with mesh size of 30x30 elements.

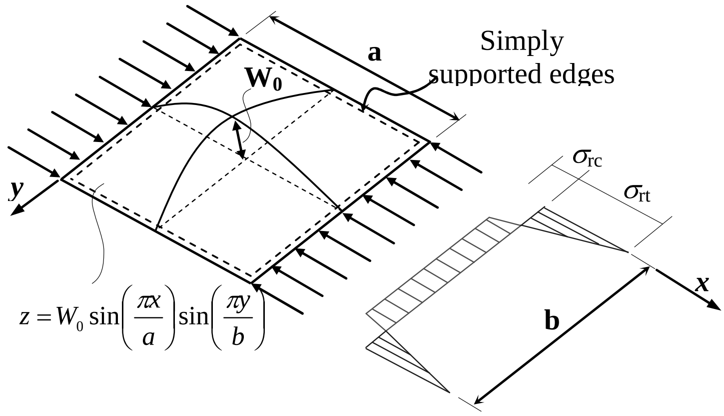

Figure 3: Idealized residual stress distribution and sinusoidal initial deflection surface

2.3 Comparison of FE results with experimental results

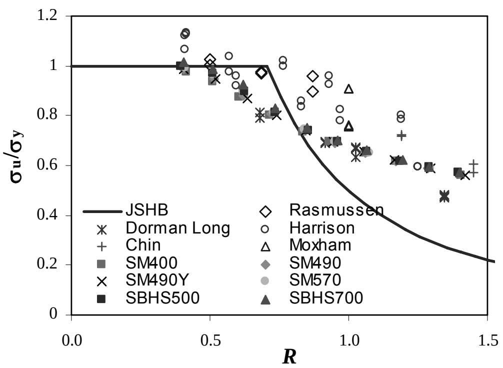

Figure 4: Comparison of current study results to previous test results

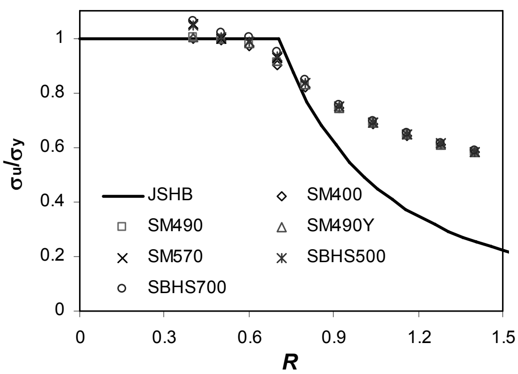

Figure 5: Normalized compressive strength of plate with 6 steel grades in the case W_0/b=1/400 and $\square_{rc}/\square_y$=0.23

The normalized compressive strengths obtained from the FE analyses as well as past experimental results (Dwight and Moxham, 1969 and Rasmussen and Hancock, 1992) are plotted in Fig. 4 as a function of R. In these analyses, an initial deflection W_0/b = 1/150 and a residual stress $\square_{rc}/\square_y$ = 0.4 are considered as a conservative assumption. As shown in figure 4, the FEM results lay the lower bound of experimental results, which corresponds to the conservative assumption.

2.4 Compressive strength of different steel grades

In this section, the normalized compressive strengths of different steel grades are compared in the case of mean values of the residual stress and the initial deflection. The mean values of normalized residual stress and initial deflection are obtained as $\square_{rc}/\square_y$=0.23 and W_0/b=1/400, respectively from the measurement data

reported in Fukumoto and Itoh (1984). In the evaluation of the mean value of the normalized initial deflection, the measurement data for W_0/b>150 are excluded owing to an allowable fabrication upper limit in JSHB.
As shown in figure 5, the compressive strengths of steel plates with 6 steel grades are quite similar in the whole range of R. The largest difference occurs at R ≈ 0.7 and R ≈ 0.4, and the normalized compressive strength of SBHS700 steel plates (maximum value among 6 steel grades) is about 6% greater than that of the SM400 steel plates (minimum value among 6 steel grades). For R > 0.4, the compressive strength of SBHS steel plates with larger YR value is greater than that of normal steel plate with lower YR value.

3. COMPRESSIVE STRENGTH SCATTERNESS

3.1 Response surface

To obtain the probability distribution of the compressive strength, Monte Carlo method is employed. However, to obtain a convergent result in the Monte Carlo simulation, it is essential to implement a large number of deterministic analyses, and accordingly it would take long time. Hence, to overcome this problem, a response surface of the normalized compressive strength, which is an approximate algebraic function of the initial deflection and residual stress, is instead of the deterministic analyses. The current study employs ten response surfaces corresponding to the 10 considered R values.

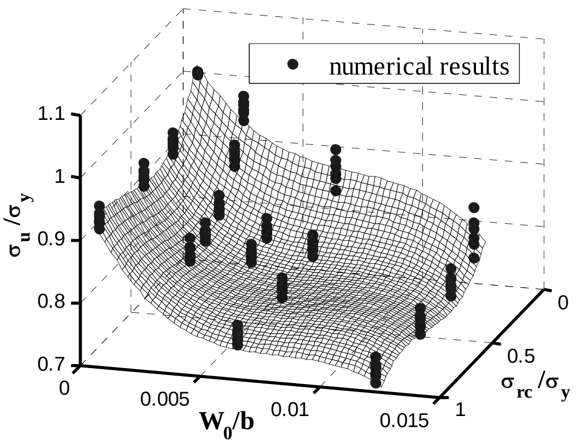

Figure 6: The response surface shape
presented along with FEM results for the case R = 0.8

The response surface is expressed as a simple algebraic function,

$$\overline{\sigma}_u = p_{00} + p_{10}\overline{\sigma}_r + p_{01}\overline{W_0} + p_{20}\overline{\sigma}_r^{\,2} + p_{11}\overline{\sigma}_r\overline{W_0} + \\ + p_{02}\overline{W_0}^{\,2} + p_{21}\overline{\sigma}_r^{\,2}\overline{W_0} + p_{12}\overline{\sigma}_r\overline{W_0}^{\,2} + p_{30}\overline{\sigma}_r^{\,3} + p_{03}\overline{W_0}^{\,3} \tag{2}$$

where $\overline{\sigma}_u = \sigma_u / \sigma_y$, $\overline{W_0} = W_0 / b$ and $\overline{\sigma}_r = \sigma_{rc} / \sigma_y$. The constants p_{ij} in equation 2 were determined from a set of 114 deterministic FE results for each steel grade and R value by using the least square method.

Figure 6 shows an obtained response surface along with FE numerical results for R=0.8. All constants of ten response surfaces are presented in Table 1. The obtained response surfaces show good fit for numerical results in the cases R≥0.7 with the coefficient of determination (R-square) > 95%. For R<0.7, the R-square values become slightly lower due to the influence of the hardening of high strength steels (SM570, SBHS500, SBHS700).

Table 1: Constant values of 10 Response surfaces

R value	p_{00}	p_{01}	p_{02}	p_{03}	p_{10}	p_{11}	p_{12}	p_{20}	p_{21}	p_{30}
0.40	1.098	-40.22	5442.0	-248100	0.007	-2.320	-48.4	-0.007	2.25	0.000
0.50	1.034	-15.15	1683.0	-90660	-0.012	-8.400	-42.4	0.069	6.72	-0.057
0.60	1.012	-1.72	-1894.0	100500	-0.087	-21.150	507.9	0.284	11.01	-0.198
0.70	1.037	-34.54	3169.0	-135000	-0.234	-32.100	1465.0	0.568	9.74	-0.342
0.80	1.047	-65.98	8382.0	-389100	-0.584	-0.520	1309.0	1.006	-15.13	-0.492
0.92	0.963	-40.44	3081.0	-112100	-0.937	57.210	-891.1	1.368	-35.91	-0.632
1.04	0.850	-23.31	1188.0	-34700	-0.788	47.270	-769.2	1.169	-29.12	-0.556
1.16	0.757	-12.66	377.6	-11430	-0.567	25.720	46.8	0.856	-20.27	-0.419
1.28	0.697	-10.08	367.4	-12430	-0.435	23.330	-269.2	0.617	-15.11	-0.288
1.40	0.650	-7.44	229.3	-8387	-0.343	18.580	-208.5	0.462	-11.63	-0.211

3.2 Stochastic inputs of initial imperfections

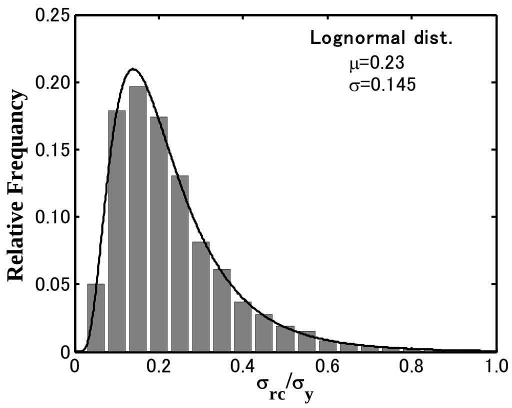

Figure 7: Generated random input of initial deflection

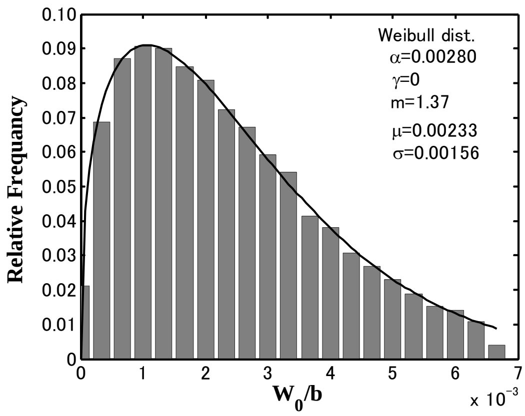

Figure 8: Generated random input of residual stress

In the Monte Carlo simulation, the probabilistic distribution of the initial deflection is assumed as the Weibull distribution, and the residual stress as the Lognormal distribution as shown in figure 7 and 8 (Fukumoto and Itoh,1984). In this figure, the generated random variables in the Monte Carlo simulation are also plotted as the histogram chart. The generated normalized initial defections more than W_0/b>1/150 are excluded in the simulation due to an allowable fabrication upper limit in JSHB.

3.3 Results of Monte Carlo simulation

The probabilistic distribution of compressive strengths is obtained by application of the response surface and a large number of random inputs of residual stress and initial deflection. The converged mean and standard deviation are obtained by processing 10000 random input couples of residual stress and initial deflection. The histogram of compressive strength with 10000 random input couples in the case of R=0.8 is shown in figure 9. Results of 10 convergent mean and standard deviation of compressive strengths are presented in Table 2.

In figure 9, the mean values of normalized compressive strength with error bar equal to two times the standard deviation are plotted along with the current JSHB design equation, mean (M) curve and mean minus 2 standard deviation (M-2S) curve proposed in Fukumoto and Itoh (1984).

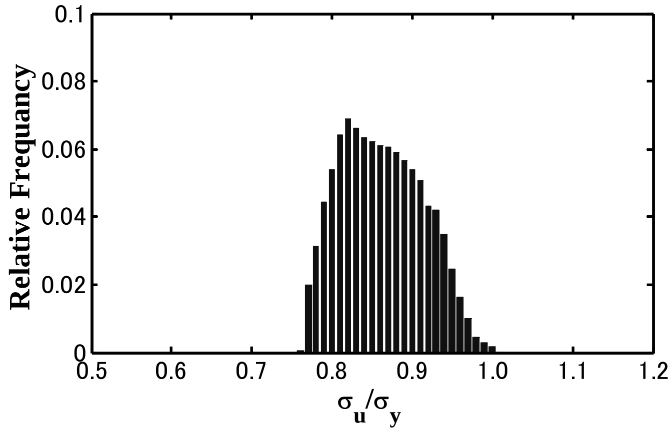

Figure 9: Probability distribution of compressive strength for R=0.8

Table 2: Mean and standard deviation of normalized compressive strength

R value	0.4	0.5	0.6	0.7	0.8	0.92	1.04	1.16	1.28	1.4
M value	1.039	1.006	0.982	0.938	0.862	0.766	0.701	0.653	0.617	0.586
S value	0.0277	0.0157	0.0212	0.0413	0.0515	0.0399	0.0294	0.0216	0.0171	0.0145

As shown in figure 9, the mean values of normalized compressive strength are similar to the mean curve reported in Fukumoto and Itoh (1984), which was proposed from test results. Within 0.65≤R≤0.85, the mean values of the current study are slightly greater than that reported in Fukumoto and Itoh (1984). One of the possible reasons is that the current study does not consider steel plates with $W_0/b>1/150$ and the influence of initial deflection on compressive strength is more significant within the mentioned range of R than other ranges. Also seen in Fig.9, the M-2S curve proposed in Fukumoto and Itoh (1984) is too conservative if compared to corresponding results of the current study.

A comparison of standard deviation of compressive strengths obtained in the current study and previous study Fukumoto and Itoh (1984) is presented in Fig.10. Within the practical range 0.6<R<1.2, the standard deviations of the current study exhibit about half of reported values in Fukumoto and Itoh (1984). As seen in the figure, the standard deviations obtained by the current study have a clearer tendency, and attained to the maximum value at R≈0.8. Within the range 0.7<R<0.9, the ultimate state of compressive plates is elastoplastic buckling, and accordingly the compressive strength is significantly influenced by both residual stress and initial deflection. For R>0.9, the standard deviation decreases, and the elastic buckling becomes dominant. The residual stress has almost no effect on the compressive strength. For R < 0.7, the compressive strength tends to attain the yield strength and is mainly influenced by initial deflection. In particular for R<0.5, the hardening behavior of high strength steel (SM570, SBHS500 and SBHS700) starts to have a significant effect on the compressive strength.

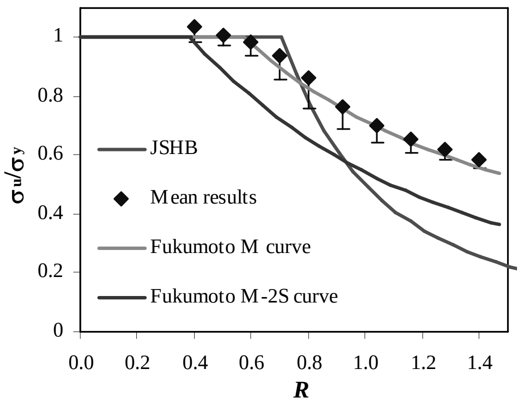

Figure 10: Comparison between current study, JSHB, 2002, and Fukumoto and Itoh (1984) results

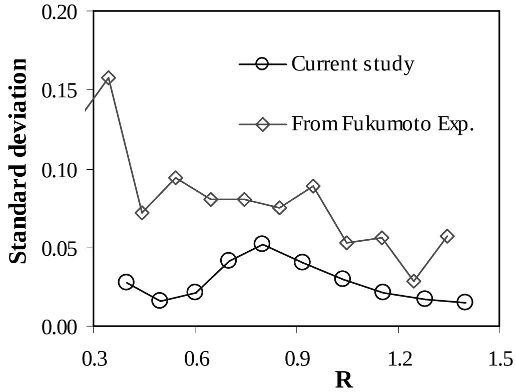

Figure 11: Comparison of standard deviation values obtained in current study and reported in Fukumoto and Itoh (1984)

4. PROPOSAL OF SAFETY FACTOR

The reliability index is used to specify a safety margin

$$\mu - \beta_T \sigma = \frac{1}{\gamma} f_N \qquad (3)$$

where σ and μ are the mean and standard deviation of normalized compressive strength, respectively; β_T stands for the target reliability index; γ and f_N are the safety factor and the corresponding nominal strength, see figure 12 for the probability density function and the approximated normal distribution at R=0.8.

Table 3. Partial safety factors in the range of 0.4≤R≤1.4

R	0.4	0.5	0.6	0.7	0.8	0.92	1.04	1.16	1.28	1.4
f_N = □	1.039	1.006	0.982	0.938	0.862	0.766	0.701	0.653	0.617	0.586
□(5%)	1.05	1.03	1.04	1.08	1.11	1.09	1.07	1.06	1.05	1.04
□(3%)	1.05	1.03	1.04	1.09	1.13	1.11	1.09	1.07	1.06	1.05
□□1%)	1.07	1.04	1.05	1.11	1.16	1.14	1.11	1.08	1.07	1.06

Assuming that the probability density of compressive strength is described by a normal distribution, and assigning non-exceedance probabilities of compressive strength to 5.0, 3.0, and 1.0%, then the corresponding target reliability incises become 1.64, 1.88, and 2.33. Furthermore, setting the nominal compressive strength equal to the mean of compressive strengths as an example, the partial safety factor can be obtained as shown in Table 3.

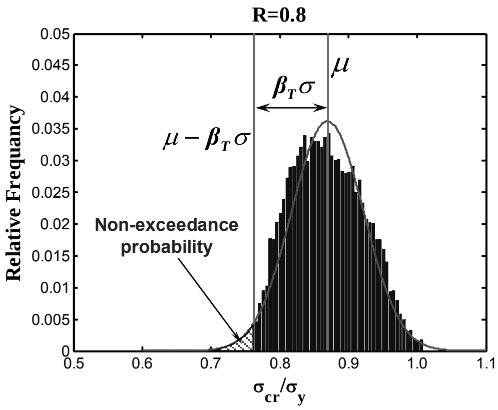

Figure 12: Explanation of equation 3

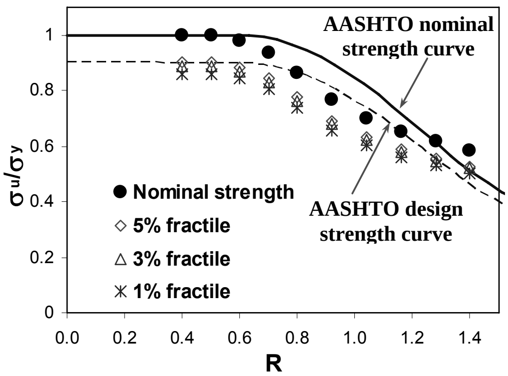

Figure 13: proposal compressive strengths

As represented above, the current study only considers the scatterness of initial imperfections and without considering scatterness of steel material yield strength, the Eq.4, the nominal compressive strength equation for simply supported steel plates is proposed based on compressive strength mean values. The comparison to AASHTO nominal curve is presented in Fig.13

$$\frac{\sigma_u}{\sigma_y} = \begin{cases} 1 & R \leq 0.55 \\ 0.399 - \dfrac{0.0775}{R} + \dfrac{0.630}{R^2} - \dfrac{0.223}{R^3} & R > 0.55 \end{cases} \tag{4}$$

The general curvature tendency of proposal nominal compressive equation is less steep than that of AASHTO. This behavior represents the difference of the steel plate compressive strength which is obtained by considering inelastic material behavior and nonlinear geometrical analysis and the ones which results from the elastic local buckling theory.

5. CONCLUSIONS

The mean values obtained in the current study are similar to those proposed in Fukumoto and Itoh (1984), but slightly greater within the range $0.7<R<0.9$. The standard deviation of compressive strength obtained in this study is about half of values reported in Fukumoto and Itoh (1984) within a range of $0.6<R<1.2$. The M-2S curve proposed in Fukumoto and Itoh (1984) is too conservative if compared to corresponding values obtained in the current study. The results of M-2S of the current study show that the current load-carrying-capacity JSHB design equation of steel plates is un-conservative within the range $0.5 < R < 0.8$ and over-conservative for $R > 0.85$.

Within the range of slenderness parameter $0.4 \leq R \leq 1.4$, the normalized compressive strengths of normal steel and SBHS steel are similar for the same

levels of R and initial imperfections. However, compressive strength of steel plates with SBHS grades with greater YR is slightly greater than that of normal steel grades.
With assumption of normal distribution function applying to probabilistic distribution of steel plate compressive strength and the compressive strength mean values considered as nominal strengths, the partial safety factors obtained are equal to 1.11, 1.13 and 1.16 corresponding to 5%, 3% and 1% fractile, respectively.

REFERENCES

American Association of State Highway and Transportation Officials, 2007. "AASHTO LRFD bridge design specification" – Fourth edition.

CEN, Eurocode3, 2004. "Design of Steel Structures", Part 1-5, plated structural elements.

CEN, Eurocode4, 1984. "Design of Composite Steel and Concrete Structures", Part 2, General rules and rules for bridges.

Dwight, J., B., Moxham K. E., 1969. "Welded steel plates in compression", *The Structural Engineer,* Vol. 47, No. 2, pp. 49-66.

Fukumoto, Y., and Itoh, Y., 1984. "Basic compressive strength of steel plates from test data", *Proc. of JSCE* No.334/I-1,

Fukumoto, Y., 1996. "New constructional steels and structural stability", *Engineering structures,* Vol.18, pp. 786-791.

International Standard ISO 2394, 1998. "General principles on reliability for structures", Third edition,

Japan Road Association, 2002. "Specifications for Highway Bridges" – part II. Steel Bridges.

Japan Road Association, 1980. "Specifications for Highway Bridges" – part II. Steel Bridges,

Japanese Industrial Standard, 2008. "JIS G 3140, Higher yield strength steel plates for bridges".

Kitada, T., Yamaguchi, T., Matsumura, M., Okada, J., Ono, K., and Ochi, N., 2002. "New technology of steel bridge in Japan", *Journal of Constructional Steel Research*, Vol.58, pp. 21-70.

Komatsu S, and Nara, S., 1983. "Statistical study on steel plate members", *Journal of Structural Engineering*, ASCE, Vol. 109, No. 4.

Rasmussen, K., J., R., and Hancock, J., G., 1992. "Plate slenderness limits for high strength steel sections", *J. Construct. Steel Research*. Vol.23, pp. 73-96.

Usami, T., and Fukumoto, Y., 1989. "Deformation analysis of locally buckled steel compression members", *Journal of Constructional Steel Research*, Vol.13, pp. 111-135.

Usami, T., 1993. "Effective width of locally buckled plates in compression and bending", *Journal of Structural Engineering, ASCE*, Vol. 119, No. 5, pp. 1358-1373.

Hybrid technology of up-flow anaerobic filter and membrane bio-reactor for recovery energy from rich organic waste stream

Thu Hang DUONG, Duc Ha TRAN, Hoai Son TRAN,
Thi Viet Nga TRAN, Bich Ngoc HOANG, Thuy Lien NGUYEN
Lecturer and Researcher, Institute of Environmental Science and Engineering,
National University of Civil Engineering, Vietnam
hatd@nuce.edu.vn

ABSTRACT

Brewery wastewater is typically one of rich organic waste streams, which concentrations of main pollutants are in the range of 970-3050 mg COD/L, 680-2150 mg BOD_5/L, 300-500 mg TSS/L and 80-90 mg TN/L. Experimental research on biological process treating brewery wastewater in Sai Gon-Hanoi Brewery Plant was set up with an up-flow anaerobic filter (UAF) followed by membrane bio-reactor (MBR). The UAF had a stable performance at room temperature (~20^0C) after 20 operating day, and a methane yield of 0.25 NL/g COD_{added} was obtained at hydraulic loading rate of 1.5 L/L.day and organic loading rate of 2-4 g COD/L.day. The highest removal efficiency of pollutants was achieved at a concentration of 7.5-8.5 g MLSS/L in the MBR, and MBR process stability was attained at flux and organic loading rate were below 9 L/m^2.h and 3 g COD/L.day, correspondingly. The treated effluent of the system was complies with the Vietnamese standard QCVN 40:2011/BTNMT (column A), which could be reused for numerous purposes in brewery plants. Additionally, sludge discharged from UAF and MBR was anaerobically stabilized at mesophilic condition (~35-37^0C), recovering approximately 150 NL of methane per 1 g $COD_{removed}$. The remarkable results of research revealed that this new hybrid technology of UAF and MBR was a sustainably saving energy solution for rich organic wastewater treatment.

Keywords: *rich organic waste stream, brewery wastewater, up-flow anaerobic filter, membrane bio-reactor, recovery energy*

1. INTRODUCTION

Wastewater discharged from food industries are generally characterized with rich organic and nutrient contents, e.g. COD ≥ 2 000 mg/L, TN ~ 100 mg/L, and tend to bring serious water environment contamination if discharged without proper treatment (Tran, 2002; Oreopoulou and Russ, 2007). Like any other food industry, the brewing industry is subject to extensive government regulations including numerous environmental protection laws. It is estimated that for the production of 1 L of beer, 3-10 L of waste effluent is generated, mostly from the brewing, rinsing and cooling processes (Brito *et al.*, 2007; Oreopoulou and Russ, 2007).

The conventional treatment of this kind of high strength wastewater is traditional anaerobic/aerobic activated sludge process which is often wasteful of resource and problematic in performance for most breweries. Besides, there are few reports on the integration of anaerobic and aerobic process for cost-effectively and stably treating of the high strength wastewater.

This research proposed the application of hybrid technology of up-flow anaerobic filter (UAF) and membrane bioreactor (MBR) for treating of rich organic waste streams. Several key points of this hybrid technology include a positive energy balance, reduced sludge production, a high biomass concentration in reactor, a very long sludge retention time resulting in the complete retention of slow-growing micro-organisms such as nitrifying bacteria, and significant low space requirements (Chae *et al.*, 2007; Hai *et al.*, 2011). In terms of energy point of view, methane produced from UAF and anaerobic processes which can be directly utilized in a boiler is firmly the preferred solution in breweries. In the context of decreasing fossil fuel reserves, energy recovery through generation of methane from rich organic waste makes a brewery more independent from external fuel supply and contributes to a more sustainable brewing process. Furthermore, membrane use can produce high quality effluent free of bacteria, offering the possibility of water reclamation. The objectives of this study are to set up a brewery wastewater treatment model at laboratory scale using up-flow anaerobic filter for pretreatment combined with membrane bio-reactor, to determine operating data and to access the efficiency and performance of wastewater treatment system. Furthermore, the study aims to examine the stabilization of sludge generated in the system and methane yield producing from excess sludge for energy recovery.

2. MATERIALS AND METHOD

2.1. Substrate and inoculum

The studied materials were wastewater and sludge provided by Sai Gon-Hanoi Brewery Plant (Vietnam). Wastewater was collected from the regulating tank, after screening, of Wastewater treatment plant (WWTP) in Sai Gon-Hanoi Brewery Plant. The inoculum sludge for the anaerobic and aerobic reactors at the laboratory was the sludge of up-flow anaerobic sludge blanket (UASB) and of sequencing batch reactors (SBR).

2.2. Experimental set up and operation

The experiment strategy was maximizing the resource recovery (methane as green energy and reuse treated wastewater) from the rich organic wastewater and from generated sludge of the wastewater system itself, characterized by two following experiments at the laboratory scale.

Experiment 1: Rich organic wastewater treatment experiment

The anaerobic filter had a dimension of DxH of 20x50 cm, with the working volume of 10 L, operating in up-flow mode (UAF) with 20 cm of Kaldnes moving-bed. The aerobic membrane bioreactor had a dimension BxLxH of

8x25x25 cm, the working volume of 6 L, equipped with the oxygen supply to maintain DO higher than 2 mg/L. The membrane module was a plate type of Kubota (type 203), made by PVDF (polyvinylidene fluoride), with the pore size of 0.4μm (MF) and area of 0.1m^2 per plate, submerged in the reactor. Scheme of the experimental system and the picture of the system are described in Figure 1.

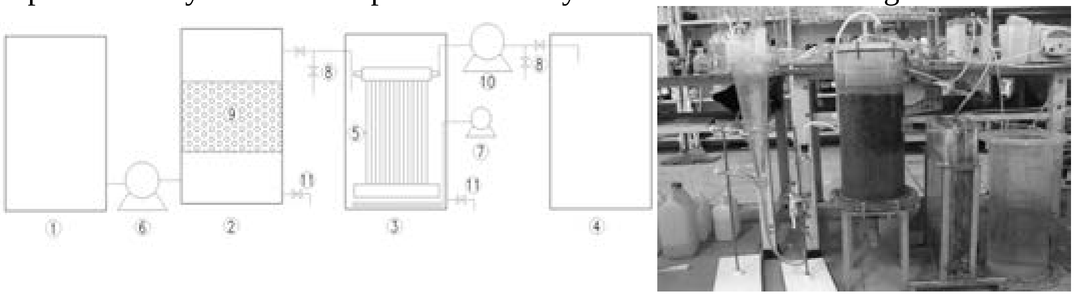

(a) (b)

Figure 1: Scheme (a) and picture (b) of the wastewater treatment experiment
(1) Influent tank, (2) UAF, (3) MBR, (4) Effluent tank, (5) Membrane module, (6) Inlet pump, (7) Aerator, (8) Water sampling, (9) Kaldnes moving-bed, (10) Outlet pump, (11) Sludge sampling

At start-up, 5L anaerobic sludge from UASB (TS: 27.5 ± 2.4 g/L; VS: 13.6 ± 3.6 g/L) and 6 L activated sludge from SBR (TS: 9.3 g/L; VS: 7.5 g/L) of the WWTP were inoculated in the UAF and MBR, correspondingly, of the experimental system. Wastewater in the influent tank was pumped into the UAF at the bottom. The water level covered the filter media by 10 cm owing to a hole-bored-plastic plate to guarantee an even flow regime. The over flow came into MBR then, the treated water was sucked through submerged membrane to effluent tank. The gas produced from the UAF was determined by the communicating vessel. Sludge generated from UAF and MBR was periodically let out according to the sludge retention time of each reactor for the sludge stabilization test. The operation regime of UAF and MBR are shown in Table 1 and 2.

Table 1: Operation strategy of UAF

Operation data	**Unit**	**Phase 1**	**Phase 2**	**Phase 3**
COD concentration of inlet UAF	mg/L	1050-2650	1283-2683	1500-2868
Hydraulic loading rate (Lq)	L/L.day	1.06	1.44	2.32
Hydraulic retention time (HRT)	H	23	17	10
Operation duration (t)	Day	25	30	30

The operation strategy was characterized by increasing of organic and hydraulic loading rate (OLR and HRT) to maximizing the pollutant treatment efficiency and methane production from the brewery wastewater of the system and investigating the optimum operation data for stable performance of each reactor.

Table 2: Operation strategy of MBR

Operation data	**Unit**	**Phase 1**	**Phase 2**	**Phase 3**	**Phase 4**
COD concentration of inlet MBR	mg/L	453-1053	333-1090	800-1108	1103-1268

Hydraulic loading rate (Lq)	L/L.day	2.04	1.32	2.76	3.72
Flux (F)	$L/m^2.h$	5.1	3	6.9-9.3	9.3
Hydraulic retention time (HRT)	h	12	18	9	6
Operation duration (t)	day	25	30	20	10

The water samples were collected at 3 points: the inlet of UAF, the outlet of UAF and the outlet of MBR (at valve 8, Figure 1). The analytical parameters including temperature (t^0C) and pH determined once a day; chemical oxygen demand (COD), total suspended solids (TSS), ammonium (NH_4^+-N), total nitrogen (TN): 2-3 times per week; biological oxygen demand (BOD_5), turbidity, color and total phosphorus (TP): 2-3 times per month. At MBR, concentration of disolved oxygen (DO) and mixed liqour suspended solid (MLSS) were determined once a day.

Experiment 2: Anaerobic fermentation of excess sludge

Sludge generated from UAF and MBR of the wastewater treatment system were digested in anaerobic condition at the batch mode for investigating the sludge stabilization and methane production. The microbial seeding, harvested from the UASB sludge of the WWTP, was added at the start to obtain the F/M ratio equal to 0.5. The reactors with the working volume of 500 mL, were continuously mixing-equipped with the magnet stir system (as Continuous flow stirred-tank reactor: CSTR), incubated in the water bath at mesophilic condition (35-37^{0}C). One reactor was set-up with the UASB sludge, incubated at the same condition for control the experiment. Methane produced from each reactor was collected through silicon tube, removed CO_2 and measured by the gas columns. Figure 2 demonstrates the scheme and picture of the experiment of sludge fermentation.

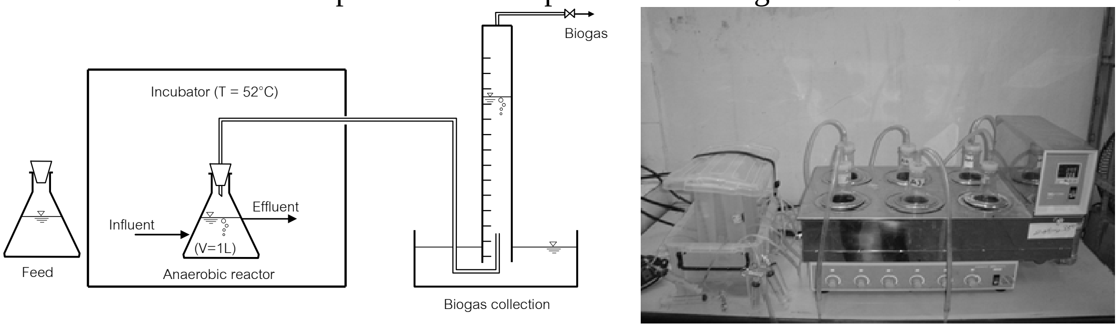

(a) (b)

Figure 2: Scheme (a) and picture (b) of the sludge fermentation experiment

In the sludge test, three sludge samples were collected from each reactor: at the beginning- after the addition of sludge substrate (day 0), after 5 operation days (day 5) and at the end of experiment-when no gas produced for 3 continuous days. The analytical parameters including total solids (TS), volatile solids (VS), pH, total COD and soluble COD, NH_4^+-N, TP were determined in the sludge samples.

2.3. Analytical methods

Gas production was measured by liquid displacement. The pH values were measured with a WM-22EP pH meter (Toaodk, Japan). The DO and MLSS were measured with HQ30d (Hach) and IM-50P (Motto, Japan), correspondingly. The alkalinity, turbidity, color, total COD (COD_{tot}) and soluble COD (COD_{sol}), BOD_5, TS, TSS, VS, NH_4^+-N, TN and TP were determined according to the the Standard Methods (APHA-AWWA-WPCF, 1999).

3. RESULTS AND DISCUSSION

3.1. Composition and characteristics of brewery wastewater

Table 3 shows the main characteristics of the substrate brewery wastewater used in the experiments.

Table 3: The main characteristics of brewery wastewater

No.	Parameters	Unit	Brewery wastewater	
			Range of value	Average value
1	pH	-	4-8	6.1
2	Biological oxygen demand, BOD_5	mg O_2/l	680-2150	1650
3	Chemical oxygen demand, COD	mg O_2/l	970-3050	1940
4	Total suspended solid, TSS	mg/l	300-500	430
5	Turbidity	NTU	400-600	490
6	Color	Pt-Co	1700-2250	1955
7	Total phosphorus, TP	mg/l	0,1-10	7
8	Total nitrogen, TN	mg N/l	80-90	87.4
9	ammonium, NH_4^+-N	mg NH_4-N/l	30-40	32.3

Brewery wastewater typically has a high COD content, mostly easily biodegradable from all the organic components (sugar, soluble starch, ethanol, volatile fatty acids, etc.) leading to COD/BOD_5 ratio of 1.1to 1.5. The effluent solids consist of spent grains and kieselguhr waste yeast. TN concentration in the tested wastewater were higher than typical brewery effluent composition (25-80 mg/L) but TP was lower (10-50 mg/L) (Brito *et al.*, 2007; Oreopoulou and Russ, 2007). Nitrogen and phosphorous levels are mainly depending on the handling of raw material and the amount of spent yeast present in the effluent. Low phosphorus levels can also result from the bio-chemicals used in the CIP unit. The ratio of COD:N: P in the wastewater was 1940 : 87 : 7 ~ 277 : 12 : 1. In the anaerobic condition, the required nitrogen content for anaerobic microorganism in rich organic substrates should be approximately COD:N ≈ 350:5 and phosphorus demand account for 1/5 to 1/7 of nitrogen. Compared to the optimum balanced nutrient ratio for anaerobic microorganism, the brewery wastewater had likely sufficient carbon and phosphorus source, but nitrogen in excess.

3.2. The UAF's performance and methane yield

As wastewater up-flows through the filter, particles were trapped and organic matter was anaerobically degraded by the biomass that was attached to the surface of filter material. Figure 3 shows the COD removal efficiency and the methane yield in UAF during the operation time.

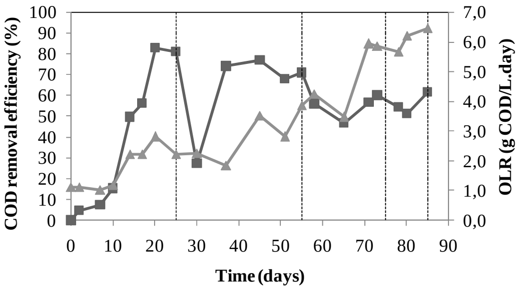

Figure 3a: Change of OLR and COD removal efficiency in UAF *(▲:OLR; ■: COD removal efficiency)*

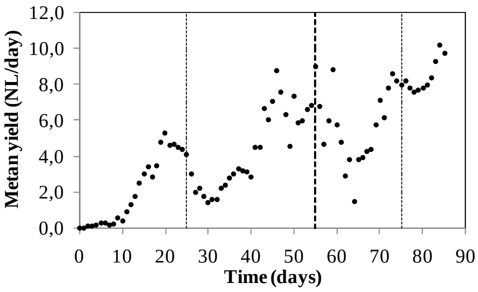

Figure 3b: Methane yield in UAF

The microbial seeding in this experiment had VSS concentration was 13.6 g/L, accordance to Elmitwalli and Chernicharo for anaerobic digestion of domestic wastewater and rich organic streams (at least 10 g VSS/L) (Elmitwalli *et al.*, 2001; Chernicharo, 2007). It had been observed that the start-up period needed for microorganism to immobilize on the moving-bed of UAF was 20 days. At the end of phase 1, COD removal efficiency reached 80%, which was agreed with the review of Chernicharo and Legginga (Lettinga *et al.*, 2001; Chernicharo, 2007) for UASB and UAF (75-85%) as well as the highest value (82%) in UAF for treating brewery wastewater in the study of Yu and Gu (Yu and Gu, 1996). The result of this research pointed out that, with the appropriate microbial seeding - already adapted to brewery wastewater, the start-up to aerobic microorganism get used to and fix on the surface of filter material of UAF remarkably decreased compared to the typical start-up duration for establishing sludge blanket in UASB of 2 to 8 months (Yu and Gu, 1996; Chong *et al.*, 2012).

Phase 2 and 3 started with the increasing of the OLR and HLR to 1.5-3 folds, the COD removal efficiency suddenly went down to below 27%, COD concentration of the effluent of UAF higher than 1 g/L. However, after 7 day, the efficiency gradually increased to approximately 70% and stabilized till the end of phase 2 although there was another increase of OLR to nearly 6 g COD/L.day, equivalent to the high range of loading rate of UAF (5 g COD/L.day) (Lettinga *et al.*, 2001; Chernicharo, 2007) but keep the HLR constant. It was found that the increasing of HLR had more severe influence on the organic matter transformation of microorganism than the increasing of OLR. It could be due to the effect of washing-out part of microorganism when high flow was applied, leading to the growing of COD in the effluent. However, when the microorganism stably attached on the filter, the 'shock' effect in the later phase became lessen. Besides, the COD removal efficiency in UAF could not achieve above 60-65% at the end of phase 3. In other words, the loading rate threshold of UAF could not surpass the value of 6 g COD/L.day or 2 L/L.day.

Figure 3 (b) showed that the result of methane yield increased in each phase, but dropped at the beginning when there was a change of loading rate. This was in accordance with the change of COD removal efficiency. This progress could be explained that the anaerobic fermentation was constituted by a chain of activities of anaerobic microorganisms and among the anaerobic microorganisms, the hydrolysis, acidogens and even acetogens microorganism likely promptly adapted to the change of organic concentration of the input stream. However the growth of methanogens was remarkably slower, about 25 times less than the growth of acetogens (Chernicharo, 2007). Then, the removal rate of hydrogen and transformation of VFAs by methanogens could not keep pace with the accumulation of VAFs, leading to the depression of pH value and intensively inhibition of methanogens in the system. However, once the VFAs reduced by the outlet and gas off, the methanogens could be strengthen upon the filter matter, hence the methane yield gradually increased in each phase. The methane yield recorded at the end of phase 1, 2 and 3 correspondingly, was 5.3, 9.0 and 10.2 NL/day, equivalent to 0.21, 0.25 and 0.16 NL/g COD_{added}. Compared to the organic loading rate and the COD removal efficiency, the efficiency of methane production in UAF in 3 phases was 65%, 74% and 70%.

3.3. The MBR performance and COD removal efficiency

The COD removal efficiency and the concentration of COD in the wastewater in-out of UAF and MBR were demonstrated in Figure 4. Figure 5 showed the change of MLSS, sludge loading rate and ratio of F/M in the MBR.

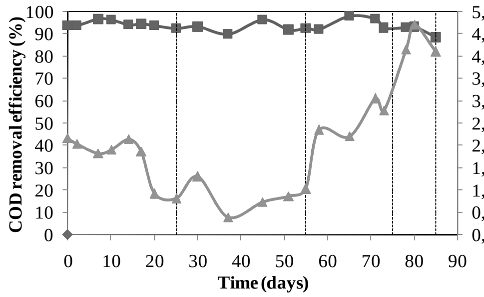

Figure 4a: Change of OLR and COD removal efficiency in MBR (▲*:OLR;* ■*:* COD removal efficiency*)*

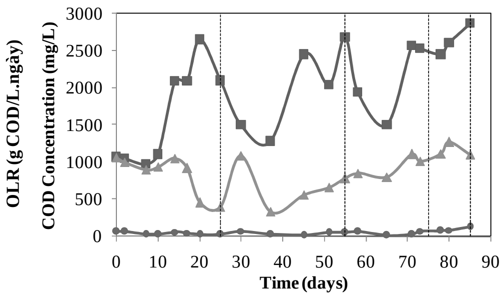

Figure 4b: Change of concentration of COD in wastewater in-out of the UAF and MBR *(■:COD of UAF inlet; ▲: COD of UAF outlet; ●: COD of MBR outlet)*

The result of this experiment shown that, right from the start, the COD removal efficiency achieved above 94% although the high COD concentration of the inflow. The MLSS remained stable at 12.5-14.0 g/L during phase 1, but depressed nearly 30% in phase 2, leading to a decrease of COD removal. It could be due to the short of organic content in the inflow of MBR resulted in the oxygenation of intracellular of activated sludge in phase 2.

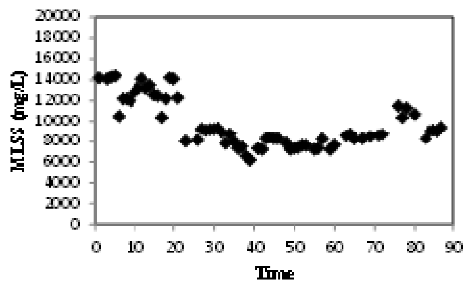

Figure 5a: MLSS in MBR

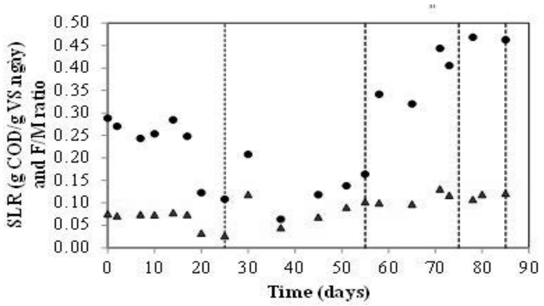

Figure 5b: Sludge loading rate and ratio of F/M in MBR *(●:*SLR*; ▲: F/M)*

In order to test the threshold and performance of MBR, phase 3 and 4 started with the continuous increase of OLR and HLR in the reactor (3-4.5 g COD/L.day and 2-4 L/L.day). At phase 3, the sludge loading rate was 0.4 g COD/g sludge.day and ratio of F/M stable at 0.1 with the hydraulic retention time of 9 hour, the efficiency of COD removal was 95%, and the COD concentration in effluent below 75 mg/L (column 1, QCVN 40:2011/BTNMT). Compared to the result of Wang, Chae and Churchouse's research, this study shown considerably achievement in MBR performance for high-strength wastewater (Churchouse, 1998; Wang ***et al.***, 2005; Chae ***et al.***, 2007). Once the sludge loading rate reached at 0.5 g COD/g sludge.day, the effluent quality declined, COD removal efficiency was below 90% and COD concentration in effluent was higher than 75 mg/L. Similarly, in the research of Chang and Churchouse, the COD removal efficiency reached at 85% at the organic loading rate of 2.7 g COD/L.day (Churchouse, 1998; Chang ***et al.***, 2007). The result of MBR performance demonstrated the great advantages of MBR system compared to the traditional activated sludge, regarding the adaptation to change of inflow, pollutant concentration and OLR of the influent, especially in the food industries. The optimum range of operation data for the best performance of MBR system in treating rich organic stream was recommended phase 3.

3.4. Assess the characteristics of effluent of hybrid technology UAF-MBR

The change of pH and ammonium concentration in the wastewater in-out of UAF-MBR was recorded in Figure 6 during operation time. The pH value of wastewater out of UAF gradually went up from approximately 5 to 7 in the first 10 days and remained constant around 7.02 ± 0.29 (within the optimum range for methanogens of 6.7-7.4), which proved the development of anaerobic microorganism and methane production in the UAF. Concurrently, the anaerobic fermentation of rich organic and nutrient matter in brewery wastewater led to the increasing of ammonium, from 32.3 ± 14.7 mg NH_4^+-N /L of the brewery wastewater to 52.5 ± 23.8 mg NH_4^+-N /L in the effluent of UAF. The change of these value proved that the hydrolysis had been strongly active at the very first beginning hence; the rate of hydrolysis was not the limiting factor of the whole anaerobic process in UAF treating easily biodegradable wastewater

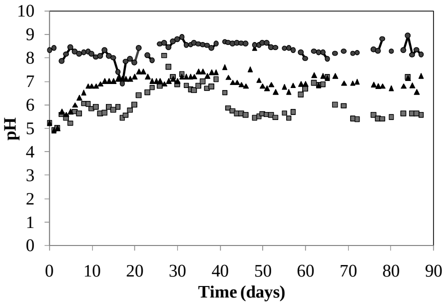

(a)

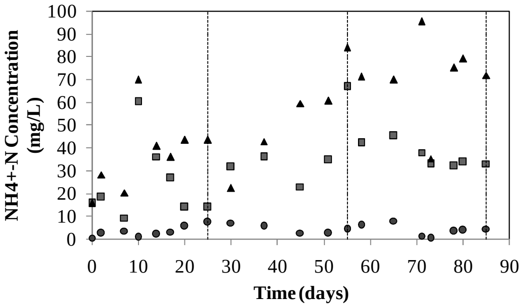

(b)

Figure 6: Change of pH value (a) and NH_4^+*-N* concentration (b) in the wastewater in-out of UAF-MBR ***(■: value of UAF inlet; ▲: value of UAF outlet; ●: value of MBR outlet)***

The concentration of ammonium in the wastewater drastically dropped in MBR due to the nitrification process and fluctuated around 4.0 ± 2.0, keep below 10 mg/L (column A, QCVN 40:2011/BTNMT) throughout the operation time. The NH_4^+-N removal effiency of MBR and of whole system (UAF-MBR) was 91.2± 7.5% and 83.6 ± 16.0%, correspondingly.

3.5. Sludge stabilization and methane production

The accumulation of volume of methane produced in three anaerobic reactors (control, UAF's sludge and MBR's sludge was shown in Figure 7. In term of energy recovery, the methane yield of 3 kinds of sludge: UASB, UAF and MBR were 174, 149 and 153 NL/g COD_{added}, equivalent to the methane production efficiency of those 50, 43 and 44%. It pointed out that, the settled sludge down in UAF consisted of mostly hard-biodegradable particulate (the easily part had been already degraded better in UAF than in UASB); hence the methane yield generated from anaerobic digestion of UAF was lower than in UASB sludge.

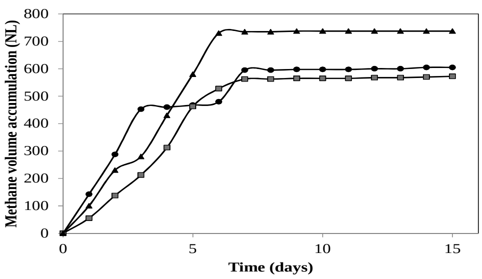

Figure 7: Accumulated volume of methane producing in anaerobic reactors in experiment 2 *(●: reactor 1 of UASB sludge; ■: reactor 2 of UAF sludge; ▲: reactor 3 of MBR sludge).*

The VS and COD removal or the stabilization of sludge efficiency of all reactors achieved about 61-66%. This result was agreed with the other research on anaerobic digestion of sewage sludge, the organic matter removal achieved only 40-70% and the methane gas production were 35-60% if sludge had not been pre-treated (Wen *et al.*, 1999; Carballa *et al.*, 2005).

4. CONCLUSION

In this paper, a laboratory scale of the UAF-MBR system was tested for treating brewery wastewater and the following results were obtained:

i. The UAF had a stable performance at room temperature (~20^0C) after 20 operating days, the COD removal efficiency of above 70% and a methane yield of 0.25 NL/g COD_{added} were obtained at hydraulic loading rate of 1.5 L/(L.day) and organic loading rate of 2-4 g COD/L.day.
ii. The MBR did not required the start-up period if obtained a sufficient microbial seeding. The highest removal efficiency of pollutants of above 94% was achieved at a concentration of 7.5-8.5 g MLSS/L. The MBR process stability was attained at flux and organic loading rate were below 9 L/(m^2.h) and 3 g COD/(L.day), correspondingly, the sludge loading rate of 0.3-0.4 g COD/L.day and ratio of F/M at around 0.1.
iii. The removal efficiencies of COD, BOD_5 và TSS in the hybrid process UAF-MBR were above 97%, 95 and 98%, correspondingly; the quality of the

effluent stable and conform the column A, QCVN 40:2011/BTNMT, which could be reuse for numerous purposes in brewing processes.

iv. Anaerobic digestion of sludge discharged from UAF and MBR at mesophilic condition (~35-37^{0}C) recovered approximately 150 NL of methane per 1 g $COD_{removed}$. The VS and COD removal or the stabilization of sludge efficiency of all reactors achieved about 61-66%.

As an effort for sustainable development in food industries and wastewater treatment, the remarkable results of this research highlighted that this hybrid technology of UAF and MBR is an effective and energy-saving solution for treating rich organic waste streams.

ACKNOWLEDGEMENT

The research is within in the framework of the scientific research “Study on design and manufacture of small-scale wastewater treatment system applying membrane bioreactor technology”, part of Project ‘Development of Vietnamese environmental industry in 2015, up to 2025, sponsored by Ministry of Industry and Trade, Vietnam.

REFERENCE

APHA-AWWA-WPCF (1999). *Standard Methods for the examination of water and wastewater*. L. S. Clesceri and Greenberg. Washington, DC 20005, American Public Health Association.

Brito, A. G., J. Peixoto, J. M. Oliveira, J. A. Oliveira, C. Costa, R. Nogueira and A. Rodrigues (2007). *Brewery and winery wastewater treatment: some focal points of design and operation*. Reykjavik, Iceland, *Springer*.

Carballa, M., F. Omil, A. C. Alder and J. M. Lema (2005). *Comparison between the conventional anaerobic digestion of sewage sludge and its combination with a chemical or thermal pre-treatment concerning the removal of pharmaceuticals and personal care products*. *4th International Symposium on Anaerobic Digestion of Solid Waste*, Copenhagen, Denmark.

Chae, S. R., S. T. Kang, S. M. Lee, E. S. Lee, S. E. Oh, Y. Watanabe and H. S. Shin (2007). "*High reuse potential of effluent from an innovative vertical submerged membrane bioreactor treating municipal wastewater*." Desalination **202**(1-3): 83-89.

Chang, T. C., S. J. You and S. H. Chuang (2007). "*Evaluation for the reclamation potential of high-tech industrial wastewater effluent treated with different membrane processes*." Environmental Engineering Science **24**(6): 762-768.

Chernicharo, C. A. d. L. (2007). *Anaerobic Reactors*. Biological Wastewater Treatment Series. London, UK, IWA Publishing. 4.

Chong, S., T. K. Sen, A. Kayaalp and H. M. Ang (2012). "*The performance enhancements of Upflow Anaerobic Sludge Blanket (UASB) reactors for domestic sludge treatment - A State of the Art Review*." Water Research.

Churchouse, S. (1998). "*Membrane bioreactors for wastewater treatment - operating experiences with the Kubota submerged membrane activated sludge process*." Membrane Technology **83**: 5-9.

Elmitwalli, T. A., J. Soellner, A. De Keizer, H. Bruning, G. Zeeman and G. Lettinga (2001). "*Biodegradability and change of physical characteristics of particles during anaerobic digestion of domestic sewage*." Water Research **35**(5): 1311-1317.

Hai, F. I., K. Yamamoto and W. Editor-in-Chief:Â Â Peter (2011). *4.16 - Membrane Biological Reactors*. Treatise on Water Science. Oxford, Elsevier: 571-613.

Lettinga, G., S. Rebac and G. Zeeman (2001). "*Challenge of psychrophilic anaerobic wastewater treatment. Trends in Biotechnology*." Biotechnology Advances **19**(9): 363-370.

Oreopoulou, V. and W. Russ, Eds. (2007). *Utilization of By-Products and Treatment of Waste in the Food Industry*. Brewery and winery wastewater treatment: some focal points of design and operation. Reykjavik, Iceland, Springer.

Tran, D. H. (2002). *Study on Wastewater treatment for brewery factories in Vietnam*, Ministry of Education and Tranining. 2/2002.

Wang, Y., X. Huang and Q. Yuan (2005). "*Nitrogen and carbon removals from food processing wastewater by an anoxic/aerobic membrane bioreactor*." Process Biochemistry **40**(5): 1733-1739.

Wen, C., X. Huang and Y. Qian (1999). "*Domestic wastewater treatment using an anaerobic bioreactor coupled with membrane filtration*." Process Biochemistry **35**(3â€“4): 335-340.

Yu, H. and G. Gu (1996). "*Biomethanation of brewery wastewater using an anaerobic upflow blanket filter*." Clearner Production **4**(3-4): 219-223.

The risk assessment by the AHP method and characteristics of the landslides in Sa Pa ,Lao Cai province northern Vietnam

Dr. Takami KANNO[1], Dr. Hiroyuki YOSHIMATSU[1]
Mse. Do Ngoc Trung[2], Sr. Eng. Nguyen Quoc Hung[2]
[1]Kawasaki Geological Engineering Co.,Ltd, Japan &
[2]Vietnam Japan Engineering Consultants Co.,Ltd, Vietnam

ABSTRACT

Sa Pa district in Lao Cai province is located at the foot of the highest peak Fansipan in Indocina, that is one of leading tourist destination in Vietnam. The slope disasters such as landslides and collapse has occurring frequently along the Highway No 4 between Sa Pa and Lao Cai, and that was forced to closed to traffic frequently.
In this project, we conducted field survey and topographical analysis based on satellite images for investigating features such as collapse and landslides along the Highway No 4 between Sa Pa and Lao Cai. Based on the results of these investigations, we have created a hazard map, and carried out risk assessment by the AHP which is one of operations research method. Furthermore, we carried out detailed investigation of topographical survey using the terrestrial LiDAR, drilling survey and high-density electrical prospecting for the typical deep-seated landslide along the Highway No 4. As results of the project, we have examined the methods for the disaster prediction, prevention and the countermeasure construction and early warning system.

Keywords: *AHP, landslide, deep-seated landslide, landslide-mapping, risk assessment, early warning system, disaster prediction, disaster prevention*

Crack identification in frame structures by using the wavelet analysis of mode shapes

TranVan Lien[1], Trinh Anh Hao[2]

ABSTRACT

Crack identification in structures is very important and attractive for many researchers. However, most of the published works deal with the simple structures such as beam or plates. There are few papers devoted to study frame structures that could be mostly investigated only by using the conventional finite element method. The present report deals firstly with a development of the dynamic stiffness method for modeling framed structure damaged to multiple cracks represented by equivalent springs. Then, the dynamic stiffness model of cracked frame is implemented to the problem of crack identification from structural vibration characteristics in conjunction with the wavelet analysis. The theoretical development was illustrated and validated by numerical examples.

Keywords: Crack Identification; Mode Shape; Wavelet Analysis; Dynamic Stiffness Method.

1. Introduction

The problem of crack identification in structure has attracted a considerable attention of engineer-researchers for several recent decades due to its practical importance. A lot of procedures have been emerged to detect and quantify cracks in structures [1]. Among the numerous proposed methods the wavelet-based approach shows to be the most effective, especially for detecting the small local damage such as crack in structures [2-5]. However, most of the published works deal with the simple structures such as beam or plates by using the analytical or the semi-analytical method. There are few papers devoted to study space frame structures that could be mostly investigated only by using the conventional finite element method (FEM).

Surace and Ruotolo [6] stated that presence of a crack in a cantilever beam can be detected by the wavelet coefficient distribution computed from the time history response measured at free end. Liew and Wang [7] demonstrated that single crack in a simply supported beam can be localized from spatial wavelet transform of free vibration response measured along the beam length at a given time moment. This study was then continued by Wang and Deng [8] for the case of impulse response of beam and plate with different boundary conditions. Douka et al. [9] have achieved at identifying both the location and size of single crack in

[1] *Corresponding Author, Associate Professor, Ph. D, Faculty of Civil Engieering, University of Civil Engineering, 55 Giai Phong Road, Hanoi, Vietnam, Tel: (84) 4 3869 1435; Email: LienTV@hotmail.com;*

[2] *Master of Civil Engieering, V-CIC, Hanoi, Vietnam, Email: TrinhAnhHao@yahoo.com*

a cantilever beam by using the wavelet coefficient distribution along the beam length of the fundamental mode shape. The crack depth is estimated by so-called the intensity factor related to the wavelet maxima coefficient. Chang and Chen [10] have proposed a method for estimating both the position and depth of multiple cracks in beam based on the spatial wavelet transform of mode shapes. The crack depth evaluation has been simplified by using the estimated crack positions and available natural frequencies. This idea was then extended by Zhang et al. [11] to multiple crack detection for stepped beam with involved the transfer matrix method. Rucka and Wilde [12] reported that choosing properly wavelet function is important for crack detection in structure. Zhong and Oyadiji [13] demonstrated that the stationary wavelet transform is a useful tool for crack detection from only the mode shape of cracked beam-like structure. Gokdag and Kopmaz [14] have proved that the approximation component of the wavelet decomposition is similar to the mode shape of undamaged structure so that it can be employed as the base-line data for conducting a damage index based on differences of the wavelet coefficients. The proposed methods for crack detection based on the spatial wavelet transform requires a high space resolution that implies also a large number of sensors needed for measuring the response signal. Zhu and Law [15] have employed the time domain response measured at a point in a beam subjected to moving load as the input signal for the wavelet analysis. The crack position can be determined easily from the continuous wavelet coefficient plotted versus position of moving load. The most of the published works have been devoted to apply the wavelet transform for crack detection in beam-like structures. A simple plan frame with cracks subjected to static load has been exceptionally investigated by Ovanesova and Suarez in reference [16] where the static response was obtained by the FEM. The actual position of crack is observable on the wavelet coefficient distribution but dominant ridges are apparent at the frame corners. Therefore, the wavelet-based approach to the crack detection for frame is a gap that has to be fulfilled.

The objective of the present report is to apply the powerful wavelet-based method for crack identification in framed structures. First, the dynamic stiffness method (DSM) is enhanced to conduct the more accurate dynamic model of multiple cracked frame structures that allows for obtaining mode shapes. Then, the stationary wavelet transform is applied for crack detection from spatial wavelet coefficient of the structure mode shapes. A case study has been accomplished to investigate also the influence of measurement noise on the wavelet coefficients.

2. The mode shapes of a multiple cracked beam element

Let us consider a beam of length L subjected to bending on surface Oxy, cross-section area $A=b\times h$, moment of inertia I and Young's modulus E, mass density ρ. Free vibration of the beam is described by the following equation [17]:

$$\frac{d^4\Phi(x,\omega)}{dx^4} - \lambda^4\Phi(x,\omega) = 0 \tag{1}$$

Where $\Phi(x,\omega)$ denotes complex amplitude of the vibration; $\lambda = \sqrt[4]{\omega^2 \frac{\rho A}{\hat{E}I_z}\left(1 - \frac{i\mu_2}{\omega}\right)}$; $i = \sqrt{-1}$ is the dynamic parameter; $\hat{E} = E(1 + i\mu_1\omega)$ is complex modulus; μ_1, μ_2 are the material and viscous damping coefficients, respectively; ω is the circular frequency (*rad/s*). When $\lambda=0$ corresponding to $\omega=0$ it is a static deformation.

Suppose that the beam has cracks at positions x_j with the depths of a_j, $j=1,2,...,n$, where $x_0 = 0 < x_1 < x_2 < ... < x_n < x_{n+1} = L$ (Fig. 1). The cracks are modeled as rotational springs with the stiffness k^z_j calculated by converting formulas [17, 18].

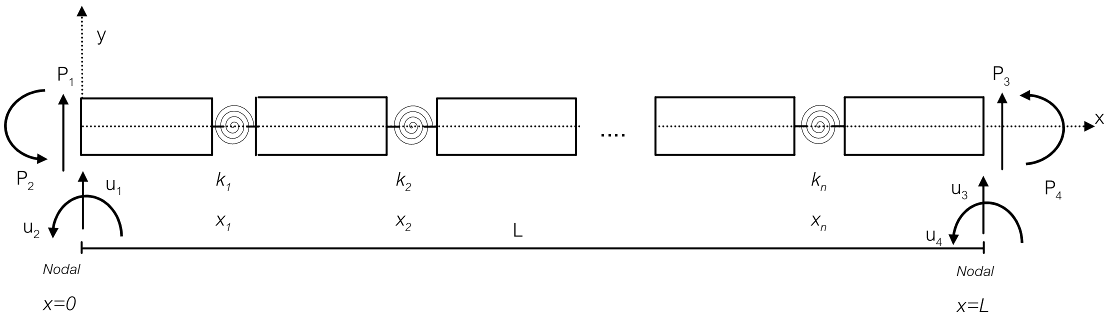

Fig. 1: Modeling of a multiple-cracked beam element

The general solution of equation (1) for the sub-segment $j=1, 2, ..., n+1$ with $x \in (x_{j-1}, x_j)$ has the form of:

$$\Phi_j(x) = K_1(\lambda\bar{x})Z^+_{j-1,1} + \frac{K_2(\lambda\bar{x})}{\lambda}Z^+_{j-1,2} + \frac{K_4(\lambda\bar{x})}{\hat{E}I_z\lambda^3}Z^+_{j-1,3} - \frac{K_3(\lambda\bar{x})}{\hat{E}I_z\lambda^2}Z^+_{j-1,4}\ ;\ \bar{x} = x - x_{j-1} \tag{2}$$

Where $K_i(x)$ are Krylov functions and $Z^+_{j-1,i}$ are initial parameters of this sub-segment:

$$K_1(x) = \frac{\cosh x + \cos x}{2};\ K_3(x) = \frac{\cosh x - \cos x}{2};\ K_2(x) = \frac{\sinh x + \sin x}{2};\ K_4(x) = \frac{\sinh x - \sin x}{2}$$

$$\{Z^+_{j-1,1}, Z^+_{j-1,2}, Z^+_{j-1,3}, Z^+_{j-1,4}\}^T = \left(\Phi(x_{j-1}+0); \Phi'(x_{j-1}+0); \hat{E}I_z\Phi'''(x_{j-1}+0); -\hat{E}I_z\Phi''(x_{j-1}+0)\right)^T$$

By using the combination of dynamic stiffness and transfer matrix methods, we yield [18]:

$$[P_1\ P_2\ P_3\ P_4]^T = [K_e].[u_1\ u_2\ u_3\ u_4]^T \tag{3}$$

The matrix $[K_e]_{4x4}$ is called the dynamic stiffness matrix for the multiple cracked beam.

Using the general solution (2) and equation (3), we can determine the free vibration shape function of multiple cracked beam elements. For example N_1, we determine the nodal forces P_1 and P_2 based on equation (3) with the following condition $u_1 = 1$; $u_2 = u_3 = u_4 = 0$

$$\begin{pmatrix} P_1 \\ P_2 \end{pmatrix} = \begin{pmatrix} k_{11} & k_{12} & k_{13} & k_{14} \\ k_{21} & k_{22} & k_{23} & k_{24} \end{pmatrix} \begin{pmatrix} 1 & 0 & 0 & 0 \end{pmatrix}^T = \begin{pmatrix} k_{11} \\ k_{21} \end{pmatrix}$$

The initial parameters of first sub-segment (*j=1*) are:

$$Z_0^+ = \left\{ Z_1^+(0) = 1; \quad Z_2^+(0) = 0; \quad Z_3^+(0) = k_{11}; \quad Z_4^+(0) = k_{21} \right\}$$

Therefore, the shape function N_1 for the first sub-segment is:

$$N_1^{(1)} = K_1(\lambda \bar{x}) + \frac{K_4(\lambda x)}{\hat{E}I_z \lambda^3} k_{11} - \frac{K_3(\lambda x)}{\hat{E}I_z \lambda^2} k_{21} \tag{4}$$

By using transfer matrix method, we get the shape function N_1 for the next sub-segment. In the case of intact beam, the shape function has the formula:

$$N_1 = K_1(\lambda x) + \frac{\tilde{K}_1 \tilde{K}_2 - \tilde{K}_3 \tilde{K}_4}{\tilde{K}_3^2 - \tilde{K}_2 \tilde{K}_4} K_4(\lambda x) - \frac{\tilde{K}_2^2 - \tilde{K}_1 \tilde{K}_3}{\tilde{K}_3^2 - \tilde{K}_2 \tilde{K}_4} K_3(\lambda x) \tag{5}$$

where $\tilde{K}_i = K_i(\lambda L)$. When damping coefficients are zeros $\mu_1 = \mu_2 = 0$, one will get the shape function N_1 determined by Leung [19].

The dynamic stiffness matrices of structure $\hat{K}(\omega)$ are assembled similarly as FEM from the dynamic stiffness matrices *[K_e]* of each beam elements. Thus, the problem of free vibration of structures with the multiple-cracked bar elements leads to the determination of natural frequencies and mode shapes from the following equation:

$$\hat{K}(\omega)U = 0 \tag{6}$$

Where the natural frequencies ω_j are determined from the equation:

$$\det \hat{K}(\omega) = 0 \tag{7}$$

The nodal displacements U corresponding to the natural frequencies ω_j will be determined by equations (6). Having obtained the nodal displacements $u_1; u_2; u_3; u_4$, we receive the mode shapes of the structure with the multiple-cracked beam elements from the expression:

$$w(x) = N_1(x)u_1 + N_2(x)u_2 + N_3(x)u_3 + N_4(x)u_4 \tag{8}$$

3. Wavelet analysis

Wavelet analysis starts by selecting a basis function from wavelet families. This function is called "*mother wavelet*" $\psi(x)$. The continuous wavelet transform

(CWT) is then defined as:

$$C(a,b)=\frac{1}{\sqrt{a}}\int_{-\infty}^{\infty} f(x)\psi\left(\frac{x-b}{a}\right)dx=\int_{-\infty}^{\infty} f(x)\psi_{a,b}(x)dx \tag{9}$$

Where $a>0$ and b are dilation scale and transition parameter; $\psi_{a,b}(x)$ is function:

$$\psi_{a,b}(x)=\frac{1}{\sqrt{a}}\psi\left(\frac{x-b}{a}\right) \tag{10}$$

The result of CWT is wavelet coefficients $C(a,b)$ showing the correlations between the wavelet function and the signal analyzed $f(x)$. Hence, sharp transitions in f(x) create wavelet coefficients with large amplitude and this precisely is the basis of the proposed identification method.

The initial signal $f(x)$ can be reconstructed from the wavelet coefficients $C(a,b)$:

$$f(x)=\frac{1}{K_\psi}\int_{-\infty}^{\infty}\int_{-\infty}^{\infty} C(a,b)\psi_{a,b}(x)\frac{dbda}{a^2} \tag{11}$$

where the constant K_ψ depends on wavelet type.

Assuming that wavelet coefficients are valid only for $a<a_0$, appropriate for high-frequency components in the signal, for $a>a_0$, seen as interference. In this case, the signal reconstruction needs the complement corresponding to $a>a_0$. To do this, another function $\phi(x)$ called “*scaled function*” is used:

$$D(a_0,b)=\frac{1}{\sqrt{a_0}}\int_{-\infty}^{\infty} f(x)\phi\left(\frac{x-b}{a_0}\right)dx=\int_{-\infty}^{\infty} f(x)\phi_{a_0,b}(x)dx \tag{12}$$

The scaled function is nessesary for numerical implementation. Instead of (11), the initial signal $f(x)$ can be reconstructed from:

$$f(x)=\frac{1}{K_\psi}\int_{a=0}^{a_0}\int_{b=-\infty}^{\infty} C(a,b)\psi_{a,b}(x)\frac{dbda}{a^2}+\frac{1}{K_\psi a_0}\int_{b=-\infty}^{\infty} D(a_0,b)\phi_{a_0,b}(x)db \tag{13}$$

One drawback of the CWT is that a very large number of wavelet coefficients $C(a,b)$ are generated during the analysis. In order to reduce the amount of computation, the discrete wavelet transform (DWT) used discrete scale and translation parameters in dyadic form: $a=2^j$; $b=k.2^j$ where j and k are integers, the integer j is referred to as the dyadic level. And the DWT is as follows:

$$C_{j,k}=2^{-j/2}\int_{-\infty}^{\infty} f(x)\psi\left(2^{-j}x-k\right)dx=\int_{-\infty}^{\infty} f(x)\psi_{j,k}(x)dx \tag{14}$$

Where $\psi_{j,k}(x)$ is discrete wavelet function:

$$\psi_{j,k}(x)=2^{-j/2}\psi\left(2^{-j}x-k\right) \tag{15}$$

Instead of (11), the signal in DWT can be reconstructed from the wavelet coefficients $C_{j,k}$:

$$f(x) = \sum_{j=-\infty}^{\infty} \sum_{k=-\infty}^{\infty} C_{j,k} 2^{-j/2} \psi\left(2^{-j} x - k\right) \tag{16}$$

The signal will be passed through a series of filters, the high-pass filters and low-pass filters, to generate high-frequency and low-frequency components, respectively. Instead of (13), the signal in DWT can be represented by approximations and details:

$$f(x) = \sum_{j=-\infty}^{J} \left(\sum_{k=-\infty}^{\infty} cD_j(k) \psi_{j,k}(x) \right) + \sum_{k=-\infty}^{\infty} cA_J(k) \phi_{j,k}(x) = \sum_{j \le J} D_j(x) + A_j(x) \tag{17}$$

Where $A_j(x)$ is the approximation at level J; $D_j(x)$ is the detail at level $j \le J$:

$$D_j(x) = \sum_{k=-\infty}^{\infty} cD_j(k) \psi_{j,k}(x);\ A_j(x) = \sum_{k=-\infty}^{\infty} cA_J(k) \phi_{j,k}(x) \tag{18}$$

cDj and cAj are detail coefficient and approximation coefficient, respectively:

$$cD_J(k) = \int_{-\infty}^{\infty} f(x) \psi_{J,k}(x) dx;\ cA_J(k) = \int_{-\infty}^{\infty} f(x) \phi_{J,k}(x) dx \tag{19}$$

For this study, we are interested in the detail signal. A it will be shown with the numerical examples, if f(x) is response signal, typically the deflection curve, the signal $D_j(x)$ contain the information necessary to detect the cracks in the structure.

But the classical DWT suffers a drawback that it is not a time-invariant transform. This means that, even with periodic signal extension, the DWT of a translated version of the original signal is not, in general, the translated version of the DWT of the original signal. To circumvent this problem, one can resort to a redundant decomposition of signal as [13]

$$\widetilde{D}_{j,k} = 2^{-j/2} \int_{-\infty}^{\infty} f(x) \psi\left(\frac{x-k}{2^j}\right) dx;\ \widetilde{A}_{j,k} = 2^{-j/2} \int_{-\infty}^{\infty} f(x) \phi\left(\frac{x-k}{2^j}\right) dx \tag{20}$$

The modified approximation and detail coefficients (20) constitute the so-called stationary wavelet transform (SWT) that has a great potential in signal processing for structural health monitoring.

It should be noted that the SWT of the origin data is not decimated. That is, the size of the SWT data does not diminish after the transform. Conversely, in DWT, the resulting transformed data are half of the original signal size. Thus, DWT is a down-sampling process which results in a poorer representation of the original signal. Conversely, SWT is an up-sampling process which leads to redundant representation of the origin signal. Therefore, the detail coefficient of DWT decomposition has less feature information than that of SWT. Consequently, SWT has great potential for feature extraction and facilitates the identification of salient features in a signal.

4 Numerical results and discussion

For illustration a planar frame consisting of 6 two-dimensional beam elements as shown in Figure 2a is considered. All the beam have the same cross section $b \times h = 0.14 \times 0.24 m^2$; Young's modulus $E = 3.5 \times 10^{10} N/m^2$; Poisson ratio ν=0.3 and mass density $\rho = 2500 kg/m^3$. Two major scenarios of cracked frame are adopted such as (a) multiple cracks of different location and depth occurred in a beam and (b) both the beam and column elements are damaged to cracks. First three mode shapes of the undamaged structure are shown in Figures 2b-d.

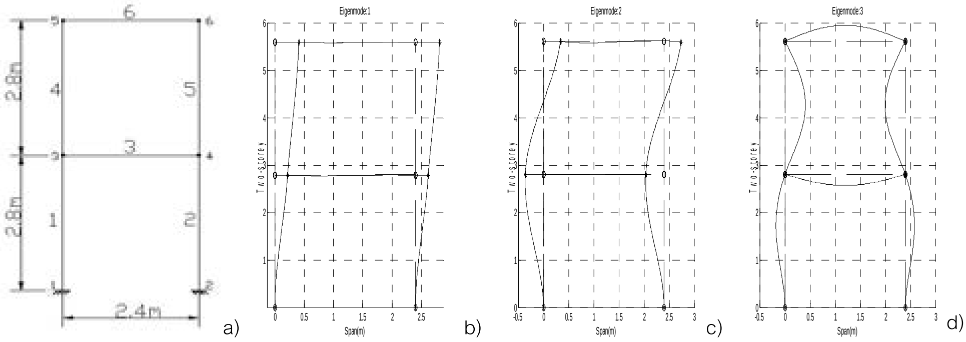

Fig. 2: A frame structure model (a) and its first three undamaged mode shapes (b-d).

Case 1: *cracked beam of number* 3. The detail wavelet coefficients of first three mode shapes in element 3 cracked at distance *0.6m* from the left end (node 3) are given in Figures 3. Obviously, crack position is not detectable from the original mode shape; however, it is apparent in the detail wavelet coefficient distribution along the beam span. Of course, the spike at the crack position gets to be higher for increasing crack depth (*10%, 20%, 30%*). The wavelet coefficients in the case of two cracks occurred at distances *0.4m* and *0.9m* from the node 3 of the element 3 are shown in Figures 4. Even the two cracks have the same depth (*10%, 20%, 30%*) the high of the wavelet coefficient spikes is different in dependence on the mode number. Namely, for the first and second modes the crack closed to the node 3 is more apparent and it is in contrary for the third mode shape.

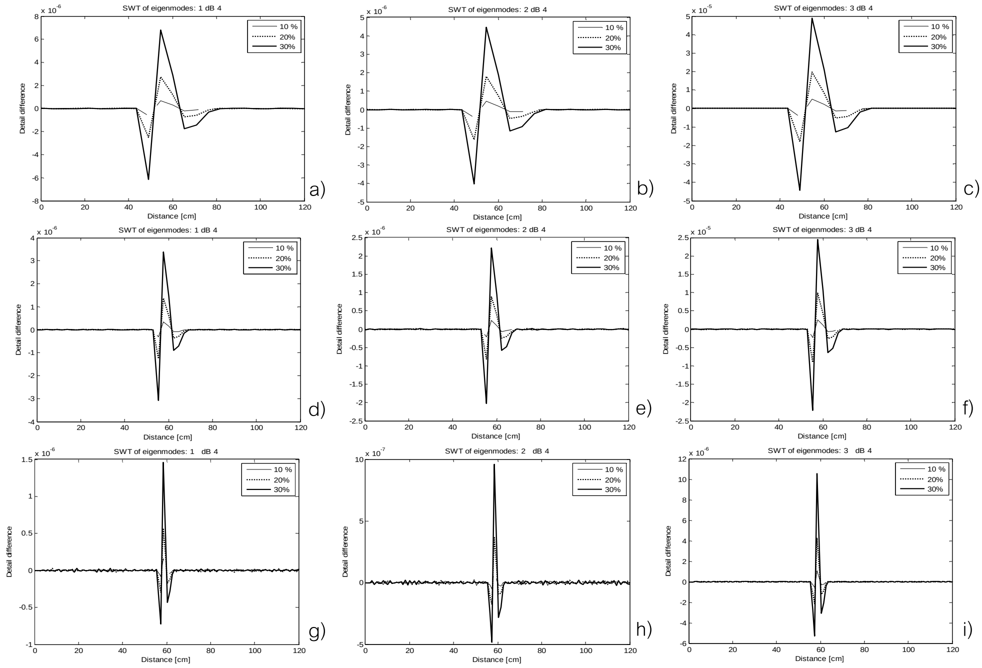

Fig. 3: The detail wavelet coefficients of first three mode shapes in the element 3 with a crack at distance 0.6m from node 3.

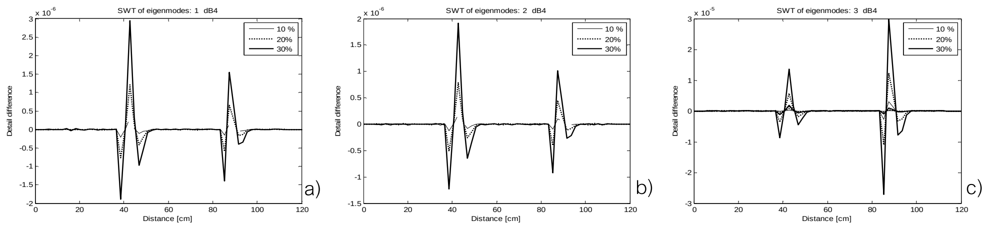

Fig. 4: Detail wavelet coefficients of the first three mode shapes for the element 3 with two cracks at distance *0.4m* and *0.9m* from the left end.

Case 2: *Cracked beam and column*. Suppose that the column (first element) and the beam (third element) are both cracked. The wavelet coefficient distribution for the first three mode shape in the case of a crack at the distance *1m* from the fixed end of column 1 and a crack at the distance *0.6m* from the left end of element 3 is plotted in Figures 5a-c. A crack at distance *2m* is added to the column element so that the frame gets to have three cracks and the wavelet coefficients of the mode shape in the frame diagram are shown in Figure 5d-f. From the Figures it can be noted that for the fundamental mode representing mostly the vibration of column the crack closer to the fixed clamp make more influence on the wavelet coefficients. In the second mode, influence of the crack closed to the node 3 increased. The crack in the horizontal beam is more detectable than that occurred at the column in the wavelet coefficient plot for the third mode shape while it is visible also in the first and second mode shape diagrams.

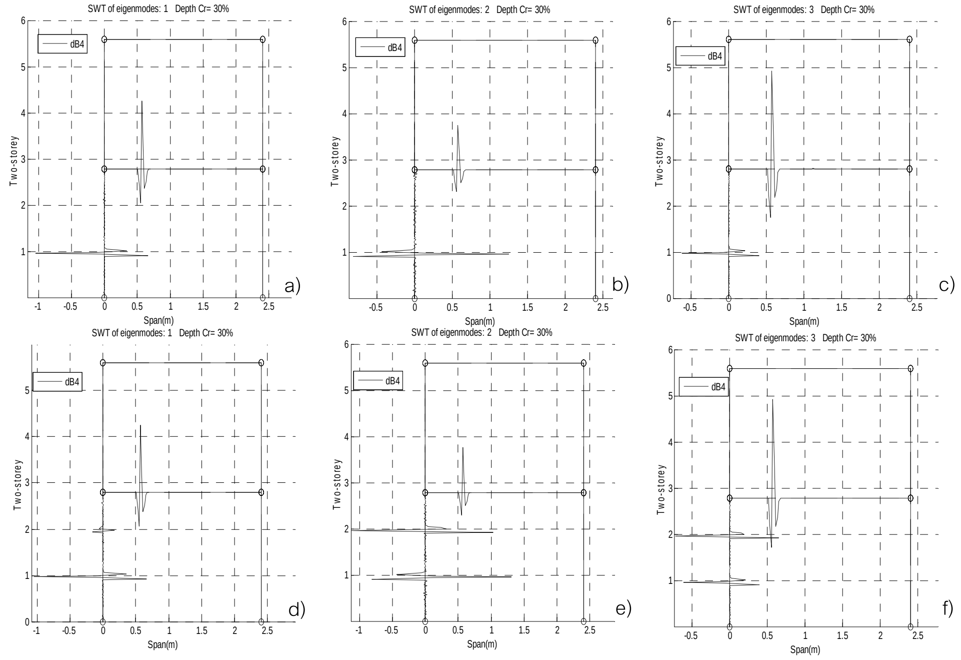

Fig. 5: The detail wavelet coefficients of first three mode shape in the case of cracked column and beam

Case 3: *influence of the noise*. The natural mode shapes of the frame cracked at distance *0.6m* of the beam element 3 have been computed and added with a Gaussian noise generated by Matlab function *Rand*(*n*). For the modal deflection of the element denoted by vector $\mathbf{Y} = \{y_1, ..., y_N\}$ the noise vector is introduced by

$$y_{noise} = \frac{y_{nr}}{norm(y_{nr})} \cdot \frac{norm(y_{intact})}{10^{(0.05 \times SNR)}} \qquad (21)$$

where $y_{nr} = Rand(size(y_{intact}))$ and *SNR* is the signal to noise ratio measured in decibel (dB). The noise level *SNR* examined in this study is of *75*, *80* and *95d*B and the wavelet coefficients of the noised first two mode shapes are given in Figure 6. It can be seen from the Figure that the crack position can be clearly detected by using fundamental mode shape if the SNR exceeds *80dB* while using the second mode shape enables a crack to be exactly localized for the noise level from 75dB.

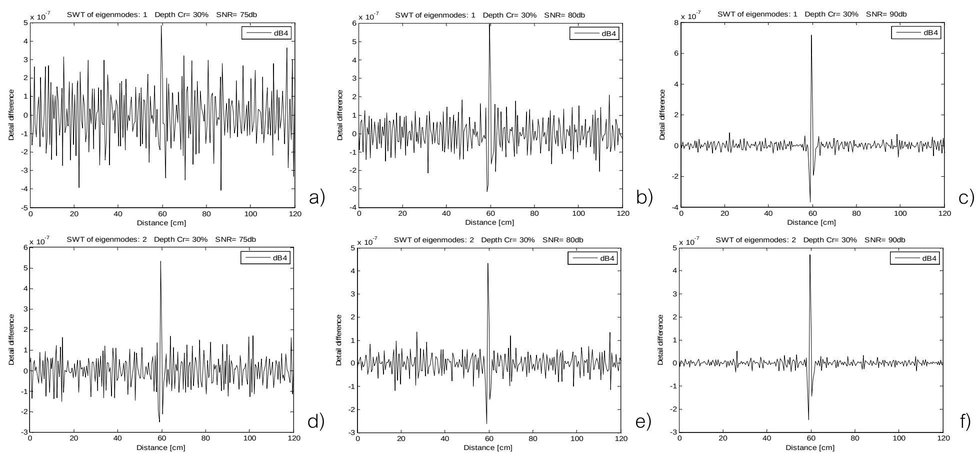

5. Conclusion

Thus, in this report the DSM has been developed for more accurate dynamic analysis of space framed structures with multiple cracked 3D beam elements; The SWT has been applied to spatial signals associated with the natural vibration mode shapes computed by using the developed DSM. The illustrating numerical results verify that the developed dynamic model of cracked frame structures combined with the SWT can be reliably employed for localization of cracks in frame structures with data contaminated with noise of SNR from 75dB. The subsequent study is to estimate crack size from the wavelet coefficients.

References

[1] H. Sohn, C.R. Farrar, F.M. Hemez et al (2004), *A Review of Health Monitoring Literature 19962001*, Los Alamos National Laboratory, Los Alamos, New Mexico, Report No LA13976-MS.

[2] W.J. Staszewski (1998), "Structural and Mechanical Damage Detection Using Wavelets", *The shock and Vibration Digest,* 36, 3443-3468.

[3] Z. Hou, M. Noori and R.St. Amand (2000), "Wavelet-Based Approach for Structural Damage Detection", *Journal of Engineering Mechanics,* Vol 126 (7), 677-683.

[4] S.T. Quek et al (2001), "Sensitivity Analysis of Crack Detection in Beams by Wavelet Technique", *International Journal of Mechanical Sciences*, 43, 2899-2910, 2001.

[5] M.M. Reda Tana et al. (2006), "Wavelet Transform for Structural Health Monitoring: A Compendium of Uses and Features", *Structural Health Monitoring*, Vol 5(3), 267-295.

[6] C. Surace and R. Ruotolo (1994), "Crack Detection of a Beam Using Wavelet Transform", *Proceedings of the* 12*th* *International Modal Analysis Conference*, Honolulu, Hawaii, pp.1141-1167.

[7] K.M. Liew and Q. Wang (1998), "Application of Wavelet Theory for Crack Identification in Structures", *Journal of Engineering Mechanics,* 124, 152–157..

[8] Q. Wang and X. Deng (1999), "Damage Detection with Spatial Wavelets", *International Journal of Solid and Structures* 36, 3443-3468.

[9] E. Douka, A. Loutridis and A. Trochidis (2003), "Crack Identification in Beam Using Wavelet Analysis", *International Journal of Solid and Structures,* 40, 3557-3569.

[10] C.C. Chang and L.W. Chen (2005), "Detection of the Location and Size of Cracks in the Multiple Cracked Beam by Spatial Wavelet Based Approach", *Mechanical Systems and Signal processing*, 19, 139-155..

[11] W. Zhang, Z. Wang and H. Ma (2009), "Crack Identification in Stepped Cantilever Beam Combining Wavelet Analysis with Transform Matrix", *Acta Mechanica Solida Sinica,* Vol 22(4), 360-368.

[12] M. Rucka and K. Wilde (2006), "Crack Identification Using Wavelets on Experimental Static Deflection Profiles", *Engineering Structures,* 28, 279-

288.

[13] S. Zhong and O. Oyadiji (2007), “Crack Detection in Simply Supported Beams without Baseline Modal Parameters by Stationary Wavelet Transform”, *Mechanical Systems and Signal processing*, 21, 1853-1884.

[14] H. Gokdag and O. Kopmaz (2009), “A New Damage Detection Approach for Beam-type Structures based on the Combination of Continuous and Discrete Wavelet Transforms”, *Journal of Sound and Vibration*, 324, 1158-1180.

[15] X.Q. Zhu and S.S. Law (2006), “Wavelet-based Crack Identification of Bridge Beam from Operational Deflection Time History”, *International Journal of Solid and Structures*, 43, 2299-2317.

[16] A.V. Ovanesova and L.E. Suáres (2004), “Applications of Wavelet Transforms to Damage Detection in Frame Structure”, *Engineering Structures*, 26, 39–49.

[17] N.T. Khiem and T.V. Lien (2001), A simplified method for natural frequency analysis of a multiple cracked beam, *Journal of Sound and vibration*, 2001, 245(4): 737-751.

[18] N.T. Khiem, T.V. Lien (2002), “The dynamic stiffness matrix method in forced vibration analysis of multiple cracked beam”, *Journal of Sound and Vibration*, 254(3), 541-555.

[19] Y.T. Leung (1993), *Dynamic Stiffness and Substructures*, Springer-Verlag, London.

[20] N.T. Khiem, T.V. Lien, D.T. Hung and T.A. Hao (2013),”Crack identification in frame structures by using the spectral element method and wavelet transform”, *Proceedings of the 6th ECCOMAS Conference on Smart Structures and Materials*, SMART2013, 24-26 June 2013, Italia.

Mechanical behavior of high damping rubber bearings at low temperatures

Dung Anh NGUYEN[1], Yoshiaki OKUI[1], Md. Shafquat HASAN[1], Hiroshi MITAMURA[2], Takashi IMAI[3],
[1] Department of Civil and Environmental Engineering, Saitama University, Japan.
s10de007@mail.saitama-u.ac.jp
[2] Civil Engineering Research Institute for Cold Region Sapporo, Japan
[3] Rubber Bearing Association, Japan

ABSTRACT

The paper is devoted to identify the mechanical behavior of high damping rubber bearings (HDRBs) at low temperatures. The rubber bearing tests were carried out in an environmental test chamber at -30°C, -20°C, and 23°C ambient temperatures. Sinusoidal loading tests with a frequency of 0.5 Hz were conducted to investigate the low temperature dependence of HDRBs. The experimental results indicate that the temperatures inside HDRBs are increased by sinusoidal loading, and the rise in the inside temperature becomes larger at lower ambient temperatures. In addition, it is shown that the stress-strain relationships of HDRBs is governed by the inside temperatures but not by the ambient temperature. Furthermore, the experimental results indicate that the hardening in the stress-strain relationship of HDRBs is significant at low temperatures. Therefore, the bilinear model cannot well represent HDRBs' behavior at low temperatures.

Keywords: *high damping rubber bearings, self-heating, inside temperature, temperature dependence.*

1. INTRODUCTION

High damping rubber bearings (HDRBs) are seismic isolating devices used widely in Japan, especially after Kobe earthquake in 1995. However, the mechanical behavior of HDRBs depends on temperatures and this dependence may affect the performance of the bearings, especially at low temperatures.
In the previous experimental investigations (Imai et al., 2010; Pinarbasi et al., 2007) considering the temperature dependence of mechanical behavior of rubber bearings, the ambient temperature in a test chamber is assumed to equal the inside temperature of rubber bearings. However, when subjected to cyclic loading, the energy dissipated by HDRBs is converted into heat and this heat may cause significant temperature rise inside rubber bearings. Takaoka et al, (2008) indicated that sinusoidal cyclic loading caused the inside temperature to rise by about 30^0C at room temperature, which leads that the yield load of bearings drops to about 80%. Therefore, the relationship between increased temperatures and the mechanical characteristics of rubber bearings is a serious concern.

In current guide specifications (AASHTO, 2000; JRA, 2002) for the seismic design of bridges with HDRBs, the nonlinear characteristics of HDRBs are expressed in terms of a bilinear model. However, the experimental observations (Bhuiyan et al., 2009; Dall' Asta and Ragni, 2006) have shown that the mechanical behavior of HDRBs is characterized by the strain hardening behavior. The current bilinear model cannot represent this behavior.
The final goal of the research project is to develop a design procedure of HDRBs at low temperatures. As the first step, rubber bearing tests were conducted to identify the mechanical behavior of HDRBs at low temperatures. The experimental results are presented in this paper to discuss the temperature dependence of HDRBs.

2. EXPERIMENTS

2.1 Specimens

All specimens had square cross-sectional shape. The reinforcing steel plates had similarly a square planar geometry with thickness of 2.3 mm. The dimensions and material properties of the specimens are given in Table 1. In order to remove stress-softening due to Mullins effect, all specimens were preloaded before the actual tests.

Table1. Dimension and material properties of HDRBs

Particulars	**Specifications**
Cross-section (mm^2)	240x240
Number of rubber layers (mm)	6
Thickness of one rubber layer (mm)	5
Thickness of one steel layer (mm)	2.3
Nominal shear modulus (MPa)	1.2

2.2 Test conditions

The rubber bearing tests were carried out in an environmental test chamber with a computer-controlled servo-hydraulic testing machine at -30°C, -20°C, and 23°C ambient temperatures. All specimens were tested under shear deformation with a constant vertical compressive average stress of 6 MPa. The displacement was applied to the top edge of the specimen and the force response was measured with two load cells. The output data were recorded by using a personal computer.
The temperatures inside the specimens are measured by installing thermocouples. The positions of temperature measurement in the central section are shown in Fig. 1. Eleven sinusoidal loading cycles were applied on the specimens with a shear strain amplitude and frequency of 1.75 and 0.5Hz, respectively.

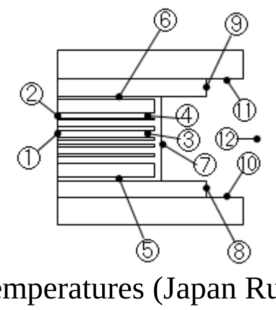

Fig.1. Measure points of temperatures (Japan Rubber Bearing Association)

3. EXPERIMENTAL RESULTS AND DISCUSSION

The measured temperatures inside the specimens and the cumulative dissipated energy are presented in Fig. 2. The cumulative dissipated energy density is calculated by

$$D = \sum_{i=1}^{11} D_i \qquad (1)$$

where D_i is the dissipated energy density of the ith cycle, and D_i can be calculated from the enclosed area of a stress-strain hysteresis loop for one cycle. Fig. 2 shows that the temperatures inside the bearings are increased by cyclic loading. The rise in the inside temperature and the cumulative dissipated energy are larger at lower ambient temperatures.

Assuming that all dissipated energy is converted into the heat energy, the temperature increase △T in a sinusoidal test is estimated from the dissipated energy density under the adiabatic condition for only rubber part:

$$DV_r = C_{pr} m_r \Delta T \qquad (2)$$

where C_{pr} is the specific heat of rubber; m_r and V_r are the mass and volume of rubber, respectively.

On the other hand, considering a rubber bearing as composite of steel and rubber, and assuming that the temperature increases in the rubber and steel are the same, the temperature increase can be estimated from

$$DV_r = \left[C_{pr} f + C_{ps} (1 - f) \right] m_r \Delta T \qquad (3)$$

where C_{ps} is the specific heat of steel; $m = m_r + m_s$ stands for the total mass; m_s is the mass of steel; $f = m_r / m$ is the mass fraction of rubber.

In this calculation, the specific heats for rubber and steel are assigned to C_{pr} = 1.732 J/g.K, and C_{ps} = 0.432 J/g.K, respectively (Uruta et al., 2004). The estimated temperatures are higher than the measured temperatures in Fig. 3 because the some heat transfers from the specimen to the ambient environment in the measurement.

In Fig. 2, the 7th cycle of the test at -30°C ambient temperature and the 4th cycle of the test at -20°C ambient temperature have the same inside temperature of -10°C. Fig. 4 presents that the stress-strain relationships of the two cycles give agreement each other. It means that the stress-strain relationships of HDRBs is governed by the inside temperatures, but not by the ambient temperature. Moreover, Takaoka et al, (2008) showed that the temperature rises in bearings are very small under an earthquake. Therefore, a seismic model for HDRBs at low temperatures should be based on the inside temperatures.

Fig. 5 presents the inside temperature dependence of stress-strain relationship of HDRBs. It is clear that the area of hysteresis loop and the strain hardening of HDRBs increase with decreasing the inside temperatures.

The shear modulus G and the damping constant h_B are calculated from the experimental results with

$$G = \frac{\tau_{\max} - \tau_{\min}}{\gamma_{\max} - \gamma_{\min}} \qquad (5)$$

$$h_B = \frac{D_i}{2\pi W} \qquad (6)$$

where W is the elastic strain energy density; τ_{max} and τ_{min} are the maximum and minimum shear stresses of rubber; and γ_{max}, γ_{min} are the corresponding shear strains at τ_{max}, τ_{min}, respectively. The values of G and h_B at different inside temperatures are shown in Fig. 6. While the inside temperature decreases from 35^{o}C to -22^{o}C, G and h_B increase 180% and 79%, respectively. It is clear that these parameters are significantly affected by the inside temperature variations.

The stress-strain relationship obtained from sinusoidal loading tests at -10^{o}C inside temperature is used to determine the parameters of the conventional bilinear model. Fig. 7 shows the comparison of the bilinear model with the sinusoidal test result. The experimental result shows significant hardening at a high strain level, but the bilinear model cannot represent this feature. This is the limitation of the bilinear model at lower temperatures.

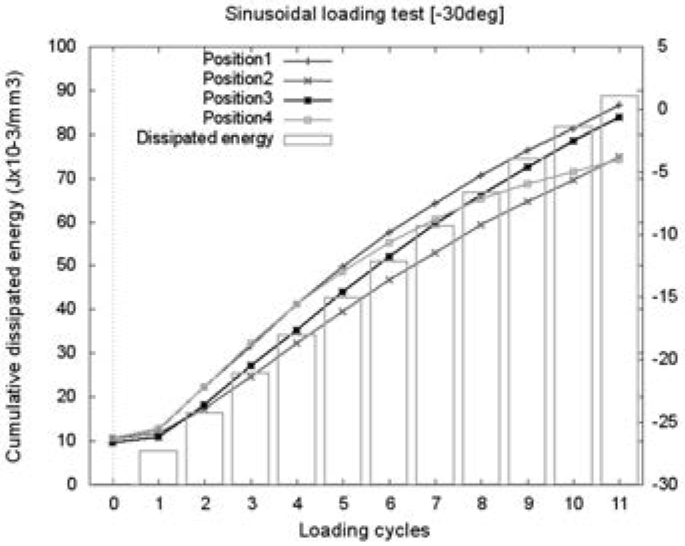

(a)

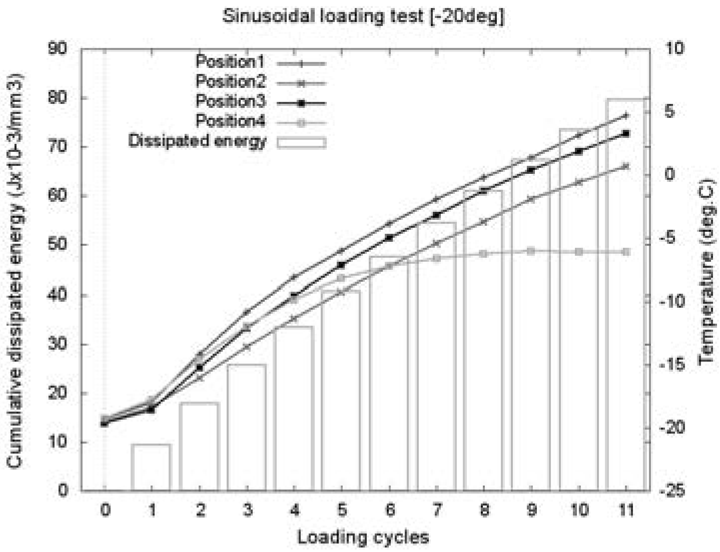

(b)

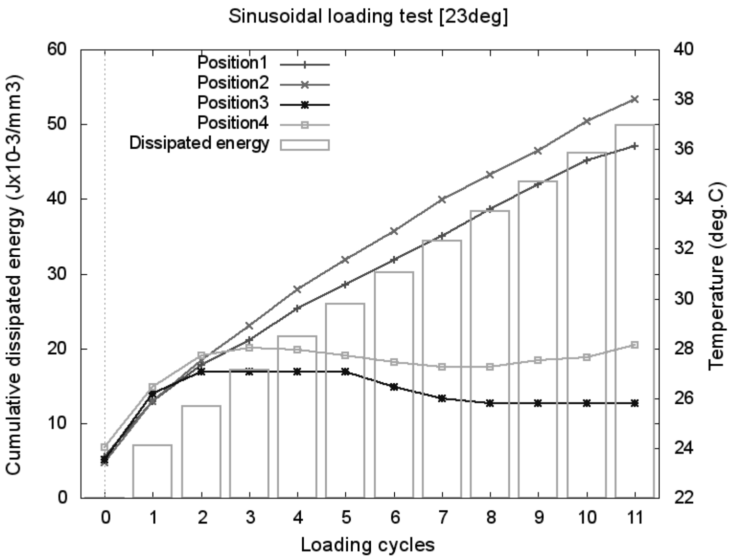

(c)

Fig.2. Cumulative dissipated energy and temperatures at ambient temperatures (a) -30°C, (b) -20°C, and (c) 23°C.

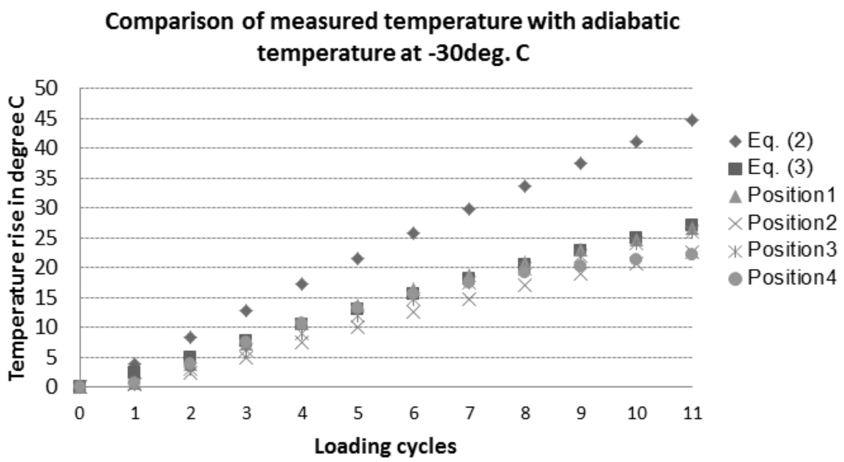

Fig.3. Comparison of measured temperature with theoretical temperature at -30°C ambient temperature.

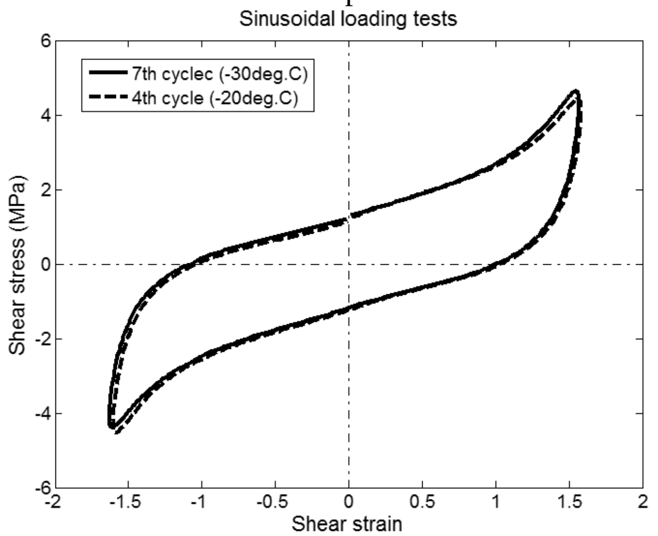

Fig.4. Stress-strain relationships at -10°C inside temperature.

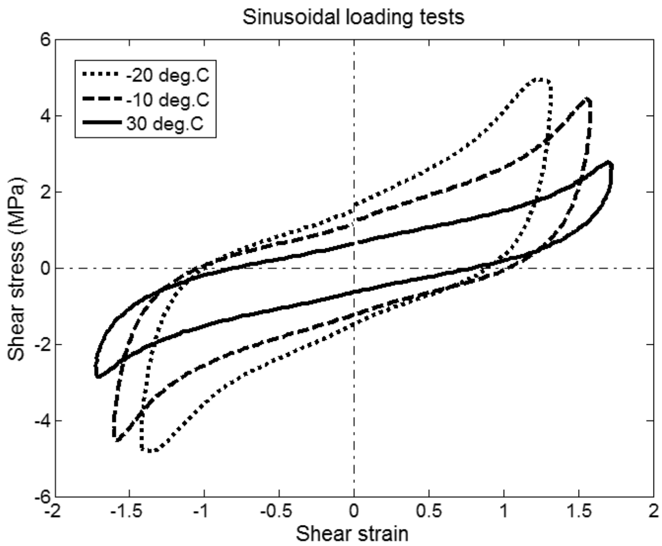

Fig.5. Stress-strain relationships of sinusoidal loading tests at different inside temperatures.

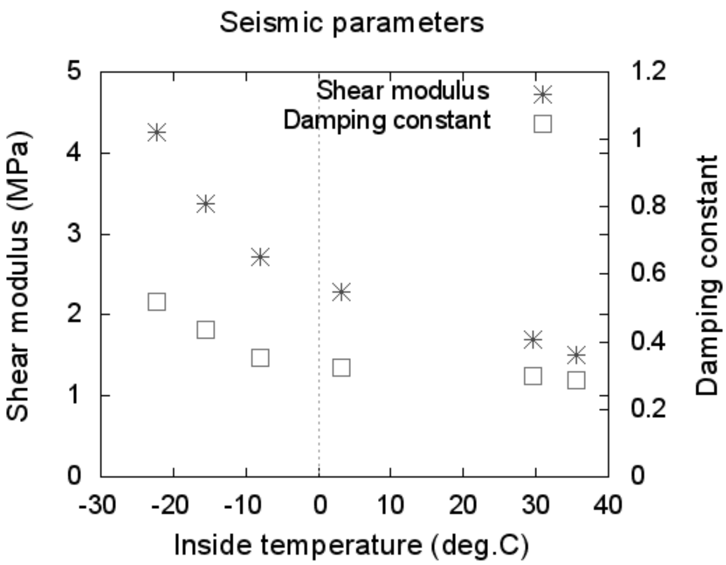

Fig.6. Temperature dependence of shear modulus and damping constant

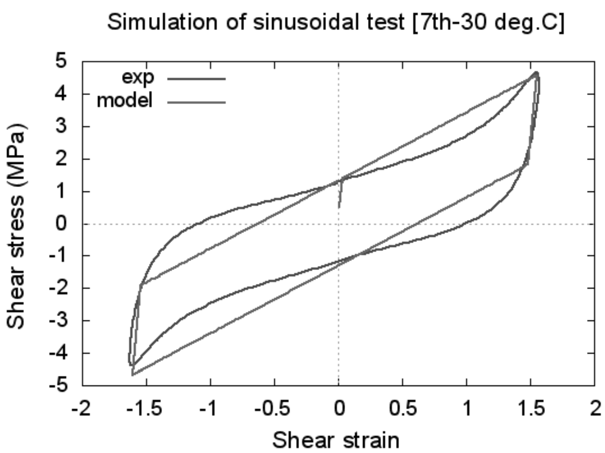

Fig.7. The comparison of the bilinear model with experimental result at -10^{0}C inside temperature

4. CONCLUSIONS

The temperatures inside HDRBs are increased by cyclic loading, and the rise in the inside temperature becomes larger at lower ambient temperatures. In addition, it is shown that the stress-strain relationships of HDRBs is governed by the inside temperatures but not by the ambient temperature.

The conventional bilinear models for HDRBs in most seismic design codes are determined based on a stress-strain relationship obtained from sinusoidal tests after several cycles of loading to remove stress-softening behavior due to Mullins effect. However, the present experimental results show that this procedure neglecting self-heating effect is not appropriate for development of seismic models for HDRBs, especially at low ambient temperatures. Since the temperature increase during an earthquake is considered not so large as that during a cycling loading test, a seismic model for HDRBs at low temperatures should be based on the inside temperatures.

In order to develop an estimation procedure of temperature increase during an arbitrary strain history, the temperature increase in a sinusoidal test is estimated from the dissipated energy under a simple adiabatic assumption. The measured temperatures are lower than the estimated temperatures because there is the heat transfer in the actual condition.

Since the hardening in the stress-strain relationship of HDRBs becomes significant at low temperatures of -20 and -30°C, the bilinear model is not well representation of HDRBs' behavior at low temperatures.

ACKNOWLEDGMENTS

The experimental works were conducted by utilizing the laboratory facilities and bearings-specimens provided by Japan Rubber Bearing Association. The authors indeed gratefully acknowledge the kind cooperation extended by them.

REFERENCES

American Association of State Highways and Transportation Officials (AASHTO), 2000. Guide Specification for Seismic Isolation Design, 2/e.

Bhuiyan, A.R., Okui, Y., Mitamura, H., Imai, T., 2009. A rheology model of high damping rubber bearings for seismic analysis : Identification of nonlinear viscosity. *International Journal of Solid and Structures* 46, 1778-1792.

Dall'Asta, A., Ragni, L., 2006. Experimental tests and analytical model of high damping rubber dissipating devices. *Engineering Structures* 28, 1974-1884.

Diani, J., Fayolle, B., Gilormini, P., 2009. A review on the Mullins effect. *European Polymer Journal* 45, 601-612.

Hwang, J.S., Hsu, T.Y., 2001. A fractional derivative model to include effect of ambient temperature on HDR bearings. *Engineering Structures* 23, 484-490.

Imai, T., Bhuiyan, A. R., Razzaq, M. K., Okui, Y., Mitamura, H., 2010. Joint conference proceedings of 7CUEE & 5ICEE, Tokyo, Japan, 1921-1928.

Japan Road Association, 2002. Specifications for Highway Bridges, Part V : Seismic Degign.

Khan, A. S., and Lopex-Pamies, O., 2002. Time and Temperature Dependent Response and Relaxation of a Soft Polymer. *Intl. J. Plast* 8, 1359-1372.

Lion, A., 1997. On the Large Deformation Behavior of Reinforced Rubber at Different Temperatures. *J. Mech. Phys. Solids* 45, 1805-1834.

Pinarbasi, S., Akyuz, U., Ozdemir, G., 2007. An experimental study on low temperature behavior of elastomeric bridge bearings. 10th world conference on seismic isolation, energy dissipation and active vibrations control of structures, Istanbul, Turkey, 28-31.

Takaoka, E., Takenaka, Y., Kondo, A., Hikita, M., Kitamura, H., 2008. Heat-Mechanics Interaction Behavior of Laminated Rubber Bearings under Large and Cyclic Lateral Deformation. The 14th World Conference on Earthquake Engineering, Beijing, China.

Uruta, H., Yamazaki, T., Ohsima, T., Nakamura, M., 2004. Experiments and numerical analysis on response of internal temperature of high damping rubber Bridge Bearing under low temperature. Proceedings of JSCE (Japan Society of Civil Engineers) Vol. I, 773, 113-123.

Examples of proposals for emergency countermeasure and research methods of landslide in Vietnam

Do Ngoc Trung [1], Nobolu Fujii[2], Seiichi Hujiwara[2] and Shinro Abe[2]
[1]Vietnam Japan Engineering Consultants Co., Ltd, Hanoi
mr.dongoctrung@gmail.com
[2]Okuyama Boring Co., Ltd, Japan

ABSTRACT

In recent years, there have been a large number of cases of new landslides occurring on road slopes, river banks and hilly areas of rapidly developing cities. This increased number of occurrences of landslides in developing cities is considered to be caused by the formation of manmade slopes due to road and residential land developments, as well as torrential rain and floods that come with climate change. Particularly in developing cities with little experience of landslides where methods for stabilization have not been established, it is essential to investigate landslides and consider countermeasures urgently. We investigated landslides occurring on the slopes along the road on the coast of Ha Long Bay: a well-known World Heritage Site in Vietnam, using 1) boring surveys with core pack tube, 2) fixed point observation to understand amount, direction, and the range of fluctuations, and 3) simple extensometers. Using these research methods which are easily prepared, installed, and observed in Vietnam, we identified the mechanisms of landslides, and proposed the emergency construction. It is thought these methods will become effective means against landslides in the developing cities as mentioned above..

Keywords: *landslide, slope disaster, landslide investigation, emergency countermeasure*

1. INTRODUCTION

In recent years, there has been a large number of cases of new landslides occurring on road slopes, river banks, and hilly areas in rapidly developing Vietnamese cities. This increased number of landslides occurring in developing cities is considered to be caused by the formation of man-made slopes because of road and residential land developments, as well as heavy rain and floods that occur with climate change. In Vietnam, where there is little experience of landslides and methods for dealing with them have not been developed yet, it is necessary to investigate landslides and urgently discuss countermeasures. For the landslides occurring on the slopes along the road on the coast of Ha Long Bay, a well-known World Heritage Site and picturesque place in Vietnam, we identified the landslide generation mechanism using survey techniques that will be easy for preparation, installation, and observations in Vietnam. We also proposed emergency construction work. It is thought that these techniques will form effective means against landslides in the aforementioned developing cities from now on.

2. Overview of landslides in the Bai Chay Bridge area

The locations studied in this study are located on the southern edge of a hilly area, at an altitude of less than 100 m, over a section of approx. 3.5 km encompassing the Bai Chay Bridge, National Route 18, over the Ha Long Bay. They all mainly correspond to cut slopes at an altitude of 10–70 m. Parts of the slopes are constructed with wet masonry or cast-in-place concrete cribwork, but they are mostly bare. On these bare slopes, a number of slope deformation through landslides or weathering and erosion, as well as unstable conditions through instance rock fall are observed.

This study is focused on site No. 10, which particularly displayed marked landslide deformations (Fig. 1).

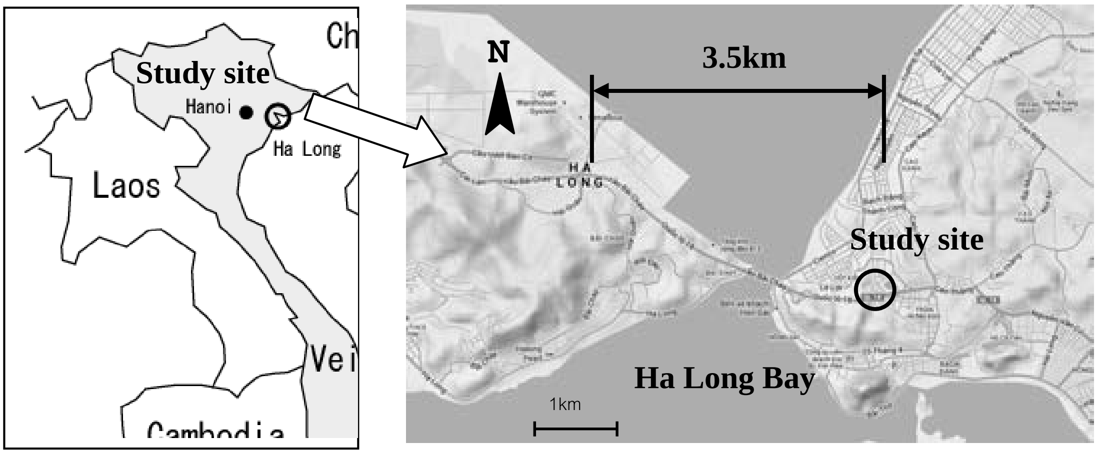

Figure 1: Survey location maps

The geology of this area is composed of sedimentary rock from the Carboniferous Period of the Paleozoic Era to the Triassic period of the Mesozoic era, such as quartz conglomerates, quartz sandstone, siltstone, claystone, and carbonaceous claystone (Department of Geology and Minerals of Vietnam, 2001) (Fig. 2).

The strike of the bed is roughly north–south, and multiple short-period folds of several tens to hundreds meters on a north–south fold axis can be observed. As National Route 18 in the area of our study traverses the northern edge of a hilly area, there are many north-facing excavated road slopes. As the road slopes in our study area are also north facing, the beds in the slope mainly dip with respect to the slope direction. Most of the landslides in this area occur as translational bedrock landslides in dip slopes in mud formations around the folding axes of the fold structures and the overfolds, amidst alternating strata of mudstone, sandstone, and conglomerates.

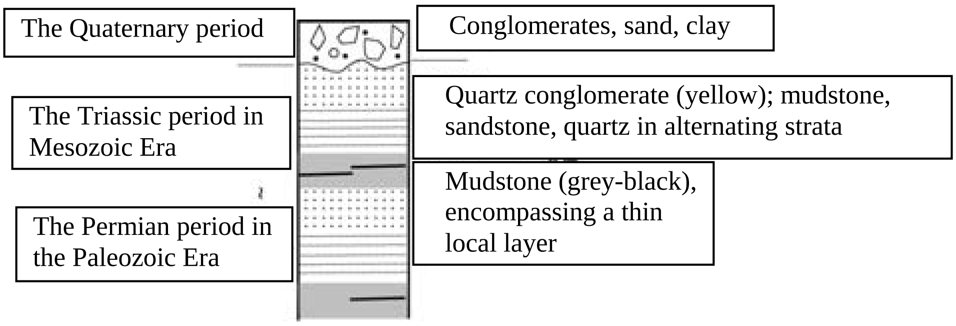

Figure 2: Pattern diagram of columnar section around the study area

3. Overview of the landslide at the study site (No. 10)

3.1 Topography, geology, and landslide conditions

Site No. 10 is a cut road slope, located on the southern edge of a hilly area at an altitude below 100 m. On this slope, a translational bedrock slide occurred covering an area of approx. 50 m wide and 60 m long (photographs 1 and 2). At the eastern edge of the landslide area, 3 m wide and 3–5 m deep openings (collapsed zones) (photograph 3) have formed. Inferring from the direction and the strike and dip of this crevice, the landslide is thought to have moved to dip in a northwesterly direction. The landslide tip is restricted by the fault on the western side, changes its direction of movement into a northerly direction, and rises up along the slope. On this slope, multiple short-period fold structures are observed, and landslides have occurred in the area where the mudstone on top of the anticline is exposed on the surface. The western edge of the landslide is in contact with the fault (photograph 1).

On this site, a φ = 1 m rock fall occurred owing to heavy rain during a typhoon in the fall of 2012.

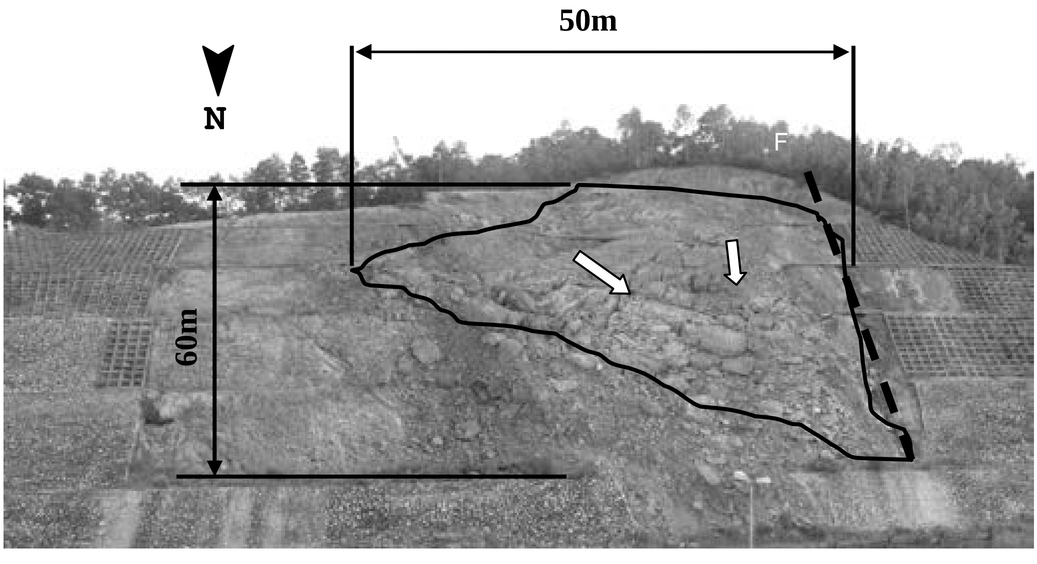

Photograph 1: Overall scene. Solid line: landslide range; Arrows: direction of movement; F: fault

Photograph 2: Landmass moving as a block

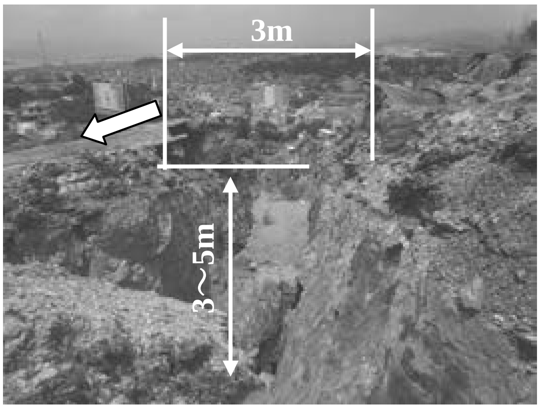

Photograph 3: Opening at the head of the landslide

3.2 Problems with the response to landslide disasters in Vietnam

During the survey of site No. 10, rock fall movement could be observed to occur during rain. Fragmentation of blocks accompanying landslides of the collapsed zone at the top and the slope was also notable, and there was a high risk of increased activity. Because National Route 18, a main route, passes at the tip of the landslide, it was desirable that a landslide survey was conducted without delay. The landslide mechanism was understood, and countermeasures were planned and implemented.

Vietnam does not, however, have any established methods for detailed landslide surveys, analysis, or countermeasure construction, and there are few past records for the development or introduction of observation equipment. Landslide disasters, therefore, either remain uninvestigated or are only analyzed through simple investigations such as boring or seismic prospecting, and countermeasures merely employ retaining walls to retain the soil or recutting at a low gradient.
We, therefore, improved the currently used technologies, employed methods of surveying, observation, and analysis using equipment that can be promptly prepared, and proposed methods for countermeasure construction.

4. Survey and countermeasure methods for site No. 10

4.1 Used survey method and results

4.1.1 Survey methods and reasons for their use

Because of the urgency, a survey was planned and implemented for this site, after a geological reconnaissance, with equipment that can be promptly prepared on site. The survey employed survey boring, fixed point observations, borehole inclinometer measurements, groundwater level measurements, and ground surface extensometers.

1. Boring surveys: In boring surveys, it is important to ascertain, by means of collected cores, the geological features, clay intercalation, and the distribution of weak planes in crevices. Because in Vietnam core, retrieval rates with the conventional core retrieving method through a single core tube (photograph 4) were poor and evaluation of the geology and slip surface was difficult, we used a double core tube and a core pack tube manufactured in Japan for improving core retrieval rates.

Photograph 4: Boring

2. Fixed point observations: In fixed point observations, simple mobile measuring points (e.g., piles, survey pins) are placed inside the landslide and the surrounding area, and the amount of horizontal and vertical movement is obtained through triangulation, distance measuring, and leveling. Through periodic measurements, the amount and direction of landslide movement can be ascertained, and this can be performed with regular measuring equipment.

3. Borehole inclinometer: Borehole inclinometers survey the borehole deformation and assess the slip surface by placing pipes using boreholes (Fig. 3). These are often used in Vietnam to survey ground deformations when digging tunnels or dam bodies.

4. Ground water level measurements: In ground water level measurements, a perforated vent pipe is placed in a borehole and consecutive ground water levels are measured with a piezometer. Assuming that ground water was supplied to this landslide area, we set up an observation hole in the collapsed zone at the head of the landslide, where the ground water level can be ascertained with a borehole of minimum depth.

5. Ground surface extensometer: Ground surface extensometers continuously ascertain landslide movement through the expansion and contraction of an inverter wire, which is placed in the moving part of the landslide and in the surrounding stationary area, spanning the crevice (Fig. 4). On this site, it was placed at the upper part of the crevice and the end. We used a Japanese battery powered extensometer.

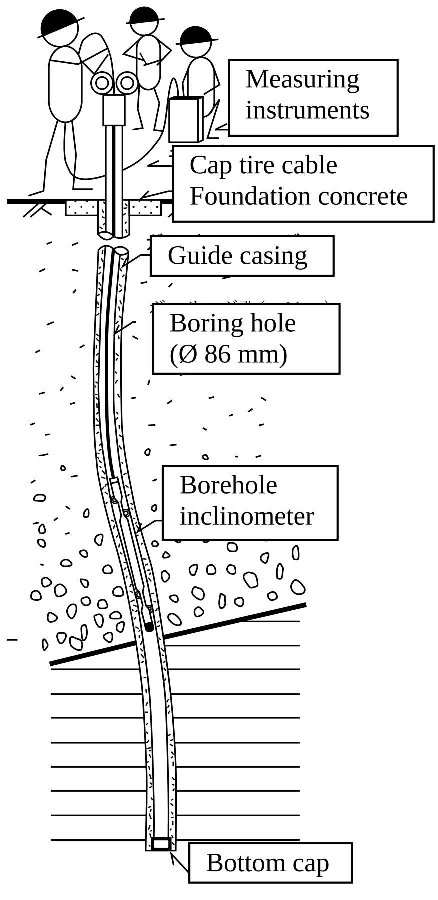

Figure 3: Borehole inclinometer measuring example

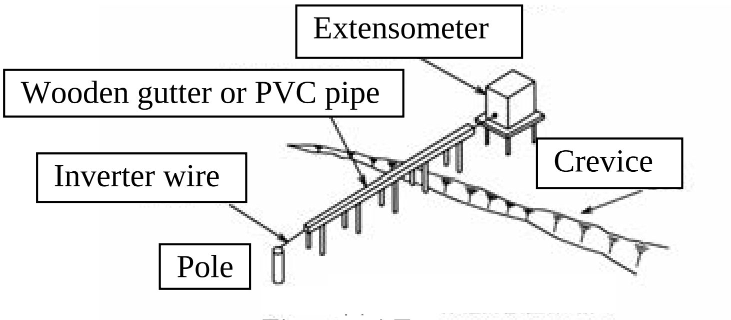

Figure . 4 Extensometer set-up

4.1.2 Survey results

1. Boring survey results

Boring core retrieval in subsurface surveys in Vietnam is generally performed using single core tubes. The fact is however that, because no casing is used or the boring machine has not been fixed, core retrieval rates are low (photograph 5). As a result of our decision to use a core packing tube, which is recently being used at Japanese landslide sites, and an excavation method, where the machine is fixed, an improvement in core retrieval rates can be observed (photograph 5).

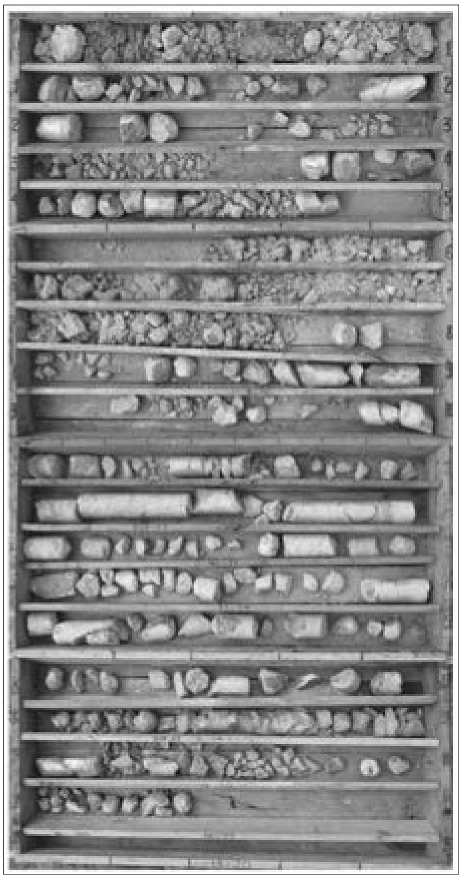

Conventional methods in Vietnam

Using a double core tube with CORE PACK

Photograph 5: Comparing boring core photographs

2. Fixed point observation results

Fixed point observation results, obtained using general surveying techniques, showed that the direction of movement is at an almost direct angle to the collapsed zone at the head. We confirmed the amount of movement to be a displacement of maximum 80 mm in approx. 1 month

We established the direction of movement to be somewhat oblique to the direction of National Route 18 (Fig. 5).

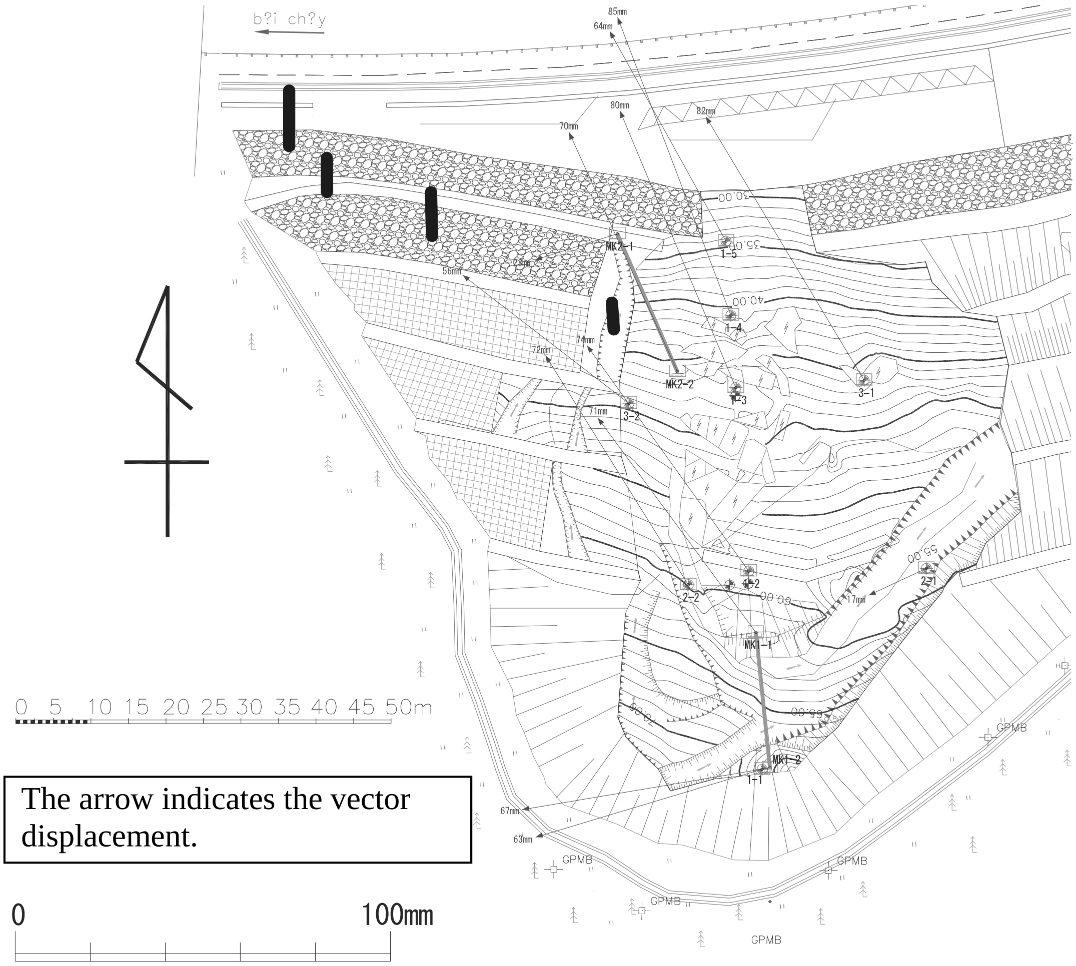

Figure 5: Fixed point– vector displacement (measuring period: 28 days)
(2012/10/22)

3. Borehole inclinometer measurement results

Bends were observed at a depth of 6.50 m in borehole BV10-1-A (Fig. 6) and at a depth of 6.00 m in borehole BV10-2-A (Fig. 7).

We ascertained that the slip surface, which was revealed by the inclinometer and the survey boring, is a so-called dip slope rockslide following the stratum gradient (Fig. 8). The slip surface angle is approx. 25°.

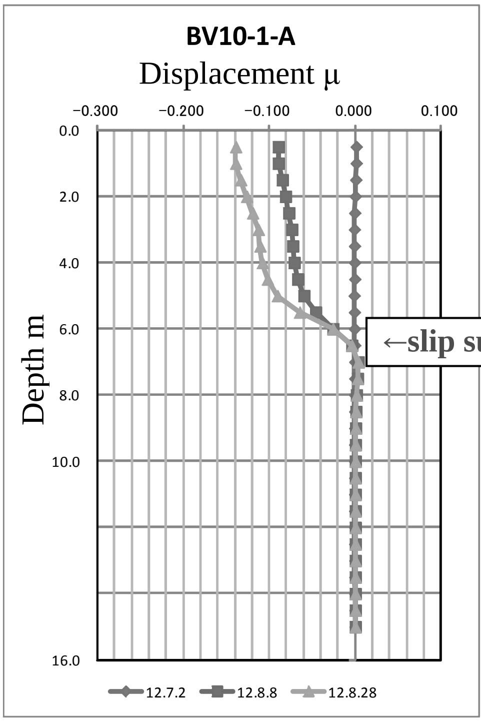

Figure 6: Borehole BV10-1-A inclinometer displacement

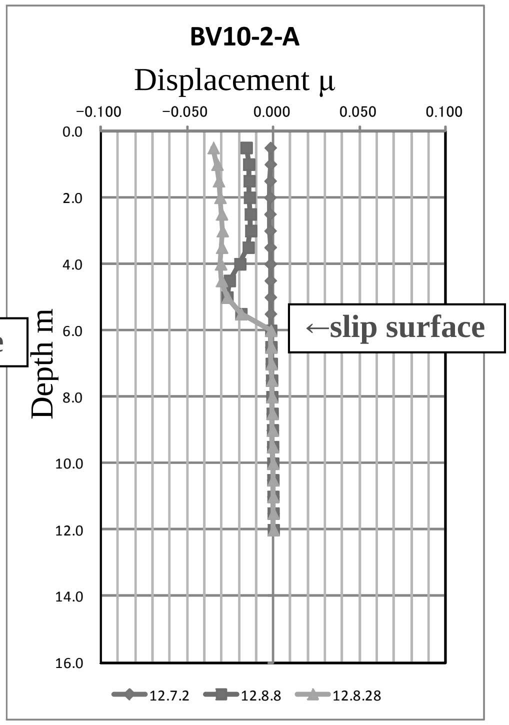

Figure 7: Borehole BV10-2-A inclinometer displacement

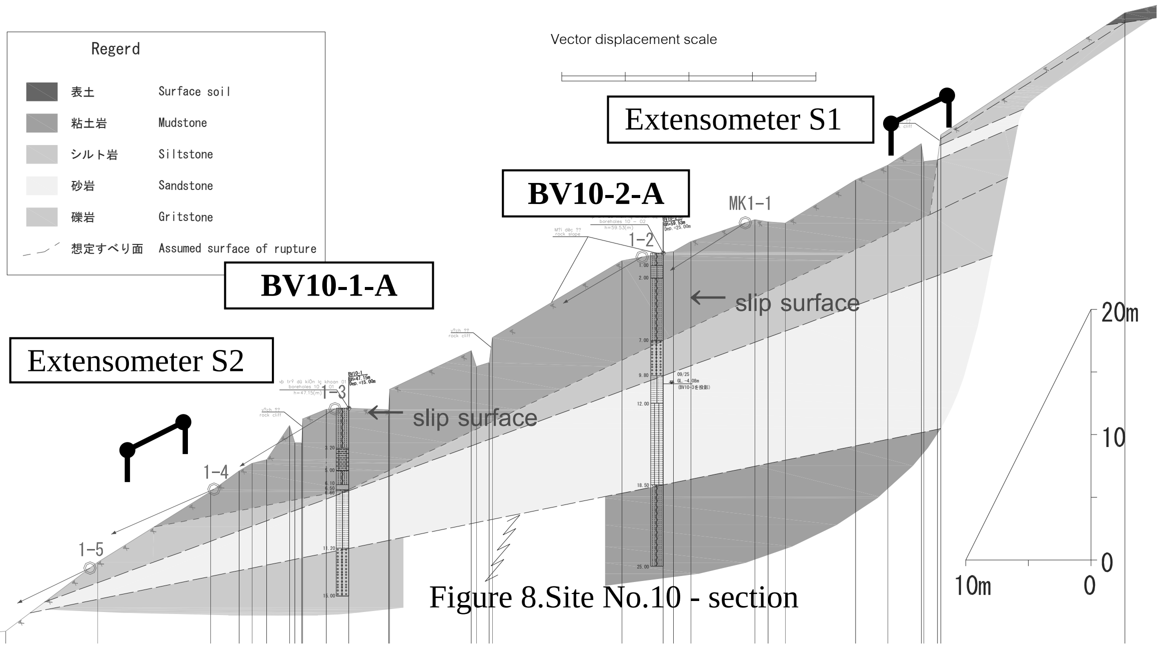

Figure 8.Site No.10 - section

4. Ground water level/extensometer results

Extensometer S-1 was set up at the head, the stretching end of the landslide; extensometer S-2 was placed at the passive tip of the landslide (Fig. 8). The movement registered by the extensometers is concordant with ground water level fluctuations, where they increased with rising ground water levels and decreased with decreasing ground water levels (Fig. 9). We could therefore affirm that the landslide at this site is greatly affected by increasing subsurface ground water level accompanied by heavy rain.

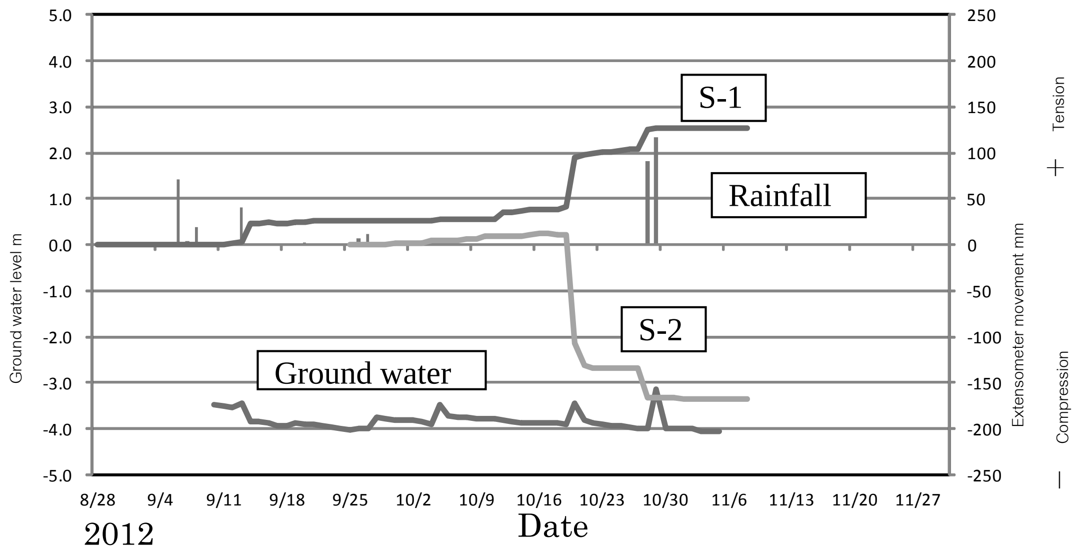

Figure 9: Rainfall/ground water level fluctuations as registered by extensometers

4.1.3 The landslide generation mechanism

On the basis of these survey results, the landslide generation mechanism can be summarized as follows.

This landslide is a rockslide, where the slip surface is formed by the mudrock formation around the fold axis and the overfold area in the fold structure. From the clear correlation that can be observed between ground water levels and landslide movement, we concluded that the rapid rise of pore water pressure at times of heavy rainfall forms the trigger for the landslide's intermittent movement.

Countermeasures for these types of landslides can be considered to deal with surface water at times of heavy rain, ground water drainage, counterweight fills, or preventive work using anchors or piles.

4.2 Countermeasure work planning

4.2.1 Stability analysis and analysis conditions

For the landslide stability analysis, the simplified Janbu method was used; for the slip surface strength, we employed C = 0 kN/m2 and φ = 22.39°, considering the slip surface gradient and the topographical incline. The design safety factor (PFs) was set at PFs = 1.20, as the subject of preservation; main road National Route 18 forms the approach route to the Bai Chay Bridge, a tourist attraction, and furthermore faces Ha Long Bay, a Unesco World Heritage Site.

Using these results, we planned emergency countermeasures focusing on counterweight fill work and ground water drainage work for the rainy season from June to September (Fig. 10).

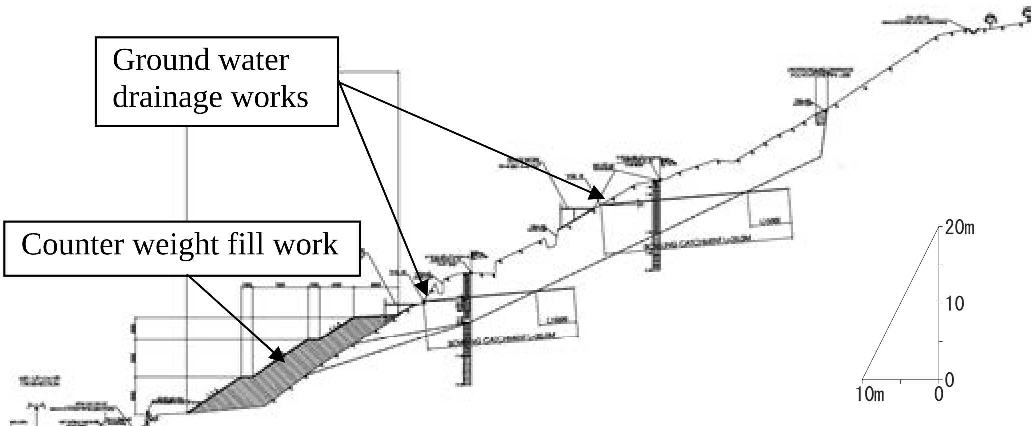

Figure 10: Cross section of the emergency countermeasure work plan

For the purpose of permanent stabilization after the emergency countermeasures, we proposed slope protection work, focusing on anchor work, to prevent destabilization by means of erosion control, with sensitivity to the surrounding scenery.

5. Conclusion

We used a core packing tube together with the boring used in Vietnam at landslide disasters and elucidated the landslide generation mechanism through economical and basic landslide survey and measuring techniques using equipment that can be prepared promptly. These included fixed point observations using mobile measuring points such as survey pins, ground surface extensometers using inverter wires and extensometers, and borehole inclinometers using porous vent pipes. We also introduced examples of countermeasure proposals.

It is thought that these will form valuable techniques against landslide disasters that are presumed to occur in future in developing cities.

Ultra rapid strength development in dry-mix shotcrete for emergency support and harsh mining conditions

Jean-Daniel LEMAY[1], Marc JOLIN[2], Richard GAGNÉ[3] and Benoît BISSONNETTE[4]
[1] Research Engineer, Université Laval, Canada
jean-daniel.lemay@gci.ulaval.ca
[2] Professor, Université Laval, Canada; marc.jolin@gci.ulaval.ca
[3] Professor, Université de Sherbrooke, Canada
[4] Professor, Université Laval, Canada

ABSTRACT

Recent development in the field of cementing materials has brought forward many nontraditional binder systems. Engineers involved in the fields of emergency repairs and rapid ground support have been on the lookout for materials that allow rapid production, placement and, most of all, very rapid strength development kinetics. One binder system that fits the description is composed of ordinary Portland Cement (OPC), calcium aluminate cement (CAC) and calcium sulfate ($\bar{S}$). However, this type of binder also sometimes exhibits difficult workability that limits its use in regular cast in-place concrete. This limitation is overcome when using dry-mix shotcrete as a placement method, since the contact between water and cement occurs in the nozzle immediately before placement, workability problem are avoided. This pneumatic placement method also offers interesting advantages when considering emergency applications: it makes use of pre-bagged material, equipment is easy to mobilize and the transport hose can easily cover hundreds of meters.
As a part of a graduate project at Laval University, 49 different mixes, including simple, binary and (mainly) ternary blends, were tested. Two majors parameters were studied, the development of compressive strength and the volumetric stability. The numerous binder compositions tested allowed the selection of a stable optimized formulation in regard of early compressive strength and volumetric stability. Finally, the selected formulation was successfully tested with industrial dry-mix shotcrete equipment to verify the large-scale placement feasibility of such a product.

Keywords: *emergency support, shotcrete, ultra high early strength*

1. INTRODUCTION

Transport and placement methods for concrete have evolved tremendously throughout history. Although cast-in place concrete is still the most common placement method, other processes have been developed; let’s simply think of the first concrete pump, self-leveling concrete or roller compacter concretes. There is also another concrete placement process developed at the beginning of the last century that has gained global acceptance. First presented to the construction industry in 1910 by Carl Akeley (ACI-506.R 2005), shotcrete is nowadays present everywhere, particularly in the mining and tunneling businesses.

Shotcrete (also know as *sprayed concrete* in many parts of the world) is a placement method for concrete. Shotcrete is defined as a mortar or concrete pneumatically projected at high velocity onto a surface (ACI-506.R 2005). The high velocity is essential to the process as it ensures an adequate compaction or consolidation and allows the material to “stick” to the sprayed surface. Without the proper compaction, quality shotcrete cannot be produce (CP-60 2009).

As any placement methods, different advantages of shotcrete make it more appropriate in certain situations. With its capacity to stick to vertical and overhead surfaces, shotcrete need only minimum, if any, formworks. To take full advantage of this specificity, shotcrete is best used in ground supports (tunnel, mine, slope stabilization, etc.), overhead civil work reparation (bridge deck and parking lower surface, etc.) and where complex formworks make cast-in place concrete very expensive (ark type bridge, circular column repairs, etc.).

Shotcrete can be produce using two different processes, the *wet-mix* and the *dry-mix*. The major differences between these processes are the conveying method of the material through the hose and the location where the water is added to the mixture.

1.1. Wet-mix shotcrete

In the wet-mix process, all the ingredients are mixed together before being pumped through the hose. Air is added at the nozzle, through an air-ring, to propel the material at high velocity onto the surface ensuring sufficient compaction. As all components are mixed together prior to pumping, wet-mix concrete is usually delivered on site by standard ready-mix truck and is feed directly into the pump.

With the exception of the set-accelerator, all admixtures are blended before pumping. When needed, the set-accelerator is added at the nozzle thought a separate valve by using a special admixture pump. Normal dosage of accelerator usually range from 2.5 to 6% but dosage of >10% of binder content is sometime used (Prudêncio Jr 1998). Accelerator dosage has to be carefully planned as it reduces long-term resistance and durability of concrete (Neville 2008).

1.2. Dry-mix shotcrete

Dry-mix shotcrete is fundamentally different from its wet-mix counter part. In this process, all the solid materials (gravel, sand, cement, additives, fibers, admixtures) are transported through the hose using compressed air. Water is added through a water ring at the nozzle or shortly before depending on the type of nozzle used. No matter the type of equipment used, the *water-binder contact* comes only a fraction of a second before placement. This particularity enables this process to bypass workability issues usually associated with the mixing and pumping of regular concrete. Figure 1 shows a schematic of a typical dry-mix shotcrete set-up.

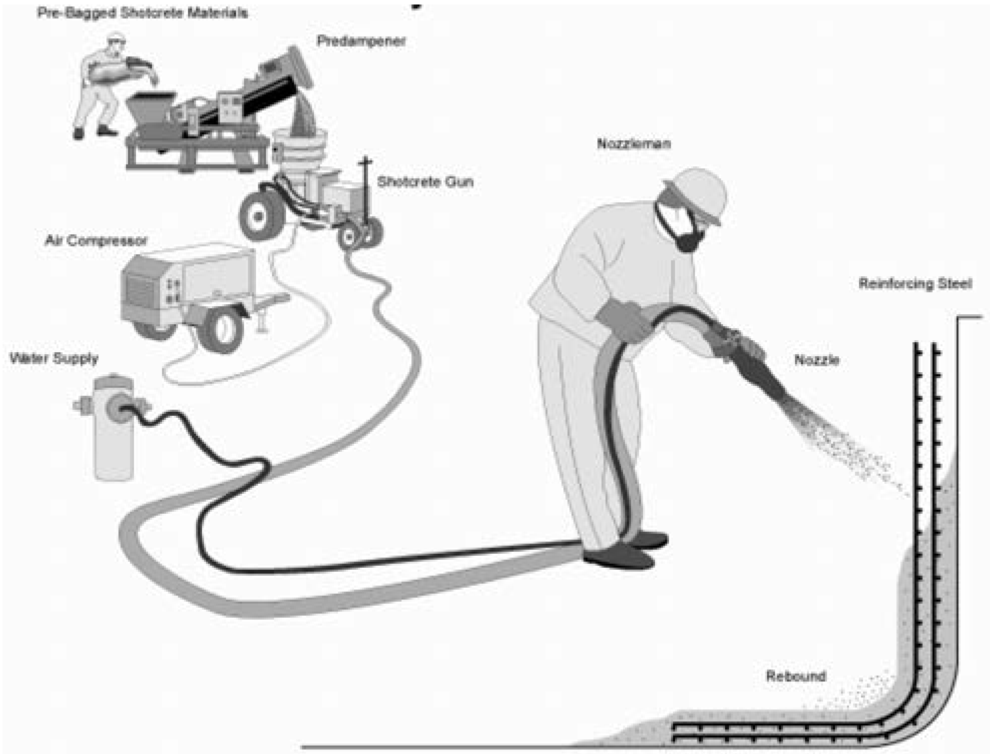

Figure 1: Typical set-up for dry-mix shotcrete operations

Since materials are introduced in the dry state in the hose, production of dry-mix shotcrete usually takes advantage of pre-bagged material. This enable easier quality control of the material as the production of such bags is done in a controlled environment.

1.3. Comparison of both process

Each process have it's own advantages and inconvenient. Wet-mix shotcrete is usually used only when high volumes of shotcrete are needed due to the important mobilization needs. On the other hand, while the dry-mix process cannot reach the production rates of the wet-mix process, its mobilization costs, preparation time and flexibility are key factors in its selection.

Table 1 : Difference between dry-mix and wet-mix process

Dry-mix process	**Wet-mix process**
PROS…	
Instantaneous adjustment of shooting consistency	Known w/cm
Delivery hose lighter to move	Rebound and Dust are lower
Start-Stop operations simple	High volume output

CONS…	
Higher rebound	High volume output sometimes difficult to manage
Low volume output	Use (and dosage) of accelerator on site

1.4. Development of new shotcrete

The development of new and alternative binder to Portland cement has opened the field of cementitious binder to a whole new variety of binder. One of those binders exhibiting very promising property is a binder composed of Portland cement (OPC), calcium aluminate cement (CAC) and calcium sulfate ($\bar{S}$) (Lamberet 2005). This type of mixture shows very rapid hardening behavior but is unfortunately often accompanied with important workability issues. With a *pot life* of less than 10 minutes, regular cast-in place application of this type of concrete is impossible without the use of numerous chemical admixtures to control set and fluidity. A mean to avoid this type of problem was sought and this is where dry-mix shotcrete becomes a very interesting process since water is added only a fraction of a second before impact onto the receiving surface, avoiding workability issues. The validity of such an hypothesis was as part of a research project at Laval University (Lemay 2013).

2. RESEARCH PROGRAM

The main objective of the project consisted in realizing a conventional dry-mix shooting session of a special mixture based on a ternary binder using standard dry-mix equipment and techniques (ACI-506.R 2005; CP-60 2009). To ensure consistent shotcreting and adequate quality control, the shotcreting took place at *Laval University's Shotcrete Laboratory*. The laboratory is equipped with full-scale shotcreting equipment in an indoor environment that is temperature controlled. The shotcrete was sprayed using a rotating barrel ALIVA 246 with a 38.1 mm (1.5 in) interior diameter hose with the water ring placed 3.0 m (10 ft.) upstream from the outlet of the nozzle – a.k.a. *hydromix nozzle*- (Figure 2).


Figure 2 : Spraying gun (left) and hydromix nozzle (right)

The mixture was shot indoors at an average temperature of 21˚C (70˚F). The *Shotcrete Laboratory*'s equipment includes an electronic air flow meter, a water flow meter and a set of electronic scales; the data acquisition system records the airflow, the water flow and the material used during the spraying operations (Figure 3). The targeted airflow is 4.25 m^3/min (180 CFM) at a working air pressure of 7 bars (105 PSI). The water flow was adjusted (by the operator holding the nozzle) to what is referred to in the industry as the *wettest stable consistency*. The evolution of the water and material flows are used as a quality control point. Irregular or non-uniform flows lead to the rejection of a mixture.

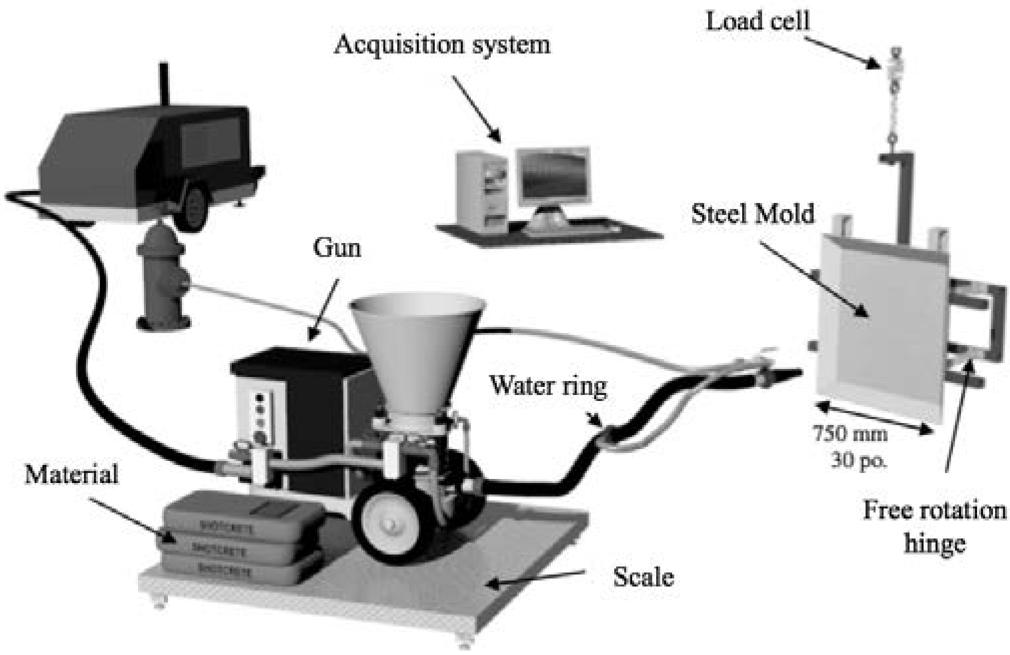

Figure 3 Schematic of the electronic acquisition system

Prior to the shotcreting operation, 780 kg of dry shotcrete material was pre-weighted and pre-blended to allow for the production of the various panels and samples needed for testing. Table 2 shows the dry proportion of the pre-blended material.

Table 2 : Dry proportion of sprayed mixture

Ternary Binder (%)	Aggregate (%)	
	Sand	Rock
19.0	52.7	28.3

To correctly assess the strength development of the ternary mixture, compressive strength test were conducted. Early age compressive strength tests (up to 3 hours) were conducting using beam specimen. These beam specimens are sprayed in steel mold to realize “End-Beam Test” (Heere and Morgan 2002), which is a common test in the mining industry. Figure 4 shows the set-up used to perform the test and an actual specimen tested.

Figure 4 : “End beam test” apparatus

To evaluate compressive strength after 3 hours, 75 mm (3 in) diameter cores were extracted from test panel (ASTM 2003; ASTM 2005). Figure 5 shows the different test panels ready for shotcreting in the “rebound chamber” in the *Shotcrete Laboratory*.

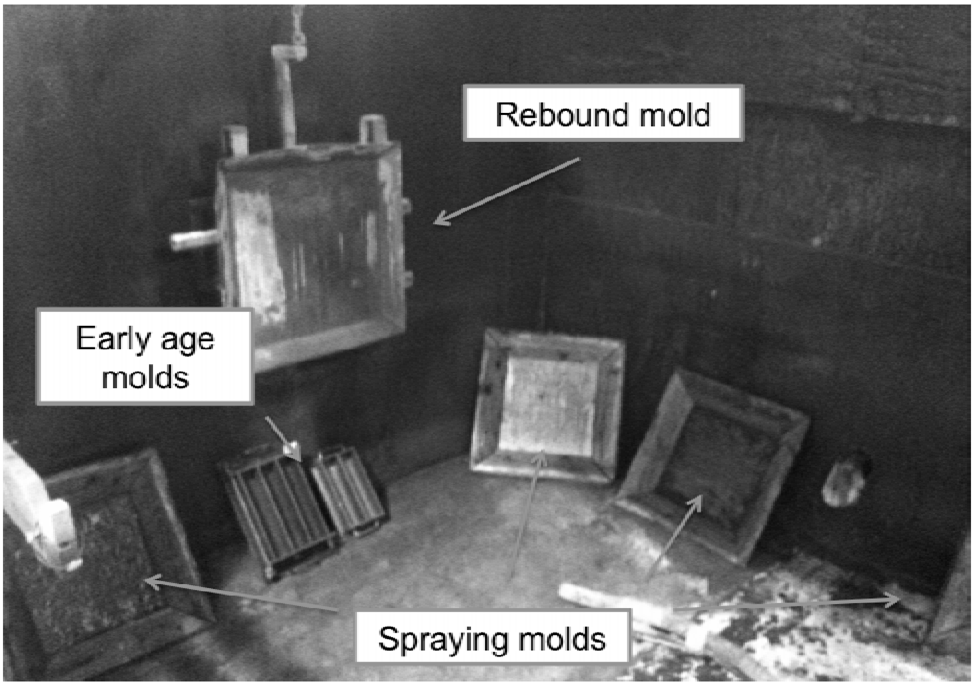

Figure 5: Rebound chamber before spraying

3. RESULTS

3.1. Placement and adhesion

The first goal of this shotcreting session is to establish whether the new type of binder allows for proper shooting and placement of dry-mix shotcrete. Using the standard equipment described above, the shotcreting was a success. Indeed, the use of the hydromix nozzle was efficient in reducing dust emission and no plugging was observed; dust and rebound were similar to those obtained with traditional dry-mix shotcrete mixture design. Later coring of the test panels confirms the homogeneity of the in-place material.

Overall, the material shot very well and allow the placement on vertical surfaces without the need of accelerator; the in-place mixture showed sufficient cohesion and adhesion to stay in place with more than 125 mm (5 in.) thickness while presenting rebound losses of approximately 20%.

3.2. Compressive strength

The spraying was successful using standard dry-mix shotcrete equipment. Particularly, the use of a hydromix nozzle where water is introduced 3 meters (10 ft) prior to its delivery through the nozzle allowed the production of homogeneous good quality shotcrete with no clogging in the equipment. Table 3 presents the average compressive strength obtained using the "End beam test" (figure 4) and using cores taken from panels.

The results presented in table 3 are actually quite impressive and are deemed a success for the mining and tunnelling industry; indeed, "typical" early age and compressive strength obtained with ordinary Portland cements based mix design and set accelerators are usually around 3 – 4 MPa. Compressive strength over 30 MPa at 3 hours with 28d compressive strength of some 50 MPa are extremely promising. On the other hand, the 1-hour results also show very interesting potential for emergency response. Structural damages caused by fire in tunnels or by natural disasters (e.g. flooding or earthquakes) on essential structures could be very rapidly be alleviated using such a mix design in combination with the dry-mix shotcrete application method. In fact, although not measured because of its rapid onset, the setting time of the mixture used is very short (< 10 minutes) which translates most probably in a few megapascals of compressive strength with minutes of its placement.

Obviously, the use of dry mix shotcrete represents an extremely well adapted method for placing such potent mixtures. Indeed, the fact that all of the dry materials are conveyed with air through the hose to the nozzle where water is added gives a very short contact time between the water and the cementing materials before it is sprayed onto the surface. By using pre-blended bulk bags that can be stored for long period of time, it becomes easy to have concrete material ready in case of emergency. Combined with the very simple mobilization of dry-mix shotcrete and absence of a need for formwork, a fast and reliable system could be obtained.

Table 3 : Compressive strength

Specimens	**Compressive strength, MPa**						
	1h	2h	3h	6h	1j	7j	28j
Prisms	***12.9***	24.9	29.6	--	--	--	--
Cores	--	--	***35.6***	47.6	54.6	51.9	***52.1***

4. CONCLUSION

The objective of this research project was to produce a dry mix shotcrete material offering a very rapid strength development. This was successfully achieved using standard shotcreting equipment.

The very rapid hardening provides extremely high early compressive strength (12 MPa at 1 hour) showing very interesting potential for emergency response. Structural damages caused by fire in tunnels or by natural disasters on essential structures could be very rapidly alleviated using such a mix design in combination with the dry-mix shotcrete application method. Along with pre-blended bulk bags and combined with the ease of mobilization of dry-mix shotcrete equipment, a fast and reliable system could be obtained for rapid “structural emergency” response.

REFERENCES

ACI-506.R (2005). *Guide to Shotcrete*, ACI International.

ASTM (2003). C 1140 - Standard Pratice for Preparing and Testing Specimens from Shotcrete Test Panels.

ASTM (2005). C 1604 - Standard Test Method for Obtaining and Testing Drilled Cores of Shotcrete.

CP-60, A. (2009). *Craftsman Workbook Publication CP-60(09)*. Farmington Hills, Michigan, USA.

Heere, R. and D. R. Morgan (2002). Determination of Early-Age Compression Strenght of Shotcrete. *American Shotcrete Association magazine*(Spring): 28-31.

Lamberet, S. (2005). *Durability of Ternary Binders Based on Portland Cement, Calcium Aluminate Cement and Calcium Sulfate*. PhD., École Polytechnique Fédérale de Lausanne.

Lemay, J.-D. (2013). *Développement de béton projeté à ultra-haute résistance initiale*. M. Sc., Canada.

Neville, A. M. (2008). *Properties of Concrete*, Pearson Prentice Hall.

Prudêncio Jr, L. R. (1998). Accelerating admixtures for shotcrete. *Cement and Concrete Composites* 20(2–3): 213-219.

A study of the behavior of a beam column joint with complex arrangement of reinforcing bars by finite element analysis

Liyanto EDDY[1] and Kohei NAGAI[2]
[1]Doctoral Student, Department of Civil Engineering
The University of Tokyo, Japan
eddy@iis.u-tokyo.ac.jp
[2]Associate Professor, International Center for Urban Safety Engineering
Institute of Industrial Science, the University of Tokyo, Japan

ABSTRACT

As many buildings experienced failures due to the previous earthquake, the performance requirement of building structures in the seismic design code becomes more stringent. To satisfy the performance requirement, more reinforcements of beams and columns are needed. Consequently, at a beam column joint, where reinforcement bars of a beam are anchored into a column, reinforcement congestion is occurred, causing difficulties during the compaction and furthermore, resulting a poor quality of construction. To reduce the reinforcement congestion in a beam column joint, a comprehensive study of the behavior of the beam column joint is needed. However, the behavior of the beam column joint has not been clarified well yet. Many aspects are involved in a relatively small dimension of a beam column joint, causing a complex stress distribution, such as material nonlinearity, the bond behavior of the anchorage, shear, and others, that even some of them are not well understood independently. In this study, by using a finite element analysis, the behavior of an example of a typical beam column joint of viaduct structures with complex arrangement of reinforcement bars is studied. In the other hand, the applicability of the finite element analysis with a complex arrangement of reinforcement bars has not been investigated. In this study, by using a complex arrangement of reinforcement bars, the applicability of the finite element analysis in predicting the beam column joint failure will be studied. Based on the analysis result, typical diagonal cracks of beam column joints, observed through the experimental work, can be simulated by the finite element analysis. However, the behavior of the beam column joint is difficult to be observed by the finite element analysis, when complicated cracks occur inside the beam column joint portion.

Keywords: *finite element analysis, beam column joint, complex arrangement of reinforcement bar, anchorage failure.*

1. INTRODUCTION

As many buildings experienced failures due to the previous earthquake, the performance requirement of building structures in the seismic design code

becomes more stringent. To satisfy the performance requirement, more reinforcements of beams and columns are needed. Consequently, at a beam column joint, where reinforcement bars of a beam are anchored into a column, reinforcement congestion is occurred, causing difficulties during the compaction and furthermore, resulting a poor quality of construction. To reduce the reinforcement congestion in a beam column joint, a comprehensive study of the behavior of the beam column joint is needed. However, the behavior of the beam column joint has not been clarified well yet. Many aspects are involved in a relatively small dimension of a beam column joint, causing a complex stress distribution, such as material nonlinearity, the bond behavior of the anchorage, shear, and others, that even some of them are not well understood independently.
In order to study the behavior of beam column joints, particularly with a complex arrangement of reinforcement bars, there are two alternatives, i.e. experimental works in laboratories and computational numerical simulations. Through experimental works, the real load-displacement relationship can be obtained easily. However, the behavior of beam column joints with complex arrangement of reinforcement bars, i.e. how the cracks propagate and how the stresses are generated, is difficult to observe because of the presence of complicated cracks and stresses. Thus, the numerical simulation will be a beneficial tool to observe the behavior of beam column joint with complex arrangement of reinforcement bars since the internal cracks and the internal strains can be obtained easily as the load changes. By finite element analysis, Salem *et al.* (2004) simulated well the bond behavior of ribbed reinforcement bars. However, the 3-dimensional arrangement of reinforcement bars was not modeled and the applicability of the finite element analysis with a complex arrangement of reinforcement bars has not been investigated. In this study, by using a complex arrangement of reinforcement bars, the applicability of the finite element analysis in predicting the beam column joint failure will be studied. Therefore, the objective of this study is to study the behavior of a beam column joint with complex arrangement of reinforcement bars by finite element analysis.

2. ANALYSIS METHOD

In this study, the simulation was carried out by 3-dimensional finite element analysis, COM3, developed by The University of Tokyo. In COM3, 3-dimensional reinforced concrete model is meshed into some solid elements. Furthermore, in this study, a beam column joint was meshed into plain concrete elements and steel elements. Details of the material models are discussed in the references (Maekawa *et.al.* (2003)).

3. ANALYSIS OF A BEAM COLUMN JOINT WITH COMPLEX ARRANGEMENT OF REINFORCEMENT BARS

3.1 Detailed Analysis

In order to study the behavior of a beam column joint with a complex arrangement of reinforcement bars, the finite element analysis was conducted for a typical beam column joint of viaduct structures. Since the purpose of this research is to study the behavior of a beam column joint with a complex arrangement of reinforcement bars, the dimensions, the reinforcement bars, including bending portion of the reinforcement bars, and the boundary condition were modeled in an accurate manner. 3-dimensional model of reinforcement bar was used. However, for the simplification of the analysis model, a rectangular shape of reinforcement bar is used, with the same area with the circular shape of the actual reinforcement bar. Furthermore, the dimensions, the reinforcement bars of the beam column joint, and the boundary condition of the analysis model, will be described below.

3.2 Analysis model

The dimension of the analysis model is shown in Figure 2. Further, the material properties of the concrete and reinforcement bars are shown in Table 1. 67314 elements are used to model the beam column joint. The size of elements in beam column joint portion is around 1 cm^3.

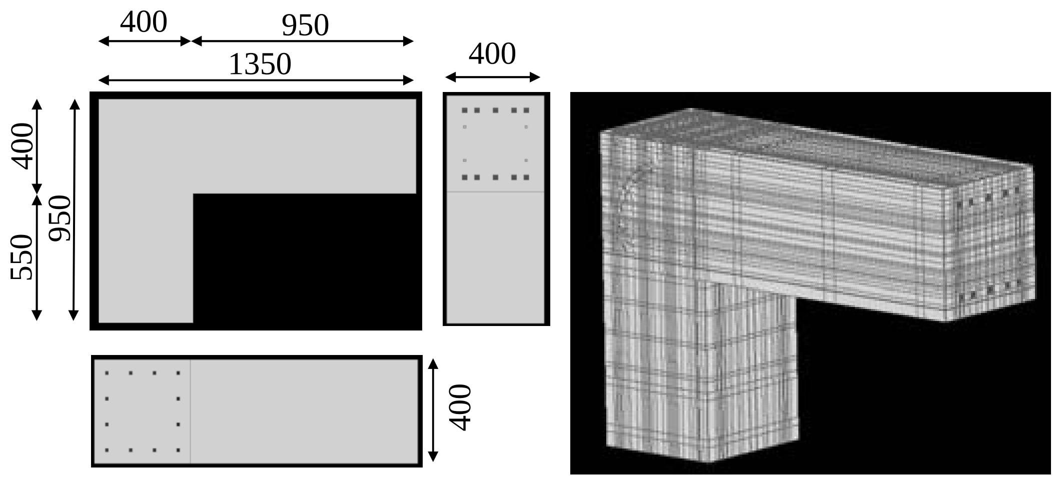

Figure 2: Analysis model (Units: mm)

For meshing simplification purpose in the numerical simulation, a rectangular shape of the reinforcement bar was used with the same area with the circular shape of the actual reinforcement bar. In the other hand, spiral stirrups of the column were simplified by increasing the yield strength of the tied stirrups of the column, and tied stirrups of the beam were simplified by enlarging the area of the tied stirrups of the beam. The bending portion of the hooked bar anchorages, located in beam column joint were modeled in an accurate manner. The reinforcement bars of the analysis model shown in Figure 3.

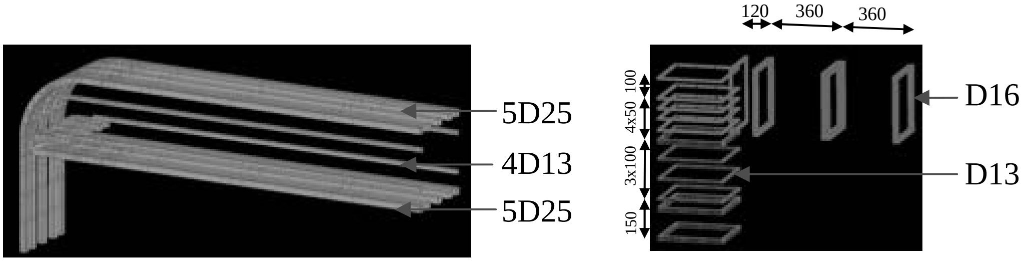

(a) Beam Re-Bars (b) Stirrups

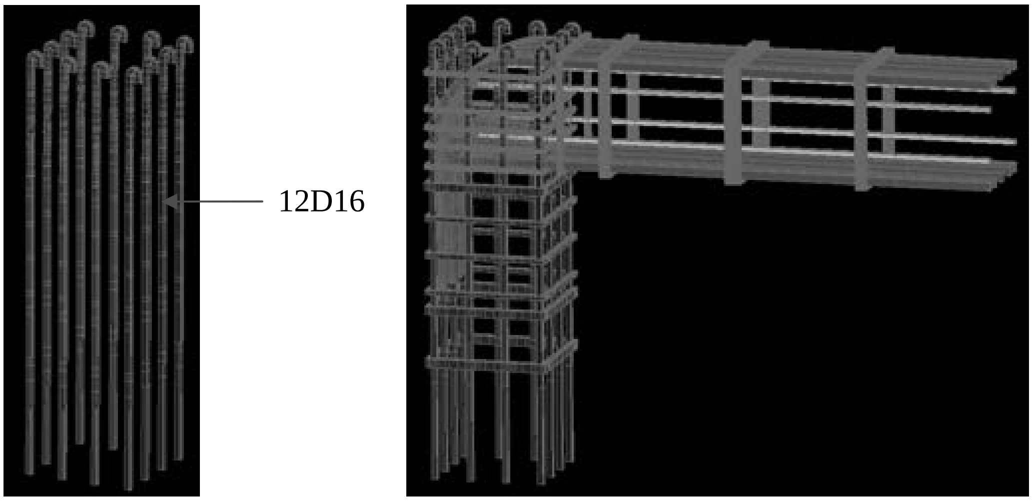

(c) Column Re-bars (d) 3-D Reinforcement Bar of Analysis model

Figure 3: Reinforcement Bars of the Analysis model

3.3 Boundary Condition

Figure 4 shows the detail of the frame loading of the analysis model, which was used as a typical frame loading in the experimental set-up. Fix condition in all direction was assumed as the boundary condition at the bottom of the steel frame. There are 3 hinges that were modeled as the boundary condition. To allow the rotation, a pin, located in the middle of the steel plates, is introduced as the connection between the steel plates (Figure 5). Furthermore, an interface element is introduced between the pin and the steel plates, with small value of shear stiffness, so that no shear force is transferred between the steel plates and the pin.

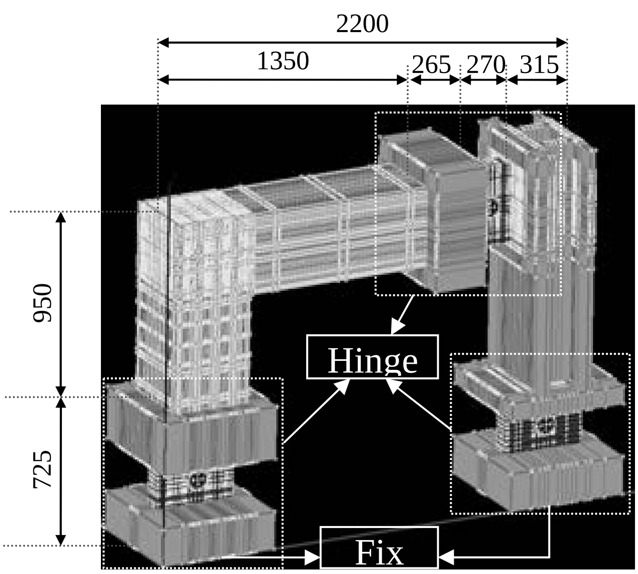

Figure 4: Detail of Frame Loading of Analysis Model

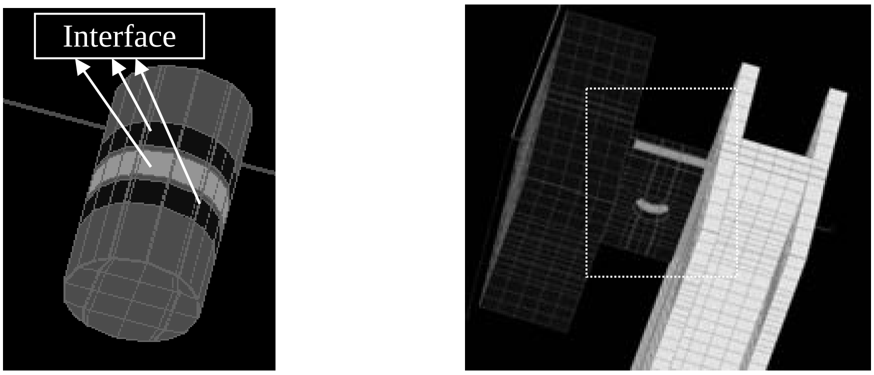

(a) Pin (b) Hinge

Figure 5: Detail of Hinge

Cyclic load of displacement control, pull load and push load alternately, was applied to the steel frame, located at the end of the beam, by the displacement control. In addition, the applied load, pull load and push load, was intended to examine the behavior of the beam column joint for a moment that tends to open and close the right angle, respectively. The same load pattern was used in the analysis model. The load was applied the steel frame which is located at the end of the beam. Figure 6 shows the load pattern of the cyclic load.

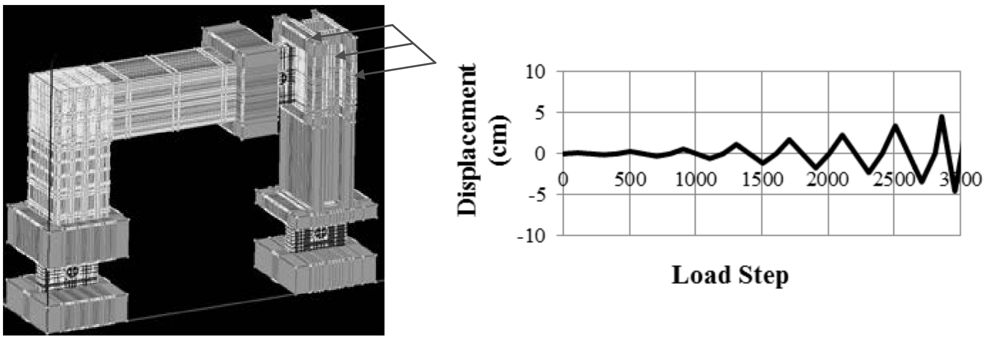

Figure 6: Load Pattern of Cyclic Load

4. ANALYSIS RESULT

4.1 Load-Displacement Relationship

Load-displacement relationship of the analysis model is shown in Figure 7 and the backbone curve of the analysis model is shown in Figure 8. The load-displacement relationship is the load and the displacement in which the load was applied.

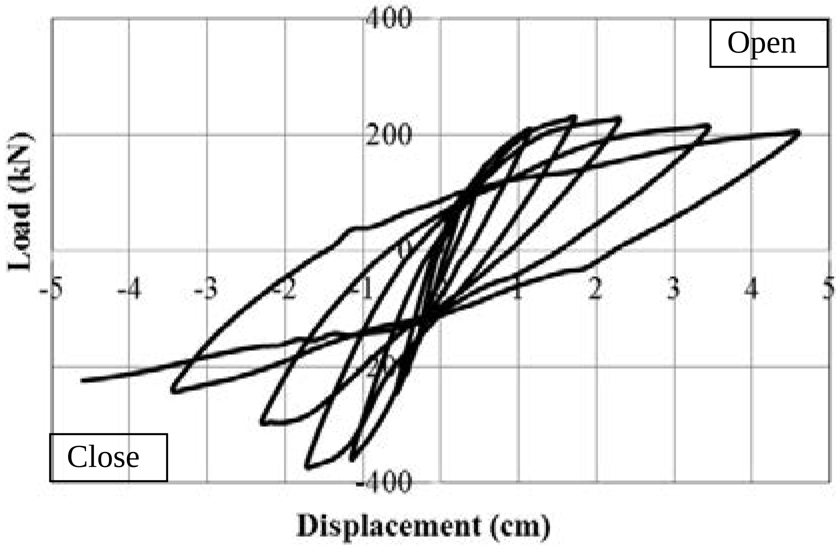

Figure 7: Load-Displacement Relationship of Analysis model

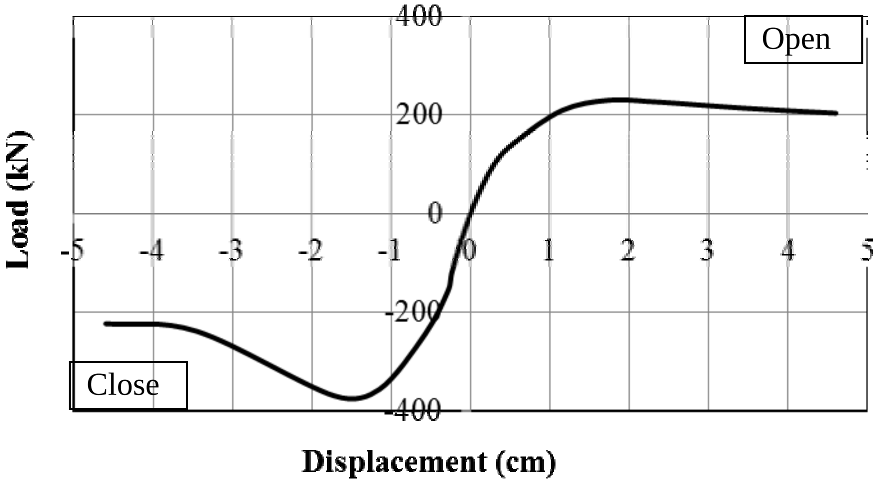

Figure 8: Backbone Curve of Analysis model

Based on the backbone curve of the analysis model, after cracks occur, the stiffness of the beam column joint decreases until the load reaches the maximum load, both under the opening load and the closing load. Under the opening load, the maximum load of the beam column joint is 229 kN at the displacement of 1.725 cm. Under the closing load, the maximum load of the beam column joint is higher than under the opening load, i.e. 370 kN at the displacement of 1.725 cm. After the load reaches the maximum load, at the displacement of 2.3 cm, the load capacity of the beam column joint does not decrease significantly under the opening load, i.e. 227 kN (98% of the maximum load), but the load capacity of the beam column joint decreases significantly under the closing load, i.e. 293 kN (80% of the maximum load) because of the anchorage failure of the longitudinal bars of the beam, as discussed later. Furthermore, to observe the failure behavior of the beam column joint by numerical simulation, the crack pattern of the beam column joint will be described below.

4.2 Crack Pattern

In this study, the crack pattern obtained by the simulation is described below. The cracks are not associated with the discrete cracks, but represent the smeared cracks. Furthermore, the cracks depend on the magnitudes of strains and element sizes.

4.2.1 Crack Pattern under Closing Load

Figure 9 shows the crack pattern of the analysis model at the displacement of 0.288 cm, 1.15 cm, and 1.75 cm, under the closing load.

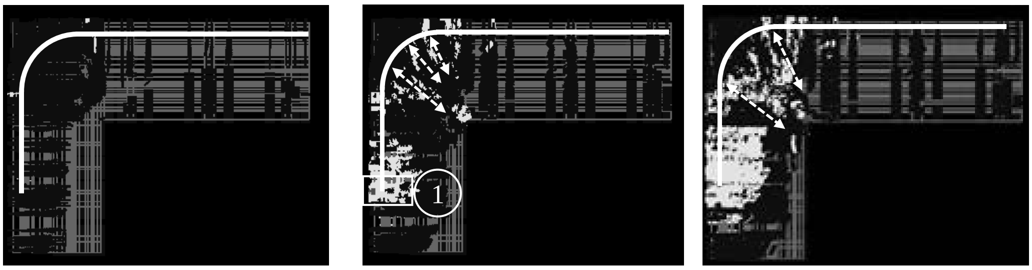

(a) 0.288 cm (b) 1.15 cm (c) 1.75 cm

Crack Width: <0.02 cm 0.02cm-0.3cm

Figure 9: Crack Pattern of the Analysis Model under Closing Load

When the applied load is relatively small, at the displacement of 0.288 cm, flexural cracks occur outside the bend of the bar anchorages, inside the beam column joint portion. As the load increases, i.e. at the displacement of 1.15 cm, cracks occur inside the bend of the bar anchorages. Furthermore, diagonal cracks, which are roughly perpendicular to the bend of the bar anchorages, occur. Before the load reaches the maximum load, large width of cracks occur at the end of the anchorages (1), and may indicate the beginning of the anchorage failure of longitudinal bars of beams. At the displacement of the maximum load, i.e. 1.75 cm, more cracks occur inside the bend of the bar anchorages.

To check the applicability of Finite Element Analysis in predicting the beam column joint failure, the crack pattern of the Finite Element Analysis is compared roughly with typical crack patterns of beam column joints from the previous experimental work. In this study, the experimental work of beam column joints of Megget (2003) is used as the comparison. Figure 10 shows the typical crack patterns of beam column joints from the previous experimental work. Red lines indicate cracks, formed under the closing load, in the other hand black line indicated cracks, formed under the opening load. The same tendency of crack patterns was observed between the finite element analysis and the experimental work. Diagonal cracks which are roughly perpendicular to the bend of the bar anchorages also occurred inside the bend of the bar anchorages of beam column joints of the experimental work, under the closing load. To understand why these diagonal cracks occur under the closing load, the reason will be described briefly.

(a) Joint A (b) Joint 14 (c) Joint 7

Figure 10: Crack Pattern of the Experimental Works (Megget (2003))

Figure 11 shows the responses of a beam column joint under the closing load, resulting moments to close the beam column joint. Forces, generated by the moments, are introduced into the beam column joint as shown in Figure 11.b. As the result, diagonal tensile stresses, shear stresses, are formed as shown in Figure 11.c. A diagonal crack occurs when the diagonal tensile stresses exceed the tensile strength of the concrete (Figure.11.d). The typical diagonal cracks, perpendicular to the bend of the bar anchorages, verify this behavior.

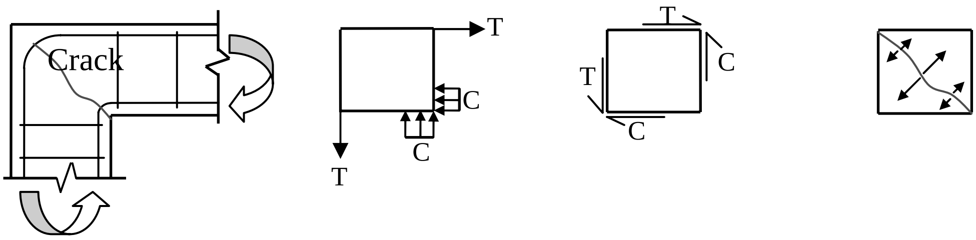

(a) Typical Cracks (b) Internal Forces (c) Shear Stress (d) Diagonal Crack

Figure 11: Response of Beam Column Joint under Closing Load

4.2.2 Crack Pattern under Opening Load

Figure 12 shows the crack pattern of the analysis model at the displacement of 0.288 cm, 1.15 cm, and 1.75 cm, under the opening load.

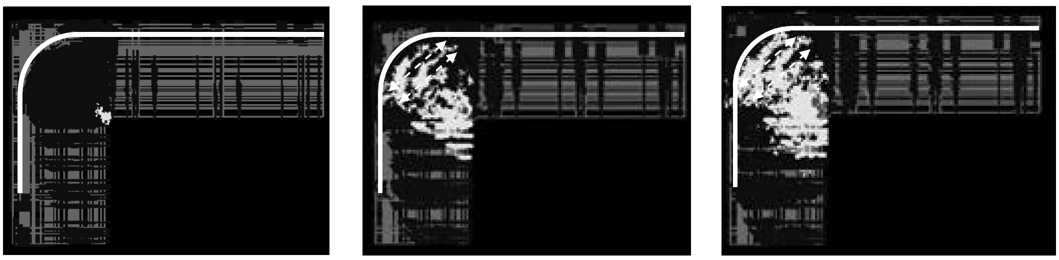

(a) 0.288 cm (b) 1.15 cm (c) 1.75 cm

Crack Width: <0.02 cm 0.02cm-0.3cm

Figure 12: Crack Pattern of the Analysis Model under Opening Load

When the applied load is relatively small, at the displacement of 0.288 cm, flexural cracks occur on the re-entrant corner of beam column joint. As the load increases, i.e. at the displacement of 1.15 cm, cracks occur inside the bend of the bar anchorages. Furthermore, diagonal cracks, which are roughly perpendicular to the cracks formed under the closing load, occur. At the displacement of the maximum load, i.e. 1.75 cm, more cracks occur inside the bend of the bar anchorages. Based on the experimental result, typical diagonal cracks, which are roughly perpendicular to the cracks formed under the closing load, also occurred inside the bend of the bar anchorages of beam column joints. To understand why these diagonal cracks occur under the opening load, the reason will be described briefly.

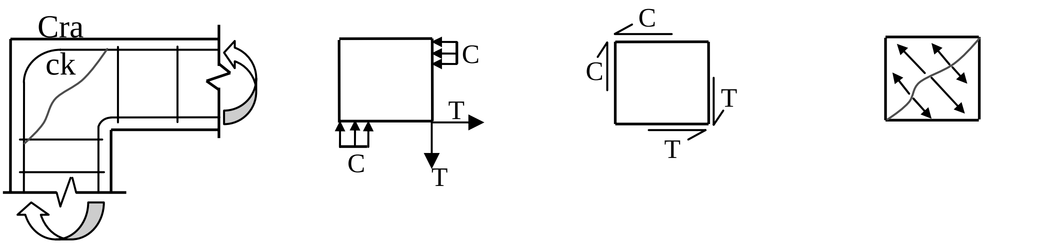

(a) Typical Cracks (b) Internal Forces (c) Shear Stress (d) Diagonal Crack

Figure 13: Response of Beam Column Joint under Opening Load

Figure 13 shows the responses of a beam column joint under the opening load, resulting moments to open the beam column joint. Forces, generated by the moments, are introduced into the beam column joint as shown in Figure 13.b. As the result, diagonal tensile stresses, shear stresses, are formed as shown in Figure 13.c. A diagonal crack, which is roughly perpendicular to the cracks formed under the closing load, occurs when the diagonal tensile stresses exceed the tensile strength of the concrete (Figure.13.d). The typical diagonal cracks verify this behavior.

4.2.3 Crack Pattern at Displacement of 2.3 cm of Closing Load

Figure 14 shows crack pattern at the displacement of 2.3 cm of the closing load. Complicated cracks occur inside the beam column joint portion of the analysis model, after loaded by several loads of the opening load and the closing load. However, the behavior of the beam column joint is difficult to be observed by finite element analysis, when the complicated cracks occur inside the beam column joint portion.

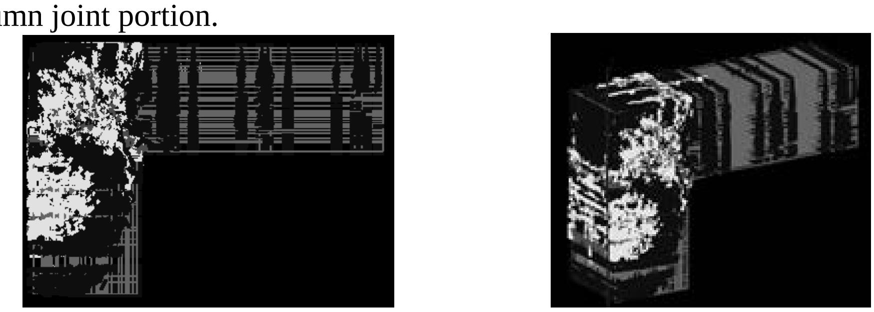

(a) Cracks of Front's Surface (b) Cracks of 3-D Model

Crack Width: <0.02 cm 0.02cm-0.3cm

Figure 14: Crack Pattern at Final Step of Load of Analysis Model

5. CONCLUSION

Based on the results of the numerical study of the behavior of a beam column joint with complex arrangement of reinforcement bars by finite element analysis, the following conclusions are made.

1. Finite element analysis could simulate the behavior of a beam column joint with complex arrangement of reinforcement bars.
2. When the push load was applied (close-mode), after the load reaches the maximum load, the load decreases significantly because of the failure of the anchorages. Diagonal cracks, which are roughly perpendicular to the bend of the bar anchorages, occur. These typical diagonal cracks were also observed from the experimental results.
3. When the pull load was applied (open-mode), after the load reaches the maximum load, the load does not decrease significantly as cracks are propagated inside the beam column-joint portion. Diagonal cracks, which are roughly perpendicular to the cracks formed under the closing load, occur. These typical diagonal cracks were also observed from the experimental results.
4. The behavior of the beam column joint is difficult to be observed by finite element analysis, after complicated cracks occur inside the beam column joint portion.

REFERENCES

Yoshitake, K., Ogawa, A., Ogira, D., and Maezono, T., 2012. The Effect of Bond Behavior of Longitudinal Reinforcement of Beam and Column on Beam Column Joint. JCI Vol.34, No.2, pp. 541-546. (*in Japanese*)

Hotta, H., Nishizawa, N., 2012. An Experimental Study on the Effect of the Position of Longitudinal Reinforcement for Reinforced Concrete Beam-Column L-shaped Joint. JCI Vol.34, No.2, pp. 282.83-282.88. (*in Japanese*)

Salem, H., Maekawa, K., 2004. Pre- and Postyield Finite Element Method Simulation of Bond of Ribbed Reinforcing Bars. Journal of Structural Engineering 2004.130:671-680.

Maekawa, K., Pimanmasm A., and Okamura, H, 2003. Nonlinear Mechanics of Reinforced Concrete. Spon Press Taylor & Francis Group, London and New York.

Megget, M. 2003. The Seismic Design and Performance of Reinforced Concrete Beam-Column Knee Joints in Buildings. Earthquake Spectra Vol.19, No.4, pp. 863-895.

Effects of crystalline admixture on compressive strength and shrinkage of concrete with pozzolanic materials

Viet TRAN HUU[1], Raktipong SAHAMITMONGKOL[2], and Somnuk TANGTERMSIRIKUL[3]
[1]Graduate student, Sirindhorn International Institute of Technology, Thammasat University. Thailand
E-mail: vietsiit@gmail.com
[2]Researcher, Construction and Maintenance Technology Research Center (CONTEC), Sirindhorn International Institute of Technology, Thammasat University, Thailand
[3]Professor, Department of Civil Engineering and Technology (CET), Sirindhorn International Institute of Technology, Thammasat University, Thailand

ABSTRACT

Crystalline admixture (CA) is a synthetic cementitious material which contains reactive silica and some crystalline catalysts. It has been used to improve the waterproofing and has a potential to improve durability properties of concrete. The effects of CA on compressive strength, autogenous shrinkage and total shrinkage of concrete with silica fume (SF) and ground granulated blast-furnace slag (SG) were investigated and compared in this study. The CA with ratio (0.5, 0.6) of total cementitious materials were applied to the specimens with two water to binder (w/b) ratios 0.4, 0.5 and replacement of SF content (5, 10%) as well as replacement of SG content (25, 60%) by weight of cement.

It was found that CA tends to increase compressive strength and autogenous shrinkage and decreasing total shrinkage of all types of concrete to different extent. The compressive strength at 91 days of almost all types of concrete was improved by CA. It is expected that the increase of compressive strength should be related with the crystal formation induced by CA. The CA also increases autogenous shrinkage of concrete. Both the increase of strength and autogenous shrinkage imply that the CA may improve the microstructure of concrete by filling some pores with crystals.

Although the autogenous shrinkage of concrete was increased by the CA, the total shrinkage of the same concrete was drastically reduced. This may be due to the fact that the CA consumes more water in its reaction and reduces average pore size so that the evaporation of water to the environment can be limited and retarded.

Keywords: *Autogenous shrinkage, Compressive strength, Crystalline admixture, Slag, Silica Fume, Total shrinkage*

1. INTRODUCTION

Concrete has been the most widely material used in the construction of civil infrastructure and industrial facilities worldwide. It was estimated that the present consumption of concrete in the word is more than 11 billion metric tons per year [1]. Along with this substantial growth of concrete demand, quality and durability of concrete have become very important issues.

As the concrete is a composite material produced from aggregates, cement, and other pozzolanic binders mixed with water. In its hardened state, the microstructure of concrete always consists of pores, capillaries, micro-cracks or voids. This porous nature of concrete is closely related to its strength as well as durability (such as shrinkage, chloride resistance, carbonation resistance, etc.) [2].

For decades, mineral additives such as silica fume (SF) and ground granulated blast-furnace slag (SG) has been added as a partial cement replacement to improve the engineering properties and performance of concrete [3, 4]. Effects of these mineral additives have been widely studied and well-documented [5-7]. Although the application of these mineral additives may beneficially modify the microstructure of concrete, the porous nature of concrete can only be reduced to some extent.

Crystalline admixture (CA) is a modern synthetic additive that has been used for improving waterproofing of concrete. Crystalline admixture contains reactive silica and some crystalline catalysts that can react with the moisture in concrete and generates a non-soluble, highly resistant crystalline formation throughout the pores and capillary tracts of concrete [8]. As this crystal formation seals the pores, it is expected to alter the mechanical properties as well as some durability properties of concrete.

Incorporating these materials into the concrete mixture not only improves quality and durability of concrete but also benefits economic and environmental considerations. The knowledge usage of crystalline admixture on different types of concrete is still very limited.

The aim of this study is to evaluate how the crystalline admixture can contribute to properties of concretes containing different binder components. The effect crystalline admixture on the compressive strength and shrinkage of concrete is emphasized and experimentally investigated.

2. EXPERIMENTAL PROGRAM

2.1 Materials and mix proportion

The cementitious materials used in this study were ordinary Portland cement type I (OPC), ground granulated blast-furnace slag (SG) and silica fume (SF). Chemical compositions and physical properties of these materials are given in Table 1. Coarse aggregate was crushed limestone with specific gravity of 2.69 and a maximum size of 20 mm. Fine aggregate was river sand with specific gravity and fineness modulus of 2.60 and 2.13, respectively. A naphthalene-based superplasticizer (SP) was used to adjust the workability of the concrete.

Concretes with two water/binder ratios (w/b = 0.4, 0.5) were tested. Cement-only concrete was tested and considered as a control concrete. For slag concrete, SG replacement percentages by weight of total binder content were 25 and 60%.

Table 1: Properties of cementitious materials

Chemical compositions (%)	OPC I	SF	SG	CA
Silicon dioxide	20.2	90.64	34.4	16.71
Aluminum oxide	4.70	2.76	9.0	3.10
Iron oxide	3.73	0.48	2.58	2.27
Calcium oxide	63.4	0.71	44.8	32.82
Magnesium oxide	1.37	2.71	4.43	1.76
Sulfur trioxide	1.22	0.36	2.26	1.27
Sodium oxide	-	0.85	0.62	-
Potassium oxide	0.28	2.26	0.5	10.02
Physical properies				
Specific gravity (g/cm^3)	3.15	2.13	2.68	2.90
Loss on ignition (%)	2.72	3.8	1.32	26.68
Blaine fineness (cm^2/g)	3430	6213	4320	5540

Table 2: Mix proportion of tested concrete (kg/m^3)

Mix proportion	Cement	Water	SP	SG	SF	CA	Sand	Gravel
0.4 OPC	382	149	3.82				801	1096
0.4 OPC 0.5	374	147	3.76			1.88	801	1096
0.4 OPC 0.6	372	146	3.74			2.25	801	1096
0.5 OPC	336	165	3.36				801	1096
0.5 OPC 0.5	329	162	3.30			1.65	801	1096
0.5 OPC 0.6	327	161	3.29			1.98	801	1096
0.4 SG 25	281	144	5.63	93.80			801	1096
0.4 SG 25 0.5	275	142	5.53	92.17		1.84	801	1096
0.4 SG 25 0.6	273	141	5.51	91.85		2.20	801	1096
0.5 SG 25	248	160	4.95	82.51			801	1096
0.5 SG 25 0.5	242	158	4.88	81.25		1.63	801	1096
0.5 SG 25 0.6	241	157	4.86	81.00		1.94	801	1096
0.4 SG 60	146	141	5.48	219.17			801	1096
0.4 SG 60 0.5	142	138	5.39	215.56		1.80	801	1096
0.4 SG 60 0.6	141	138	5.37	214.83		2.15	801	1096
0.5 SG 60	129	160	4.84	193.50			801	1096
0.5 SG 60 0.5	125	158	4.77	190.60		1.59	801	1096
0.5 SG 60 0.6	125	157	4.75	190.04		1.90	801	1096
0.4 SF 5	360	145	6.81		18.92		801	1096
0.4 SF 5 0.5	351	142	6.69		18.59	1.86	801	1096
0.4 SF 5 0.6	350	142	6.67		18.53	2.22	801	1096
0.5 SF 5	316	160	5.59		16.63		801	1096
0.5 SF 5 0.5	309	158	5.89		16.32	1.64	801	1096
0.5 SF 5 0.6	308	157	5.88		16.32	1.96	801	1096
0.4 SF 10	337	143	6.74		37.45		801	1096
0.4 SF 10 0.5	329	141	6.62		36.80	1.84	801	1096
0.4 SF 10 0.6	328	140	6.60		36.68	2.20	801	1096
0.5 SF 10	297	159	5.93		32.95		801	1096
0.5 SF 10 0.5	290	156	5.84		32.45	1.62	801	1096
0.5 SF 10 0.6	289	156	5.82		32.35	1.94	801	1096

For silica fume concrete, SF replacement percentages by weight of total binder content were 5 and 10%. For all types of concretes, comparative concrete mixtures with crystalline admixtures (CA) were produced and tested. The chemical composition of the CA is also provided in Table 1. Two dosages of crystalline admixtures (0.5 and 0.6% by weight of total binder content) were investigated in this study.

Table 2 shows the mix proportions of eighteen concrete mixtures tested in this study. The term 'OPC I' represents ordinary Portland cement (Type I), SG represents ground granulated blast-furnace slag, whereas SF represents silica fume. An example of description of the mixture designation is as follow: "0.5 SF 5 X 0.5" means the sample which has water to binder ratio of 0.5, silica fume replacement ratio of 5% and 0.5% of crystalline admixture.

2.2 Test Methods

2.2.1 Compressive strength

The compressive strength was tested in accordance with ASTM C39. Concrete cylinder specimens with a diameter of 100mm and height of 200 mm were cast and demolded at 24 hours after casting. After that, all specimens were sealed by plastic wrap and kept in controlled condition (28 ± 1 ^{o}C and RH 50-70%) until the age of testing. The compressive strength was tested at the ages of 7, 28 and 91 days. The universal testing machine (UTM) was applied for loading. The values of the compressive strengths are average from three tested samples.

2.2.2 Autogenous shrinkage

Shrinkage was evaluated by investigating the length change of concrete prisms in accordance with ASTM C157. The size of concrete prism specimens was 75x75x285 mm. Initial lengths of the specimens were measured just after demoulding at 24 hours after casting. The samples were subsequently double-layered sealed with plastic wrap and aluminum foil in order to prevent moisture loss to the environment. The loss of water was monitored by measuring the weight of concrete sample. All autogenous shrinkage samples have less than 1% weight loss throughout the test period.

The length of each specimen was measured periodically until the age of 91 days by using length comparator. Free expansion and free shrinkage strain can be calculated by using the following equations (positive value for shrinkage):

$$\Delta L = L_i - L_t \quad (1)$$

$$\varepsilon = (\Delta L / L_i) \times 10^6 \quad (2)$$

Where ΔL is the length change of specimen at the time t (mm), L_i is the initial length of specimen (mm), L_t is the length of specimen (mm) at the time t, and ε is the shrinkage strain.

2.2.3 Total shrinkage

The term 'total shrinkage' refers to an absolute volume change of concrete over time. In this study, it is assumed that the total shrinkage represents a summation of 'autogenous shrinkage' and 'drying shrinkage'. All temperature effects are ignored since the temperature was kept at 28± 1^{o}C throughout the test.

Concrete prism specimens for total shrinkage measurement were prepared in accordance with ASTM C 157. After casting, the plastic sheet was used to cover the specimens to avoid moisture loss to the environment. The specimen were demoulded at 24 hours after casting and immediately taken for the initial length measurement. The specimens were subsequently kept in a controlled environment (28 ± 1 ^{o}C and RH 50-70%). The length change measurements were conducted periodically until 91 days.

3. EXPERIMENTAL RESULTS AND DISCUSSION

3.1 Compressive strength

Figure 1 compares the compressive strengths of cement-only concrete and the cement-only concrete with CA. The results indicate that CA can increases the compressive strength of cement-only concrete at all ages (7, 28, 91 days). By adding CA, compressive strength of concrete can be increased for approximately 10%. For instance, in the case that the dosage of CA was 0.6% total binder content and water to binder ratio was 0.4, the CA can increase 28-days and 91-days compressive strengths for 10.34% and 12.26%, respectively. While, in the case that the dosage of CA was 0.6% total binder content and water to binder ratio was 0.5, the 28-day and 91-day strengths increase for 14.4 and 14.5%, respectively. More improvement of compressive strength can be expected in concrete with higher water-to-binder ratio and more dosage of CA. It is also noted here that, for cement-only, concrete, the strength improvement at 91 days are, in all cases, higher than the strength improvement at 28 days.

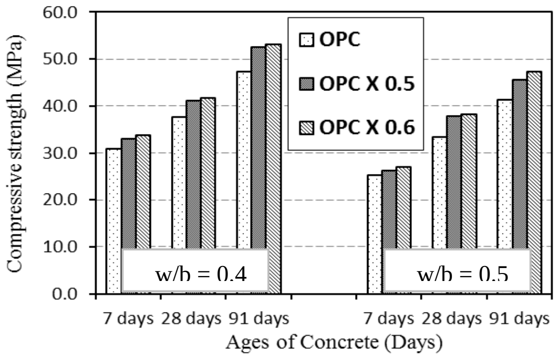

Figure 1: Compressive strength of cement-only concrete with/without CA

Figure 2 shows the effects of CA on compressive strength of the slag concrete Figure 2a and Figure 2b show the results of concrete with 25% and 60% slag replacement, respectively. It is clearly shown that, when cement is partially replaced by slag (25% or 60%), compressive strengths at 7 and 28 days are reduced while the compressive strengths at 91 days are increased. This is because the reaction of slag is slower than cement and requires $Ca(OH)_2$ from cement hydration to react. The results also show that CA can improve the compressive strength of slag concrete.

Figure 3 shows the effects of CA on compressive strength of the silica fume concrete. Figure 3a and Figure 3b show the results of concrete with 5% and 10% silica fume replacement, respectively. The results show that the effect of CA on the compressive strength of silica fume concrete at the age of 7 days and 28 days is not so good and reductions of compressive strength can be observed in some cases. However, the CA can increase the compressive strength of all silica fume concretes at 91 days. The deficiency of the CA during the early age may be due to very high reactivity of silica fume which may considerably consume $Ca(OH)_2$ in the early age period. The CA thus cannot react well in such period.

In spite of slight difference in strength development characteristics of all type concrete, it is proved that the CA can improve long-term strengths of all concrete. The strength improvement was found to be higher in older concrete. This result also suggests that the crystal formed by CA contributes as a permanent component of the cementitious microstructure system.

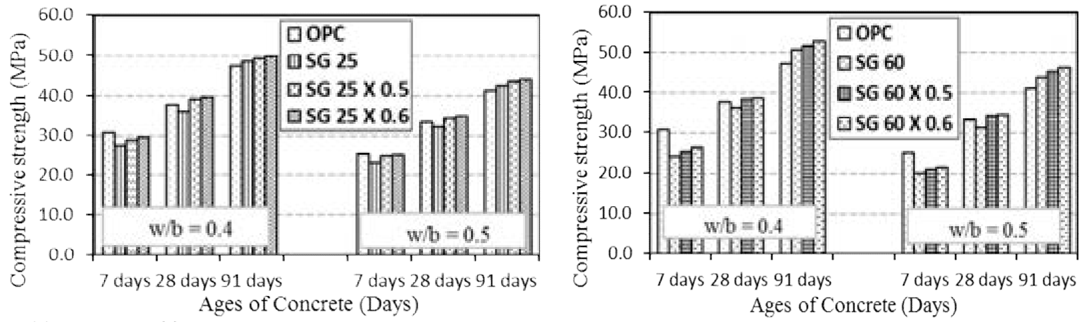

(a) Concrete with 25% Slag (b) Concrete with 60% Slag

Figure 2: Compressive strength of slag concrete with/without CA

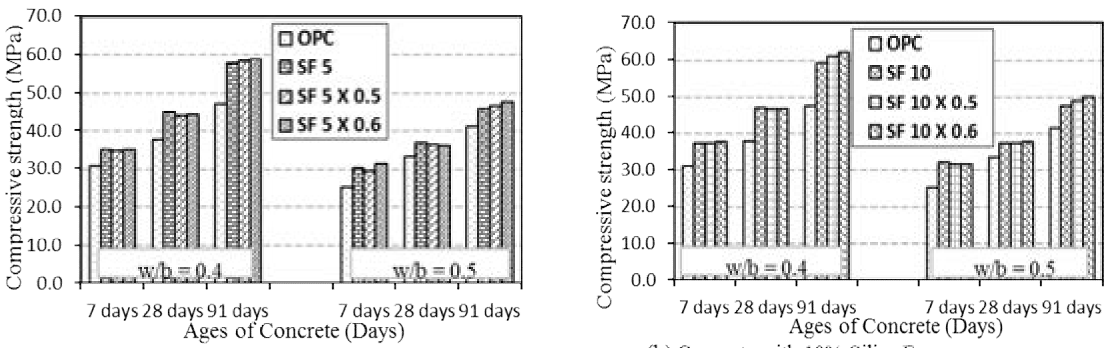

(a) Concrete with 5% Silica Fume (b) Concrete with 10% Silica Fume

Figure 3: Compressive strength of silica fume concrete with/without CA

3.2 Autogenous Shrinkage

The effect of CA on autogenous shrinkage of cement-only concrete is shown in Figure 4. The autogenous shrinkage at both w/b ratios 0.4 and 0.5 was increased by the addition of CA (Figure 4a and Figure 4b). In this case, the autogenous shrinkage may increase because the formation of crystals by CA changes pore structure and also consumes free water. The presence of CA in the system thus increases the self-desiccation.

Figure 5 shows the autogenous shrinkage of slag concrete. For concrete with 25% slag replacement (Figure 5a and Figure 5b), in the early age period, the autogenous shrinkage of slag concrete was smaller than that of cement-only concrete. However, at longer period, concrete with 25% slag has clearly more autogenous shrinkage. For concrete with 60% slag replacement (Figure 5c and Figure 5d), an early-age expansion can be observed and the final autogenous shrinkage is remarkably reduced. The early-age expansion may be induced by the formation of ettrigite since the slag contains higher content of sulfate (see Table 1). For all slag concrete mixtures, adding CA results in relatively higher autogenous shrinkage.

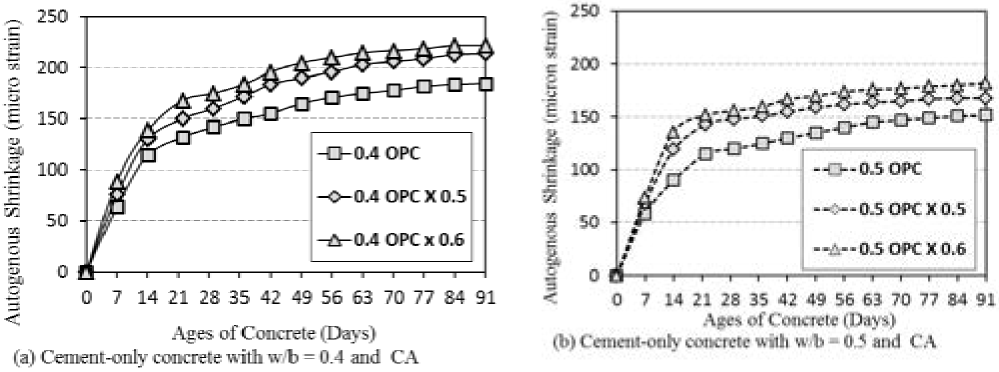

Figure 4: Autogenous shrinkage of cement only - concrete with/without CA

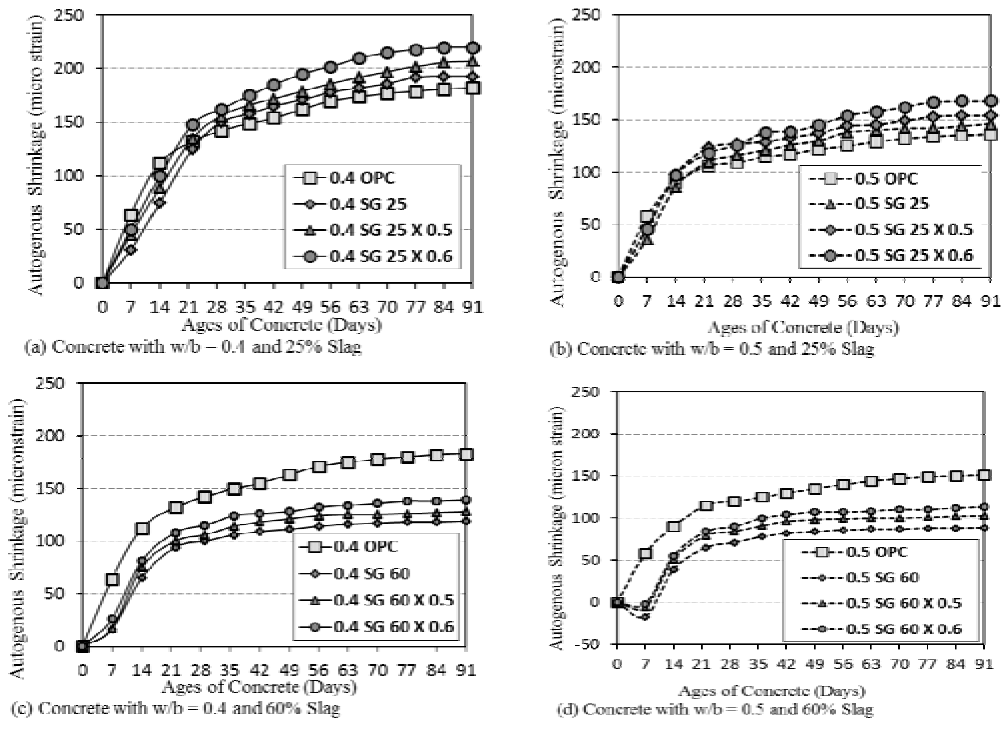

Figure 5: Autogenous shrinkage of slag concrete with/without CA

Figure 6 shows the autogenous shrinkage of silica fume concrete. When silica fume is added to concrete the autogenous shrinkage of concrete is drastically increased. For the silica fume concrete with w/b = 0.4 (Figure 6a and Figure 6c), the autogenous shrinkages at 7 days were approximately double of those of cement-only concrete. This is due to a high reactivity and reaction rate of silica fume. As the rate of reaction is accelerated, the autogenous shrinkage became larger. Adding CA into silica fume concrete additionally increase the autonomous shrinkage.

The test results clearly show that the CA increases the autogenous shrinkage of all types of concretes. The increase of autogenous shrinkage should be related to the modification of microstructure by the crystal formation. Although the higher value autogenous shrinkage indicates higher risk of shrinkage crack. It, at the same time, implies that the microstructure of concrete became denser by the incorporation of CA. Furthermore, the risk of shrinkage crack should be evaluated by considering the total shrinkage not merely the autogenous shrinkage.

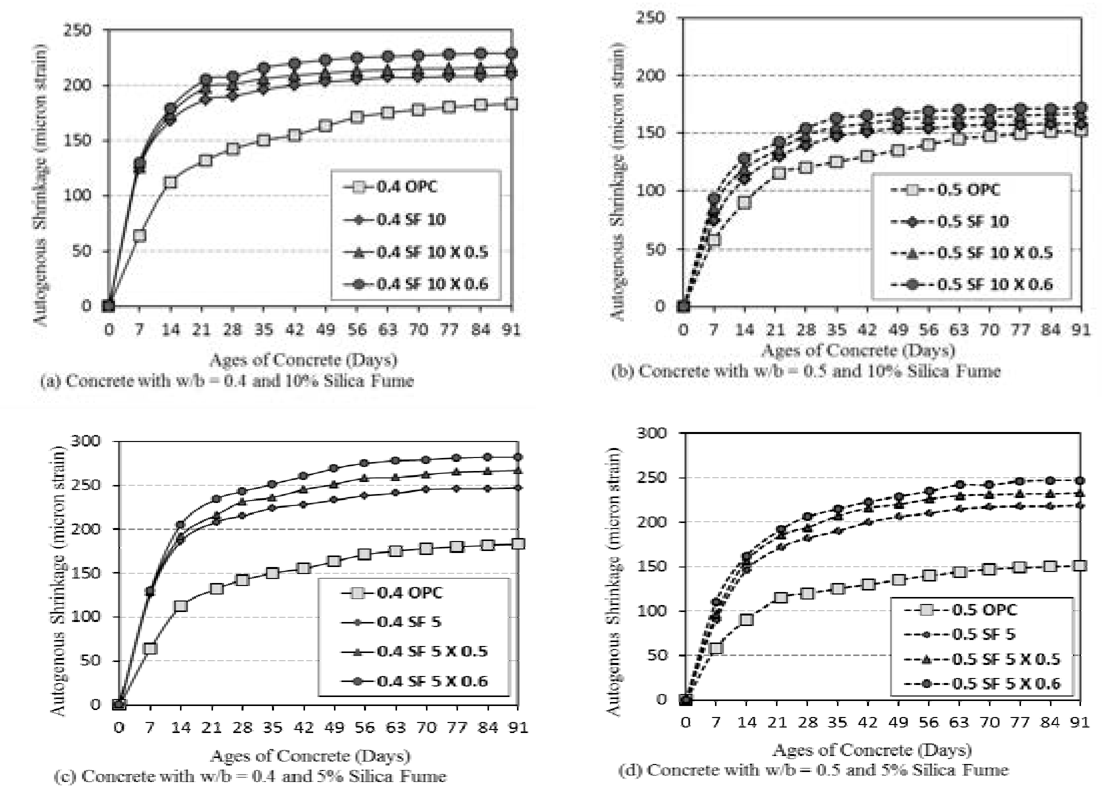

Figure 6: Autogenous shrinkage of silica fume concrete with/without CA

3.3 Total shrinkage

Figure 7 shows the total shrinkage of cement-only concrete. Higher water-to-binder ratio (w/b) results in higher total shrinkage although the autogenous shrinkage is reduced (see Figure 4). This is because the concrete with higher water content, in same drying condition, encounter more evaporation of free water and more drying shrinkage.

Figure 8 and Figure 9 shows the total shrinkage of slag concrete (Figure 8a and Figure 8b) and silica fume concrete (Figure 9a and Figure 9b), respectively. In this experiment, it was found that the partial replacement of cement by slag or silica fume can reduce the total shrinkage to a certain extent although the autogenous shrinkage was found to be larger (see Figure 5 and Figure 6).

This is probably related to the small size of test concrete prisms and their high surface area. With this high surface area to total volume (S/V), the drying shrinkage dominates the total shrinkage behavior. It is noted here that the contribution from drying shrinkage should be proportionally lower in the case of the real concrete structural element.

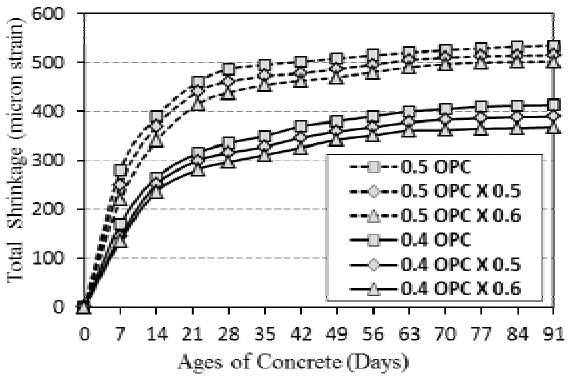

Figure 7: Total shrinkage of cement only - concrete with/without CA

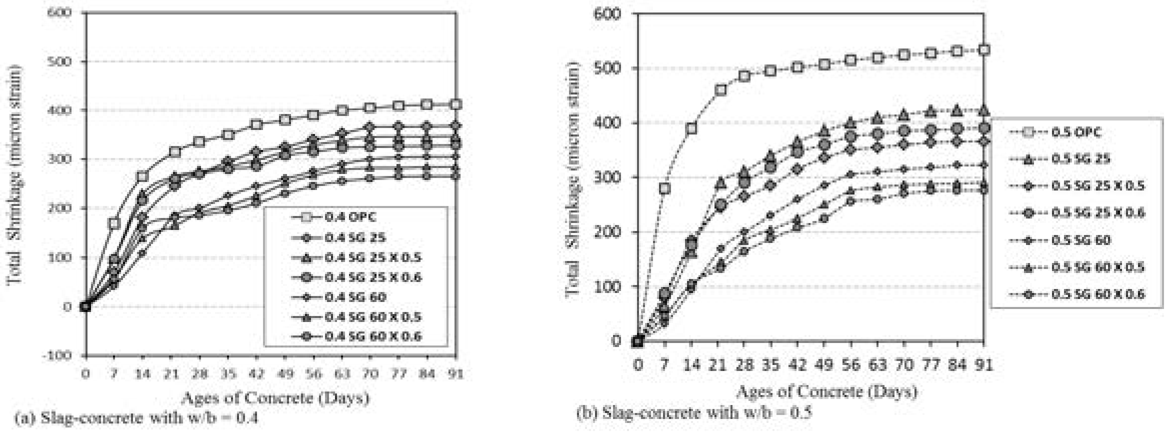

Figure 8: Total shrinkage of slag concrete with/without CA

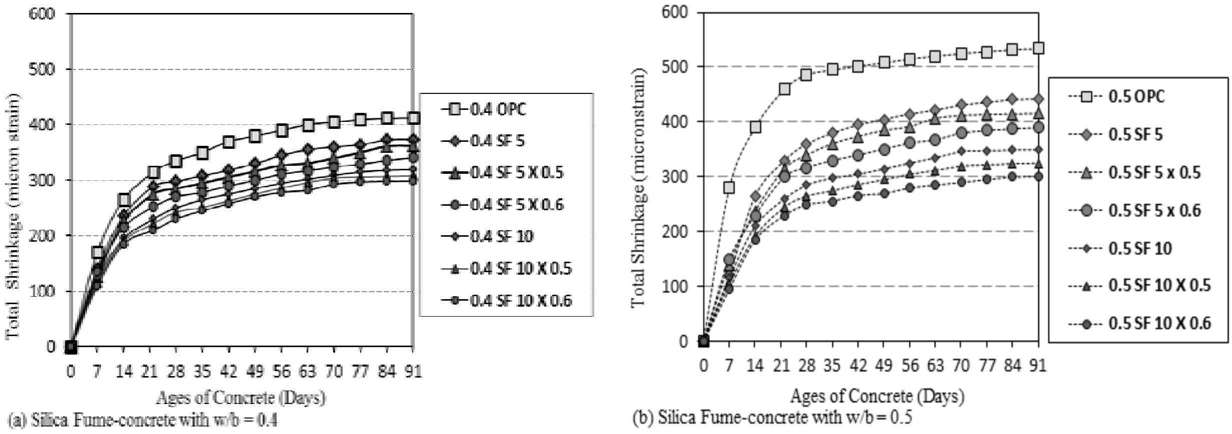

Figure 9: Total shrinkage of silica fume concrete with/without CA

The results of all types of concrete also demonstrate that the addition of CA into concrete reduces the total shrinkage (see Figures 7, 8, and 9) although it was reported to induce higher autogenous shrinkage (see Figures 4, 5, and 6). It is possible that CA consumes free water in its reaction and reduces evaporable water content. At the same time, the average pore size is expected to be reduced by the crystal formation. This smaller pore can retard the evaporation of free water to environment. As a result, the drying shrinkage can be reduced when CA is added.

Figures 10, 11, and 12 show the effects of CA on the drying shrinkage of cement-only concrete, slag concrete, and silica fume concrete, respectively. The drying shrinkage was calculated by subtracting the total shrinkage with the autogenous shrinkage of the same mix. The results clearly show the drying shrinkage of all types of concrete can be drastically reduced by the incorporation of CA. Especially, in the case of concrete with 10% silica fume replacement, the CA can reduce drying shrinkage remarkably low (lower than 90).

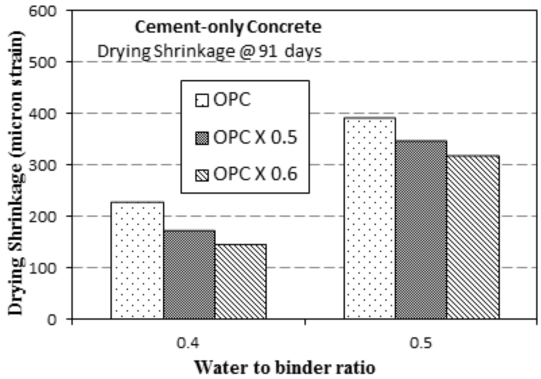

Figure 10: Drying shrinkage of cement only - concrete with/without CA

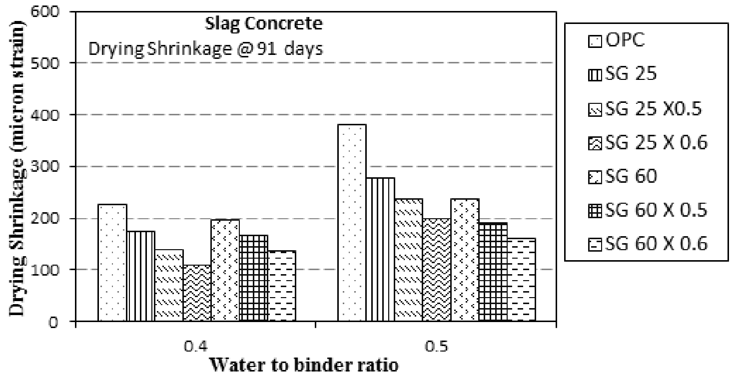

Figure 11: Drying shrinkage of slag concrete with/without CA

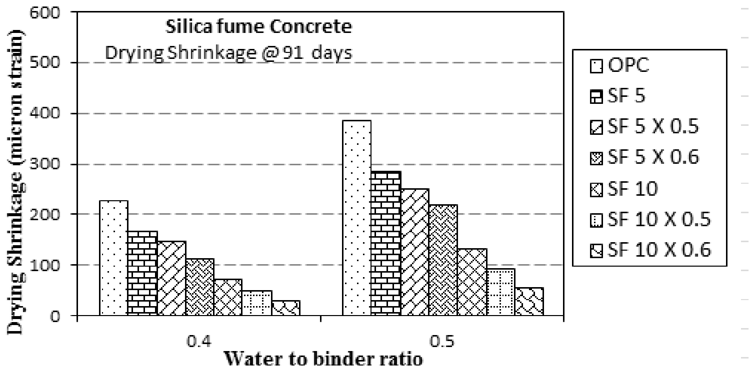

Figure 12: Drying shrinkage of silica fume concrete with/without CA

4. CONCLUSIONS

- Crystalline admixture (CA) increases compressive strength, especially at long-term of all types of concrete (cement-only concrete, slag concrete, and silica fume concrete).
- The increase of strength is more at long-term. This suggests that the improvement by CA is permanent.
- Although CA increased the autogenous shrinkage of concrete, the total shrinkage was favorably reduced. This is related to ability of CA to reduce the evaporation of free water from the concrete specimens.

REFERENCES

[1] Mehta, P.K., Monteiro. Paulo J.M, 2006. *Concrete, Microstructure, properties, and Materials,* 3rd Edition.
[2] Tangtermsirikul, S., 2003. *Durability and Mix design of concrete,* 1st Edition.
[3] Malhotra, V.M., and Mehta, P.K., 1996. *Pozzolanic and cementitious materials, Advances in Concrete Technology,* Gordon and Breach, London.
[4] K.E. Hassan, J.G. Cabrera, R.S. Maliehe, 2000. *The effect of mineral admixtures on the properties of high-performance concrete*, Cement and Concrete Composites, 267-271.
[5] Bouikni, A, Swarmy, R.N., and Bali, A., 2009. *Durability properties of concrete containing 50% and 65% slag*, Construction and Building Materials, 2836-2845.
[6] Lee, K.M., Lee, H.K., Lee, S.H., and Kim, G.Y., 2006. *Autogenous shrinkage of concrete containing granuated blast-furnace slag*, Cement and Concrete Research, 1279-1285.
[7] Zhang, M.H., Tam, C.T., Leow, M.P., 2003. *Effect of water-to-cementitious materials ratio and silica fume on the autogenous shrinkage of concrete*, Cement and Concrete Research, 1687-1694.
[8] Yodmalai, D., Sahamitmongkol, R., Tangtermsirikul, S., Lawtrakul, L., 2010. *Water sorptivity, water permeability, autogenous shrinkage, and compressive strength of concrete with crystalline materials* , 15th National Convention on Civil Engineering, Ubon Ratchathani, Thailand.

Effect of heating and re-curing on crack characteristics in cement paste

Yuto HARAGUCHI[1], Michael HENRY[2], Ivan Sandi DARMA[3], and Takafumi SUGIYAMA[4]
[1]Master student, Division of Field Engineering for the Environment, Graduate School of Engineering, Hokkaido University, Japan
knmrhtkemsn@gmail.com
[2]Assistant professor, Division of Field Engineering for the Environment, Faculty of Engineering, Hokkaido University, Japan
[3]Ph.D. student, Division of Field Engineering for the Environment, Graduate School of Engineering, Hokkaido University, Japan
[4]Professor, Division of Field Engineering for the Environment, Faculty of Engineering, Hokkaido University, Japan

ABSTRACT

After fire, concrete performance degrades due to dehydration of the cement paste, which leads to coarsening of microstructure and the formation of cracks. Healing of cracks has been observed under water re-curing, and these may have a large influence on the recovery of concrete performance, but it is necessary to better understand the effects of heating and subsequent re-curing on crack characteristics. In this research, the changes in microstructure and cracks due to heating and re-curing were investigated by applying X-ray CT and image analysis techniques, which enable non-destructive examination of the internal microstructure of a material. Results showed that, in the cement paste specimen, radial cracks formed during heating due to shrinkage by dehydration. Under water re-curing, these cracks grew larger and new cracks formed due to expansion by rehydration. The growth of the cracks in the cement paste under water re-curing may be due to the rehydration of calcium oxide into calcium hydroxide under water supply which led to expansion of the specimen.

Keywords: *fire damage, re-curing, microstructure, crack recovery, rehydration, repair*

1. INTRODUCTION

After fire, concrete performance degrades due to dehydration and cracks caused by shrinking, so it is necessary to restore performance to the same state as before the fire for resuming use of concrete structure. Restoring performance generally involves repair operations, including demolition of the damaged concrete, but these require extensive labor and time which may contribute to an increased environmental impact.

Some past research has reported that concrete performance can be recovered by re-curing the fire-damaged concrete in water. This leads to self-healing of cracks and decrease in air voids due to rehydration of cement hydrates (Suzuki et al., 2010; Henry et al., 2011). The healing of cracks under re-curing may have a large influence on the recovery of concrete performance, but crack formation and recovery under fire loading and re-curing have not been studied in depth. Therefore, in this research the formation and change in cracks after heating and re-curing was investigated using X-ray CT, which can non-destructively examine the internal microstructure of a material.

2. EXPERIMENTAL PROCEDURE

2.1 Overview

An overview of the experimental flow is shown in Figure 1. High-strength cement paste with a W/C of 30% was made using ordinary Portland cement, and specimens were cured in water for 13 weeks. After curing, specimens were heated at 600ºC in an electric furnace for 1 hour. After heating, specimens were re-cured in water for up to 13 weeks. In this research, two experiments were carried out: X-ray CT and TG/DTA (Thermogravimetry Differential Thermal Analysis). Specimens were examined before heating, after heating and after 1 (TG/DTA only), 4 and 13 weeks water re-curing.

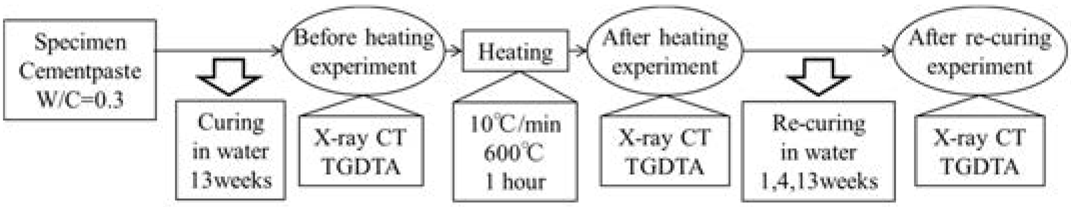

Figure 1: Experimental flow

2.2 Specimens

Two types of specimens were prepared: cylinders (100×200 mm) and beams (40×40×160 mm). As shown in Figure 2, after curing for 4 weeks cores 20 mm in diameter were extracted from the cylinder specimens and cut to a length of 20 mm. The beam specimens were also sliced (40×40×2 mm) at the same time, and the small test specimens were returned to the water for 9 more weeks.

2.3 Heating and re-curing

After 13 weeks of curing, the test specimens were exposed to high temperatures in an electric furnace. The heating curve and electric furnace picture are shown Figure 3. The rate of heat increase was set at 10ºC per minute and the target temperature of 600ºC was held for 1 hour. After heating, specimens were cooled naturally in the air for 1 hour then re-cured in water of at 20ºC for up to 13 weeks.

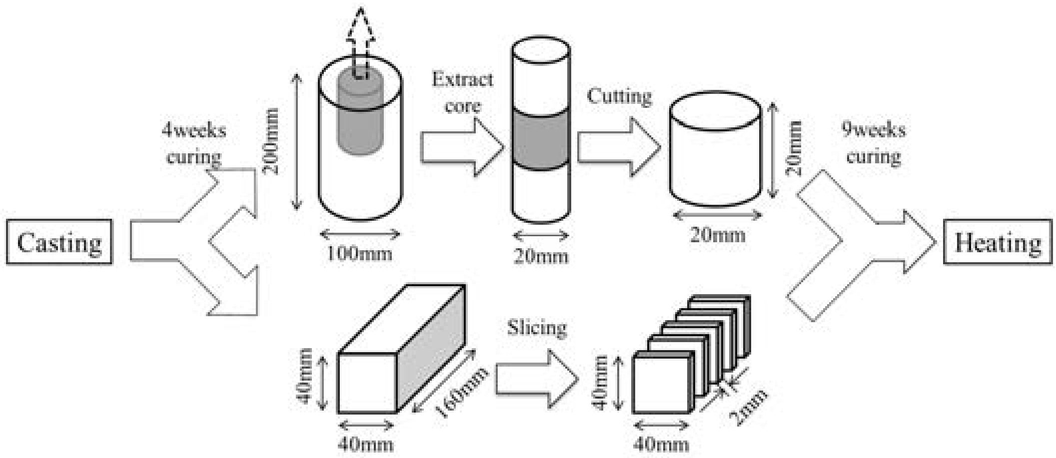

Figure 2: Flow of specimen preparation and curing

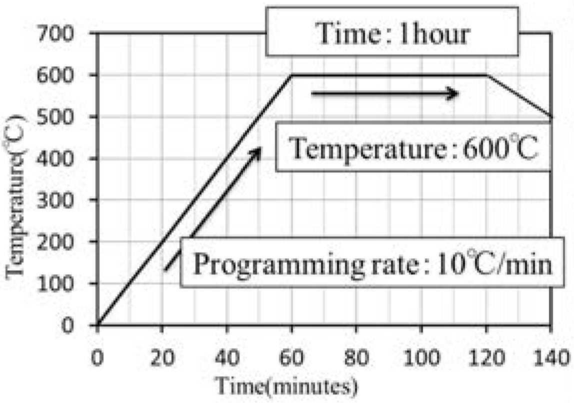

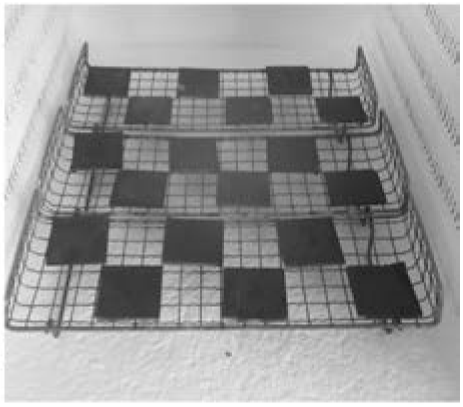

Figure 3: Heating curve (left) and specimen heating conditions (right)

2.4 Image capture using X-ray CT

As summarized by Promentilla and Sugiyama (2010) and Landis and Keane (2010), the concept of X-ray microtomography is similar to that of Computed Axial Tomography (CAT or CT) scans in the medical field, in which a three-dimensional (3D) digital image is reconstructed from a series of two-dimensional (2D) images or "slices." Each voxel (3D pixel) within the 3D digital image has an associated X-ray absorption value which can be correlated to material density, and thus the internal structure can be determined based on the arrangement of the voxels in a 3D space.

The setup for acquiring the X-ray CT images is shown in Figure 4 and the details of the X-ray CT specimen are shown in Figure 5. Image acquisition in the specimens occurred in the illustrated focus area, which was approximately 11 mm in height, 20 mm in diameter, and roughly centered on the specimen. In this area, 351 slices of 33 microns thick were obtained. Each slice was 1024 x 1024 pixels in size, with each pixel 20 x 20 microns, for a voxel size of 20 x 20 x 33 microns.

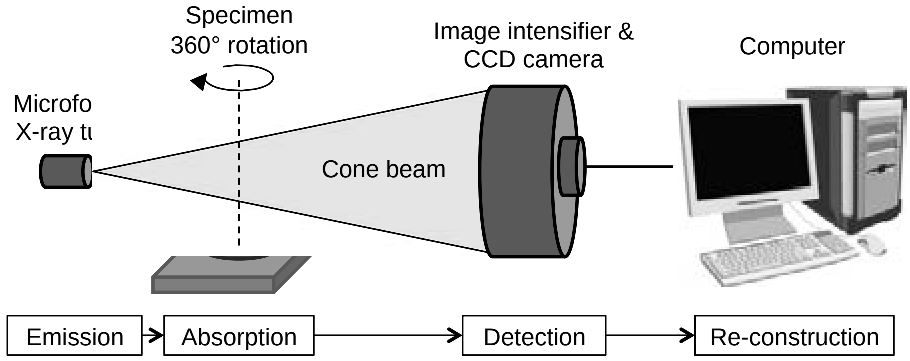

Figure 4: X-ray CT system setup for image capture

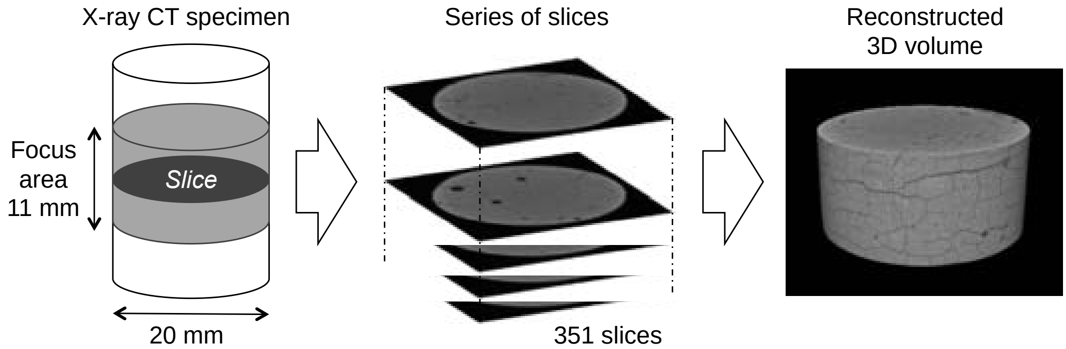

Figure 5: Details of the X-ray CT specimen and 3D image reconstruction

2.5 Chemical analysis

In this research, TG/DTA (Thermogravimetry Differential Thermal Analysis) was carried to analyze the chemical composition. TG measures the weight change of the heated sample, while DTA measures the temperature gap between the sample and a reference material (alumina is used as the reference). In this research, the analysis conditions were a heating rate of 10ºC/minute and a target temperature of 100ºC.

3. RESULTS AND DISCUSSION

3.1 X-ray CT images

Figure 6 shows the cross-sectional images of the cement paste specimen at various heights (measured from the bottom of the specimen) before and after heating and after re-curing. After heating, it is difficult to visually identify the cracks, but they can be observed to occur radially due to shrinkage caused by heating. After water re-curing for 4 weeks, the crack width appeared to increase; in addition, some new cracks formed which appeared to bridge between crack tips inside the specimen. From 4 to 13 weeks, however, the crack widths appeared to be mostly unchanged. From these images it is difficult to fully capture the cracking behavior under heating and re-curing so, quantitative evaluation is necessary.

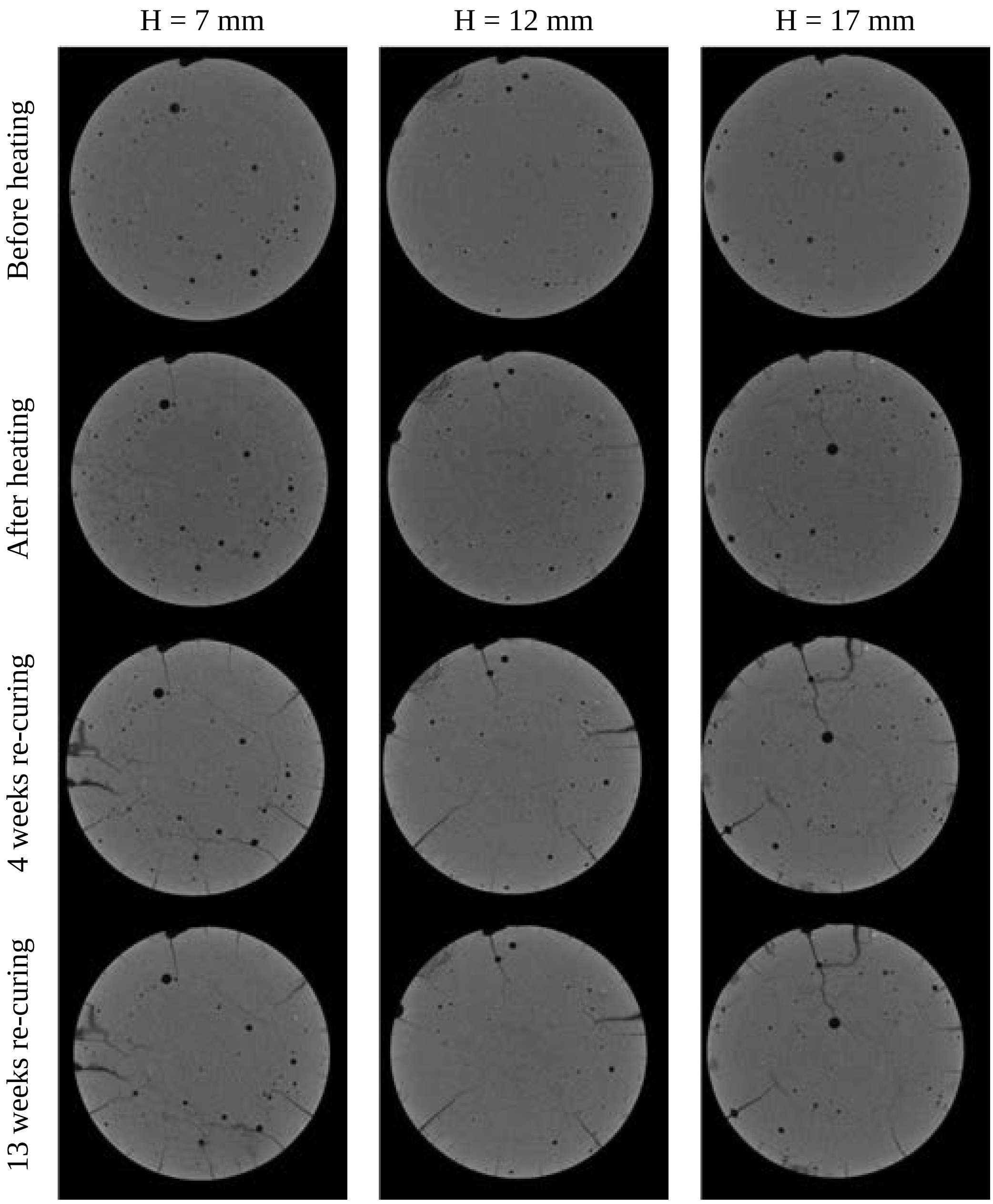

Figure 6: Slice images of the cement paste specimen

3.2 Crack width analysis method and results

In order to quantitatively evaluate the change in crack characteristics due to water re-curing, some cracks were selected and their widths measured. The method for measuring crack width is illustrated in Figure 7. Segments which intersected a selected cracks were drawn on the CT image at various depths from the specimen surface, and the width were measured based on the extracted CT value distribution along the segment.

The results for two cracks are shown in Figure 8. After heating, the cracks shapes are such that the width becomes smaller further away from the surface. After 4 weeks re-curing, the crack width increased between 10 to 70 μm. For Crack #1, the width increased less at the surface and more at away from the surface. For Crack #2, the width appeared to increase evenly along the whole length. After 13 weeks re-curing, the crack width generally increased from 4 weeks, but did decrease slightly at a few points. Particularly in Crack #1, the change in crack width from 4 to 13 weeks was greater near the surface but much less deeper along the crack. Overall, when comparing the crack widths after heating and after 13 weeks water re-curing, the crack widths increased between 25 to 125 μm.

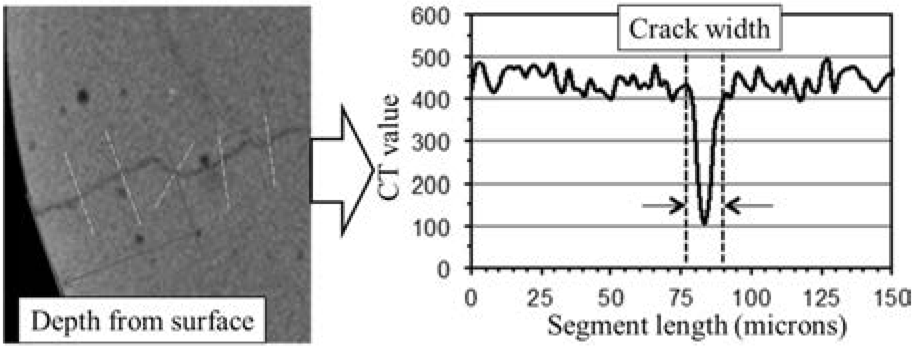

Figure 7: Crack width analysis method

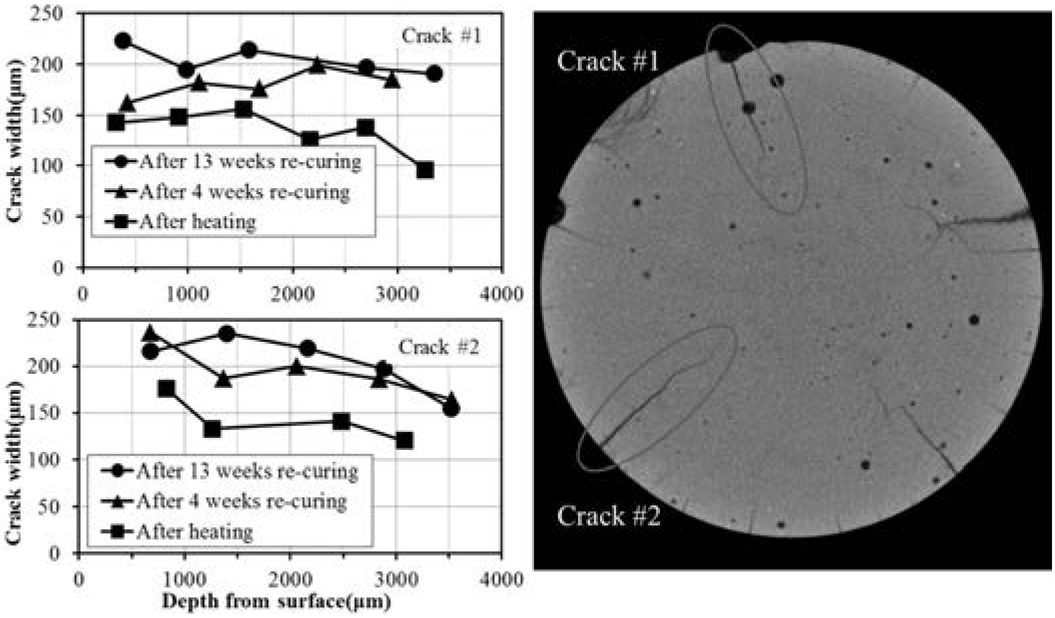

Figure 8: Crack width analysis results (left) and selected cracks (right)

3.3 Reconstruction of 3D crack network

The connected cracks and air voids were extracted used a segmentation method to separate solids and voids and convert the slice to a binary (black and white) image. After carrying out the segmentation for all slices, a 3D reconstruction of the crack network (after 4 weeks water re-curing) could be prepared by compiling the slice stack. The result is shown in Figure 9. It can be clearly seen that cracks propagate radially inwards from the specimen surface and propagate both vertically and horizontally. Some cracks also intersect air voids in the specimen.

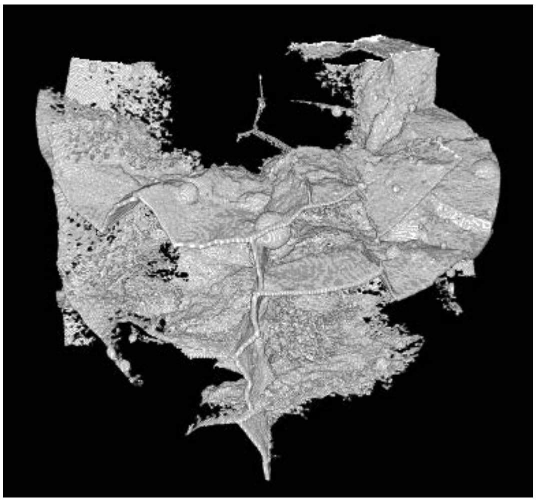

Figure 9: 3D crack network after 4 weeks water re-curing

3.4 Chemical analysis results

In order to understand why the crack widths increased, chemical analysis was conducted. Under exposure to temperatures between 400 and 500ºC, $Ca(OH)_2$ in concrete decomposes to calcium oxide (CaO) and water (H_2O). The reverse reaction occurs during rehydration (CaO changes to $Ca(OH)_2$). It has been reported that rehydration can cause expansion in a specimen due to the larger volumetric size of CaO compared to $Ca(OH)_2$ (Hewlett, 1998). Therefore, the analysis focused on the change in calcium hydroxide ($Ca(OH)_2$).

Figure 10 shows the TG/DTA test results, where the change in calcium hydroxide is reported as a percentage of the pre-heating condition. After heating, the amount of calcium hydroxide decreased by 60%, but after 1 week of water re-curing the amount returned to a similar value as before heating. However, between 1 and 13 weeks of water re-curing little change was observed. Therefore, rehydration of calcium hydroxide appeared to finish in just one week of water re-curing.

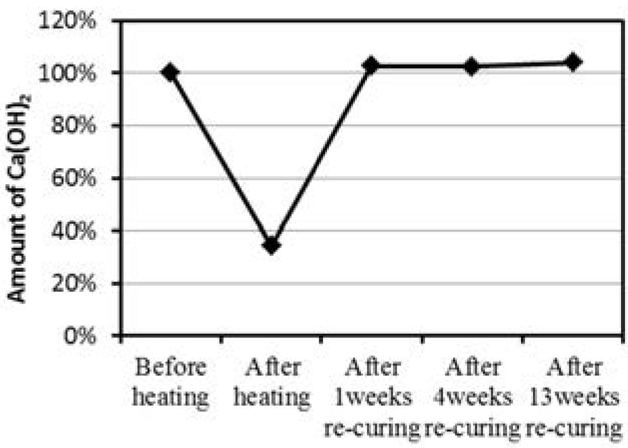

Figure 10: Change in calcium hydroxide
(as a percent of the pre-heating amount) due to heating and re-curing

As mentioned previously, it has been reported that rehydration can cause expansion in a specimen, which would lead to an increase in crack width and growth of new cracks. Based on the obtained chemical analysis results, as well as observations of the cracking pattern, the recovery of $Ca(OH)_2$ under water re-curing is believed to be the cause of the increase in cracks width and growth of new cracks as seen in the X-ray CT images and crack width analysis results.

4. CONCLUSION

The objective of this research was to non-destructively investigate the changes in cracks in cement paste material due to heating and re-curing by applying X-ray CT and image analysis techniques. After heating, cracks occurred radially but were difficult to observe. Through image analysis, it was shown that re-curing lead to an increase in crack width of 25 to 125 μm, along with the formation of new cracks which bridged between radial cracks inside the specimen. The formation of these cracks is believed to be caused by expansion due to the rehydration of CaO into $Ca(OH)_2$. From 4 weeks to 13 weeks, cracks appeared to remain mostly unchanged and there was little change in the mass of $Ca(OH)_2$.

This study has several limitations which need to be addressed in the future. First, cracks were only examined in 2D images but they occurred in 3D space. Second, the change in other cement hydrates such as such as C-S-H need to be examined to better clarify the re-curing mechanism. Finally, the observed changes in the crack space and microstructure need to be related to changes in mechanical properties such as strength or durability.

ACKNOWLEDGMENT

This research was partially supported by the Japan Society for the Promotion of Science (Scientific Research B, no. 23360187).

REFERENCES

Hewlett, P.C., 1998. Lea's Chemistry of Cement and Concrete, 4th Ed., Elsevier, Oxford.

Landis, E.N., Keane, D.T., 2010. X-ray microtomography. Materials Characterization Vol. 61, pp. 1305-1316.

Henry, M., Suzuki, M., Kato, Y., 2011. Behavior of fire-damaged mortar under variable re-curing conditions. ACI Materials Journal, 108(3), pp. 281-289

Promentilla, M.A.B., Sugiyama, T., 2010. X-ray microtomography of mortars exposed to freezing-thawing action, Journal of Advanced Concrete Technology Vol. 8 No. 2, pp. 97-111.

Suzuki, M., Henry, M., Kato, Y., Katsuki, F., 2010. Influence of re-curing on physio-chemical properties of mortar exposed to fire. Cement Science and Concrete Technology No. 63, pp. 148-154. (in Japanese)

Introduction of CAESAR’s research activity utilizing decommissioned bridge in Japan

Akiko HIROE[1], Hidetaka HOMMA[2], and Yoshitomi KIMURA[3]
[1]Researcher, Bridge and Structural Engineering Research Group, CAESAR, PWRI, Japan
hiroe@pwri.ge.jp
[2]Senior Researcher, Bridge and Structural Engineering Research Group, CAESAR, PWRI, Japan
[3]Chief Researcher, Bridge and Structural Engineering Research Group, CAESAR, PWRI, Japan

ABSTRACT

In Japan, approximately 50% of the bridges will become more than 50 years old in next decade and numerous bridges have been damaged while they are in service. Needs for inspection, assessment, repair and rehabilitation of existing bridges are rapidly increasing. Center for Advanced Engineering Structural Assessment and Research (CAESAR) was established as one of the organization of Public Works Research Institute (PWRI) in Japan to tackle such current infrastructural issue. For safe and sustainable use, CAESAR focuses on a “clinical study” which utilizes decommissioned bridges. The final goal of the study is to establish evaluation methods for deteriorated bridges. We introduce current condition of Japanese highway bridges and its management in this paper. Concerning concrete bridges, examples of defects of bridges and CAESAR’s research activity utilizing decommissioned bridges are also described.

Keywords: *decommissioned bridge, defect of bridge, bridge maintenance*

1. INTRODUCTION

Center for Advanced Engineering Structural Assessment and Research (CAESAR) was established in April, 2008 as one of four research institutes and centers in Public Works Research Institute (PWRI). At that time, an issue of aging infrastructure had become apparent as represented by the collapse of the bridge in Minneapolis, Minnesota, U.S., August 2007. In Japan, a fracture of a truss member covered in concrete deck was found in Kiso River Oh-hashi Bridge in the same period. CAESAR tackles such infrastructural issues related to bridges. One of the pillars of its research activity is a “clinical study.” Similar to the medical research, it requires accumulation of cases of defects and specimens of damaged bridges. As a part of clinical study, CAESAR conducts studies utilizing decommissioned bridges or its components.

2. CURRENT CONDITION OF HIGHWAY BRIDGES IN JAPAN

Figure 1 shows the number of highway bridges in Japan sharply increased from 1950s to 1970s. This period was Japan's high economic growth period and during the time, early enrichment of infrastructure was desired. Since bridges were intensively constructed in a short period, the percentage of aging bridges increases rapidly after 2000. Figure 2 portrays that the percentage of highway bridges older than 50 years. In both figures, bridges longer than 15 m are counted. The statistical data indicate that, by 2031, 53% of Japan's highway bridges will be older than 50 years, where the total number of existing bridges is approximately 157,000 as of April 1, 2010.

Figure 3 shows the percentage of bridges by damage level on designated national highway. The data was obtained from inspection of bridges longer than 2 m. From the figure, it is found that about 40% of bridges have damages that require immediate remedial action.

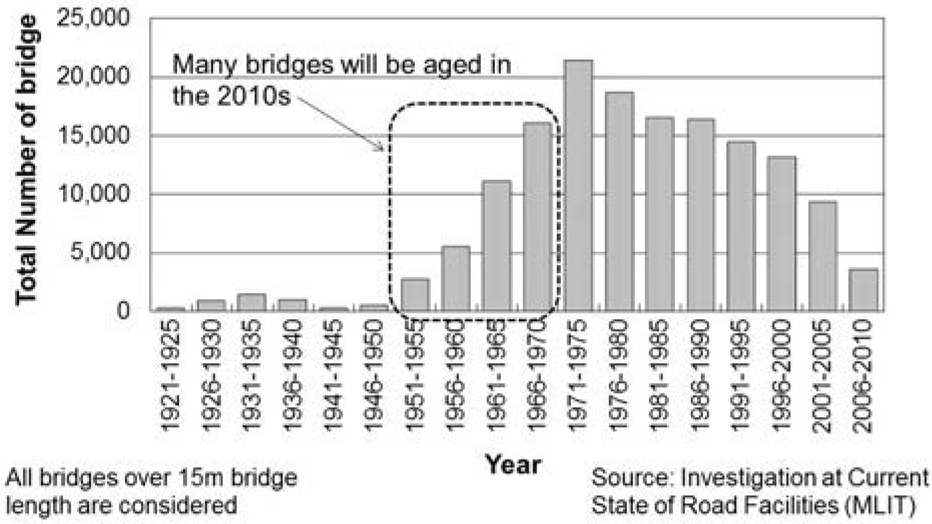

Figure 1: Transition of the Construction Number of Highway Bridges by Fiscal Year of in Japan

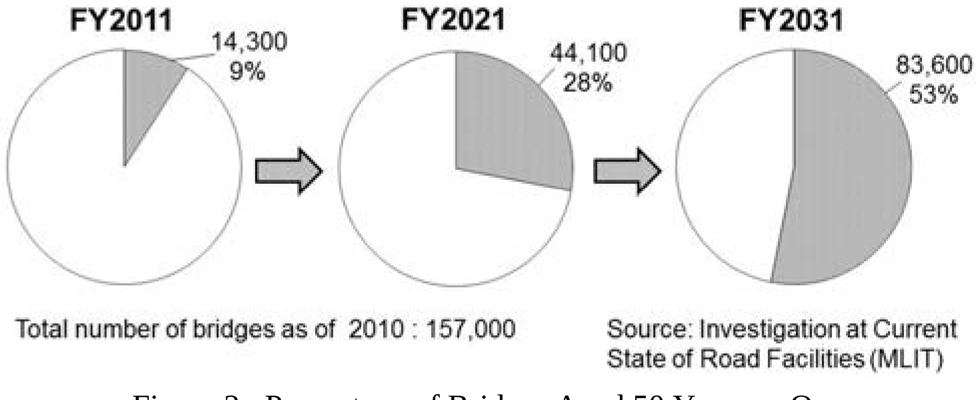

Figure 2: Percentage of Bridges Aged 50 Years or Over (bridge length of 15 m or more)

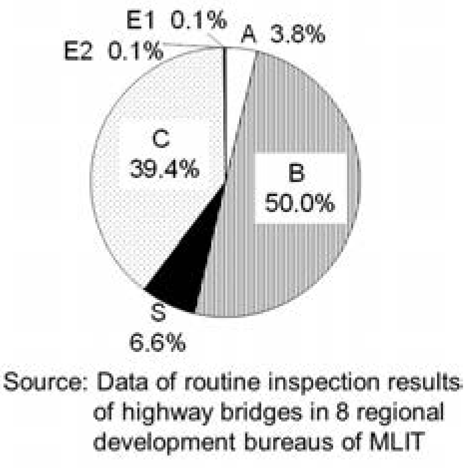

Remedial Action Criterion

Level	Remedial Action
A	No or negligible damage No remedial action is required
B	Depending on situation
C	Immediate action is required
E1	Urgent action is required from the view point of structural safety
E2	Urgent action is required by other reason
M	As a part of ordinary maintenance work
S	Detailed survey is required

Figure 3: Percentage of Bridges by Damage Level on Designated National Highway (bridge length of 2 m or more)

3. HIGHWAY BRIDGES INSPECTION IN JAPAN

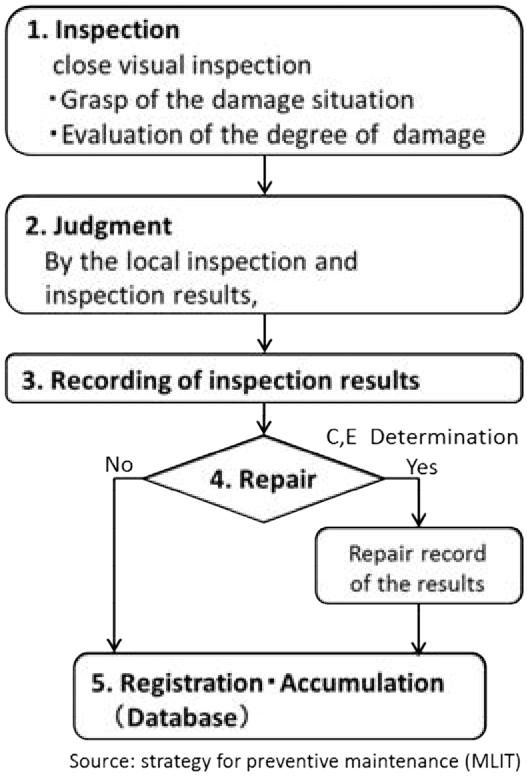

Figure 4: Flowchart of Highway Bridges Inspection in Japan

Figure 4 shows the flowchart of Japanese highway bridges inspection. In 2004, revised inspection manual for bridge was released by Ministry of Land, Infrastructure, Transport and Tourism (MLIT), which is promoting preventive maintenance and long duration of infrastructures. In this revision, some contents are modified considerably. The first point is the introduction of the initial inspection. It is conducted within 2 years from construction to find out initial deficiencies such as bulging, peeling of paint, leakage or ponding by malfunction of drainage structure or water proof system, initial crack on concrete and so on. The second point is the shortening of the periodic inspection interval. The pre-manual recommended periodic inspections once in 10 years but the revised manual shortens them to once in 5 years in order to prevent from risks to miss indications of deterioration and rapid progress of deficiencies. The visual inspection is conducted every 5 years and each part composing bridge is inspected by a proximate observation. Highway operators make a chart for each bridge based on the results of inspections. Bridges are categorized with the remedial action criterion, which is on right side of Figure 3. If the bridge is given C, E1 or E2, it needs some remedial action immediately.

4. RECENT CASES OF BRIDGE DAMAGE

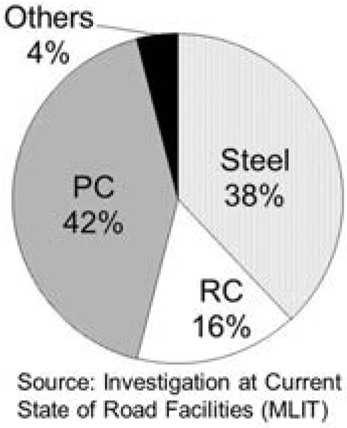

Figure 4: Percentage of Bridges by materials in Japan

Figure 4 shows the percentage of bridges by their materials. In Japan, bridges are mainly constructed with steel and concrete. According to the figure, the percentage of prestressed concrete bridges is almost equal to that of steel bridges, and 58 % of bridges are constructed with concrete. It reveals that concrete is the one of popular material for bridge construction in Japan. Therefore, some recent cases of damage of bridges in Japan are reported with focusing on concrete bridge in this section.

4.1 Chloride-Induced Deterioration

Chloride-induced deterioration is one of the major issues in the maintenance of concrete bridges. It occurs in coastal area, especially in Okinawa, which is the southernmost part of Japan and northern Japan sea side. That is because wind brings salinity from sea; Okinawa is frequently struck by typhoons every year and northern Japan sea side is hit by northwest seasonal wind. The cold districts are also the area where chloride-induced deterioration occurs because sometimes antifreezing agent including chloride is used on bridges.
Figure 5 shows the collapse of concrete bridge in Okinawa in 2010. Before collapse, many rebars had been already fractured because of the corrosion induced by chloride. This bridge was closed to traffic when it collapsed, so that it did not cause injury. Other bridges’ chloride-induced deterioration is on Figure 6.

(a) before collapse (b) after collapse

Figure 5: Collapsed Concrete Bridge in Okinawa


(a) falling off of concrete　(b) crack by expansion pressure of corroded PC cables

Figure 6: Chloride-Induced Deterioration

4.2 Alkali-Silica Reaction (ASR)

Some aggregate in concrete causes a chemical reaction with alkali despite inside of concrete being alkaline environment. Substance that results from a chemical reaction makes its volume increase because of the water absorption and cracks occur on a surface of concrete. In some cases of ASR, breakages of rebars because of the expanding pressure of concrete were found. This may have a significant effect against structural integrity.

Figure 7 shows cracks induced by ASR. Map crack appears on the structure with non-directional binding, e.g. structure which has a small amount of rebar, and a horizontal crack found on the structure with strong binding, e.g. structure which has a large amount of rebar or prestress. For the prestressed structures suffering ASR, it is known that longitudinal cracks along prestressing direction may appear.


(a) map crack on pier　(b) horizontal crack on precast hollow girder (PC)

Figure 7: Cracks Occurred by ASR

5. RECENT CASES OF CLINICAL STUDY

To encouraging preventive maintenance and long duration of bridges, the establishment of evaluation method for aging and damaged bridges is essential. “Clinical study” is conducted with decommissioned bridges by CAESAR in order to reveal behaviors of deteriorated bridges, to detect the internal deficiencies of bridges, to assess non-destructive testing (NDT) technologies, and so on.

CAESAR wrestles with the problems of aging bridges by it. Some cases of clinical study are introduced in this section.

5.1 Loading Test

It is very important to assess the remaining strength of deteriorated bridges when the operator judges its serviceability, timing of repair or demolition. Although it is desirable to conduct full scale loading test using whole bridge, it is quite expensive and subjects to restriction of loading facilities. Therefore, CAESAR samples members of bridges as large as possible and conducts loading test.

Figure 8 shows Kuratani Bridge. It was 2-span simply-supported reinforced concrete slab bridge constructed in 1959. The bridge was located on near the coast line of western Japan and suffered chloride induced deterioration. When the operator decided to demolish the bridge in 2010, large area of cover concrete on the bottom surface of the deck was already separated or fell off because of the expanding pressure of corroded rebars (Figure 9). Loading test was conducted with sampled bridge slab deck (Figure 10). From the test, the correlation between the ultimate strength and the area loss of rebars were revealed as Figure 11 shows.

Figure 8: Kuratani Bridge before Demolition

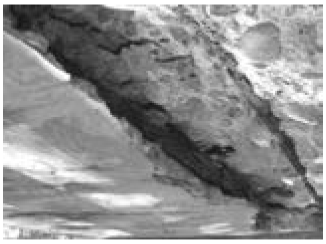

Figure 9: Corroded Rebars and Separated Concrete Cover

Figure 10: Loading Test using Sampled Bridge Slab

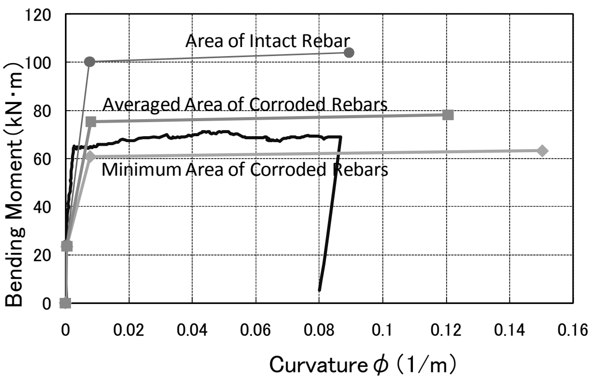

Figure 11: Curvature and Bending Moment

5.2 Anatomical Study

Anatomical study is done for detecting internal deficiencies of bridge members, such as corrosion of steel member inside concrete, chlorine content in core specimens, condition of cracks, or insufficient grouting in post tension prestressed concrete. Through anatomical study using decommissioned bridge members, it is expected to accumulate the knowledge regarding such issues.

Tsuha Bridge (Figure 5) was simply-supported reinforced concrete girder bridge constructed 1931 in Okinawa and collapsed in 2010 mainly because of chloride induced deterioration. As mentioned in 4.1, Okinawa is one of the harsh places for concrete bridges. It was thought that the concrete had large amount of salt inside from the beginning of its service when the quality control was not well established. CAESAR sampled some portions of girders (Figure 12) and conducted anatomical study. As Figure 13 shows, rebars under cover concrete corroded less despite while the exposed rebars lost almost all their cross section. Figure 14 and Figure 15 reveals that the chloride ion concentration is higher than the marginal concentration of corrosion occurrence at the main reinforcements or stirrups. However, deep portion of concrete has not much chloride ion. That indicates that the amount of initial salt in the concrete might be carefully controlled.

Figure 12: Sampled girder of Tsuha Bridge

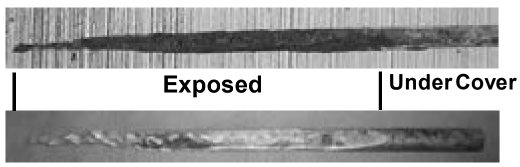

Figure 13: Diminishment of Rebar

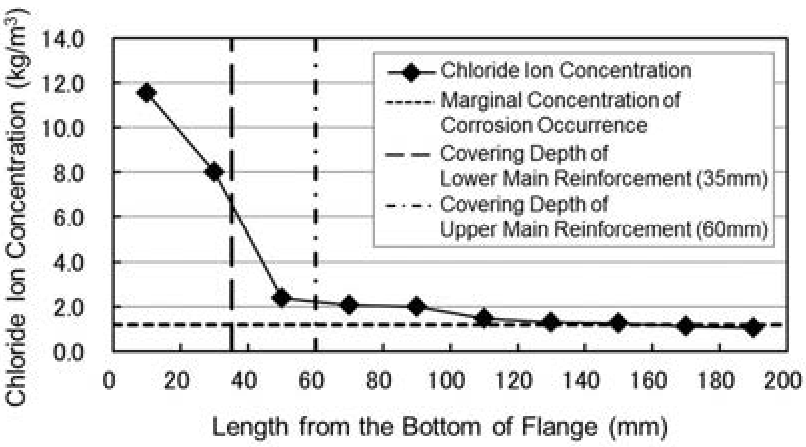

Figure 14: Chloride Ion Vertical Distribution in the Girder

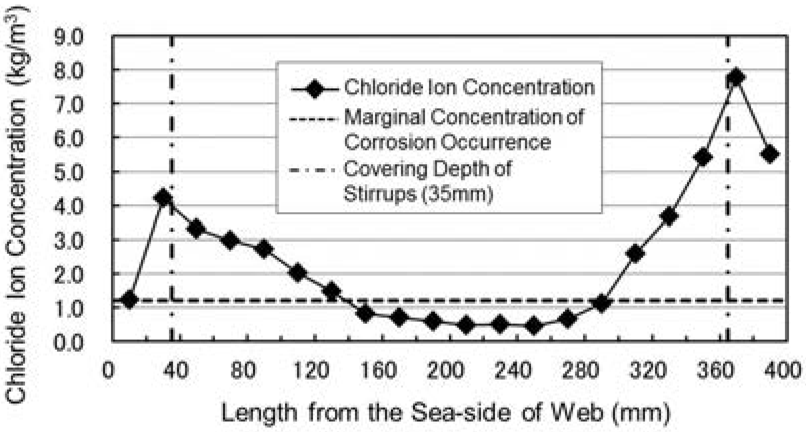

Figure 15: Chloride Ion Horizontal Distribution in the Girder

5.3 Non-Destructive Testing (NDT)

The NDT is demanded to inspect the invisible portions, such as the inside of concrete, without causing damage to the bridge. The development of NDT technologies has been progressing and many kinds of NDT devices have been produced. Decommissioned bridges with various deficiencies are good fields to evaluate performance of NDT devices.

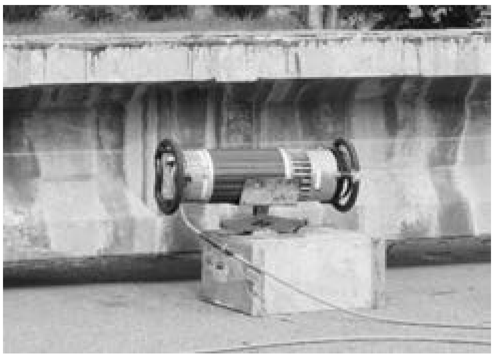

Figure 16: X-ray Generator (300keV)

X-Ray Tomography is one of the well-known NDT technologies. Figure 16 shows the X-ray generator whose energy output is 300keV. It is utilized in bridge inspections. X-ray images of the decommissioned bridge were taken by this device. The results are shown in Figure 17. It is possible to discriminate rebars, PC cables and voids in sheathes.

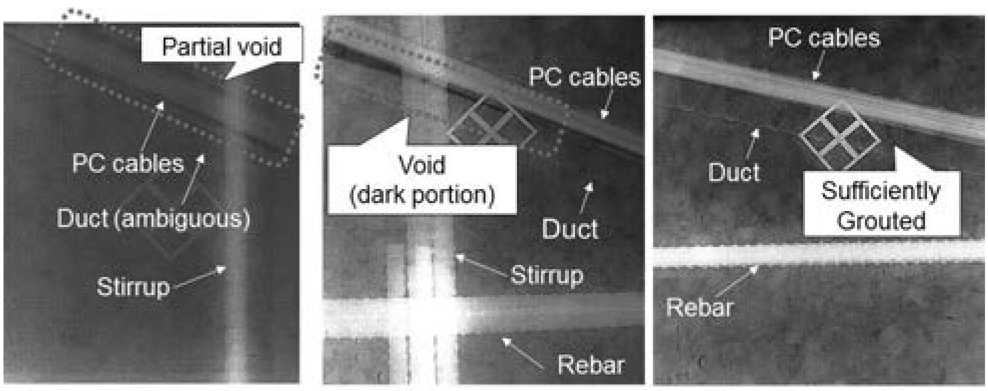

(a) Thickness: 400mm
(Irradiation time: 60 min)

(b) Thickness: 160mm (Irradiation time: 3 min)

Figure 17: X-ray Image of Decommissioned Bridge

However, the image of the 400 mm thickness area is unclear compared with those of 160 mm thickness area. In addition, thicker part need much more time than thinner part. It reveals that more improvement is necessary to get clearer image by X-ray.

As Figure 18 shows, other kinds of NDT devices are also evaluated concerning their performance with utilizing decommissioned bridges or deteriorated bridge.

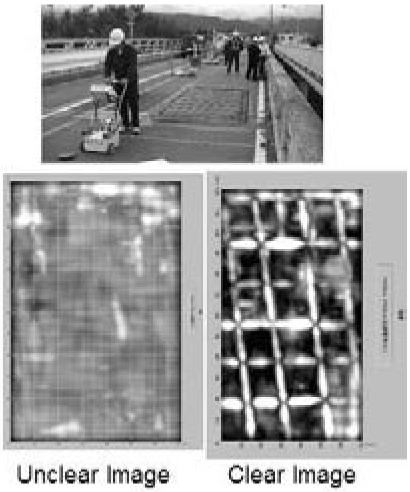

(a) Electromagnetic Radar

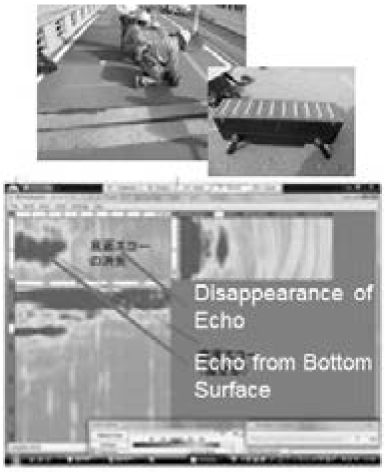

(b) Ultrasonic

Figure 18: Examples of NDT Devices Evaluation

6. CONCLUSION

The bridges in Japan are now facing their aging and deterioration. Therefore, the maintenance of the bridges is essential to sustain society of Japan. Development of inspection methods and repair methods for bridges is expected. We, CAESAR, tackle to those issues with our research activities. The clinical study utilizing decommissioned bridges is just a case study now and still there is difficulty to reveal the comprehensive method. Thus, CAESAR will continue the accumulation of cases and analyze them in order to summarize practical manuals or specifications for more rational maintenance of bridges.

REFERENCES

Hanai, T., Ohishi, R., Kuwabara, T., Hoshikuma, J., and Murakoshi, J., 2011. Research Activity Utilizing Decommissioned Bridge. *Proceedings of the 2011 International Forum on Bridge Engineering*, 203-223

Tamakoshi, T., Okubo, M., and Yokoi, Y., 2012. Annual report of basic data on road structures in FY 2011. *Technical Note of National Institute for Land and Infrastructure Management*, No.693, Japan, (in Japanese)

Performance of different sacrificial anode materials on corrosion protection of reinforcing steel

Pakawat SANCHAROEN[1], Aris MAHASIRIPANA[2]
and Somnuk TANGTERMSIRIKUL[3]
[1]Researcher, Construction and Maintenance Technology Research Center,
Sirindhorn International Institute of Technology, Thammasat University, Thailand
pakawat@siit.tu.ac.th
[2]Graduate Student, School of Civil Engineering and Technology,
Sirindhorn International Institute of Technology, Thammasat University, Thailand
[3]Professor, School of Civil Engineering and Technology,
Sirindhorn International Institute of Technology, Thammasat University, Thailand

ABSTRACT

Sacrificial anode cathodic protection is one of prevention and repairing methods of corrosion of reinforcing steel in RC structure. Its performance mainly depends on anode material and electrical resistivity of concrete. This study determined performance of different sacrificial anode materials which are aluminum alloy, zinc alloy and alkaline activated zinc alloy to protect corrosion if reinforcing steel in different concrete mix proportion. Half-cell potential and corrosion current density of reinforcing steel at different distance from sacrificial anode were measure weekly. The results showed that aluminum alloy has the highest performance of corrosion protection because of its lowest natural potential. Higher chloride content in concrete and lower water to binder ratio caused higher electrical resistivity of concrete reducing the performance of corrosion protection of sacrificial anode. The results can be used for designing sacrificial anode to protect corrosion of reinforcing steel in RC structure.

Keywords: *corrosion, cathodic protection, sacrificial anode, maintenance*

1. INTRODUCTION

Corrosion of reinforcing steel in reinforced concrete structure is one of the most important problems around the world. Thailand is also now approaching the aging infrastructure era. The effective maintenance methods are needs to be concerned in order to ensure safety of structures and resources saving. Cathodic protection is one of promised methods to prevent or delay corrosion deterioration of RC structures (Sancharoen et al., 2008 and DNV, 2010). Impressed current and sacrificial anode are two major categories of cathodic protection. One needs the supply of external electricity while another requires 2 metals with different potential in galvanic series. This study mainly focused on effectiveness of sacrificial anode system. In case of normal reinforcing steel in RC structure, aluminum alloy and zinc alloy are widely used as sacrificial anode due to their potential is more negative than that of steel. Unfortunately, current design guidelines of cathodic protection systems (DNV, 2010) are generally concerned about underground or underwater steel structure. In case of RC structure, there is little information regarding to the design of sacrificial anode for RC structures. So this study aims to study the effectiveness of different sacrificial anode materials to protect reinforcing steel in different concrete mix proportions from corrosion due to chloride attack. The results can be used as the guideline for material selections, system designing and installation and service life evaluation of repairing structure by sacrificial anode.

2. EXPERIMENTAL PROGRAM

2.1 Materials

2.1.1 Concrete

As electrical resistivity of concrete affects the effectiveness of sacrificial anode, various concrete mix proportions were prepared. Cement is ordinary Portland cement type 1 accordingly to ASTM C150. Sand and gravel are natural river sand and crushed limestone aggregate according to ASTM C33. Water to cement ratio were varied as 0.4, 0.5 and 0.6 as shown in Table 1. Chloride was initially mixed in mixing water in form of sodium chloride (NaCl) in order to obtain chloride concentration as 1%, 2% and 4% of chloride by weight of cement.

2.1.2 Reinforcing steel

Reinforcing steel used in this study was DB12 grade SD40 according to TIS 20-2543. It was cut to the length of 140 mm. Then, reinforcing steel was polished its surface by wire brush to remove rust and oxide films. Electrical wire was connected to one end. Exposed surface area of steel for testing was controlled by coating both ends of steel by epoxy coating. The exposed steel length was 80 mm in the center. Before casting, steel surface was degreased by acetone and clean by distilled water. Prepared reinforcing steel was shown in Figure 1.

Table 1: Concrete Mix Proportions

Name	W/C	Unit content (kg/m^3)				
		Cement	Water	Sand	Gravel	NaCl
0.4OPC-4%CL	0.4	454	182	720	1032	18.16
0.5OPC-1%CL	0.5	399	199	720	1032	4.02
0.5OPC-2%CL	0.5	399	199	720	1032	8.01
0.5OPC-4%CL	0.5	399	199	720	1032	15.96
0.6OPC-4%CL	0.6	355	213	720	1032	14.20

Figure 1: Prepared reinforcing steel

2.1.3 Sacrificial anode

Al anode and Zn anode were used as sacrificial anode. They were prepared and supported by Thai Naval Dockyard, Royal Thai Navy. Their chemical compositions and electrochemical properties were shown in Table 2 and Table 3. However, some literatures showed that Zn anode has problem about formed zinc oxide film that reduced current discharge. Therefore, this study also prepared zinc sacrificial anode coated by high alkalinity mortar backfill. Lithium hydroxide (LiOH) were mixed in the mortar to increase pH around zinc sacrificial anode and dissolve the zinc oxide film and maintain current flow of zinc alloy. Prepared sacrificial anodes were shown in Figure 2.

Table 2: Chemical Compositions of Sacrificial Anode

Anode	**Chemical Composition (% by weight)**								
	Fe	**Pb**	**Cd**	**Sn**	**Al**	**Cu**	**In**	**Zn**	**Si**
Al	0.090	-	-	0.001	Remain-der	0.004	0.014-0.020	4.0-6.5	0.08-0.20
Zn	0.005	0.006	0.025-0.07	-	0.1-0.5	0.005	-	Remain-der	-

Table 3: Electrochemical Properties of Sacrificial Anode

Anode	**Density (g/cm^3)**	**Potential (mV vs. Ag/AgCl)**	**Current capacity (Ah/kg)**	**Consumption rate (g/Ah)**
Al	2.699	1050.67	2566.06	0.390
Zn	7.133	1006.33	783.41	1.276

2.2 Specimen preparation

RC specimen designed specially to study effectiveness of sacrificial anode cathodic protection as shown in Figure 3. Specimen size was 100 cm in length and 10 cm × 10 cm in cross section. Reinforcing steel were installed at varying distance from anode as the 1st to the 5th positions of steel was 5 cm interval, the 5th to the 7th was 10 cm interval and the 7th to the 9th was 20 cm interval.

(a) (b) (c)

Figure 2: Prepared sacrificial anode (a) Aluminum alloy anode (b) Zinc alloy anode (c) Coated zinc alloy anode

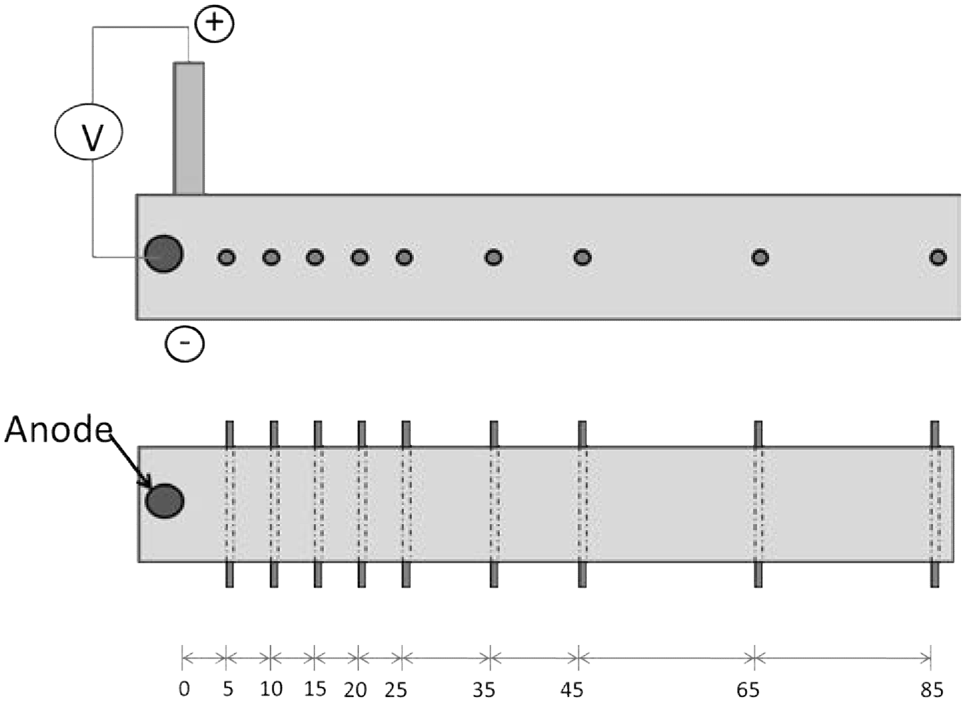

Figure 3: Specimen Preparation

Sacrificial anode was installed far from the 1st steel position for 8 cm. Concrete was casted and let harden in the mold for 1 day. Then, specimens were cured by being covered with wet cloth for another 7 days.

2.3 Measurements

2.3.1 Half-cell potential measurement

Half-cell potential measurement (HCP) at concrete surface was conducted for all reinforcing steel positions and anode in each concrete specimen as shown in Figure 3. Copper/copper sulfate electrode ($Cu^{2+}/CuSO_4$) was used. HCP testing was conducted at three conditions; on potential, instant-off potential and off potential, according to NACE standard. On potential condition was tested when anode and steel were always connected by electrical wire. Instant-off condition was tested when anode was disconnected from steel within 15 minutes. Off potential condition was tested when anode disconnected from steel more than 4 hours. The external switching box was used to disconnect electrical connection between anode and steel.

2.3.2 Current flow measurement

Sacrificial anode current density flow is very important to effectively design sacrificial anode cathodic protection in concrete. So, current density requirements to protect reinforcing steel were shown in Table 4.

Current flow between sacrificial anode and steel was conducted by measuring electrical voltage dropped across the external resistor as shown in Figure 4. By Ohm's law, current flow can be calculated as shown in Equation (1)

$$V = IR \tag{1}$$

Where V = Electrical voltage dropped across external resistor (Volt), I = Current Flow (Amp), R = Resistance of external electrical resistor (Ohm)

2.3.3 Concrete resistivity

Resistivity of concrete is very important factor affecting performance of sacrificial anode system. Resistivity was measured by commercial Wenner's four probes according to AASHTO TP 95-11 as shown in Figure 4.

Table 4: Current Density Requirements to Protect Corrosion of Reinforcing Steel

Environment surrounding reinforcing steel	Current density requirement (mA/m^2)
Alkaline, no corrosion, low oxygen	0.1
Alkaline, no corrosion, exposed structure	1-3
Alkaline, chloride present, dry	3-7
Chloride present, wet, poor quality concrete and general corrosion	8-20
High chloride level, wet fluctuating environment, high oxygen level, hot, severe corrosion on steel	30-50

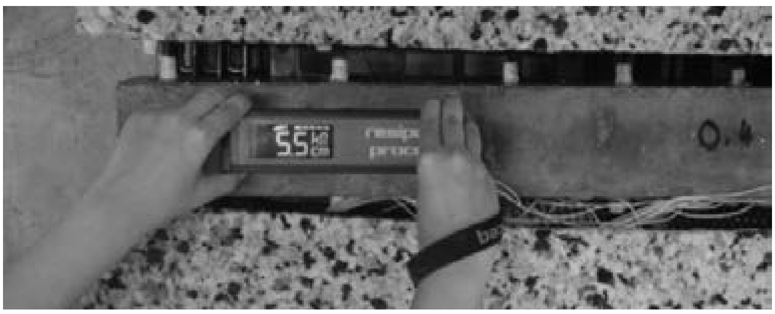

Figure 4: Concrete Resistivity Measurement

3. RESULTS AND DISCUSSION

3.1 General

Figure 5 shows general results of half-cell potential measurement at different conditions as initial, on-potential, instant off-potential and off-potential. The results showed half-cell potential of steel at distance 5cm, 35cm and 85cm from anode. As shown, on-potential showed the lowest value meaning steel was polarized by anode. However, please be noted that polarized potential criteria of acceptance sacrificial anode system according to DNV and NACE standard at -850mV cannot be used for RC structure because of very high electrical resistivity of concrete compared to soil or water. The 100mV decay shift of potential between instant off-potential and off-potential criteria was used instead.

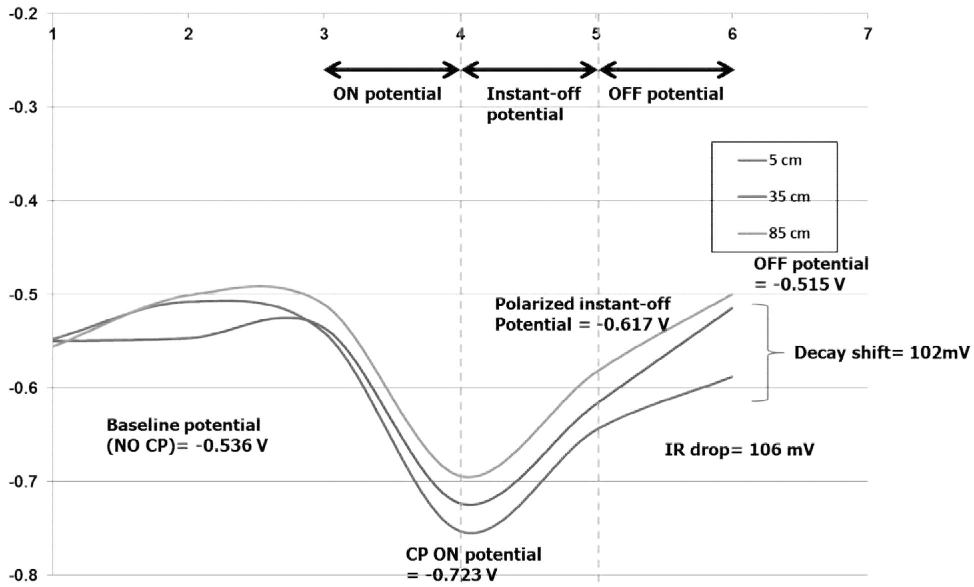

Figure 5: General of Half-cell Potential Results

3.2 Effect of different sacrificial anodes

Figure 6 shows the results of half-cell potential of steel polarized by different sacrificial anode. As shown, none of all sacrificial anodes passed the -850mV criteria of NACE standard. However, aluminum alloy anode can polarize steel to be the lowest potential due to its more negative potential than zinc alloy anode. Comparison between result of zinc alloy and coated zinc alloy anodes shows clearly the benefit of high alkalinity around zinc alloy. As pH more than 13.2, calcium hydroxyzincate film was destroyed. Therefore, potential and current flow from coated zinc anode to steel was improved.

Similarly, due to higher current capacity of aluminum alloy anode, discharged current density of aluminum anode was higher than that of zinc as shown in Figure 7. Also the improvement of current discharge due to high alkalinity mortar coated zinc anode can be observed in Figure 7.

3.3 Effect of different concrete mix proportions on half-cell potential

Figure 8 shows effects of different water to cement ratio on half-cell potential of steel. As shown, there is no significantly different on polarized potential of steel at different concrete mix proportion. This may due to thee testing condition is wet condition. So concrete is continuously wet causing no significantly different in concrete resistivity as shown in Figure 9.

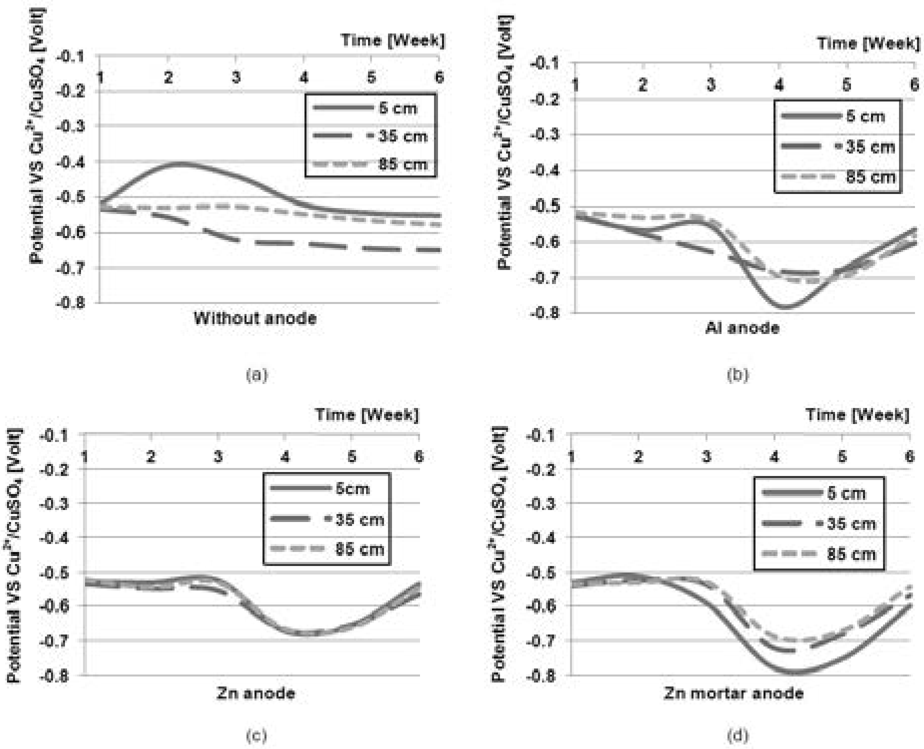

Figure 6: Effect of Different Sacrificial Anodes on Half-cell Potential

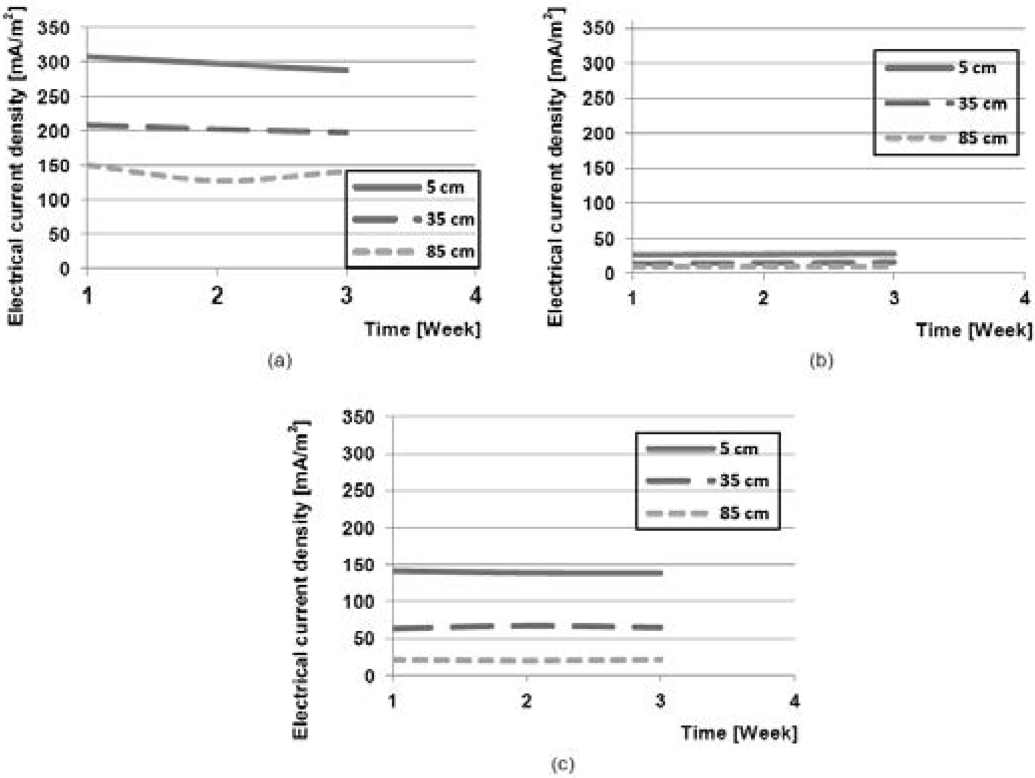

Figure 7: Effect of Different Sacrificial Anodes on Current Density (a) Aluminum anode (b) Zinc anode (c) Coated zinc anode

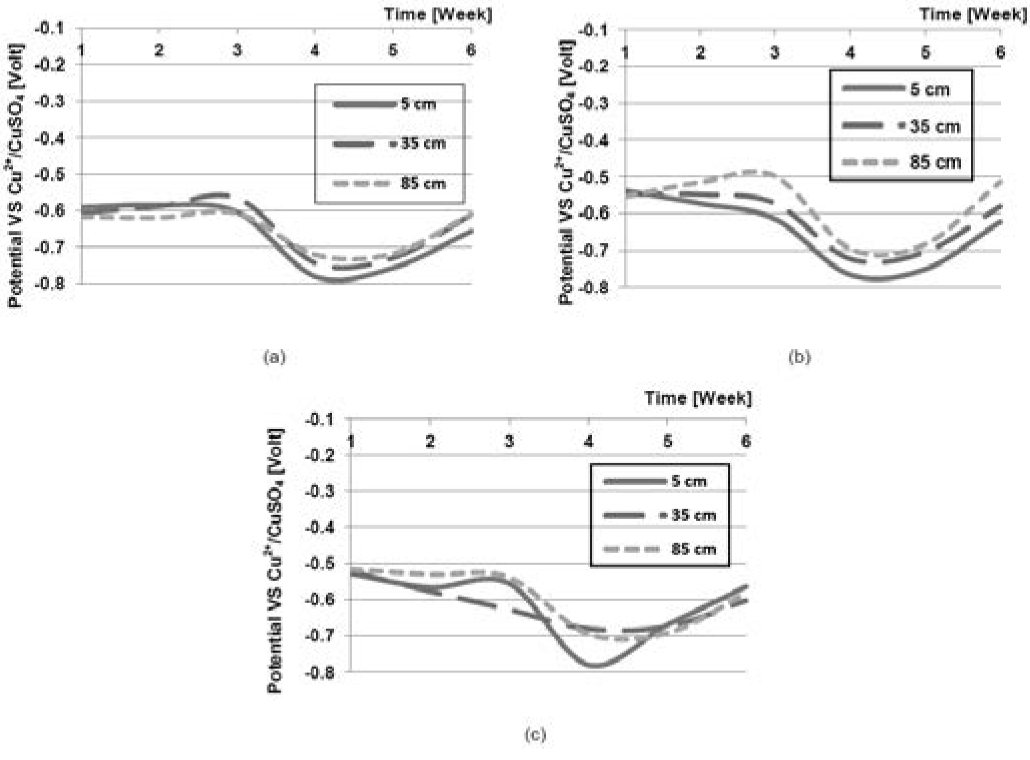

Figure 8: Effect of Water to Cement Ratio on Half-cell Potential (a) w/c = 0.4 (b) w/c = 0.5 (c) w/c = 0.6

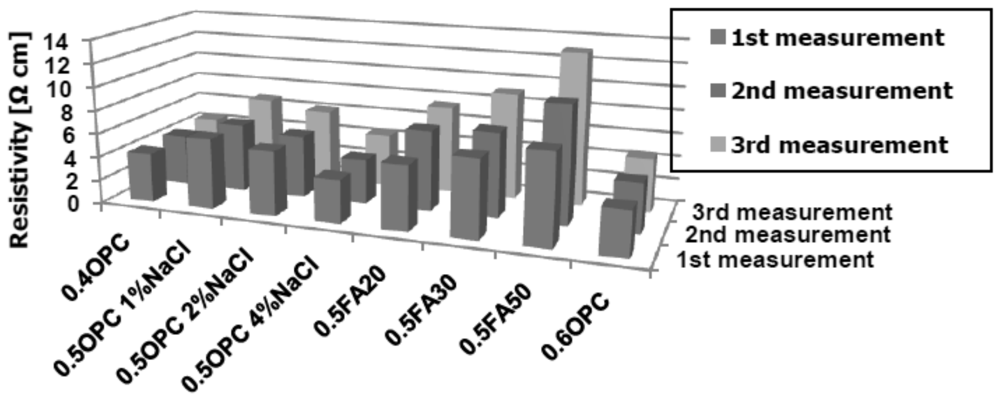

Figure 9: Results of Concrete Resistivity

Figure 10 shows effects of different chloride content on half-cell potential of steel. As shown, steel was polarized to be more negative potential when chloride content was increased. This is due to the significantly change, almost 50% reduction, of concrete resistivity as shown in Figure 9. Similarly, current density of higher chloride content specimen was higher than that of lower chloride content as shown in Figure 11. This was due to lower concrete resistivity and severe corrosion of reinforcing steel in higher chloride content.

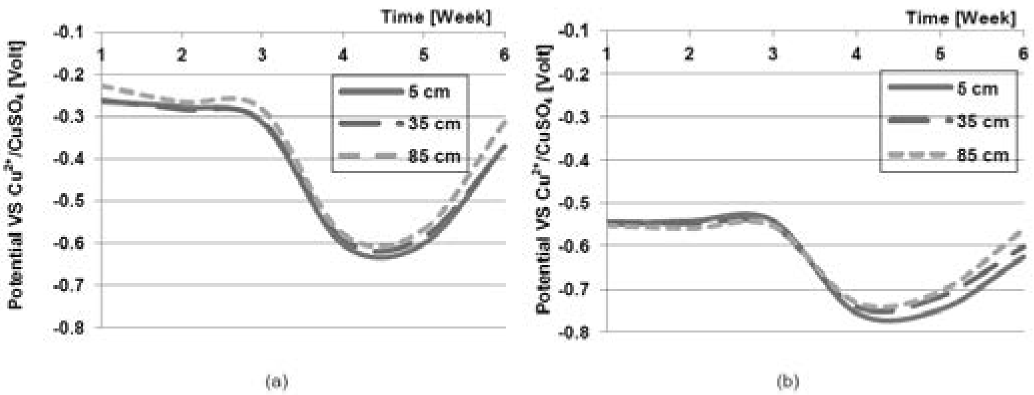

Figure 10: Effect of Chloride Content on Half-cell Potential (a) 0.5OPC-1%CL (b) 0.5OPC-4%CL

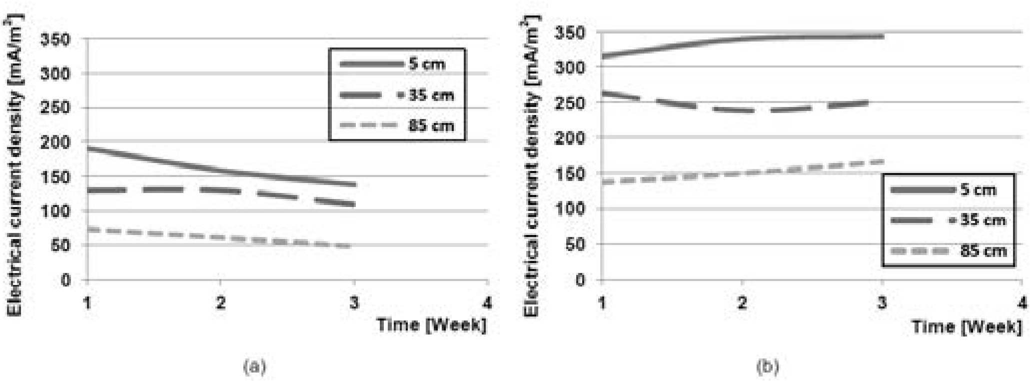

Figure 11: Effect of Chloride Content on Current Density (a) 0.5OPC-1%CL (b) 0.5OPC-4%CL

4. CONCLUSIONS

Based on 100mV decay shift criteria, all of anodes can protect reinforcing steel in wet concrete from corrosion even at the distance of 85 cm from anode. Polarized potential and current density of steel connected to zinc anode was the worst due to formed passive film which can be solved by coating zinc by high alkalinity mortar. Water to cement ratio did not significantly affect effectiveness of sacrificial anode because testing was conducted in wet condition. More severe conditions as wet-dry and dry condition are conducting. Higher chloride content in concrete reduced concrete resistivity significantly and caused more severe corrosion. Therefore, potential and current density were affected. The results can be used as a guideline to design sacrificial anode system to protect corrosion of reinforcing steel more effectively.

ACKNOWLEDGEMENTS

Sacrificial anodes were supported by Thai Naval dockyard, Royal Thai Navy.

REFERENCES

DNV-RP-B401, 2010. *Cathodic protection design*. Recommended practice of DET NORSKE VERITAS.

Sancharoen, P., Kato, Y., and Uomoto, T., 2008, *Probability-based maintenance planning for RC structures attacked by chloride*, Journal of Advanced Concrete Technology, Vol.6, No.3, pp.481-495.

Yeomans, S. R., 2004, *Galvanized Steel Reinforcement in Concrete,* Elsevier Science, United Kingdom

Investigation on performance of concrete and mortar using active compound powder

Parnthep JULNIPITAWONG[1], Chalermchai WANICHLAMLERT[2]
[1,2]Researcher, Construction and Maintenance Technology Research Center,
Sirindhorn International Institute of Technology, Thammasat University, Thailand
parnthep@siit.tu.ac.th

ABSTRACT

The early-age properties of low slump concrete and mortar with the active compound were investigated. The active compound was used as an additive and replacement material with varied content. The expansion of mortar samples containing the active compound stored in water and the autoclave expansion of paste bar samples containing the active compound were used to determine durability properties. The long term durability property such as carbonation resistance was also investigated. It was found that as consequence of using the active compound as an additive material the early-age compressive strength and slump of concrete were improved. The expansion of mortar due to storage in water was in the limit of the standard when incorporated with limestone powder. The autoclave expansion of paste bar sample containing the active compound was less than that of the control sample. The carbonation resistance of concrete was much obviously improved

Keywords: *active compound, early-age, additive material*

1. INTRODUCTION

In concrete industry nowadays, the demand for high early strength concrete is apparently increasing for reasons of high business competition. The application of high early strength concrete includes old as well as new structures. According to its fast strength development, it is excellent for concrete repair work, especially where the concrete structures cannot be closed for a long period. High early strength concrete is very useful for opening up concrete pavements to traffic earlier than conventional concrete mixtures. Moreover, high early strength concrete is also excellent for the precast concrete industry as the faster the strength gain is, the faster the production process will be. There are several ways to achieve high early strength of concrete. The most common way is to use high early strength cement (Portland cement type 3). In Thailand, even though the Portland cement type 3 is available in the construction market, but it costs about 10% more than ordinary Portland cement type 1. Furthermore, the cost of concrete is the main criterion for user to decide whether that type of concrete shall be selected or not. Another alternative to make concrete achieve high early strength is to use mineral admixtures such as pozzolanic materials, fillers etc. to partially replace some amounts of the cement. In previous days, most of the mineral admixtures were reactive powder materials which obtained from other industries as by-products. At present, scientists can synthesize and create special selective mineral admixtures to improve the reaction under certain circumstance as needed. This synthesis admixture is able to be directly involved in the hydration reaction of cement. This type of admixture usually has a chemical composition similar to those of cement compositions that provide the reaction at early-age stage. However, overdosing of this kind of admixture could lead to the problem of excessive expansion. The existence of any mineral admixtures in concrete can be considered as the modification of cement in both terms of physical properties and chemical composition, which affects concrete properties. The concrete properties can be separated according to the age of concrete as early-age properties, and long term properties. The early-age properties are investigated in a preliminary study to determine whether a certain admixture could be used in concrete without adverse effects. These concrete properties include workability, setting time, compressive strength development. The long term properties which mostly are related to durability properties have to be determined to ensure that the desired engineering properties are maintained.

2. OBJECTIVES AND SCOPES OF THE STUDY

This research is aimed to investigate performance of concrete and mortar using an active compound by comparing the workability, mechanical and durability properties with those of the control concrete and mortar without an active compound.

3. MATERIALS AND MIX PROPORTIONS

Ordinary Portland cement type 1, fly ash, limestone powder with mean particle size of 3 micron and the active compound were used in this study. The active compound was used as a mineral admixture. For simplification, the following notations are used to specify each type of materials; OPC1 is Ordinary Portland cement type 1. FA is fly ash. LP is limestone powder and AC is the active compound.

Chemical compositions and physical properties of the OPC1, fly ash and active compound are tabulated in Table 1.

2.2 Mix proportions

To study the influence of active compound powder on performance of concrete and mortar, OPC1 and OPC1 with LP were blended with the active compound powder using different addition and replacement percentages. The addition and replacement percentages of active compound powder were calculated by weight of cement in case of OPC1 mixture whereas calculated by weight of OPC1 and LP in case of OPC1 - LP mixture. The selected addition and replacement percentages of active powder were 5.5%, 6.5% and 7.5%. Mix proportions for investigating workability, compressive strength and carbonation resistance are shown in Table

2. For the early durability properties investigation, the mix proportions shown in Table 3 were used. Note that admixture was used in order to achieve the designed slump criteria.

Table 1 Chemical and physical properties of OPC, fly ash and active compound

Chemical and Physical Properties		OPC1	Fly ash	Active compound
Chemical Compositions*	SiO_2	17.72	33.41	1.76
	Al_2O_3	3.78	18.74	0.36
	Fe_2O_3	3.64	15.03	0.31
	CaO	66.76	20.01	43.96
	MgO	1.42	2.02	0.24
	SO_3	4.32	5.19	48.79
	Na_2O	0.24	1.27	0.60
	K_2O	0.60	2.92	0.08
	TiO_2	0.25	0.49	0.02
	P_2O_5	0.07	0.22	0.01
Physical properties	Density	3.15	2.24	2.95
	Blaine surface area (cm^2/g)	3300	2578	2984
	Loss on ignition	1.06	0.23	3.78

(*) by XRF analysis

4. METHODOLOGY

4.1 Workability and compressive strength measurements

The initial slump of all concrete was controlled at 50±20 mm. The slump loss was measured every 15 minutes.

The compressive strength of concrete was measured on seal-cured cube samples with dimension of 100x100x100 mm. The testing ages were 18 hrs, 1 day and 3 days.

4.2 Durability properties measurements

Regarding the high content of SO_3 in the active compound the measurement of volume stability of the sample is significant. The selected measurements were autoclave expansion (ASTM C151) and expansion of mortar bars stored in water (ASTM 1038). The paste bars and mortar bars with dimension of 25x25x285 mm were cast for autoclave test and the expansion of mortar bars stored in water test, respectively. The carbonation depth of 100x100x100 mm concrete samples containing the active compound was investigated and compared to those of the control samples. The concrete samples were seal-cured until 7 days before storing in the carbonation chamber. The concrete samples were carbonated under a carbon dioxide concentration of 4% (40,000 ppm) in the accelerated carbonation chamber for periods of 4 weeks. The temperature and relative humidity in the carbonation chamber were controlled at 40°C and 55±5% relative humidity.

Table 2 Mix proportions for investigating workability compressive strength and carbonation resistance of concrete

Mix	□	**w/b**	**C (kg/m^3)**	**LP (kg/m^3)**	**AC (kg/m^3)**	**W (kg/m^3)**	**S (kg/m^3)**	**G (kg/m^3)**	**Admix-ture (cc/m^3)**
OPC1 g1.38	1.38	0.30	554	-	-	159	742	980	7473
OPC1+AC5.5 (add)	1.38	0.30	554	-	30	161	742	980	5536
OPC1+AC6.5 (add)	1.38	0.30	554	-	36	161	742	980	5536
OPC1+AC7.5 (add)	1.38	0.30	554	-	42	161	742	980	5536
OPC1 g1.4	1.40	0.30	562	-	-	163	736	972	5618
OPC1+AC5.5 (replace)	1.40	0.30	530	-	30	164	736	972	4239
OPC1+AC6.5 (replace)	1.40	0.30	524	-	36	164	736	972	4193
OPC1+AC7.5 (replace)	1.40	0.30	518	-	42	164	736	972	4147
OPC+LP10	1.30	0.30	465	52	0	149	765	1011	6193
OPC1+LP10+ AC5.5 (add)	1.30	0.30	465	52	28	150	765	1011	4645
OPC1+LP10+ AC6.5 (add)	1.30	0.30	465	52	34	150	765	1011	4645
OPC1+LP10+ AC7.5 (add)	1.30	0.30	465	52	39	150	765	1011	4645
OPC+LP10 g1.4	1.40	0.30	501	56	0	162	736	972	5013
OPC1+LP10+ AC5.5 (replace)	1.40	0.30	470	56	31	164	736	972	3152
OPC1+LP10+ AC6.5 (replace)	1.40	0.30	464	56	36	164	736	972	3118
OPC1+LP10+ AC7.5 (replace)	1.40	0.30	458	56	42	164	736	972	3084
OPC1**	1.20	0.50	362	-	-	181	1050	795	-
OPC1+FA20**	1.20	0.50	281	-	FA*=70	175	1050	795	-
OPC1+RK5.5 add**	1.20	0.50	362	-	20	181	1050	795	-
OPC1+RK6.5 add**	1.20	0.50	362	-	24	181	1050	795	-

OPC1+RK7.5 add**	1.20	0.50	362	-	27	181	1050	795	-
OPC1+RK5.5 replace**	1.20	0.50	341	-	20	181	1050	795	-
OPC1+RK6.5 replace**	1.20	0.50	338	-	24	181	1050	795	-
OPC1+RK7.5 replace**	1.20	0.50	334	-	27	181	1050	795	-

(*) FA is fly ash, (**) mix proportions of carbonation test

Table 3 Mix proportions for investigating durability properties of mortars

Mix	OPC (%)	LP (%)	AC (%)
OPC1	100	-	-
OPC1+AC5.5 (add)	100	-	5.5
OPC1+AC6.5 (add)	100	-	6.5
OPC1+AC7.5 (add)	100	-	7.5
OPC1+AC5.5 (replace)	94.5	-	5.5
OPC1+AC6.5 (replace)	93.5	-	6.5
OPC1+AC7.5 (replace)	92.5	-	7.5
OPC+LP10	90	10	-
OPC1+LP10+ AC5.5 (add)	90	10	5.5
OPC1+LP10+ AC6.5 (add)	90	10	6.5
OPC1+LP10+ AC7.5 (add)	90	10	7.5
OPC1+LP10+ AC5.5 (replace)	84.5	10	5.5
OPC1+LP10+ AC6.5 (replace)	83.5	10	6.5
OPC1+LP10+ AC7.5 (replace)	82.5	10	7.5

5. RESULTS AND DISCUSSIONS

5.1 Slump Loss

The slump loss results of OPC1 containing different percentages of active compound (AC) are shown in Fig. 5.1 (a) and (b) for both addition and replacement cases. From the Fig. 5.1 (a) addition case, it was found that slump retention of concrete containing active compound was better than that of the OPC1 concrete. Fig. 5.1 (b) shows that using the active compound as replacement material caused longer slump retention.

In the case of concrete containing limestone powder, using the active compound as additive material (% by weight of binder) increased slump retention and slump retention was longer than that of the OPC1 concrete (Fig. 5.2 (a)).

Using the active compound as replacement material, the concrete mixture with 7.5% of active compound (% by weight of binder) increased slump retention while the other replacement percentages did not show different slump retention from the control mix as shown in Fig. 5.2 (b).

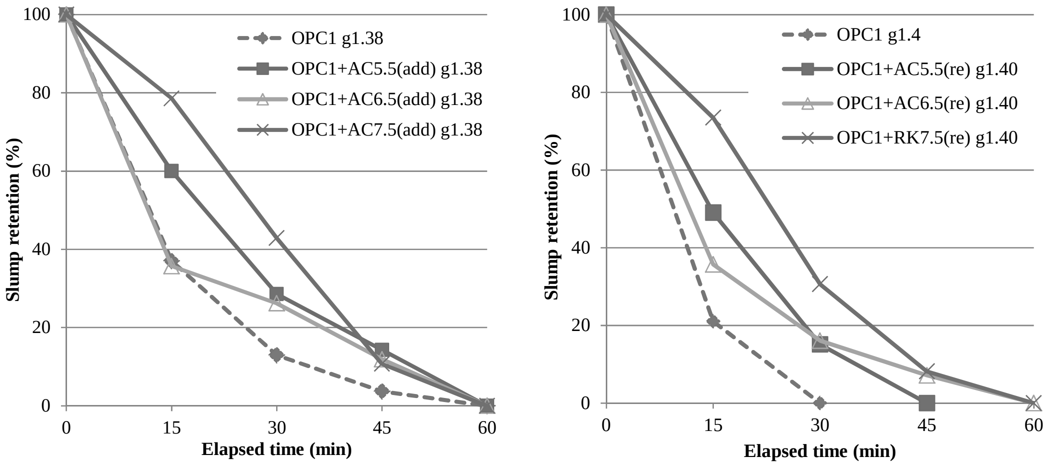

(a) addition case **(b) replacement case**

Fig. 5.1 Slump loss of OPC1 concrete with and without active compound

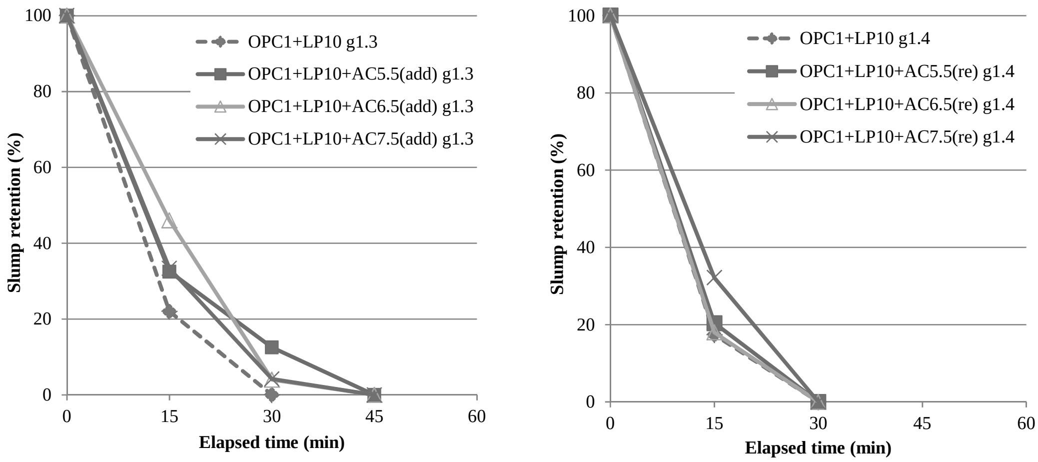

(a) **(b)**

Fig. 5.2 Slump loss of OPC1-LP concrete with and without active compound

5.2 Compressive strength

From Fig. 5.3, using active compound as additive material was effective in increasing early-age compressive strength of OPC1 concrete at the ages of 18 hrs, 1 day, 3 days. Especially at the age of 18 hrs the compressive strength of OPC1 was increased to 16% when using 6.5% of the active compound.

However, by using the active compound as replacement material, the compressive strength of OPC1 concrete containing the active compound were lower than that of OPC1 concrete at early-ages (Fig.5.4) when using 5.5% and 7.5% of the active compound.

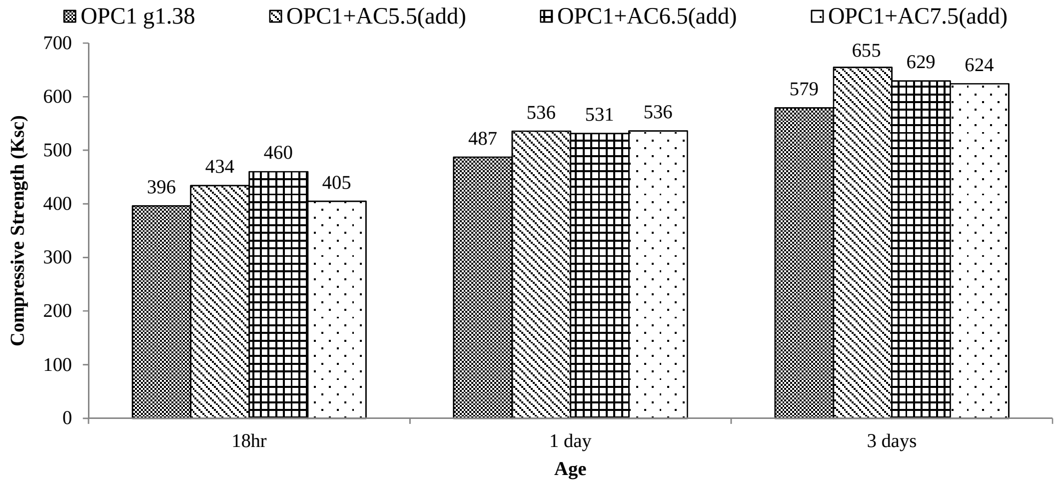

Fig. 5.3 - Compressive strength of OPC1 concrete with and without active compound (addition case)

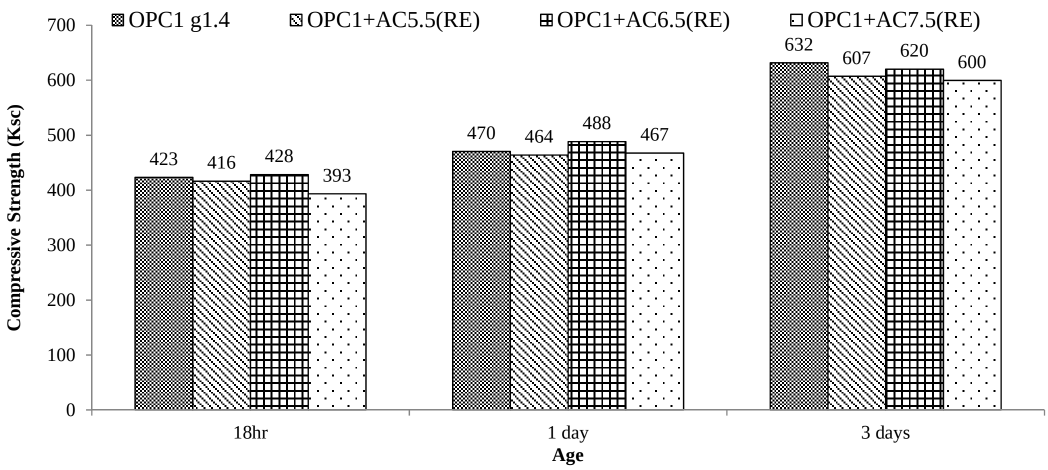

Fig. 5.4 Compressive strength of OPC1 concrete with and without active compound (replacement case)

Fig. 5.5 and Fig. 5.6 show the compressive strength results of limestone powder concrete containing the active compound as an additive and replacement material (% by weight of binder). It can be seen from Fig. 5.5 that using the active compound as aan dditive material resulted in increase in compressive strength of limestone powder concrete at the ages of 18hrs, 1 day and 3 days. At the age of 18hrs the compressive strength of concrete containing 6.5% of active compound obviously increased up to 20% of that of the control concrete sample.

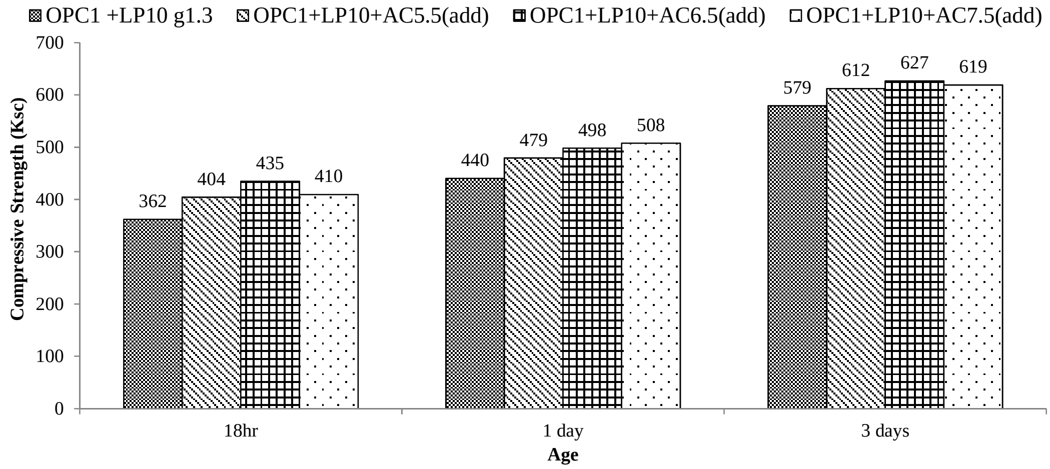

Fig. 5.5 Compressive strength of OPC1-LP concrete with and without active compound (addition case)

On the contrary, using more the active compound as replacement material caused reduction in compressive strength at the ages of 18hrs and 1 day (Fig. 5.6).

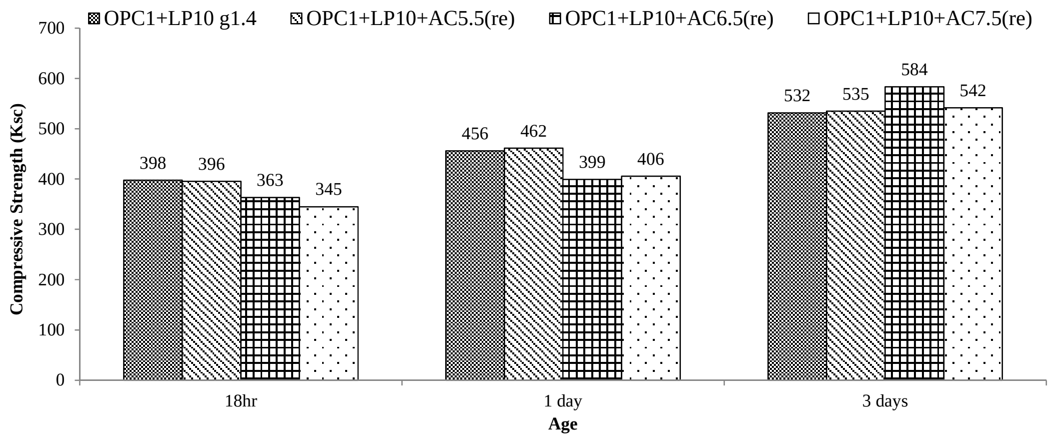

Fig. 5.6 Compressive strength of OPC1-LP concrete with and without active compound (replacement case)

5.3 Volume stability

Fig. 5.7 (a) shows the length change in microns where (+) sign means expansion and (-) means shrinkage of mortar bar samples containing OPC1 with and without the active compound as an additive and replacement material. The figure showed that using higher percentages of addition or replacement of active compound increased the expansion of the samples when stored in water. Moreover, the expansion of the mortar samples exceeded 200 microns as specified by ASTM C150 in some mixtures. The expansions of limestone powder mortar samples with the active compound are shown in Fig. 5.7 (b). It is also obviously seen that the higher the content of active compound used, the more expansion of mortar sample was obtained. In specific case the expansion of samples exceeded 200 microns as specified by ASTM C150.

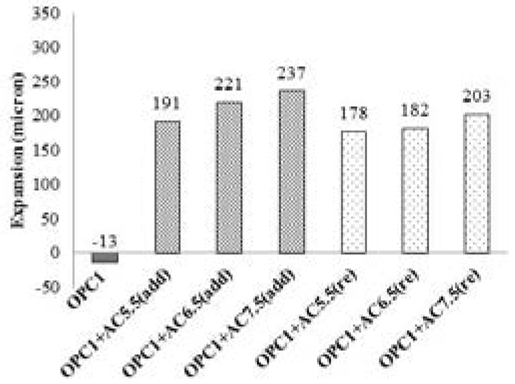

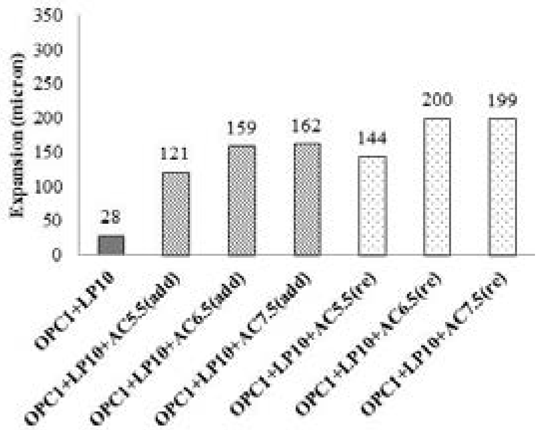

(a) OPC1 mortar samples **(b) OPC1-LP mortar samples**

Fig. 5.7 Expansion of mortar samples after 14 days stored in water

From Fig. 5.8 (a), it can be seen that all cement paste bars with the active compound as an additive and replacement material showed less expansion (+ means shrinkage) than that of the OPC1 paste sample. The test results passed the ASTM C151 standard which allows 0.8% maximum autoclave expansion. The OPC1-LP paste samples containing active compound showed shrinkage results and were below 0.8% as shown in the Fig 5.8 (b).

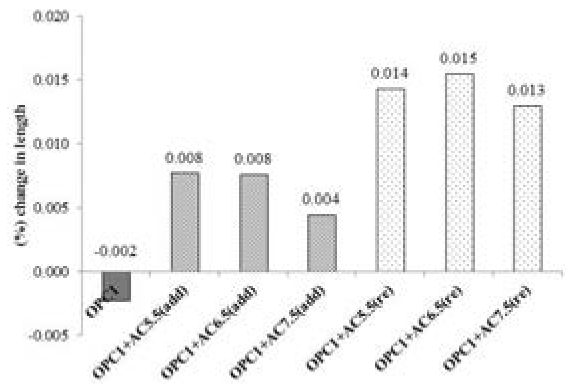

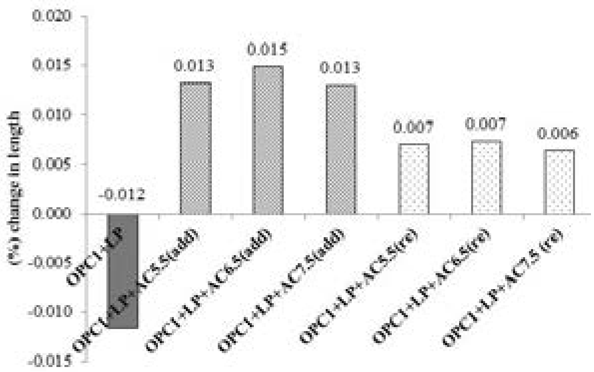

(a) OPC1 paste samples **(b) OPC1-LP paste samples**

Fig. 5.8 Expansion of mortar samples after autoclave test

5.4 Carbonation

From Fig. 5.9 (a) and (b) considering the 7-day seal-cured samples, all carbonation depths of concrete samples containing the active compound were lower than those of the control samples. Concrete samples containing the active compound as additive material showed increase in carbonation depth when the active compound content was increased. On the contrary, the carbonation depths of concrete samples decreased when increasing the active compound content in case of using the active compound as replacement material.

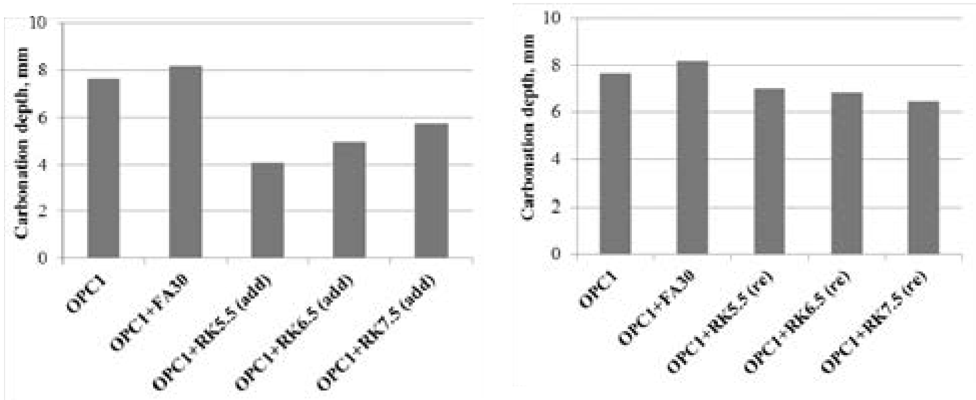

(a) addition case **(b) replacement case**

Fig. 5.9 Carbonation depth of 7-day seal-cured concrete samples containing active compound compared with those of the control samples at 28 days

6. CONCLUSIONS

In general the application of active compound powder as an additive material in concrete mixture improves fresh and hardened concrete properties, i.e., increasing slump retention, increasing early compressive strength especially in case of using the active compound as an additive material in the OPC1-LP mixture. The increase in compressive strength can be attributed to decrease in porosity (Chan et al., 2000). Regarding durability of concrete containing the active compound it is found that the autoclave expansion of mixtures containing the active compound are under 0.8% as specified by ASTM 151 standard. Higher addition content of the active compound causes an increase in expansion in water but less than 200 microns as prescribed by ASTM 150, when incorporated with limestone powder. However, this standard test has shortcomings for the evaluation of internal sulfate attack. Yan et al. (1997) reported that in some cases samples showing an expansion less than 0.02% at 14 days had much higher expansion five years later. In case of carbonation resistance using the active compound as additive material, between 5.5% and 6.5% and seal curing generally provide better carbonation resistance of concrete than those of the control samples.

7. REFERENCES

ASTM 150-00, Standard specification for Portland cement, *Annual Book of ASTM Standards,* Vol. 4.01, 2000.

ASTM C151-00, Standard test method for autoclave expansion of Portland cement, *Annual Book of ASTM Standards,* Vol. 4.01, 2000

ASTM C1038-00, Standard test method for expansion of Portland cement mortar bars stored in water, *Annual Book of ASTM Standards,* Vol. 4.02, 2000.

Chan, Y.N., Luo, X., Sun, W, 2000. Compressive strength and pore structure of high-performance concrete after exposure to high temperature up to 800°C. *Cement and Concrete Reasearch* 30, 247-251.

Yan, F., Jian, D., J.J., Beaudoin., 1997. Expansion of Portland cement mortar due to internal sulphate attack. Cement and Concrete Research 27, 1299-1306.

A simple method to determine the unsaturated soil shear strength with respect to a wide range of matric suction

Hoang Viet NGUYEN[1] and Thi Dieu Chinh LUU[2]
[1] Lecturer, Soil Mechanics and Foundation Department,
National University of Civil Engineering, Vietnam
nhvdhxd@gmail.com
[2] Lecturer, Water Resources and Hydropower Department,
National University of Civil Engineering, Vietnam

ABSTRACT

To determine the shear strength parameters of unsaturated soils, normally a sophisticated and time consuming testing programme needs to be carried out. This paper proposes a simple method, which based on two types of test series: the first series is used to determine the soil water characteristics curve by filter paper method; and the second series is the direct shear tests carried out on the soil at unsaturated state with different water contents. Finally, the nonlinear characteristic of shear strength envelope of unsaturated soils with respect to a large range of matric suction (up to 15600 kPa) is introduced.

Keywords: *unsaturated soil, shear strength, filter paper, direct shear test, matric suction*

1. INTRODUCTION

There is no doubt that unsaturated soil mechanics has already played an important role in geotechnical engineering practice. However, there are some challenges, which have been contributing to the complex, time consuming attributes of unsaturated soil mechanics. The shear strength properties of unsaturated soil are far more complicated than those of saturated soils. It is not only because of laboratory apparatuses used to measure unsaturated soils properties are the technically demanding and quite complex to operate, but also highly negative pore-water pressure is difficult to measure, particularly, in the field (i.e., matric suctions greater than 100 kPa) (Fredlund 2006). In addition, the surface tension of the water-air interface in unsaturated soil also causes more difficulty to extend the formulas for describing the behavior of saturated soils to unsaturated soils (Ye et al. 2010).

The triaxial or direct shear apparatus, that modified to allow for the control and measurement of pore-air and pore-water pressures, are often used (Bishop et al. 1960; Escario & Saez 1986; Gan, Fredlund & Rahardjo 1988; Ho & Fredlund 1982; De Campos & Carrillo 1995; Oloo & Fredlund 1996). However, the equipment and level of expertise required for the characterization of using these tests are beyond the capabilities of most geotechnical laboratories. Furthermore, the time required to perform the tests runs into weeks or even months depending on the coefficient of permeability of the soil being tested (Oloo & Fredlund 1996).

Although, the unsaturated shear strength can also be predicted by combining the shear strength parameters determined at saturated state with the Soil – Water Characteristic Curve (SWCC) property. Several procedures have been proposed in the literature to predict the shear strength of an unsaturated soil (Fredlund et al. 1996; Vanapalli et al. 1996; Öberg & Sällfors 1997; Khalili & Khabbaz 1998). However, these models are still shows remarkable divergence on a wide range of suction when the predicted values are compared with the measured values (Vanapalli & Fredlund 2000).

Several test methods have been developed to establish the SWCC. They can be divided into direct or indirect methods. The direct method measures the negative pore water pressure due to suction directly, whereas the indirect method requires the measurement of other parameters such as relative humidity, resistivity, conductivity or water content and then relates the results to the suction through calibration (Nam et al. 2010). The filter paper method is identified as one of two methods which are having widespread appeal for the measurement of suctions (Ridley et al. 2003).

Since early, Donald (1956) conducted a series of direct shear tests on fine sands and coarse silts subjected to a negative pore-water pressure. The direct shear apparatus modified to apply a negative pore water pressure by applying a constant negative head to the water phase through a membrane at the base of the specimen, while the soil specimens were exposed to the atmosphere to maintain a pore air pressure, of zero gauge pressure. However, this apparatus limited the applied matric suction, to 101 (kPa) due to water cavities in the measuring system at a negative gauge pressure approaching 101 kPa. To solve that problem, Hilf (1956) suggested that pore-air and pore-water pressures could both be raised to positive pressure in order to apply matric suctions higher than 101 kPa without cavitation in measuring system. The proposed procedure is referred to as the axis-translation technique. This technique is performed with the use of a high air entry disc that allows the passage of water but prevents the passage of air. As a result, the pore-air and pore-water pressures can be controlled or measured independently as long as matric suction of the soil does not exceed the air entry value of the ceramic disc (Gan, Fredlund & Rahardjo 1988).

Using the axis-translation technique, Escario (1980) modified the conventional direct shear test to be capable of controlling suction during test. A direct shear test box is placed inside a chamber into which nitrogen under pressure may be introduced to the upper part of the soil sample through a coarse grained porous stone. The lower face of the sample is in contact with water at atmospheric pressure through a high air entry value porous stone (1500 kPa). When equilibrium is reached, the suction in the pore-water is equal to the applied air pressure. The vertical and lateral forces and displacements are monitored with appropriate push rods (Escario and Saez 1986). Later, the conventional direct shear test apparatus modified has widely used to study the unsaturated soil shear strength (Escario & Saez 1986; Gan, Fredlund & Rahardjo 1988; De Campos & Carrillo 1995).

It is obvious that the unsaturated soil shear strength often requires advanced apparatus and time consuming test. It becomes an obstacle to apply in engineering practice. Consequently, there have been a number of efforts to simplify the testing procedure for determining the unsaturated soil shear strength parameters. However, it is still a big challenge for geotechnical researchers. Oloo et al. (1996) proposed a quite simple method for determining the unsaturated soil shear strength parameter ϕ^b for statically compacted soils at different water content. The test can be performed on a conventional direct shear apparatus. The angle obtained using the proposed procedure was shown to be comparable to that obtained using the modified direct shear test. Or Vilar (2006) proposed a simplified procedure to estimate the shear strength envelope of unsaturated soils, which is based on an empirical hyperbolic function. The function requires two input values, namely the shear strength of saturated sample and the shear strength of an air-dried sample tested without the need for suction control. Nevertheless, the range of matric suction investigated in the study of Oloo et al. is limited (less than 450 kPa).

In this paper, a more simpler method is proposed to investigate the unsaturated soil shear strength with respect to a wide range of matric suction. The method bases on two types of test series: the first series is used to determine the soil water characteristics curve by filter paper method; and the second series is the direct shear tests carried out on the soil at unsaturated state with different water contents.

2. SOIL MATERIAL

The soil used in this study is a slightly expansive soil taken from a cut slope construction of highway project. After obtaining samples from the site, the soil was exposed in laboratory under non-controlled temperature and humidity condition. A wooden hammer was used to beat the soil lumps, when its water content was dry enough. After the treatment, an amount of soil grains larger than 2 mm in size was discarded by dry sieving. This process was used to obtain soil specimens with the original soil structure thoroughly destroyed. In addition, the specific gravity of soil particles, the liquid and plastic limits of the fines were determined. Their values are shown in Table 1 as below:

Table 1: Physical Soil Properties

Specific Gravity	Liquid Limit	Plastic Limit	Plasticity Index
G_s	W_L (%)	W_P (%)	I_P
2.7	32.39	20.11	12.28

The soil specimens used in the SWCC test series are the same as those used in the direct shear test series. They are reconstituted by the static compaction method.

The dimension of soil specimen is 61.8 mm in diameter and 20 mm in height. To prepare the soil for compaction, the dry soil material is first thoroughly mixed with distilled water to achieve a water content of 14% by weight; after that it is sealed in plastic bag about 24 hours in order to ensure the moisture is uniform over the whole soil bag. After that the soil material is compacted inside a mould to required dry density of 1.738 g/cm^3. Finally, the specimens are saturated by creating a vacuum pressure about 100 kPa to evacuate air bubbles for at least 45 minutes, and then water is slowly filling into the voids of specimens.

3. TEST PROCEDURE

3.1 Soil Water Characteristic Curve Tests

In order to estimate the SWCC, 30 points covering the SWCC are proposed to be carried out by the filter paper method. The calibration filter paper used in this study is Whatman No. 42. The calibration for Whatman No. 42 filter paper reported by a number of authors and summarized by Crilly, M. S. and R. J. Chandler (1993) suggest that the measurements fall within a range that is typically ±25% of the mean. However, by adopting good, consistent methods it is though that better accuracy (e.g. ±10%) can be achieved.

In order to obtain one value on the SWCC, it is required to prepare two soil specimens and three filter paper discs. The diameter of three filter paper discs needs to be a little bit less than the diameter of soil specimens (about 54 to 58 mm). The two soil specimens are taken out of their cut rings together. They are dried up by the natural evaporation process simultaneously until the gravity water contents of two samples approximately reaching the design value. The three filter papers are placed on the top surface of one soil specimen. For the contact procedure, the middle filter paper disc is generally used for the suction measurement, while the upper and lower filter paper discs are primarily used to protect the middle disc from soil contamination. Another soil specimen is placed directly on the three filter paper discs. It means that the intimate contact between the three filter paper discs and two soil specimens needs to be guaranteed during equalization period of water content.

Due to the time period required for establishing the equilibrium of water content between two soil specimens and three filter paper discs is at least 07 days. Consequently, the 02 soil specimens accompanied with the 03 filter paper discs at the middle are wrapped in layers of cling film to prevent the decrease in water content of two soil specimens by evaporation. At the end of the equalization period, the filter papers are removed by using a pair of tweezers, and the water content of the middle filter paper disc is determined. It is used to interpret the matric suction of two soil specimens.

3.2 Direct Shear Tests

After the soil specimens are saturated by vacuum chamber, they are exposed to atmospheric to let the water in the soil specimens evaporate until their gravimetric water contents reach the design value. Before the soil specimens are installed on the standard direct shear apparatus, the specimens are tested to determine both its mass and volume due to slightly change in volume during evaporation. Then the unconsolidated-quick shear condition is applied to all the five groups. During shearing process, the displacement rate of 1.2 mm/minute is imposed (Oloo and Fredlund (1996) used a fast rate of 1 mm/minute). Failure usually occurs within 6 minutes of shearing, thus the change in matric suction during the shearing process is minimized.

The first group includes fifteen saturated soil samples, the others four groups were unsaturated at different gravimetric water content ranges. The gravimetric water content of the soil samples before shearing, w_{Begin} and after shearing, w_{End} were measured by weight. The unsaturated soil specimens and its water contents of the four groups are summarized in Table 2.

Table 2: Summary of Unsaturated Direct Shear Tests

ID	σ (kPa)	m_{unsat} (g)	m_{dry} (g)	m_w (g)	w_{Begin} (%)	w_{End} (%)	Range w_{Begin} (%)	Range w_{End} (%)
S1	50	122.1	104.3	17.8	17.10	18.18	16.53-18.35	16.71-18.57
S2	100	122.8	104.3	18.5	17.77	18.57		
S3	150	123.3	104.3	19.0	18.25	18.12		
S4	200	122.4	104.3	18.1	17.39	17.09		
S5	250	123.1	104.3	18.8	18.06	17.28		
S6	300	121.5	104.3	17.2	16.53	16.71		
S11	50	115.2	104.3	10.9	10.49	10.89	7.90-10.87	7.48-11.26
S12	100	115.0	104.3	10.7	10.29	10.79		
S13	150	114.5	104.3	10.2	9.81	10.94		
S14	200	114.0	104.3	9.7	9.33	10.66		
S15	250	112.5	104.3	8.2	7.90	7.48		
S16	300	113.6	104.3	9.3	8.95	9.35		
S25	50	108.2	104.3	3.9	3.77	3.31	3.58-4.44	2.86-4.23
S24	100	108.2	104.3	3.9	3.77	3.51		
S23	150	108.1	104.3	3.8	3.68	4.23		
S22	200	108.2	104.3	3.9	3.77	3.61		
S21	250	108.0	104.3	3.7	3.58	3.75		
S26	300	108.0	104.3	3.7	3.58	3.51		
S31	50	120.0	104.3	15.7	15.09	14.89	13.65-15.09	13.64-15.19
S32	100	119.9	104.3	15.6	14.99	15.00		
S33	150	119.3	104.3	15.0	14.42	14.81		
S34	200	119.6	104.3	15.3	14.71	15.00		
S35	250	118.9	104.3	14.6	14.03	13.76		
S36	300	118.5	104.3	14.2	13.65	14.67		

4. TEST RESULT AND DISCUSSION

The extended Mohr-Coulomb failure criterion proposed by Fredlund et al. (1978) is widely accepted for analyzing unsaturated soil shear strength, and it also applied to analyze the test result from direct shear tests. Nevertheless, the direct shear test series was carried out on the standard direct shear apparatus at atmospheric condition. Hence, the pore-air pressure gauge is equal to zero ($u_a = 0$). In order to simplify the analysis of the test results of the unsaturated direct shear tests, the extended Mohr-Coulomb equation can be rewritten as follows:

$$\tau_f = c + \sigma_V \tan\phi + S \tan\phi^b \qquad (1)$$

where τ_f is the shear strength (i.e. the maximum shear stress); σ_V is the vertical stress applied on the soil specimen during shear (unchanged during shear); S is the matric suction at failure condition (the maximum duration of shearing is about 7 minutes, thus the matric suction at failure is assumed to equal the matric suction at the beginning of shearing); c is the cohesion; ϕ is the internal friction angle; ϕ^b is the angle indicating the rate of increase in shear strength relative to the matric suction.

In the plane $\tau - \sigma$, the extended Mohr-Coulomb failure criterion is expressed by the linear line; the equation of the failure criterion can be changed to:

$$\tau_f = c_{apparent} + \sigma_V \tan\phi \qquad (2)$$

where $c_{apparent}$ is the apparent cohesion parameter, equals $c + S\tan\phi^b$.

At failure, the shear stresses along shear surface $\left(\tau_f\right)$ were measured, they are depicted again the corresponding applied vertical stress for each test together in Figure 1. Consequently, the extended Mohr-Coulomb failure envelope of each group are gained by using a linear least square fitting method, and also illustrated in the figure. Thus, the apparent cohesion and internal friction angle shear strength parameters are deduced for each group of separated water content, and presented in Table 3.

Table 3: Shear Strength Parameters for the consistent range of vertical stress

Group	Gravimetric Water Content - w_{Begin} (%)	$c_{apparent}(kPa)$	$\tan(\phi)$	$\phi(^0)$
Saturation	20.50%	2.84	0.54396	28.5
Unsaturation	16.53 ~ 18.35%	14.75	0.54396	28.5
	13.65 ~ 15.09%	48.45	0.67753	34.1
	7.90 ~ 10.87%	128.77	0.89482	41.8
	3.58 ~ 4.44%	205.94	1.17110	49.5

Figure 1 shows that the tendency of the increase in the apparent cohesion and internal friction angle parameters with the decrease in the gravimetric water content is obvious, and it is similar to the conclusion reported by Escario & Saez (1986), and Oloo & Fredlund (1996).

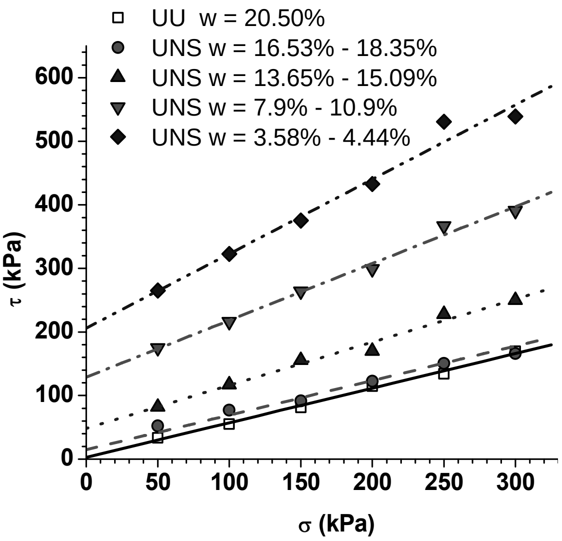

Figure 1: Mohr-Coulomb Failure Envelopes

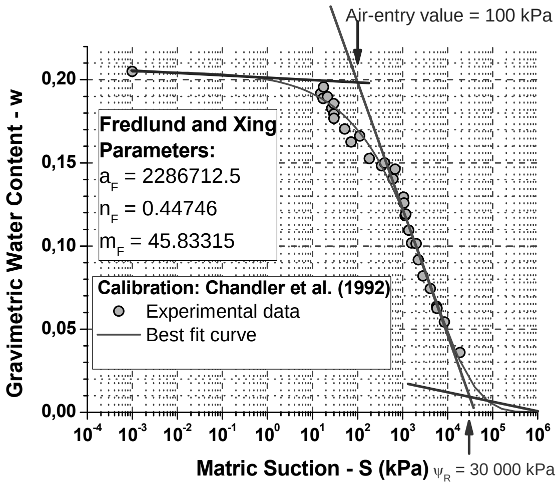

Figure 2: SWCC model (Fredlund & Xing 1994)

In order to investigate the dependence of the shear strength on the matric suction, the relationship between water content and matric suction needs to be determined. Based on the results from SWCC test series, when the equilibrium of water content of the filter paper is achieved, the average gravimetric water content of the two soil specimens for each test is measured. Simultaneously the water content of the middle filter paper pieces is also measured, then the corresponding matric suction of the couple of soil specimens is interpreted from the calibration for Whatman No. 42 filter paper reported by Chandler et al. (1992). After that, the SWCC is gained by fitting the Fredlund and Xing (1994) model with the measured data (Figure 2). The fitted parameters are presented in Table 4 as follows:

Table 4: Fit Model Parameters of SWCC

Parameters	A	n	m	ψ_R (kPa)	$\psi_{AEV}\,(kPa)$
Value	2286712	0.447	45.83	30000	100

In the model of Fredlund and Xing, the gravimetric water content is a function of the variable matric suction, but the equation also can be inversed to that the matric suction is a function of the gravimetric water content variable as Equation (3) below:

$$\psi = a\left[e^{(w_S/w)^{(1/m)}} - e\right]^{\frac{1}{n}} \tag{3}$$

Using Equation (3) the matric suction in soil samples at the beginning of shearing can be deduced from the gravimetric water content measured. Hence, the shear strength of each test can also be illustrated against the matric suction as Figure 3. In addition, the shear stresses at failure are depicted against the applied vertical stress and matric suction in shear stress – vertical stress – matric suction space as Figure 4. In the figure, the shear strength surface envelope is fitted from the observed data. The two figures clearly evidence that the failure surface of unsaturated soil is strongly nonlinear. It means that the shear strength parameter is not constant on the wide range of matric suction.

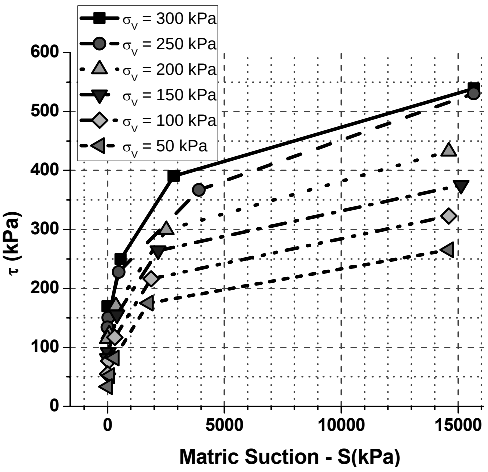

Figure 3: Shear Strength versus Matric Suction

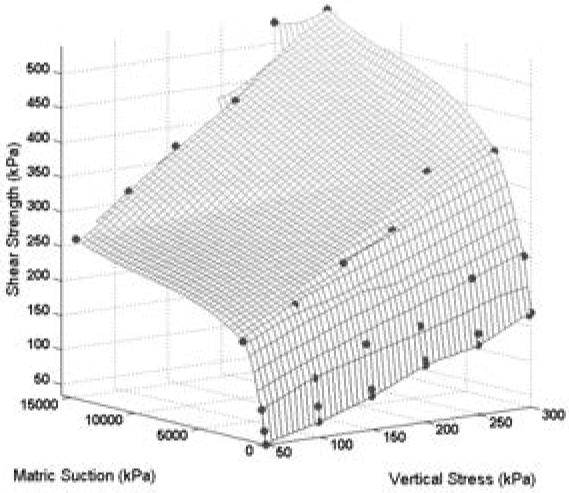

Figure 4: Shear Strength Surface Envelope

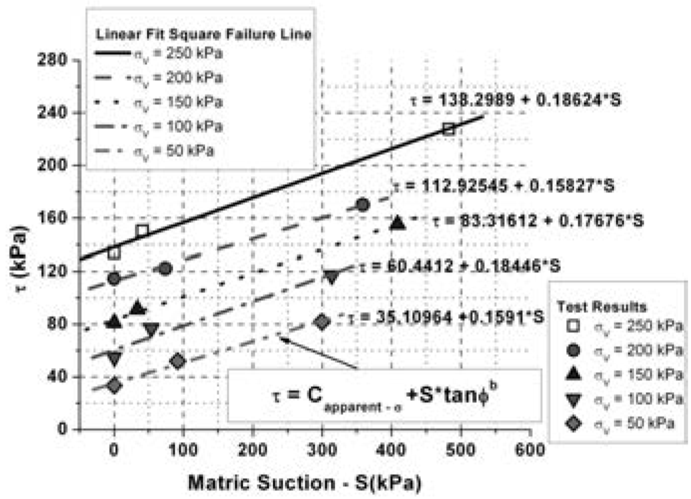

Figure 5: Shear Strength versus Matric Suction

In order to determine the ϕ^b parameter, it is assumed that the ϕ^b parameter is constant when the matrix suction is less than 500 kPa, and the test results at high matric suction (greater than 500 kPa) are ignored. The extended Mohr-Coulomb failure criterion in the $\tau - s$ plane is considered to be linear. The equation of the failure criterion in that plane is reformulated as follow:

$$\tau_f = c_{apparent-\sigma} + s\tan\phi^b \tag{4}$$

where $c_{apparent-\sigma}$ is also the apparent cohesion parameter, equals $c + \sigma_V \tan\phi$.

In plane $\tau - s$, the shear stresses at failure are plotted against the matric suction, hence the corresponding shear strength envelope of each group of the same value of applied vertical stress are obtained by linear least squares fitting method as Figure 5. Hence, the apparent cohesion (in the plane) and ϕ^b parameters are deduced, their values are shown in Table 5. The average deviation of 0.636 reveals that the angle 9.8118 degrees taken average from the five values corresponding to different group under different vertical stress applied 50, 100, 150, 200, and 250 kPa respectively is consistent.

Table 5: Shear Strength Parameter Respect to Matric Suction (S<500 kPa)

Test Series	Vertical Stress	$c_{apparent-\sigma}$	$\tan\phi^b$	ϕ^b
	(kPa)	(kPa)	/	$\left(^{0}\right)$
D250	250	138.2989	0.1862	10.55
D200	200	112.9255	0.1583	8.99
D150	150	83.3161	0.1768	10.02
D100	100	60.4412	0.1845	10.45
D50	50	35.1096	0.1591	9.04
Average		/	/	9.81
Aver. Deviation		/	/	0.64

5. CONCLUSIONS

In this paper, a simple method has proposed to investigate unsaturated soil shear strength characteristic. The testing method is a combination of the two types of test series: the first series is used to determine the soil water characteristics curve by filter paper method; and the second series is the direct shear tests carried out on the soil at unsaturated state with different water contents. Applying this method enables geotechnical engineers to measure the unsaturated soil shear strength with respect to a large range of matric suction (up to 15600 kPa).

ACKNOWLEDGMENTS

The authors appreciate the support from the Key Laboratory of Ministry of Education for Geomechanics and Embankment Engineering and Geotechnical Research Institute of Hohai University.

REFERENCES

Bishop, A. W., Alpan, I., Blight, G. & Donald, I., 1960. Factors controlling the strength of partly saturated cohesive soils. *Proc.Colorado Conference*, 503–532.

De Campos, T. & Carrillo, C., 1995. Direct shear testing on an unsaturated soil from Rio de Janeiro. *Proceedings of The First International Conference on Unsaturated Soils*, Paris, France, vol. 1.
Crilly, S., Chandler, R. J. & Establishment, B. R., 1993. *A Method of Determining the State of Desiccation in Clay Soils*. Building Research Establishment.
Chandler, R., Crilly, M., Smith, M., Smith, M. G. & BRE, 1992. A low-cost method of assessing clay desiccation for low rise buildings. *Proceedings of the ICE - Civil Engineering*, vol. 92, no. 2, 82–89.
Donald, I. B., 1956. Shear strength measurements in unsaturated, non-cohesive soils with negative pore pressure. *Proceedings of the 2nd Australia and New Zealand Conference on Soil Mechanics and Foundation Engineering*, 200–205.
Escario, V. & Saez, J., 1986. The shear strength of partly saturated soils. *Geotechnique*, vol. 36, 453–456.
Fredlund, D. G., 2006. Unsaturated Soil Mechanics in Engineering Practice. *Journal of Geotechnical and Geoenvironmental Engineering*, vol. 132, no. 3, 286–321.
Fredlund, D. G., Morgenstern, N. R. & Widger, R. A., 1978. Shear Strength of Unsaturated Soils. *Canadian Geotechnical Journal*, vol. 15, 313–321.
Fredlund, D. G. & Xing, A., 1994. Equations for the soil-water characteristic curve. *Canadian Geotechnical Journal*, vol. 31, no. 4, 521–532.
Fredlund, D. G., Xing, A., Fredlund, M. D. & Barbour, S. L., 1996. The relationship of the unsaturated soil shear strength to the soil-water characteristic curve. *Canadian Geotechnical Journal*, vol. 33, no. 3, 440–448.
Gan, J. K. M., Fredlund, D. G. & Rahardjo, H., 1988. Determination of the shear strength parameters of an unsaturated soil using the direct shear test. *Canadian Geotechnical Journal*, vol. 25, no. 3, 500–510.
Hilf, J. W., 1956. *An investigation of pore water pressure in compacted codesive soils*. Technical Memorandum, Denver.
Ho, D. Y. & Fredlund, D. G., 1982. A Multistage Triaxial Test for Unsaturated Soil. *American Society for Testing and Materials*.
Khalili, N. & Khabbaz, M. H., 1998. A unique relationship for χ for the determination of the shear strength of unsaturated soils. *Géotechnique*, vol. 48, no. 5, 681–687.
Nam, S., Gutierrez, M., Diplas, P., Petrie, J., Wayllace, A., Lu, N. & Muñoz, J. J., 2010. Comparison of testing techniques and models for establishing the SWCC of riverbank soils. *Engineering Geology*, vol. 110, no. 1–2, 1–10.
Öberg, A. L. & Sällfors, G., 1997. Determination of shear strength parameters of unsaturated silts and sands based on the water retention curve. *ASTM geotechnical testing journal*, vol. 20, no. 1, 40–48.
Oloo, S. Y. & Fredlund, D. G., 1996. A method for determination of ϕb for statically compacted soils. *Canadian Geotechnical Journal*, vol. 33, no. 2, 272–280.
Vilar, O. M., 2006. A simplified procedure to estimate the shear strength envelope of unsaturated soils. *Canadian Geotechnical Journal*, vol. 43, no. 10, 1088–1095.
Ridley, A. M., Dineen, K., Burland, J. B. & Vaughan, P. R., 2003. Soil matrix suction: some examples of its measurement and application in geotechnical engineering. *Géotechnique*, vol. 53, no. 2, 241–253.

Vanapalli, S. K. & Fredlund, D. G., 2000. Comparison of Different Procedures to Predict Unsaturated Soil Shear Strength. *Advances in Unsaturated Geotechnics*, American Society of Civil Engineers, 195–209.

Vanapalli, S. K, Fredlund, D. G., Pufahl, D. E. & Clifton, A. W., 1996. Model for the prediction of shear strength with respect to soil suction. *Canadian Geotechnical Journal*, vol. 33, no. 3, 379–392.

Ye, W. M., Zhang, Y. W., Chen, B. & Zhang, S. F., 2010. Characteristics of Shear Strength of Unsaturated Weak Expansive Soil. In Y Chen, L Zhan & X Tang (editors), *Advances in Environmental Geotechnics*, Springer Berlin Heidelberg, 505–510.

Large prefabricated pile foundation, a solution for high-rise buildings in Hanoi

Bao Viet NGUYEN
National University of Civil Engineering, Hanoi, Vietnam
nbviet@sdh.nuce.edu.vn

ABSTRACT

In order to supply housing for people living in Hanoi and also the other big cities of Vietnam where population is highly dense, buildings with multi storeys are required. In general, most high-rise buildings were based on a strong foundation with bored piles. Normally in construction of bored piles, soils must be drilled and taken out of the ground. The soils and betonite slurry used in the construction are big problems for not only the site but also for environment. The treatment requires a lot of efforts, money and times. Foundation with large prefabricated piles is a solution which could overcome that issue. The solution has been applied to 20 storeys twin buildings in Hanoi. The results show that large prefabricated piles could replace bored piles for high-rise building with advantages of low cost, cleaner site, lack of construction trash.

Keywords: *large prefabricated piles, low cost, construction trash.*

1. INTRODUCTION

Since the mid-1980s, after the "Đổi Mới" reform, Vietnam economy has experienced rapid growth. Nowadays, Vietnam's economy continues to expand at an annual rate in excess of 7%, one of the fastest growing in the world. Together

(a) (b)

Figure 1: Construction site of (a) bored piles and (b) prefabricated piles

with the economic growing, the population of the big cities is increasing rapidly with very highly dense, especially in Ha Noi and Ho Chi Minh city.
In order to supply residential places for the people, a lot of multi storey buildings are rising. The buildings with huge of self-weight and loads require a firm foundation. Till now, foundation based on bored piles is the most common choice for the buildings whose number of storeys higher than 15. Bored pile has large bearing capacity because of large size, long length with toe on the expected hard soils. But the limitation of bored pile is a lot of construction trash induced in the construction and so on. Figure 1a shows a swampy site with bored piles under construction. The poor situation obstruct significantly all the actions in site therefore construction time would be extended. Furthermore, huge amount of soils taken out from the ground and the used betonite slurry need to be removed out of site and treated as particular solid wastes.
Because of the occurrence of high ability rigs in driving pile, recently large prefabricated pile is an alternative solution for the high-rise buildings. Foundation based on the piles of bearing capacity up to 4,000 kN, could sustain all the loads of a building up to 30 storeys. Applying the prefabricated piles would overcome the limitation of the bored piles. The trash induced in the pile construction and the environmental consequence will be eliminated. Figure 1 illustrates the big differences between a swampy site using bored piles and a clean site using prefabricated piles.

2. GEOLOGICAL CONDITIONS OF HANOI

Ha Noi is located in the delta of Hong River in the northern of Viet Nam. The average elevation of Ha Noi is about +8,00m above sea level.
Stratum structure of Ha Noi might be divided into two parts. The upper part contain of various type of soils from weak to pretty hard. Figure 2 illustrates the distribution of major types of the upper part in the area of old Ha Noi. Characteristics of soils in the upper part are listed in the Table 1.
The lower part from about 30m below ground level includes 2 layers a) coarse sand, medium stiff and b) gravels with SPT value about 100. These layers are available to sustain heavy loads so pile foundation of the high-rise buildings is usually required lay on this part.

Figure 2: Distribution maps of soil types in area of old Ha Noi

Table 1: Description of main soil strata types in the area of old Ha Noi

Sub-soil type	**Name**	**Description**	**Distribution**
A Single	A1	Clayed soils, up to 30m thick, PI=0.15~0.4, SPT=12~15, E_0=10Mpa	West Từ Liêm; Đông Anh

layer	A2	Clayed soils, up to 30m thick, PI=0.35~0.6, SPT=8~12, E_0=5~8Mpa	Hà Nội center
B Two layers	B1	Upper layer: Clayed soils, up to 10m thick, PI=0.15~0.4, SPT=12~15, E_0>10Mpa; Lower layer: Medium sand, medium dense, up to 20m thick, SPT≈30,E_0>20Mpa.	North Đông Anh
	B2	Upper layer: Clayed soils, 5~10m thick, PI=0.35~0.6, SPT=9 Lower layer: small sand, medium dense, up to 20m thick, SPT≈12, E_0>10Mpa;	South Đông Anh and Thanh Trì; Gia Lâm
C Multi layers with weak soil	C1	Upper layer: Clayed soils, up to 10m thick, PI=0.15~0.4, SPT=12~15, E_0=10Mpa; Middle layer: Organic soils, up to 10m thick, PI>0.8, SPT=5, E_0=3~5Mpa; Lower layer: Medium sand, up to 10m thick, SPT≈30, E_0≈20Mpa;	North Đông Anh
	C2-3	Upper layer: Clayed soils, up to 10m thick, PI=0.35~0.6, SPT=5~8, E_0=6~8Mpa; Middle layer: Organic soils, up to 15m thick, PI>1.2, SPT=2~4, E_0=3Mpa; Lower layer: Sandy soil, up to 10m thick, SPT≈20, E_0≈15Mpa;	Đông Anh, Gia Lâm (small area) Thanh Trì, South Từ Liêm

3. PREFABICATED PILES FOUNDATION

The most important work in foundation design is decision of size and length of piles then analyses of its bearing capacity. Since mid-1990s, bored piles have been used in Viet Nam. At that time, bored piles are the unique choice of the high-rise buildings foundation. Recently, driving ability of prefabricated piles had remarkable steps. Occurrence of big jack-in rigs for pile driving with pressing force up to 10,000kN has ensured that large prefabricated piles with allowable bearing capacity up to 4,000kN is completely feasible. These piles certainly could be used for the high-rise buildings. It should be said that the rigs are complete combination with counter-weight, cranes and mechanical moving system so that the pile driving could be carried out easily with highly efficient. Furthermore, applying the prefabricated pile will eliminate most of construction trash of bored pile construction such as drilled soils and betonite mud.

To investigate the applicability of the prefabricated piles in Ha Noi area, the following assumptions are used:

a) Number of storeys of the buildings is 15, 20, 25 and 30;

b) Total vertical loads (dead and live loads) on a floor are 15kPa; self-weight and loads of basement are 60kPa;

c) Loads of winds and earthquake on foundation would be considered as 50% of the total vertical loads.

d) Distances between piles (center to center) are 4 times of the pile size;

e) Pile is rectangular and ratio of pile length and pile size is 70.

g) Nominal values of soil properties and layer thickness listed in Table 1 are applied in analyses;

From the assumption a); b); and c), the total loading on foundation, *p*, could be calculated by the following equation and the results are showed on Table 2

$$p = 1.5(15n + 60) \tag{1}$$

Where n = number of storeys.

Table 2 Total loading acting on foundation (kPa)

Building with Number of storeys	15	20	25	30
Loading on foundation	427,5	540	652,5	765

Based on assumptions e) and g), allowable bearing capacity, Q_a, of prefabricated piles are estimated according to equation A.4 in Vietnamese code TCXD 205-1998, "Pile foundation – Specification for design". The results showed in Table 3.

$$Q_a = \frac{q_p.A_p + u\sum f_i.l_i}{FS} \tag{2}$$

Where q_p = soil resistance at pile toe tabulated depend on soil type and depth;
A_p = cross section area of pile;
f_i = soil friction at i^{th} segment tabulated depend on soil type and depth;
l_i = length of i^{th} pile segment;
u = perimeter of pile cross section;
FS = factor of safety = 2.

According to assumption d), the minimum area, A_{min}, required for one pile with size of 35, 40, 45 and 50 are 1.96, 2.56, 3.24, 4.00 sqm, respectively. In order to indicate which size of piles is available for foundation of the high-rise buildings, the bearing capacity of piles should be showed also in term of $Q_{aua} = Q_a/A_{min}$. The term expresses allowable bearing capacity of the pile foundation on a unit of area so that it is easy to compare with the loads of the buildings tabulated in Table 2. The values of Q_a and Q_{aua} are tabulated in the Table 3.

Table 3 Allowable bearing capacity of the piles Q_a (kN) and Q_{aua} (kPa)

Pile size (cm) / **Sub-soil type**	35x35		40x40		45x45		50x50	
	Q_a	Q_{aua}	Q_a	Q_{aua}	Q_a	Q_{aua}	Q_a	Q_{aua}
A1	1260	643	1730	676	2620	809	3250	813
A2	710	362	950	371	1990	614	2550	638
B1	1420	724	1970	770	2970	917	3630	908
B2	950	485	1300	508	2380	735	2980	745
C1	950	485	1430	559	2360	728	2970	743
C2-3	780	398	1180	461	1630	503	2060	515

To assess applicability of the pile foundation to the high-rise buildings, feasibility ratio, R_{fea}, defined as a ratio of allowable bearing capacity of pile foundation on a unit of area, Q_{aua}, and total loading acting on foundation, p.

$$R_{fea} = Q_{aua} / p \tag{3}$$

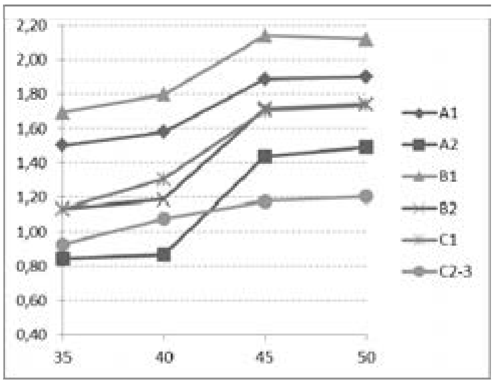

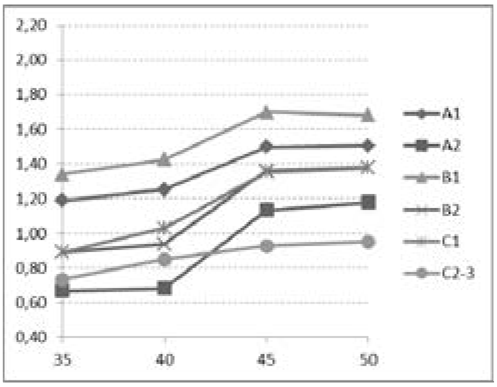

(a) Buildings with storeys of 15 (b) Buildings with storeys of 20

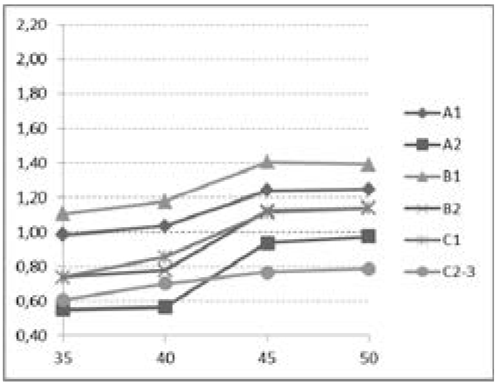

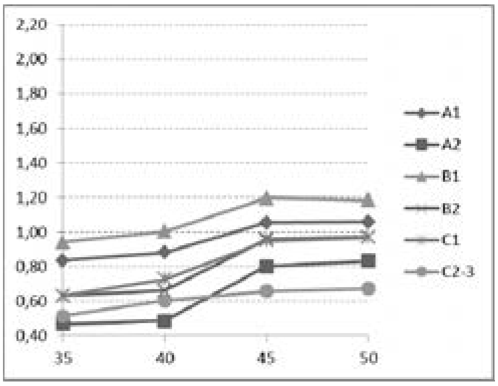

(c) Buildings with storeys of 25 (d) Buildings with storeys of 30

Figure 3: feasibility ratio of prefabricated piles

The values of the feasibility ratio, R_{fea}, are illustrated in Figure 3 for the high-rise building of 15, 20, 25, 30 storeys. Based on value of R_{fea}, it might be divided the applicability degree into three ranges: a) high applicability with $R_{fea}>=1.0$; b) medium applicability with $1.0>R_{fea}>=0.8$ and, c) low applicability with $R_{fea}<0.8$.
Figure 3a showed that 15 storeys buildings could use most of pile sizes for all types of soil strata. In case of A2, C2-3 soil types, pile with size of 35x35cm and 40x40cm might be used if thickness of the soft soils in the sites is thin enough so the pile toe can reach to the stiff sand layer below.
Value of R_{fea} in Figure 3b&c indicated that for 20 or 25 storey buildings, the application of the pile in sites of C2-3 and A2 soil types needs to be considered carefully. A1 and B1 soil types are the 2 stiffest then they are available for all the size of piles. The other types of soil are suitable for pile with size of 45x45cm and 50x50cm.

The applicability of the piles for 30 storeys buildings are showed in Figure 3d. Because of very heavy loads, only pile size of 45x45cm and 50x50cm could be used for soil types of A1 and B1. It is considerably risk if soil types are A2 and C2-3 whatever the pile sizes are. The piles with size of 45x45cm and 50x50cm might be used for B2, C1 soil types with careful consideration.

4. CASE HISTORY

A project of 20 storey twin buildings located in Gia Lam district area is one of the first projects using large prefabricated pile. Strata at the site may be classified into B2 type in the Table 1, the details showed in エラー**!** 参照元が見つかりません。.

Foundation of 45x45cm piles with effective length of 30m was applied for the buildings. Based on the above mentioned approach and results of static load test, the allowable bearing capacity with FS=2.0 are 2,000kN and 1,700kN respectively. Structural bearing capacity of the pile with high strength concrete is of 5,000kN.

Structural analysis results showed that dead and live loads of about 520MN. The vertical load plus wind and earthquake loads transfer to 386 piles of the foundation. The maximum loading acting on one pile is about 1,500kN which is in safety range of 1,700kN.

It should be noted that with total floor area of 41,440sqm, the total vertical loading acting on foundation is about only 12.55kPa much smaller than the proposed value of 15kPa. In addition, the feasibility ratio is about 1.66 much greater than the value evaluated in part 3, Figure 3b. Furthermore, the assumption c) (wind and earthquake load is about 50% of vertical loading) seems to be conservative for 20 storey buildings (the loads of analysis results is only about 10% of the vertical loads).

All the above results have proved the applicability of the piles in term of bearing capacity. On the other hand, the serviceability conditions must be also satisfied. The estimated settlement is even about 10cm but when most of concrete and brick works already finish (70% total loads), the measurement settlement was about 1.0cm. However, it should be noted that the measurement works started a little late, after the 4th floor finish.

Generally, the application of prefabricated pile

Figure 4: Twin buildings

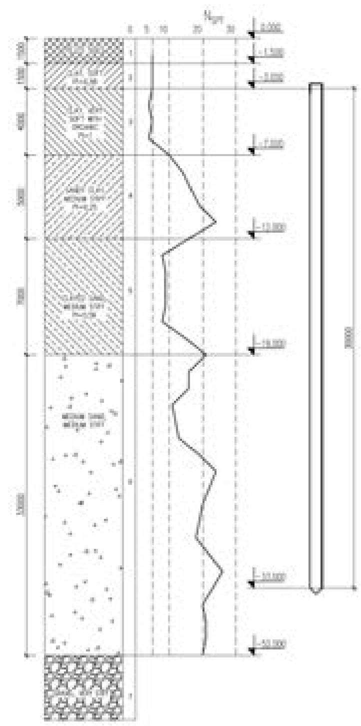

Figure 5: Soil strata of the twin buildings

foundation to the 20 storey twin buildings in Ha Noi was success. The results would open an alternative approach for high-rise foundation with number of advantages such as environmental and economic efficiency, as well as construction time reduced.
Pile driving activities in the site of the twin buildings showed that occasionally the pile toe could not reach to the expected depth even the jack pressure was large enough to destroy the pile head. The cause may be the sandwiched sand layers. If a soft layer is just below the pile toe then the settlements of the buildings may be increase significantly. Hence, in case of sandwiched sand layers, it is necessary to consider carefully application of the prefabricated pile foundation.

5. CONCLUSIONS

The analysis results of both hypothetic and practice indicated that the large prefabricated pile foundation could be applied to the high-rise buildings up to 30 storeys. In case of the 20 storeys twin buildings, the 45x45cm prefabricated piles saved 20% of budgets for foundation. In addition, this approach did not make lot of construction trash like bored pile construction so that the trash treatment was not necessary. Last but not least, the construction site was pretty clean therefore the construction works of foundation could be carried out smoothly.
In Ha Noi, soil types of A1 and B1 is most suitable for prefabricated pile foundation of buildings up to 30 storeys. In case of B2, C1 soil types, the applicability of the piles for buildings up to 25 storeys is highly reliable. If the loads are heavy like buildings of 30 storeys, then pile sizes of 45x45cm and 50x50cm are required with carefully consideration. Buildings of 15 storeys and buildings of 20 storeys could be settled on C2-3 and A2 soil types, respectively, with large size of pile (45x45cm and 50x50cm). When the loads become greater, C2-3 and A2 is not much suitable for the piles.
It should be carefully considered to apply the prefabricated pile foundation in case of soil strata has sandwiched sand layers which could obstruct driving pile to the design locations.

REFERENCES

Geotechnical and Construction Engineering Institute, 2010. *Calculation report of the twin buildings*. Unpublished documents in Vietnamese.
Inspection testing and environment JSC, 2012. *Settlement monitoring report of the twin buildings*. Unpublished documents in Vietnamese.
Nguyen Huy Phuong, et al., 2004. *Collect and verify the existing documents, to study and complement for mapping the distribution of soft soils in Hanoi*. General report of key topics of Hanoi, TC-ĐT/06-02-03, Ha Noi, Viet Nam.
Vietnamese code TCXD 205-1998. *Pile foundation – Specification for design*.

Sustainability in the concrete industry for construction of mega cities

Kiên TONG[1], Thành LE[2] and Lanh PHAM[3]
[1] National University of Civil Engineering, Vietnam
kientt@nuce.edu.vn
[2] Ministry of Construction, Vietnam
[3]Construction Technical College No 1, Vietnam

ABSTRACT

In the last 150 years, concrete has become one of the most widely used building materials for construction of large cities in the world. The use of concrete has a significant impact on sustainability. Environmental responsibility is certainly part of it, but any form of construction must also be socially beneficial and economically viable. A building material, to be truly sustainable, must address all three of these criteria. This paper presents some ideas on using raw materials for sustainable development in the concrete industry. The first is reusing construction demolition waste as recycled aggregate to form an environmental- friendly concrete. The second is using industrial wastes (Fly ash, Blastfurnace slag, glass, silica dust, steel slag, etc.) as replacement materials to both cement and aggregate for concrete. These more sustainable concrete are expected to play a key role in construction of safer mega cities in the coming time as it can help to cut down large volume of carbon dioxide emitted from cement production and also reduce pollution from exploitation of natural raw materials.

Keywords: *Recycled Aggregates (RAs), Construction Demolition Waste (CDW), Recycled Concrete Aggregate (RCA), Sustainable Concrete, Fly ash (FA).*

1. SUSTAINABLE BUILT ENVIRONMENT CONCRETE

There are three general pillars of sustainability in regard to economic, environmental, and social aspects (Tom et al., 2012). When activities are sustainable, no pillar is ignored; instead, a workable balance between the three aspects must be found. Together, the three pillars form what is commonly called the “triple bottom line”. This concept can be expressed graphically as shown in Figure 1.

Concrete has become one of the most widely used building materials on earth. Throughout history, the use of concrete as a building material has contributed significantly to the built environment (Tarun, 2008). Annual global cement production has reached 3.2 billion tonnes, and is expected to increase to some 3.5 billion tonnes per year in 2015 (Martin and Verein, 2011). According to Metha P. K. (Mehta, 2002), if a typical concrete mix contains about 12% cement, 8%

mixing water and 80% aggregate by mass then in addition to 3.2 billion tonnes of cement used worldwide, the concrete industry is consuming 21.3 billion tonnes of sand and rock, and 2.2 billion tons of mixing water annually. In total, the concrete industry, which uses 26.7 billion tonnes of raw materials each year, is the largest user of natural resources in the world. Associated with concrete industry is the inevitable carbon dioxide emissions estimated to be responsible for 5 to 7% of the total global production of carbon dioxide.

Figure 1. Three general pillars of sustainability (Tom et al., 2012)

The long-term approach to lower the enviroment impact of using any materials in development of sustainable concrete industry is to reduce rate consumption of concrete. In the short-term, we must begin practicing industrial ecology for sustainable industrial development (Mehta, 2002). The practice of industrial ecology involves recycling the waste products of one industry by substituting them for the virgin raw materials of another industry, thereby reducing the environmental impact of both.

A sustainable concrete structure is commonly fabricated to ensure that the total environmental impact during its life cycle, including its use, will be minimal (Tarun, 2008). Sustainable concrete should have a very low inherent energy requirement, be produced with little waste, be made from some of the most plentiful resources on earth, produce durable structures, have a very high thermal mass, and be made with recycled materials.
Buildings that are constructed to be both durable and environmentally friendly often lead to higher productivity because the buildings generally lead to better air quality and therefore higher productivity.

For the sustainability of the cement and concrete industries, water and portland cement should be used less and blended cements and organic chemical admixtures should be used more (Mehta, 2002). Bearing in mind that the devastation of air is a global problem, regardless of the locality in which the pollution is created.

2. SUPPLEMENTARY CEMENTITIOUS MATERIALS

The use of cement substitution and of recycled aggregate substitution is being acknowledged recently by many countries in over the world. To date, concrete building solutions for green credits through a level of cement reduction by using supplementary cementitious materials (SCMs) such as fly ash or blast furnace slag. Portland cement is not considered as an environmentally friendly material, because its manufacture creates greenhouse gas emissions. Therefore, engineers must reduce the use of portland cement in concrete (Malhotra, 2004). We must use more blended cements rather than portland cement clinker by blending clinker with other puzolan materials or use SCMs. This also leads to reduce the need of raw materials for manufacturing cement.

2.1. Supplementary Cementitious Materials

A significant proportion of concrete produced contains SCMs as part of the total cementitious component or binder (CCAA, 2010). The three types of SCMs commonly used are puzolan materials such as: ground granulated blast-furnace slag (slag), fly ash and amorphous silica. When blended with portland cement in certain proportions, they impart many beneficial properties to concrete. By reducing the amount of manufactured cement required in a given concrete mix, the use of SCMs further reduces concrete’s environmental impact. SCMs also lead to better economic outcomes for concrete construction - being industrial by-products, they can be produred at a lower cost than cement.

Ground granulated blast furnace slag (GGBS): Slag is a by-product of the manufacture of steel in a blast furnace. It is formed simultaneously with iron; when cooled rapidly it produces a non-metallic product that can be ground and used as an SCM in concrete. In Vietnam, slag has been used in quantities of up to 60% of the mass for slag cement, 20-40% for blended cement or sulfate ressistant cements, 50-60% for low heat cements (VIBM, 2008). The use of GGBS as a partial replacement of cement revealed the different behavior of compressive strength development. Our recent research results on Ultra-High Performance Concrete (UHPC) using GGBS (Thang et al., 2013) revealed that the compressive strength of UHPC was in excess of 150MPa with using 20% of GGBS under normal curing and up to 30% with steam curing. When GGBS was used, the compressive strength of the sample curing at 20^{o}C increased slowly at early age but strength gained faster at 90 days and did not match that of the 90^{o}C curing specimens. After 90 days, under 90^{o}C curing, compressive strength of all UHPC samples could reach 150 MPa with the GGBS replacement up to 50% (fig. 2).

Fly ash (FA): is one of the residues generated in the combustion of coal. FA used as an SCM in concrete is recovered from the electrostatic precipitators before the chimneys in coal-fired power stations. Fly ashes damage the environment when illegally dumped, occupy large volume when disposed of in landfill sites, and could be harmful to human and animal health. The recycling of FA in beneficial products would therefore be useful to alleviate its aforementioned adverse implications. Recycling FA in construction, including concrete, is a major approach to tackle this problem. When replacing cement, FA could indirectly reduce the CO_2 emission linked to cement production as well as decrease landfill area.

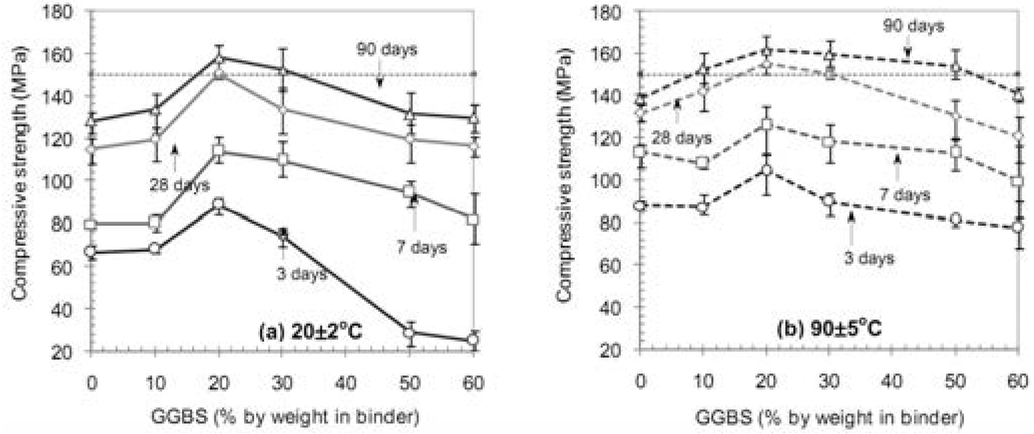

Figure 2. Effect of GGBS on compressive strength of UHPC, w/b = 0.16, (a) 20 ± 2^0C, (b) 90 ± 5^0C (Thang et al., 2013)

In Vietnam, FA is typically used up to 40% of the mass of the total cement, 20-40% for blended cement or sulfate resistant cements, 20-30% for low heat cements (VIBM, 2008). The research results of a high strength concrete (compressive strength of above 80 MPa) investigated in National University of Civil Engineering (Pham et al., 2011b; Tong, 2009) showed that high strength concrete can be manufactured using high content of fly ash as a cement replacement for the structures in Vietnamese marine environment. 35% fly ash added in a 80 MPa compressive strength concrete showed more advantageous in mechanical properties comprising flexural strength, water permeability, chloride penetration and abrasion resistance, when being compared with a typical concrete which is usually used for the structures in Vietnamese marine environment. The use of this concrete probably helps extend the service-life of the infrastructures and also helps reduce a large amount of an industrial waste (Fly ash) discharged from Vietnamese thermal power plants. This will be able to improve all three aspects of a sustainable construction which comprises economy, natural resource and environment.

Amorphous silica: covers a range of products, from a naturally-occurring material to by-products of the silicon and ferrosilicon production processes. The latter is sometimes referred to as silica dust, silica powder, silica flour or microsilica. The name most commonly used is silica fume (SF). In Vietnam, silicafume is typically used 5-10% or up to 15% of the mass of the total cement for specific applications, e.g. high-strength concretes, UHPC. The total cement replacement by using a blend of GGBS and SF can reach to 55% (45% GGBS and 10% SF) in UHPC, the compressive strength of all samples in excess of 150 MPa under 90^oC curing and at 90 days (Thang et al., 2013). Another amorphous silica used in Vietnam is rice husk ash (RHA), which is come from an enormous quantity of waste discharged from Vietnamese rice paddy has been processed to become a mineral admixture for using in concrete products. For example, 20% rice husk ash has been utilised to partially replace cement in a 70- 90 MPa high strength concrete or in lightweight foamed concrete with 4-6 MPa compressive strength and 700-900 kg/m^3 density (Pham et al., 2011a).

2.2. New types of binders

New types of binders and material concepts *Alkali activated cements* (or Geopolymer) is a name used for a large group of binders which solidify after the activation of a reactive solid in a highly alkaline environment. The setting and strength development can mainly be ascribed to polycondensation reactions which form three dimensional networks of amorphous inorganic aluminosilicates. Geopolymers can be produced on the basis of natural sources of aluminosilicates, e.g. kaolin, or on the basis of waste materials like fly ash, slag. The characteristics of geopolymer binders strongly depend on the source material and the activation conditions. Possible advantages of these materials can be a high early and/or final strength, a high resistance against chemical attack, the good passivation of reinforcement, a very dense microstructure and heat resistance (Schneider et al., 2011). According to Davidoits (Davidovits, 2002), geopolymer concrete can reduce 26-45% of green house gas CO_2 compare to conventional concrete. This due to the production of 1 tonnes cement generates 0.55 tonnes of CO_2 and needs the burn of carbon-fuel into 0.42 tonnes of CO_2. To simplify: 1T cement = 1T CO_2. However, the production of 1 tonne of Geopolymeric cement generates 0.180 tones of CO_2, from combustion carbon-fuel, compared with 1.00 tones of CO_2 for Portland cement. Geo-polymeric cement generates six times less CO_2 during manufacture than Portland cement. This simply means that, in newly industrialising countries, six times more cement for infrastructure and building applications might be manufactured, for the same emission of green house gas CO_2. Since January 2013, some of preliminary investigations have been conducted into geopolymer materials at National University of Civil Engineering. These investigations have been based around geopolymer mortars using low-Ca FA and GGBS in Vietnam as the sole pozzolanic solids, the type of alkaline activator is a combination of NaOH and Na-silicate solution. The compressive strength of mortar using recyled fine agregates can reach 50-70Mpa for binder geopolymer based on GGBS under normal curing but only give 10-30Mpa for binder geopolymer based on FA under dry curing at 70^0C depen on alkali dosage was varied from 7.5% to 15% and Alkali modulus in the activator solution.

Novacem is reported as a cement based on magnesium oxide and hydrated magnesium carbonates (Novacem, 2010). According to the inventors of this binder, the raw material is based on magnesium silicates which are globally available in large quantities. During hardening, Novacem absorbs carbon dioxide from ambient air. So it may be reduce environment impact of concrete industry.
Calcium sulfoaluminate (CSA) cements are binders mainly based in the phases yeelimite (C_4A_3S'), belite, CAF and gypsum in varying ratios (Schneider et al., 2011). The solidification of these binders is mainly based on the formation of ettringite and CSH phases. Due to the lower temperatures and the lower content of calcium, the specific CO_2 emissions of CSA cements are lower than those of Portland cement clinker.

3. RECYCLING MATERIALS FOR ENVIRONMENTAL-FRIENDLY CONCRETE

Recycling concrete is not an end in itself, a full Life Cycle Assessment of the concrete structure, including the recycling phase at the end of its life, is required to assess the overall sustainable credentials of the structure (CCANZ, 2011). As regards the concrete manufacturing phase, much effort has gone into reducing the environmental footprint of cement manufacture. Transportation and delivery at all stages of concrete production is the second greatest source of impact. So that, recycling concrete waste for new concrete tends to produce environmental benefit by preserving natural aggregate and water, a finite resource.

It is estimated that 1 billion tonnes of construction and demolition waste (CDW) are generated annually worldwide. Whether CDW originates from clearing operations after natural disasters (e.g., major earthquakes) or from human-controlled activities, the utilization of such waste by recycling can provide not only economically advantages but in addition local recycling minimizes environmental impact by reducing the carbon footprint, embodied energy, and emissions and enhances social products by reducing the need for landfills and the extraction of nonrenewable raw materials. Achieving this goal ensures that a balance is struck among the economic, environmental, and social factors. This is especially efficient in regions of high population density where the limitation of availability of construction materials often leads to cost-effective options for recycling concrete.

Within a life cycle analysis, the use of recovered concrete can lower overall environmental impact:

- Failing to use recovered materials increases landfill and associated environmental and health costs;
- Failing to use recovered materials means virgin materials are used instead;
- Recovered concrete is generally inert;
- In some cases, transportation needs for recycled concrete can be lower than virgin materials (often not located in urban development areas) and as such fuel consumption, CO_2 emissions and road and vehicle use can be reduced.

However, processing technology for recovery of concrete should consider possible air and noise pollution impacts as well as energy consumption, although there is little difference to natural aggregates processing.

3.1. Reusing water and aggregate in concrete mixture

The use of water in concrete production has been a source of debate and research over many years. The acceptability of recycled water for use in concrete is decided by its effect on workability, strength and durability of the concrete. One of the most common methods of recycling water in the concrete batching process is to use water run-off or slurry from concrete production operations (CCAA, 2010). If the batching plant has a reclaiming facility, aggregates can be reclaimed from returned concrete. Unused concrete which is returned to a plant in a plastic state goes through a separation process washing cement slurry from the aggregates, figure 3.

Trucks returning from the site to be washed out discharge into 'concrete reclaimer' where the aggregates are then re-graded from the liquid fines, and are available for use in freshly batched concrete. Recycling washout material reduces the amout of fresh water required for mix operations whilst minimising the amout of solid material which has to be disposed of.

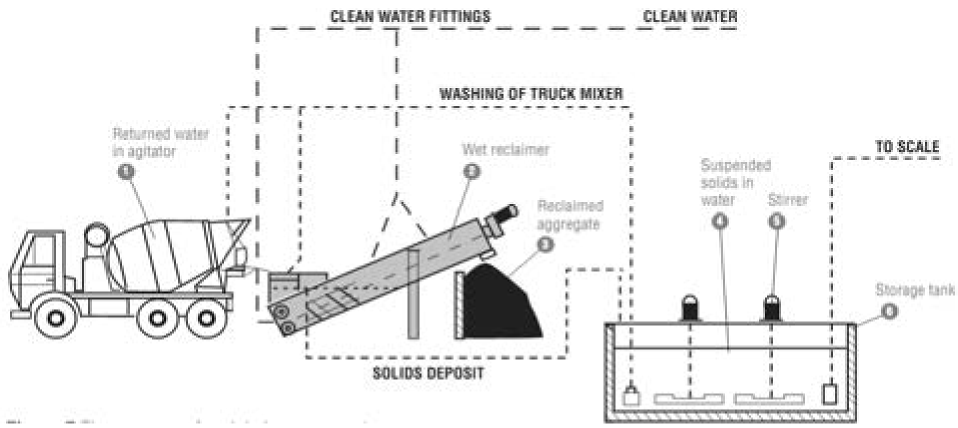

Figure 3. Typical system for recycling wash water/aggregate recovery

3.2. Reproduce hardened concrete and construction demolition waste into recycled aggregate

In many countries, recycled concrete aggregates have been proven to be practical for structural concretes. A number of manufactured and recycled aggregate plants are readily available in over the world as well in Vietnam (Tong, 2011). We have carried out some research projects regarding CDW and found that recycled construction demolition waste from concrete and masonry can be utilised as natural aggregates as well as natural materials for all subgrade, base and subase layers of road foundation without cement treated (Kien et al., 2013; Tong, 2011). When using recycled fine aggregate (RFA) for lower base layer of the high performance pavement structures, it should be reinforced with 7.5% cement for RFA from concrete debris and 10.5% cement for RFA from masonry debris. 10.5% and 12.5% cement respectively from concrete and masonry debris, which using RFA for upper layer of the high performance pavement structures and the bituminous pavements.

In the recycled aggregate plants, both coarse recycled aggregates and fine recycled aggregates are produced and/or dredged for use in new concrete. This use makes up only a small portion of the total extractive industry output, most of which is used in asphalt, road base, civil works and site works. Currently, most concrete producers utilise aggregates sourced from the nearest quarries, and their concrete mixes design to suit with the aggregates. This leads to a lower overall cost, lower environmental impact due to minimising transportation, and often underpins the local economy, especially in rural areas. A fully system for recycling aggregate is showed in figure 4. This can reduce up to 80% freshwater using in the plant and recovery about 90% CDW into high quality recycled aggregate.

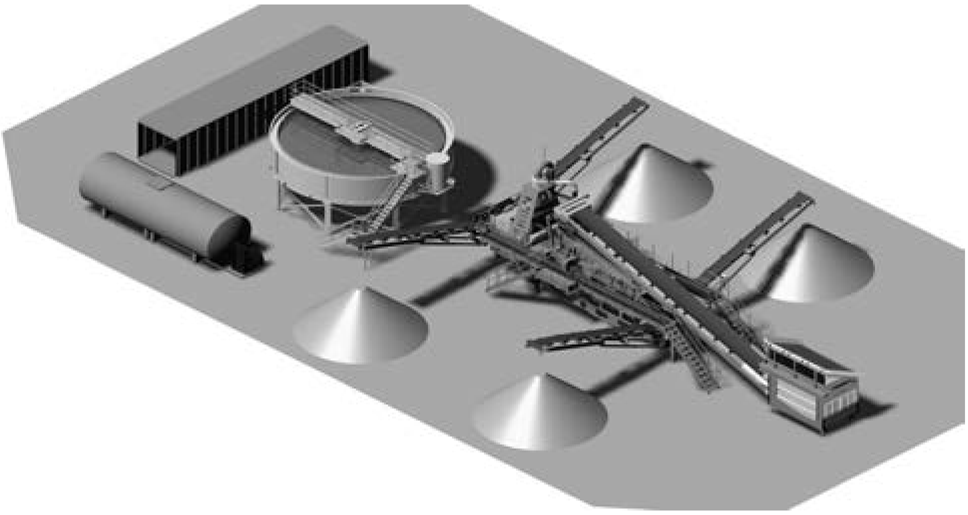

Figure 4. Fully diagram of the recycled aggrgate washing plant, M2500 from construction demolition waste (source: www.cdeglobal.com)

For example, in the UK, the cost of using 10,000 tonnes recycled concrete-derived aggregate as a substitute for limestone aggregate, see Table 1 (Tang, 2008). A direct saving of £89,800 is noted. It mainly arises from the reduction in transportation costs. Significant environmental benefits are also achieved, i.e. a reduction of 31.5 tonnes of CO^2 emission by avoiding the long distance delivery of importing limestone from North Wales. Otherwise, it will take 43 trees approximately 100 years to offset this amount of CO_2.

Table 1. Economic and environmental benefits from using recycled demolition aggregate

Total cost of using quarried limestone (10,000 tonnes)					**Total cost of using recycled aggregate (10,000 tonnes of concrete rubbles as coarse aggregate)**				**Direct saving from using recycled aggregate**	
Gate price, £		Transportation cost			Gate price cost, £	Transportation cost			In cost, £	In CO2, tonne
Min	Max	Cost, £	Total travel distance, mile	CO2 emission, tonne		Cost, £	Total travel distance, mile	CO2 emission, tonne		
£109,500	£122,600	40,000 +20,0	47,059 +4000	38	£59,700	20,000	8,824	6.5	>£89,800	31.5

		00								

There are several barriers to recycling CDW. The most significant barrier is the potential inability on the part of project managers and solid waste authorities to identify markets for the debris. Another barrier is the difficulty in accurately characterizing CDW, CDW is highly variable in both content and quantity. This variability is due to the nature of the waste, the dispersion of construction and demolition activities, inconsistent waste management regulations, range of disposal options, and the variance in cost of disposal options.

5. BARRIERS TO DEVELOP SUSTAINABILE CONCRETE INDUSTRY IN VIETNAM

In Vietnam, natural material sources are commonly availabe, exploration tax of the resources is relatively low meanwhile there are not many economic policies to encourage investors and concrete producers invest on research and production of sustainable concrete. There is no clear plan for disposal CDW area separately and the discharge of leftover fresh concrete in concrete plants.

Building standards are another institutional barrier that discourages the use of recycled materials. Vietnam has not specification requirements for raw materials in processing sustainable concrete, particularly reused and recycled materials. Some out-of-date codes specify the use of particular materials and mixture proportions for a job rather than specifying a particular standard of performance. There are no standards for specification requirements, checking and taking over the buildings which use recycled concrete structures.

A third institutional barrier is lack of a holistic approach in engineering education and research. Currently, structural design teaching at universities is mostly focussed on technical and economic issues. Environmental factors such as global warming and social factors such as noise and dust pollution are largely ignored. The design/selection by civil engineers on construction materials, structure styles and methods of construction/ maintenance clearly has a significant effect on the environment and society. The shift from reductionistic to holistic construction practices must begin by reforming the present system of education and research in the fields of concrete science and technology. Sustainable development of the entire concrete construction industry will have to proceed for a better future in construction of mega cities.

6. CONCLUSION

There are some ways discussed to gain sustainability for concrete: reusing construction demolition waste as recycled aggregate to form an environmental-friendly concrete; and using industrial wastes (Fly ash, Blastfurnace slag, glass, silica dust, steel slag, etc.) as replacement materials to both cement and aggregate for concrete. The more sustainable concrete are expected to play a key role in construction of safer mega cities in the coming time as it can help to cut down large volume of carbon dioxide emitted from cement production and also reduce pollution from exploitation of natural raw materials.

Development of sustainability in the concrete industry to build more sustainable mega cities really needs the support from policy makers and governments. Unnecessary restrictions or barriers on the use of recycling materials should be removed. Crafting precise specifications, taking into account sustainability requirements, educating structural engineers, designers, contractors, and the construction community on new construction materials and technologies, and enforcing contract plans during construction, are the keys to the wide utilisation of sustainable concrete.

REFERENCES

CCAA. 2010. Sustainable Concrete Materials. *Briefing 11 April 2010, Cement Concrete & Aggregates Australia* [Online]. Available: www.ccaa.com.au [Accessed 2012].

CCANZ. 2011. *Best Practice Guide for the use of Recycled Aggregates in New Concrete.* Cement & Concrete Association of New Zealand.

DAVIDOVITS, J. 2002. Environmentally Driven Geopolymer Cement Applications. Geopolymer Institute, 02100 Saint-Quentin, France.

KIEN, T. T., THANH, L. T. & LU, P. V. 2013. Utilisation of construction demolition waste as stabilised materials for road base applications. *In:* The international Conference on Sustainable Built Environment for Now and the Future, 26 -27 March 2013, 2013 Hanoi, Vietnam. Construction publishing house, Page 285-293.

MALHOTRA, V. M. 2004. Role of supplementary cementing materials and superplasticizers in reducing greenhouse gas emissions. *In:* Proc.,ICFRC Int. Conf. on Fiber Composites, High-Performance Concrete, and Smart Materials, Indian Institute of Technology, 2004 Chennai, India. 489-499.

MARTIN, S. & VEREIN, D. Z. 2011. New technology in cement manufactory. *Global Cement Magazine.*

MEHTA, P. K. 2002. Greening of the concrete industry for sustainable development. *ACI Concrete International*, Vol. 24 (7)**,** 23–28.

NOVACEM, L. 2010. *NovacemCarbon Negative Cement: Presentation for SCI 25 November 2010* [Online]. Available: http://novacem.com/wp-content/uploads/2010/12/20101125-Technical-update.pdf [Accessed 2011].

PHAM, H. H., BUI, D. D., TONG, K. T., LE, T. T. & NGUYEN, T. V. 2011a. Development of sustainable building materials at national university of civil engineering of Vietnam. *In:* The international Conference on Innovation and sustainable construction in developing countries, 1 -3 November 2011, 2011a Hanoi, Vietnam. Construction publishing house, Page 201-206.

PHAM, H. H., TONG, K. T. & LE, T. T. 2011b. High strength cncrete using fly ash for structures in Vietnamese marine environment for sustainability. *In:* The international Conference on Innovation and sustainable construction in developing countries, 1 -3 November 2011, 2011b Hanoi, Vietnam. Construction publishing house, Page 173-177.

SCHNEIDER, M., ROMER, M., TSCHUDIN, M. & BOLIO, H. 2011. Sustainable cement production- present and future. *Cement and Concrete Research,* Vol. 41**,** 642–650.

TANG, K. K. 2008. *Precast concrete paving products made with recycled demolition aggregate* Doctor of Philosophy, University of Liverpool (English).

TARUN, N. R. 2008. Sustainability of concrete construction *Practice periodical on structural design and construction, ASCE May 2008***,** pages 98-103.

THANG, N. C., TUAN, N. V., THANH, L. T., HANH, P. H. & GUANG, Y. 2013. Ultra High Performance Concrete using a combination of Silica Fume and Ground Granulated Blast-Furnace Slag in Vietnam. *In:* The international Conference on Sustainable Built Environment for Now and the Future, 26 -27 March 2013, 2013 Hanoi, Vietnam. Construction publishing house, Page 303-309.

TOM, D. V., PETER, T., GARY, F., DAVID, G., MARTHA, V. & EMILY, L. 2012. *Sustainable concrete pavements: A manual of practice.* National Concrete Pavement Technology Center, Iowa State University

TONG, T. K. 2009. *Fine aggregate concrete for the structures in Vietnamese marine environment.* Master of Engineering, National University of Civil Engineering, (In Vietnamese).

TONG, T. K. 2011. *Studying the posibility of recycling demolition watste to produce construction materials.* Final report of University project, National University of Civil Engineering, (In Vietnamese).

VIBM. 2008. *Using artificial mineral materials for manufacturing of portland cement blended and special cements.* Vietnam Institute of Building Materials, (In Vietnamese).

Slump control of fresh concrete by re-dosing polycarboxylic based superplasticizer and comparison with naphthalene based

Ram Hari DHAKAL[1]*, Pitisan KRAMMART[2], Chalermchai WANICHLAMLERT3 and Akarawit NARONGKUL2
1Graduate Student, School of Civil Engineering, Sirindhorn International Institute of Technology(SIIT), Thammasat University, Pathumthani, Thailand
*e-mail of corresponding author: dhakalramhari@gmail.com
2Department of Civil Engineering, Rajamangala University of Technology Thanyaburi, Pathumthani, Thailand
3Construction and Maintenance Technology Research Center, SIIT, Thammasat University, Pathumthani, Thailand

ABSTRACT

This research was made to solve slump loss problem of ready mix concrete during delivery time. Research was focused to find the possibility of slump control in concrete by adding second dose of superplasticizer (SP), after it losses certain percentage of slump. Concrete mix designed for test specimen was prepared with the paste (ratio of volume of cement to volume of void in the aggregate) contain of 1.1 and 1.2, water to cement ratio 0.63, initial dose of SP 0.5% for Naphthalene(NP) and 0.18% for Polycarboxylic(PC) based by weight of cement. Re-dosing of SP was done in 30, 60, 90 minutes respectively. The research was concluded that addition of second dose of SP is possible to regain the slump in field and there is certain relation between percentage slump loss and second dose of SP. But for addition of second dose, NP based SP seems easier practically than PC based. It is also found that there is not any adverse affect on compressive strength of concrete (28 days) due to addition of second dose of SP in concrete.

Keywords: *Concrete, Naphthalene, Polycarboxylic, Re-dosing, Slump*

1. INTRODUCTION

The workability of fresh concrete can be defined by many ways. Workability is the ability of a fresh concrete mix to fill the form/mold properly with the desired work (vibration) and without reducing the concrete's quality. Workability of concrete is defined as the amount of useful internal work necessary to produce full compaction. [1] The ASTM C 125-00 defines workability of the concrete as “that property determines the effort required to manipulate a freshly mixed quantity of concrete with the minimum loss of homogeneity” [2].

The superplasticizer are chemical additives which are introduced to concrete mix to reduce amount of water in the mix, hence reduce capillary porosity of the hardened cementations materials and to maintain a specified workability of fresh concrete for reasonable period of time even at low water cement ratio. [3] This is achieved without undesirable side effects such as excessive air entrainment or set retardation. Major three types of raw materials used in SP, are Sulfonated naphthalene formaldehyde (SNF), Sulfonated melamine formaldehyde (SMF) and Polyacrylates. The dispersing mechanism for water reducing admixtures (i.e. Lignosulfonate based) and SP (Naphthalene and Melamine based) is based on Electrostatic stabilization shown in Figure 1 [4]

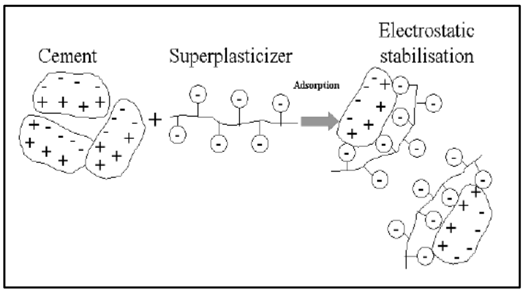

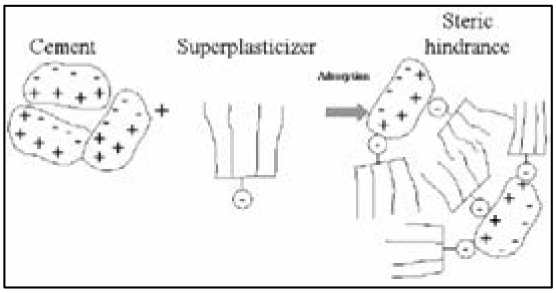

Figure 1: Electrostatic stabilization

Figure 2: Steric hindrance

The dispersing mechanisms for polycarboxylate and comb polymers are based on electrostatic stabilization with Steric hindrance together shown in Figure 2 [4].

Ready mix concrete is ordered based on workability (slump) and strength class. SP is added in concrete which make concrete workable at ready mix factory to get desired slump. In practice workability is a desirable property of concrete at site when pouring and compacting it, but during fresh stage it loses workability with elapsed of time. In case of long haul involved specially in delivering ready-mixed concrete to the site it is needed to retain the workability for longer period. Sometimes the concrete batch does not meet the job requirement when it reaches to the construction site and leads to reject.

There are three possible options to retard or restore the slump loss in concrete; making high initial slump, re-tempering with water and re-tempering with SP after certain interval of time. Making initial slump high is not a reliable option, because it is usually not possible to estimate the time needed before discharge of concrete, re-tempering with water significantly reduces the strength of concrete even though the slump is restored, re-tempering with SP can restores the slump with less adverse effect on concrete properties [5, 6]

2. MATERIALS AND TEST METHODS

2.1 Materials

<u>Cement:</u> Ordinary Portland cement Type I was used. The physical and chemical compositions of cement are shown in the table 2

Table: 1 Chemical/ Physical Properties of Cement

Ingredients	Value	Ingredients	Value
CaO (%)	64.28	K_2O (%)	0.48

SiO_2 (%)	20.35	SO_3 (%)	2.92
Al_2O_3 (%)	5.02	Specific Gravity	3.1
Fe_2O_3 (%)	3.18	Blaine Finesse (cm^2/gm)	3440
MgO (%)	2.03	Loss of Ignition (%)	1.42
Na_2O (%)	0.20		

Aggregate: Normal weight fine and course aggregate was used in this research. The natural river sand passing through sieve no. 4 and naturally found in Thailand was used as the fine aggregate and crushed limestone with the maximum size of 25mm conformed to ASTM C 33 was used as the coarse aggregate. The physical properties of coarse and fine aggregates (gravel and sand) are shown in the table 2.

Table: 2 Physical Properties of Aggregate

Physical Properties	Value		Remarks
	Gravel	Sand	
Specific gravity	2.71	2.6	
Fineness modulus	7.98	2.45	
Water absorption (%)	0.7	1.06	

Water: Tap water available in civil engineering laboratory SIIT, Thammasat University was used.

Chemical Admixture (Superplasticizer): NP based, brand name MXT, and PC based, brand name ADVA 208 SP commercially available and widely used in Thailand was used.

2.2 Mix Proportion

The water cement ratio of mix was 0.63 and the paste contain and of mix was 1.1 and 1.2. Initial dose of SP was 0.55% and 0.18% by weight of cement for NP based and PC based respectively. The minimum void in aggregate was found in for sand/gravel ratio of 0.42 and was 23.5.

2.3 Concrete Mixing Procedure

The drum type concrete mixture was used. Initially, cement, course aggregate and fine aggregate were weighted and put in the mixture and dry mixed for one minute. Then weighted amount of water was added and mixed for one minute. Finally the weighted amount of SP was added and mixed for two minutes. Total mixing time was around four minute.

2.4 Slump Measurement and Re-dosing of SP

The slump was measured immediately after the mixing procedure was finished and recorded as the initial slump. Then the concrete was kept in the tray with the plastic cover to prevent loss of water by evaporation. Then the sample of concrete was used to measure the slump value at stipulated time of 30, 60 and 90 minutes respectively. The measured slump was recorded as the slump before re-does. Before measuring the slump, sample was mixed for two minutes to make it homogenous.

Then guess weighted amount of SP was added to the concrete as a second dose and mixed for two minutes to make it homogenous. Again slump was measured and recorded as slump after second dose of SP. The process was repeated until the original slump was regained. That amount of SP which regains the exact original slump taken as the second dose of SP to regained the slump. The amount of second dose was varied from 0.1 to 1.5 % by weight of cement.

The test method described on the ASTM C143-90 was followed to test the slump.

3. RESULT AND DISCUSSION

3.1. Slump Loss

The rate of slum loss depends on various factors such as initial slump, type and dose of SP, ambient temperature, water binder ratio, type of cement and amount of cement. The figure 3 gives the relation between slump losses with time for NP based and PC based admixture with different cement content. The figure shows that mix with NP based SP loss the slump faster than mix with PC based although dose of NP is higher than PC. This may be due to that NP based type SP dispersing mechanism; it is strongly affected by ionic strength of pore solution. The higher the ionic strength the lower the repulsive force. Negative charges induced between 20 to 40 mV [7]. Workability loss occurs when adsorbed polyelectrolyte layer are compressed by the ionic concentration in pore solution can re-flocculation of cement particles [8]. Molecular structure of PC based SP has side chains which can provide sufficient distance between cement particles, so that Van der Waals force cannot act and its negative charge induced less than 10 mV (Ionic strength of pore solution is lower than NP based)[9]. In practice, admixtures based on steric hindrance can provide sufficient workability for longer period than NP based. Workability loss occurs when side chains are incorporated by growing hydration layers [9].

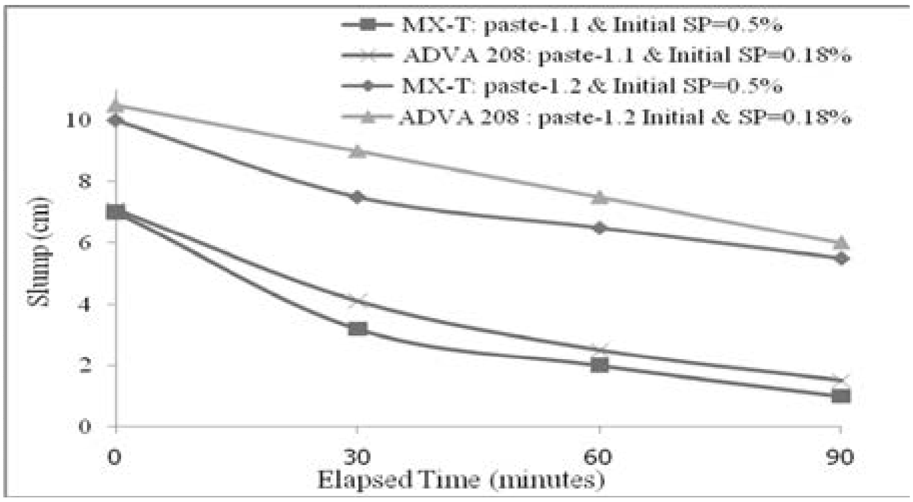

Figure 3: Slump Loss of Concrete

3.2. Second Dose of SP to Regain Original Slump

The figure 4 shows that when the SP is re-dosed the slump of concrete is regained. SP are surface acting agents absorbed on the cement and fine particles giving surface charge and made then repulsion. Addition of SP may increase zeta potential of cement, at the same time viscosity decreased. Increased zeta potentials help to disperse the cement particles and make the concrete more workable and slump is regained. [10]

Figure 5 shows the relation between the percentage slump loss and second dose of SP to regain the original slump. It shows that even for the same percentage slump loss amount of second dose of SP required is more for mix with NP based SP as compare with PC based SP. PC based SP; amount of second dose of SP is between 0.1 and 0.2 percentages by weight of cement for eight percentage slump losses. This is because of the water reducing efficiency of each SP. Figure 6 shows water reducing efficiency of both NP and PC based SP. PC based SP has significantly higher water reducing efficiency than NP based especially in lower SP dose.

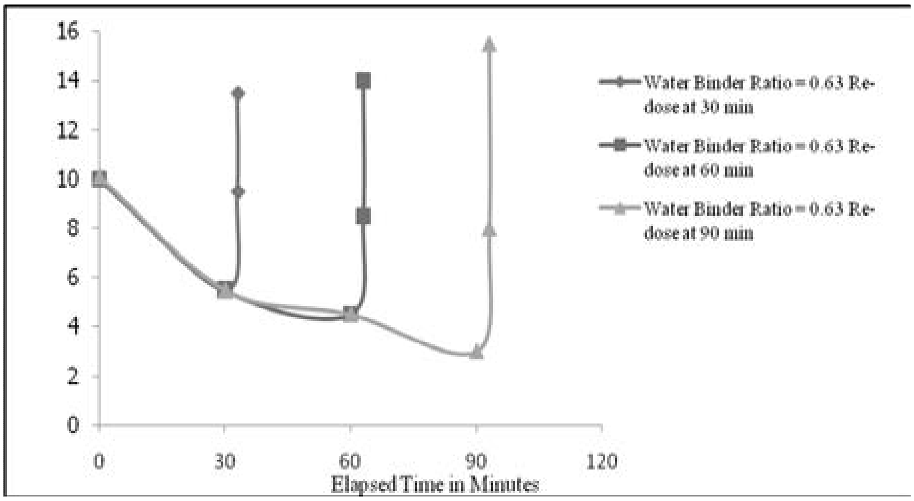

Figure 4: Concept of Re-Dose

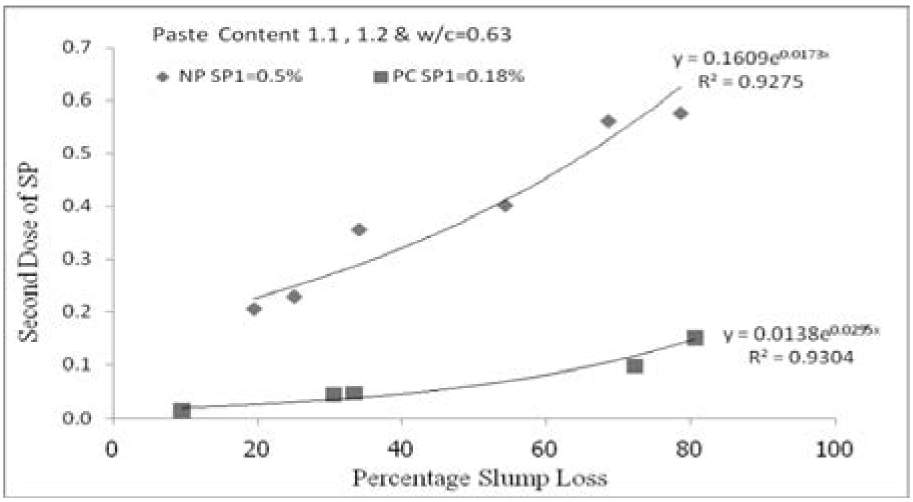

Figure 5: Relation between Percentage Slump loss and Second Dose

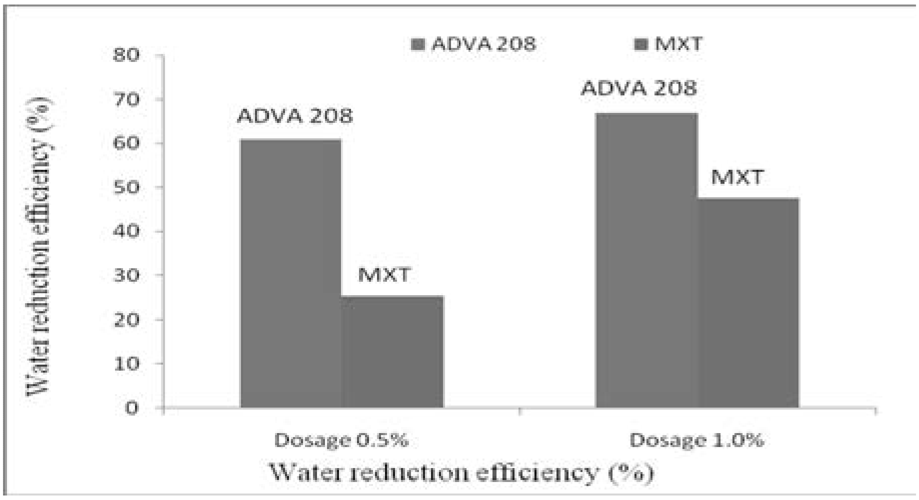

Figure 6: Water reducing efficiency of NP (MXT) and PC (ADVA 208)

From the figure 5 general relation between second dose of SP and percentage slump loss is given by

$$y = ae^{(bx)}$$

Where, ‘a’ and ‘b’: constant, y: percentage of second dose of SP with the total binder, x: percentage of slump loss with respect to original slump.
The value of ‘a’ = 0.161, 0.0138, ‘b’=0.017, 0.029 for NP based and PC based SP respectively for particular water binder ratio and initial dose of SP.

3.3. Effect on Compressive Strength

Figure 7 and 8 shows the compressive strength of concrete with and without re-dose, concrete with paste content 1.1 and 1.2 and water binder ratio 0.63. It was found that variation of compressive strength is less than ten percentages.

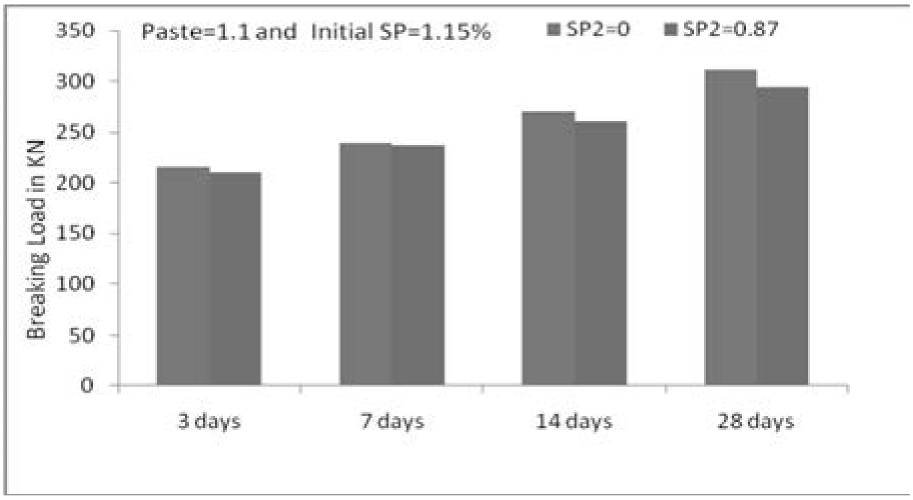

Figure 7: Compressive Strength in 3, 7, 14 and 28 Days with and without Re-dosing (Paste content 1.1 water=0.63)

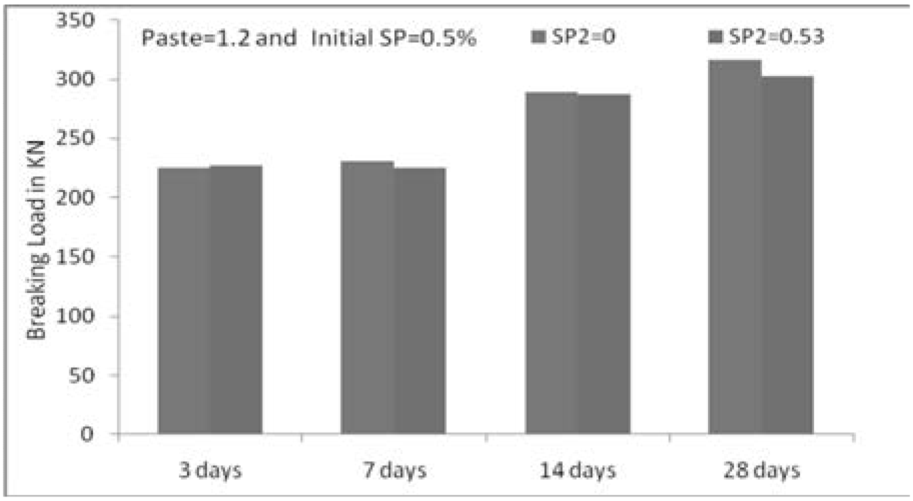

Figure 8: Compressive Strength in 3, 7, 14 and 28 Day with and without Re-dosing
(Paste content 1.2 and water binder = 0.63)

4. CONCLUSION

From the experimental data it has been concluded that, the second dose of SP basically depend up on percentage of slump loss and type of SP used for the particular mix. Second dose of PC based SP is too less even for high percentage loss so it seems that addition of second dose of SP in the field, NP based SP seems easier practically than PC based (difficult to re-dose mix and make homogenous at site). There is no any significant effect on the compressive strength due to the addition of second dose of SP.

ACKNOWLEDGMENTS

Authors would like to thank all team members of Civil Engineering Laboratory, SIIT and all members of CONTEC, SIIT for their valuable suggestion and help during the experiment time. Authors would like special thank to Mr.Wittawat Pattaranawic for helping to collect some data.

REFERENCES

[1]Glanville W H et al 1947, "*The grading of aggregate and workability of concrete*," Road and research Tech. Paper No. 5
[2]ASTM 125-00 "Standard Terminology Relating to Concrete and Concrete Aggregates"
[3]ACI Committee 212, *Chemical Admixture for concrete*, in ACI Manual of concrete Practice, Vol. 1 , PP 212R to 212R-22, 1996

[4]Olafur H. Wallevik and Stefan Kubens, 2008 "*Effect of Water, Superplasticizer, Air- entraining agent and Water to Cement Ratio on Rheological Properties of Mortar*", Innovation Center Iceland, IBRI-Rheocenter.

[5]Wanichlamlert C., Tangtermsirikul S. October 2011, "*2nd Dose of Superplasticizer and Slump Recovery of Concrete Using Naphthalene Based Superplasticizer"* 10th International Symposium on New Technology for Urban Safety of Mega Cities in Asia.

[6]Erdog S. 2005, "*Effect of Retempering with Superplasticizer Admixtures on Slump Loss and Compressive Strength of Concrete Subjected to Prolonged Mixing*", Cement and Concrete Research 35 (2005) 907– 912

[7]Li, C.Z., et al., 2005 "*Effects of Polyethlene Oxide Chains on the Performance of Polycarboxylate-Type Water Reducers*", Cement and Concrete Research 35, pp.867-873.

[8]Kong, H.J., et al., 2006 "*Effects of a Strong Polyelectrolyte on the Rheological Properties of Concentrated Cementitious Suspensions*", Cement and Concrete Research 36, pp.851-857.

[9]Yoshioka, K., et al., 1997 "*Role of Steric Hindrance in the Performance of Water Reducers for Concrete*", Journal of Amercian Ceramic Society 80 (10), p.2667-2672.

[10] Helge Hodne, 2007 "*Rheological Performance of Cementitious Materials Used in Well Cementing*", Doctoral Thesis, University of Stavanger, Norway.

International Center for Urban Safety Engineering
Institute of Industrial Science, The University of Tokyo
4-6-1 Komaba, Meguro-ku,
Tokyo 153-8505, Japan
Tel: +81-3-5452-6472
Fax: +81-3-5452-6476
http://icus.iis.u-tokyo.ac.jp
E-mail: icus@iis.u-tokyo.ac.jp